

Assessment of Mitigation Systems on Vapor Intrusion: Temporal Trends, Attenuation Factors, and Contaminant Migration Routes under Mitigated And Non-mitigated Conditions

Assessment of Mitigation Systems on Vapor Intrusion: Temporal Trends, Attenuation Factors, and Contaminant Migration Routes under Mitigated and Non-mitigated Conditions

Prepared for

U.S. Environmental Protection Agency
National Exposure Research Laboratory
Las Vegas, Nevada

Prepared by

RTI International
3040 E. Cornwallis Road
Research Triangle Park, NC 27709

and

ARCADIS U.S., Inc.
4915 Prospectus Drive, Suite F
Durham, NC 27713

EPA Contract EP-C-11-036, Task Order 009

Although this work was reviewed by EPA and approved for publication, it may not necessarily reflect official Agency policy. Mention of trade names and commercial products does not constitute endorsement or recommendation for use.

U.S. Environmental Protection Agency
Office of Research and Development
Washington, DC 20460

Table of Contents

| | | |
|---------|---|------|
| 1.0 | Executive Summary | 1-1 |
| 1.1 | Background | 1-1 |
| 1.2 | Purpose and Objectives | 1-1 |
| 1.3 | Methods | 1-2 |
| 1.4 | Conclusions | 1-3 |
| 1.4.1 | Conceptual Site Model: VOC Data..... | 1-3 |
| 1.4.2 | Mitigation System Performance—Radon | 1-3 |
| 1.4.3 | Mitigation System Performance—VOCs | 1-4 |
| 1.4.4 | Meteorological Effects on Vapor Intrusion | 1-5 |
| 1.4.5 | Preferential Pathways and Conceptual Site Model: Helium Tracer and Geophysical Tests | 1-6 |
| 1.4.6 | Temporal Variability and Trends..... | 1-8 |
| 1.4.7 | Summary | 1-8 |
| 2.0 | Introduction | 2-1 |
| 2.1 | Background | 2-2 |
| 2.1.1 | Variability in Vapor Intrusion Studies | 2-4 |
| 2.1.1.1 | Spatial Variability | 2-5 |
| 2.1.1.2 | Temporal Variability | 2-7 |
| 2.1.1.3 | Measurement Variability | 2-8 |
| 2.1.2 | Vapor Attenuation Factors..... | 2-9 |
| 2.1.3 | Potential for Use of Radon as a Surrogate for VOC Vapor Intrusion..... | 2-9 |
| 2.1.4 | Passive VOC Sampling..... | 2-12 |
| 2.2 | Objectives | 2-16 |
| 2.2.1 | Time Scale and Measurement of Independent and Dependent Variables..... | 2-18 |
| 2.2.2 | Data Quality Objectives and Criteria..... | 2-18 |
| 3.0 | Methods..... | 3-1 |
| 3.1 | Site Description | 3-1 |
| 3.1.1 | Area Geology/Hydrogeology | 3-1 |
| 3.1.2 | Area Potential Sources | 3-1 |
| 3.1.3 | Building Description..... | 3-7 |
| 3.1.3.1 | Building Age, Condition, and HVAC | 3-7 |
| 3.1.3.2 | Building Utilities/Potential Entry Points | 3-8 |
| 3.1.4 | Building Occupancy During Sampling..... | 3-9 |
| 3.1.5 | Investigation History..... | 3-9 |
| 3.2 | Evolution of Conceptual Site Model | 3-10 |
| 3.2.1 | Prior to 2011–2012 Investigations | 3-10 |
| 3.2.2 | After 2011–2012 Investigations (U.S. EPA, 2012a)..... | 3-10 |
| 3.2.3 | Refinements in Conceptual Site Model Sought in this 2012–2013 Study | 3-11 |

| | | |
|-------|--|------|
| 3.3 | Building Renovation and Mitigation | 3-12 |
| 3.3.1 | Subslab Depressurization Mitigation System Installation | 3-12 |
| 3.4 | Monitoring, Sampling, and Analysis | 3-19 |
| 3.4.1 | Indoor and Outdoor Air VOC Monitoring | 3-19 |
| 3.4.2 | Subslab and Soil Gas (TO-17) | 3-21 |
| 3.4.3 | Online Gas Chromatograph | 3-22 |
| 3.4.4 | Groundwater | 3-23 |
| 3.4.5 | Subslab Depressurization System Stack Gas Sampling | 3-24 |
| 3.5 | Radon Sampling and Analysis | 3-24 |
| 3.5.1 | Indoor Air Radon Sampling and Analysis | 3-24 |
| 3.5.2 | Subslab and Soil Gas Radon Sampling and Analysis | 3-25 |
| 3.5.3 | Continuous (Real-Time) Indoor Air Radon Sampling and Analysis | 3-26 |
| 3.6 | Physical Parameters Monitoring | 3-26 |
| 3.6.1 | On-Site Weather Station | 3-26 |
| 3.6.2 | Indoor Temperature | 3-28 |
| 3.6.3 | Soil Temperature | 3-28 |
| 3.6.4 | Soil Moisture | 3-28 |
| 3.6.5 | Potentiometric Surface/Water Levels | 3-29 |
| 3.6.6 | Differential Pressure | 3-29 |
| 3.6.7 | Air Exchange Rate | 3-30 |
| 3.6.8 | Crack Monitoring | 3-30 |
| 3.7 | Data Aggregation Methods | 3-31 |
| 4.0 | Results and Discussion: Quality Assurance Checks of Individual Data Sets | 4-1 |
| 4.1 | VOC Sampling—Indoor Air—Passive—Air Toxics Ltd. (ATL) | 4-1 |
| 4.1.1 | Blanks | 4-1 |
| 4.1.2 | Surrogate Recoveries | 4-3 |
| 4.1.3 | Laboratory Control Sample Recoveries | 4-3 |
| 4.1.4 | Duplicates | 4-4 |
| 4.2 | VOC Sampling—Subslab and Soil Gas (TO-17)—U.S. EPA | 4-5 |
| 4.2.1 | Blanks | 4-5 |
| 4.2.2 | Calibration Verification | 4-7 |
| 4.2.3 | Internal Standard Recoveries | 4-8 |
| 4.2.4 | Surrogate Recoveries | 4-8 |
| 4.2.5 | Laboratory Control Sample Recoveries | 4-9 |
| 4.2.6 | Field Duplicates | 4-9 |
| 4.3 | Online Gas Chromatograph (Soil Gas and Indoor Air) | 4-10 |
| 4.3.1 | Blanks | 4-10 |
| 4.3.2 | Initial Calibration | 4-10 |
| 4.3.3 | Continuing Calibration | 4-11 |
| 4.3.4 | Calibration Check via Comparison to Fixed Laboratory (TO-15 vs. Online GC) | 4-12 |
| 4.3.5 | Agreement of Online GC Results with TO-17 Verification Samples | 4-14 |

| | | |
|-------|---|------|
| 4.3.6 | Agreement of Integrated Online GC Results with Passive Samplers | 4-16 |
| 4.3.7 | Overall Assessment of Online GC Data | 4-37 |
| 4.4 | Radon | 4-43 |
| 4.4.1 | Indoor Air: Comparison of Electrets Field, ARCADIS to Charcoal Analyzed by U.S. EPA R&IE National Laboratory | 4-43 |
| 4.4.2 | Comparison of Average of Real-Time AlphaGUARD to Electrets and Charcoal Canisters..... | 4-45 |
| 4.4.3 | Quality Assurance Checks of Electrets..... | 4-48 |
| 4.5 | On-Site Weather Station vs. National Weather Service (NWS) | 4-48 |
| 4.6 | Groundwater Analysis—EPA NERL | 4-51 |
| 4.6.1 | Blanks | 4-51 |
| 4.6.2 | Surrogate Recoveries | 4-53 |
| 4.7 | Groundwater Analysis—Pace Laboratories | 4-54 |
| 4.8 | Database | 4-54 |
| 4.8.1 | Checks on Laboratory Reports..... | 4-54 |
| 4.8.2 | Database Checks | 4-54 |
| 4.9 | Air Exchange Rate Measurements | 4-55 |
| 5.0 | Subslab Depressurization Mitigation System Monitoring Results..... | 5-1 |
| 5.1 | Differential Pressure and Mitigation System Flow | 5-1 |
| 5.1.1 | Radon System Design Standards for Differential Pressure | 5-1 |
| 5.1.2 | Differential Pressure Monitoring of this SSD System..... | 5-3 |
| 5.1.3 | Mitigation System Flow..... | 5-21 |
| 5.2 | Radon Monitoring: Hourly and Weekly Time Scales | 5-21 |
| 5.3 | VOC Monitoring During Mitigation Testing | 5-30 |
| 5.3.1 | Descriptive Statistics..... | 5-33 |
| 5.3.2 | Effect of Mitigation System Status on Indoor Air VOC Levels..... | 5-45 |
| 5.3.3 | Discussion..... | 5-46 |
| 5.4 | Stack Gas Monitoring..... | 5-47 |
| 5.4.1 | Is Stack Gas an Indicator of System Performance in Protecting Indoor Air?..... | 5-47 |
| 5.4.2 | Air Exchange Rate Measurements..... | 5-50 |
| 5.4.3 | Stack Gas Measurements to Define Flux to Structure..... | 5-53 |
| 6.0 | Results and Discussion: VOC Concentration Temporal Trends and Relationship to HVAC and Mitigation | 6-1 |
| 6.1 | VOC Seasonal Trends Based on Weekly, Biweekly, and Monthly Measurements for 52+ Weeks..... | 6-1 |
| 6.1.1 | Indoor Air | 6-1 |
| 6.1.2 | Subslab Soil Gas | 6-4 |
| 6.1.3 | Shallow and Deep Soil Gas..... | 6-15 |
| 6.2 | Radon Seasonal Trends (based on Weekly Measurements)..... | 6-45 |
| 6.3 | VOC Short-Term Variability (Based on Daily and Hourly VOC Sampling)..... | 6-45 |
| 6.3.1 | Indoor Air | 6-45 |

| | | |
|---------|---|------|
| 6.3.1.1 | Chloroform | 6-45 |
| 6.3.2 | Subsurface Soil Gas Data..... | 6-51 |
| 6.3.2.1 | Chloroform | 6-51 |
| 6.3.2.2 | Tetrachloroethylene (PCE)..... | 6-53 |
| 6.4 | Radon Short-Term Variability (Based on Daily and More Frequent Measurements)..... | 6-58 |
| 6.5 | Outdoor Climate/Weather Data..... | 6-59 |
| 6.5.1 | Indianapolis Weather Compared with VOCs and Radon | 6-65 |
| 6.5.1.1 | Wall Port VOC Concentrations as a Function of Barometric Pressure and Wind Speed | 6-51 |
| 7.0 | Results and Discussion: Establishing the Relationship between VOCs and Radon in Subslab/Subsurface Soil Gas and Indoor Air | 7-1 |
| 7.1 | Previously Reported Tests of Radon as a Semiquantitative VOC Tracer | 7-1 |
| 7.2 | Understanding the Performance of the Radon Tracer During Mitigation Testing | 7-1 |
| 7.3 | Attenuation Factors Derived Using the Radon Tracer | 7-4 |
| 7.4 | Radon Tracer in Statistical Time Series Analysis | 7-4 |
| 8.0 | Results and Discussion: Attenuation of Soil Gas VOCs and Radon..... | 8-1 |
| 8.1 | Calculation of Daily Attenuation Factors without Mitigation..... | 8-1 |
| 8.1.1 | Daily Radon Attenuation Factors without Mitigation..... | 8-2 |
| 8.1.2 | Daily VOC Attenuation Factors without Mitigation..... | 8-2 |
| 8.2 | Subslab and Soil Gas to Indoor Air Weekly Attenuation Factors..... | 8-8 |
| 8.2.1 | Radon Weekly Attenuation Factors | 8-8 |
| 8.2.2 | VOC Weekly Attenuation Factors | 8-11 |
| 8.3 | Effect of Mitigation | 8-19 |
| 8.3.1 | Subslab to Indoor Air Daily Attenuation..... | 8-20 |
| 8.3.2 | Subslab and Soil Gas to Indoor Air Weekly Attenuation | 8-23 |
| 9.0 | Results and Discussion: Determine If Observed Changes in Indoor Air Concentration of Volatile Organics of Interest are Mechanistically Attributable to Changes in Vapor Intrusion | 9-1 |
| 9.1 | Large Differential Pressures, Pressure Changes and Meteorological Factors Analysis with Mitigation Off | 9-1 |
| 9.1.1 | Temperature Effects on Differential Pressure..... | 9-1 |
| 9.1.2 | Barometric Pressure Effects on Differential Pressure..... | 9-4 |
| 9.1.3 | Precipitation Effects on Differential Pressure..... | 9-8 |
| 9.1.4 | Wind Effects on Differential Pressure | 9-10 |
| 9.1.5 | Assessment of Whether High Observed Differential Pressures Could be Artifactual | 9-16 |
| 9.1.6 | Examination of High-Resolution Time Series Data for Individual Extreme Differential Pressure Events | 9-16 |
| 9.2 | Influence of Meteorological Conditions on Indoor VOC Concentration; Mitigation Off | 9-44 |
| 9.2.1 | Temperature Effect on VOCs | 9-44 |

| | | |
|--------|---|-------|
| 9.2.2 | Barometric Pressure Effect on VOCs | 9-47 |
| 9.2.3 | Precipitation Effects on VOCs..... | 9-47 |
| 9.2.4 | Effect of Wind on VOC Concentrations..... | 9-52 |
| 9.3 | Summary of Meteorological Effects on Vapor Intrusion—Evidence Presented in Sections 6 and 9..... | 9-59 |
| 10.0 | Time Series Analysis..... | 10-1 |
| 10.1 | Time Series Analysis of Indoor Radon Data (AlphaGUARD) Aggregated with 1-Day Time Resolution | 10-2 |
| 10.2 | Correlation between Radon Concentration and Categorical Predictors | 10-18 |
| 10.3 | Correlation between Radon Concentration Time Series for 422 Basement South in 2011–2012 (X422BN-1) and Continuous Predictor Variables..... | 10-19 |
| 10.4 | Correlation between Radon Concentration Time Series for 422 2nd Floor Office (2011–2012) and Predictor Variables..... | 10-25 |
| 10.5 | Correlation between Radon Concentration Time Series for 422 Basement South (2012–2013) and Predictor Variables..... | 10-32 |
| 10.6 | Correlation between Radon Concentration Time Series for 422 Office on 2nd Floor and Predictor Variables | 10-37 |
| 10.7 | Correlation between VOC (Radiello) Time Series and Predictor Variables in 422 Basement South..... | 10-41 |
| 10.7.1 | Stationarity and Serial Correlation Analysis..... | 10-41 |
| 10.7.2 | Predictor Variables Modeled and Their Potential for Autocorrelation..... | 10-50 |
| 10.7.3 | Time Series Analysis Results for 2011–2012 Chloroform Data Set..... | 10-53 |
| 10.7.4 | Time Series Analysis Results for 2011–2012 PCE Data Set..... | 10-57 |
| 10.7.5 | Time Series Analysis of 422 Basement South Chloroform Data Set from the period Sept 2012–Apr 2013 | 10-65 |
| 10.7.6 | Time Series Analysis Results of 422 Basement South PCE Data from Sept 2012 through April 2013..... | 10-71 |
| | Addendum..... | 10-79 |
| 11.0 | Results and Discussion: Do Groundwater Concentrations Control Soil Gas Concentrations at this Site? And Thus Indoor Air Concentrations? | 11-1 |
| 11.1 | Groundwater Level Changes | 11-1 |
| 11.2 | Groundwater Concentration Trends | 11-2 |
| 11.2.1 | Is the Groundwater Concentration Trend Correlated to Well or Water Table Depth?..... | 11-5 |
| 11.3 | Revision to the Conceptual Model—Is the Groundwater Concentration Related to Soil Gas and Indoor Air Concentrations?..... | 11-6 |
| 12.0 | Results and Discussion: Special Studies | 12-2 |
| 12.1 | Summary of Geophysics Study | 12-2 |
| 12.2 | Summary of Tracer Testing..... | 12-4 |
| 12.2.1 | Introduction to Tracer Testing | 12-4 |
| 12.2.2 | Tracer Testing Objective..... | 12-4 |
| 12.2.3 | Tracer Test Experimental Methods..... | 12-4 |

| | | |
|--------|--|-------|
| 12.2.4 | Tracer Test Results and Discussion | 12-5 |
| 12.2.5 | Summary of Tracer Test Conclusions..... | 12-16 |
| 12.3 | Testing Utility of Consumer Grade Radon Device (Safety Siren Pro)..... | 12-16 |
| 12.3.1 | Introduction to the Use of Consumer Grade Radon Monitoring Equipment in Vapor Intrusion..... | 12-16 |
| 12.3.2 | Objective of Consumer-Grade Radon Device Testing | 12-16 |
| 12.3.3 | Methods of Consumer-Grade Radon Device Testing..... | 12-16 |
| 12.3.4 | Consumer Grade Radon Detector Results and Discussion | 12-17 |
| 13.0 | Conclusions and Recommendations..... | 13-1 |
| 13.1 | Conclusions | 13-1 |
| 13.1.1 | Mitigation System Performance | 13-2 |
| 13.1.2 | Meteorological Effects on Vapor Intrusion | 13-4 |
| 13.1.3 | Preferential Pathways and Revisions to Conceptual Site Model: Helium Tracer and Geophysical Tests | 13-5 |
| 13.1.4 | Revisions to Conceptual Site Model: VOC Data..... | 13-7 |
| 13.1.5 | Temporal Trends..... | 13-8 |
| 13.2 | Practical Implications for Practitioners | 13-9 |
| 13.2.1 | Mitigation Design Implications | 13-9 |
| 13.2.2 | Sampling Planning Implications | 13-9 |
| 13.2.3 | Delineating Preferential Pathways..... | 13-10 |
| 13.3 | Recommendations | 13-10 |
| 14.0 | References..... | 14-1 |

Appendix A. Radon Mitigation System Photos and Field Diagnostic Report

Appendix B. Geophysics Report

Appendix C. Additional Statistical Analysis of Effect of Mitigation on Indoor VOC Concentrations

List of Figures

| | | |
|-------|--|------|
| 1-1. | Temporal coverage of data sets collected (red line indicates the cutoff date for this report)..... | 1-5 |
| 1-2. | Indoor air concentrations of PCE (top panel) and radon (middle and bottom panels) with mitigation on (black bars), passive mitigation (no fan, gray bars), and mitigation off (no bar). Snow and frozen ground events are indicated by blue bars and red dots. | 1-9 |
| 2-1. | An overview of important vapor intrusion pathways (U.S. EPA graphic). | 2-3 |
| 2-2. | Soil gas and groundwater concentrations below a slab (Schumacher et al., 2010)..... | 2-6 |
| 3-1. | Lithological fence diagram showing the major soil types beneath the 422/420 house..... | 3-2 |
| 3-2. | Aerial view of duplex, 420/422 East 28th Street, showing nearby sanitary and storm sewers..... | 3-3 |
| 3-3. | East side of house (on right) and adjoining commercial quadraplex visible (left). | 3-4 |
| 3-4. | Roof of adjacent commercial quadraplex. | 3-4 |
| 3-5. | Looking toward southeast corner of adjacent commercial quadraplex..... | 3-5 |
| 3-6. | Visual evidence of historic dry cleaners in area. | 3-6 |
| 3-7. | Front view of house during summer 2011 sampling, with fan testing and weather station..... | 3-7 |
| 3-8. | Front view of duplex under winter conditions showing designation of sides and HVAC setup. | 3-8 |
| 3-9. | 422 (left) and 420 East 28th Street in January 2011. | 3-9 |
| 3-10. | Map view of the 422-side basement showing SSD mitigation system legs, subslab soil gas extraction pits (red circles), and the position of the passive “sampling racks.” Horizontal divisions are walls between “north” (top in figure), “central,” and “south” (bottom in figure) sections of basement with open walkways between (cistern is in the central basement). | 3-14 |
| 3-11. | Map view of the 420-side basement showing the SSD mitigation system legs, subslab soil gas extraction pits (red circles), and the passive “sampling racks.” Horizontal divisions are walls between “north” (top in figure), “central,” and “south” (bottom in figure) sections of basement with open walkways between (cistern is in the central basement). | 3-15 |
| 3-12. | Photos of mitigation system: (left) SSD blower and stack on northeast corner of duplex; right) SSD extraction point, showing valve and U-tube manometer. | 3-16 |
| 3-13. | Cross-section showing the general layout of the 422/420 north and central basements with the positioning of the extraction legs, exterior blower, and exhaust stack. | 3-17 |
| 3-14. | Subsurface soil gas monitoring probes (SGP), subslab sampling ports (SSP), and groundwater monitoring wells (MW). Horizontal divisions are walls between “north,” “central,” and “south” sections of basement with open walkways between (cisterns are in the central basements). Probes/ports in red were sampled by the on-site GC. Soil temperature and moisture probes were installed in the 422 basement between SGP 8 and MW 3 and in the backyard to the north of MW 2..... | 3-18 |
| 3-15. | Passive indoor air sampling rack: 422 first floor. | 3-20 |
| 3-16. | Ambient sampler shelters on telephone pole near duplex..... | 3-21 |
| 3-17. | Monitoring well MW-3, installed in the basement and completed on the first floor..... | 3-26 |

| | | |
|-------|--|------|
| 3-18. | Front view of 420/422 duplex with location of weather station sensors indicated with red arrow..... | 3-27 |
| 3-19. | Calibrated crack monitor..... | 3-30 |
| 4-1. | TCE Continuing Calibration Standard Analyses, Hartman 3 Period..... | 4-12 |
| 4-2. | XY Comparison plot of Radiello and GC indoor air concentration measurements ($\mu\text{g}/\text{m}^3$), Hartman 1 sampling period..... | 4-30 |
| 4-3. | XY Comparison plot of Radiello and GC indoor air concentration measurements ($\mu\text{g}/\text{m}^3$), Hartman 2 sampling period..... | 4-31 |
| 4-4. | Time series comparison of field GC and passive sampling data: 422 basement, Hartman Period 2, chloroform. Horizontal gray line is calculated GC reporting limit. Red hash marks on y-axis indicate missing values..... | 4-33 |
| 4-5. | Time series comparison of field GC and passive sampling data: 422 first floor, Hartman Period 2, chloroform. Horizontal gray line is calculated GC reporting limit. Red hash marks on y-axis indicate missing values..... | 4-34 |
| 4-6. | Time series comparison of field GC and passive sampling data: 422 basement, Hartman Period 2, PCE. Horizontal gray line is calculated GC reporting limit. Red hash marks on y-axis indicate missing values..... | 4-35 |
| 4-7. | Time series comparison of field GC and passive sampling data: 422 first floor, Hartman Period 2, PCE. Horizontal gray line is calculated GC reporting limit. Red hash marks on y-axis indicate missing values..... | 4-36 |
| 4-8. | XY Plot of field GC vs. passive sampler data, Hartman Period 3..... | 4-38 |
| 4-9. | Time series comparison of field GC and passive sampling data: 422 basement, Hartman Period 3, chloroform. Horizontal gray line is calculated GC reporting limit. Red hash marks on y-axis indicate missing values..... | 4-39 |
| 4-10. | Time series comparison of field GC and passive sampling data: 422 first floor, Hartman Period 3, chloroform. Horizontal gray line is calculated GC reporting limit. Red hash marks on y-axis indicate missing values..... | 4-40 |
| 4-11. | Time series comparison of field GC and passive sampling data: 422 Basement, Hartman Period 3, PCE. Horizontal gray line is calculated GC reporting limit. Red hash marks on y-axis indicate missing values..... | 4-41 |
| 4-12. | Time series comparison of field GC and passive sampling data: 422 first floor, Hartman Period 3, PCE. Horizontal gray line is calculated GC reporting limit. Red hash marks on y-axis indicate missing values (none in this case)..... | 4-42 |
| 4-13. | Correlation between radon measured using the electret and charcoal methods..... | 4-45 |
| 4-14. | Aerial view of study house, showing potential influences on wind velocity, red arrow indicates study house..... | 4-49 |
| 4-15. | Comparison of National Weather Service Indianapolis temperature data to weather station at 422 East 28th Street..... | 4-50 |
| 4-16. | Comparison of National Weather Service Indianapolis relative humidity to weather station at 422 East 28th Street..... | 4-50 |
| 4-17. | Comparison of National Weather Service wind speed data to weather station at 422 East 28th Street..... | 4-51 |

| | | |
|-------|---|------|
| 5-1. | Subslab vs. basement differential pressure: 422 side during mitigation testing. | 5-19 |
| 5-2. | Subslab vs. basement differential pressure: 420 side during mitigation testing. | 5-20 |
| 5-3. | Deep soil gas vs. shallow soil gas differential pressure during mitigation testing..... | 5-21 |
| 5-4. | Basement vs. upstairs differential pressure: 422 side during mitigation testing. | 5-22 |
| 5-5. | Basement vs. exterior differential pressure: 422 side during mitigation testing. | 5-22 |
| 5-6. | Stack gas flow velocity from SSD system. | 5-23 |
| 5-7. | Real-time radon monitoring: 422 basement..... | 5-23 |
| 5-8. | Real-time radon monitoring: 422 second floor. | 5-24 |
| 5-9. | Weekly integrated radon (electret) during mitigation testing. | 5-24 |
| 5-10. | Passive sampler monitoring of PCE during mitigation testing. | 5-31 |
| 5-11. | Passive sampler monitoring of chloroform during mitigation period. | 5-31 |
| 5-12. | Indoor air PCE, real-time monitoring during mitigation testing. | 5-32 |
| 5-13. | Boxplots of mitigation effect on indoor air concentrations. | 5-46 |
| 5-14. | Stack gas monitoring during mitigation testing: chloroform. | 5-48 |
| 5-15. | 422 first floor versus stack gas chloroform concentrations: mitigation on. | 5-48 |
| 5-16. | Stack gas monitoring during mitigation testing: PCE..... | 5-49 |
| 5-17. | Stack gas versus 422 first floor PCE concentrations: mitigation on. | 5-49 |
| 6-1. | PCE concentrations in indoor and ambient air vs. time (7-day Radiello samples)..... | 6-2 |
| 6-2. | Chloroform concentrations in indoor and ambient air vs. time (7-day Radiello samples). | 6-2 |
| 6-3. | Benzene concentrations in indoor air. | 6-3 |
| 6-4. | Toluene concentrations in indoor air. | 6-4 |
| 6-5. | Interior and exterior sampling port locations. Sampling ports sampled by the on-site GC are shown in red, with parenthetical notes indicating which SGP depths were sampled by the GC. | 6-5 |
| 6-6a. | Plot of subslab chloroform concentrations vs. time (TO-17 data). | 6-6 |
| 6-6b. | Plot of subslab chloroform concentrations vs. time, first intensive sampling period (TO- 17 data). | 6-6 |
| 6-6c. | Plot of subslab chloroform concentrations vs. time mitigation testing period (TO-17 data). | 6-7 |
| 6-7a. | Plot of subslab PCE concentrations vs. time. (TO-17 data)..... | 6-7 |
| 6-7b. | Plot of subslab PCE concentrations vs. time, first intensive sampling period. (TO-17 data). | 6-8 |
| 6-7c. | Plot of subslab PCE concentrations vs. time, mitigation testing period (TO-17 data). | 6-8 |
| 6-7d. | Plot of subslab PCE concentrations vs. time, mitigation testing period; real time GC..... | 6-9 |
| 6-8a. | Plot of wall port chloroform concentrations vs. time (method TO-17). | 6-11 |

| | | |
|-------|--|------|
| 6-8b. | Plot of WP-3 chloroform concentrations vs. time (online GC). | 6-12 |
| 6-9a. | Plot of wall port PCE concentrations vs. time (method TO-17). | 6-13 |
| 6-9b. | Plot of WP-3; PCE concentrations vs. time (online GC). | 6-14 |
| 6-10. | Chloroform concentrations at subslab and 6-ft soil gas ports directly under the 420 side of duplex. | 6-18 |
| 6-11. | PCE concentrations at 6-ft soil gas ports and subslab immediately below the 420 side of the duplex. | 6-19 |
| 6-12. | Chloroform concentrations at 9-ft soil gas ports below 420 side of the duplex. | 6-20 |
| 6-13. | PCE concentrations at soil gas points 9 ft below the 420 side of duplex. | 6-21 |
| 6-14. | Chloroform concentrations in soil gas at 13 ft below the 420 side of the duplex. | 6-22 |
| 6-15. | PCE concentrations in soil gas at 13 ft below the 420 side of duplex. | 6-23 |
| 6-16. | Chloroform concentrations in soil gas at 16.5 ft below the 420 side of duplex. | 6-24 |
| 6-17. | PCE concentrations in soil gas at 16.5 ft below the 420 side of the duplex. | 6-25 |
| 6-18. | Chloroform concentrations in 6-ft soil gas and subslab ports immediately below the 422 side of the duplex. | 6-26 |
| 6-19. | PCE concentrations in 6-ft soil gas ports and subslab ports directly below the 422 side of the duplex. | 6-27 |
| 6-20. | Chloroform concentrations in soil gas port at 9-ft depth below 422 side of duplex. | 6-28 |
| 6-21. | PCE concentrations in soil gas at 9 ft below the 422 side of the duplex. | 6-29 |
| 6-22. | Chloroform concentrations in soil gas at 13 ft below the 422 side of the duplex. | 6-30 |
| 6-23. | PCE concentrations in soil gas at 13 ft below the 422 side of the duplex. | 6-31 |
| 6-24. | Chloroform concentrations at 16.5 ft below the 422 side of the duplex. | 6-32 |
| 6-25. | PCE concentrations at 16.5 ft below the 422 side of the duplex. | 6-33 |
| 6-26. | Chloroform concentrations in exterior soil gas at 3.5 ft bls. | 6-34 |
| 6-27. | PCE concentrations in exterior soil gas at 3.5 ft bls. | 6-35 |
| 6-28. | Chloroform concentrations in exterior soil gas at 6 ft. bls. | 6-36 |
| 6-29. | PCE concentrations in exterior soil gas at 6 ft bls. | 6-37 |
| 6-30. | Chloroform concentrations in exterior soil gas at 9 ft bls. | 6-38 |
| 6-31. | PCE concentrations in exterior soil gas at 9 ft bls. | 6-39 |
| 6-32. | Chloroform concentrations in exterior soil gas at 13 ft bls. | 6-40 |
| 6-33. | PCE concentrations in exterior soil gas at 13 ft bls. | 6-41 |
| 6-34. | Chloroform concentrations in exterior soil gas at 16.5 ft bls. | 6-42 |
| 6-35. | PCE concentrations in exterior soil gas at 16.5 ft bls. | 6-43 |
| 6-36. | Subslab PCE concentrations over a 1-week period during the first intensive round. | 6-44 |
| 6-37. | Subslab PCE concentrations over a 1-week period during the second intensive round. | 6-44 |
| 6-38. | Radon: Weekly time integrated samples (electret). | 6-45 |

| | | |
|-------|--|------|
| 6-39. | Online GC chloroform indoor air data for 422 first floor..... | 6-46 |
| 6-40. | Online GC chloroform indoor air data for 422 basement..... | 6-47 |
| 6-41. | Online GC chloroform indoor air data for 420 first floor..... | 6-47 |
| 6-42. | Online GC chloroform indoor air data for 420 basement..... | 6-48 |
| 6-43. | Online GC PCE indoor air data for 422 first floor..... | 6-49 |
| 6-44. | Online GC PCE indoor air data for 422 basement..... | 6-49 |
| 6-45. | Online GC PCE indoor air data for 420 first floor..... | 6-50 |
| 6-46. | Online GC PCE indoor air data for 420 basement..... | 6-50 |
| 6-47. | Online GC subsurface chloroform soil gas data—Phase 1 and Phase 2..... | 6-52 |
| 6-48. | Online GC subsurface chloroform soil gas data—Phase 1..... | 6-52 |
| 6-49. | Online GC subsurface chloroform soil gas data—Phase 2..... | 6-53 |
| 6-50. | Online GC subsurface PCE soil gas data—Phase 1 and Phase 2..... | 6-54 |
| 6-51. | Online GC subsurface PCE soil gas data—Phase 1..... | 6-54 |
| 6-52. | Online GC subsurface PCE soil gas data—Phase 2..... | 6-55 |
| 6-53. | Method TO-17 data for SSP-4..... | 6-55 |
| 6-54. | Online GC PCE measurements in SSP-4..... | 6-57 |
| 6-55. | Comparison of online GC measurements of PCE and chloroform in SGP9 at 6 ft..... | 6-57 |
| 6-56. | Real-time radon levels (422 basement) 2011–2013..... | 6-58 |
| 6-57. | Real-time radon levels (422, 2 nd floor office), 2011–2013..... | 6-59 |
| 6-58. | Temperature records from the external temperature monitor and the HOBO devices at seven indoor locations on the 422 and 420 sides of the house..... | 6-61 |
| 6-59. | Stacked hydrological graph with rainfall in inches (top—green line), depth to water in feet (middle—red circles), and discharge at Fall Creek in ft ³ /s (bottom—blue line)..... | 6-62 |
| 6-60. | Plot of high wind speed for measurement period, wind run and wind speed (average over measurement period) at 422/420 house over time..... | 6-63 |
| 6-61. | Weather variables measured inside 422 office (2nd floor) and on roof: a. barometric pressure (in Hg); b. indoor air density, c. indoor air equilibrium moisture content, d, indoor percent humidity, f. outdoor percent humidity, g. rain (inches total in measurement period), h. rain rate—the most intense rainfall during the measurement period in inches/hour..... | 6-64 |
| 6-62. | Snow depth vs. time (data are from NCDC records for the Indianapolis International Airport)..... | 6-65 |
| 6-63. | GC Phase 2 VOCs at WP-3 compared with 422/420 house external pressure..... | 6-66 |
| 6-64. | GC Phase 3 VOCs at WP-3 compared with 422/420 house external pressure..... | 6-67 |
| 6-65. | GC Phase 2 VOCs at WP-3 compared with 422/420 house external wind speed..... | 6-68 |
| 6-66. | GC Phase 3 VOCs at WP-3 compared with 422/420 house external wind speed..... | 6-69 |

| | | |
|-------|---|------|
| 6-67. | GC chloroform at subslab and soil gas ports versus radon from stationary AlphaGUARDS..... | 6-72 |
| 6-68. | GC PCE at subslab ports versus radon from stationary AlphaGUARDS..... | 6-73 |
| 6-69. | GC chloroform in indoor air versus radon from stationary AlphaGUARDS..... | 6-74 |
| 6-70. | GC PCE in indoor air versus radon from stationary AlphaGUARDS..... | 6-75 |
| 6-71. | GC chloroform concentrations in indoor air, 420 first floor..... | 6-76 |
| 6-72. | GC chloroform concentrations in indoor air, 420 basement south..... | 6-76 |
| 6-73. | GC PCE concentrations in indoor air, 420 first floor..... | 6-77 |
| 6-74. | GC PCE concentrations in indoor air, 420 basement south..... | 6-77 |
| 7-1. | Comparison of mean concentrations among wall and subslab ports under different mitigation conditions (heat on data only): radon (top), PCE (middle), and chloroform (bottom)..... | 7-2 |
| 7-2. | Long-term trends in radon and VOCs with shading showing mitigation status during Phase 2..... | 7-5 |
| 8-1. | AlphaGUARD concentrations and daily radon attenuation factors (number of samples indicated below each bar graph pair). Sample pairs represented indicated along x-axis. SSP-7 is on the 420 side of the building and so may not be representative of subslab attenuation as the other sample pairs. Sampling period = January 2011–May 2013, mitigation system off..... | 8-3 |
| 8-2. | Daily indoor air and soil gas PCE concentrations used in attenuation factor calculations (number of samples with heat on and off are indicated below each bar graph pair)..... | 8-4 |
| 8-3. | Daily PCE attenuation factors (number of samples indicated below each bar graph pair)..... | 8-5 |
| 8-4. | Daily chloroform concentrations used in attenuation factor calculations (number of samples indicated below each bar graph pair)..... | 8-6 |
| 8-5. | Daily chloroform attenuation factors (number of samples indicated below each bar graph pair)..... | 8-7 |
| 8-6. | Electret radon concentrations used in weekly attenuation factor calculations. Number of measurements indicated below each box and whiskers pair..... | 8-9 |
| 8-7. | AlphaGUARD soil gas radon concentrations (pCi/L) used in weekly attenuation factor calculations. Number of measurements noted below each box and whiskers pair. Note that these concentrations represent averages across all samples taken at the same depth and time (e.g., subslab samples are averages across all subslab points)..... | 8-10 |
| 8-8. | Weekly radon attenuation factors (number of samples indicated below each bar graph pair). Note that these attenuation factors were calculated from indoor air and soil gas concentrations averaged at the same depth and time (as described in Figure 8-7)..... | 8-11 |
| 8-9. | Radiello PCE concentrations used in attenuation factor calculations. Numbers at the bottom of each column indicate the number of available readings for unheated (left) and heated (right) conditions..... | 8-12 |
| 8-10. | TO-17 PCE concentrations used in attenuation factor calculations..... | 8-13 |
| 8-11. | Weekly PCE attenuation factors (numbers of samples indicated by numbers beneath each bar graph pair)..... | 8-14 |

| | | |
|-------|--|------|
| 8-12. | Radiello chloroform concentrations used as numerators for weekly attenuation factor calculations. | 8-15 |
| 8-13. | TO-17 chloroform concentrations used as denominators for weekly attenuation factor calculations. | 8-16 |
| 8-14. | Weekly chloroform attenuation factors (number of samples indicated below each bar graph pair)..... | 8-17 |
| 8-15. | Attenuation of PCE, chloroform, and radon juxtaposed..... | 8-18 |
| 8-16. | Mitigation status and schedule..... | 8-19 |
| 8-17. | Radon indoor air and soil gas concentrations used in daily attenuation factor calculations..... | 8-20 |
| 8-18. | Daily radon attenuation factors..... | 8-21 |
| 8-19. | Daily PCE attenuation factors..... | 8-22 |
| 8-20. | Daily chloroform attenuation factors..... | 8-23 |
| 8-21. | Electret indoor radon concentrations..... | 8-24 |
| 8-22. | AlphaGUARD subsurface radon concentrations (pCi/L)..... | 8-25 |
| 8-23. | Weekly radon attenuation..... | 8-26 |
| 8-24. | Radiello indoor air PCE concentrations..... | 8-27 |
| 8-25. | TO-17 soil gas PCE concentrations..... | 8-28 |
| 8-26. | Weekly PCE attenuation..... | 8-29 |
| 8-27. | Radiello weekly indoor air chloroform concentrations..... | 8-30 |
| 8-28. | TO-17 soil gas chloroform concentrations..... | 8-31 |
| 8-29. | Weekly chloroform attenuation factors..... | 8-32 |
| 8-30. | Attenuation of PCE, chloroform, and radon juxtaposed..... | 8-33 |
| 9-1. | Long-term trend in subslab vs. basement differential pressure (Pa) compared with exterior temperature and the first derivative of exterior temperature (°F)..... | 9-2 |
| 9-2. | XY plot of subslab vs. basement differential pressure vs. daily low exterior temperature..... | 9-3 |
| 9-3. | XY plot of daily low exterior temperature vs. (subslab vs. basement differential pressure)..... | 9-4 |
| 9-4. | Long term pressure trends in subslab vs. basement differential pressure (Pa) compared with external barometric pressure (inches) with derivative plots..... | 9-5 |
| 9-5. | XY plot of external barometric pressure vs. (422 subslab vs. basement differential pressure)..... | 9-6 |
| 9-6. | XY plot of barometric pressure drop (per hour) vs. (422 subslab vs. basement differential pressure)..... | 9-7 |
| 9-7. | Long term trends in subslab vs. basement pressure (Pa) compared to rainfall and snow depth (inches)..... | 9-8 |
| 9-8. | XY graph of total daily rainfall vs. (subslab vs. basement differential pressure)..... | 9-9 |
| 9-9. | XY graph of total snow depth (inches) vs. differential pressures (Pa)..... | 9-10 |

| | | |
|-------|---|------|
| 9-10. | Long-term trends in subslab vs. basement differential pressure (Pa) compared to maximum wind speed and average wind speed data (mph)..... | 9-11 |
| 9-11. | Long-term trend in subslab vs. basement differential pressure (Pa) vs. wind direction parameters (change in direction, maximum direction, average direction) (degrees)..... | 9-12 |
| 9-12. | XY plot of daily high wind speed vs. (subslab vs. basement differential pressure)..... | 9-13 |
| 9-13. | XY plot of daily average wind speed vs. (subslab vs. basement differential pressure)..... | 9-14 |
| 9-14. | XY plot of wind direction effects on subslab vs. basement differential pressure (upper plot) and radon concentrations in the 422 basement (lower plot)..... | 9-15 |
| 9-15. | Extreme Event 1: subslab vs. basement differential pressure (positive difference indicates flow into the structure)..... | 9-17 |
| 9-16. | Extreme Event 2: subslab vs. basement differential pressure (positive difference indicates flow into the structure)..... | 9-18 |
| 9-17. | Extreme Event 3: subslab vs. basement differential pressure (positive difference indicates flow into the structure)..... | 9-19 |
| 9-18. | Extreme Event 4: subslab vs. basement differential pressure (positive difference indicates flow into the structure)..... | 9-20 |
| 9-19. | Extreme Event 5: subslab vs. basement differential pressure (positive difference indicates flow into the structure)..... | 9-21 |
| 9-20. | Extreme Events 6/7: subslab vs. basement differential pressure (positive difference indicates flow into the structure)..... | 9-22 |
| 9-21. | Detailed time series of unusual pressure Event 1 showing barometric pressure changes (barometric pressure in inches of Hg, differential pressure in Pa)..... | 9-23 |
| 9-22. | Detailed time series of unusual pressure Event 1 showing precipitation events (rainfall in inches, snow depth in inches, differential pressure in Pa)..... | 9-24 |
| 9-23. | Detailed time series of unusual pressure Event 2 showing barometric pressure changes (barometric pressure in inches of Hg, differential pressure in Pa)..... | 9-25 |
| 9-24. | Detailed time series of unusual pressure Event 2 showing temperature changes (differential pressure in Pa, temperature in °F)..... | 9-26 |
| 9-25. | Detailed time series of unusual pressure Event 3 showing barometric pressure changes (barometric pressure in inches of Hg, differential pressure in Pa)..... | 9-27 |
| 9-26. | Detailed time series of unusual pressure Event 3 showing temperature changes (differential pressure in Pa, temperature in °F)..... | 9-28 |
| 9-27. | Detailed time series of unusual pressure Event 3 showing wind direction variables (wind direction-related variables in degrees, differential pressure in Pa)..... | 9-29 |
| 9-28. | Detailed time series of unusual pressure Event 3 showing PCE and radon..... | 9-30 |
| 9-29. | Detailed time series of Event 4 showing wind direction variables (wind direction-related variables in degrees, differential pressure in Pa)..... | 9-32 |
| 9-30. | Detailed time series of Event 4 showing wind speed variables (wind speed variables in MPH, differential pressure in Pa)..... | 9-33 |
| 9-31. | Detailed time series of Event 4 showing temperature variables (differential pressure in Pa, temperature in °F)..... | 9-34 |

| | | |
|-------|---|------|
| 9-32. | Detailed time series of Event 5 showing precipitation event (rainfall in inches, snow depth in inches, differential pressure in Pa)..... | 9-35 |
| 9-33. | Detailed time series of Event 5 showing wind speed variables (wind direction-related variables in degrees, differential pressure in Pa). | 9-36 |
| 9-34. | Detailed time series of Event 5 showing wind direction variables. | 9-37 |
| 9-35. | Detailed time series of Event 5 showing temperature variables (differential pressure in Pa, temperature in °F). | 9-38 |
| 9-36. | Detailed time series of Event 5 showing PCE and radon..... | 9-39 |
| 9-37. | Detailed time series of Event 6/7 showing barometric pressure (barometric pressure in inches of Hg, differential pressure in Pa)..... | 9-40 |
| 9-38. | Detailed time series of Event 6/7 showing precipitation (rainfall in inches, snow depth in inches, differential pressure in Pa). | 9-41 |
| 9-39. | Detailed time series of Event 6/7 showing wind speed variables (wind direction-related variables in degrees, differential pressure in Pa). | 9-42 |
| 9-40. | Detailed time series of Event 6/7 showing wind direction variables (wind direction-related variables in degrees, differential pressure in Pa)..... | 9-43 |
| 9-41. | Detailed time series of Event 6/7 showing radon and PCE. | 9-44 |
| 9-42. | XY graph of total heating degree days per week vs. weekly PCE concentration (Radiello data). | 9-45 |
| 9-43. | XY graph of heating degree days vs. chloroform concentration (weekly Radiello data). | 9-46 |
| 9-44. | XY graph of average weekly barometric pressure vs. PCE concentration. | 9-47 |
| 9-45. | XY graph of weekly average snow depth vs. PCE concentration..... | 9-48 |
| 9-46. | XY graph of weekly average snow depth vs. chloroform concentration. | 9-49 |
| 9-47. | XY graph of weekly average snow depth vs. radon concentration..... | 9-50 |
| 9-48. | XY graph of total weekly rainfall vs. PCE concentration in indoor air. | 9-51 |
| 9-49. | XY graph of total weekly rainfall vs. chloroform concentration in indoor air. | 9-52 |
| 9-50. | XY graph of wind direction vs. PCE concentration in indoor air in 422 basement..... | 9-53 |
| 9-51. | XY graph of wind direction vs. chloroform concentration in indoor air in 422 basement. | 9-54 |
| 9-52. | XY graph of wind direction vs. radon concentration in indoor air in 422 basement. | 9-55 |
| 9-53. | Modeled effect of building wind loads on ground surface and subslab gauge pressure distribution (adapted from U.S. EPA, 2012d)..... | 9-56 |
| 9-54. | Modeled effect of building wind load on subslab soil vapor distribution for recalcitrant and aerobically biodegradable VOCs (adapted from U.S. EPA, 2012d). | 9-57 |
| 9-55. | XY graph of wind speed vs. PCE concentration in indoor air in 422 basement. | 9-58 |
| 9-56. | XY graph of wind speed vs. chloroform concentration in indoor air in 422 basement. | 9-59 |

| | | |
|--------|---|-------|
| 10-1. | Daily time series of radon concentrations (pCi/L) 422 basement north, 2011–2012 with rolling-averages, and autocorrelation (ACF) and partial autocorrelation function (PACF) plots..... | 10-4 |
| 10-2. | Time series of first difference of daily radon concentrations (pCi/L) 422 basement north, 2011–2012 with rolling-averages, and autocorrelation (ACF) and partial autocorrelation function (PACF) plots..... | 10-5 |
| 10-3. | Daily time series of radon concentrations (pCi/L) 422 basement north, 2012–2013 with rolling-averages, and autocorrelation (ACF) and partial autocorrelation function (PACF) plots..... | 10-6 |
| 10-4. | Time series of first difference of daily radon concentrations (pCi/L) 422 basement north, 2012–2013 with rolling-averages, and autocorrelation (ACF) and partial autocorrelation function (PACF) plots..... | 10-7 |
| 10-5. | Time series of daily radon concentrations: 422 office (2nd floor), 2011–2012 with rolling-averages, and autocorrelation (ACF) and partial autocorrelation function (PACF) plots..... | 10-8 |
| 10-6. | Time series of first difference of daily radon concentrations: 422 office (2nd floor), 2011–2012 with rolling-averages, and autocorrelation (ACF) and partial autocorrelation function (PACF) plots..... | 10-9 |
| 10-7. | Time series of radon concentrations: 422 office (2nd floor), 2012–2013 with rolling-averages, and autocorrelation (ACF) and partial autocorrelation function (PACF) plots. | 10-10 |
| 10-8. | Time series of differences of daily radon concentrations: 422 office (2nd floor), 2012–2013 with rolling-averages, and autocorrelation (ACF) and partial autocorrelation function (PACF) plots..... | 10-11 |
| 10-9. | Correlation between radon concentration and predictors for both sites (basement north and office 2nd floor). Time period 2011–2012. NOTE: See Table 10-2 for “Plain Language” key of abbreviations used in this figure..... | 10-16 |
| 10-10. | Correlation between radon concentration and predictors for both sites (basement north and office 2nd floor). Time period 2012–2013. NOTE: See Table 10-2 for “Plain Language” key of abbreviations used in this figure..... | 10-17 |
| 10-11. | Time series plot, ACF and PACF for weekly Radiello chloroform. Location X422 basement south. Time period: Jan 5, 2011–Feb 15, 2012..... | 10-42 |
| 10-12. | Time series plot, ACF and PACF for first difference of weekly Radiello. Chloroform. Location X422 basement south. Time period: Jan 5, 2011–Feb 15, 2012..... | 10-43 |
| 10-13. | Time series plot, ACF and PACF for weekly Radiello PCE. Location X422 basement south. Time period: Jan 5, 2011–Feb 15, 2012..... | 10-44 |
| 10-14. | Time series plot, ACF and PACF for weekly chloroform. Location X422 basement south. Time period: Sept 26, 2012–April 10, 2013..... | 10-46 |
| 10-15. | Time series plot, ACF and PACF for first difference weekly Radiello CHCl ₃ -2 (X422BaseS_Radiello_Weekly_CHCl ₃). Location X422 basement south. Time period: Sept 26, 2012–April 10, 2013..... | 10-47 |
| 10-16. | Time series plot, ACF and PACF for weekly Radiello PCE-2 (X422BaseS_Radiello_Weekly_PCE). Location X422 basement south. Time period: Sept 26, 2012–April 10, 2013..... | 10-48 |

| | | |
|--------|--|-------|
| 10-17. | Time series plot, ACF and PACF for first difference weekly Radiello PCE-2 (X422BaseS_Radiello_Weekly_PCE). Location X422 basement south. Time period: Sept 26, 2012–April 10, 2013. | 10-49 |
| 10-18. | XY plot of weekly average snow depth vs. PCE concentration. | 10-63 |
| 10-19. | XY Plot of change in weekly average snow depth vs. PCE concentration. | 10-64 |
| 10-20. | XY Plot of weekly average snow depth vs. change in PCE. | 10-65 |
| 11-1. | Stacked hydrological graph with rainfall in inches (top—green line), depth to water in feet (middle—red circles), and discharge at Fall Creek in ft ³ /s (bottom—blue line). | 11-1 |
| 11-2. | Actual groundwater levels along with the daily time series predicted from Fall Creek gage height data. | 11-2 |
| 11-3. | Groundwater concentrations over time for Indianapolis duplex. | 11-4 |
| 11-4. | PCE groundwater concentrations over time, showing concentrations by individual well and soil gas ports. | 11-4 |
| 11-5. | Plot of groundwater PCE and chloroform concentrations against well screen (or soil gas port) depth (well depth measured to top of screen). | 11-5 |
| 11-6. | Plot of groundwater PCE and chloroform concentrations against groundwater depth. | 11-6 |
| 12-1. | Response at all locations to first helium injection in front yard. | 12-5 |
| 12-2. | Response at all locations to second helium injection in front yard. | 12-6 |
| 12-3. | Response at all locations to third helium injection in backyard. | 12-6 |
| 12-4. | Response at all locations to fourth helium injection in backyard. | 12-7 |
| 12-5. | Helium response at SGP2 cluster (south of duplex) directly above injection point after injections 1 (top graph, mitigation off) and 2 (bottom graph, mitigation on). | 12-8 |
| 12-6. | Helium response at SGP6 cluster at SGP6 cluster (north of duplex) directly above injection point after injections 3 (top graph, mitigation off) and 4 (bottom graph, mitigation on). | 12-9 |
| 12-7. | Helium response at SGP1 cluster (south of duplex, approximately 6 ft closer to duplex than injection point) after first Injection (top graph, mitigation off) and second injection (bottom graph, mitigation on). | 12-10 |
| 12-8. | Helium response at SGP5 cluster (north of duplex, approximately 6 ft closer to duplex than injection point) after third injection (top graph, mitigation off) and fourth injection (bottom graph, mitigation on). | 12-11 |
| 12-9. | Helium response to first and second helium injections at SGP9 (interior). | 12-12 |
| 12-10. | Helium response to third and fourth helium injections at SGP10 (interior). | 12-12 |
| 12-11. | Cross-section view of helium tracer arrival at 6-ft depth intervals. | 12-14 |
| 12-12. | Comparison of electret and Safety Siren results for first phase of the project (top graph) and second project phase (bottom graph). | 12-17 |
| 12-13. | Comparison between the 422 office Safety Siren and electret. | 12-22 |
| 12-14. | Comparison between the 422 basement N Safety Siren and electret. | 12-22 |

List of Tables

| | | |
|-------|--|------|
| 1-1. | Summary of Lines of Evidence for Meteorological Factors Influencing Vapor Intrusion in This Study (Blank cells reflect types of analysis not completed for a given parameter)..... | 1-7 |
| 2-1. | VOC Indoor Air Sampling Method Options..... | 2-15 |
| 2-2. | Continuing Project Objectives Addressed in this Document..... | 2-17 |
| 2-2. | Continuing Project Objectives Addressed in this Document (continued) | 2-18 |
| 2-3. | Factors Causing Temporal Change in Vapor Intrusion and How They are Observed and Measured..... | 2-19 |
| 2-4. | Data Quality Objectives and Criteria..... | 2-20 |
| 3-1. | Pressure Readings Taken During Extraction Point Testing..... | 3-13 |
| 3-2. | Data Aggregation Applied to Predictor Variables | 3-31 |
| 4-1. | Indoor Air Passive Field Blank Summary—Radiello 130..... | 4-2 |
| 4-2. | Indoor Air Passive Trip Blank Summary—Radiello 130 | 4-2 |
| 4-3. | Indoor Air Passive Laboratory Blank Summary—Radiello 130 | 4-2 |
| 4-4. | Indoor Air Passive Surrogate Summary—Radiello 130 | 4-3 |
| 4-5. | Indoor Air Passive LCS Summary—Radiello 130 | 4-4 |
| 4-6. | Indoor Air Passive Laboratory Precision (LCS/LCSD) Summary—Radiello 130..... | 4-4 |
| 4-7. | Subslab and Soil Gas—EPA Field Blank Summary—TO-17 | 4-5 |
| 4-8. | Subslab and Soil Gas—EPA Trip Blank Summary—TO-17 | 4-6 |
| 4-9. | Subslab and Soil Gas—EPA Laboratory Blank Summary—TO-17..... | 4-6 |
| 4-10. | Subslab and Soil Gas—EPA Fridge Blank Summary—TO-17 | 4-7 |
| 4-11. | EPA TO-17 Calibration Verification (CV) Summary | 4-8 |
| 4-12. | EPA TO-17 Internal Standard (IS) Summary | 4-8 |
| 4-13. | EPA TO-17 Surrogate Recovery Summary | 4-9 |
| 4-14. | EPA TO-17 Laboratory Control Sample (LCS) Summary | 4-9 |
| 4-15. | EPA TO-17 Field Duplicate Summary | 4-10 |
| 4-16. | Field GC Estimated Minimum Detection Limits and Practical Quantitation Limits..... | 4-11 |
| 4-17. | Result of Repeated TCE Calibration Standard Analyses on On-line GC in March 2013 (Hartman Period 3) | 4-14 |
| 4-18. | Results of Repeated PCE Calibration Standard Analyses on Online GC in March 2013 (Hartman Period 3) | 4-14 |
| 4-19. | Interlaboratory Results: Spiked Verification Samples..... | 4-15 |
| 4-20. | Interlaboratory Statistics: Spiked Verification Samples | 4-16 |
| 4-21. | Comparison of Online GC to Radiello Results by Week..... | 4-17 |

| | | |
|-------|--|------|
| 4-22. | Comparison between Electrets and Charcoal Canisters at the 422/420 EPA House from January 19–26, 2011 | 4-43 |
| 4-23. | Comparison of Electret and Charcoal Canister Data from April 27 to May 4, 2011 | 4-44 |
| 4-24. | Comparison of Charcoal and Electret Radon December 28, 2011, to January 4, 2012 | 4-44 |
| 4-25. | Comparison between 422 Basement N AlphaGUARDs and Electrets from March 30, 2011, and May 18, 2011 | 4-45 |
| 4-26. | Comparison of Real-Time AlphaGUARD to Integrated Electret August through October | 4-46 |
| 4-27. | Comparison of Real-Time AlphaGUARD to Integrated Electret Measurements December 28, 2011, to January 4, 2012..... | 4-46 |
| 4-28. | Comparison of Real-Time AlphaGUARD to Integrated Electret Measurements January through March 2012..... | 4-47 |
| 4-29. | Comparison of Real-Time AlphaGUARD to Integrated Electret Measurements January through March 2013..... | 4-47 |
| 4-29. | Comparison of Real-Time AlphaGUARD to Integrated Electret Measurements January through March 2013..... | 4-48 |
| 4-30. | Groundwater (5 mL)—EPA Field Blank Summary | 4-52 |
| 4-31. | Groundwater (5 mL)—EPA Laboratory Blank Summary—TO-17 | 4-52 |
| 4-32. | Groundwater (25 mL)—EPA Field Blank Summary—TO-17 | 4-52 |
| 4-33. | Groundwater (25 mL)—EPA Laboratory Blank Summary—TO-17 | 4-53 |
| 4-34. | EPA Groundwater (5 mL) Surrogate Recovery Summary | 4-53 |
| 4-35. | EPA Groundwater (25 mL) Surrogate Recovery Summary | 4-53 |
| 5-1. | Subslab vs. Basement Differential Pressures Measured with Handheld Micromanometer at Permanent SSPs (negative pressure indicates flow out of building; yellow indicates mitigation off)..... | 5-4 |
| 5-2. | Wall Port vs. Basement Differential Pressure Measured with Handheld Micromanometer (negative pressure indicates flow out of building)..... | 5-8 |
| 5-3. | Shallow Interior SGP (6 ft bls) vs. Basement Differential Pressure Measured with Handheld Micromanometer (negative pressure indicates flow out of building)..... | 5-9 |
| 5-4. | Shallow Exterior SGP (3.5 ft and 6 ft bls) vs. Basement Differential Pressure Measured with a Handheld Micromanometer (negative pressure indicates flow out of building)..... | 5-10 |
| 5-5. | Deep Interior SGP (9 ft and 13 ft bls) vs. Basement Differential Pressure Measured by ARCADIS with Handheld Micromanometer (negative pressure indicates flow out of building)..... | 5-12 |
| 5-6. | Deep Exterior SGP (9 ft and 13 ft bls) vs. Basement Differential Pressure Measured by ARCADIS with Handheld Micromanometer (negative pressure indicates flow out of building)..... | 5-15 |
| 5-7. | Comparison of Setra Continuous Sensor Differential Pressure vs. Airdata Multimeter ADM-870 with SSD System Operating: December 29, 2012 (yellow shaded data reflects an “off scale” response on the Setra) | 5-20 |
| 5-8. | Electret Radon Descriptive Statistics by Mitigation and Heating Status (pCi/L)..... | 5-25 |

| | | |
|-------|--|-------|
| 5-9. | Indoor Air Radon Descriptive Statistics by Mitigation and Heating Status: From Stationary Real Time AlphaGUARD (pCi/L) | 5-26 |
| 5-10. | Indoor Radon Descriptive Statistics—Individual Locations by Mitigation and Heating Status: Electret Data (pCi/L)..... | 5-26 |
| 5-11. | Descriptive Statistics: Radon in Subslab and Wall Ports by Individual Location and Mitigation and Heating Status (pCi/L) | 5-28 |
| 5-12. | Radon Descriptive Statistics by Location Type and Mitigation and Heating Status (pCi/L) | 5-30 |
| 5-13. | Descriptive Statistics of Weekly Passive VOC Measurements ($\mu\text{g}/\text{m}^3$) in Indoor Air by Mitigation Status and Heating Use (yellow indicates statistics during active mitigation)..... | 5-33 |
| 5-14. | Distribution of Concentrations ($\mu\text{g}/\text{m}^3$) by VOC and Mitigation and Heating Status: Indoor Air, Week-Long Passive Samples (yellow indicates statistics during active mitigation)..... | 5-34 |
| 5-15. | Descriptive Statistics of Indoor VOC Concentrations ($\mu\text{g}/\text{m}^3$) During Mitigation Testing by Location and Mitigation and Heating Status (yellow indicates statistics during active mitigation)..... | 5-35 |
| 5-16. | Descriptive Statistics: Average Subslab and Wall Port VOC Concentrations ($\mu\text{g}/\text{m}^3$) by Mitigation and Heating Status (yellow indicates statistics during active mitigation)..... | 5-39 |
| 5-17. | Distribution of Subslab and Wall Port VOC Concentrations ($\mu\text{g}/\text{m}^3$) by Mitigation and Heating Status (yellow indicates statistics during active mitigation) | 5-40 |
| 5-18. | Descriptive Statistics of Subslab and Wall Port VOC Concentrations ($\mu\text{g}/\text{m}^3$) by Location and Mitigation and Heating Status (yellow indicates statistics during active mitigation) | 5-41 |
| 5-19. | April/May 2011 Air Exchange Rate Measurement Results | 5-51 |
| 5-20. | September 2011 Air Exchange Rate Measurement Results..... | 5-51 |
| 5-21. | October 2011 Air Exchange Measurement Results (during and after fan testing) | 5-52 |
| 5-22. | April 2013 Air Exchange Measurement Results (During Mitigation)..... | 5-52 |
| 5-23. | National Survey of Air Exchange Rates, Reprinted from the <i>EPA Exposure Factor Handbook</i> (U.S. EPA, 2011)..... | 5-52 |
| 5-23. | National Survey of Air Exchange Rates, Reprinted from the <i>EPA Exposure Factor Handbook</i> (U.S. EPA, 2011) (continued) | 5-53 |
| 5-24. | Stack Gas Discharge Measurements During Mitigation..... | 5-54 |
| 6-1. | Frequency of Nondetectable Samples (%) by Soil Gas Point or Cluster | 6-16 |
| 6-2. | Frequency of Nondetects in TO-17 VOC Data by Soil Gas Sampling Depth | 6-16 |
| 6-3. | Summary Meteorological Data for Central Indiana Note that the symbols “^” and “v” mean “above” and “below” normal, respectively, and that the weekly values show how the weekly averages differ from normal (from Scheeringa and Hudson, 2012, 2013) | 6-60 |
| 6-4. | Summary of Meteorological Data During the 2012/2013 Snow and Ice Events | 6-78 |
| 9-1. | Summary of Qualitative Lines of Evidence for Meteorological Factors Influencing Vapor Intrusion in This Study..... | 9-60 |
| 10-1. | Significant Lags for ACF and PACF for Each Time Series and Regression Model | 10-12 |
| 10-2. | Significant Lag and AR Model by Predictor and Site Location | 10-13 |

| | | |
|--------|--|-------|
| 10-3. | Model Parameters, Standard Errors by Model, Predictor and Time Series: All Radon Time Periods, Categorical Variables | 10-18 |
| 10-4. | Model Parameters, Standard Errors by Model and Predictor for X422baseN_AG_radon (X422BN-1): 2011–2012, Lag 1 Models..... | 10-20 |
| 10-5. | Model Parameters, Standard Errors by Predictor for X422baseN_AG_radon (X422BN-1): 2011–1012, Lag 2 Models..... | 10-25 |
| 10-6. | Model Parameters, Standard Errors by Predictor for X422baseN_AG_radon (X422BN-1), Lag 4 Models | 10-25 |
| 10-7. | Model Parameters, Standard Errors by Predictor for X422office_2nd_AG_radon Concentration (X422OF2-1): 2011–2012, No Lag Terms in Model | 10-26 |
| 10-8. | Model Parameters, Standard Errors by Model and Predictor for Time Series Analysis of Radon in 422 Office: 2011–2012, Lag 1 Models..... | 10-26 |
| 10-9. | Model Parameters, Standard Errors by Predictor for X422office_2nd_AG_radon Concentration (X422OF2-1): 2011–2012. Lag 2 Models..... | 10-32 |
| 10-10. | Model Parameters, Standard Errors by Predictor for X422baseN_AG_radon (X422OF2-1): 2011–2012. Lag4 Models | 10-32 |
| 10-11. | Model Parameters, Standard Errors by Predictor for 422 Basement Radon: 2012–2013. No Lag Terms in Model..... | 10-33 |
| 10-12. | Model Parameters, Standard Errors by Model and Predictor for 422 Basement Radon: 2012–2013 Lag 1 Models | 10-33 |
| 10-13. | Model Parameters, Standard Errors by Predictor for X422office_2nd_AG_radon Concentration (X422OF2-2): 2012–2013. No Lag Terms in Model | 10-37 |
| 10-14. | Model Parameters, Standard Errors by Model and Predictor for X422office_2nd_AG_radon Concentration (X422OF2-2): 2012–2013 Lag 1 Models..... | 10-38 |
| 10-15. | Name, Periodicity, Time Period, and Location of Time Series (Outcome) Considered..... | 10-41 |
| 10-16. | Transformation and Terms Required by Time Series | 10-45 |
| 10-17. | Continuous Covariates by Time Period | 10-50 |
| 10-18. | Analysis for Outcome First Difference of X422BaseS_Radiello_Weekly_CHCl ₃ . Variables That Did Not Need Lag Terms. Period Jan 5, 2011–Feb 15, 2012..... | 10-53 |
| 10-19. | Analysis for Outcome X422BaseS_Radiello_Weekly_CHCl ₃ . Variables that Needed a lag-1 Term. Period Jan 5, 2011–Feb 15, 2012 | 10-54 |
| 10-20. | Analysis for Outcome X422BaseS_Radiello_Weekly_CHCl ₃ . Variables that Needed Lag-1 and Lag-2 Terms. Period Jan 5, 2011–Feb 15, 2012 | 10-58 |
| 10-21. | Time Series Analysis for Outcome First Difference of 422 Basement South PCE Concentration Variables that Did Not Need Lag Terms. Period Jan 2011 to Feb 2012 | 10-59 |
| 10-22. | Analysis for PCE Concentration at 42 Base South, Variables that Needed a Lag-1 Term. Period Jan 2011 to Feb 2012..... | 10-60 |
| 10-23. | Analysis for PCE Concentration at 422 Base South Variables that Needed Both Lag-1 Week And Lag-2 Week Terms. Period Jan 2011 to Feb 2012..... | 10-64 |
| 10-24. | Analysis for First Difference of Chloroform Concentration at 422 Basement South. Variables that Did Not Need Lag Terms. Period Sept 2012 to April 2013 | 10-66 |

| | | |
|--------|--|-------|
| 10-25. | Analysis Chloroform Concentration at 422 Base South. Variables that Needed A Lag-1 One Week Term. Period Sept 2012 to April 2013 | 10-67 |
| 10-26. | Analysis for Chloroform Concentration at 422 Base South. Variables Needing Lag-1 and Lag-2 Week Terms. Period Sept 2012 to April 2013 | 10-71 |
| 10-27. | Analysis for First Difference of 422 Base South PCE Concentration. Variables that Did Not Need Lag Terms. Period Sept 2012 to April 2013 | 10-72 |
| 10-28. | Analysis for 422 Base South PCE Concentration. Variables that Needed A Lag-1 Week Term. Period Sept 2012 to April 2013 | 10-73 |
| 10-29. | Analysis for PCE Concentration at 422 Base South. Variables Needing Both Lag-1 And Lag-2 Week Terms. Period Sept 2012 to April 2013 | 10-77 |
| 11-1. | Groundwater Monitoring Locations. | 11-3 |
| 12-1. | Data Quality Objectives and Performance/Acceptance Criteria for Special Studies..... | 12-2 |
| 12-2. | Comparison of Safety Siren, AlphaGUARD, and Electret Radon Data | 12-18 |
| 12-3. | Comparison of Safety Siren and Electret Radon Data | 12-20 |
| 13-1. | Summary of Lines of Evidence for Meteorological Factors Influencing Vapor Intrusion in This Study | 13-6 |

Notice

The information in this document has been funded wholly by the United States Environmental Protection Agency under contract number EP-C-11-036 to the Research Triangle Institute. It has been subjected to external peer review as well as the Agency's peer and administrative review and has been approved for publication as an EPA document. Mention of trade names or commercial products does not constitute endorsement or recommendation for use.

Preface

This report entitled, "Assessment of Mitigation Systems on Vapor Intrusion: Temporal Trends, Attenuation Factors, and Contaminant Migration Routes under Mitigated and Non-mitigated Conditions" (EPA/600/R-13/241) is the second in a series of reports based on research performed to look at vapor intrusion into a historical duplex in Indianapolis, Indiana. The research is being conducted to look at the general principles of how vapors enter into this single residence.

The study was initiated in 2011 with the primary initial goal to investigate distributional changes in VOC and radon concentrations in the indoor air, subslab, and subsurface soil gas from an underground source (groundwater source and/or vadose zone source) proximal to a residence. Currently, the study has extended more than 3.5 years in order to evaluate the effects due to seasonal variations on radon and VOC vapor intrusion. As a result, a significant dataset has been generated that can be used to advance and inform the understanding of vapor intrusion.

A series of at least four (4) reports are anticipated from the research at the Indianapolis duplex.

- The initial report entitled, "Fluctuation of Indoor Radon and VOC Concentrations Due to Seasonal Variations" (EPA/600/R-12/673) examined the distributional changes in VOC and radon concentrations in the indoor air, subslab, and subsurface from the ground water source into a residence.
- This second report examines: (a) subsurface conditions that influence the movement of VOCs and radon into the home; (b) effects of an installed mitigation system on VOC and radon concentration into the residence; and (c) the influence of a winter capping event on vapor movement into the home.
- The third report entitled, "Simple, Efficient, and Rapid Methods to Determine the Potential for Vapor Intrusion into the Home: Temporal Trends, Vapor Intrusion Forecasting, Sampling Strategies, and Contaminant Migration Routes" (EPA/600/R-15/XXX) will examine the use of radon and other variables; such as weather data changes in temperature and differential pressure between indoors and outdoors, as potential low-cost, easily monitored indicators of when to sample for vapor intrusion events and when to turn on the mitigation system to reduce vapor intrusion exposure to the residents. Select data trends through the years of study at this site are also presented.
- The fourth report will provide information regarding the effectiveness of a soil vapor extraction system in preventing vapor intrusion into the residence.

In general, because this work was conducted at a single residential duplex, it cannot be representative of all sites and site conditions subject to vapor intrusion. However, it should be useful to compare the results of this study of an older building in a temperate Midwest climate with other ongoing detailed studies, such as the one conducted in a newer home in Layton, Utah for common threads that can be applied across all vapor intrusion sites.

A separate research report will be looking at the performance of passive sorbers for the monitoring of vapor intrusion at multiple sites, including the Indianapolis duplex. It is anticipated that this report will be released in late 2015.

It is anticipated that research will continue as new areas of scientific concern are identified and build on the research that has been conducted to date. The publication of peer-reviewed journal articles on select topics is also anticipated.

Acknowledgments

This project was conceived, directed, and managed by Brian Schumacher and John Zimmerman of U.S. EPA NERL. Robert Truesdale (RTI International) and Chris Lutes (ARCADIS) led the project, with report input by Brian Cosky (ARCADIS), Breda Munoz and Robert Norberg (RTI), Heidi Hayes (Air Toxics Ltd.), and Blayne Hartman (Hartman Environmental Geoscience). The authors would also like to thank the following for their valuable input to the project:

- Leigh Riley Evens, Executive Director of Mapleton-Fall Creek Development Corporation, the not for profit that provided the house used for this work.
- Dale Greenwell, U.S. EPA NRMRL, and Ron Mosley (retired), radon and equipment support
- Gregory Budd, U.S. EPA Radiation and Indoor Environments National Laboratory, radon QC sample analysis and instrument support
- Ausha Scott, analytical support, Air Toxics Ltd.
- Alan Williams and Jade Morgan, U.S. EPA NERL, TO-17 analytical support
- Robert Uppencamp ARCADIS – field, data interpretation, and site selection support; Sara Jonker, ARCADIS, field support
- Rebecca Forbort and Valerie Kull, ARCADIS, Shu-yi Lin, RTI, data management and analysis
- Scott Forsberg, Harvard School of Public Health, air exchange rate measurement support
- Susan Beck and Sharon Barrell, RTI, document preparation and editing support.

Table of Contents

| | | |
|-------|--|-----|
| 1.0 | Executive Summary | 1-1 |
| 1.1 | Background | 1-1 |
| 1.2 | Purpose and Objectives | 1-1 |
| 1.3 | Methods..... | 1-2 |
| 1.4 | Conclusions | 1-3 |
| 1.4.1 | Conceptual Site Model: VOC Data..... | 1-3 |
| 1.4.2 | Mitigation System Performance-Radon..... | 1-3 |
| 1.4.3 | Mitigation System Performance-VOCs | 1-4 |
| 1.4.4 | Meteorological Effects on Vapor Intrusion | 1-5 |
| 1.4.5 | Preferential Pathways and Conceptual Site Model: Helium Tracer and Geophysical Tests | 1-5 |
| 1.4.6 | Temporal Variability and Trends..... | 1-8 |
| 1.4.7 | Discussion..... | 1-8 |

List of Figures

| | | |
|------|---|-----|
| 1-1. | Temporal coverage of data sets collected (red line indicates the cutoff date for this report)..... | 1-4 |
| 1-2. | Indoor air concentrations of PCE (top panel) and radon (middle and bottom panels) with mitigation on (black bars), passive mitigation (no fan, gray bars), and mitigation off (no bar). Snow and frozen ground events are indicated by blue bars and red dots | 1-8 |

List of Tables

| | | |
|------|--|-----|
| 1-1. | Summary of Lines of Evidence for Meteorological Factors Influencing Vapor Intrusion in This Study (Blank cells reflect types of analysis not completed for a given parameter)..... | 1-6 |
|------|--|-----|

1.0 Executive Summary

1.1 Context in Overall Research Program

Vapor intrusion is the migration of subsurface vapors, including radon and volatile organic compounds (VOCs),¹ in soil gas from the subsurface to indoor air. Vapor intrusion happens because there are pressure and concentration differentials between indoor air and soil gas. Indoor environments are often negatively pressurized with respect to outdoor air and soil gas, for example, from exhaust fans or the stack effect,² and this pressure difference allows soil gas containing subsurface contaminant vapors to flow into indoor air through advection. In addition, concentration differentials cause VOCs and radon to migrate from areas of higher to lower concentrations through diffusion, which can lead to vapor intrusion.

While vapor intrusion investigations have been ongoing for many years, several issues still remain. Vapor intrusion site investigation costs are driven higher by the need for multiple samples per structure to characterize the commonly observed spatial and temporal variability in indoor, subslab, and deep soil gas concentrations. However, relatively few vapor intrusion assessment data sets have been published that include both long-term monitoring and high-frequency sample collection for VOCs. Temporal variability in VOC concentrations in indoor air is expected to be driven by variation in barometric pressure, house operations, temperature, water table, and soil moisture. These phenomena have known but irregular cycles on multiple time scales.

Subslab depressurization (SSD) is the predominant technology used for mitigating vapor intrusion. Design practices for SSD systems have been adapted essentially verbatim from radon mitigation experience. Few highly detailed long-term data sets have been published from tests of the effectiveness of SSD mitigation systems on indoor air VOC concentrations from vapor intrusion.

1.2 Purpose and Objectives

The main initial goal of this project was to investigate distributional changes in VOC and radon concentrations in the indoor air, subslab, and subsurface soil gas from an underground source (groundwater source and/or vadose zone source) proximal to a residence. The time frame of this study was more than 2.5 years in order to evaluate the effects due to seasonal variations on radon and VOC vapor intrusion. Because this work was conducted at a single residential duplex, it cannot be representative of all sites and site conditions subject to vapor intrusion. However, it should be useful to compare the results of this study of an older building in a temperate mid-West climate with other ongoing detailed studies, such as the one conducted in a newer home in Logan, Utah (Johnson et al., 2012; Holton et al., 2013) for common threads that can be applied across all vapor intrusion sites.

We reported previously on our results from studies conducted in 2011–2012 prior to mitigation testing (U.S. Environmental Protection Agency [EPA], 2012a). Here we report primarily new results of studies conducted in 2012–2013, additional analyses of temporal variability encompassing the entire data set collected, and the results of continuing research on six objectives initially established for the previous (U.S. EPA, 2012a) research effort:

¹Mercury in certain forms is sufficiently volatile and toxic to pose a vapor risk, but mercury vapor investigations are very site specific and much rarer than those addressing VOCs and radon. As a result, mercury vapor intrusion is not discussed further in this document.

²The stack effect is the movement of air into, upwards, and out of buildings, chimneys, flue gas stacks, or other containers resulting from indoor/outdoor air density differences due to temperature and moisture gradients between indoor and outdoor air.

1. Identify seasonal fluxes in radon and VOC concentrations as they relate to a typical use of heating, ventilation, and air conditioning (HVAC) in the building.
2. Establish relationship between subslab/subsurface soil gas and indoor air concentrations of VOCs and radon.
3. Determine the relationship of radon to VOC concentrations in, around, and underneath the building.
4. Characterize the near-building environment sufficiently to explain the observed variation of VOCs and radon in indoor air.
5. Determine whether the observed changes in indoor air concentration of volatile organics of interest can be mechanistically attributed to changes in vapor intrusion.
6. Evaluate the extent to which groundwater concentrations and/or vadose zone sources control soil gas and indoor air VOC concentrations at this site.

New objectives established for the 2012–2013 studies include the following:

- Better define the particular subsurface conditions that influence the movement of VOCs and radon into this home. These conditions were expected to include differences in air permeability on a spatial scale of 1 to 20 ft in the vadose zone beneath and immediately adjacent to the structure, along with information on potential preferential pathways and conditions beneath the foundation slab.
- Design, install, and monitor a mitigation system based on the predominant vapor intrusion mitigation technology—SSD. We wish to determine how well the mitigation system worked in reducing indoor radon and VOC concentrations for this particular well-studied duplex.
- Capture a winter snow/ice capping event to monitor its influence on radon and VOC vapor movement into the home.

Because this report is the second report in a series of four, it should be regarded as an interim field report that provides results through the spring of 2013 along with initial information on the performance of the mitigation system at the duplex. Additional studies and reports are in progress that will test some of the associations developed from this study and provide longer term tests of mitigation system performance. As a result, interpretations and conclusions drawn in this report are subject to change as additional information and insights are gained on vapor intrusion processes at this duplex.

1.3 Methods

This study was conducted at a highly instrumented pre-1920 residential duplex. The house was devoid of potential indoor VOC sources, but one half of the structure was operated as if occupied (provision of heating and cooling). To characterize the basement of this residential duplex, serving as a vapor intrusion research house, several sampling devices have been installed: seven conventional subslab ports, four ports similar to conventional subslab ports, seven external nested soil gas points (5 depths per point), and five nested soil gas points below the basement (4 depths per point). This provides for collection of an unusually comprehensive data set to formulate three-dimensional visualizations of seasonal VOC concentrations.

In our overall study design, we used weekly measurements to observe our dependent variable—indoor air concentration. We expected the indoor air concentration to depend on the flux from vapor intrusion from soil gas. Our dependent variable is thus controlled by a series of independent variables with different time cycles that affect the vapor intrusion process, including air temperature, barometric pressure, wind, soil moisture, soil temperature, groundwater level, and HVAC operation. In the course of this study, we

monitored or measured most of these independent variables or their surrogates and different frequencies balancing on the general desire for continuous measurements against logistic considerations.

The strategy for the SSD mitigation system installation was to select an experienced radon and VOC mitigation contractor and ask them to perform a “typical” active SSD system installation but with greater documentation and reporting for the research purpose. We also added some additional valves and sampling ports to the “typical” system to facilitate much more intensive monitoring than is usually conducted for an SSD mitigation system designed for radon.

Figure 1-1 shows the various types of samples and sampling frequency employed for each across this study. The more continuous variables (shown with black lines) are used in time series analysis in Sections 9 and 10. With respect to radon measurements, continuous measurements (weeklong electrets or continuous AlphaGUARD data) were taken for indoor air, while short-term grab samples were used to characterize soil gas. Similarly, the primary VOC measurements were weeklong Radiello samples (for the entire project) and continuous measurements with an on-site gas chromatograph (GC) (during critical project phases) for indoor air, with TO-17 grab samples to characterize soil gas on a weekly basis. Meteorological, observational, and pressure differential (Setra) data were collected essentially continuously during the entire project.

1.4 Conclusions

As noted above, this document is a field report updating results of a study in progress. Because measurements and analyses are ongoing and future work is planned to test the validity of some of the correlations and conclusions drawn at this point in the project, the results should be regarded as preliminary and subject to change in the third and fourth reports of this series.

1.4.1 Conceptual Site Model: VOC Data

Although chloroform was detected in groundwater, the currently measured concentrations were too low to account for the peak chloroform concentrations observed in soil gas. This suggests that there may be (1) other sources of chloroform such as combined sewers³ or drinking water mains⁴ that leak below grade, (2) higher groundwater concentrations at some locations near the site, or (3) chloroform mass stored in the vadose zone from a historic release. For PCE, the results indicate a groundwater source, but the narrow range of variability in PCE concentrations over time make it unlikely that variability in groundwater concentrations is the only source of the observed changes in soil gas or indoor air concentrations observed in this study. The variability in indoor air PCE concentrations is also influenced by subsurface, building-related, and meteorological variables. The potential that other sources of PCE may exist in the vadose zone or combined sewer lines cannot be ruled out at this point.

1.4.2 Mitigation System Performance—Radon

The mitigation system installed in the duplex met or exceeded all conventional performance tests as well as more comprehensive tests involving pressure differentials and continuous indoor radon monitoring. Radon reductions greater than 90% were observed, and all measured radon levels were below 4 picocuries per liter (pCi/L) with the mitigation system on.

³Chloroform can form in sewers that receive bleach-containing products.

⁴Groundwater chloroform concentrations at this duplex are lower than the mean and peak drinking water concentrations for Indianapolis (19 ppb and 82 ppb).

1.4.3 Mitigation System Performance—VOCs

The mitigation system did not perform as well with VOCs as it did with radon. During 7 months of mitigation system operation, immediate VOC reductions in indoor air were observed but the system only achieved a reduction of just over 60% of VOC indoor air concentrations before mitigation. However, additional decreases in indoor VOC levels were observed near the end of the monitoring period reported in this document (May 2013). During these periods of mitigation system operation, the system was also observed to increase soil gas levels below the slab and at depth below the duplex, suggesting that VOCs are being redistributed by the mitigation system and that soil gas concentrations close to the building may be enhanced by drawing higher concentrations of VOCs from greater depths. In addition, several snow events corresponded to increases in indoor air VOC levels during mitigation that were not observed for radon.

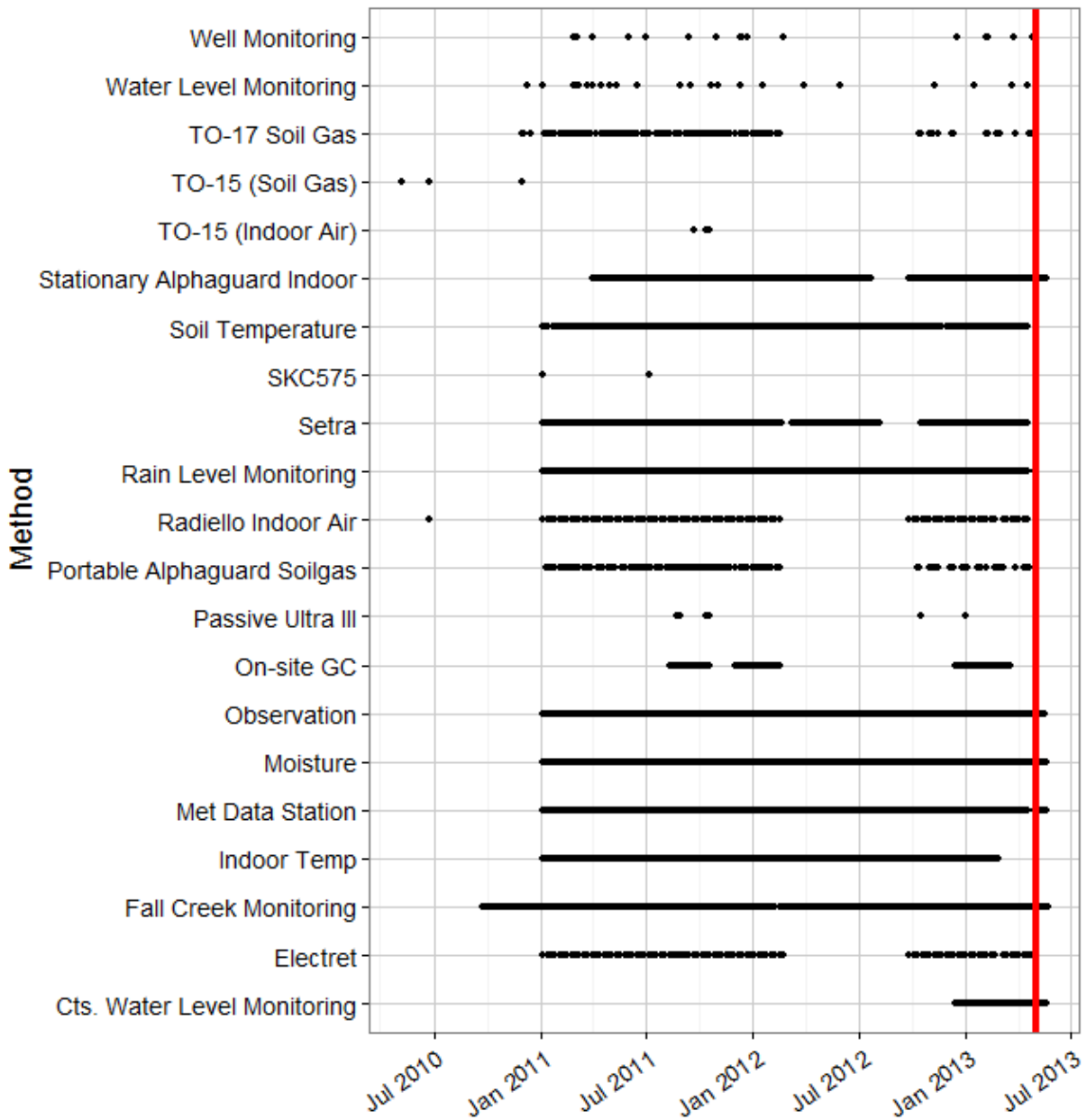


Figure 1-1. Temporal coverage of data sets collected (red line indicates the cutoff date for this report).

Dots represent discrete sampling events. Bars represent continuous sampling methods. The red line indicates the cutoff date for data used in this study (May 2013). TO-15 is a summa cannister sampler; TO-17 is an active (pumped) sorbent tube sampler; SKC 575 and Ultra III are badge-style passive sorbent samplers; Setra is a differential pressure measurement device; GC = gas chromatograph; Electret and AlphaGUARD are radon measurement devices; Cts = continuous. See Section 3 for additional information on measurements and methods.

1.4.4 Meteorological Effects on Vapor Intrusion

To assess the relationship between meteorological parameters and vapor intrusion, we used visual examination of temporal trends in stacked plots of indoor air, soil gas, and subslab concentration data

along with quantitative time series methods. Results from these lines of evidence are summarized in **Table 1-1**. In summary, the data suggest that multiple meteorological variables likely interact in complex ways to affect VOC vapor intrusion at this duplex.

As expected, based on stack effects, cold temperatures contributed to greater vapor intrusion. This was expected from knowledge of the stack effect mechanism. The evidence also indicates that both snowfall and snow/ice accumulation can increase VOC vapor intrusion, although this effect may be absent for radon and is complex for VOCs. Snow varies in moisture content and; thus, air permeability from one snow event to another and as a snow accumulation ages over time. There is relatively little evidence of rain effects on VOCs, but there is evidence suggestive of a rain effect on radon. Barometric pressure change appears to have effects on radon and probably VOCs, although the interactions are complex and additional work on the time series data is needed to determine how best to analyze the effects of barometric pumping on vapor intrusion in the duplex. There also is evidence of an association between winds from westerly directions with vapor intrusion in the 422 portion of the duplex, but the evidence for an effect of wind velocity is equivocal. Additional study is needed to assess how to best model the complex interactions between meteorological variables and vapor intrusion at this site, as well as to see how different meteorological and building conditions can lead to different results at other sites.

1.4.5 Preferential Pathways and Conceptual Site Model: Helium Tracer and Geophysical Tests

Four helium tracer tests performed pairwise with common subsurface injection locations yielded similar overall patterns of tracer distribution in soil gas outside the building with and without mitigation system operation. The variability between paired tests (mitigation on and mitigation off) was more pronounced beneath the building where the mitigation system would have been expected to have the most significant influence on airflow. The similar patterns between tests performed in different subsurface areas (i.e., different injection points) suggest control by common features of soil stratigraphy or the building envelope. Helium tracer concentrations suggest easy horizontal migration toward the building over distances of up to 20 ft and rapid vertical migration from 13 ft to 6 ft bls at the injection cluster. However, lower helium concentrations at certain ports suggest subsurface heterogeneity and preferential flow paths that could not be fully mapped with only the four tests conducted.

Geophysical tests confirmed the location of many known features in and around the duplex, including the shallow, moist silty clay layer overlying the deeper sand/gravel outwash layer and the shallower (7–7.5 ft bls) silt/clay layer. Ground penetrating radar (GPR) results suggest that the concrete slab varies from 0.5 to 0.7 ft in thickness with an irregular undulating contact with the underlying fill material and resulting gaps where soil gas may pool or move preferentially.

Table 1-1. Summary of Lines of Evidence for Meteorological Factors Influencing Vapor Intrusion in This Study (Blank cells reflect types of analysis not completed for a given parameter)

| | Snowfall | Snow or Ice Accumulation on Ground | Cold Exterior Temperatures (or Substantial Change in temperatures) | Rain Events/ Rainfall Amount | Barometric Pressure Changes | West to NW Winds | High Wind Velocity |
|---|-------------------|---|--|------------------------------|-----------------------------|--------------------------------|--------------------------------|
| Apparent Temporal Association with VOC Concentrations in Indoor Air (Section 6, also EPA 2012a) | Yes | Yes | Yes | Possibly for chloroform | | | |
| Apparent Temporal Association with VOC Concentrations in Wall Ports or Subslab Ports (Section 6) | Yes | Yes | | | Weak | | Some |
| Apparent Temporal Association with Large Subslab to Indoor Differential Pressure Events (Section 9.1) | Yes in some cases | | Yes in some cases | | Yes in some cases | Yes in a few cases | Yes in a few cases |
| Apparent Trend in XY Graph of Meteorological Parameter vs. Subslab/Indoor Differential Pressure (Section 9.1 and EPA 2012a) | | | Yes | No | | Yes | No |
| Apparent Trend in XY Graph of Meteorological Parameter vs. VOC Concentration (Section 9.2) | | Yes for PCE, not definitive for chloroform | Yes | No clear relationship | Not definitive | Yes for PCE, No for chloroform | No for PCE, Yes for chloroform |
| Correlation with Radon in Quantitative Time Series Analysis (sections 10.1 to 10.4); 422 Basement and Office | No | No | Yes in most analyses | Yes in some analyses | Yes in most analyses | | Yes in some analyses |
| Correlation with Chloroform in Quantitative Time Series Analysis (Sections 10.5 and 10.7); 422 Basement | | Yes in one of two cases with opposite signs for the coefficients of the current and past weeks. | Yes | No | Yes in some analyses | | |
| Correlation with PCE in Quantitative Time Series Analysis (Sections 10.6 and 10.8), 422 Basement | | Yes in one of two cases but with an unexpectedly negative coefficient for the current week. | Yes, although coefficients are both positive and negative | No | Yes | No | No |

1.4.6 Temporal Variability and Trends

PCE levels in indoor air follow the general trend of starting higher at the beginning of the project (January 2011), dropping to a low in early summer, and rising slightly and leveling out through the end of the intensive premitigation study period (February 2012). This general trend was attributed primarily to temperature, because the winter of 2010–2011 was much more severe than the winter of 2011–2012.

During mitigation testing, which began in October 2012, radon dropped quickly with mitigation and remained low, while indoor air PCE concentrations first dropped then rose to levels above those observed in the March 2011 to September 2012 time period (see February and March period in **Figure 1-1**). Given that soil gas levels also tended to rise at times during mitigation, we postulate that VOCs can be moved close to the structure either by a cumulative stack effect during a severe winter or by operation of an SSD mitigation system. It is unknown whether this VOC migration effect toward the slab will be common at sites with other geological formations or contaminant distributions or whether it would continue to occur at this site with longer operation of the mitigation system. Because our mitigation testing included several on-off cycles over one winter, we also do not know whether more substantial reductions in indoor air VOC concentrations would be achieved with continuous operation of the SSD mitigation system. However, spatial patterns changed dramatically when mitigation was operating, indicating that at least during initial operation the mitigation system was influencing both soil gas and indoor air concentrations.

1.4.7 Summary

These results suggest that current chemical vapor intrusion mitigation system designs, based on radon systems experience, may produce designs that are highly effective for radon but not as effective for VOCs, *at least during the initial months of system operation*. This finding suggests a need for longer term confirmation of post-mitigation VOC concentrations and replication of this study's findings in other environments. Specifically, buildings of other ages/designs in conditions similar to this (15 to 20 ft to groundwater, moderate strength source, and coarse deep geology) should be tested. This finding should also prompt more intensive studies of long-term mitigation system performance in commercial buildings and in other geographies. The current trend of TCE being managed based on short-term exposure thresholds provides additional impetus for such studies, because radon and other VOCs are not usually managed based on short-term health effects.

The results reported here provide little support for the common guidance that vapor intrusion sampling must be timed around rain events greater than one half inch. While there may have been some effects on vapor intrusion of major seasonal flooding events that changed the local water table by approximately 5 ft, there was not any apparent effect on indoor air concentrations from more moderate rain events. The results reported here do suggest that snow events, snow cover, and/or frozen soils may temporarily increase vapor intrusion.

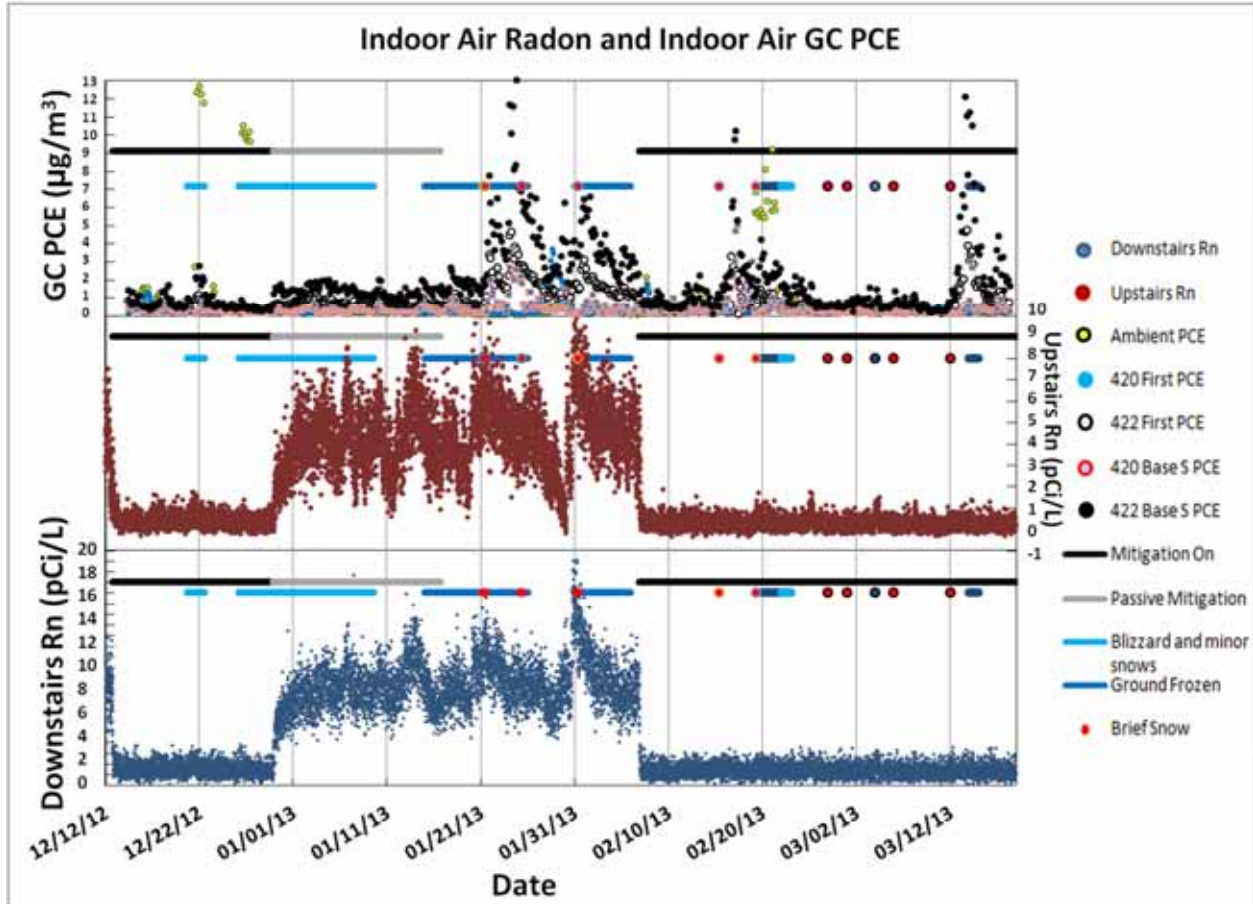


Figure 1-2. Indoor air concentrations of PCE (top panel) and radon (middle and bottom panels) with mitigation on (black bars), passive mitigation (no fan, gray bars), and mitigation off (no bar). Snow and frozen ground events are indicated by blue bars and red dots.

A large number of variables have been shown here to most likely have an interactive effect on VOC vapor intrusion, including cold temperatures, snow/ice, barometric pressure, and wind direction. Practitioners should thus expect to not be able to explain in detail temporal patterns drawn from small data sets (for example, three or four rounds of VOC sampling). However, after results from this study are confirmed in studies of other buildings, it may be possible to develop recommendations to guide selection of “near worst case” indoor air sampling conditions for specific sites based on each site’s known characteristics such as climate, stratigraphy, and source characteristics.

Table of Contents

2.0 Introduction2-1

2.1 Background2-2

2.1.1 Variability in Vapor Intrusion Studies.....2-4

 2.1.1.1 Spatial Variability2-5

 2.1.1.2 Temporal Variability.....2-7

 2.1.1.3 Measurement Variability.....2-8

2.1.2 Vapor Attenuation Factors.....2-9

2.1.3 Potential for Use of Radon as a Surrogate for VOC Vapor Intrusion.....2-9

2.1.4 Passive VOC Sampling.....2-12

2.2 Objectives.....2-16

2.2.1 Time Scale and Measurement of Independent and Dependent Variables.....2-18

2.2.2 Data Quality Objectives and Criteria.....2-18

List of Figures

2-1. An overview of important vapor intrusion pathways (U.S. EPA graphic).2-3

2-2. Soil gas and groundwater concentrations below a slab (Schumacher et al., 2010).....2-6

List of Tables

2-1. VOC Indoor Air Sampling Method Options.....2-15

2-2. Continuing Project Objectives Addressed in this Document.....2-17

2-2. Continuing Project Objectives Addressed in this Document (continued)2-18

2-3. Factors Causing Temporal Change in Vapor Intrusion and How They are Observed and Measured.....2-19

2-4. Data Quality Objectives and Criteria.....2-20

2.0 Introduction

Vapor intrusion is the migration of subsurface vapors, including radon and volatile organic compounds (VOCs), in soil gas from the subsurface to indoor air. Vapor intrusion happens because there are pressure and concentration differentials between indoor air and soil gas. Indoor environments are often negatively pressurized with respect to outdoor air and soil gas, for example, from exhaust fans or the stack effect,⁵ and this pressure difference allows soil gas containing subsurface contaminant vapors to flow into indoor air through advection. In addition, concentration differentials cause VOCs and radon to migrate from areas of higher to lower concentrations through diffusion, which is another cause of vapor intrusion.

For VOCs, the vapor intrusion exposure pathway extends from the contaminant source, which can be free product (nonaqueous phase liquids or NAPLs), VOCs sorbed to the geologic matrix, or contaminated groundwater, to indoor air exposure points. Contaminated matrices may include groundwater, soil, soil gas, and indoor air. VOC contaminants of concern typically include halogenated solvents such as trichloroethene (TCE), tetrachloroethene (PCE), chloroform, and the degradation products of TCE and PCE, including dichloroethenes and vinyl chloride. These halogenated VOCs were widely used and are toxic and degrade very slowly in the subsurface, making them priority contaminants of concern through the vapor intrusion exposure pathway at many hazardous waste sites nationwide. Petroleum hydrocarbons, such as the aromatic VOCs of benzene, toluene, ethylbenzene, and xylenes (BTEX), are also contaminants of concern for vapor intrusion, but because they degrade much more readily in the subsurface, they are much less likely to lead to a vapor intrusion problem (U.S. Environmental Protection Agency [U.S. EPA], 2012p).

Radon is a colorless radioactive gas that is released by radioactive decay of radionuclides in soil, where it migrates into homes through vapor intrusion in a similar fashion to VOCs. Radon is high in areas where the radioactive precursors to radon occur at relatively high concentrations in soil (as with the subject house of this investigation) and affects many more homes across the United States than halogenated VOCs. Low-cost testing and effective mitigation methods are available for radon, and the radon exposure pathway has been studied extensively by EPA and other organizations and thus contributes to a conceptual understanding of the vapor intrusion process.

VOC vapor intrusion is less well studied than radon and is the primary focus of this research project. In particular, the study focuses on halogenated VOCs, which are relatively recalcitrant (resistant) to biodegradation in aerobic soils and groundwater (with typical half-lives of a year or more; Howard et al., 1991); in contrast, radon has a radioactive half-life of about 3.8 days (Cohen, 1971). Of the two primary VOCs subject to investigation under this project, PCE is generally considered quite recalcitrant, with an aerobic half-life in groundwater of 1 to 2 years (Howard et al., 1991). Studies of chloroform biodegradation under aerobic conditions are mixed, with some showing recalcitrance (e.g., a 0.2- to 5-year half-life in Howard et al., 1991) and others showing moderate cometabolic biodegradation with methylene chloride and chloromethane as sequential degradation products (Air Force Center for Environmental Excellence [AFCEE], 2004; Agency for Toxic Substances and Disease Registry [ATSDR], 1997).

Current practice for evaluating the vapor intrusion pathway involves a multiple line of evidence approach based on direct measurements in groundwater, external soil gas, subslab soil gas, and/or indoor air. Modeling approaches ranging from simple constructs, such as attenuation factors to one-dimensional models to three-dimensional models, are frequently used as an aid to data interpretation and predictive

⁵The stack effect is the overall upward movement of air inside a building that results from heated air rising and escaping through openings in the building super structure, thus causing an indoor pressure level lower than that in the soil gas beneath or surrounding the building foundation (<http://www.epa.gov/iaq/glossary.html>).

tool. No single line of evidence is considered definitive, and direct measurements can be costly, especially where significant spatial and temporal variability require repeated measurements at multiple locations to assess the chronic risks of long-term VOC exposure accurately.

The main focus of this report is to better characterize this variability by collecting a detailed long-term data set of week-long measurements of subslab soil gas, external soil gas, and indoor air, on a single building that is affected by vapor intrusion of radon and VOCs. By examining both short-term and long-term (average annual) concentrations, the project provides valuable information on how to best take and evaluate measurements to estimate long-term, chronic risk for VOCs. Special attention was paid to snow/ice events and flooding events as potential causes of dramatic temporal variability. We then implemented a common mitigation technology—subslab depressurization (SSD)—to evaluate the effectiveness of this approach as a tool for reducing indoor concentrations and the temporal variability. Radon concentration fluctuations were also measured because if radon can be shown to indicate when there is a potential for chemical (i.e., VOC) vapor intrusion, radon, which is much cheaper to measure than VOCs, could be an important tool in improving the investigation and mitigation of chemical vapor intrusion using SSD. In addition, there is much research on radon intrusion into indoor air that could provide valuable lessons for chemical vapor intrusion.

The study reported here is an extension of work conducted and published in a previous report (U.S. EPA, 2012a). The earlier study examined the:

- passive sorbent performance over various timescales,
- an evaluation of the usefulness of soil gas samples taken externally to the building,
- heating, ventilation, and air conditioning (HVAC) system cycles,
- the use of temporary vs. permanent subslab ports, and
- induced depressurization within a building as a vapor intrusion evaluation strategy (fan testing).

The previous study helped define additional research questions addressed in this study such as the:

- specific geologic and anthropogenic features that influence contaminant transport in this specific case (and by implication may be important in other similar urban neighborhoods),
- relative role of groundwater and vadose zone sources, and
- control of radon and VOC vapor intrusion variability through SSD mitigation.

In addition to the effects of installing and operating an SSD mitigation system on VOC and radon levels in soil gas and indoor air, the new research report provides additional research on the effect of snow and frozen ground cover on vapor intrusion, as well as a longer term data set. For topics where significant new data were obtained after September 2012, we interpret the new evidence in conjunction with that reported previously.

2.1 Background

An overview of the VOC vapor intrusion pathway is shown in **Figure 2-1**; the building in which exposure occurs is shown in the center. Three main routes of VOC migration have been defined:

- Movement of VOC vapors from shallow soil sources through the unsaturated (vadose) zone
- Transport of VOCs through groundwater, followed by partitioning of VOCs from the most shallow layer of groundwater into vadose zone soil gas
- Vapor movement through preferential pathways such as utility corridors

In portions of these three routes, advective forces predominate, and in others diffusive forces dominate transport. The final step of vapor intrusion typically involves soil gas moving from immediately below the building slab into the indoor air, which is normally envisioned as an advective process for most slabs, although it may be diffusive with very well-sealed slabs. This subslab space is often significantly more permeable than the bulk vadose zone soil, either because a gravel drainage layer was intentionally used or the soils have shrunk back from the slab in places. In those cases, the subslab space is expected to serve as a common plenum allowing the lateral mixing of VOCs that reach the building through multiple pathways. In other cases, the subslab space may not be so interconnected, resulting in differing subslab VOC concentrations at different locations across the slab.

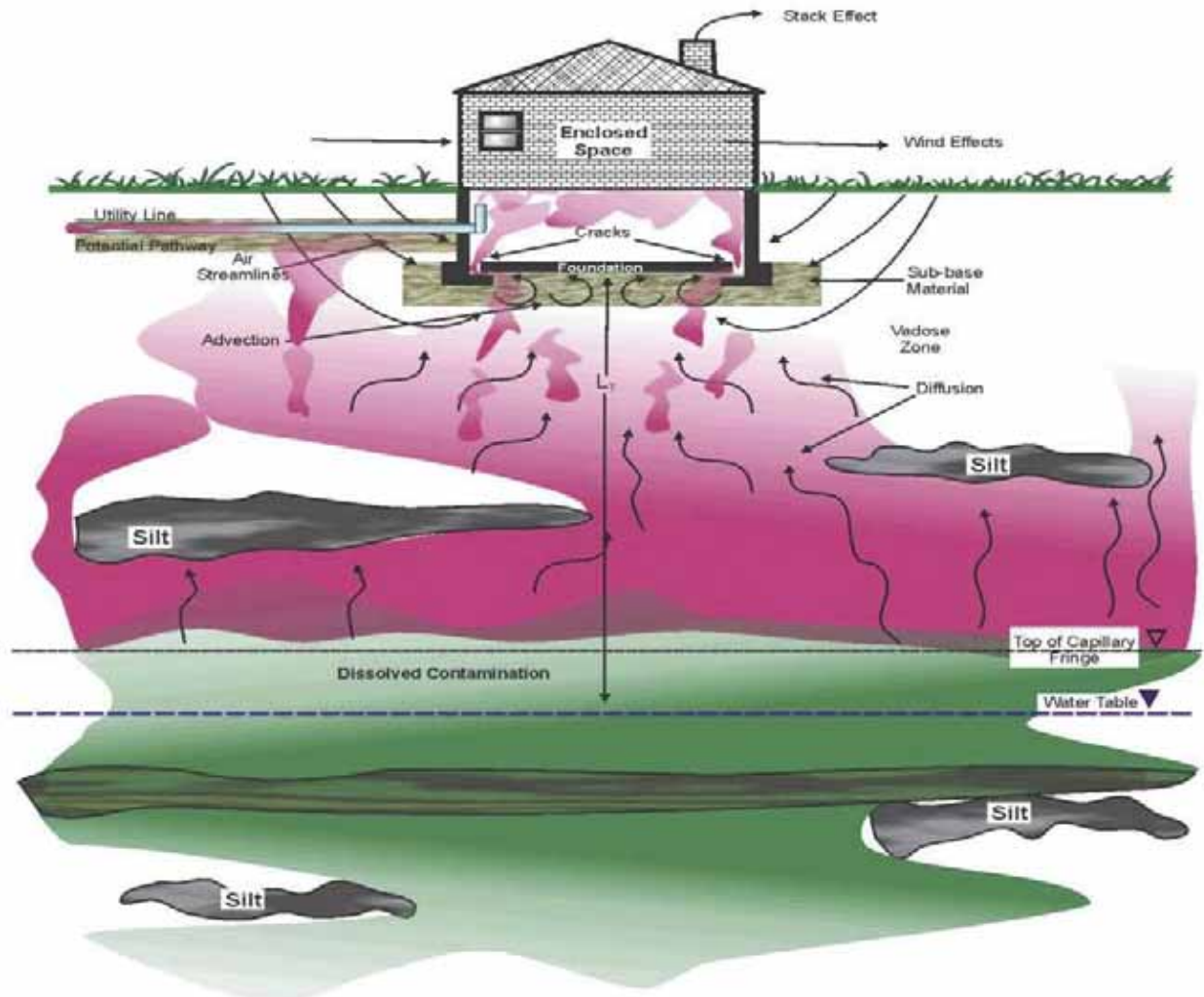


Figure 2-1. An overview of important vapor intrusion pathways (U.S. EPA graphic).

It has been argued that in addition to the average advective force, there is an important and even dominant role in transport under some conditions (such as high permeability) for the fluctuating element of the pressure field, which, like diffusion, contributes to the movement of mass from high to low concentration zones (Robinson and Sextro, 1997; Robinson, Sextro and Fisk, 2007; DeVaul 2012, 2013).

Vapor and liquid transport processes and their interactions with various geologic and physical site settings (including building construction and design), under given meteorological conditions, control migration

through the vapor intrusion pathway. Variations in building design, construction, use, maintenance, and subslab composition and temporal variation in meteorological factors (e.g., atmospheric pressure, temperature, and precipitation and its infiltration) all influence vapor intrusion. Utility corridors, such as the backfill around water lines or partially full sanitary or combined sewers, can provide routes of preferential migration through the vadose zone. Advective flow into a building can occur through cracks in the floor, below grade walls, or at incompletely sealed utility penetrations in the building envelope. NJ DEP (2013) summarizes other important factors that can affect vapor intrusion at many sites:

- biodegradation of VOCs as they migrate in the vadose zone,
- site stratigraphy,
- soil moisture and groundwater recharge,
- fluctuations in water table elevation, and
- temporal and inter-building variations in the operation of ventilation systems in commercial/industrial buildings.

These and other factors combine to create a complex and dynamic system controlling vapor intrusion at a particular site.

This project explored and further developed several promising cost-effective techniques to evaluate the vapor intrusion pathway and improve data quality. Two primary tools were investigated: (1) using modified sorbent-based measurement techniques for time-integrated measurements of indoor air VOCs and (2) using radon measurements for assessing VOC vapor intrusion. The project also investigated measurements of pressure differentials (subslab vs. indoor), meteorological conditions, crack size, and air exchange rates in the context of the chemical-specific measurements described above. These physical measurements are not stand-alone tools nor are they the emphases of the current research program, but are necessary supporting tools for developing a conceptual understanding of spatial variability, temporal seasonal effects, and a mass balance around a building subject to vapor intrusion.

2.1.1 Variability in Vapor Intrusion Studies

This project focused on observing changes in vapor intrusion over a >2-year period both with and without SSD mitigation. In order to express quantitatively our goals for this project, it is necessary to understand the causes and typical ranges of spatial and temporal variation in various matrices studied for vapor intrusion assessment.

Through measurements of radon and VOC vapor intrusion under various conditions, several studies have provided insight into the complexity of temporal variability in indoor air concentrations attributable to vapor intrusion—the primary focus of this work. Nazaroff et al. (1987) studied how induced-pressure variations can influence radon transport from soil into buildings with roughly hourly resolution. In a more recent study, Mosley (2007) presented the results of experiments, showing that induced building-pressure variations influence both the temporal and spatial variability of both radon and chlorinated VOCs (CVOCs) in subslab samples and in indoor air (hourly sampling for radon). Schuver and Mosley (2009) have also reviewed numerous studies of radon indoor concentrations, in which multiple repeated indoor air samples were collected with hourly, daily, weekly, monthly, 3-month, and annual sample durations for study periods of up to 3 years; however, detailed soil gas radon data sets are much rarer.

Several radon studies have demonstrated that barometric pressure fluctuations can affect the transport of soil gas into buildings (Robinson and Sextro, 1997; Robinson et al., 1997). The impact of barometric pressure fluctuations on indoor air is influenced by the interaction of the building structures and conditions, as well as other concurrent factors, such as wind (Luo et al., 2006, 2009). Changes in

atmospheric conditions (e.g., pressure, wind) and building conditions (e.g., open doors and windows) may temporarily over- or under-pressurize a building. Based on long-term pressure differential data sets acquired by ARCADIS and EPA's National Risk Management Research Laboratory (NRMRL) at a different Indianapolis study site (the Wheeler building) at which both radon and VOCs are being measured in both subslab and indoor air, other factors that may cause temporal and spatial variability in soil vapor and indoor air concentrations include:

- fluctuation in building air exchange rates due to resident behavior/HVAC operations,
- fluctuations in outdoor/indoor temperature difference, and
- rainfall events and resultant infiltration and fluctuations in the water table elevation.

The pressure difference between a house-sized building and the surrounding soil is usually most significant within 1 to 2 m of the structure, but measurable effects have been reported up to 5 m from the structure (Nazaroff et al., 1987). Temperature differences or unbalanced mechanical ventilation are likely to induce a symmetrical pressure distribution in the subsurface, but the wind load on a building adds an asymmetrical component to the pressure and distribution of contaminants in soil gas.

Folkes et al. (2009) summarized several large groundwater, subslab, and indoor air data sets collected with sampling frequencies ranging from quarterly to annually during investigations of vapor intrusion from chlorinated VOC plumes beneath hundreds of homes in Colorado and New York. They analyzed these data sets to illustrate the temporal and spatial distributions in the concentration of VOCs. Their analysis demonstrated that although the areal extent of structures affected by vapor intrusion mirrored the plume of chlorinated VOCs in groundwater, not all structures above the plume were affected. In addition, they found that measured concentrations of VOCs in indoor air and subslab soil gas can vary considerably from month to month and season to season, and that sampling results from a single location or point in time cannot be expected to represent the range of conditions that may exist spatially or at other times.

In a study of the vapor intrusion pathway at the Raymark Superfund site, DiGiulio et al. (2006) showed that measured concentrations of CVOCs in subslab exhibited spatial and temporal variability between neighboring houses and within individual houses. Similar variability in subslab CVOC concentrations within and between houses has been observed during vapor intrusion evaluations of several sites in New York State (Wertz and Festa, 2007).

In scenarios with coarser soils (e.g., sands, gravels), the soil gas permeability is high, and changes in building pressurization may affect the airflow field and the resultant soil vapor concentration profiles near buildings. In scenarios with fine-grained soils (e.g., silts, clays), the soil gas permeability is low and soil gas flow rates (Q_s) may be negligible and not affect the subsurface concentration. Nevertheless, in both soil-type scenarios, over-pressurization of the building may still significantly reduce the indoor air concentration because of the reversal of soil gas flow direction from the building into the soil (Abreu and Johnson, 2005, 2006).

A wind-induced, non-uniform pressure distribution on the ground surface on either side of a house may cause spatial and temporal variability in the subslab soil vapor concentration distribution if the wind is strong and the soil gas permeability is high (Luo et al., 2006, 2009). In addition, during or after a rainfall event, the subsurface beneath the building may have a lower moisture content than the adjacent areas because of water infiltration.

2.1.1.1 Spatial Variability

Spatially, reports of several orders of magnitude variability without apparent patterns between indoor air and subslab concentrations for adjacent structures in a neighborhood are very common (see, for example,

U.S. EPA, 2012c). Six orders of magnitude in subslab concentration variability were reported by Eklund and Burrows (2009) for a commercial building of 8,290 sq ft. As shown in **Figure 2-2**, Schumacher and coworkers (2010) observed more than three orders of magnitude concentration variability in shallow soil gas below a slab over a span of 50 lateral feet, suggesting a strong effect of impervious surfaces both in limiting soil gas exchange with the atmosphere and in maintaining relatively high concentrations of VOCs in shallow groundwater. They also observed two orders of magnitude concentration variability with a depth change of 10 ft in the unsaturated zone within one borehole. Although these publications, unlike this study, are for larger nonresidential properties, they do support the general conclusion that spatial variability can be over several orders of magnitude at vapor intrusion sites.

Lee and coworkers (2010) observed two orders of magnitude variability in subslab concentration beneath a small townhouse. Studies by McHugh and others (2007) have generally found markedly less variability in indoor air concentrations than in subslab concentrations, probably due to the greater degree of mixing in the indoor environment.



Measured Soil Gas Profile for TCE – Phase 2

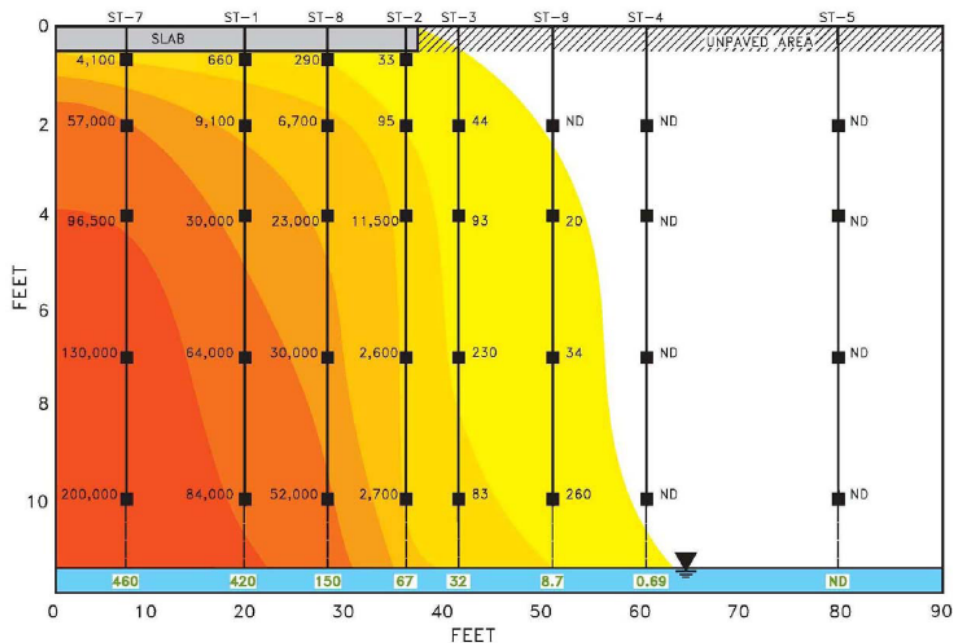


Figure 2-2. Soil gas and groundwater concentrations below a slab (Schumacher et al., 2010).

2.1.1.2 Temporal Variability

Temporal variability has been summarized by ITRC (2007), which states in Section D.4.10:

Variations in soil gas concentrations due to temporal effects are principally due to temperature changes, precipitation, and activities within any overlying structure. Variations are greater in samples taken close to the surface and dampen with increasing depth. In 2006 there were a number of studies on temporal variation in soil gas concentrations, and more are under way or planned in 2007 by USEPA and independent groups. To date these studies have shown that short-term variations in soil gas concentrations at depths 4 feet or deeper are less than a factor of 2 and that seasonal variations in colder climates are less than a factor of 5 (Hartman 2006). Larger variations may be expected in areas of greater temperature variation and during heavy periods of precipitation, as described below.

**Temporal Variability Example:
IBM site, Endicott, New York**

Recent data from a large site in Endicott, New York, collected over a 15-month period showed soil gas concentration variations of less than a factor of 2 at depths greater than 5 feet bls.

- **Temperature.** *Effects on soil gas concentrations due to actual changes in the vadose zone temperature are minimal. The bigger effect is due to changes in an overlying heating or HVAC system and the ventilation of the structure due to open doors and windows. In colder climates, worse-case scenarios are most likely in the winter season. The radon literature suggests that temporal variations in soil gas are typically less than a factor of 2 and that seasonal effects are less than a factor of 5. If soil gas values are more than a factor of 5 below acceptable levels, repeated sampling is likely not necessary regardless of the season. If the measured values are within a factor of 5 of allowable risk levels, then repeated sampling may be appropriate.*
- **Precipitation.** *Infiltration from rainfall can potentially impact soil gas concentrations by displacing the soil gas, dissolving VOCs, and by creating a “cap” above the soil gas. In many settings, infiltration from large storms penetrates into only the uppermost vadose zone. In general, soil gas samples collected at depths greater than about 3–5 feet bgs or under foundations or areas with surface cover are unlikely to be significantly affected. Soil gas samples collected closer to the surface (<3 feet) with no surface cover may be affected. If the moisture has penetrated to the sampling zone, it typically can be recognized by difficulty in collecting soil gas samples. If high vacuum readings are encountered when collecting a sample or drops of moisture are evident in the sampling system or sample, measured values should be considered as minimum values.*
- **Barometric Pressure.** *Barometric pressure variations are unlikely to have a significant effect on soil gas concentrations at depths exceeding 3–5 feet bgs unless a major storm front is passing by. A recent study in Wyoming (Luo et al. 2006) has shown little to no relationship between barometric pressure and soil gas oxygen concentrations for a site with a water table at ~15 feet bgs.*

In summary, temporal variations in soil gas concentrations, even for northern climates, are minor compared with the conservative nature of the risk-based screening levels. If soil gas values are a factor of 5–10 times below the risk-based screening levels, there likely is no need to do repeated sampling unless a major change in conditions occurs at the site (e.g., elevated water table, significant seasonal change in rainfall)...

And in Section D.8 of the same document, ITRC notes:

Short-term temporal variability in subsurface vapor intrusion occurs in response to changes in weather conditions (temperature, wind, barometric pressure, etc.), and the variability in indoor air samples generally decreases as the duration of the sample increases because the influences tend to average out over longer intervals. Published information on temporal variability in indoor air quality shows concentrations with a range of a factor of 2–5 for 24-hour samples (Kuehster, Folkes, and Wannamaker 2004; McAlary et al. 2002). If grab samples are used to assess indoor air quality, a factor of safety (at least a factor of 5) should be used to adjust for short-term fluctuations before comparing the results to risk-based target concentrations. Long-term integrated average samples (up to several days) are technically feasible, using a slower flow rate this is the USEPA recommended approach for radon monitoring). Indoor air sampling during unusual weather conditions should generally be avoided.

In Section D.11.8, ITRC goes on to discuss the effect of meteorological changes on vapor intrusion:

A variety of weather conditions can influence soil gas or indoor air concentrations. The radon literature suggests that temporal variations in the soil gas are typically less than a factor of 2 during a season and less than a factor of 5 from season to season). Recent soil gas data from Endicott, New York and Casper, Wyoming are in agreement with the radon results. For soil gas, the importance of these variables will be greater the closer the samples are to the surface and are unlikely to be important at depths greater than 3–5 feet below the surface or structure foundation.

The most frequent time interval of observation in routine vapor intrusion practice has been 8- to 24-hour integrated samples. In this project, multiple durations of observation of indoor air concentrations were compared, including automated discrete samples collected on 3-hour intervals and passive samples with varying integration times: 24–48 hours, 7 days, 14 days, 28 days, 91 days, 182 days, and 364 days.

A team led by Paul Johnson (Johnson et al., 2012; Holton et al., 2013) reported more than 2 years of high frequency observation of a home overlying a chlorinated solvent groundwater plume in Layton, Utah. At the time of this report, key preliminary observations at that site with regard to temporal variability included the following:

- Indoor air variability in TCE of about three orders of magnitude was observed.
- The near-source data, such as deep soil gas, were more consistent in time than the near-surface data sets such as subslab air or indoor air.
- The temporal trend was characterized by “long periods of relative VI inactivity with sporadic VI activity” and “long periods of relative VI activity with sporadic VI inactivity” (Johnson, 2012).
- “24-h samples are not a very practicable option at the resolution required for robust VI pathway assessment” (Holton, 2013).

2.1.1.3 Measurement Variability

Beyond spatial and temporal variability, the underlying uncertainty of the measurements used to assess vapor intrusion must also be considered. Many measurements of vapor intrusion, both in indoor air and subslab soil gas, have traditionally relied on Summa canister samples analyzed by methods TO-14/TO-15. (U.S. EPA, 1999a, 1999b). Method TO-15 specifies an audit accuracy of 30% and a replicate precision of 25% as performance criteria. But even those figures do not fully convey the interlaboratory variability observed for these methods when applied to the low concentrations typical of indoor air studies. As Lutes and coworkers (2010) reported:

- “In two recent TO-15 or 8260 interlaboratory comparisons administered by the company ERA for gas phase samples the acceptance range for tetrachloroethylene results were: 4.31–22.3 ppbv (July–Sept 2009 study) and 31.6–74.1 µg/L (October–November 2007 study).”

- “For comparison in a 2007 TO-14/TO-15 study conducted by Scott Specialty Gasses the reported values for toluene reported by 12 labs varied from 3.1 to 18.6 ppbv.”

2.1.2 Vapor Attenuation Factors

One common way of evaluating the impact of subsurface vapors on indoor air quality is to compute the ratio of indoor air concentration to subslab soil vapor concentration. EPA has defined the resulting “attenuation factor” as follows: “The attenuation factor, α , is a proportionality constant relating indoor air concentrations ($C_{\text{indoor air}}$) to the concentrations of vapors in soil gas ($C_{\text{soil gas}}$) or groundwater ($C_{\text{groundwater}}$) concentrations.” For soil gas to indoor air, the equation is as follows:

$$C_{\text{indoor air}} = \alpha_{\text{SG}} \times C_{\text{soil gas}}$$

For groundwater, a similar equation is used except that the dimensionless Henry’s Law Constant (H) is used to convert the dissolved VOC concentration in groundwater to the corresponding equilibrium vapor concentration:

$$C_{\text{indoor air}} = \alpha_{\text{GW}} \times C_{\text{groundwater}} \times H.$$

A larger α indicates less attenuation, and a smaller value indicates more attenuation. The greater the attenuation factor, the greater the indoor air concentration.

Note that both of these equations assume that all of the indoor air VOC concentration ($C_{\text{indoor air}}$) is from vapor intrusion. In many cases, this is not the case because of VOC-containing products in the indoor environment. At this site, VOCs are not in use because the house is not occupied, so all VOCs over the outdoor ambient air concentration can be attributed to vapor intrusion.

Within any one given site, the attenuation factors

- between groundwater and indoor air typically vary 2 to 3 orders of magnitude and
- between external soil gas and indoor air typically vary 2 to 4 orders of magnitude.

Subslab soil gas and indoor air typically vary 2 to 4 orders of magnitude (Dawson and Schuver, 2010). EPA recently published a compilation of attenuation factor data (U.S. EPA, 2012c) that analyzes spatial and temporal variability. Because the case with the most rounds of data discussed in the compilation as an example of temporal variability has only six rounds, this report is expected to provide a valuable addition to the literature regarding attenuation factors in a residential structure.

2.1.3 Potential for Use of Radon as a Surrogate for VOC Vapor Intrusion

Radon, a naturally occurring radioactive gas, is a potentially useful surrogate for assessing VOC vapor intrusion because the physics of radon intrusion into indoor air is similar to VOC vapor intrusion. Radon is ubiquitous in the soil and present at measurable quantities in soil gas throughout the United States. Indeed, much of the research in VOC vapor intrusion is an expansion of earlier work on radon intrusion. Applications of radon as a VOC surrogate have been proposed for the following reasons (Lutes, 2009; Mosley, 2007; Mosley, 2008; Schuver, 2009):

- Estimating attenuation factors, with the measured radon attenuation factor serving as a surrogate for the attenuation that may be occurring for VOCs
- Screening of large populations of housing units/buildings, with the presence of radon above ambient levels in indoor air serving as evidence of soil gas influence

- Use as a line of evidence to help distinguish indoor sources of VOCs where VOC indoor concentrations are higher than would be inferred based on the radon attenuation factor. Also, differing responses of radon and VOCs to building pressurization/depressurization tests could be used to assess the potential for indoor sources
- Locating soil gas entry points, when higher radon readings are observed near entry points
- Verifying SSD mitigation system performance based on the reduction of indoor air radon concentrations during SSD system operation.

Radon provides a nearly unique surrogate for VOC vapor intrusion because its presence in the indoor environment is usually a result of radon in the soil gas immediately surrounding a building. In theory, the entry mechanisms are believed to be the same for VOCs and radon in soil gas. Thus, measured radon entry rates should be a good predictor of relative entry rates for VOCs. The advantages of using radon as a surrogate measure for VOC vapor intrusion characterization include:

- Measurements of radon are easier, more accurate and precise, and much less expensive than canister measurements of VOCs (typically less than 10% of the VOC analysis cost). Passive indoor sampling for radon costs approximately \$5 to \$20 per sample. Active radon sampling (indoor air and subslab) uses some of the same equipment and setup as for VOCs. This minimizes sampling times and cost. Continuous measurement devices for radon are also available ranging from consumer grade devices under \$150 to professional grade instruments under \$10,000.
- High levels of indoor radon identify buildings that are vulnerable to soil gas entry.
- Because of the low sampling/analytical costs for radon, it is possible to conduct more field measurements than with VOCs. This, in turn, can increase confidence in the field evaluation.
- Because the SSD mitigation systems can be expected to behave similarly for radon and VOCs in the vicinity of the building, radon measurements before and after installation of vapor intrusion mitigation systems may be useful for assessing SSD mitigation system performance for VOCs as well.

In summary, the limited data gathered to date suggest that radon measurement may be an inexpensive, semi-quantitative surrogate for VOC measurement when characterizing vapor intrusion and may significantly enhance vapor intrusion characterization and decision making, particularly when used in conjunction with subslab sampling. However, several key aspects and assumptions of this approach need to be verified before it can be put into widespread use. For radon to be a valuable surrogate for VOCs:

- Radon detection in building interiors should be quantitatively possible across the wide range of subslab concentrations encountered in the United States. Ideally these measurements can be made with inexpensive passive methods (i.e., charcoal or electrets).
- The radon route and mechanism of entry should be similar to that of VOCs of interest, once both species are present in the subslab soil gas. This would imply that the subslab attenuation factors for radon and VOCs are similar.
- Variance in the natural vadose zone (unsaturated soil) radon concentration across a given building footprint should be low enough to allow radon to be a useful indicator.
- Concentrations of radon and the VOCs of concern should be well correlated in subslab soil gas. This would not necessarily be expected based on the fact that radon and VOCs have different sources. However, they may indeed be approximately correlated if the VOC(s) of interest and radon are both widely dispersed in deep soil gas. In this case, the concentrations of both radon and VOCs at various locations in the subslab may be controlled primarily by the ratio of flow from the deep soil gas to the flow from ambient air (in which both VOC and radon concentrations would be expected to be low).

- Interior sources of radon should be negligible.

The loss rates to sink effects in the indoor environment should be similar or negligible for radon and VOCs so that the air exchange rate forms the primary control on indoor air concentration once vapor intrusion has occurred.

To our knowledge, this concept was first applied in a relatively small study (Cody et al., 2003) at the Raymark Superfund Site in Connecticut. The study compared the intrusion behavior of radon and individual VOCs by determining attenuation factors between the subslab and indoor (basement) air in 11 houses. The results indicated that the use of radon measurements in the subslab and basement areas was promising as a conservative predictor of indoor VOC concentrations when the subslab VOC concentrations were known. Further work at the Raymark site (U.S. EPA, 2005b) statistically compared basement and subslab concentration ratios for radon and VOCs associated with vapor intrusion. Of six test locations, three showed that basement/subslab concentration ratios for radon and VOCs associated with subsurface contamination were similar. Three had statistically different ratios, suggesting that further research was needed to evaluate the usefulness of radon in evaluating vapor intrusion. Conservative VOCs (those believed to be associated only with subsurface contamination) were a better predictor of other individual volatile compounds associated with vapor intrusion than was radon.

A three-building complex, commercial case study of the radon tracer approach was published by Wisbeck et al. (2006). Radon and indoor air attenuation factors were calculated for five sampling points and were generally well correlated. Subslab radon concentrations varied by approximately a factor of 10 across the five sampling points.

Results of an earlier test program at Orion Park Housing units at Moffett Field have been preliminarily reported (Mosley, 2007). Results showed:

- Low levels of radon can be measured with sufficient accuracy to be used in analysis of vapor intrusion problems.
- Radon is a promising, low-cost surrogate for soil gas contaminants; however, as with VOCs themselves, the complete distribution under the slab must be known in order to properly interpret its impact on indoor measurements.
- Unexpectedly, the subslab areas under each unit were segmented. The four subslab sampling points installed in one unit were not in good communication with one another. An introduced tracer, SF₆, moved very slowly and not very uniformly under the slab.
- Results showed that for soils like these with poor communication, a subslab measurement at a single point is not very reliable for estimating potential vapor intrusion problems. The average value of subslab measurements at several locations also may not yield a reliable estimate of indoor concentrations. When subslab communication is poor, one must identify a connection between subslab contaminants and a viable entry path.

The potential usefulness of the radon tracer was studied in 2007 to 2010 by EPA NRMRL at Moffett Field in California and in the Wheeler building in Indianapolis. These studies are summarized in three draft peer-reviewed papers that have been submitted for EPA internal review:

- *Vapor Intrusion Evaluation Using Radon as a Naturally Occurring Tracer*: In this paper, we compile data from five study sites where radon has been used in VOC vapor intrusion investigations and attenuation factors were calculated. A total of 17 buildings are included in the data set, a mix of commercial and residential, in a wide variety of geographical areas within the United States. Attenuation factors were roughly correlated between radon and VOCs.

- *Randomized Experiment on Radon Tracer Screening for Vapor Intrusion in a Renovated Historical Building Complex*: This study focused on a renovated former industrial facility now being reused as residential, public, and office space. Fifty locations within the complex were originally screened for radon using passive sampling techniques. Then two subsets of these sample locations were selected for passive VOC sampling, one randomly and the other based on the radon information. The upstairs radon-guided samples were significantly higher in TCE than the randomly selected locations. The portions of the building complex where the radon guidance appeared to provide predictive power were understandable in terms of the building design and the concept of the open basement serving as a common plenum.
- *Case Study: Using Multiple Lines of Evidence to Distinguish Indoor and Vapor Intrusion Sources in a Historic Building*: This paper uses data sets developed at the Southeast Neighborhood Development Corporation (SEND) Wheeler Arts Building site in Indianapolis, Indiana, to demonstrate the use of multiple lines of evidence in distinguishing indoor from subsurface sources in a complex multiuse, multiunit building. The use of radon as a quantitative tracer for vapor intrusion source discrimination is shown as well as the use of differential pressure data as an additional line of evidence. Box and whisker plots of the distribution of indoor air pollutants on multiple floors are used to distinguish pollutants with predominant slab sources from those with predominant indoor sources. Those pollutants that the box and whisker analysis suggest have indoor sources are also corroborated from the literature as having very common indoor sources expected in this building, including arts and crafts activities, human exhalation, consumer products, and tobacco smoking.

A recent review presentation by Schuver (2013) thus summarizes the usefulness of radon as a “qualitative/semi-quantitative indicator of building specific susceptibility to near-surface soil-gas/vapor intrusion” and “a signature of the building-specific responses to environmental changes” and a “key (3rd-strike) evidence basis for demonstrated-potential for chem-VI.” Steck (2012) summarizes an EPA document currently under development that describes lessons learned from radon that can be applied in vapor intrusion research and practices.

2.1.4 Passive VOC Sampling

Sorbent-based methods are an emerging technology for vapor intrusion assessment. Current standard practices for indoor air VOC monitoring in the United States include the use of negatively pressurized, ultra-clean, passivated, stainless steel canisters for sample collection. Practitioners frequently use 8- to 48-hour integrated samples with Summa canisters in an attempt to average over an exposure period. This is the U.S. “gold standard” for indoor air analysis, but it is expensive to implement. Professional experience, shows that the flow controllers currently used in commercial practice are subject to substantial flow rate and final pressure errors when set for integration times in excess of 24 hours (Hayes, 2008).

Active and passive sorbent sampling techniques are already in use in the United States for personal air monitoring for industrial workers and are outlined in both the Occupational Safety and Health Administration (OSHA) Sampling and Analytical Methods (<http://www.osha.gov/dts/sltc/methods/toc.html>) and National Institute for Occupational Safety and Health (NIOSH) *Manual of Analytical Methods* (<http://www.cdc.gov/niosh/nmam/>). Typical sampling scenarios involve the collection of active or passive samples to monitor a single chemical used in the workplace over a period of up to 10 hours. These methods are designed to meet OSHA permissible exposure limits (PELs), which are typically in the ppm range and consequently several orders of magnitude higher than risk-based indoor air screening levels and not suitable for ambient air measurements without modification.

Active sorbent methods (i.e., TO-17) have also been published by EPA for VOC measurements in ambient air (U.S. EPA, 1999c). However, in those methods, air samples are normally actively collected

over 1 hour, using a sample pump with a sampling rate of 16.7 mL/min to 66.7 mL/min, yielding total sample volumes between 1 and 4 liters. Sampling intervals can be extended beyond 1 hour; however, care must be taken to ensure breakthrough volumes are not exceeded in order to quantitatively retain the compounds of interest on the sorbent tube. Given the minimum pump flow rate cited in TO-17 of 10 mL/min, the practical upper limit for chlorinated VOCs using a multi-bed thermal desorption sorbent tube is on the order of 10 liters up to 20 L for select VOCs yielding a corresponding maximum collection period of 8 to 24 hours (Marotta et al., 2012).

One way to lower the detection limits and control day-to-day variability is to sample over a longer period of time. Recent studies have shown that it may be feasible to use passive sorbent samplers to collect a continuous indoor air sample over several weeks. This approach would provide a lower detection limit, be cost-effective, and result in a time-integrated composite sample. Laboratory and field evaluations of passive samplers for ambient and indoor air applications have been published and showed promising results for sampling durations of up to 14 days. Exposure of badge-type charcoal passive samplers to controlled atmospheres of 10 to 200 ppb benzene, toluene, and m-xylene showed good performance when deployed for 14 days (Oury et al., 2006). A field study published by Begerow et al. (1999) showed comparability between two charcoal-based passive sampler geometries, badge and tube-style for 4-week indoor and outdoor air samples. Field evaluations were also conducted using radial charcoal and thermal desorption Radiello[®] samplers to determine performance over a 14-day period. Ambient BTEX measurements using the Radiello samplers compared well to active sorbent sampling results (Cocheo et al., 2009).

Testing at Orion Park, Moffett Field in California by EPA NRMRL Air Pollution Prevention and Control Division (APPCD), EPA Region IX, and ARCADIS compared measurements of VOCs by Method TO-15 to three different radial and axial tube-type sorbent systems⁶:

7. Radial: activated charcoal (with carbon disulfide [CS₂] extraction: gas chromatography–mass spectrometry [GC/MS])
8. Radial: carbograph 4 (TO-17: thermal desorption [TD] GC/MS)
9. Axial: chromosorb 106 thermal desorption tube (TO-17: TD GC/MS)

Performance for the two radial methods was superior to the axial method (Lutes, 2010). Testing was also performed at the Wheeler site in Indianapolis comparing Summa canisters to Radiello radial solvent-extracted samplers. Across the two sites, the Radiello solvent extracted showed good agreement to TO-15 and precision at both sites for chlorinated compounds. Agreement was poor for polar compounds: ethanol, methyl ethyl ketone (MEK), methyl isobutyl ketone (MIBK), and acetone. Radiello TD correlated well with Summa TO-15 but gave noticeably lower concentrations, suggesting that 2 weeks is too long an integration time for these samplers. The agreement of the axial (tube) method was inferior (Mosley et al., 2008; Lutes et al., 2010).

Table 2-1 compares the characteristics of commercially available passive sampler geometries and available sorbent configurations. The geometry of the sampler (radial, badge, or axial tube) largely determines the sampling rate or uptake rate with the radial design resulting in the highest sampling rate and the tube-style the lowest sampling rate. The permeation sampler relies on permeation of the vapor-phase compound through the polydimethylsiloxane (PDMS) membrane and adsorption to the sorbent bed behind the membrane. The greater the sampling rate, the greater the mass of VOCs adsorbed onto the sorbent bed. In addition to the passive geometries available, sorbent pairings fall into two main

⁶Radial samplers are sorbent-containing tubes where diffusion from the surrounding air occurs radially along the entire length of the tube. Axial samplers are tubes containing sorbent where diffusion occurs axially through one open end of the tube. Because of the higher surface area exposed for diffusion, radial samplers have higher uptake rates than axial tube-type samplers.

categories—charcoal based and thermally desorbable. Charcoal-based materials are characterized as very strong sorbents with a large surface area and a corresponding high adsorption capacity. To efficiently extract adsorbed compounds for measurement in the laboratory, an aggressive solvent extraction is required. The thermally desorbable sorbents are generally much weaker than charcoal with a smaller surface area, allowing for analysis of the adsorbed compounds through thermal extraction. As Table 2-1 shows, when comparing the same passive geometry, the thermally desorbed model provides the lowest detection limits, while the charcoal-based solvent-extracted system allows for longer sampling times as well as a greater dynamic range because the high capacity of the charcoal minimizes sorbent saturation under conditions of high analyte or background matrix.

European agencies have developed standard methods for passive sampling for VOCs that are applicable to the range of concentrations and durations to be tested in this project:

- Methods for the Determination of Hazardous Substances (MDHS) 88: *Volatile Organic Compounds in Air: Laboratory Method Using Diffusive Samplers, Solvent Desorption and Gas Chromatography*, December 1997. Published by the Health and Safety Executive of the United Kingdom: <http://www.hse.gov.uk/index.htm>.
- MDHS 80: *Volatile Organic Compounds in Air: Laboratory Method Using Diffusive Solid Sorbent Tubes, Thermal Desorption and Gas Chromatography*, August 1995. Published by the Health and Safety Executive of the United Kingdom: <http://www.hse.gov.uk/index.htm>.
- Ambient air quality: *Standard Method for Measurement of Benzene Concentrations—Part 4: Diffusive Sampling Followed by Thermal Desorption and Gas Chromatography*, EN 14662-4:2005. Published by the European Committee of Standardization.
- Ambient air quality: *Standard Method for Measurement of Benzene Concentrations—Part 5: Diffusive Sampling Followed by Solvent Desorption and Gas Chromatography*, EN 14662-5:2005. Published by the European Committee of Standardization. (Also published as the British Standard BS EN 14662-5:2005).

Indoor air quality: *Diffusive Samplers for Determination of Concentrations of Gases and Vapors: Guide for Selection, Use, and Maintenance*, EN 14412:2004. Published by the European Committee of Standardization.

Table 2-1. VOC Indoor Air Sampling Method Options

| Parameter | Whole Air | Sorbent-Active | Sorbent-Diffusive | | | | | | |
|--|--|---|------------------------------------|---------------------------------------|---|--|--|--------------------------------------|--------------------------------------|
| | | | Radial: Charcoal (Radiello 130) | Radial: TD sorbent (Radiello 145) | Badge: Charcoal type (SKC 575, 3M OVM3500) | Badge: TD sorbents selected by deployment time: (SKC Ultra I, II, III) | Tube: TD sorbents (e.g., Chromosorb 106) | Permeation: Charcoal type (WMS™) | Permeation: TD sorbent (WMS™) |
| Collection media | Summa canister (TO-15) | Multi-bed ATD sorbent tubes (TO-17) | Radial: Charcoal (Radiello 130) | Radial: TD sorbent (Radiello 145) | Badge: Charcoal type (SKC 575, 3M OVM3500) | Badge: TD sorbents selected by deployment time: (SKC Ultra I, II, III) | Tube: TD sorbents (e.g., Chromosorb 106) | Permeation: Charcoal type (WMS™) | Permeation: TD sorbent (WMS™) |
| Ease of deployment | Good | Good | Excellent | Excellent | Excellent | Excellent | Excellent | Excellent | Excellent |
| Estimated media & shipping cost ^b | \$\$\$ | \$\$ | \$ | \$\$ | \$ | \$\$ | \$\$ | \$ | \$ |
| Method and analysis | TO-15 GC/MS | TO-17 GC/MS | Solvent Extraction GC/MS or GC/FID | TO-17 GC/MS | Solvent extraction GC/MS or GC/FID | TO-17 GC/MS | TO-17 GC/MS | Solvent extraction GC/MS | TO-17 GC/MS |
| Estimated analytical reporting limit | 0.05–0.1 µg/m ³ | 1–10 ng | 100–200 ng | 1–10 ng | 75–200 ng | 1–10 ng | 1–10 ng | 50–200 ng | 1–10 ng |
| Expected sampling rate | 0.5–3.5 mL/min | 10–200 mL/min | ~60 mL/min | ~25 mL/min | ~10 mL/min SKC ~30 mL/min 3M | ~10 mL/min | ~0.5 mL/min | ~0.5–5 mL/min | ~0.5–5 mL/min |
| Recommended sampling duration | Typically 24 hours | 8–24 hours | Up to 30 days | Up to 7 days for chlorinated solvents | Up to 4 weeks | 1–7 days | In general, up to 4 weeks) | Up to 30 days | Up to 30 days |
| Estimated sample reporting limits ^a | ~0.05 (SIM)–0.1 µg/m ³ | ~0.1–1 µg/m ³ | ~0.1–0.4 µg/m ³ | ~0.005–0.05 µg/m ³ | ~0.25–2 µg/m ³ | ~0.01–0.1 µg/m ³ | ~0.2–2 µg/m ³ | ~1–40 µg/m ³ | ~1–40 µg/m ³ |
| Applicable range of chlorinated solvents (based on available sampling rates) | TCE/PCE and all breakdown products including vinyl chloride (VC) | TCE/PCE and all breakdown products including VC | TCE, PCE, 111-TCA, chloroform | TCE, PCE, 111-TCA | Validated for a wide range of chlorinated solvents for 8 hours, several for up to 30 days | TCE, PCE, DCE, 111-TCA, chloroform, 12-DCA, cis-12-DCE, trans-12-DCE, 11-DCA | TCE, PCE, 111-TCA | TCE, PCE and most breakdown products | TCE, PCE and most breakdown products |

Approximate costs: \$ ≤\$50, \$\$ = \$50 to \$100, \$\$\$ ≥\$100.

^b Normalized to a 7-day period for diffusive samplers.

Given the wide range of sampling durations required for this project, several diffusive sampler configurations are recommended to meet anticipated project objectives for indoor air measurements. For short-term samples (less than 7 days), the sampler must have sufficient sensitivity to measure the low VOC concentrations that are expected in the indoor air. Thermally desorbable sorbents paired with a badge or radial-style geometry can be used effectively for the 24-hour samples and yield low reporting limits. The badge style is recommended over the radial style given the larger number of chlorinated compounds for which sampling rates have been generated and validated. For durations of greater than 7 days, stronger sorbents with higher adsorptive capacity are recommended, which require solvent extraction. Although the solvent extraction is less sensitive than thermal desorption, the high sampling rate of the radial sampler geometry over durations of 7 to 30 days will result in sample reporting limits essentially equivalent to or lower than those generated using the thermal desorption technique.

Very few studies have evaluated VOC measurements using diffusive samplers beyond 30 days, and determining if this is possible is one objective of this study. The sorbent selection, the sampler geometry, and the target chemical's volatility all may have a significant impact on the successful application of diffusive samplers to extended deployment periods. The few published studies evaluating sampling intervals greater than 30 days are largely focused on measuring BTEX (Bertoni et al., 2001; Brown and Crump, 1993), and the stability of chlorinated compounds on sorbents in the presence of humidity and the variability of the sampling rate past 30 days are not well understood for any of the diffusive samplers under consideration for this study.

Given the previous studies discussed above and the existence of standard methods for this application in Europe, the 1- and 2-week Radiello passive samplers for VOCs are considered sufficiently accurate and precise to be the primary VOC measurement tool in this project and are used as a basis of comparison for longer duration samples.

Results from our previous report on studies of this house (U.S. EPA, 2012a) led to these conclusions regarding the performance of the solvent extracted radial style charcoal passive sampler:

- Excellent agreement was observed between numerical averages of successive 7-day exposure samples with the results of single passive samplers exposed for 14 days (almost always within +/- 30%) for all compounds despite dramatic temporal variability. This suggests uniform uptake rates for these time periods.
- PCE, benzene, hexane, and toluene performed well for 28 days.
- PCE and toluene performed well for 91, 182, and 364 days.
- Temporal variability is substantial and for certain compounds passive samplers allow cost-effective acquisition of long-term average concentration data.
- Compound vapor pressure correlates with the relative performance of different compounds with the passive samplers. Method accuracy over different durations increases with increasing vapor pressure because of better sorbent retention of the VOC.

2.2 Objectives

The overall goal of this project was to investigate distributional changes in VOC and radon concentrations in the indoor air, slab, and subsurface soil gas of a residential building from an underground (groundwater or vadose zone) source adjacent to the residence. The time frame of this study was more than 2 years in order to evaluate the effects due to seasonal variations on radon and VOC vapor intrusion. This report describes the second phase of this project, with the first phase described in U.S. EPA (2012a). Several objectives that were established for the initial, first phase research effort were continued in this study:

10. Identify seasonal fluxes in radon and VOC concentrations as they relate to a typical use of HVAC in the building.
11. Establish relationship between slab/subsurface soil gas and indoor air concentrations of VOCs and radon.
12. Determine the relationship of radon to VOC concentrations in, around, and underneath the building.
13. Characterize the near-building environment sufficiently to explain the observed variation of VOCs and radon in indoor air.
14. Determine whether the observed changes in indoor air concentration of volatile organics of interest can be mechanistically attributed to changes in vapor intrusion.
15. Evaluate the extent to which groundwater concentrations and/or vadose zone sources control soil gas and indoor air VOC concentrations at this site.

In October 2012, we critically evaluated our progress against these objectives, assessed the additional information that could be gained from further study, and used that assessment to define the objectives of this study. **Table 2-2** provides additional detail on the objective statements continued from the previous project. Data quality objectives for these objectives can be found in U.S. EPA (2012a).

Table 2-2. Continuing Project Objectives Addressed in this Document

| Original Statement of Objective | Current/Ongoing Status |
|--|--|
| Determine relationship of radon to VOC concentrations. | This study continued to address how radon relates to VOC vapor intrusion, including statistical analysis of correlations. The relative effect of SSD mitigation on radon and VOC concentrations and attenuation factors was also addressed. |
| Establish relationship between slab/subsurface soil gas and indoor air concentrations of VOCs and radon. | Soil gas and indoor air concentrations are compared graphically in a similar fashion as the previous project. In general, soil gas concentrations continue to increase with depth and appear to drive indoor air concentrations. |
| Identify any seasonal fluxes in radon and VOC concentrations as they relate to a typical use of HVAC in the building. | Although the previous report adequately addressed this objective, it left unexplained why the relationship between stack effect driving force and indoor concentration appears to be nonlinear. This study examined the interactions of multiple meteorological factors. In this study we also investigated how the HVAC and the SSD mitigation system interact to influence vapor intrusion processes |
| Determine if observed changes in indoor air concentration of volatile organics of interest are mechanistically attributable to changes in vapor intrusion. | The current study looked at both preferential flow pathways using helium tracer and geophysical tests. We also looked at the effects of a frozen soil capping event and conducted a more detailed time series analysis of how meteorological and building factors (such as differential pressures) interact to influence vapor intrusion. |
| Characterize the near-building environment sufficiently to allow future 3D modeling of this site. | Helium tracer tests, groundwater level monitoring, and a geophysical investigation were conducted to provide a better understanding of the near-building subsurface conditions. |
| Evaluate the extent to which groundwater concentrations control soil gas concentrations at this site and thus indoor air concentrations (as distinguished from vadose zone sources). | Previous work established that soil gas concentrations of both chloroform and PCE peak just above the water table. PCE groundwater concentrations measured continued to correlate well with deep soil gas, but although analytical improvements (lower detection limits) enabled chloroform to be detected in groundwater, current concentrations were too low to drive the measured soil gas chloroform concentrations. |

(continued)

Table 2-2. Continuing Project Objectives Addressed in this Document (cont.)

| Original Statement of Objective | Current/Ongoing Status |
|--|--|
| Collect additional data to evaluate the possibility of a “capping” effect from snow and ice cover. | A colder 2012/2013 winter allowed us to collect the additional data on the capping effect. We showed that both snow/ice cover and snowfall events without accumulation appear to affect vapor intrusion. |
| Evaluate the ability of a low-cost (\$129) consumer-grade radon detector provide a continuous indication of soil gas entry into the structure. | Continued testing during SSD system installation and manipulation to test the commercial radon detector under varying radon levels, and confirm good performance at and below 4 pCi/L and good utility overall in spite of a high bias at higher radon concentrations. |

The following additional studies were undertaken with new objectives developed for this report:

- Better define the particular subsurface conditions that influence the movement of VOCs and radon into this home. Conditions investigated include differences in vadose zone air permeability beneath and immediately adjacent to the structure; definition of entry routes for soil gas into the building envelope; the degree to which utility corridors function as preferential transport pathways, either through the vadose zone or through the building envelope; and how the structure of the foundation may subdivide the subslab air space.
- Design, install, and monitor a mitigation system based on the predominant vapor intrusion mitigation technology—SSD—with the objective of determining how efficiently SSD works for mitigating radon and VOCs in this particular well-studied case. We monitored VOCs and radon from the SSD system exhaust pipe along with flow with the objectives to calculate flux through the system and to determine if this flux can be usefully correlated with indoor VOC and radon concentrations.
- Capture an additional winter snow/ice capping event to monitor its influence on vapor movement into the home with an SSD mitigation system installed.

Characteristics of the experimental design and data quality objectives developed to meet these objectives are described below.

2.2.1 Time Scale and Measurement of Independent and Dependent Variables

In our overall study design, we used weekly measurements to observe our dependent variable—indoor air concentration. We expected the indoor air concentration to be dependent on the flux from vapor intrusion from soil gas. Our dependent variable is thus controlled by a series of independent variables with different time cycles that affect the vapor intrusion process, including air temperature, barometric pressure, wind, soil moisture, soil temperature, groundwater level, and HVAC operation.

In the course of this study we monitored or measured most of these independent variables or their surrogates and different frequencies balancing on the general desire for continuous measurements against logistic considerations. **Table 2-3** was prepared to consider these time-scale issues and the implications they may have for our test matrix. Figures in Nazaroff and Nero (1988) show examples of how such independent variables controlled indoor radon concentrations in previous studies.

2.2.2 Data Quality Objectives and Criteria

Table 2-4 summarizes the data quality objectives and criteria for the new elements of this project. Each objective is expressed first qualitatively and then each objective is expressed in quantitative and statistical terms where possible. The measurements that were used to achieve each objective are also listed. More details on the specific test methods used are provided in Section 3 of this report. Specific sampling and

analytical data quality objectives can be found in the quality assurance/quality control section of this report (Section 4).

Table 2-3. Factors Causing Temporal Change in Vapor Intrusion and How They are Observed and Measured

| Independent Variables/ Causes of Variability | Expected Time Cycle | Indoor VOC & Soil Gas Measurement Intervals Available to Observe at these Time Scales | Measurements of Independent Variables Available |
|--|--|---|--|
| HVAC system on/off | <ul style="list-style-type: none"> ▪ 10 min–1 hour | The influence of the HVAC system in general was observed on a scale of days and weeks by comparing sides of the duplex and periods of “on” and “off” for AC units. Although the individual cycles of the forced air heating system were not visible in measurements taken over a 24 hours or longer time scale or even in the 2-hour online GC data, the cumulative impact of heating system “on” and “off” over exposure periods of weeks to was relevant. | Measurement with data logger was planned every 5 minutes within heating season. |
| Diurnal temperature/ wind (night/day) | <ul style="list-style-type: none"> ▪ 24 hour | Measurements with the online GC and continuous radon instruments have sufficient time resolution on the scale of hours to observe this. | Weather station: at least one data point per hour. |
| Barometric pumping from weather fronts | <ul style="list-style-type: none"> ▪ 2–3 days typical | Weekly, except for daily samples and continuous measurements during intensive sampling events. | Weather station: ambient pressure logging with at least one data point per hour. |
| Water table fluctuations | <ul style="list-style-type: none"> ▪ Barometric pressure: 2–3 days ▪ Rain events: irregular ▪ Seasonal climate: monthly ▪ Surface water level: hours | Weekly and monthly integrated indoor air samples. Measurements with the continuous radon and on-site GC instruments have time resolution on the scale of minutes to hours. | Monthly water-level measurements; supplemented beginning in fall 2012 with real-time data logger at one station on site; strong correlation of gauge height and groundwater level enabled hind casting of groundwater levels for entire project. |
| Soil and groundwater temperature change | <ul style="list-style-type: none"> ▪ Annual/ seasonal | Weekly, biweekly, and quarterly samples of indoor air and soil gas. | Soil temperature logging with thermocouples: one or more points per hour. Groundwater temperature monthly during sampling. |
| Vadose zone moisture change | <ul style="list-style-type: none"> ▪ Seasonal major rain events? | Weekly samples of indoor air and soil gas. Measurements with the online GC and continuous radon instruments have time resolution on the scale of hours. | Once per hour at five depths. |
| Stack-effect, heating vs. cooling season | <ul style="list-style-type: none"> ▪ Daily and seasonal | Weekly samples of indoor air and soil gas. Measurements with the online GC and continuous radon instruments have time resolution on the scale of hours. | Differential pressures, indoor temperatures: 15-minute rolling average. |

Table 2-4. Data Quality Objectives and Criteria

| Task Order Objective | Study Purpose/Objectives | Study Questions | Measurement Used To Support Study Questions | Measurement Performance or Acceptance Criteria |
|--|--|--|---|---|
| Determine subsurface effects on building envelop | Better define the particular subsurface conditions that influence the movement of VOCs and radon into this home. | What is the nature of the subsurface environment—fine features of the stratigraphic environment that influence contaminant transport? | Geophysical techniques, including ground penetrating radar (GPR), electromagnetic resistivity (EM), electrical resistivity (ER), vacuum testing, and subsurface tracer testing (to be addressed in a separate geophysical report) | Geophysical data to be acquired from multiple transects within each third of the basement. Vacuum testing from at least two extraction points. At least two helium tracer injections with monitoring on 1-hour frequency at five or more locations. Continue data analysis of soil gas information to provide data for a three-dimensional picture of radon and VOC concentration changes at different locations over time to discern seasonal patterns, whether caused by temperature or water level. Observe effect of on/off cycles of the SSD system on contaminant movement. (NOTE: analytical data quality objectives are defined in Section 4) |
| | Determine the effects of utility corridors on subsurface movements of VOCs and radon. | How do the house foundation features and utility corridors affect subsurface movements of VOCs and radon? | Active and passive sampling methods. Geophysical measurements (GPR) (to be addressed in future reports). | |
| Determine effect of SSD mitigation on VOC and radon levels | Install and monitor an SSD mitigation system for VOCs and radon. | How efficiently does the SSD system work at this particular location? | Active and passive VOC and radon sampling of both the subslab environment and the stack with the SSD system on and off in 1-week intervals. Indoor air VOC and radon data, differential pressure data (differential pressure to be addressed in a future report). | At least three on/off cycles of the SSD system. One 6-week period of on-site GC operation for soil gas, indoor air, and ambient VOC levels. Continuous indoor air radon measurements during entire test period. Weekly VOC and radon measurements during entire test period. Weekly radon and VOC grab samples from soil gas ports (subslab and deeper). Continuous Setra differential pressure measurements (NOTE: analytical data quality objectives are defined in Section 4) |
| | | Can a relationship be established between the flux of VOC/radon exhausted from the stack and the effectiveness of the system in reducing indoor air concentrations? | | |
| | | What is the differential pressure required to counter the observed substantial seasonal variability in VOC concentrations? | | |
| | | Does the effect of the SSD system reduce the variable component of the vapor intrusion driving force (in addition to changing the average differential pressure)? ^a | | |

(continued)

Table 2-4. Data Quality Objectives and Criteria (cont.)

| Task Order Objective | Study Purpose/Objectives | Study Questions | Measurement Used To Support Study Questions | Measurement Performance or Acceptance Criteria (for this question/# of data points anticipated) |
|---|---|---|--|---|
| Determine the effect of a winter ice cap on vapor intrusion | Capture a winter ice capping event and monitor its influence on vapor movement into the home. | Does a winter ice capping event or heavy snowfall affect VOC and radon concentrations? | Active and passive sampling in an intensive mode. Reports of snow cover made during week days by ARCADIS on-site personnel. We supplemented these observations with publically available information from the National Climatic Data Center/National Weather Service for the Indianapolis International Airport http://www.ncdc.noaa.gov/snow-and-ice/dly-data.php . | Multiple snow and ice events (as observed in the winter of 2012/2013); Statistical data analyses (also performed for previous winters). 8 weeks of online GC for VOCs Continuous AlphaGUARD data for radon Maintain index of snow cover for the long-term analysis of the indoor air data set. (NOTE: analytical data quality objectives are defined in Section 4) |
| | | If so, through what mechanism does the winter event affect concentrations (increase in subslab concentration? effects on stack effect induced pressure field?)? | | |
| | | Can an effect of snow/ice cover outside the residence be discerned that is separate from the effect of temperature? | | |

Table of Contents

| | | |
|-------|---|------|
| 3.0 | Methods..... | 3-1 |
| 3.1 | Site Description | 3-1 |
| 3.1.1 | Area Geology/Hydrogeology..... | 3-1 |
| 3.1.2 | Area Potential Sources..... | 3-1 |
| 3.1.3 | Building Description..... | 3-7 |
| | 3.1.3.1 Building Age, Condition, and HVAC..... | 3-7 |
| | 3.1.3.2 Building Utilities/Potential Entry Points..... | 3-8 |
| 3.1.4 | Building Occupancy During Sampling..... | 3-9 |
| 3.1.5 | Investigation History..... | 3-9 |
| 3.2 | Evolution of Conceptual Site Model | 3-10 |
| 3.2.1 | Prior to 2011–2012 Investigations | 3-10 |
| 3.2.2 | After 2011–2012 Investigations (U.S. EPA, 2012a)..... | 3-10 |
| 3.2.3 | Refinements in Conceptual Site Model Sought in this 2012–2013 Study | 3-11 |
| 3.3 | Building Renovation and Mitigation..... | 3-12 |
| 3.3.1 | Subslab Depressurization Mitigation System Installation | 3-12 |
| 3.4 | Monitoring, Sampling, and Analysis..... | 3-17 |
| 3.4.1 | Indoor and Outdoor Air VOC Monitoring..... | 3-17 |
| 3.4.2 | Subslab and Soil Gas (TO-17)..... | 3-23 |
| 3.4.3 | Online Gas Chromatograph | 3-22 |
| 3.4.4 | Groundwater | 3-23 |
| 3.4.5 | Subslab Depressurization System Stack Gas Sampling..... | 3-24 |
| 3.5 | Radon Sampling and Analysis | 3-24 |
| 3.5.1 | Indoor Air Radon Sampling and Analysis | 3-24 |
| 3.5.2 | Subslab and Soil Gas Radon Sampling and Analysis..... | 3-25 |
| 3.5.3 | Continuous (Real-Time) Indoor Air Radon Sampling and Analysis..... | 3-26 |
| 3.6 | Physical Parameters Monitoring | 3-26 |
| 3.6.1 | On-Site Weather Station | 3-26 |
| 3.6.2 | Indoor Temperature | 3-28 |
| 3.6.3 | Soil Temperature..... | 3-28 |
| 3.6.4 | Soil Moisture..... | 3-28 |
| 3.6.5 | Potentiometric Surface/Water Levels | 3-29 |
| 3.6.6 | Differential Pressure | 3-29 |
| 3.6.7 | Air Exchange Rate | 3-30 |
| 3.6.8 | Crack Monitoring..... | 3-30 |
| 3.7 | Data Aggregation Methods | 3-31 |

List of Figures

| | | |
|------|--|-----|
| 3-1. | Lithological fence diagram showing the major soil types beneath the 422/420 house..... | 3-4 |
|------|--|-----|

| | | |
|-------|--|------|
| 3-2. | Aerial view of duplex, 420/422 East 28th Street, showing nearby sanitary and storm sewers..... | 3-5 |
| 3-3. | East side of house (on right) and adjoining commercial quadraplex visible (left). | 3-6 |
| 3-4. | Roof of adjacent commercial quadraplex. | 3-6 |
| 3-5. | Looking toward southeast corner of adjacent commercial quadraplex..... | 3-7 |
| 3-6. | Visual evidence of historic dry cleaners in area. | 3-8 |
| 3-7. | Front view of house during summer 2011 sampling, with fan testing and weather station..... | 3-9 |
| 3-8. | Front view of duplex under winter conditions showing designation of sides and HVAC setup..... | 3-10 |
| 3-9. | 422 (left) and 420 East 28th Street in January 2011. | 3-11 |
| 3-10. | Map view of the 422-side basement showing SSD mitigation system legs, subslab soil gas extraction pits (red circles), and the position of the passive “sampling racks.” Horizontal divisions are walls between “north” (top in figure), “central,” and “south” (bottom in figure) sections of basement with open walkways between (cistern is in the central basement). | 3-14 |
| 3-11. | Map view of the 420-side basement showing the SSD mitigation system legs, subslab soil gas extraction pits (red circles), and the passive “sampling racks.” Horizontal divisions are walls between “north” (top in figure), “central,” and “south” (bottom in figure) sections of basement with open walkways between (cistern is in the central basement). | 3-15 |
| 3-12. | Photos of mitigation system: (left) SSD blower and stack on northeast corner of duplex; right) SSD extraction point, showing valve and U-tube manometer. | 3-16 |
| 3-13. | Cross-section showing the general layout of the 422/420 north and central basements with the positioning of the extraction legs, exterior blower, and exhaust stack. | 3-17 |
| 3-14. | Subsurface soil gas monitoring probes (SGP), subslab sampling ports (SSP), and groundwater monitoring wells (MW). Horizontal divisions are walls between “north,” “central,” and “south” sections of basement with open walkways between (cisterns are in the central basements). Probes/ports in red were sampled by the on-site GC. Soil temperature and moisture probes were installed in the 422 basement between SGP 8 and MW 3 and in the backyard to the north of MW 2..... | 3-18 |
| 3-15. | Passive indoor air sampling rack: 422 first floor. | 3-20 |
| 3-16. | Ambient sampler shelters on telephone pole near duplex..... | 3-21 |
| 3-17. | Monitoring well MW-3, installed in the basement and completed on the first floor. | 3-24 |
| 3-18. | Front view of 420/422 duplex with location of weather station sensors indicated with red arrow. | 3-27 |
| 3-19. | Calibrated crack monitor..... | 3-30 |

List of Tables

| | | |
|------|--|------|
| 3-1. | Pressure Readings Taken During Extraction Point Testing..... | 3-13 |
| 3-2. | Data Aggregation Applied to Predictor Variables | 3-31 |

3.0 Methods

3.1 Site Description

The test house is a vacant residential duplex at 420/422 East 28th Street in the Mapleton Fall Creek neighborhood of Indianapolis. This area of Indianapolis was initially a farming settlement known as Mapleton founded in the 1840s. The primary residential development in this area occurred in the late 1800s and early 1900s. Commercial development on the immediate cross street, Central Avenue, began in the 1920s.

3.1.1 Area Geology/Hydrogeology

Several soil borings were advanced in the area immediately surrounding the house, during monitoring well (MW) construction and soil gas port installation. SGP-1A, SGP-1B, and SGP-1C, as well as MW-1A and MW-1B, were installed April 29, 2010. All additional soil gas ports and MWs on the exterior of the house were installed between August 30 and September 1, 2010. Soil gas ports and MW-3 located below the footprint of the house were installed in September 2010. 3-D visualizations of subsurface lithology are presented in **Figure 3-1**. Boring logs are included in **Appendix A**.

In the southern portion of the property, topsoil extends down to about 0.5 to 1 ft. Beneath the topsoil is found sand or silt mixed with cinders, coal fragments, or ash to about 1.5 ft. Then to between 5 and 6 ft is silt or silty sand with varying amounts of clay. Some trace gravels start at about 7 ft, and underlying that layer are sands and gravels to between 15 and 16 ft. beneath that sand and gravel is generally sand.

To the east side of the property, at the surface are soils with a visibly high organic content and gravel or a concrete sidewalk. Underlying that from 1 to 3 ft is sand or clayey sand, with some gravel and coal fragments in some borings. Beneath that layer down to 7 ft is predominantly clay with some sand or silt. Underlying that is sand with some clay and gravel down to about 12 to 14 ft. Down to 16.25 ft is sand, with gravel added down to 16.5 ft.

To the north side of the property, the first foot is fill, sand, and gravel. Beneath that to 3 ft is brick, with sand and weathered brick to 3.5 ft. The brick constituent in this location is possibly a remnant of a former exterior basement stairwell. To 6.25 ft is silty, sandy clay. Down to 8 ft is sand, with sand, gravel, and some clay down to 12 ft. From 12 to 16 ft is sand.

On the west side of the property, the first half-foot beneath the surface is the concrete sidewalk. Underlying that to 1.25 ft is fill, cinders, and gravel. Down to 6.75 ft is silty, sandy clay with trace gravel. The layer beneath that to 15.5 ft is sand and gravel with some clay followed by sand to the end of the boring at 16.5 ft. See Section 6.1 for additional information on site soils.

In the top figure, the view is toward the north from the street in front of the house. The bottom figure shows a view toward the south from the backyard. The empty white area at the top of the soil figure represents the house's basement. In the immediate vicinity of the house, silt and clay (brown) are present until 7.5 to 8 ft below land surface. After that, sand and gravel (burnt orange) alternate with layers of sand (orange).

3.1.2 Area Potential Sources

The site location, as illustrated in **Figure 3-2**, is bounded to the north by 29th St., to the west by N. New Jersey St., and to the east by Central Avenue. There is a river, Fall Creek, approximately 300 ft to the

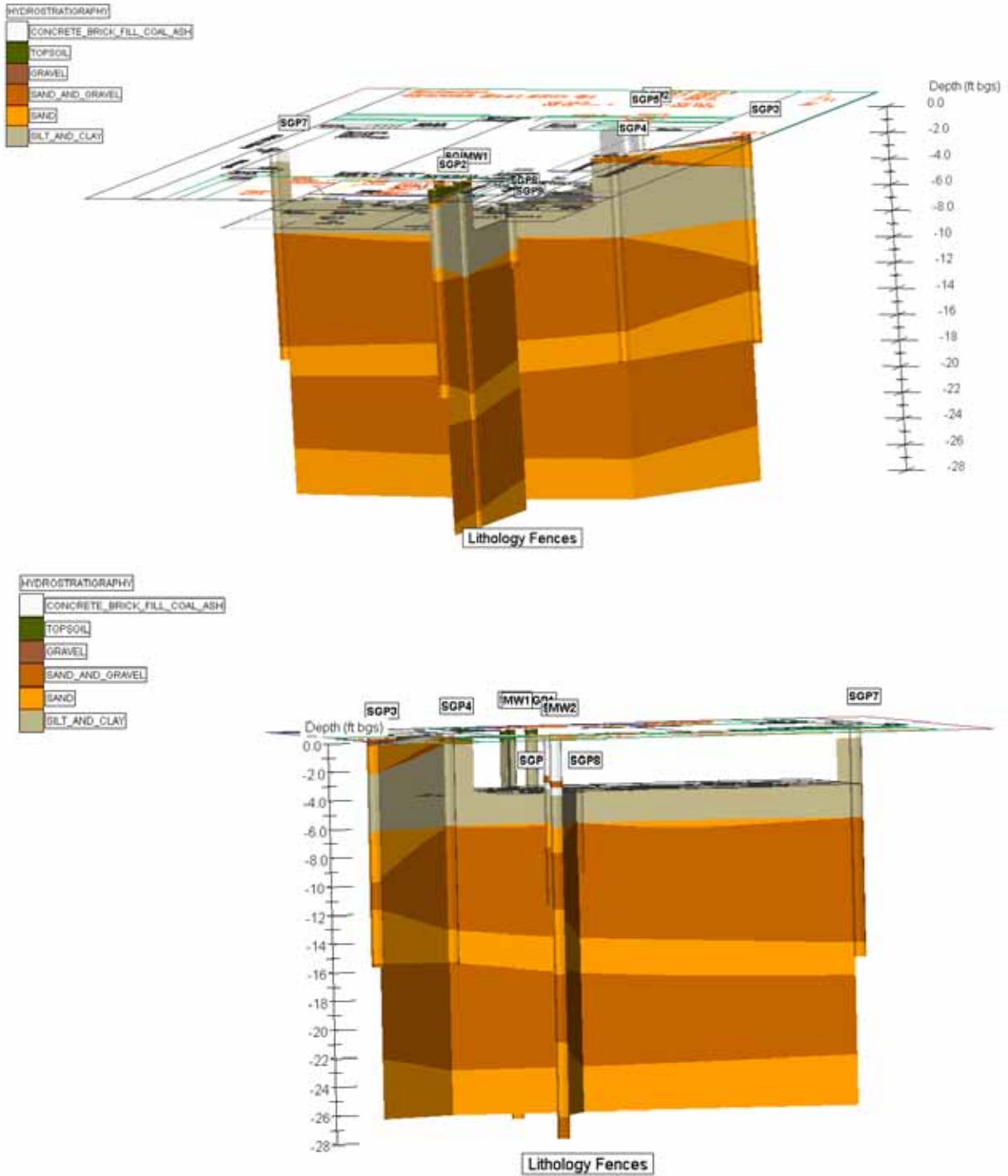


Figure 3-1. Lithological fence diagram showing the major soil types beneath the 422/420 house.

south of the site toward which groundwater flow generally trends. Across the street south of the site, there is a parking lot and to the east there is an open field. Across an alley to the west of the site, there is an open lot with a grassy area and a paved parking lot. Adjacent to the north side of the site there are backyards of the residential buildings along Central Avenue.

420 E. 28th St, Indianapolis, IN

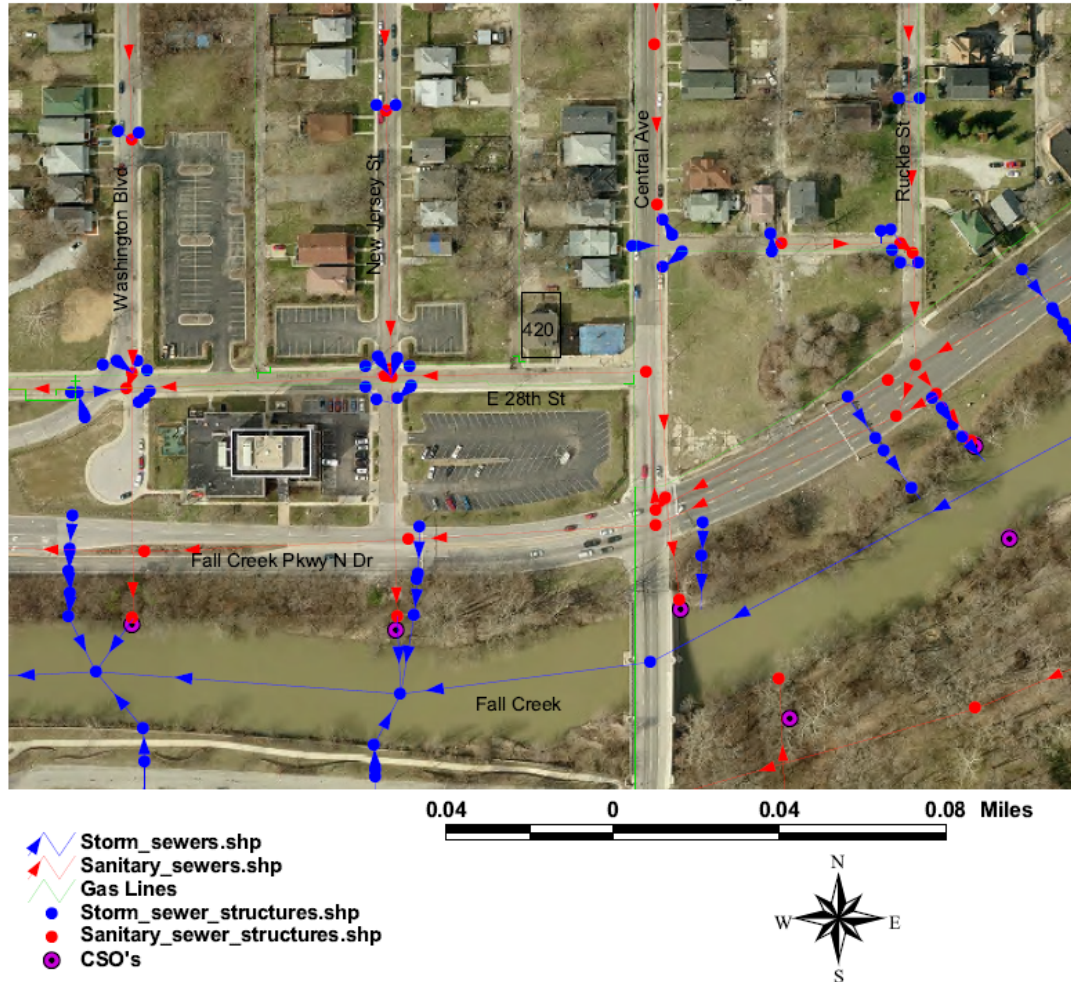


Figure 3-2. Aerial view of duplex, 420/422 East 28th Street, showing nearby sanitary and storm sewers.

Immediately adjacent to the studied duplex (approximately 10 ft east) lies a small commercial/residential quadraplex (**Figures 3-3, 3-4, and 3-5**) with a diverse, primarily commercial history dating back to 1930. The four portions of the building are numbered as 424 East 28th Street, 426 East 28th Street, 2802 Central Avenue, and 2804 Central Avenue.

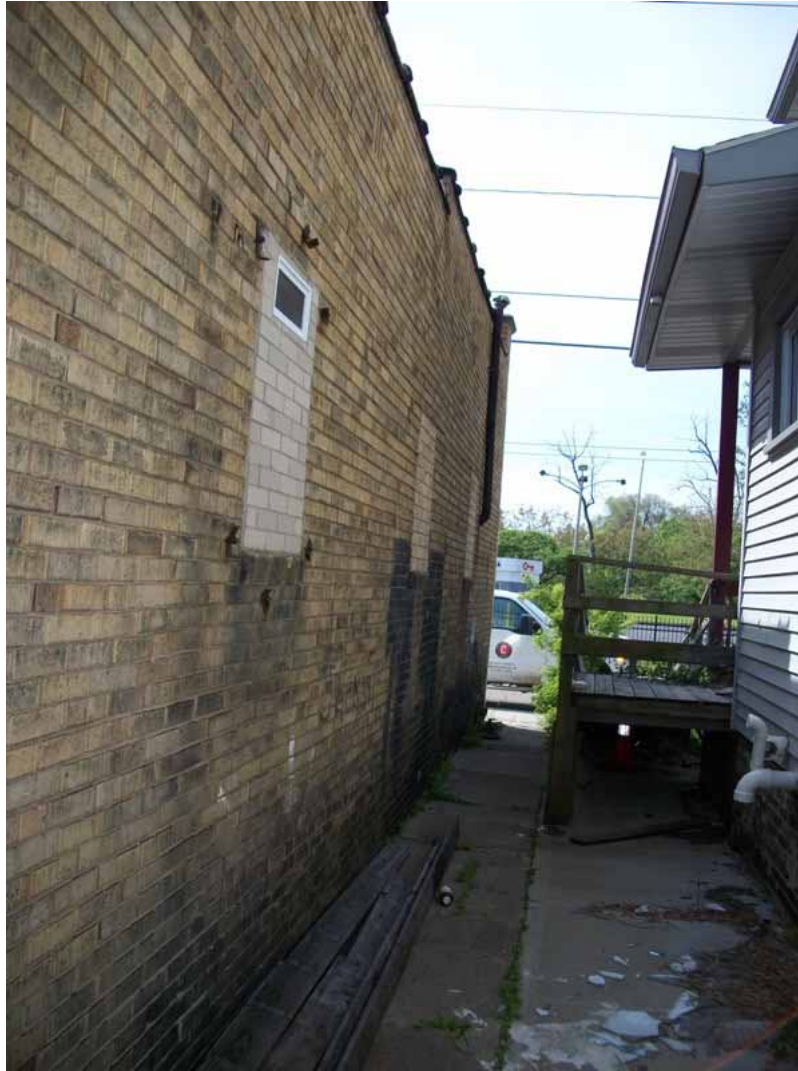


Figure 3-3. East side of house (on right) and adjoining commercial quadraplex visible (left).



Figure 3-4. Roof of adjacent commercial quadraplex.

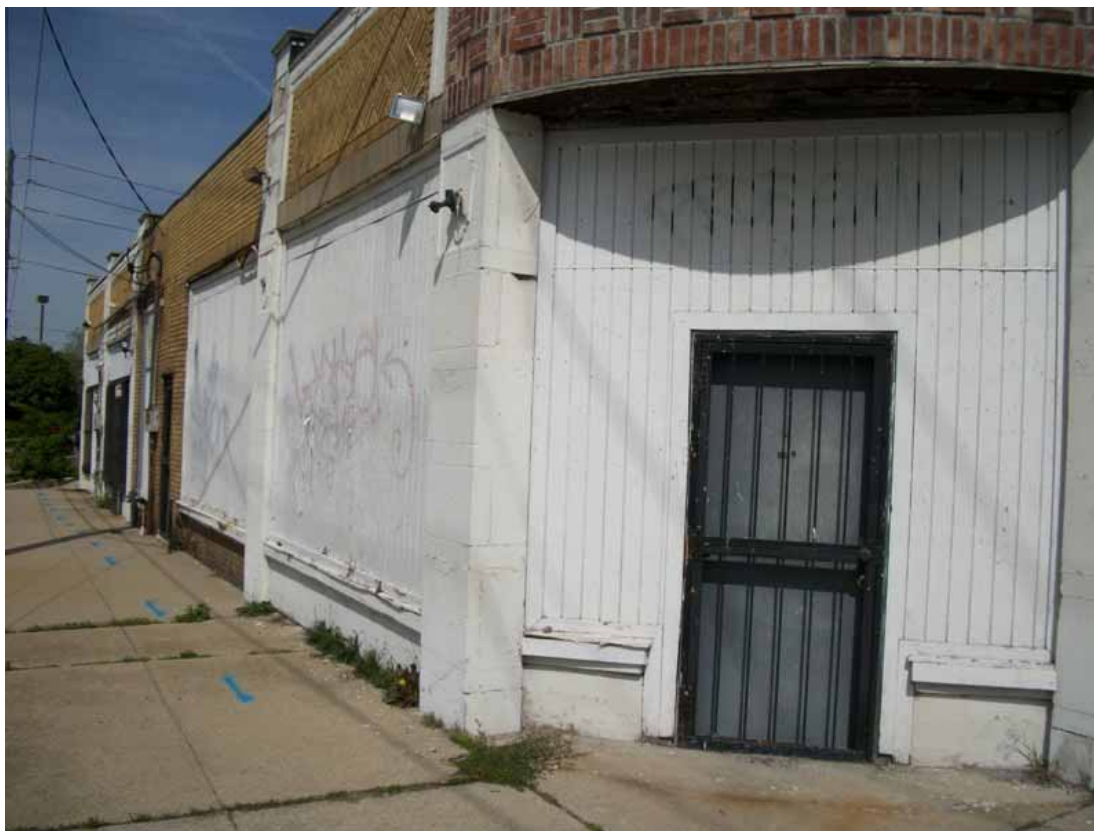


Figure 3-5. Looking toward southeast corner of adjacent commercial quadrangle.

Among the historic uses of parts of that building were a pharmacy, beauty supply, radio shop, fur store, and detector companies. Regarding most of the businesses that occupied that space, only their name is currently known, and those names do not match any businesses with a current local or Internet presence. Thus, chemical uses, though probable, are not documented. The back part of the adjacent building at 2804 Central Ave has historically been occupied by “Wolf Fur Co.” Later in 1954, the same location was occupied by the “Avideo Detectors Telaveta.” In 1930 it was occupied by Gould & Schildmoler ENEN and Home Radio Co. The records for the adjacent buildings (424 to 428 East 28th Street and 2802 to 2804 Central Avenue) show a number of drug store and beauty shop uses. There are substantial gaps in the records for these properties, and there seems to be little or nothing reported about what was occupying these locations between 1970 and 2000.

There were 9 to 10 historic laundry cleaners located less than a quarter of a mile to the north of the 422/420 house, and one was a quarter of a mile to the west (**Figure 3-6**). These were listed as hand and steam laundries, pressers, and driers. The most recent laundry was present in 1970 (EDR Radius Map, June 15, 2010). In the fall of 2010, we observed Mapleton/Fall Creek Development Corporation (MFCDC) staff excavating an underground storage tank that appeared to contain product at a dry cleaners several blocks upgradient from the house.

There were three historic gas stations or auto service and repair shops within a quarter of a mile to the north as well. The most recent auto repair shop was present in 1990 (EDR Radius Map, June 15, 2010).



Figure 3-6. Visual evidence of historic dry cleaners in area.

The property southwest of the intersection of East 28th and Central Avenue was historically mildly impacted with petroleum hydrocarbons and managed as a brownfield named “Mapleton-Fall Creek Site” or “Fall Creek Central Project.” This site was closed after tank and soil removal. One round of VOC groundwater data was acquired at that location that showed detectable chloroform at 8.9 to 22.1 $\mu\text{g/L}$ in a June 2005 sampling event. These previous studies showed that the study area has sand and gravel geology from approximately 7 to 25 ft below land surface (bls) and groundwater at approximately at 16 ft bls. The upper 7 ft of the stratigraphy is heterogeneous, variously described as including fill materials, loam, and silty and moist sandy clay.

Based on the general topography of the area and professional experience in this portion of Indianapolis, groundwater is thought to flow from the north of the 422/420 house south of the house to Fall Creek. Thus, many of the historic laundries or auto shops that are potential contaminant sources are generally upgradient of the study house.

The 422/420 house is located between Central Avenue and its associated alleyway on 28th Street. The immediate area receives a moderate amount of traffic, but the Central Avenue/Fall Creek Parkway intersection is very busy throughout most of the day. This could be a contributing factor to petroleum-based contaminants in surface soils and ambient air.

3.1.3 Building Description

3.1.3.1 Building Age, Condition, and HVAC

The tested house located at 422/420 East 28th Street, Indianapolis, IN (**Figure 3-7**) is an early twentieth century duplex, dating from before 1915 because it is present on the 1915 Sanborn map of the area. Based on the mirrored floor plans of the two sides, it is likely that the house was always a duplex. Construction is wood frame on a brick foundation with a poured concrete basement floor. Interior floor materials include tile, carpet, and wood flooring.



Figure 3-7. Front view of house during summer 2011 sampling, with fan testing and weather station.

The duplex at 422/420 was initially abandoned and is now owned by MFCDC in Indianapolis. Before our involvement, the house had been vandalized and stripped of all valuable metals and fixtures (e.g., copper wiring and tubing, most plumbing fixtures, many outlets) and destroyed the previous HVAC unit.

A staff member from the Indianapolis ARCADIS office acquired the use of the house for the duration of the project through the generosity of the MFCDC. A small rent is now being paid by ARCADIS to MFCDC for use of the house for this study.

Power was restored to the house in September 2010. A gas-fired forced air HVAC unit was installed on the 422 side in October 2010 by Edwards Electric and Mechanical for use in this project (**Figure 3-8**). The house had no air conditioning (AC) system, and we chose to install window-mounted units, which would have been the likely type used by any tenants in this house.



Figure 3-8. Front view of duplex under winter conditions showing designation of sides and HVAC setup.

There are internal and external visual clues indicating (**Figure 3-9**) the house has been updated several times. For example, visual clues suggest that a previous HVAC unit had been installed that was not native to the house's original construction. In the basement, there is evidence of former coal chutes (possibly) and cisterns on both the 420 and 422 sides. The probable coal chutes and old windows had been blocked by cinder blocks before ARCADIS occupancy. The cisterns had also been cemented over. Comments made by electricians in the basement suggest that at one time the house had been heated by an old style furnace, indicated by cemented-over holes in the walls, but that it had been gone for some time.

3.1.3.2 Building Utilities/Potential Entry Points

The electric lines connect to the house at the northwest corner of the 420 side. Since all original wiring native to the house had been removed by vandals before the project, we had to have the junction box rewired to the city electrical line and run new lines within the house to new outlets at designated points. The gas line connects only to the furnace from an access line in the south wall of the 422 side. Both the electrical lines and the gas line were emplaced by Edwards Electrical and Mechanical during the furnace installation and enter the house at the original entry points for each utility.

Sanitary sewer lines run immediately south of the house along East 28th Street. Sanitary and combined sewer lines run less than one block east and west of the house along Central Avenue and New Jersey Street (see previous **Figure 3-2**). There is a sewer lateral running beneath the basement floor along the length of the 422 side from north to south that was buried and cemented over sometime after the floor's original construction. PVC drain lines join this lateral from the plumbing on both sides of the duplex. The HVAC unit drains condensation into a floor grill leading to the lateral. A nonfunctional water line enters the house from the south. Large, cinder-blocked portions of the north interior basement walls of both sides of the duplex along with brick strata in borings have been observed. We interpret these to be vestigial entranceways to the basement from a time when the basement was accessed from the back yard, rather than from an interior basement door.



Figure 3-9. 422 (left) and 420 East 28th Street in January 2011.

3.1.4 Building Occupancy During Sampling

The initial concept for the 422/420 house was to create an environment free from lifestyle-related indoor air sources, but operated as though the space were occupied in order to simulate a residential environment free from indoor VOC sources. The 422/420 house was borrowed (and is now rented) from MFCDC that owns the property. The house was an ideal location for this study because even though it is an older residence typical of this area of Indianapolis, it had no occupants, was not subject to any use beyond the project, was in a good location and price range, and had vapor intrusion present. Because the house was unoccupied and in poor condition, we could set up ports, wells, and sensors for observations and install a mitigation system without having to consider the occupants' comfort or convenience.

To more closely approach a living environment, a field scientist worked on site for several months before sampling began. During most normal work weeks during the periods of active VOC sampling, the field scientist was at the house at least 4 days per week. During the down times between VOC sampling efforts (such as April to September 2012), visits to the house were less frequent. The intent during VOC sampling periods was to have an individual who would open doors and windows, move through the environment, and make temperature adjustments similar to the way a homeowner would. The constant close proximity of the worker to the work zone also allowed for quick responses to environmental changes and any issues with the sampling devices. A second floor bedroom on the 422 side of the duplex was minimally modified and used as an office for the sampling staff member.

3.1.5 Investigation History

The selection and screening of this duplex was conducted in April to June 2010 as described in the first report on this series of projects (U.S. EPA, 2012a). That report describes the design and results of an

extensive 14-month soil gas, groundwater, and indoor air sampling program conducted from December 2010 to March 2012. This report covers VOC and radon samples taken after that date, prior to and after the October 2012 installation of an SSD mitigation system, and until May 2013. In many cases, the results and analysis in this report build on the results presented in U.S. EPA (2012a). This report also describes the effects of the SSD mitigation system on radon and VOC levels in the duplex and investigates the factors that influence VOC and radon levels in and under the duplex. Where sampling locations and techniques are common to both stages of the investigation, the descriptions from U.S. EPA (2012a) are repeated here.

3.2 Evolution of Conceptual Site Model

This report provides an opportunity to document how a conceptual site model can evolve through intensive study of the vapor intrusion situation surrounding a single building as one of the goals of this study. This discussion updates the conceptual site model from the previous report (U.S. EPA, 2012a). Subsequent reports in this series will make any updates to the conceptual site model that are made necessary as additional information is collected about the site.

3.2.1 Prior to 2011–2012 Investigations

During site selection, the initial conceptual site model for this structure was that a vapor intrusion source was most likely present in shallow and subslab soil gas due to historical dry cleaning facilities and adjacent commercial uses. Radon impacts were suspected because Marion County, Indiana, is in EPA's Zone 1—highest risk for radon. Detectable concentrations of chlorinated hydrocarbons were detected during initial site screening and responded to depressurization of the structure by fans (U.S. EPA, 2012a).

The source of the primary VOCs (PCE and chloroform) observed at this duplex was initially suspected to be transport of contaminants either:

- through a groundwater pathway from upgradient dry cleaners or
- released into the shallow vadose zone during the operations of the adjacent commercial quadraplex.

Later observations and discussions suggested that disinfection byproducts in city drinking water could be an additional potential source for chloroform detected in soil gas.

3.2.2 After 2011–2012 Investigations (U.S. EPA, 2012a)

The detailed 2011–2012 site investigation and monitoring work described in U.S. EPA (2012a) added the following details to our conceptual site model of this duplex and the vapor intrusion exposure pathway:

- The groundwater and nearby Fall Creek are intimately connected. The groundwater level beneath the house is subject to rapid swings of up to 5 ft over the course of a few days during seasonal flooding in the creek. There also could be connections to the combined sewers that discharge into Fall Creek.
- The stack effect caused by indoor/outdoor temperature differentials operates not only during the heating season, but also during the summer as well, due to the “solar stack effect” and the storage of heat in the building during cool late summer/fall nights. Differential pressure measurements indicate that changes in building differential pressure are reflected in a measureable advective driving force between the 13-ft depth near the water table and the 6-ft depth directly beneath the basement. Therefore, in this case, advection may be the primary cause of VOC migration through the deeper portions of the vadose zone.

- The heterogeneity of the subslab concentrations and geophysical result suggests the absence of an engineered gravel layer beneath the duplex. Thus, the subslab does not behave here as a well-mixed plenum.
- PCE is apparently widely spatially distributed in site groundwater at concentrations well below the current 5 µg/L MCL (U.S. EPA, 2012a). These shallow groundwater concentrations apparently control deep soil gas concentrations. Only a moderate degree of attenuation occurs in those deep soil concentrations as they are drawn toward the basement of the structure. Substantial attenuation occurs in the upper 6 ft of the site external soil gas, which is finer grained materials than the sandy deeper materials. It is currently unclear whether this is due to gas permeability contrasts, sorption processes, or most likely barometric pumping dilution. Substantial attenuation also occurs across the building envelope between subslab and indoor air.
- Chloroform is present in highest concentration in deep soil gas. Substantial chloroform has been historically been detected in groundwater on a site 200 ft to the southwest. Chloroform was also detected in groundwater at this house in preliminary sampling and at low levels (< 0.6 µ/L) in the spring of 2013. Studies were conducted that determined that the lack of detections in recent groundwater samples on site is not from losses in the sampling and analysis process. Chloroform attenuation in soil gas is substantial between the area just above the water table and the 6-ft depth below the structure. Chloroform is also substantially attenuated between subslab air and indoor air.
- The relative importance of the potential sources of PCE and chloroform—historic dry cleaners, historical activities in the adjacent commercial/industrial quadraplex, and leaking storm sewers/drinking water lines—is unclear.
- Sewer lines and laterals likely play some role in contaminant fate and transport in this system. Elevated concentrations of PCE and chloroform were present in the headspace of sewer gas (U.S. EPA, 2012a). As described in U.S. EPA (2012a), their role as a direct entry pathway has been minimized through plumbing trap and vent maintenance and blocking the drains in the house. Their role in lateral transport through the vadose zone and into the subslab of the duplex will be elucidated through future geotechnical studies.
- There is a strong seasonal component to the PCE and chloroform indoor concentrations (see Section 11, **Figure 11-12**). The seasonal component is partially but not completely correlated to the strength of the stack effect (Section 10, **Figures 10-10** and **10-11**).
- Concentrations of benzene, hexane, and toluene in indoor air are quite similar to ambient levels and appear to move in lockstep with ambient air, although there are some traces of benzene in soil gas (Section 11, **Figure 11-12**). TCE in indoor air also tracks ambient concentrations when TCE is low, but are very similar to the PCE plots when concentrations were high at the beginning of the study, suggesting a contribution of subsurface sources to TCE indoor air concentrations.

3.2.3 Refinements in Conceptual Site Model Sought in this 2012–2013 Study

In the Quality Assurance Project Plan (QAPP) for the current work, we defined several goals related to improving our conceptual site model based on the investigation results available at that time:

- Better define the particular subsurface conditions that influence the movement of VOCs and radon into this home. These conditions are expected to include differences in air permeability on a spatial scale of 1 to 20 ft in the vadose zone beneath and immediately adjacent to the structure.
- Better define the particular entry routes of soil gas into the building envelope. Define the degree to which utility corridors function as preferential transport pathways—either through the vadose zone or through the building envelope.

- Determine how the structure of the foundation may subdivide the subslab air space.
- Capture a winter capping event to monitor its influence on vapor movement into the home.

Uncertainty remains about the relative importance of a groundwater source. The detected concentrations in groundwater in the installed wells are able to account for the highest current deep soil gas concentrations through a Henry's law calculation for PCE within a factor of 3, but the chloroform soil gas concentrations were 12 times higher than the vapor concentrations calculated using Henry's Law of the groundwater concentrations. The highest soil gas concentrations are generally on the downgradient (SE) side of the house. However, generally the highest concentrations observed in soil gas are just above the water table. There is a large and rapid response of the potentiometric surface to rainfall, perhaps related to the presence of combined sewers and surface water bodies in the vicinity of the study duplex. There is a visual correlation between chloroform trends and changes in hydrogeology. Also, at a site 200 ft to the southeast, substantial chloroform was previously detected in groundwater (U.S. EPA, 2012a, Section 11 and Section 13.1.6).

Several hypotheses could explain these observations:

- The primary stored mass is in the deep vadose zone either sorbed to soil particles, present in soil moisture, or present as soil gas in the least permeable portions of the soils. (Others have hypothesized that vadose zone soils will retain mass for a substantial time period after an associated groundwater plume naturally attenuates).
- The primary source is affected groundwater lateral to the duplex location not observed by our monitoring wells, but perhaps suggested by prior off-site detections. The primary source is from water that is periodically transported along deep combined sewers and leaked water from those sewers percolating downward toward the water table. This might manifest in higher VOC concentrations in soil moisture in the vadose zone or in the capillary fringe than in the sampled shallowest portion of the saturated zone.

General support for the importance of these hypotheses at other sites can be found in the literature (Carr, 2011; Christ, 2010). Particularly relevant is this statement from Carr (2010): "*The common perception that VI potential is largely a function of contemporaneous groundwater quality is flawed.*"

3.3 Building Renovation and Mitigation

Details of the original building renovations were presented in U.S. EPA (2012a). Generally, the house was rewired, a heating system was installed on the 422 side of the building, window air conditions were added, and locks and a security system were installed. The primary renovation for this phase was the installation of the SSD mitigation system.

3.3.1 Subslab Depressurization Mitigation System Installation

The strategy for the SSD mitigation system installation was to select an experienced radon and VOC mitigation contractor and ask them to perform a "typical" active SSD system installation but with greater documentation and reporting for the research purpose. We also added some additional valves and sampling ports to the "typical" system to facilitate monitoring.

On October 16, 2012, Brian Schumacher and John Zimmerman of EPA were present on site with ARCADIS and our radon mitigation subcontractor Radon Environmental to oversee the installation of the SSD mitigation system under both sides of the 422/420 duplex. The initial plan for the installation planned for two extraction pits to be installed at the northern basement sections on the 422 and 420 sides

of the house. After installation, if pressures with only the two initial legs proved insufficient, two more could be installed to provide the necessary negative pressures beneath the subslab.

Prior to the drilling start time, all Radiello passive VOC sampling was stopped, the electrets were read, and SKC Ultra III badges were begun for the duration of the drilling/installation. This was to ensure potential increases in radon and VOCs could be monitored during installation or would not interfere with normal VOC monitoring for the time period.

Drilling began in the north basements at 10:00 am and used the core drill method to install the subslab suction system. A section of the concrete slab was drilled out with a core drill, and schedule 40 3 in. PVC piping was fit into the slab hole. The piping was then arranged in the basement to intersect a main line, which would lead out of the basement and connect to a fan. The fan (or blower) was a Radon Away RP 265 high-flow fan unit. The fan has an on/off switch and each extraction leg possesses a ball valve, so the whole system can be shut off or only select legs of the system can be shut off.

The initial two legs in each of the north basements were initially turned on at 16:30 on October 16, 2012. After initial pressure drop testing the project team decided that pressures were insufficient (generally < -0.04 in. WC; see **Table 3-1**) and that two additional legs would need to be installed the following day by Radon Environmental in each of the central basement areas. The full system, then consisting of four extraction legs total (**Figures 3-10** and **3-11**), was turned on at 17:20 on October 17, 2012. Additionally, sampling ports for the SSD mitigation system were drilled into the positive side of the SSD mitigation system stack (i.e., above the blower). The ports were drilled for WMS Waterloo samplers, AlphaGUARD sampling, and a port for insertion of an airfoil velocity measurement attachment for the micromanometer that was used to test the system after installation but prior to monitoring. **Figure 3-12** shows external and internal photographs of the system, and **Figure 3-13** is a cross-section diagram showing the general layout of the 422/420 north and central basements with the positioning of the extraction legs, exterior blower, and exhaust stack. Additional system photographs and details on system testing can be found in **Appendix A**.

After installation and testing, the system was operated and monitored for three on periods, two passive periods, and one fully off period. The three on periods ran from October 17, 2012, to November 14, 2012; December 12, 2012, to December 29, 2012; and February 6, 2013, to April 24, 2013. The two passive periods ran from November 14, 2012, to December 12, 2012, and from December 29, 2012, to January 16, 2013. The fully off period ran from January 16, 2013, to February 6, 2013.

Table 3-1. Pressure Readings Taken During Extraction Point Testing

| Date: 10/16/12 with two suction lines activated, one in 422 basement north, and one in 420 basement north. | |
|---|---------------------------|
| Location | Pressure Reading (in WC) |
| 1 | -0.155 |
| 2 | -0.058 |
| 3 | -0.020 |
| 4 | -0.018 |
| 5 | -0.006 |
| 6 | -0.035 |
| 7 | -0.038 |
| 8 | -0.017 |
| 9 | -0.011 |
| 10 | -0.003 |
| Date: 10/17/12 with the two in each of the north basement sections and two in each of the center basement sections. | |
| Location | Pressure Reading (in. WC) |
| 1 | -0.092 |
| 2 | -0.089 |
| 3 | -0.046 |
| 4 | -0.046 |
| 5 | -0.009 |
| 6 | -0.065 |
| 7 | -0.066 |
| 8 | -0.040 |
| 9 | -0.035 |
| 10 | -0.006 |

in. WC = inches water column

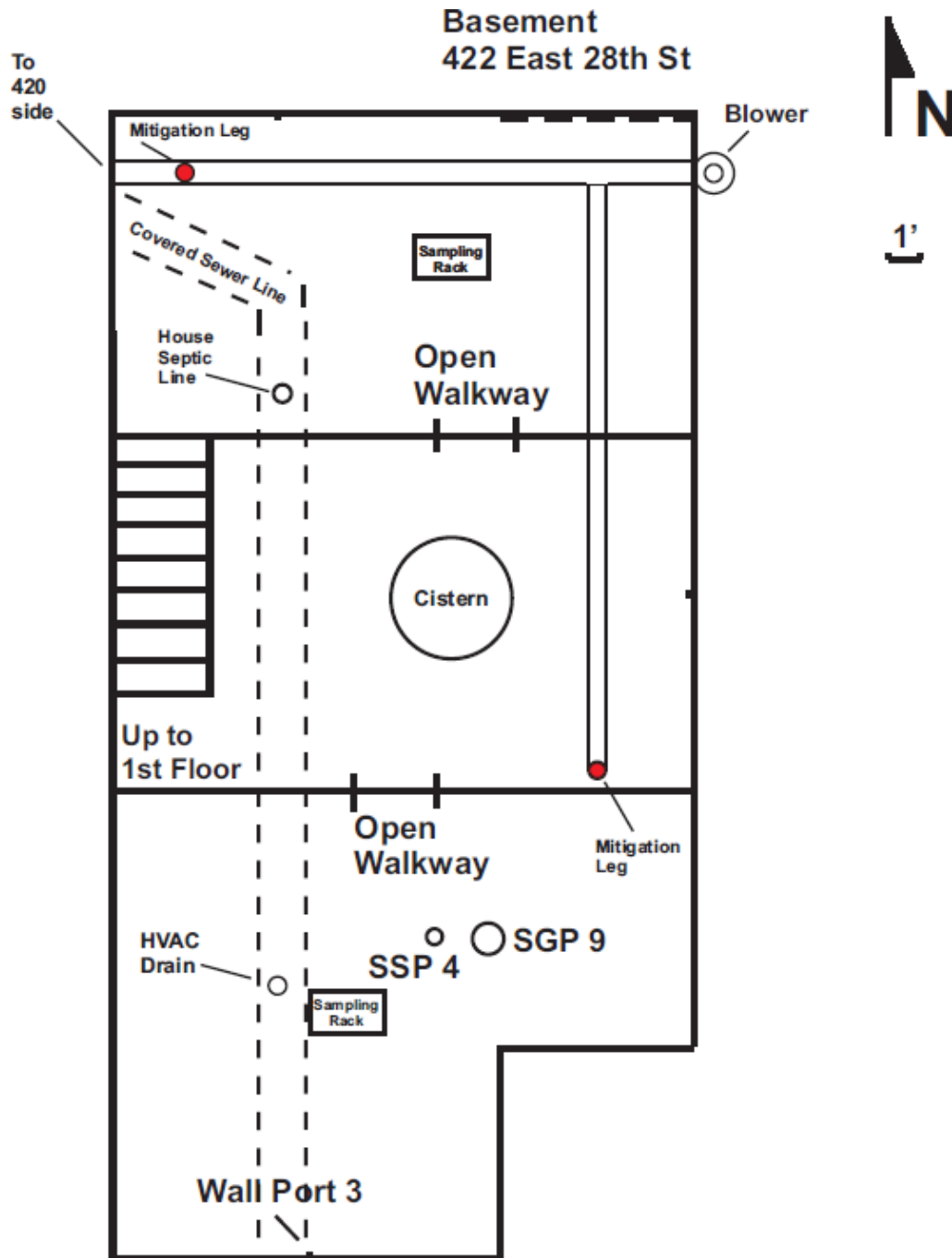


Figure 3-10. Map view of the 422-side basement showing SSD mitigation system legs, subslab soil gas extraction pits (red circles), and the position of the passive “sampling racks.” Horizontal divisions are walls between “north” (top in figure), “central,” and “south” (bottom in figure) sections of basement with open walkways between (cistern is in the central basement).

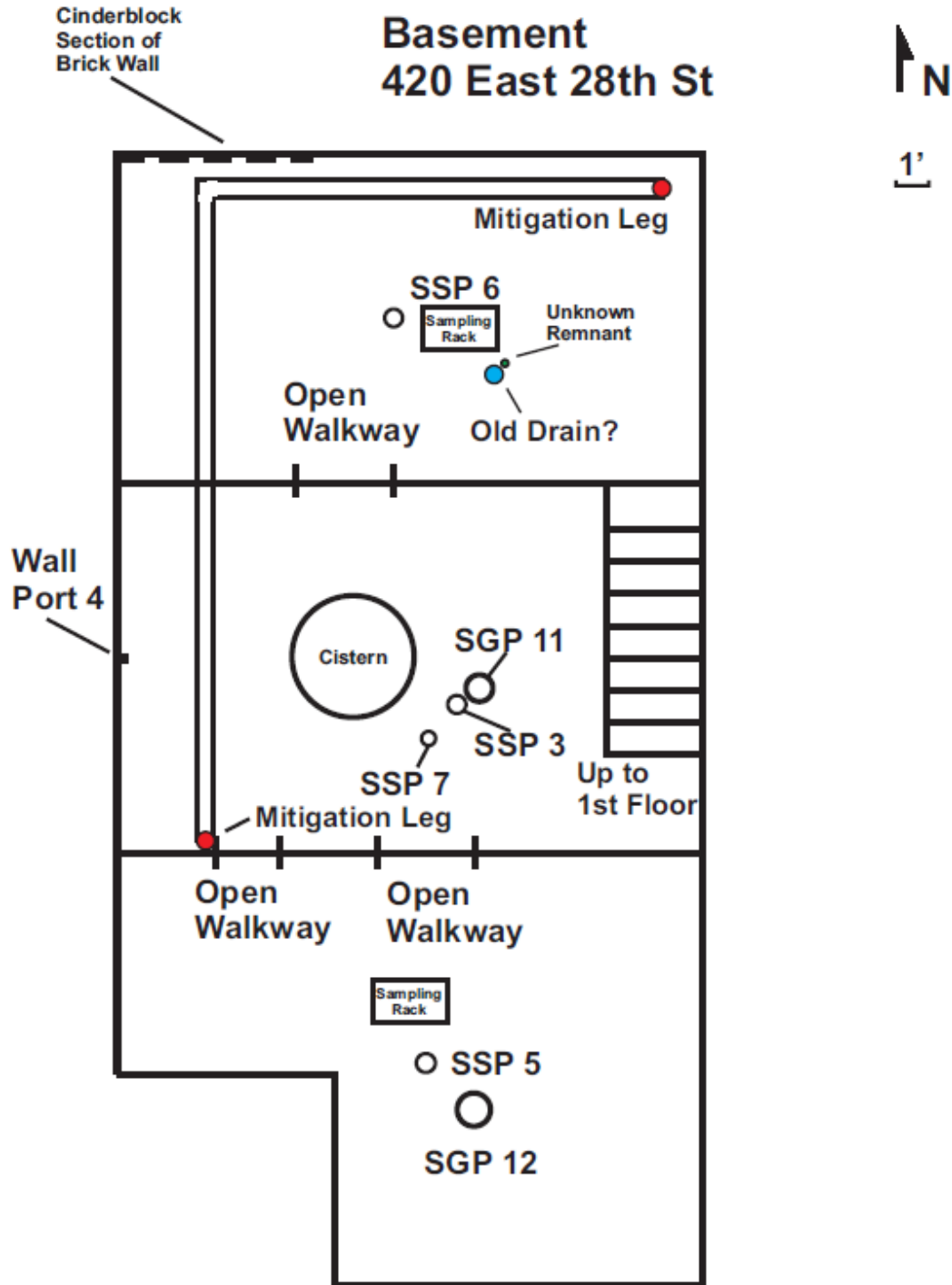


Figure 3-11. Map view of the 420-side basement showing the SSD mitigation system legs, subslab soil gas extraction pits (red circles), and the passive “sampling racks.” Horizontal divisions are walls between “north” (top in figure), “central,” and “south” (bottom in figure) sections of basement with open walkways between (cistern is in the central basement).



Figure 3-12. Photos of mitigation system: (left) SSD blower and stack on northeast corner of duplex; (right) SSD extraction point, showing valve and U-tube manometer.

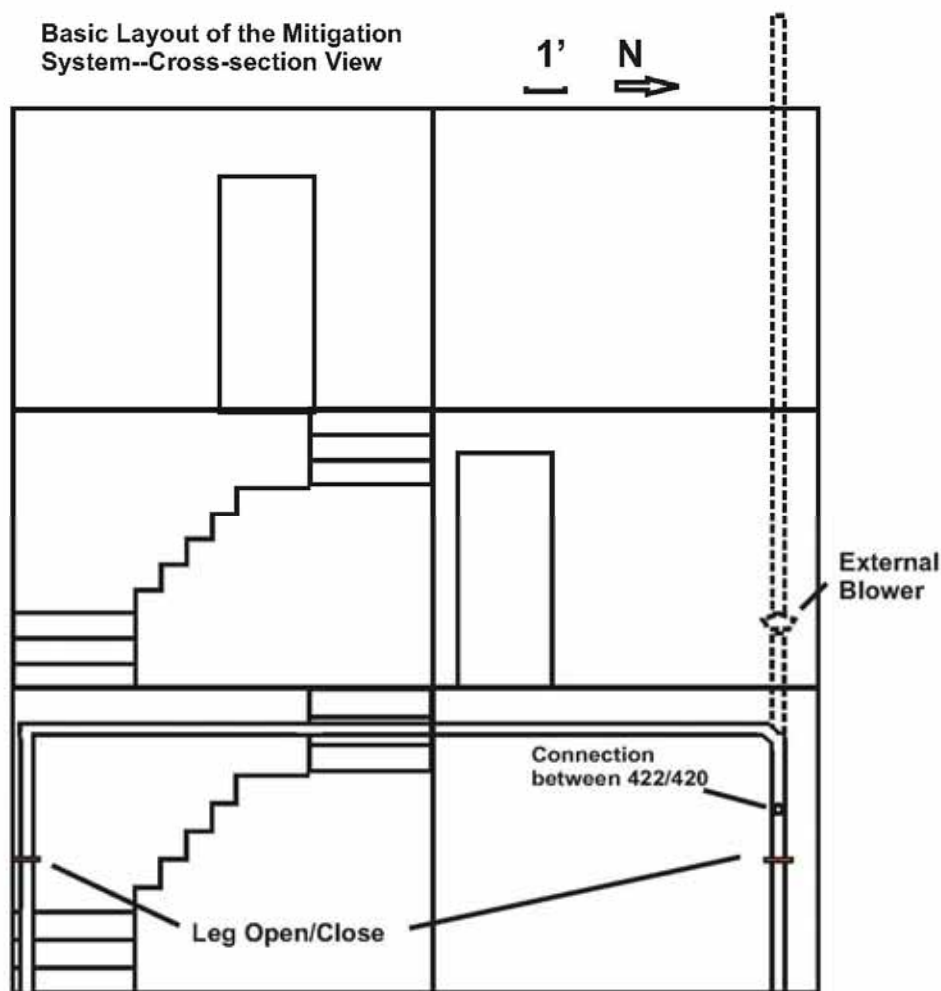


Figure 3-13. Cross-section showing the general layout of the 422/420 north and central basements with the positioning of the extraction legs, exterior blower, and exhaust stack.

3.4 Monitoring, Sampling, and Analysis

Section 3 in the previous project report (U.S. EPA, 2012a) provided details on the design and installation of the monitoring infrastructure used in this project including wells, soil gas monitoring ports, soil temperature and moisture sensors, differential pressure sensors, weather data, and indoor and outdoor monitoring for VOCs and radon. This report updates the previous report, with this section summarizing and updating the previous report's text on the VOC sampling configurations used for soil gas, air, and groundwater monitoring. Section 3.5 describes radon sampling, and Section 3.6 describes monitoring of physical parameters like weather, indoor temperature, and differential pressures. **Figure 3-14** maps the subsurface monitoring points including soil gas sampling ports and groundwater monitoring wells.

3.4.1 Indoor and Outdoor Air VOC Monitoring

The overwhelming majority of the indoor passive sampling was done with Radiello 130s supplied by and analyzed by Air Toxics Ltd. For comparison, two different types of SKC badges were also used that were specifically adapted to use at very short or long sampling durations.

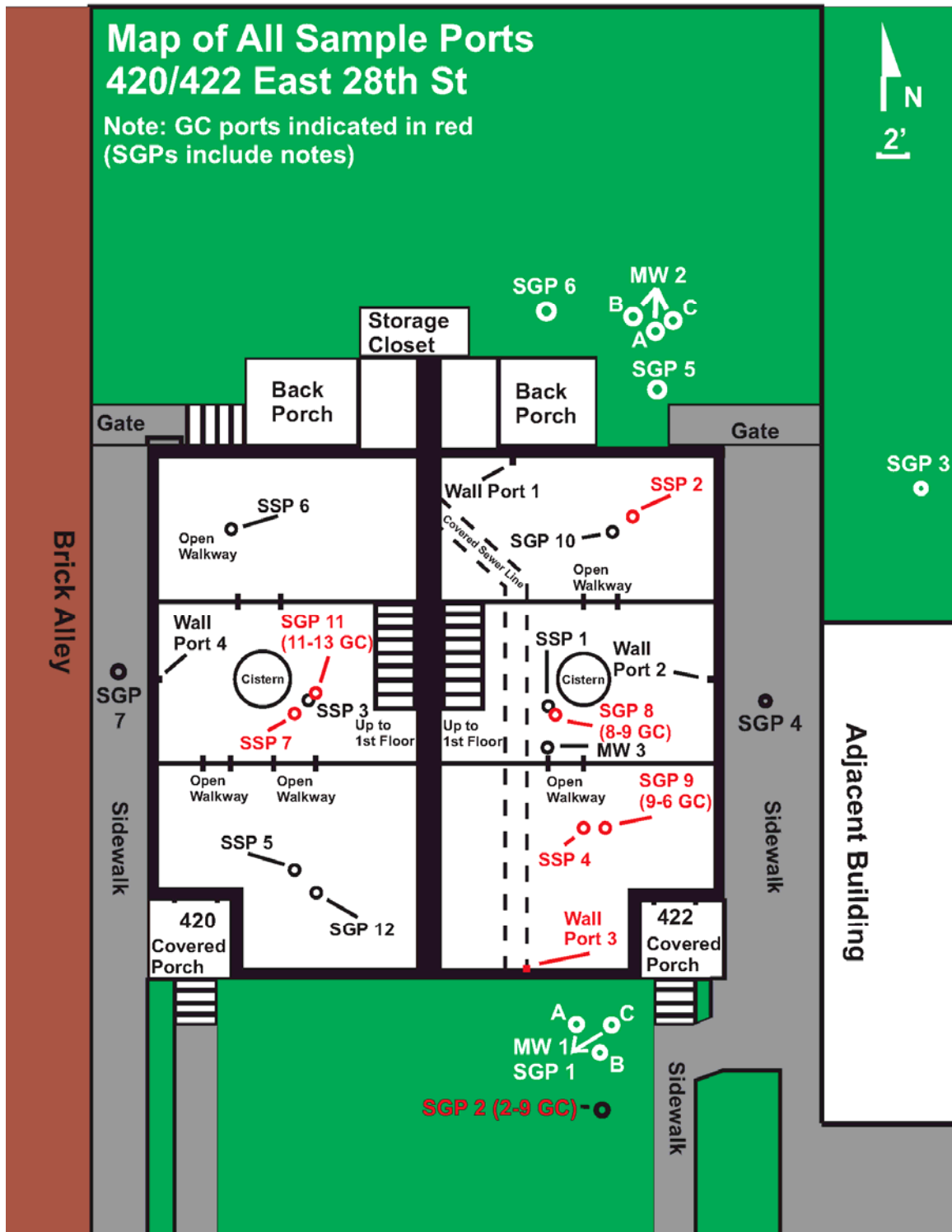


Figure 3-14. Subsurface soil gas monitoring probes (SGP), subslab sampling ports (SSP), and groundwater monitoring wells (MW). Horizontal divisions are walls between “north,” “central,” and “south” sections of basement with open walkways between (cisterns are in the central basements). Probes/ports in red were sampled by the onsite GC. Soil temperature and moisture probes were installed in the 422 basement between SGP 8 and MW 3 and in the backyard to the north of MW 2.

For passive sampling, several racks were set up to facilitate arranging groups of samplers in consistent locations for different durations during the run of the project. These racks were ordinary laundry drying racks that can be purchased inexpensively at most department stores (**Figure 3-15**). The racks were ideal in that they allowed multiple samplers to be placed at the same, or similar, levels within the normal breathing zone. One rack was placed in the first floor center room of 420 and 422 and in the northern and southern areas of each basement.

At each rack, a specific location was assigned for one of several day durations each approximately 6 in. apart to minimize the potential for starvation effects. Durations of 7, 14, 28, 91, 182, and 364 days were used from January 2011 to March 2012 to study the performance of varying durations of passive samplers as well as temporal variability. From October 2012 through May 2013, the primary emphasis of the passive sampling was to study the effects of the SSD mitigation system and snow/ice effects on VOC and radon levels using weekly and quarterly sampling durations. Enough spaces on the rack remained for duplicates of those durations, plus special locations occupied during intensive rounds. SKC badges were primarily hung on the back portion of the racks, in a similar manner to the Radiellos.

In addition to these indoor racks, a special outdoor (ambient) location had to be made to accommodate the samplers. A hood was purchased to house the samplers and mounted on a telephone pole by the alley near the house (**Figure 3-16**). This hood housed all of the Radiellos and badges for the different day durations.

Sampling of Radiellos consisted of removing the white diffusive body from its backing shield, opening the glass vial that contained the new screened Radiello 130, and allowing it to slide into the white body; then the white body was replaced in its backing plate with a new sample number. The old one was then sealed in a glass vial for shipping. Each week, Radiellos of the appropriate durations were stopped and replacements were started. For example, when the 7- and 14-day Radiellos were stopped, new ones were put up in their places. The 7-day samples were taken down the following week, followed by the 14-day samples the week after. This arrangement allowed us to compare the results of different time durations to each other (ex. four weekly samples against the monthly for the same time period). Additionally, during some of the intensive rounds, daily Radiellos were taken to compare them to the weekly time increments.

SKC 575 badges with the secondary diffusion cover were used for comparing the longest Radiello durations (the 182- and 364-day time periods). These solvent-extracted charcoal badges have been used in the literature for durations of 4 weeks and longer. SKC Ultra Badges (thermally desorbed) were used for 24-hour and 7-day sampling during an intensive round and short-term sampling during a fan test. Both Radiellos and SKC badges were provided by and returned to Air Toxics Ltd. for analysis.

Summa canisters (6 liter) were only used for preliminary site screening and indoor air before and after the fan testing (Method TO-15). These were acquired from and returned to Air Toxics Ltd. for analysis.



Figure 3-15. Passive indoor air sampling rack: 422 first floor.



Figure 3-16. Ambient sampler shelters on telephone pole near duplex.

3.4.2 Subslab and Soil Gas (TO-17)

The primary method of subslab and soil gas sampling for VOCs during the second phase of the project was by TO-17. In this method, a thermo-desorption tube, with a female Swagelok end, was connected to each sampling port in turn. Each port had its own male union connected to a valve. Before sampling, the port was purged with an SKC Universal XR pump set to 1L/min. Five well volumes were then purged via an exhaust line that ran away from the operator for exterior ports or out of a basement window in the case of the interior ports. The fittings were attached with wrenches, and an air tight syringe was mounted onto the other end of the TO-17 tube. Once this was done, the port's valve was opened, and the syringe was used to draw 200 mL of air through the TO-17 tube over a period of a minute. After this, the port valve was closed, and the TO-17 tube was removed and sealed for shipping.

Samples were taken from the operational ports positioned at three (interior probes) or four (exterior probes) depths each week from January 2011 through February 2012. Sampling was performed at least monthly from October 2012 through May 2013. During this time period, sampling was also performed

more frequently at time points selected to observe the effects of snow/ice events and flooding events. Initially, the preferred depths to sample were 3.5, 9, and 16.5 ft bls exterior and 6, 9, and 16.5 ft bls interior. However, a higher than expected water table prevented the sampling of the 16.5 ft depths for most of the duration of the project. Unusually high water tables or perched/infiltrating water occasionally made other soil gas ports inoperative. In addition, all wall ports were sampled during most sampling rounds, as well as a subset of the subslab ports. Details of the subslab, wall port, and soil gas probe locations and construction can be found in U.S. EPA (2012a).

The majority of the TO-17 tubes collected were prepared by and analyzed by the EPA National Exposure Research Laboratory (NERL) in Las Vegas, NV. For the extensive sampling of the intensive rounds conducted in 2011 to 2012, additional TO-17 tubes were prepared by and analyzed by Air Toxics. An intercomparison study of the two TO-17 laboratories was conducted in the previous project and showed acceptable agreement between the two laboratories (see Section 4.2.4 of U.S. EPA [2012a]). During the intensive rounds, all functioning ports (not made inoperative by water) were sampled at least once each day of the round. For a few days of each round, several locations were sampled multiple times of the day with the intention of comparing hourly and daily variability to the normal weekly variability.

3.4.3 Online Gas Chromatograph

An automated sampling and analysis system was provided by Hartman Environmental Geoscience for two periods during the previous project and from December until early March for this project, and system design and deployment are described here for all three sampling periods. The system consisted of the following elements:

- gas chromatograph (GC) with an electron capture detector (ECD),
- 16-port stream selection valve,
- sample injection valve with an adsorbent trap or 1 cc sample loop,
- computerized data acquisition system (Peaksimple by SRI Instruments), and
- remote connection via wireless.

The GC was connected by gas tight tubing from selected sample points for first floor indoor air, soil gas, subslab soil gas, and ambient air samples. The tubing from each sample location was connected to the stream selector valve. At any time, one of the entering tubes was connected to the adsorbent trap or sample loop depending on the position of the stream selector valve. A low-flow vacuum pump drew the vapor sample through the tubing at a rate of 25 cc/min to 40 cc/minute for 30 to 90 seconds to purge the sample tubing and ensure the sample in the sample loop was from the selected sample location. When purging was complete, the sample injection valve would rotate and inject the sample into the GC for analysis. Cycle time from start of purging to the end of the analysis was approximately 10 to 15 minutes. When the analysis was complete, the stream selector valve advanced to the next position (next sample location) and the process repeated itself. This sequence continued uninterrupted until stopped by the operator. Approximately seven (7) to nine (9) samples from each sample location were analyzed each day.

The data acquisition software (Peaksimple) acquired the chromatographic data and also controlled the stream-selector valve, sample injection, and GC analysis and stored the data to a summary file on a laptop. Remote access to the laptop and the data was enabled by a WiFi connection installed at the house for this purpose.

The 16 sampling ports were distributed as follows: one was initially connected to a nitrogen tank but later was connected to a line to outdoor air (~4 ft from the house), one was connected to a TCE standard

periodically, and two were blanks used to clear the instrument after each run. There were 12 sample locations: four indoor air, three subslab ports, one wall port, and three house-interior and one exterior soil gas probes with soil gas ports at multiple depths (3 ft, 6 ft, 9 ft, and 16.5 ft bls) in the subsurface. The 6 ft bls soil gas probes corresponded to the subslab probes in terms of depth.

All sampling lines were constructed of 1/16 in. OD stainless steel tubing (except the 420 first floor line had approximately a 20 ft section of 1/8 in. OD stainless steel tubing at the sampling end). The tubing for all lines ran from the stream selector valve at the GC along interior walls to the sampling points. At the sample locations, the indoor air lines hung suspended over passive sampler racks, within the breathing zone. For soil gas ports and subslab ports, each tube was connected to a sampling port by means of Swage-Lok male/female fittings.

In the first phase of the automated program (August 2011 to October 2011), the vapor sample from each location was concentrated onto an adsorbent trap. Volumes passed over the trap were adjusted depending on the vapor concentration at each location and ranged from 20 cc to 80 cc. Higher volumes were collected on the trap for lower concentration locations such as indoor air. Lower volumes were used for soil gas. Cycle time from start of purging to the end of the analysis was approximately 10 minutes. Approximately nine (9) samples from each sample location were analyzed each day.

In the second phase of the program (December 2011 to February 2012), the adsorbent trap was eliminated and the sample was passed through a 1 cc sample lop for direct injection into the GC. This modification was made to minimize carry-over between the high-concentration soil gas samples and the low-concentration indoor air samples and to speed up the analysis. Cycle time from start of purging to the end of the analysis was approximately 10 minutes. Approximately nine (9) samples from each sample location were analyzed each day.

In the third phase of the program (December 2012 to March 2013), the adsorbent trap was eliminated and the sample was passed through a 1 cc sample loop for direct injection into the GC. The analysis was also slowed down to enable lower detection limits for chloroform. Cycle time from start of purging to the end of the analysis was approximately 15 minutes. Approximately seven (7) samples from each sample location were analyzed each day.

3.4.4 Groundwater

Groundwater samples were taken approximately monthly with permeable diffusion bags (PDBs) from EON Products Inc. However, because of difficulties sampling the indoor 1-inch well (MW-3) by PDB, samples were taken by bailers from February 6, 2013, onward. The 422/420 duplex has six exterior MWs (two clusters of three) and one single-depth interior well installed in the basement and completed on the first floor (**Figure 3-17**). The exterior wells are arranged in groups of three in the front and the back yards. Each group of three is divided into depths of 16 to 21 ft, 21 to 24 ft, and 24 to 26 ft bls. The interior well (MW-3) is about 18 ft bls, but the casing extends up to the first floor for ease of access, so it is about 24 ft deep at its access point. The exterior wells are 2 inches in diameter, and the internal well is 1 inch in diameter. PDBs for the exterior wells are 12 by 1.75 inches, and the interior is 18 by 0.75 inches. PDBs were deployed for at least 2 weeks, and a new set of PDBs was cycled through almost monthly. PDBs were filled initially with deionized water provided by the EPA NERL laboratory. Most groundwater samples were shipped to EPA NERL-Las Vegas for VOC analysis by Method 8260. A few samples were analyzed by Pace laboratories in Indianapolis as a quality control check.

Groundwater samples were also collected from soil gas points when they were temporarily flooded using a peristaltic pump. Peristaltic pump samples were also collected from the monitoring wells for comparison purposes.



Figure 3-17. Monitoring well MW-3, installed in the basement and completed on the first floor.

3.4.5 Subslab Depressurization System Stack Gas Sampling

Passive sampling from the stack for VOCs was done with a passive sampler, the Waterloo Membrane Sampler. The Waterloo Membrane Sampler is preferred for sampling from the SSD stack because its design makes it resistant to changes in air velocity and because of its small size. The sampler and its validation are described at <http://www.sirem-lab.com/images/PDF/wms.pdf> (last accessed 10/9/2012). Radon readings in the stack were taken using the portable AlphaGUARD instrument used for soil gas. Stack velocity readings were taken with a Shortridge AND-870C Multimeter with the Airfoil Velocity measurement probe.

3.5 Radon Sampling and Analysis

3.5.1 Indoor Air Radon Sampling and Analysis

The primary radon sampling method was electrets ion chambers collecting radon samples passively in indoor air for the same 7-day intervals as Radiellos-collected VOCs. The following secondary methods were, however, also used for radon in indoor air:

- stationary AlphaGUARDs at two locations to provide greater time resolution,
- carbon absorbers for a QC comparison, and
- consumer grade ionization chamber-based detector (Safety Siren Pro Series 3 manufactured by Family Safety Products Inc.) for comparison.

Each method is described in detail below.

We used Rad Elec, E-Perm, ST-type (short-term) electrets according to EPA 402-R-92-004 (U.S. EPA, 1992). These were primarily deployed in s-chambers, but h-chambers were used on a few occasions. To

sample, electrets were opened within their chambers at their assigned locations for a week. After a week, the chambers were closed, all electrets were allowed to equilibrate for an hour to the room temperature where they would be read, and then their voltages were read on a Rad Elec electret voltage reader. Start and stop times, as well as voltages, were recorded and the electrets redeployed. The voltages, configurations (e.g., ST electrets in s-chambers), dates, and times would then be incorporated into a calculation used to convert voltage to picroCuries per liter (pCi/L) (pCi/L), with background gamma correction.

The electrets reader was calibrated weekly with three standards. In addition, an electret blank test was run weekly to test for effects of the chamber on the electrets. In this test, an electret not used during the sampling was inserted into one of the used electret chambers (closed) and then read to determine whether there had been any voltage drop from the previous week's reading.

Electrets were hung in mesh bags, one at each of the same locations used for sampling Radiellos, plus a duplicate at one location (three locations on the 422 side of the house and three on the 420 side). The ambient electret was kept in a permeable bag and hung from a wooden dowel about 2 ft from the house. Since December 28, 2011, a new electret was added in the 422 second floor office to be used in conjunction with the radon siren testing.

Charcoal canisters from the U.S. EPA Radiation and Indoor Environments (R&IE) National Laboratory in Las Vegas, NV, were set out on the sampling racks on three separate occasions to check the accuracy of the electret readings (U.S. EPA, 1990). They were simply opened for a week (matching an electret sampling period), closed, and shipped back to EPA for testing. Section 3.5.3 discusses the stationary AlphaGUARDS that were also used on the project for indoor air radon measurement.

Consumer-grade radon detector (Safety Siren) testing was a later addition to the project. Six Pro Series 3 Safety Siren radon gas detectors were deployed on December 23, 2011, and in use until March 1, 2012. They were tested again from October 2012 to May 2013 during a period of mitigation on/off testing. Each was installed at one of six locations: 422 second floor office, 422 first floor center room, 422 basement south, 422 basement north, 420 first floor center room (stolen October 11, 2012, not replaced), and 420 basement south. The intention of the test was to determine the agreement among the radon Safety Sirens, electrets, stationary AlphaGUARDS, and (for 1 week) charcoal canisters. The Safety Sirens can be read once each week, so their readings were taken when the other data types were being acquired and their readings compared.

3.5.2 Subslab and Soil Gas Radon Sampling and Analysis

Radon readings were collected weekly in 2011–2012 and approximately monthly or as meteorological conditions required in 2012–2013 with a portable AlphaGUARD Professional Radon Monitor from Genitron instruments. Operations were based on EPA guidelines for using continuous radon monitors (U.S. EPA, 1992). More information on the AlphaGUARD can be found at www.genitron.de/products/products.html. During routine sampling, this device was connected to subslab, soil gas, and wall ports with an SKC Universal XR pump set to 1 L/min. Tubes connected the sample port to the pump (with a moisture filter on the sampling end) and the pump to the AlphaGUARD. A purge line led away from the operator for exterior sampling and out of basement windows for interior sampling locations. The AlphaGUARD requires a 10-minute cycle of uninterrupted air flow from the sample location for an accurate reading. Because a certain amount of time was needed for movement between, one 10-minute cycle was spent relocating and then another to sample at the next location. Thus, each sample port needed 20 minutes to sample.

Because radon has a short half-life (3.8 days) and the migration time from substantial depths for soil gas is estimated to be months to years (Kurtz and Folkes, 2008; Carr et al., 2011), radon sampling focused on

the shallowest depths and, thus, differed from the VOC sampling strategy. Exterior sampling consisted of the shallowest ports available of the wells closest to the house. Usually, these were the 3.5- and 6-ft deep ports of SGPs 1, 7, 4, and 5. Periodically, these depths would not yield a sample, presumably because of moisture infiltration. In such cases, the next shallowest depths were chosen. Routine interior sampling included all wall ports, five of the subslab ports, and the shallowest intervals of the nested interior soil gas ports.

For routine sampling, first an ambient reading was taken outdoors and ~20 ft away from the 422/420 house. Then, lines to be sampled would be purged with the SKC pump (five soil gas point volumes, calculated based on the depth). Finally, the pump would be connected to the AlphaGUARD to acquire a full 10-minute sample.

The AlphaGUARD has a readout screen that details the results of the analysis at the end of each 10-minute cycle. The data provided are radon concentration (Bq/m^3), relative humidity (%), pressure (mbar), and temperature ($^{\circ}\text{C}$). These data were recorded each week in a spreadsheet and the Bq/m^3 converted to pCi/L .

3.5.3 Continuous (Real-Time) Indoor Air Radon Sampling and Analysis

The real-time AlphaGUARDs are essentially the same as the handheld AlphaGUARD instrument used to sample from the soil gas ports, except they are not fitted with the same nozzle type, because they are not connected to external pumps. Rather, in this application they are operated in a diffusion mode. These AlphaGUARDs are intended to be placed to give readings in specific rooms. In the case of the 422/420 duplex, one unit was placed in the 422 second floor office, and the other was placed in the 422 north basement area. These units stayed in their locations, except for brief, periodic data downloadings. These units were first regularly deployed on March 31, 2011, and were in near-continuous operation until May 2013 except for a period of off-site recalibration in late July through late September 2012.

The data are produced by the instrument in the same units as the portable AlphaGUARD (requiring conversion to pCi/L), and data points are collected every 10 minutes. However, because these devices were not moved, all 10-minute cycles are usable. The real-time AlphaGUARDs are used in conjunction with Data Expert software, also from Genitron Instruments. Once each week, the AlphaGUARDs were connected to the computer (the one in the basement required briefly moving the instrument to download), and the software downloaded the readings for the week. These were then saved as text files for later conversion to Excel spreadsheet files.

3.6 Physical Parameters Monitoring

3.6.1 On-Site Weather Station

This project used a Davis Vantage Vue Weather Station on site with Weather Link data logger and software (**Figure 3-18**). The components consist of the outdoor monitoring unit, the indoor receiver, and the computer connection. The outdoor monitoring unit was mounted on an accessible portion of the 422/420 house roof. The unit was mounted on steel pipes, but 5 ft above the highest roof deck (that of the attic dormer).

The outdoor unit contains all the exterior monitoring equipment (e.g., wind speed cups, rain gauge) and has a solar panel/battery backup for power. The outdoor unit transmits a radio signal to the indoor receiver, which also records the data every half hour. The indoor unit is human readable and can also be used to set a variety of parameters. The indoor unit also records the house interior data at its location, in this case the 422 second floor office. Once each week, the data were downloaded from the indoor unit onto the computer containing the Weather Link software. These data were saved as a text file and later

compiled in an Excel spreadsheet file. Many parameters are recorded; the key ones required for this project are temperature (degrees F, interior and exterior), relative humidity (%), wind speed (mph), and wind direction (16 points [22.5°] on compass rose).

Initially, and at least every 6 months, the results from this on-site system were compared with other nearby weather stations in Indianapolis using at least 1 day's observations. The National Weather Service (NWS) Indianapolis International Airport (KIND) is approximately 15 miles southwest from the site. The Indianapolis NWS station at Eagle Creek Airpark (KEYE) is approximately 9 miles west of the site. There is also a private weather station available online closer to the site in Indianapolis, IN (KININDIA33).



Figure 3-18. Front view of 420/422 duplex with location of weather station sensors indicated with red arrow.

During the autumn months of 2012, it was discovered that the weather station stopped recording data for brief periods each day, usually for approximately 2 hours in the early morning. It was determined in the winter of 2012 that the house exterior station needed its battery changed. Because the station's height made it inaccessible under ordinary conditions, a subcontractor was hired. As soon as the winter ice

conditions allowed (January 15, 2013), Ping's Tree Service was hired to access the external station's battery with a bucket truck. After the battery was changed, no further interruptions in data occurred.

3.6.2 Indoor Temperature

Although the indoor weather station unit can record temperature, it only does this in the 422 second floor office where it is located. Because temperature readings were required at all sample locations to allow adjustment of the passive sampler data for uptake rate variation due to temperature, another form of data collection was necessary. HOBOs data loggers, made by Onset (<http://www.onsetcomp.com/>), were placed—one at each of the six passive sampler racks in the house. HOBOs record temperature (degrees F) and relative humidity (%) every 30 minutes. Once a week, these data were recorded by taking them to the computer with the Hoboware reading software and later importing those data to an Excel spreadsheet file. Special spreadsheets were created to provide this information for the different Radiello time durations to the passive sampler analytical laboratory.

3.6.3 Soil Temperature

Soil temperature was recorded by thermocouples from Omega (Type T, hermetically sealed tip insulated thermocouples, HSTC-TT-T-24S-120). During the initial house set up, holes were drilled beneath the 422 basement slab and backyard soils of the duplex (see **Figure 3-14**) to accommodate thermocouple probes with end points set at different depths. Wires were inserted in ~2-in diameter holes with weights loosely attached near the ends. The holes were allowed to cave in and backfill naturally. The thermocouple wires run from their holes to male/female connectors (sealed from the elements in rubber “boots”) and from there to a data acquisition system (PDAQ 56 by IOtech), where the data were recorded to the software on the computer. A reading was taken approximately every 15 minutes. The thermocouples wired to the PDAQ roughly corresponded to the depths of the soil gas ports: inside at 6, 9, 13, and 16.5 ft bls; outside at 1, 3.5, 6, and 13 ft bls. However, there is one thermocouple (outside 16.5 ft) that is wired into an Omega data logger (OM-EL-USB-TC). The thermocouple data were most typically collected at 15-minute intervals.

3.6.4 Soil Moisture

Soil moisture was recorded by implanted Watermark moisture sensors. The units of measurement for the soil moisture sensors are explained by Smajstrla and Harrison (2002):

Water potential is commonly measured in units of bars (and centibars in the English system of measurement) or kilopascals (in metric units). One bar is approximately equal to one atmosphere (14.7 lb/in²) of pressure. One centibar is equal to one kilopascal. Because water is held by capillary forces within unsaturated soil pore spaces, its water potential is negative, indicating that the water is under tension and that work must be done to extract water from the soil. A water potential reading of 0 indicates that the soil is saturated, and plant roots may suffer from lack of oxygen. As the soil dries, water becomes less available and the water potential becomes more negative. The negative sign is usually omitted for convenience when soil water potentials are measured.

The soil water matrix potential can be converted into volumetric water content using known equations. Moisture content is often measured in fixed laboratories as gravimetric water content. To convert gravimetric water content to volumetric water, multiply the gravimetric water content by the bulk specific gravity of the material.

These sensors were also installed in the holes drilled during the house set up. Before insertion, the sensors had to be presoaked in water to prepare them. The sensors are pill-shaped devices at the end of a wire. The wire was run up through a PVC pipe of the appropriate length for the depth and the wire grasped

manually. The sensor could then be placed to the appropriate depth within the hole, the PVC pipe withdrawn, and the soil backfill allowed to fill in naturally. Wires extend to the Watermark 900M monitor, which reads and records the data every 30 minutes. Once each week these data were downloaded to the Watergraph 3.1 software on the computer. Data were recorded in centibars. Soil moisture probes were installed near the soil temperature probes in the 422 basement and backyard (see **Figure 3-14**). The sensors were installed to approximately correspond to the soil gas port depths: inside at 6, 13, and 16.5 ft bls and outside at 3.5, 6, 9, 13, and 16.5 ft bls.

3.6.5 Potentiometric Surface/Water Levels

Water levels in the seven wells (three clusters) on site were taken periodically with a Solinst water-level meter. The water-level results were compared against U.S. Geological Survey (USGS) stream gauge data for Fall Creek at Millersville, site 03352500 near the house.

For this new phase of the project, a Solinst water Levelogger Model 3001 was used to obtain higher time resolution, starting November 9, 2012; data are taken each half hour by the device. The device was installed in the deepest well (1A, ~26 ft) of the south yard monitoring well cluster (MW1). Installation made use of the existing tether system originally used with PDB sampling. Approximately each month, the water logger is retrieved and connected to a computer via a USB port. Using the Levelogger Series 4 Software, the data are downloaded from the logger and entered into a spreadsheet. The spreadsheet contains formulas for converting the recorded height of the water column to one corrected for outdoor pressure (using outdoor pressures from the weather station). Each month, depth to water is also manually measured using a Solinst water level indicator for comparison to the data logger. Readings differ by approximately 0.3 ft. The logger is then restarted and redeployed on its tether back in MW1-A.

3.6.6 Differential Pressure

Differential pressure readings were monitored by Setra Model 264 low differential pressure transducer. These units contain a pressure-sensitive diaphragm that measures pressure changes from the exterior high/low poles. The poles had tubing connected that ran from the areas to be measured. Some Setra poles were left open as an interior reference at a particular location. The configurations on the 422 side were as follows: subslab versus basement, basement versus upstairs, deep soil gas versus shallow soil gas, and basement versus exterior (out of the basement window). Only one unit was located on the 420 side, and it was used for subslab versus basement. Three lines used soil gas ports as access points: 422 deep soil gas versus shallow soil gas used SGP8-6 and SGP8-13, 422 subslab versus basement used SSP-1, and 420 subslab versus basement used SGP11-9. When these locations had to be sampled for VOCs, the ports would be closed, disconnected from the Setras, purged, and sampled. Afterward, the ports would be reconnected to the Setras and opened again.

The four Setras on the 422 side of the house are wired into the Personal Measurement Device, PMD-1208LS from Measurement Computing. The PMD is connected to the computer and uses TracerDaq software. Readings are taken every 15 minutes. The one Setra on the 420 side is connected to the PDAQ device and also takes a reading every 15 minutes (but not necessarily the same 15-minute interval as the PMD Setras).

In the beginning of the project, the Setras were laid flat on their supporting surfaces. In February 2011, manufacturer's guidance was found indicating that they should be mounted vertically. The manufacturer stated that correcting for the different mounting could be done by blocking the poles in the horizontal position to determine their "zero readings" and then recording those same readings in the vertical position to determine the offset. The offset could then be factored in to change the horizontal position data to vertical. By March 31, 2011, all were hung in this manner, and the early data corrected.

3.6.7 Air Exchange Rate

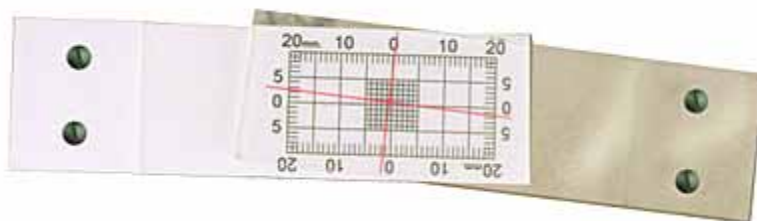
To determine the air exchange rate, capillary adsorption tubes (CATs) were used in conjunction with perfluorodimethylcyclohexane (PDCH) and perfluoromethylcyclohexane (PMCH) emitters, provided by the Harvard School of Public Health (HSPH) (EPA Method IP-4). The emitters are small metal shells containing a fluid (either PDCH or PMCH), and the shells are contained within a foam wrapping. The fluid releases a tracer gas at a measured constant rate, which is picked up by the CATs when in place. One stopper end of the CAT is removed when the samplers were deployed for periods of 1 week to allow sampling of the tracer gas by the adsorbent medium.

On April 22, 2011, in the 422 side of the house, 10 of the PDCH emitters were placed in the basement, 10 PMCH emitters were placed on the first floor, and 9 PMCH emitters were placed on the second floor. Care was taken that emitters be placed far enough from each other and from walls (about 3 to 4 ft). The placement locations also allowed unrestricted air flow.

CATs were used for sampling for air exchange rate measurement on four occasions. The first was from April 27, 2011, to May 4, 2011; the second was from September 23, 2011, to September 29, 2011; the third was from October 13, 2011, to October 14, 2011 and from October 18, 2011, to October 19, 2011; and the fourth was from April 2, 2013, to April 9, 2013. On the first occasion, CATs were deployed—one on the 422 first floor (center room) and two in the 422 basement (one duplicate). One was also placed in 420 on the first floor (center room) and in the 420 basement (center room). On the second occasion, CATs were only deployed on the 422 side of the house. One was in the 422 office on the second floor, one on the first floor (center room), and two were placed in the basement center room (one duplicate). On the fourth occasion, CATs were deployed on the 422 second floor office, the 422 first floor central room, the 422 basement central room (and a duplicate there), and the 420 first floor central room. When sampling, CATs were placed on their sides with one cap removed and slightly tipped at one end so the open end pointed toward the ground. After sampling, the CATs were sealed and sent to HSPH for analysis.

3.6.8 Crack Monitoring

The basement floors and walls were visually inspected for significant cracks (i.e., ones where vapors could infiltrate from subsurface soils). For the three most significant cracks, we installed a calibrated crack monitor as shown in the **Figure 3-19**. This device consists of two plates that move independently. One plate is white with a black millimeter grid; the other is transparent with red crosshairs centered over the grid. Once the monitor is secured with epoxy or screws across a crack, the crosshairs shift vertically or horizontally on the grid, making crack movement easily visible and trackable. It was installed with a 5-Minute® Epoxy, a rapid-curing, general-purpose adhesive that bonds rigid, durable substrates such as metals, glass, ceramics, concrete, and wood in all combinations. The position of the monitor was recorded monthly and indicated that the monitored cracks did not move during the course of the study.



BEN MEADOWS Calibrated Crack Monitor

Figure 3-19. Calibrated crack monitor.

3.7 Data Aggregation Methods

In order to conduct statistical time series analysis in Sections 9 and 10, data had to be arranged into files that contained one value for each predictor (independent) variable for each value of an outcome (dependent) variable. Because of methodological constraints, not all data sets were acquired with exactly the same time intervals. Therefore data were aggregated at the level of individual days and weeks for data analysis. Professional judgment was used to determine the most appropriate method of aggregation for a given parameter (e.g., mean, sum, mode, maximum); in most cases, the mean or mode was used as a central tendency estimate to avoid any bias in the aggregated variable. The methods of aggregation for each variable are provided in **Table 3-2**.

Table 3-2. Data Aggregation Applied to Predictor Variables

| Variable Name (Plain Language) | Variable Code | Method of Aggregation |
|---|-------------------------|-----------------------|
| <i>Building Variables</i> | | |
| 420 air conditioning status (on/on briefly/off) | AC_on-off_420_daily | Mode |
| 422 air conditioning status (on/on briefly/off) | AC_on-off_422_daily | Mode |
| 422 fan status (on/off) (Note: fan was never used on 420) | Fan_on-off_422_daily | Mode |
| 420 side heating status (on/off) | Heat_on-off_420_daily | Mode |
| 422 heating status (on/off) | Heat_on-off_422_daily | Mode |
| House Mitigation Status (not yet installed/on/passive/off) | Mitigation_Status_Daily | Mode |
| <i>Building Environment Variables</i> | | |
| Air density interior | AirDens_422 | Mean |
| Dew point, interior, Fahrenheit | Dew_pt_422_F | Mean |
| Humidity interior | Hum_422_%. | Mean |
| Interior heating Index | Indoor_Heat_Index | Mean |
| 420, subslab vs. basement differential pressure | Setra_420ss.base_Pa | Mean |
| 422 basement vs. exterior differential pressure, Pascals | Setra_422base.out_Pa | Mean |
| 422, basement vs. upstairs differential pressure, Pascals | Setra_422base.upst_Pa | Mean |
| 422, deep vs. shallow soil gas differential pressure, Pascals | Setra_422SGdp.ss_Pa | Mean |
| 422, subslab vs. basement differential pressure, Pascals | Setra_422ss.base_Pa | Mean |
| Temperature at 420 basement north sampling location from HOBO | T_420baseN_C | Mean |
| Temperature at 420 basement south sampling location from HOBO | T_420baseS_C | Mean |
| Temperature at 420 first floor sampling location from HOBO | T_420first_C | Mean |
| Temperature, 422 first floor from weather station | T_422_F | Mean |
| Temperature 422 basement north from HOBO | T_422baseN_C | Mean |
| Temperature 422 first floor from HOBO | T_422baseS_C | Mean |
| Temperature on first floor of 422 of duplex from HOBO | T_422first_C | Mean |
| <i>Subsurface and Stream Variables</i> | | |
| Height Measured at Fall Creek Stream Gauge in feet | Fall_Crk_Gage_ht_ft | Mean |
| Soil moisture, 13 ft bls beneath structure, cbar | Soil_H2O_In13._cbar | Mean |
| Soil moisture 16.5 ft bls beneath structure, cbar | Soil_H2O_In16.5._cbar | Mean |
| Soil moisture 6 ft bls beneath structure, cbar | Soil_H2O_In6._cbar | Mean |
| Soil moisture 13 ft bls exterior, cbar | Soil_H2O_Out13._cbar | Mean |

(continued)

Table 3-2. Data Aggregation Applied to Predictor Variables (cont.)

| Variable Name (Plain Language) | Variable Code | Method of Aggregation |
|---|-----------------------|--------------------------------|
| Soil moisture, 3.5 ft bls exterior, cbar | Soil_H2O_Out3.5._cbar | Mean |
| Soil moisture 6 ft bls exterior, cbar | Soil_H2O_Out6._cbar | Mean |
| Soil temperature 13 ft bls beneath structure | Soil_T_C_MW3.13 | Mean |
| Soil temperature 16.4 ft bls beneath structure | Soil_T_C_MW3.16.5 | Mean |
| Soil temperature 6 ft bls beneath structure | Soil_T_C_MW3.6 | Mean |
| Soil temperature 9 ft bls beneath structure | Soil_T_C_MW3.9 | Mean |
| Soil temperature 1 ft bls exterior | Soil_T_C_OTC.1 | Mean |
| Soil temperature 13 ft bls exterior | Soil_T_C_OTC.13 | Mean |
| Soil temperature 16.5 ft bls exterior | Soil_T_C_OTC.16.5 | Mean |
| Soil temperature 6 ft bls exterior | Soil_T_C_OTC.6 | Mean |
| <i>Weather Variables</i> | | |
| Barometric pressure rate of change in inches of mercury per hour | Bar_drop_.Hg.hr | Mean |
| Barometric pressure in inches of mercury | Bar_in_Hg | Mean |
| Net barometric pressure change over measurement period in inches of mercury | BP_Net_Change | First-Last, by date/time |
| Standard deviation of barometric pressure change over measurement period in inches of mercury | BP_Pump_Speed | Standard Deviation |
| Largest barometric pressure change over measurement period ("stroke length" of barometric pumping) in inches of mercury | BP_Stroke_Length | Maximum-Minimum |
| Cooling degree days | Cool_Degree_Day | Sum |
| Dew point, exterior | Dew_pt_out_F | Mean |
| Heating degree days | Heat_Degree_Day | Sum |
| Exterior Heating Index – calculated based on temperature and humidity | Heat_Index_F | Mean |
| Humidity exterior | Hum_out_%. | Mean |
| Rain (inches) totaled during observation period | Rain_In_met | Sum |
| Rain highest rate during observation period in inches/hour | Rain_IPH | Maximum |
| Depth of snow on the ground, inches | Snowdepth_daily | Mean |
| Temperature exterior from HOBO | T_out_C | Mean |
| Exterior temperature from weather station (°F) | T_out_F | Mean |
| Temperature exterior, high during data collection period | T_out_Hi_F | Maximum |
| Lowest exterior temperature in Fahrenheit | T_out_Lo_F | Minimum |
| Temperature, humidity, and wind index | THW_F | Mean |
| Wind chill | Wind_Chill_F | Mean |
| Average wind direction in degrees | Wind_Dir | Trigonometric Mean |
| Wind direction of high speed during measurement period in Degrees | Wind_Dir_Hi | Direction paired to high speed |
| Wind run is a function of wind speed and duration | Wind_Run_mi | Sum |
| High wind speed during measurement period | Wind_Speed_Hi_MPH | Maximum |
| Average wind speed during measurement period | Wind_Speed_MPH | Mean |

(continued)

Table 3-2. Data Aggregation Applied to Predictor Variables (cont.)

| Variable Name (Plain Language) | Variable Code | Method of Aggregation |
|---|--------------------------------|---|
| <i>Chemical Concentration Measurements</i> | | |
| Chloroform concentration at 420 basement north sampling location, in $\mu\text{g}/\text{m}^3$, as measured by Radiello sample | 420BaseN_Radiello_Weekly_CHCl3 | Randomly choose (when more than one per week) |
| Chloroform concentration at 420 basement south sampling location, in $\mu\text{g}/\text{m}^3$, as measured by Radiello sample | 420BaseS_Radiello_Weekly_CHCl3 | Randomly choose (when more than one per week) |
| Chloroform concentration at 422 basement north sampling location, in $\mu\text{g}/\text{m}^3$, as measured by Radiello sample | 422BaseN_Radiello_Weekly_CHCl3 | Randomly choose (when more than one per week) |
| Chloroform concentration at 422 basement south sampling location, in $\mu\text{g}/\text{m}^3$, as measured by Radiello sample | 422BaseS_Radiello_Weekly_CHCl3 | Randomly choose (when more than one per week) |
| Chloroform concentration at 422 first floor sampling location, in $\mu\text{g}/\text{m}^3$, as measured by Radiello sample | 420First_Radiello_Weekly_CHCl3 | Randomly choose (when more than one per week) |
| Chloroform concentration at 422 first floor sampling location, in $\mu\text{g}/\text{m}^3$, as measured by Radiello sample | 422First_Radiello_Weekly_CHCl3 | Randomly choose (when more than one per week) |
| Chloroform concentration at outside sampling location, in $\mu\text{g}/\text{m}^3$, as measured by Radiello sample | Out_Radiello_Weekly_CHCl3 | Randomly choose (when more than one per week) |
| Tetrachloroethene concentration at 420 basement north sampling location, in $\mu\text{g}/\text{m}^3$, as measured by Radiello sample | 420BaseN_Radiello_Weekly_PCE | Randomly choose (when more than one per week) |
| Tetrachloroethene concentration at 420 basement south sampling location, in $\mu\text{g}/\text{m}^3$, as measured by Radiello sample | 420BaseS_Radiello_Weekly_PCE | Randomly choose (when more than one per week) |
| Tetrachloroethene concentration at 422 basement north sampling location, in $\mu\text{g}/\text{m}^3$, as measured by Radiello sample | 422BaseN_Radiello_Weekly_PCE | Randomly choose (when more than one per week) |
| Tetrachloroethene concentration at 422 basement south sampling location, in $\mu\text{g}/\text{m}^3$, as measured by Radiello sample | 422BaseS_Radiello_Weekly_PCE | Randomly choose (when more than one per week) |
| Tetrachloroethene concentration at 422 first floor sampling location, in $\mu\text{g}/\text{m}^3$, as measured by Radiello sample | 420First_Radiello_Weekly_PCE | Randomly choose (when more than one per week) |
| Tetrachloroethene concentration at 422 first floor sampling location, in $\mu\text{g}/\text{m}^3$, as measured by Radiello sample | 422First_Radiello_Weekly_PCE | Randomly choose (when more than one per week) |
| Tetrachloroethene concentration at outside sampling location, in $\mu\text{g}/\text{m}^3$, as measured by Radiello sample | Out_Radiello_Weekly_PCE | Randomly choose (when more than one per week) |
| Radon concentration at 422 basement north sampling location, in pCi/L, as measured by AlphaGUARD sample | 422baseN_AG_radon | Mean |
| Radon concentration at 422 office sampling location, in pCi/L, as measured by AlphaGUARD sample | 422office_2nd_AG_radon | Mean |

(continued)

Table 3-2. Data Aggregation Applied to Predictor Variables (cont.)

| Variable Name (Plain Language) | Variable Code | Method of Aggregation |
|--|------------------|-----------------------|
| Tetrachloroethene concentration at 420 basement south sampling location, in $\mu\text{g}/\text{m}^3$, as measured by GC sample during the first period of GC sampling | 420baseS_GC1_PCE | Mean |
| Tetrachloroethene concentration at 422 basement south sampling location, in $\mu\text{g}/\text{m}^3$, as measured by GC sample during the first period of GC sampling | 422baseS_GC1_PCE | Mean |
| Tetrachloroethene concentration at 420 first sampling location, in $\mu\text{g}/\text{m}^3$, as measured by GC sample during the first period of GC sampling | 420first_GC1_PCE | Mean |
| Tetrachloroethene concentration at 422 first sampling location, in $\mu\text{g}/\text{m}^3$, as measured by GC sample during the first period of GC sampling | 422first_GC1_PCE | Mean |
| Tetrachloroethene Concentration at Wall Port 3 sampling location, in $\mu\text{g}/\text{m}^3$, as measured by GC sample during the first period of GC sampling | WP3_GC1_PCE | Mean |
| Tetrachloroethene concentration at Subslab Port 2 sampling location, in $\mu\text{g}/\text{m}^3$, as measured by GC sample during the first period of GC sampling | SSP2_GC1_PCE | Mean |
| Tetrachloroethene concentration at Subslab Port 4 sampling location, in $\mu\text{g}/\text{m}^3$, as measured by GC sample during the first period of GC sampling | SSP4_GC1_PCE | Mean |
| Tetrachloroethene concentration at Subslab Port 7 sampling location, in $\mu\text{g}/\text{m}^3$, as measured by GC sample during the first period of GC sampling | SSP7_GC1_PCE | Mean |
| Tetrachloroethene concentration at Soil Gas Port 11 sampling location at a depth of 13 feet, in $\mu\text{g}/\text{m}^3$, as measured by GC sample during the first period of GC sampling | SGP11-13_GC1_PCE | Mean |
| Tetrachloroethene concentration at Soil Gas Port 2 sampling location at a depth of 9 feet, in $\mu\text{g}/\text{m}^3$, as measured by GC sample during the first period of GC sampling | SGP2-9_GC1_PCE | Mean |
| Tetrachloroethene concentration at Soil Gas Port 8 sampling location at a depth of 9 feet, in $\mu\text{g}/\text{m}^3$, as measured by GC sample during the first period of GC sampling | SGP8-9_GC1_PCE | Mean |
| Tetrachloroethene concentration at Soil Gas Port 9 sampling location at a depth of 6 feet, in $\mu\text{g}/\text{m}^3$, as measured by GC sample during the first period of GC sampling | SGP9-6_GC1_PCE | Mean |
| Tetrachloroethene concentration at 420 basement south sampling location, in $\mu\text{g}/\text{m}^3$, as measured by GC sample during the second period of GC sampling | 420baseS_GC2_PCE | Mean |
| Tetrachloroethene concentration at 422 basement south sampling location, in $\mu\text{g}/\text{m}^3$, as measured by GC sample during the second period of GC sampling | 422baseS_GC2_PCE | Mean |
| Tetrachloroethene concentration at 420 first sampling location, in $\mu\text{g}/\text{m}^3$, as measured by GC sample during the second period of GC sampling | 420first_GC2_PCE | Mean |
| Tetrachloroethene concentration at 422 first sampling location, in $\mu\text{g}/\text{m}^3$, as measured by GC sample during the second period of GC sampling | 422first_GC2_PCE | Mean |

(continued)

Table 3-2. Data Aggregation Applied to Predictor Variables (cont.)

| Variable Name (Plain Language) | Variable Code | Method of Aggregation |
|---|------------------|-----------------------|
| Tetrachloroethene concentration at Wall Port 3 sampling location, in $\mu\text{g}/\text{m}^3$, as measured by GC sample during the second period of GC sampling | WP3_GC2_PCE | Mean |
| Tetrachloroethene concentration at Subslab Port 2 sampling location, in $\mu\text{g}/\text{m}^3$, as measured by GC sample during the second period of GC sampling | SSP2_GC2_PCE | Mean |
| Tetrachloroethene concentration at Subslab Port 4 sampling location, in $\mu\text{g}/\text{m}^3$, as measured by GC sample during the second period of GC sampling | SSP4_GC2_PCE | Mean |
| Tetrachloroethene concentration at Subslab Port 7 sampling location, in $\mu\text{g}/\text{m}^3$, as measured by GC sample during the second period of GC sampling | SSP7_GC2_PCE | Mean |
| Tetrachloroethene concentration at Soil Gas Port 11 sampling location at a depth of 13 feet, in $\mu\text{g}/\text{m}^3$, as measured by GC sample during the second period of GC sampling | SGP11-13_GC2_PCE | Mean |
| Tetrachloroethene concentration at Soil Gas Port 2 sampling location at a depth of 9 feet, in $\mu\text{g}/\text{m}^3$, as measured by GC sample during the second period of GC sampling | SGP2-9_GC2_PCE | Mean |
| Tetrachloroethene concentration at Soil Gas Port 8 sampling location at a depth of 9 feet, in $\mu\text{g}/\text{m}^3$, as measured by GC sample during the second period of GC sampling | SGP8-9_GC2_PCE | Mean |
| Tetrachloroethene concentration at Soil Gas Port 9 sampling location at a depth of 6 feet, in $\mu\text{g}/\text{m}^3$, as measured by GC sample during the second period of GC sampling | SGP9-6_GC2_PCE | Mean |
| Tetrachloroethene concentration at 420 basement south sampling location, in $\mu\text{g}/\text{m}^3$, as measured by GC sample during the third period of GC sampling | 420baseS_GC3_PCE | Mean |
| Tetrachloroethene concentration at 422 basement south sampling location, in $\mu\text{g}/\text{m}^3$, as measured by GC sample during the third period of GC sampling | 422baseS_GC3_PCE | Mean |
| Tetrachloroethene concentration at 420 first sampling location, in $\mu\text{g}/\text{m}^3$, as measured by GC sample during the third period of GC sampling | 420first_GC3_PCE | Mean |
| Tetrachloroethene concentration at 422 first sampling location, in $\mu\text{g}/\text{m}^3$, as measured by GC sample during the third period of GC sampling | 422first_GC3_PCE | Mean |
| Tetrachloroethene concentration at Wall Port 3 sampling location, in $\mu\text{g}/\text{m}^3$, as measured by GC sample during the third period of GC sampling | WP3_GC3_PCE | Mean |
| Tetrachloroethene concentration at Subslab Port 2 sampling location, in $\mu\text{g}/\text{m}^3$, as measured by GC sample during the third period of GC sampling | SSP2_GC3_PCE | Mean |
| Tetrachloroethene concentration at Subslab Port 4 sampling location, in $\mu\text{g}/\text{m}^3$, as measured by GC sample during the third period of GC sampling | SSP4_GC3_PCE | Mean |
| Tetrachloroethene concentration at Subslab Port 7 sampling location, in $\mu\text{g}/\text{m}^3$, as measured by GC sample during the third period of GC sampling | SSP7_GC3_PCE | Mean |

(continued)

Table 3-2. Data Aggregation Applied to Predictor Variables (cont.)

| Variable Name (Plain Language) | Variable Code | Method of Aggregation |
|--|------------------|-----------------------|
| Tetrachloroethene concentration at Soil Gas Port 11 sampling location at a depth of 13 feet, in $\mu\text{g}/\text{m}^3$, as measured by GC sample during the third period of GC sampling | SGP11-13_GC3_PCE | Mean |
| Tetrachloroethene concentration at Soil Gas Port 2 sampling location at a depth of 9 feet, in $\mu\text{g}/\text{m}^3$, as measured by GC sample during the third period of GC sampling | SGP2-9_GC3_PCE | Mean |
| Tetrachloroethene concentration at Soil Gas Port 8 sampling location at a depth of 9 feet, in $\mu\text{g}/\text{m}^3$, as measured by GC sample during the third period of GC sampling | SGP8-9_GC3_PCE | Mean |
| Tetrachloroethene concentration at Soil Gas Port 9 sampling location at a depth of 6 feet, in $\mu\text{g}/\text{m}^3$, as measured by GC sample during the third period of GC sampling | SGP9-6_GC3_PCE | Mean |

Table of Contents

| | | |
|-------|--|------|
| 4.0 | Results and Discussion: Quality Assurance Checks of Individual Data Sets | 4-1 |
| 4.1 | VOC Sampling—Indoor Air-Passive—Air Toxics Ltd. (ATL)..... | 4-1 |
| 4.1.1 | Blanks | 4-1 |
| 4.1.2 | Surrogate Recoveries | 4-3 |
| 4.1.3 | Laboratory Control Sample Recoveries..... | 4-3 |
| 4.1.4 | Duplicates | 4-4 |
| 4.2 | VOC Sampling—Subslab and Soil Gas (TO-17)—U.S. EPA | 4-5 |
| 4.2.1 | Blanks | 4-5 |
| 4.2.2 | Calibration Verification | 4-7 |
| 4.2.3 | Internal Standard Recoveries | 4-8 |
| 4.2.4 | Surrogate Recoveries | 4-8 |
| 4.2.5 | Laboratory Control Sample Recoveries..... | 4-9 |
| 4.2.6 | Field Duplicates | 4-9 |
| 4.3 | Online Gas Chromatograph (Soil Gas and Indoor Air)..... | 4-10 |
| 4.3.1 | Blanks | 4-10 |
| 4.3.2 | Initial Calibration..... | 4-10 |
| 4.3.3 | Continuing Calibration | 4-11 |
| 4.3.4 | Calibration Check via Comparison to Fixed Laboratory (TO-15 vs. Online GC)..... | 4-12 |
| 4.3.5 | Agreement of Online GC Results with TO-17 Verification Samples..... | 4-14 |
| 4.3.6 | Agreement of Integrated Online GC Results with Passive Samplers | 4-16 |
| 4.3.7 | Overall Assessment of Online GC Data | 4-37 |
| 4.4 | Radon | 4-43 |
| 4.4.1 | Indoor Air: Comparison of Electrets Field, ARCADIS to Charcoal Analyzed by U.S. EPA R&IE National Laboratory..... | 4-43 |
| 4.4.2 | Comparison of Average of Real-Time AlphaGUARD to Electrets and Charcoal Canisters..... | 4-45 |
| 4.4.3 | Quality Assurance Checks of Electrets..... | 4-48 |
| 4.5 | On-Site Weather Station vs. National Weather Service (NWS) | 4-48 |
| 4.6 | Groundwater Analysis—EPA NERL | 4-51 |
| 4.6.1 | Blanks | 4-51 |
| 4.6.2 | Surrogate Recoveries | 4-53 |
| 4.7 | Groundwater Analysis—Pace Laboratories | 4-54 |
| 4.8 | Database | 4-54 |
| 4.8.1 | Checks on Laboratory Reports..... | 4-54 |
| 4.8.2 | Database Checks | 4-54 |
| 4.9 | Air Exchange Rate Measurements | 4-55 |

List of Figures

| | | |
|-------|---|------|
| 4-1. | TCE Continuing Calibration Standard Analyses, Hartman 3 Period. | 4-12 |
| 4-2. | XY Comparison plot of Radiello and GC indoor air concentration measurements ($\mu\text{g}/\text{m}^3$), Hartman 1 sampling period. | 4-30 |
| 4-3. | XY Comparison plot of Radiello and GC indoor air concentration measurements ($\mu\text{g}/\text{m}^3$), Hartman 2 sampling period. | 4-31 |
| 4-4. | Time series comparison of field GC and passive sampling data: 422 basement, Hartman Period 2, chloroform. Horizontal gray line is calculated GC reporting limit. Red hash marks on y-axis indicate missing values. | 4-33 |
| 4-5. | Time series comparison of field GC and passive sampling data: 422 first floor, Hartman Period 2, chloroform. Horizontal gray line is calculated GC reporting limit. Red hash marks on y-axis indicate missing values. | 4-34 |
| 4-6. | Time series comparison of field GC and passive sampling data: 422 basement, Hartman Period 2, PCE. Horizontal gray line is calculated GC reporting limit. Red hash marks on y-axis indicate missing values. | 4-35 |
| 4-7. | Time series comparison of field GC and passive sampling data: 422 first floor, Hartman Period 2, PCE. Horizontal gray line is calculated GC reporting limit. Red hash marks on y-axis indicate missing values. | 4-36 |
| 4-8. | XY Plot of field GC vs. passive sampler data, Hartman Period 3. | 4-38 |
| 4-9. | Time series comparison of field GC and passive sampling data: 422 basement, Hartman Period 3, chloroform. Horizontal gray line is calculated GC reporting limit. Red hash marks on y-axis indicate missing values. | 4-39 |
| 4-10. | Time series comparison of field GC and passive sampling data: 422 first floor, Hartman Period 3, chloroform. Horizontal gray line is calculated GC reporting limit. Red hash marks on y-axis indicate missing values. | 4-40 |
| 4-11. | Time series comparison of field GC and passive sampling data: 422 Basement, Hartman Period 3, PCE. Horizontal gray line is calculated GC reporting limit. Red hash marks on y-axis indicate missing values. | 4-41 |
| 4-12. | Time series comparison of field GC and passive sampling data: 422 first floor, Hartman Period 3, PCE. Horizontal gray line is calculated GC reporting limit. Red hash marks on y-axis indicate missing values (none in this case). | 4-42 |
| 4-13. | Correlation between radon measured using the electret and charcoal methods. | 4-45 |
| 4-14. | Aerial view of study house, showing potential influences on wind velocity, red arrow indicates study house. | 4-49 |
| 4-15. | Comparison of National Weather Service Indianapolis temperature data to weather station at 422 East 28th Street. | 4-50 |
| 4-16. | Comparison of National Weather Service Indianapolis relative humidity to weather station at 422 East 28th Street. | 4-50 |
| 4-17. | Comparison of National Weather Service wind speed data to weather station at 422 East 28th Street. | 4-51 |

List of Tables

| | | |
|-------|--|------|
| 4-1. | Indoor Air Passive Field Blank Summary—Radiello 130 | 4-2 |
| 4-2. | Indoor Air Passive Trip Blank Summary—Radiello 130 | 4-2 |
| 4-3. | Indoor Air Passive Laboratory Blank Summary—Radiello 130 | 4-2 |
| 4-4. | Indoor Air Passive Surrogate Summary—Radiello 130 | 4-3 |
| 4-5. | Indoor Air Passive LCS Summary—Radiello 130 | 4-4 |
| 4-6. | Indoor Air Passive Laboratory Precision (LCS/LCSD) Summary—Radiello 130 | 4-4 |
| 4-7. | Subslab and Soil Gas—EPA Field Blank Summary—TO-17 | 4-5 |
| 4-8. | Subslab and Soil Gas—EPA Trip Blank Summary—TO-17 | 4-6 |
| 4-9. | Subslab and Soil Gas—EPA Laboratory Blank Summary—TO-17..... | 4-6 |
| 4-10. | Subslab and Soil Gas—EPA Fridge Blank Summary—TO-17 | 4-7 |
| 4-11. | EPA TO-17 Calibration Verification (CV) Summary | 4-8 |
| 4-12. | EPA TO-17 Internal Standard (IS) Summary | 4-8 |
| 4-13. | EPA TO-17 Surrogate Recovery Summary | 4-9 |
| 4-14. | EPA TO-17 Laboratory Control Sample (LCS) Summary | 4-9 |
| 4-15. | EPA TO-17 Field Duplicate Summary | 4-10 |
| 4-16. | Field GC Estimated Minimum Detection Limits and Practical Quantitation Limits | 4-11 |
| 4-17. | Result of Repeated TCE Calibration Standard Analyses on On-line GC in March 2013 (Hartman Period 3) | 4-14 |
| 4-18. | Results of Repeated PCE Calibration Standard Analyses on Online GC in March 2013 (Hartman Period 3) | 4-14 |
| 4-19. | Interlaboratory Results: Spiked Verification Samples | 4-15 |
| 4-20. | Interlaboratory Statistics: Spiked Verification Samples | 4-16 |
| 4-21. | Comparison of Online GC to Radiello Results by Week..... | 4-17 |
| 4-22. | Comparison between Electrets and Charcoal Canisters at the 422/420 EPA House from January 19–26, 2011 | 4-43 |
| 4-23. | Comparison of Electret and Charcoal Canister Data from April 27 to May 4, 2011 | 4-44 |
| 4-24. | Comparison of Charcoal and Electret Radon December 28, 2011, to January 4, 2012 | 4-44 |
| 4-25. | Comparison between 422 Basement N AlphaGUARDS and Electrets from March 30, 2011, and May 18, 2011 | 4-45 |
| 4-26. | Comparison of Real-Time AlphaGUARD to Integrated Electret August through October | 4-46 |
| 4-27. | Comparison of Real-Time AlphaGUARD to Integrated Electret Measurements December 28, 2011, to January 4, 2012..... | 4-46 |
| 4-28. | Comparison of Real-Time AlphaGUARD to Integrated Electret Measurements January through March 2012..... | 4-47 |
| 4-29. | Comparison of Real-Time AlphaGUARD to Integrated Electret Measurements January through March 2013..... | 4-47 |

| | | |
|-------|--|------|
| 4-29. | Comparison of Real-Time AlphaGUARD to Integrated Electret Measurements January through March 2013..... | 4-48 |
| 4-30. | Groundwater (5 mL)—EPA Field Blank Summary | 4-52 |
| 4-31. | Groundwater (5 mL)—EPA Laboratory Blank Summary—TO-17 | 4-52 |
| 4-32. | Groundwater (25 mL)—EPA Field Blank Summary—TO-17 | 4-52 |
| 4-33. | Groundwater (25 mL)—EPA Laboratory Blank Summary—TO-17 | 4-53 |
| 4-34. | EPA Groundwater (5 mL) Surrogate Recovery Summary | 4-53 |
| 4-35. | EPA Groundwater (25 mL) Surrogate Recovery Summary | 4-53 |

4.0 Results and Discussion: Quality Assurance Checks of Individual Data Sets

This section describes the sampling and analytical quality assurance/quality control (QA/QC) checks conducted for passive VOC sampling using Radiello samplers (4.1),*⁷ active sorbent tube sampling per method TO-17 for soil gas samples (4.2)*, the on-site gas chromatograph used for continuous monitoring of indoor air and soil gas (4.3), radon measurements by AlphaGUARD and electret instruments (4.4)*, weather station measurements (4.5), groundwater sampling and analysis (4.6 and 4.7)*, and entry of the compiled data into the project databases (4–8). Additional details on each of the sampling methods can be found in Section 3.

4.1 VOC Sampling—Indoor Air—Passive—Air Toxics Ltd. (ATL)

QA/QC checks for the passive Radiello 130 samplers used for indoor and outdoor air sampling are described in the following sections for blanks (4.1.1), surrogate recoveries (4.1.2), and laboratory control surrogate (LCS) recoveries (4.1.3). For blanks, chloroform showed no detections, while PCE showed an acceptably small percentage (3 to 9%) of detectable concentrations between the detection and reporting limits. All surrogate recoveries met the laboratory control acceptance criteria. Chloroform failed to meet the LCS recovery limits five times, while all PCE LCS recoveries met the control limits. These results being above the control limits suggest that a minority of the time the laboratory may be overestimating the concentration of chloroform and hexane by a factor of two times or less, which is acceptable quality for the study's data quality objectives.

4.1.1 Blanks

Field blanks, trip blanks, and laboratory blanks were used to evaluate false positives and/or high bias due to transport, storage, sample handling, and sorbent contamination.

- **Field blanks** were collected using a blank Radiello 130 cartridge from the media sample batch sent to the field from the laboratory. The cartridge was removed from the sealed storage vial and transferred to the diffusive housing in a similar manner to sample deployment. The cartridge was then immediately removed from the housing, returned to the storage vial, and sealed for shipment back to the laboratory with the field samples. In general, a field blank was collected with each shipment to the laboratory. A total of 67 field blanks were submitted over the duration of the project.
- **Trip blanks** were also assigned as blank Radiello cartridges from the media batches. The cartridge was not opened or removed from the storage vial but was sent back to the laboratory along with the field samples. There were 23 trip blanks submitted for analysis.
- For the **laboratory blanks**, a Radiello 130 cartridge was extracted with each analytical batch to measure background from the sorbent and the extraction process. A total of 120 unique lab blanks were analyzed and reported over the duration of the project.

To assist in data interpretation, all blank samples and all field sample results were evaluated down to the method detection limit (MDL). The results of the field, trip, and laboratory blanks are summarized in **Tables 4-1, 4-2, and 4-3**. The number of blanks with detections above the reporting limit (RL) and MDL are tabulated. Summary statistics were then calculated on this subset of positive detections.

⁷Measurements marked with an asterisk are designated as critical in the project QAPP.

Table 4-1. Indoor Air Passive Field Blank Summary—Radiello 130

| | RL (µg) | # FB Analyzed | FB Conc. > RL | RL > FB Conc. > MDL | % of Field Blanks with Detections | Mean Blank Conc. (µg) | Std. Dev. (µg) | Min (µg) | Max (µg) |
|--------------|---------|---------------|---------------|---------------------|-----------------------------------|-----------------------|----------------|----------|----------|
| Benzene | 0.4 | 67 | 0 | 58 | 87 | 0.122 | 0.04 | 0.04 | 0.21 |
| Chloroform | 0.1 | 67 | 0 | 0 | 0 | NA | NA | NA | NA |
| cis-1, 2-DCE | 0.1 | 67 | 0 | 0 | 0 | NA | NA | NA | NA |
| Hexane | 0.1 | 67 | 4 | 13 | 19 | 0.099 | 0.091 | 0.033 | 0.35 |
| PCE | 0.1 | 67 | 0 | 4 | 6 | 0.032 | 0.02 | 0.007 | 0.05 |
| Toluene | 0.1 | 67 | 1 | 25 | 37 | 0.044 | 0.037 | 0.014 | 0.17 |
| TCE | 0.1 | 67 | 0 | 5 | 7 | 0.015 | 0.009 | 0.006 | 0.03 |

NA= Not Applicable

Table 4-2. Indoor Air Passive Trip Blank Summary—Radiello 130

| | RL (µg) | # FB Analyzed | FB Conc. > RL | RL > FB Conc. > MDL | % of Trip Blanks with Detections | Mean Blank Conc. (µg) | Std. Dev. (µg) | Min (µg) | Max (µg) |
|--------------|---------|---------------|---------------|---------------------|----------------------------------|-----------------------|----------------|----------|----------|
| Benzene | 0.4 | 23 | 0 | 21 | 91 | 0.102 | 0.039 | 0.042 | 0.16 |
| Chloroform | 0.1 | 23 | 0 | 0 | 0 | NA | NA | NA | NA |
| cis-1, 2-DCE | 0.1 | 23 | 0 | 0 | 0 | NA | NA | NA | NA |
| Hexane | 0.1 | 23 | 0 | 10 | 43 | 0.049 | 0.012 | 0.036 | 0.07 |
| PCE | 0.1 | 23 | 0 | 2 | 9 | 0.015 | 0.009 | 0.009 | 0.02 |
| Toluene | 0.1 | 23 | 0 | 18 | 78 | 0.02 | 0.008 | 0.012 | 0.041 |
| TCE | 0.1 | 23 | 0 | 4 | 17 | 0.024 | 0.016 | 0.009 | 0.043 |

NA= Not Applicable

Table 4-3. Indoor Air Passive Laboratory Blank Summary—Radiello 130

| | RL (µg) | # LB Analyzed | LB Conc. > RL | RL > LB Conc. > MDL | % of Lab Blanks with Detections | Mean Blank Conc. (µg) | Std. Dev. (µg) | Min (µg) | Max (µg) |
|--------------|---------|---------------|---------------|---------------------|---------------------------------|-----------------------|----------------|----------|----------|
| Benzene | 0.4 | 120 | 9 | 113 | 94 | 0.1 | 0.056 | 0.038 | 0.34 |
| Chloroform | 0.1 | 120 | 10 | 0 | 0 | NA | NA | NA | NA |
| cis-1, 2-DCE | 0.1 | 120 | 0 | 0 | 0 | NA | NA | NA | NA |
| Hexane | 0.1 | 120 | 1 | 36 | 30 | 0.303 | 0.022 | 0.034 | 0.14 |
| PCE | 0.1 | 120 | 0 | 3 | 3 | 5.5 | 0.000 | 0.008 | 0.01 |
| Toluene | 0.1 | 120 | 3 | 72 | 60 | 0.454 | 0.026 | 0.005 | 0.13 |
| TCE | 0.1 | 120 | 0 | 5 | 4 | 0.372 | 0.006 | 0.013 | 0.03 |

NA= Not Applicable

Benzene was detected above the MDL but below the RL in a majority of the field, trip, and lab blanks at similar background levels. The average of the positive detections was 0.121, 0.102, and 0.1 µg for the field, trip, and lab blanks, respectively. The benzene blank levels are largely due to benzene contamination present in the carbon disulfide extraction solvent. Although the laboratory used high purity (99.99%) carbon disulfide reagent, benzene is present as a common contaminant in this solvent (White, 1964).

Although the benzene background levels were below the RL, a positive bias is expected for the daily Radiello and a large subset of the weekly indoor air samples. Longer duration samples would normally collect more mass and thus would not be significantly affected.

Hexane and toluene were also commonly detected in the field, trip, and lab blanks above the MDL. In the case of the field and lab blanks, some had concentrations above the RL for hexane and toluene. All detections in the trip blanks were below the RL but above the MDL. Similar to benzene, a positive bias for hexane and toluene is anticipated for the daily Radiello samples due to the blank levels.

Because benzene, hexane, and toluene have a relatively constant low level blank contribution from the media, the blank problems are more significant for the shortest duration samples (i.e., daily and to a lesser extent weekly). See Section 4.1.1 of U.S. EPA (2012a) for a full discussion of these issues.

No detections of chloroform or cis-1,2-dichloroethene (cis-1,2-DCE) were measured in any of the blanks. For a small percentage of the blanks, low concentration detections above the MDL were measured for tetrachloroethene (PCE) and trichloroethene (TCE).

In summary, the contaminants of most concern in this study showed either no blank detections (for chloroform) or an acceptably small percentage (3 to 9%) of low concentrations between the detection and reporting limits (for PCE). The contaminants with highest blank detections (benzene, toluene, and hexane) were not a primary focus for this study in that they were attributed to ambient outdoor air sources and did not come from vapor intrusion.

4.1.2 Surrogate Recoveries

To monitor extraction efficiency, 5.0 µg of toluene-d8 was spiked into each field sample and QC sample Radiello 130 cartridge immediately prior to extraction. The recoveries were evaluated against laboratory limits of 70 to 130%. All surrogate recoveries met the laboratory criterion, and summary statistics are presented in **Table 4-4**.

Table 4-4. Indoor Air Passive Surrogate Summary—Radiello 130

| Parameter | Result |
|---|--------|
| Number of surrogate recoveries measures | 1,681 |
| Average recovery (%R) | 103 |
| Standard deviation (%R) | 5.4 |
| Minimum recovery (%R) | 86 |
| Maximum recovery (%R) | 122 |

4.1.3 Laboratory Control Sample Recoveries

Accuracy of the extraction and analysis step for the target compounds was evaluated by analyzing an LCS. An unused Radiello cartridge was spiked with a standard containing 5.0 µg of each compound of

interest. The laboratory acceptance criterion for LCS recovery was 70 to 130%. Chloroform and hexane failed to meet the control limits five times each. These results being above the control limits suggest that a minority of the time the laboratory may be overestimating the concentration of chloroform and hexane by a factor of two times or less. Benzene, cis-1, 2-DCE, toluene, and TCE failed to meet the control limits once each. PCE LCS recoveries met the control limits. Summary statistics are presented in **Table 4-5**.

Table 4-5. Indoor Air Passive LCS Summary—Radiello 130

| | Number of LCS Analyzed | Mean LCS % Recovery | LCS Std Dev (%R) | Min (%R) | Max (%R) |
|-------------|------------------------|---------------------|------------------|----------|----------|
| Benzene | 113 | 96 | 14 | 70 | 147 |
| Chloroform | 113 | 100 | 17 | 70 | 206 |
| cis-1,2-DCE | 113 | 99 | 14 | 72 | 192 |
| Hexane | 113 | 103 | 20 | 71 | 219 |
| PCE | 113 | 100 | 11 | 80 | 130 |
| Toluene | 113 | 97 | 11 | 76 | 131 |
| TCE | 113 | 101 | 11 | 78 | 148 |

4.1.4 Duplicates

Sample precision was evaluated by collecting field duplicates and by analyzing LCSDs. Field duplicates were collected for approximately every 10 field samples, and an LCSD was prepared and analyzed with each sample preparation batch. Because the LCSD was a second cartridge prepared and extracted in the same manner as the LCS, the relative percentage difference (%RPD) represents the precision of the analytical method from extraction through analysis. The method precision is summarized in **Table 4-6**. The laboratory acceptance criterion of %RPD < 25% was met by PCE, toluene, and TCE but exceeded in 2 batches by benzene, 5 by chloroform, 1 by cis-1, 2-DCE, and 11 by hexane.

Table 4-6. Indoor Air Passive Laboratory Precision (LCS/LCSD) Summary—Radiello 130

| | Number of LCSD Analyzed | Mean %RPD | Std Dev. (%RPD) | Min (%RPD) | Max (%RPD) | Number of Exceedances |
|-------------|-------------------------|-----------|-----------------|------------|------------|-----------------------|
| Benzene | 113 | 9 | 8 | 0 | 42 | 2 |
| Chloroform | 113 | 10 | 8 | 0 | 35 | 0 |
| cis-1,2-DCE | 113 | 5 | 5 | 0 | 31 | 0 |
| Hexane | 113 | 13 | 11 | 0 | 47 | 5 |
| PCE | 113 | 4 | 4 | 0 | 19 | 0 |
| Toluene | 113 | 5 | 5 | 0 | 19 | 0 |
| TCE | 113 | 5 | 4 | 0 | 20 | 0 |

4.2 VOC Sampling—Subslab and Soil Gas (TO-17)—U.S. EPA

4.2.1 Blanks

Field, trip, refrigerator, and laboratory blanks were used to evaluate false positives and/or high bias due to transport, storage, sample handling, and sorbent contamination. Field blanks were collected using a blank Tenax TA TO-17 sorbent tube from the media sample batch sent to the field from the laboratory. The Swagelok end caps were removed as if to prepare for sample collection; however, no soil vapor was pulled through the tube. The end caps were immediately replaced, and the tube was sent back to the laboratory with the field samples. Typically, a field blank was collected with each shipment to the laboratory. A total of 121 field blanks were submitted over the duration of the project.

Blank Tenax TA TO-17 sorbent tubes from the media batches were also assigned as trip blanks. The tube remained capped and wrapped in aluminum foil and was sent from the laboratory to the field and back to the laboratory along with the field samples. There were 111 trip blanks submitted for analysis.

In the case of the laboratory blank, a Tenax TA TO-17 tube was analyzed with each analytical batch to measure background from the sorbent tubes and instrumentation. A total of 387 lab blanks were analyzed and reported over the duration of the project.

For a refrigerator (fridge) blank, a Tenax TA TO-17 tube was stored and analyzed with each sample batch to measure background from the sample storage refrigerator. The tubes were stored in the refrigerator capped and sealed in a zip lock bag on top of the jars containing the samples that were received as a batch. The fridge blanks were placed in the refrigerator with a sample batch and remained in the refrigerator with the batch until all the samples from that batch had been analyzed. So, the fridge blanks were in the refrigerator longer than some of the samples within a batch. A total of 61 fridge blanks were analyzed and reported over the duration of the project.

To assist in data interpretation, all blank samples and all field sample results were evaluated down to the MDL. The results of the field, trip, laboratory, and fridge blanks are summarized in **Tables 4-7, 4-8, 4-9, and 4-10**. The number of blanks with detections above the RL and MDL are tabulated. Summary statistics were then calculated on this subset of positive detections.

Table 4-7. Subslab and Soil Gas—EPA Field Blank Summary—TO-17

| | RL (ng) | Number of Field Blanks | | | % of Field Blanks with Detections | Mean Blank Conc. (ng) | Std. Dev. (ng) | Min (ng) | Max (ng) |
|--------------------|---------|------------------------|------------|------------------|-----------------------------------|-----------------------|----------------|----------|----------|
| | | Analyzed | Conc. > RL | RL > Conc. > MDL | | | | | |
| Benzene | 5.0 | 121 | 0 | 53 | 44 | 1.4 | 0.5 | 0.81 | 3.0 |
| Carbon disulfide | 5.0 | 121 | 0 | 9 | 7 | 3.4 | 1.4 | 1.7 | 6.4 |
| Chloroform | 2.0 | 121 | 5 | 0 | 4 | 72 | 110 | 3.0 | 260 |
| cis-1,2-DCE | 2.0 | 121 | 0 | 1 | 1 | 1.5 | N/A | 1.5 | 1.5 |
| Hexane | 10 | 121 | 0 | 2 | 2 | 1.6 | 1.5 | 2.2 | 4.4 |
| Methylene chloride | 50 | 121 | 0 | 9 | 9 | 8.7 | 5.2 | 2.5 | 19 |
| PCE | 2.0 | 121 | 9 | 0 | 7 | 9.6 | 4.3 | 2.1 | 10 |
| Toluene | 5.0 | 121 | 0 | 18 | 15 | 2.2 | 2.0 | 1.1 | 7.7 |
| TCE | 2.0 | 121 | 1 | 0 | 1 | 2.8 | N/A | 2.8 | 2.8 |

N/A = Not Applicable

Table 4-8. Subslab and Soil Gas—EPA Trip Blank Summary—TO-17

| | RL (ng) | Number of Trip Blanks | | | % of Trip Blanks with Detections | Mean Blank Conc. (ng) | Std. Dev. (ng) | Min (ng) | Max (ng) |
|--------------------|---------|-----------------------|------------|----------------|----------------------------------|-----------------------|----------------|----------|----------|
| | | Analyzed | Conc. > RL | RL>Conc. > MDL | | | | | |
| Benzene | 5.0 | 111 | 0 | 38 | 34 | 1.3 | 0.5 | 0.81 | 2.6 |
| Carbon disulfide | 5.0 | 111 | 0 | 9 | 8 | 2.6 | 0.8 | 1.6 | 4.0 |
| Chloroform | 2.0 | 111 | 6 | 1 | 6 | 32 | 41 | 2.0 | 120 |
| cis-1,2-DCE | 2.0 | 111 | 0 | 0 | 0 | 0 | 0 | 0 | 0 |
| Hexane | 10 | 111 | 0 | 2 | 2 | 2.0 | 1.5 | 1.0 | 3.0 |
| Methylene chloride | 50 | 111 | 0 | 4 | 4 | 2.8 | 0.8 | 2.2 | 4.0 |
| PCE | 2.0 | 111 | 4 | 0 | 4 | 18 | 11 | 2.3 | 27 |
| Toluene | 5.0 | 111 | 3 | 20 | 21 | 3.1 | 4.1 | 1.0 | 19 |
| TCE | 2.0 | 111 | 2 | 0 | 2 | 3.7 | 2.0 | 2.3 | 5.2 |

Table 4-9. Subslab and Soil Gas—EPA Laboratory Blank Summary—TO-17

| | RL (ng) | Number of Lab Blanks | | | % of Lab Blanks with Detections | Mean Blank Conc. (ng) | Std. Dev. (ng) | Min (ng) | Max (ng) |
|--------------------|---------|----------------------|------------|----------------|---------------------------------|-----------------------|----------------|----------|----------|
| | | Analyzed | Conc. > RL | RL>Conc. > MDL | | | | | |
| Benzene | 5.0 | 387 | 7 | 99 | 27 | 1.8 | 1.9 | 0.80 | 12 |
| Carbon disulfide | 5.0 | 387 | 4 | 42 | 12 | 9.6 | 9.2 | 0.87 | 52 |
| Chloroform | 2.0 | 387 | 16 | 2 | 5 | 3.4 | 1.7 | 1.3 | 5.8 |
| cis-1,2-DCE | 2.0 | 387 | 0 | 4 | 1 | 4.1 | 0.7 | 4.9 | 3.4 |
| Hexane | 10 | 387 | 1 | 10 | 3 | 4.9 | 5.6 | 1.5 | 21 |
| Methylene chloride | 50 | 387 | 0 | 8 | 2 | 3.2 | 1.2 | 2.4 | 5.6 |
| PCE | 2.0 | 387 | 4 | 8 | 3 | 1.8 | 1.2 | 0.7 | 4.1 |
| Toluene | 5.0 | 387 | 5 | 47 | 13 | 2.7 | 3.4 | 1.0 | 16 |
| TCE | 2.0 | 387 | 4 | 3 | 2 | 5.6 | 5.3 | 1.4 | 16 |

N/A = Not Applicable

Table 4-10. Subslab and Soil Gas—EPA Fridge Blank Summary—TO-17

| | RL (ng) | Number of Fridge Blanks | | | % of Fridge Blanks with Detections | Mean Blank Conc. (ng) | Std. Dev. (ng) | Min (ng) | Max (ng) |
|--------------------|------------|-------------------------|---------------|-------------------|--|--------------------------------|----------------------|-------------|-------------|
| | | Analyzed | Conc. > RL | RL>Conc. > MDL | | | | | |
| Benzene | 5.0 | 61 | 0 | 22 | 36 | 1.2 | 0.40 | 0.81 | 1.8 |
| Carbon disulfide | 5.0 | 61 | 0 | 2 | 3 | 2.3 | 0.69 | 1.8 | 2.8 |
| Chloroform | 2.0 | 61 | 2 | 0 | 3 | 2.3 | 0.29 | 2.1 | 2.5 |
| cis-1,2-DCE | 2.0 | 61 | 0 | 0 | 0 | 0 | 0 | 0 | 0 |
| Hexane | 10 | 61 | 0 | 3 | 5 | 1.0 | 0.08 | 0.88 | 1.0 |
| Methylene chloride | 50 | 61 | 0 | 4 | 7 | 6.1 | 7.5 | 1.8 | 17 |
| PCE | 2.0 | 61 | 6 | 4 | 16 | 3.2 | 1.7 | 0.8 | 3.5 |
| Toluene | 5.0 | 61 | 5 | 11 | 26 | 8.5 | 20 | 0.96 | 82 |
| TCE | 2.0 | 61 | 8 | 1 | 15 | 7.4 | 4.6 | 1.5 | 17 |

Benzene was detected above the MDL in 44%, 34%, 27%, and 36% of the field (Figure 4-7), trip (Figure 4-8), laboratory (Figure 4-9), and fridge (Figure 4-10) blanks, respectively. The average of the positive detections was 1.4, 1.3, 1.8, and 1.2 nanogram (ng) for the field, trip, lab, and fridge blanks, respectively. Seven laboratory blanks had benzene concentrations above the RL of 5.0 ng. The benzene blank levels are largely due to background contribution from the Tenax TA polymer, which can break down during the heating step to generate low levels of benzene (Middleditch, 1989).

The concentrations of benzene in the TO-17 soil vapor samples were similar in magnitude to those measured in the field blanks. Of the 2844 TO-17 soil vapor samples analyzed by EPA, 59% of the samples had a positive detection of benzene. Of the samples that had a positive detection for benzene, only 2% had a detected concentration above the RL of 5.0 ng. The second most common contaminant in these blank samples was toluene, which has also been reported as a Tenax breakdown product (MacLeod and Ames, 1986; Cao and Hewitt, 1994).

Detections of the key compounds that form the focus of this work—PCE, chloroform, and TCE—occurred in 3% or less of the hundreds of samples and field, trip, and lab blanks analyzed. However, the percentage of refrigerator blanks with PCE and TCE contamination was considerably higher—16%.

4.2.2 Calibration Verification

The calibration relationship established during the initial calibration was verified at the beginning of each 24-hour analytical shift using a calibration verification standard concentration equal to the mid-point of the initial calibration range. If the analyte concentration was within $\pm 30\%$ (40% for Carbon Disulfide and Methylene Chloride) of the expected concentration of the calibration verification standard, then the initial calibration was considered valid, and the analysis of samples was continued. Most analyte calibration verification standard recoveries met the QAPP established criterion, and summary statistics are presented in **Table 4-11**.

Table 4-11. EPA TO-17 Calibration Verification (CV) Summary

| | Number of CV Analyzed | Mean CV % Recovery | CV Std Dev (%R) | Min (%R) | Max (%R) | CV Recovery Limits | Number of Exceedances |
|--------------------|-----------------------|--------------------|-----------------|----------|----------|--------------------|-----------------------|
| Benzene | 665 | 97 | 18 | 2 | 276 | 70–130% | 22 |
| Carbon disulfide | 665 | 84 | 52 | 0 | 664 | 60–140% | 251 |
| Chloroform | 665 | 91 | 19 | 0 | 298 | 70–130% | 53 |
| cis-1,2-DCE | 665 | 95 | 20 | 0 | 268 | 70–130% | 45 |
| Hexane | 665 | 93 | 20 | 0 | 262 | 70–130% | 51 |
| Methylene chloride | 665 | 94 | 67 | 0 | 818 | 60–140% | 266 |
| PCE | 665 | 87 | 17 | 0 | 262 | 70–130% | 75 |
| Toluene | 665 | 98 | 18 | 0 | 286 | 70–130% | 23 |
| TCE | 665 | 95 | 17 | 0 | 276 | 70–130% | 19 |

4.2.3 Internal Standard Recoveries

Two internal standards were utilized in the calibration of the TO-17 analytical instrumentation, 1,4-difluorobenzene and chlorobenzene-d5. 4.7 ng of 1,4-difluorobenzene and 4.8 ng of chlorobenzene-d5 in a gas phase standard were automatically introduced into the sample flow path by the instrumentation during the initial tube desorption of all samples. The internal standard calibration was used to account for routine variation in the response of the chromatographic system as well as variations in the exact volume of sample introduced into the chromatographic system. The recoveries were evaluated against the QAPP established criteria of 60 to 140% recovery. Most internal standard recoveries met the QAPP established criterion, and summary statistics are presented in **Table 4-12**.

Table 4-12. EPA TO-17 Internal Standard (IS) Summary

| | Number of IS Analyzed | Mean IS % Recovery | IS Std Dev (%R) | Min (%R) | Max (%R) | IS Recovery Limits | Number of Exceedances |
|---------------------|-----------------------|--------------------|-----------------|----------|----------|--------------------|-----------------------|
| 1,4-Difluorobenzene | 4620 | 99 | 34 | 15 | 373 | 60–140% | 907 |
| Chlorobenzene-d5 | 4620 | 99 | 30 | 18 | 358 | 60–140% | 776 |

4.2.4 Surrogate Recoveries

To monitor analytical efficiency, 5.3 ng of bromochloromethane were loaded onto each QC and field sample sorbent tube along with the vapor phase internal standard mix during sample analysis. Field surrogates were not included in the scope of this project. The recoveries were evaluated against laboratory limits of 70 to 130%. Most surrogate recoveries met the QAPP established criterion, and summary statistics are presented in **Table 4-13**.

Table 4-13. EPA TO-17 Surrogate Recovery Summary

| Parameter | Result |
|---|--------|
| Number of surrogate recoveries measured | 4,620 |
| Average recovery (%R) | 105 |
| Standard deviation (%R) | 14 |
| Minimum recovery (%R) | 22 |
| Maximum recovery (%R) | 360 |

4.2.5 Laboratory Control Sample Recoveries

Analytical accuracy was evaluated by analyzing an LCS. Two clean Tenax TA TO-17 sorbent tubes were spiked with a calibration standard from a source independent from the primary calibration standard and analyzed after each initial calibration. The spike contained approximately 100 nanograms of each target compound. The performance of the EPA TO-17 LCS spikes is summarized in **Table 4-14**. A total of 10 LCS samples were evaluated, and all met the laboratory RLs with the exceptions of five outliers for carbon disulfide, four outliers for methylene chloride, and one outlier for cis-1,2-DCE.

Table 4-14. EPA TO-17 Laboratory Control Sample (LCS) Summary

| | Number of LCS Analyzed | Mean LCS % Recovery | LCS Std Dev (%R) | Min (%R) | Max (%R) | LCS Recovery Limits | Number of Exceedances |
|--------------------|------------------------|---------------------|------------------|----------|----------|---------------------|-----------------------|
| Benzene | 10 | 101 | 11 | 86 | 118 | 70–130% | 0 |
| Carbon disulfide | 10 | 117 | 64 | 24 | 272 | 70–130% | 5 |
| Chloroform | 10 | 96 | 11 | 82 | 122 | 70–130% | 0 |
| cis-1,2-DCE | 10 | 105 | 10 | 96 | 133 | 70–130% | 1 |
| Hexane | 10 | 98 | g11 | 72 | 120 | 70–130% | 0 |
| Methylene chloride | 10 | 111 | 71 | 29 | 291 | 70–130% | 4 |
| PCE | 10 | 85 | 8.1 | 71 | 97 | 70–130% | 0 |
| Toluene | 10 | 102 | 13 | 80 | 128 | 70–130% | 0 |
| TCE | 10 | 100 | 12 | 80 | 120 | 70–130% | 0 |

4.2.6 Field Duplicates

Sample precision was evaluated by collecting field duplicates. Field duplicates were collected for approximately every 10 field samples. The sample precision is summarized in **Table 4-15**. The laboratory acceptance criterion of %RPD < 50% was met by PCE, toluene, and TCE but exceeded in 2 batches by benzene, 5 by chloroform, 1 by cis-1, 2-DCE, and 11 by hexane.

Table 4-15. EPA TO-17 Field Duplicate Summary

| | Number Analyzed | Mean %RPD | Std Dev. (%RPD) | Min (%RPD) | Max (%RPD) | Number of Sample Exceedances |
|-------------|-----------------|-----------|-----------------|------------|------------|------------------------------|
| Benzene | 173 | 40 | 36 | 0 | 163 | 35 |
| Chloroform | 173 | 30 | 49 | 0 | 197 | 26 |
| cis-1,2-DCE | 173 | 21 | 32 | 1 | 106 | 2 |
| Hexane | 173 | 45 | 34 | 13 | 119 | 5 |
| PCE | 173 | 23 | 40 | 0 | 197 | 20 |
| Toluene | 173 | 27 | 23 | 0 | 91 | 8 |
| TCE | 173 | 38 | 50 | 0 | 173 | 8 |

4.3 Online Gas Chromatograph (Soil Gas and Indoor Air)

The online GC was used in three distinct mobilization periods each of which had some differences in instrument setup. These analyses were provided by Hartman Environmental Geosciences with logistical support from ARCADIS. Therefore, we refer to these data sets in this discussion of QA checks as

- Hartman 1 = August 11, 2011, to October 17, 2011;
- Hartman 2 = December 1, 2011, to February 26, 2012; and
- Hartman 3 = December 14, 2012, to March 8, 2013.

4.3.1 Blanks

Instrument blanks were analyzed at least once per analysis cycle of the 12 sampling locations. Nitrogen or outdoor air was analyzed at the beginning of the analysis cycle (stream selector valve port #1). System blanks (no vapor sample injected) were analyzed twice per analysis cycle at the end of the analysis cycle (stream selector valve ports #15 and #16) from August 26, 2011, through February 26, 2012.

Environmental analytical data are normally compared with blank data using approaches suitable for very small numbers of samples (often just one blank vs. one sample). For example, data are often qualified if the sample does not exceed a certain multiple of the blank concentration.⁸ However, this approach is no longer a mandatory requirement of the EPA functional guidelines for low concentration VOCs (U.S. EPA, 2008b). Those guidelines now call for professional judgment in cases where the sample result exceeds the blank result itself. In this case, given that we have hundreds of measurements of indoor air and either a blank or atmospheric air taken with the same instrument, it is appropriate to use other statistical tests to judge whether the samples are significantly different from the blank (or atmospheric air control).

4.3.2 Initial Calibration

For Hartman Period 1 (August 11, 2011, to October 17, 2011), initial calibration curves for PCE and chloroform were performed at the start of the monitoring program as follows:

- PCE: Two points at concentrations of 14 $\mu\text{g}/\text{m}^3$ and 70 $\mu\text{g}/\text{m}^3$

⁸http://140.194.76.129/publications/eng-manuals/EM_200-1-10/c-10.pdf

- CHCl₃: A single point at a concentration 10 µg/m³, with a separate linearity study after the initial deployment

Additional calibration points were not possible because of uncertainties with the calibration standards brought to the site during instrument set-up.

For Hartman Period 2 (December 1, 2011, to February 16, 2012), initial calibrations were as follows:

- PCE low range: six points at concentrations from 0.7 µg/m³ to 23 µg/m³
- PCE high range: three points at concentrations from 3.5 µg/m³ to 69 µg/m³
- CHCl₃ low range: four points at concentrations from 3.3 µg/m³ to 55 µg/m³
- CHCl₃ high range: three points at concentrations from 55 µg/m³ to 270 µg/m³

For Hartman Period 3, the chloroform and PCE calibration ranges were:

- CHCl₃: 1.0 to 250 µg/m³, 6 calibration points
- TCE: 5.5 to 220 µg/m³, 6 calibration points
- PCE: 0.69 to 280 µg/m³, 8 calibration points

Although a formal MDL determination was not conducted for the Hartman 1 and Hartman 2 field GC periods, a formal MDL determination based on seven repetitive injections of a standard was performed for Hartman 3. For the other periods, the MDL was estimated based on three times the concentration observed in repetitive injections of nitrogen blanks or background air. This field MDL and PQL information and its basis are summarized in **Table 4-16**. As discussed in Section 4.5.1, this three-times blank (or ambient air) definition of a detection is more stringent than required by current EPA functional guidelines and probably does not adequately capture the sensitivity of a data set with hundreds of repetitive analyses of both the target atmosphere and the blank (or ambient air).

Table 4-16. Field GC Estimated Minimum Detection Limits and Practical Quantitation Limits

| Period | Dates | CHCl ₃ | | PCE | PQL Low Cal µg/m ³ |
|-----------|----------------|--------------------------|----------------------------------|--------------------------|----------------------------------|
| | | MDL µg/m ³ | PQL Low Cal µg/m ³ | MDL µg/m ³ | |
| Hartman 1 | 8/2011–10/2011 | 1 | 10 | 0.84 | 14 |
| Hartman 2 | 12/2011–2/2012 | 0.7 | 0.6 | 0.9–1.2 | 0.69 |
| Hartman 3 | 12/2012–3/2013 | 0.7 | 1.0 | 0.7 | 0.69 |

Notes:

MDLs computed as three times air blanks

CHCl₃ MDL from actual analyses; PCE from three times air blank

MDLs for PCE calculated from 14 runs of a low concentration standard

4.3.3 Continuing Calibration

Continuing calibration was not performed using the compounds of primary interest because of the concern that the calibration standard could contaminate the indoor air values (since it necessarily would be stored within the study duplex). Instead a surrogate compound, TCE, was used for continuing calibration. The TCE was plumbed to stream selector port #14 with the intent it would be analyzed in every analytical cycle of the 16 ports. However, during both the Hartman 1 and 2 periods of the program, the TCE calibration standard quickly ran out because of a leak at port 14 in the stream selector valve. As

an alternative, a calibration check comparing the performance of the field instrument to a laboratory-based instrument with site sample was performed as discussed in the next section for those periods. The valve was replaced before Hartman 3.

The Hartman 3 data set had a continuing calibration standard that was repeatedly analyzed for 332 successive analyses over the first 48 days of the operational period until it was exhausted (**Figure 4-1**). For those analyses, the mean was $74.20 \mu\text{g}/\text{m}^3$ with a standard deviation of 0.99, indicating a very stable measurement with a variability range well within $\pm 2 \mu\text{g}/\text{m}^3$. The TCE concentration in this standard was measured at $32 \mu\text{g}/\text{m}^3$ by H&P Laboratories.

After the continuing calibration standard was exhausted on January 31, attempts were made to provide additional calibration standards. These culminated in a final calibration run between March 7 and March 11 reported in Section 4.5.4. Taken together, these approaches to continuing calibration suggest that the instrument maintained precision well within the quality assurance project plan (QAPP) established precision goal of $\pm 25\%$.

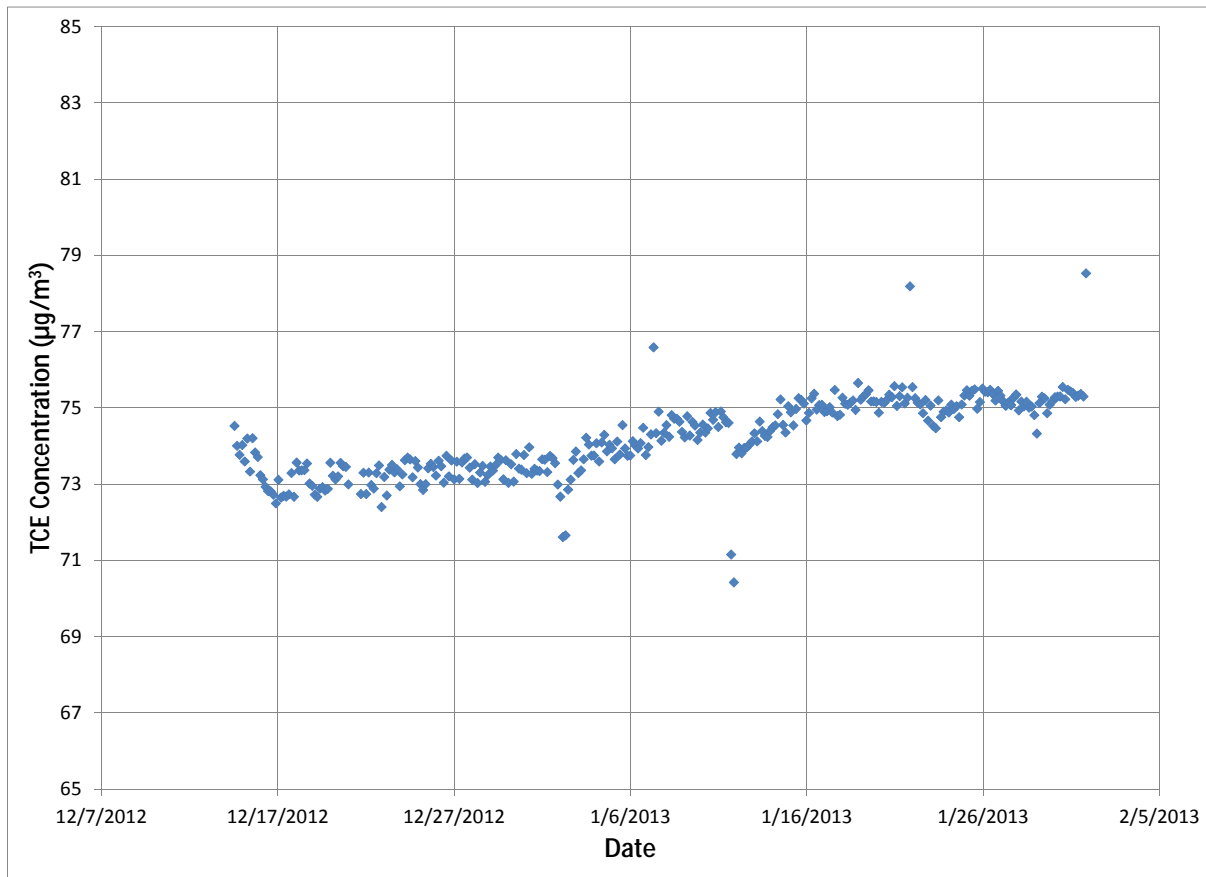


Figure 4-1. TCE Continuing Calibration Standard Analyses, Hartman 3 Period.

4.3.4 Calibration Check via Comparison to Fixed Laboratory (TO-15 vs. Online GC)

Verification samples were collected and analyzed by H&P Mobile Geochemistry during each sampling period as follows. The H&P fixed base lab is certified for a variety of tests such as EPA 8260B, EPA TO-15, and CA LUFT/8015m. Key certifying bodies include:

- U.S. Department of Defense, Environmental Laboratory Accreditation Program (DoD-ELAP) - PJLA Accreditation No. 69070 - Certificate No. L11-175 (Methods: H&P-SOP 8260SV; EPA 8260B; EPA TO15; EPA TO14A; H&P-SOP-TO15M)
- California Department of Public Health, Environmental Laboratory Accreditation Program, (ELAP) Certificate No. 2741; and
- New York State Department of Health, National Environmental Laboratory Accreditation Conference (NELAC) Standards Certificate Lab ID No. 11845

Hartman Period 1: An indoor air sample was collected from the 422 first floor on October 11, 2011, and compared with the on-site instrument to check on the reported concentration values. The results were as follows ($\mu\text{g}/\text{m}^3$):

| | On-site GC | H&P TO-15 |
|-------------------|------------|-----------|
| CHCl ₃ | 1.7 | 0.8 |
| PCE | 3 | 1.3 |

In addition, a 24-hour time composite indoor air sample was collected from the 422 first floor and the basement on September 22, 2011, and compared with the on-site instruments values over the same time period to check on the reported low concentration values. The results were as follows ($\mu\text{g}/\text{m}^3$):

| | On-site GC | ATL TO-15 |
|-------------------------|------------|-----------|
| <i>422 first floor:</i> | | |
| CHCl ₃ | 1.0 | 0.24 |
| PCE | 1.75 | 0.40 |
| <i>422 basement:</i> | | |
| CHCl ₃ | 1.7 | 0.41 |
| PCE | 3.5 | 0.94 |

Based on these data and the data summarized in Section 4.5.6, we decided that the online GC chloroform low values ($<5 \mu\text{g}/\text{m}^3$) could be adjusted down by a factor of 2 and the online GC PCE low values ($<5 \mu\text{g}/\text{m}^3$) could be adjusted down by a factor of 3. Alternatively, the generally low bias exhibited by the Hartman Period 1 samples could be adequate justification to not use these data in subsequent analysis or at least to regard any conclusions drawn as less reliable than those drawn from the Periods 2 and 3 data.

Hartman Period 2: A sample was collected from probe SP8-9 on December 11, 2011, and compared with the on-site instrument. The results were as follows ($\mu\text{g}/\text{m}^3$):

| | On-site GC | H&P TO-15 |
|-------------------|------------|-----------|
| CHCl ₃ | 118 | 100 |
| PCE | 140 | 160 |

Based on these results, no adjustments in the online GC data were made.

Hartman Period 3: A final calibration check was performed between March 7 and March 11, 2013. During that period, 26 successive analyses of the same Hartman Environmental-prepared standard⁹ were performed and the results compared with an analysis of the standard performed at a fixed based

⁹The standard was prepared in a Tedlar bag by diluting a liquid standard into 1,000 cc and was analyzed using TO-15 and the auto GC. The target concentration range was 10 to 100 $\mu\text{g}/\text{m}^3$.

laboratory. The results indicated excellent precision and good accuracy for TCE (**Table 4-17**) and PCE (**Table 4-18**).

Table 4-17. Result of Repeated TCE Calibration Standard Analyses on On-line GC in March 2013 (Hartman Period 3)

| TCE | | | |
|------------|-----------|-------|-------------------|
| Hartman GC | Average | 9.68 | µg/m ³ |
| | Stdevp | 0.57 | µg/m ³ |
| %RPD | Precision | 5.9% | |
| | H&P value | 8.12 | µg/m ³ |
| Accuracy | % RPD | 17.6% | |

Table 4-18. Results of Repeated PCE Calibration Standard Analyses on Online GC in March 2013 (Hartman Period 3)

| PCE | | | |
|------------|-----------|--------|-------------------|
| Hartman GC | Average | 6.99 | µg/m ³ |
| | Stdevp | 0.51 | µg/m ³ |
| | Precision | 7.3% | |
| | H&P Value | 8.25 | µg/m ³ |
| Accuracy | % RPD | -16.5% | |

4.3.5 Agreement of Online GC Results with TO-17 Verification Samples

Early in the Hartman 1 period, ATL prepared four 3 L Tedlar bags each containing approximately 2 L of vapor labeled A, B, C, and D and sent them to the Indianapolis field site. Bags A and B were duplicate nitrogen blanks. Bags C and D were duplicate spikes with chloroform, TCE, and PCE drawn from a common Summa canister. Analyses were performed of these bags using the online GC and by ARCADIS staff collecting TO-17 samples directly from the bags and submitting them to NERL for analysis. ATL also performed analyses before sending the bags to Indianapolis and after their return from the field. Results of these interlaboratory comparisons are provided in **Table 4-19**, and statistical comparison is provided in **Table 4-20**. The agreement between the two fixed based laboratories where the RPD is <25% is excellent; this is a considerably narrower range than is often seen in method VOC method intercomparison studies (Lutes 2010B). The agreement between the field instrument and the fixed based laboratories with all RPDs <50% is somewhat lesser, but still reasonable given that RPDs that large are sometimes seen between fixed based laboratories running the same method (Lutes, 2010b) and that this comparison is between methods - between an automated GC-ECD and an attended GC-MS.

Table 4-19. Interlaboratory Results: Spiked Verification Samples

| Bag | Laboratory | Subsample Date | Analysis Date | PCE flag | PCE ug/m ³ | PCE ppbv | TCE flag | TCE ug/m ³ | TCE ppbv | Chloroform Flag | Chloroform ug/m ³ | Chloroform ppbv |
|-----|------------|----------------|---------------|----------|-----------------------|----------|----------|-----------------------|----------|-----------------|------------------------------|-----------------|
| D | Air Toxics | 8/9/2011 | 8/9/2011 | | | 21 | | | 34 | | | 42 |
| A | Hartmann | 8/11/2011 | 8/11/2011 | < | | 2 | < | | 2 | < | | 2 |
| B | Hartmann | 8/11/2011 | 8/11/2011 | < | | 2 | < | | 2 | < | | 2 |
| C | Hartmann | 8/11/2011 | 8/11/2011 | | | 20 | | | 28 | | | 40 |
| D | Hartmann | 8/11/2011 | 8/11/2011 | | | 20 | | | 23 | | | 40 |
| C | Air Toxics | 8/12/2011 | 8/12/2011 | | | 13 | | | 16 | | | 20 |
| D | Air Toxics | 8/12/2011 | 8/12/2011 | | | 12 | | | 16 | | | 21 |
| B | EPA NERL | 8/10/2011 | 8/14/2011 | U | 8.5 | 1.2 | U | 6.7 | 1.2 | B | 12 | 2.4 |
| A | EPA NERL | 8/10/2011 | 8/14/2011 | U | 8.5 | 1.2 | U | 6.7 | 1.2 | U | 6.2 | 1.3 |
| D | EPA NERL | 8/10/2011 | 8/14/2011 | | 85 | 12.3 | | 110 | 20.1 | | 140 | 28.2 |
| B | EPA NERL | 8/10/2011 | 8/14/2011 | U | 8.5 | 1.2 | U | 6.7 | 1.2 | B | 12 | 2.4 |
| A | EPA NERL | 8/10/2011 | 8/14/2011 | U | 8.5 | 1.2 | U | 6.7 | 1.2 | B | 11 | 2.2 |
| D | EPA NERL | 8/10/2011 | 8/14/2011 | | 80 | 11.6 | | 110 | 20.1 | | 130 | 26.2 |
| C | EPA NERL | 8/10/2011 | 8/14/2011 | | 89 | 12.9 | | 110 | 20.1 | | 140 | 28.2 |
| C | EPA NERL | 8/10/2011 | 8/14/2011 | | 84 | 12.2 | | 110 | 20.1 | | 130 | 26.2 |

Table 4-20. Interlaboratory Statistics: Spiked Verification Samples

| Data Summary for Interlab Data | | Interlab Comparison | | | | | |
|--------------------------------|----------------|--|----------------|----------------|--------------------------|------------------------|------------------------|
| | | Standard Samples after Pooling c and d: Interlab Comparison Using Standard Results | | | | | |
| | | Mean (ppbv) | | | % Difference (% error)** | | |
| Chemical | Actual (TO-15) | Air Toxics (N=3) | EPA NERL (N=4) | Hartmann (N=2) | Air Toxics vs. EPA NERL | Air Toxics vs. Hartman | Air Toxics vs. Hartman |
| Chloroform | 42 | 27.7 | 27.2 | 40.0 | 1.64 | 38.03 | 36.45 |
| Tetrachloroethene | 21 | 15.3 | 12.3 | 20.0 | 22.24 | 47.95 | 26.42 |
| Trichloroethene | 34 | 22.0 | 20.1 | 25.5 | 8.80 | 23.46 | 14.74 |

4.3.6 Agreement of Integrated Online GC Results with Passive Samplers

4.3.6.1 Hartman Periods 1 and 2

Table 4-21 and **Figures 4-2** and **4-3** compare the concentrations measured by the 1-week Radiello samples to the concentrations calculated by averaging the online GC results. In **Figures 4-2** and **4-3**, the Radiello chloroform (red) and PCE (aqua) concentrations are plotted against their corresponding weekly average GC values for Hartman 1 and Hartman 2, respectively. The grey line in each figure has a slope of 1 and an intercept of 0 and represents the ideal case where GC and Radiello measurements match exactly. Most of the time, the weekly GC sample averages are higher than the corresponding Radiello weekly samples, suggesting a consistent positive bias for the GC or a negative bias for the Radiellos. However, this difference is small (mostly less than a factor of 2; **Table 4-21**), and the data are still usable, given the purpose of the GC and weekly Radiello data, to measure short-term and long-term variability in indoor air VOC concentrations.

For chloroform, agreement is generally remarkably good for the first 4 weeks of instrument operation. The results for this period are generally within 50 relative percent difference, which we considered good for this comparison between two different methods, given that variability in interlaboratory comparisons for split samples of VOCs using one method can be larger. Expressed as a ratio during this period the online GC result is always between 0.6 and 1.9 times the Radiello result.

However, for chloroform, agreement is noticeably worse in succeeding weeks (after September 14, 2011). Generally the chloroform values reported from the online GC are one to three times higher than the values from the corresponding Radiello sample, although higher ratios up to six times higher were occasionally observed, associated with the lowest concentration Radiello results. During the period when ambient samples were also collected with the online GC, those results tended to be a more significant fraction of the measured indoor air values than was seen in the Radiello samples. This suggests the possible existence of an elevated baseline in the online GC data.

Results were considerably improved in Hartman Period 2 over the results in the later portions of Period 1 (see **Figure 4-2**). This may be due to the instrument setup changes that were made (as described in Section 3.4.3). This may also be due to the higher concentrations available for analysis in the field samples. In general, the agreement across all periods is better at higher concentration levels (>0.5 µg/m³). Hartman Period 1 was the only period conducted under summer conditions.

For PCE, the relationship between the online GC and the Radiello samples appears more stable with the vast majority of the results showing online GC results one to three times higher than the corresponding Radiello data.

Table 4-21. Comparison of Online GC to Radiello Results by Week

| Start Date Time | Stop Date Time | Period | Location | Compound | Radiello ($\mu\text{g}/\text{m}^3$) | GC: Missing Values = 1/2 MDL ($\mu\text{g}/\text{m}^3$) | GC: Missing values = MDL ($\mu\text{g}/\text{m}^3$) | GC: Missing values = NGC ($\mu\text{g}/\text{m}^3$) | RPD Calculated with Missing Values = 1/2 MDL | RPD Calculated with Missing values = MDL | RPD Calculated with Missing values = NGC | Ratio (online GC/Radiello) Calculated with Missing Values = 1/2 MDL | Ratio (online GC/Radiello) Calculated with Missing values = MDL | Ratio (online GC/Radiello) Calculated with Missing values = NGC |
|-----------------|-----------------|----------|----------|-------------------|--|---|---|---|---|---|---|---|---|---|
| 8/17/2011 22:55 | 8/24/2011 21:21 | Hartman1 | 420BaseS | Tetrachloroethene | 0.38 | 0.695027 | 0.701027 | 0.699013 | 59% | 59% | 59% | 1.83 | 1.84 | 1.84 |
| 8/24/2011 21:22 | 8/31/2011 20:51 | Hartman1 | 420BaseS | Tetrachloroethene | 0.4 | 0.624743 | 0.624743 | 0.624743 | 44% | 44% | 44% | 1.56 | 1.56 | 1.56 |
| 8/31/2011 20:52 | 9/7/2011 20:34 | Hartman1 | 420BaseS | Tetrachloroethene | 0.36 | 0.539148 | 0.546148 | 0.541167 | 40% | 41% | 40% | 1.50 | 1.52 | 1.50 |
| 9/7/2011 20:36 | 9/14/2011 23:09 | Hartman1 | 420BaseS | Tetrachloroethene | 0.36 | 0.588986 | 0.588986 | 0.588986 | 48% | 48% | 48% | 1.64 | 1.64 | 1.64 |
| 9/14/2011 23:11 | 9/21/2011 22:23 | Hartman1 | 420BaseS | Tetrachloroethene | 0.63 | 0.633948 | 0.689419 | 0.666505 | 1% | 9% | 6% | 1.01 | 1.09 | 1.06 |
| 9/21/2011 22:25 | 9/28/2011 21:09 | Hartman1 | 420BaseS | Tetrachloroethene | 0.27 | 0.516929 | 0.706606 | 0.596752 | 63% | 89% | 75% | 1.91 | 2.62 | 2.21 |
| 9/28/2011 21:12 | 10/6/2011 21:41 | Hartman1 | 420BaseS | Tetrachloroethene | 0.52 | 0.755773 | 0.80244 | 0.797745 | 37% | 43% | 42% | 1.45 | 1.54 | 1.53 |
| 8/17/2011 22:36 | 8/24/2011 21:14 | Hartman1 | 420First | Tetrachloroethene | 0.3 | 0.655622 | 0.655622 | 0.655622 | 74% | 74% | 74% | 2.19 | 2.19 | 2.19 |
| 8/24/2011 21:16 | 8/31/2011 20:44 | Hartman1 | 420First | Tetrachloroethene | 0.33 | 0.578883 | 0.578883 | 0.578883 | 55% | 55% | 55% | 1.75 | 1.75 | 1.75 |
| 8/31/2011 20:46 | 9/7/2011 20:27 | Hartman1 | 420First | Tetrachloroethene | 0.23 | 0.65351 | 0.66751 | 0.661562 | 96% | 97% | 97% | 2.84 | 2.90 | 2.88 |
| 9/7/2011 20:29 | 9/14/2011 22:48 | Hartman1 | 420First | Tetrachloroethene | 0.22 | 0.777222 | 0.777222 | 0.777222 | 112% | 112% | 112% | 3.53 | 3.53 | 3.53 |
| 9/14/2011 22:49 | 9/21/2011 22:18 | Hartman1 | 420First | Tetrachloroethene | 0.35 | 0.870784 | 0.93418 | 0.950923 | 85% | 91% | 92% | 2.49 | 2.67 | 2.72 |
| 9/21/2011 22:20 | 9/28/2011 20:58 | Hartman1 | 420First | Tetrachloroethene | 0.18 | 0.696707 | 0.872836 | 0.896551 | 118% | 132% | 133% | 3.87 | 4.85 | 4.98 |
| 9/28/2011 21:00 | 10/6/2011 21:32 | Hartman1 | 420First | Tetrachloroethene | 0.34 | 0.830614 | 0.894781 | 0.904659 | 84% | 90% | 91% | 2.44 | 2.63 | 2.66 |
| 8/17/2011 22:17 | 8/24/2011 20:58 | Hartman1 | 422BaseS | Tetrachloroethene | 0.53 | 0.83145 | 0.83145 | 0.83145 | 44% | 44% | 44% | 1.57 | 1.57 | 1.57 |
| 8/24/2011 21:00 | 8/31/2011 20:24 | Hartman1 | 422BaseS | Tetrachloroethene | 0.2 | 0.538404 | 0.538404 | 0.538404 | 92% | 92% | 92% | 2.69 | 2.69 | 2.69 |
| 8/31/2011 20:26 | 9/7/2011 20:20 | Hartman1 | 422BaseS | Tetrachloroethene | 0.52 | 0.745522 | 0.752522 | 0.751039 | 36% | 37% | 36% | 1.43 | 1.45 | 1.44 |
| 9/7/2011 20:22 | 9/14/2011 22:27 | Hartman1 | 422BaseS | Tetrachloroethene | 0.89 | 1.160058 | 1.160058 | 1.160058 | 26% | 26% | 26% | 1.30 | 1.30 | 1.30 |
| 9/14/2011 22:29 | 9/21/2011 22:02 | Hartman1 | 422BaseS | Tetrachloroethene | 0.94 | 1.082404 | 1.114102 | 1.136477 | 14% | 17% | 19% | 1.15 | 1.19 | 1.21 |
| 9/21/2011 22:05 | 9/28/2011 20:39 | Hartman1 | 422BaseS | Tetrachloroethene | 0.6 | 0.877887 | 1.033693 | 1.147923 | 38% | 53% | 63% | 1.46 | 1.72 | 1.91 |
| 9/28/2011 20:42 | 10/6/2011 21:18 | Hartman1 | 422BaseS | Tetrachloroethene | 0.73 | 1.136962 | 1.184286 | 1.228005 | 44% | 47% | 51% | 1.56 | 1.62 | 1.68 |

(continued)

Table 4-21. Comparison of Online GC to Radiello Results by Week (cont.)

| Start Date Time | Stop Date Time | Period | Location | Compound | Radiello ($\mu\text{g}/\text{m}^3$) | GC: Missing Values = 1/2 MDL ($\mu\text{g}/\text{m}^3$) | GC: Missing values = MDL ($\mu\text{g}/\text{m}^3$) | GC: Missing values = NGC ($\mu\text{g}/\text{m}^3$) | RPD Calculated with Missing Values = 1/2 MDL | RPD Calculated with Missing values = MDL | RPD Calculated with Missing values = NGC | Ratio (online GC/Radiello) Calculated with Missing Values = 1/2 MDL | Ratio (online GC/Radiello) Calculated with Missing values = MDL | Ratio (online GC/Radiello) Calculated with Missing values = NGC |
|------------------|------------------|----------|----------|-------------------|--|---|---|---|---|---|---|---|---|---|
| 8/17/2011 21:34 | 8/24/2011 20:44 | Hartman1 | 422First | Tetrachloroethene | 0.21 | 0.505163 | 0.511078 | 0.506379 | 83% | 84% | 83% | 2.41 | 2.43 | 2.41 |
| 8/24/2011 20:47 | 8/31/2011 20:10 | Hartman1 | 422First | Tetrachloroethene | 0.11 | 0.284921 | 0.284921 | 0.284921 | 89% | 89% | 89% | 2.59 | 2.59 | 2.59 |
| 8/31/2011 20:12 | 9/7/2011 20:10 | Hartman1 | 422First | Tetrachloroethene | 0.43 | 0.460549 | 0.460549 | 0.460549 | 7% | 7% | 7% | 1.07 | 1.07 | 1.07 |
| 9/7/2011 20:12 | 9/14/2011 21:57 | Hartman1 | 422First | Tetrachloroethene | 0.77 | 0.768224 | 0.768224 | 0.768224 | 0% | 0% | 0% | 1.00 | 1.00 | 1.00 |
| 9/14/2011 21:59 | 9/21/2011 21:50 | Hartman1 | 422First | Tetrachloroethene | 0.33 | 0.546832 | 0.546832 | 0.546832 | 49% | 49% | 49% | 1.66 | 1.66 | 1.66 |
| 9/21/2011 21:53 | 9/28/2011 20:08 | Hartman1 | 422First | Tetrachloroethene | 0.27 | 0.504122 | 0.504122 | 0.504122 | 60% | 60% | 60% | 1.87 | 1.87 | 1.87 |
| 9/28/2011 20:11 | 10/6/2011 20:57 | Hartman1 | 422First | Tetrachloroethene | 0.43 | 0.611999 | 0.611999 | 0.611999 | 35% | 35% | 35% | 1.42 | 1.42 | 1.42 |
| 12/7/2011 23:13 | 12/14/2011 21:20 | Hartman2 | 420BaseS | Tetrachloroethene | 0.41 | 0.762772 | 0.762772 | 0.762772 | 60% | 60% | 60% | 1.86 | 1.86 | 1.86 |
| 12/9/2011 17:57 | 12/15/2011 20:46 | Hartman2 | 420BaseS | Tetrachloroethene | 0.34 | 0.835366 | 0.835366 | 0.835366 | 84% | 84% | 84% | 2.46 | 2.46 | 2.46 |
| 12/14/2011 21:21 | 12/22/2011 22:26 | Hartman2 | 420BaseS | Tetrachloroethene | 0.16 | 0.280202 | 0.304444 | 0.266737 | 55% | 62% | 50% | 1.75 | 1.90 | 1.67 |
| 12/22/2011 22:28 | 12/28/2011 21:48 | Hartman2 | 420BaseS | Tetrachloroethene | 0.14 | NGC | NGC | NGC | NGC | NGC | NGC | NGC | NGC | NGC |
| 12/28/2011 21:50 | 1/4/2012 22:13 | Hartman2 | 420BaseS | Tetrachloroethene | 0.11 | 0.072088 | 0.078681 | 0.066222 | -42% | -33% | -50% | 0.66 | 0.72 | 0.60 |
| 1/4/2012 22:19 | 1/11/2012 22:19 | Hartman2 | 420BaseS | Tetrachloroethene | 0.2 | 0.307347 | 0.307347 | 0.307347 | 42% | 42% | 42% | 1.54 | 1.54 | 1.54 |
| 1/11/2012 20:01 | 1/18/2012 20:01 | Hartman2 | 420BaseS | Tetrachloroethene | 0.19 | 0.298824 | 0.298824 | 0.298824 | 45% | 45% | 45% | 1.57 | 1.57 | 1.57 |
| 1/18/2012 20:11 | 1/25/2012 20:56 | Hartman2 | 420BaseS | Tetrachloroethene | 0.21 | 0.39 | 0.39 | 0.39 | 60% | 60% | 60% | 1.86 | 1.86 | 1.86 |
| 12/7/2011 22:51 | 12/14/2011 21:09 | Hartman2 | 420First | Tetrachloroethene | 0.31 | 0.597327 | 0.597327 | 0.597327 | 63% | 63% | 63% | 1.93 | 1.93 | 1.93 |
| 12/9/2011 17:41 | 12/15/2011 20:43 | Hartman2 | 420First | Tetrachloroethene | 0.25 | 0.789146 | 0.789146 | 0.789146 | 104% | 104% | 104% | 3.16 | 3.16 | 3.16 |
| 12/14/2011 21:42 | 12/22/2011 22:12 | Hartman2 | 420First | Tetrachloroethene | 0.09 | 0.2337 | 0.2457 | 0.226224 | 89% | 93% | 86% | 2.60 | 2.73 | 2.51 |
| 12/22/2011 22:15 | 12/28/2011 21:43 | Hartman2 | 420First | Tetrachloroethene | 0.1 | NGC | NGC | NGC | NGC | NGC | NGC | NGC | NGC | NGC |
| 12/28/2011 21:45 | 1/4/2012 21:53 | Hartman2 | 420First | Tetrachloroethene | 0.081 | 0.013407 | 0.013407 | 0.013407 | -143% | -143% | -143% | 0.17 | 0.17 | 0.17 |
| 1/4/2012 21:55 | 1/11/2012 21:55 | Hartman2 | 420First | Tetrachloroethene | 0.17 | 0.183673 | 0.183673 | 0.183673 | 8% | 8% | 8% | 1.08 | 1.08 | 1.08 |

(continued)

Table 4-21. Comparison of Online GC to Radiello Results by Week (cont.)

| Start Date Time | Stop Date Time | Period | Location | Compound | Radiello ($\mu\text{g}/\text{m}^3$) | GC: Missing Values = 1/2 MDL ($\mu\text{g}/\text{m}^3$) | GC: Missing values = MDL ($\mu\text{g}/\text{m}^3$) | GC: Missing values = NGC ($\mu\text{g}/\text{m}^3$) | RPD Calculated with Missing Values = 1/2 MDL | RPD Calculated with Missing values = MDL | RPD Calculated with Missing values = NGC | Ratio (online GC/Radiello) Calculated with Missing Values = 1/2 MDL | Ratio (online GC/Radiello) Calculated with Missing values = MDL | Ratio (online GC/Radiello) Calculated with Missing values = NGC |
|------------------|------------------|----------|----------|-------------------|--|---|---|---|---|---|---|---|---|---|
| 1/11/2012 19:56 | 1/18/2012 19:56 | Hartman2 | 420First | Tetrachloroethene | 0.14 | 0.240686 | 0.240686 | 0.240686 | 53% | 53% | 53% | 1.72 | 1.72 | 1.72 |
| 1/18/2012 20:01 | 1/25/2012 20:50 | Hartman2 | 420First | Tetrachloroethene | 0.15 | 0.198229 | 0.198229 | 0.198229 | 28% | 28% | 28% | 1.32 | 1.32 | 1.32 |
| 12/7/2011 22:10 | 12/14/2011 20:41 | Hartman2 | 422BaseS | Tetrachloroethene | 0.93 | 1.81 | 1.816 | 1.822222 | 64% | 65% | 65% | 1.95 | 1.95 | 1.96 |
| 12/9/2011 17:33 | 12/15/2011 20:35 | Hartman2 | 422BaseS | Tetrachloroethene | 0.9 | 1.862195 | 1.869512 | 1.877778 | 70% | 70% | 70% | 2.07 | 2.08 | 2.09 |
| 12/14/2011 20:42 | 12/22/2011 23:16 | Hartman2 | 422BaseS | Tetrachloroethene | 0.62 | 1.550495 | 1.562376 | 1.569697 | 86% | 86% | 87% | 2.50 | 2.52 | 2.53 |
| 12/22/2011 23:18 | 12/28/2011 21:37 | Hartman2 | 422BaseS | Tetrachloroethene | 0.61 | NGC | NGC | NGC | NGC | NGC | NGC | NGC | NGC | NGC |
| 12/28/2011 21:40 | 1/4/2012 19:56 | Hartman2 | 422BaseS | Tetrachloroethene | 0.64 | 1.14382 | 1.150562 | 1.15 | 56% | 57% | 57% | 1.79 | 1.80 | 1.80 |
| 1/4/2012 19:58 | 1/11/2012 19:58 | Hartman2 | 422BaseS | Tetrachloroethene | 0.71 | 1.305102 | 1.305102 | 1.305102 | 59% | 59% | 59% | 1.84 | 1.84 | 1.84 |
| 1/11/2012 19:50 | 1/18/2012 19:50 | Hartman2 | 422BaseS | Tetrachloroethene | 1.1 | 2.179208 | 2.185149 | 2.195 | 66% | 66% | 66% | 1.98 | 1.99 | 2.00 |
| 1/18/2012 19:44 | 1/25/2012 20:45 | Hartman2 | 422BaseS | Tetrachloroethene | 1.1 | 2.136082 | 2.142268 | 2.152083 | 64% | 64% | 65% | 1.94 | 1.95 | 1.96 |
| 1/25/2012 20:47 | 2/1/2012 20:24 | Hartman2 | 422BaseS | Tetrachloroethene | 0.81 | 1.557647 | 1.575294 | 1.586667 | 63% | 64% | 65% | 1.92 | 1.94 | 1.96 |
| 2/1/2012 20:32 | 2/8/2012 20:03 | Hartman2 | 422BaseS | Tetrachloroethene | 0.57 | 1.065795 | 1.072614 | 1.071149 | 61% | 61% | 61% | 1.87 | 1.88 | 1.88 |
| 2/8/2012 20:04 | 2/15/2012 18:19 | Hartman2 | 422BaseS | Tetrachloroethene | 0.65 | 1.265215 | 1.265215 | 1.265215 | 64% | 64% | 64% | 1.95 | 1.95 | 1.95 |
| 12/7/2011 21:19 | 12/14/2011 20:27 | Hartman2 | 422First | Tetrachloroethene | 0.48 | 0.991188 | 0.991188 | 0.991188 | 69% | 69% | 69% | 2.06 | 2.06 | 2.06 |
| 12/9/2011 17:12 | 12/15/2011 20:08 | Hartman2 | 422First | Tetrachloroethene | 0.47 | 1.066341 | 1.066341 | 1.066341 | 78% | 78% | 78% | 2.27 | 2.27 | 2.27 |
| 12/14/2011 20:28 | 12/22/2011 22:52 | Hartman2 | 422First | Tetrachloroethene | 0.32 | 0.646768 | 0.664949 | 0.648229 | 68% | 70% | 68% | 2.02 | 2.08 | 2.03 |
| 12/22/2011 22:54 | 12/28/2011 21:26 | Hartman2 | 422First | Tetrachloroethene | 0.27 | NGC | NGC | NGC | NGC | NGC | NGC | NGC | NGC | NGC |
| 12/28/2011 21:29 | 1/4/2012 19:23 | Hartman2 | 422First | Tetrachloroethene | 0.3 | 0.400787 | 0.421011 | 0.393837 | 29% | 34% | 27% | 1.34 | 1.40 | 1.31 |
| 1/4/2012 19:24 | 1/11/2012 19:24 | Hartman2 | 422First | Tetrachloroethene | 0.35 | 0.572449 | 0.572449 | 0.572449 | 48% | 48% | 48% | 1.64 | 1.64 | 1.64 |
| 1/11/2012 19:38 | 1/18/2012 19:38 | Hartman2 | 422First | Tetrachloroethene | 0.54 | 0.927647 | 0.933529 | 0.930891 | 53% | 53% | 53% | 1.72 | 1.73 | 1.72 |
| 1/18/2012 19:23 | 1/25/2012 20:34 | Hartman2 | 422First | Tetrachloroethene | 0.53 | 0.888557 | 0.894742 | 0.891563 | 51% | 51% | 51% | 1.68 | 1.69 | 1.68 |

(continued)

Table 4-21. Comparison of Online GC to Radiello Results by Week (cont.)

| Start Date Time | Stop Date Time | Period | Location | Compound | Radiello ($\mu\text{g}/\text{m}^3$) | GC: Missing Values = 1/2 MDL ($\mu\text{g}/\text{m}^3$) | GC: Missing values = MDL ($\mu\text{g}/\text{m}^3$) | GC: Missing values = NGC ($\mu\text{g}/\text{m}^3$) | RPD Calculated with Missing Values = 1/2 MDL | RPD Calculated with Missing values = MDL | RPD Calculated with Missing values = NGC | Ratio (online GC/Radiello) Calculated with Missing Values = 1/2 MDL | Ratio (online GC/Radiello) Calculated with Missing values = MDL | Ratio (online GC/Radiello) Calculated with Missing values = NGC |
|------------------|------------------|----------|----------|-------------------|--|---|---|---|---|---|---|---|---|---|
| 1/25/2012 20:37 | 2/1/2012 20:05 | Hartman2 | 422First | Tetrachloroethene | 0.42 | 0.644571 | 0.644571 | 0.644571 | 42% | 42% | 42% | 1.53 | 1.53 | 1.53 |
| 2/1/2012 20:13 | 2/8/2012 19:57 | Hartman2 | 422First | Tetrachloroethene | 0.33 | 0.460449 | 0.460449 | 0.460449 | 33% | 33% | 33% | 1.40 | 1.40 | 1.40 |
| 2/8/2012 20:00 | 2/15/2012 18:14 | Hartman2 | 422First | Tetrachloroethene | 0.32 | 0.437412 | 0.437412 | 0.437412 | 31% | 31% | 31% | 1.37 | 1.37 | 1.37 |
| 12/7/2011 22:33 | 12/14/2011 22:00 | Hartman2 | Outside | Tetrachloroethene | 0.23 | 0.425545 | 0.425545 | 0.425545 | 60% | 60% | 60% | 1.85 | 1.85 | 1.85 |
| 12/9/2011 18:17 | 12/15/2011 21:12 | Hartman2 | Outside | Tetrachloroethene | 0.21 | 0.629277 | 0.629277 | 0.629277 | 100% | 100% | 100% | 3.00 | 3.00 | 3.00 |
| 12/14/2011 22:01 | 12/22/2011 21:49 | Hartman2 | Outside | Tetrachloroethene | 0.094 | 0.492198 | 0.492198 | 0.492198 | 136% | 136% | 136% | 5.24 | 5.24 | 5.24 |
| 12/22/2011 21:53 | 12/28/2011 21:59 | Hartman2 | Outside | Tetrachloroethene | 0.091 | NGC | NGC | NGC | NGC | NGC | NGC | NGC | NGC | NGC |
| 12/28/2011 22:01 | 1/4/2012 21:37 | Hartman2 | Outside | Tetrachloroethene | 0.074 | 0.141099 | 0.167473 | 0.12 | 62% | 77% | 47% | 1.91 | 2.26 | 1.62 |
| 1/4/2012 21:39 | 1/11/2012 21:39 | Hartman2 | Outside | Tetrachloroethene | 0.18 | 0.274796 | 0.274796 | 0.274796 | 42% | 42% | 42% | 1.53 | 1.53 | 1.53 |
| 1/11/2012 20:13 | 1/18/2012 20:13 | Hartman2 | Outside | Tetrachloroethene | 0.067 | 0.077723 | 0.077723 | 0.077723 | 15% | 15% | 15% | 1.16 | 1.16 | 1.16 |
| 1/18/2012 20:32 | 1/25/2012 21:09 | Hartman2 | Outside | Tetrachloroethene | 0.08 | 0.245104 | 0.251354 | 0.241368 | 102% | 103% | 100% | 3.06 | 3.14 | 3.02 |
| 1/25/2012 21:12 | 2/1/2012 21:02 | Hartman2 | Outside | Tetrachloroethene | 0.11 | 0.274706 | 0.274706 | 0.274706 | 86% | 86% | 86% | 2.50 | 2.50 | 2.50 |
| 2/1/2012 21:07 | 2/8/2012 20:08 | Hartman2 | Outside | Tetrachloroethene | 0.13 | 0.262045 | 0.262045 | 0.262045 | 67% | 67% | 67% | 2.02 | 2.02 | 2.02 |
| 2/8/2012 20:10 | 2/15/2012 17:58 | Hartman2 | Outside | Tetrachloroethene | 0.071 | 0.184235 | 0.184235 | 0.184235 | 89% | 89% | 89% | 2.59 | 2.59 | 2.59 |
| 12/19/2012 23:30 | 12/26/2012 15:49 | Hartman3 | 420BaseS | Tetrachloroethene | 0.17 | 0.26644 | 0.26644 | 0.26644 | 44% | 44% | 44% | 1.57 | 1.57 | 1.57 |
| 12/19/2012 23:33 | 12/26/2012 15:51 | Hartman3 | 420BaseS | Tetrachloroethene | 0.24 | 0.26644 | 0.26644 | 0.26644 | 10% | 10% | 10% | 1.11 | 1.11 | 1.11 |
| 12/26/2012 15:50 | 1/2/2013 21:30 | Hartman3 | 420BaseS | Tetrachloroethene | 0.16 | 0.227258 | 0.227258 | 0.227258 | 35% | 35% | 35% | 1.42 | 1.42 | 1.42 |
| 1/2/2013 21:32 | 1/9/2013 20:24 | Hartman3 | 420BaseS | Tetrachloroethene | 0.25 | 0.255719 | 0.255719 | 0.255719 | 2% | 2% | 2% | 1.02 | 1.02 | 1.02 |
| 1/9/2013 20:26 | 1/16/2013 19:37 | Hartman3 | 420BaseS | Tetrachloroethene | 0.35 | 0.326374 | 0.326374 | 0.326374 | -7% | -7% | -7% | 0.93 | 0.93 | 0.93 |
| 1/16/2013 19:39 | 1/23/2013 21:11 | Hartman3 | 420BaseS | Tetrachloroethene | 0.36 | 0.473815 | 0.481106 | 0.476449 | 27% | 29% | 28% | 1.32 | 1.34 | 1.32 |
| 1/23/2013 21:13 | 1/30/2013 18:12 | Hartman3 | 420BaseS | Tetrachloroethene | 1 | 0.944917 | 0.944917 | 0.944917 | -6% | -6% | -6% | 0.94 | 0.94 | 0.94 |

(continued)

Table 4-21. Comparison of Online GC to Radiello Results by Week (cont.)

| Start Date Time | Stop Date Time | Period | Location | Compound | Radiello ($\mu\text{g}/\text{m}^3$) | GC: Missing Values = 1/2 MDL ($\mu\text{g}/\text{m}^3$) | GC: Missing values = MDL ($\mu\text{g}/\text{m}^3$) | GC: Missing values = NGC ($\mu\text{g}/\text{m}^3$) | RPD Calculated with Missing Values = 1/2 MDL | RPD Calculated with Missing values = MDL | RPD Calculated with Missing values = NGC | Ratio (online GC/Radiello) Calculated with Missing Values = 1/2 MDL | Ratio (online GC/Radiello) Calculated with Missing values = MDL | Ratio (online GC/Radiello) Calculated with Missing values = NGC |
|------------------|------------------|----------|----------|-------------------|--|---|---|---|---|---|---|---|---|---|
| 1/23/2013 21:18 | 1/30/2013 18:18 | Hartman3 | 420BaseS | Tetrachloroethene | 1 | 0.944917 | 0.944917 | 0.944917 | -6% | -6% | -6% | 0.94 | 0.94 | 0.94 |
| 1/30/2013 18:14 | 2/6/2013 0:59 | Hartman3 | 420BaseS | Tetrachloroethene | 0.36 | 0.349814 | 0.349814 | 0.349814 | -3% | -3% | -3% | 0.97 | 0.97 | 0.97 |
| 1/30/2013 18:20 | 2/6/2013 1:03 | Hartman3 | 420BaseS | Tetrachloroethene | 0.34 | 0.349814 | 0.349814 | 0.349814 | 3% | 3% | 3% | 1.03 | 1.03 | 1.03 |
| 2/6/2013 1:00 | 2/13/2013 19:50 | Hartman3 | 420BaseS | Tetrachloroethene | 0.29 | 0.330543 | 0.330543 | 0.330543 | 13% | 13% | 13% | 1.14 | 1.14 | 1.14 |
| 2/6/2013 1:04 | 2/13/2013 19:54 | Hartman3 | 420BaseS | Tetrachloroethene | 0.28 | 0.330543 | 0.330543 | 0.330543 | 17% | 17% | 17% | 1.18 | 1.18 | 1.18 |
| 2/13/2013 19:52 | 2/20/2013 21:35 | Hartman3 | 420BaseS | Tetrachloroethene | 0.67 | 0.814083 | 0.814083 | 0.814083 | 19% | 19% | 19% | 1.22 | 1.22 | 1.22 |
| 2/13/2013 19:56 | 2/20/2013 21:39 | Hartman3 | 420BaseS | Tetrachloroethene | 0.64 | 0.814083 | 0.814083 | 0.814083 | 24% | 24% | 24% | 1.27 | 1.27 | 1.27 |
| 3/6/2013 20:20 | 3/14/2013 22:53 | Hartman3 | 420BaseS | Tetrachloroethene | 0.28 | 0.335229 | 0.335229 | 0.335229 | 18% | 18% | 18% | 1.20 | 1.20 | 1.20 |
| 3/6/2013 20:24 | 3/14/2013 23:04 | Hartman3 | 420BaseS | Tetrachloroethene | 0.27 | 0.335229 | 0.335229 | 0.335229 | 22% | 22% | 22% | 1.24 | 1.24 | 1.24 |
| 12/19/2012 23:26 | 12/26/2012 15:45 | Hartman3 | 420First | Tetrachloroethene | 0.13 | 0.248347 | 0.248347 | 0.248347 | 63% | 63% | 63% | 1.91 | 1.91 | 1.91 |
| 12/26/2012 15:46 | 1/2/2013 21:20 | Hartman3 | 420First | Tetrachloroethene | 0.12 | 0.193949 | 0.193949 | 0.193949 | 47% | 47% | 47% | 1.62 | 1.62 | 1.62 |
| 1/2/2013 21:22 | 1/9/2013 20:19 | Hartman3 | 420First | Tetrachloroethene | 0.18 | 0.18147 | 0.18147 | 0.18147 | 1% | 1% | 1% | 1.01 | 1.01 | 1.01 |
| 1/9/2013 20:22 | 1/16/2013 19:32 | Hartman3 | 420First | Tetrachloroethene | 0.21 | 0.263481 | 0.263481 | 0.263481 | 23% | 23% | 23% | 1.25 | 1.25 | 1.25 |
| 1/16/2013 19:34 | 1/23/2013 21:05 | Hartman3 | 420First | Tetrachloroethene | 0.22 | 0.202046 | 0.202046 | 0.202046 | -9% | -9% | -9% | 0.92 | 0.92 | 0.92 |
| 1/23/2013 21:07 | 1/30/2013 18:07 | Hartman3 | 420First | Tetrachloroethene | 0.73 | 0.8585 | 0.8585 | 0.8585 | 16% | 16% | 16% | 1.18 | 1.18 | 1.18 |
| 1/30/2013 18:09 | 2/6/2013 0:51 | Hartman3 | 420First | Tetrachloroethene | 0.2 | 0.114152 | 0.122486 | 0.1084 | -55% | -48% | -59% | 0.57 | 0.61 | 0.54 |
| 2/6/2013 0:54 | 2/13/2013 19:44 | Hartman3 | 420First | Tetrachloroethene | 0.16 | 0.401728 | 0.401728 | 0.401728 | 86% | 86% | 86% | 2.51 | 2.51 | 2.51 |
| 2/13/2013 19:46 | 2/20/2013 21:29 | Hartman3 | 420First | Tetrachloroethene | 0.34 | 0.288124 | 0.288124 | 0.288124 | -17% | -17% | -17% | 0.85 | 0.85 | 0.85 |
| 3/6/2013 20:11 | 3/14/2013 22:47 | Hartman3 | 420First | Tetrachloroethene | 0.22 | 0.261475 | 0.261475 | 0.261475 | 17% | 17% | 17% | 1.19 | 1.19 | 1.19 |
| 12/19/2012 23:20 | 12/26/2012 15:39 | Hartman3 | 422BaseS | Tetrachloroethene | 0.09 | 0.87325 | 0.87325 | 0.87325 | 163% | 163% | 163% | 9.70 | 9.70 | 9.70 |
| 12/26/2012 15:39 | 1/2/2013 21:13 | Hartman3 | 422BaseS | Tetrachloroethene | 0.68 | 0.902784 | 0.902784 | 0.902784 | 28% | 28% | 28% | 1.33 | 1.33 | 1.33 |

(continued)

Table 4-21. Comparison of Online GC to Radiello Results by Week (cont.)

| Start Date Time | Stop Date Time | Period | Location | Compound | Radiello ($\mu\text{g}/\text{m}^3$) | GC: Missing Values = 1/2 MDL ($\mu\text{g}/\text{m}^3$) | GC: Missing values = MDL ($\mu\text{g}/\text{m}^3$) | GC: Missing values = NGC ($\mu\text{g}/\text{m}^3$) | RPD Calculated with Missing Values = 1/2 MDL | RPD Calculated with Missing values = MDL | RPD Calculated with Missing values = NGC | Ratio (online GC/Radiello) Calculated with Missing Values = 1/2 MDL | Ratio (online GC/Radiello) Calculated with Missing values = MDL | Ratio (online GC/Radiello) Calculated with Missing values = NGC |
|------------------|------------------|----------|----------|-------------------|--|---|---|---|---|---|---|---|---|---|
| 1/2/2013 21:15 | 1/9/2013 20:13 | Hartman3 | 422BaseS | Tetrachloroethene | 1.2 | 1.458409 | 1.458409 | 1.458409 | 19% | 19% | 19% | 1.22 | 1.22 | 1.22 |
| 1/9/2013 20:15 | 1/16/2013 19:24 | Hartman3 | 422BaseS | Tetrachloroethene | 1.2 | 1.239126 | 1.239126 | 1.239126 | 3% | 3% | 3% | 1.03 | 1.03 | 1.03 |
| 1/16/2013 19:27 | 1/23/2013 20:58 | Hartman3 | 422BaseS | Tetrachloroethene | 1.8 | 2.545342 | 2.545342 | 2.545342 | 34% | 34% | 34% | 1.41 | 1.41 | 1.41 |
| 1/23/2013 21:01 | 1/30/2013 18:01 | Hartman3 | 422BaseS | Tetrachloroethene | 4.1 | 4.94923 | 4.94923 | 4.94923 | 19% | 19% | 19% | 1.21 | 1.21 | 1.21 |
| 1/30/2013 18:03 | 2/6/2013 0:41 | Hartman3 | 422BaseS | Tetrachloroethene | 2.7 | 3.791853 | 3.791853 | 3.791853 | 34% | 34% | 34% | 1.40 | 1.40 | 1.40 |
| 2/6/2013 0:43 | 2/13/2013 19:38 | Hartman3 | 422BaseS | Tetrachloroethene | 0.98 | 1.075208 | 1.075208 | 1.075208 | 9% | 9% | 9% | 1.10 | 1.10 | 1.10 |
| 2/13/2013 19:41 | 2/20/2013 21:22 | Hartman3 | 422BaseS | Tetrachloroethene | 2.2 | 2.383663 | 2.383663 | 2.383663 | 8% | 8% | 8% | 1.08 | 1.08 | 1.08 |
| 3/6/2013 20:05 | 3/14/2013 22:41 | Hartman3 | 422BaseS | Tetrachloroethene | 1.9 | 2.358331 | 2.358331 | 2.358331 | 22% | 22% | 22% | 1.24 | 1.24 | 1.24 |
| 12/19/2012 23:12 | 12/26/2012 15:31 | Hartman3 | 422First | Tetrachloroethene | 0.32 | 0.448193 | 0.448193 | 0.448193 | 33% | 33% | 33% | 1.40 | 1.40 | 1.40 |
| 12/26/2012 15:33 | 1/2/2013 21:01 | Hartman3 | 422First | Tetrachloroethene | 0.3 | 0.450698 | 0.450698 | 0.450698 | 40% | 40% | 40% | 1.50 | 1.50 | 1.50 |
| 1/2/2013 21:05 | 1/9/2013 20:02 | Hartman3 | 422First | Tetrachloroethene | 0.62 | 0.678085 | 0.678085 | 0.678085 | 9% | 9% | 9% | 1.09 | 1.09 | 1.09 |
| 1/9/2013 20:04 | 1/16/2013 19:12 | Hartman3 | 422First | Tetrachloroethene | 0.57 | 0.585404 | 0.585404 | 0.585404 | 3% | 3% | 3% | 1.03 | 1.03 | 1.03 |
| 1/16/2013 19:13 | 1/23/2013 20:47 | Hartman3 | 422First | Tetrachloroethene | 0.98 | 1.116247 | 1.116247 | 1.116247 | 13% | 13% | 13% | 1.14 | 1.14 | 1.14 |
| 1/23/2013 20:48 | 1/30/2013 17:51 | Hartman3 | 422First | Tetrachloroethene | 1.6 | 1.991854 | 1.991854 | 1.991854 | 22% | 22% | 22% | 1.24 | 1.24 | 1.24 |
| 1/30/2013 17:52 | 2/6/2013 0:21 | Hartman3 | 422First | Tetrachloroethene | 1.2 | 1.658681 | 1.658681 | 1.658681 | 32% | 32% | 32% | 1.38 | 1.38 | 1.38 |
| 2/6/2013 0:24 | 2/13/2013 19:28 | Hartman3 | 422First | Tetrachloroethene | 0.34 | 0.524513 | 0.524513 | 0.524513 | 43% | 43% | 43% | 1.54 | 1.54 | 1.54 |
| 2/13/2013 19:31 | 2/20/2013 21:10 | Hartman3 | 422First | Tetrachloroethene | 0.76 | 0.871925 | 0.871925 | 0.871925 | 14% | 14% | 14% | 1.15 | 1.15 | 1.15 |
| 3/6/2013 19:44 | 3/14/2013 22:28 | Hartman3 | 422First | Tetrachloroethene | 0.76 | 0.973867 | 0.973867 | 0.973867 | 25% | 25% | 25% | 1.28 | 1.28 | 1.28 |
| 12/19/2012 23:42 | 12/26/2012 15:54 | Hartman3 | Outside | Tetrachloroethene | 0.1 | 2.867612 | 2.867612 | 2.867612 | 187% | 187% | 187% | 28.68 | 28.68 | 28.68 |
| 12/26/2012 16:00 | 1/2/2013 21:53 | Hartman3 | Outside | Tetrachloroethene | 0.095 | 1.594169 | 1.594169 | 1.594169 | 178% | 178% | 178% | 16.78 | 16.78 | 16.78 |
| 1/2/2013 21:55 | 1/9/2013 20:40 | Hartman3 | Outside | Tetrachloroethene | 0.15 | 0.17637 | 0.17637 | 0.17637 | 16% | 16% | 16% | 1.18 | 1.18 | 1.18 |

(continued)

Table 4-21. Comparison of Online GC to Radiello Results by Week (cont.)

| Start Date Time | Stop Date Time | Period | Location | Compound | Radiello ($\mu\text{g}/\text{m}^3$) | GC: Missing Values = 1/2 MDL ($\mu\text{g}/\text{m}^3$) | GC: Missing values = MDL ($\mu\text{g}/\text{m}^3$) | GC: Missing values = NGC ($\mu\text{g}/\text{m}^3$) | RPD Calculated with Missing Values = 1/2 MDL | RPD Calculated with Missing values = MDL | RPD Calculated with Missing values = NGC | Ratio (online GC/Radiello) Calculated with Missing Values = 1/2 MDL | Ratio (online GC/Radiello) Calculated with Missing values = MDL | Ratio (online GC/Radiello) Calculated with Missing values = NGC |
|-----------------|-----------------|----------|----------|-------------------|--|---|---|---|---|---|---|---|---|---|
| 1/9/2013 20:42 | 1/16/2013 19:57 | Hartman3 | Outside | Tetrachloroethene | 0.13 | 0.268352 | 0.268352 | 0.268352 | 69% | 69% | 69% | 2.06 | 2.06 | 2.06 |
| 1/16/2013 19:59 | 1/23/2013 21:29 | Hartman3 | Outside | Tetrachloroethene | 0.095 | 0.154371 | 0.154371 | 0.154371 | 48% | 48% | 48% | 1.62 | 1.62 | 1.62 |
| 1/23/2013 21:32 | 1/30/2013 18:32 | Hartman3 | Outside | Tetrachloroethene | 0.14 | 0.234515 | 0.234515 | 0.234515 | 50% | 50% | 50% | 1.68 | 1.68 | 1.68 |
| 1/30/2013 18:34 | 2/6/2013 1:27 | Hartman3 | Outside | Tetrachloroethene | 0.095 | 0.168551 | 0.168551 | 0.168551 | 56% | 56% | 56% | 1.77 | 1.77 | 1.77 |
| 2/6/2013 1:29 | 2/13/2013 20:03 | Hartman3 | Outside | Tetrachloroethene | 0.095 | 0.388508 | 0.388508 | 0.388508 | 121% | 121% | 121% | 4.09 | 4.09 | 4.09 |
| 2/13/2013 20:06 | 2/20/2013 21:51 | Hartman3 | Outside | Tetrachloroethene | 0.095 | 1.506992 | 1.506992 | 1.506992 | 176% | 176% | 176% | 15.86 | 15.86 | 15.86 |
| 3/6/2013 20:42 | 3/14/2013 23:15 | Hartman3 | Outside | Tetrachloroethene | 0.08 | 0.192146 | 0.192146 | 0.192146 | 82% | 82% | 82% | 2.40 | 2.40 | 2.40 |
| 8/17/2011 22:55 | 8/24/2011 21:21 | Hartman1 | 420BaseS | Chloroform | 0.13 | 0.200157 | 0.200157 | 0.200157 | 42% | 42% | 42% | 1.54 | 1.54 | 1.54 |
| 8/24/2011 21:22 | 8/31/2011 20:51 | Hartman1 | 420BaseS | Chloroform | 0.19 | 0.250638 | 0.250638 | 0.250638 | 28% | 28% | 28% | 1.32 | 1.32 | 1.32 |
| 8/31/2011 20:52 | 9/7/2011 20:34 | Hartman1 | 420BaseS | Chloroform | 0.34 | 0.33628 | 0.33628 | 0.33628 | -1% | -1% | -1% | 0.99 | 0.99 | 0.99 |
| 9/7/2011 20:36 | 9/14/2011 23:09 | Hartman1 | 420BaseS | Chloroform | 0.26 | 0.297065 | 0.297065 | 0.297065 | 13% | 13% | 13% | 1.14 | 1.14 | 1.14 |
| 9/14/2011 23:11 | 9/21/2011 22:23 | Hartman1 | 420BaseS | Chloroform | 0.25 | 0.681553 | 0.681553 | 0.681553 | 93% | 93% | 93% | 2.73 | 2.73 | 2.73 |
| 9/21/2011 22:25 | 9/28/2011 21:09 | Hartman1 | 420BaseS | Chloroform | 0.089 | 0.45143 | 0.45143 | 0.45143 | 134% | 134% | 134% | 5.07 | 5.07 | 5.07 |
| 9/28/2011 21:12 | 10/6/2011 21:41 | Hartman1 | 420BaseS | Chloroform | 0.34 | 0.63844 | 0.666218 | 0.646583 | 61% | 65% | 62% | 1.88 | 1.96 | 1.90 |
| 8/17/2011 22:36 | 8/24/2011 21:14 | Hartman1 | 420First | Chloroform | 0.18 | 0.163392 | 0.163392 | 0.163392 | -10% | -10% | -10% | 0.91 | 0.91 | 0.91 |
| 8/24/2011 21:16 | 8/31/2011 20:44 | Hartman1 | 420First | Chloroform | 0.24 | 0.194262 | 0.194262 | 0.194262 | -21% | -21% | -21% | 0.81 | 0.81 | 0.81 |
| 8/31/2011 20:46 | 9/7/2011 20:27 | Hartman1 | 420First | Chloroform | 0.16 | 0.236445 | 0.236445 | 0.236445 | 39% | 39% | 39% | 1.48 | 1.48 | 1.48 |
| 9/7/2011 20:29 | 9/14/2011 22:48 | Hartman1 | 420First | Chloroform | 0.21 | 0.283872 | 0.283872 | 0.283872 | 30% | 30% | 30% | 1.35 | 1.35 | 1.35 |
| 9/14/2011 22:49 | 9/21/2011 22:18 | Hartman1 | 420First | Chloroform | 0.26 | 0.694797 | 0.694797 | 0.694797 | 91% | 91% | 91% | 2.67 | 2.67 | 2.67 |
| 9/21/2011 22:20 | 9/28/2011 20:58 | Hartman1 | 420First | Chloroform | 0.094 | 0.573214 | 0.573214 | 0.573214 | 144% | 144% | 144% | 6.10 | 6.10 | 6.10 |
| 9/28/2011 21:00 | 10/6/2011 21:32 | Hartman1 | 420First | Chloroform | 0.22 | 0.702489 | 0.723322 | 0.711292 | 105% | 107% | 106% | 3.19 | 3.29 | 3.23 |

(continued)

Table 4-21. Comparison of Online GC to Radiello Results by Week (cont.)

| Start Date Time | Stop Date Time | Period | Location | Compound | Radiello ($\mu\text{g}/\text{m}^3$) | GC: Missing Values = 1/2 MDL ($\mu\text{g}/\text{m}^3$) | GC: Missing values = MDL ($\mu\text{g}/\text{m}^3$) | GC: Missing values = NGC ($\mu\text{g}/\text{m}^3$) | RPD Calculated with Missing Values = 1/2 MDL | RPD Calculated with Missing values = MDL | RPD Calculated with Missing values = NGC | Ratio (online GC/Radiello) Calculated with Missing Values = 1/2 MDL | Ratio (online GC/Radiello) Calculated with Missing values = MDL | Ratio (online GC/Radiello) Calculated with Missing values = NGC |
|------------------|------------------|----------|----------|------------|--|---|---|---|---|---|---|---|---|---|
| 8/17/2011 22:17 | 8/24/2011 20:58 | Hartman1 | 422BaseS | Chloroform | 0.17 | 0.225866 | 0.225866 | 0.225866 | 28% | 28% | 28% | 1.33 | 1.33 | 1.33 |
| 8/24/2011 21:00 | 8/31/2011 20:24 | Hartman1 | 422BaseS | Chloroform | 0.099 | 0.161171 | 0.161171 | 0.161171 | 48% | 48% | 48% | 1.63 | 1.63 | 1.63 |
| 8/31/2011 20:26 | 9/7/2011 20:20 | Hartman1 | 422BaseS | Chloroform | 0.49 | 0.431763 | 0.431763 | 0.431763 | -13% | -13% | -13% | 0.88 | 0.88 | 0.88 |
| 9/7/2011 20:22 | 9/14/2011 22:27 | Hartman1 | 422BaseS | Chloroform | 0.71 | 0.72271 | 0.72271 | 0.72271 | 2% | 2% | 2% | 1.02 | 1.02 | 1.02 |
| 9/14/2011 22:29 | 9/21/2011 22:02 | Hartman1 | 422BaseS | Chloroform | 0.38 | 1.094928 | 1.094928 | 1.094928 | 97% | 97% | 97% | 2.88 | 2.88 | 2.88 |
| 9/21/2011 22:05 | 9/28/2011 20:39 | Hartman1 | 422BaseS | Chloroform | 0.22 | 0.768588 | 0.768588 | 0.768588 | 111% | 111% | 111% | 3.49 | 3.49 | 3.49 |
| 9/28/2011 20:42 | 10/6/2011 21:18 | Hartman1 | 422BaseS | Chloroform | 0.34 | 0.90011 | 0.921236 | 0.917761 | 90% | 92% | 92% | 2.65 | 2.71 | 2.70 |
| 8/17/2011 21:34 | 8/24/2011 20:44 | Hartman1 | 422First | Chloroform | 0.15 | 0.129456 | 0.129456 | 0.129456 | -15% | -15% | -15% | 0.86 | 0.86 | 0.86 |
| 8/24/2011 20:47 | 8/31/2011 20:10 | Hartman1 | 422First | Chloroform | 0.12 | 0.100367 | 0.100367 | 0.100367 | -18% | -18% | -18% | 0.84 | 0.84 | 0.84 |
| 8/31/2011 20:12 | 9/7/2011 20:10 | Hartman1 | 422First | Chloroform | 0.46 | 0.23895 | 0.23895 | 0.23895 | -63% | -63% | -63% | 0.52 | 0.52 | 0.52 |
| 9/7/2011 20:12 | 9/14/2011 21:57 | Hartman1 | 422First | Chloroform | 0.59 | 0.449548 | 0.449548 | 0.449548 | -27% | -27% | -27% | 0.76 | 0.76 | 0.76 |
| 9/14/2011 21:59 | 9/21/2011 21:50 | Hartman1 | 422First | Chloroform | 0.23 | 0.507337 | 0.507337 | 0.507337 | 75% | 75% | 75% | 2.21 | 2.21 | 2.21 |
| 9/21/2011 21:53 | 9/28/2011 20:08 | Hartman1 | 422First | Chloroform | 0.14 | 0.422027 | 0.422027 | 0.422027 | 100% | 100% | 100% | 3.01 | 3.01 | 3.01 |
| 9/28/2011 20:11 | 10/6/2011 20:57 | Hartman1 | 422First | Chloroform | 0.3 | 0.514956 | 0.514956 | 0.514956 | 53% | 53% | 53% | 1.72 | 1.72 | 1.72 |
| 12/7/2011 23:13 | 12/14/2011 21:20 | Hartman2 | 420BaseS | Chloroform | 0.3 | 0.583333 | 0.583333 | 0.583333 | 64% | 64% | 64% | 1.94 | 1.94 | 1.94 |
| 12/9/2011 17:57 | 12/15/2011 20:46 | Hartman2 | 420BaseS | Chloroform | 0.26 | 0.602273 | 0.602273 | 0.602273 | 79% | 79% | 79% | 2.32 | 2.32 | 2.32 |
| 12/14/2011 21:21 | 12/22/2011 22:26 | Hartman2 | 420BaseS | Chloroform | 0.12 | 0.71 | 0.71 | 0.71 | 142% | 142% | 142% | 5.92 | 5.92 | 5.92 |
| 12/22/2011 22:28 | 12/28/2011 21:48 | Hartman2 | 420BaseS | Chloroform | 0.15 | NGC | NGC | NGC | NGC | NGC | NGC | NGC | NGC | NGC |
| 12/28/2011 21:50 | 1/4/2012 22:13 | Hartman2 | 420BaseS | Chloroform | 0.1 | 0.350989 | 0.697143 | 0.44 | 111% | 150% | 126% | 3.51 | 6.97 | 4.40 |
| 1/4/2012 22:19 | 1/11/2012 22:19 | Hartman2 | 420BaseS | Chloroform | 0.14 | 0.343163 | 0.521735 | 0.336042 | 84% | 115% | 82% | 2.45 | 3.73 | 2.40 |
| 1/11/2012 20:01 | 1/18/2012 20:01 | Hartman2 | 420BaseS | Chloroform | 0.14 | 0.301863 | 0.336176 | 0.29663 | 73% | 82% | 72% | 2.16 | 2.40 | 2.12 |
| 1/18/2012 20:11 | 1/25/2012 20:56 | Hartman2 | 420BaseS | Chloroform | 0.11 | 0.319789 | 0.341895 | 0.317753 | 98% | 103% | 97% | 2.91 | 3.11 | 2.89 |

(continued)

Table 4-21. Comparison of Online GC to Radiello Results by Week (cont.)

| Start Date Time | Stop Date Time | Period | Location | Compound | Radiello ($\mu\text{g}/\text{m}^3$) | GC: Missing Values = 1/2 MDL ($\mu\text{g}/\text{m}^3$) | GC: Missing values = MDL ($\mu\text{g}/\text{m}^3$) | GC: Missing values = NGC ($\mu\text{g}/\text{m}^3$) | RPD Calculated with Missing Values = 1/2 MDL | RPD Calculated with Missing values = MDL | RPD Calculated with Missing values = NGC | Ratio (online GC/Radiello) Calculated with Missing Values = 1/2 MDL | Ratio (online GC/Radiello) Calculated with Missing values = MDL | Ratio (online GC/Radiello) Calculated with Missing values = NGC |
|------------------|------------------|----------|----------|------------|--|---|---|---|---|---|---|---|---|---|
| 12/7/2011 22:51 | 12/14/2011 21:09 | Hartman2 | 420First | Chloroform | 0.22 | 0.380952 | 0.380952 | 0.380952 | 54% | 54% | 54% | 1.73 | 1.73 | 1.73 |
| 12/9/2011 17:41 | 12/15/2011 20:43 | Hartman2 | 420First | Chloroform | 0.18 | 0.4 | 0.4 | 0.4 | 76% | 76% | 76% | 2.22 | 2.22 | 2.22 |
| 12/14/2011 21:42 | 12/22/2011 22:12 | Hartman2 | 420First | Chloroform | 0.067 | 0.325 | 0.325 | 0.325 | 132% | 132% | 132% | 4.85 | 4.85 | 4.85 |
| 12/22/2011 22:15 | 12/28/2011 21:43 | Hartman2 | 420First | Chloroform | 0.12 | NGC | NGC | NGC | NGC | NGC | NGC | NGC | NGC | NGC |
| 12/28/2011 21:45 | 1/4/2012 21:53 | Hartman2 | 420First | Chloroform | 0.092 | 0.321978 | 0.598901 | 0.215789 | 111% | 147% | 80% | 3.50 | 6.51 | 2.35 |
| 1/4/2012 21:55 | 1/11/2012 21:55 | Hartman2 | 420First | Chloroform | 0.12 | 0.313673 | 0.477959 | 0.281538 | 89% | 120% | 80% | 2.61 | 3.98 | 2.35 |
| 1/11/2012 19:56 | 1/18/2012 19:56 | Hartman2 | 420First | Chloroform | 0.11 | 0.301765 | 0.418431 | 0.277647 | 93% | 117% | 86% | 2.74 | 3.80 | 2.52 |
| 1/18/2012 20:01 | 1/25/2012 20:50 | Hartman2 | 420First | Chloroform | 0.087 | 0.29617 | 0.378085 | 0.279722 | 109% | 125% | 105% | 3.40 | 4.35 | 3.22 |
| 12/7/2011 22:10 | 12/14/2011 20:41 | Hartman2 | 422BaseS | Chloroform | 0.86 | 1.081 | 1.081 | 1.081 | 23% | 23% | 23% | 1.26 | 1.26 | 1.26 |
| 12/9/2011 17:33 | 12/15/2011 20:35 | Hartman2 | 422BaseS | Chloroform | 0.8 | 1.096296 | 1.096296 | 1.096296 | 31% | 31% | 31% | 1.37 | 1.37 | 1.37 |
| 12/14/2011 20:42 | 12/22/2011 23:16 | Hartman2 | 422BaseS | Chloroform | 0.61 | 0.797895 | 0.834737 | 0.850588 | 27% | 31% | 33% | 1.31 | 1.37 | 1.39 |
| 12/22/2011 23:18 | 12/28/2011 21:37 | Hartman2 | 422BaseS | Chloroform | 0.46 | NGC | NGC | NGC | NGC | NGC | NGC | NGC | NGC | NGC |
| 12/28/2011 21:40 | 1/4/2012 19:56 | Hartman2 | 422BaseS | Chloroform | 0.71 | 0.973596 | 0.977528 | 0.980682 | 31% | 32% | 32% | 1.37 | 1.38 | 1.38 |
| 1/4/2012 19:58 | 1/11/2012 19:58 | Hartman2 | 422BaseS | Chloroform | 0.68 | 0.951656 | 0.951656 | 0.951656 | 33% | 33% | 33% | 1.40 | 1.40 | 1.40 |
| 1/11/2012 19:50 | 1/18/2012 19:50 | Hartman2 | 422BaseS | Chloroform | 0.73 | 1.074851 | 1.078317 | 1.0821 | 38% | 39% | 39% | 1.47 | 1.48 | 1.48 |
| 1/18/2012 19:44 | 1/25/2012 20:45 | Hartman2 | 422BaseS | Chloroform | 0.69 | 1.017216 | 1.020825 | 1.024167 | 38% | 39% | 39% | 1.47 | 1.48 | 1.48 |
| 1/25/2012 20:47 | 2/1/2012 20:24 | Hartman2 | 422BaseS | Chloroform | 0.51 | 0.81 | 0.820294 | 0.823939 | 45% | 47% | 47% | 1.59 | 1.61 | 1.62 |
| 2/1/2012 20:32 | 2/8/2012 20:03 | Hartman2 | 422BaseS | Chloroform | 0.5 | 0.667273 | 0.67125 | 0.67092 | 29% | 29% | 29% | 1.33 | 1.34 | 1.34 |
| 2/8/2012 20:04 | 2/15/2012 18:19 | Hartman2 | 422BaseS | Chloroform | 0.61 | 0.764167 | 0.764167 | 0.764167 | 22% | 22% | 22% | 1.25 | 1.25 | 1.25 |
| 12/7/2011 21:19 | 12/14/2011 20:27 | Hartman2 | 422First | Chloroform | 0.39 | 0.639375 | 0.639375 | 0.639375 | 48% | 48% | 48% | 1.64 | 1.64 | 1.64 |
| 12/9/2011 17:12 | 12/15/2011 20:08 | Hartman2 | 422First | Chloroform | 0.36 | 0.648533 | 0.648533 | 0.648533 | 57% | 57% | 57% | 1.80 | 1.80 | 1.80 |

(continued)

Table 4-21. Comparison of Online GC to Radiello Results by Week (cont.)

| Start Date Time | Stop Date Time | Period | Location | Compound | Radiello ($\mu\text{g}/\text{m}^3$) | GC: Missing Values = 1/2 MDL ($\mu\text{g}/\text{m}^3$) | GC: Missing values = MDL ($\mu\text{g}/\text{m}^3$) | GC: Missing values = NGC ($\mu\text{g}/\text{m}^3$) | RPD Calculated with Missing Values = 1/2 MDL | RPD Calculated with Missing values = MDL | RPD Calculated with Missing values = NGC | Ratio (online GC/Radiello) Calculated with Missing Values = 1/2 MDL | Ratio (online GC/Radiello) Calculated with Missing values = MDL | Ratio (online GC/Radiello) Calculated with Missing values = NGC |
|------------------|------------------|----------|----------|------------|--|---|---|---|---|---|---|---|---|---|
| 12/14/2011 20:28 | 12/22/2011 22:52 | Hartman2 | 422First | Chloroform | 0.26 | 0.533019 | 0.533019 | 0.533019 | 69% | 69% | 69% | 2.05 | 2.05 | 2.05 |
| 12/22/2011 22:54 | 12/28/2011 21:26 | Hartman2 | 422First | Chloroform | 0.22 | NGC | NGC | NGC | NGC | NGC | NGC | NGC | NGC | NGC |
| 12/28/2011 21:29 | 1/4/2012 19:23 | Hartman2 | 422First | Chloroform | 0.3 | 0.491573 | 0.629213 | 0.583333 | 48% | 71% | 64% | 1.64 | 2.10 | 1.94 |
| 1/4/2012 19:24 | 1/11/2012 19:24 | Hartman2 | 422First | Chloroform | 0.22 | 0.516939 | 0.531224 | 0.524043 | 81% | 83% | 82% | 2.35 | 2.41 | 2.38 |
| 1/11/2012 19:38 | 1/18/2012 19:38 | Hartman2 | 422First | Chloroform | 0.36 | 0.552549 | 0.55598 | 0.554554 | 42% | 43% | 43% | 1.53 | 1.54 | 1.54 |
| 1/18/2012 19:23 | 1/25/2012 20:34 | Hartman2 | 422First | Chloroform | 0.31 | 0.537835 | 0.537835 | 0.537835 | 54% | 54% | 54% | 1.73 | 1.73 | 1.73 |
| 1/25/2012 20:37 | 2/1/2012 20:05 | Hartman2 | 422First | Chloroform | 0.26 | 0.520286 | 0.520286 | 0.520286 | 67% | 67% | 67% | 2.00 | 2.00 | 2.00 |
| 2/1/2012 20:13 | 2/8/2012 19:57 | Hartman2 | 422First | Chloroform | 0.25 | 0.395843 | 0.395843 | 0.395843 | 45% | 45% | 45% | 1.58 | 1.58 | 1.58 |
| 2/8/2012 20:00 | 2/15/2012 18:14 | Hartman2 | 422First | Chloroform | 0.28 | 0.420235 | 0.420235 | 0.420235 | 40% | 40% | 40% | 1.50 | 1.50 | 1.50 |
| 12/7/2011 22:33 | 12/14/2011 22:00 | Hartman2 | Outside | Chloroform | 0.13 | 0.511667 | 0.511667 | 0.511667 | 119% | 119% | 119% | 3.94 | 3.94 | 3.94 |
| 12/9/2011 18:17 | 12/15/2011 21:12 | Hartman2 | Outside | Chloroform | 0.12 | 0.569 | 0.569 | 0.569 | 130% | 130% | 130% | 4.74 | 4.74 | 4.74 |
| 12/14/2011 22:01 | 12/22/2011 21:49 | Hartman2 | Outside | Chloroform | 0.051 | 0.612 | 0.612 | 0.612 | 169% | 169% | 169% | 12.00 | 12.00 | 12.00 |
| 12/22/2011 21:53 | 12/28/2011 21:59 | Hartman2 | Outside | Chloroform | 0.087 | NGC | NGC | NGC | NGC | NGC | NGC | NGC | NGC | NGC |
| 12/28/2011 22:01 | 1/4/2012 21:37 | Hartman2 | Outside | Chloroform | 0.093 | 0.35 | 0.7 | NGC | 116% | 153% | NGC | 3.76 | 7.53 | NGC |
| 1/4/2012 21:39 | 1/11/2012 21:39 | Hartman2 | Outside | Chloroform | 0.1 | 0.323878 | 0.538163 | 0.282632 | 106% | 137% | 95% | 3.24 | 5.38 | 2.83 |
| 1/11/2012 20:13 | 1/18/2012 20:13 | Hartman2 | Outside | Chloroform | 0.09 | 0.317525 | 0.52198 | 0.271905 | 112% | 141% | 101% | 3.53 | 5.80 | 3.02 |
| 1/18/2012 20:32 | 1/25/2012 21:09 | Hartman2 | Outside | Chloroform | 0.075 | 0.345313 | 0.392708 | 0.344578 | 129% | 136% | 128% | 4.60 | 5.24 | 4.59 |
| 1/25/2012 21:12 | 2/1/2012 21:02 | Hartman2 | Outside | Chloroform | 0.075 | 0.374706 | 0.374706 | 0.374706 | 133% | 133% | 133% | 5.00 | 5.00 | 5.00 |
| 2/1/2012 21:07 | 2/8/2012 20:08 | Hartman2 | Outside | Chloroform | 0.1 | 0.337955 | 0.337955 | 0.337955 | 109% | 109% | 109% | 3.38 | 3.38 | 3.38 |
| 2/8/2012 20:10 | 2/15/2012 17:58 | Hartman2 | Outside | Chloroform | 0.1 | 0.33119 | 0.339524 | 0.330732 | 107% | 109% | 107% | 3.31 | 3.40 | 3.31 |

(continued)

Table 4-21. Comparison of Online GC to Radiello Results by Week (cont.)

| Start Date Time | Stop Date Time | Period | Location | Compound | Radiello ($\mu\text{g}/\text{m}^3$) | GC: Missing Values = 1/2 MDL ($\mu\text{g}/\text{m}^3$) | GC: Missing values = MDL ($\mu\text{g}/\text{m}^3$) | GC: Missing values = NGC ($\mu\text{g}/\text{m}^3$) | RPD Calculated with Missing Values = 1/2 MDL | RPD Calculated with Missing values = MDL | RPD Calculated with Missing values = NGC | Ratio (online GC/Radiello) Calculated with Missing Values = 1/2 MDL | Ratio (online GC/Radiello) Calculated with Missing values = MDL | Ratio (online GC/Radiello) Calculated with Missing values = NGC |
|------------------|------------------|----------|----------|------------|--|---|---|---|---|---|---|---|---|---|
| 12/19/2012 23:30 | 12/26/2012 15:49 | Hartman3 | 420BaseS | Chloroform | 0.14 | 0.348638 | 0.690305 | 0.2928 | 85% | 133% | 71% | 2.49 | 4.93 | 2.09 |
| 12/19/2012 23:33 | 12/26/2012 15:51 | Hartman3 | 420BaseS | Chloroform | 0.075 | 0.348638 | 0.690305 | 0.2928 | 129% | 161% | 118% | 4.65 | 9.20 | 3.90 |
| 12/26/2012 15:50 | 1/2/2013 21:30 | Hartman3 | 420BaseS | Chloroform | 0.13 | 0.35 | 0.7 | NGC | 92% | 137% | NGC | 2.69 | 5.38 | NGC |
| 1/2/2013 21:32 | 1/9/2013 20:24 | Hartman3 | 420BaseS | Chloroform | 0.13 | 0.348713 | 0.691266 | 0.2895 | 91% | 137% | 76% | 2.68 | 5.32 | 2.23 |
| 1/9/2013 20:26 | 1/16/2013 19:37 | Hartman3 | 420BaseS | Chloroform | 0.16 | 0.348979 | 0.661745 | 0.3404 | 74% | 122% | 72% | 2.18 | 4.14 | 2.13 |
| 1/16/2013 19:39 | 1/23/2013 21:11 | Hartman3 | 420BaseS | Chloroform | 0.19 | 0.363157 | 0.633611 | 0.40789 | 63% | 108% | 73% | 1.91 | 3.33 | 2.15 |
| 1/23/2013 21:13 | 1/30/2013 18:12 | Hartman3 | 420BaseS | Chloroform | 0.16 | 0.351707 | 0.636591 | 0.359175 | 75% | 120% | 77% | 2.20 | 3.98 | 2.24 |
| 1/23/2013 21:18 | 1/30/2013 18:18 | Hartman3 | 420BaseS | Chloroform | 0.16 | 0.351707 | 0.636591 | 0.359175 | 75% | 120% | 77% | 2.20 | 3.98 | 2.24 |
| 1/30/2013 18:14 | 2/6/2013 0:59 | Hartman3 | 420BaseS | Chloroform | 0.14 | 0.349288 | 0.658591 | 0.34388 | 86% | 130% | 84% | 2.49 | 4.70 | 2.46 |
| 1/30/2013 18:20 | 2/6/2013 1:03 | Hartman3 | 420BaseS | Chloroform | 0.14 | 0.349288 | 0.658591 | 0.34388 | 86% | 130% | 84% | 2.49 | 4.70 | 2.46 |
| 2/6/2013 1:00 | 2/13/2013 19:50 | Hartman3 | 420BaseS | Chloroform | 0.11 | 0.348683 | 0.678872 | 0.326733 | 104% | 144% | 99% | 3.17 | 6.17 | 2.97 |
| 2/6/2013 1:04 | 2/13/2013 19:54 | Hartman3 | 420BaseS | Chloroform | 0.15 | 0.348683 | 0.678872 | 0.326733 | 80% | 128% | 74% | 2.32 | 4.53 | 2.18 |
| 2/13/2013 19:52 | 2/20/2013 21:35 | Hartman3 | 420BaseS | Chloroform | 0.14 | 0.354646 | 0.690063 | 0.4615 | 87% | 133% | 107% | 2.53 | 4.93 | 3.30 |
| 2/13/2013 19:56 | 2/20/2013 21:39 | Hartman3 | 420BaseS | Chloroform | 0.12 | 0.354646 | 0.690063 | 0.4615 | 99% | 141% | 117% | 2.96 | 5.75 | 3.85 |
| 3/6/2013 20:20 | 3/14/2013 22:53 | Hartman3 | 420BaseS | Chloroform | 0.092 | 0.349513 | 0.686785 | 0.3366 | 117% | 153% | 114% | 3.80 | 7.47 | 3.66 |
| 3/6/2013 20:24 | 3/14/2013 23:04 | Hartman3 | 420BaseS | Chloroform | 0.096 | 0.349513 | 0.686785 | 0.3366 | 114% | 151% | 111% | 3.64 | 7.15 | 3.51 |
| 12/19/2012 23:26 | 12/26/2012 15:45 | Hartman3 | 420First | Chloroform | 0.075 | 0.35 | 0.7 | NGC | 129% | 161% | NGC | 4.67 | 9.33 | NGC |
| 12/26/2012 15:46 | 1/2/2013 21:20 | Hartman3 | 420First | Chloroform | 0.12 | 0.35 | 0.7 | NGC | 98% | 141% | NGC | 2.92 | 5.83 | NGC |
| 1/2/2013 21:22 | 1/9/2013 20:19 | Hartman3 | 420First | Chloroform | 0.14 | 0.35 | 0.7 | NGC | 86% | 133% | NGC | 2.50 | 5.00 | NGC |
| 1/9/2013 20:22 | 1/16/2013 19:32 | Hartman3 | 420First | Chloroform | 0.12 | 0.350142 | 0.69285 | 0.3568 | 98% | 141% | 99% | 2.92 | 5.77 | 2.97 |
| 1/16/2013 19:34 | 1/23/2013 21:05 | Hartman3 | 420First | Chloroform | 0.12 | 0.349995 | 0.683329 | 0.3499 | 98% | 140% | 98% | 2.92 | 5.69 | 2.92 |

(continued)

Table 4-21. Comparison of Online GC to Radiello Results by Week (cont.)

| Start Date Time | Stop Date Time | Period | Location | Compound | Radiello ($\mu\text{g}/\text{m}^3$) | GC: Missing Values = 1/2 MDL ($\mu\text{g}/\text{m}^3$) | GC: Missing values = MDL ($\mu\text{g}/\text{m}^3$) | GC: Missing values = NGC ($\mu\text{g}/\text{m}^3$) | RPD Calculated with Missing Values = 1/2 MDL | RPD Calculated with Missing values = MDL | RPD Calculated with Missing values = NGC | Ratio (online GC/Radiello) Calculated with Missing Values = 1/2 MDL | Ratio (online GC/Radiello) Calculated with Missing values = MDL | Ratio (online GC/Radiello) Calculated with Missing values = NGC |
|------------------|------------------|----------|----------|------------|--|---|---|---|---|---|---|---|---|---|
| 1/23/2013 21:07 | 1/30/2013 18:07 | Hartman3 | 420First | Chloroform | 0.12 | 0.350661 | 0.668843 | 0.357275 | 98% | 139% | 99% | 2.92 | 5.57 | 2.98 |
| 1/30/2013 18:09 | 2/6/2013 0:51 | Hartman3 | 420First | Chloroform | 0.12 | 0.347683 | 0.681017 | 0.30135 | 97% | 140% | 86% | 2.90 | 5.68 | 2.51 |
| 2/6/2013 0:54 | 2/13/2013 19:44 | Hartman3 | 420First | Chloroform | 0.075 | 0.35 | 0.7 | NGC | 129% | 161% | NGC | 4.67 | 9.33 | NGC |
| 2/13/2013 19:46 | 2/20/2013 21:29 | Hartman3 | 420First | Chloroform | 0.12 | 0.35 | 0.7 | NGC | 98% | 141% | NGC | 2.92 | 5.83 | NGC |
| 3/6/2013 20:11 | 3/14/2013 22:47 | Hartman3 | 420First | Chloroform | 0.06 | 0.35 | 0.7 | NGC | 141% | 168% | NGC | 5.83 | 11.67 | NGC |
| 12/19/2012 23:20 | 12/26/2012 15:39 | Hartman3 | 422BaseS | Chloroform | 0.26 | 0.38025 | 0.613583 | 0.44075 | 38% | 81% | 52% | 1.46 | 2.36 | 1.70 |
| 12/26/2012 15:39 | 1/2/2013 21:13 | Hartman3 | 422BaseS | Chloroform | 0.29 | 0.49425 | 0.62725 | 0.582661 | 52% | 74% | 67% | 1.70 | 2.16 | 2.01 |
| 1/2/2013 21:15 | 1/9/2013 20:13 | Hartman3 | 422BaseS | Chloroform | 0.54 | 0.690777 | 0.690777 | 0.690777 | 25% | 25% | 25% | 1.28 | 1.28 | 1.28 |
| 1/9/2013 20:15 | 1/16/2013 19:24 | Hartman3 | 422BaseS | Chloroform | 0.6 | 0.789715 | 0.789715 | 0.789715 | 27% | 27% | 27% | 1.32 | 1.32 | 1.32 |
| 1/16/2013 19:27 | 1/23/2013 20:58 | Hartman3 | 422BaseS | Chloroform | 0.85 | 1.537021 | 1.537021 | 1.537021 | 58% | 58% | 58% | 1.81 | 1.81 | 1.81 |
| 1/23/2013 21:01 | 1/30/2013 18:01 | Hartman3 | 422BaseS | Chloroform | 0.77 | 1.328185 | 1.328185 | 1.328185 | 53% | 53% | 53% | 1.72 | 1.72 | 1.72 |
| 1/30/2013 18:03 | 2/6/2013 0:41 | Hartman3 | 422BaseS | Chloroform | 0.85 | 1.474558 | 1.474558 | 1.474558 | 54% | 54% | 54% | 1.73 | 1.73 | 1.73 |
| 2/6/2013 0:43 | 2/13/2013 19:38 | Hartman3 | 422BaseS | Chloroform | 0.2 | 0.467058 | 0.698191 | 0.694672 | 80% | 111% | 111% | 2.34 | 3.49 | 3.47 |
| 2/13/2013 19:41 | 2/20/2013 21:22 | Hartman3 | 422BaseS | Chloroform | 0.28 | 0.409804 | 0.511888 | 0.434429 | 38% | 59% | 43% | 1.46 | 1.83 | 1.55 |
| 3/6/2013 20:05 | 3/14/2013 22:41 | Hartman3 | 422BaseS | Chloroform | 0.22 | 0.393565 | 0.584475 | 0.445844 | 57% | 91% | 68% | 1.79 | 2.66 | 2.03 |
| 12/19/2012 23:12 | 12/26/2012 15:31 | Hartman3 | 422First | Chloroform | 0.18 | 0.346621 | 0.663288 | 0.314525 | 63% | 115% | 54% | 1.93 | 3.68 | 1.75 |
| 12/26/2012 15:33 | 1/2/2013 21:01 | Hartman3 | 422First | Chloroform | 0.22 | 0.362552 | 0.642552 | 0.41276 | 49% | 98% | 61% | 1.65 | 2.92 | 1.88 |
| 1/2/2013 21:05 | 1/9/2013 20:02 | Hartman3 | 422First | Chloroform | 0.37 | 0.4194 | 0.545996 | 0.458727 | 13% | 38% | 21% | 1.13 | 1.48 | 1.24 |
| 1/9/2013 20:04 | 1/16/2013 19:12 | Hartman3 | 422First | Chloroform | 0.32 | 0.425666 | 0.537368 | 0.461134 | 28% | 51% | 36% | 1.33 | 1.68 | 1.44 |
| 1/16/2013 19:13 | 1/23/2013 20:47 | Hartman3 | 422First | Chloroform | 0.43 | 0.686704 | 0.693847 | 0.693719 | 46% | 47% | 47% | 1.60 | 1.61 | 1.61 |
| 1/23/2013 20:48 | 1/30/2013 17:51 | Hartman3 | 422First | Chloroform | 0.4 | 0.593417 | 0.593417 | 0.593417 | 39% | 39% | 39% | 1.48 | 1.48 | 1.48 |

(continued)

Table 4-21. Comparison of Online GC to Radiello Results by Week (cont.)

| Start Date Time | Stop Date Time | Period | Location | Compound | Radiello ($\mu\text{g}/\text{m}^3$) | GC: Missing Values = 1/2 MDL ($\mu\text{g}/\text{m}^3$) | GC: Missing values = MDL ($\mu\text{g}/\text{m}^3$) | GC: Missing values = NGC ($\mu\text{g}/\text{m}^3$) | RPD Calculated with Missing Values = 1/2 MDL | RPD Calculated with Missing values = MDL | RPD Calculated with Missing values = NGC | Ratio (online GC/Radiello) Calculated with Missing Values = 1/2 MDL | Ratio (online GC/Radiello) Calculated with Missing values = MDL | Ratio (online GC/Radiello) Calculated with Missing values = NGC |
|------------------|------------------|----------|----------|------------|--|---|---|---|---|---|---|---|---|---|
| 1/30/2013 17:52 | 2/6/2013 0:21 | Hartman3 | 422First | Chloroform | 0.39 | 0.694886 | 0.694886 | 0.694886 | 56% | 56% | 56% | 1.78 | 1.78 | 1.78 |
| 2/6/2013 0:24 | 2/13/2013 19:28 | Hartman3 | 422First | Chloroform | 0.07 | 0.383526 | 0.680696 | 0.572113 | 138% | 163% | 156% | 5.48 | 9.72 | 8.17 |
| 2/13/2013 19:31 | 2/20/2013 21:10 | Hartman3 | 422First | Chloroform | 0.16 | 0.350648 | 0.693356 | 0.3811 | 75% | 125% | 82% | 2.19 | 4.33 | 2.38 |
| 3/6/2013 19:44 | 3/14/2013 22:28 | Hartman3 | 422First | Chloroform | 0.11 | 0.349662 | 0.655116 | 0.347343 | 104% | 142% | 104% | 3.18 | 5.96 | 3.16 |
| 12/19/2012 23:42 | 12/26/2012 15:54 | Hartman3 | Outside | Chloroform | 0.08 | 0.489826 | 0.774709 | 1.101563 | 144% | 163% | 173% | 6.12 | 9.68 | 13.77 |
| 12/26/2012 16:00 | 1/2/2013 21:53 | Hartman3 | Outside | Chloroform | 0.075 | 0.424082 | 0.724082 | 0.868571 | 140% | 162% | 168% | 5.65 | 9.65 | 11.58 |
| 1/2/2013 21:55 | 1/9/2013 20:40 | Hartman3 | Outside | Chloroform | 0.12 | 0.35 | 0.7 | NGC | 98% | 141% | NGC | 2.92 | 5.83 | NGC |
| 1/9/2013 20:42 | 1/16/2013 19:57 | Hartman3 | Outside | Chloroform | 0.075 | 0.347365 | 0.660906 | 0.3247 | 129% | 159% | 125% | 4.63 | 8.81 | 4.33 |
| 1/16/2013 19:59 | 1/23/2013 21:29 | Hartman3 | Outside | Chloroform | 0.075 | 0.361402 | 0.678069 | 0.469725 | 131% | 160% | 145% | 4.82 | 9.04 | 6.26 |
| 1/23/2013 21:32 | 1/30/2013 18:32 | Hartman3 | Outside | Chloroform | 0.075 | 0.34572 | 0.640039 | 0.3231 | 129% | 158% | 125% | 4.61 | 8.53 | 4.31 |
| 1/30/2013 18:34 | 2/6/2013 1:27 | Hartman3 | Outside | Chloroform | 0.075 | 0.360212 | 0.702072 | 0.7891 | 131% | 161% | 165% | 4.80 | 9.36 | 10.52 |
| 2/6/2013 1:29 | 2/13/2013 20:03 | Hartman3 | Outside | Chloroform | 0.075 | 0.353025 | 0.650194 | 0.370038 | 130% | 159% | 133% | 4.71 | 8.67 | 4.93 |
| 2/13/2013 20:06 | 2/20/2013 21:51 | Hartman3 | Outside | Chloroform | 0.075 | 0.42005 | 0.68255 | 0.6302 | 139% | 160% | 157% | 5.60 | 9.10 | 8.40 |
| 3/6/2013 20:42 | 3/14/2013 23:15 | Hartman3 | Outside | Chloroform | 0.065 | 0.349014 | 0.692764 | 0.2948 | 137% | 166% | 128% | 5.37 | 10.66 | 4.54 |

Note: NGC = No GC data available for comparison

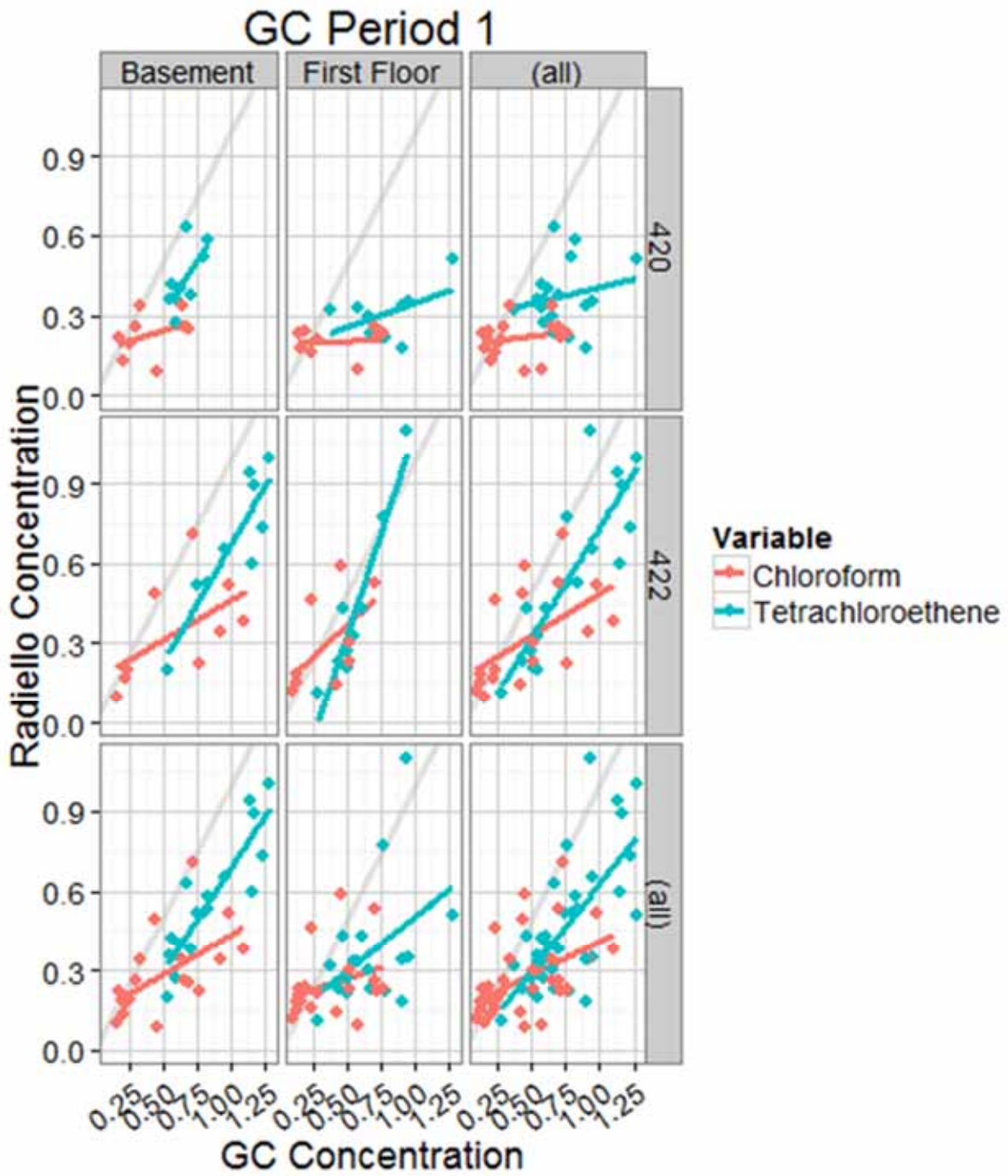


Figure 4-2. XY Comparison plot of Radiello and GC indoor air concentration measurements ($\mu\text{g}/\text{m}^3$), Hartman 1 sampling period.

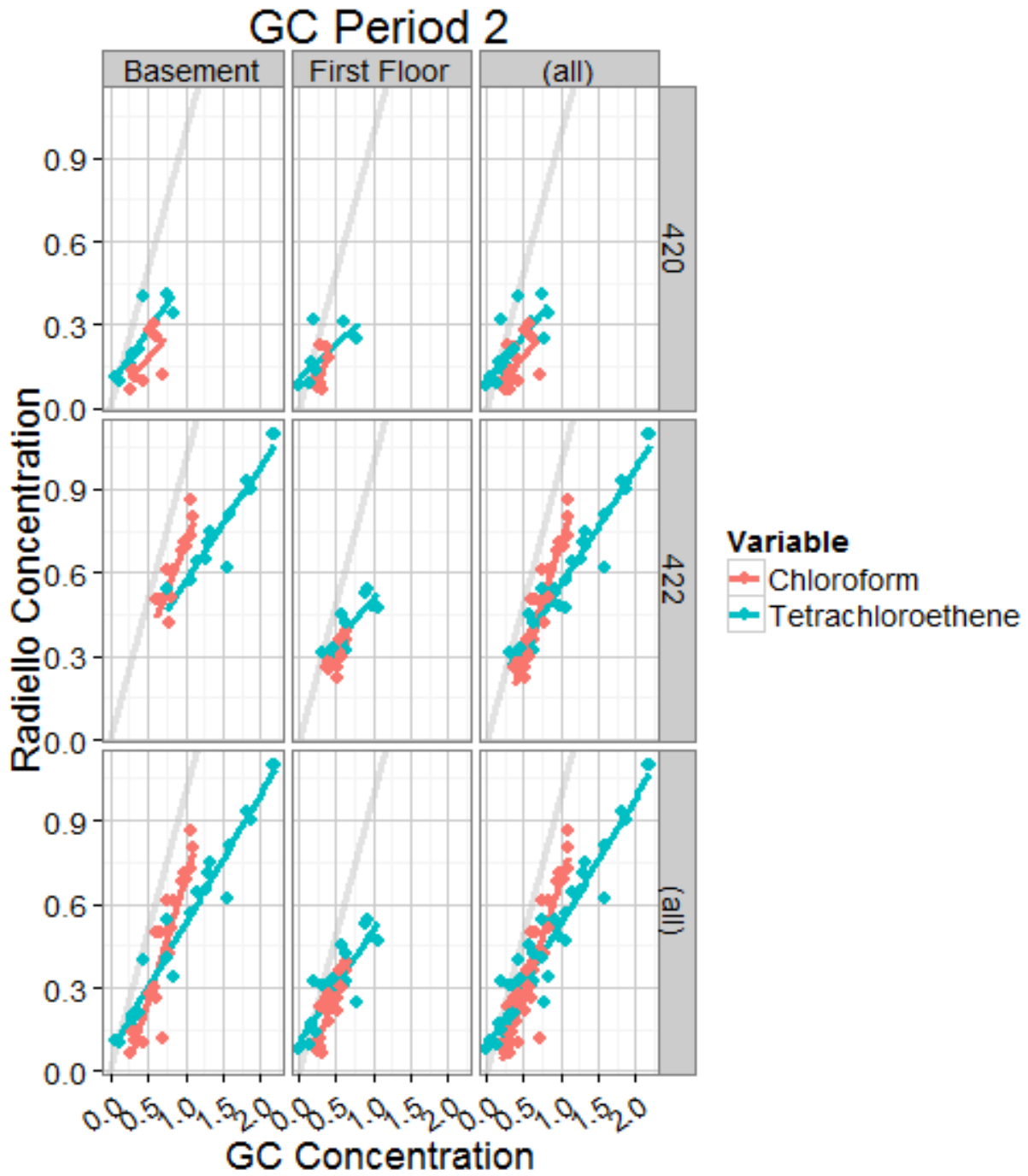


Figure 4-3. XY Comparison plot of Radiello and GC indoor air concentration measurements ($\mu\text{g}/\text{m}^3$), Hartman 2 sampling period.

The effect of these differences can also be visualized in the time series. In the time series plots (such as **Figures 4-4** through **4-7**), the individual GC measurements occurring approximately every 2 hours are shown as faint grey dots. Orange, green, and blue bars represent the weeklong averages of those GC measurements after applying different treatments to time periods when there was no signal recorded on the GC. When the treatment of the no signal data was immaterial, a single green bar marks the average GC results. The individual occasions when no signal was detected on the GC are shown as red hash marks just above the X axis. The calculated detection/reporting limit of the online GC (see Section 4.3.2) is shown as a dark grey line bisecting the graph. The concentration measured by the passive Radiello sampler exposed for 1 week is shown as a lavender bar. From these **Figures 4-4** through **4-7**, it is apparent that the weekly average GC measurements and passive sampler measurements move in parallel trends and the online GC results almost always exceed the passive sampler results. The agreement of temporal trends is best when the indoor air concentrations are relatively high (where the vast majority of the GC runs identified a peak and concentrations were $>0.5 \mu\text{g}/\text{m}^3$). This provides qualitative confidence that the high spikes seen in the online GC data likely reflect real events of vapor intrusion. As expected, the weekly averaged data are less “jagged” than the data collected every 2 hours.

Other studies have also generally showed that online GC results and/or fixed laboratory TO-15 sample results are generally slightly higher than those obtained with passive samplers under low concentration ambient or indoor air conditions (Odenchantz et al., 2008; Lutes et al., 2010b; Allen et al., 2007).

Despite the substantial differences between the absolute values for either compound measured by the two methods, when the data are examined in terms of the ratio of concentrations on the first floor to concentrations measured in the basement, there is reasonably close agreement between the two instruments. Correlation between the two methods is better for Hartman 2 (**Figure 4-3**) and Hartman 3 (discussed in next section).

For brevity, a full set of plots of the correlation of the online GC to the weeklong passive samples at all locations is appended (Appendix B).

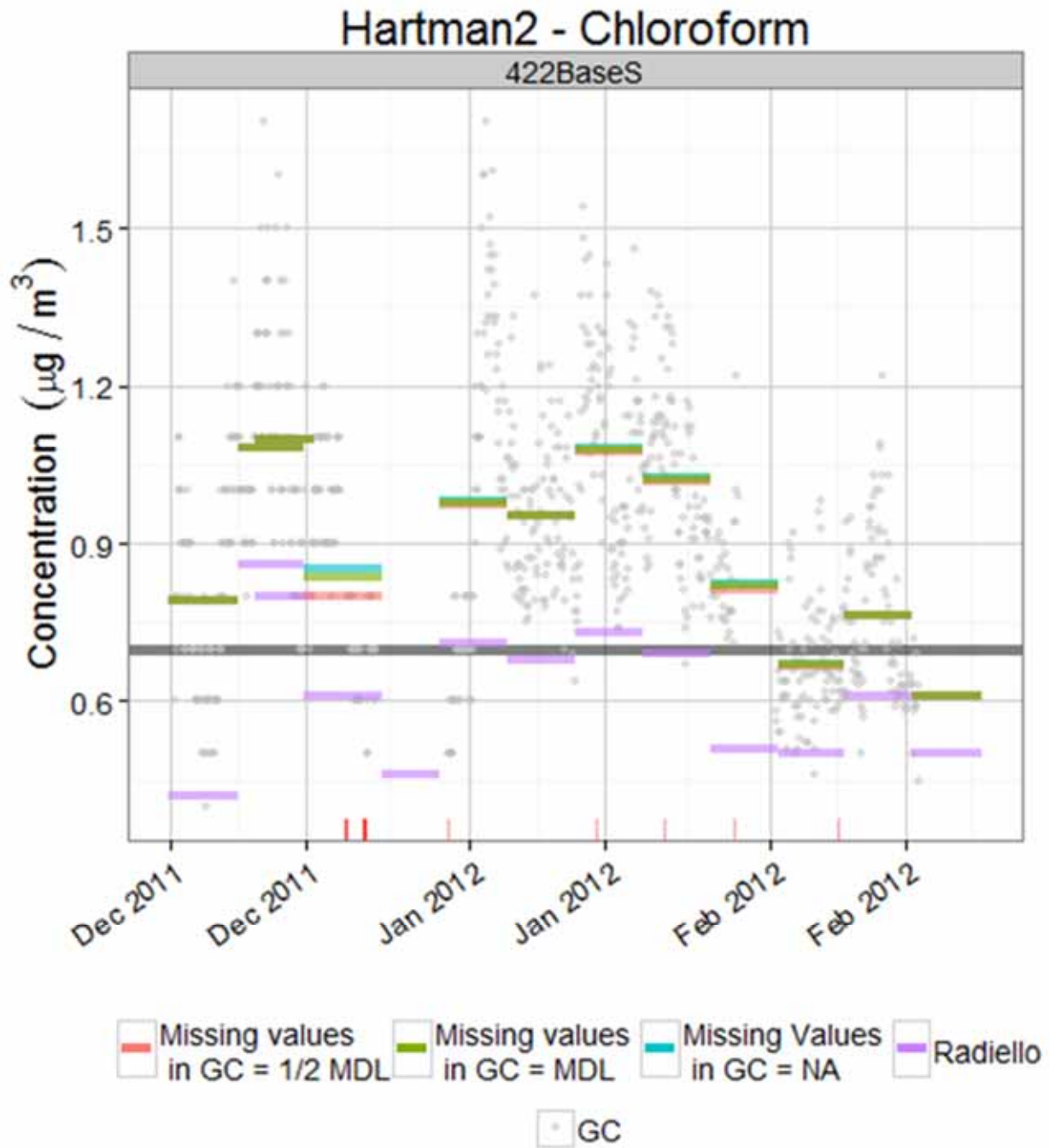


Figure 4-4. Time series comparison of field GC and passive sampling data: 422 basement, Hartman Period 2, chloroform. Horizontal gray line is calculated GC reporting limit. Red hash marks on y-axis indicate missing values.

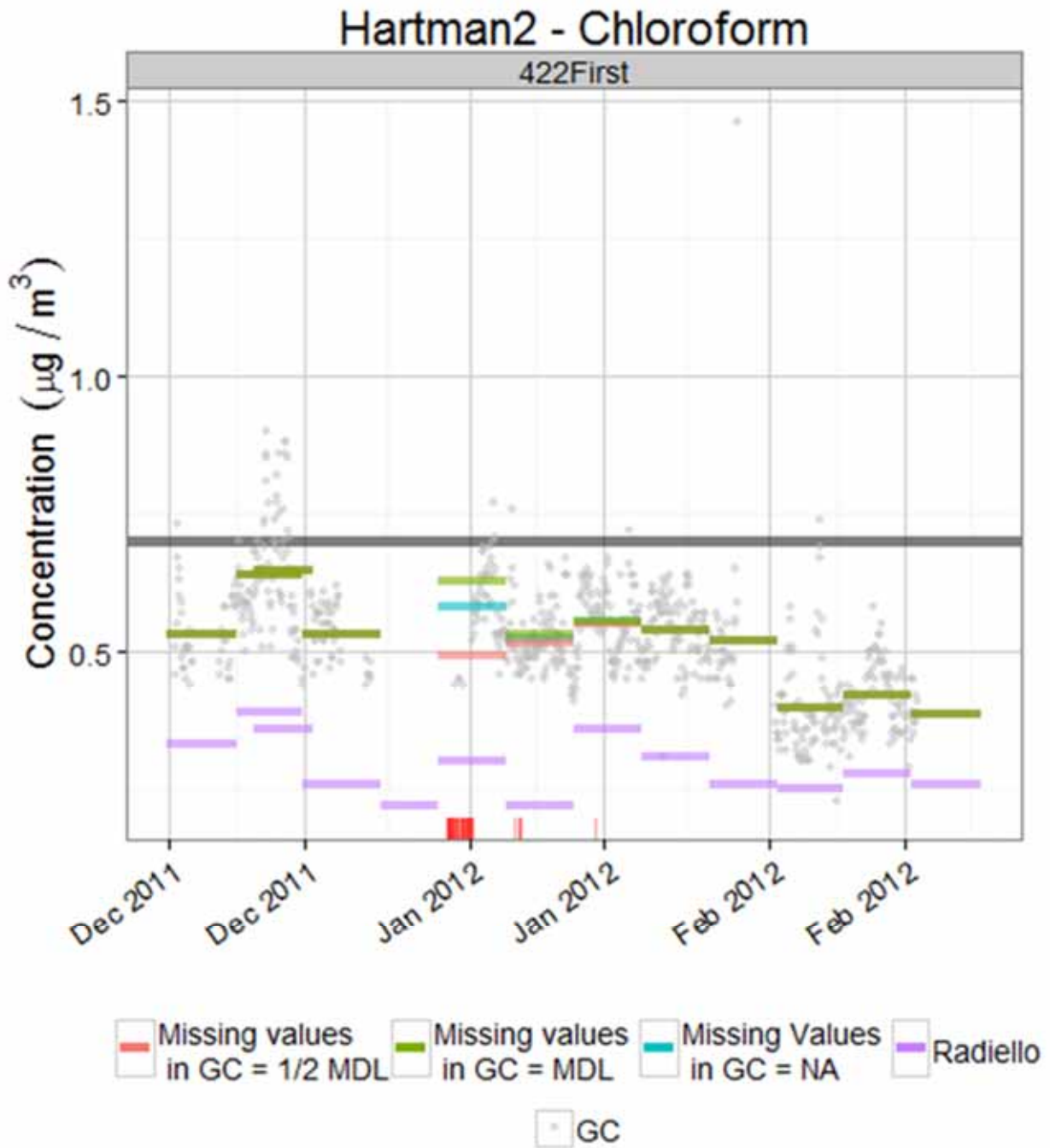


Figure 4-5. Time series comparison of field GC and passive sampling data: 422 first floor, Hartman Period 2, chloroform. Horizontal gray line is calculated GC reporting limit. Red hash marks on y-axis indicate missing values.

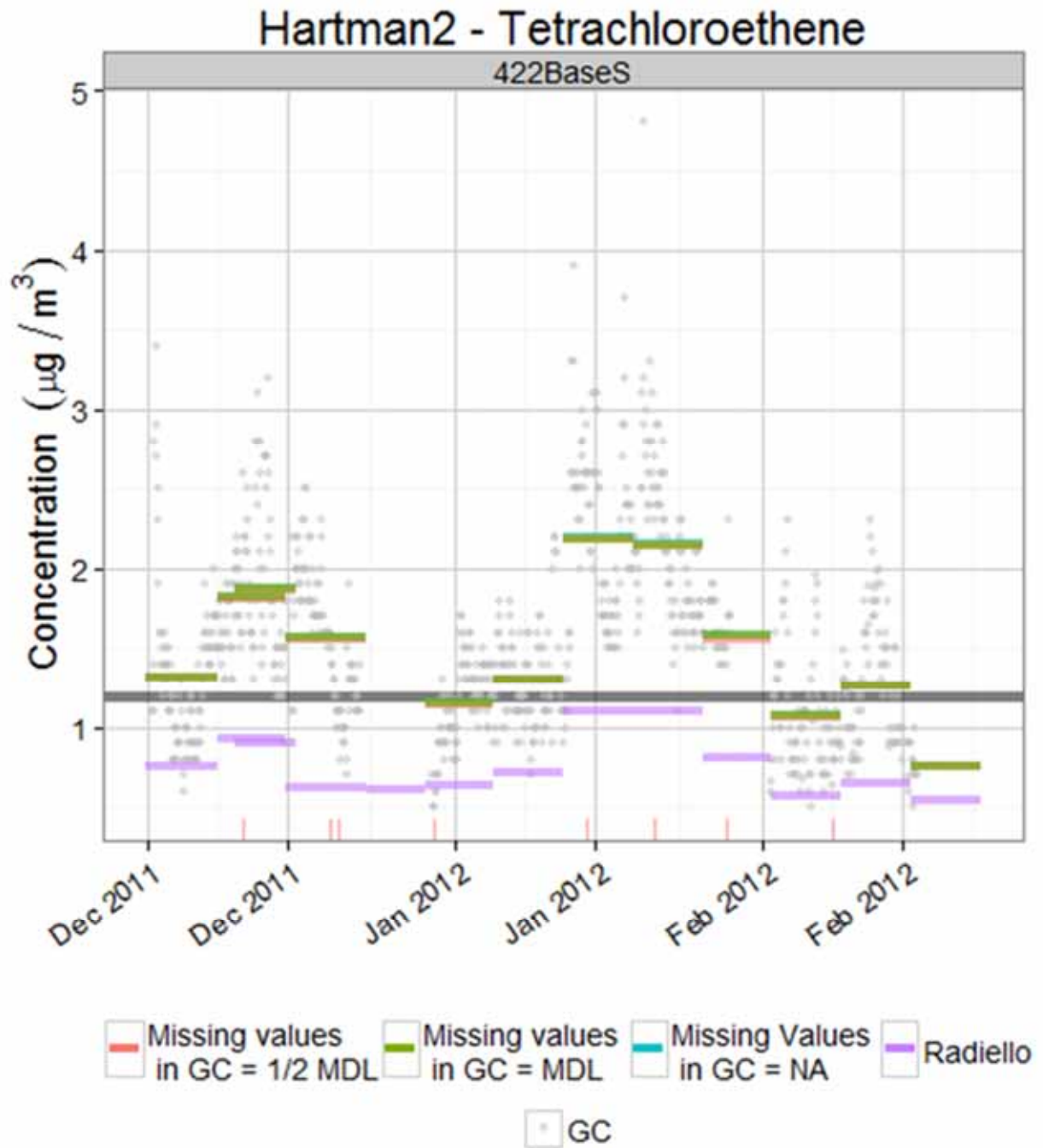


Figure 4-6. Time series comparison of field GC and passive sampling data: 422 basement, Hartman Period 2, PCE. Horizontal gray line is calculated GC reporting limit. Red hash marks on y-axis indicate missing values.

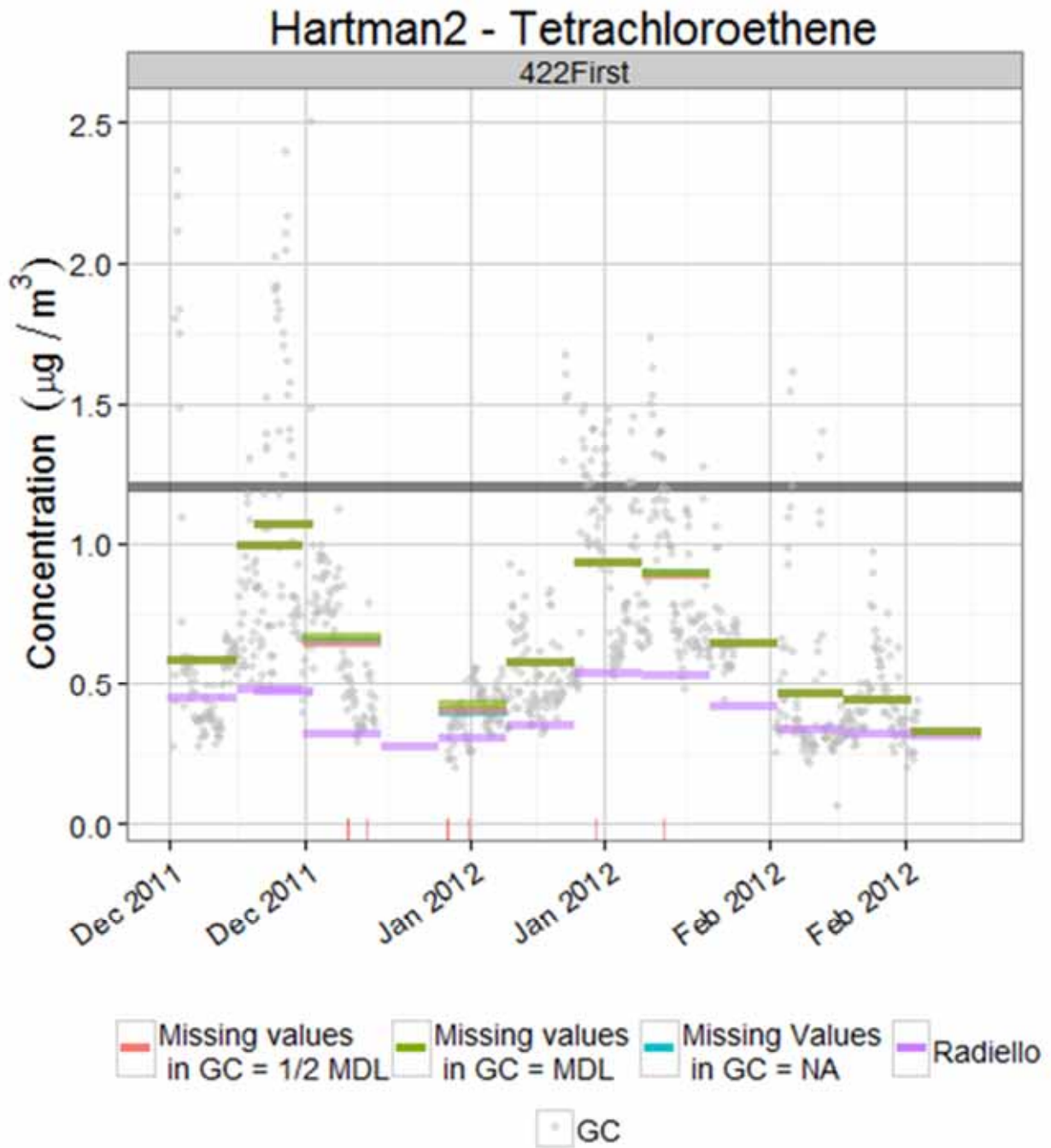


Figure 4-7. Time series comparison of field GC and passive sampling data: 422 first floor, Hartman Period 2, PCE. Horizontal gray line is calculated GC reporting limit. Red hash marks on y-axis indicate missing values.

4.3.6.2 Hartman Period 3

The agreement between the field GC and the Radiello data is generally, although not always, better during this period (**Table 4-21, Figure 4-8**). A majority of the comparisons are within the stated accuracy objective of 40% RPD. All PCE cases where both instruments found the concentration to be $>0.5 \mu\text{g}/\text{m}^3$ met this accuracy objective. There were very few cases where the Radiello indoor chloroform exceeded the $>0.7 \mu\text{g}/\text{m}^3$ stated MDL for the GC. Those cases showed RPDs between 50 and 60%. Overall the correlation between the methods is strong, especially at higher concentration levels (**Figure 4-8**).

We also plotted the time series of the weekly average field GC results against the passive sampler results (**Figures 4-9 through 4-12**). As was seen for Hartman 2 a parallel movement is seen between the two data sets. Weeks that exhibited high peaks in the online GC (and thus had high average concentrations) were also high in the passive sampler results.

In cases where the concentrations registered a peak on the GC (where the amount of missing data was low), the temporal agreement between the field GC and the Radiello was good. This suggests that the peaks above the detection limit observed by the field GC likely reflect real events of vapor intrusion.

4.3.7 Overall Assessment of Online GC Data

Several overarching assessments can be reached regarding these data sets:

- Agreement with other methods/instruments is best for the first 4 weeks of period Hartman Period 1 and for the entirety of Hartman Period 2 and Hartman Period 3. The later portion of Hartman 1 appears to contain a substantial high bias.
- Agreement is better for the higher concentrations (those well above the MDL) as would be expected. Thus, the agreement is best in the winter data sets (Hartman Periods 2 and 3). This also suggests that agreement is generally best in the 422 basement where the concentrations are highest.
- Because of the biases exhibited in the Hartman Period 1 data (most likely due to the lower VOC concentrations exhibited in the summer months), data analysis results for this period should be considered less reliable than those drawn from Hartman Periods 2 and 3.

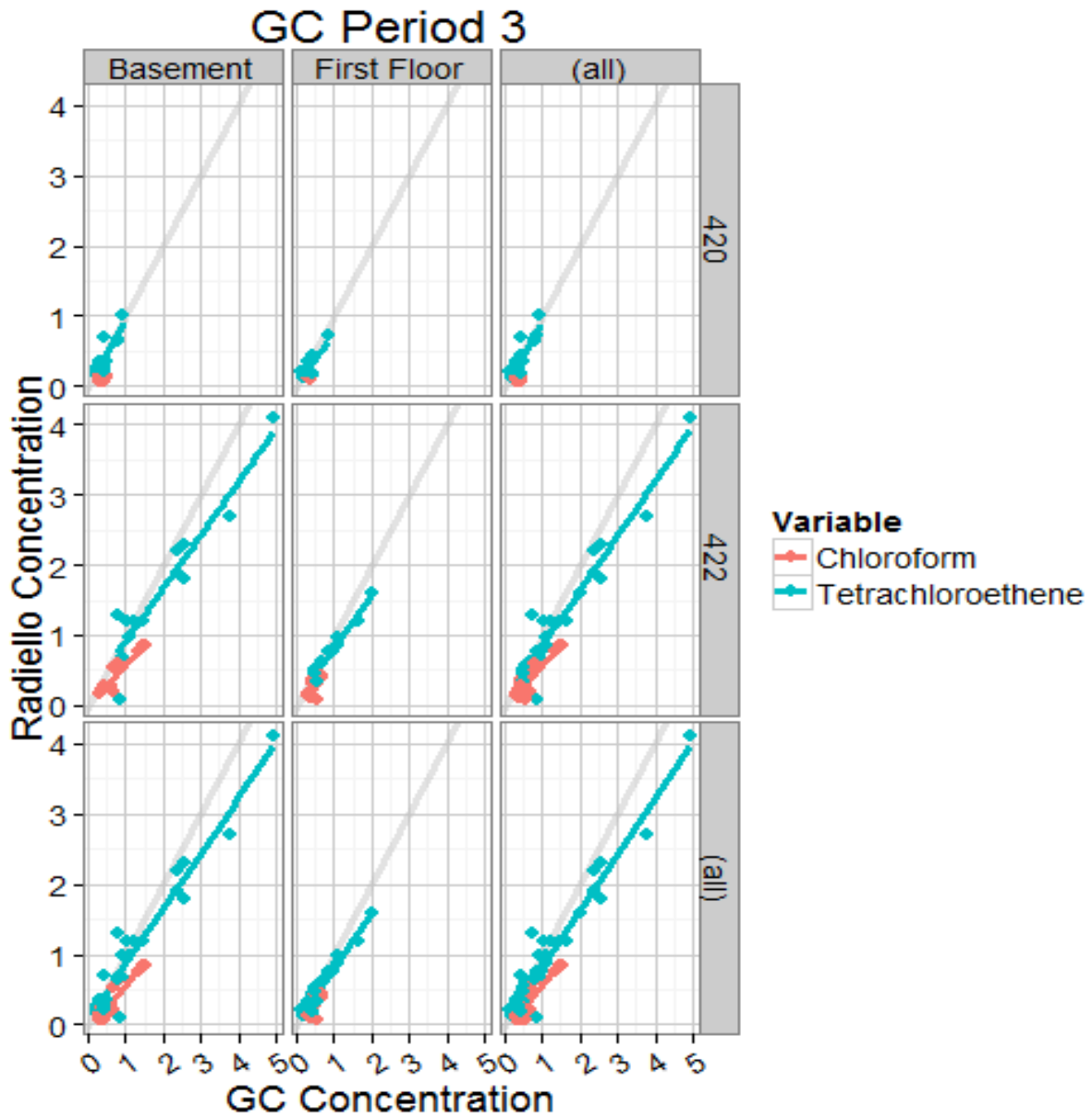


Figure 4-8. XY Plot of field GC vs. passive sampler data, Hartman Period 3.

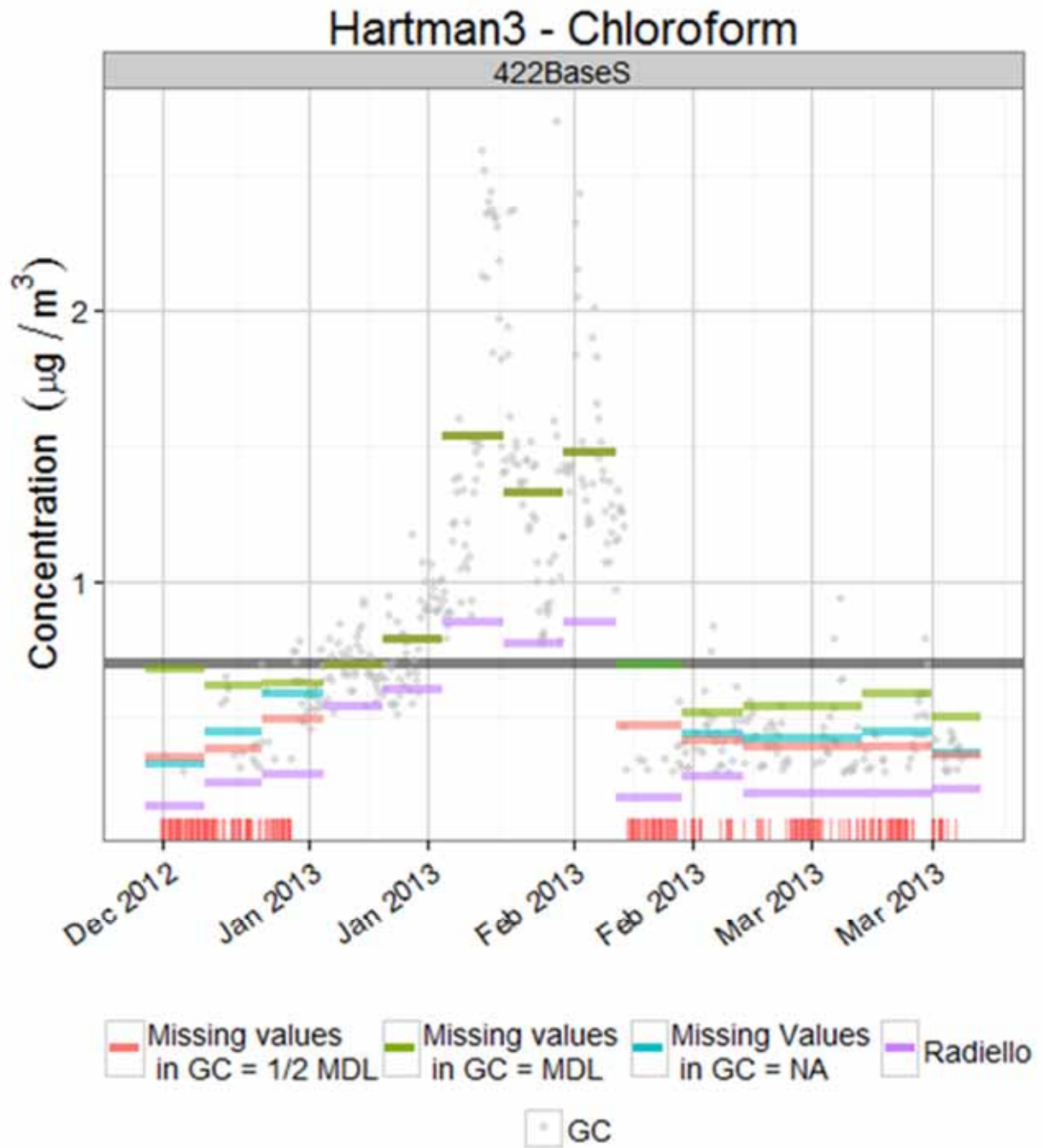


Figure 4-9. Time series comparison of field GC and passive sampling data: 422 basement, Hartman Period 3, chloroform. Horizontal gray line is calculated GC reporting limit. Red hash marks on y-axis indicate missing values.

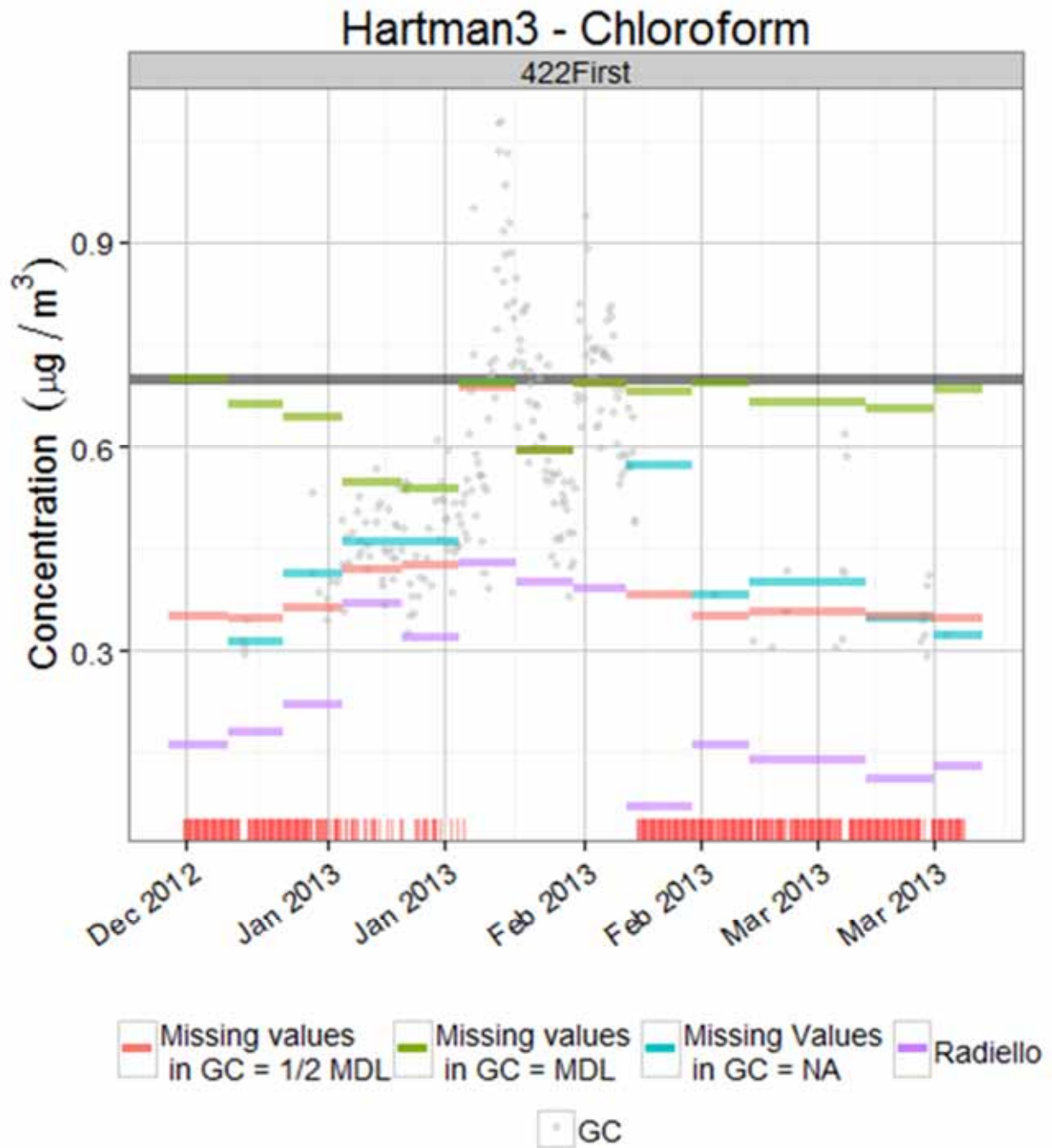


Figure 4-10. Time series comparison of field GC and passive sampling data: 422 first floor, Hartman Period 3, chloroform. Horizontal gray line is calculated GC reporting limit. Red hash marks on y-axis indicate missing values.

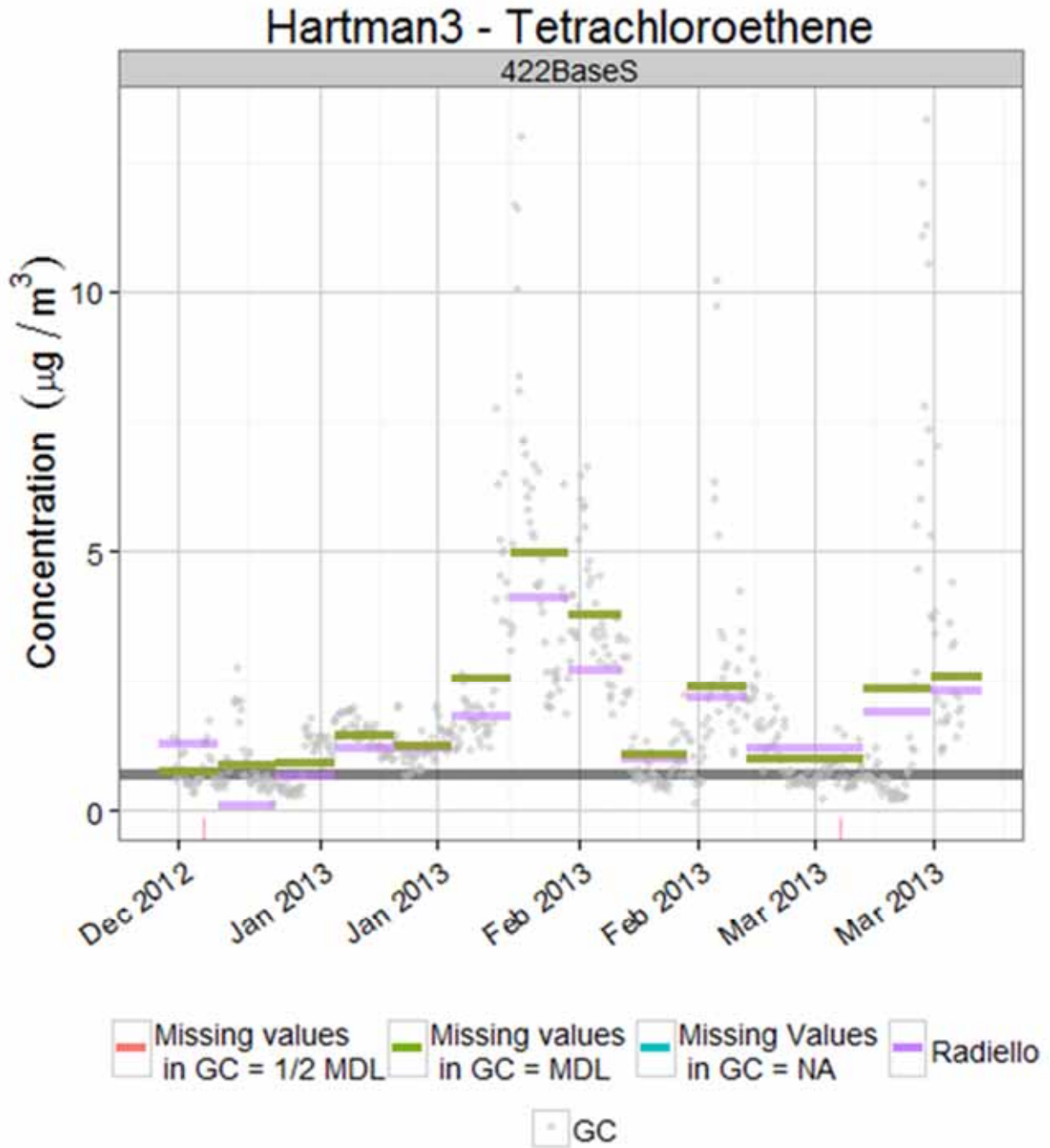


Figure 4-11. Time series comparison of field GC and passive sampling data: 422 Basement, Hartman Period 3, PCE. Horizontal gray line is calculated GC reporting limit. Red hash marks on y-axis indicate missing values.

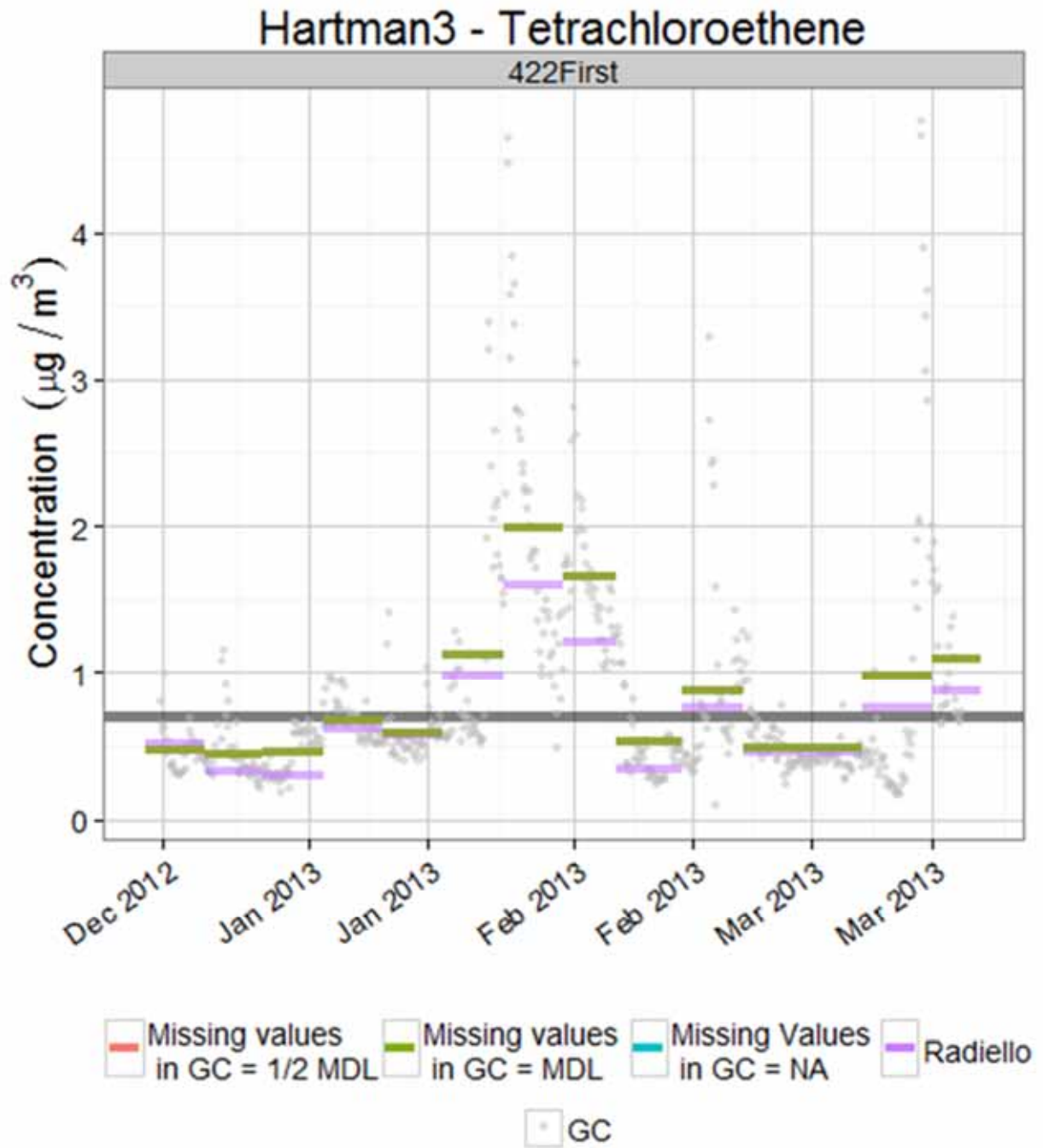


Figure 4-12. Time series comparison of field GC and passive sampling data: 422 first floor, Hartman Period 3, PCE. Horizontal gray line is calculated GC reporting limit. Red hash marks on y-axis indicate missing values (none in this case).

4.4 Radon

4.4.1 Indoor Air: Comparison of Electrets Field, ARCADIS to Charcoal Analyzed by U.S. EPA R&IE National Laboratory

Three comparisons were made between electrets and charcoal canisters. Charcoal canisters were provided and analyzed by EPA's Radiation and Indoor Environments National Laboratory Center for Indoor Environments in Las Vegas, Nevada. ARCADIS collected charcoal canister samples and electret samples. Electrets were obtained from Rad Elec (Frederick, Maryland) and read by ARCADIS on site before and after deployment. The charcoal canisters were used as a QC check on three separate occasions: January 19, 2011, to January 26, 2011, April 27, 2011, to May 4, 2011, and December 28, 2011, to January 4, 2012. A further test with charcoal canisters occurred on June 19, 2013, through June 26, 2013, with results pending analysis of the canisters by EPA. Charcoal canisters (plus duplicates) were placed at indoor locations and the ambient locations that were routinely being used for electret monitoring. When the results were received, the sample plus its duplicate were averaged together to obtain a result for the location. This was then compared with the electret result for that location and time period.

For the first occasion, the relative percentage difference between the two methods was 20% or less (**Table 4-22**). The maximum absolute difference was 0.63 pCi. A relative percentage difference could not be calculated for the ambient, which was below the detection limit with the charcoal method (BDL).

On the second occasion, five of six comparisons showed a relative percentage difference of 20% or less and four of the six comparisons were within 0.5 pCi/L of each other (**Table 4-23**).

The exceptions were 422 basement north and 420 basement south, which were within 0.9 pCi/L of each other. The ambient was again BDL by the charcoal method, as would have been predicted from the electret data.

For the third occasion, December 28, 2011, to January 4, 2012, the absolute difference between the methods is at or below 0.3 pCi/L and RPD is <6% for all samples (**Table 4-24**). The ambient charcoal sample was below the detection limit and that detection limit was equal to the ambient value reported by the electret method.

Table 4-22. Comparison between Electrets and Charcoal Canisters at the 422/420 EPA House from January 19–26, 2011

| Sample Location | Electret Rn (pCi/L) | Charcoal Rn (pCi/L) | Charcoal Average | Absolute Difference (pCi/l) | RPD (%) |
|-----------------|---------------------|---------------------|------------------|-----------------------------|---------|
| 422First | 5.14 | 4.8 | 4.7 | 0.44 | 6.84% |
| 422First | | 4.6 | | | |
| 422BaseN | 8.44 | 8 | 8.4 | 0.04 | 5.35% |
| 422BaseN | | 8.8 | | | |
| 420First | 1.68 | 1.7 | 1.65 | 0.03 | -1.18% |
| 420First | | 1.6 | | | |
| 420BaseN | 3.98 | 3.3 | 3.35 | 0.63 | 18.68% |
| 420BaseN | | 3.4 | | | |
| Ambient | 0.03 | <0.5 | <0.5 | | |
| Ambient | | <0.5 | | | |

Table 4-23. Comparison of Electret and Charcoal Canister Data from April 27 to May 4, 2011

| Location | Electret Data (pCi/l) | Charcoal Canister Radon Activity (pCi/l) | Charcoal Canister Average Radon Activity (pCi/l) | Absolute Difference (pCi/l) | RPD (%) |
|----------------|-----------------------|--|--|-----------------------------|---------|
| Ambient | 0.47 | <0.5 | | | |
| Ambient Dup | | <0.5 | | | |
| 422 First | 2.72 | 2.8 | 2.6 | 0.12 | 4.51% |
| 422 First Dup | | 2.4 | | | |
| 422 Base S | 7.39 | 7.3 | 7 | 0.39 | 5.42% |
| 422 Base S Dup | | 6.7 | | | |
| 422 Base N | 7.14 | 6.3 | 6.05 | 0.905 | 13.92% |
| 422 Base N Dup | 6.77 | 5.8 | | | |
| 420 First | 0.98 | 1.3 | 1.4 | -0.42 | -35.29% |
| 420 First Dup | | 1.5 | | | |
| 420 Base S | 4.58 | 3.8 | 3.75 | 0.83 | 19.93% |
| 420 Base S Dup | | 3.7 | | | |
| 420 Base N | 4.48 | 4.2 | 3.95 | 0.53 | 12.57% |
| 420 Base N Dup | | 3.7 | | | |
| Field blank | NA | <0.5 | | | |
| Field blank | NA | <0.5 | | | |

NA = Not Available

Table 4-24. Comparison of Charcoal and Electret Radon December 28, 2011, to January 4, 2012

| Canister ID | Radon Activity (pCi/l) | Charcoal Average (pCi/l) | Location | Electrets (pCi/L) | Absolute Difference (pCi/L) | RPD (%) |
|-------------|------------------------|--------------------------|---------------|-------------------|-----------------------------|---------|
| 877138 | 3.1 | 3.2 | 420BaseN | 3.34 | -0.2 | -5.86% |
| 877113 | 3.2 | | 420BaseN Dup | | | |
| 877137 | 2.8 | 2.8 | 420BaseS | 2.72 | 0.0 | 1.10% |
| 877115 | 2.7 | | 420BaseS Dup | | | |
| 877133 | 1.1 | 1.1 | 420First | 1.09 | 0.0 | -3.74% |
| 877107 | 1.0 | | 420First Dup | | | |
| 877139 | 10.0 | 10.0 | 422BaseN | 10.22 | -0.3 | -2.67% |
| 877136 | 9.9 | | 422BaseN Dup | 10.35 | | |
| 877128 | 9.6 | 9.5 | 422BaseS | 9.57 | -0.1 | -0.73% |
| 877111 | 9.4 | | 422BaseS Dup | | | |
| 877108 | 4.8 | 4.8 | 422First | 4.86 | -0.1 | -2.29% |
| 877140 | 4.7 | | 422First Dup | | | |
| 877110 | 5.0 | 5.2 | 422Office | 4.92 | 0.2 | 4.57% |
| 877131 | 5.3 | | 422Office Dup | | | |
| 877130 | <0.5 | | Ambient | 0.5 | NA | NA |

NA = Not Available

Figure 4-13 shows the correlations from Tables 4-22 to 4-24 in graphical form.

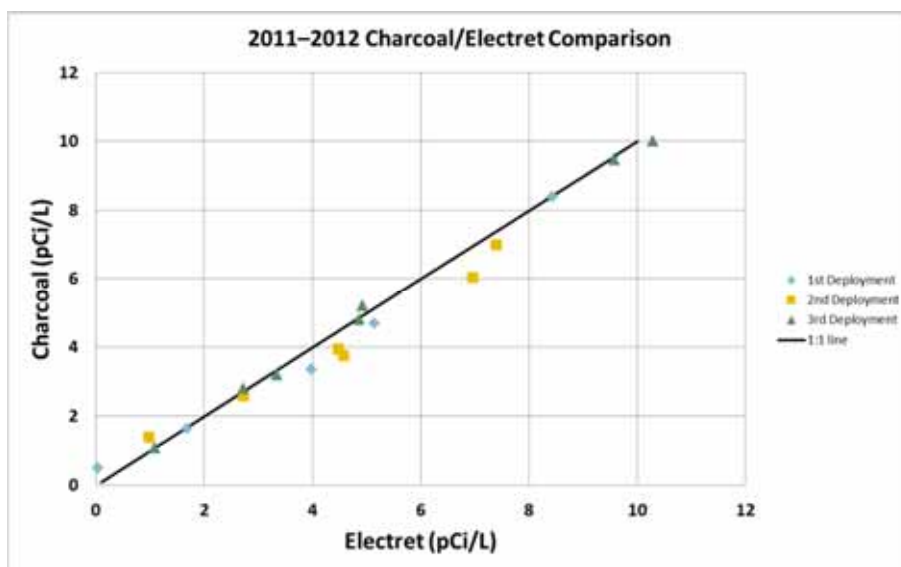


Figure 4-13. Correlation between radon measured using the electret and charcoal methods.

4.4.2 Comparison of Average of Real-Time AlphaGUARD to Electrets and Charcoal Canisters

Stationary AlphaGUARD units provided by EPA were used for real-time monitoring of indoor air radon at two locations (422 basement north and 422 office (2nd floor)). Several comparisons were made between the stationary AlphaGUARD data and electrets located nearby (at 422 basement north at first and both 422 basement north and 422 office later).

The first comparison took place over several weeks between March 30, 2011, and May 18, 2011 (Table 4-25). The absolute difference ranged from -0.04 pCi/L to 1.44 pCi/L. The relative percentage difference ranged from 0.50% to 26.04%.

Table 4-25. Comparison between 422 Basement N AlphaGUARDs and Electrets from March 30, 2011, and May 18, 2011

| Date Range | AlphaGUARD Reading (pCi/l) | Electret (pCi/l) | Electret Dup(pCi/l) | Electret Ave (pCi/L) | Absolute Difference (pCi/L) | Relative Percentage Difference |
|-------------|----------------------------|------------------|---------------------|----------------------|-----------------------------|--------------------------------|
| 03/30-04/07 | 6.18 | 6.30 | 4.98 | 5.64 | 0.54 | 9.14% |
| 04/07-04/13 | 5.90 | 4.94 | 5.87 | 5.41 | 0.50 | 8.76% |
| 04/13-04/20 | 8.41 | 6.97 | 7.83 | 7.40 | 1.01 | 12.78% |
| 04/20-04/27 | 6.25 | 4.04 | 5.58 | 4.81 | 1.44 | 26.04% |
| 04/27-05/04 | 6.92 | 7.14 | 6.77 | 6.96 | -0.04 | -0.50% |
| 05/04-05/11 | 4.66 | 2.93 | 4.50 | 3.72 | 0.95 | 22.57% |
| 05/11-05/18 | 6.15 | 5.81 | 6.01 | 5.91 | 0.24 | 3.98% |

For the second comparison, which occurred from August 3, 2011, to October 6, 2011, in the 422 basement north location, the absolute difference ranged from -1.11 pCi/L to 2.42 pCi/L. The relative percentage difference ranged from -40.18% to 30.76% (Table 4-26).

Table 4-26. Comparison of Real-Time AlphaGUARD to Integrated Electret August through October

| End Date/ Time | Rn (pCi/L) A Guard (averaged over a week) | Rn (pCi/L) Electrets 422 Base N | Rn (pCi/L) Electrets 422 Base N Dup | Average of Duplicate Electrets (pCi/L) | Absolute Difference (pCi/L) | Relative Percentage Difference |
|-------------------|--|---------------------------------------|---|---|-----------------------------------|--------------------------------------|
| 8/3/2011 | 6.85 | 6.85 | 5.14 | 6.00 | 0.85 | 13.26% |
| 8/10/2011 | 7.24 | 7.25 | 6.79 | 7.02 | 0.22 | 3.09% |
| 8/17/2011 | 8.38 | 7.53 | 7.20 | 7.37 | 1.02 | 12.91% |
| 8/24/2011 | 3.84 | 3.48 | 3.00 | 3.24 | 0.60 | 16.93% |
| 8/31/2011 | 2.21 | 2.17 | 4.46 | 3.32 | -1.11 | -40.18% |
| 9/7/2011 | 4.34 | 4.52 | 1.84 | 3.18 | 1.16 | 30.76% |
| 9/14/2011 | 6.09 | 5.68 | 5.44 | 5.56 | 0.53 | 9.16% |
| 9/21/2011 | 8.69 | 8.03 | 7.84 | 7.94 | 0.75 | 9.05% |
| 9/28/2011 | 12.51 | 11.67 | 11.44 | 11.56 | 0.96 | 7.97% |
| 10/6/2011 | 10.33 | 7.83 | 7.99 | 7.91 | 2.42 | 26.53% |

During the third comparison, electrets, the AlphaGUARD, and the charcoal canisters were compared from December 28, 2011, to January 4, 2012. Only the 422 office and 422 basement north were compared by all three methods during this time. The absolute difference between the canisters and AlphaGUARD ranged from -0.05 pCi/L to 0.15pCi/L, and the absolute difference between the electrets and AlphaGUARD ranged from -0.08pCi/L to 0.29pCi/L. The relative percentage difference between canisters and AlphaGUARD ranged from -0.50% to 2.96%, and the relative percentage difference between electrets and AlphaGUARD ranged from -1.61% to 2.81% (Table 4-27).

Table 4-27. Comparison of Real-Time AlphaGUARD to Integrated Electret Measurements December 28, 2011, to January 4, 2012

| Location | Canister Radon Activity (pCi/l) | Dup Canister Radon Activity (pCi/L) | Canister Average (pCi/L) | Electret (pCi/L) | Electret Dup (pCi/L) | Electret Average (pCi/L) | 422 Base N AlphaGUARD Approximation (pCi/L) | Absolute Difference between Canisters and AlphaGUARDs (pCi/L) | Absolute Difference between Electrets and AlphaGUARDs (pCi/L) | Relative Percent Difference between Canisters and AlphaGUARD | Relative Percent Difference between Electrets and AlphaGUARD |
|------------|------------------------------------|--|--------------------------|------------------|----------------------|--------------------------|---|---|---|---|---|
| 422BaseN | 10.00 | 9.90 | 9.95 | 10.22 | 10.35 | 10.29 | 10.00 | -0.05 | 0.29 | -0.50% | 2.81% |
| 422 Office | 5.00 | 5.30 | 5.15 | 4.92 | | | 5.00 | 0.15 | -0.08 | 2.96% | -1.61% |

The fourth comparison occurred between January 4, 2012, and March 1, 2012, for both the 422 office and 422 basement north locations. The absolute difference between 422 basement north AlphaGUARDs and electrets ranged from -0.52 pCi/L to 1.79 pCi/L, and the absolute difference between 422 office AlphaGUARDs and electrets ranged from 0.05 pCi/L to 0.77 pCi/L. The relative percentage difference for 422 basement north ranged from -5.95% to 26.15%, and the relative percentage difference for the 422 office ranged from 1.05% to 17.68% (Table 4-28).

Table 4-28. Comparison of Real-Time AlphaGUARD to Integrated Electret Measurements January through March 2012

| Date Range | 422 Base N AlphaGUARD Reading (pCi/L) | Office AlphaGUARD Reading (pCi/L) | 422 Base N Electret (pCi/L) | 422 Base N Dup Electret (pCi/L) | 422 Base N Electret Average (pCi/L) | Office Electret (pCi/L) | Absolute Difference between 422 Base N AlphaGUARDs and Electrets (pCi/L) | Absolute Difference between Office AlphaGUARDs and Electrets (pCi/L) | 422 Base N Relative Percent Difference | Office Relative Percent Difference |
|-------------------|---------------------------------------|-----------------------------------|-----------------------------|---------------------------------|-------------------------------------|-------------------------|--|--|--|------------------------------------|
| ?-01/04/12 | 10 | 5 | 10.22 | 10.35 | 10.29 | 4.92 | -0.29 | 0.08 | -2.81% | 1.61% |
| 01/04/12-01/11/12 | 8.78 | 4.69 | 9.05 | 9.11 | 9.08 | 4.56 | 0.30 | 0.13 | -3.36% | 2.81% |
| 01/11/12-01/18/12 | 9.73 | 5.09 | 9.34 | 9.73 | 9.54 | 4.88 | 0.19 | 0.21 | 2.02% | 4.21% |
| 01/18/12-01/25/12 | 8.52 | 4.79 | 7.83 | 7.98 | 7.91 | 4.74 | 0.61 | 0.05 | 7.49% | 1.05% |
| 01/25/12-02/01/12 | 7.71 | 4.46 | 8.24 | 8.03 | 8.14 | 4.15 | -0.43 | 0.31 | -5.36% | 7.20% |
| 02/01/12-02/08/12 | 8.68 | 4.78 | 8.60 | 8.62 | 8.61 | 4.58 | 0.06 | 0.20 | 0.81% | 4.27% |
| 02/08/12-02/15/12 | 8.44 | 4.80 | 8.28 | 7.47 | 7.88 | 4.41 | 0.56 | 0.39 | 6.93% | 8.47% |
| 02/15/12-02/22/12 | 7.74 | 4.3 | 6.08 | 5.82 | 5.95 | 3.68 | 1.79 | 0.62 | 26.15% | 15.54% |
| 02/22/12-03/01/12 | 8.48 | 4.74 | 9.00 | 9.00 | 9.00 | 3.97 | -0.52 | 0.77 | -5.95% | 17.68% |

The fifth comparison covers the time period from the week of January 2, 2013, through March 6, 2013 (Table 4-29). It compares the stationary AlphaGUARDs and electrets at both the 422 basement north and the 422 office. The normal and duplicate electrets at the 422 basement north location are averaged. The agreement was within 12% RPD when the mitigation system was in a passive mode and the radon concentrations were above the EPA action level. The portion of the comparison that corresponded with the mitigation on period (February 6 through April 24, 2013) showed much greater RPDs. However, the paired results during these weeks are within +/- 0.7 pCi/l. The high RPDs are due to the tiny absolute value of the radon present as indicated by both methods. This suggests that results below 1.5 pCi/l may have a higher percentage uncertainty.

Table 4-29. Comparison of Real-Time AlphaGUARD to Integrated Electret Measurements January through March 2013

| Week Start Date | 422 Basement North AlphaGUARD (pCi/L) | 422 Basement North Ave Electret (pCi/L) | 422 Office AlphaGUARD (pCi/L) | 422 Office Electret (pCi/L) | Absolute Difference 422 Basement North AlphaGUARD and Electrets (pCi.L) | Absolute Difference 422 Office AlphaGUARD and Electrets (pCi.L) | Relative Percentage Difference 422 Basement North AlphaGUARD and Electrets (%) | Relative Percentage Difference 422 Office AlphaGUARD and Electrets (%) |
|-----------------|---------------------------------------|---|-------------------------------|-----------------------------|---|---|--|--|
| 01/02/13 | 8.0 | 8.7 | 4.3 | 4.5 | -0.7 | -0.2 | -8.50 | -3.88 |
| 01/09/13 | 8.4 | 9.4 | 4.4 | 4.7 | -1.0 | -0.3 | -11.02 | -6.59 |
| 01/16/13 | 8.8 | 9.5 | 4.6 | 4.6 | -0.7 | 0.0 | -7.65 | 0.65 |
| 01/23/13 | 8.3 | 8.2 | 3.9 | 4.0 | 0.2 | -0.1 | 1.82 | -2.28 |

(continued)

Table 4-29. Comparison of Real-Time AlphaGUARD to Integrated Electret Measurements January through March 2013

| Week Start Date | 422 Basement North Alpha-GUARD (pCi/L) | 422 Basement North Ave Electret (pCi/L) | 422 Office Alpha-GUARD (pCi/L) | 422 Office Electret (pCi/L) | Absolute Difference 422 Basement North Alpha-GUARD and Electrets (pCi.L) | Absolute Difference 422 Office Alpha-GUARD and Electrets (pCi.L) | Relative Percentage Difference 422 Basement North Alpha-GUARD and Electrets (%) | Relative Percentage Difference 422 Office Alpha-GUARD and Electrets (%) |
|-----------------|--|---|--------------------------------|-----------------------------|--|--|---|---|
| 01/30/13 | 9.4 | 9.2 | 5.0 | 4.7 | 0.3 | 0.3 | 2.70 | 5.76 |
| 02/06/13 | 1.3 | 0.6 | 0.8 | 0.2 | 0.7 | 0.6 | 68.04 | 116.83 |
| 02/13/13 | 0.4 | 0.5 | 0.3 | 0.1 | -0.1 | 0.2 | -26.09 | 100.00 |
| 02/20/13 | 0.4 | 0.5 | 0.3 | 0.1 | -0.1 | 0.3 | -22.22 | 142.86 |
| 03/06/13 | 0.3 | 0.5 | 0.2 | 0.0 | -0.2 | 0.2 | -44.16 | 147.83 |

4.4.3 Quality Assurance Checks of Electrets

QC was performed on the electret reader and on the chambers holding the electrets. The QC check on the reader was performed by placing reference electrets within the reader each week to measure any deviation from the standard. The standard reference electrets were of 0 V, 245 V, and 250 V. Over the duration of the project, the readings on the 0 V electret fluctuated but stayed within 4 V of its nominal value. The 245 V electret, with only two exceptions stayed within 20 V of its stated value. It steadily declined over the duration of the project, hitting a low before slowly rising toward the end of the project. The 250 V electret stayed within 6 V of its nominal value, showing a slight decline toward the end of the project.

To check for drift within the electret chambers, a normal electret was placed in a closed electret chamber each week and then read on the voltage meter to measure any change in the voltage from the previous week's readings. This would indicate any deviation caused by the chambers. Near the beginning of the project, this electret dropped an average of 5 V/4 weeks or 1.25 V per week. The rate was even lower in the second half of the project to a drop of 5 V/30 weeks or 0.16 V per week. These rates of drift are insignificant because the actual observed voltage change at the indoor sampling locations was typically 25 V per week or more.

4.5 On-Site Weather Station vs. National Weather Service (NWS)

A VantageVue weather station from Davis Instruments was installed at the 422/420 house. Because it was not safe to mount the station directly on the peak of the roof, it was mounted on vertical rods raised to the approximate peak elevation from the edge of the second story roof. The trees near the house, especially to the north, are quite tall, equal to or higher than the weather station. Branches extend close to the house on the northwest corner. The house is much taller than the neighboring building to the east. There is also a neighboring two-story residential structure to the northeast, approximately 30 to 40 ft away. A seven-story commercial structure is approximately 150 ft southwest of the studied duplex. Essentially, the only side completely free from all air current obstructions is the southern side, which borders 28th Street (Figure 4-14).

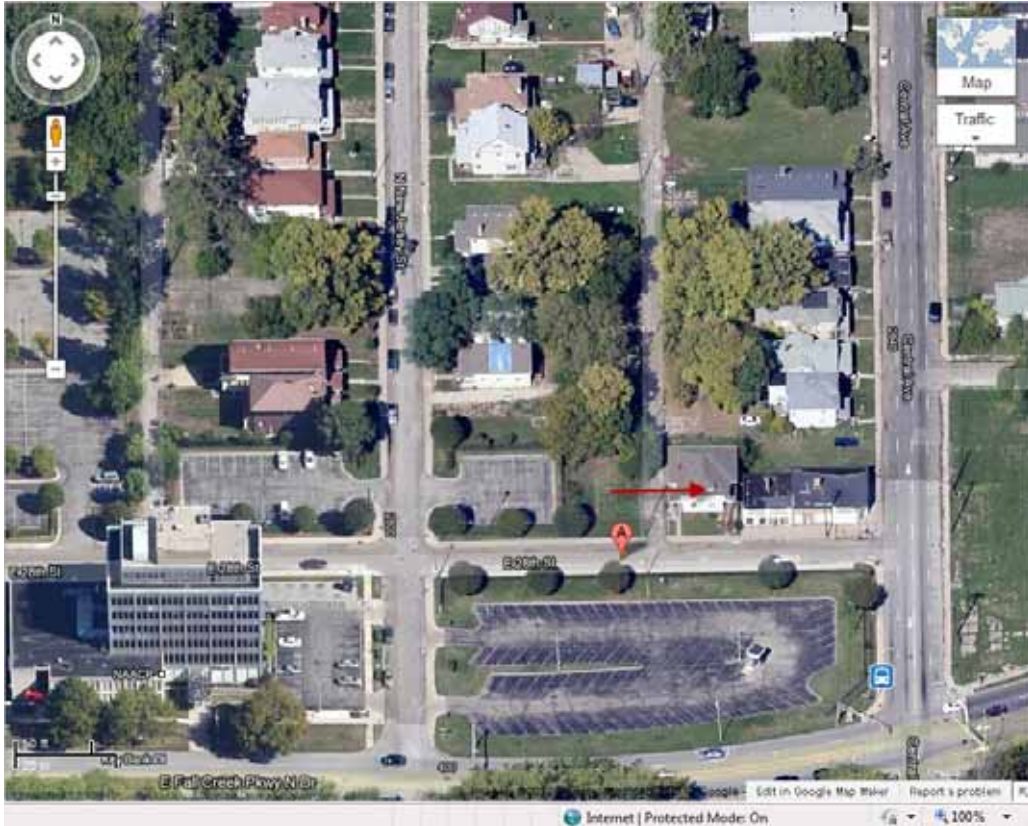


Figure 4-14. Aerial view of study house, showing potential influences on wind velocity, red arrow indicates study house.

From roughly mid-October of 2012 through mid-January of 2013, the 422 house weather station would periodically stop reporting data in the early morning hours, for roughly 15 minutes to 2 hours, and then restart. Eventually, it was determined that this was attributable to a weakness in the solar-recharged battery in the exterior weather sensor. When weather conditions were safe enough, Ping’s Tree Service was called on January 15, 2013, to use a bucket truck to change the sensor’s battery. Changing the battery solved the problem.

A 3-month comparison between the house weather station data and NWS data was made from January 1, 2013, to March 31, 2013, as a QC check. Three parameters were compared: temperature, relative humidity, and wind speed. For temperature, the data from the two weather stations match well, only differing by an average of 2 degrees F (**Figure 4-15**). Relative humidity at both weather stations differed by an average of ~4% (**Figure 4-16**). House wind speed and that of the NWS differed by an average of ~6 mph; the airport weather station was generally higher. This difference is likely due to the local NWS station being at the Indianapolis International Airport. The KIND weather station is located in the middle of the runways at the Indianapolis Airport approximately 500 meters from the nearest building. Thus, the readings obtained at the house are probably a better representation of the wind speeds that directly impinge on the house (**Figure 4-17**).

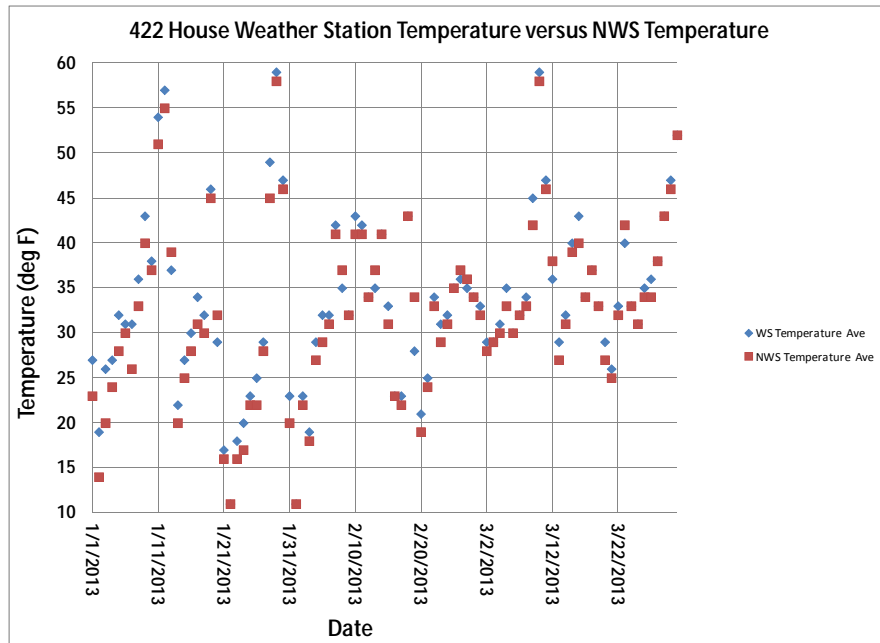


Figure 4-15. Comparison of National Weather Service Indianapolis temperature data to weather station at 422 East 28th Street.

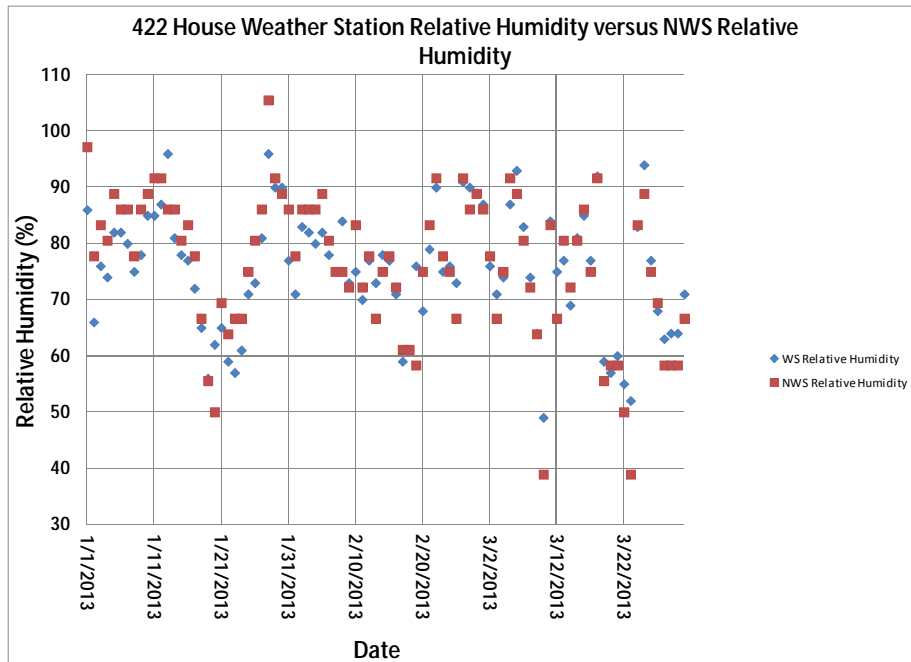


Figure 4-16. Comparison of National Weather Service Indianapolis relative humidity to weather station at 422 East 28th Street.

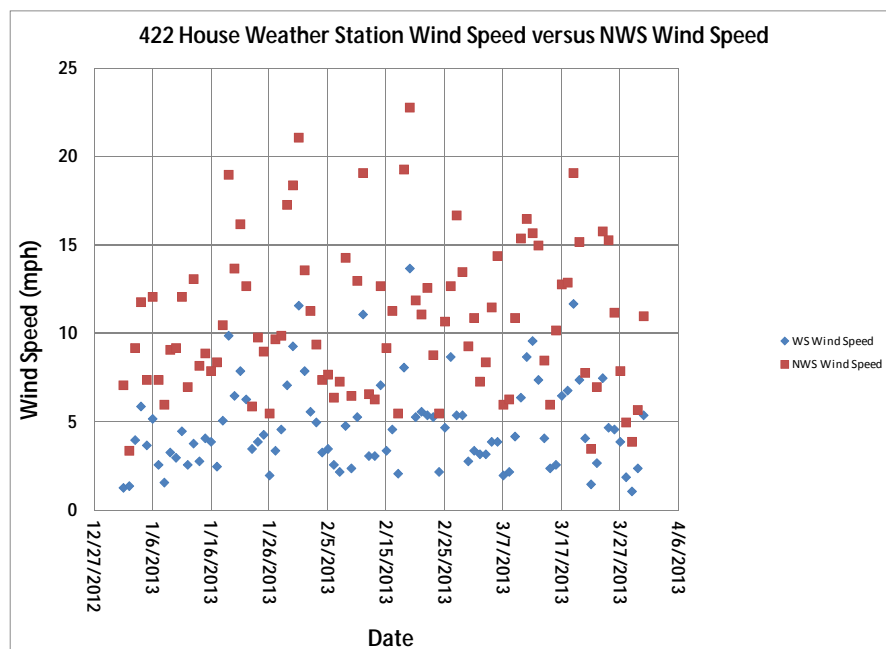


Figure 4-17. Comparison of National Weather Service wind speed data to weather station at 422 East 28th Street.

4.6 Groundwater Analysis—EPA NERL

4.6.1 Blanks

Field and laboratory blanks were used to evaluate false positives and/or high bias due to transport, storage, and sample handling. Field blanks were collected by filling a VOA vial with deionized (DI) water (provided by the laboratory) at the field site, then sealing and including the vial with the samples sent to the laboratory for analysis. Typically, a field blank was collected with each shipment to the laboratory. A total of 17 field blanks were submitted over the duration of the project.

In the case of the laboratory blank, a VOA vial of laboratory DI water was analyzed with each analytical batch to measure background from the instrumentation. A total of 27 lab blanks were analyzed and reported over the duration of the project.

To assist in data interpretation, all blank samples and all field sample results were evaluated down to the MDL. During the first phase of this project, the volume of sample analyzed was 5 mL, and during the second phase the volume of sample analyzed was increased to 25 mL to lower the detection limits. The results of the field and laboratory blanks for the 5 mL sample size are summarized in **Tables 4-30** and **4-31**. The results of the field and laboratory blanks for the 25 mL sample size are summarized in **Tables 4-32** and **4-33**. The number of blanks with detections above the RL and MDL are tabulated. Summary statistics were then calculated on this subset of positive detections.

Table 4-30. Groundwater (5 mL)—EPA Field Blank Summary

| | RL (ng) | MDL (ng) | Number of Field Blanks | | | % of Field Blanks with Detections | Mean Blank Conc. (ng) | Std. Dev. (ng) | Min (ng) | Max (ng) |
|-------------|------------|-------------|------------------------|---------------|-------------------|---|--------------------------------|----------------------|-------------|-------------|
| | | | Analyzed | Conc. > RL | RL>Conc. > MDL | | | | | |
| Benzene | 25 | 1.4 | 11 | 0 | 5 | 45 | 1.8 | 0.9 | 1.4 | 4.6 |
| Chloroform | 25 | 10 | 11 | 0 | 0 | 0 | 10 | NA | 10 | 10 |
| cis-1,2-DCE | 25 | 13 | 11 | 0 | 0 | 0 | 13 | NA | 13 | 13 |
| PCE | 25 | 14 | 11 | 0 | 0 | 0 | 13 | NA | 17 | 17 |
| Toluene | 25 | 14 | 11 | 0 | 0 | 0 | 10 | NA | 10 | 10 |
| TCE | 25 | 17 | 11 | 0 | 0 | 0 | 13 | NA | 13 | 13 |

NA = Not Applicable

Table 4-31. Groundwater (5 mL)—EPA Laboratory Blank Summary—TO-17

| | RL (ng) | MDL (ng) | Number of Field Blanks | | | % of Field Blanks with Detections | Mean Blank Conc. (ng) | Std. Dev. (ng) | Min (ng) | Max (ng) |
|-------------|------------|-------------|------------------------|---------------|-------------------|---|--------------------------------|----------------------|-------------|-------------|
| | | | Analyzed | Conc. > RL | RL>Conc. > MDL | | | | | |
| Benzene | 25 | 1.4 | 17 | 0 | 8 | 47 | 1.6 | 0.7 | 1.4 | 3.5 |
| Chloroform | 25 | 10 | 17 | 0 | 3 | 18 | 11 | 1.9 | 10 | 14 |
| cis-1,2-DCE | 25 | 13 | 17 | 0 | 0 | 0 | 13 | NA | 13 | 13 |
| PCE | 25 | 14 | 17 | 0 | 0 | 0 | 14 | NA | 14 | 14 |
| Toluene | 25 | 14 | 17 | 0 | 0 | 0 | 14 | NA | 14 | 14 |
| TCE | 25 | 17 | 17 | 0 | 0 | 0 | 17 | NA | 17 | 17 |

NA = Not Applicable

Table 4-32. Groundwater (25 mL)—EPA Field Blank Summary—TO-17

| | RL (ng) | MDL (ng) | Number of Field Blanks | | | % of Field Blanks with Detections | Mean Blank Conc. (ng) | Std. Dev. (ng) | Min (ng) | Max (ng) |
|-------------|------------|-------------|------------------------|---------------|-------------------|---|--------------------------------|----------------------|-------------|-------------|
| | | | Analyzed | Conc. > RL | RL>Conc. > MDL | | | | | |
| Benzene | 13 | 1.2 | 6 | 0 | 0 | 0 | 1.2 | NA | 1.2 | 1.2 |
| Chloroform | 13 | 1.3 | 6 | 0 | 0 | 0 | 1.3 | NA | 1.3 | 1.3 |
| cis-1,2-DCE | 13 | 1.7 | 6 | 0 | 0 | 0 | 1.7 | NA | 1.7 | 1.7 |
| PCE | 13 | 1.2 | 6 | 0 | 1 | 17 | 7.1 | NA | 1.2 | 7.1 |
| Toluene | 13 | 1.1 | 6 | 0 | 2 | 33 | 1.7 | 0.04 | 1.1 | 1.8 |
| TCE | 13 | 1.6 | 6 | 0 | 0 | 0 | 1.6 | NA | 1.6 | 1.6 |

NA = Not Applicable

Table 4-33. Groundwater (25 mL)—EPA Laboratory Blank Summary—TO-17

| | RL (ng) | MDL (ng) | Number of Field Blanks | | | % of Field Blanks with Detections | Mean Blank Conc. (ng) | Std. Dev. (ng) | Min (ng) | Max (ng) |
|-------------|------------|-------------|------------------------|---------------|--------------------|--|--------------------------------|----------------------|-------------|-------------|
| | | | Analyzed | Conc. > RL | RL>Conc . > MDL | | | | | |
| Benzene | 13 | 1.2 | 10 | 0 | 1 | 10 | 1.6 | 0.7 | 1.2 | 3.5 |
| Chloroform | 13 | 1.3 | 10 | 1 | 0 | 10 | 14 | NA | 1.3 | 14 |
| cis-1,2-DCE | 13 | 1.7 | 10 | 0 | 5 | 50 | 3.0 | 2.2 | 1.7 | 7.0 |
| PCE | 13 | 1.2 | 10 | 0 | 0 | 0 | 1.2 | NA | 1.2 | 1.2 |
| Toluene | 13 | 1.1 | 10 | 0 | 1 | 10 | 2.1 | NA | 1.1 | 2.1 |
| TCE | 13 | 1.6 | 10 | 0 | 1 | 10 | 5.5 | NA | 1.6 | 5.5 |

NA = Not Applicable

4.6.2 Surrogate Recoveries

To monitor analytical efficiency, 200 ng of dibromofluoromethane, 1,4-dichloroethane-d4, and toluene-d8 were added into each QC and field sample with the vapor phase internal standard mix during sample analysis. Field surrogates were not included in the scope of this project. The recoveries were evaluated against laboratory limits of 70 to 130%. Most surrogate recoveries met the laboratory criterion, and summary statistics are presented in **Tables 4-34** and **4-35**.

Table 4-34. EPA Groundwater (5 mL) Surrogate Recovery Summary

| Parameter | Dibromofluoromethane Result | 1,4-dichloroethane-d4 Result | Toluene-d8 Results |
|---|--------------------------------|---------------------------------|-----------------------|
| Number of surrogate recoveries measured | 111 | 111 | 111 |
| Average recovery (%R) | 105 | 95 | 98 |
| Standard deviation (%R) | 10 | 4 | 8 |
| Minimum recovery (%R) | 79 | 85 | 83 |
| Maximum recovery (%R) | 131 | 106 | 117 |

Table 4-35. EPA Groundwater (25 mL) Surrogate Recovery Summary

| Parameter | Dibromofluoromethane Result | 1,4-dichloroethane-d4 Result | Toluene-d8 Results |
|---|--------------------------------|---------------------------------|-----------------------|
| Number of surrogate recoveries measured | 105 | 105 | 105 |
| Average recovery (%R) | 98 | 94 | 98 |
| Standard deviation (%R) | 8 | 5 | 5 |
| Minimum recovery (%R) | 77 | 82 | 86 |
| Maximum recovery (%R) | 115 | 113 | 108 |

4.7 Groundwater Analysis—Pace Laboratories

On two occasions, split groundwater samples were submitted to Pace Laboratories. The intent of this work was to provide an independent check on the groundwater analyses and also to evaluate whether air transport to the EPA laboratory was having an impact on the chloroform results. A total of seven samples and two trip blanks were submitted.

The surrogate recovery limits were:

- Dibromofluoromethane: 83–123%
- 4-Bromofluorobenzene: 72–135%
- Toluene-d8: 81–114%

All samples were well within these limits.

There were no detections in either the trip blank or method blank for either sample batch.

Results of the LCS were well within the stated acceptance limits:

- PCE: 57–125%
- Chloroform: 73–122%.

In summary all reported QA/QC parameters were in control for these two batches.

4.8 Database

4.8.1 Checks on Laboratory Reports

Throughout the project, the ARCADIS project manager briefly reviewed laboratory reports as they were received from the VOC analytical laboratories. The primary focus of these checks was on blanks and ambient samples as a sampling performance indicator as well as the general consistency and reasonableness of the trends in reported concentrations for the primary analytes: PCE and chloroform.

The ARCADIS project manager also performed a manual review of the electrets radon computations in the spreadsheet used for those calculations. He also reviewed that data set regularly and interacted with the field scientist collecting this data when any anomalous results were observed.

The lead analyst (from Hartmann Environmental Geosciences), an ARCADIS principal scientist, and an RTI scientist were all involved in reviewing the online GC calculations. For suspect values QC checks performed included calibration checks and chromatogram reviews

4.8.2 Database Checks

An Access database was developed and used to compile results for VOCs (TO-17, TO-15, and passive indoor air) and radon in indoor air and soil gas (electret and AlphaGUARD).

The following QC checks were performed on this database:

- The ARCADIS field scientist responsible for the majority of the field sampling performed a check of the reports received from laboratories against his own records. He checked for the following: approximate number of each sample type (to determine what reports were still pending) and a line-by-line check of the sample times, dates, and sample numbers of each

sample type. The assignment of sample locations was also reviewed. Notes of any discrepancies and corrections were sent to the ARCADIS database manager.

- During the initial portions of the project, the ATL technical director manually prepared an Excel spreadsheet from laboratory reports comparing the results of passive samplers exposed at the same location for multiple durations and calculating percentage bias. The ARCADIS project manager then used that spreadsheet to spot check the calculations of percentage bias performed in the database. After correcting for slight differences in the percentage bias formula used, excellent agreement was found. This indicates that, at least for the calculations spot checked, both the calculation and the importation of the underlying concentration data from electronic deliverable files into the database are being performed correctly.
- During the initial portions of the project, the ATL technical director manually prepared an Excel spreadsheet of indoor air VOC results from laboratory reports. The Excel spreadsheet was used to prepare temporal trend plots of indoor concentrations for key analytes for the first 18 weeks of the project before the Access database was fully implemented. The ARCADIS project manager then confirmed that the essential features of these temporal trend plots (such as range of concentrations and overall temporal trends) were consistent between these plots and similar plots generated from the Access database. This indicates for this period that the importation of the underlying concentration data from electronic deliverable files into the database is being performed correctly.
- The ARCADIS project manager provided to the database manager a design document for the reports to be generated, including definitions of key formulas and variables. The design document was prepared based on the project objectives in the QAPP. As database reports were prepared, the ARCADIS project manager reviewed their format and content and requested changes as necessary.
- The ARCADIS project manager and database manager both spot checked the transfer of the NERL results for groundwater into the database.
- The ARCADIS Project manager and RTI statistical intern both reviewed the data sets for outliers, queried them and addressed any problems identified.
- Database reports were run to identify samples that were collected but for which data was not received. These samples were investigated and often determined to be due to problems that occurred in the analytical laboratory. These lost samples were notated in the project database.

4.9 Air Exchange Rate Measurements

In this report we present the results of air exchange rate measurements made on three occasions not presented in our previous report (EPA 2012a). A total of 10 primary samples were analyzed and reported.

In each round we conducted one duplicate measurement, the relative percent difference of the tracer measurement were:

- October 13–14, 2011: 0.9%
- October 18–19, 2011: 4.7%
- April 2013: 8%

Two trip blanks were analyzed in October 2013. Both trip blanks yielded between 1.9 and 2.0 picoliters (pl) of PMCH and no reported PDCH. The PMCH concentration in the trip blank for the fan test on condition could have significantly influenced the measurement of the air exchange rate on the first floor because the concentration in that sample was only 6.21 pl. No blank correction was performed. If a blank correction had been performed, the increase in air exchange rate under the fan-on condition discussed in Section 5 would have been more dramatic. In the other cases, the blank concentration was <15% of the

concentration in the primary sample and thus would have had little influence on the calculated air exchange rates (AERs).

One trip blank was analyzed in April 2013 and showed 3 pl of PMCH and 9 pl of PDCH. The blank concentration was <15% of the concentration in the primary sample and thus would have had little influence on the calculated AERs.

Table of Contents

| | | |
|-------|--|------|
| 5.0 | Subslab Depressurization Mitigation System Monitoring Results..... | 5-1 |
| 5.1 | Differential Pressure and Mitigation System Flow | 5-1 |
| 5.1.1 | Radon System Design Standards for Differential Pressure | 5-1 |
| 5.1.2 | Differential Pressure Monitoring of this SSD System..... | 5-3 |
| 5.1.3 | Mitigation System Flow..... | 5-21 |
| 5.2 | Radon Monitoring: Hourly and Weekly Time Scales | 5-21 |
| 5.3 | VOC Monitoring During Mitigation Testing | 5-30 |
| 5.3.1 | Descriptive Statistics..... | 5-33 |
| 5.3.2 | Effect of Mitigation System Status on Indoor Air VOC Levels | 5-45 |
| 5.3.3 | Discussion..... | 5-46 |
| 5.4 | Stack Gas Monitoring..... | 5-47 |
| 5.4.1 | Is Stack Gas an Indicator of System Performance in Protecting Indoor Air?..... | 5-47 |
| 5.4.2 | Air Exchange Rate Measurements..... | 5-50 |
| 5.4.3 | Stack Gas Measurements to Define Flux to Structure | 5-53 |

List of Figures

| | | |
|-------|---|------|
| 5-1. | Subslab vs. basement differential pressure: 422 side during mitigation testing. | 5-19 |
| 5-2. | Subslab vs. basement differential pressure: 420 side during mitigation testing. | 5-20 |
| 5-3. | Deep soil gas vs. shallow soil gas differential pressure during mitigation testing..... | 5-21 |
| 5-4. | Basement vs. upstairs differential pressure: 422 side during mitigation testing..... | 5-22 |
| 5-5. | Basement vs. exterior differential pressure: 422 side during mitigation testing..... | 5-22 |
| 5-6. | Stack gas flow velocity from SSD system..... | 5-23 |
| 5-7. | Real-time radon monitoring: 422 basement..... | 5-23 |
| 5-8. | Real-time radon monitoring: 422 second floor..... | 5-24 |
| 5-9. | Weekly integrated radon (electret) during mitigation testing. | 5-24 |
| 5-10. | Passive sampler monitoring of PCE during mitigation testing. | 5-31 |
| 5-11. | Passive sampler monitoring of chloroform during mitigation period..... | 5-31 |
| 5-12. | Indoor air PCE, real-time monitoring during mitigation testing..... | 5-32 |
| 5-13. | Boxplots of mitigation effect on indoor air concentrations. | 5-46 |
| 5-14. | Stack gas monitoring during mitigation testing: chloroform..... | 5-48 |
| 5-15. | 422 first floor versus stack gas chloroform concentrations: mitigation on..... | 5-48 |
| 5-16. | Stack gas monitoring during mitigation testing: PCE..... | 5-49 |
| 5-17. | Stack gas versus 422 first floor PCE concentrations: mitigation on..... | 5-49 |

List of Tables

5-1. Subslab vs. Basement Differential Pressures Measured with Handheld Micromanometer at Permanent SSPs (negative pressure indicates flow out of building; yellow indicates mitigation off) 5-4

5-2. Wall Port vs. Basement Differential Pressure Measured with Handheld Micromanometer (negative pressure indicates flow out of building) 5-8

5-3. Shallow Interior SGP (6 ft bls) vs. Basement Differential Pressure Measured with Handheld Micromanometer (negative pressure indicates flow out of building)..... 5-9

5-4. Shallow Exterior SGP (3.5 ft and 6 ft bls) vs. Basement Differential Pressure Measured with a Handheld Micromanometer (negative pressure indicates flow out of building)..... 5-10

5-5. Deep Interior SGP (9 ft and 13 ft bls) vs. Basement Differential Pressure Measured by ARCADIS with Handheld Micromanometer (negative pressure indicates flow out of building)..... 5-12

5-6. Deep Exterior SGP (9 ft and 13 ft bls) vs. Basement Differential Pressure Measured by ARCADIS with Handheld Micromanometer (negative pressure indicates flow out of building)..... 5-15

5-7. Comparison of Setra Continuous Sensor Differential Pressure vs. Airdata Multimeter ADM-870 with SSD System Operating: December 29, 2012 (yellow shaded data reflects an “off scale” response on the Setra) 5-20

5-8. Electret Radon Descriptive Statistics by Mitigation and Heating Status (pCi/L) 5-25

5-9. Indoor Air Radon Descriptive Statistics by Mitigation and Heating Status: From Stationary Real Time AlphaGUARD (pCi/L) 5-26

5-10. Indoor Radon Descriptive Statistics—Individual Locations by Mitigation and Heating Status: Electret Data (pCi/L)..... 5-26

5-11. Descriptive Statistics: Radon in Subslab and Wall Ports by Individual Location and Mitigation and Heating Status (pCi/L) 5-28

5-12. Radon Descriptive Statistics by Location Type and Mitigation and Heating Status (pCi/L) 5-30

5-13. Descriptive Statistics of Weekly Passive VOC Measurements ($\mu\text{g}/\text{m}^3$) in Indoor Air by Mitigation Status and Heating Use (yellow indicates statistics during active mitigation)..... 5-33

5-14. Distribution of Concentrations ($\mu\text{g}/\text{m}^3$) by VOC and Mitigation and Heating Status: Indoor Air, Week-Long Passive Samples (yellow indicates statistics during active mitigation)..... 5-34

5-15. Descriptive Statistics of Indoor VOC Concentrations ($\mu\text{g}/\text{m}^3$) During Mitigation Testing by Location and Mitigation and Heating Status (yellow indicates statistics during active mitigation)..... 5-35

5-16. Descriptive Statistics: Average Subslab and Wall Port VOC Concentrations ($\mu\text{g}/\text{m}^3$) by Mitigation and Heating Status (yellow indicates statistics during active mitigation)..... 5-39

5-17. Distribution of Subslab and Wall Port VOC Concentrations ($\mu\text{g}/\text{m}^3$) by Mitigation and Heating Status (yellow indicates statistics during active mitigation) 5-40

5-18. Descriptive Statistics of Subslab and Wall Port VOC Concentrations ($\mu\text{g}/\text{m}^3$) by Location and Mitigation and Heating Status (yellow indicates statistics during active mitigation) 5-41

5-19. April/May 2011 Air Exchange Rate Measurement Results 5-51

| | | |
|-------|--|------|
| 5-20. | September 2011 Air Exchange Rate Measurement Results..... | 5-51 |
| 5-21. | October 2011 Air Exchange Measurement Results (during and after fan testing) | 5-52 |
| 5-22. | April 2013 Air Exchange Measurement Results (During Mitigation)..... | 5-52 |
| 5-23. | National Survey of Air Exchange Rates, Reprinted from the <i>EPA Exposure Factor Handbook</i> (U.S. EPA, 2011)..... | 5-52 |
| 5-23. | National Survey of Air Exchange Rates, Reprinted from the <i>EPA Exposure Factor Handbook</i> (U.S. EPA, 2011) (continued) | 5-53 |
| 5-24. | Stack Gas Discharge Measurements During Mitigation..... | 5-54 |

5.0 Subslab Depressurization Mitigation System Monitoring Results

Installation and testing of the subslab depressurization (SSD) mitigation system is described in Section 3.2. After the system was installed and tested, a program of SSD mitigation system monitoring was carried out to investigate the ability of the system to control radon and VOC levels in both active (fan on) and passive (fan off) modes. In addition, the SSD mitigation system was installed with valves in the depressurization lines to simulate a house without a mitigation system in place. The SSD mitigation system had a single fan that served the entire duplex with a total of four extraction points. As described in Section 3.2, SSD mitigation monitoring involved measuring radon and VOC levels with the SSD mitigation system in active mode (fan on), passive mode (fan off, valves open), and completely off (fan off, valves closed). To simplify data interpretation, the on/passive/off mitigation switches were always conducted on a Wednesday, which was the day when new week-long integrated radon and VOC samples were begun.

5.1 Differential Pressure and Mitigation System Flow

5.1.1 Radon System Design Standards for Differential Pressure

U.S. EPA's (1993a) most extensive guidance for radon SSD systems states a standard in terms of inches of water column (in. WC), which is also known as inches of water gauge (in. WG):

Were the system to function solely by the primary mechanism discussed earlier, i.e., by maintaining a measurable depressurization in the soil everywhere that it contacts the foundation, a soil depressurization of about 0.015 in. WG, measured during mild weather, would nominally be required to ensure that subsequent cold weather and winds would rarely depressurize the house sufficiently to overwhelm the system. If exhaust appliances were off during the measurement, the soil would nominally have to be depressurized by an additional 0.01 to 0.02 in. WG to ensure that the system would not be overwhelmed when these appliances were turned on. However, some experience suggests that the other mechanisms mentioned earlier, including soil gas dilution and perhaps air-barrier shielding, can come into play to varying degrees, depending upon the circumstances. These other mechanisms could explain why good radon reductions are often achieved by SSD systems even in cases where portions of the sub-slab are only marginally depressurized, to an extent far less than the nominally required 0.025 to 0.035 in. WG.

U.S. EPA (1993a) goes on to describe in detail that the 0.025 to 0.035 in. WG criteria is meant to take into account the typical maximum depressurization potentially produced by building HVAC systems of 0.02 in WG attributable to central furnace fans, clothes dryers, and exhaust fans. U.S. EPA (1993) further notes that achieving a particular numerical target for depressurization “may in fact not be necessary” and that a less stringent standard of 0.001 to 0.002 in WG can be applied if measured under worst case conditions:

Depending upon site-specific factors, there may not necessarily be a significant impact on long-term average indoor concentration if the pressure differential across some portion of the slab is occasionally reversed by operation of these exhaust fans. Moreover, since SSD seems to work by mechanisms in addition to soil depressurization (in particular, by soil gas dilution), it may in fact not be necessary to guarantee that the sub-slab depressurizations being established by the system are greater at every sub-slab location than every potential basement depressurization that the system may ever encounter. However, where the SSD system can reasonably be designed to provide sub-slab depressurizations of about 0.01 to 0.02 in. WG everywhere during cold weather with

the appliances off, in order to ensure that the system will essentially never be overwhelmed, it is advisable to do so.

And elsewhere:

Where slab pressure measurements are made during cold weather with exhaust appliances on - i.e., with the system experiencing its worst-case challenge - any measurable sub-slab depressurization should be sufficient (0.001 to 0.002 in. WG)

U.S. EPA's 1994 guidance for *Radon Prevention in the Design and Construction of Schools and Other Large Buildings* states, "A minimum subslab pressure of -0.002 in the water column (WC) is required at all test holes for an effective ASD system."

U.S. EPA (1993a) also identifies backdrafting as a potential risk of systems with a high degree of depressurization. U.S. EPA (1993a) explicitly describes the 0.025 to 0.035 in. WG design goal as conservative:

If sub-slab depressurizations being created by a SSD system were being measured during mild weather with exhaust appliances off, the conservative rule of thumb would thus be that the system should be designed to maintain a depressurization of at least 0.015 in. WG everywhere to avoid being overwhelmed by the stack effect when cold weather arrives. In addition, to avoid being overwhelmed by the incremental basement depressurization created when exhaust appliances are turned on during cold weather, the SSD system should nominally maintain an additional sub-slab depressurization of up to 0.01 to 0.02 in. WG, as discussed previously in Section 2.3.1b. Thus, ideally, sub-slab depressurizations measured during mild weather with appliances off should total about 0.025 to 0.035 inch WG everywhere in order to ensure that the system will never be overwhelmed during cold weather with the appliances on.

But as re-iterated several places in this document, this target depressurization is usually a very conservative design goal. Commonly, sub-slab depressurizations much less than these ideal targets will still provide satisfactory SSD performance. Thus, an expensive upgrade of a SSD system in an attempt to achieve these high depressurizations is often unnecessary. However, where the SSD system can reasonably be designed to achieve such depressurizations, it is probably advisable to do so.

Furthermore, this conservative maximum basement depressurization of 0.025 to 0.035 in. WG due to thermal and appliance effects is thought to be high for many cases..... In addition, the upper end of the range assumes that the major depressurizing appliances are operating during the coldest weather; among these appliances, whole-house and attic fans will in fact not be operated in cold weather, and clothes driers will be operated only intermittently. Combustion appliances in the basement would backdraft if depressurizations as great as 0.035 in. WG were actually maintained for any extended period.

Fourteen years later, this same numerical criterion was restated in the much briefer ITRC VI guidance document (2007) without reprinting the detailed discussion of the basis for the recommendation:

Active SSD systems are the most reliable, cost effective, and efficient technique for controlling vapor intrusion in the majority of cases, which concentration reductions in the 90%-99% range (USEPA 1993b) and 99.5% or greater in carefully designed and installed systems (Folkes 2002). Subslab depressurization in the range of 0.025-0.035 inches H₂O is generally sufficient to maintain downward pressure gradients (USEPA 1993b).

SSD mitigation systems with very similar hardware can provide indoor air quality benefits through two separate mechanisms described as subslab depressurization and subslab ventilation. These mechanisms are described in U.S. EPA (2008):

The hardware used in sub-slab ventilation (SSV) systems and sub-slab depressurization (SSD) systems is similar. The two names describe the different mechanisms through which the system can be effective in keeping soil gas contaminants out of the building. When the surrounding soil has a relatively high permeability, the fan pulls large quantities of air (largely from the atmosphere) down through the soil thus diluting the contaminant in the sub-slab region resulting in reduced entry into the building. This mechanism predominates in a sub-slab ventilation system. It is important to ensure that openings in the slab and foundation are adequately sealed to prevent large quantities of conditioned indoor air being pulled into the mitigation system. Sealing as part of SSD system installation is discussed in EPA 1993b, section 4.7 and in NYSDOH, 2006, section 4.3.1. When the soil is much less permeable, less air flows and the fan generates a larger negative pressure in the subslab region (thus sub-slab depressurization occurs). The result is a larger negative pressure gradient across the slab. The system works because the negative pressure gradient ensures that the flow is in the direction from indoors to the soil and dilution of sub-slab gases is less important in this SSD case. In extreme cases of low permeability and low flows, it may be necessary to specify a special blower to ensure that adequate pressure gradients are generated.

Thus, a system operating in an SSV mode would be expected to show substantial reduction in subslab concentration but relatively low differential pressures across the slab. A system operating in an SSD mode would show little reduction in subslab concentration but substantial and sustained pressure differential across the slab.

5.1.2 Differential Pressure Monitoring of this SSD System

After SSD system installation, the mitigation subcontractor conducted tests typical of a commercially installed residential SSD mitigation system. They tested differential pressure across the SSD system using a portable micromanometer at a series of 10 temporary pressure monitoring points. As indicated in the tabulated data in **Table 3-8**, the differential pressure at 8 of 10 of these locations immediately following the October installation met and sometimes substantially exceeded the most conservative EPA depressurization criteria 0.025 to 0.035 in. WC (6–9 Pa). All 10 of the monitoring points substantially exceeded the 0.002 in. WC (0.5 Pa) criterion that was considered applicable here because the testing occurred in mid-October and there are no exhaust appliances in the duplex.

After initial testing, we monitored the U-tube micromanometer supplied with the system, which would be the tool that a homeowner would use to verify that a residential installation of SSD was functional. U-tube manometers connected to each leg of the mitigation system were routinely monitored during on periods to determine whether pressures remained constant. At no time during the monitoring did the pressures deviate from the norm (0.3 in. WC on the 422 side, 0.25 in. WC on the 420 side).

We subsequently conducted several additional rounds of vacuum influence monitoring using a separate handheld micromanometer at the permanent subslab ports (**Table 5-1**), wall ports (WPs) (**Table 5-2**), and both shallow (**Tables 5-3 and 5-4**) and deep (**Tables 5-5 and 5-6**) interior and exterior soil gas ports. Note that yellow highlighted rows in these tables represent periods when the mitigation system was off (valve off or in passive mode).

Testing using the permanent SSPs (**Table 5-1**) and the conventionally constructed soil gas ports just below the slab (**Table 5-3**) generally indicated that the system was functioning well in maintaining

vacuum influence across the slab in the desired direction (away from the building). A few exceptions were observed:

- at SSP-4 on February 22, 2013 (relatively strong driving force into the building of 0.12 to 0.13 in. WC)
- at SSP-7 on December 29, 2012 (pressures fluctuating strongly from +0.18 to -0.10 in. WC)
- at SGP11-6 on April 21, 2013 (pressures fluctuating strongly from +0.2225 to -0.26 in. WC)

Table 5-1. Subslab vs. Basement Differential Pressures Measured with Handheld Micromanometer at Permanent SSPs (negative pressure indicates flow out of building; yellow indicates mitigation off)

| Date | Time | Negative ^a End of Manometer | Positive ^a End of Manometer | Reading (in. WC) | Mitigation System On/Off |
|------------|-------|--|--|------------------|--------------------------|
| 12/7/2012 | 11:19 | Basement | SSP-1 | 0.0028 | Off |
| 12/7/2012 | 11:20 | Basement | SSP-1 | 0.0036 | Off |
| 12/7/2012 | 11:21 | Basement | SSP-1 | 0.0042 | Off |
| 11/8/2012 | 12:18 | Basement | SSP-1 | -0.2297 | On |
| 11/14/2012 | 18:39 | Basement | SSP-1 | -0.2247 | On |
| 11/14/2012 | 18:40 | Basement | SSP-1 | -0.2280 | On |
| 11/14/2012 | 18:41 | Basement | SSP-1 | -0.2287 | On |
| 12/29/2012 | 13:14 | Basement | SSP-1 | -0.2135 | On |
| 12/29/2012 | 13:15 | Basement | SSP-1 | -0.2154 | On |
| 12/29/2012 | 13:16 | Basement | SSP-1 | -0.2126 | On |
| 2/22/2013 | 12:59 | Basement | SSP-1 | -0.1258 | On |
| 2/22/2013 | 13:00 | Basement | SSP-1 | -0.1386 | On |
| 2/22/2013 | 13:01 | Basement | SSP-1 | -0.1214 | On |
| 2/22/2013 | 13:02 | Basement | SSP-1 | -0.1341 | On |
| 2/22/2013 | 13:03 | Basement | SSP-1 | -0.1333 | On |
| 4/20/2013 | 15:05 | Basement | SSP-1 | -0.2124 | On |
| 4/20/2013 | 15:05 | Basement | SSP-1 | -0.2176 | On |
| 4/20/2013 | 15:05 | Basement | SSP-1 | -0.2179 | On |
| 4/22/2013 | 15:02 | Basement | SSP-1 | -0.2206 | On |
| 4/22/2013 | 15:02 | Basement | SSP-1 | -0.2170 | On |
| 4/22/2013 | 15:03 | Basement | SSP-1 | -0.2166 | On |
| 12/7/2012 | 11:38 | Basement | SSP-2 | 0.0038 | Off |
| 12/7/2012 | 11:39 | Basement | SSP-2 | 0.0039 | Off |
| 12/7/2012 | 11:40 | Basement | SSP-2 | 0.0038 | Off |
| 12/29/2012 | 13:34 | Basement | SSP-2 | -0.0299 | On |
| 12/29/2012 | 13:35 | Basement | SSP-2 | -0.0293 | On |
| 12/29/2012 | 13:35 | Basement | SSP-2 | -0.0319 | On |
| 2/22/2013 | 12:31 | Basement | SSP-2 | -0.0317 | On |
| 2/22/2013 | 12:32 | Basement | SSP-2 | -0.0325 | On |
| 2/22/2013 | 12:33 | Basement | SSP-2 | -0.0311 | On |
| 2/22/2013 | 12:34 | Basement | SSP-2 | -0.0318 | On |
| 2/22/2013 | 12:35 | Basement | SSP-2 | -0.0324 | On |
| 4/20/2013 | 15:06 | Basement | SSP-2 | -0.0394 | On |

(continued)

Table 5-1. Subslab vs. Basement Differential Pressures Measured with Handheld Micromanometer at Permanent SSPs (negative pressure indicates flow out of building; yellow indicates mitigation off) (cont.)

| Date | Time | Negative ^a End of Manometer | Positive ^a End of Manometer | Reading (in. WC) | Mitigation System On/Off |
|------------|-------|--|--|------------------|--------------------------|
| 4/20/2013 | 15:07 | Basement | SSP-2 | -0.0399 | On |
| 4/20/2013 | 15:07 | Basement | SSP-2 | -0.0386 | On |
| 4/22/2013 | 15:04 | Basement | SSP-2 | -0.0417 | On |
| 4/22/2013 | 15:04 | Basement | SSP-2 | -0.0424 | On |
| 4/22/2013 | 15:05 | Basement | SSP-2 | -0.0421 | On |
| 12/7/2012 | 11:57 | Basement | SSP-3 | -0.0007 | Off |
| 12/7/2012 | 11:58 | Basement | SSP-3 | 0.0000 | Off |
| 12/7/2012 | 11:59 | Basement | SSP-3 | 0.0002 | Off |
| 12/29/2012 | 16:53 | Basement | SSP-3 | -0.1079 | On |
| 12/29/2012 | 16:53 | Basement | SSP-3 | -0.1082 | On |
| 12/29/2012 | 16:53 | Basement | SSP-3 | -0.1037 | On |
| 2/22/2013 | 14:13 | Basement | SSP-3 | -0.1122 | On |
| 2/22/2013 | 14:14 | Basement | SSP-3 | -0.1109 | On |
| 2/22/2013 | 14:15 | Basement | SSP-3 | -0.1113 | On |
| 2/22/2013 | 14:20 | Basement | SSP-3 | -0.1123 | On |
| 2/22/2013 | 14:21 | Basement | SSP-3 | -0.1098 | On |
| 4/20/2013 | 15:15 | Basement | SSP-3 | -0.1139 | On |
| 4/20/2013 | 15:16 | Basement | SSP-3 | -0.1133 | On |
| 4/20/2013 | 15:16 | Basement | SSP-3 | -0.1138 | On |
| 4/22/2013 | 15:12 | Basement | SSP-3 | -0.1118 | On |
| 4/22/2013 | 15:12 | Basement | SSP-3 | -0.1136 | On |
| 4/22/2013 | 15:13 | Basement | SSP-3 | -0.1141 | On |
| 12/7/2012 | 11:34 | Basement | SSP-4 | 0.0038 | Off |
| 12/7/2012 | 11:35 | Basement | SSP-4 | 0.0041 | Off |
| 12/7/2012 | 11:36 | Basement | SSP-4 | 0.0031 | Off |
| 12/29/2012 | 13:31 | Basement | SSP-4 | -0.0291 | On |
| 12/29/2012 | 13:31 | Basement | SSP-4 | -0.0408 | On |
| 12/29/2012 | 13:32 | Basement | SSP-4 | -0.0451 | On |
| 2/22/2013 | 13:44 | Basement | SSP-4 | 0.1247 | On |
| 2/22/2013 | 13:45 | Basement | SSP-4 | 0.1311 | On |
| 2/22/2013 | 13:46 | Basement | SSP-4 | 0.1315 | On |
| 2/22/2013 | 13:47 | Basement | SSP-4 | 0.1315 | On |
| 2/22/2013 | 13:48 | Basement | SSP-4 | 0.1347 | On |

(continued)

Table 5-1. Subslab vs. Basement Differential Pressures Measured with Handheld Micromanometer at Permanent SSPs (negative pressure indicates flow out of building; yellow indicates mitigation off) (cont.)

| Date | Time | Negative ^a End of Manometer | Positive ^a End of Manometer | Reading (in. WC) | Mitigation System On/Off |
|------------|-------|--|--|------------------|--------------------------|
| 4/20/2013 | 15:09 | Basement | SSP-4 | -0.0531 | On |
| 4/20/2013 | 15:09 | Basement | SSP-4 | -0.0534 | On |
| 4/20/2013 | 15:10 | Basement | SSP-4 | -0.0515 | On |
| 4/22/2013 | 15:07 | Basement | SSP-4 | -0.0539 | On |
| 4/22/2013 | 15:07 | Basement | SSP-4 | -0.0545 | On |
| 4/22/2013 | 15:07 | Basement | SSP-4 | -0.0542 | On |
| 12/7/2012 | 12:03 | Basement | SSP-5 | 0.0004 | Off |
| 12/7/2012 | 12:04 | Basement | SSP-5 | 0.0009 | Off |
| 12/7/2012 | 12:05 | Basement | SSP-5 | 0.0009 | Off |
| 12/29/2012 | 16:54 | Basement | SSP-5 | -0.0213 | On |
| 12/29/2012 | 16:54 | Basement | SSP-5 | -0.0183 | On |
| 12/29/2012 | 16:55 | Basement | SSP-5 | -0.0337 | On |
| 2/22/2013 | 15:08 | Basement | SSP-5 | -0.0208 | On |
| 2/22/2013 | 15:09 | Basement | SSP-5 | -0.0200 | On |
| 2/22/2013 | 15:10 | Basement | SSP-5 | -0.0224 | On |
| 2/22/2013 | 15:11 | Basement | SSP-5 | -0.0206 | On |
| 2/22/2013 | 15:12 | Basement | SSP-5 | -0.0210 | On |
| 4/20/2013 | 15:19 | Basement | SSP-5 | -0.0265 | On |
| 4/20/2013 | 15:19 | Basement | SSP-5 | -0.0261 | On |
| 4/20/2013 | 15:19 | Basement | SSP-5 | -0.0261 | On |
| 4/22/2013 | 15:15 | Basement | SSP-5 | -0.0259 | On |
| 4/22/2013 | 15:15 | Basement | SSP-5 | -0.0266 | On |
| 4/22/2013 | 15:16 | Basement | SSP-5 | -0.0265 | On |
| 12/7/2012 | 11:48 | Basement | SSP-6 | 0.0001 | Off |
| 12/7/2012 | 11:49 | Basement | SSP-6 | 0.0002 | Off |
| 12/7/2012 | 11:50 | Basement | SSP-6 | 0.0004 | Off |
| 12/29/2012 | 16:49 | Basement | SSP-6 | -0.0350 | On |
| 12/29/2012 | 16:49 | Basement | SSP-6 | -0.0379 | On |
| 12/29/2012 | 16:50 | Basement | SSP-6 | -0.0351 | On |
| 2/22/2013 | 14:02 | Basement | SSP-6 | -0.0388 | On |
| 2/22/2013 | 14:03 | Basement | SSP-6 | -0.0387 | On |
| 2/22/2013 | 14:04 | Basement | SSP-6 | -0.0399 | On |
| 2/22/2013 | 14:05 | Basement | SSP-6 | -0.0373 | On |

(continued)

Table 5-1. Subslab vs. Basement Differential Pressures Measured with Handheld Micromanometer at Permanent SSPs (negative pressure indicates flow out of building; yellow indicates mitigation off) (cont.)

| Date | Time | Negative ^a End of Manometer | Positive ^a End of Manometer | Reading (in. WC) | Mitigation System On/Off |
|------------|-------|--|--|------------------|--------------------------|
| 2/22/2013 | 14:06 | Basement | SSP-6 | -0.0401 | On |
| 4/20/2013 | 15:13 | Basement | SSP-6 | -0.0403 | On |
| 4/20/2013 | 15:14 | Basement | SSP-6 | -0.0387 | On |
| 4/20/2013 | 15:14 | Basement | SSP-6 | -0.0412 | On |
| 4/22/2013 | 15:10 | Basement | SSP-6 | -0.0420 | On |
| 4/22/2013 | 15:11 | Basement | SSP-6 | -0.0434 | On |
| 4/22/2013 | 15:11 | Basement | SSP-6 | -0.0434 | On |
| 12/7/2012 | 12:00 | Basement | SSP-7 | -0.0005 | Off |
| 12/7/2012 | 12:01 | Basement | SSP-7 | -0.0010 | Off |
| 12/7/2012 | 12:02 | Basement | SSP-7 | -0.0006 | Off |
| 11/8/2012 | 12:27 | Basement | SSP-7 | 0.1726 | On |
| 11/14/2012 | 18:44 | Basement | SSP-7 | -0.1145 | On |
| 11/14/2012 | 18:45 | Basement | SSP-7 | -0.1144 | On |
| 11/14/2012 | 18:46 | Basement | SSP-7 | -0.1131 | On |
| 12/29/2012 | 17:07 | Basement | SSP-7 | 0.1491 | On |
| 12/29/2012 | 17:07 | Basement | SSP-7 | 0.1889 | On |
| 12/29/2012 | 17:07 | Basement | SSP-7 | -0.1031 | On |
| 12/29/2012 | 17:08 | Basement | SSP-7 | -0.1046 | On |
| 12/29/2012 | 17:09 | Basement | SSP-7 | -0.1045 | On |
| 12/29/2012 | 17:09 | Basement | SSP-7 | -0.1066 | On |
| 12/29/2012 | 17:10 | Basement | SSP-7 | -0.1044 | On |
| 2/22/2013 | 14:21 | Basement | SSP-7 | -0.1102 | On |
| 2/22/2013 | 14:22 | Basement | SSP-7 | -0.1093 | On |
| 2/22/2013 | 14:23 | Basement | SSP-7 | -0.1105 | On |
| 2/22/2013 | 14:24 | Basement | SSP-7 | -0.1099 | On |
| 2/22/2013 | 14:25 | Basement | SSP-7 | -0.1115 | On |
| 4/20/2013 | 15:17 | Basement | SSP-7 | -0.1143 | On |
| 4/20/2013 | 15:17 | Basement | SSP-7 | -0.1129 | On |
| 4/20/2013 | 15:17 | Basement | SSP-7 | -0.1129 | On |
| 4/22/2013 | 15:13 | Basement | SSP-7 | -0.1129 | On |
| 4/22/2013 | 15:14 | Basement | SSP-7 | -0.1113 | On |
| 4/22/2013 | 15:14 | Basement | SSP-7 | -0.1120 | On |

^aIn Tables 5-1 through 5-6, the “negative end” is the low pressure manometer port and the “positive end” is the high pressure manometer port.

Table 5-2. Wall Port vs. Basement Differential Pressure Measured with Handheld Micromanometer(negative pressure indicates flow out of building)

| Date | Time | Negative End of Manometer | Positive End of Manometer | Reading (in. WC) | Mitigation System On/Off |
|-----------|-------|---------------------------|---------------------------|------------------|--------------------------|
| 2/22/2013 | 12:25 | Basement | WP-1 | -0.0007 | On |
| 2/22/2013 | 12:26 | Basement | WP-1 | -0.0010 | On |
| 2/22/2013 | 12:28 | Basement | WP-1 | -0.0012 | On |
| 2/22/2013 | 12:29 | Basement | WP-1 | -0.0014 | On |
| 2/22/2013 | 12:30 | Basement | WP-1 | -0.0008 | On |
| 4/21/2013 | 18:27 | Basement | WP-1 | -0.0031 | On |
| 4/21/2013 | 18:27 | Basement | WP-1 | -0.0044 | On |
| 4/21/2013 | 18:28 | Basement | WP-1 | -0.0043 | On |
| 2/22/2013 | 12:51 | Basement | WP-2 | -0.0024 | On |
| 2/22/2013 | 12:52 | Basement | WP-2 | -0.0027 | On |
| 2/22/2013 | 12:53 | Basement | WP-2 | -0.0043 | On |
| 2/22/2013 | 12:54 | Basement | WP-2 | -0.0037 | On |
| 2/22/2013 | 12:55 | Basement | WP-2 | -0.0039 | On |
| 4/21/2013 | 18:33 | Basement | WP-2 | -0.0034 | On |
| 4/21/2013 | 18:34 | Basement | WP-2 | -0.0060 | On |
| 4/21/2013 | 18:34 | Basement | WP-2 | -0.0059 | On |
| 2/22/2013 | 13:33 | Basement | WP-3 | 0.0063 | On |
| 2/22/2013 | 13:34 | Basement | WP-3 | 0.0070 | On |
| 2/22/2013 | 13:35 | Basement | WP-3 | 0.0052 | On |
| 2/22/2013 | 13:36 | Basement | WP-3 | 0.0076 | On |
| 2/22/2013 | 13:37 | Basement | WP-3 | 0.0054 | On |
| 4/21/2013 | 18:47 | Basement | WP-3 | -0.0002 | On |
| 4/21/2013 | 18:47 | Basement | WP-3 | 0.0000 | On |
| 4/21/2013 | 18:48 | Basement | WP-3 | 0.0000 | On |
| 2/22/2013 | 14:08 | Basement | WP-4 | -0.0051 | On |
| 2/22/2013 | 14:09 | Basement | WP-4 | -0.0063 | On |
| 2/22/2013 | 14:10 | Basement | WP-4 | -0.0033 | On |
| 2/22/2013 | 14:11 | Basement | WP-4 | -0.0051 | On |
| 2/22/2013 | 14:12 | Basement | WP-4 | -0.0035 | On |
| 4/21/2013 | 18:50 | Basement | WP-4 | -0.0090 | On |
| 4/21/2013 | 18:51 | Basement | WP-4 | -0.0084 | On |
| 4/21/2013 | 18:51 | Basement | WP-4 | -0.0073 | On |

(continued)

Table 5-3. Shallow Interior SGP (6 ft bls) vs. Basement Differential Pressure Measured with Handheld Micromanometer (negative pressure indicates flow out of building)

| Date | Time | Negative End of Manometer | Positive End of Manometer | Reading (in. WC) | Mitigation System On/Off |
|-----------|-------|---------------------------|---------------------------|------------------|--------------------------|
| 2/22/2013 | 12:38 | Basement | SGP10-6 | -0.0425 | On |
| 2/22/2013 | 12:39 | Basement | SGP10-6 | -0.0434 | On |
| 2/22/2013 | 12:40 | Basement | SGP10-6 | -0.0423 | On |
| 2/22/2013 | 12:41 | Basement | SGP10-6 | -0.0418 | On |
| 2/22/2013 | 12:42 | Basement | SGP10-6 | -0.0427 | On |
| 4/21/2013 | 18:29 | Basement | SGP10-6 | -0.0537 | On |
| 4/21/2013 | 18:29 | Basement | SGP10-6 | -0.0542 | On |
| 4/21/2013 | 18:30 | Basement | SGP10-6 | -0.0535 | On |
| 11/8/2012 | 12:28 | Basement | SGP11-6 | -0.0768 | On |
| 2/22/2013 | 14:25 | Basement | SGP11-6 | -0.1446 | On |
| 2/22/2013 | 14:26 | Basement | SGP11-6 | -0.1593 | On |
| 2/22/2013 | 14:27 | Basement | SGP11-6 | -0.1835 | On |
| 2/22/2013 | 14:28 | Basement | SGP11-6 | -0.2157 | On |
| 2/22/2013 | 14:29 | Basement | SGP11-6 | -0.2276 | On |
| 4/21/2013 | 18:52 | Basement | SGP11-6 | 0.2225 | On |
| 4/21/2013 | 18:52 | Basement | SGP11-6 | 0.0910 | On |
| 4/21/2013 | 18:53 | Basement | SGP11-6 | 0.0046 | On |
| 4/21/2013 | 18:53 | Basement | SGP11-6 | 0.0650 | On |
| 4/21/2013 | 18:54 | Basement | SGP11-6 | 0.0486 | On |
| 4/21/2013 | 18:54 | Basement | SGP11-6 | -0.1308 | On |
| 4/21/2013 | 18:55 | Basement | SGP11-6 | -0.2641 | On |
| 4/21/2013 | 18:55 | Basement | SGP11-6 | -0.2458 | On |
| 4/22/2013 | 15:17 | Basement | SGP11-6 | -0.0781 | On |
| 4/22/2013 | 15:17 | Basement | SGP11-6 | -0.0786 | On |
| 4/22/2013 | 15:17 | Basement | SGP11-6 | -0.0781 | On |
| 4/22/2013 | 15:18 | Basement | SGP11-6 | -0.0783 | On |
| 4/22/2013 | 15:18 | Basement | SGP11-6 | -0.0778 | On |
| 2/22/2013 | 14:56 | Basement | SGP12-6 | -0.0463 | On |
| 2/22/2013 | 14:57 | Basement | SGP12-6 | -0.0792 | On |
| 2/22/2013 | 14:58 | Basement | SGP12-6 | -0.1263 | On |
| 2/22/2013 | 14:59 | Basement | SGP12-6 | -0.1610 | On |
| 2/22/2013 | 15:00 | Basement | SGP12-6 | -0.1937 | On |
| 4/21/2013 | 18:59 | Basement | SGP12-6 | -0.0213 | On |
| 4/21/2013 | 18:59 | Basement | SGP12-6 | -0.0214 | On |

(continued)

Table 5-3. Shallow Interior SGP (6 ft bls) vs. Basement Differential Pressure Measured with Handheld Micromanometer (negative pressure indicates flow out of building) (cont.)

| Date | Time | Negative End of Manometer | Positive End of Manometer | Reading (in. WC) | Mitigation System On/Off |
|-----------|-------|---------------------------|---------------------------|------------------|--------------------------|
| 4/21/2013 | 19:00 | Basement | SGP12-6 | -0.0196 | On |
| 11/8/2012 | 12:21 | Basement | SGP8-6 | -0.1719 | On |
| 2/22/2013 | 13:03 | Basement | SGP8-6 | -0.1633 | On |
| 2/22/2013 | 13:04 | Basement | SGP8-6 | -0.1636 | On |
| 2/22/2013 | 13:05 | Basement | SGP8-6 | -0.1631 | On |
| 2/22/2013 | 13:06 | Basement | SGP8-6 | -0.1647 | On |
| 2/22/2013 | 13:07 | Basement | SGP8-6 | -0.1647 | On |
| 4/21/2013 | 18:35 | Basement | SGP8-6 | -0.1690 | On |
| 4/21/2013 | 18:36 | Basement | SGP8-6 | -0.1702 | On |
| 4/21/2013 | 18:36 | Basement | SGP8-6 | -0.1710 | On |
| 2/22/2013 | 13:24 | Basement | SGP9-6 | -0.0471 | On |
| 2/22/2013 | 13:25 | Basement | SGP9-6 | -0.0488 | On |
| 2/22/2013 | 13:26 | Basement | SGP9-6 | -0.0472 | On |
| 2/22/2013 | 13:27 | Basement | SGP9-6 | -0.0481 | On |
| 2/22/2013 | 13:28 | Basement | SGP9-6 | -0.0489 | On |
| 4/21/2013 | 18:41 | Basement | SGP9-6 | -0.0580 | On |
| 4/21/2013 | 18:42 | Basement | SGP9-6 | -0.0580 | On |
| 4/21/2013 | 18:42 | Basement | SGP9-6 | -0.0579 | On |

Table 5-4. Shallow Exterior SGP (3.5 ft and 6 ft bls) vs. Basement Differential Pressure Measured with a Handheld Micromanometer (negative pressure indicates flow out of building)

| Date | Time | Negative End of Manometer | Positive End of Manometer | Reading (in. WC) | Mitigation System On/Off |
|-----------|-------|---------------------------|---------------------------|------------------|--------------------------|
| 2/20/2013 | 13:57 | Basement | SGP2-3.5 | -0.0035 | On |
| 2/20/2013 | 13:58 | Basement | SGP2-3.5 | -0.0088 | On |
| 2/20/2013 | 13:59 | Basement | SGP2-3.5 | -0.0027 | On |
| 2/20/2013 | 14:00 | Basement | SGP2-3.5 | -0.0012 | On |
| 2/20/2013 | 14:01 | Basement | SGP2-3.5 | 0.0108 | On |
| 4/23/2013 | 14:27 | Basement | SGP2-3.5 | -0.0084 | On |
| 4/23/2013 | 14:28 | Basement | SGP2-3.5 | -0.0016 | On |
| 4/23/2013 | 14:28 | Basement | SGP2-3.5 | -0.0048 | On |
| 2/20/2013 | 14:02 | Basement | SGP2-6 | 0.0032 | On |
| 2/20/2013 | 14:03 | Basement | SGP2-6 | 0.0016 | On |
| 2/20/2013 | 14:04 | Basement | SGP2-6 | -0.0054 | On |

(continued)

Table 5-4. Shallow Exterior SGP (3.5 ft and 6 ft bls) vs. Basement Differential Pressure Measured by ARCADIS with Handheld Micromanometer (negative pressure indicates flow out of building) (cont.)

| Date | Time | Negative End of Manometer | Positive End of Manometer | Reading (in. WC) | Mitigation System On/Off |
|-----------|-------|---------------------------|---------------------------|------------------|--------------------------|
| 2/20/2013 | 14:05 | Basement | SGP2-6 | 0.0019 | On |
| 2/20/2013 | 14:06 | Basement | SGP2-6 | 0.0049 | On |
| 4/23/2013 | 14:29 | Basement | SGP2-6 | 0.0009 | On |
| 4/23/2013 | 14:30 | Basement | SGP2-6 | -0.0131 | On |
| 4/23/2013 | 14:30 | Basement | SGP2-6 | 0.0073 | On |
| 2/21/2013 | 12:20 | Basement | SGP3-3.5 | 0.0564 | On |
| 2/21/2013 | 12:21 | Basement | SGP3-3.5 | -0.4021 | On |
| 2/21/2013 | 12:22 | Basement | SGP3-3.5 | -0.7826 | On |
| 2/21/2013 | 12:23 | Basement | SGP3-3.5 | -1.0090 | On |
| 2/21/2013 | 12:24 | Basement | SGP3-3.5 | -0.9012 | On |
| 4/24/2013 | 13:04 | Basement | SGP3-3.5 | 1.1480 | On |
| 4/24/2013 | 13:04 | Basement | SGP3-3.5 | 0.2347 | On |
| 4/24/2013 | 13:05 | Basement | SGP3-3.5 | -0.0053 | On |
| 2/21/2013 | 12:28 | Basement | SGP3-6 | -0.0077 | On |
| 2/21/2013 | 12:29 | Basement | SGP3-6 | -0.2139 | On |
| 2/21/2013 | 12:30 | Basement | SGP3-6 | -0.1523 | On |
| 2/21/2013 | 12:31 | Basement | SGP3-6 | -0.0588 | On |
| 2/21/2013 | 12:32 | Basement | SGP3-6 | -0.1876 | On |
| 4/24/2013 | 13:05 | Basement | SGP3-6 | 0.1260 | On |
| 4/24/2013 | 13:06 | Basement | SGP3-6 | 0.0659 | On |
| 4/24/2013 | 13:06 | Basement | SGP3-6 | -0.0082 | On |
| 4/23/2013 | 14:46 | Basement | SGP4-3.5 | -0.0461 | On |
| 4/23/2013 | 14:47 | Basement | SGP4-3.5 | -0.0472 | On |
| 4/23/2013 | 14:47 | Basement | SGP4-3.5 | -0.0713 | On |
| 2/21/2013 | 13:10 | Basement | SGP5-6 | -0.0045 | On |
| 2/21/2013 | 13:11 | Basement | SGP5-6 | -0.0091 | On |
| 2/21/2013 | 13:12 | Basement | SGP5-6 | 0.0277 | On |
| 2/21/2013 | 13:13 | Basement | SGP5-6 | -0.0129 | On |
| 2/21/2013 | 13:14 | Basement | SGP5-6 | 0.0042 | On |
| 4/24/2013 | 13:12 | Basement | SGP5-6 | -0.0273 | On |
| 4/24/2013 | 13:12 | Basement | SGP5-6 | -0.0321 | On |
| 4/24/2013 | 13:12 | Basement | SGP5-6 | -0.0388 | On |

(continued)

Table 5-4. Shallow Exterior SGP (3.5 ft and 6 ft bls) vs. Basement Differential Pressure Measured by ARCADIS with Handheld Micromanometer (negative pressure indicates flow out of building) (cont.)

| Date | Time | Negative End of Manometer | Positive End of Manometer | Reading (in. WC) | Mitigation System On/Off |
|-----------|-------|---------------------------|---------------------------|------------------|--------------------------|
| 2/21/2013 | 14:41 | Basement | SGP6-6 | -0.0783 | On |
| 2/21/2013 | 14:42 | Basement | SGP6-6 | 0.1263 | On |
| 2/21/2013 | 14:43 | Basement | SGP6-6 | 0.1289 | On |
| 2/21/2013 | 14:44 | Basement | SGP6-6 | -0.1172 | On |
| 2/21/2013 | 14:45 | Basement | SGP6-6 | -0.1588 | On |
| 4/24/2013 | 13:22 | Basement | SGP6-6 | 0.1805 | On |
| 4/24/2013 | 13:23 | Basement | SGP6-6 | 0.0933 | On |
| 4/24/2013 | 13:23 | Basement | SGP6-6 | 0.0137 | On |

Table 5-5. Deep Interior SGP (9 ft and 13 ft bls) vs. Basement Differential Pressure Measured by ARCADIS with Handheld Micromanometer (negative pressure indicates flow out of building)

| Date | Time | Negative End of Manometer | Positive End of Manometer | Reading (in. WC) | Mitigation System On/Off |
|-----------|-------|---------------------------|---------------------------|------------------|--------------------------|
| 2/20/2013 | 14:23 | Basement | SGP7-9 | -0.4040 | On |
| 2/20/2013 | 14:24 | Basement | SGP7-9 | -0.0439 | On |
| 2/20/2013 | 14:25 | Basement | SGP7-9 | -0.0595 | On |
| 2/20/2013 | 14:26 | Basement | SGP7-9 | -0.0674 | On |
| 2/20/2013 | 14:27 | Basement | SGP7-9 | -0.0608 | On |
| 4/23/2013 | 14:40 | Basement | SGP7-9 | -0.2718 | On |
| 4/23/2013 | 14:40 | Basement | SGP7-9 | -0.2725 | On |
| 4/23/2013 | 14:41 | Basement | SGP7-9 | -0.2784 | On |
| 2/20/2013 | 14:28 | Basement | SGP7-13 | -0.3053 | On |
| 2/20/2013 | 14:29 | Basement | SGP7-13 | -0.1442 | On |
| 2/20/2013 | 14:30 | Basement | SGP7-13 | -0.2961 | On |
| 2/20/2013 | 14:31 | Basement | SGP7-13 | -0.2985 | On |
| 2/20/2013 | 14:32 | Basement | SGP7-13 | -0.3074 | On |
| 4/23/2013 | 14:42 | Basement | SGP7-13 | -0.3162 | On |
| 4/23/2013 | 14:43 | Basement | SGP7-13 | -0.3713 | On |
| 4/23/2013 | 14:43 | Basement | SGP7-13 | -0.3536 | On |
| 11/8/2012 | 12:22 | Basement | SGP8-9 | -0.0999 | On |
| 2/22/2013 | 13:19 | Basement | SGP8-9 | -0.0927 | On |
| 2/22/2013 | 13:20 | Basement | SGP8-9 | -0.0911 | On |
| 2/22/2013 | 13:21 | Basement | SGP8-9 | -0.0911 | On |
| 2/22/2013 | 13:22 | Basement | SGP8-9 | -0.0956 | On |
| 2/22/2013 | 13:23 | Basement | SGP8-9 | -0.0946 | On |

(continued)

Table 5-5. Deep Interior SGP (9 ft and 13 ft bls) vs. Basement Differential Pressure Measured by ARCADIS with Handheld Micromanometer (negative pressure indicates flow out of building) (cont.)

| Date | Time | Negative End of Manometer | Positive End of Manometer | Reading (in. WC) | Mitigation System On/Off |
|-----------|-------|---------------------------|---------------------------|------------------|--------------------------|
| 4/21/2013 | 18:37 | Basement | SGP8-9 | -0.1038 | On |
| 4/21/2013 | 18:38 | Basement | SGP8-9 | -0.1059 | On |
| 4/21/2013 | 18:38 | Basement | SGP8-9 | -0.1026 | On |
| 11/8/2012 | 12:22 | Basement | SGP8-13 | -0.0477 | On |
| 2/22/2013 | 13:08 | Basement | SGP8-13 | -0.0408 | On |
| 2/22/2013 | 13:09 | Basement | SGP8-13 | -0.0379 | On |
| 2/22/2013 | 13:10 | Basement | SGP8-13 | -0.0428 | On |
| 2/22/2013 | 13:11 | Basement | SGP8-13 | -0.0411 | On |
| 2/22/2013 | 13:12 | Basement | SGP8-13 | -0.0394 | On |
| 4/21/2013 | 18:39 | Basement | SGP8-13 | -0.0594 | On |
| 4/21/2013 | 18:39 | Basement | SGP8-13 | -0.0603 | On |
| 4/21/2013 | 18:39 | Basement | SGP8-13 | -0.0611 | On |
| 2/22/2013 | 13:28 | Basement | SGP9-9 | -0.0492 | On |
| 2/22/2013 | 13:29 | Basement | SGP9-9 | -0.0471 | On |
| 2/22/2013 | 13:30 | Basement | SGP9-9 | -0.0479 | On |
| 2/22/2013 | 13:31 | Basement | SGP9-9 | -0.0501 | On |
| 2/22/2013 | 13:32 | Basement | SGP9-9 | -0.0482 | On |
| 4/21/2013 | 18:43 | Basement | SGP9-9 | -0.0580 | On |
| 4/21/2013 | 18:43 | Basement | SGP9-9 | -0.0588 | On |
| 4/21/2013 | 18:43 | Basement | SGP9-9 | -0.0588 | On |
| 2/22/2013 | 13:38 | Basement | SGP9-13 | -0.0178 | On |
| 2/22/2013 | 13:39 | Basement | SGP9-13 | -0.0139 | On |
| 2/22/2013 | 13:40 | Basement | SGP9-13 | -0.0138 | On |
| 2/22/2013 | 13:41 | Basement | SGP9-13 | -0.0171 | On |
| 2/22/2013 | 13:42 | Basement | SGP9-13 | -0.0128 | On |
| 4/21/2013 | 18:44 | Basement | SGP9-13 | -0.0328 | On |
| 4/21/2013 | 18:44 | Basement | SGP9-13 | -0.0285 | On |
| 4/21/2013 | 18:45 | Basement | SGP9-13 | -0.0299 | On |
| 2/22/2013 | 12:42 | Basement | SGP10-9 | 0.2429 | On |
| 2/22/2013 | 12:43 | Basement | SGP10-9 | -0.0314 | On |
| 2/22/2013 | 12:44 | Basement | SGP10-9 | -0.0347 | On |
| 2/22/2013 | 12:45 | Basement | SGP10-9 | -0.0375 | On |
| 2/22/2013 | 12:46 | Basement | SGP10-9 | -0.0365 | On |
| 4/21/2013 | 18:30 | Basement | SGP10-9 | -0.0465 | On |
| 4/21/2013 | 18:31 | Basement | SGP10-9 | -0.0471 | On |
| 4/21/2013 | 18:31 | Basement | SGP10-9 | -0.0445 | On |
| 2/22/2013 | 12:46 | Basement | SGP10-13 | -0.0195 | On |
| 2/22/2013 | 12:47 | Basement | SGP10-13 | -0.0269 | On |

(continued)

Table 5-5. Deep Interior SGP (9 ft and 13 ft bls) vs. Basement Differential Pressure Measured by ARCADIS with Handheld Micromanometer (negative pressure indicates flow out of building; yellow indicates mitigation off) (cont.)

| Date | Time | Negative End of Manometer | Positive End of Manometer | Reading (in. WC) | Mitigation System On/Off |
|------------|-------|---------------------------|---------------------------|------------------|--------------------------|
| 2/22/2013 | 12:48 | Basement | SGP10-13 | -0.0197 | On |
| 2/22/2013 | 12:49 | Basement | SGP10-13 | -0.0228 | On |
| 2/22/2013 | 12:50 | Basement | SGP10-13 | -0.0267 | On |
| 4/21/2013 | 18:32 | Basement | SGP10-13 | -0.0362 | On |
| 4/21/2013 | 18:32 | Basement | SGP10-13 | -0.0370 | On |
| 4/21/2013 | 18:32 | Basement | SGP10-13 | -0.0375 | On |
| 11/8/2012 | 12:29 | Basement | SGP11-9 | -0.0652 | On |
| 12/7/2012 | 11:52 | Basement | SGP11-9 | -0.0005 | Off |
| 12/7/2012 | 11:53 | Basement | SGP11-9 | -0.0002 | Off |
| 12/7/2012 | 11:54 | Basement | SGP11-9 | -0.0001 | Off |
| 12/7/2012 | 11:55 | Basement | SGP11-9 | 0.0000 | Off |
| 12/7/2012 | 11:56 | Basement | SGP11-9 | -0.0006 | Off |
| 12/29/2012 | 16:47 | Basement | SGP11-9 | -0.0579 | On |
| 12/29/2012 | 16:47 | Basement | SGP11-9 | -0.0603 | On |
| 12/29/2012 | 16:48 | Basement | SGP11-9 | -0.0556 | On |
| 2/22/2013 | 14:30 | Basement | SGP11-9 | -0.2417 | On |
| 2/22/2013 | 14:31 | Basement | SGP11-9 | -0.2678 | On |
| 2/22/2013 | 14:32 | Basement | SGP11-9 | -0.2689 | On |
| 2/22/2013 | 14:33 | Basement | SGP11-9 | -0.2657 | On |
| 2/22/2013 | 14:34 | Basement | SGP11-9 | -0.2690 | On |
| 4/21/2013 | 18:56 | Basement | SGP11-9 | -0.0664 | On |
| 4/21/2013 | 18:56 | Basement | SGP11-9 | -0.0645 | On |
| 4/21/2013 | 18:56 | Basement | SGP11-9 | -0.0637 | On |
| 11/8/2012 | 12:30 | Basement | SGP11-13 | -0.0380 | On |
| 2/22/2013 | 14:51 | Basement | SGP11-13 | -0.0382 | On |
| 2/22/2013 | 14:52 | Basement | SGP11-13 | -0.0310 | On |
| 2/22/2013 | 14:53 | Basement | SGP11-13 | -0.0283 | On |
| 2/22/2013 | 14:54 | Basement | SGP11-13 | -0.0355 | On |
| 2/22/2013 | 14:55 | Basement | SGP11-13 | -0.0362 | On |
| 4/21/2013 | 18:57 | Basement | SGP11-13 | -0.0416 | On |
| 4/21/2013 | 18:58 | Basement | SGP11-13 | -0.0443 | On |
| 4/21/2013 | 18:58 | Basement | SGP11-13 | -0.0427 | On |
| 2/22/2013 | 15:00 | Basement | SGP12-9 | -0.0194 | On |
| 2/22/2013 | 15:01 | Basement | SGP12-9 | -0.0192 | On |
| 2/22/2013 | 15:02 | Basement | SGP12-9 | -0.0198 | On |
| 2/22/2013 | 15:03 | Basement | SGP12-9 | -0.0180 | On |
| 2/22/2013 | 15:04 | Basement | SGP12-9 | -0.0171 | On |

(continued)

Table 5-5. Deep Interior SGP (9 ft and 13 ft bls) vs. Basement Differential Pressure Measured by ARCADIS with Handheld Micromanometer (negative pressure indicates flow out of building) (cont.)

| Date | Time | Negative End of Manometer | Positive End of Manometer | Reading (in. WC) | Mitigation System On/Off |
|-----------|-------|---------------------------|---------------------------|------------------|--------------------------|
| 4/21/2013 | 19:00 | Basement | SGP12-9 | -0.0244 | On |
| 4/21/2013 | 19:01 | Basement | SGP12-9 | -0.0230 | On |
| 4/21/2013 | 19:01 | Basement | SGP12-9 | -0.0215 | On |
| 2/22/2013 | 15:04 | Basement | SGP12-13 | -0.0065 | On |
| 2/22/2013 | 15:05 | Basement | SGP12-13 | -0.0196 | On |
| 2/22/2013 | 15:06 | Basement | SGP12-13 | -0.0168 | On |
| 2/22/2013 | 15:07 | Basement | SGP12-13 | -0.1048 | On |
| 2/22/2013 | 15:08 | Basement | SGP12-13 | -0.0979 | On |
| 4/21/2013 | 19:02 | Basement | SGP12-13 | -0.0303 | On |
| 4/21/2013 | 19:02 | Basement | SGP12-13 | -0.0320 | On |
| 4/21/2013 | 19:02 | Basement | SGP12-13 | -0.0292 | On |

Table 5-6. Deep Exterior SGP (9 ft and 13 ft bls) vs. Basement Differential Pressure Measured by ARCADIS with Handheld Micromanometer (negative pressure indicates flow out of building)

| Date | Time | Negative End of Manometer | Positive End of Manometer | Reading (in. WC) | Mitigation System On/Off |
|-----------|-------|---------------------------|---------------------------|------------------|--------------------------|
| 2/20/2013 | 13:29 | Basement | SGP1-13 | -0.0124 | On |
| 2/20/2013 | 13:30 | Basement | SGP1-13 | -0.0153 | On |
| 2/20/2013 | 13:31 | Basement | SGP1-13 | -0.0337 | On |
| 2/20/2013 | 13:32 | Basement | SGP1-13 | -0.0149 | On |
| 2/20/2013 | 13:33 | Basement | SGP1-13 | -0.0146 | On |
| 4/23/2013 | 14:25 | Basement | SGP1-13 | -0.0293 | On |
| 4/23/2013 | 14:25 | Basement | SGP1-13 | -0.0273 | On |
| 4/23/2013 | 14:25 | Basement | SGP1-13 | -0.0321 | On |
| 2/20/2013 | 13:18 | Basement | SGP1-9 | 0.1209 | On |
| 2/20/2013 | 13:19 | Basement | SGP1-9 | -0.2483 | On |
| 2/20/2013 | 13:20 | Basement | SGP1-9 | -0.0130 | On |
| 2/20/2013 | 13:21 | Basement | SGP1-9 | -0.0100 | On |
| 2/20/2013 | 13:22 | Basement | SGP1-9 | -0.0125 | On |
| 4/23/2013 | 14:23 | Basement | SGP1-9 | -0.1319 | On |
| 4/23/2013 | 14:24 | Basement | SGP1-9 | -0.1363 | On |
| 4/23/2013 | 14:24 | Basement | SGP1-9 | -0.1954 | On |
| 2/20/2013 | 14:06 | Basement | SGP2-13 | -0.0089 | On |
| 2/20/2013 | 14:07 | Basement | SGP2-13 | 0.0000 | On |
| 2/20/2013 | 14:08 | Basement | SGP2-13 | 0.0018 | On |
| 2/20/2013 | 14:09 | Basement | SGP2-13 | -0.0169 | On |
| 2/20/2013 | 14:10 | Basement | SGP2-13 | -0.0134 | On |

(continued)

Table 5-6. Deep Exterior SGP (9 ft and 13 ft bls) vs. Basement Differential Pressure Measured by ARCADIS with Handheld Micromanometer (negative pressure indicates flow out of building) (cont.)

| Date | Time | Negative End of Manometer | Positive End of Manometer | Reading (in. WC) | Mitigation System On/Off |
|-----------|-------|---------------------------|---------------------------|------------------|--------------------------|
| 4/23/2013 | 14:32 | Basement | SGP2-13 | -0.0316 | On |
| 4/23/2013 | 14:32 | Basement | SGP2-13 | -0.0240 | On |
| 4/23/2013 | 14:33 | Basement | SGP2-13 | -0.0141 | On |
| 2/20/2013 | 13:24 | Basement | SGP2-9 | -0.0025 | On |
| 2/20/2013 | 13:25 | Basement | SGP2-9 | -0.0079 | On |
| 2/20/2013 | 13:26 | Basement | SGP2-9 | -0.0080 | On |
| 2/20/2013 | 13:27 | Basement | SGP2-9 | -0.0084 | On |
| 2/20/2013 | 13:28 | Basement | SGP2-9 | -0.0032 | On |
| 4/23/2013 | 14:31 | Basement | SGP2-9 | -0.2818 | On |
| 4/23/2013 | 14:31 | Basement | SGP2-9 | -0.3829 | On |
| 4/23/2013 | 14:31 | Basement | SGP2-9 | -0.4583 | On |
| 2/21/2013 | 12:37 | Basement | SGP3-13 | -0.0253 | On |
| 2/21/2013 | 12:38 | Basement | SGP3-13 | -0.0191 | On |
| 2/21/2013 | 12:39 | Basement | SGP3-13 | -0.0168 | On |
| 2/21/2013 | 12:40 | Basement | SGP3-13 | -0.0310 | On |
| 2/21/2013 | 12:41 | Basement | SGP3-13 | -0.0194 | On |
| 4/24/2013 | 13:08 | Basement | SGP3-13 | -0.0240 | On |
| 4/24/2013 | 13:08 | Basement | SGP3-13 | -0.0250 | On |
| 4/24/2013 | 13:08 | Basement | SGP3-13 | -0.0343 | On |
| 2/21/2013 | 12:32 | Basement | SGP3-9 | 3.3110 | On |
| 2/21/2013 | 12:33 | Basement | SGP3-9 | 2.6090 | On |
| 2/21/2013 | 12:34 | Basement | SGP3-9 | 2.3070 | On |
| 2/21/2013 | 12:35 | Basement | SGP3-9 | 2.0440 | On |
| 2/21/2013 | 12:36 | Basement | SGP3-9 | 2.0850 | On |
| 4/24/2013 | 13:06 | Basement | SGP3-9 | -0.0804 | On |
| 4/24/2013 | 13:07 | Basement | SGP3-9 | -0.1652 | On |
| 4/24/2013 | 13:07 | Basement | SGP3-9 | -0.1840 | On |
| 2/21/2013 | 12:53 | Basement | SGP4-13 | -0.0601 | On |
| 2/21/2013 | 12:54 | Basement | SGP4-13 | -0.0490 | On |
| 2/21/2013 | 12:55 | Basement | SGP4-13 | -0.0388 | On |
| 2/21/2013 | 12:56 | Basement | SGP4-13 | -0.0351 | On |
| 2/21/2013 | 12:57 | Basement | SGP4-13 | -0.0351 | On |
| 4/23/2013 | 14:48 | Basement | SGP4-13 | -0.0375 | On |
| 4/23/2013 | 14:48 | Basement | SGP4-13 | -0.0413 | On |
| 4/23/2013 | 14:48 | Basement | SGP4-13 | -0.0570 | On |
| 2/21/2013 | 12:48 | Basement | SGP4-9 | -0.8140 | On |
| 2/21/2013 | 12:49 | Basement | SGP4-9 | -0.4402 | On |
| 2/21/2013 | 12:50 | Basement | SGP4-9 | -0.3766 | On |

(continued)

Table 5-6. Deep Exterior SGP (9 ft and 13 ft bls) vs. Basement Differential Pressure Measured by ARCADIS with Handheld Micromanometer (negative pressure indicates flow out of building) (cont.)

| Date | Time | Negative End of Manometer | Positive End of Manometer | Reading (in. WC) | Mitigation System On/Off |
|-----------|-------|---------------------------|---------------------------|------------------|--------------------------|
| 2/21/2013 | 12:51 | Basement | SGP4-9 | -0.3957 | On |
| 2/21/2013 | 12:52 | Basement | SGP4-9 | -0.3744 | On |
| 2/21/2013 | 13:21 | Basement | SGP5-13 | -0.0231 | On |
| 2/21/2013 | 13:22 | Basement | SGP5-13 | -0.0289 | On |
| 2/21/2013 | 13:23 | Basement | SGP5-13 | -0.0189 | On |
| 2/21/2013 | 13:24 | Basement | SGP5-13 | -0.0433 | On |
| 2/21/2013 | 13:25 | Basement | SGP5-13 | -0.0338 | On |
| 4/24/2013 | 13:16 | Basement | SGP5-13 | -0.0137 | On |
| 4/24/2013 | 13:16 | Basement | SGP5-13 | -0.1725 | On |
| 4/24/2013 | 13:16 | Basement | SGP5-13 | -0.1781 | On |
| 2/21/2013 | 13:16 | Basement | SGP5-9 | -0.0200 | On |
| 2/21/2013 | 13:17 | Basement | SGP5-9 | -0.0205 | On |
| 2/21/2013 | 13:18 | Basement | SGP5-9 | -0.0181 | On |
| 2/21/2013 | 13:19 | Basement | SGP5-9 | -0.0095 | On |
| 2/21/2013 | 13:20 | Basement | SGP5-9 | -0.0120 | On |
| 4/24/2013 | 13:14 | Basement | SGP5-9 | -0.0314 | On |
| 4/24/2013 | 13:15 | Basement | SGP5-9 | -0.0361 | On |
| 4/24/2013 | 13:15 | Basement | SGP5-9 | -0.0315 | On |
| 2/21/2013 | 14:58 | Basement | SGP6-13 | -0.0688 | On |
| 2/21/2013 | 14:59 | Basement | SGP6-13 | -0.0403 | On |
| 2/21/2013 | 15:00 | Basement | SGP6-13 | -0.0144 | On |
| 2/21/2013 | 15:01 | Basement | SGP6-13 | -0.0350 | On |
| 2/21/2013 | 15:02 | Basement | SGP6-13 | -0.0256 | On |
| 4/24/2013 | 13:25 | Basement | SGP6-13 | -0.0259 | On |
| 4/24/2013 | 13:25 | Basement | SGP6-13 | -0.0240 | On |
| 4/24/2013 | 13:25 | Basement | SGP6-13 | -0.0228 | On |
| 2/21/2013 | 14:53 | Basement | SGP6-9 | -0.1667 | On |
| 2/21/2013 | 14:54 | Basement | SGP6-9 | -0.1361 | On |
| 2/21/2013 | 14:55 | Basement | SGP6-9 | -0.1582 | On |
| 2/21/2013 | 14:56 | Basement | SGP6-9 | -0.2463 | On |
| 2/21/2013 | 14:57 | Basement | SGP6-9 | -0.0993 | On |
| 4/24/2013 | 13:24 | Basement | SGP6-9 | 0.1724 | On |
| 4/24/2013 | 13:24 | Basement | SGP6-9 | -0.3384 | On |
| 4/24/2013 | 13:24 | Basement | SGP6-9 | -0.5029 | On |
| 2/20/2013 | 14:28 | Basement | SGP7-13 | -0.3053 | On |
| 2/20/2013 | 14:29 | Basement | SGP7-13 | -0.1442 | On |
| 2/20/2013 | 14:30 | Basement | SGP7-13 | -0.2961 | On |

(continued)

Table 5-6. Deep Exterior SGP (9 ft and 13 ft bls) vs. Basement Differential Pressure Measured by ARCADIS with Handheld Micromanometer (negative pressure indicates flow out of building) (cont.)

| Date | Time | Negative End of Manometer | Positive End of Manometer | Reading (in. WC) | Mitigation System On/Off |
|-----------|-------|---------------------------|---------------------------|------------------|--------------------------|
| 2/20/2013 | 14:31 | Basement | SGP7-13 | -0.2985 | On |
| 2/20/2013 | 14:32 | Basement | SGP7-13 | -0.3074 | On |
| 4/23/2013 | 14:42 | Basement | SGP7-13 | -0.3162 | On |
| 4/23/2013 | 14:43 | Basement | SGP7-13 | -0.3713 | On |
| 4/23/2013 | 14:43 | Basement | SGP7-13 | -0.3536 | On |
| 2/20/2013 | 14:23 | Basement | SGP7-9 | -0.4040 | On |
| 2/20/2013 | 14:24 | Basement | SGP7-9 | -0.0439 | On |
| 2/20/2013 | 14:25 | Basement | SGP7-9 | -0.0595 | On |
| 2/20/2013 | 14:26 | Basement | SGP7-9 | -0.0674 | On |
| 2/20/2013 | 14:27 | Basement | SGP7-9 | -0.0608 | On |
| 4/23/2013 | 14:40 | Basement | SGP7-9 | -0.2718 | On |
| 4/23/2013 | 14:40 | Basement | SGP7-9 | -0.2725 | On |
| 4/23/2013 | 14:41 | Basement | SGP7-9 | -0.2784 | On |

This testing would not have been required for residential SSD systems in many jurisdictions but may have been conducted in some cases. For example, ITRC (2007) states the following in its section on operation, maintenance, and monitoring of SSD mitigation systems:

Suction field extension testing may be warranted if manometer readings indicate reduced suction levels or indoor air tests show increasing trends.

Vacuum influence monitoring through a series of wall ports (**Table 5-2**), shallow exterior soil gas ports (**Table 5-4**), deep interior soil gas ports (**Table 5-5**), and deep exterior soil gas ports (**Table 5-6**) was also conducted in this research project. Such monitoring is not a feature of normal residential SSD system operation. The results at the wall ports (**Table 5-3**) showed that the vacuum influence was weak (which is reasonable given that the extraction ports were beneath the floor and the wall ports are closer to the surface of the soil). Three of the wall ports showed weak influence but in the desired direction. WP-3, located on the south wall of the 422 basement, was the exception, showing several readings indicative of weak driving forces into the basement.

The differential pressure between the shallow exterior ports and the basement (**Table 5-4**) was much less consistent. This result would be expected because the SSD system is not designed to depressurize the area outside of the building footprint.

The differential pressure between the deep interior ports (9 and 13 ft bls = 3 and 6 ft below the basement floor) is consistent and shows that the driving force is moving out of the building (**Table 5-5**). There was only a single exception to this pattern at SGP 10-9, which could have been an artifact because it was the first reading at that location on that day. The differential pressure between the deep exterior ports and the basement was also generally negative, indicating a driving force out of the building (**Table 5-6**).

ARCADIS monitored differential pressure continuously at five locations (methods described in Section 3.3.6). Such continuous monitoring would rarely be performed on a residential SSD system in current practice but is more common in evaluating commercial building systems. As shown in **Figure 5-1**, the

subslab vs. basement differential pressure monitored near the center of the 422 building but 7 feet from the nearest extraction point consistently showed depressurization to some degree during active SSD operation. The exception is a period from October 22 to 25, when readings of approximately 0.5 Pa greater pressurization in the subslab than in the building were observed. However, during those 3 days, no anomalous radon results were seen in continuous monitoring.

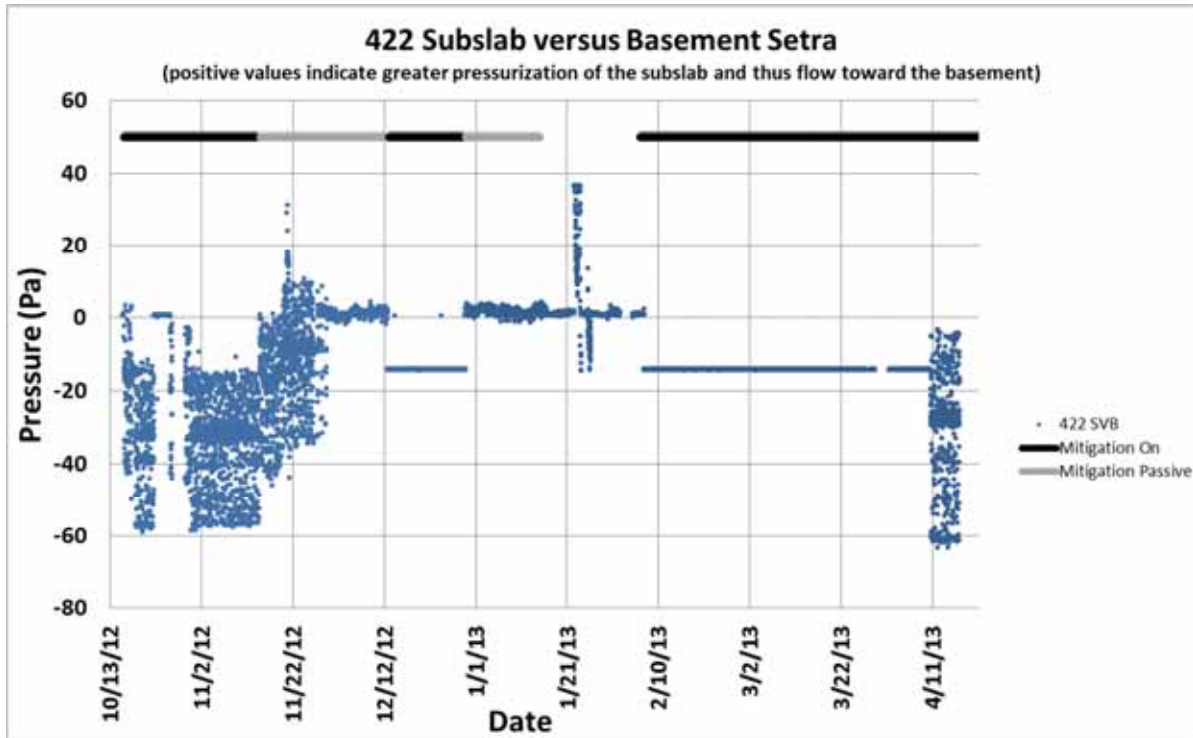


Figure 5-1. Subslab vs. basement differential pressure: 422 side during mitigation testing.

In most cases, readings at or beyond the design capacity of the micromanometer +15 Pa to –15 Pa (0.06 to –0.06 in. WC) were observed. According to our discussions with the manufacturer of the Setra sensors, when the pressure goes above the designed range, the values should be considered semi-quantitative. The Setra sensor may also at times give a constant result of –15 Pa to indicate the pressure is off scale. We evaluated this over-range performance on the Setra sensors by comparing it with the Airdata Multimeter ADM-870 handheld micromanometer, which has a greater design range. These results show that the two instruments agree well up to approximately double the differential pressure design range of the Setra sensor which is 0.12 in. WC. However, an essentially constant reading of –0.058 in. WC (–14.3 Pa) was recorded when the Airdata instrument found a differential pressure more than three times the design range of the Setra (**Table 5-7**)—0.213 in. WC (–53 Pa).

In general, the subslab vs. basement differential pressure on the 422 side of the duplex responded as a square wave to the turning on and off of the SSD system. However, unexpectedly, the relaxation of the vacuum in the first off cycle was gradual over as long as 10 days from November 16 to 26, 2012 (**Figure 5-1**). On the 420 side of the duplex (**Figure 5-2**), the subslab vs. basement differential pressure responded as a square wave to the turning on and off of the SSD system with the exception of two time periods when vacuum control was apparently lost and the driving force swung toward the building. These occurred on December 24–28, 2012, and April 16, 2013. These dates corresponded to a major blizzard and a major storm event from the evening of the April 16th until the late night. The storm produced much rain, and the Fall Creek stream gauge read over 2,000 cf/s.

Table 5-7. Comparison of Setra Continuous Sensor Differential Pressure vs. Airdata Multimeter ADM-870 with SSD System Operating: December 29, 2012 (yellow shaded data reflects an “off scale” response on the Setra)

| Location | Airdata ADM-870 Replicate Readings (in WC) Taken within about 2 min per Location | Setra data, Replicate Readings Bracketing the Airdata Data (in WC); Data Points at 14-min. Intervals |
|--|--|--|
| 422 Basement vs. Upstairs | 0.0013 0.0012 0.0012 | 0.002941 0.001885 0.001885 0.001885 |
| 422 Subslab vs. Basement | -0.2135 -0.2154 -0.2126 | -0.05761 -0.05761 -0.05814 -0.05814 |
| 422 Deep Soil Gas vs. Shallow Soil Gas | 0.1248 0.1229 0.1268 | 0.124052 0.125373 0.125638 0.12511 |
| 422 Basement vs. Exterior | -0.0189 -0.0147 -0.0139 | -0.01028 -0.01107 -0.00922 -0.00922 |
| 420 Subslab vs. Basement | -0.0579 -0.0603 -0.0556 | -0.05791 -0.05791 -0.05853 -0.05815 |

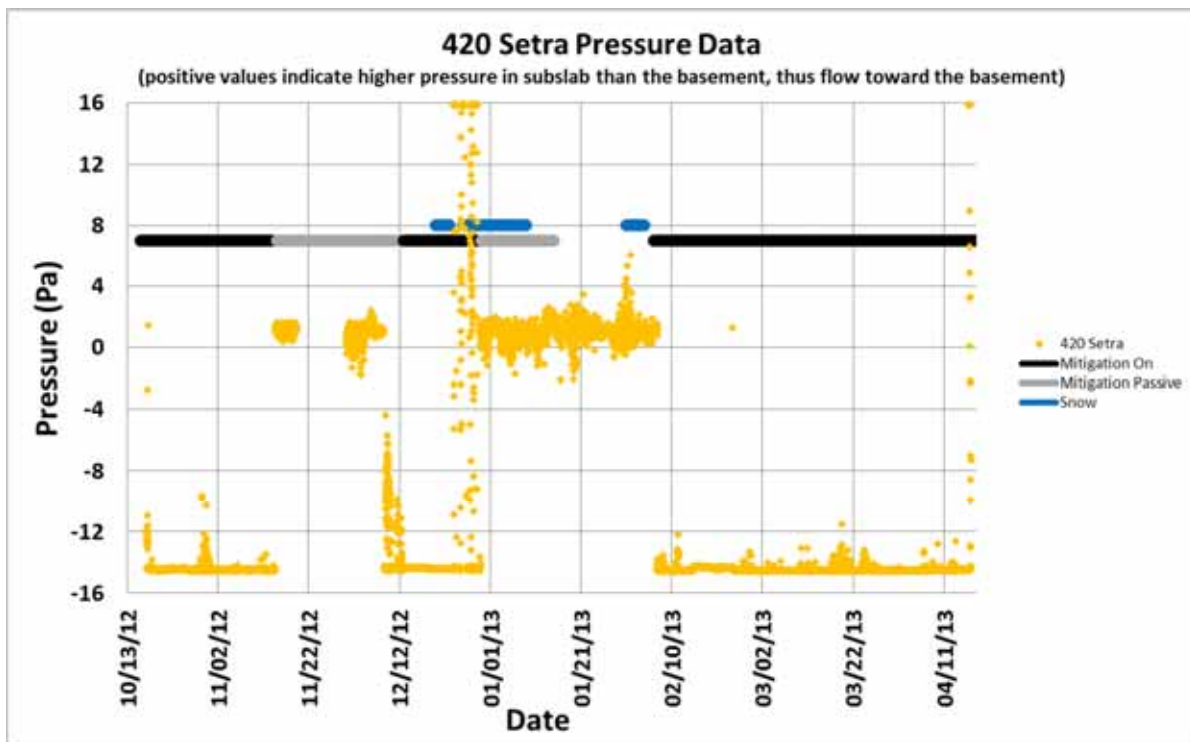


Figure 5-2. Subslab vs. basement differential pressure: 420 side during mitigation testing.

Differential pressure monitoring also indicates that during mitigation the driving force is generally from the 13 ft bls soil gas depth to a 6 ft bls (subslab) soil gas depth (**Figure 5-3**). With some temporary exceptions, this suggests that the mitigation system is drawing in soil gas from above the water table, which could enhance contaminant migration toward the structure. This effect has been previously hypothesized as a reason to not overpower SSD systems (Lutes, 2010b).

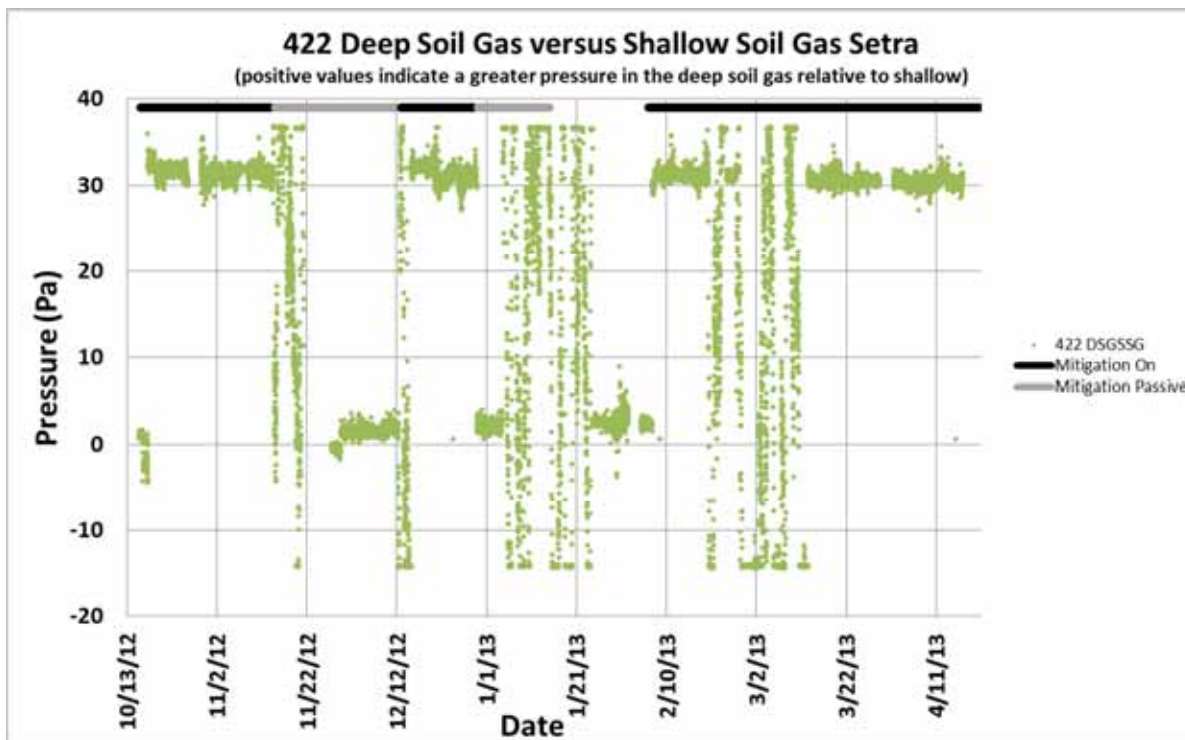


Figure 5-3. Deep soil gas vs. shallow soil gas differential pressure during mitigation testing.

The SSD system has little or no effect on the driving force from the basement to the upstairs within the structure (**Figure 5-4**). There is relatively little driving force between these zones of the house, most likely because there is little resistance to flow between floors as a result of poor air sealing. The basement vs. exterior differential pressure (**Figure 5-5**) shows some variability, including a sharp drop off in late November 2012, but no clear correlation of that variability to mitigation status.

5.1.3 SSD Mitigation System Flow

Flow through the SSD system discharge stack is relatively consistent between 1,540 and 1,819 fpm when the SSD system is on (**Figure 5-6**). As expected, when the SSD system was in the passive mode, flows were much lower and variable in direction.

5.2 Radon Monitoring: Hourly and Weekly Time Scales

As expected, radon concentrations show a near immediate substantial drop when the SSD system is turned on and quickly return to high (premitigation) concentrations when the SSD system is turned off. This is shown for the 422 side of the duplex based on continuous AlphaGUARD data, which were collected on 10-min intervals (**Figures 5-7 and 5-8**). This is shown for all monitored interior locations with weekly integrated electret samples (**Figure 5-9**). The weekly data include an ambient location and show that during active SSD operation radon concentrations in the interior closely approached ambient levels.

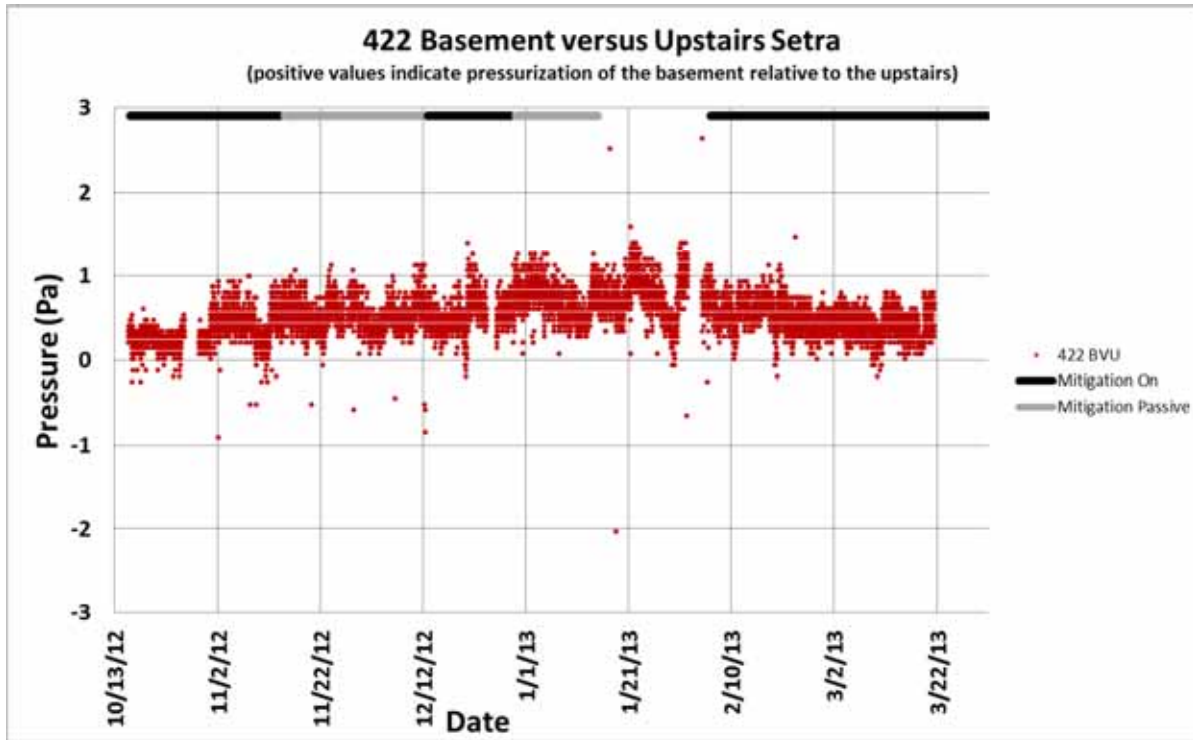


Figure 5-4. Basement vs. upstairs differential pressure: 422 side during mitigation testing.

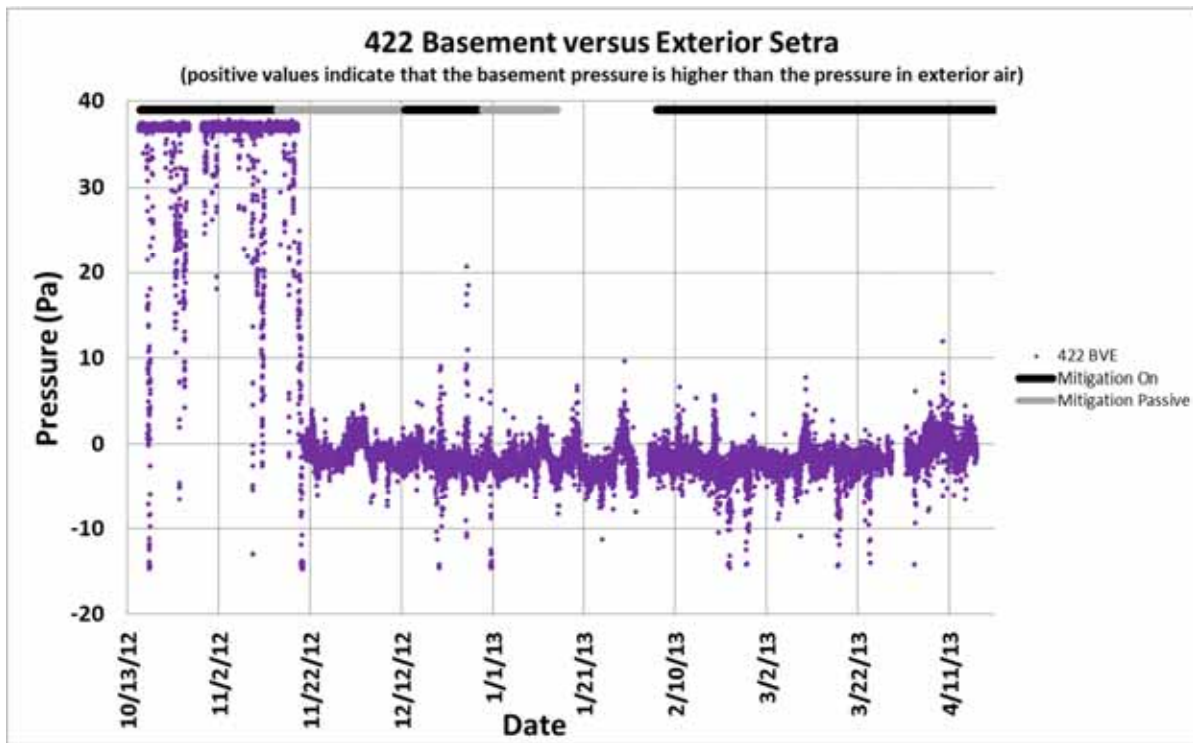


Figure 5-5. Basement vs. exterior differential pressure: 422 side during mitigation testing.

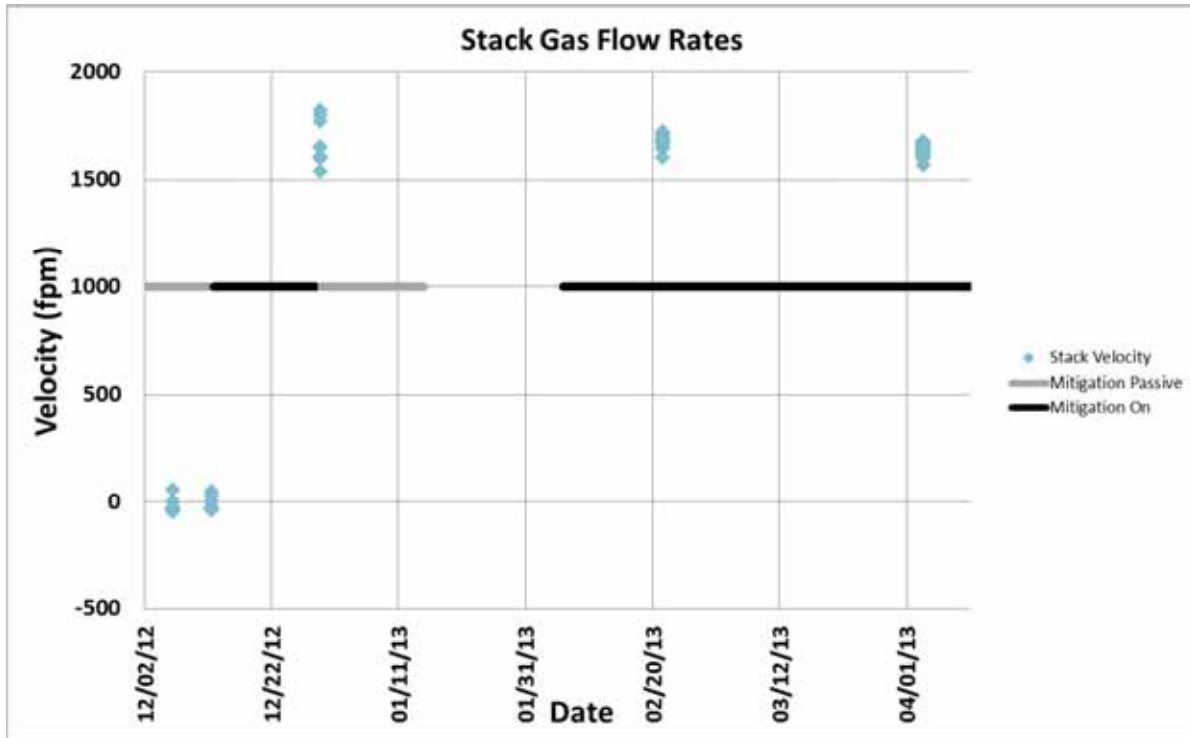


Figure 5-6. Stack gas flow velocity from SSD system.

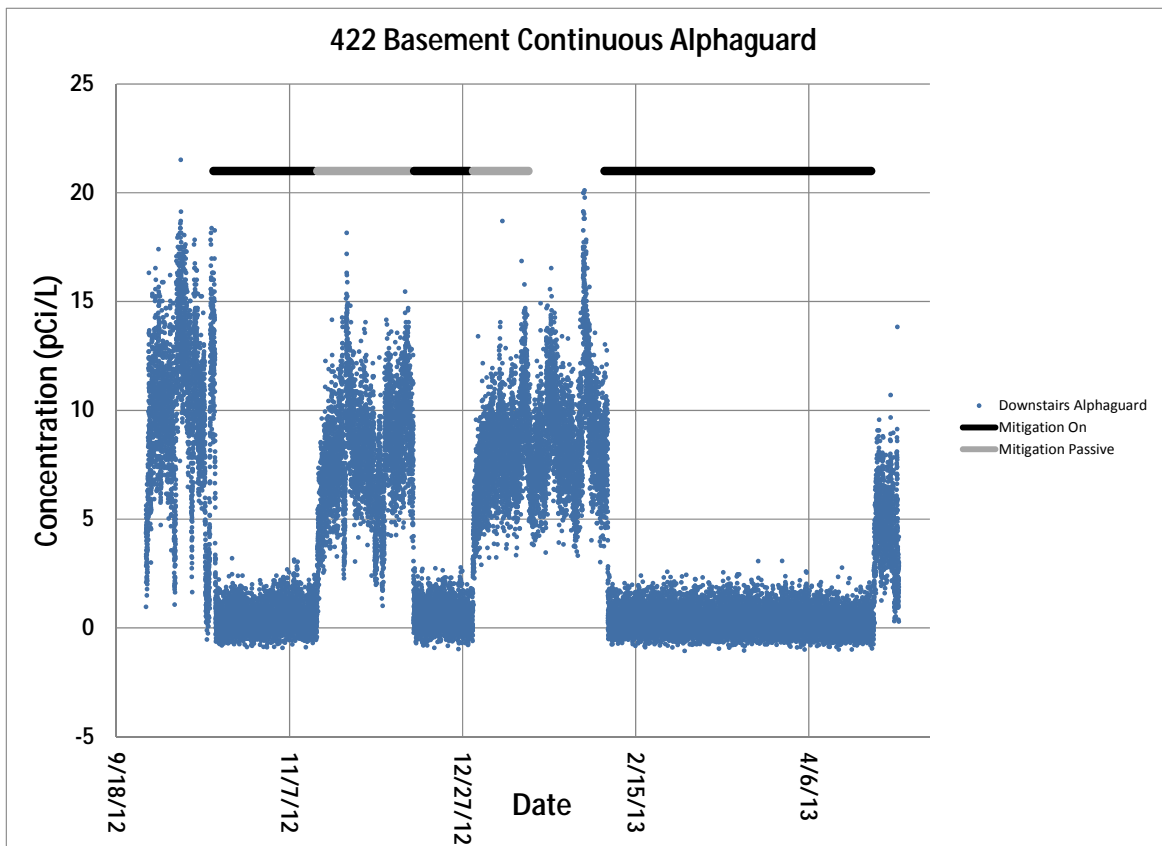


Figure 5-7. Real-time radon monitoring: 422 basement.

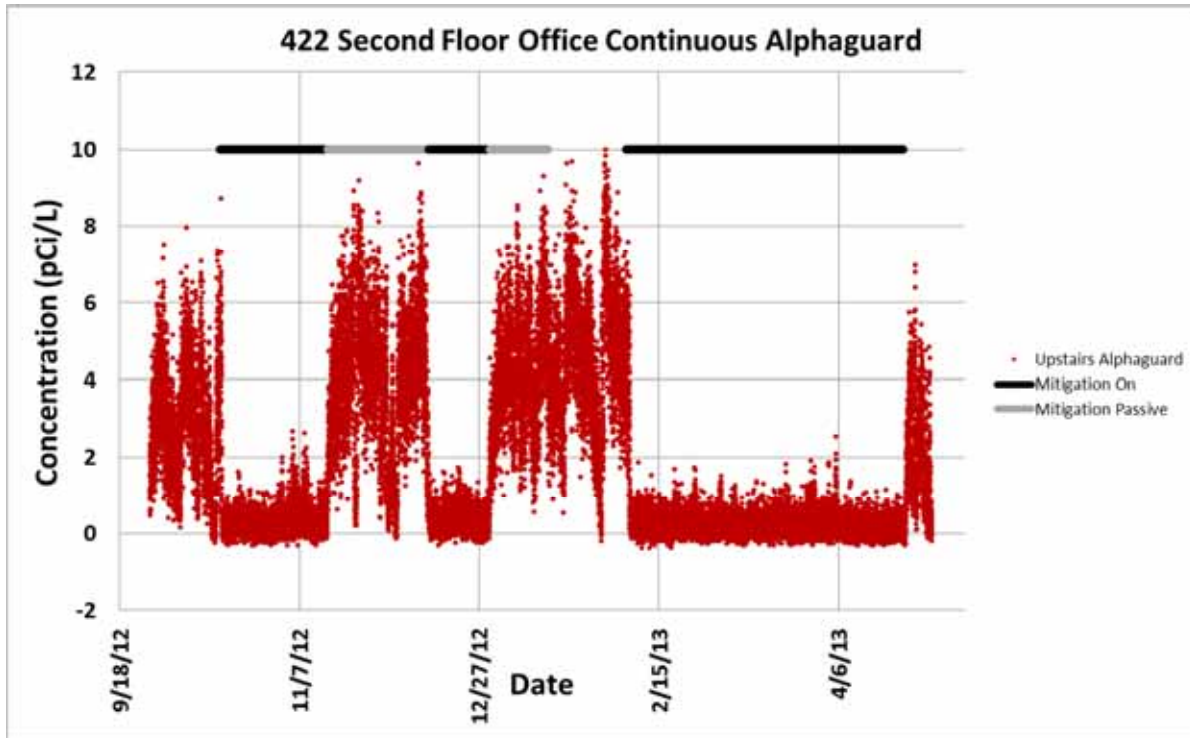


Figure 5-8. Real-time radon monitoring: 422 second floor.

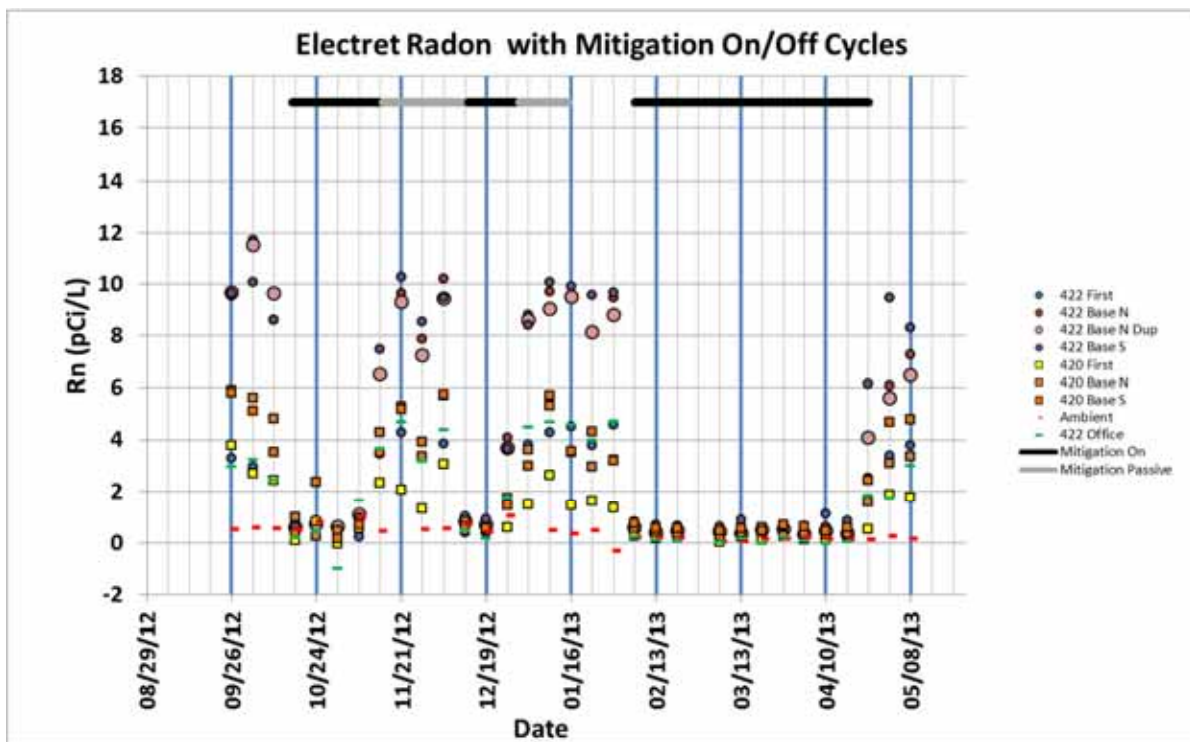


Figure 5-9. Weekly integrated radon (electret) during mitigation testing.

Operating the SSD system in a passive mode provided little benefit for radon. It is possible that this reflects the design of the SSD system, which involved an exterior stack. SSD systems intended to be primarily run in a passive mode are frequently designed with a stack running up through the center of the structure to maximize stack effects.

Descriptive statistics for the electret measurements are presented in **Table 5-8**. The descriptive statistics have been broken up into four mitigation status categories defined as follows:

- Not installed—data collected prior to installing the SSD system
- Off—data collected after the SSD system was installed and first operated, but with the SSD system powered off and valves off as a test
- Passive—data collected after the SSD system was installed and first operated, but with the SSD system powered off but with the valves open
- On—data collected with the SSD system powered on and valves open.

The descriptive statistics have also been broken up into two heating status categories:

- Off—includes data from the 420 side where the heating system was not installed, as well as summer data for both sides of the duplex
- On—heating system in operation (during the heating season, on the 422 side this was the normal state). Weekly duration data are coded as “on” for the 420 side if the heating system was on the 422 side, this is reasonable because thermocouple data suggest that the 420 side stays above ambient temperatures in winter due to heat leakage.

It should be noted that not all possible combinations of mitigation and heating status were tested. For example, passive mitigation was not tested outside of the heating season.

Table 5-8. Electret Radon Descriptive Statistics by Mitigation and Heating Status (pCi/L)

| Mitigation | Heating | Number Samples | Mean | SD | CV | geoMean | geoSD | geoCV |
|---------------|---------|----------------|------|------|------|---------|-------|-------|
| Not installed | Off | 221 | 4.70 | 3.54 | 0.75 | 2.66 | 8.28 | 3.11 |
| Not installed | On | 284 | 5.07 | 3.36 | 0.66 | 3.99 | 2.15 | 0.54 |
| Off | On | 27 | 4.39 | 2.84 | 0.65 | 3.55 | 2.02 | 0.57 |
| Passive | On | 49 | 4.85 | 2.68 | 0.55 | 4.09 | 1.87 | 0.46 |
| On | Off | 14 | 0.66 | 0.56 | 0.85 | 0.50 | 2.19 | 4.37 |
| On | On | 91 | 0.47 | 0.33 | 0.70 | 0.28 | 6.54 | 23.50 |

The data presented in **Table 5-8** include all the indoor sampling locations and show very similar arithmetic mean radon concentrations prior to SSD system installation, with the SSD system completely off and with the SSD system in the passive mode. The SSD system substantially reduces the indoor radon concentration both within the heating season and outside of the heating season. The reduction was approximately 91% (comparing SSD on during the heating season to SSD not installed during the heating season). The ability to achieve and measure a greater radon reduction was probably limited by the ambient concentration of radon (i.e., SSD systems should not be expected to reduce concentrations in indoor air below ambient air levels). The operating mitigation systems achieved concentrations well below the EPA recommended action level of 4 pCi/L. EPA states that “reducing radon levels below 2 pCi/L is difficult” (U.S. EPA, 2012g), so the SSD system performs very well for radon. **Table 5-9** shows nearly identical trends when the data from the real time stationary AlphaGUARD measurements of radon

are tabulated. For example, the mean at the 422 basement north location was reduced by 93% with the SSD system turned on during the heating season. **Table 5-10** shows that very similar trends also hold in the electret data at each location within the duplex.

Table 5-9. Indoor Air Radon Descriptive Statistics by Mitigation and Heating Status: From Stationary Real Time AlphaGUARD (pCi/L)

| Location1 | Mitigation | Heating | Number Samples | Mean | SD | CV | geoMean | geoSD | geoCV |
|-----------|---------------|---------|----------------|------|------|------|---------|-------|--------|
| 422BaseN | Not installed | Off | 29,472 | 7.18 | 3.98 | 0.55 | 5.23 | 3.75 | 0.72 |
| 422BaseN | Not installed | On | 42,125 | 7.13 | 3.22 | 0.45 | 6.12 | 2.11 | 0.35 |
| 422BaseN | Off | Off | 382 | 9.62 | 3.60 | 0.37 | 8.91 | 1.50 | 0.17 |
| 422BaseN | Off | On | 6,479 | 7.83 | 3.16 | 0.40 | 6.56 | 2.90 | 0.44 |
| 422BaseN | Passive | On | 6,483 | 7.93 | 2.34 | 0.30 | 7.49 | 1.54 | 0.21 |
| 422BaseN | On | Off | 2,304 | 0.78 | 2.20 | 2.84 | 0.06 | 44.43 | 751.27 |
| 422BaseN | On | On | 15,543 | 0.47 | 0.91 | 1.95 | 0.05 | 43.31 | 828.75 |
| | | | | | | | | | |
| 422Office | Not installed | Off | 29,645 | 2.65 | 2.12 | 0.80 | 1.60 | 4.60 | 2.87 |
| 422Office | Not installed | On | 41,857 | 3.36 | 2.02 | 0.60 | 2.41 | 3.18 | 1.32 |
| 422Office | Off | Off | 381 | 2.36 | 1.69 | 0.72 | 1.64 | 2.66 | 1.62 |
| 422Office | Off | On | 6,480 | 3.38 | 1.98 | 0.59 | 2.30 | 4.22 | 1.84 |
| 422Office | Passive | On | 6,443 | 4.04 | 1.65 | 0.41 | 3.51 | 2.02 | 0.57 |
| 422Office | On | Off | 2,304 | 0.37 | 0.83 | 2.24 | 0.06 | 24.29 | 414.78 |
| 422Office | On | On | 15,544 | 0.33 | 0.50 | 1.54 | 0.08 | 19.72 | 251.68 |

Table 5-10. Indoor Radon Descriptive Statistics—Individual Locations by Mitigation and Heating Status: Electret Data (pCi/L)

| Location1 | Mitigation | Heating | Number Samples | Mean | SD | CV | geoMean | geoSD | geoCV |
|-----------|---------------|---------|----------------|------|------|------|---------|-------|-------|
| 420BaseN | Not installed | Off | 44 | 4.58 | 2.01 | 0.44 | 3.28 | 5.43 | 1.65 |
| 420BaseN | Not installed | On | 40 | 3.31 | 1.40 | 0.42 | 3.03 | 1.55 | 0.51 |
| 420BaseN | Off | On | 4 | 2.82 | 0.86 | 0.30 | 2.70 | 1.44 | 0.53 |
| 420BaseN | Passive | On | 7 | 4.19 | 1.41 | 0.34 | 3.93 | 1.51 | 0.39 |
| 420BaseN | On | Off | 2 | 0.64 | 0.50 | 0.79 | 0.53 | 2.42 | 4.59 |
| 420BaseN | On | On | 13 | 0.47 | 0.18 | 0.39 | 0.44 | 1.46 | 3.32 |
| | | | | | | | | | |
| 420BaseS | Not installed | Off | 43 | 5.64 | 2.21 | 0.39 | 5.23 | 1.49 | 0.28 |
| 420BaseS | Not installed | On | 40 | 4.24 | 2.02 | 0.48 | 3.85 | 1.55 | 0.40 |
| 420BaseS | Off | On | 4 | 3.37 | 0.78 | 0.23 | 3.30 | 1.27 | 0.38 |
| 420BaseS | Passive | On | 7 | 4.07 | 1.59 | 0.39 | 3.73 | 1.63 | 0.44 |
| 420BaseS | On | Off | 2 | 1.37 | 1.41 | 1.03 | 0.94 | 3.68 | 3.90 |
| 420BaseS | On | On | 13 | 0.56 | 0.15 | 0.27 | 0.54 | 1.44 | 2.68 |

(continued)

Table 5-10. Indoor Radon Descriptive Statistics—Individual Locations by Mitigation and Heating Status: Electret Data (pCi/L) (cont.)

| Location1 | Mitigation | Heating | Number Samples | Mean | SD | CV | geoMean | geoSD | geoCV |
|-----------|---------------|---------|----------------|------|------|------|---------|-------|----------|
| 420First | Not installed | Off | 42 | 2.68 | 1.23 | 0.46 | 1.99 | 5.03 | 2.53 |
| 420First | Not installed | On | 40 | 1.28 | 0.67 | 0.52 | 1.12 | 1.74 | 1.56 |
| 420First | Off | On | 4 | 1.25 | 0.48 | 0.39 | 1.15 | 1.67 | 1.45 |
| 420First | Passive | On | 7 | 1.93 | 0.84 | 0.43 | 1.73 | 1.74 | 1.01 |
| 420First | On | Off | 2 | 0.46 | 0.52 | 1.12 | 0.28 | 4.56 | 16.12 |
| 420First | On | On | 13 | 0.24 | 0.18 | 0.76 | 0.11 | 9.59 | 83.79 |
| 422BaseN | Not installed | Off | 30 | 6.37 | 3.67 | 0.58 | 3.90 | 8.05 | 2.07 |
| 422BaseN | Not installed | On | 53 | 7.31 | 1.90 | 0.26 | 7.01 | 1.36 | 0.19 |
| 422BaseN | Off | On | 3 | 7.70 | 3.10 | 0.40 | 7.18 | 1.62 | 0.23 |
| 422BaseN | Passive | On | 7 | 8.11 | 2.19 | 0.27 | 7.80 | 1.38 | 0.18 |
| 422BaseN | On | Off | 2 | 0.67 | 0.03 | 0.04 | 0.67 | 1.04 | 1.56 |
| 422BaseN | On | On | 13 | 0.60 | 0.20 | 0.33 | 0.57 | 1.41 | 2.47 |
| 422BaseS | Not installed | Off | 30 | 7.04 | 6.41 | 0.91 | 3.85 | 8.55 | 2.22 |
| 422BaseS | Not installed | On | 53 | 9.07 | 3.78 | 0.42 | 8.66 | 1.31 | 0.15 |
| 422BaseS | Off | On | 4 | 8.82 | 1.79 | 0.20 | 8.66 | 1.26 | 0.15 |
| 422BaseS | Passive | On | 7 | 8.27 | 2.27 | 0.27 | 7.90 | 1.43 | 0.18 |
| 422BaseS | On | Off | 2 | 0.74 | 0.17 | 0.22 | 0.73 | 1.25 | 1.72 |
| 422BaseS | On | On | 13 | 0.73 | 0.18 | 0.25 | 0.71 | 1.27 | 1.78 |
| 422First | Not installed | Off | 29 | 2.44 | 2.09 | 0.86 | 0.50 | 38.29 | 76.72 |
| 422First | Not installed | On | 53 | 3.76 | 1.25 | 0.33 | 3.46 | 1.59 | 0.46 |
| 422First | Off | On | 4 | 3.85 | 0.96 | 0.25 | 3.75 | 1.32 | 0.35 |
| 422First | Passive | On | 7 | 3.52 | 0.91 | 0.26 | 3.38 | 1.40 | 0.41 |
| 422First | On | Off | 2 | 0.41 | 0.20 | 0.49 | 0.39 | 1.68 | 4.35 |
| 422First | On | On | 13 | 0.50 | 0.25 | 0.51 | 0.45 | 1.55 | 3.45 |
| 422Office | Not installed | Off | 3 | 2.87 | 0.41 | 0.14 | 2.85 | 1.16 | 0.41 |
| 422Office | Not installed | On | 5 | 4.16 | 0.36 | 0.09 | 4.15 | 1.09 | 0.26 |
| 422Office | Off | On | 4 | 3.78 | 1.34 | 0.35 | 3.54 | 1.57 | 0.44 |
| 422Office | Passive | On | 7 | 3.83 | 1.08 | 0.28 | 3.65 | 1.43 | 0.39 |
| 422Office | On | Off | 2 | 0.32 | 0.16 | 0.51 | 0.30 | 1.71 | 5.75 |
| 422Office | On | On | 13 | 0.15 | 0.55 | 3.62 | 0.03 | 29.03 | 1,108.10 |
| Outside | Not installed | Off | 29 | 0.42 | 0.67 | 1.62 | 0.12 | 22.87 | 185.41 |
| Outside | Not installed | On | 45 | 0.18 | 1.14 | 6.49 | 0.06 | 29.96 | 488.54 |

(continued)

Table 5-10. Indoor Radon Descriptive Statistics—Individual Locations by Mitigation and Heating Status: Electret Data (pCi/L) (cont.)

| Location1 | Mitigation | Heating | Number Samples | Mean | SD | CV | geoMean | geoSD | geoCV |
|-----------|------------|---------|----------------|------|------|------|---------|-------|----------|
| Outside | Off | On | 4 | 0.17 | 0.35 | 2.06 | 0.04 | 55.95 | 1,420.99 |
| Outside | Passive | On | 5 | 0.62 | 0.24 | 0.38 | 0.60 | 1.38 | 2.32 |
| Outside | On | Off | 2 | 0.67 | 0.21 | 0.31 | 0.65 | 1.37 | 2.10 |
| Outside | On | On | 12 | 0.30 | 0.29 | 0.99 | 0.21 | 2.35 | 11.38 |

Table 5-11 shows that in all cases the concentration of radon was reduced by the SSD system operation in the subslab sampling ports, wall ports, and shallowest interior soil gas ports. **Table 5-12** shows that this effect is, on average, about a 60% reduction in the subslab sampling ports and 80% in the wall ports. Comparing this result with the reductions observed in indoor air suggests that the SSD system is operating at this duplex to reduce radon in indoor air through two mechanisms—both diluting the air beneath the slab with lower concentration air (presumably atmospheric) as well as reversing the pressure differential across the slab.

Table 5-11. Descriptive Statistics: Radon in Subslab and Wall Ports by Individual Location and Mitigation and Heating Status (pCi/L)

| Location1 | Mitigation | Heating | Number Samples | Mean | SD | CV | geoMean | geoSD | geoCV |
|-----------|---------------|---------|----------------|-------|-----|------|---------|-------|-------|
| SGP8-6 | Not installed | Off | 27 | 1,277 | 213 | 0.17 | 1,258 | 1.19 | 0.00 |
| SGP8-6 | Not installed | On | 56 | 1,321 | 190 | 0.14 | 1,306 | 1.17 | 0.00 |
| SGP8-6 | Off | On | 1 | 911 | NA | NA | 911 | NA | NA |
| SGP8-6 | On | On | 7 | 386 | 100 | 0.26 | 375 | 1.28 | 0.00 |
| SGP8-6 | Passive | On | 3 | 1,223 | 86 | 0.07 | 1,221 | 1.07 | 0.00 |
| SGP9-6 | Not installed | Off | 31 | 1,696 | 129 | 0.08 | 1,691 | 1.08 | 0.00 |
| SGP9-6 | Not installed | On | 61 | 1,598 | 212 | 0.13 | 1,581 | 1.17 | 0.00 |
| SGP9-6 | Off | On | 1 | 1,349 | NA | NA | 1,349 | NA | NA |
| SGP9-6 | On | On | 7 | 248 | 80 | 0.32 | 240 | 1.31 | 0.01 |
| SGP9-6 | Passive | On | 2 | 1,566 | 323 | 0.21 | 1,549 | 1.23 | 0.00 |
| SSP-1 | Not installed | Off | 26 | 776 | 323 | 0.42 | 642 | 2.27 | 0.00 |
| SSP-1 | Not installed | On | 62 | 929 | 199 | 0.21 | 909 | 1.24 | 0.00 |
| SSP-1 | Off | On | 1 | 749 | NA | NA | 749 | NA | NA |
| SSP-1 | On | On | 7 | 531 | 97 | 0.18 | 524 | 1.18 | 0.00 |
| SSP-1 | Passive | On | 3 | 545 | 195 | 0.36 | 524 | 1.40 | 0.00 |
| SSP-2 | Not installed | Off | 11 | 1,179 | 158 | 0.13 | 1,169 | 1.14 | 0.00 |
| SSP-2 | Not installed | On | 10 | 984 | 518 | 0.53 | 555 | 5.33 | 0.01 |
| SSP-2 | Off | On | 1 | 1,268 | NA | NA | 1,268 | NA | NA |
| SSP-2 | On | Off | 1 | 181 | NA | NA | 181 | NA | NA |
| SSP-2 | On | On | 6 | 227 | 66 | 0.29 | 219 | 1.32 | 0.01 |
| SSP-2 | Passive | On | 2 | 1,338 | 42 | 0.03 | 1,338 | 1.03 | 0.00 |
| SSP-3 | Not installed | Off | 7 | 551 | 364 | 0.66 | 378 | 3.24 | 0.01 |

(continued)

Table 5-11. Descriptive Statistics: Radon in Subslab and Wall Ports by Individual Location and Mitigation and Heating Status (pCi/L) (cont.)

| Location1 | Mitigation | Heating | Number Samples | Mean | SD | CV | geoMean | geoSD | geoCV |
|-----------|---------------|---------|----------------|-------|-----|------|---------|-------|-------|
| SSP-3 | Off | Off | 1 | 1,086 | NA | NA | 1,086 | NA | NA |
| SSP-3 | On | Off | 8 | 248 | 35 | 0.14 | 246 | 1.16 | 0.00 |
| SSP-3 | Passive | Off | 2 | 331 | 86 | 0.26 | 325 | 1.30 | 0.00 |
| SSP-4 | Not installed | Off | 32 | 1,996 | 158 | 0.08 | 1,990 | 1.08 | 0.00 |
| SSP-4 | Not installed | On | 60 | 1,850 | 423 | 0.23 | 1,688 | 1.93 | 0.00 |
| SSP-4 | Off | On | 1 | 1,854 | NA | NA | 1,854 | NA | NA |
| SSP-4 | On | On | 7 | 733 | 22 | 0.03 | 733 | 1.03 | 0.00 |
| SSP-4 | Passive | On | 2 | 1,896 | 170 | 0.09 | 1,892 | 1.09 | 0.00 |
| SSP-5 | Not installed | Off | 75 | 1,245 | 127 | 0.10 | 1,238 | 1.12 | 0.00 |
| SSP-5 | Off | Off | 1 | 1,178 | NA | NA | 1,178 | NA | NA |
| SSP-5 | On | Off | 8 | 195 | 56 | 0.29 | 189 | 1.29 | 0.01 |
| SSP-5 | Passive | Off | 1 | 1,341 | NA | NA | 1,341 | NA | NA |
| SSP-6 | Not installed | Off | 74 | 1,585 | 269 | 0.17 | 1,552 | 1.26 | 0.00 |
| SSP-6 | Off | Off | 1 | 1,827 | NA | NA | 1,827 | NA | NA |
| SSP-6 | On | Off | 8 | 321 | 124 | 0.39 | 291 | 1.68 | 0.01 |
| SSP-6 | Passive | Off | 2 | 1,634 | 128 | 0.08 | 1,631 | 1.08 | 0.00 |
| SSP-7 | Not installed | Off | 91 | 495 | 388 | 0.78 | 300 | 3.41 | 0.01 |
| SSP-7 | Off | Off | 1 | 1,214 | NA | NA | 1,214 | NA | NA |
| SSP-7 | On | Off | 8 | 263 | 62 | 0.24 | 255 | 1.32 | 0.01 |
| SSP-7 | Passive | Off | 2 | 219 | 175 | 0.80 | 181 | 2.47 | 0.01 |
| WP-1 | Not installed | Off | 21 | 213 | 84 | 0.39 | 194 | 1.61 | 0.01 |
| WP-1 | Not installed | On | 45 | 245 | 155 | 0.64 | 194 | 2.21 | 0.01 |
| WP-1 | Off | On | 2 | 173 | 29 | 0.17 | 172 | 1.19 | 0.01 |
| WP-1 | On | Off | 1 | 50 | NA | NA | 50 | NA | NA |
| WP-1 | On | On | 8 | 46 | 9 | 0.19 | 45 | 1.20 | 0.03 |
| WP-1 | Passive | On | 2 | 165 | 11 | 0.06 | 165 | 1.07 | 0.01 |
| WP-2 | Not installed | Off | 24 | 76 | 34 | 0.44 | 68 | 1.69 | 0.03 |
| WP-2 | Not installed | On | 44 | 37 | 28 | 0.74 | 31 | 1.84 | 0.06 |
| WP-2 | Off | On | 2 | 22 | 7 | 0.30 | 22 | 1.36 | 0.06 |
| WP-2 | On | Off | 1 | 28 | NA | NA | 28 | NA | NA |
| WP-2 | On | On | 8 | 23 | 3 | 0.12 | 23 | 1.12 | 0.05 |
| WP-2 | Passive | On | 2 | 29 | 8 | 0.28 | 28 | 1.33 | 0.05 |
| WP-3 | Not installed | Off | 24 | 82 | 39 | 0.47 | 73 | 1.66 | 0.02 |
| WP-3 | Not installed | On | 50 | 78 | 45 | 0.57 | 67 | 1.78 | 0.03 |
| WP-3 | Off | On | 2 | 181 | 137 | 0.76 | 153 | 2.33 | 0.02 |
| WP-3 | On | Off | 1 | 289 | NA | NA | 289 | NA | NA |

(continued)

Table 5-11. Descriptive Statistics: Radon in Subslab and Wall Ports by Individual Location and Mitigation and Heating Status (pCi/L) (cont.)

| Location1 | Mitigation | Heating | Number Samples | Mean | SD | CV | geoMean | geoSD | geoCV |
|-----------|---------------|---------|----------------|------|----|------|---------|-------|-------|
| WP-3 | On | On | 7 | 122 | 31 | 0.25 | 119 | 1.25 | 0.01 |
| WP-3 | Passive | On | 2 | 124 | 37 | 0.29 | 121 | 1.35 | 0.01 |
| WP-4 | Not installed | Off | 86 | 50 | 34 | 0.67 | 40 | 2.00 | 0.05 |
| WP-4 | Off | Off | 2 | 17 | 2 | 0.13 | 17 | 1.14 | 0.07 |
| WP-4 | On | Off | 9 | 9 | 6 | 0.67 | 7 | 1.97 | 0.28 |
| WP-4 | Passive | Off | 2 | 25 | 2 | 0.07 | 25 | 1.07 | 0.04 |

Table 5-12. Radon Descriptive Statistics by Location Type and Mitigation and Heating Status (pCi/L)

| Location Type | Mitigation | Heating | Number Samples | Mean | SD | CV | geoMean | geoSD | geoCV |
|---------------|---------------|---------|----------------|-------|-----|------|---------|-------|-------|
| Subslab | Not installed | Off | 316 | 1,129 | 583 | 0.52 | 839 | 2.79 | 0.00 |
| Subslab | Not installed | On | 132 | 1,352 | 571 | 0.42 | 1,160 | 2.09 | 0.00 |
| Subslab | Off | Off | 4 | 1,326 | 338 | 0.25 | 1,298 | 1.26 | 0.00 |
| Subslab | Off | On | 3 | 1,290 | 553 | 0.43 | 1,207 | 1.58 | 0.00 |
| Subslab | Passive | Off | 7 | 816 | 689 | 0.84 | 534 | 2.96 | 0.01 |
| Subslab | Passive | On | 7 | 1,158 | 631 | 0.54 | 989 | 1.90 | 0.00 |
| Subslab | On | Off | 33 | 254 | 86 | 0.34 | 240 | 1.42 | 0.01 |
| Subslab | On | On | 20 | 510 | 219 | 0.43 | 454 | 1.71 | 0.00 |
| Wall | Not installed | Off | 155 | 81 | 69 | 0.86 | 59 | 2.26 | 0.04 |
| Wall | Not installed | On | 139 | 119 | 129 | 1.08 | 74 | 2.71 | 0.04 |
| Wall | Off | Off | 2 | 17 | 2 | 0.13 | 17 | 1.14 | 0.07 |
| Wall | Off | On | 6 | 126 | 102 | 0.81 | 83 | 3.04 | 0.04 |
| Wall | Passive | Off | 2 | 25 | 2 | 0.07 | 25 | 1.07 | 0.04 |
| Wall | Passive | On | 6 | 106 | 65 | 0.61 | 83 | 2.36 | 0.03 |
| Wall | On | Off | 12 | 37 | 81 | 2.18 | 13 | 3.73 | 0.29 |
| Wall | On | On | 23 | 61 | 45 | 0.74 | 48 | 2.01 | 0.04 |

5.3 VOC Monitoring During Mitigation Testing

SSD mitigation reduced the indoor air concentration of the primary VOCs at the site PCE and chloroform but not as dramatically or consistently as the reduction seen for radon. As shown in **Figures 5-10** and **5-11** in the week immediately after installation, the SSD system appeared to have reduced the VOC concentrations to ambient levels. The concentrations then rose over the next 2 weeks of operation. During the two subsequent operational periods—December 12, 2012, to December 29, 2012 and February 6, 2013, to April 24, 2013—concentrations were reduced compared with the unmitigated periods but did not reach ambient concentrations again until late in April 2013 when temperatures had moderated.

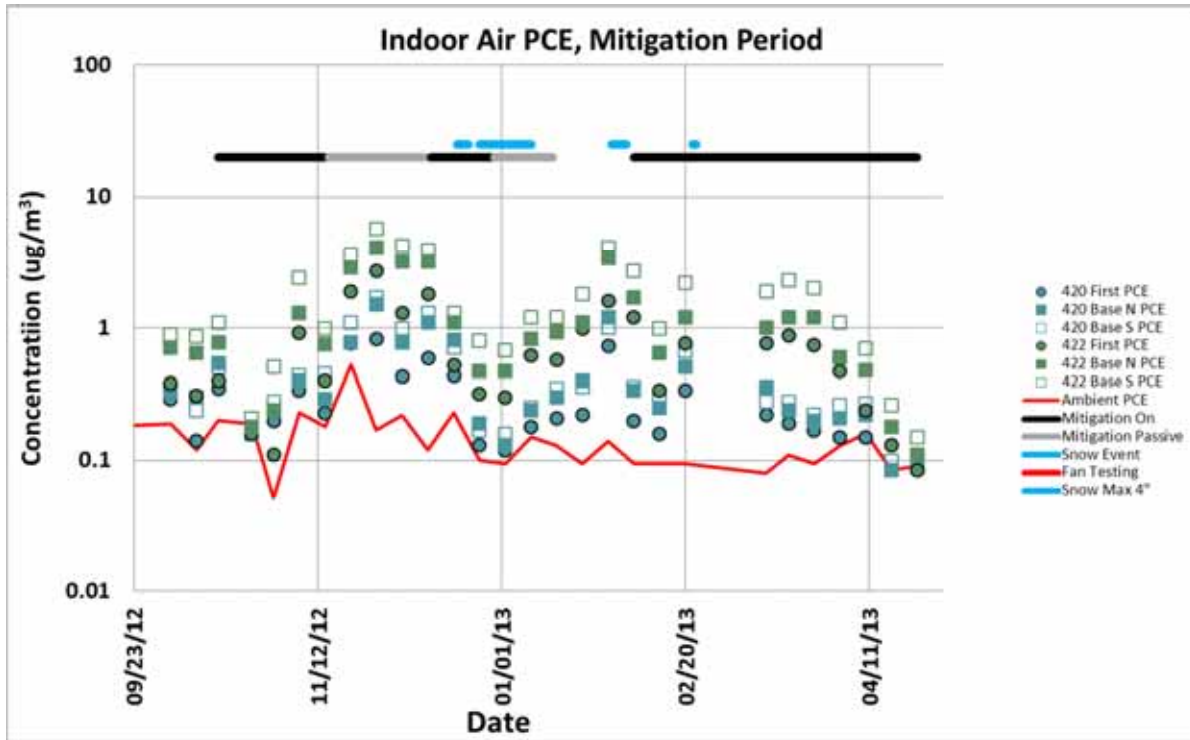


Figure 5-10. Passive sampler monitoring of PCE during mitigation testing.

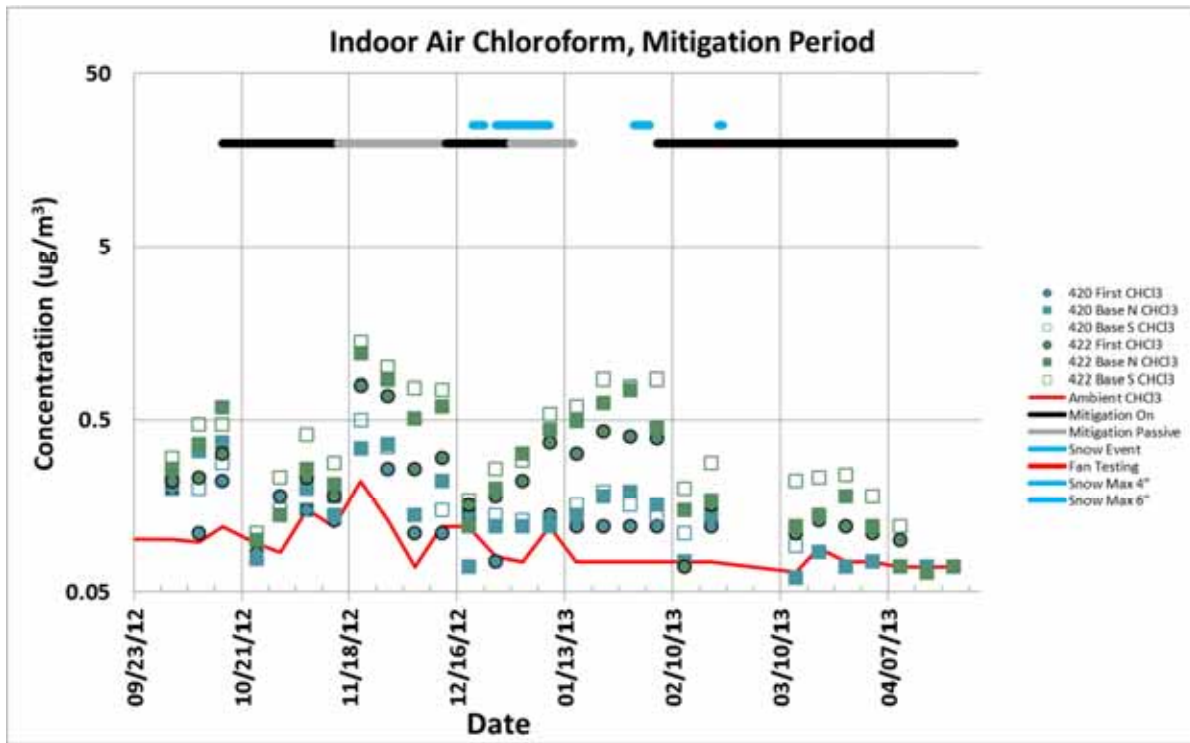


Figure 5-11. Passive sampler monitoring of chloroform during mitigation period.

Real-time GC data were also available for a portion of the mitigation testing (see **Figure 5-12** for PCE). This shows two distinct upward spikes during the February 6 through April period when the SSD system was on. These are prominent in the 422 basement south GC plot. One occurred on February 16 and 17 (with a secondary peak on February 19) and the other on March 12–15 with a secondary peak on March 17. Brief snow events were noted on February 15, February 19, and March 12. Both peaks were also associated with west northwest to west winds which as we will show in Section 9 are associated with high differential pressures and radon concentrations (see **Figure 9-14**). February 16 and 17 had rather low temperatures (average 23° F both days) as compared to the surrounding days. However during both GC peaks the 422 subslab versus basement differential pressure remained at -15 Pa and the 420 subslab versus basement differential pressure showed very little deflection remaining at -13 to -15 Pa.

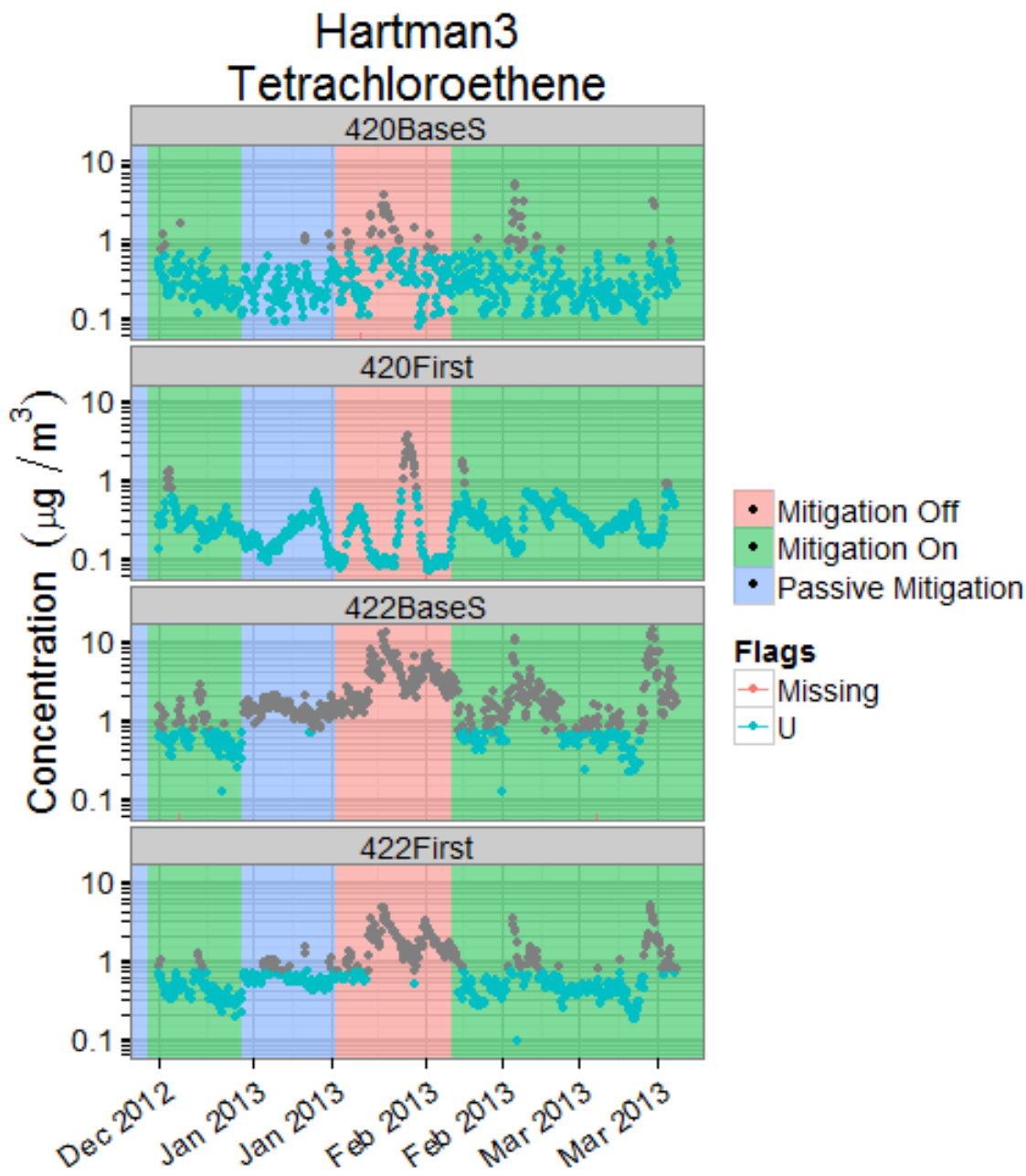


Figure 5-12. Indoor air PCE, real-time monitoring during mitigation testing.

5.3.1 Descriptive Statistics

Descriptive statistics (**Table 5-13**) show a 68% reduction in the mean chloroform concentration in indoor air with the SSD system turned on during the heating season. The corresponding reduction in mean PCE with active mitigation in the heating season was 61%. These reductions are both less than those achieved for radon in this house (about 91%) and substantially less than the 99% reduction generally considered to be possible for SSD systems operating in high initial concentration vapor intrusion situations (U.S. EPA, 2008).

Table 5-13. Descriptive Statistics of Weekly Passive VOC Measurements ($\mu\text{g}/\text{m}^3$) in Indoor Air by Mitigation Status and Heating Use (yellow indicates statistics during active mitigation)

| Variable | Mitigation | Heating | Number Samples | Mean | SD | CV | geoMean | geoSD | geoCV |
|-------------------|---------------|---------|----------------|------|------|------|---------|-------|-------|
| Chloroform | Not installed | Off | 135 | 0.21 | 0.13 | 0.61 | 0.18 | 1.78 | 10.00 |
| Chloroform | Not installed | On | 235 | 0.41 | 0.50 | 1.23 | 0.26 | 2.45 | 9.34 |
| Chloroform | Off | On | 20 | 0.36 | 0.27 | 0.74 | 0.28 | 2.09 | 7.54 |
| Chloroform | Passive | On | 43 | 0.40 | 0.31 | 0.76 | 0.31 | 2.09 | 6.75 |
| Chloroform | On | Off | 14 | 0.13 | 0.05 | 0.35 | 0.13 | 1.40 | 10.96 |
| Chloroform | On | On | 90 | 0.13 | 0.07 | 0.52 | 0.11 | 1.59 | 14.19 |
| | | | | | | | | | |
| Tetrachloroethene | Not installed | Off | 135 | 0.39 | 0.22 | 0.56 | 0.34 | 1.72 | 5.04 |
| Tetrachloroethene | Not installed | On | 235 | 1.36 | 2.77 | 2.05 | 0.53 | 3.34 | 6.33 |
| Tetrachloroethene | Off | On | 20 | 1.24 | 1.08 | 0.87 | 0.87 | 2.45 | 2.83 |
| Tetrachloroethene | Passive | On | 43 | 1.40 | 1.35 | 0.97 | 0.88 | 2.78 | 3.17 |
| Tetrachloroethene | On | Off | 14 | 0.22 | 0.10 | 0.43 | 0.21 | 1.43 | 6.90 |
| Tetrachloroethene | On | On | 90 | 0.53 | 0.52 | 0.98 | 0.36 | 2.41 | 6.76 |

The distribution of the VOC data (**Table 5-14**) shows that the primary effect of the SSD system was to cut off the highest end of the distribution (90th and 95th percentiles). The trend of the active mitigation improving indoor air, but to a lesser extent than would have been predicted from radon, holds at all of the individual monitoring locations (**Table 5-15**). An explanation for this surprising finding is that the VOC concentrations in the area immediately outside the building envelope (subslab and wall ports) were increased by the SSD system, especially for PCE (**Table 5-16**). Because the concentration of radon decreased substantially in these areas, this suggests that air is being drawn into the area around the building envelope at least in part from a zone of high VOC concentration and lower radon concentration. This effect is seen most dramatically in the higher concentration portion of the distribution for PCE. For example, during the heating season, the 75th percentile of the subslab data with the mitigation on exceeds the 95th percentile with the mitigation off (**Table 5-17**). This trend holds for most, although not all, subslab and wall ports (**Table 5-18**). In some cases, the increases are dramatic; for example, PCE increased 875% at SSP-3, 575% at SSP-4, and 2,000% at SSP-7. Given the observed pressure differentials, this most likely indicates that the mitigation system is drawing VOCs in from near the water table. Such an effect has been previously hypothesized (Lutes, 2010b) but not to our knowledge published in detail.

Table 5-14. Distribution of Concentrations ($\mu\text{g}/\text{m}^3$) by VOC and Mitigation and Heating Status: Indoor Air, Week-Long Passive Samples (yellow indicates statistics during active mitigation)

| Variable | Mitigation | Heating | Number Samples | 5th Percentile | 10th Percentile | 25th Percentile | 50th Percentile | 75th Percentile | 90th Percentile | 95th Percentile |
|-------------------|---------------|---------|----------------|----------------|-----------------|-----------------|-----------------|-----------------|-----------------|-----------------|
| Chloroform | Not installed | Off | 135 | 0.07 | 0.09 | 0.11 | 0.18 | 0.26 | 0.37 | 0.47 |
| Chloroform | Not installed | On | 235 | 0.07 | 0.09 | 0.13 | 0.23 | 0.50 | 0.93 | 1.20 |
| Chloroform | Off | On | 20 | 0.12 | 0.12 | 0.16 | 0.19 | 0.50 | 0.78 | 0.85 |
| Chloroform | Passive | On | 43 | 0.12 | 0.12 | 0.14 | 0.32 | 0.53 | 0.78 | 0.99 |
| Chloroform | On | Off | 14 | 0.08 | 0.09 | 0.10 | 0.13 | 0.15 | 0.21 | 0.22 |
| Chloroform | On | On | 90 | 0.07 | 0.07 | 0.07 | 0.12 | 0.16 | 0.21 | 0.25 |
| | | | | | | | | | | |
| Tetrachloroethene | Not installed | Off | 135 | 0.14 | 0.17 | 0.24 | 0.33 | 0.52 | 0.69 | 0.87 |
| Tetrachloroethene | Not installed | On | 235 | 0.11 | 0.15 | 0.22 | 0.40 | 0.92 | 3.64 | 6.63 |
| Tetrachloroethene | Off | On | 20 | 0.22 | 0.33 | 0.36 | 1.00 | 1.63 | 2.77 | 3.44 |
| Tetrachloroethene | Passive | On | 43 | 0.16 | 0.22 | 0.45 | 0.93 | 1.75 | 3.52 | 4.08 |
| Tetrachloroethene | On | Off | 14 | 0.14 | 0.16 | 0.17 | 0.19 | 0.24 | 0.28 | 0.36 |
| Tetrachloroethene | On | On | 90 | 0.09 | 0.10 | 0.20 | 0.31 | 0.71 | 1.20 | 1.63 |

Table 5-15. Descriptive Statistics of Indoor VOC Concentrations ($\mu\text{g}/\text{m}^3$) During Mitigation Testing by Location and Mitigation and Heating Status (yellow indicates statistics during active mitigation)

| Location1 | Variable | Mitigation | Heating | Number Samples | Mean | SD | CV | geoMean | geoSD | geoCV |
|-----------|-------------------|---------------|---------|----------------|------|------|------|---------|-------|-------|
| 420BaseN | Chloroform | Not installed | Off | 22 | 0.20 | 0.10 | 0.52 | 0.17 | 1.78 | 10.45 |
| 420BaseN | Chloroform | Not installed | On | 37 | 0.18 | 0.12 | 0.68 | 0.15 | 1.76 | 11.41 |
| 420BaseN | Chloroform | Off | On | 3 | 0.18 | 0.02 | 0.09 | 0.18 | 1.09 | 6.20 |
| 420BaseN | Chloroform | On | Off | 2 | 0.11 | 0.04 | 0.40 | 0.10 | 1.51 | 14.47 |
| 420BaseN | Chloroform | On | On | 13 | 0.10 | 0.04 | 0.44 | 0.09 | 1.45 | 16.26 |
| 420BaseN | Chloroform | Passive | On | 7 | 0.21 | 0.10 | 0.51 | 0.19 | 1.61 | 8.69 |
| 420BaseN | Tetrachloroethene | Not installed | Off | 22 | 0.31 | 0.12 | 0.39 | 0.29 | 1.46 | 5.05 |
| 420BaseN | Tetrachloroethene | Not installed | On | 37 | 0.82 | 1.94 | 2.36 | 0.32 | 2.94 | 9.09 |
| 420BaseN | Tetrachloroethene | Off | On | 3 | 0.65 | 0.48 | 0.74 | 0.55 | 1.99 | 3.63 |
| 420BaseN | Tetrachloroethene | On | Off | 2 | 0.20 | 0.06 | 0.28 | 0.20 | 1.33 | 6.80 |
| 420BaseN | Tetrachloroethene | On | On | 13 | 0.30 | 0.19 | 0.65 | 0.25 | 1.86 | 7.49 |
| 420BaseN | Tetrachloroethene | Passive | On | 7 | 0.69 | 0.50 | 0.73 | 0.51 | 2.45 | 4.79 |
| 420BaseS | Chloroform | Not installed | Off | 25 | 0.18 | 0.08 | 0.47 | 0.16 | 1.66 | 10.53 |
| 420BaseS | Chloroform | Not installed | On | 44 | 0.18 | 0.17 | 0.95 | 0.15 | 1.87 | 12.83 |
| 420BaseS | Chloroform | Off | On | 5 | 0.16 | 0.02 | 0.13 | 0.16 | 1.13 | 7.22 |
| 420BaseS | Chloroform | On | Off | 4 | 0.15 | 0.05 | 0.38 | 0.14 | 1.43 | 10.34 |
| 420BaseS | Chloroform | On | On | 25 | 0.10 | 0.04 | 0.36 | 0.10 | 1.41 | 14.40 |
| 420BaseS | Chloroform | Passive | On | 8 | 0.25 | 0.16 | 0.62 | 0.21 | 1.80 | 8.38 |
| 420BaseS | Tetrachloroethene | Not installed | Off | 25 | 0.35 | 0.12 | 0.35 | 0.33 | 1.43 | 4.38 |
| 420BaseS | Tetrachloroethene | Not installed | On | 44 | 0.92 | 2.29 | 2.50 | 0.36 | 2.85 | 7.84 |
| 420BaseS | Tetrachloroethene | Off | On | 5 | 0.61 | 0.35 | 0.58 | 0.54 | 1.77 | 3.30 |
| 420BaseS | Tetrachloroethene | On | Off | 4 | 0.23 | 0.06 | 0.27 | 0.22 | 1.31 | 5.93 |
| 420BaseS | Tetrachloroethene | On | On | 25 | 0.30 | 0.17 | 0.57 | 0.26 | 1.81 | 6.98 |
| 420BaseS | Tetrachloroethene | Passive | On | 8 | 0.85 | 0.55 | 0.64 | 0.65 | 2.38 | 3.66 |

(continued)

Table 5-15. Descriptive Statistics of Indoor VOC Concentrations ($\mu\text{g}/\text{m}^3$) During Mitigation Testing by Location and Mitigation and Heating Status (yellow indicates statistics during active mitigation) (cont.)

| Location1 | Variable | Mitigation | Heating | Number Samples | Mean | SD | CV | geoMean | geoSD | geoCV |
|-----------|-------------------|---------------|---------|----------------|------|------|------|---------|-------|-------|
| 420First | Chloroform | Not installed | Off | 22 | 0.16 | 0.06 | 0.40 | 0.14 | 1.56 | 10.86 |
| 420First | Chloroform | Not installed | On | 37 | 0.22 | 0.26 | 1.18 | 0.15 | 2.09 | 13.50 |
| 420First | Chloroform | Off | On | 3 | 0.12 | 0.00 | 0.00 | 0.12 | 1.00 | 8.33 |
| 420First | Chloroform | On | Off | 2 | 0.13 | 0.07 | 0.51 | 0.12 | 1.71 | 13.94 |
| 420First | Chloroform | On | On | 13 | 0.09 | 0.03 | 0.35 | 0.09 | 1.38 | 15.86 |
| 420First | Chloroform | Passive | On | 7 | 0.17 | 0.09 | 0.53 | 0.16 | 1.58 | 10.20 |
| 420First | Tetrachloroethene | Not installed | Off | 22 | 0.24 | 0.10 | 0.42 | 0.22 | 1.53 | 6.95 |
| 420First | Tetrachloroethene | Not installed | On | 37 | 1.34 | 3.89 | 2.90 | 0.27 | 4.06 | 14.82 |
| 420First | Tetrachloroethene | Off | On | 3 | 0.38 | 0.30 | 0.78 | 0.32 | 2.06 | 6.47 |
| 420First | Tetrachloroethene | On | Off | 2 | 0.19 | 0.01 | 0.07 | 0.19 | 1.08 | 5.68 |
| 420First | Tetrachloroethene | On | On | 13 | 0.21 | 0.11 | 0.51 | 0.19 | 1.64 | 8.86 |
| 420First | Tetrachloroethene | Passive | On | 7 | 0.44 | 0.29 | 0.64 | 0.36 | 2.14 | 6.03 |
| 422BaseN | Chloroform | Not installed | Off | 22 | 0.24 | 0.14 | 0.60 | 0.20 | 1.91 | 9.73 |
| 422BaseN | Chloroform | Not installed | On | 37 | 0.48 | 0.30 | 0.62 | 0.40 | 1.89 | 4.71 |
| 422BaseN | Chloroform | Off | On | 3 | 0.61 | 0.15 | 0.24 | 0.59 | 1.29 | 2.17 |
| 422BaseN | Chloroform | On | Off | 2 | 0.12 | 0.03 | 0.24 | 0.12 | 1.27 | 10.72 |
| 422BaseN | Chloroform | On | On | 13 | 0.14 | 0.06 | 0.41 | 0.13 | 1.56 | 11.76 |
| 422BaseN | Chloroform | Passive | On | 7 | 0.63 | 0.30 | 0.48 | 0.58 | 1.55 | 2.68 |
| 422BaseN | Tetrachloroethene | Not installed | Off | 22 | 0.49 | 0.21 | 0.42 | 0.45 | 1.59 | 3.57 |
| 422BaseN | Tetrachloroethene | Not installed | On | 37 | 1.52 | 2.34 | 1.54 | 0.84 | 2.57 | 3.06 |
| 422BaseN | Tetrachloroethene | Off | On | 3 | 2.07 | 1.19 | 0.58 | 1.85 | 1.77 | 0.95 |
| 422BaseN | Tetrachloroethene | On | Off | 2 | 0.21 | 0.04 | 0.20 | 0.21 | 1.23 | 5.90 |
| 422BaseN | Tetrachloroethene | On | On | 13 | 0.79 | 0.41 | 0.52 | 0.64 | 2.16 | 3.35 |
| 422BaseN | Tetrachloroethene | Passive | On | 7 | 2.23 | 1.45 | 0.65 | 1.72 | 2.36 | 1.37 |

(continued)

Table 5-15. Descriptive Statistics of Indoor VOC Concentrations ($\mu\text{g}/\text{m}^3$) During Mitigation Testing by Location and Mitigation and Heating Status (yellow indicates statistics during active mitigation) (cont.)

| Location1 | Variable | Mitigation | Heating | Number Samples | Mean | SD | CV | geoMean | geoSD | geoCV |
|-----------|-------------------|---------------|---------|----------------|------|------|------|---------|-------|-------|
| 422BaseS | Chloroform | Not installed | Off | 22 | 0.28 | 0.17 | 0.61 | 0.23 | 1.89 | 8.10 |
| 422BaseS | Chloroform | Not installed | On | 40 | 0.71 | 0.41 | 0.58 | 0.59 | 1.87 | 3.14 |
| 422BaseS | Chloroform | Off | On | 3 | 0.82 | 0.05 | 0.06 | 0.82 | 1.06 | 1.29 |
| 422BaseS | Chloroform | On | Off | 2 | 0.17 | 0.08 | 0.50 | 0.16 | 1.68 | 10.59 |
| 422BaseS | Chloroform | On | On | 13 | 0.21 | 0.09 | 0.45 | 0.19 | 1.71 | 9.17 |
| 422BaseS | Chloroform | Passive | On | 7 | 0.76 | 0.36 | 0.47 | 0.69 | 1.64 | 2.39 |
| 422BaseS | Tetrachloroethene | Not installed | Off | 22 | 0.65 | 0.25 | 0.38 | 0.59 | 1.58 | 2.65 |
| 422BaseS | Tetrachloroethene | Not installed | On | 40 | 2.38 | 3.61 | 1.51 | 1.30 | 2.63 | 2.03 |
| 422BaseS | Tetrachloroethene | Off | On | 3 | 2.87 | 1.16 | 0.40 | 2.71 | 1.51 | 0.56 |
| 422BaseS | Tetrachloroethene | On | Off | 2 | 0.36 | 0.21 | 0.59 | 0.33 | 1.87 | 5.72 |
| 422BaseS | Tetrachloroethene | On | On | 13 | 1.26 | 0.83 | 0.66 | 0.87 | 2.96 | 3.41 |
| 422BaseS | Tetrachloroethene | Passive | On | 7 | 2.93 | 1.90 | 0.65 | 2.29 | 2.26 | 0.99 |
| 422First | Chloroform | Not installed | Off | 22 | 0.22 | 0.14 | 0.66 | 0.18 | 1.76 | 9.61 |
| 422First | Chloroform | Not installed | On | 40 | 0.67 | 0.92 | 1.37 | 0.39 | 2.53 | 6.43 |
| 422First | Chloroform | Off | On | 3 | 0.41 | 0.02 | 0.05 | 0.41 | 1.05 | 2.59 |
| 422First | Chloroform | On | Off | 2 | 0.12 | 0.03 | 0.24 | 0.12 | 1.27 | 10.72 |
| 422First | Chloroform | On | On | 13 | 0.13 | 0.05 | 0.39 | 0.12 | 1.49 | 12.38 |
| 422First | Chloroform | Passive | On | 7 | 0.42 | 0.22 | 0.53 | 0.38 | 1.63 | 4.30 |
| 422First | Tetrachloroethene | Not installed | Off | 22 | 0.33 | 0.22 | 0.67 | 0.28 | 1.73 | 6.11 |
| 422First | Tetrachloroethene | Not installed | On | 40 | 1.17 | 1.80 | 1.55 | 0.61 | 2.77 | 4.55 |
| 422First | Tetrachloroethene | Off | On | 3 | 1.26 | 0.31 | 0.25 | 1.23 | 1.28 | 1.04 |
| 422First | Tetrachloroethene | On | Off | 2 | 0.14 | 0.04 | 0.26 | 0.13 | 1.30 | 9.82 |
| 422First | Tetrachloroethene | On | On | 13 | 0.50 | 0.28 | 0.56 | 0.41 | 2.10 | 5.10 |
| 422First | Tetrachloroethene | Passive | On | 7 | 1.31 | 0.87 | 0.66 | 1.04 | 2.22 | 2.14 |

(continued)

Table 5-15. Descriptive Statistics of Indoor VOC Concentrations ($\mu\text{g}/\text{m}^3$) During Mitigation Testing by Location and Mitigation and Heating Status (yellow indicates statistics during active mitigation) (cont.)

| Location1 | Variable | Mitigation | Heating | Number Samples | Mean | SD | CV | geoMean | geoSD | geoCV |
|-----------|-------------------|---------------|---------|----------------|------|------|------|---------|-------|-------|
| Outside | Chloroform | Not Installed | Off | 22 | 0.09 | 0.03 | 0.29 | 0.09 | 1.36 | 15.98 |
| Outside | Chloroform | Not Installed | On | 41 | 0.08 | 0.02 | 0.28 | 0.08 | 1.30 | 16.99 |
| Outside | Chloroform | Off | On | 3 | 0.08 | 0.00 | 0.00 | 0.08 | 1.00 | 13.33 |
| Outside | Chloroform | On | Off | 2 | 0.09 | 0.01 | 0.08 | 0.09 | 1.08 | 12.04 |
| Outside | Chloroform | On | On | 13 | 0.09 | 0.03 | 0.30 | 0.08 | 1.30 | 15.38 |
| Outside | Chloroform | Passive | On | 7 | 0.12 | 0.05 | 0.45 | 0.11 | 1.51 | 14.08 |
| Outside | Tetrachloroethene | Not installed | Off | 22 | 0.16 | 0.08 | 0.50 | 0.15 | 1.46 | 9.95 |
| Outside | Tetrachloroethene | Not installed | On | 41 | 0.12 | 0.05 | 0.39 | 0.12 | 1.47 | 12.62 |
| Outside | Tetrachloroethene | Off | On | 3 | 0.11 | 0.03 | 0.24 | 0.11 | 1.25 | 11.57 |
| Outside | Tetrachloroethene | On | Off | 2 | 0.12 | 0.10 | 0.81 | 0.10 | 2.50 | 25.15 |
| Outside | Tetrachloroethene | On | On | 13 | 0.13 | 0.05 | 0.41 | 0.12 | 1.45 | 12.04 |
| Outside | Tetrachloroethene | Passive | On | 7 | 0.20 | 0.15 | 0.74 | 0.17 | 1.76 | 10.23 |

Table 5-16. Descriptive Statistics: Average Subslab and Wall Port VOC Concentrations ($\mu\text{g}/\text{m}^3$) by Mitigation and Heating Status (yellow indicates statistics during active mitigation)

| Location Type | Variable | Mitigation | Heating | Number Samples | Mean | SD | CV | geoMean | geoSD | geoCV |
|---------------|-------------------|---------------|---------|----------------|--------|--------|------|---------|-------|-------|
| Subslab | Chloroform | Not installed | Off | 244 | 22.73 | 51.84 | 2.28 | 6.93 | 3.56 | 0.51 |
| Subslab | Chloroform | Not installed | On | 115 | 147.86 | 80.55 | 0.54 | 110.47 | 2.80 | 0.03 |
| Subslab | Chloroform | Off | Off | 10 | 20.50 | 19.62 | 0.96 | 15.39 | 2.04 | 0.13 |
| Subslab | Chloroform | Passive | On | 3 | 207.37 | 245.97 | 1.19 | 52.06 | 17.25 | 0.33 |
| Subslab | Chloroform | Passive | Off | 4 | 2.10 | 0.00 | 0.00 | 2.10 | 1.00 | 0.48 |
| Subslab | Chloroform | On | Off | 32 | 51.10 | 54.24 | 1.06 | 19.27 | 5.61 | 0.29 |
| Subslab | Chloroform | On | On | 24 | 85.32 | 122.98 | 1.44 | 21.81 | 7.48 | 0.34 |
| | | | | | | | | | | |
| Subslab | Tetrachloroethene | Not installed | Off | 244 | 54.82 | 57.97 | 1.06 | 33.40 | 2.80 | 0.08 |
| Subslab | Tetrachloroethene | Not installed | On | 115 | 230.47 | 197.25 | 0.86 | 182.27 | 2.17 | 0.01 |
| Subslab | Tetrachloroethene | Off | Off | 10 | 64.17 | 59.40 | 0.93 | 38.61 | 3.06 | 0.08 |
| Subslab | Tetrachloroethene | Passive | Off | 4 | 21.91 | 8.89 | 0.41 | 20.26 | 1.63 | 0.08 |
| Subslab | Tetrachloroethene | Passive | On | 3 | 492.63 | 420.54 | 0.85 | 162.14 | 13.69 | 0.08 |
| Subslab | Tetrachloroethene | On | Off | 32 | 154.54 | 278.40 | 1.80 | 42.33 | 5.08 | 0.12 |
| Subslab | Tetrachloroethene | On | On | 24 | 359.46 | 489.24 | 1.36 | 61.93 | 12.45 | 0.20 |
| | | | | | | | | | | |
| Wall | Chloroform | Not installed | Off | 107 | 12.33 | 68.16 | 5.53 | 4.04 | 2.26 | 0.56 |
| Wall | Chloroform | Not installed | On | 116 | 5.35 | 10.13 | 1.90 | 3.69 | 1.86 | 0.50 |
| Wall | Chloroform | Off | Off | 1 | 4.00 | NA | NA | 4.00 | NA | NA |
| Wall | Chloroform | Passive | Off | 1 | 2.10 | NA | NA | 2.10 | NA | NA |
| Wall | Chloroform | Passive | On | 3 | 2.10 | 0.00 | 0.00 | 2.10 | 1.00 | 0.48 |
| Wall | Chloroform | On | Off | 6 | 2.10 | 0.00 | 0.00 | 2.10 | 1.00 | 0.48 |
| Wall | Chloroform | On | On | 18 | 14.11 | 20.08 | 1.42 | 5.35 | 3.99 | 0.75 |
| | | | | | | | | | | |
| Wall | Tetrachloroethene | Not installed | Off | 107 | 13.02 | 74.46 | 5.72 | 4.88 | 1.95 | 0.40 |
| Wall | Tetrachloroethene | Not installed | On | 116 | 14.63 | 50.70 | 3.47 | 5.73 | 2.33 | 0.41 |
| Wall | Tetrachloroethene | Off | Off | 1 | 1.80 | NA | NA | 1.80 | NA | NA |
| Wall | Tetrachloroethene | Passive | Off | 1 | 1.75 | NA | NA | 1.75 | NA | NA |
| Wall | Tetrachloroethene | Passive | On | 3 | 46.47 | 72.40 | 1.56 | 12.03 | 8.93 | 0.74 |
| Wall | Tetrachloroethene | On | Off | 6 | 2.19 | 1.08 | 0.49 | 2.04 | 1.46 | 0.71 |
| Wall | Tetrachloroethene | On | On | 18 | 60.82 | 150.56 | 2.48 | 7.03 | 7.58 | 1.08 |

Table 5-17. Distribution of Subslab and Wall Port VOC Concentrations ($\mu\text{g}/\text{m}^3$) by Mitigation and Heating Status (yellow indicates statistics during active mitigation)

| Location Type | Variable | Mitigation | Heating | Number Samples | 5th Percentile | 10th Percentile | 25th Percentile | 50th Percentile | 75th Percentile | 90th Percentile | 95th Percentile |
|---------------|-------------------|---------------|---------|----------------|----------------|-----------------|-----------------|-----------------|-----------------|-----------------|-----------------|
| Subslab | Chloroform | Not installed | Off | 244 | 3 | 3 | 3 | 3 | 11 | 75 | 139 |
| Subslab | Chloroform | Not installed | On | 115 | 6 | 58 | 82 | 140 | 210 | 266 | 273 |
| Subslab | Chloroform | Off | Off | 10 | 10 | 10 | 10 | 10 | 15 | 56 | 58 |
| Subslab | Chloroform | Passive | On | 3 | 16 | 30 | 71 | 140 | 310 | 412 | 446 |
| Subslab | Chloroform | Passive | Off | 4 | 2 | 2 | 2 | 2 | 2 | 2 | 2 |
| Subslab | Chloroform | On | Off | 32 | 2 | 2 | 2 | 28 | 82 | 129 | 159 |
| Subslab | Chloroform | On | On | 24 | 2 | 2 | 2 | 42 | 135 | 187 | 216 |
| | | | | | | | | | | | |
| Subslab | Tetrachloroethene | Not installed | Off | 244 | 7 | 9 | 17 | 31 | 75 | 120 | 180 |
| Subslab | Tetrachloroethene | Not installed | On | 115 | 91 | 105 | 150 | 190 | 240 | 336 | 457 |
| Subslab | Tetrachloroethene | Off | Off | 10 | 10 | 10 | 17 | 28 | 128 | 140 | 140 |
| Subslab | Tetrachloroethene | Passive | Off | 4 | 12 | 14 | 19 | 23 | 26 | 29 | 30 |
| Subslab | Tetrachloroethene | Passive | On | 3 | 78 | 148 | 359 | 710 | 735 | 750 | 755 |
| Subslab | Tetrachloroethene | On | Off | 32 | 6 | 7 | 11 | 32 | 95 | 456 | 613 |
| Subslab | Tetrachloroethene | On | On | 24 | 2 | 2 | 5 | 104 | 640 | 907 | 1336 |
| | | | | | | | | | | | |
| Wall | Chloroform | Not installed | Off | 107 | 3 | 3 | 3 | 3 | 3 | 8 | 15 |
| Wall | Chloroform | Not installed | On | 116 | 2 | 3 | 3 | 3 | 3 | 7 | 13 |
| Wall | Chloroform | Off | Off | 1 | 4 | 4 | 4 | 4 | 4 | 4 | 4 |
| Wall | Chloroform | Passive | Off | 1 | 2 | 2 | 2 | 2 | 2 | 2 | 2 |
| Wall | Chloroform | Passive | On | 3 | 2 | 2 | 2 | 2 | 2 | 2 | 2 |
| Wall | Chloroform | On | Off | 6 | 2 | 2 | 2 | 2 | 2 | 2 | 2 |
| Wall | Chloroform | On | On | 18 | 2 | 2 | 2 | 2 | 23 | 43 | 55 |
| | | | | | | | | | | | |
| Wall | Tetrachloroethene | Not installed | Off | 107 | 4 | 4 | 4 | 4 | 4 | 5 | 8 |
| Wall | Tetrachloroethene | Not installed | On | 116 | 4 | 4 | 4 | 4 | 5 | 10 | 24 |
| Wall | Tetrachloroethene | Off | Off | 1 | 2 | 2 | 2 | 2 | 2 | 2 | 2 |
| Wall | Tetrachloroethene | Passive | Off | 1 | 2 | 2 | 2 | 2 | 2 | 2 | 2 |
| Wall | Tetrachloroethene | Passive | On | 3 | 2 | 3 | 5 | 8 | 69 | 106 | 118 |
| Wall | Tetrachloroethene | On | Off | 6 | 2 | 2 | 2 | 2 | 2 | 3 | 4 |
| Wall | Tetrachloroethene | On | On | 18 | 2 | 2 | 2 | 2 | 43 | 129 | 288 |

Table 5-18. Descriptive Statistics of Subslab and Wall Port VOC Concentrations ($\mu\text{g}/\text{m}^3$) by Location and Mitigation and Heating Status (yellow indicates statistics during active mitigation)

| Location1 | Variable | Mitigation | Heating | Number Samples | Mean | SD | CV | geoMean | geoSD | geoCV |
|-----------|-------------------|---------------|---------|----------------|------|--------|------|---------|-------|-------|
| SSP-1 | Chloroform | Not installed | Off | 35 | 74 | 91.30 | 1.23 | 37 | 3.32 | 0.09 |
| SSP-1 | Chloroform | Not installed | On | 67 | 121 | 57.72 | 0.48 | 104 | 1.94 | 0.02 |
| SSP-1 | Chloroform | Off | Off | 2 | 58 | 2.12 | 0.04 | 57 | 1.04 | 0.02 |
| SSP-1 | Chloroform | On | On | 8 | 43 | 47.49 | 1.11 | 20 | 4.74 | 0.23 |
| SSP-1 | Chloroform | Passive | On | 1 | 140 | NA | NA | 140 | NA | NA |
| SSP-1 | Tetrachloroethene | Not installed | Off | 35 | 115 | 47.51 | 0.41 | 102 | 1.92 | 0.02 |
| SSP-1 | Tetrachloroethene | Not installed | On | 67 | 292 | 237.05 | 0.81 | 244 | 1.74 | 0.01 |
| SSP-1 | Tetrachloroethene | Off | Off | 2 | 140 | 0.00 | 0.00 | 140 | 1.00 | 0.01 |
| SSP-1 | Tetrachloroethene | On | On | 8 | 192 | 225.55 | 1.18 | 120 | 2.68 | 0.02 |
| SSP-1 | Tetrachloroethene | Passive | On | 1 | 760 | NA | NA | 760 | NA | NA |
| | | | | | | | | | | |
| SSP-2 | Chloroform | Not installed | Off | 2 | 8 | 4.56 | 0.55 | 8 | 1.80 | 0.24 |
| SSP-2 | Chloroform | Not installed | On | 3 | 4 | 2.19 | 0.50 | 4 | 1.59 | 0.39 |
| SSP-2 | Chloroform | Off | Off | 2 | 10 | 0.00 | 0.00 | 10 | 1.00 | 0.10 |
| SSP-2 | Chloroform | On | On | 8 | 5 | 6.82 | 1.51 | 3 | 2.27 | 0.81 |
| SSP-2 | Chloroform | Passive | On | 1 | 2 | NA | NA | 2 | NA | NA |
| SSP-2 | Tetrachloroethene | Not installed | Off | 2 | 12 | 2.51 | 0.21 | 12 | 1.23 | 0.10 |
| SSP-2 | Tetrachloroethene | Not installed | On | 3 | 5 | 1.88 | 0.35 | 5 | 1.39 | 0.27 |
| SSP-2 | Tetrachloroethene | Off | Off | 2 | 10 | 0.21 | 0.02 | 10 | 1.02 | 0.10 |
| SSP-2 | Tetrachloroethene | On | On | 8 | 3 | 1.84 | 0.62 | 3 | 1.74 | 0.67 |
| SSP-2 | Tetrachloroethene | Passive | On | 1 | 8 | NA | NA | 8 | NA | NA |
| | | | | | | | | | | |
| SSP-3 | Chloroform | Not installed | Off | 9 | 8 | 8.52 | 1.10 | 6 | 2.14 | 0.38 |
| SSP-3 | Chloroform | Off | Off | 2 | 10 | 0.00 | 0.00 | 10 | 1.00 | 0.10 |
| SSP-3 | Chloroform | On | Off | 8 | 65 | 29.80 | 0.46 | 58 | 1.65 | 0.03 |
| SSP-3 | Chloroform | Passive | Off | 1 | 2 | NA | NA | 2 | NA | NA |

(continued)

Table 5-18. Descriptive Statistics of Subslab and Wall Port VOC Concentrations ($\mu\text{g}/\text{m}^3$) by Location and Mitigation and Heating Status (yellow indicates statistics during active mitigation) (cont.)

| Location1 | Variable | Mitigation | Heating | Number Samples | Mean | SD | CV | geoMean | geoSD | geoCV |
|-----------|-------------------|---------------|---------|----------------|------|--------|------|---------|-------|-------|
| SSP-3 | Tetrachloroethene | Not installed | Off | 9 | 21 | 21.38 | 1.02 | 16 | 2.09 | 0.13 |
| SSP-3 | Tetrachloroethene | Off | Off | 2 | 18 | 2.83 | 0.16 | 18 | 1.17 | 0.07 |
| SSP-3 | Tetrachloroethene | On | Off | 8 | 184 | 208.14 | 1.13 | 83 | 4.51 | 0.05 |
| SSP-3 | Tetrachloroethene | Passive | Off | 1 | 22 | NA | NA | 22 | NA | NA |
| | | | | | | | | | | |
| SSP-4 | Chloroform | Not installed | Off | 15 | 101 | 69.30 | 0.69 | 64 | 3.72 | 0.06 |
| SSP-4 | Chloroform | Not installed | On | 45 | 198 | 82.20 | 0.42 | 151 | 3.03 | 0.02 |
| SSP-4 | Chloroform | Off | Off | 2 | 15 | 0.00 | 0.00 | 15 | 1.00 | 0.07 |
| SSP-4 | Chloroform | On | On | 8 | 209 | 142.97 | 0.68 | 182 | 1.66 | 0.01 |
| SSP-4 | Chloroform | Passive | On | 1 | 480 | NA | NA | 480 | NA | NA |
| SSP-4 | Tetrachloroethene | Not installed | Off | 15 | 188 | 91.43 | 0.49 | 124 | 4.02 | 0.03 |
| SSP-4 | Tetrachloroethene | Not installed | On | 45 | 153 | 32.88 | 0.21 | 150 | 1.25 | 0.01 |
| SSP-4 | Tetrachloroethene | Off | Off | 2 | 125 | 7.07 | 0.06 | 125 | 1.06 | 0.01 |
| SSP-4 | Tetrachloroethene | On | On | 8 | 884 | 493.99 | 0.56 | 770 | 1.78 | 0.00 |
| SSP-4 | Tetrachloroethene | Passive | On | 1 | 710 | NA | NA | 710 | NA | NA |
| | | | | | | | | | | |
| SSP-5 | Chloroform | Not installed | Off | 67 | 11 | 29.72 | 2.77 | 5 | 2.52 | 0.55 |
| SSP-5 | Chloroform | Off | Off | 2 | 10 | 0.00 | 0.00 | 10 | 1.00 | 0.10 |
| SSP-5 | Chloroform | On | Off | 8 | 11 | 12.54 | 1.13 | 5 | 3.68 | 0.68 |
| SSP-5 | Chloroform | Passive | Off | 1 | 2 | NA | NA | 2 | NA | NA |
| SSP-5 | Tetrachloroethene | Not installed | Off | 67 | 44 | 29.66 | 0.67 | 34 | 2.18 | 0.06 |
| SSP-5 | Tetrachloroethene | Off | Off | 2 | 28 | 4.24 | 0.15 | 28 | 1.16 | 0.04 |
| SSP-5 | Tetrachloroethene | On | Off | 8 | 25 | 8.83 | 0.36 | 23 | 1.44 | 0.06 |
| SSP-5 | Tetrachloroethene | Passive | Off | 1 | 32 | NA | NA | 32 | NA | NA |
| | | | | | | | | | | |
| SSP-6 | Chloroform | Not installed | Off | 70 | 5 | 12.84 | 2.46 | 4 | 1.74 | 0.48 |
| SSP-6 | Chloroform | On | Off | 8 | 15 | 28.67 | 1.92 | 4 | 4.26 | 0.95 |
| SSP-6 | Chloroform | Passive | Off | 1 | 2 | NA | NA | 2 | NA | NA |

(continued)

Table 5-18. Descriptive Statistics of Subslab and Wall Port VOC Concentrations ($\mu\text{g}/\text{m}^3$) by Location and Mitigation and Heating Status (yellow indicates statistics during active mitigation) (cont.)

| Location1 | Variable | Mitigation | Heating | Number Samples | Mean | SD | CV | geoMean | geoSD | geoCV |
|-----------|-------------------|---------------|---------|----------------|------|--------|------|---------|-------|-------|
| SSP-6 | Tetrachloroethene | Not installed | Off | 70 | 37 | 27.57 | 0.74 | 29 | 2.00 | 0.07 |
| SSP-6 | Tetrachloroethene | On | Off | 8 | 64 | 160.04 | 2.50 | 12 | 4.58 | 0.39 |
| SSP-6 | Tetrachloroethene | Passive | Off | 1 | 10 | NA | NA | 10 | NA | NA |
| | | | | | | | | | | |
| SSP-7 | Chloroform | Not installed | Off | 46 | 6 | 5.00 | 0.86 | 5 | 1.72 | 0.36 |
| SSP-7 | Chloroform | On | Off | 8 | 114 | 55.98 | 0.49 | 98 | 1.95 | 0.02 |
| SSP-7 | Chloroform | Passive | Off | 1 | 2 | NA | NA | 2 | NA | NA |
| SSP-7 | Tetrachloroethene | Not installed | Off | 46 | 17 | 11.93 | 0.71 | 13 | 1.99 | 0.15 |
| SSP-7 | Tetrachloroethene | On | Off | 8 | 345 | 450.57 | 1.30 | 141 | 4.91 | 0.03 |
| SSP-7 | Tetrachloroethene | Passive | Off | 1 | 24 | NA | NA | 24 | NA | NA |
| | | | | | | | | | | |
| WP-1 | Chloroform | Not installed | Off | 17 | 4 | 2.59 | 0.69 | 3 | 1.48 | 0.43 |
| WP-1 | Chloroform | Not installed | On | 41 | 3 | 1.02 | 0.31 | 3 | 1.35 | 0.42 |
| WP-1 | Chloroform | On | On | 6 | 6 | 8.63 | 1.54 | 3 | 2.67 | 0.85 |
| WP-1 | Chloroform | Passive | On | 1 | 2 | NA | NA | 2 | NA | NA |
| WP-1 | Tetrachloroethene | Not installed | Off | 17 | 4 | 0.64 | 0.16 | 4 | 1.25 | 0.31 |
| WP-1 | Tetrachloroethene | Not installed | On | 41 | 4 | 0.71 | 0.17 | 4 | 1.23 | 0.29 |
| WP-1 | Tetrachloroethene | On | On | 6 | 2 | 0.00 | 0.00 | 2 | 1.00 | 0.57 |
| WP-1 | Tetrachloroethene | Passive | On | 1 | 2 | NA | NA | 2 | NA | NA |
| | | | | | | | | | | |
| WP-2 | Chloroform | Not installed | Off | 18 | 4 | 2.06 | 0.56 | 3 | 1.39 | 0.40 |
| WP-2 | Chloroform | Not installed | On | 39 | 6 | 14.80 | 2.53 | 4 | 1.85 | 0.51 |
| WP-2 | Chloroform | Off | Off | 1 | 4 | NA | NA | 4 | NA | NA |
| WP-2 | Chloroform | On | On | 6 | 6 | 9.94 | 1.61 | 3 | 2.81 | 0.88 |
| WP-2 | Chloroform | Passive | On | 1 | 2 | NA | NA | 2 | NA | NA |
| WP-2 | Tetrachloroethene | Not installed | Off | 18 | 7 | 11.49 | 1.65 | 5 | 1.82 | 0.37 |
| WP-2 | Tetrachloroethene | Not installed | On | 39 | 4 | 0.43 | 0.10 | 4 | 1.13 | 0.26 |
| WP-2 | Tetrachloroethene | Off | Off | 1 | 2 | NA | NA | 2 | NA | NA |

(continued)

Table 5-18. Descriptive Statistics of Subslab and Wall Port VOC Concentrations ($\mu\text{g}/\text{m}^3$) by Location and Mitigation and Heating Status (yellow indicates statistics during active mitigation) (cont.)

| Location1 | Variable | Mitigation | Heating | Number Samples | Mean | SD | CV | geoMean | geoSD | geoCV |
|-----------|-------------------|---------------|---------|----------------|------|--------|------|---------|-------|-------|
| WP-2 | Tetrachloroethene | On | On | 6 | 2 | 1.31 | 0.57 | 2 | 1.53 | 0.73 |
| WP-2 | Tetrachloroethene | Passive | On | 1 | 8 | NA | NA | 8 | NA | NA |
| | | | | | | | | | | |
| WP-3 | Chloroform | Not installed | Off | 14 | 12 | 20.72 | 1.80 | 6 | 2.64 | 0.44 |
| WP-3 | Chloroform | Not installed | On | 36 | 7 | 9.49 | 1.34 | 4 | 2.30 | 0.52 |
| WP-3 | Chloroform | On | On | 6 | 31 | 26.66 | 0.87 | 15 | 4.87 | 0.32 |
| WP-3 | Chloroform | Passive | On | 1 | 2 | NA | NA | 2 | NA | NA |
| WP-3 | Tetrachloroethene | Not installed | Off | 14 | 7 | 8.41 | 1.16 | 6 | 1.80 | 0.32 |
| WP-3 | Tetrachloroethene | Not installed | On | 36 | 38 | 87.50 | 2.33 | 11 | 3.55 | 0.32 |
| WP-3 | Tetrachloroethene | On | On | 6 | 178 | 228.42 | 1.28 | 95 | 3.41 | 0.04 |
| WP-3 | Tetrachloroethene | Passive | On | 1 | 130 | NA | NA | 130 | NA | NA |
| | | | | | | | | | | |
| WP-4 | Chloroform | Not installed | Off | 58 | 18 | 91.99 | 5.19 | 4 | 2.57 | 0.63 |
| WP-4 | Chloroform | On | Off | 6 | 2 | 0.00 | 0.00 | 2 | 1.00 | 0.48 |
| WP-4 | Chloroform | Passive | Off | 1 | 2 | NA | NA | 2 | NA | NA |
| WP-4 | Tetrachloroethene | Not installed | Off | 58 | 19 | 100.87 | 5.34 | 5 | 2.20 | 0.44 |
| WP-4 | Tetrachloroethene | On | Off | 6 | 2 | 1.08 | 0.49 | 2 | 1.46 | 0.71 |
| WP-4 | Tetrachloroethene | Passive | Off | 1 | 2 | NA | NA | 2 | NA | NA |

5.3.2 Effect of Mitigation System Status on Indoor Air VOC Levels

Figure 5-13 compares the distributions of PCE and chloroform concentrations from weekly Radiello samples by indoor air sampling location and mitigation status. The SSD system appears to reduce the variability of the indoor air concentrations (as shown by the smaller green boxes for mitigation on in the figure) and at all locations, the distributions VOCs in indoor air were lower with mitigation on. To test the significance of this difference, we first investigated whether the populations (mitigation on and mitigation off by location and compound) are log-normally distributed, have the same variance, and are independent from one another.

As shown in **Appendix C**, all 24 sampling locations/mitigation status/compound combinations tested had the same variance (based on an F-test) and only six of the 24 failed a Shapiro-Wilk test of log-normality. With respect to the assumption of independence, we believe that VOC concentrations from consecutive weeks are not autocorrelated due to the known air exchange rate and results from other published research, but significant autocorrelation beyond a week was found in our data analysis in some cases (see Chapter 10). However, because the data being examined in this section do not span an entire year, the data cannot be detrended and this may contribute to the observed autocorrelation. If the data were autocorrelated across weeks, the data in each of the two populations considered for each comparison (the two populations are mitigation "On" observations and mitigation "Off" observations) would be more similar among themselves than truly randomly chosen observations from each population would be.

That being said, the results are quite convincing. Using a two sided two sample t-test to test the difference between the log-concentrations with mitigation "On" and "Off" with the null hypothesis that the difference between the two populations is 0 (that is to say that the null hypothesis is that mitigation has no effect) provides p-values for that hypothesis that were well below 0.05 for all mitigation status/location/compound cases tested, with the highest p-value observed being 0.019. Additional details on this analysis and these results can be found in **Appendix C**.

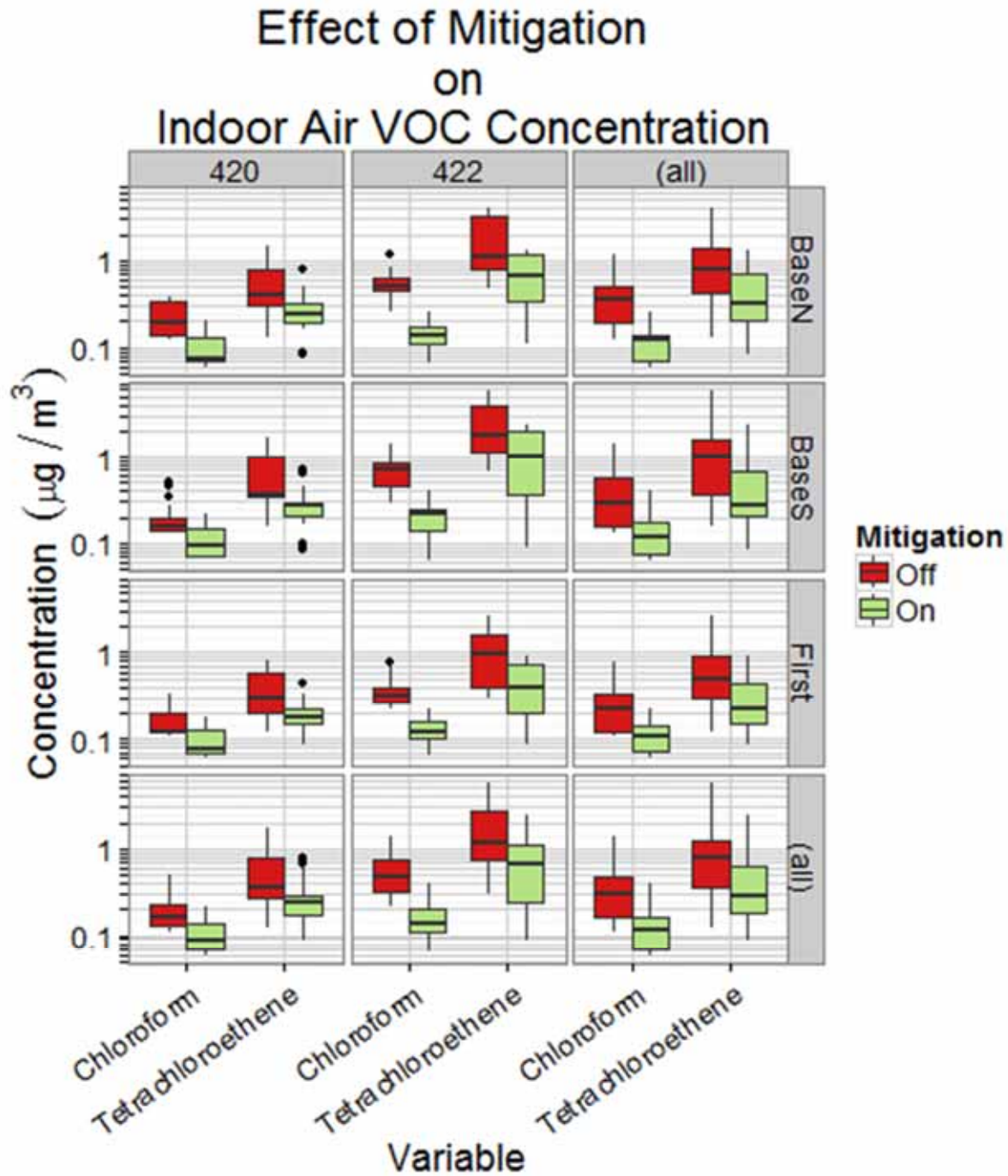


Figure 5-13. Boxplots of mitigation effect on indoor air concentrations.

5.3.3 Discussion

The effect of the SSD system on subslab and wall ports was shown in **Table 5-16**. Comparing heating on and mitigation not installed vs. heating on and mitigation on that table shows:

- Chloroform went down on average in subslab but PCE went up in subslab.
- Chloroform and PCE both went up on average in wall ports.

The effect of mitigation on certain particular subslab and wall ports is also shown graphically later in this document in **Figures 6-6, 6-7, and 7-1**.

An alternate way of understanding why mitigation could be more effective for radon than VOCs can be stated as follows:

- Radon is formed from the radioactive decay of radium, and then must leave the soil grain and travel into the fluid filled pore space to produce a risk (a process called emanation). As a first approximation, the concentration of radon in soil gas is controlled by the emanation rate and the soil air permeability. The exhalation rate, or the rate of radon release from a soil surface, in turn depends on the radium concentration of the soil, its moisture content, and temperature (Lewis and Houle, 2009). However the exhalation rate is not expected to be changed significantly by increasing the air flow rate through the soil. Therefore assuming a relatively uniform soil profile with regard to exhalation rate, the concentration of radon in the soil gas may be depleted with additional flow.
- Given its short half-life, radon in soil gas entering a structure must have emanated within a few days of its entry into and therefore fairly near the house in question.
- Subsurface VOCs are usually present as a sorbed or free-phase source that is essentially infinite over the time span of interest. Increasing airflow rates up to a certain point will increase mass removal by increasing mass transfer (Le Chatelier's principle). However if the system is diffusion limited or the soils dry out, further increases in air flow rate may not further increase volatilization (Rorech, 2001; Thomas 1990).
- VOC concentration profiles at sites distant from the point of release, when transport is primarily through groundwater are typically characterized by decreasing concentration with depth. Because PCE and TCE are only slowly degraded in aerobic soils (with half-lives over 1 year versus 3.8 days for radon), the PCE entering the structure may have migrated over many weeks or even years from the source area, and from much greater distances than radon. Thus, enhanced airflow caused by SSD may draw in higher concentration soil gas from deep soils, but is less likely to increase the radon concentration.

5.4 Stack Gas Monitoring

5.4.1 Is Stack Gas an Indicator of SSD System Performance in Protecting Indoor Air?

The stack gas week-long integrated chloroform concentration as measured by the Waterloo passive sampler is highest during periods of active SSD operation as expected (**Figure 5-14**). The stack gas concentration has some variability during periods with the mitigation on (8.9 to 33 $\mu\text{g}/\text{m}^3$). For chloroform, the concentration in the stack gas is not a strong predictor of the indoor air concentration at the 422 first floor location (**Figure 5-15**) during SSD operation ($R^2 = 0.26$). This could reflect infiltration of outside air as indoor air levels are within the upper end of the range of outdoor air chloroform levels.

The stack gas week-long integrated PCE concentration as measured by the Waterloo passive sampler is highest during periods of active SSD operation as expected (**Figure 5-16**). The stack gas concentration has high variability during periods with the mitigation on (13 to 98 $\mu\text{g}/\text{m}^3$). In contrast to the result for chloroform, there is a good correlation between stack gas and the 422 first floor indoor concentration (**Figure 5-17**) during SSD operation ($R^2 = 0.70$).

This would suggest that stack gas monitoring in conjunction with verification of SSD operational status could provide some information about whether the SSD system is increasing or decreasing concentrations in the subslab area. Although SSD systems need not decrease subslab concentrations to effectively protect indoor air, systems that exhibit increased concentration in the subslab area during SSD system operation

may require more careful monitoring to ensure that control of flow across the slab is maintained at the vast majority of times and locations.

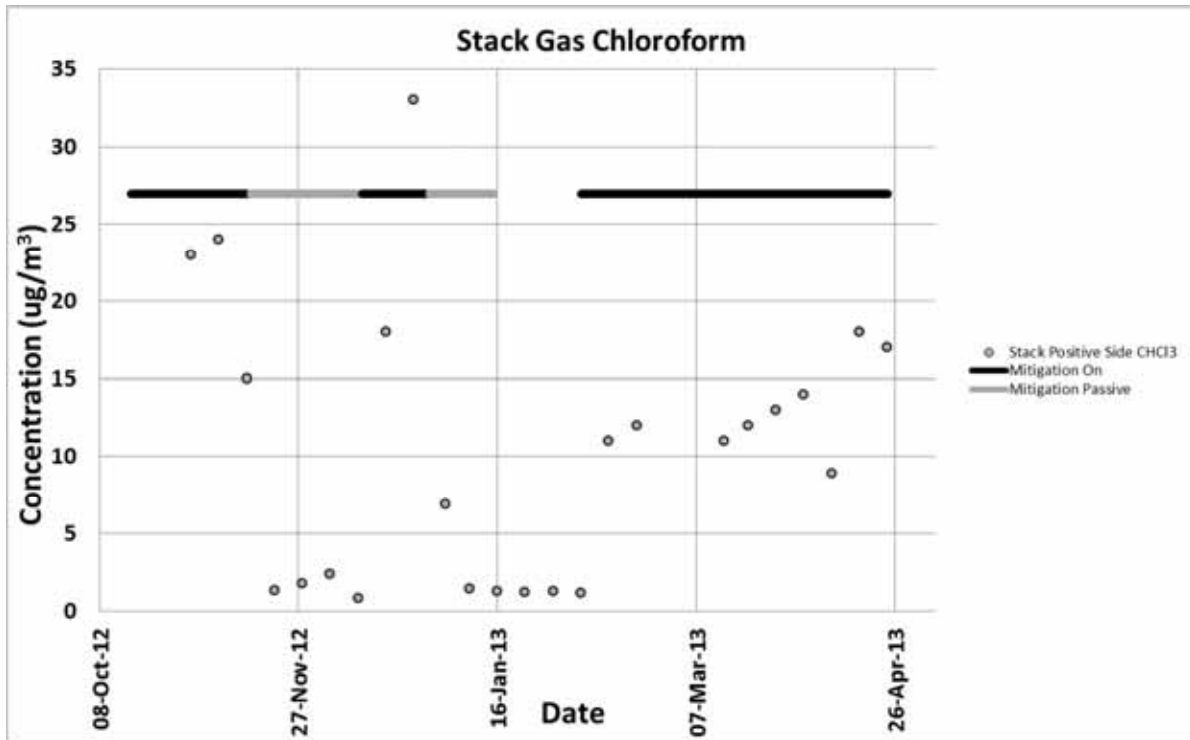


Figure 5-14. Stack gas monitoring during mitigation testing: chloroform.

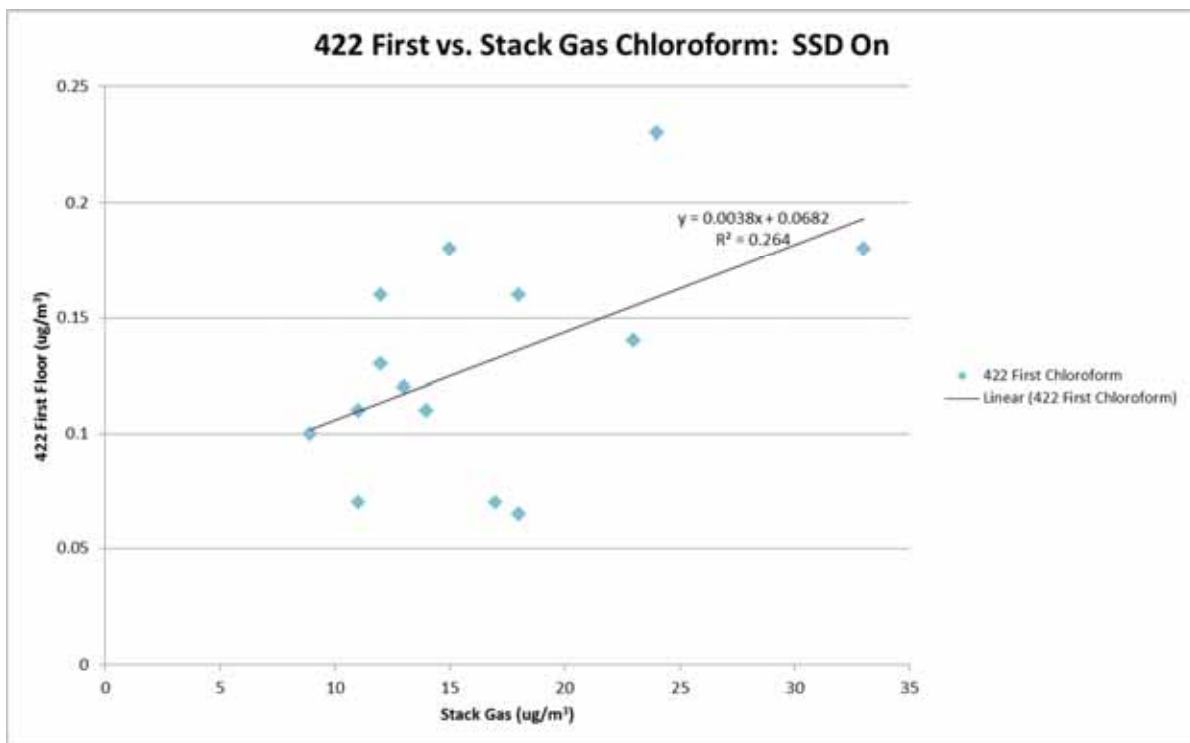


Figure 5-15. 422 first floor versus stack gas chloroform concentrations: mitigation on.

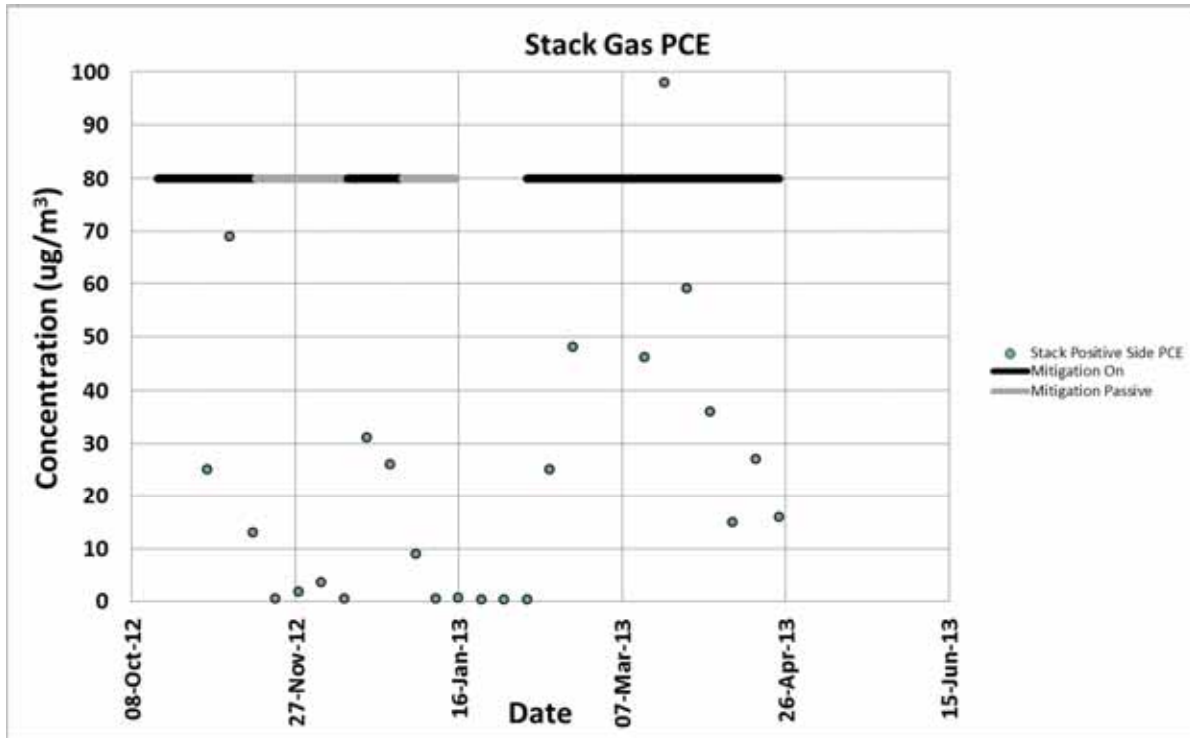


Figure 5-16. Stack gas monitoring during mitigation testing: PCE.

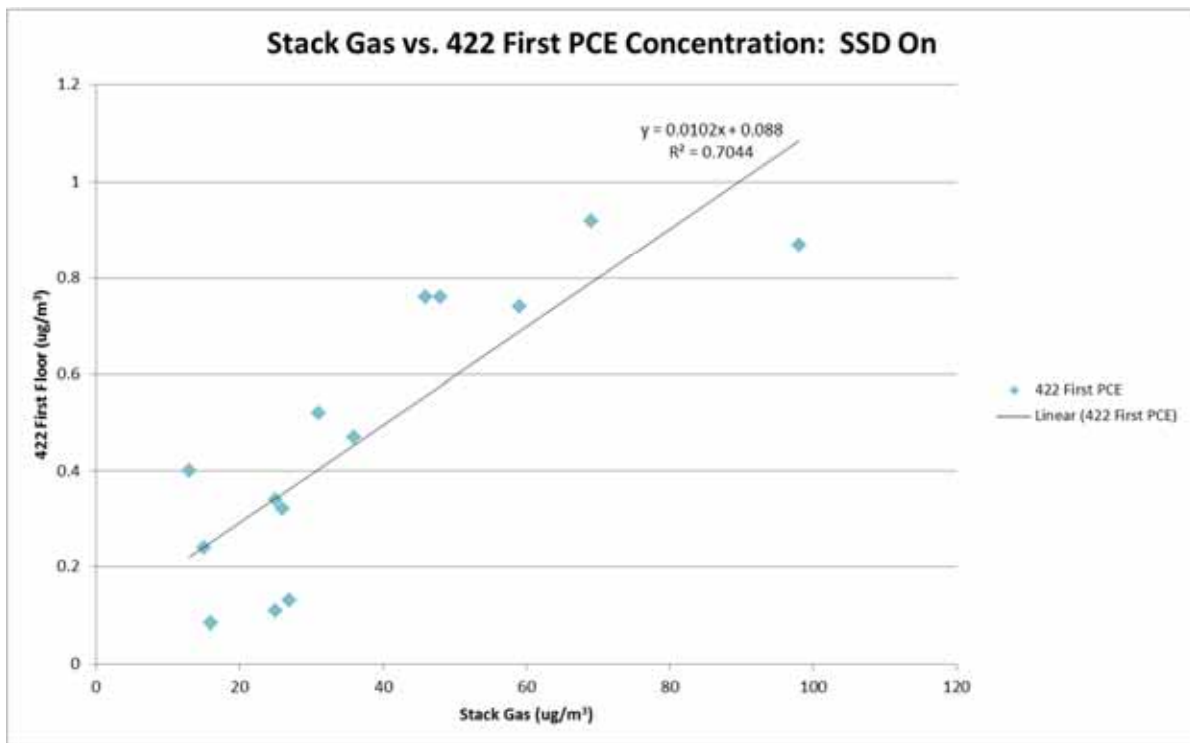


Figure 5-17. Stack gas versus 422 first floor PCE concentrations: mitigation on.

5.4.2 Air Exchange Rate Measurements

Air exchange rate measurements were performed using EPA Method IP-4A, which uses passive emitters and passive samplers known as capillary adsorption tube samplers (CATS) from

- April 27 to May 11, 2011 (heating system on)
- September 23 to September 29, 2011 (heating system off).¹⁰
- October 13 to October 14, 2011 (during fan test I¹¹, see description of fan tests in Section 12.2 of U.S. EPA [2012a], heating system off).
- October 18 to October 19, 2011 (after fan testing, heating system off)
- April 2 to April 9, 2013 (with mitigation system operating, heating system on)

During these periods, the house was operated as usual—with windows closed and the doors opened only as needed to maintain the house and the sampling equipment.

The emitters were evenly spaced across their respective floors of the 422 side of the duplex:

- 10 PDCH emitters in the basement
- 10 PMCH emitters on the first floor
- 9 PMCH emitters on the second floor (10 in some tests)

No emitters were placed on the 420 side of the duplex, but CATS measurements were made there in the April/May 2011 round and April 2013 to estimate the amount of airflow between sides of the duplex. The emitters were deployed on April 22, 2011, to allow the building to come to equilibrium before sampling and were essentially left in place throughout the measurement periods with one change out to fresh emitters.

As shown in **Table 5-19**, the April/May 422 basement air exchange rates showed excellent agreement for the duplicates (both 0.74/hour). As shown in **Table 5-20**, the September measurements for the basement (0.64/hour and 0.72/hour) are slightly more variable but quite similar to the April/May measurements. The first floor measurements were lower in both measurement periods (0.56 in April/May and 0.55 in September). The September measurements show a pattern of decreasing air exchange rates up through the building (basement through second floor office).

Measurements performed in April/May 2012 did not show any detectable crossover of either tracer into the 420 side of the duplex. The detection limit of the method is approximately 1 pl per sample and the lowest amount of tracer collected in one of the rooms with the emitters for that tracer present was 126 pl. So less than 1% of the tracer concentration detected in the 422 zones where it was released was present on the 420 side of the duplex.

The concentration of the tracer released in the basement (PDCH) was about 20% of the basement concentration on the first floor. The concentration of the tracer released on the first and second floors (PMCH) was detected at about 2% of the first floor concentration in the basement. These percentages suggest that during that measurement period more flow was up from the basement to the first floor, although some flow did come from the first floor down into the basement.

¹⁰Fan testing had ended on September 14 and resumed on October 6. These first two tests were reported previously in section 10 of U.S. EPA (2012a). All five tests are reported here. There have been minor corrections to the calculations from the September 2011 data set.

¹¹Fan tests were attempts to induce worst case vapor intrusion by using box fans, in this case to exhaust air from the basement up the stairway to the first floor.

Table 5-19. April/May 2011 Air Exchange Rate Measurement Results

| Date Deployed | Date Collected | CAT ID | PMCH Amount (pl) | PDCH Amount (pl) | Location | Primary Tracer Deployed | Interior Temperature (°F) | Calculated AER 1/hr | Volume Ft ³ | Duration of Test Minutes |
|---------------|----------------|--------|------------------|------------------|------------------|-------------------------|---------------------------|---------------------|------------------------|--------------------------|
| 4/27/2011 | 5/4/2011 | 11015 | 30.74 | 127.51 | 422 basement | PDCH | 61.29 | 0.74 | 4,547 | 10,368 |
| 4/27/2011 | 5/4/2011 | 8441 | 28.96 | 126.67 | 422 basement dup | PDCH | 61.29 | 0.74 | 4,547 | 10,367 |
| 4/27/2011 | 5/4/2011 | 779 | 301.47 | 25.03 | 422 first | PMCH | 67.82 | 0.56 | 9,002 | 10,364 |
| 4/27/2011 | 5/4/2011 | 9167 | 0 | 0 | 420 basement | None | 58.17 | NA | 4,547 | 10,354 |
| 4/27/2011 | 5/4/2011 | 5273 | 0 | 0 | 420 first | None | 61.19 | NA | 9,002 | 10,352 |
| 4/27/2011 | 5/4/2011 | 6963 | 0.75 | 0 | Travel blank | None | 68 | NA | 0 | 0 |

Table 5-20. September 2011 Air Exchange Rate Measurement Results

| Date Deployed | Date Collected | CAT ID | PMCH Amount (pl) | PDCH Amount (pl) | Location | Primary Tracer Deployed | Interior Temperature (°F) | AER 1/hr | Volume Ft ³ | Duration of Test Minutes |
|---------------|----------------|--------|------------------|------------------|------------------|-------------------------|---------------------------|-------------|------------------------|--------------------------|
| 9/23/2011 | 9/29/2011 | 12621 | 406.42 | 28.96 | 422 office | PMCH | 72.416 | 0.34 | 9,002 | 8,594 |
| 9/23/2011 | 9/29/2011 | 18744 | 253.51 | 38.35 | 422 first | PMCH | 72.416 | 0.55 | 9,002 | 8,594 |
| 9/23/2011 | 9/29/2011 | 18185 | 5.94 | 108.79 | 422 basement | PDCH | 67.77 | 0.72 | 4,547 | 8,591 |
| 9/23/2011 | 9/29/2011 | 9024 | 4.48 | 121.27 | 422 basement dup | PDCH | 67.77 | 0.64 | 4,547 | 8,591 |

During fan test “I” the air exchange rates were about a factor of 2 to 4 higher (**Table 5-21**) in a 1-day measurement. The increase was actually less than we would have calculated if the observed fan flow 1,224 cfm (Section 12.2.2 of U.S. EPA [2012a]) was completely removing the air from the basement in a “one pass” sense. It is likely that the air being removed from the basement during the fan tests is being recirculated within the house. Evidence for this is provided by the nearly equal concentrations of the PMCH and PDCH tracers found in both the basement and the first floor. Recall that PDCH was released only in the basement and PMCH on the upper floors. This suggests that there is much more flow both ways between floors with the fan on.

The 1-day test done after the fan testing was completed (**Table 5-21**) showed somewhat higher air exchange rates than seen in the previous longer term tests done without the fan. During that day, exterior temperatures were in the mid-40s °F. It is possible that a stronger stack effect thus explains the higher air exchange rate than the April 2011 test (40s to 70s °F) or September 2011 test (mid-50s to mid-60s °F).

The April 2013 tests (**Table 5-22**) were conducted with the SSD system on during a period of very wide-ranging exterior temperatures (20s to 70s °F). If the SSD system was drawing all the exhausted air from the basement, then we would expect the AER of the basement to increase by approximately 1 air exchange per hour. Because the air exchange rates measured with the SSD system on were increased by somewhat less than 1 air exchange per hour, it is likely (as theory would suggest) that the mitigation system is drawing air from both the structure and elsewhere in the soil column/atmosphere into the subslab region and hence out the exhaust pipe.

Table 5-21. October 2011 Air Exchange Measurement Results (during and after fan testing)

| Date Deployed | Date Collected | CAT ID | PMCH Amount (pl) | PDCH Amount (pl) | Location | Primary Tracer deployed | Interior Temperature (°F) | AER 1/hr | Volume ft ³ | Duration of Test minutes | Conditions |
|---------------|----------------|--------|------------------|------------------|------------------|-------------------------|---------------------------|----------|------------------------|--------------------------|-------------|
| 10/13/2011 | 10/14/2011 | 11067 | 16.43 | 4.80 | 422 Office | PMCH | 75.0 | 1.42 | 9,002 | 1,440 | Fan test on |
| 10/13/2011 | 10/14/2011 | 18277 | 6.21 | 5.08 | 422 First | PMCH | 72.7 | 3.76 | 9,002 | 1,439 | Fan test on |
| 10/13/2011 | 10/14/2011 | 2502 | 4.64 | 4.49 | 422 Basement | PDCH | 69.0 | 2.91 | 4,547 | 1,440 | Fan test on |
| 10/13/2011 | 10/14/2011 | 17707 | 4.51 | 4.45 | 422 Basement Dup | PDCH | 69.0 | 2.94 | 4,547 | 1,440 | Fan test on |
| | | 10002 | 1.98 | 0.00 | Trip blank | PMCH | 71.4 | | 9,002 | | |
| 10/18/2011 | 10/19/2011 | 7229 | 38.92 | 1.76 | 422 Office | PMCH | 63.8 | 0.60 | 9,002.00 | 1,441.00 | Fan off |
| 10/18/2011 | 10/19/2011 | 18654 | 23.30 | 1.66 | 422 First | PMCH | 62.4 | 1.06 | 9,002.00 | 1,441.00 | Fan off |
| 10/18/2011 | 10/19/2011 | 15758 | 2.59 | 10.27 | 422 Basement | PDCH | 62.2 | 1.27 | 4,547.00 | 1,441.00 | Fan off |
| 10/18/2011 | 10/19/2011 | 9271 | 2.70 | 10.76 | 422 Basement Dup | PDCH | 62.2 | 1.21 | 4,547.00 | 1,440.00 | Fan off |
| | | 6739 | 1.90 | 0.00 | Trip blank | | 62.7 | | | | Fan off |

Table 5-22. April 2013 Air Exchange Measurement Results (During Mitigation)

| Date Deployed | Date Collected | CAT ID | PMCH Amount (pl) | PDCH Amount (pl) | Location | Primary Tracer deployed | Interior Temperature (°F) | AER 1/hr | Volume ft ³ | Duration of Test minutes |
|---------------|----------------|--------|------------------|------------------|-------------------------|-------------------------|---------------------------|----------|------------------------|--------------------------|
| 4/2/2013 | 4/9/2013 | 7247 | 166.00 | 21.00 | 422 Second Floor Office | PMCH | 74.4 | 1.03 | 9,002 | 10,040 |
| 4/2/2013 | 4/9/2013 | 17946 | 126.00 | 16.00 | 422 First Floor Center | PMCH | 69.7 | 1.36 | 9,002 | 10,033 |
| 4/2/2013 | 4/9/2013 | 14883 | 12.00 | 65.00 | 422 Basement Center | PDCH | 60.2 | 1.40 | 4,547 | 10,030 |
| 4/2/2013 | 4/9/2013 | 9304 | 10.00 | 60.00 | 422 Basement Center Dup | PDCH | 60.2 | 1.52 | 4,547 | 10,030 |
| 4/2/2013 | 4/9/2013 | 15680 | 0 | 7 | 420 1st | PMCH | 57.2 | | 9,002 | 10,022 |

The measurements of air exchange rate (not during fan tests) are almost all between the 50th and 90th percentile of the range of Midwestern values compiled in EPA’s *Exposure Factor Handbook* (U.S. EPA, 2011; **Table 5-23**).

Table 5-23. National Survey of Air Exchange Rates, Reprinted from the *EPA Exposure Factor Handbook* (U.S. EPA, 2011)

| Summary Statistics for Residential Air Exchange Rates (in AER, 1/hr ³), by Region | | | | | |
|---|-------------|----------------|------------------|--------------|-------------|
| | West Region | Midwest Region | Northeast Region | South Region | All Regions |
| Arithmetic mean | 0.66 | 0.57 | 0.71 | 0.61 | 0.63 |
| Arithmetic standard deviation | 0.87 | 0.63 | 0.60 | 0.51 | 0.65 |
| Geometric mean | 0.47 | 0.39 | 0.54 | 0.46 | 0.46 |
| Geometric standard deviation | 2.11 | 2.36 | 2.14 | 2.28 | 2.25 |

(continued)

Table 5-23. National Survey of Air Exchange Rates, Reprinted from the *EPA Exposure Factor Handbook* (U.S. EPA, 2011) (cont.)

| Summary Statistics for Residential Air Exchange Rates (in AER, 1/hr ^a), by Region | | | | | |
|---|-------------|----------------|------------------|--------------|-------------|
| | West Region | Midwest Region | Northeast Region | South Region | All Regions |
| 10th percentile | 0.20 | 0.16 | 0.23 | 0.16 | 0.18 |
| 50th percentile | 0.43 | 0.35 | 0.49 | 0.49 | 0.45 |
| 90th percentile | 1.25 | 1.49 | 1.33 | 1.21 | 1.26 |
| Maximum | 23.32 | 4.52 | 5.49 | 3.44 | 23.32 |

^aAER = ACH = Air exchanges per hour.

Source: Koontz and Rector, 1995, as cited in U.S. EPA (2011), Table 19-24.

5.4.3 Stack Gas Measurements to Define Flux to Structure

From stack velocity measurements (multiple instantaneous) and Waterloo sampler VOC concentrations in the stack (typically integrated over one week) we calculated estimates of the mass of PCE and chloroform emitted by the SSD system over time (**Table 5-24**). Although the values expressed as micrograms may seem large at first the average emission of PCE can also be expressed as 0.11 grams/day or 0.000010 pounds per hour. Some perspective on these values can be provided by noting that:

- Controls are often required on VOC sources with emission rates exceeding 3 pounds per hour and 3.1 tons per year (U.S. EPA, 2008).
- Heggie and Stavropoulos (2010) measured a TCE flux rate between 41 and 312 $\mu\text{g}/\text{m}^2/\text{h}$ for an Australian vapor intrusion site. Our average PCE flux converts to 40 $\mu\text{g}/\text{m}^2/\text{h}$.
- These discharges are, however, considerably higher than those reported for Altus AFB and Hill AFB buildings, which expressed as deep soil gas to subslab discharge¹² ranged from 0.16 to 467 $\mu\text{g}/\text{day}$ (GSI, 2008).
- Without mitigation, we can estimate the discharge of VOCs into the Indianapolis structure as follows: Assume the 422 basement, with an air exchange rate of 0.74 per hour (**Table 5-19**) and a volume of 129 m^3 . Apply the mean 422 Base South sampling location concentration of 0.65 $\mu\text{g}/\text{m}^3$ (**Table 5-16** of this report); this yields a VOC mass discharge of 1,500 $\mu\text{g}/\text{day}$ (0.0015 grams/day) for the half of the duplex that has generally higher concentrations.

This brief analysis suggests that the mass flux and discharge rates measured are reasonable and are likely increased under mitigation on conditions. This agrees with the finding discussed in Section 6.1.2 that SSD system operation increases the concentration in subslab soil gas in many of our measurements.

¹²Reported as “mass flux” in GSI (2008)

Table 5-24. Stack Gas Discharge Measurements During Mitigation

| Stack Discharge Measurement Summary—SSD Mitigation On | | | |
|--|--------------------------------|--|---|
| VOC Sample Date Collected | Flow Data Date Acquired | Stack Discharge of PCE (µg/day) | Stack Discharge of Chloroform (µg/day) |
| 12/26/2012 | 12/28/2012 | 87,000 | 110,000 |
| 12/26/2012 | 12/28/2012 | 86,000 | 110,000 |
| 2/20/2013 | 2/21/2013 | 160,000 | 40,000 |
| 4/3/2013 | 4/3/2013 | 120,000 | 46,000 |
| 4/3/2013 | 4/3/2013 | 120,000 | 46,000 |
| Average | | 114,000 | 70,000 |

Note: PCE and chloroform stack discharges are rounded to 2 significant figures

Table of Contents

| | | |
|-------|---|------|
| 6.0 | Results and Discussion: VOC Concentration Temporal Trends and Relationship to HVAC and Mitigation | 6-1 |
| 6.1 | VOC Seasonal Trends Based on Weekly, Biweekly, and Monthly Measurements for 52+ Weeks..... | 6-1 |
| 6.1.1 | Indoor Air | 6-1 |
| 6.1.2 | Subslab Soil Gas | 6-4 |
| 6.1.3 | Shallow and Deep Soil Gas..... | 6-15 |
| 6.2 | Radon Seasonal Trends (based on Weekly Measurements)..... | 6-46 |
| 6.3 | VOC Short-Term Variability (Based on Daily and Hourly VOC Sampling)..... | 6-46 |
| 6.3.1 | Indoor Air | 6-46 |
| 6.3.2 | Subsurface Soil Gas Data..... | 6-52 |
| 6.4 | Radon Short-Term Variability (Based on Daily and More Frequent Measurements)..... | 6-59 |
| 6.5 | Outdoor Climate/Weather Data..... | 6-60 |
| 6.5.1 | Indianapolis Weather Compared with VOCs and Radon | 6-66 |

List of Figures

| | | |
|-------|---|------|
| 6-1. | PCE concentrations in indoor and ambient air vs. time (7-day Radiello samples)..... | 6-2 |
| 6-2. | Chloroform concentrations in indoor and ambient air vs. time (7-day Radiello samples). | 6-2 |
| 6-3. | Benzene concentrations in indoor air..... | 6-3 |
| 6-4. | Toluene concentrations in indoor air. | 6-4 |
| 6-5. | Interior and exterior sampling port locations. Sampling ports sampled by the on-site GC are shown in red, with parenthetical notes indicating which SGP depths were sampled by the GC. | 6-5 |
| 6-6a. | Plot of subslab chloroform concentrations vs. time (TO-17 data)..... | 6-6 |
| 6-6b. | Plot of subslab chloroform concentrations vs. time, first intensive sampling period (TO-17 data). | 6-6 |
| 6-6c. | Plot of subslab chloroform concentrations vs. time mitigation testing period (TO-17 data). | 6-7 |
| 6-7a. | Plot of subslab PCE concentrations vs. time. (TO-17 data)..... | 6-7 |
| 6-7b. | Plot of subslab PCE concentrations vs. time, first intensive sampling period. (TO-17 data). | 6-8 |
| 6-7c. | Plot of subslab PCE concentrations vs. time, mitigation testing period (TO-17 data). | 6-8 |
| 6-7d. | Plot of subslab PCE concentrations vs. time, mitigation testing period; real time GC..... | 6-9 |
| 6-8a. | Plot of wall port chloroform concentrations vs. time (method TO-17). | 6-11 |
| 6-8b. | Plot of WP-3 chloroform concentrations vs. time (online GC). | 6-12 |
| 6-9a. | Plot of wall port PCE concentrations vs. time (method TO-17)..... | 6-13 |
| 6-9b. | Plot of WP-3; PCE concentrations vs. time (online GC)..... | 6-14 |

| | | |
|-------|--|------|
| 6-10. | Chloroform concentrations at subslab and 6-ft soil gas ports directly under the 420 side of duplex..... | 6-18 |
| 6-11. | PCE concentrations at 6-ft soil gas ports and subslab immediately below the 420 side of the duplex..... | 6-19 |
| 6-12. | Chloroform concentrations at 9-ft soil gas ports below 420 side of the duplex..... | 6-20 |
| 6-13. | PCE concentrations at soil gas points 9 ft below the 420 side of duplex..... | 6-21 |
| 6-14. | Chloroform concentrations in soil gas at 13 ft below the 420 side of the duplex..... | 6-22 |
| 6-15. | PCE concentrations in soil gas at 13 ft below the 420 side of duplex..... | 6-23 |
| 6-16. | Chloroform concentrations in soil gas at 16.5 ft below the 420 side of duplex..... | 6-24 |
| 6-17. | PCE concentrations in soil gas at 16.5 ft below the 420 side of the duplex..... | 6-25 |
| 6-18. | Chloroform concentrations in 6-ft soil gas and subslab ports immediately below the 422 side of the duplex..... | 6-26 |
| 6-19. | PCE concentrations in 6-ft soil gas ports and subslab ports directly below the 422 side of the duplex..... | 6-27 |
| 6-20. | Chloroform concentrations in soil gas port at 9-ft depth below 422 side of duplex..... | 6-28 |
| 6-21. | PCE concentrations in soil gas at 9 ft below the 422 side of the duplex..... | 6-29 |
| 6-22. | Chloroform concentrations in soil gas at 13 ft below the 422 side of the duplex..... | 6-30 |
| 6-23. | PCE concentrations in soil gas at 13 ft below the 422 side of the duplex..... | 6-31 |
| 6-24. | Chloroform concentrations at 16.5 ft below the 422 side of the duplex..... | 6-32 |
| 6-25. | PCE concentrations at 16.5 ft below the 422 side of the duplex..... | 6-33 |
| 6-26. | Chloroform concentrations in exterior soil gas at 3.5 ft bls..... | 6-34 |
| 6-27. | PCE concentrations in exterior soil gas at 3.5 ft bls..... | 6-35 |
| 6-28. | Chloroform concentrations in exterior soil gas at 6 ft. bls..... | 6-36 |
| 6-29. | PCE concentrations in exterior soil gas at 6 ft bls..... | 6-37 |
| 6-30. | Chloroform concentrations in exterior soil gas at 9 ft bls..... | 6-38 |
| 6-31. | PCE concentrations in exterior soil gas at 9 ft bls..... | 6-39 |
| 6-32. | Chloroform concentrations in exterior soil gas at 13 ft bls..... | 6-40 |
| 6-33. | PCE concentrations in exterior soil gas at 13 ft bls..... | 6-41 |
| 6-34. | Chloroform concentrations in exterior soil gas at 16.5 ft bls..... | 6-42 |
| 6-35. | PCE concentrations in exterior soil gas at 16.5 ft bls..... | 6-43 |
| 6-36. | Subslab PCE concentrations over a 1-week period during the first intensive round..... | 6-44 |
| 6-37. | Subslab PCE concentrations over a 1-week period during the second intensive round..... | 6-44 |
| 6-38. | Radon: Weekly time integrated samples (electret)..... | 6-45 |
| 6-39. | Online GC chloroform indoor air data for 422 first floor..... | 6-46 |
| 6-40. | Online GC chloroform indoor air data for 422 basement..... | 6-47 |
| 6-41. | Online GC chloroform indoor air data for 420 first floor..... | 6-47 |

*Section 6—Results and Discussion:
VOC Concentration Temporal Trends and Relationship to HVAC and Mitigation*

| | | |
|-------|---|------|
| 6-42. | Online GC chloroform indoor air data for 420 basement. | 6-48 |
| 6-43. | Online GC PCE indoor air data for 422 first floor. | 6-49 |
| 6-44. | Online GC PCE indoor air data for 422 basement. | 6-49 |
| 6-45. | Online GC PCE indoor air data for 420 first floor. | 6-50 |
| 6-46. | Online GC PCE indoor air data for 420 basement. | 6-50 |
| 6-47. | Online GC subsurface chloroform soil gas data—Phase 1 and Phase 2. | 6-52 |
| 6-48. | Online GC subsurface chloroform soil gas data—Phase 1. | 6-52 |
| 6-49. | Online GC subsurface chloroform soil gas data—Phase 2. | 6-53 |
| 6-50. | Online GC subsurface PCE soil gas data—Phase 1 and Phase 2. | 6-54 |
| 6-51. | Online GC subsurface PCE soil gas data—Phase 1. | 6-54 |
| 6-52. | Online GC subsurface PCE soil gas data—Phase 2. | 6-55 |
| 6-53. | Method TO-17 data for SSP-4. | 6-55 |
| 6-54. | Online GC PCE measurements in SSP-4. | 6-57 |
| 6-55. | Comparison of online GC measurements of PCE and chloroform in SGP9 at 6 ft. | 6-57 |
| 6-56. | Real-time radon levels (422 basement) 2011–2013. | 6-58 |
| 6-57. | Real-time radon levels (422, 2 nd floor office), 2011–2013. | 6-59 |
| 6-58. | Temperature records from the external temperature monitor and the HOBO devices at seven indoor locations on the 422 and 420 sides of the house. | 6-61 |
| 6-59. | Stacked hydrological graph with rainfall in inches (top—green line), depth to water in feet (middle—red circles), and discharge at Fall Creek in ft ³ /s (bottom—blue line). | 6-62 |
| 6-60. | Plot of high wind speed for measurement period, wind run and wind speed (average over measurement period) at 422/420 house over time. | 6-63 |
| 6-61. | Weather variables measured inside 422 office (2nd floor) and on roof: a. barometric pressure (in Hg); b. indoor air density, c. indoor air equilibrium moisture content, d, indoor percent humidity, f. outdoor percent humidity, g. rain (inches total in measurement period), h. rain rate—the most intense rainfall during the measurement period in inches/hour. | 6-64 |
| 6-62. | Snow depth vs. time (data are from NCDC records for the Indianapolis International Airport). | 6-65 |
| 6-63. | GC Phase 2 VOCs at WP-3 compared with 422/420 house external pressure. | 6-66 |
| 6-64. | GC Phase 3 VOCs at WP-3 compared with 422/420 house external pressure. | 6-67 |
| 6-65. | GC Phase 2 VOCs at WP-3 compared with 422/420 house external wind speed. | 6-68 |
| 6-66. | GC Phase 3 VOCs at WP-3 compared with 422/420 house external wind speed. | 6-69 |
| 6-67. | GC chloroform at subslab and soil gas ports versus radon from stationary AlphaGUARDS. | 6-72 |
| 6-68. | GC PCE at subslab ports versus radon from stationary AlphaGUARDS. | 6-73 |
| 6-69. | GC chloroform in indoor air versus radon from stationary AlphaGUARDS. | 6-74 |

| | | |
|-------|--|------|
| 6-70. | GC PCE in indoor air versus radon from stationary AlphaGUARDS..... | 6-75 |
| 6-71. | GC chloroform concentrations in indoor air, 420 first floor..... | 6-76 |
| 6-72. | GC chloroform concentrations in indoor air, 420 basement south. | 6-76 |
| 6-73. | GC PCE concentrations in indoor air, 420 first floor. | 6-77 |
| 6-74. | GC PCE concentrations in indoor air, 420 basement south. | 6-77 |

List of Tables

| | | |
|------|--|------|
| 6-1. | Frequency of NondetecSamples (%) by Soil Gas Point or Cluster..... | 6-16 |
| 6-2. | Frequency of Nondetects in TO-17 VOC Data by Soil Gas Sampling Depth | 6-16 |
| 6-3. | Summary Meteorological Data for Central Indiana Note that the symbols “^” and “v” mean “above” and “below” normal, respectively, and that the weekly values show how the weekly averages differ from normal (from Scheeringa and Hudson, 2012, 2013) | 6-60 |
| 6-4. | Summary of Meteorological Data During the 2012/2013 Snow and Ice Events | 6-78 |

6.0 Results and Discussion: VOC Concentration Temporal Trends and Relationship to HVAC and Mitigation

6.1 VOC Seasonal Trends Based on Weekly, Biweekly, and Monthly Measurements for 52+ Weeks

6.1.1 Indoor Air

Figures 6-1 and **6-2** show PCE and chloroform concentrations over time, respectively, at all six indoor air monitoring locations, in addition to the ambient location (see **Figure 3-10a and b** for the placement of the indoor air sampling racks). PCE concentrations at all six indoor locations follow the same general trend of starting higher at the beginning of the project, dropping to a low in spring, and rising slightly and leveling out through the end of the premitigation period. Indoor air sampling was discontinued from February 2012 to October 2012 because of funding limitations. However, the concentrations in October 2012 before the mitigation system was installed were very similar to those observed in October 2011. The timing of the spring minimum differed substantially for the unheated side of the duplex (when it occurred in late March) from the heated side of the duplex (where the minimum was reached in July). The highest readings were generally found at 422 basement south except during brief periods when first floor concentrations were higher, which occurred mostly during operation of a basement depressurization fan in 422 (see U.S. EPA, 2012a, Section 12.2).

Highlights of the PCE concentration patterns shown in **Figure 6-1** are:

1. Indoor air PCE concentrations during the first period of active mitigation rose to levels not seen in the duplex since February 2011. The concentrations continued to rise after the mitigation system was switched into a passive mode, reaching a maximum of $5.7 \mu\text{g}/\text{m}^3$ in November 2012. Indoor air concentrations higher than $5.7 \mu\text{g}/\text{m}^3$ had not been observed at the duplex since January and February 2011.
2. In discussions and comments during conference presentations (Schumacher et al., 2013; Lutes et al., 2012a, 2012b, 2012c, 2012d) on the earlier PCE data set (through February 2012), questions were raised about whether the highest PCE concentrations observed in January and February 2011 were artifacts. At the time, the authors offered other lines of evidence (such as the lack of indoor sources, preparation of the house prior to sampling) as support for the observed levels. The observation of higher PCE post-mitigation during the winter of 2012 to 2013 does confirm that the subsurface can yield enough vapor intrusion-derived PCE to account for the January 2011 concentrations. We postulate that VOCs can be moved close to the structure either by a cumulative stack effect during a severe winter or by an SSD system, at least during its initial period of operation. How VOC levels will change over time as the mitigation system continues to operate remains to be seen.

Chloroform concentration patterns (see **Figure 6-2**) were generally similar to PCE and can be summarized as follows:

1. Broadly, the six indoor locations show a general concentration decline from a localized maximum at the beginning of the sampling interval in January 2011. The minimum was reached at the end of spring on the 422 side of the house (early July), as with PCE. Also similar to PCE's behavior, the chloroform minimum concentration on the 420 side of the house occurred much earlier in the year (March).

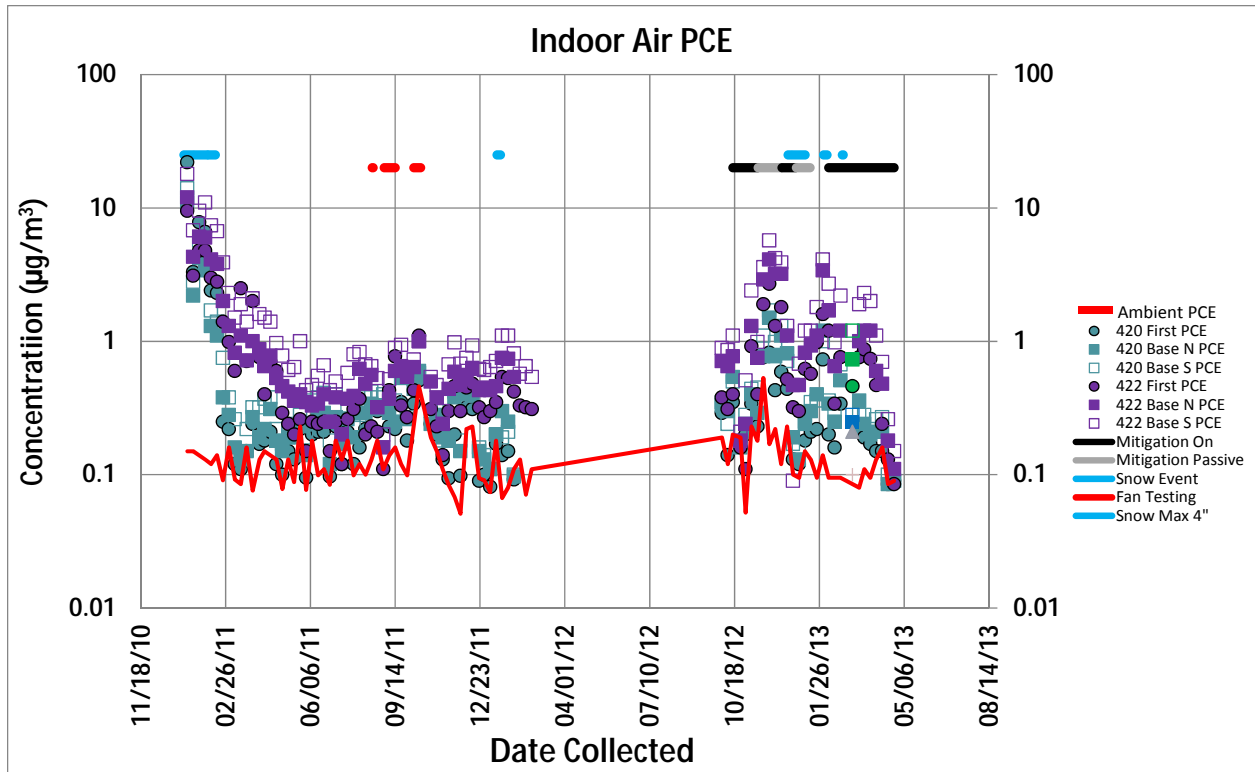


Figure 6-1. PCE concentrations in indoor and ambient air vs. time (7-day Radiello samples).

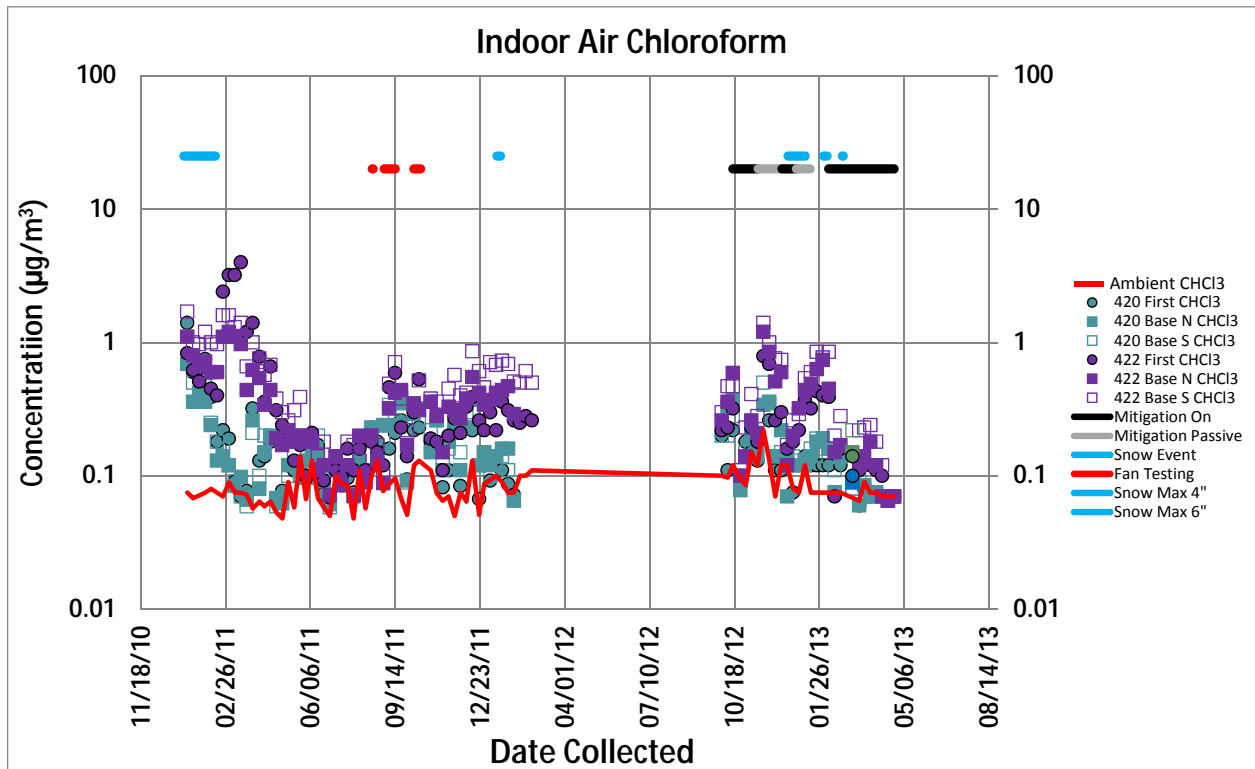


Figure 6-2. Chloroform concentrations in indoor and ambient air vs. time (7-day Radiello samples).

2. The levels at the 422 first floor sampling location rose abruptly to a maximum in March 2011 immediately after the first brief drop in January. During this maximum, the first floor concentrations exceeded those of even the basement stations. The 422 basement sampling stations showed a less dramatic rise in this period.
3. Chloroform concentrations reached a minimum in July 2011 and began steadily increasing thereafter, forming a generally U-shaped curve. The winter 2012 levels more closely approached their 2011 highs than do the corresponding PCE results.
4. The second maximum concentration for chloroform occurred in October 2011 for the 420 (unheated) locations and was followed by a considerable decline through the winter months. A second peak occurred later (December 2012) on the 422 (heated) side of the duplex and concentrations stayed near that maximum until February 2012.
5. The concentrations of chloroform in October 2012 when sampling was restarted after a break since February 2012 were similar to those observed in October 2011.

With the exception of the elevated chloroform from late February to late March 2011, the highest chloroform levels were found at 422 basement south, the same station that was generally highest for PCE (Figures 6-1 and 6-2).

Figures 6-3 and 6-4 show benzene and toluene indoor air concentrations at 422 basement south over time, along with ambient concentrations of benzene and toluene. Although both benzene and toluene concentrations are above their action levels (benzene = $0.31\mu\text{g}/\text{m}^3$; toluene = $0.0052\mu\text{g}/\text{m}^3$; RSL Summary Table, Nov., 2011), each tends to trend similarly to its respective ambient concentrations; this is not the case with PCE or chloroform concentrations, which are almost always considerably higher than in the ambient air. This suggests that benzene and toluene indoor air concentrations are controlled by ambient air, not vapor intrusion.

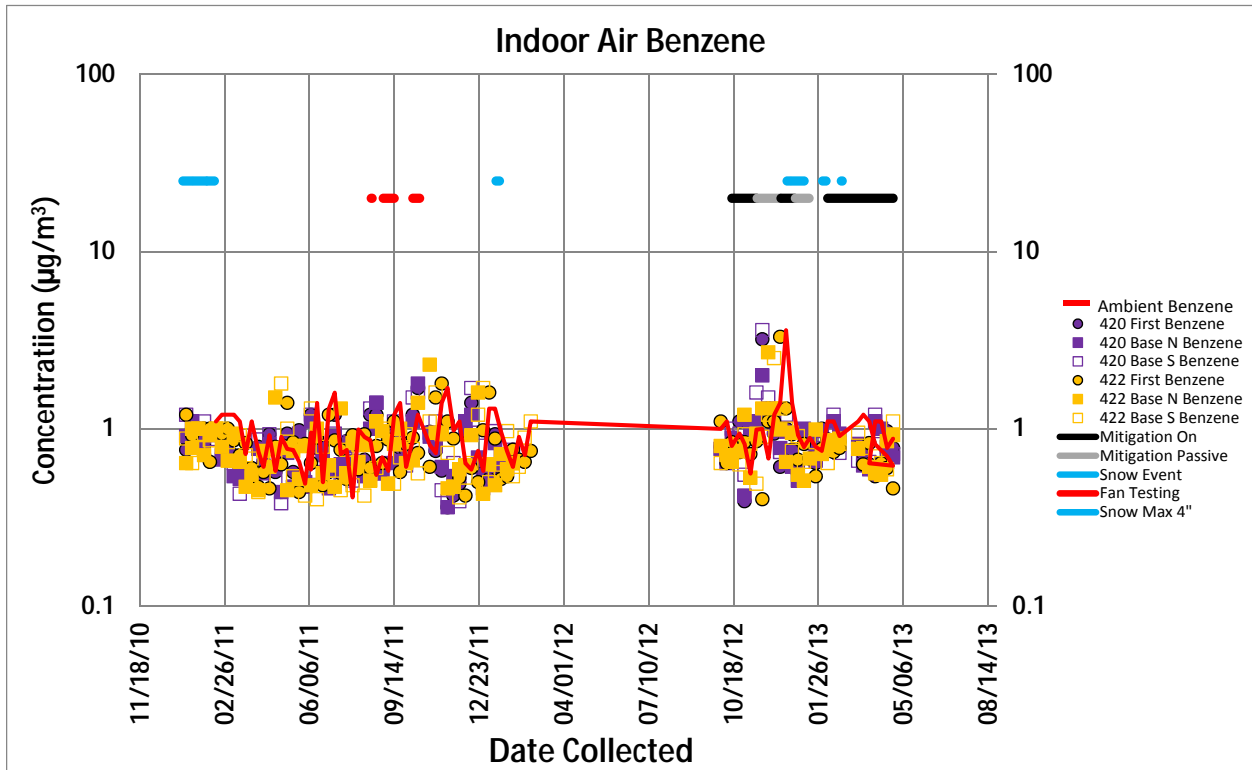


Figure 6-3. Benzene concentrations in indoor air.

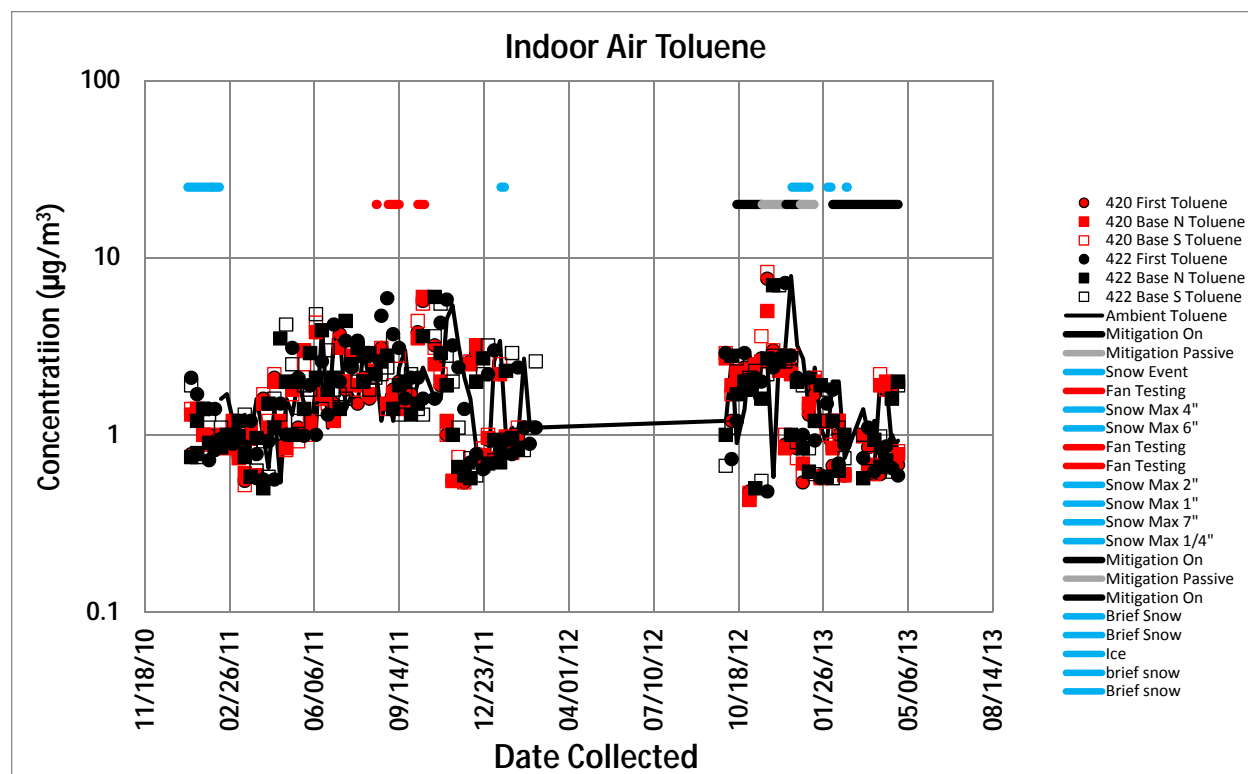


Figure 6-4. Toluene concentrations in indoor air.

6.1.2 Subslab Soil Gas

Subslab sampling ports (SSPs) were placed throughout the basement of both the 420 and 422 sides of the duplex, as shown in **Figure 6-5**. Interior soil gas probes (SGPs) are also shown in this figure, with each probe having multiple sampling ports at 6 ft, 9 ft, 13 ft, and 16.5 ft, with the 6 ft SGP's being at an equivalent depth bls to the SSPs. Given the low initial concentration of SSP-2 and its nearness to SGP10-6, SSP-2 was sampled relatively infrequently. On the 420 side of the house are SSP-3 and SSP-5 through -7 and WP-4. The basements of both sides of the duplex are each divided into thirds in the interior. There is generally one SSP per basement division, with one section on the 420 side having two. The wall ports are located on the exterior walls of the duplex. WP-1 and 3 are each located in the centers of the north and south ends of the 422 basement, and WP-2 is in the center of the east side of the 422 basement. WP-4 is located in the center of the west wall of the 420 basement (**Figure 6-5**). The wall ports are approximately 3 ft bls.

Figures 6-6a, 6-6b, and 6-6c (for chloroform) and **6-7a, 6-7b, and 6-7c** (PCE) plot VOC concentrations over time. Figures 6-6a and 6-7a present an overview of subslab TO-17 data, the b versions of these figures represent intensive sampling periods, and the c sections focus on the mitigation testing period.¹³ For chloroform, as shown in **Figure 6-6a**, most of the ports on the unheated 420 side (the various crosses and the square) were generally stable for most of the duration of the project prior to mitigation. However, some subslab ports, such as SSP-4 and SSP-7, reached new high concentrations after mitigation began. Yet within the mitigation testing period there is no clear visible VOC concentration trend as the system is switched on and off (**Figure 6-6c**), perhaps because of the limited amount of available data (see also the discussion of the descriptive statistics for these concentrations in Section 5.3).

¹³During the normal times, the subslab samples were collected during regular daytime working hours, while the intensive periods involved two shifts of personnel, allowing up to three samples to be collected, generally early morning, midday, and evening.

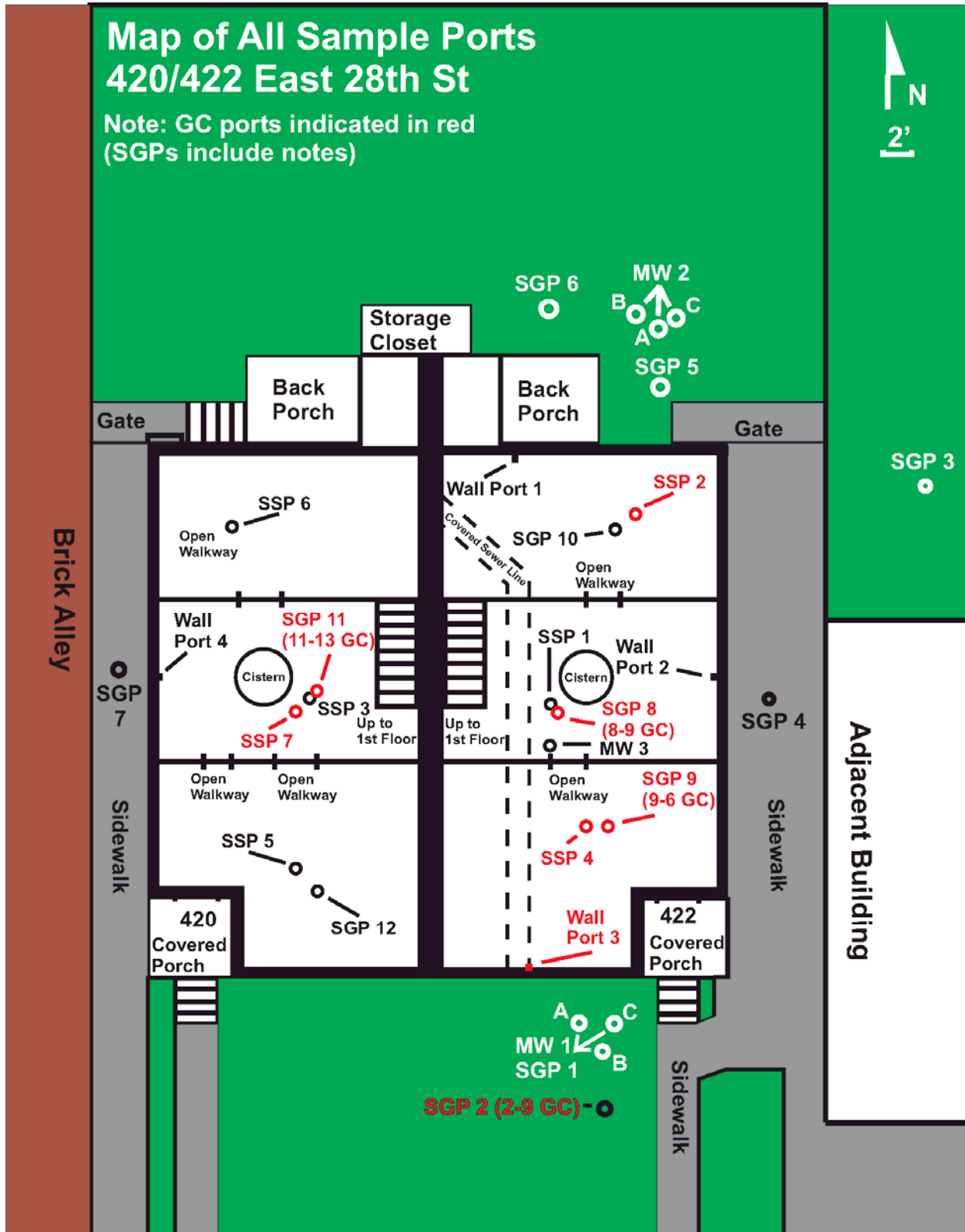


Figure 6-5. Interior and exterior sampling port locations. Sampling ports sampled by the on-site GC are shown in red, with parenthetical notes indicating which SGP depths were sampled by the GC.

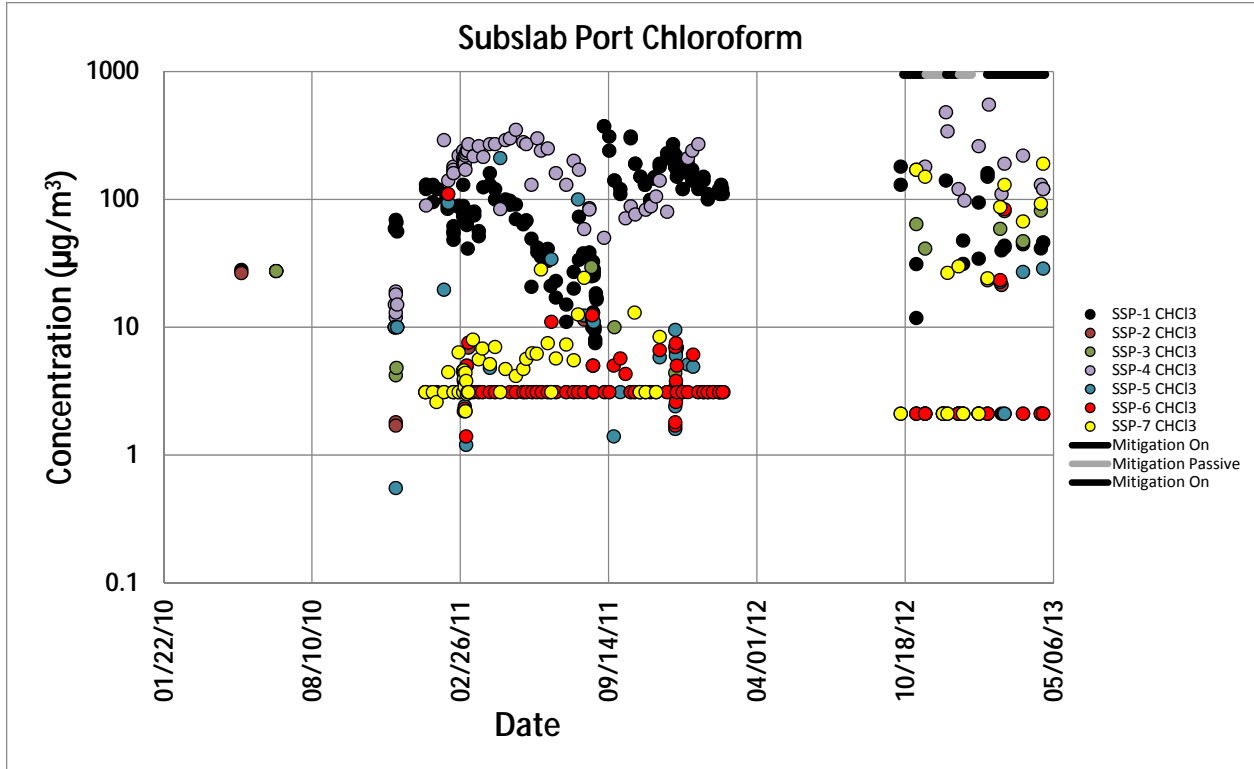


Figure 6-6a. Plot of subslab chloroform concentrations vs. time (TO-17 data).

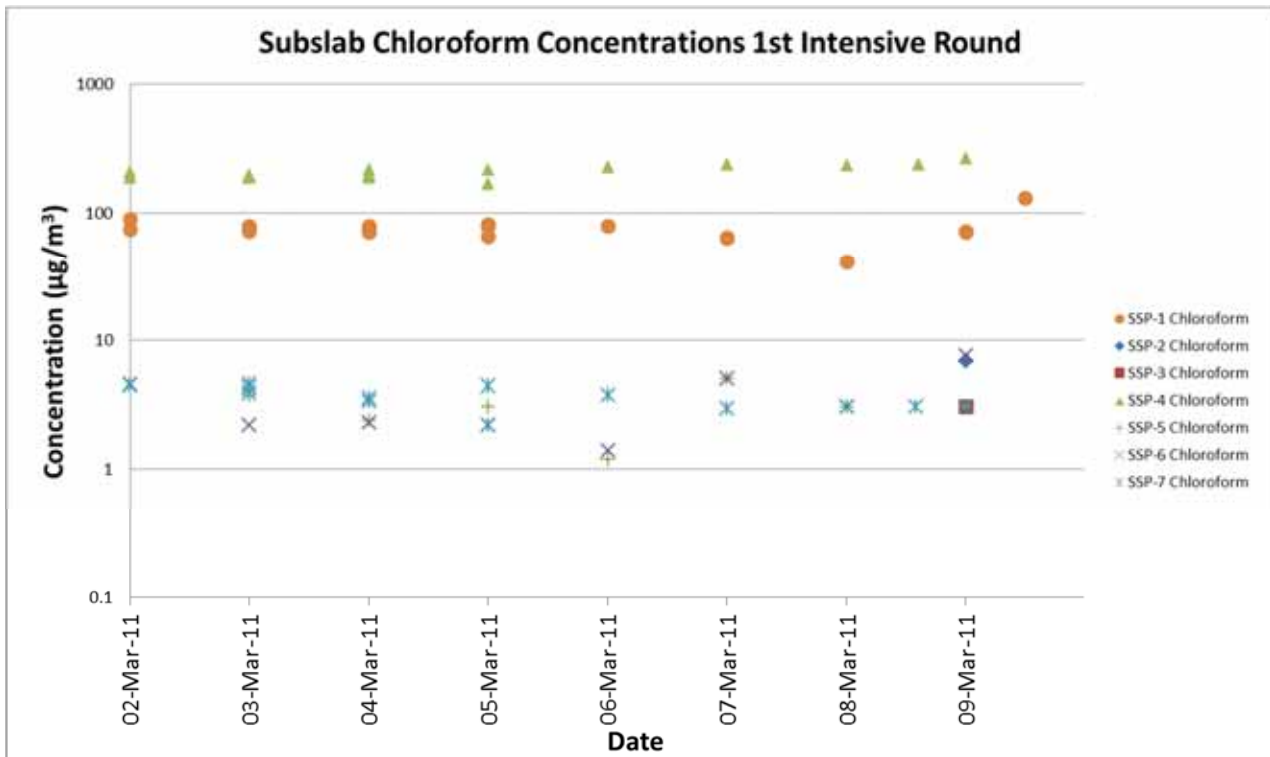


Figure 6-6b. Plot of subslab chloroform concentrations vs. time, first intensive sampling period (TO-17 data).

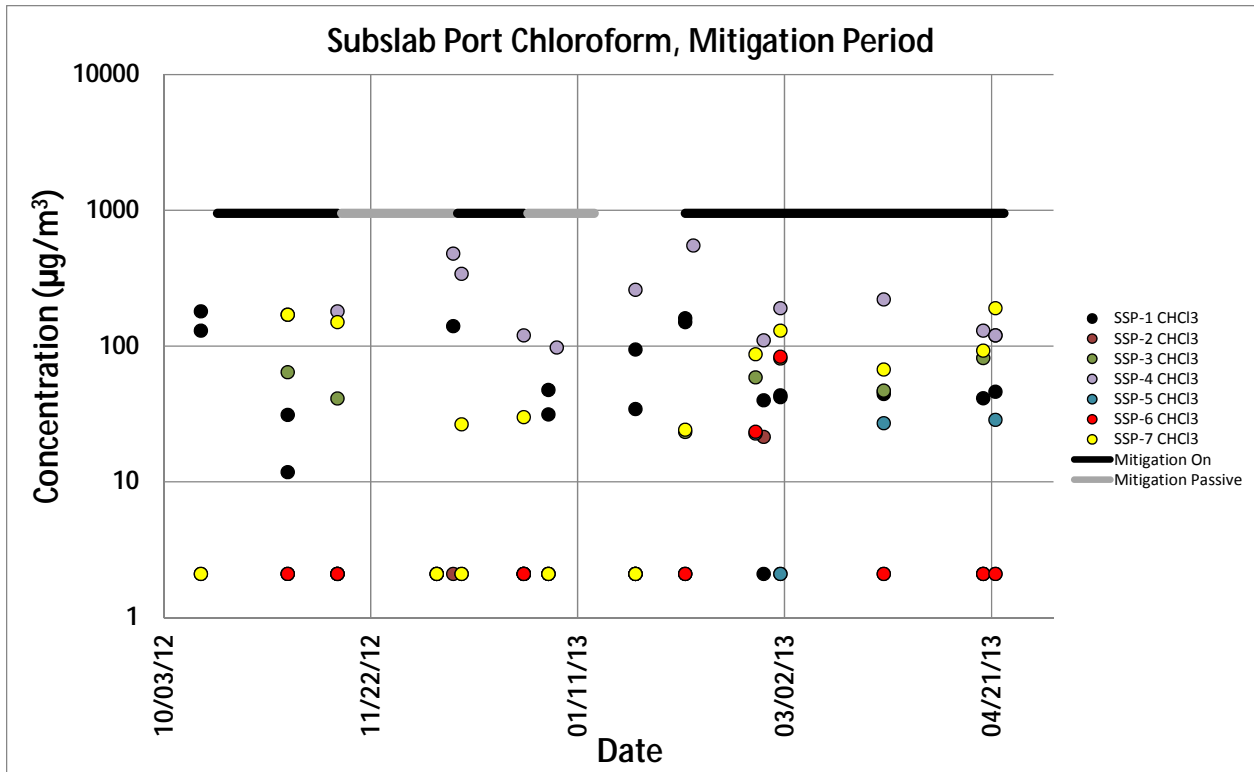


Figure 6-6c. Plot of subslab chloroform concentrations vs. time mitigation testing period (TO-17 data).

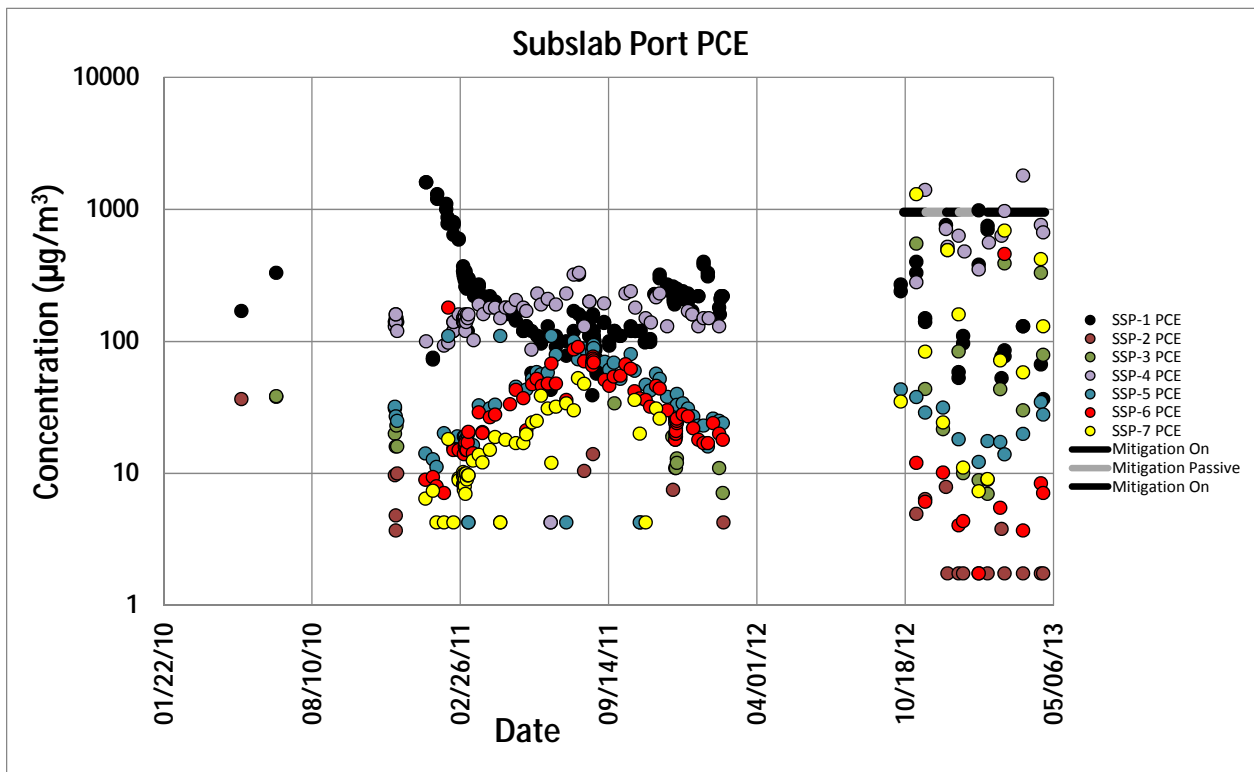


Figure 6-7a. Plot of subslab PCE concentrations vs. time. (TO-17 data).

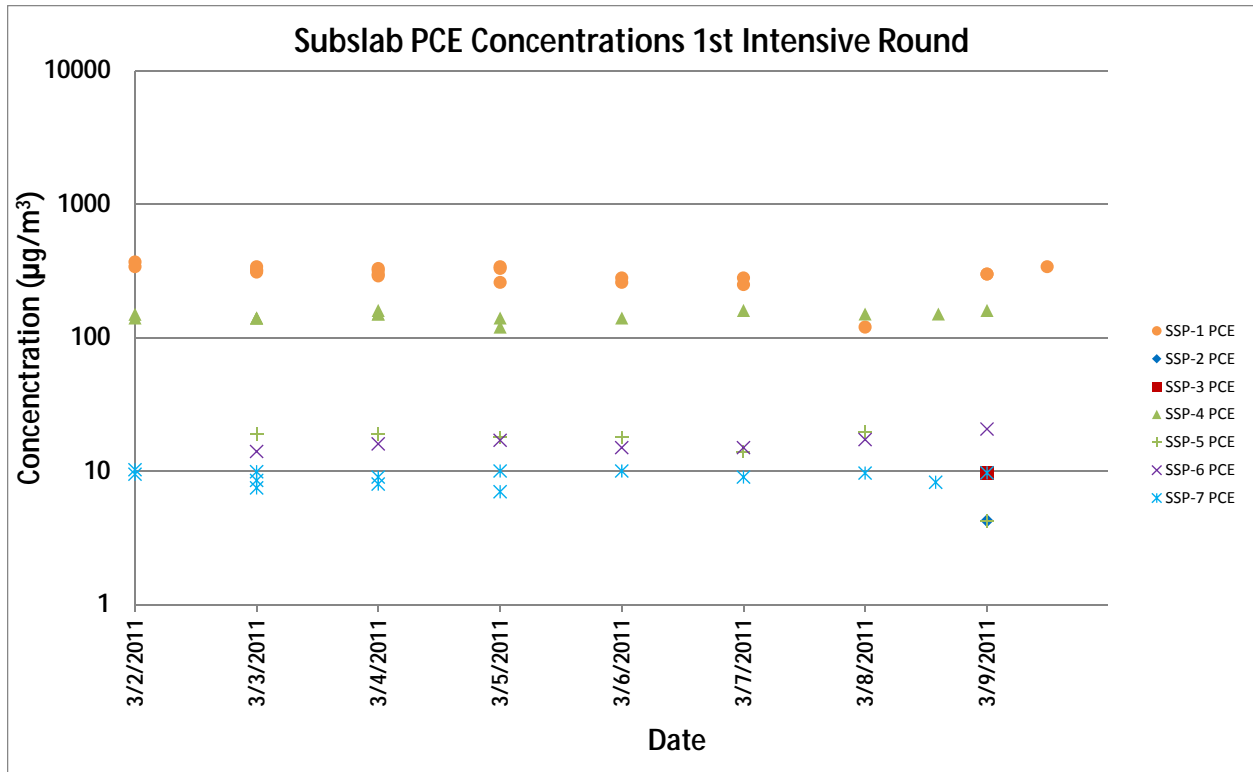


Figure 6-7b. Plot of subslab PCE concentrations vs. time, first intensive sampling period. (TO-17 data).

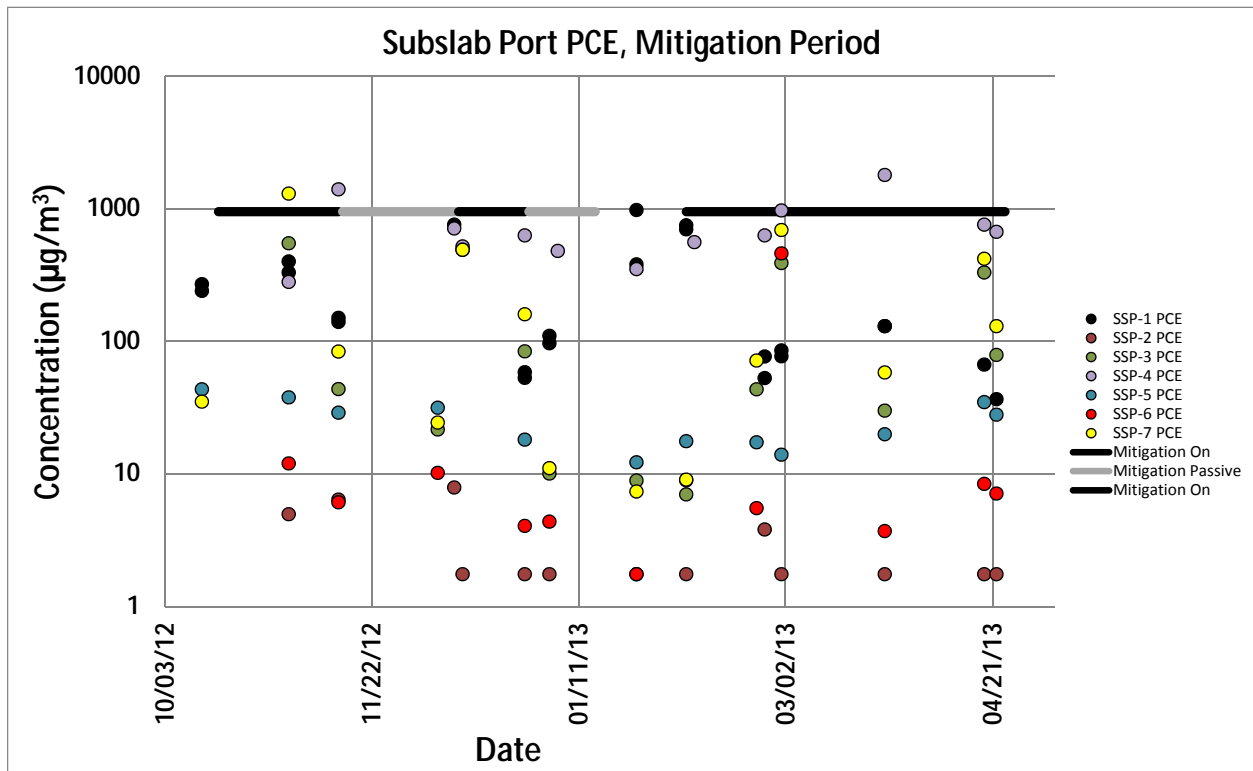


Figure 6-7c. Plot of subslab PCE concentrations vs. time, mitigation testing period (TO-17 data).

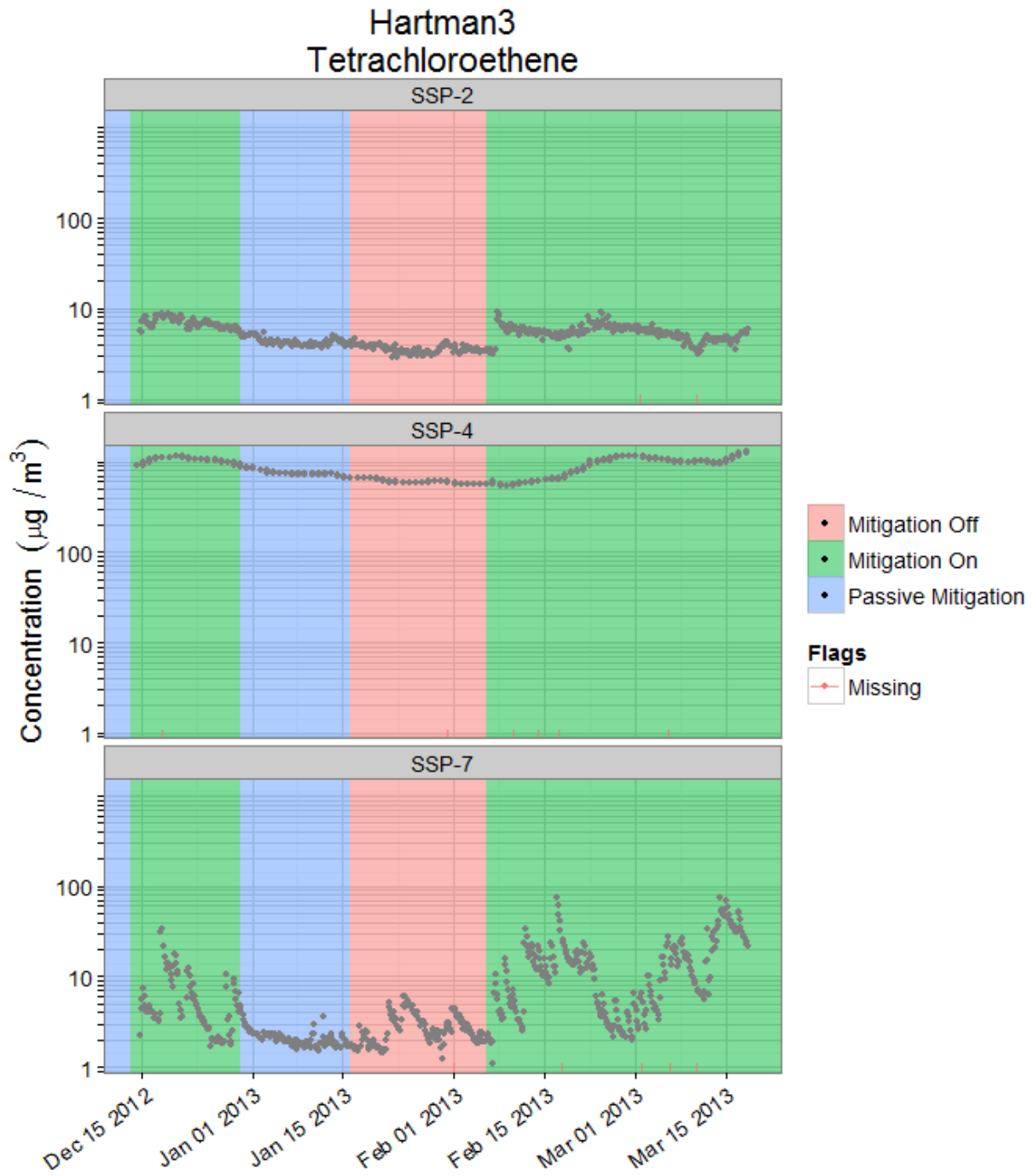


Figure 6-7d. Plot of subslab PCE concentrations vs. time, mitigation testing period; real time GC.

Another exception to the general pattern of chloroform stability is vertical alignment of data points on the plot (indicating concentration variability over a short time period) that occurred during intensive periods of sampling. This may indicate that there was a diurnal pattern in the subslab sampling that was only perceptible during the intensive periods (**Figures 6-6b** and **6-7b**).¹⁴ Another noteworthy observation on the 420 side occurred from July 14, 2011, to August 3, 2011, between the time when thieves stole the house window unit air conditioners (ACs) from both sides of the duplex and when they were replaced on the 422 side only. Chloroform approached its highest levels on the 420 side during this time. Chloroform on the 422 side (shown in **Figure 6-6a** as the circles, diamonds, and triangles) showed a rough sinusoidal concentration trend over months, although the different ports are somewhat out of phase. These trends generally show lows during the warmer months (SSP-1 and SSP-4 seem to both reach a minimum in August/September 2011) and highs during cooler months. It is also notable that the concentration increases abruptly two orders of magnitude between August 27 and September 8, 2011, a period of time during which a series of fan tests (coded B and F) intended to simulate the stack effect expected under winter conditions were conducted (as discussed in Section 12.2 of U.S. EPA [2012a]). Another smaller rise occurs from September 30 to October 14, 2011. Fan test “T” was conducted from October 6 to October 14, 2011.

The subslab ports on the 422 side (heated) have higher concentrations of PCE and chloroform than those on the 420 (unheated) side of the structure. In **Figure 6-7a**, subslab port PCE concentrations versus time more prominently display a simple pattern of high and low concentration changes during warmer and cooler months, respectively, across the range of ports. Most of the ports on the 420 side of the house and SSP-4 on the 422 side showed highs during the warmer months and lows during the cooler months. A notable exception is SSP-1, which showed the opposite PCE concentration trend to all the others. Essentially, there is much more spatial variability among the subslab ports in winter than in summer.

As occurred with chloroform concentrations, some ports—SSP-3, SSP-6, and SSP-7—reached new high PCE values after mitigation began (**Figure 6-7c**). As discussed in the descriptive statistical analysis in Section 5.3, there was a clear trend in PCE concentrations within the mitigation testing period of higher subslab PCE concentrations being associated with the mitigation on.

The higher temporal resolution data from the online GC (**Figure 6-7d**) shows that two subslab ports on either end of the 422 side of the duplex were relatively stable in PCE during mitigation testing (SSP-2 and SSP-4). In contrast, a subslab port near the center of the 420 side of the duplex, SSP-7, showed approximately two orders of magnitude temporal variability during the mitigation testing period. It appears that turning the mitigation system on drew VOCs toward that port. However, even during a long period of having the mitigation system on, more than an order of magnitude of temporal variability was observed at that port.

Neither compound when graphed for the wall ports (**Figure 6-8** nor **Figure 6-9**) shows the same clear patterns of highs and lows found during the changing seasons for the subslab ports in **Figures 6-6a** and **6-7a**. **Figure 6-8a** plots chloroform concentrations at the four wall ports versus time, and **Figure 6-8b** shows more detail of WP-3 based on online GC data. These chloroform levels do not show the same kind of spike during the period when the ACs were stolen as for the chloroform subslab port. Highs for WP-3 in January through February and September through October 2011 seem to suggest influence of the snow and ice and fan testing, respectively. The greater temporal fluctuations of the wall ports as compared with the subslab ports may be attributable to their more shallow depths (approximately 1.5 ft bls) and their position through the exterior basement wall, which results in a greater atmospheric influence and lesser building effects. The detailed data in **Figure 6-8b** show that WP-3 experienced multiday chloroform concentration peaks and valleys during all mitigation periods.

¹⁴ During normal times, the subslab samples were collected during regular daytime working hours, while the intensive periods involved two shifts of personnel, allowing up to three samples to be collected, generally early morning, midday, and evening.

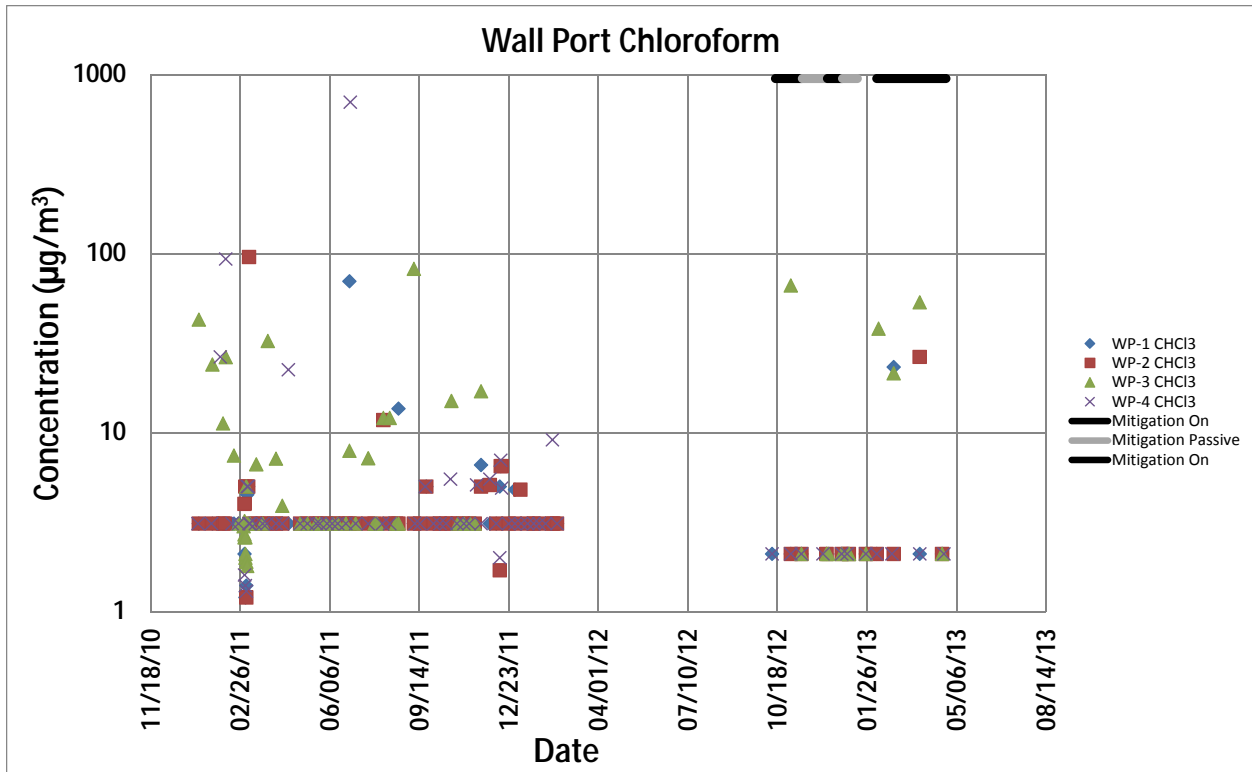


Figure 6-8a. Plot of wall port chloroform concentrations vs. time (method TO-17).

Figure 6-9a plots PCE concentrations at the four wall ports versus time. The wall port concentrations, although generally modest, show more variability than the subslab ports. The high concentrations of PCE in WP-3 at the beginning of the project could be due to the snow and ice capping event during the severe winter of January and February 2011. Highs in September and October 2011 might be attributable to the fan testing during that time. Relatively high VOC concentrations at WP-3 were also reached after the mitigation testing began. This suggests that the SSD system may be drawing VOCs closer to the building envelope.

Higher temporal resolution data using the online GC were obtained for PCE at WP-3 (**Figure 6-9b**). This shows nearly two orders of magnitude of variability in wall port PCE concentrations during the mitigation testing period, including multiday concentration peaks and valleys during all mitigation periods that are similar to those observed for chloroform in **Figure 6-8b**.

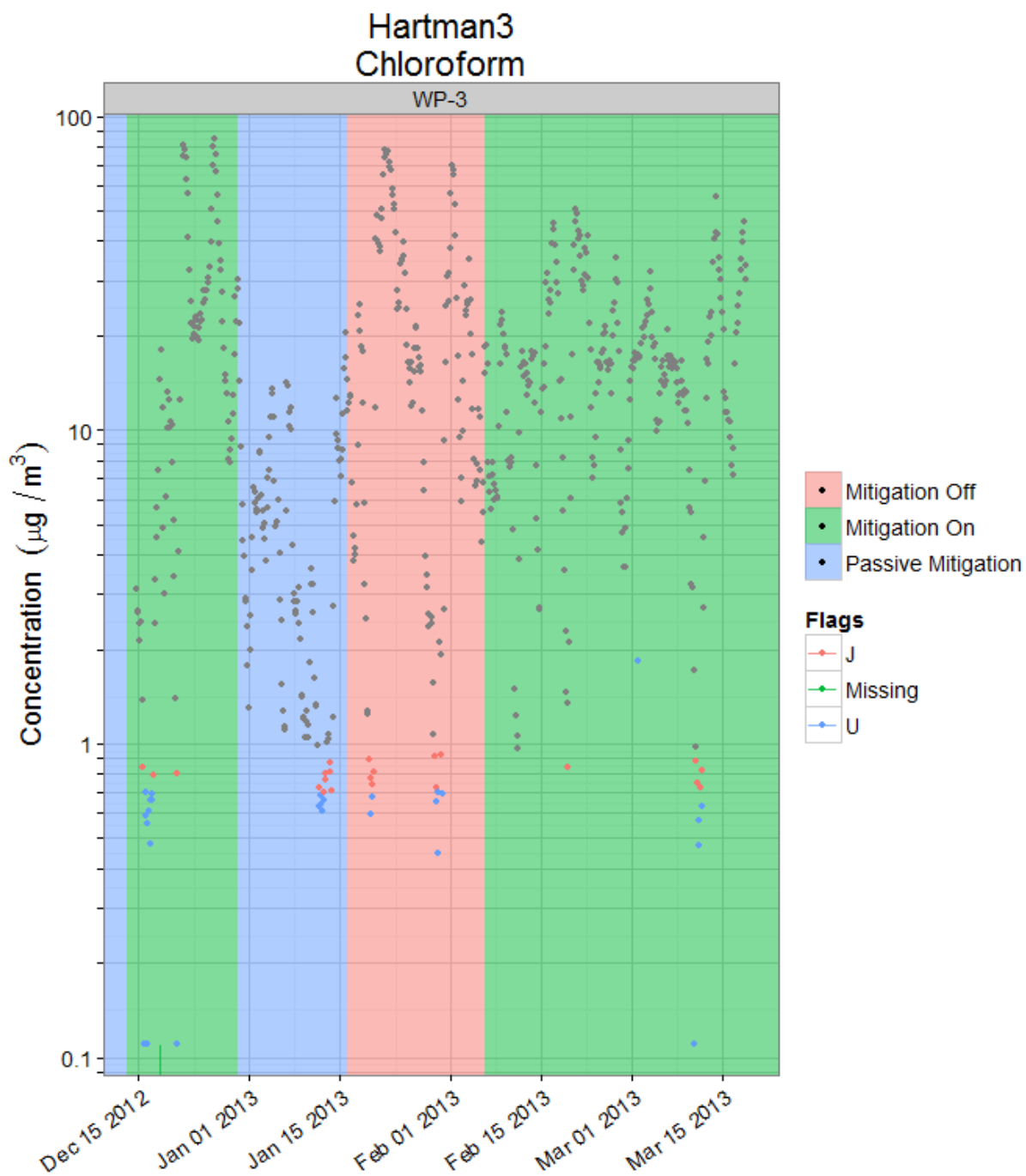


Figure 6-8b. Plot of WP-3 chloroform concentrations vs. time (online GC).

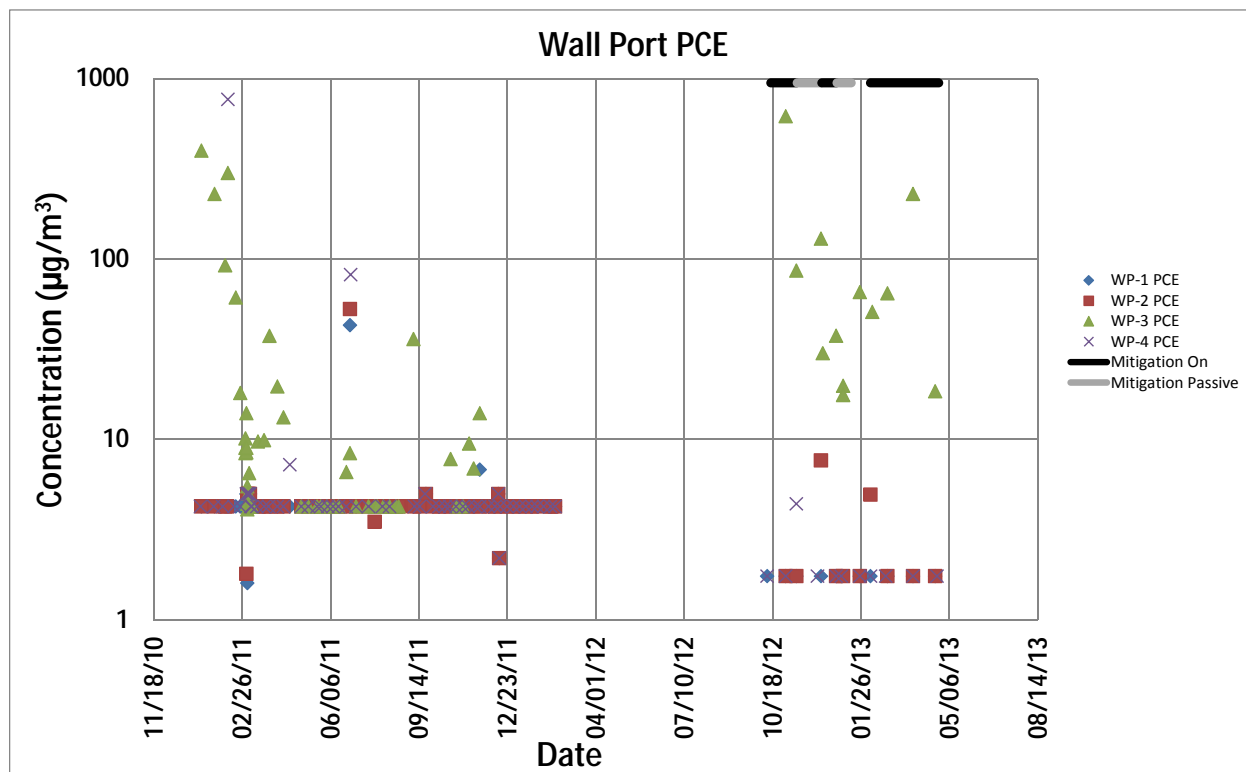


Figure 6-9a. Plot of wall port PCE concentrations vs. time (method TO-17).

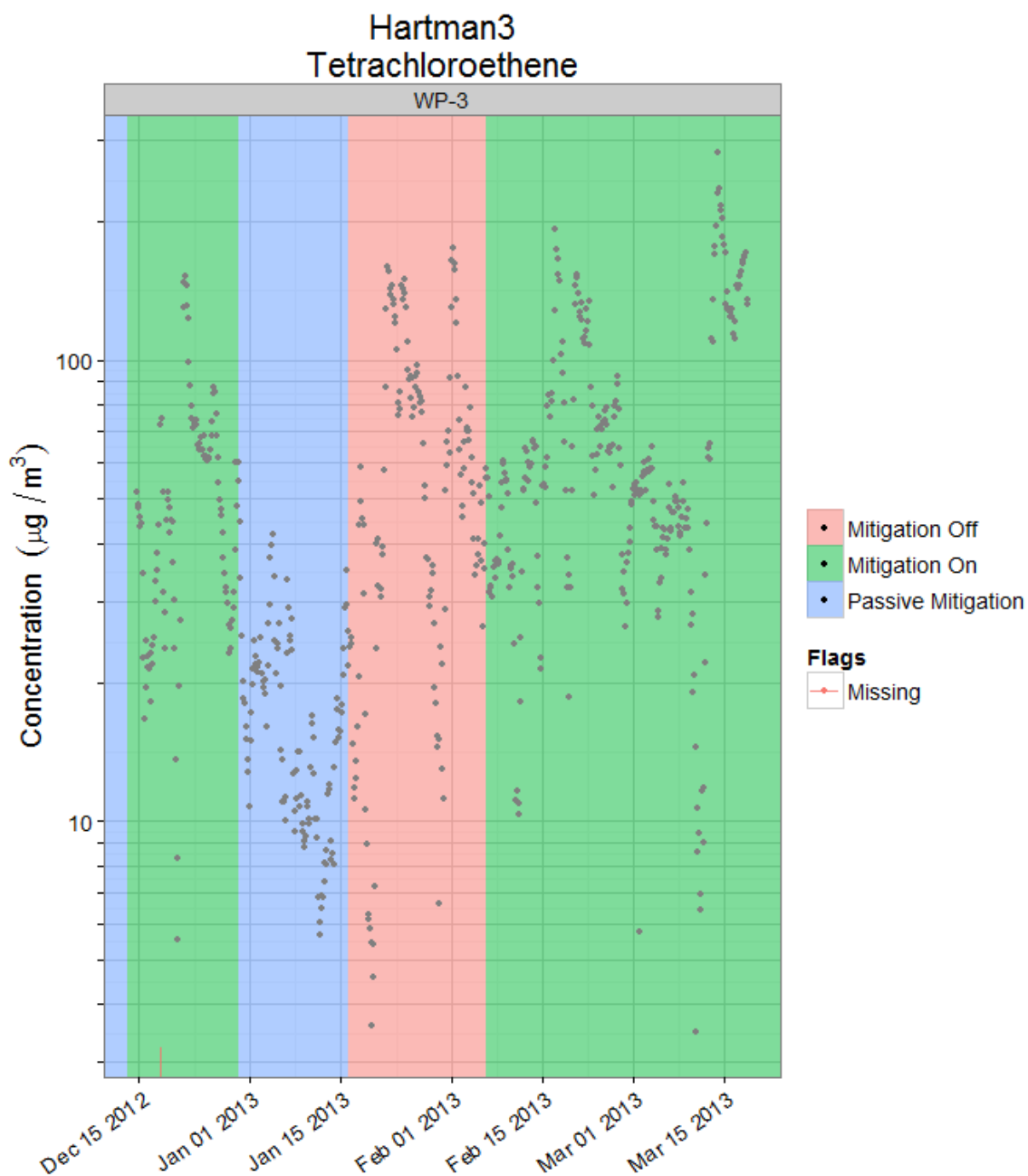


Figure 6-9b. Plot of WP-3; PCE concentrations vs. time (online GC).

6.1.3 Shallow and Deep Soil Gas

A series of 12 nested soil gas ports surround the 420/422 house or originate in the basements of either side of the duplex (**Figure 6-5**). The five depths at each of the external nested locations are as follows: 3.5 ft bls, 6 ft bls, 9 ft bls, 13 ft bls, and 16.5 ft bls. Internal to the house are the nested locations notated SGP8 through 12. Each individual port is notated based on its location and its depth (e.g., SGP1-3.5 for the 3.5-ft depth at the SGP1 location). At the internal nested locations, there are only four depths; the 3.5-ft depth is omitted because the basement floor is at ~5 ft bls. The internal soil gas VOC concentration data are graphed in **Figures 6-10** through **6-17** for the 420 side of the duplex and **Figures 6-18** to **6-25** for the 422 side of the duplex. External to the house, there are seven nested locations, notated SGP1 through 7 and graphed as **Figures 6-26** to **6-35**.

Groundwater levels varied throughout the project but remained high enough most of the time to render the 16.5-ft depths inaccessible for soil gas sampling for much of the project. Based on subsurface profiles from core data described in Section 3.1.1, the predominant subsurface lithology of the nested probe depths can be described as follows:

- 3.5 ft bls: silt and silty sand with some clay and evidence of fill material (e.g., cinders, ash, coal fragments, organic material)
- 6 ft bls: transition zone between finer silt and silty sand with clay above over coarser sand below
- 9 ft bls: sand and gravel outwash with some clay
- 13.5 ft bls: sand and gravel coarsening with depth
- 16 ft bls: sand, gravel, some cobbles

Thus, the general stratigraphy under the house is about 6 ft finer grain sediments (from fill or till) overlying coarse to very coarse glacial outwash deposits (i.e., sand, gravel, and cobbles). Cobbles were encountered during the drilling of MW-3, just to the south of SSP-1 and SGP-8 on the 422 side of the duplex. The coarseness of the deeper material at the site is evidenced by the rapidity of the water table rise after an increase in the gage height at nearby Falls Creek (see Section 11).

Prior to mitigation, VOC concentrations were generally highest in the deepest ports of each cluster and decrease at shallower depths. This pattern is consistent with expectations for attenuation of vapor intrusion of VOCs originating from a deep source (whether in the vadose zone or groundwater). This attenuation pattern appears to be more pronounced for chloroform (frequently two to three orders of magnitude) than for PCE (generally one order of magnitude).

An analysis of the frequencies of nondetects was performed for each compound by borehole and depth. Of the boreholes outside the house footprint, only SGP1 (south of the 422 part of the duplex) has less than a 20% frequency of nondetects for both PCE and chloroform (**Table 6-1**).

Table 6-1. Frequency of Nondetectable Samples (%) by Soil Gas Point or Cluster

| Location ID | Percent Nondetect Samples | | | | | | |
|------------------------------|---------------------------|-----|-----|---------|---------|--------|-------|
| | Chloroform | PCE | TCE | Benzene | Toluene | Hexane | Radon |
| Soil Gas Probes | | | | | | | |
| SGP1 | 22 | 13 | 74 | 33 | 67 | 79 | 0 |
| SGP2 | 40 | 38 | 75 | 32 | 65 | 82 | 0 |
| SGP3 | 70 | 83 | 91 | 34 | 78 | 89 | 0 |
| SGP4 | 55 | 22 | 90 | 35 | 76 | 87 | 0 |
| SGP5 | 45 | 55 | 91 | 37 | 77 | 92 | 0 |
| SGP6 | 53 | 42 | 93 | 39 | 79 | 92 | 0 |
| SGP7 | 51 | 38 | 91 | 36 | 80 | 90 | 0 |
| SGP8 | 8 | 14 | 75 | 35 | 68 | 80 | 0 |
| SGP9 | 10 | 6 | 79 | 33 | 71 | 81 | 0 |
| SGP10 | 41 | 15 | 92 | 43 | 80 | 91 | 0 |
| SGP11 | 20 | 5 | 89 | 34 | 77 | 89 | 0 |
| SGP12 | 30 | 8 | 91 | 36 | 81 | 89 | 0 |
| Subslab Ports | | | | | | | |
| SSP-1 | 8 | 7 | 55 | 19 | 50 | 67 | 0 |
| SSP-2 | 63 | 50 | 81 | 56 | 50 | 81 | 0 |
| SSP-3 | 30 | 5 | 75 | 50 | 40 | 80 | 0 |
| SSP-4 | 10 | 8 | 65 | 28 | 66 | 80 | 0 |
| SSP-5 | 58 | 9 | 79 | 26 | 68 | 78 | 0 |
| SSP-6 | 70 | 8 | 82 | 28 | 67 | 80 | 0 |
| SSP-7 | 33 | 13 | 78 | 29 | 73 | 80 | 0 |
| Wall Ports (Basement) | | | | | | | |
| WP-1 | 82 | 86 | 86 | 32 | 75 | 86 | 0 |
| WP-2 | 78 | 83 | 88 | 37 | 78 | 86 | 0 |
| WP-3 | 49 | 37 | 75 | 28 | 74 | 82 | 0 |
| WP-4 | 75 | 83 | 85 | 28 | 74 | 85 | 0 |

All of the wall ports have more than 20% nondetects for all compounds (**Table 6-2**). Nondetects are infrequent (<20%) in almost all the subslab ports for PCE but more frequent for chloroform and the 420 side of the duplex.

Interestingly, SSP-1 and SSP-4 are consistently detectable (>80%) for benzene as well—in the center and on the south end of the 422 side of the duplex. Benzene is also consistently detectable at the 16.5-ft depth.

Table 6-2. Frequency of Nondetects in TO-17 VOC Data by Soil Gas Sampling Depth

| Depth bls (ft) | Probe Type | Percent Nondetect Samples | | | | | | |
|----------------|------------|---------------------------|-----|-----|---------|---------|--------|-------|
| | | Chloroform | PCE | TCE | Benzene | Toluene | Hexane | Radon |
| 3 | Wall Port | 72 | 73 | 84 | 31 | 75 | 85 | 0 |
| 3.5 | Soil Gas | 85 | 86 | 95 | 39 | 82 | 95 | 0 |
| 6 | Soil Gas | 38 | 19 | 79 | 30 | 68 | 80 | 0 |
| 6 | Subslab | 35 | 10 | 71 | 27 | 61 | 76 | 0 |
| 9 | Soil Gas | 35 | 23 | 79 | 32 | 71 | 82 | 0 |
| 13 | Soil Gas | 13 | 14 | 97 | 50 | 81 | 95 | 0 |
| 16.5 | Soil Gas | 11 | 20 | 98 | 15 | 84 | 94 | 0 |

bls = below land surface; PCE = tetrachloroethene; TCE = trichloroethene

Note that a depth of 4 is assigned to the wall ports and a depth of 5 is assigned to the subslab ports.

For the trend in nondetects by depth, we see about what we would expect for a deep vapor intrusion source; there are fewer nondetects at lower depths. PCE is under 20% nondetects at subslab ports (depth = 5) as mentioned before and from 6 ft down in soil gas ports it is also under 20%. Chloroform is under 20% nondetects only at a depth of 13 ft or deeper. Benzene is under 20% nondetects only at the deepest depth of 16 ft. No other compounds were consistently detectable. Thus, the shallowest depths (3.5 ft) were generally the most stable, with little fluctuation because most results were below the detection limit (**Figure 6-25** and **Figure 6-26**). The 9-ft depths had periods of stability as well (see **Figures 6-12, 6-20, 6-30, and 6-31**). Notable exceptions to the shallow stability can be found at SGP1 and, to differing degrees, all of the indoor ports, SGP8 through 12 where the shallow concentrations were higher and thus less affected by nondetects. At each of those ports, shallow concentrations seem to partially track the seasonal variations seen in the deeper ports (see **Figures 6-13, 6-14, 6-15, 6-23, 6-30, and 6-33**). At SGP3 and 4, the deeper ports are often low or stable (see **Figures 6-32 through 6-34**). At the 6-ft depths, PCE concentrations on the 420 side (**Figure 6-11**) rose toward the summer of 2011 and then fell off. A similar trend is also seen at 9 ft. That trend is not seen in **Figure 6-19** for the 422 side where PCE concentrations in SGP8-6 and SSP-1 showed a decline.

Many of the deeper ports at each location (9 ft through 13 ft, sometimes 16.5 ft) showed what appears to be a rough cycle responding to seasonal changes (see **Figures 6-13, 6-14, 6-15, 6-23, 6-30, and 6-33**), that is, VOC concentrations were higher in the cooler months and lower in the warmer months (**Figures 6-13, 6-15, 6-20, 6-23, and 6-20**). SGP3 and 4 were too diffuse to show much of a trend. SGP1 and 2 showed the opposite PCE concentration trend, at SGP1-6 (see **Figures 6-28 and 6-29**).

TO-17 VOC concentrations at some sampling locations (SSP-5, -6, and -7 in **Figure 6-6a**) varied only within a narrow range of two or three times over 1 year, suggesting that multiple samples or time-integrated samples may have limited benefit. However, at some locations (SSP-1 and -4 in **Figure 6-6a** and SGP11-9 and 12-9 in **Figure 6-12**), 10-times changes in soil gas VOC concentrations occur over 1 year, suggesting that there would be significant additional information provided from additional soil gas sampling rounds at these locations.

Some features among the figures might be attributed to natural or project-related phenomena. Although samples were taken multiple times per week, and in some cases per day, during the intensive rounds (yielding as many as >12 successive samples at some locations during a week), there were no discernible or notable concentration trends in the data. This suggests that there is probably not a strong diurnal variance in subslab soil gas VOC concentrations at this duplex and that the frequency of sampling (and thus, the artificial volumetric flow in the subsurface induced by frequent sampling) does not appear to be significant (for example, see **Figures 6-36 and 6-37**). High concentrations found at the beginning of the project but tapering off toward the spring could be due to the period of heavy snow and ice in the very cold winter of January and February 2011 (for example, see **Figures 6-14 and 6-20**).

During the mitigation testing period PCE appeared to be gradually depleted at a number of 9- and 13-ft ports (such as 11-9, 12-9; 6-13, 8-13, 9-13 and 10-13; -see **Figures 6-13, 6-15, 6-23 and 6-33**). In contrast, PCE concentrations were increasing in other ports such as 8-9 and 9-9 and chloroform concentrations increased in 8-13 and 9-13 (**Figures 6-21 and 6-22**).

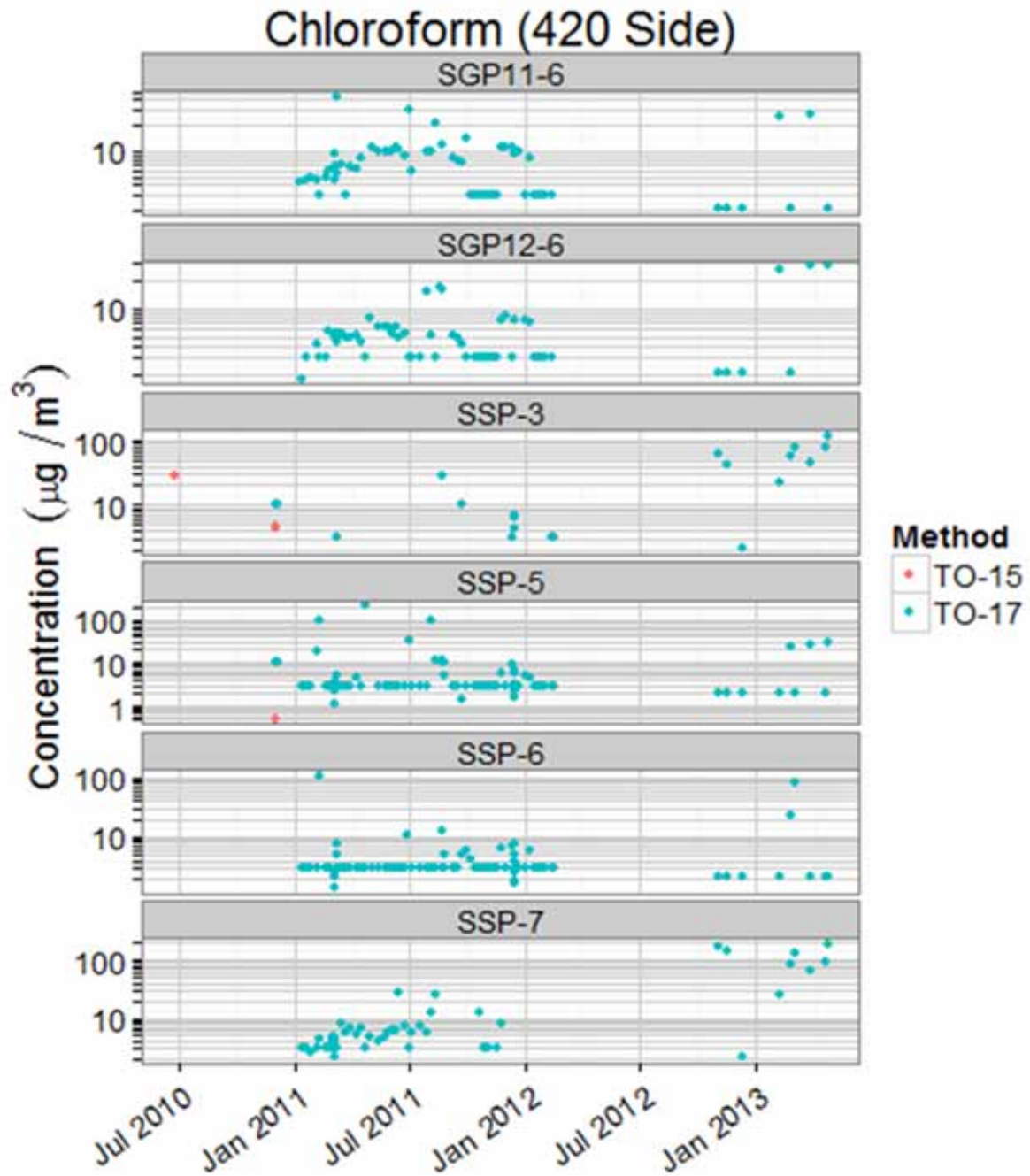


Figure 6-10. Chloroform concentrations at subslab and 6-ft soil gas ports directly under the 420 side of duplex.

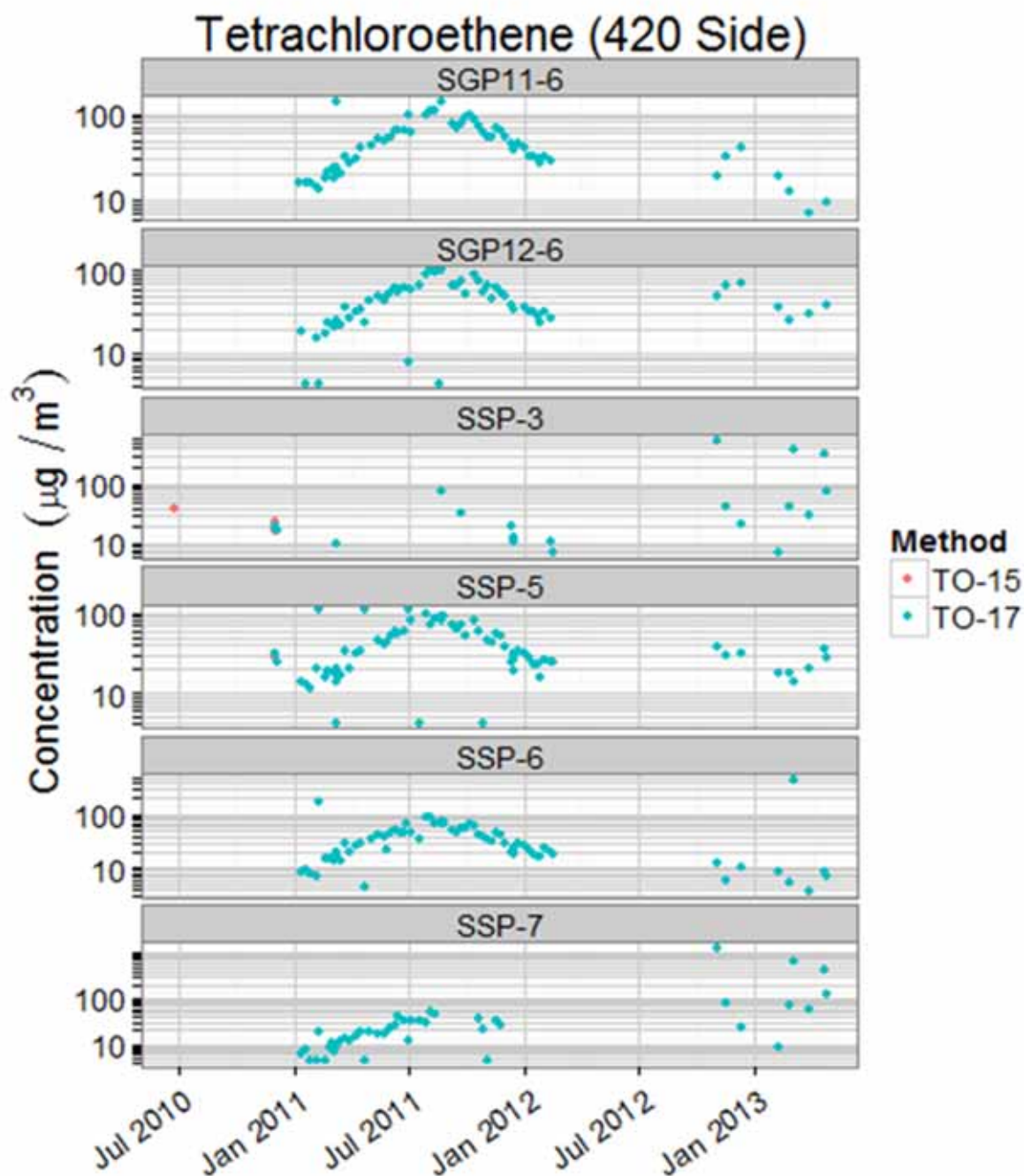


Figure 6-11. PCE concentrations at 6-ft soil gas ports and subslab immediately below the 420 side of the duplex.

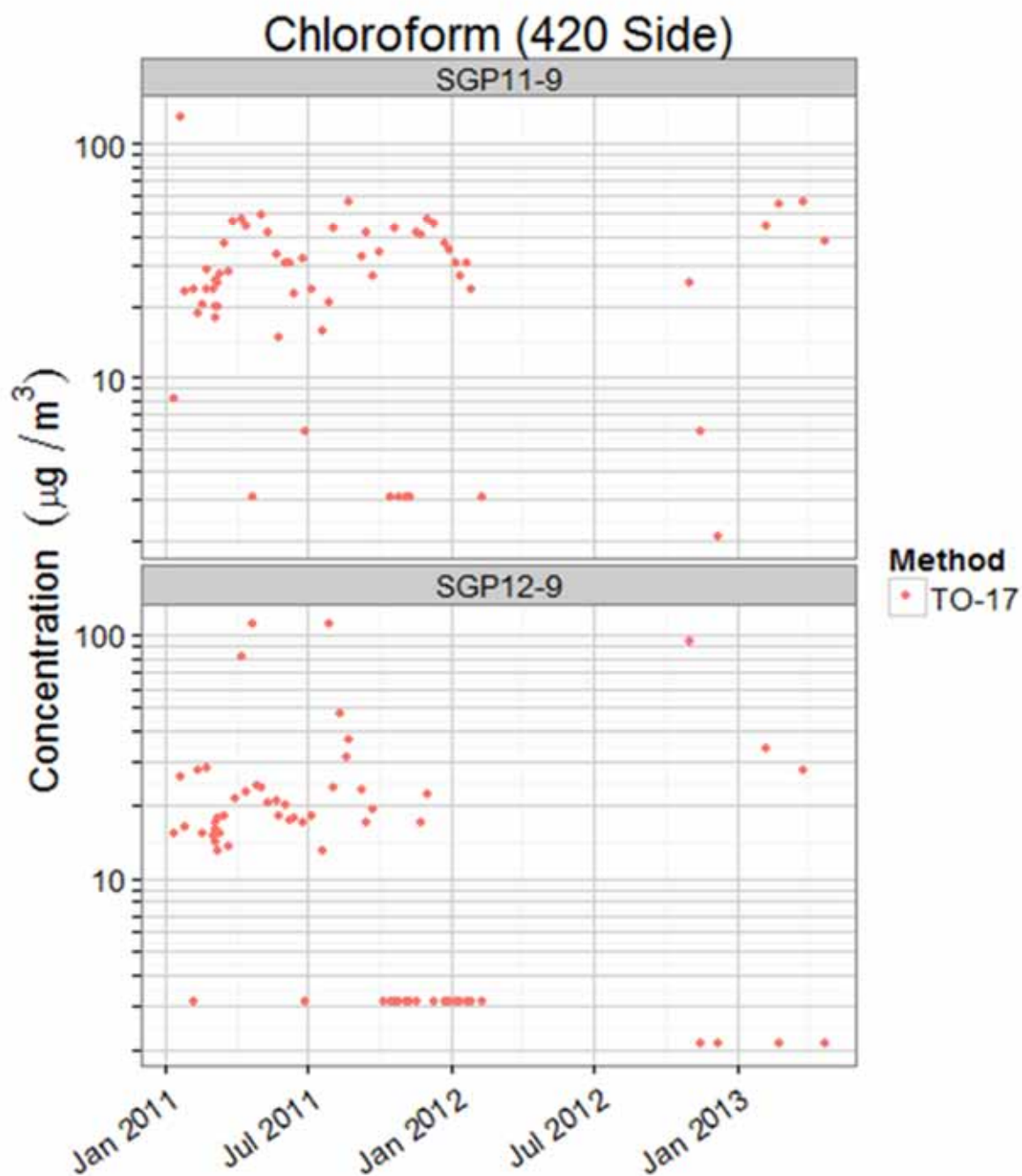


Figure 6-12. Chloroform concentrations at 9-ft soil gas ports below 420 side of the duplex.

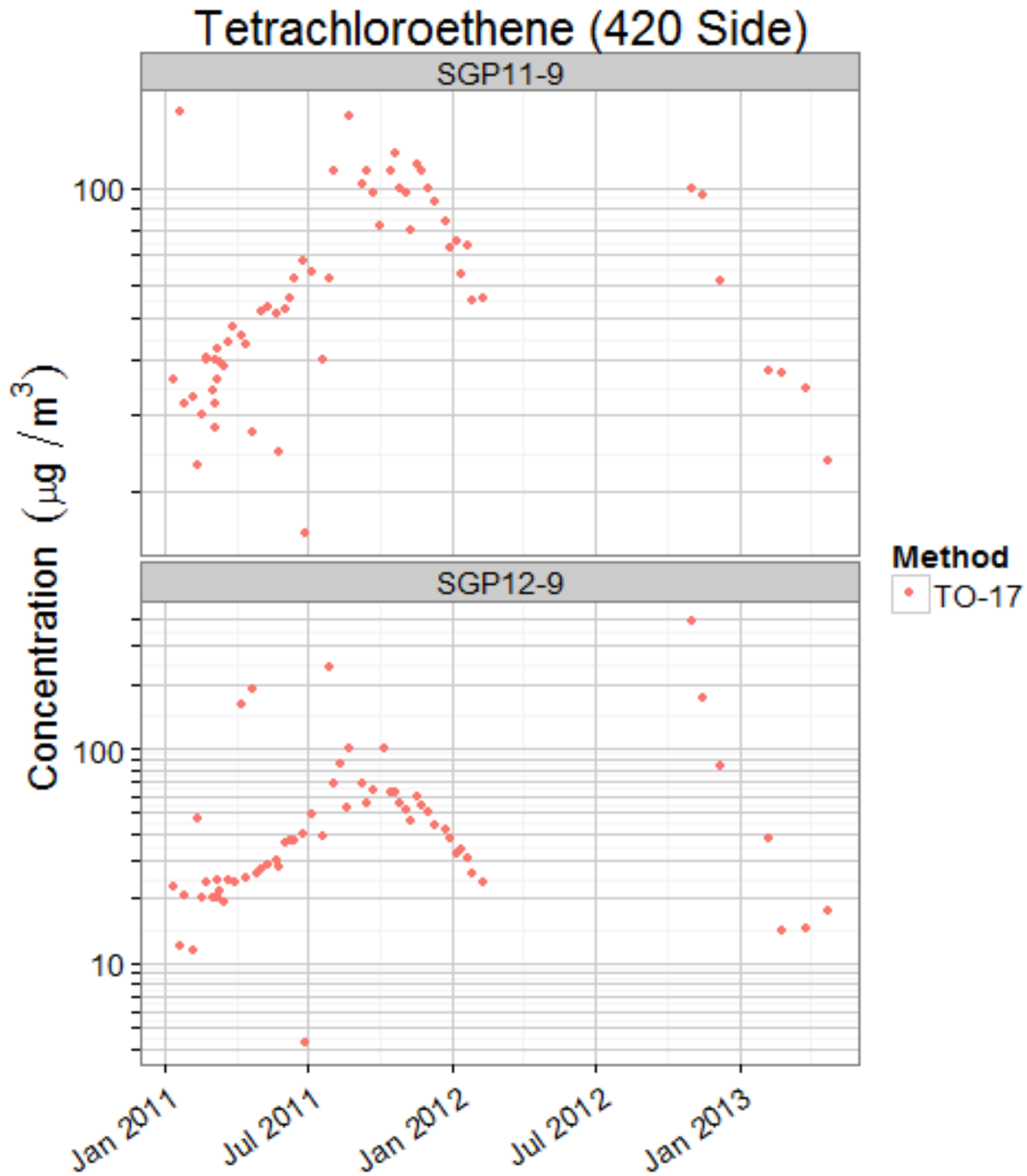


Figure 6-13. PCE concentrations at soil gas points 9 ft below the 420 side of duplex.

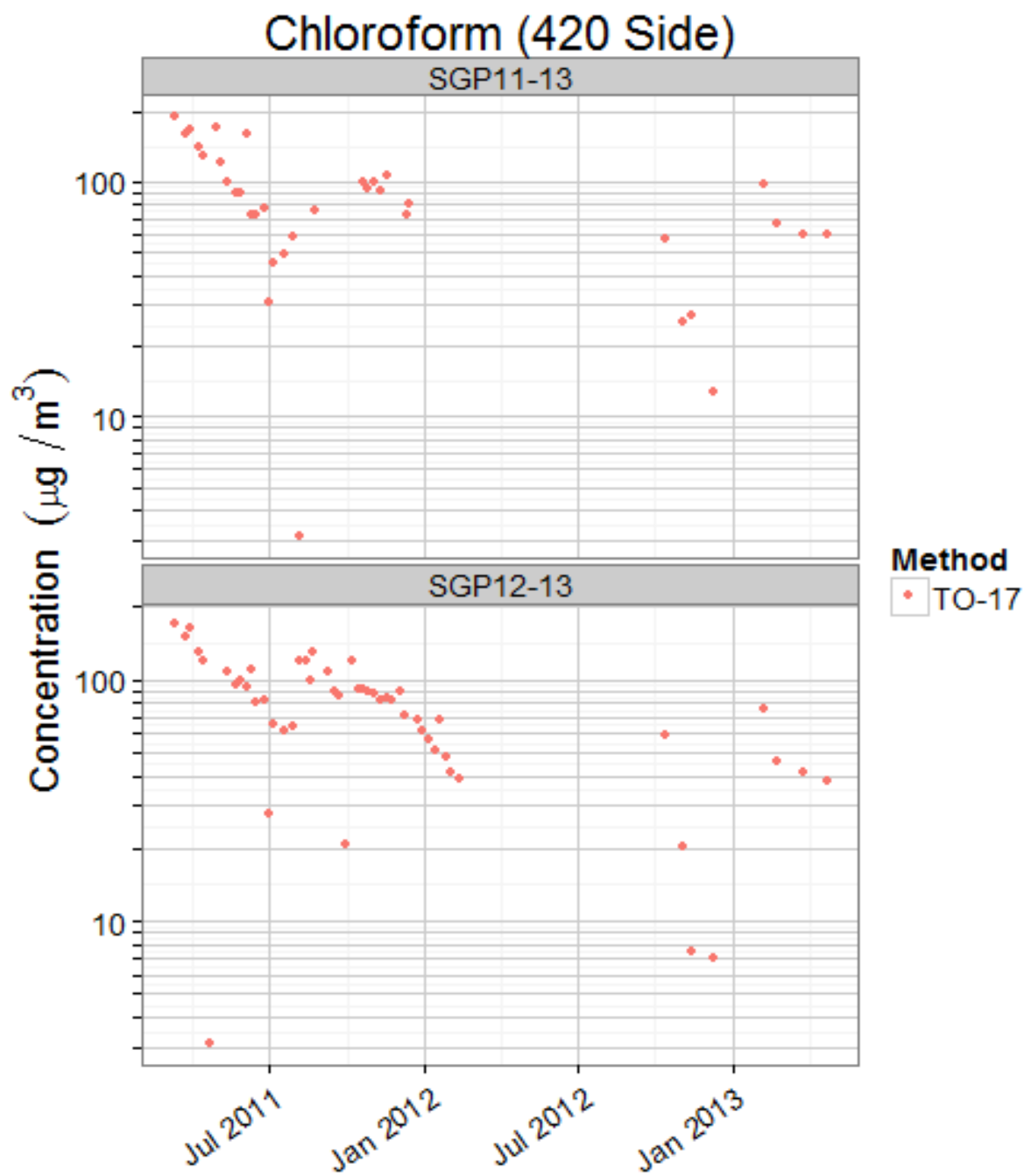


Figure 6-14. Chloroform concentrations in soil gas at 13 ft below the 420 side of the duplex.

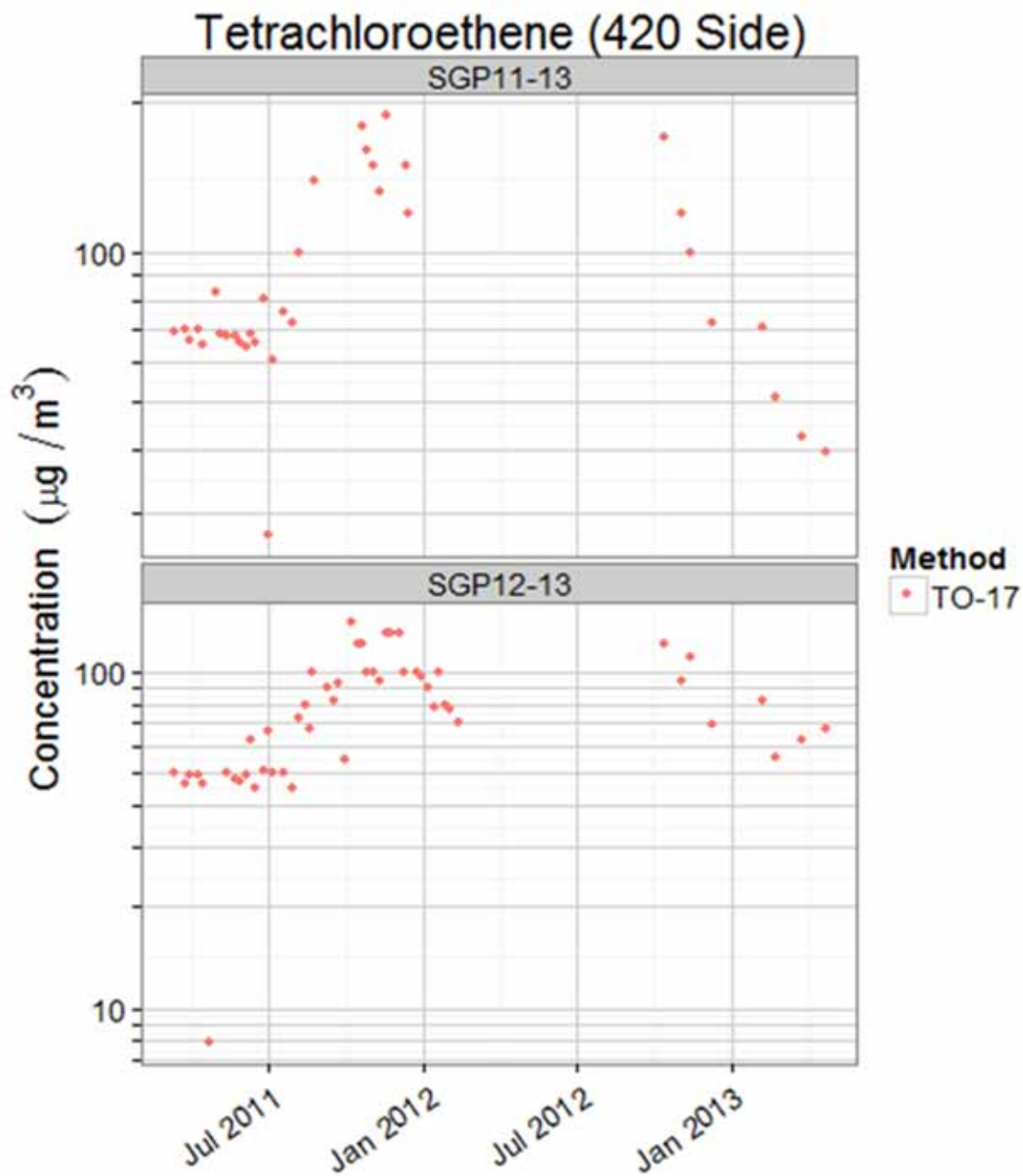


Figure 6-15. PCE concentrations in soil gas at 13 ft below the 420 side of duplex.

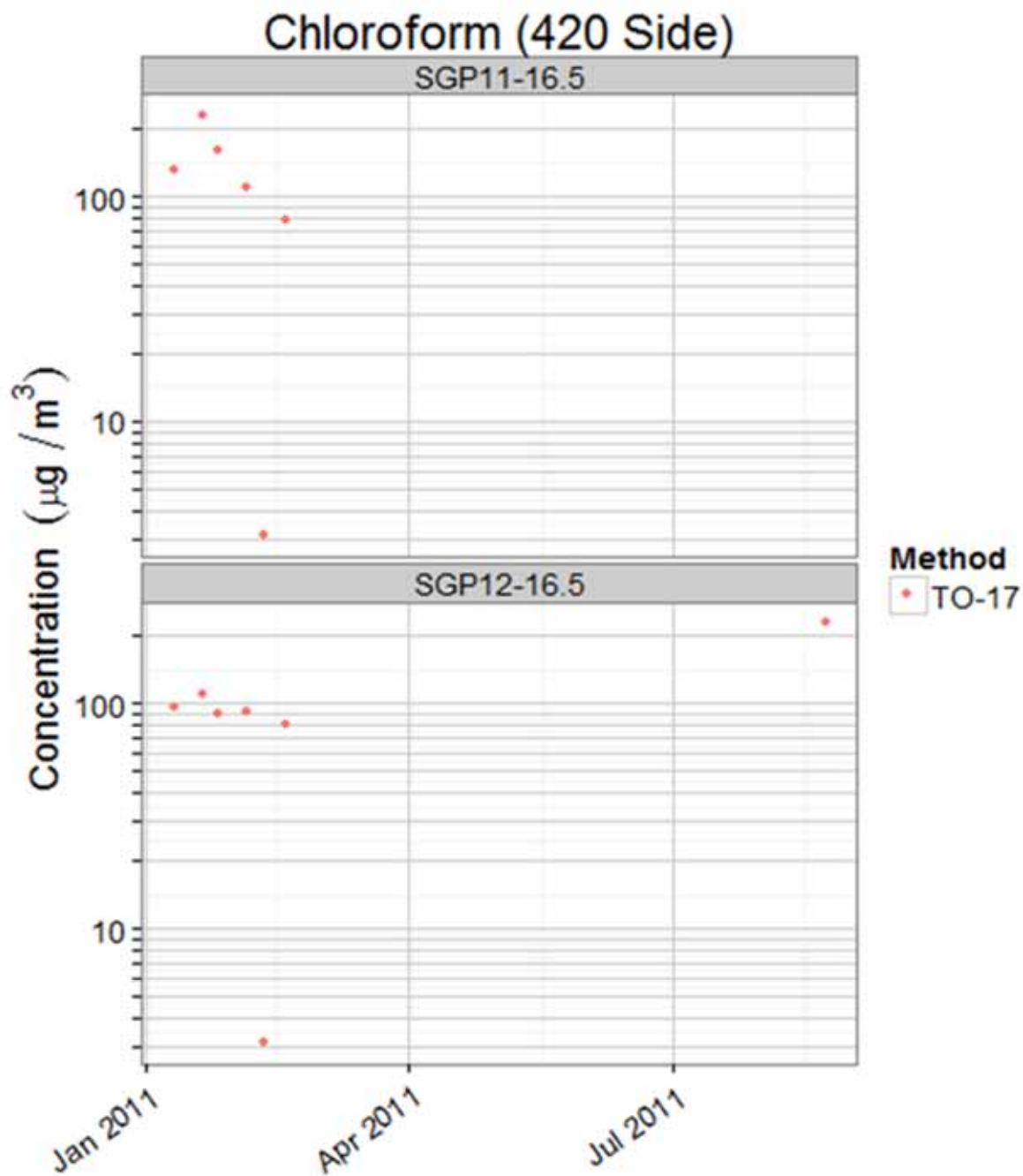


Figure 6-16. Chloroform concentrations in soil gas at 16.5 ft below the 420 side of duplex.

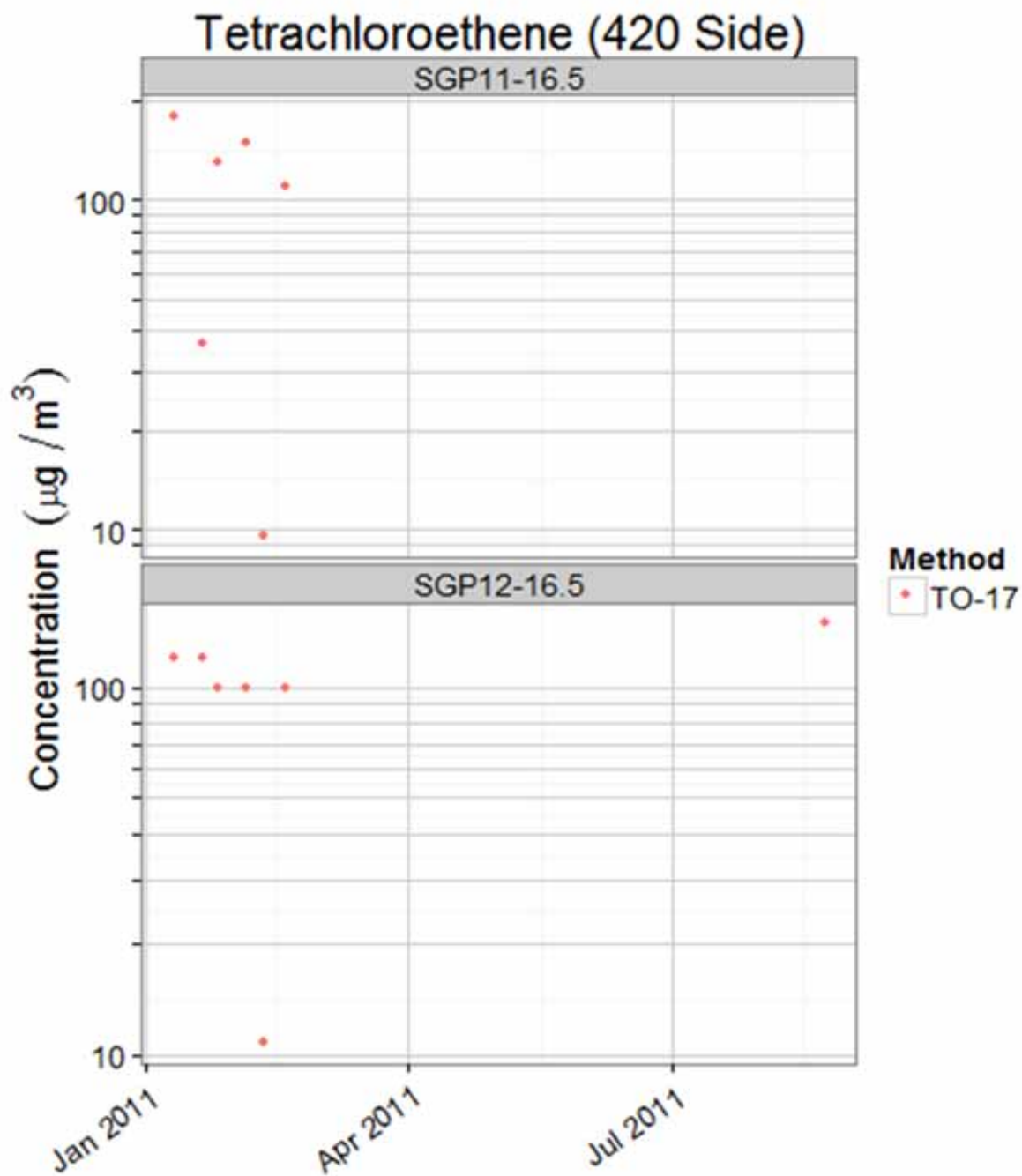


Figure 6-17. PCE concentrations in soil gas at 16.5 ft below the 420 side of the duplex.

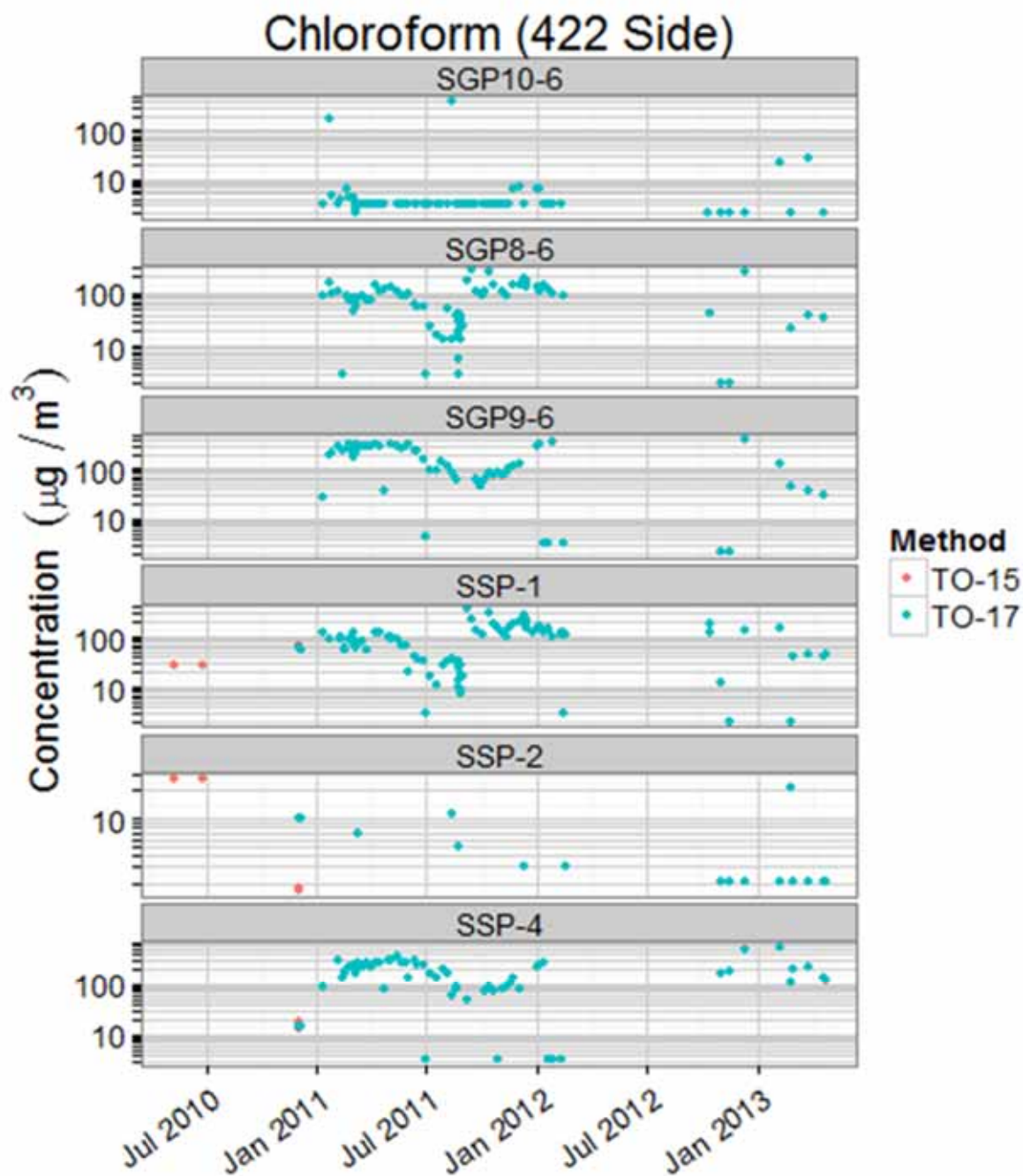


Figure 6-18. Chloroform concentrations in 6-ft soil gas and subslab ports immediately below the 422 side of the duplex.

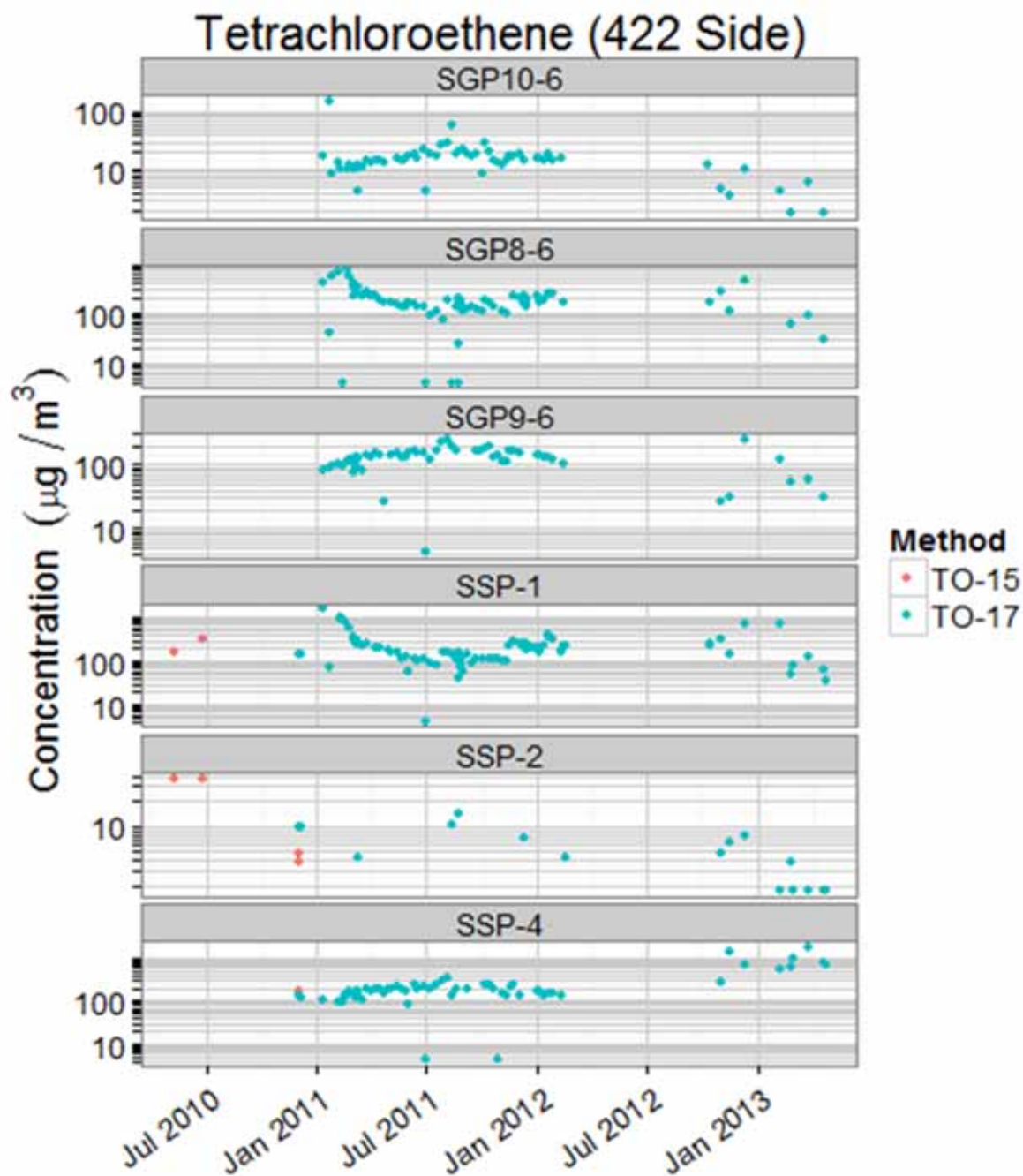


Figure 6-19. PCE concentrations in 6-ft soil gas ports and subslab ports directly below the 422 side of the duplex.

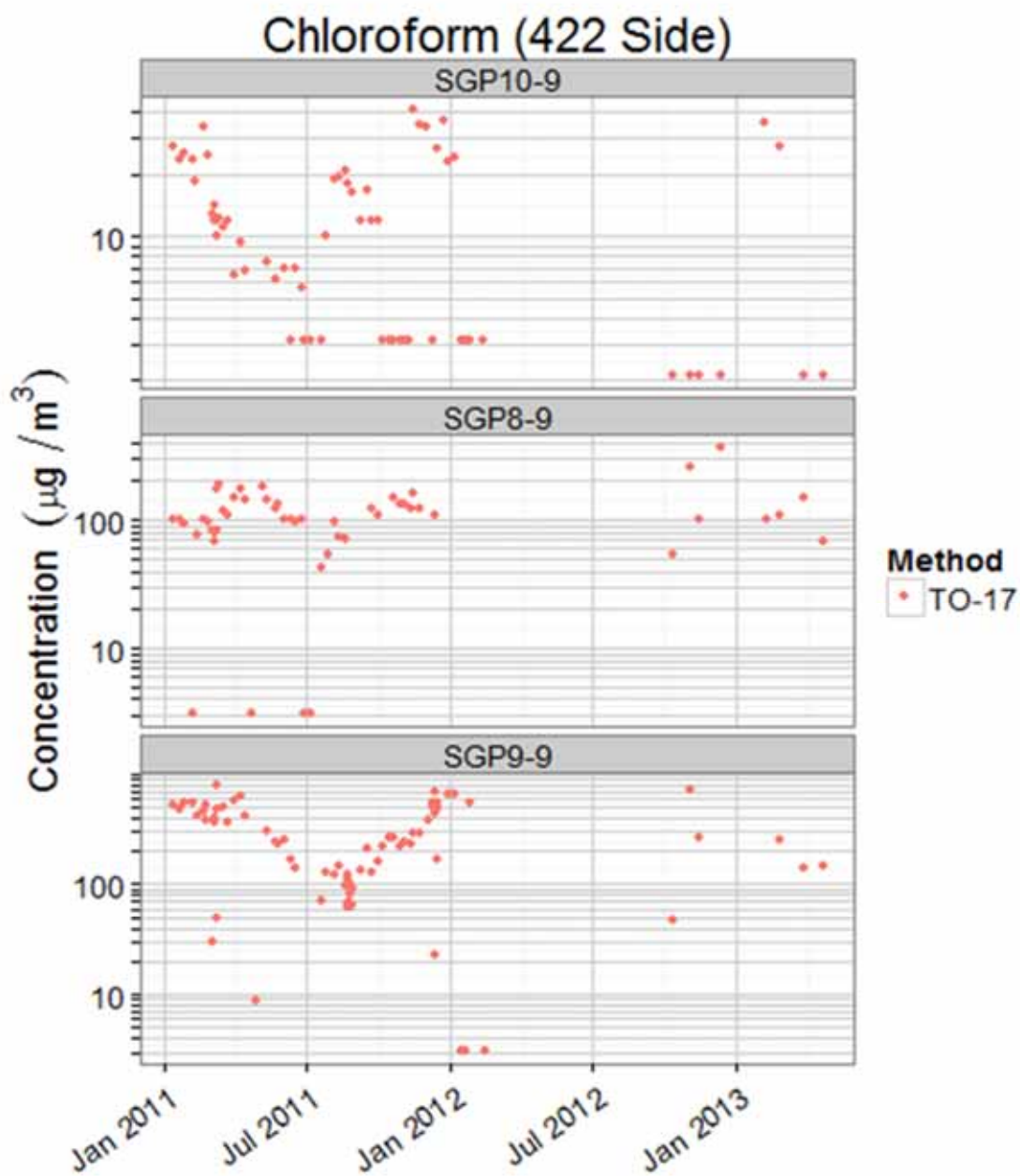


Figure 6-20. Chloroform concentrations in soil gas port at 9-ft depth below 422 side of duplex.

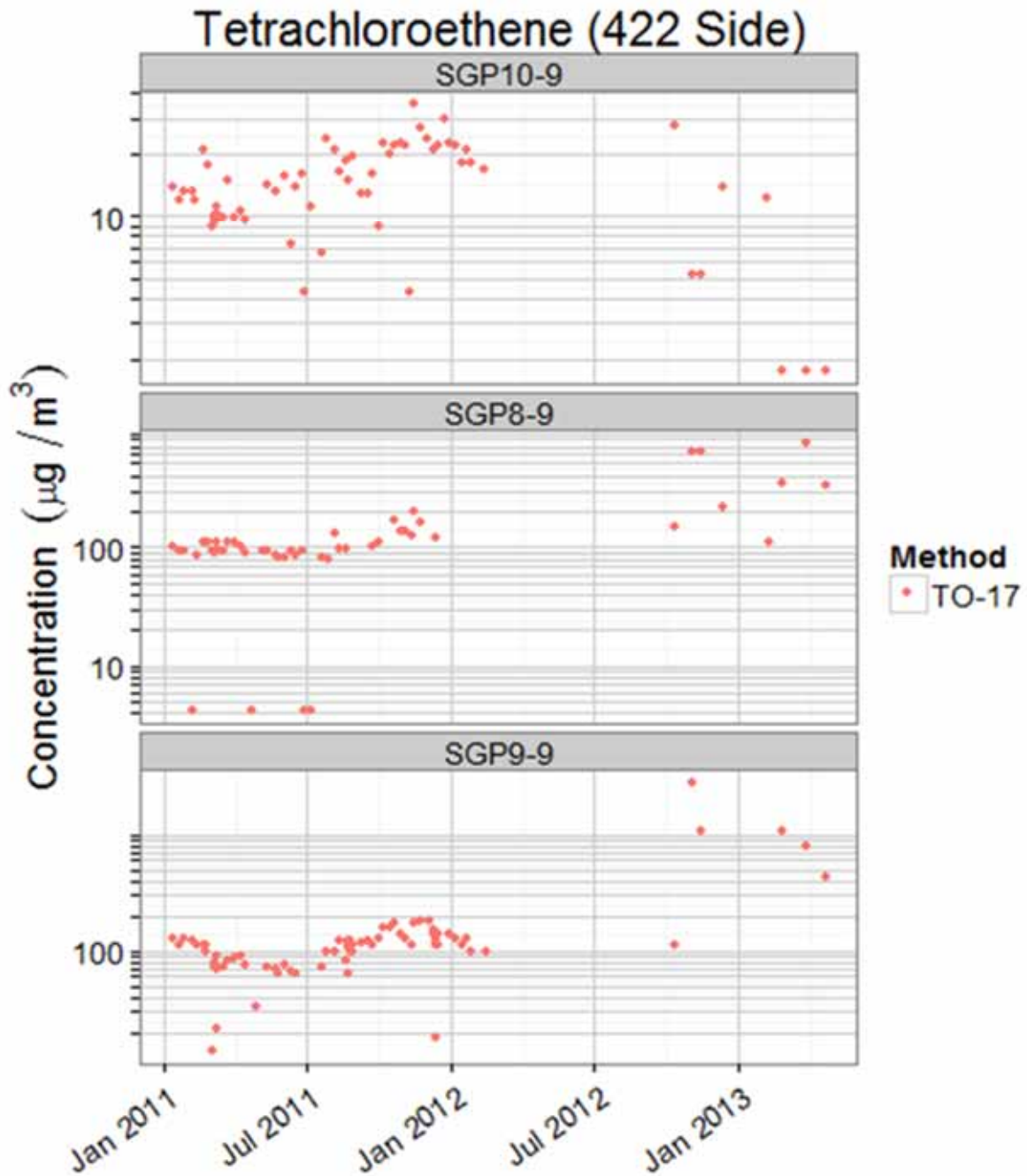


Figure 6-21. PCE concentrations in soil gas at 9 ft below the 422 side of the duplex.

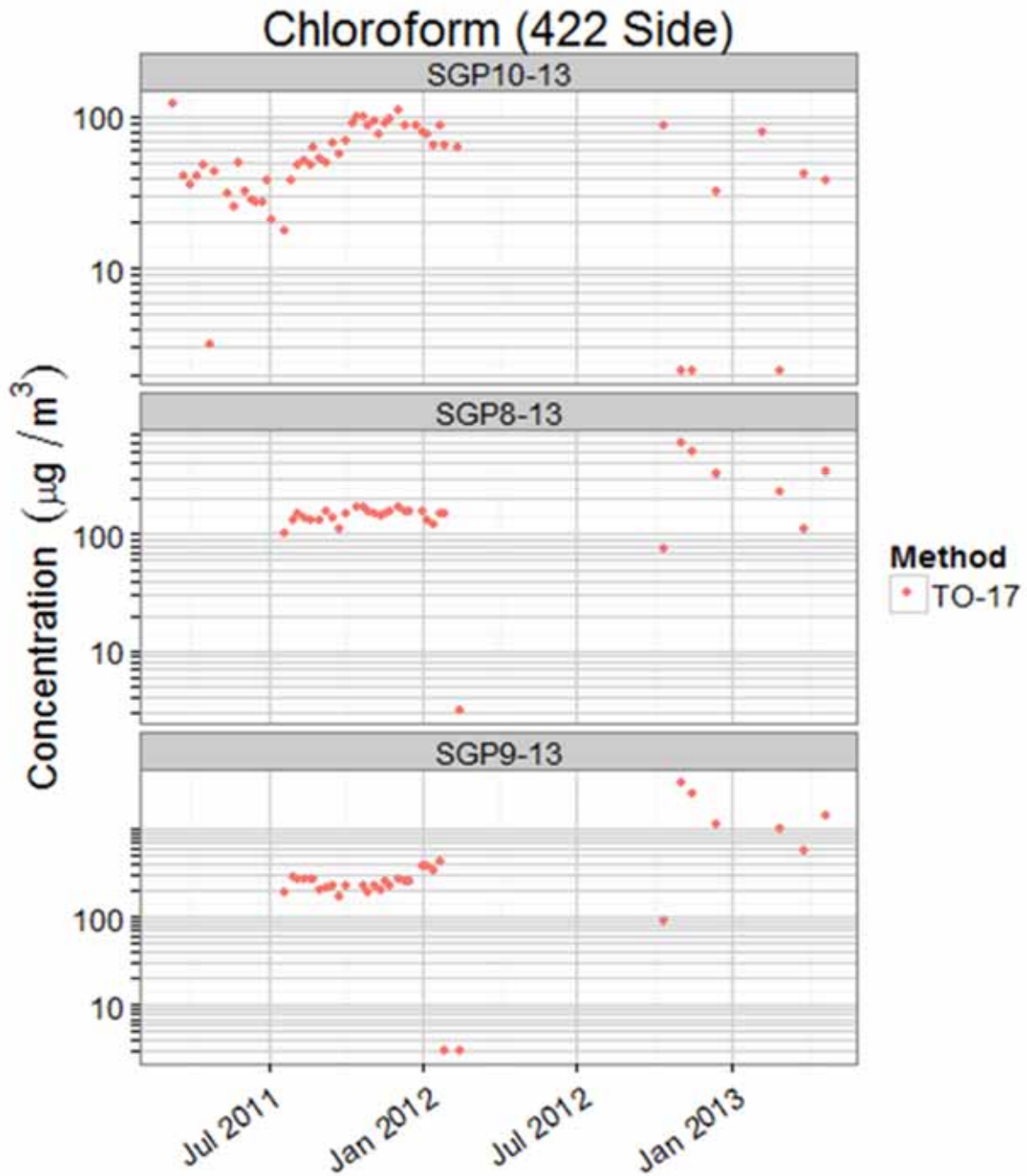


Figure 6-22. Chloroform concentrations in soil gas at 13 ft below the 422 side of the duplex.

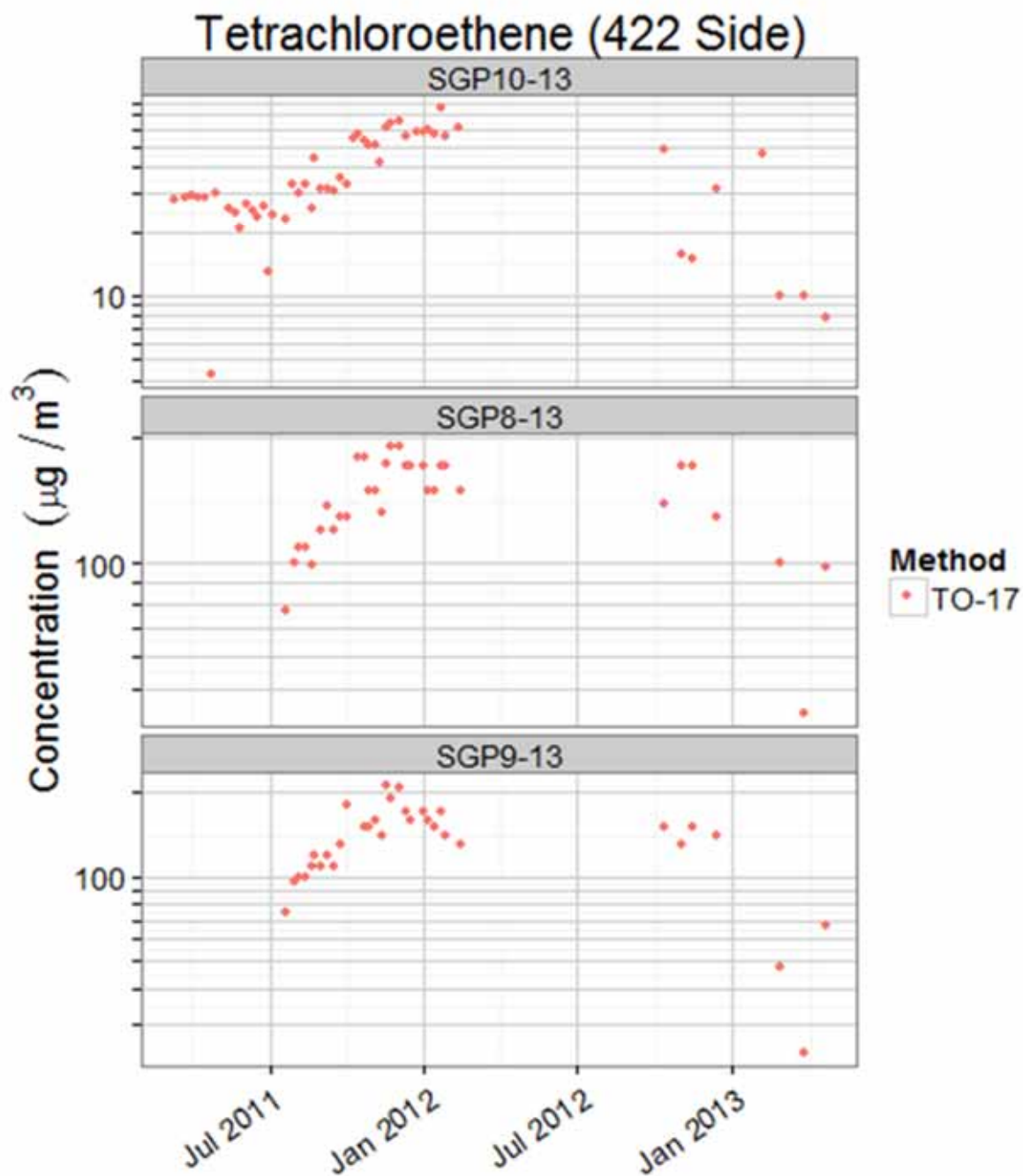


Figure 6-23. PCE concentrations in soil gas at 13 ft below the 422 side of the duplex.

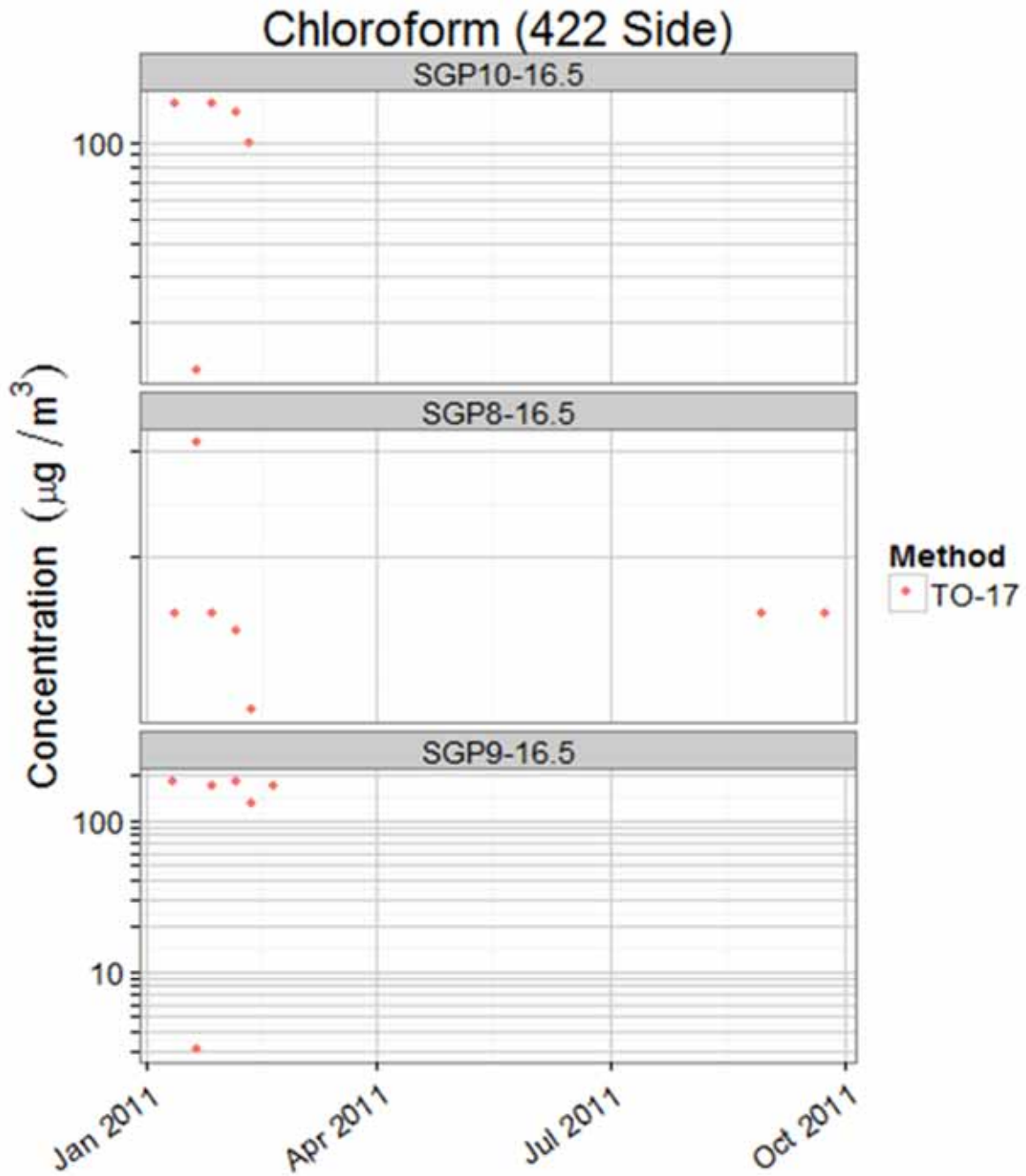


Figure 6-24. Chloroform concentrations at 16.5 ft below the 422 side of the duplex.

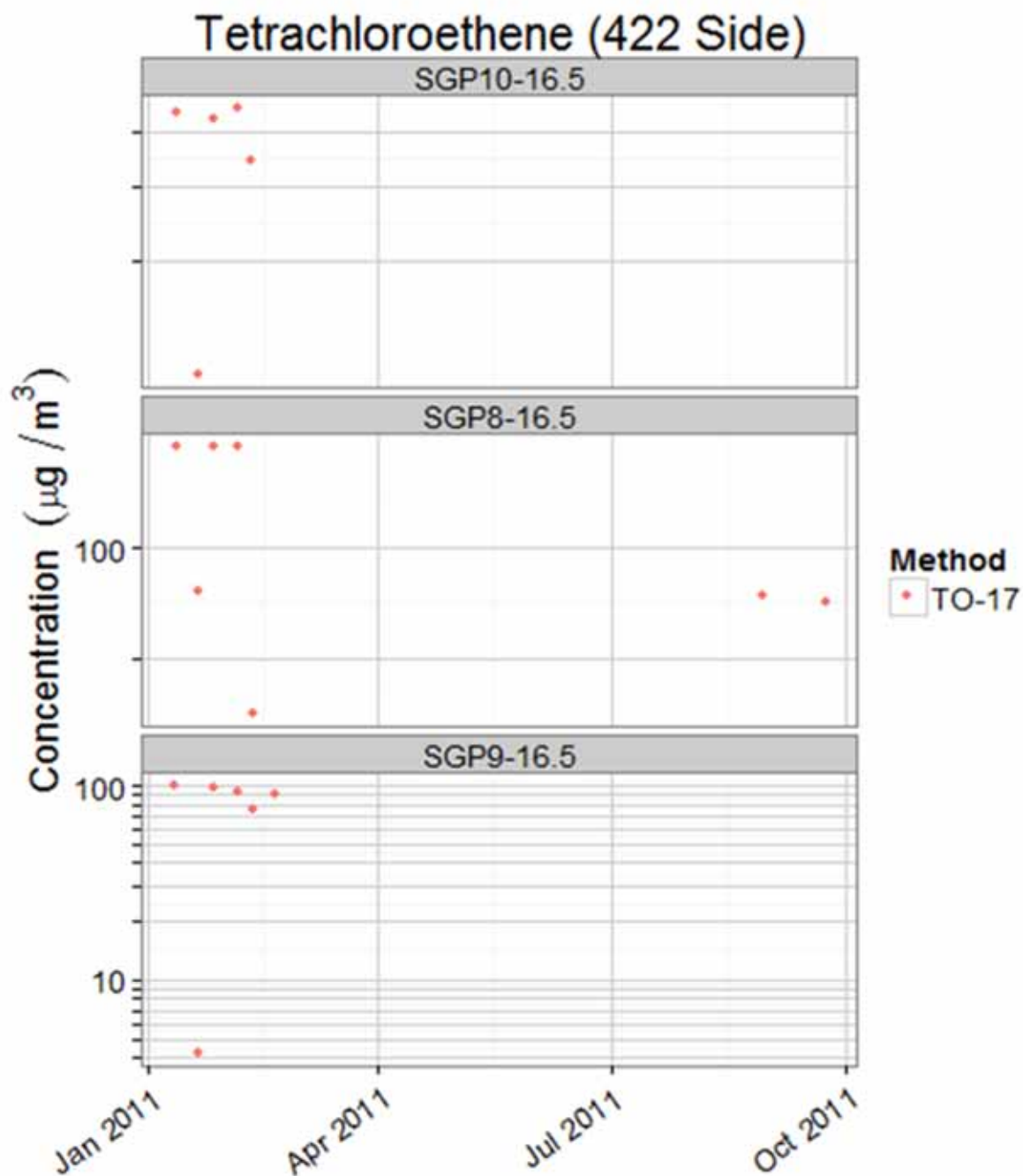


Figure 6-25. PCE concentrations at 16.5 ft below the 422 side of the duplex.

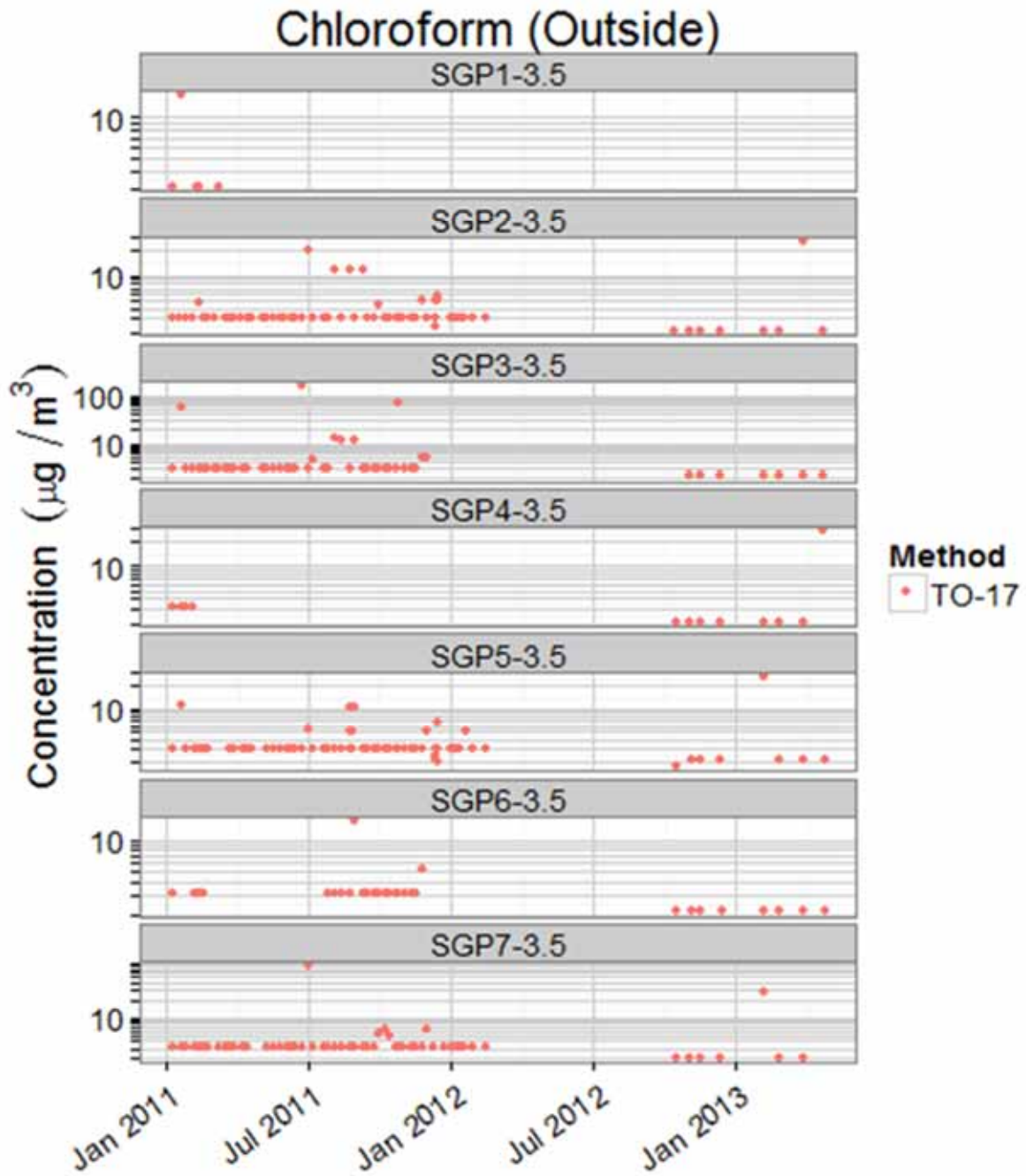


Figure 6-26. Chloroform concentrations in exterior soil gas at 3.5 ft bls.

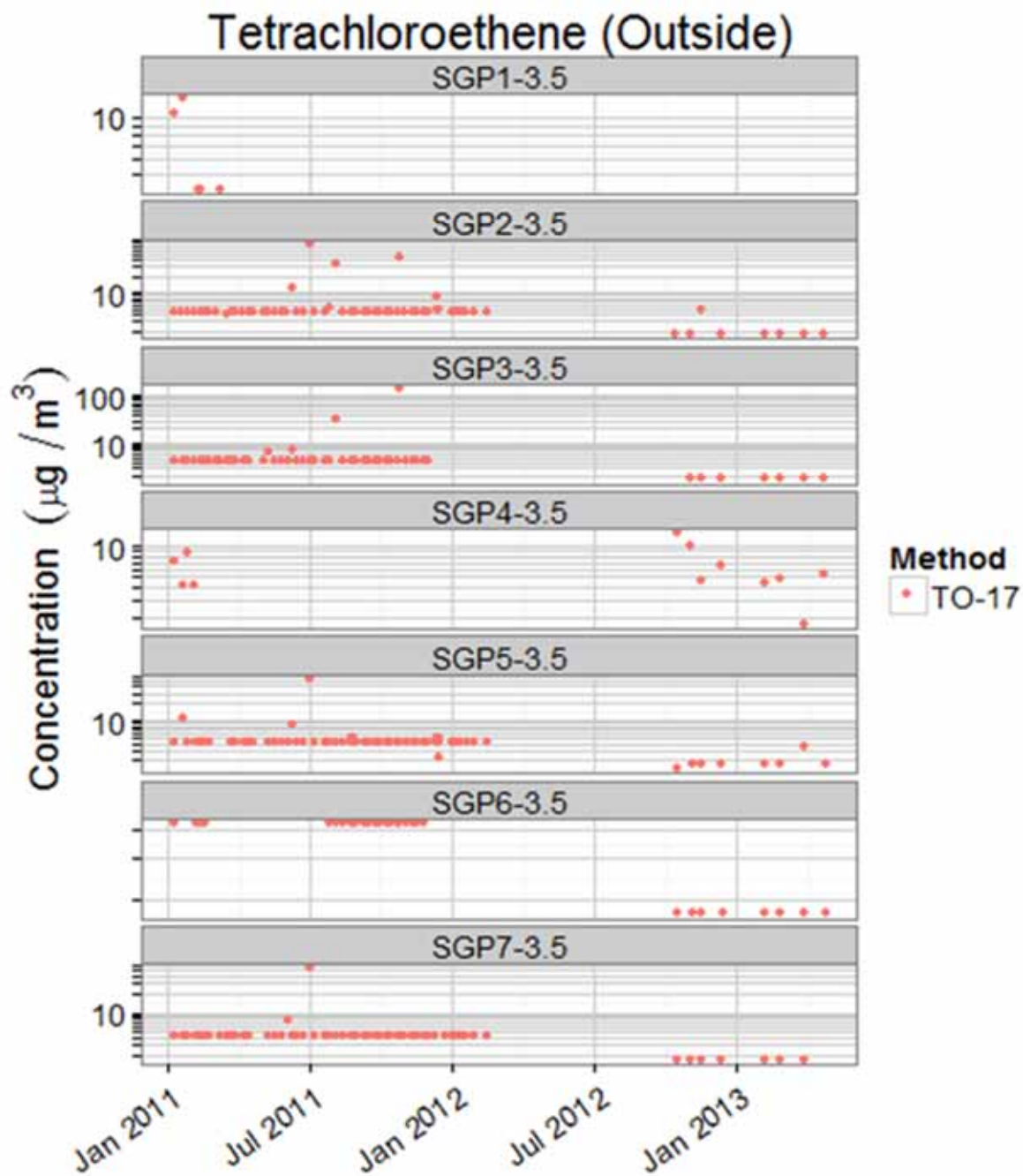


Figure 6-27. PCE concentrations in exterior soil gas at 3.5 ft bls.

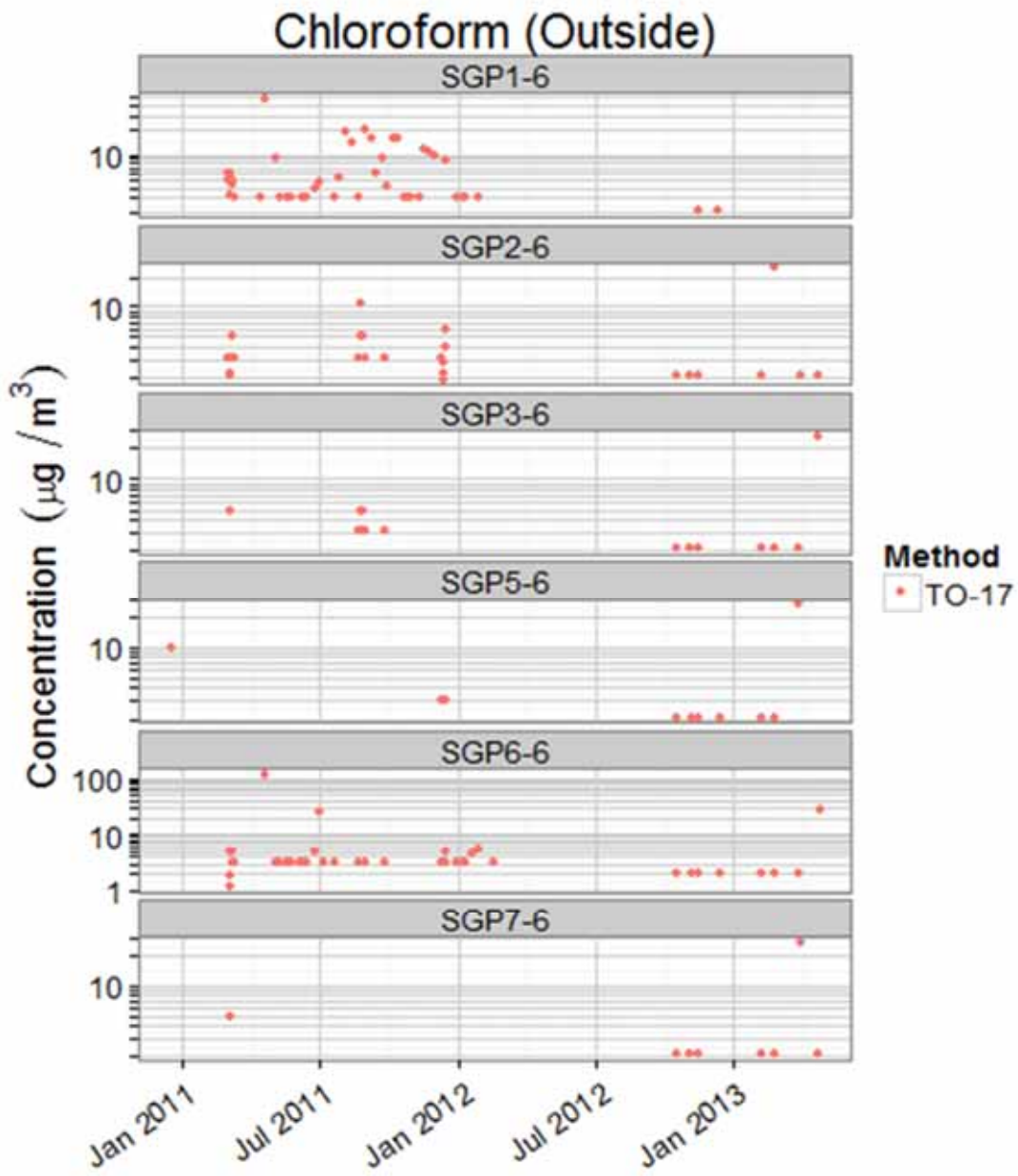


Figure 6-28. Chloroform concentrations in exterior soil gas at 6 ft. bls.

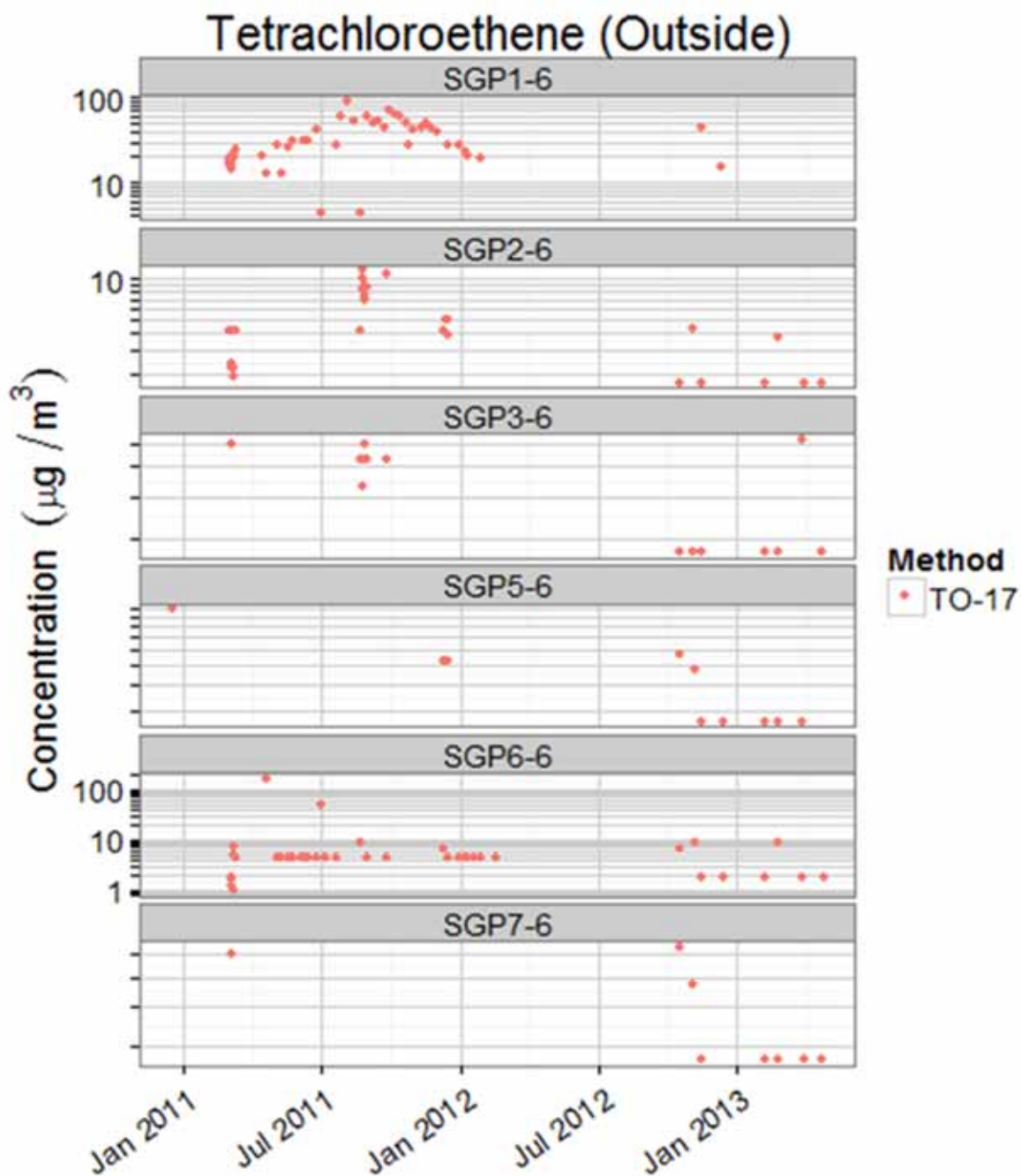


Figure 6-29. PCE concentrations in exterior soil gas at 6 ft bls.

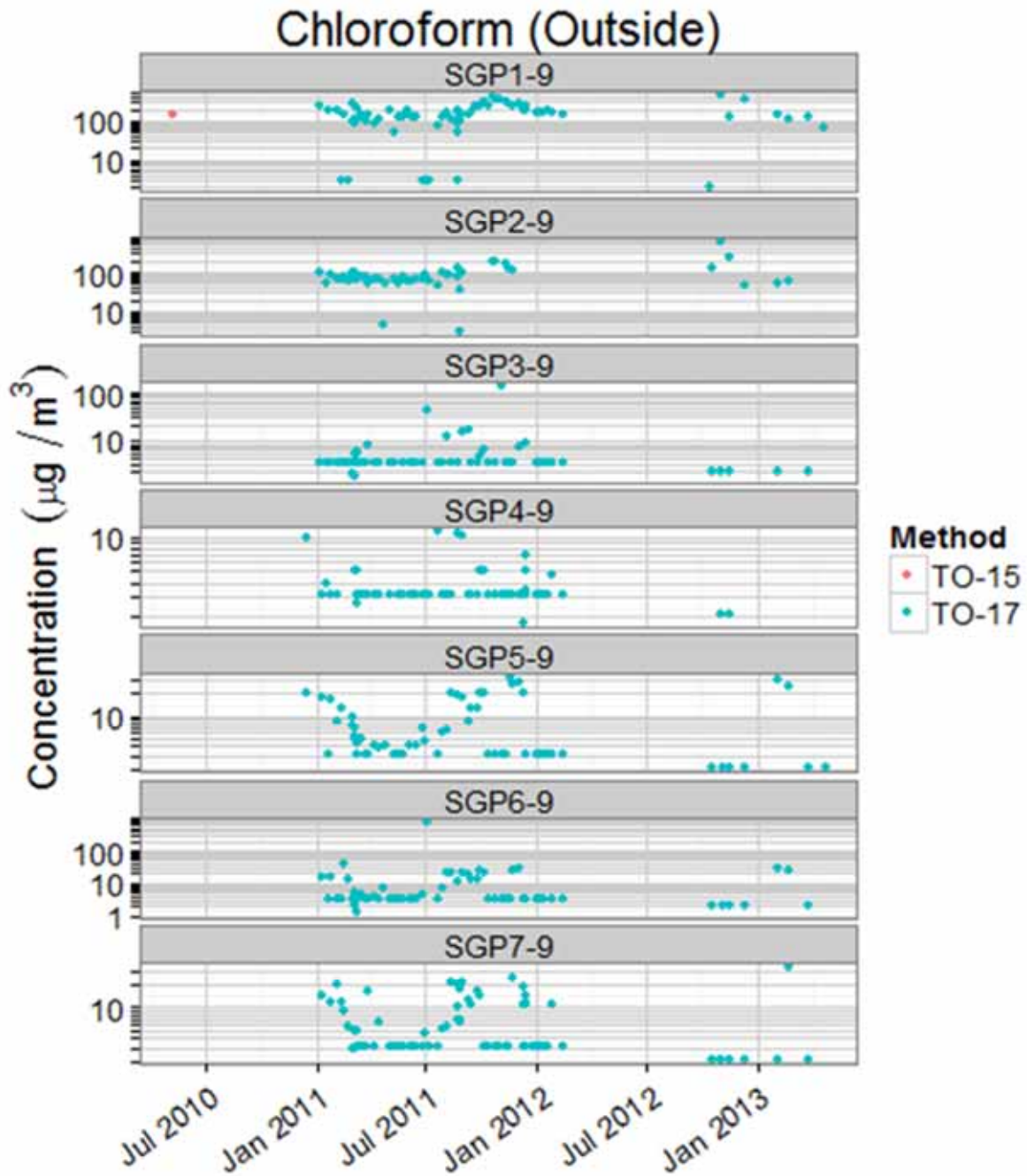


Figure 6-30. Chloroform concentrations in exterior soil gas at 9 ft bls.

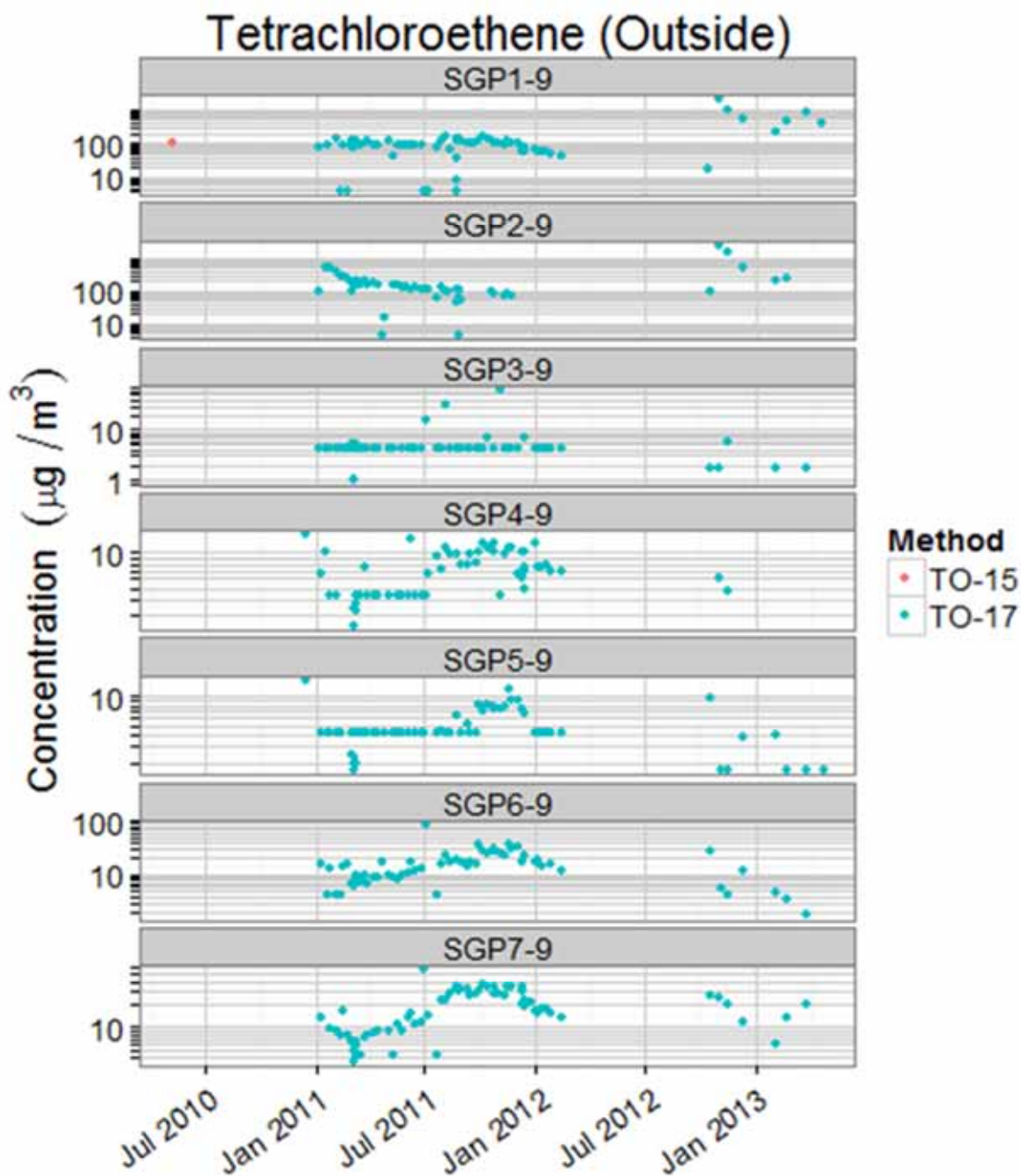


Figure 6-31. PCE concentrations in exterior soil gas at 9 ft bls.

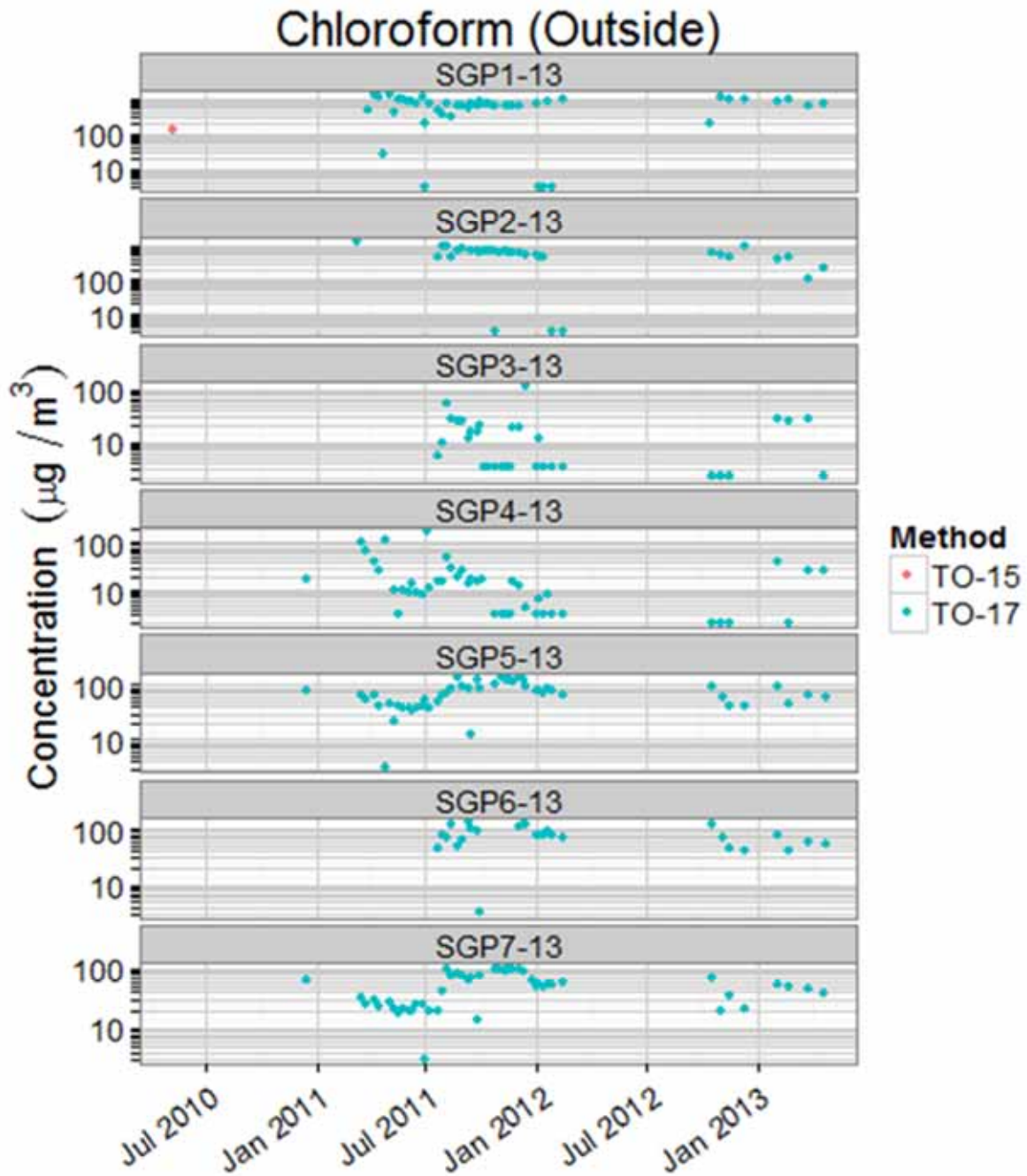


Figure 6-32. Chloroform concentrations in exterior soil gas at 13 ft bls.

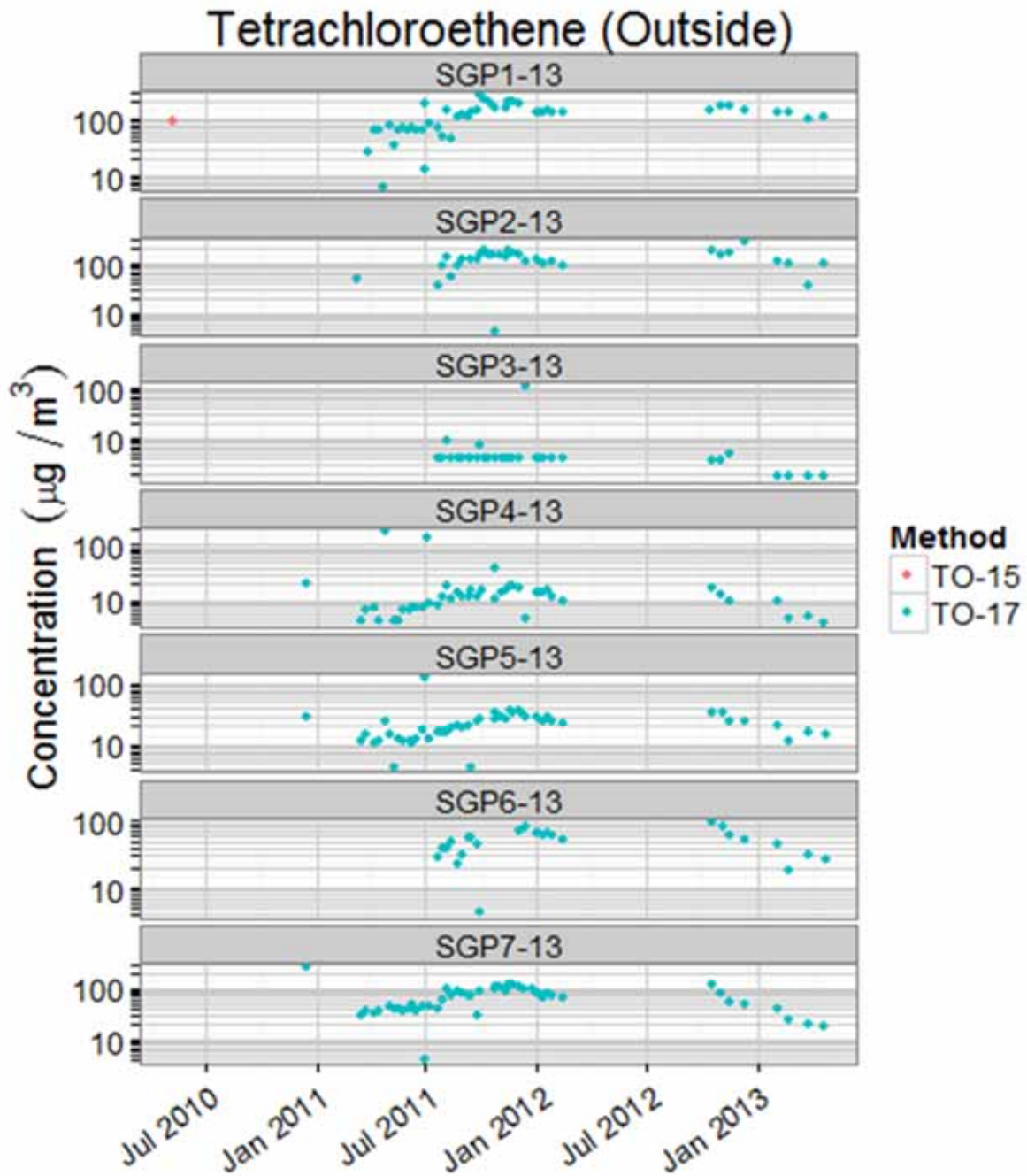


Figure 6-33. PCE concentrations in exterior soil gas at 13 ft bls.

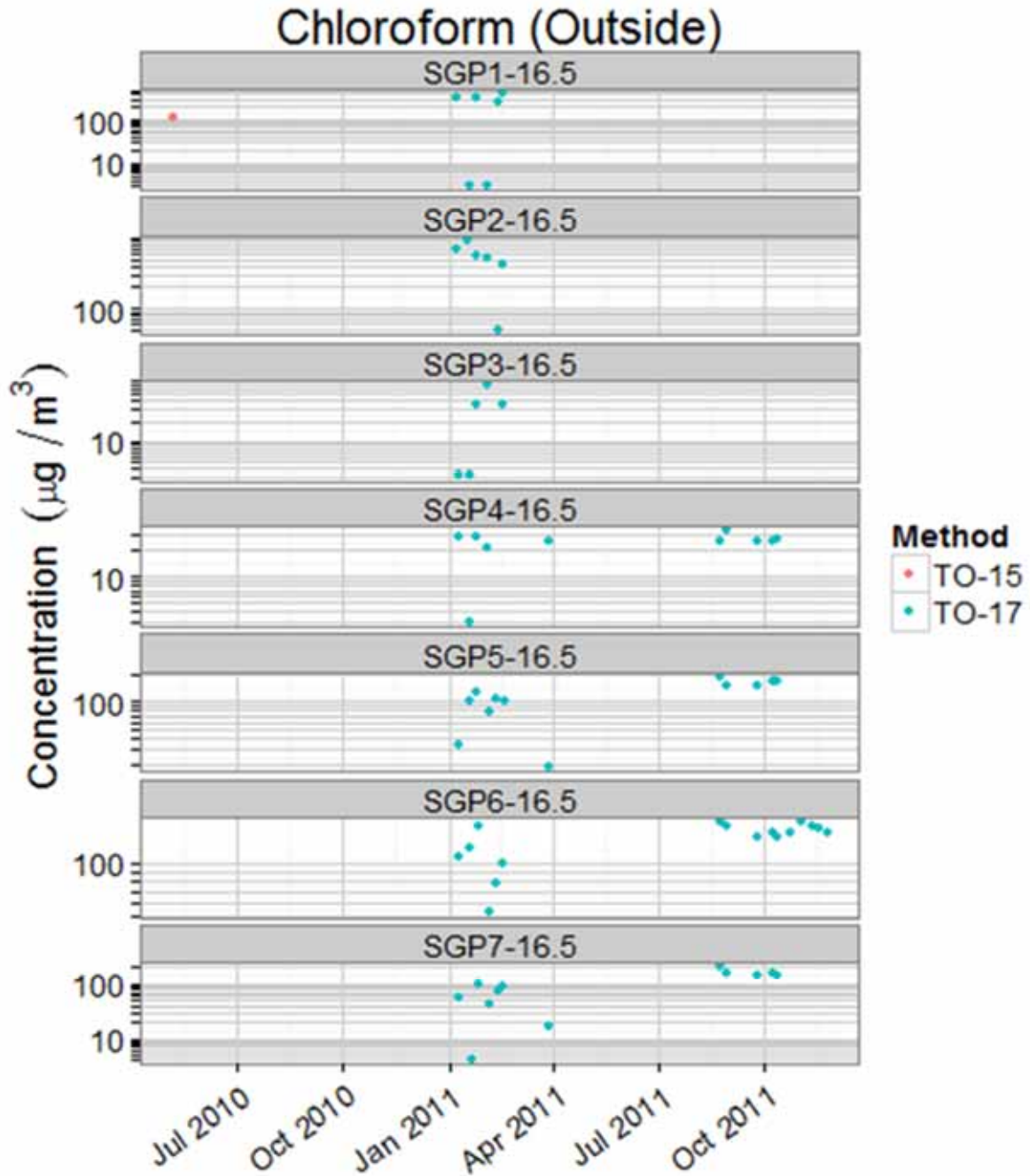


Figure 6-34. Chloroform concentrations in exterior soil gas at 16.5 ft bls.

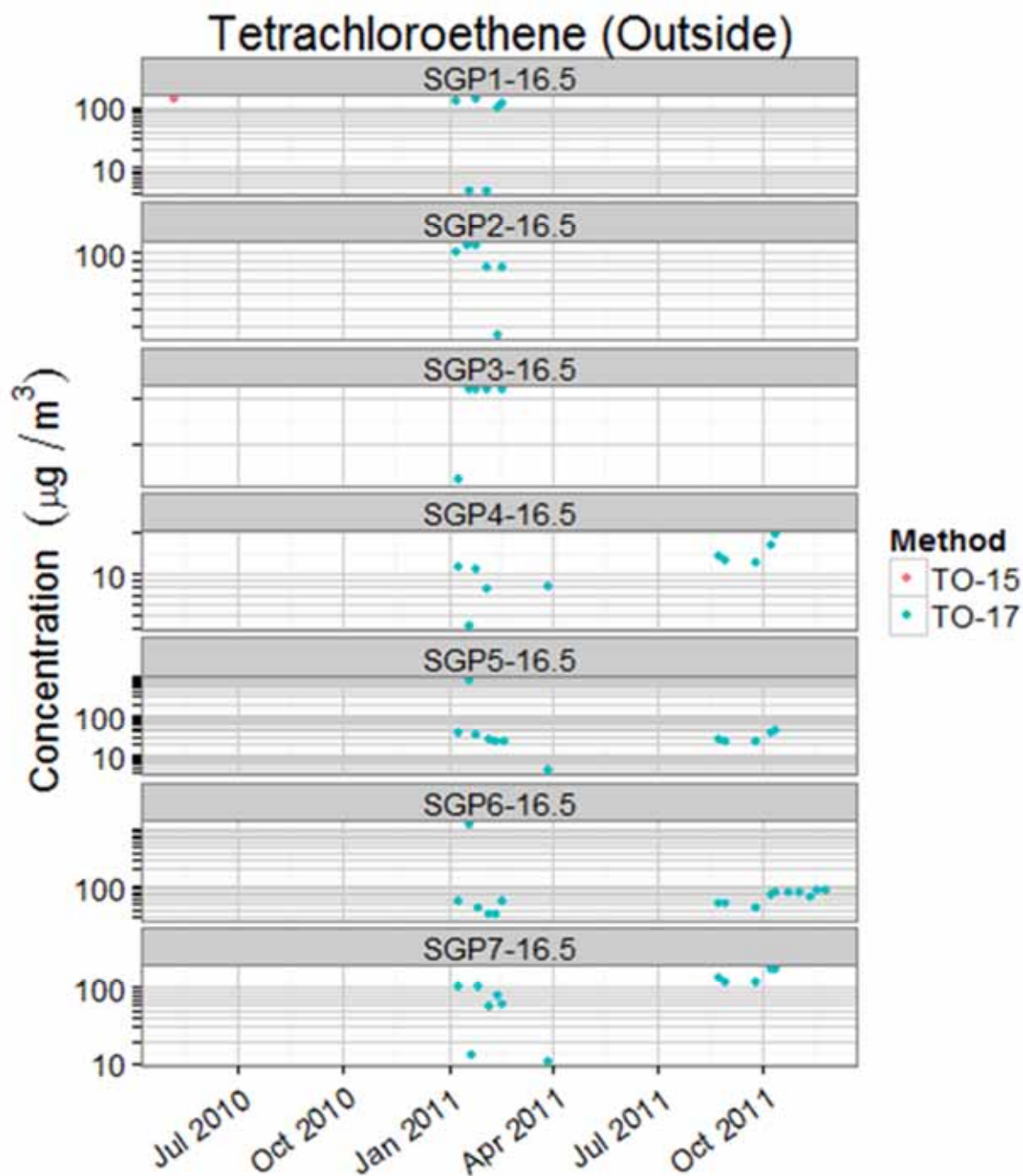


Figure 6-35. PCE concentrations in exterior soil gas at 16.5 ft bls.

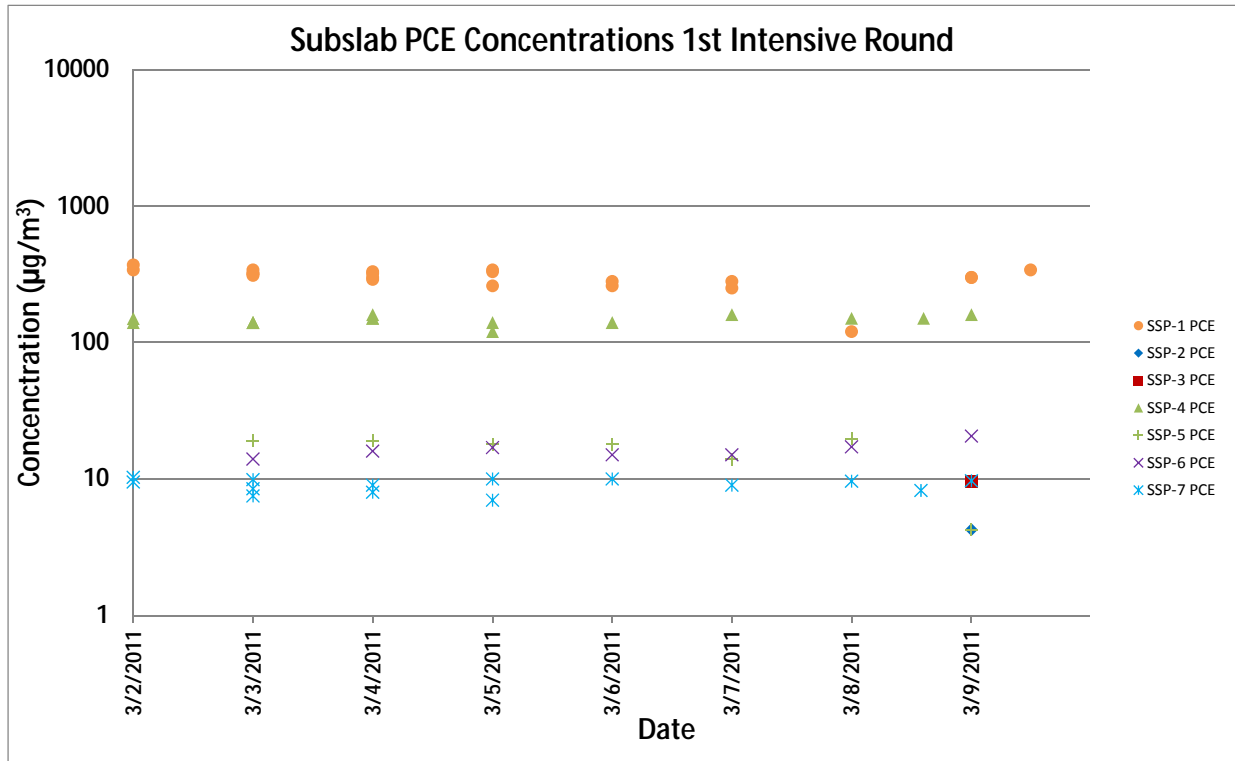


Figure 6-36. Subslab PCE concentrations over a 1-week period during the first intensive round.

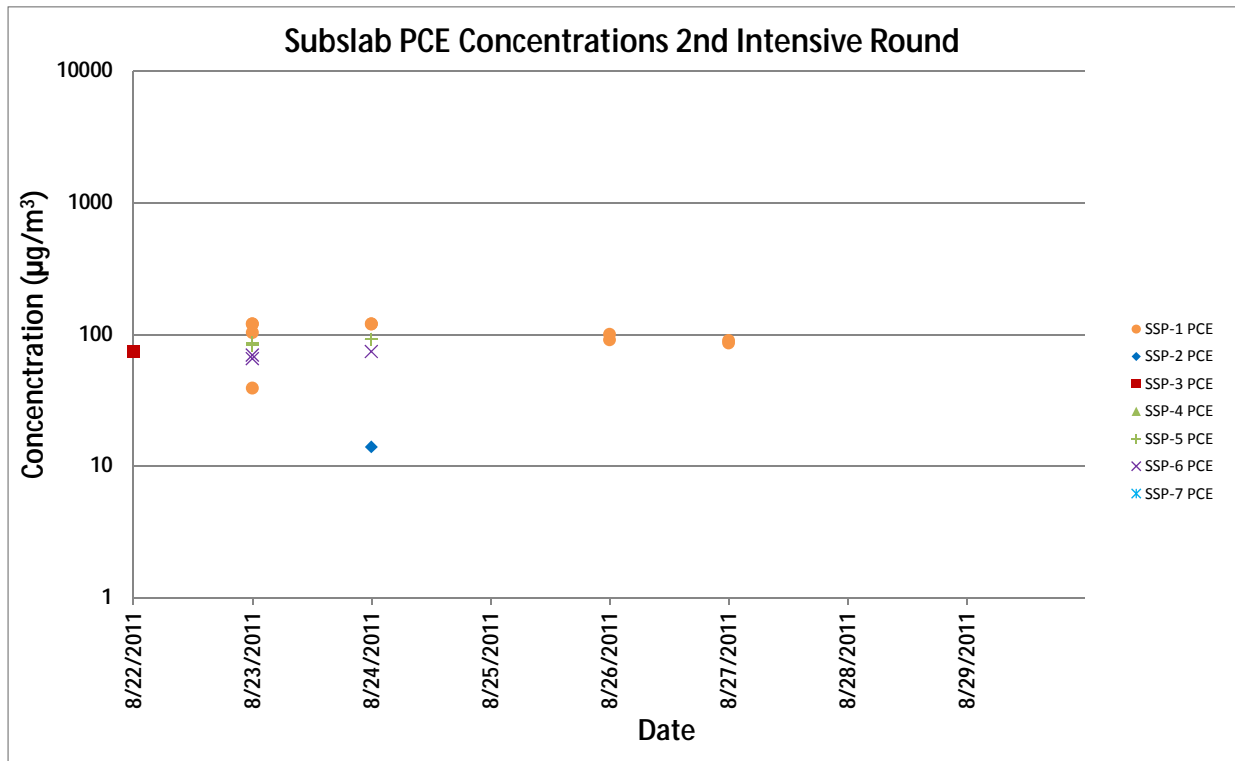


Figure 6-37. Subslab PCE concentrations over a 1-week period during the second intensive round.

6.2 Radon Seasonal Trends (based on Weekly Measurements)

Please see Section 5.2 of U.S. EPA (2012a) for a complete discussion of this topic based on the 2011–2012 data sets, and Section 5.2 of the current report for a discussion of the effects of the mitigation system on radon concentrations. The periodic operations of the mitigation system, while having dramatic short-term effects in reducing radon levels, appear to have not changed the long-term concentrations observed in periods when the system was not on (**Figure 6-38**).

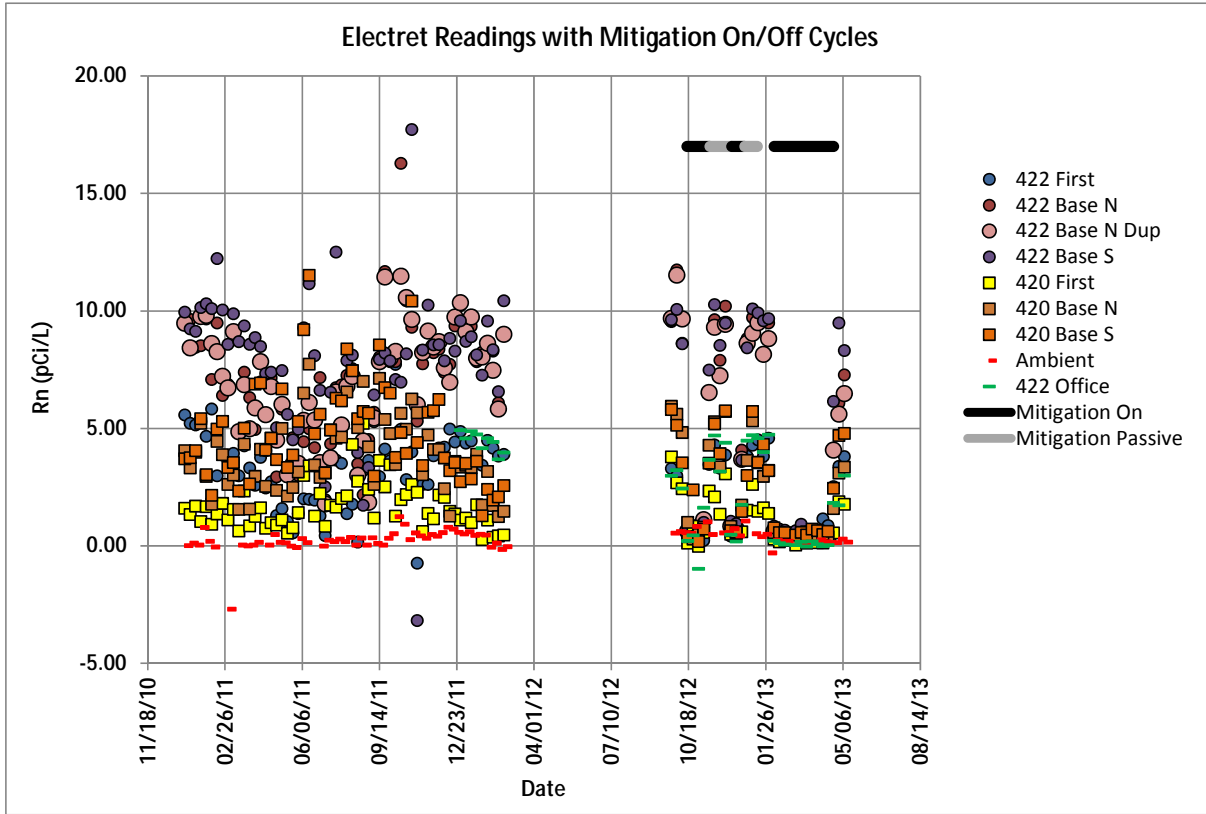


Figure 6-38. Radon: Weekly time integrated samples (electret).

6.3 VOC Short-Term Variability (Based on Daily and Hourly VOC Sampling)

Online GC data were used to assess short-term variability in VOC concentrations in indoor air and samples from selected soil gas ports. When interpreting the magnitude of variability during the first phase of GC operation, the use of a ventilation fan during parts of this period should be taken into account (see Section 12.3).

6.3.1 Indoor Air

6.3.1.1 Chloroform

Measured chloroform concentrations for 422 first floor ranged from detection level ($\sim 0.1 \mu\text{g}/\text{m}^3$) to $\sim 1.0 \mu\text{g}/\text{m}^3$. There was a notable increase in concentration by approximately a factor of 4 to 5 starting in September, and concentrations remained at that level until the end of the program in February (**Figure 6-39**). It is possible; however, that some of this could be attributable to instrument drift (see discussion in Section 4). Short-term temporal variations were less than a factor of 2.

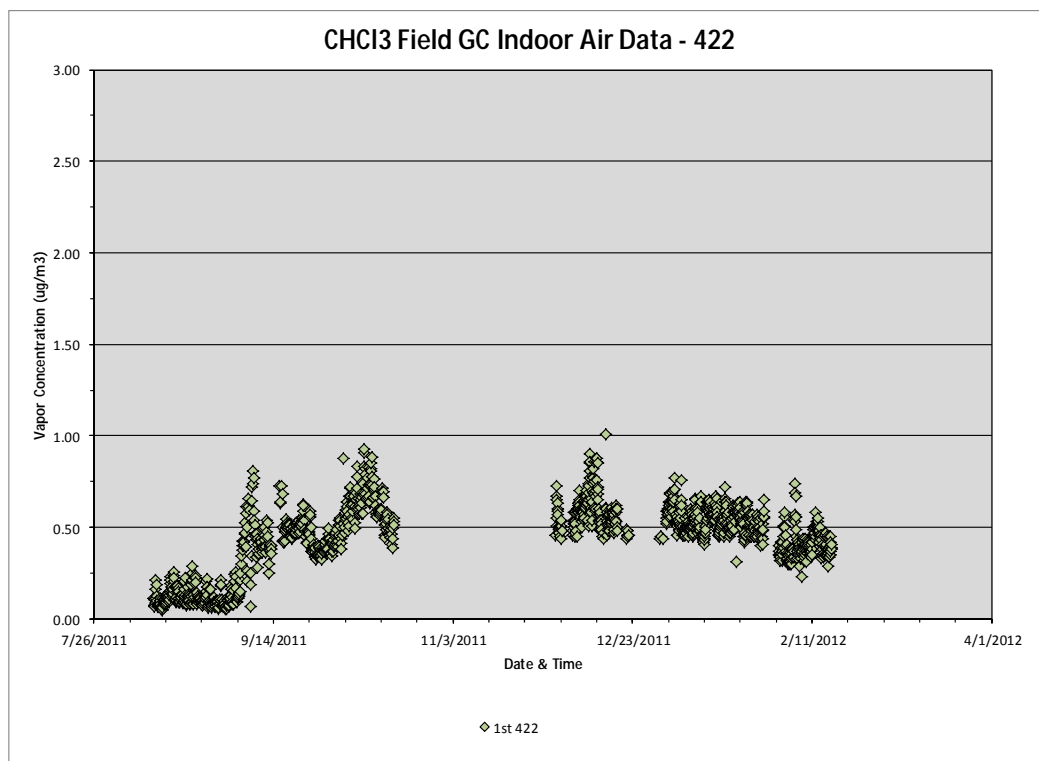


Figure 6-39. Online GC chloroform indoor air data for 422 first floor.

Measured chloroform concentrations for 422 basement were generally slightly higher than on the first floor, ranging from detection level ($\sim 0.1 \mu\text{g}/\text{m}^3$) to $\sim 1.7 \mu\text{g}/\text{m}^3$. Similar to the first floor, there was a notable increase in concentration by approximately a factor of 5 starting in September, and concentrations remained at that level until the end of the program in February (**Figure 6-40**). Short-term temporal variations were less than a factor of 3.

Measured chloroform concentrations for 420 first floor (the non-climate controlled part of the house) ranged from detection level ($\sim 0.1 \mu\text{g}/\text{m}^3$) to $\sim 1.0 \mu\text{g}/\text{m}^3$. Concentrations were about the same as measured in 422 first floor for the first phase, but slightly lower than 422 during the second phase and showed less scatter. Similar to 422, there was an increase in concentration starting in September and continuing into October (**Figure 6-41**). Other than these step changes, short-term temporal variations were generally less than a factor of 2.

Measured chloroform concentrations for 420 basement ranged from $\sim 0.3 \mu\text{g}/\text{m}^3$ to $\sim 1.0 \mu\text{g}/\text{m}^3$ (**Figure 6-42**). A less distinct step change is seen at this point in late September. Aside from that step change, short-term temporal variations were generally less than a factor of 2. Values were slightly lower than values measured in 422 basement especially during the second phase.

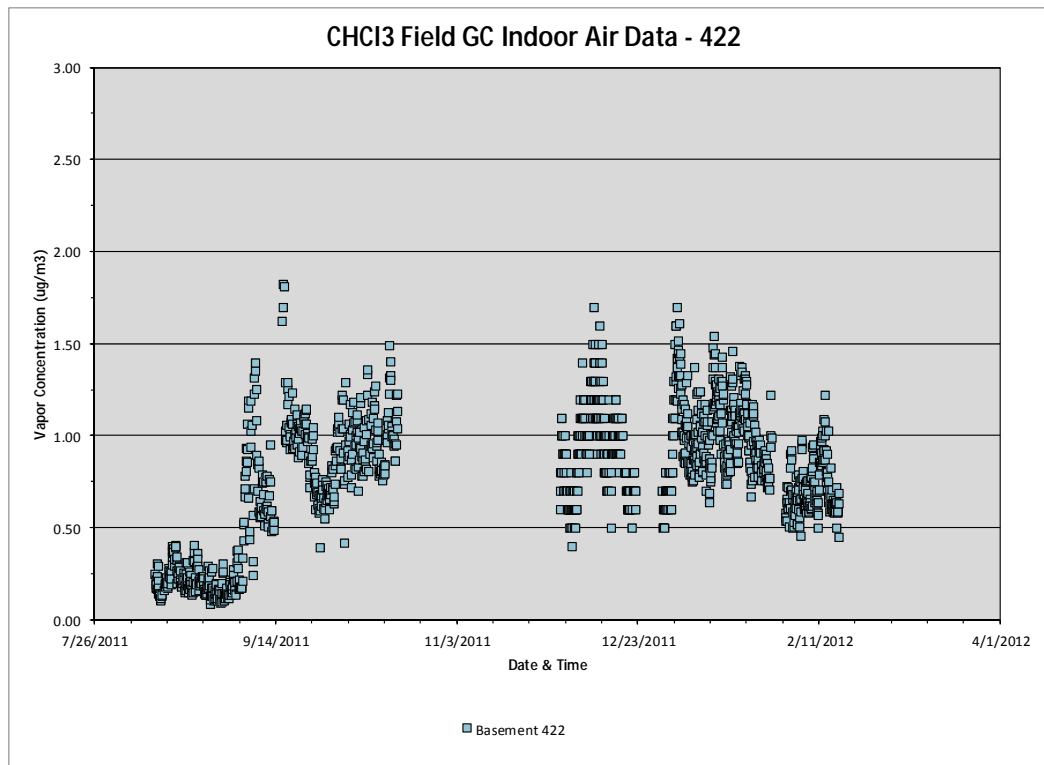


Figure 6-40. Online GC chloroform indoor air data for 422 basement.

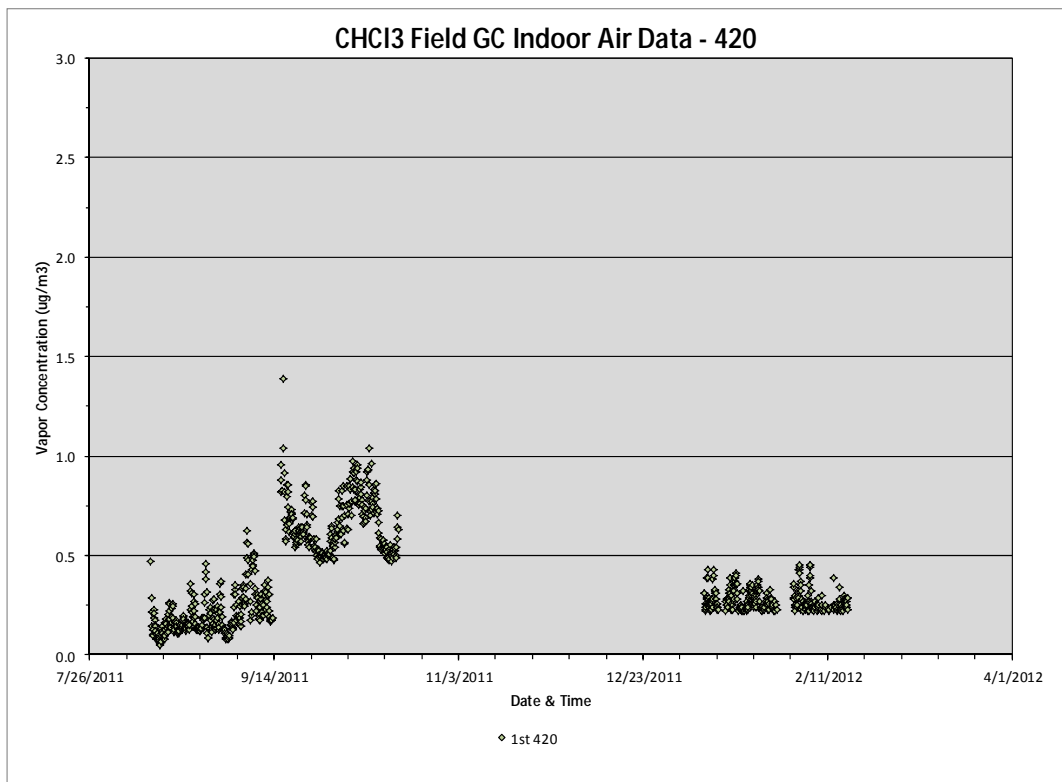


Figure 6-41. Online GC chloroform indoor air data for 420 first floor.

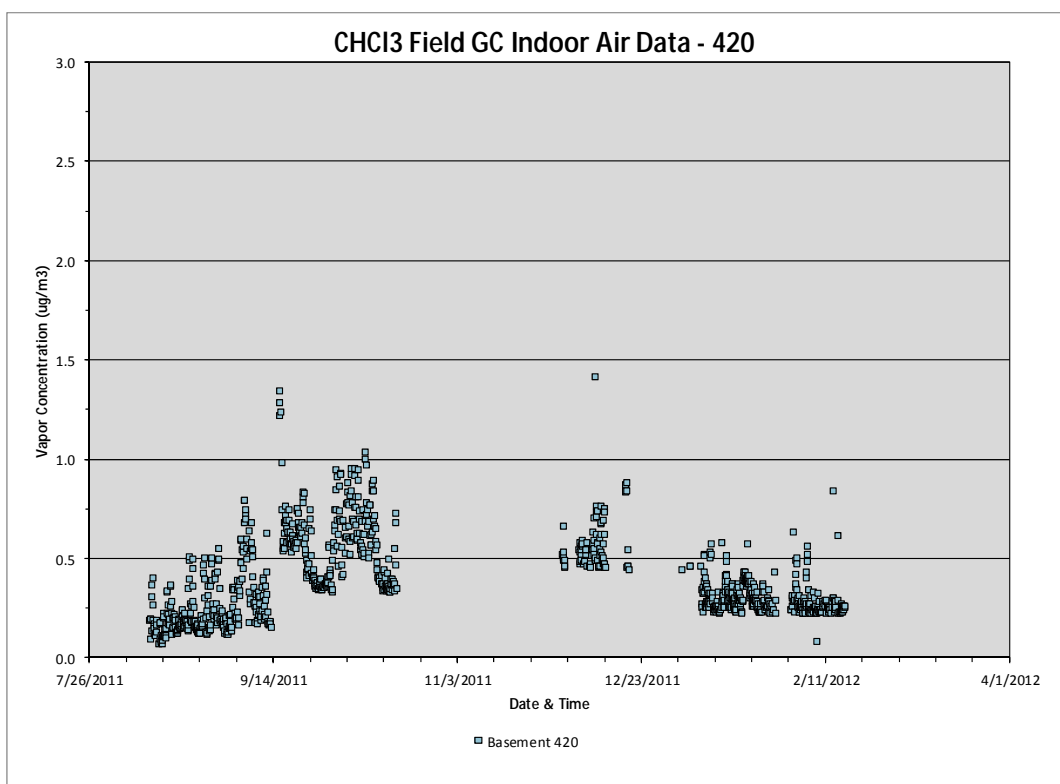


Figure 6-42. Online GC chloroform indoor air data for 420 basement.

6.3.1.2 Tetrachloroethylene (PCE)

Measured PCE concentrations for 422 first floor ranged from 0.2 $\mu\text{g}/\text{m}^3$ to $\sim 2.2 \mu\text{g}/\text{m}^3$, although the vast majority of values ranged from 0.5 $\mu\text{g}/\text{m}^3$ to 1.0 $\mu\text{g}/\text{m}^3$ (Figure 6-43). Generally, PCE concentrations were similar for both sampling phases, although there were periods of higher values in the second phase. Short-term temporal variations in the second phase were up to a factor of 4.

Measured PCE concentrations for 422 basement ranged from $\sim 0.3 \mu\text{g}/\text{m}^3$ to $\sim 3.2 \mu\text{g}/\text{m}^3$. Short-term temporal variations in the second phase were up to a factor of 4, similar to the variations seen on the first floor (Figure 6-44).

Measured PCE concentrations for 420 first floor (the non-climate controlled part of the house) ranged from detection level ($\sim 0.1 \mu\text{g}/\text{m}^3$) to $\sim 2.2 \mu\text{g}/\text{m}^3$ (Figure 6-45). Generally, the concentrations were higher in the first phase with little temporal variation and much greater short-term variation during the second phase. Temporal variation during the first phase was generally less than a factor of 2, but short-term temporal variations in the second phase were up to a factor of 10.

Measured PCE concentrations for 420 basement ranged from detection level ($\sim 0.1 \mu\text{g}/\text{m}^3$) to $\sim 2.2 \mu\text{g}/\text{m}^3$. Patterns were similar to those seen on the first floor with little temporal variation during the first phase ($<2\times$) and higher short-term variations during the second phase of a factor of 10 (Figure 6-46).

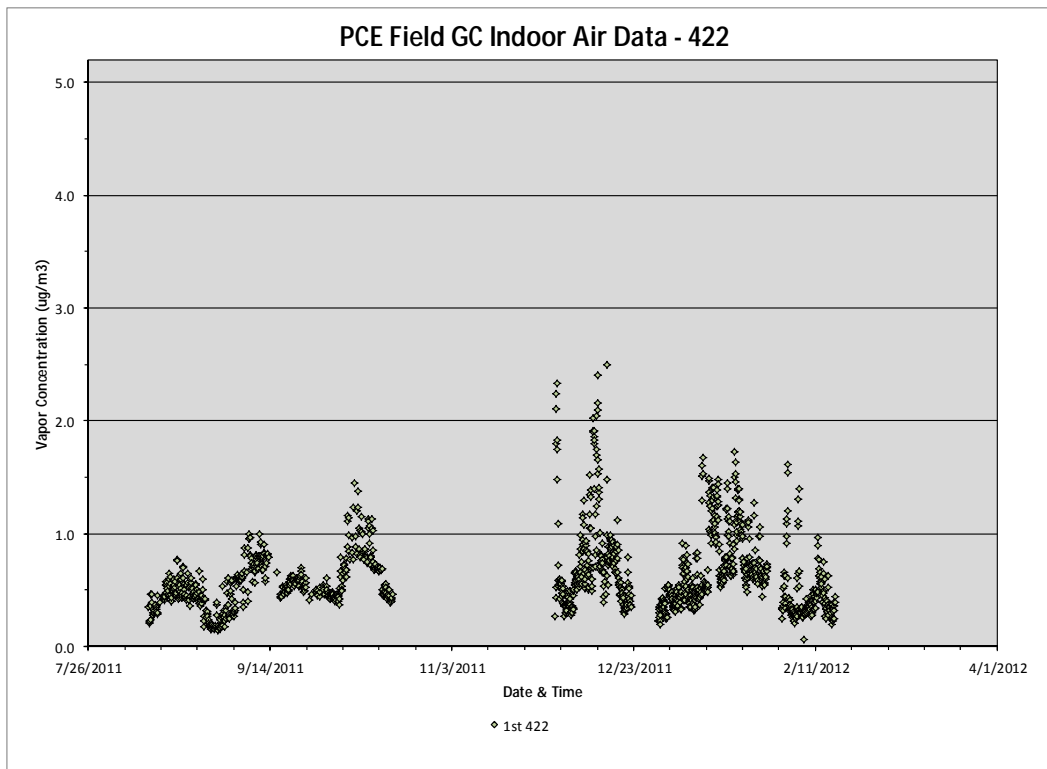


Figure 6-43. Online GC PCE indoor air data for 422 first floor.

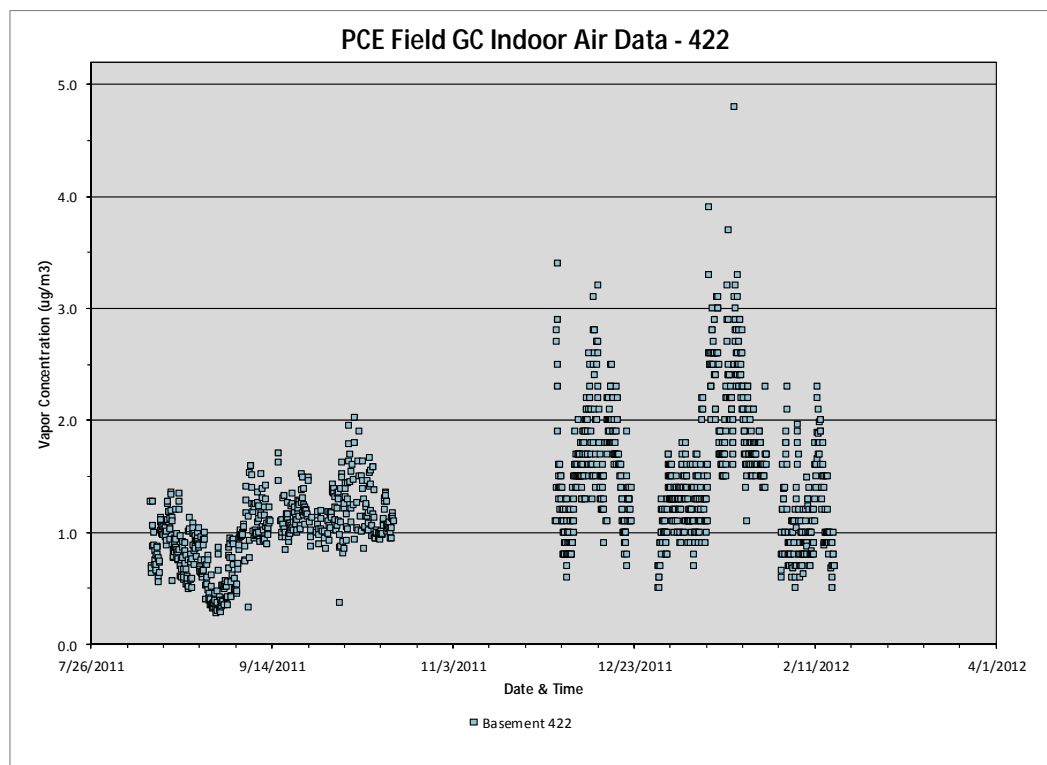


Figure 6-44. Online GC PCE indoor air data for 422 basement.

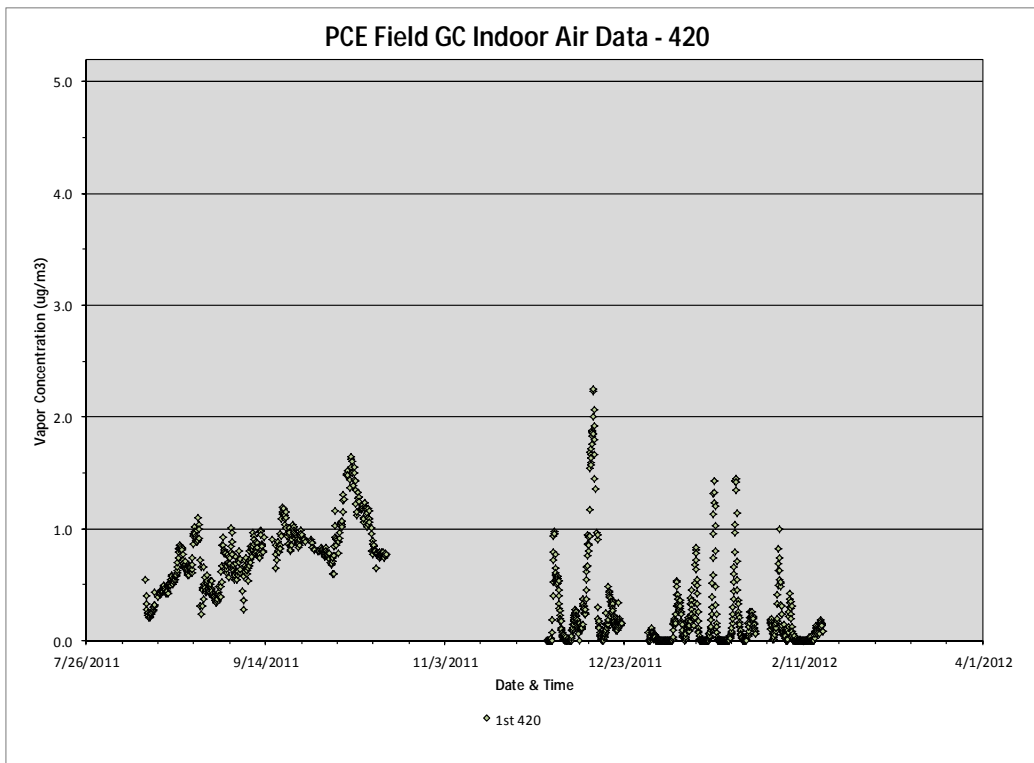


Figure 6-45. Online GC PCE indoor air data for 420 first floor.

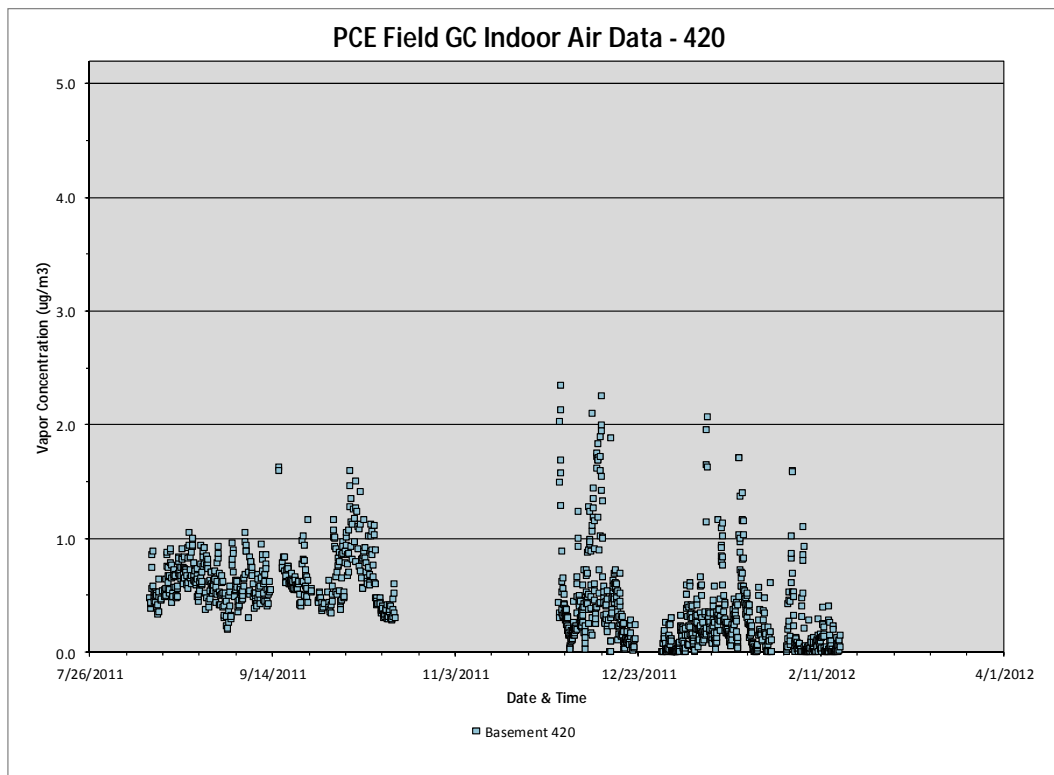


Figure 6-46. Online GC PCE indoor air data for 420 basement.

6.3.2 Subsurface Soil Gas Data

Subsurface VOC concentrations were monitored at eight locations with the automated GC:

- three subslab locations: SSP-2, SSP-4, and SSP-7
- four soil gas locations: SGP2-9 ft, SGP8-9 ft, SGP9-6 ft, and SGP11-13 ft
- one location in the wall on the side of the basement (WP-3).

Approximately 600 measurements per location were collected in Phase 1, and approximately 900 measurements per location were collected in Phase 2 at each of these eight locations.

6.3.2.1 Chloroform

The chloroform concentration data from the automated GC for all locations for both sampling phases are summarized in **Figure 6-47** and for the separate phases in **Figures 6-48** and **6-49**.

In the first phase of the program, chloroform concentrations were relatively constant until approximately September 13. At that time, the instrument inexplicably stopped and was not restarted until 2 days later on September 15. Upon restart, there was an abrupt increase in all the chloroform concentrations but not the PCE concentrations. This shift occurred because of a change in the chloroform baseline definition by the integration software and is not due to changes in the actual chloroform concentrations.

The following chloroform concentration behaviors were observed in the first phase (**Figure 6-48**):

- Temporal variation is generally less than a factor of 2 at all the sample locations during this phase except for location WP-3. However, several ports showed what appeared to be low frequency bimodal behavior. For example, SGP9-6, SGP11-13, SSP-2, SSP-4 show substantial number of points at a second level offset by more than order of magnitude from the most common level.
- At probe WP-3, concentrations show smoothly varying high and low variations of a factor of 3 to 5 times occurring over time scales of several days. WP-3 was the only location to exhibit this behavior.

In the second phase of the program (**Figure 6-49**), the following behaviors were observed:

- Probe WP-3 continued showing the same oscillations in chloroform concentrations as in the first phase.
- Probes SGP9-6 ft and SSP-4 showed a continual rise in chloroform concentrations throughout the sampling period, increasing by approximately 2 to 2.5 times above the starting concentration of the second phase. This same increase in chloroform concentrations at SGP9-6 ft was also observed in the TO-17 grab soil gas samples as a trend running from late August to December. This pattern was not seen in the first phase of the program. Despite this large concentration increase of chloroform soil gas concentrations during this second phase, there was no concurrent increase in the indoor air concentrations of chloroform measured by the online GC in either the basement or first floor of unit 422 (**Figure 6-39**).
- SSP-2 had approximately one order of magnitude variation but at relatively low chloroform concentration levels.

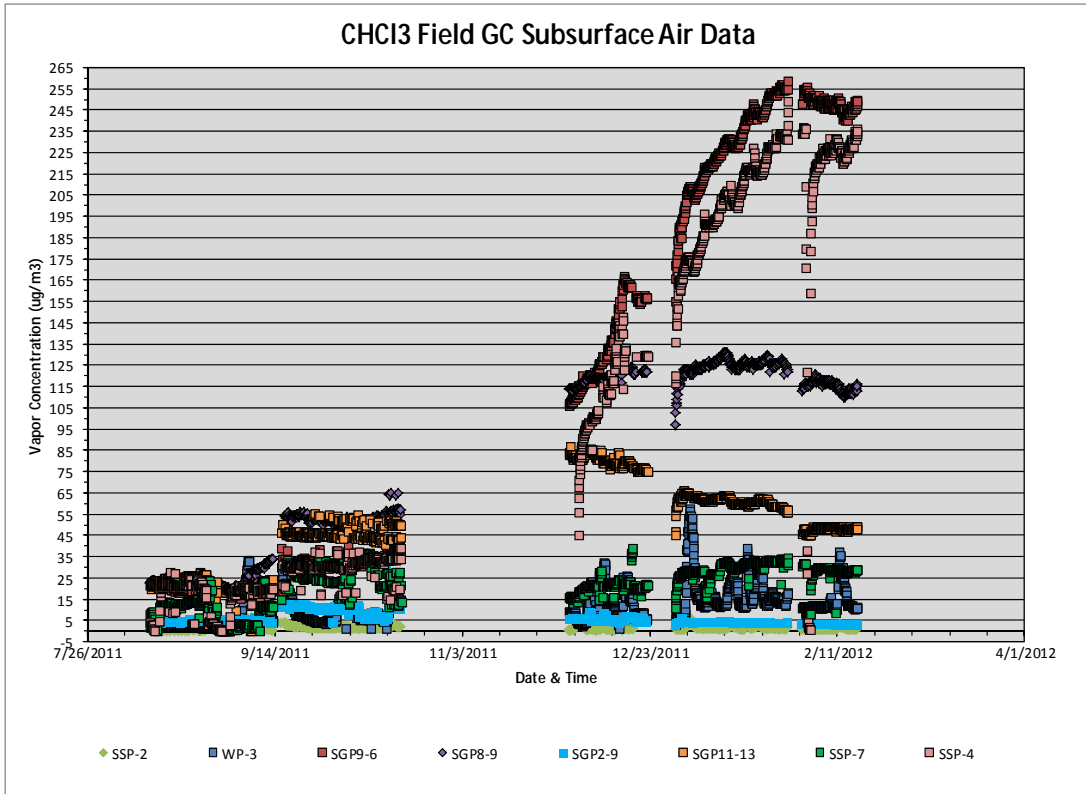


Figure 6-47. Online GC subsurface chloroform soil gas data—Phase 1 and Phase 2.

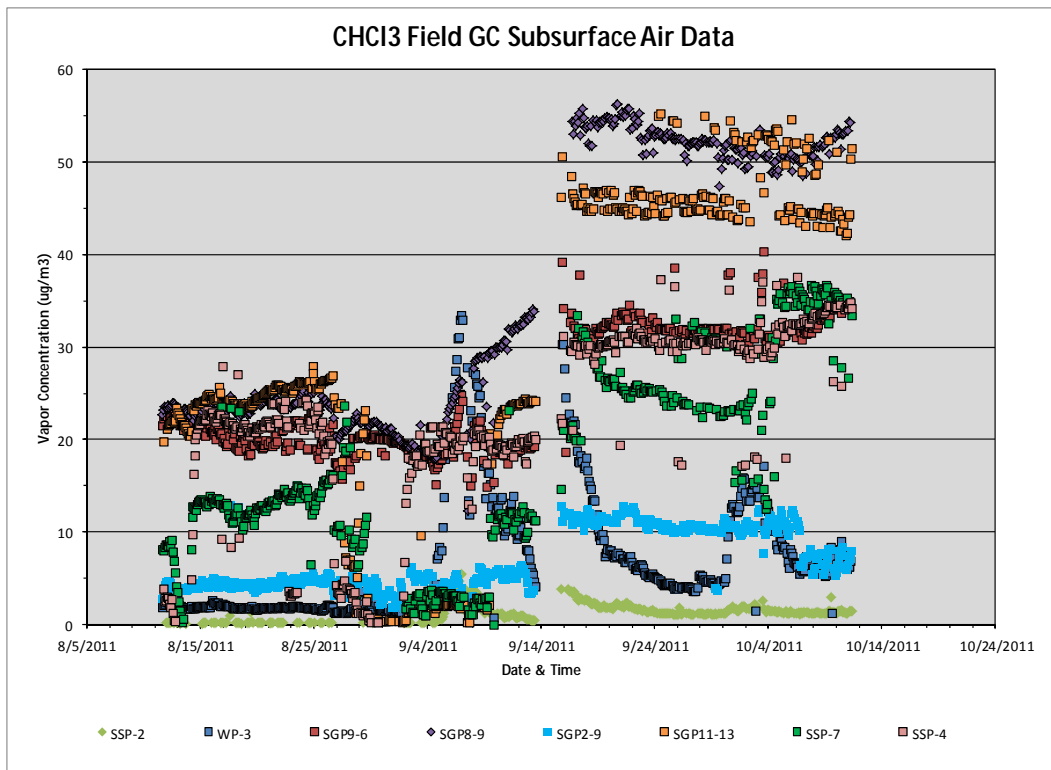


Figure 6-48. Online GC subsurface chloroform soil gas data—Phase 1.

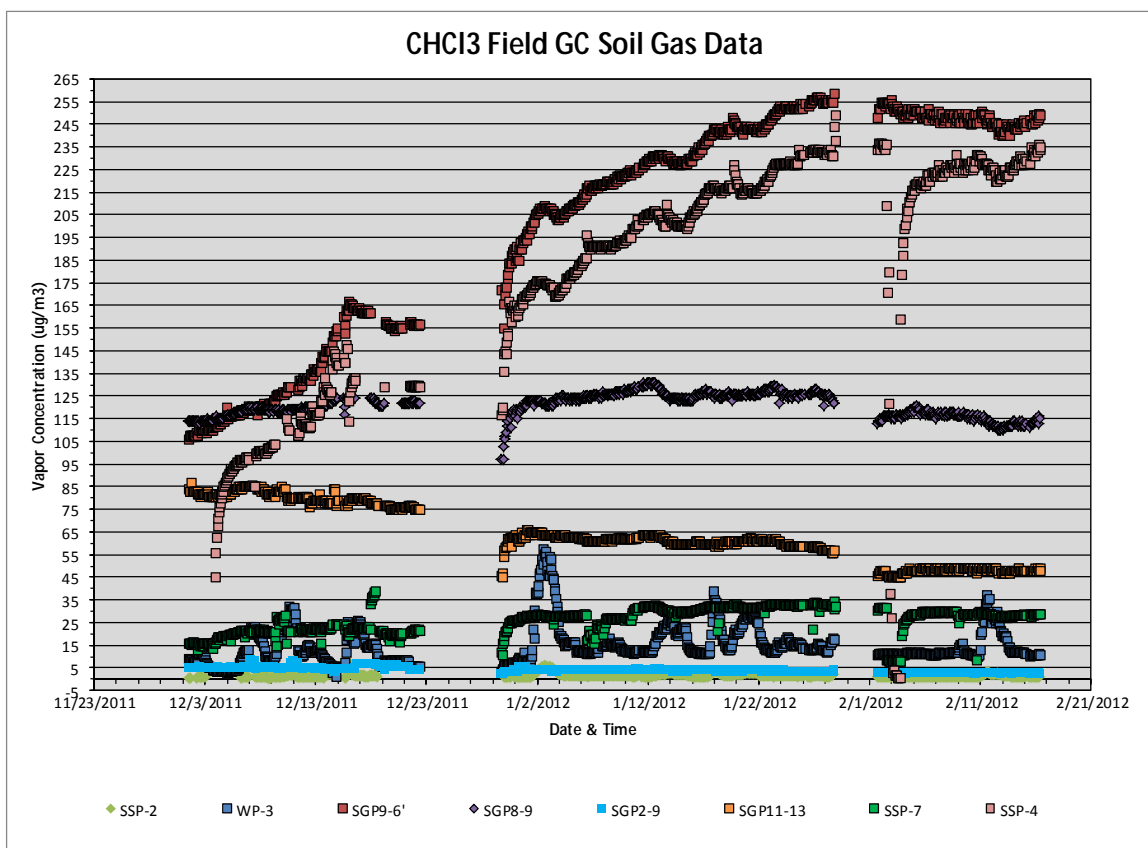


Figure 6-49. Online GC subsurface chloroform soil gas data—Phase 2.

6.3.2.2 Tetrachloroethylene (PCE)

The PCE concentration data from the automated GC for all locations for both sampling phases are summarized in **Figure 6-50** and for the separate phases in **Figures 6-51** and **6-52**.

In the first phase of the program (**Figure 6-51**), it appears as if there is a lot of fluctuation in the subsurface PCE concentrations. However, inspection of the individual locations shows the following:

- Probes SGP2-9 ft, SGP8-9 ft, and SGP9-6 ft show only slight temporal variations of 20% to 50%, except for some very infrequent outliers.
- There are two probes that field records suggest may have been inadvertently closed for a period of time:
 SGP11-13 ft 8/29/11 @ 15:16 closed; 9/9/11 between 14:00 and 15:00 opened
 SSP-7 ft 8/29/11 @ 15:36 closed; 9/9/11 between 14:00 and 15:00 opened
- Probes SSP-4 and SSP-2 also show less than a factor of 2 temporal variation over most of the sampling period. However, both of these probes contain a group of analyses when the PCE concentrations dropped rapidly by large amounts and then increased rapidly back to the prior values (**Figure 6-51**). The cause for this behavior is not clear. The drop in SSP-2 data occurred at times that may suggest an effect of the fan tests (discussed in Section 12.2). The SSP-4 drop offs happen more frequently and do not appear to be caused by the fan tests. The TO-17 data for SSP-4 PCE over the whole year also did show considerable variability (**Figure 6-53**). The pattern of this subslab probe’s plot is reminiscent of Johnson et al’s (2012) observation of data from another house: “There are long periods of relative VI activity with sporadic VI inactivity.”

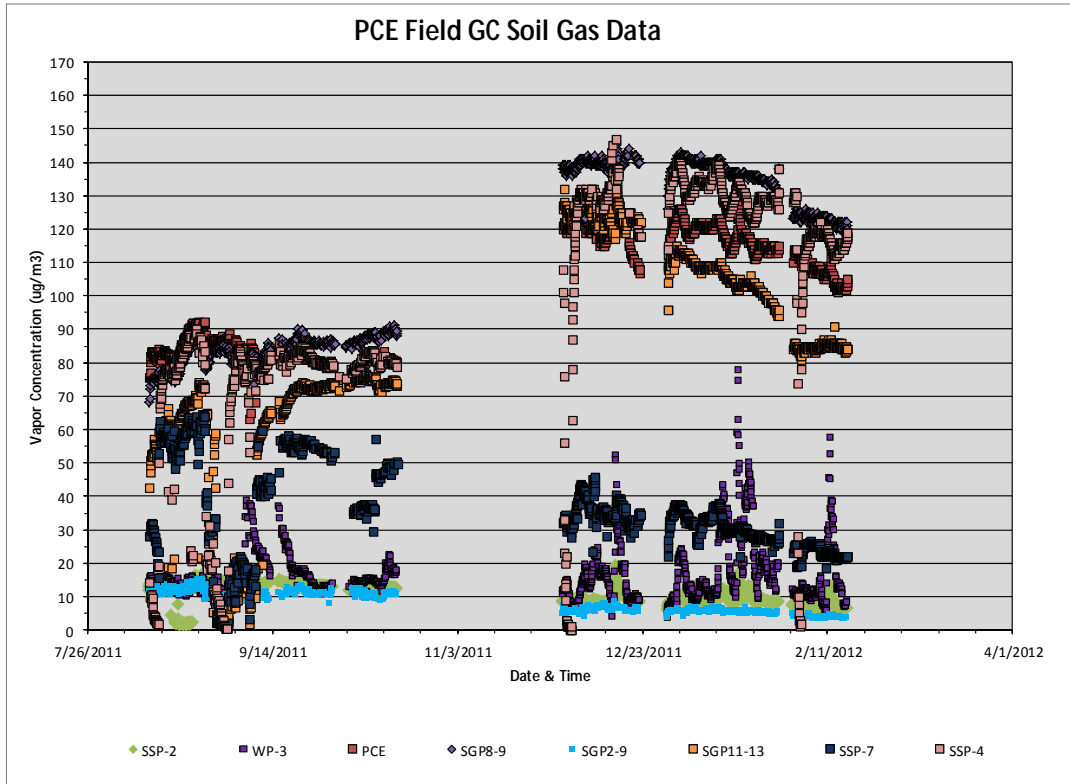


Figure 6-50. Online GC subsurface PCE soil gas data—Phase 1 and Phase 2.

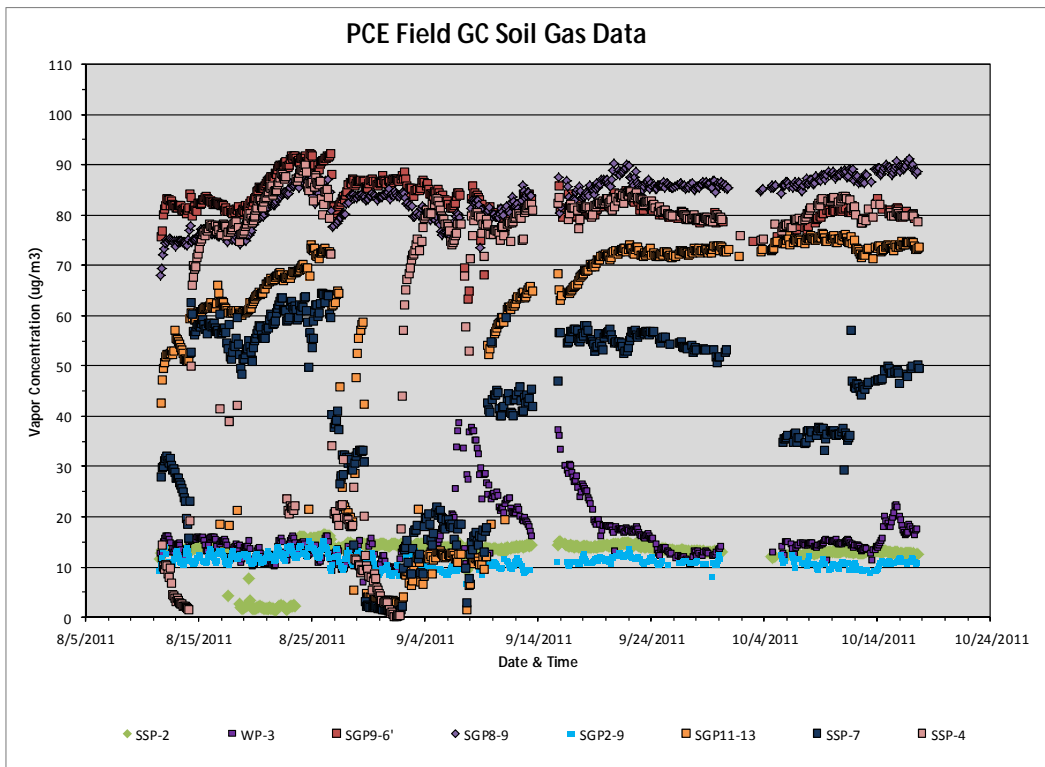


Figure 6-51. Online GC subsurface PCE soil gas data—Phase 1.

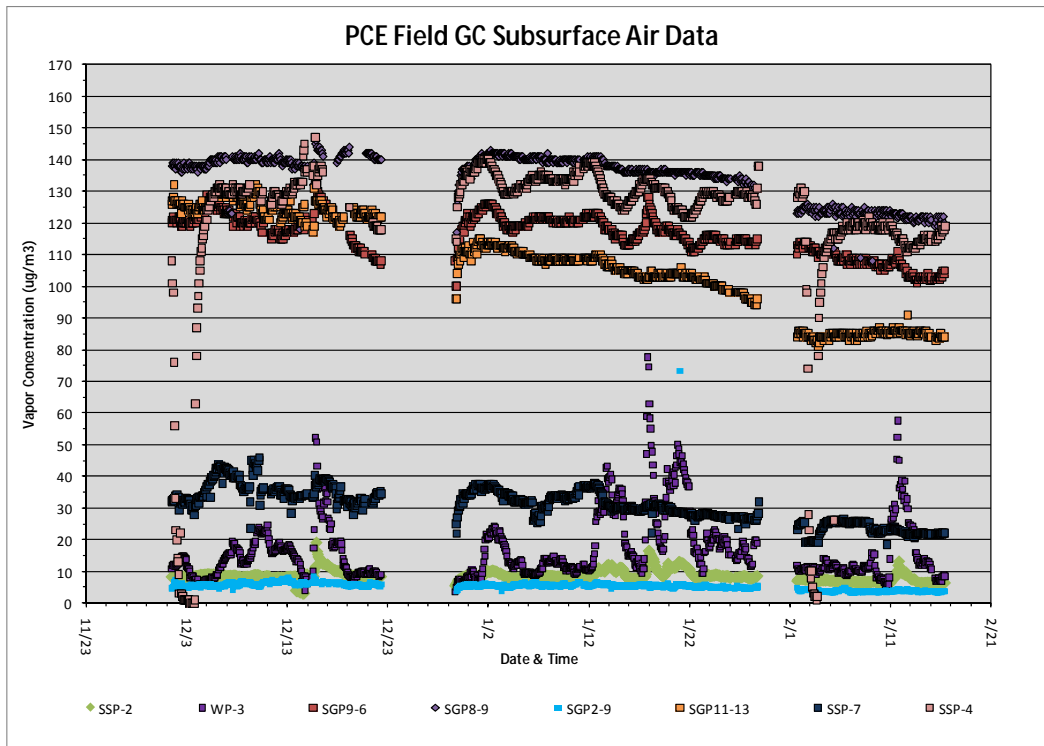


Figure 6-52. Online GC subsurface PCE soil gas data—Phase 2.

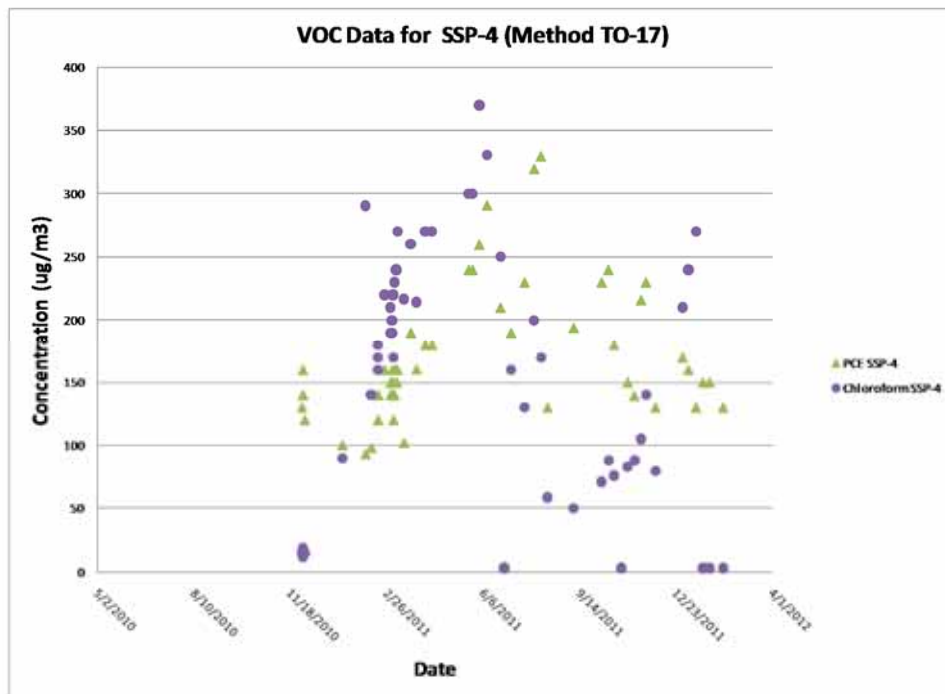


Figure 6-53. Method TO-17 data for SSP-4.

- Probe WP-3 PCE concentrations show repeated high and low variations of a factor of 3 to 5 times occurring over weekly time scales. These fluctuations are similar to the chloroform variations seen in this same probe.

In the second phase of the program (**Figure 6-52**), the following behaviors were observed:

- Probes SGP2-9 ft, SGP8-9 ft, SGP9-6 ft, SGP11-13 ft, and SSP-7 show slight temporal variations of 20% to 50% over the sampling period. Probes SGP2-9 and SGP11-13 have a gradual downward drift over several months.
- Probe SSP-4 is constant within 25% for most of this phase of observation but shows one period of a rapid drop in PCE concentrations down to near-zero values and then a quick rebound to the pre-drop values (**Figure 6-54**). This probe is located very close both spatially and within 18 inches vertically to probe SGP9-6 ft. SGP9-6 ft had similar PCE concentrations and did not show the same rapid variations. However, the drop in values is also seen in the method TO-17 samples of location SSP-4 at other times. This suggests that the behavior at SSP-4 was due to air leakage in the thin void zone that often exists under concrete slabs (DePersio and Fitzgerald, 1995) and, thus, had less influence on the SGP9-6 ft probe, which had a wider screened interval.
- Probe SSP-2 was characterized by low PCE concentrations that varied up to an order of magnitude.
- Probes SGP11-13 ft and SSP-7 did not show the rapid drop in concentrations seen during the first phase, suggesting that the behavior in the first phase might indeed be due to valve closure, not actual variations in the soil gas PCE concentrations as discussed above.
- Probe WP-3 continued to show the same oscillations as in the first phase with slightly greater variations of a factor of 5 to 8 times occurring over time scales of several days. These fluctuations are similar to the variations in chloroform concentrations seen in this same probe.
- The PCE concentrations at locations SGP9-6 ft and SSP-4 decreased slightly over the sampling period in contrast to the CHCl₃ concentrations, which showed large increases in these two probes over the same time period (**Figure 6-55** shows data from SGP9-6). This trend was also observed in the TO-17 sampling of this port during the same time period. This is indicative of different sources for the chloroform and tetrachloroethylene.

In summary, except for probe WP-3, the regular short time scale (< 14 day) temporal variations in PCE concentrations seen in all the subsurface probes are typically less than an order of magnitude. Probe WP-3 is located closest to the ground surface (~3; bls) so the variations detected might be due to surface influences. SSP-4 showed long periods at relatively steady elevated concentrations punctuated by short intervals of dramatically lower concentrations.

Variations in soil gas PCE concentration that were observed at WP-3, and to a lesser extent at SSP-2, occurred over a period of days, indicating that there is little advantage to collecting 24-hour composite samples versus instantaneous grab samples at this probe.

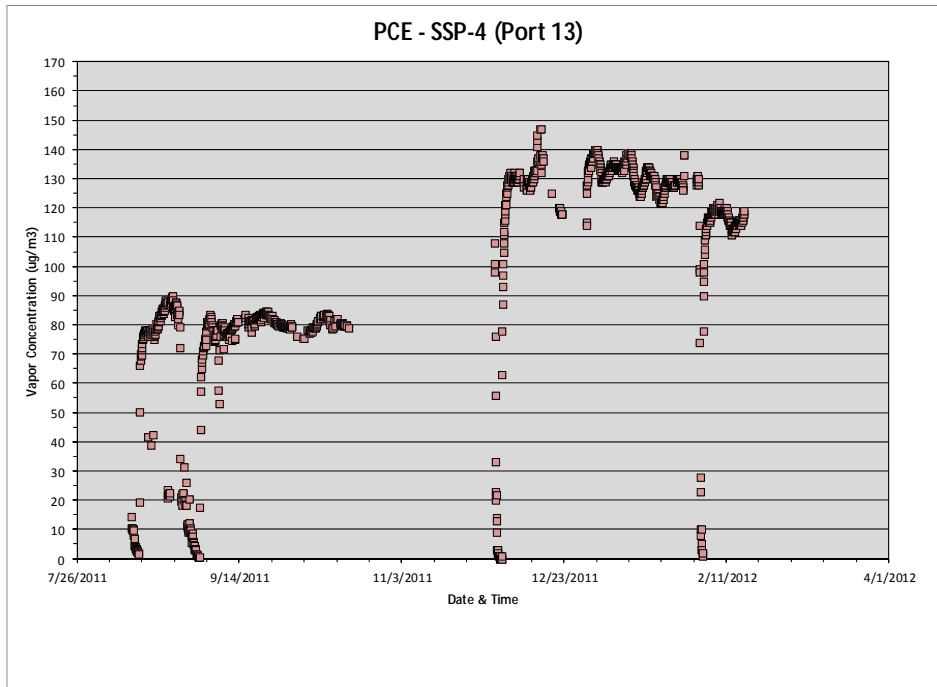


Figure 6-54. Online GC PCE measurements in SSP-4.

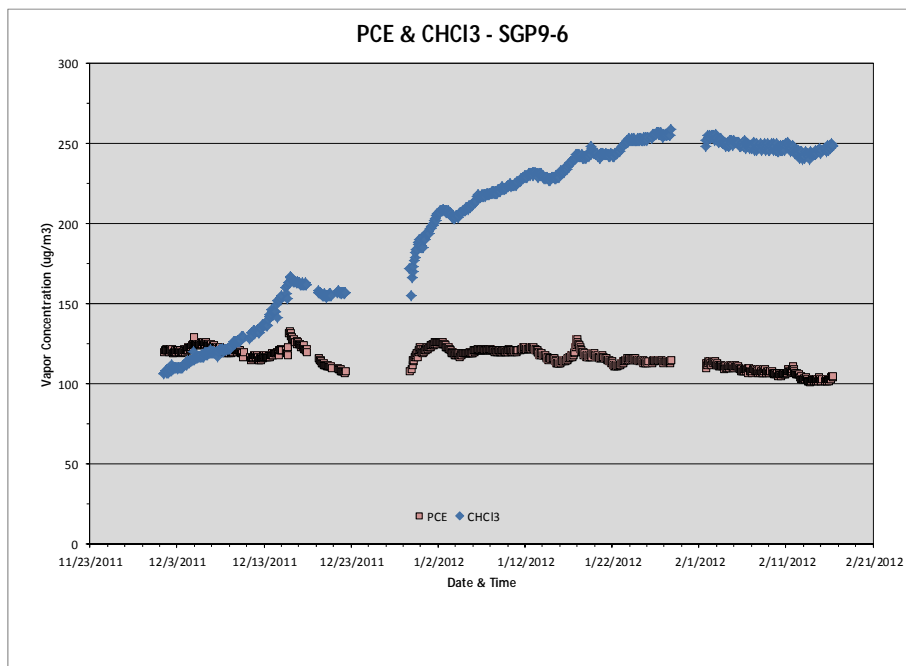


Figure 6-55. Comparison of online GC measurements of PCE and chloroform in SGP9 at 6 ft.

6.4 Radon Short-Term Variability (Based on Daily and More Frequent Measurements)

This section discusses the short term variability in indoor radon levels measured by the stationary AlphaGUARD instruments located in the basement and in the second floor office of the 422 side of the duplex. For additional discussion of the stationary AlphaGUARD data, please see the discussion in Section 5.4 of U.S. EPA (2012a) regarding the 2011–2012 data and Section 5.2 of the current report regarding the effect of mitigation system. Section 5.4 of U.S. EPA (2012a) discussed electret radon in indoor air and a breakdown of electret and stationary AlphaGUARD data during intensive periods. Regular sampling with the portable AlphaGUARD was summarized as well.

The stationary AlphaGUARD data set now includes more than 110,000 measurements at each of two locations. The degree of short-term variability in radon concentration observed when the mitigation system is not on, but after it began operating, is quite similar to the long-term trend. Dramatic variations of as much as 15 pCi/L within a few days are common in the basement data set, collected every 10 minutes in indoor air when the mitigation system is not operating (**Figure 6-56**). During the “mitigation on” periods the vast majority of the data is confined to a narrower absolute range from -0.5 to 2.3 pCi/L (note the negative readings are not physically realistic, but likely reflect a small offset error).

The office data set (422 side 2nd floor) has a somewhat smaller range of short-term variation (about 8 pCi/L is typical) but shows a similar response to mitigation (**Figure 6-57**). During the period of mitigation the variation is confined to a smaller absolute range, approximately 0 to 2.5 pCi/L.

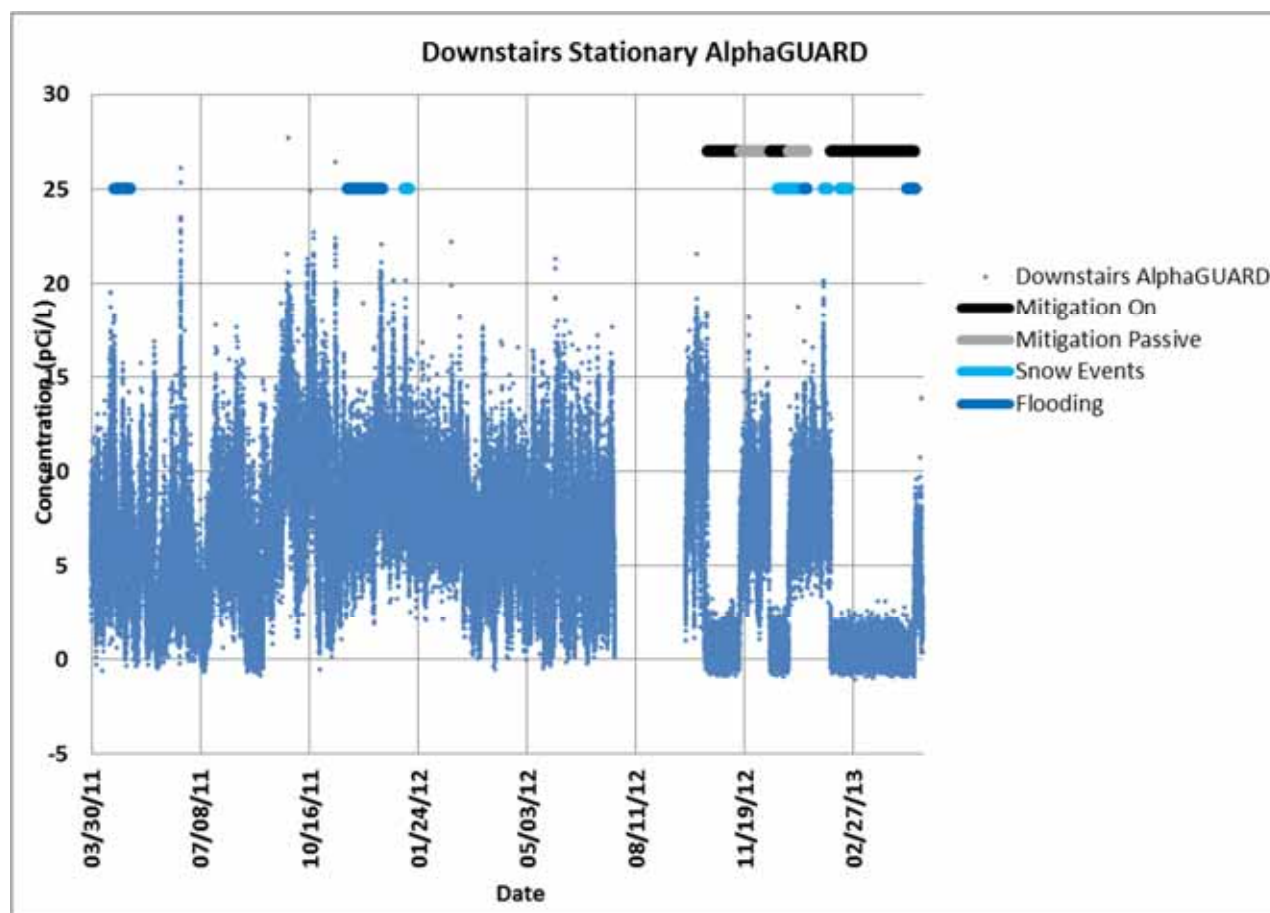


Figure 6-56. Real-time radon levels (422 basement) 2011–2013.

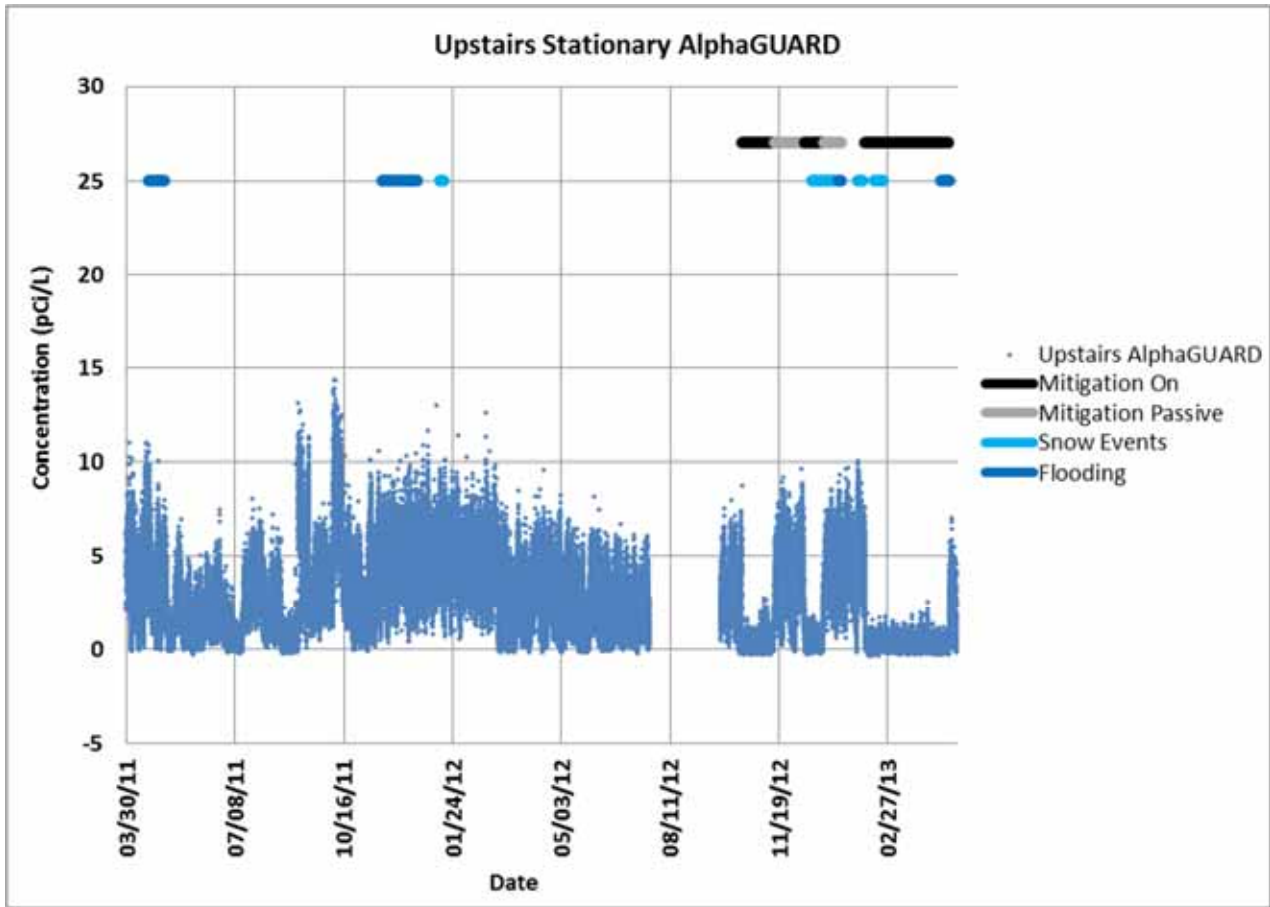


Figure 6-57. Real-time radon levels (422, 2nd floor office), 2011–2013.

6.5 Outdoor Climate/Weather Data

External and internal weather parameters were measured at the 422/420 house on a Vantage Vue weather monitor. Internal temperatures were recorded by HOBO data loggers. Barometric pressure readings were taken about every 15 minutes by Setra pressure sensors. Data were downloaded from these sources approximately once per week. Well water levels were measured approximately once per month during the first portion of the study but then continuously in late 2012 early 2013. The 2011 through 2013 weather data were presented and analyzed in Section 5.5 of U.S. EPA (2012a). This section thus focuses on the 2012 through 2013 weather situation.

Table 6-3 presents data from monthly weather summaries for 2012 and 2013 published by the Indiana State Climate Office (Scheeringa, 2012–2013). The 2012 through 2013 project year was very different from the previous year. The year began with less rain than normal, which quickly led to months of drought conditions for much of Indiana. The summer of 2012 saw heat waves followed by the third warmest July in Indiana record. However, as the year proceeded to autumn, weather became wetter and cooler than normal. A warmer than average December finally yielded to winter on December 21, leading to cooler conditions and even a blizzard the day after Christmas. The winter of 2013 began much wetter than normal, with wild temperature swings and precipitation in February. In 2012, March had been the warmest March recorded, but March 2013 was 20 °F colder than the one March 2012, falling 6 °F below average for the state (Table 5-3 and Scheeringa and Hudson, 2012–2013).

Table 6-3. Summary Meteorological Data for Central Indiana Note that the symbols “^” and “v” mean “above” and “below” normal, respectively, and that the weekly values show how the weekly averages differ from normal (from Scheeringa and Hudson, 2012, 2013)

| Month/Year | State Ave T (°F) | Central IN Ave T (°F) | State Ave Precipitation (in) | Central Ave Precipitation (in) | Special Notes on Central IN | Week 1 T ave (°F) | Week 2 T ave (°F) | Week 3 T ave (°F) | Week 4 T ave (°F) |
|----------------|------------------|-----------------------|------------------------------|--------------------------------|-------------------------------|-------------------|-------------------|-------------------|-------------------|
| April 2012 | 53.0, 1.7 ^ | 52.4, 1.6 ^ | 2.32, 1.62 v | 2.47, 1.44 v | Cool, hard freezes, less rain | 9 ^ normal | 1 v normal | 3 ^ normal | 3 v normal |
| May 2012 | 67.8, 5.8 ^ | 67.6, 5.9 ^ | 2.79, 1.61 v | 3.19, 1.2 v | Mod drought | 10 ^ normal | normal | 3 ^ normal | 16 ^ normal |
| June 2012 | 72.1, 1.2 ^ | 71.9, 1.3 ^ | 1.3, 2.89 v | 0.86, 3.24 v | Heat wave, severe drought | 4 v normal | 1 ^ normal | 5 ^ normal | 4 ^ normal |
| July 2012 | 80.5, 5.9 ^ | 80.5, 6.2 ^ | 2.45, 1.65 v | 1.75, 2.51 v | Drought, 3rd warmest July | 11 ^ normal | 3 ^ normal | 5 ^ normal | 6 ^ normal |
| August 2012 | 72.3, 0.3 v | 71.9, 0.3 v | 3.95, 0.17 ^ | 4.47, 0.72 ^ | Drought broken, windy | 3 ^ normal | 3 v normal | 5 v normal | 1 ^ normal |
| September 2012 | 64.2, 1.5 v | 63.6, 1.7 v | 5.38, 2.29 ^ | 6.40, 3.42 ^ | Cool, above normal rain | 4 ^ normal | 3 v normal | 5 v normal | 3 v normal |
| October 2012 | 51.7, 2.2 v | 51.2, 2.3 v | 3.97, 1.07 ^ | 4.44, 1.62 ^ | Cooler and wetter than normal | 4 v normal | 6 v normal | 3 ^ normal | 5 v normal |
| November 2012 | 40.2, 2.2 v | 39.8, 2.1 v | 1.02, 2.57 v | 1.19, 2.45 v | Cold, dry, and uneventful | 19 v normal | 1 v normal | 2 ^ normal | 2 v normal |
| December 2012 | 37.3, 6.2 ^ | 37.0, 6.3 ^ | 3.22, 0.16 ^ | 3.22, 0.24 ^ | Warmer and wetter than ave. | 13 ^ normal | 5 ^ normal | 10 ^ normal | 7 v normal ? |
| January 2013 | 29.7, 3.7 ^ | 28.9, 3.6 ^ | 4.7, 2.26 ^ | 5.18, 2.84 ^ | Precipitation 210% normal | 4 v normal | 14 ^ normal | 8 v normal | 2 ^ normal |
| February 2013 | 29.8, 0.6 v | 29.3, 0.3 v | 2.24, 0.04 v | 2.13, 0.14 v | Wild swings in T and precip. | 1 v normal | 9 ^ normal | 15 v normal | 3 v normal |
| March 2013 | 34.8, 6 v | 34.3, 6.2 v | 2.41, 1 v | 2.14, 1.14 v | 20 deg colder than last March | 6 v normal | <1 v normal | 9 v normal | 7 v normal |
| April 2013 | 50.9, 0.5 v | 50.9, norm | 6.45, 2.51 ^ | 7.45, 3.54 ^ | Winds and heavy precip. | 6 v normal | 7 ^ normal | 15 v normal | 3 v normal |

Note that the symbols “^” and “v” mean “above” and “below” normal, respectively, and that the weekly values show how the weekly averages differ from normal (from Scheeringa and Hudson, 2012, 2013)

Figure 6-58 shows the temperature record from the external temperature monitor and HOBO devices placed at seven indoor locations on the 422 and 420 sides of the house.

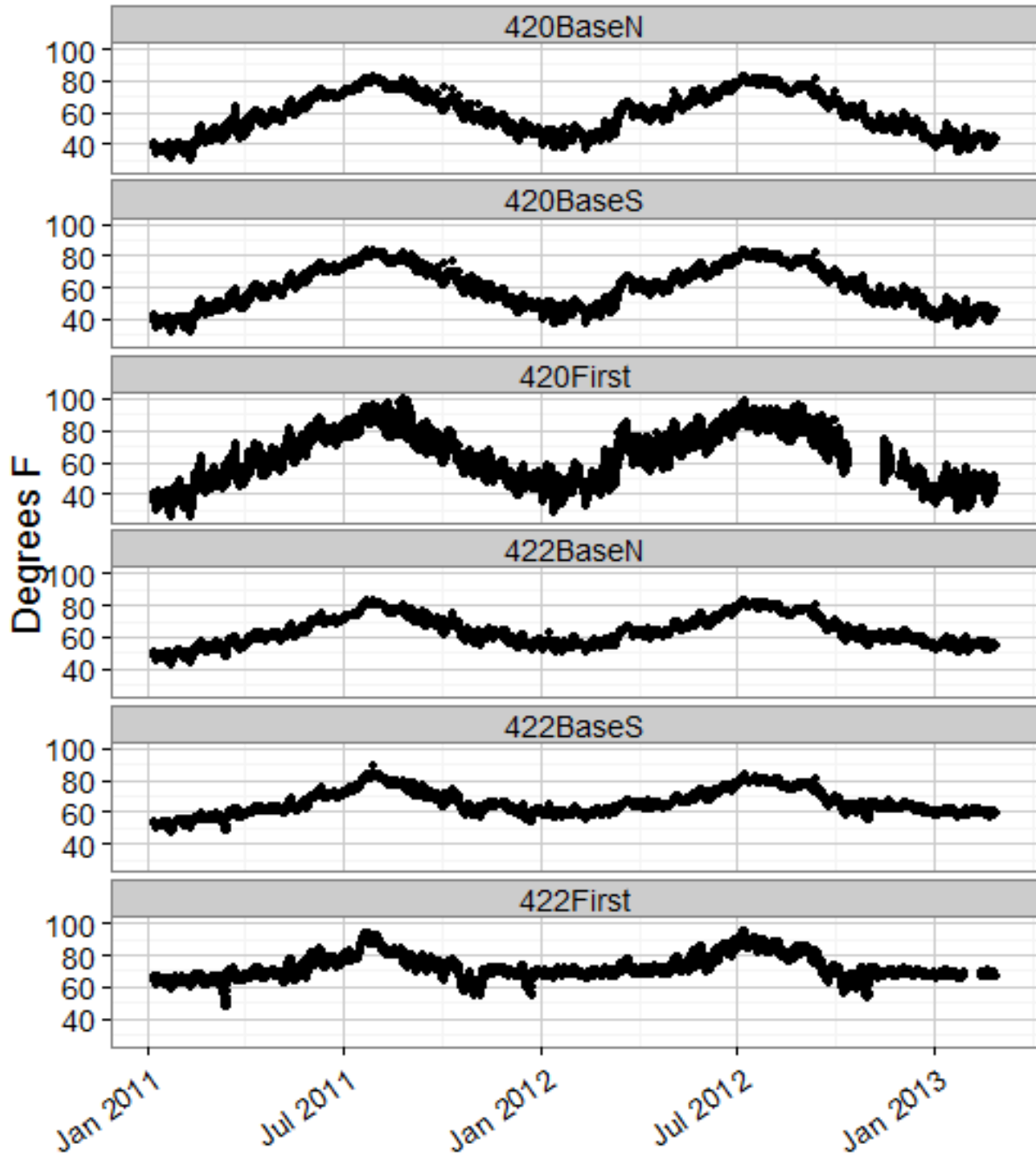


Figure 6-58. Temperature records from the external temperature monitor and the HOBO devices at seven indoor locations on the 422 and 420 sides of the house.

The same general trend can be seen in both figures, cycling from the winter lows to the summer highs. However, indoor temperatures reflect the moderating effects of the thermal mass of the building, HVAC systems (422), and air conditioning (both sides of the duplex at times).

As stated in Section 3.2.1, the gas-fired furnace was run from November 19, 2010, until June 22, 2011, then from November 7, 2011, until June 1, 2012, and then from October 31, 2012, through May 22, 2013 on the 422 side only, with no heating unit on the 420 side. Initially, window-mounted ACs ran on both sides of the duplex from June 29, 2011, until July 12, 2011. When the ACs were replaced, they were replaced on the 422 side only and ran from March 3, 2011, until October 24, 2011. **Figures 5-73 and 5-74** show some of the highest temperatures occurring during the period between the AC theft and when they were replaced on the 422 side, along with higher temperatures on the 420 side where the AC units were not replaced. The higher temperatures between AC periods could be a result of the solar stack effect, which may have been driving the higher radon and VOC concentrations observed during that time (see Section 5.2.1).

The most obvious features of the stacked hydrological graph of **Figure 6-59** are the prominent highs in rainfall and stream discharge, coupled with the high water levels measured during gauging. These highs align well with the period of heavy snowfall and rain experienced in central Indiana (see Table 6-3). Dips in stream discharge and the lower depths during well gauging match well with the much hotter drier summer period.

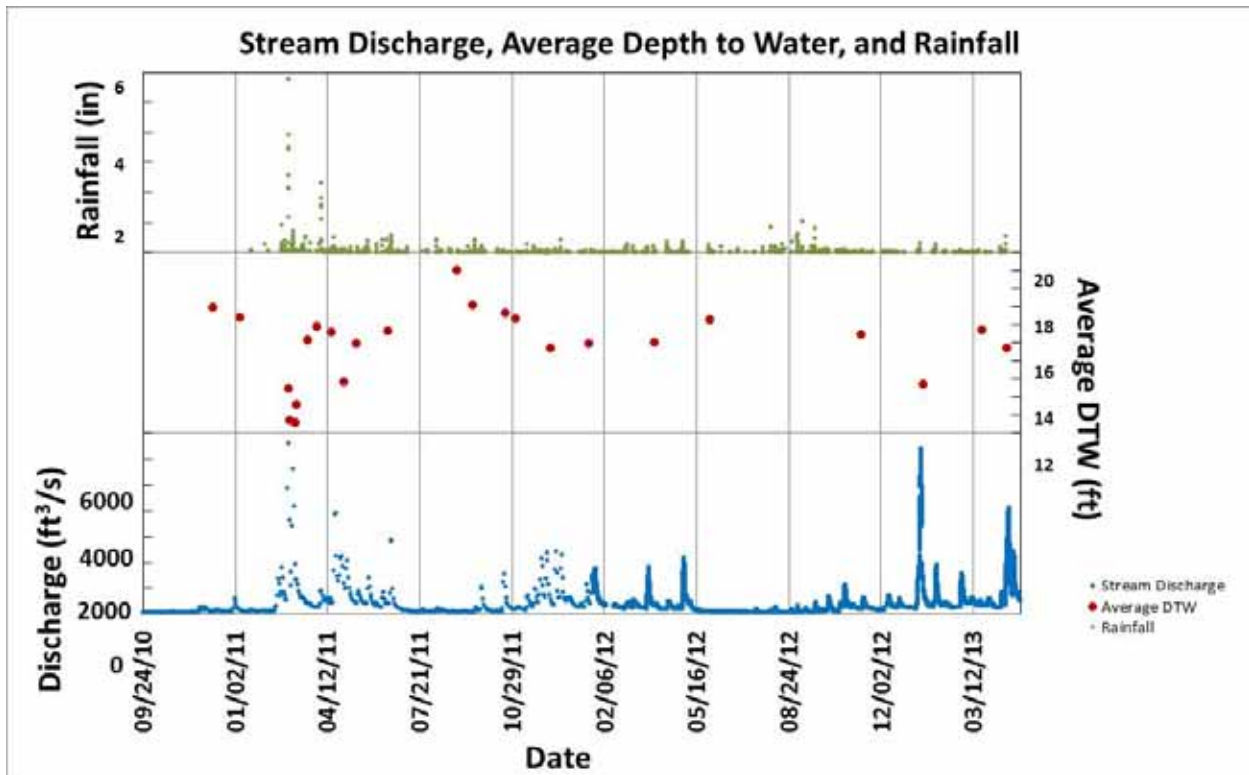


Figure 6-59. Stacked hydrological graph with rainfall in inches (top—green line), depth to water in feet (middle—red circles), and discharge at Fall Creek in ft³/s (bottom—blue line).

Various indices related to wind speed are shown in **Figure 6-60**. Generally, wind speeds are lowest in summer at this house. As shown in **Figure 6-61**, summer is also the period of least barometric pressure variation at this house. Figure 6-61 also shows that indoor humidity is much more stable over short time scales than outdoor humidity. In addition, the bottom graphs on Figure 6-61 include rainfall in inches/hour and total amounts (“Rain”) to show how the high rates correlate with significant total rainfall amounts. **Figure 6-62** shows snow depths in inches. The first winter 2010 to 2011, with a depth of 6 inches, and third winter (2012 to 2013), with a depth of approximately 7 inches, were more severe regarding snowfall than the second winter (2011 to 2012).

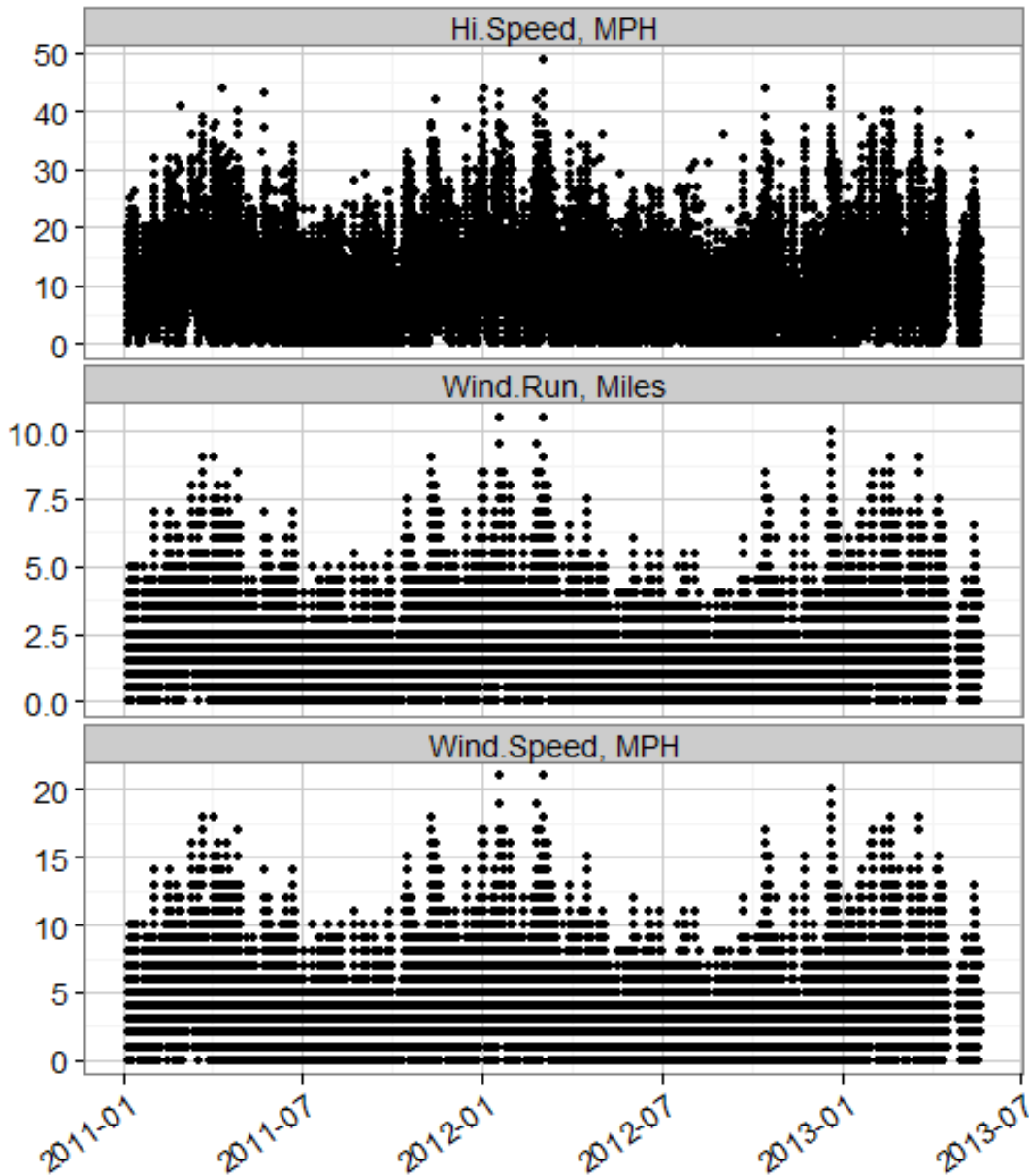


Figure 6-60. Plot of high wind speed for measurement period, wind run and wind speed (average over measurement period) at 422/420 house over time.

Wind run is calculated by multiplying the wind speed by the measurement period and summing over time.

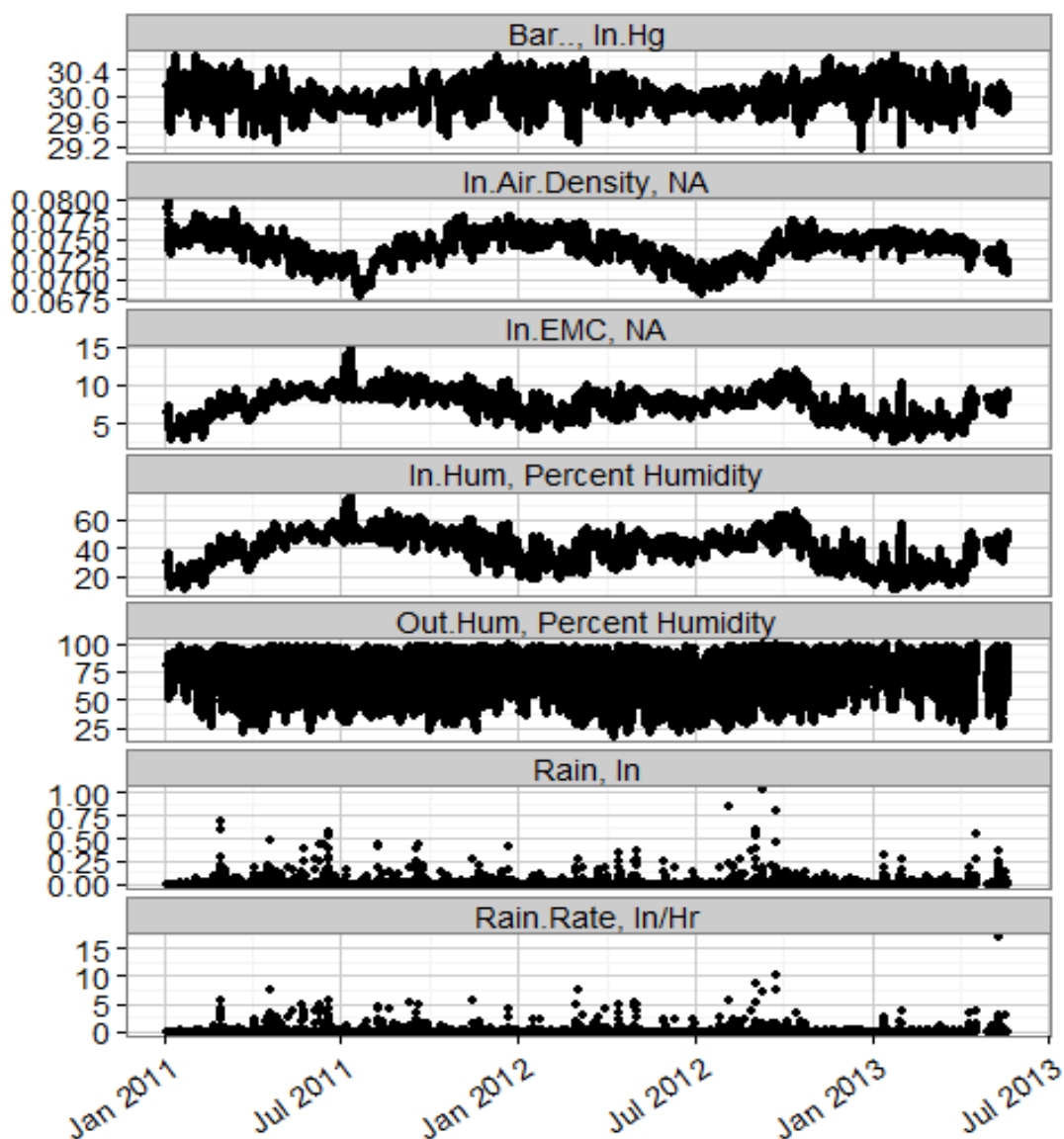


Figure 6-61. Weather variables measured inside 422 office (2nd floor) and on roof: a. barometric pressure (in Hg); b. indoor air density, c. indoor air equilibrium moisture content, d, indoor percent humidity, f. outdoor percent humidity, g. rain (inches total in measurement period), h. rain rate—the most intense rainfall during the measurement period in inches/hour.

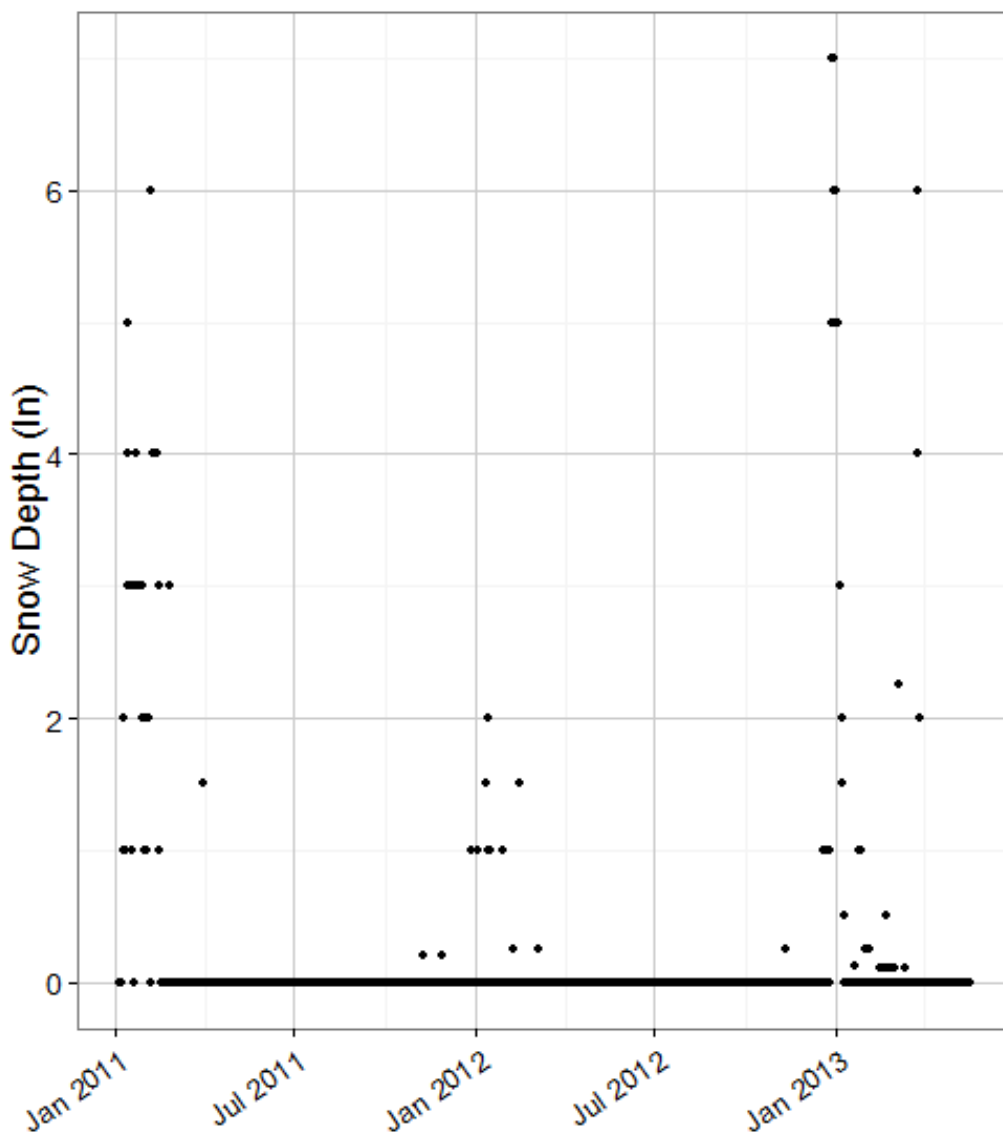


Figure 6-62. Snow depth vs. time (data are from NCDL records for the Indianapolis International Airport).

6.5.1 Indianapolis Weather Compared with VOCs and Radon

6.5.1.1 Wall Port VOC Concentrations as a Function of Barometric Pressure and Wind Speed

Sudden peaks and troughs in real-time VOC and radon data appear to have a qualitative relationship to weather phenomena. **Figures 6-63** and **6-64** (from Hartman 2 and 3, respectively) compare PCE and chloroform data for WP-3 in the 422 basement wall from the GC to barometric pressure changes recorded on the 422/420 house weather monitor. From theory we would expect a decrease in barometric pressure to be associated with higher vapor intrusion. Note that the general patterns of peaks and troughs in the wall port PCE and chloroform data only bear a rough resemblance to some of the highs and lows in the pressure data. Also note that although a late December 2012 low pressure trough might correspond with a

high peak in the PCE concentration trend, a similar late February 2012 high PCE concentration does not show a corresponding pressure drop. This suggests that multiple factors control the PCE concentration, and because of this complexity, the relationship between barometric pressure and PCE concentration is not strongly supported by either of the GC phases.

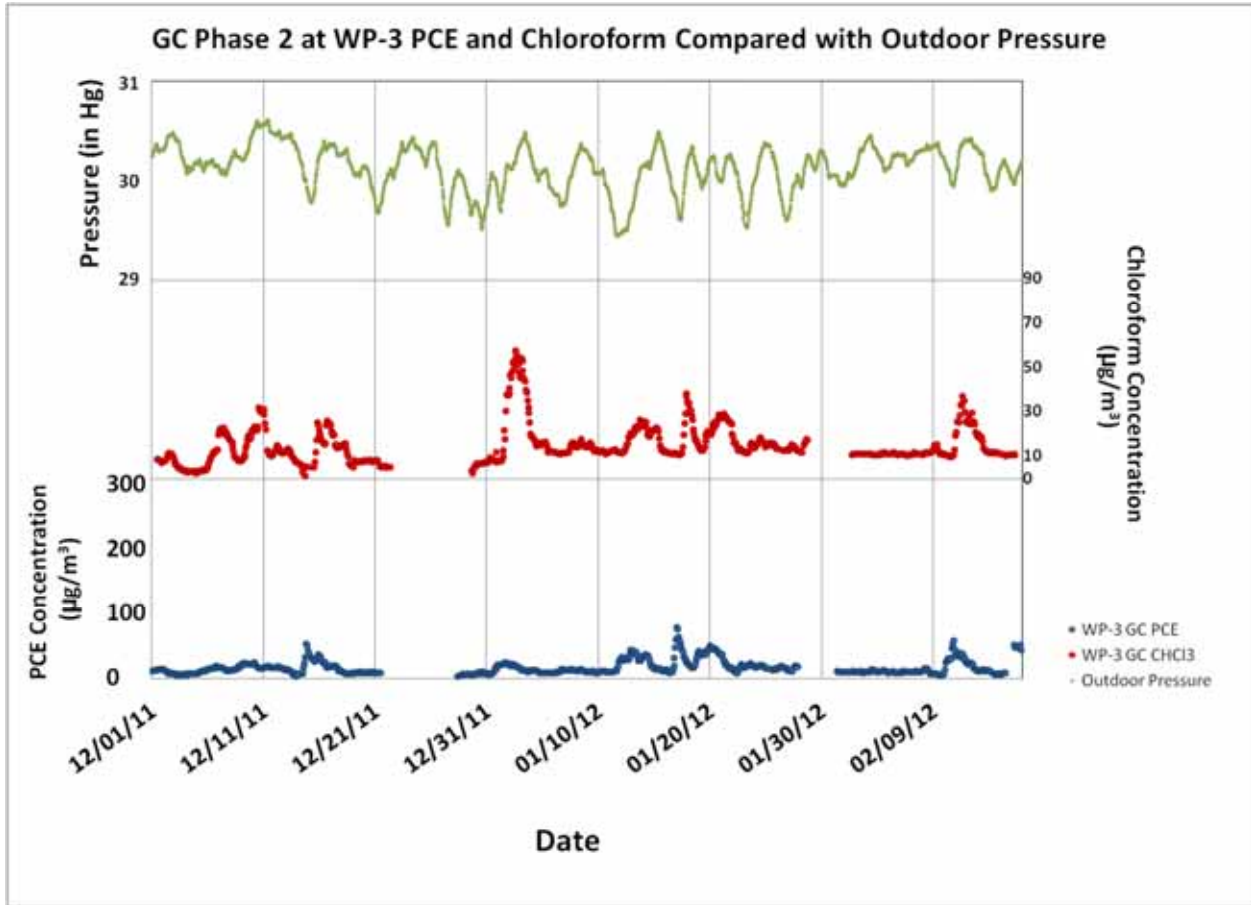


Figure 6-63. GC Phase 2 VOCs at WP-3 compared with 422/420 house external pressure.

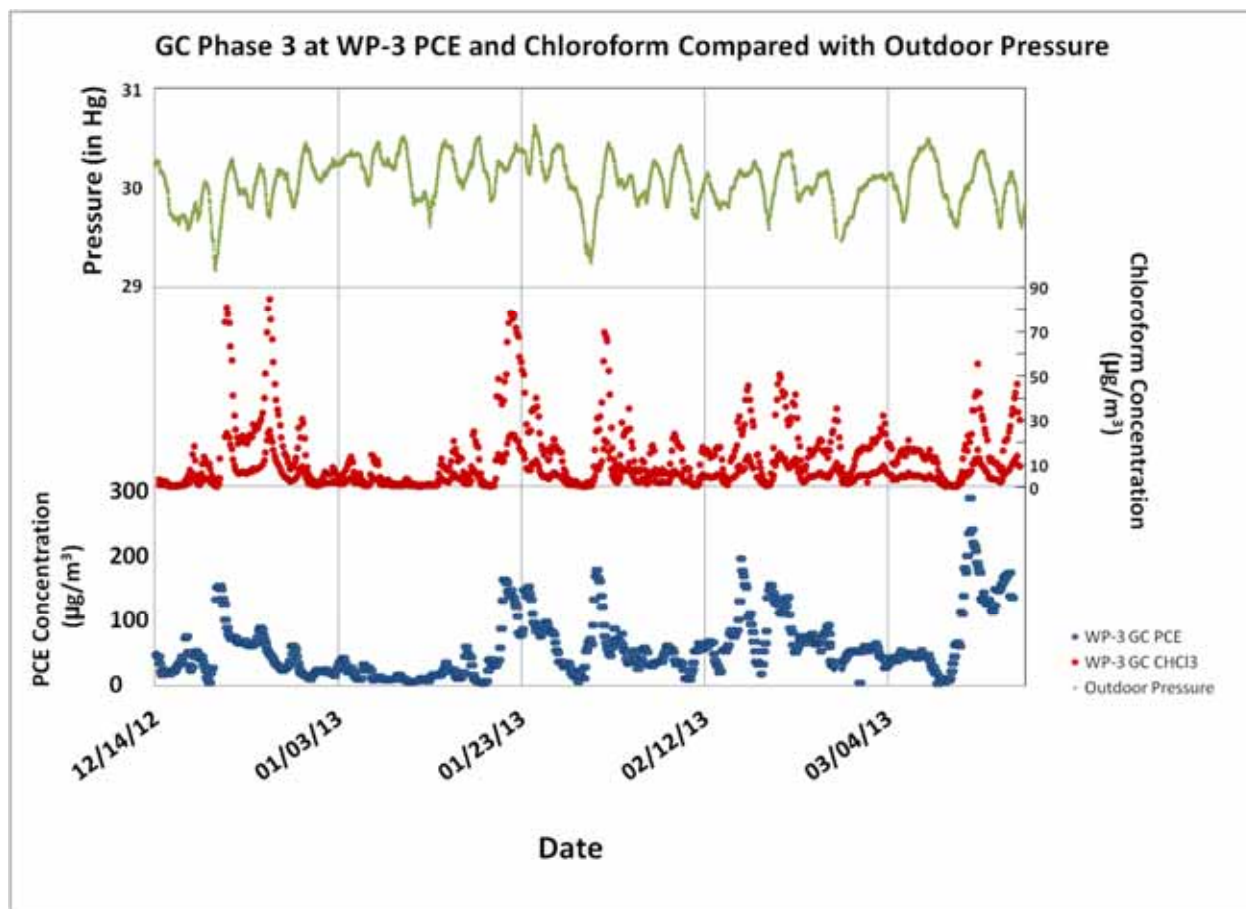


Figure 6-64. GC Phase 3 VOCs at WP-3 compared with 422/420 house external pressure.

Figures 6-65 and 6-66 (from Hartman 2 and 3, respectively) compare the same GC VOC data for WP-3 with wind speed recorded by the 422/420 house weather station. Again, there is a rough correspondence between highs and lows within the data sets. And again, as with the pressure data, high wind spikes might correspond in time to some peaks in PCE and chloroform data, but not in a constant ratio. It is possible that a relatively continuous dramatic change in wind speed has more of an effect than just a high speed alone (compare for example January 2012 with December 2012). Modeling studies would suggest that both the speed and direction of wind would be associated with vapors being driven up on one side of a building. In this case north or northwesterly winds would be likely to increase concentrations at WP-3.

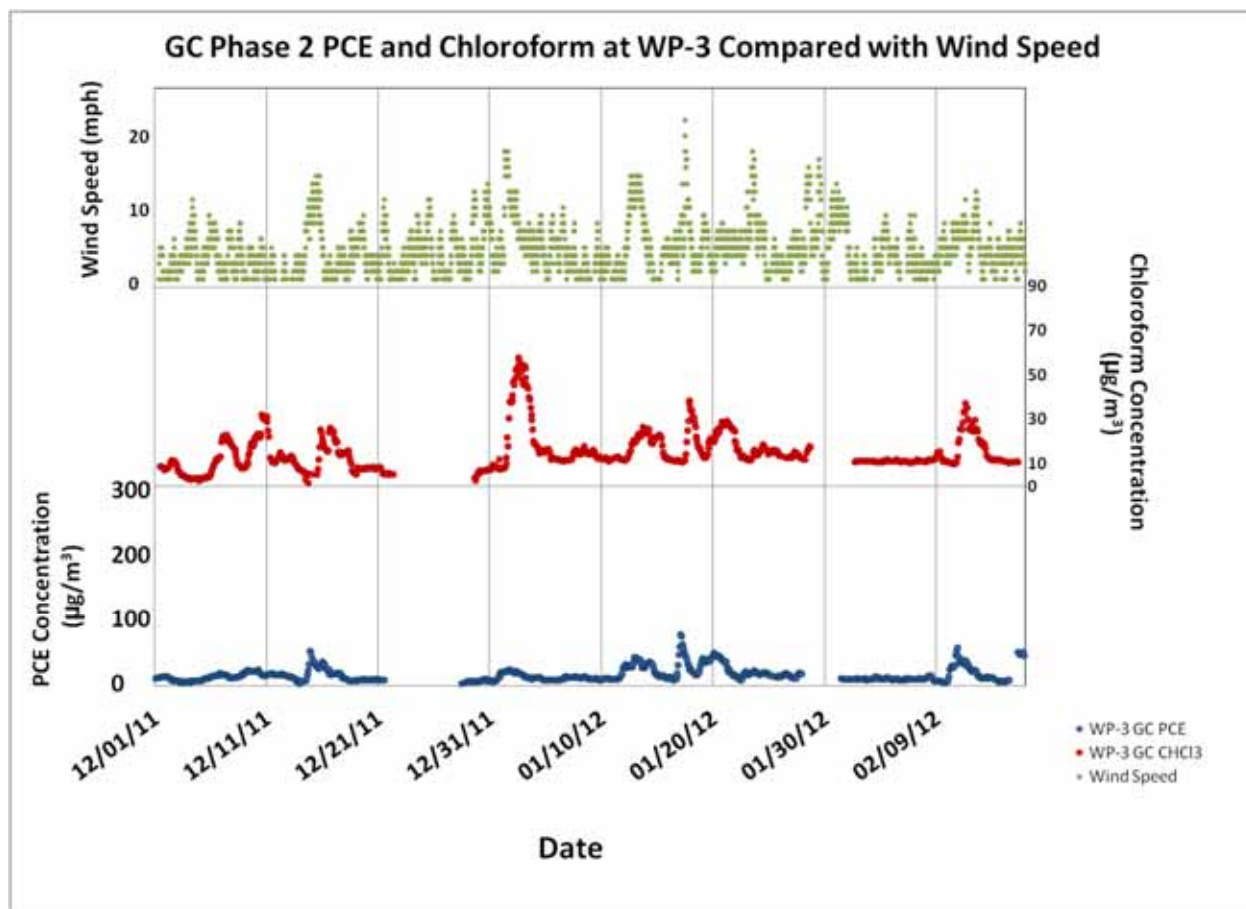


Figure 6-65. GC Phase 2 VOCs at WP-3 compared with 422/420 house external wind speed.

6.5.1.2 Effects of Snow and Ice on Radon and VOCs

It has been hypothesized that frozen soil, snow packs, or ice packs could affect vapor intrusion by providing a “cap” that limits interaction between shallow soil gas and the atmosphere (ITRC, 2007). A snow/ice pack did develop at the Indianapolis site in the winter of 2011 (see previous **Figures 3-9, 3-16, and 6-62**). Impervious surface caps have been shown to have a substantial effect on VOC distribution in soil gas (Schumacher, 2010). The air permeability of a snow layer is a complex function of pore size, grain size, ice fraction, density (Armstrong, 2008; Bender, 1957; Conway and Abrahamson, 1984). A recent North Battleford Saskatchewan vapor intrusion study showed little effect on petroleum vapor intrusion from a foot deep, light snow pack. However, since that study focused on biodegradable VOCs, it may indicate only that oxygen was successfully able to be delivered to soil microorganisms through the snow; thus, this study may not predict the effects of snow on recalcitrant VOCs (Hers et al., 2011). Investigators in that study planned in the future to create an ice lens to see if it had an effect. A successful field demonstration was conducted at Oak Ridge, TN, of the use of an engineered frozen soil barrier to hydraulically isolate a volume of radioactive waste to prevent its migration (DOE, 2009).

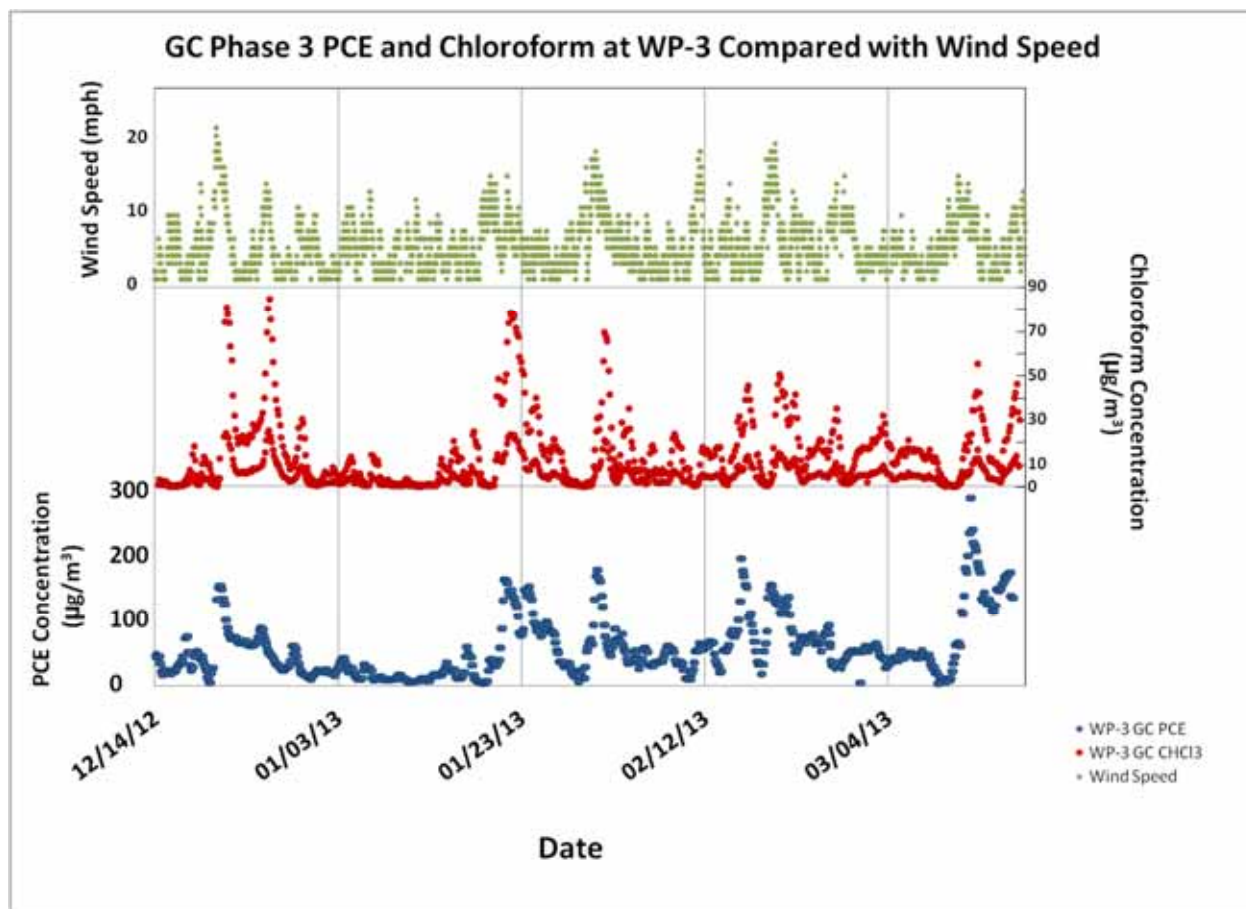


Figure 6-66. GC Phase 3 VOCs at WP-3 compared with 422/420 house external wind speed.

The EPA research team observed a potentially weather-induced phenomenon in the winter of 2011. During a period of extensive snow and ice fall, observers noted an increase in VOCs and radon matching the period of a firm snow and ice cover in the surrounding grounds of the 422/420 house. Unfortunately, the following winter, this snow/ice period did not repeat itself; however, a mini-intensive sampling period conducted during a brief snowfall in 2012 did manifest similar characteristics, to a much smaller degree, to the 2011 snow/ice period.

Figures 6-67 through 6-69 plot GC VOC data and radon data from December 2012 through March 2013. In each, the radon data are from the 422/420 house stationary AlphaGUARDs and are repeated on each figure. Each of these figures further compares the GC VOC (chloroform and PCE) data and radon data with mitigation on/off cycles and visually observed winter weather conditions. Observed winter weather conditions included long and short periods of snow cover on the 422/420 house yard and periods of the front and backyards being frozen.

Radon (any of **Figures 6-67 through 6-69**) shows a dramatic decrease during the mitigation on periods, but little to no change during periods of passive mitigation (as discussed in Section 5). The upstairs and downstairs AlphaGUARDs are separated by two floors, yet they show nearly the same general trend in radon levels (although at lower absolute values for the upstairs AlphaGUARD). This suggests that the separation between the basement and upstairs HVAC zones and outside air dilution provides little delay and do not significantly change the pattern of the radon time series.

Radon fluctuations in indoor air appear to be somewhat related to periods of snow fall or frozen ground. For example the prominent radon peaks on 1/21 and 1/31 appear to coincide with brief snow events. Previous studies have suggested that snow cover can block the usual effects of diurnal pressure variations on radon concentrations (Moses, 1963). However, Moses, Lucas, and Zerbe (1963) concluded that “a snow cover on the order of four inches or less, probably offers little obstruction to the release of radon from the soil. Yamazawa (2005) and coworkers,¹⁵ however, found that either frozen ground or snow cover can reduce radon flux from surface soils.

Subslab VOCs (chloroform in **Figure 6-67** and PCE in **Figure 6-68**) appear to be controlled more by the mitigation on/off cycles than by weather fluctuations. However, WP-3 (purple symbols) does appear to have highs associated with some periods of snow cover or frozen ground. In **Figure 6-66**, SGP2-9 (green symbols) also appears to fluctuate greatly but not associated with any period of snow cover or frozen ground.

Figures 6-69 and **6-70** show indoor air chloroform and PCE concentration time series, respectively. Both chloroform and PCE concentrations peak during the mitigation off period, roughly coinciding with two periods of snow cover and frozen ground (1/21 and 1/31/2013 peaks). It is not clear whether the influence comes from the snow event, snow cover, frozen ground, or a combination of those factors.

Even during mitigation on cycles, there appears to be a relationship between a rise in chloroform and PCE concentrations and periods of frozen ground. PCE (**Figure 6-68**) shows its most dramatic increases in concentration during periods of snow cover or frozen ground. It is very interesting to note is that VOC concentrations rose to nearly equivalent levels during periods of snow or frozen ground whether the mitigation system was on or off. Yet the mitigation system provides very effective protection from radon even during snow events.

We cannot yet fully explain why the mitigation system provided less protection for VOCs than for radon. But we note that an extensive literature exists on interactions between organic pollutants (primarily semivolatiles) and snow/ice packs (see review by Wania et al., 1998). The known effects include adsorption to liquid layers within the snow/ice, scavenging of VOCs from the atmosphere, as well as retardation of the air exchange from the surface soil. Snow is modeled as including air filled pore spaces, liquid water, organic matter, and an air-ice interface (Wania et al., 1998). Aaltonen et al. (2012) found that certain biogenic volatile organics emanating from soil were trapped by the snow pack. The air permeability of snow varies greatly among snows of different textures and changes as the snow pack ages (Conway and Abrahamson, 1984). The State of Alaska vapor intrusion guidance states without citation that “*Caps around a building, such as an asphalt driveway or frozen ground, may reduce volatilization to outdoor air and increase the concentration of contaminants near the building foundation.*”¹⁶

An EPA review of VOC behavior in soil stated, “*Yeates and Nielsen (1987) noted that differences between winter and summer concentrations occur when the frozen soil acts as a ‘lid,’ creating higher soil gas concentrations during winter because release to the atmosphere is inhibited.*”

Figures 6-71 through **6-74** plot PCE and chloroform in indoor air on the 420 side of the house as measured by the online GC. The 420 side of the house is unheated, so the conditions there are roughly as though that half of the duplex were unoccupied. When looking at radon concentrations (in **Figures 6-67** through **6-70**), it is possible to interpret elevated radon concentrations on the 422 side as being controlled by increased HVAC activity due to colder temperatures causing the heater to turn on and not snow cover or frozen ground. This could also be true for the higher VOC concentrations in indoor air (**Figures 6-69**

¹⁵Radon exhalation from a ground surface during a cold snow season

¹⁶State of Alaska. Department of Environmental Conservation

and **6-70**). However, the 420 side of the house has no HVAC system and is considerably cooler than the 422 side during the winter (**Figure 6-58**). **Figures 6-71** and **6-72** plot chloroform concentrations of the first floor and southern basement, respectively. The chloroform data do weakly suggest increased concentrations during periods of snow or frozen ground, although ambient and indoor air concentrations are similar, suggesting that outdoor air may be controlling chloroform levels during this period. PCE concentration data suggest a stronger relationship between increased concentrations and periods of snow or frozen ground, although, the alignment between events and concentration increases is not perfect (**Figures 6-73** and **6-74**).

Each of our data sets (**Figures 6-67** through **6-74**) suggests a relationship between indoor air quality and winter weather conditions (snow cover, frozen ground) to a greater or lesser degree. However, those correlations were not always uniform. Snow events, from a light dusting of less than a quarter of an inch to a blizzard producing 7 or more inches, seemed to have varying effects. The amount of snow fall and depth of accumulation did not seem to matter significantly as effects were seen even with no accumulation, just flurries. These snow flurry effects might suggest that snow events may be a marker for other meteorological events, like barometric pressure drops and wind shifts, rather than being a direct physical influence on soil gas concentrations. Alternatively, perhaps the flurries are sufficient to provide the scavenging followed by melting described by Wania (1998). The winter 2012–2013 snow events and other meteorological circumstances surrounding them have been summarized in **Table 6-4**. Some of the highest observed concentrations for VOCs and radon seemed to occur in conjunction with periods of frozen ground or when a snow event occurred after the ground was already frozen. But not every period of frozen ground produced increased concentrations in VOCs and radon at every location (especially for some of the latter periods of snow and frozen ground in **Figures 6-73** and **6-74**). Additionally, the peak radon and VOC concentrations sometimes occurred partway through a period of frozen ground and not at its beginning (**Figures 6-69** and **6-70**). Increased radon and VOC concentrations could occur immediately before, during, or after the snow and frozen ground events. Although the observed behavior at this house is complex, the literature of air permeability of snow packs and interactions between hydrophobic organics and snow/ice layers suggests that complex, multifaceted behavior is possible depending on snow type and its aging after fall. This is consistent with our observation that there appears to be no clear relationship between snow conditions and indoor air quality at this duplex; there are suggestions of a relationship in some cases, but not in all. Additional work is needed to understand this issue and the complex influences of meteorological variables on vapor intrusion processes.

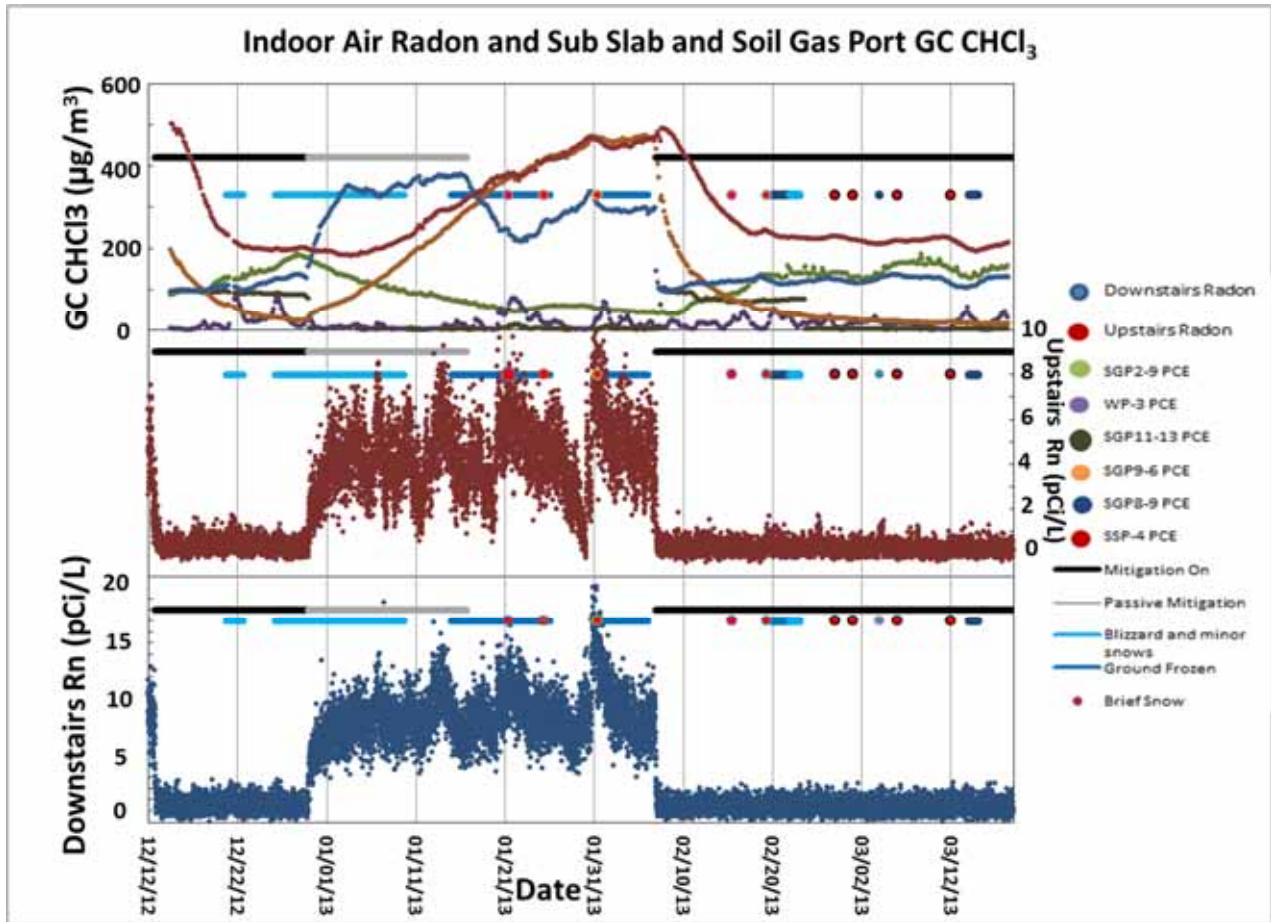


Figure 6-67. GC chloroform at subslab and soil gas ports versus radon from stationary AlphaGUARDs.

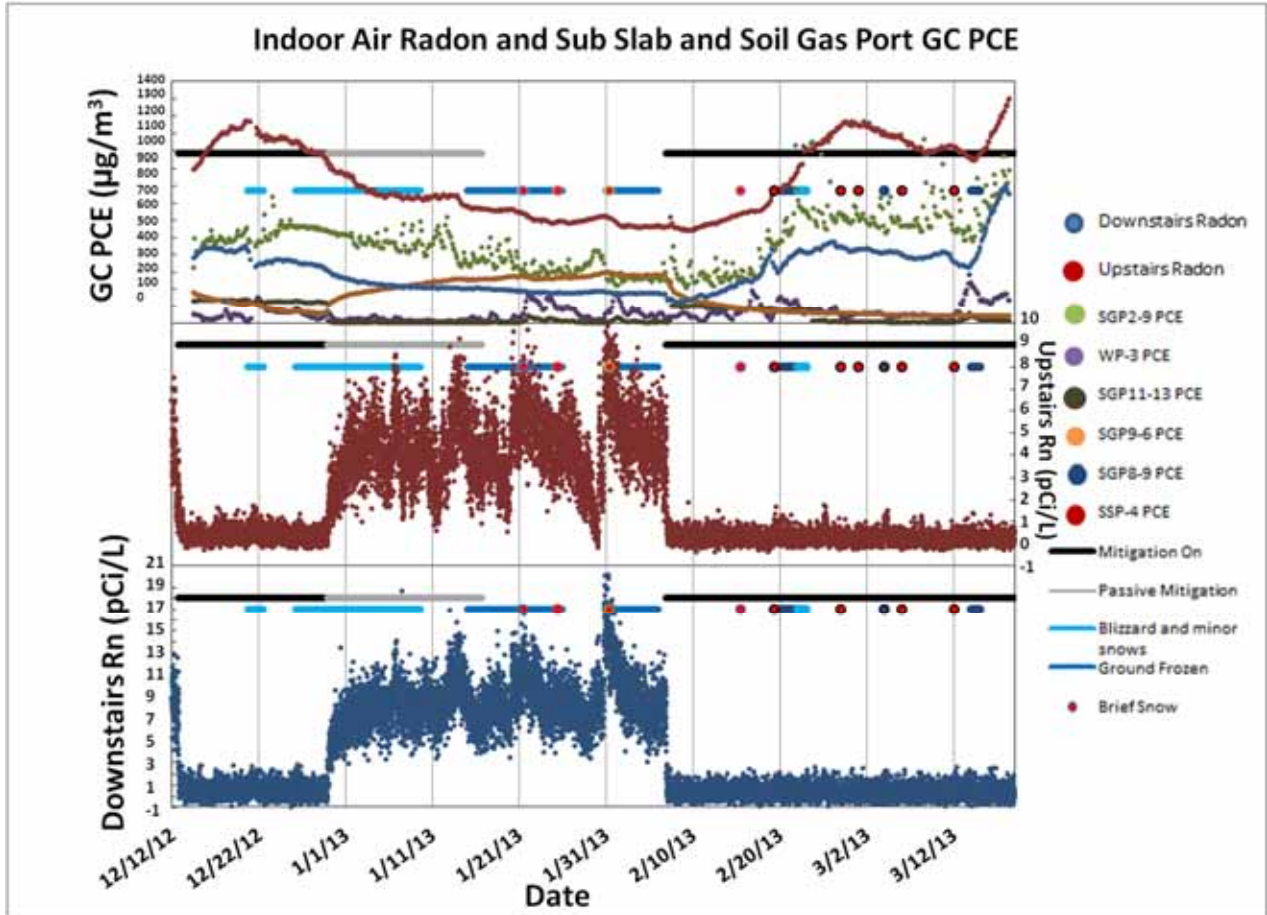


Figure 6-68. GC PCE at subslab ports versus radon from stationary AlphaGUARDS.

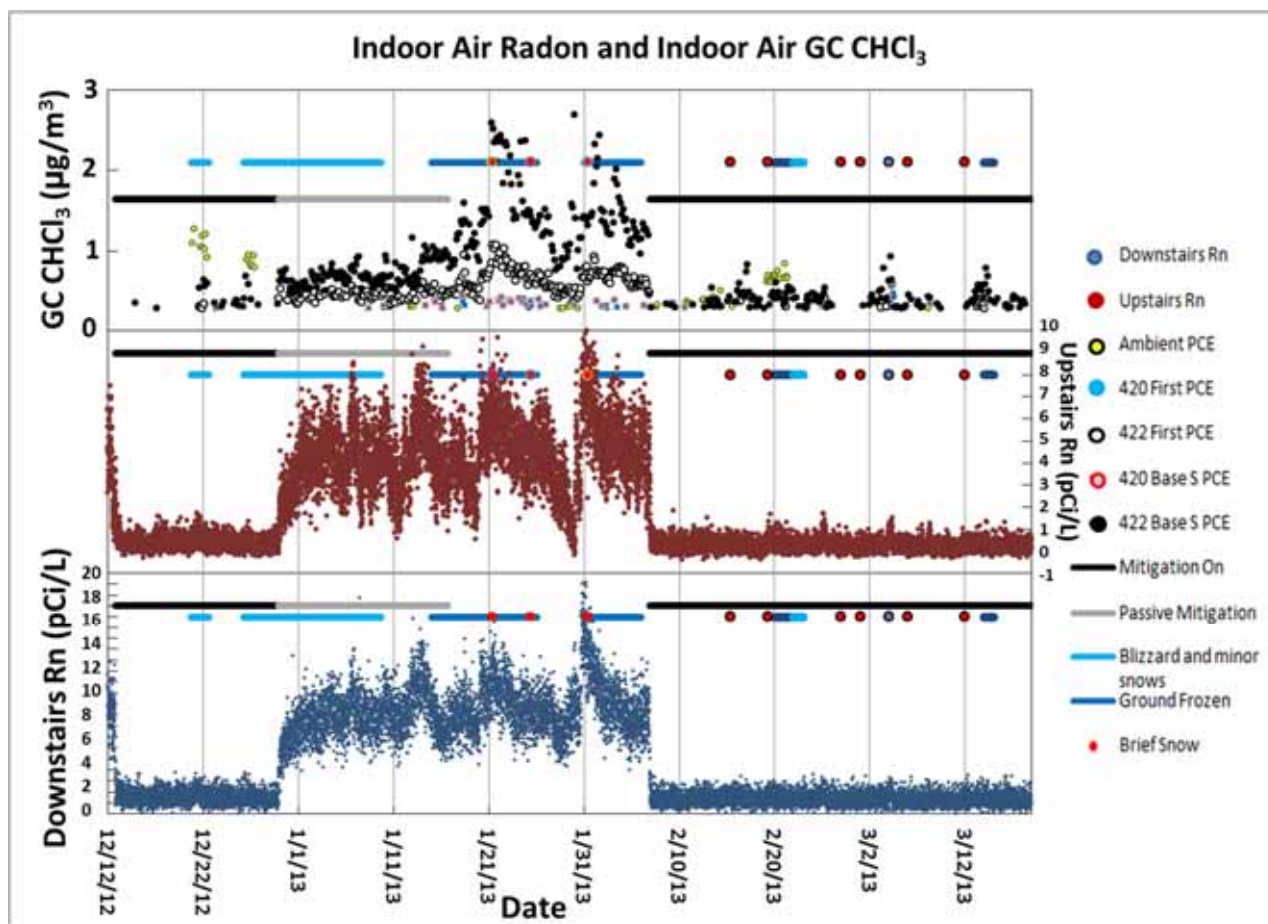


Figure 6-69. GC chloroform in indoor air versus radon from stationary AlphaGUARDs.

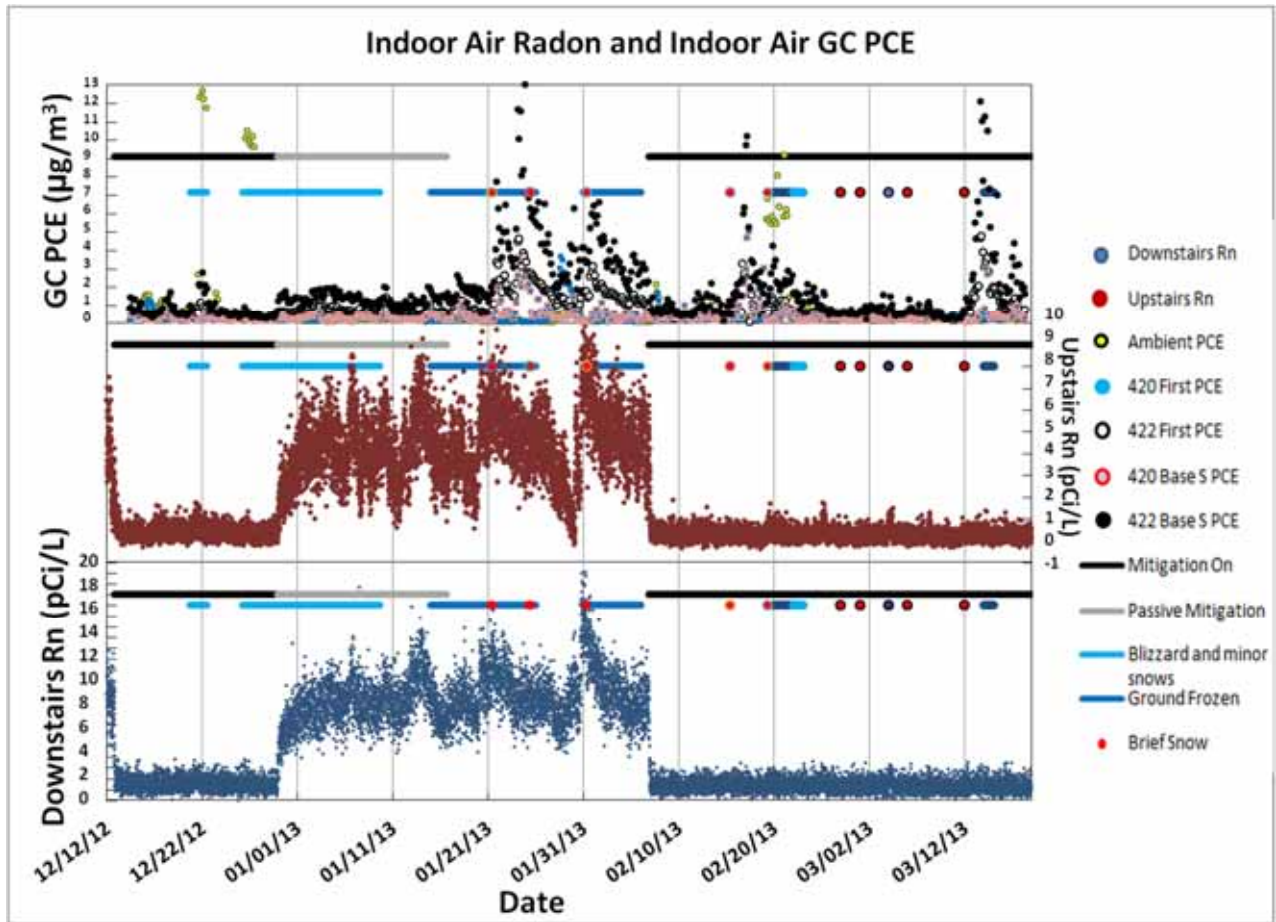


Figure 6-70. GC PCE in indoor air versus radon from stationary AlphaGUARDS.

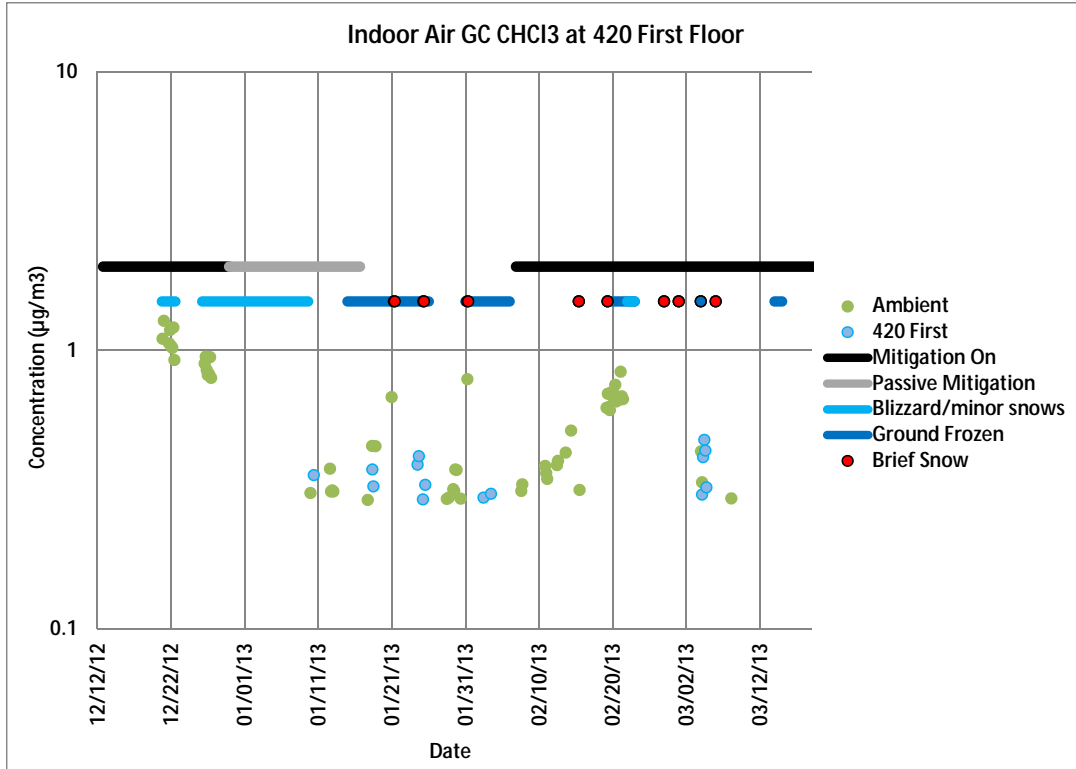


Figure 6-71. GC chloroform concentrations in indoor air, 420 first floor.

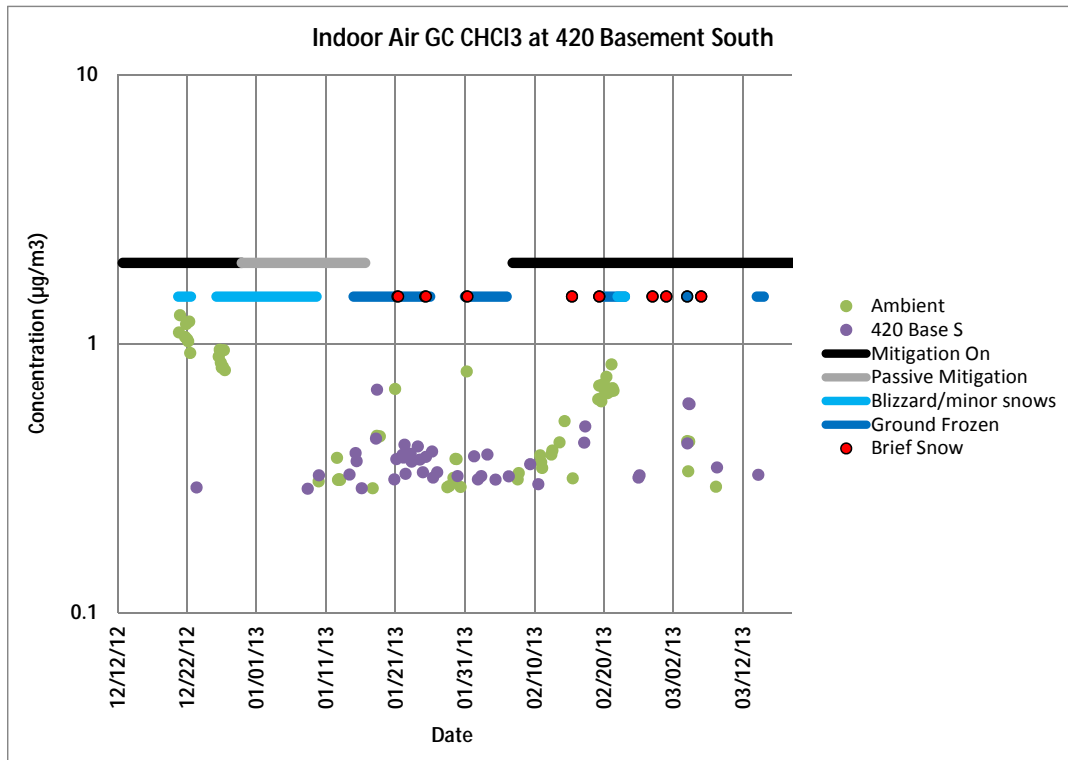


Figure 6-72. GC chloroform concentrations in indoor air, 420 basement south.

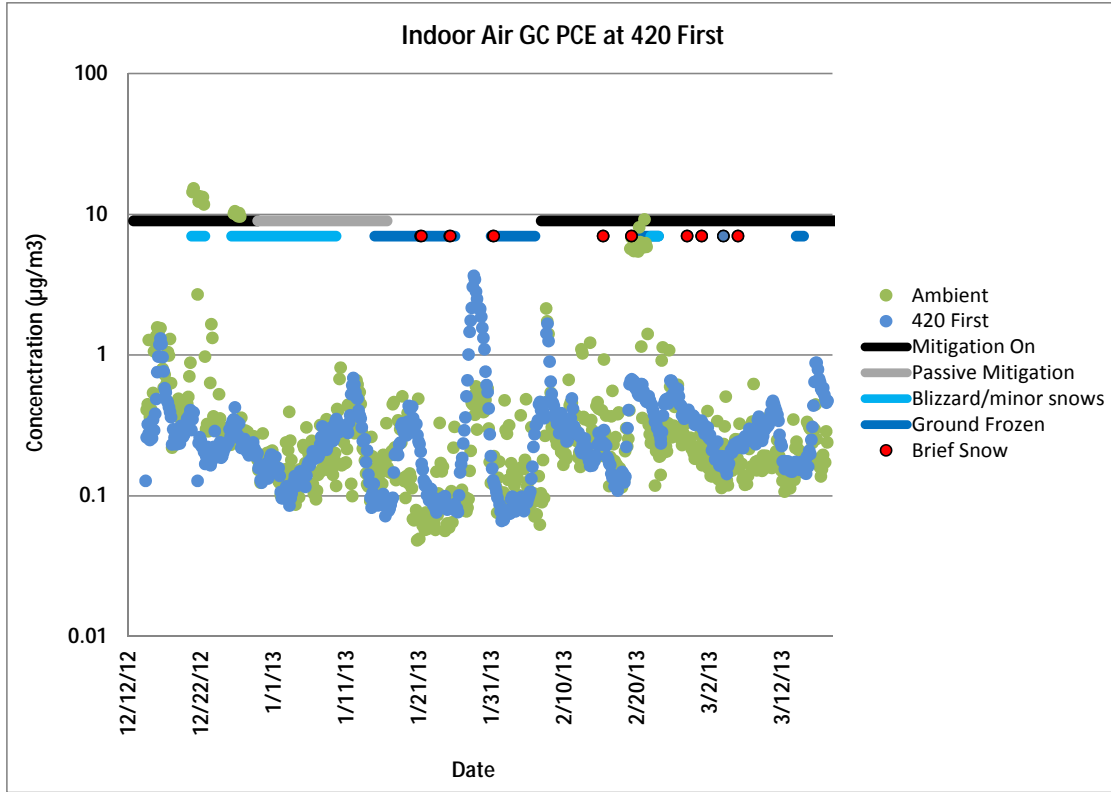


Figure 6-73. GC PCE concentrations in indoor air, 420 first floor.

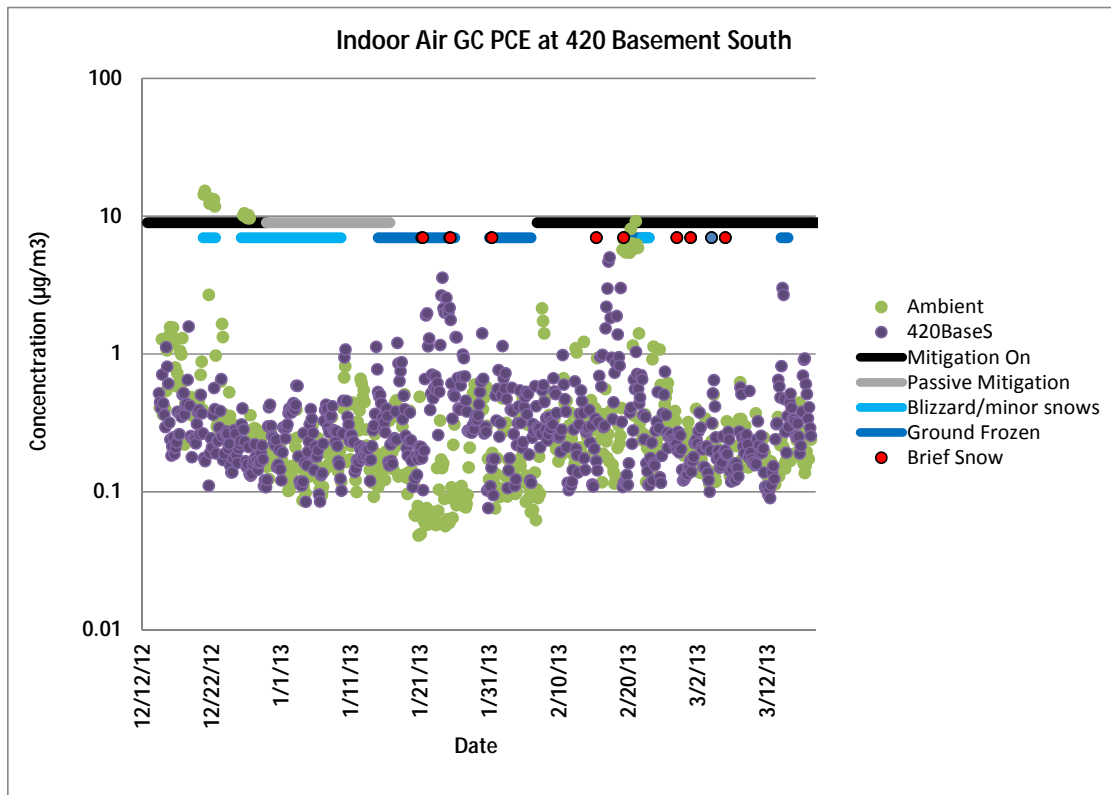


Figure 6-74. GC PCE concentrations in indoor air, 420 basement south.

Table 6-4. Summary of Meteorological Data During the 2012/2013 Snow and Ice Events

| Date and Estimated Time | Snow Event | Mitigation Status | Predominant Wind Direction | Time Surrounding Storm Average Wind Speeds MPH | Indoor Air PCE Peak? Present? | Indoor Air Chloroform Peak? Present? | Radon Peak 422 Basement? | Temperature °F |
|-------------------------|--------------------------|-------------------|----------------------------|---|---|--------------------------------------|--------------------------|----------------|
| 12/20/12 18:00 | Minor snow (~1") | On | WSW | 12–20 | 422 basement ambient | Ambient | Tiny | 30–40 |
| 12/26/12 6:00 | Blizzard and minor snows | On | NE | 10–12 | 420 first floor 422 basement Weak | Ambient | Tiny | ~30 |
| 1/21/13 7:00 | Brief snow | Off | WNW | 7–10 | 422 basement 422 first floor 420 basement | 422 first floor 422 basement | Strong | 16–20 |
| 1/25/13 7:00 | Minor snow (1") | Off | SE | 1–5 | 422 basement | | Moderate | 19–21 |
| 1/31/13 7:00 | Minor snow (1/4") | Off | WNW-W | 7–15 | 422 basement 422 first floor | 422 First Floor 422 Basement | Strong | 22–24 |
| 2/15/13 10:00 | Brief snow | On | WNW | 4–10 | 422 basement 420 basement 422 first floor | Ambient 422 basement | None | 32–34 |
| 2/19/13 8:00 | Brief snow | On | WNW | 10–17 | Ambient 422 basement 420 basement | Ambient | Tiny | 24–28 |
| 2/22/13 1:00 | Ice | On | E | 4–10 | 422 basement 420 basement | | | 28–32 |
| 2/27/13 12:30 | Brief snow | On | WSW | 8–10 | None | | | 34–35 |
| 3/1/13 1:00 | Brief snow | On | WNW | 2–4 | Weak 422 first floor | 422 first floor 422 Basement | | 31–33 |
| 3/6/13 1:00 | Brief snow | On | WNW | 2–4 | 422 basement 422 first floor | | Tiny | 28–30 |
| 3/12/13 23:00 | Brief snow | On | WNW | 6–12 | 422 basement 422 first floor 420 basement | 422 first floor 422 basement | | 30–34 |

Table of Contents

| | | |
|-----|--|-----|
| 7.0 | Results and Discussion: Establishing the Relationship between VOCs and Radon in Subslab/Subsurface Soil Gas and Indoor Air | 7-1 |
| 7.1 | Previously Reported Tests of Radon as a Semiquantitative VOC Tracer | 7-1 |
| 7.2 | Understanding the Performance of the Radon Tracer During Mitigation Testing | 7-1 |
| 7.3 | Attenuation Factors Derived Using the Radon Tracer | 7-4 |
| 7.4 | Radon Tracer in Statistical Time Series Analysis | 7-4 |

List of Figures

| | | |
|------|---|-----|
| 7-1. | Comparison of mean concentrations among wall and subslab ports under different mitigation conditions (heat on data only): radon (top), PCE (middle), and chloroform (bottom). | 7-2 |
| 7-2. | Long-term trends in radon and VOCs with shading showing mitigation status during Phase 2. | 7-5 |

7.0 Results and Discussion: Establishing the Relationship between VOCs and Radon in Subslab/Subsurface Soil Gas and Indoor Air

7.1 *Previously Reported Tests of Radon as a Semiquantitative VOC Tracer*

In Section 2 of this report, we discuss the conditions under which radon is expected to be a useful semiquantitative tracer of vapor intrusion. The most difficult to satisfy condition at this study site is the need for radon and VOCs to be similarly distributed in subsurface air just outside the building envelope and thus for entry routes to be similar.

Our previous report (U.S. EPA, 2012a) contained an extensive discussion of radon-to-VOC correlation in our 2011–2012 data set leading to the following conclusions:

- Radon concentrations in subslab air were much steadier than VOC concentrations, presumably because the shallow soils themselves were the dominant source of radon and VOCs originated at a greater depth/distance.
- Radon concentrations in indoor air varied over approximately an order of magnitude short-term—apparently greater short-term variation than was observed for VOCs.
- However, with a 1-week integration time, radon had less seasonal variability than VOCs in indoor air.
- Statistical cross-correlation testing found that radon and VOCs were positively cross-correlated at most indoor air sampling locations (5% critical level). Some cross-correlations of radon and VOCs were observed at soil gas ports, but these cross-correlations were less consistent/strong.
- Radon was clearly a marker for soil gas in this system. Thus, radon was a useful aid to VOC data interpretation. But long-term radon exposure would not have completely predicted VOC exposure in this house over all time scales.

7.2 *Understanding the Performance of the Radon Tracer During Mitigation Testing*

Additional data on the correlation between radon and VOCs were gathered in 2012–2013, during a period of time when the mitigation system was being tested by being turned on and off. In Section 5 of this report, we show that radon does not seem to be a sensitive indicator of mitigation system performance vs. PCE. The performance of the mitigation system was substantially better and more consistent for radon than it was for VOCs. We observed a 91 to 93% reduction in indoor radon. **Table 5-11** showed that in all cases the concentration of radon was reduced by the SSD system operation in the subslab sampling ports, wall ports, and shallowest interior soil gas ports. **Table 5-12** showed that this effect is, on average, about a 60% reduction in the subslab sampling ports and 80% in the wall ports. Comparing this result with the reductions observed in indoor air suggests that the SSD system is operating at this duplex to reduce radon in indoor air through two mechanisms—both by diluting the air beneath the slab with lower concentration air (presumably atmospheric) and reversing the pressure differential across the slab. Our discussion in Section 5 focused on mitigation performance and causes for that performance. Our discussion in this section focuses on the performance of the radon tracer technique and why the tracer was or was not useful.

As shown in **Figure 7-1**, prior to mitigation (blue bars) the distribution of radon among various subslab and wall ports was more continuous/smoothly varying than it was for PCE and chloroform. Concentrations of radon were generally reduced or only slightly increased under the mitigation on condition (purple bars). PCE and chloroform concentrations increased dramatically at some locations with

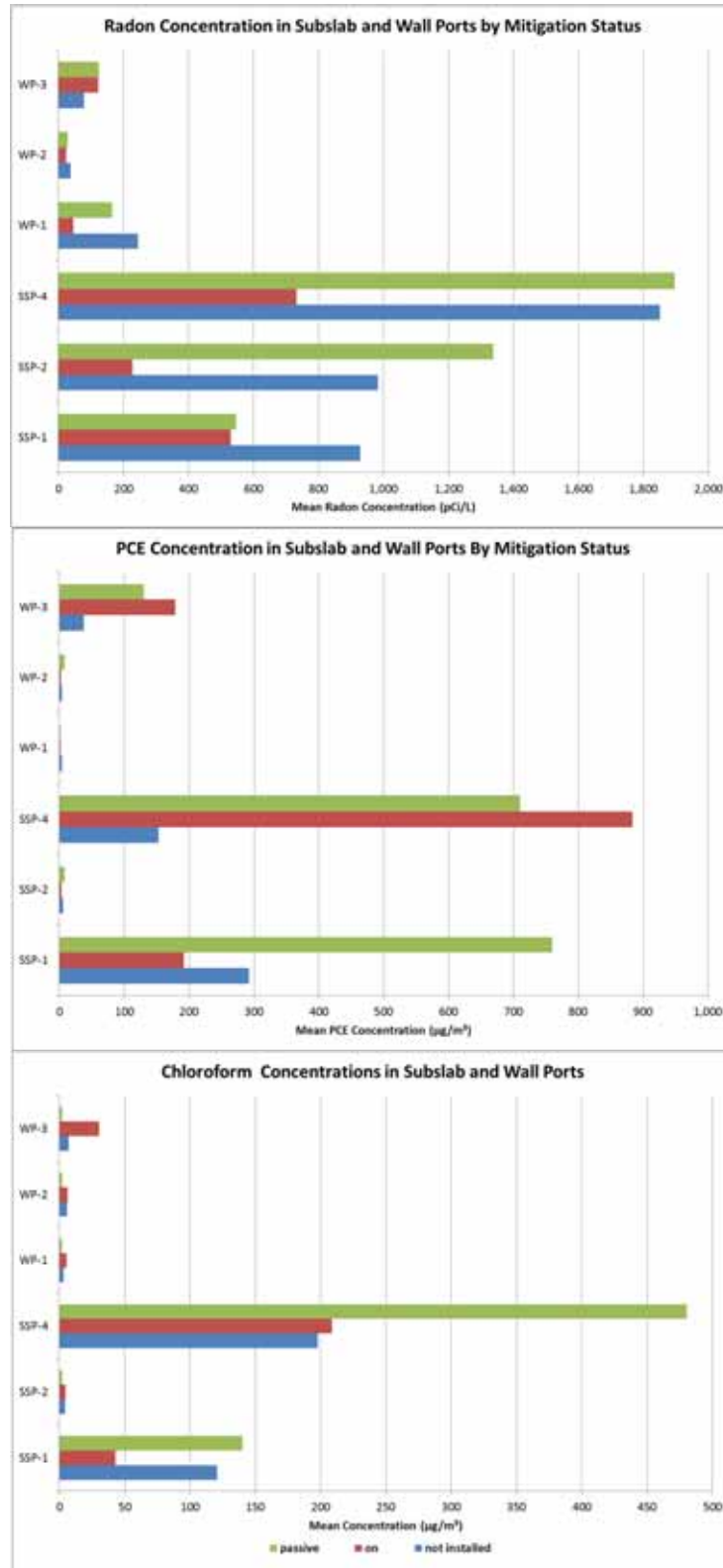


Figure 7-1. Comparison of mean concentrations among wall and subslab ports under different mitigation conditions (heat on data only): radon (top), PCE (middle), and chloroform (bottom).

the mitigation on. Under post-mitigation conditions, there were still more dramatic differences in concentration between ports for PCE than for radon.

The flow of soil gas into the building is expected to be very nonuniform with some areas of soil gas just outside the building envelope near major cracks/gaps dominating the total flow into the building. Mitigation may change the particular locations from which the predominant flow is coming. Thus, the greater homogeneity of the radon concentrations as compared to VOC concentrations can explain why the percentage improvement in indoor air concentrations is not the same for radon and VOCs.

Similarly, **Figure 6-70** showed that several day-long peaks in PCE in indoor air were observed under mitigation on conditions that were not observed in indoor air radon (neither with the professional grade AlphaGUARD instrument, integrated electret measurements, nor Safety Siren Consumer grade detector). Those peaks were also much less prominent for chloroform. We discuss in Section 5 that those PCE peaks were not necessarily accompanied by a loss of differential pressure control in the center of the subslab areas where continuous differential pressure observations were being made. A likely explanation for those two sets of observations is that differential pressure control was lost in only a portion of the building envelope, but high PCE concentrations were present in the soil gas adjacent to those portions of the building envelope where pressure control was lost. Although radon would have been expected to have also been present in the soil gas, the greater variability in soil gas PCE concentrations could cause a more dramatic PCE peak relative to baseline. The lack of a distinct peak in the radon concentration plots during this time period provides useful mechanistic information; it suggests that during these PCE peaks the mitigation system is still effective in substantially limiting the total amount of soil gas entering the structure.

Fundamentally, we can understand the potential for radon and VOCs to have different behavior in mitigation systems in terms of travel time of the gas flowing into the extraction points (and subslab area more generally). We can envision the subslab depressurization system for some purposes as a tiny soil vapor extraction (SVE) system, although we do not advocate using SSD for mass removal. Gas travel times to extraction wells in SVE systems can be much larger than the radon half-life of 3.8 days (Falta, 2006). Thus, because the sources of radon and VOCs are generally both diffusion-controlled processes that originate from sources in the fine soil particles, we can understand that as the SSD continues to operate and draws in gas with long travel times, the temporal profiles of radon and VOC concentrations could differ.

As discussed above in our premitigation studies, the relative amount of variability of radon and VOCs was compared as follows:

- Radon concentrations in subslab air were much steadier than VOC concentrations.
- Radon concentrations in indoor air varied over approximately an order of magnitude short-term—apparently greater short-term variation than was observed for VOCs.
- However, with a 1-week integration time, radon had less seasonal variability than VOCs in indoor air.

Figure 7-2 illustrates long-term trends in VOC and radon concentrations both before the mitigation testing and during the mitigation testing. Note that radon concentrations respond very quickly to mitigation system on/off cycles, forming essentially a “square wave” as the mitigation system is shut on and off. The PCE and chloroform concentration profiles trace a less responsive-looking pattern, with a minimum occurring during the week after the mitigation system was turned on and maximums, higher than before mitigation, when the system was shut down in December and in early January. This differs from the typical pattern seen with soil vapor extraction systems in which extracted concentrations generally decline with time as the system is operated. For example, Thomson and Flynn (2000) describe a first extraction stage of high concentration soil gas that is assumed to be in equilibrium with NAPL and a final stage where extraction is mass transfer limited by gas and aqueous phase diffusion into preferential gas flow pathways. This may reflect that SVE wells are usually intentionally screened in areas of high soil gas concentrations, while the SSD extraction points in this case are more distant from the source zone.

Also note that **Figure 7-2** shows the behavior of each contaminant in indoor air when compared with outside ambient air concentrations measured at the duplex. The chemicals fall into two main groups: those whose indoor air concentrations follow ambient air concentrations very closely (benzene, toluene, and hexane) and those with indoor concentrations mostly above ambient levels (radon, chloroform, and PCE). Indoor air concentrations of benzene, toluene, and hexane are clearly derived from outdoor air sources, probably influenced by the traffic on the busy road south of the duplex. Radon, chloroform, and PCE are well above ambient levels, although the ambient levels clearly influence chloroform and PCE concentrations over time to a greater degree than can be observed for radon, probably because outdoor air concentrations are closer to indoor air concentrations for chloroform and PCE than for radon. Note that TCE behaves similarly to chloroform and PCE at the higher concentrations observed early in the study but mirrors the outdoor air concentrations when TCE concentrations decrease to close to ambient later in the study, although there is a small increase over background when the mitigation system was first shut off, which could reflect the same causes as the similar increases observed for PCE and chloroform.

7.3 Attenuation Factors Derived Using the Radon Tracer

As shown in Section 8, radon predicts reasonably well the attenuation factor from wall port to indoor air and from subslab to indoor air. The agreement is much less good for deeper soil gas to indoor air. Thus, radon serves as a reasonable tracer for the portion of the vapor intrusion process across the slab or building envelope but is less effective as a tracer for VOC attenuation from deeper media. The reason for that is also very clear in Section 8; there is substantial reduction in chloroform concentration and PCE concentration from 13 to 6 ft bls. However, radon concentrations are quite similar at 6, 9 and 13 ft depths. Thus, radon can be seen as a reasonable surrogate for the portion of the attenuation factor that describes attenuation across the building envelope (AF_{bldg} , as defined in U.S. EPA, 2012c). As might be expected, radon does a much poorer job of describing the portion of the attenuation factor that is due to subsurface migration processes (AF_{soil}).

7.4 Radon Tracer in Statistical Time Series Analysis

In Section 10, we present time series analyses for both radon and VOCs in which we examine potential correlations to a wide variety of meteorological and soil conditions. For the purposes of the current section, two primary lessons stand out:

- In most of the analyses including mitigation, mitigation was shown to have a significant beneficial effect for radon at either the 1% or 5% level of significance. In contrast, in the VOC

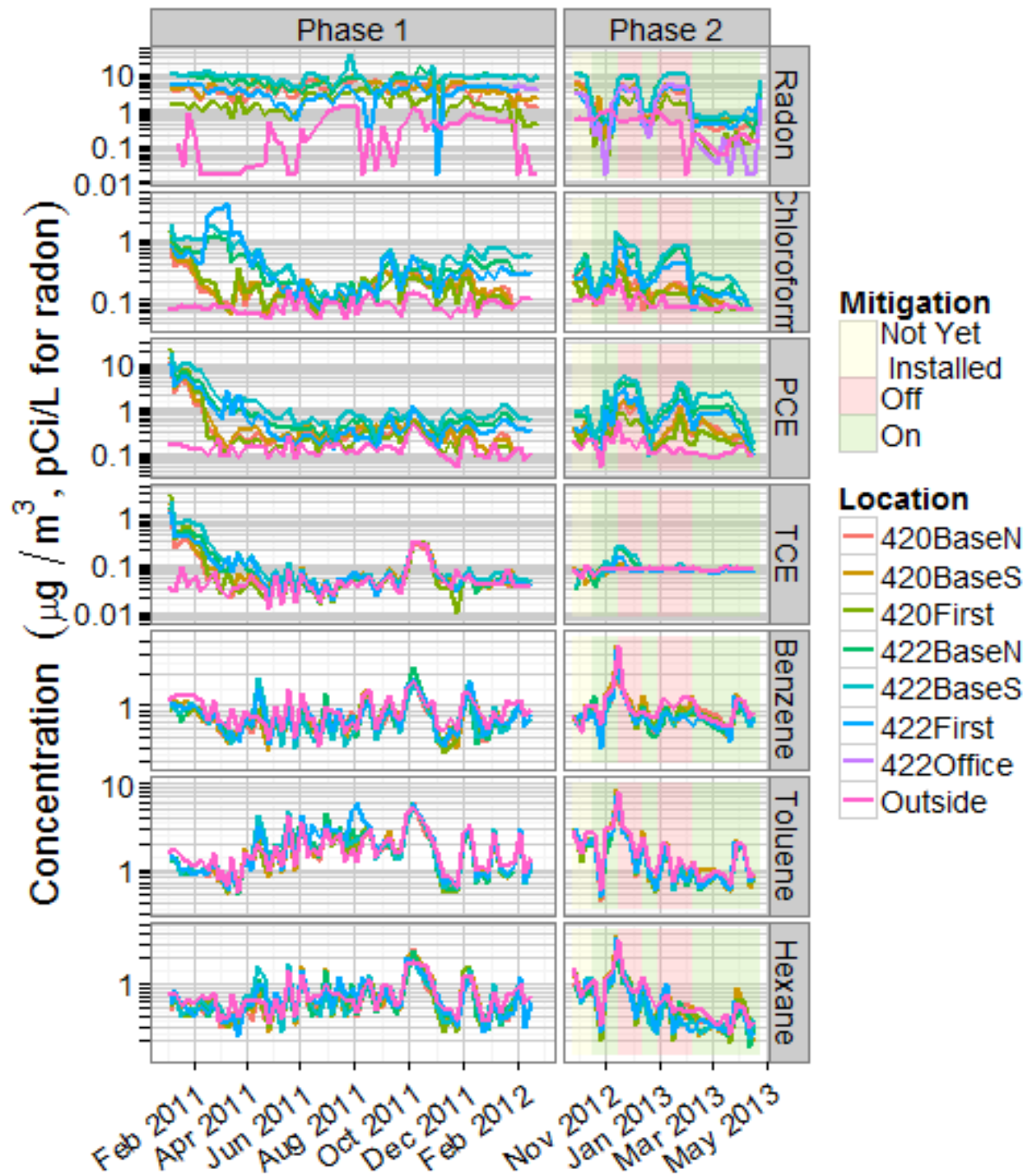


Figure 7-2. Long-term trends in radon and VOCs with shading showing mitigation status during Phase 2.

time series results, although mitigation generally appeared beneficial, it was not statistically significant. This agrees with the other modes of mitigation analysis discussed previously in this section and in Section 5.

- In the radon time series analysis, many meteorological variables (often a majority of the variables tested) were found to be statistically correlated to indoor radon concentrations. In contrast, for the VOCs, a smaller proportion of the variables tested rose to statistical significance. It is possible that this is an artifact of the sample size. Alternatively, this may be a more formal mathematical confirmation of two phenomena discussed earlier:
 - As described in Section 6.4, radon responds almost immediately to both “mitigation on” and “mitigation off” cycles. After decreasing to near ambient air background (a range of 0 to 2.5 pCi/L) with the mitigation system on, it quickly returns to more elevated levels and a more dramatic range (4 to 15 pCi/L) when the mitigation system is turned off. VOCs tended to show a slower and more variable response to mitigation than radon, at least during the initial operation of the system described in this report.
 - Radon’s concentration in indoor air may be more simply defined as a first approximation based on the amount of transport across the building envelope, while VOCs have a more heterogeneous spatial and temporal patterns of concentration in soil gas. Therefore, radon’s behavior may be easier to predict using statistical models with a limited number of variables (in this case, one variable at a time was tested, plus the mitigation on/off variable).

In essence, radon responded more quickly, cleanly, and repeatedly to changes in subslab depressurization because the radon entering the house is generated very near the house because radon’s relatively short half-life (3.8 days) does not allow it to travel far from its point of generation before decaying. VOCs, with their much longer half-lives (generally over a year or longer), have a much longer transport path than radon, making them more subject to processes along this path and leading to a much wider source area than is typical for radon, along with a greater medium to long-term (daily to weekly) variability both during and before mitigation with subslab depressurization.

Table of Contents

8.0 Results and Discussion: Attenuation of Soil Gas VOCs and Radon.....8-1

8.1 Calculation of Daily Attenuation Factors without Mitigation.....8-1

8.1.1 Daily Radon Attenuation Factors without Mitigation.....8-5

8.1.2 Daily VOC Attenuation Factors without Mitigation.....8-5

8.2 Subslab and Soil Gas to Indoor Air Weekly Attenuation Factors.....8-8

8.2.1 Radon Weekly Attenuation Factors.....8-8

8.2.2 VOC Weekly Attenuation Factors.....8-11

8.3 Effect of Mitigation.....8-19

8.3.1 Subslab to Indoor Air Daily Attenuation.....8-20

8.3.2 Subslab and Soil Gas to Indoor Air Weekly Attenuation.....8-23

List of Figures

8-1. AlphaGUARD concentrations and daily radon attenuation factors (number of samples indicated below each bar graph pair). Sample pairs represented indicated along x-axis. SSP-7 is on the 420 side of the building and so may not be representative of subslab attenuation as the other sample pairs. Sampling period = January 2011–May 2013, mitigation system off.8-3

8-2. Daily indoor air and soil gas PCE concentrations used in attenuation factor calculations (number of samples with heat on and off are indicated below each bar graph pair).8-4

8-3. Daily PCE attenuation factors (number of samples indicated below each bar graph pair).....8-5

8-4. Daily chloroform concentrations used in attenuation factor calculations (number of samples indicated below each bar graph pair).8-6

8-5. Daily chloroform attenuation factors (number of samples indicated below each bar graph pair).....8-7

8-6. Electret radon concentrations used in weekly attenuation factor calculations. Number of measurements indicated below each box and whiskers pair.....8-9

8-7. AlphaGUARD soil gas radon concentrations (pCi/L) used in weekly attenuation factor calculations. Number of measurements noted below each box and whiskers pair. Note that these concentrations represent averages across all samples taken at the same depth and time (e.g., subslab samples are averages across all subslab points).8-10

8-8. Weekly radon attenuation factors (number of samples indicated below each bar graph pair). Note that these attenuation factors were calculated from indoor air and soil gas concentrations averaged at the same depth and time (as described in Figure 8-7).8-11

8-9. Radiello PCE concentrations used in attenuation factor calculations. Numbers at the bottom of each column indicate the number of available readings for unheated (left) and heated (right) conditions.8-12

8-10. TO-17 PCE concentrations used in attenuation factor calculations.....8-13

8-11. Weekly PCE attenuation factors (numbers of samples indicated by numbers beneath each bar graph pair).....8-14

| | | |
|-------|--|------|
| 8-12. | Radiello chloroform concentrations used as numerators for weekly attenuation factor calculations. | 8-15 |
| 8-13. | TO-17 chloroform concentrations used as denominators for weekly attenuation factor calculations. | 8-16 |
| 8-14. | Weekly chloroform attenuation factors (number of samples indicated below each bar graph pair)..... | 8-17 |
| 8-15. | Attenuation of PCE, chloroform, and radon juxtaposed..... | 8-18 |
| 8-16. | Mitigation status and schedule..... | 8-19 |
| 8-17. | Radon indoor air and soil gas concentrations used in daily attenuation factor calculations..... | 8-20 |
| 8-18. | Daily radon attenuation factors..... | 8-21 |
| 8-19. | Daily PCE attenuation factors..... | 8-22 |
| 8-20. | Daily chloroform attenuation factors..... | 8-23 |
| 8-21. | Electret indoor radon concentrations..... | 8-24 |
| 8-22. | AlphaGUARD subsurface radon concentrations (pCi/L)..... | 8-25 |
| 8-23. | Weekly radon attenuation..... | 8-26 |
| 8-24. | Radiello indoor air PCE concentrations..... | 8-27 |
| 8-25. | TO-17 soil gas PCE concentrations..... | 8-28 |
| 8-26. | Weekly PCE attenuation..... | 8-29 |
| 8-27. | Radiello weekly indoor air chloroform concentrations..... | 8-30 |
| 8-28. | TO-17 soil gas chloroform concentrations..... | 8-31 |
| 8-29. | Weekly chloroform attenuation factors..... | 8-32 |
| 8-30. | Attenuation of PCE, chloroform, and radon juxtaposed..... | 8-33 |

8.0 Results and Discussion: Attenuation of Soil Gas VOCs and Radon

In this section, we explore the relationship between radon and VOC levels in indoor air and concentrations measured in subslab and deeper soil gas, which is usually portrayed through the vapor intrusion attenuation factor. As described in Section 2, the vapor intrusion attenuation factor is the indoor air concentration divided by a subsurface soil gas concentration at the same time and location. For example, if subslab soil gas concentrations are 100 times greater in the indoor air concentration measured at the same time, the subslab has a 100-fold attenuation and the attenuation factor would be 0.01.

The previous report on the first phase of this project (U.S. EPA, 2012a) described and compared the temporal variability of attenuation factors based on individual paired points and whole site averages for subslab and deeper soil gas attenuation factors for VOCs and radon. This report updates the U.S. EPA (2012a) data sets and compares radon and VOC attenuation factors with and without operation of the subslab depressurization mitigation system discussed in Section 3.

8.1 Calculation of Daily Attenuation Factors without Mitigation

Daily attenuation factors were calculated for radon and VOCs for the entire project period, including the phases before and after the mitigation system was installed on 10/15/2012, through the end of this reporting period in early May 2013. To calculate the daily attenuation factors, we averaged subsurface and indoor air concentrations measured on the same day and divided these indoor air concentration averages for each day by the nearest (temporally and spatially) subsurface concentrations available. This would be within a 24-hour range or within 24 hours from each sample point (i.e., no daily attenuation sample pairs are more than 24 hours apart).

In terms of the lag time between subsurface and indoor air (i.e., how long it takes for a radon or VOC molecule to move from the surface into indoor air), we believe it is reasonable for a radon or VOC molecule to travel from the subslab or outside the wall into the basement indoor air in 24 hours or less and that a daily resolution for attenuation factors is therefore informative. The most interesting daily attenuation factors are the attenuation from subslab ports and wall ports to basement indoor air. The time of travel from subslab or wall exterior to basement indoor air should be relatively quick, so “same day” averaging is appropriate. Although we expect that attenuation from deeper soil gas will take longer, because the deeper vadose zone is very coarse grained, we think that advective flow is likely operative and assumed that it would take longer than 24 hours for VOCs in deep soil gas to reach indoor air in the building.

As described in Section 3, subsurface concentration measurements were taken from the soil gas and subslab sampling ports using a portable AlphaGUARD sampler for radon and TO-17 active sorbent tubes for VOCs. These measurements serve as the soil gas concentrations (denominator) for all radon or VOC attenuation factor calculations, and although they are grab samples, we assumed they are representative of the average soil gas concentrations for the day or week during which they were taken. In other words, for both radon and VOCs, we assumed that the subsurface soil gas concentrations, which were TO-17 grab samples taken approximately weekly, remain relatively constant.

Radon was measured in indoor air using stationary AlphaGUARD monitors as well as electret sampler badges. The more continuous indoor AlphaGUARD measurements allow the calculation of a daily indoor air radon concentration for the daily attenuation factors while the electret samplers provide a weekly physical average attenuation factor that could be used directly. Similarly, VOCs were measured fairly continuously (every hour or so) in indoor air during the periods of on-site GC operation, and these

measurements were used to calculate daily average concentrations for the periods of online GC operation. The weekly indoor air Radiello sampler concentrations, which are available for the entire project period, were used to calculate the weekly VOC attenuation factors.

8.1.1 Daily Radon Attenuation Factors without Mitigation

Indoor AlphaGUARD measurements were only taken on the 422 side of the duplex, so daily radon attenuation factors are only computed for pairs of locations on the 422 side. This allowed us to observe the effect of heating because only the 422 side was heated. **Figure 8-1** compares the distributions of daily radon attenuation factors with the heat on and off and the mitigation system either off or not installed and shows the ranges of the indoor air and subslab concentrations used to calculate them. In general, attenuation is slightly lower when the heat is on, as would be expected given increased stack effect for a building when the heat is on, which tends to increase indoor VOC concentrations. Also as expected, the wall port shows much less attenuation (i.e., higher attenuation factors) than the two subslab ports on the 422 side of the building (SSP-2 and SSP-4) because of the lower soil gas (denominator) concentrations in the wall port due to its stronger connections with the atmosphere. SSP-2 and SSP-4 attenuation factors are similar because of similar subslab concentrations. SSP-7, which is on the 420 side of the duplex, is included in the figure and calculations, but because it represents 420 subslab data with 422 indoor air data, it is not as representative of subslab attenuation as SSP-2 and SSP-4.

8.1.2 Daily VOC Attenuation Factors without Mitigation

The on-site GC data allow daily subslab to indoor air attenuation factors with very high time coverage for the three periods when the on-site GC was in operation at the site, two periods before and one period after the mitigation system was installed (see Section 3). The on-site GC has 2 basement sampling points: the south side of the 420 and 422 basements. As with the radon data, the data also include three subslab locations: SSP-7 on the 420 side and SSP-2 and SSP-4 on the 422 side. Because of differences in instrument calibration (see Section 4), the two periods prior to mitigation are treated as disjointed data, but the two periods are juxtaposed in the following figures because the heat was off for the entirety of the first period of GC monitoring and on throughout the second period.¹⁷

Figure 8-2 provides the range of daily indoor air and soil gas concentrations used to calculate the PCE attenuation factors and **Figure 8-3** provides the range of those attenuation factors for the individual indoor air/subslab pairs calculated for PCE. Note that for PCE in indoor air, only the 422 basement and SSP-4 show the increase in PCE concentrations with the heat on, which is as expected because SSP-7 is on the unheated 420 side of the building and WP-3 is shallow and likely affected by atmospheric air. On the 420 side, both the basement and SSP-7 show a decrease in VOC levels in the heated (winter) months, suggesting that perhaps lower temperatures decrease vapor intrusion driving forces. Also, SSP-2, on the north side of 422, was not expected to show the measured decrease in PCE concentration with the heat on, suggesting that the subslab area sampled by SSP-2 is not strongly connected to the 422 indoor air environment and/or there is atmospheric air diluting the subslab concentrations at this point.

¹⁷Note that five zero PCE concentration values for the 420 basement were replaced with 0.005 (the smallest positive concentration value at that location). While the zero values would still yield a finite attenuation value (0), they were replaced with 0.005 so they can be plotted on log-scaled figures.

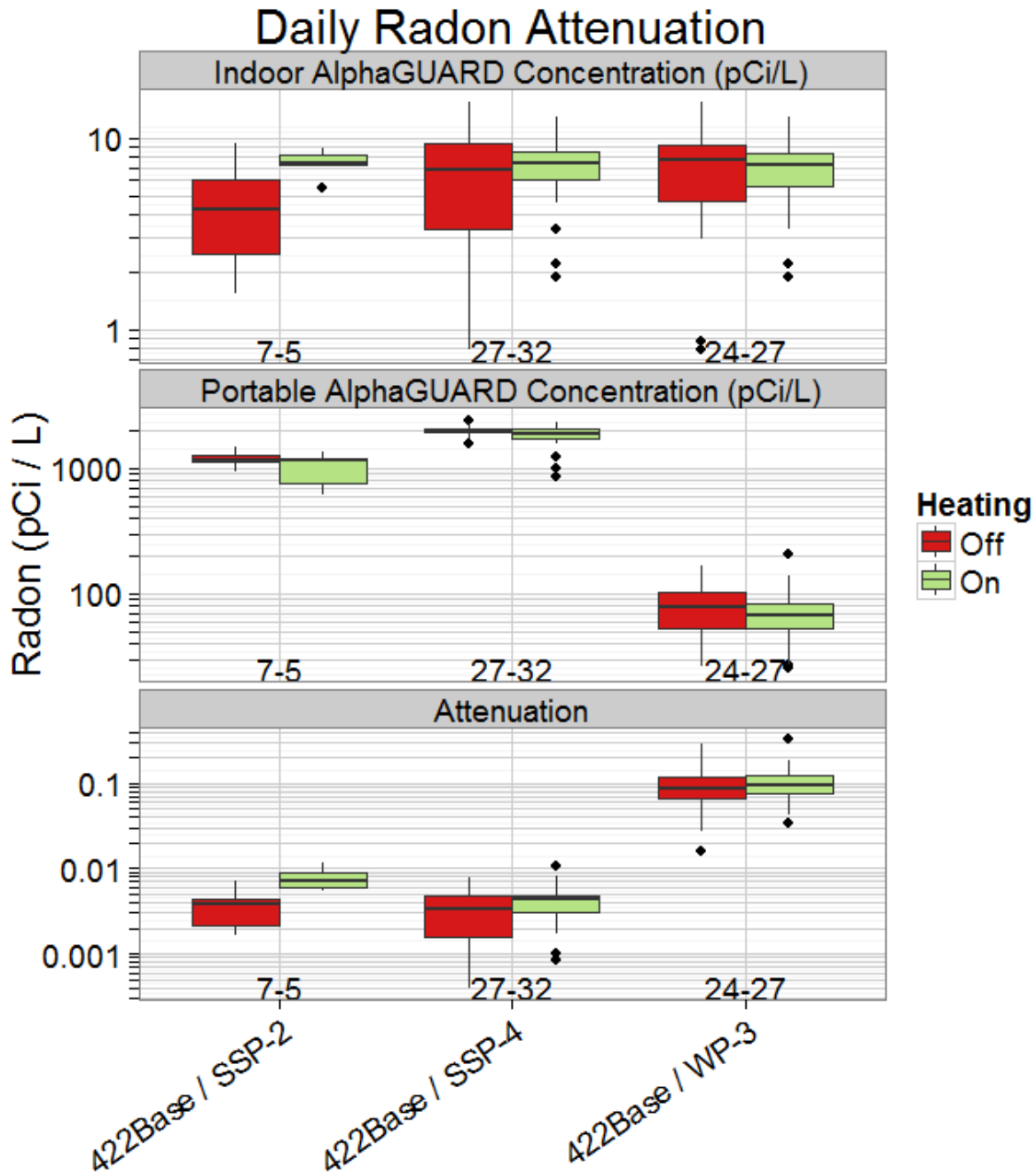


Figure 8-1. AlphaGUARD concentrations and daily radon attenuation factors (number of samples indicated below each bar graph pair). Sample pairs represented indicated along x-axis. Sampling period = January 2011–May 2013, mitigation system off.

As far as attenuation is concerned, the 422 basement / SSP-4 attenuation factor shows a small decrease (i.e., more attenuation) with heating because the SSP-4 concentration increased more than the 422 basement indoor air concentration with heating on. Also, SSP-2 and WP-3 show very low attenuation

(with an attenuation factor around 1), which would be expected if the soil gas at these ports was connected to the atmosphere.

Similar patterns can be seen for chloroform in **Figures 8-4** and **8-5** except that WP-3 does not show the decrease in chloroform concentrations and increase in attenuation factors with heating as seen for PCE. As with PCE, the anomalously high attenuation factors for WP-3 and (especially) SSP-2 suggest atmospheric leakage and that the VOC levels in indoor air is not greatly influenced by soil gas from these locations.

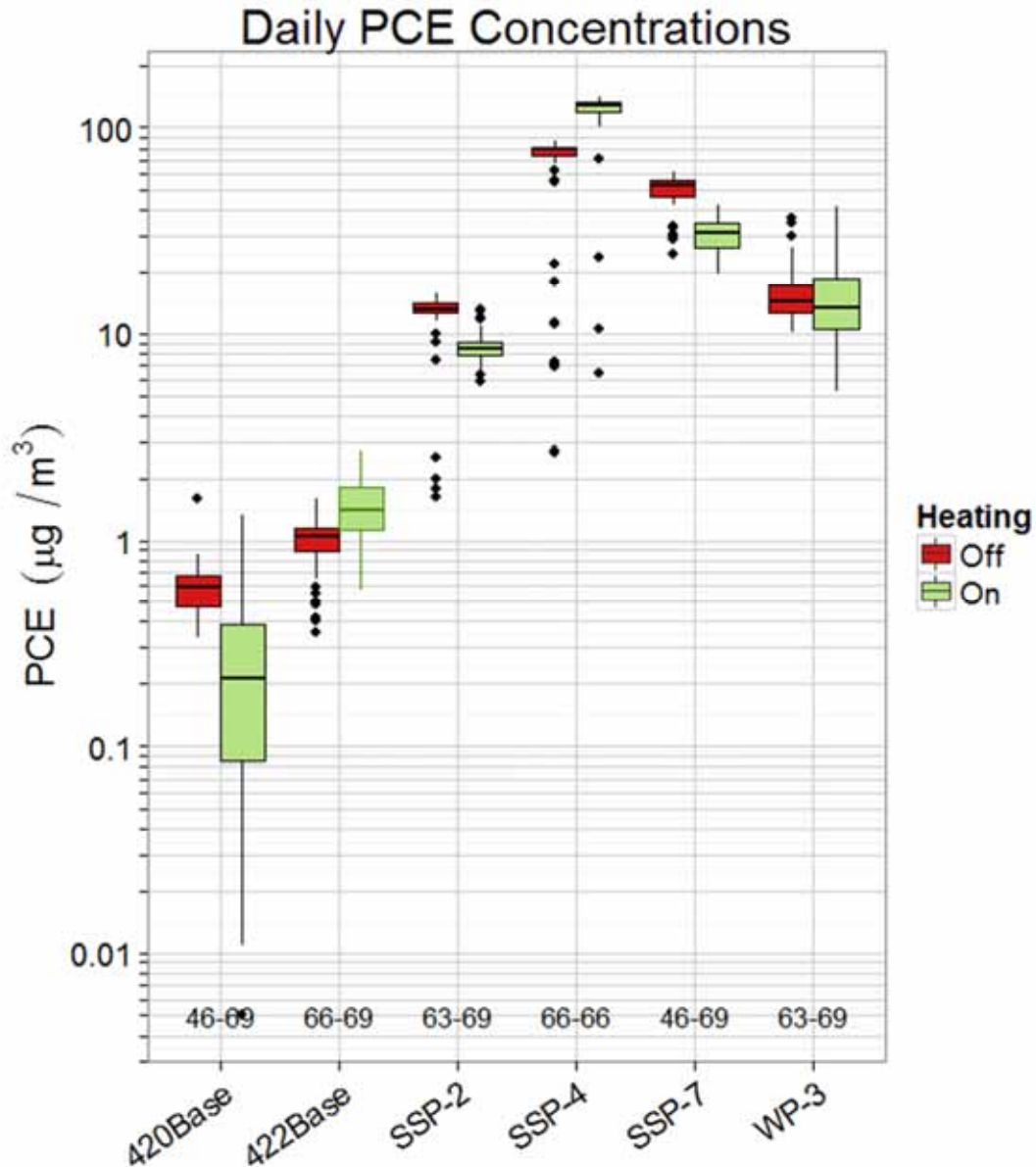


Figure 8-2. Daily indoor air and soil gas PCE concentrations used in attenuation factor calculations (number of samples with heat on and off are indicated below each bar graph pair).

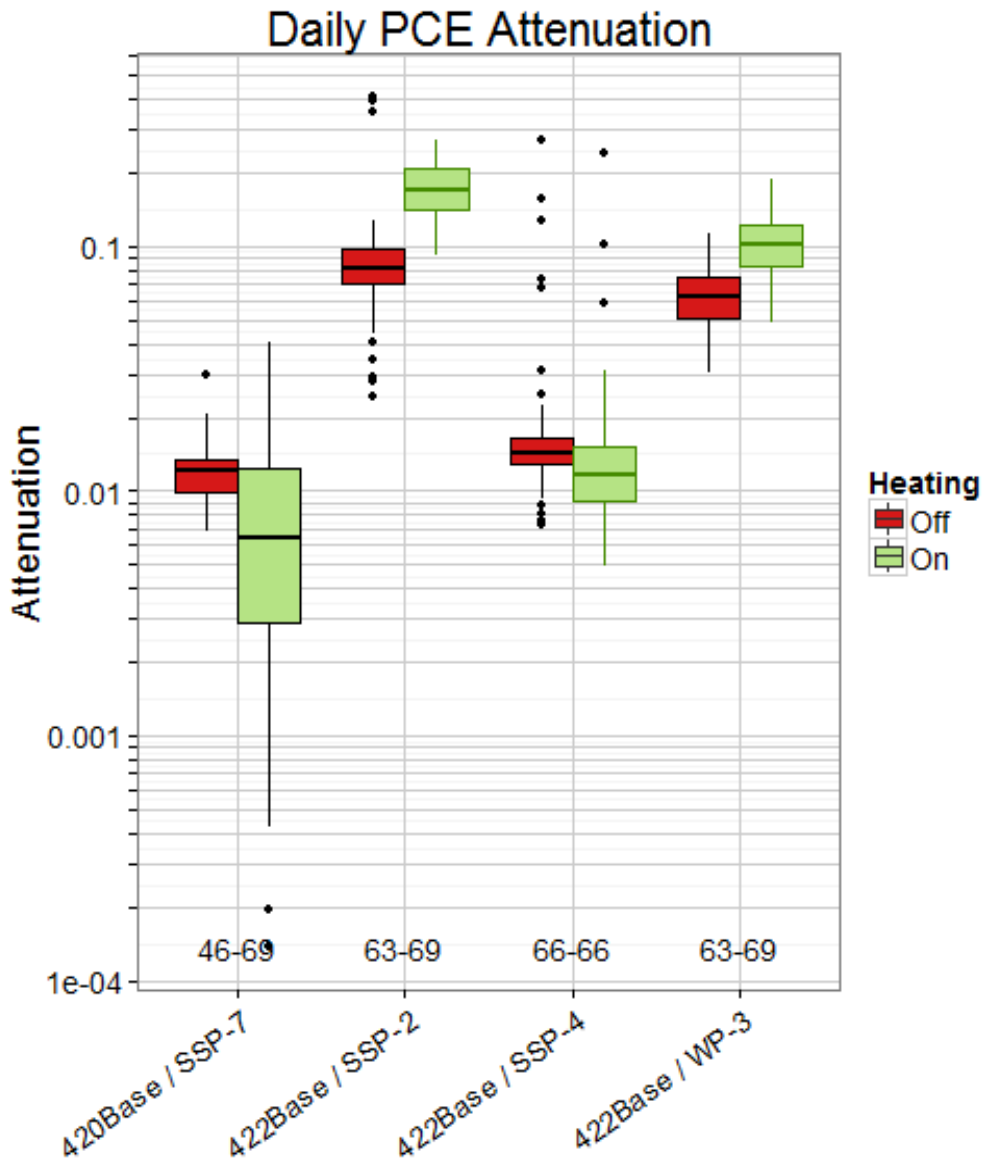


Figure 8-3. Daily PCE attenuation factors (number of samples indicated below each bar graph pair).

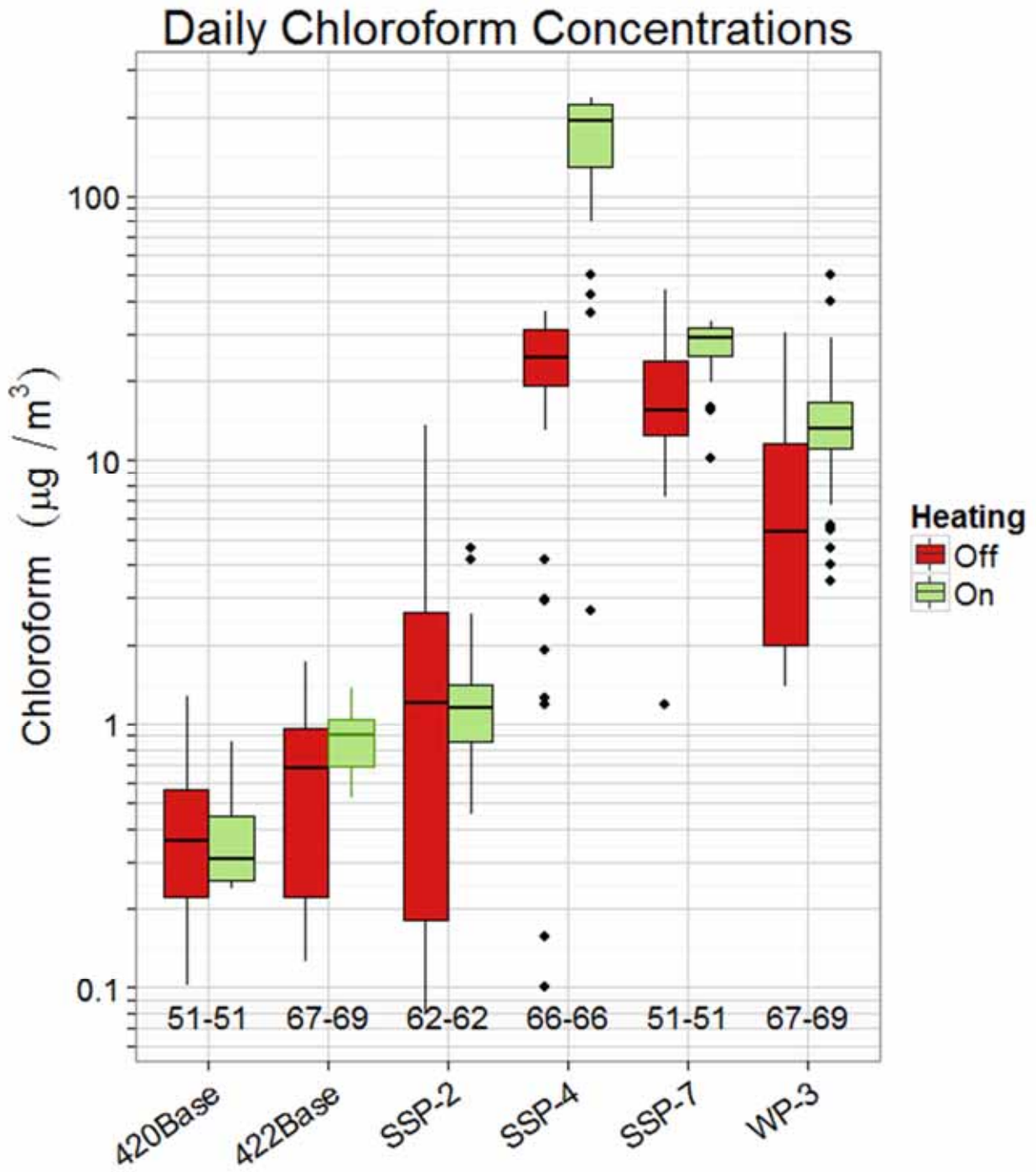


Figure 8-4. Daily chloroform concentrations used in attenuation factor calculations (number of samples indicated below each bar graph pair).

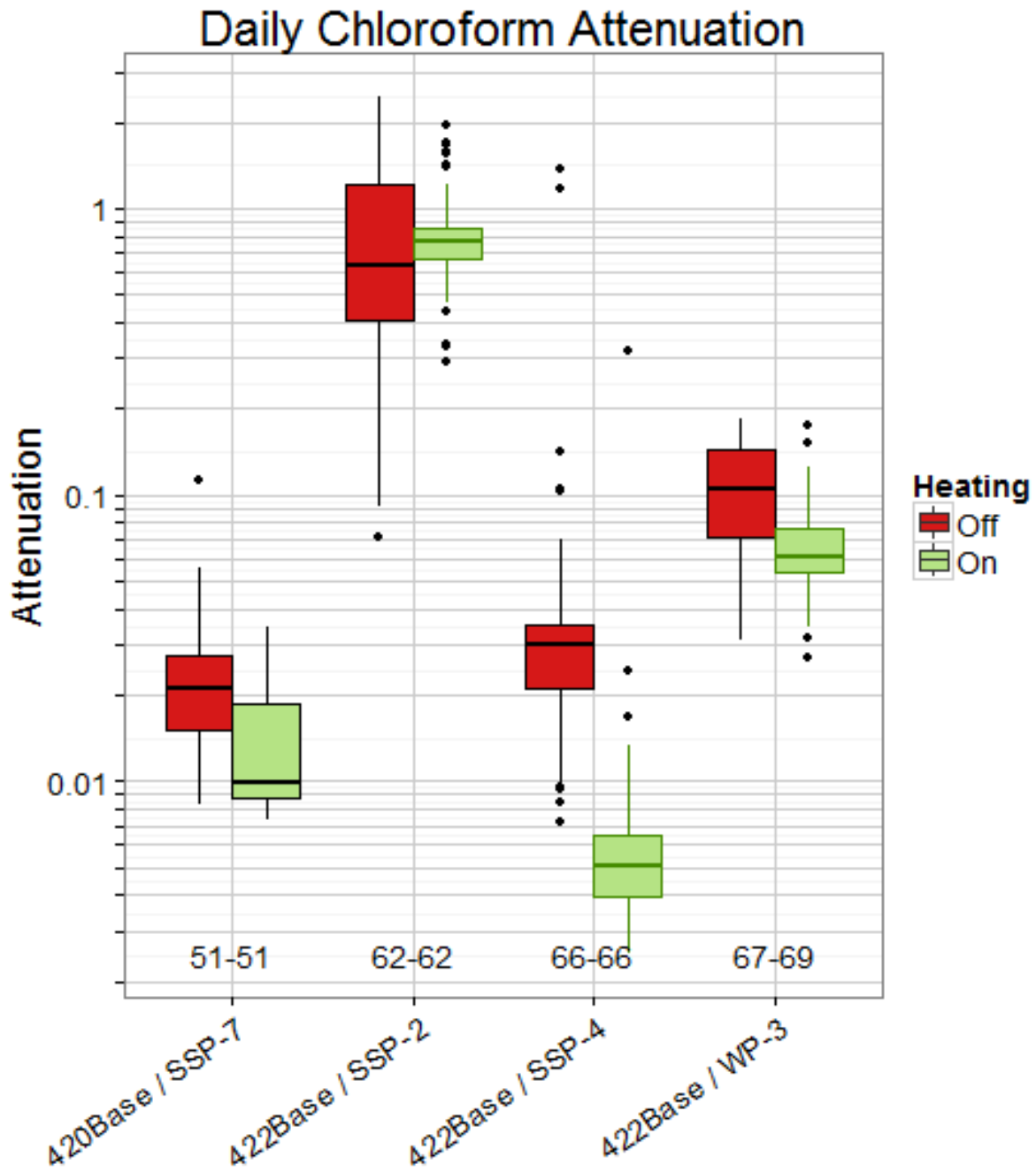


Figure 8-5. Daily chloroform soil gas to indoor air attenuation factors (number of samples indicated below each bar graph pair).

8.2 Subslab and Soil Gas to Indoor Air Weekly Attenuation Factors

8.2.1 Radon Weekly Attenuation Factors

Week-long attenuation factors for radon were calculated by averaging all subsurface radon measurements that coincide with an indoor air electret badge exposure period and pairing that average to the electret measurement. The attenuation between deeper soil gas and indoor air is interesting on a weekly scale because the soil gas has time to travel from deep in the soil to the indoor air. Given the duration of the measurement, it also makes sense to average soil gas samples from the same depth. Similarly, basement samples are lumped together, so the south (420BaseS) and north (420BaseN) samples are all classified as 420 basement (420Base).

Because of the way electrets are read, there were some small negative and 0 values in the indoor air concentrations. For the sake of calculating attenuation these values were replaced with the smallest non-negative value in the data series.

As with the daily attenuation figures, the weekly figures depict the data segregated by heat on and off, but only the 422 side was heated. **Figure 8-6** is an overview of all indoor air electret concentrations that were used to calculate attenuation factors.

As with the daily data, indoor air concentrations are higher during the heating season for the heated 422 side of the duplex, while radon concentrations actually decreased during the colder months on the unheated 420 side. **Figure 8-7** shows the subsurface soil gas radon concentrations measured with the portable AlphaGUARD instrument. In this case, the shallower soil gas samples (subslab, wall port, 3.5 ft, and 6 ft) show a decrease in radon concentrations while the deeper soil gas samples (9 ft, 13 ft, and 16.5 ft) show an increase during the heating season. This observation needs additional research because it is opposite of what might be expected, at least for the 422 side of the house with the increasing stack effect during the heating season. The same is true with respect to the observation that the difference between periods of heat on and off in subslab concentrations mirrors the 420 side indoor air rather than the 422 side indoor air. This was not expected as the stack effect created by heating should affect the subslab air. It is also not immediately obvious that the radon concentrations in soil gas fall off with depth, but the decrease is greater in the summer months.

Figure 8-8 shows the attenuation factors for the weekly radon samples. Weekly attenuation factors for the 420 and 422 basements are similar, ranging from 0.005 to 0.01 for the subslab and deeper soil gas, and without any obvious trends with depth. Wall port attenuation factors are higher than the others, but these results are difficult to evaluate because of the multiple influences (soil gas, atmospheric, building pressures) on these shallow samples.

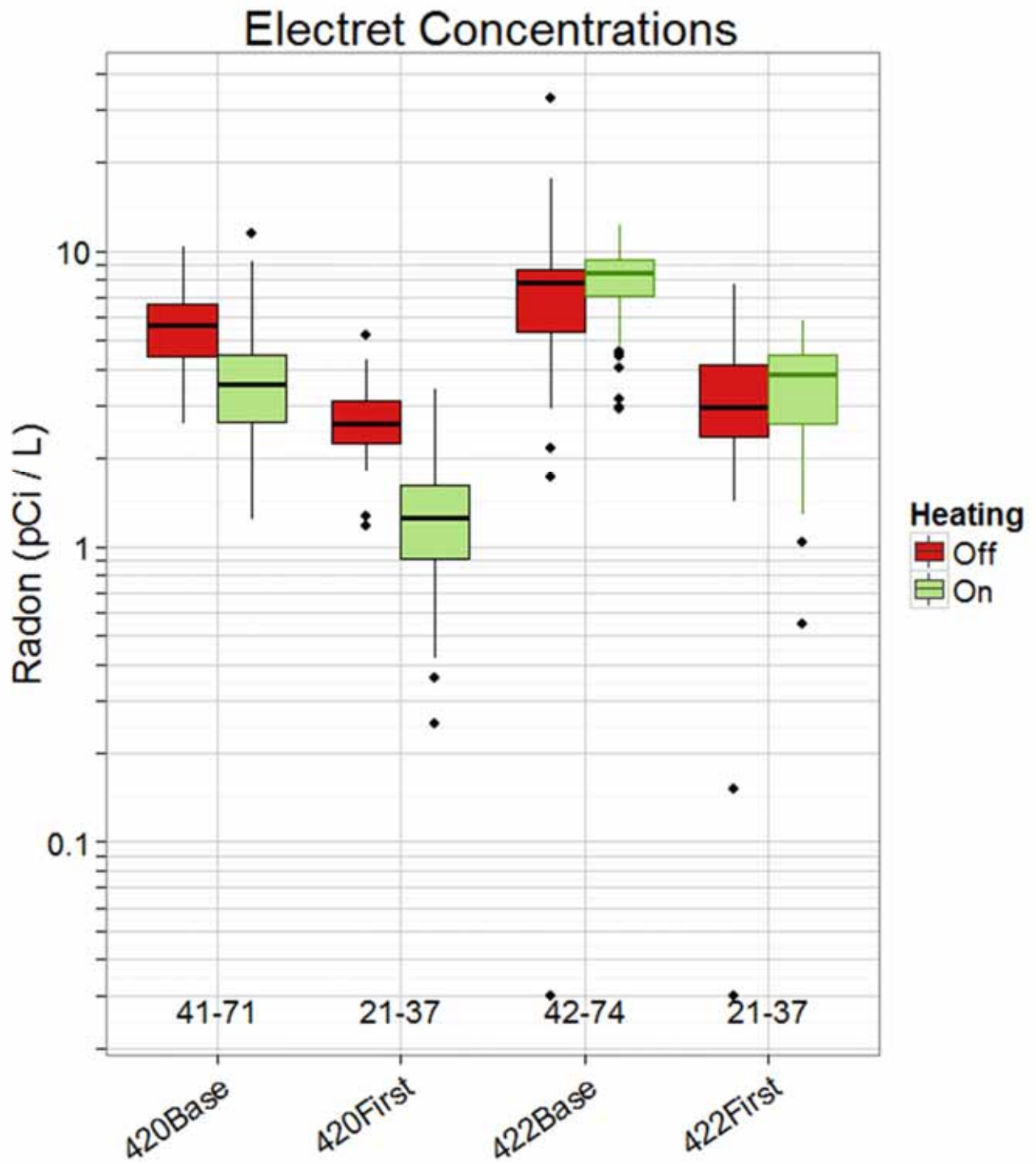


Figure 8-6. Electret radon indoor air concentrations used in weekly attenuation factor calculations. Number of measurements indicated below each box and whiskers pair.

AlphaGUARD Soil Gas Radon Concentrations

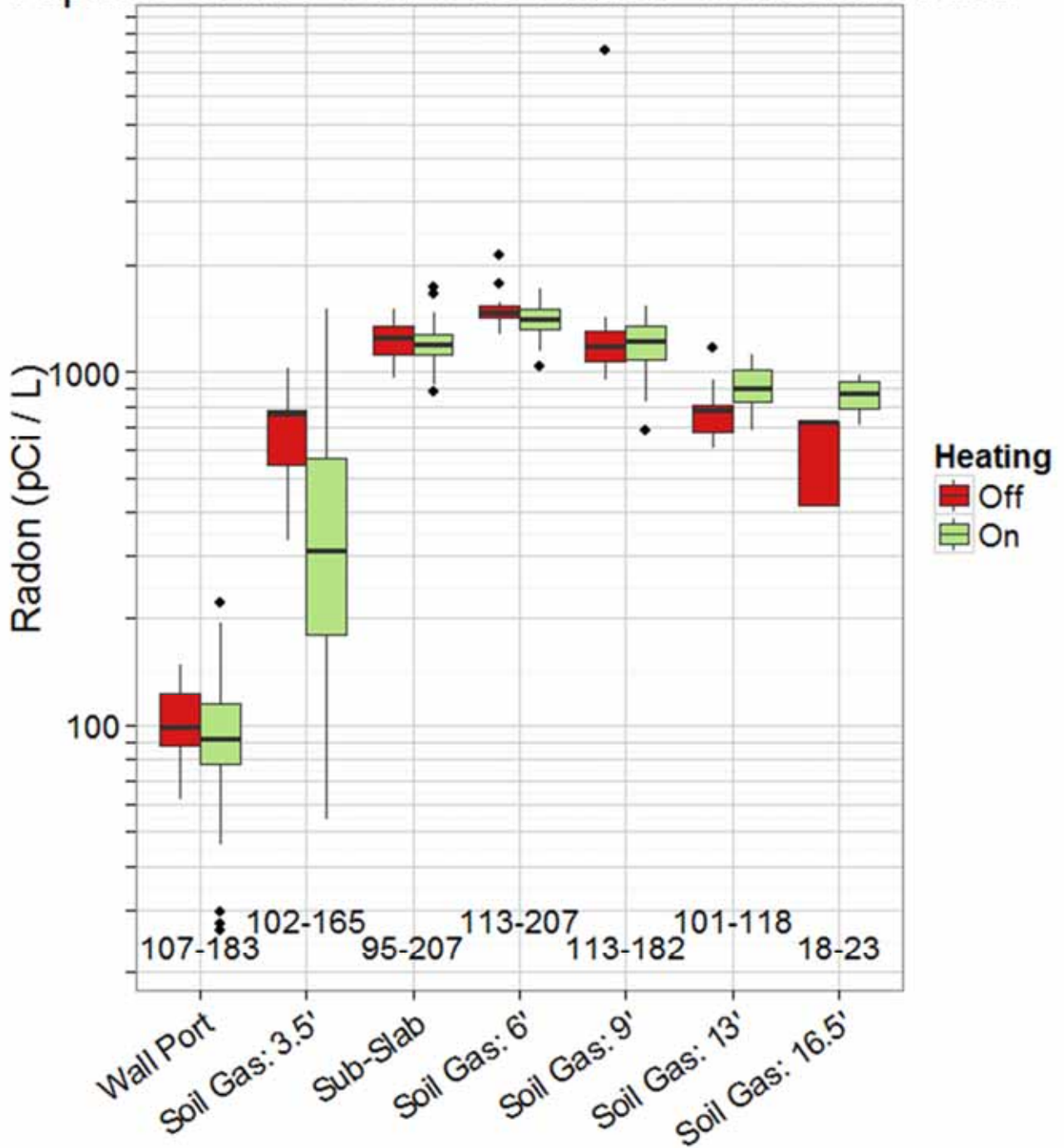


Figure 8-7. AlphaGUARD soil gas radon concentrations (pCi/L) used in weekly attenuation factor calculations. Number of measurements noted below each box and whiskers pair. Note that these concentrations represent averages across all samples taken at the same depth and time (e.g., subslab samples are averages across all subslab points).

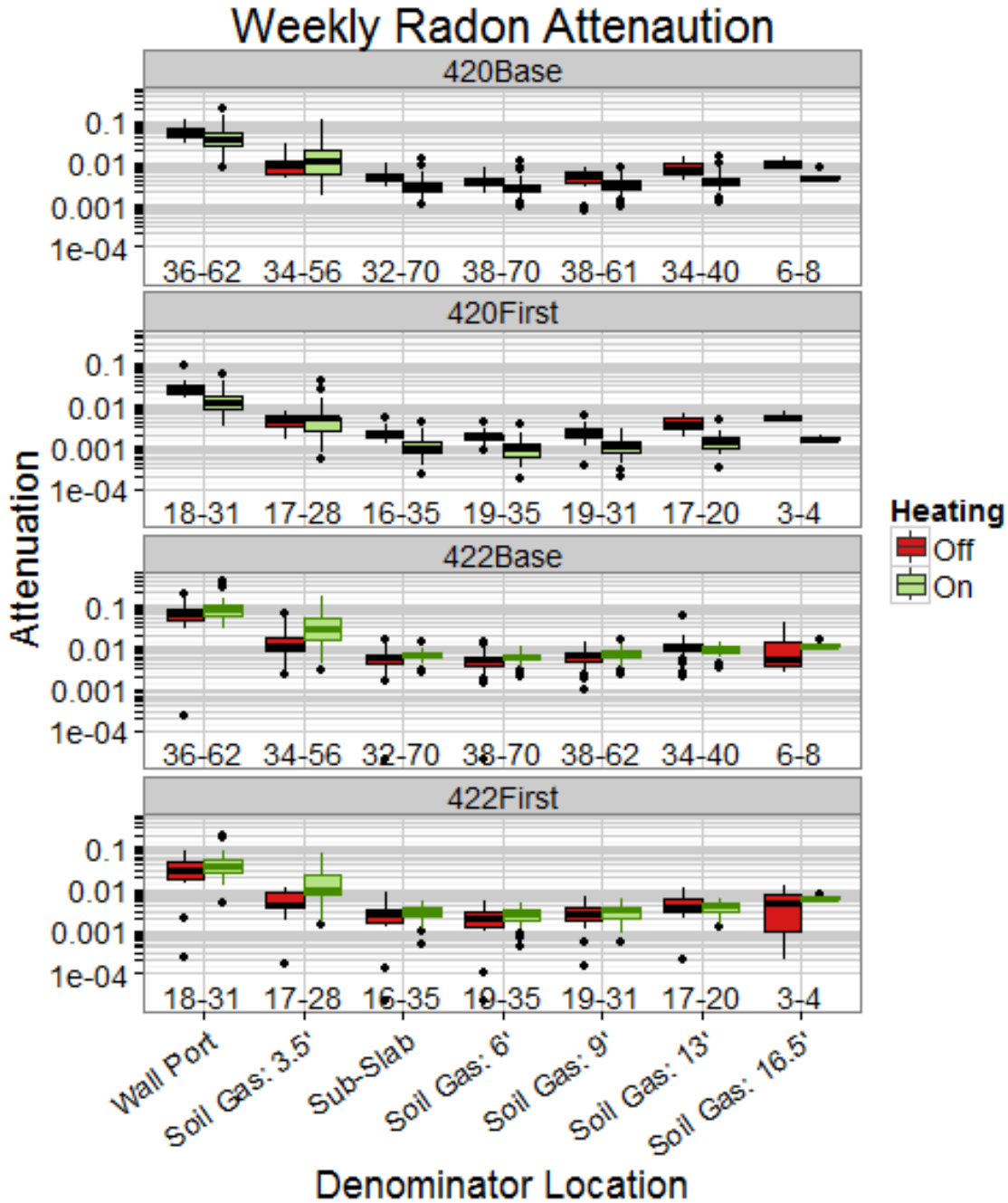


Figure 8-8. Weekly radon attenuation factors (number of samples indicated below each bar graph pair). Note that these attenuation factors were calculated from indoor air and soil gas concentrations averaged at the same depth and time (as described in Figure 8-7).

8.2.2 VOC Weekly Attenuation Factors

The attenuation factors calculated from the Radiello/TO-17 data for VOCs are comparable to the electret/portable AlphaGUARD attenuation factors calculated for radon in that they represent weekly indoor air averages against grab subsurface samples taken about once per week. **Figure 8-9** shows the weekly Radiello indoor air sample concentrations used in these calculations, which show a drop off in

winter concentrations on the unheated 420 side of the building, which was statistically significant for the basement ($p = 0.04$, simple T-test, null hypothesis = there is no decrease in concentration with mitigation) but not for the first floor ($p = 0.04$). This could reflect a weaker stack effect in this colder, unheated side of the building. The heated 422 side showed the expected increase in concentrations during the heated period, which was statistically significant for both the basement ($p = 0.0004$) and the first floor ($p = 0.01$). Both sides exhibited the higher basement VOC concentrations (than first floor) that would be expected at a vapor intrusion site.

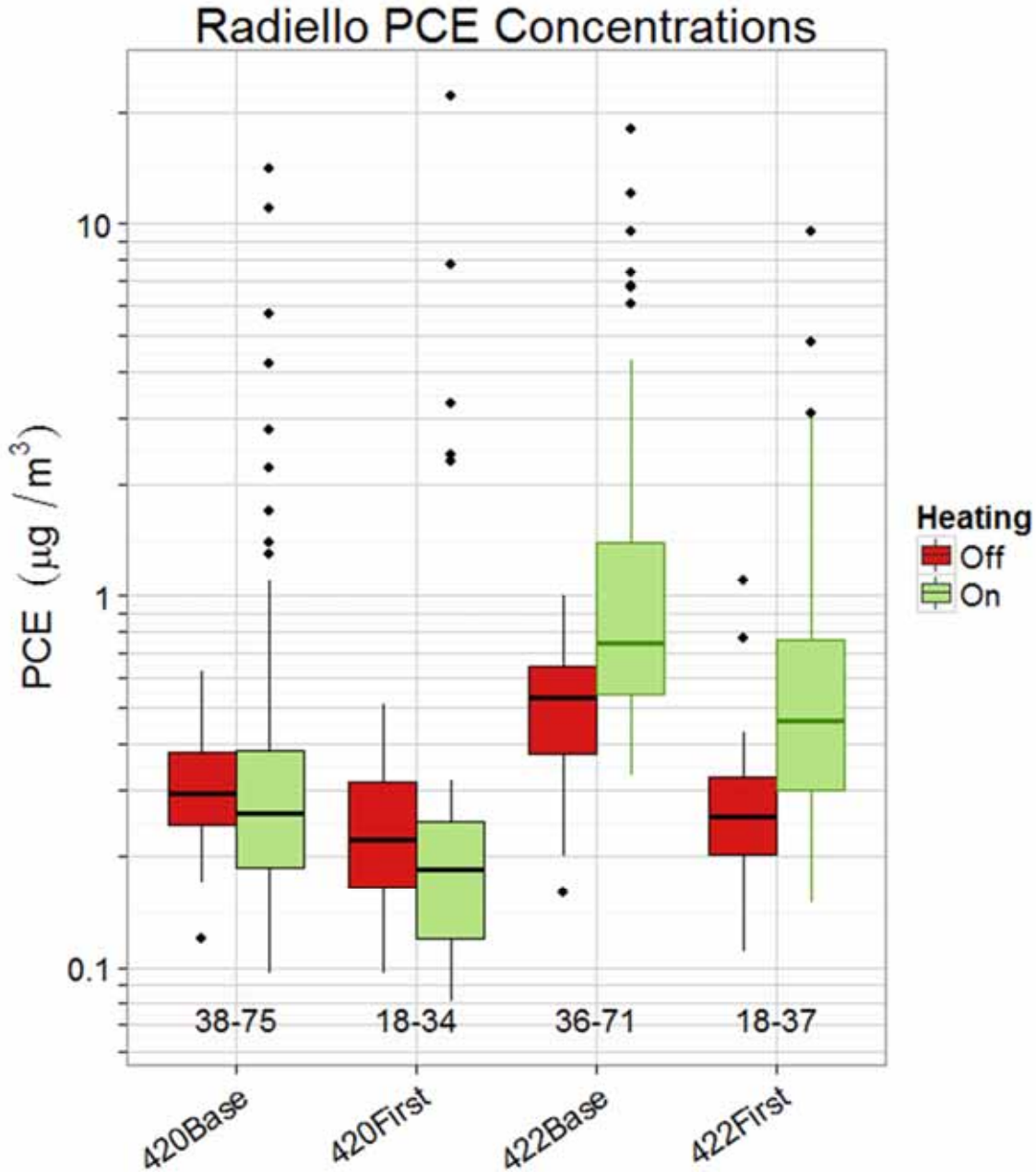


Figure 8-9. Radiello PCE indoor air concentrations used in attenuation factor calculations. Numbers at the bottom of each column indicate the number of available readings for unheated (left) and heated (right) conditions.

Figure 8-10 shows the TO-17 grab samples taken from the subsurface sampling ports used as a denominator in calculating the PCE attenuation factors. PCE concentrations tend to drop off with depth between subslab and the deeper soil gas, with the winter/summer differences not showing any consistent trends. The much lower concentrations observed in the wall port and shallow exterior soil gas samples are consistent with and serve to validate the conceptual models of shallow soil gas concentrations modeled and pictured in Abreu and Johnson (2005) and U.S. EPA (2012d).

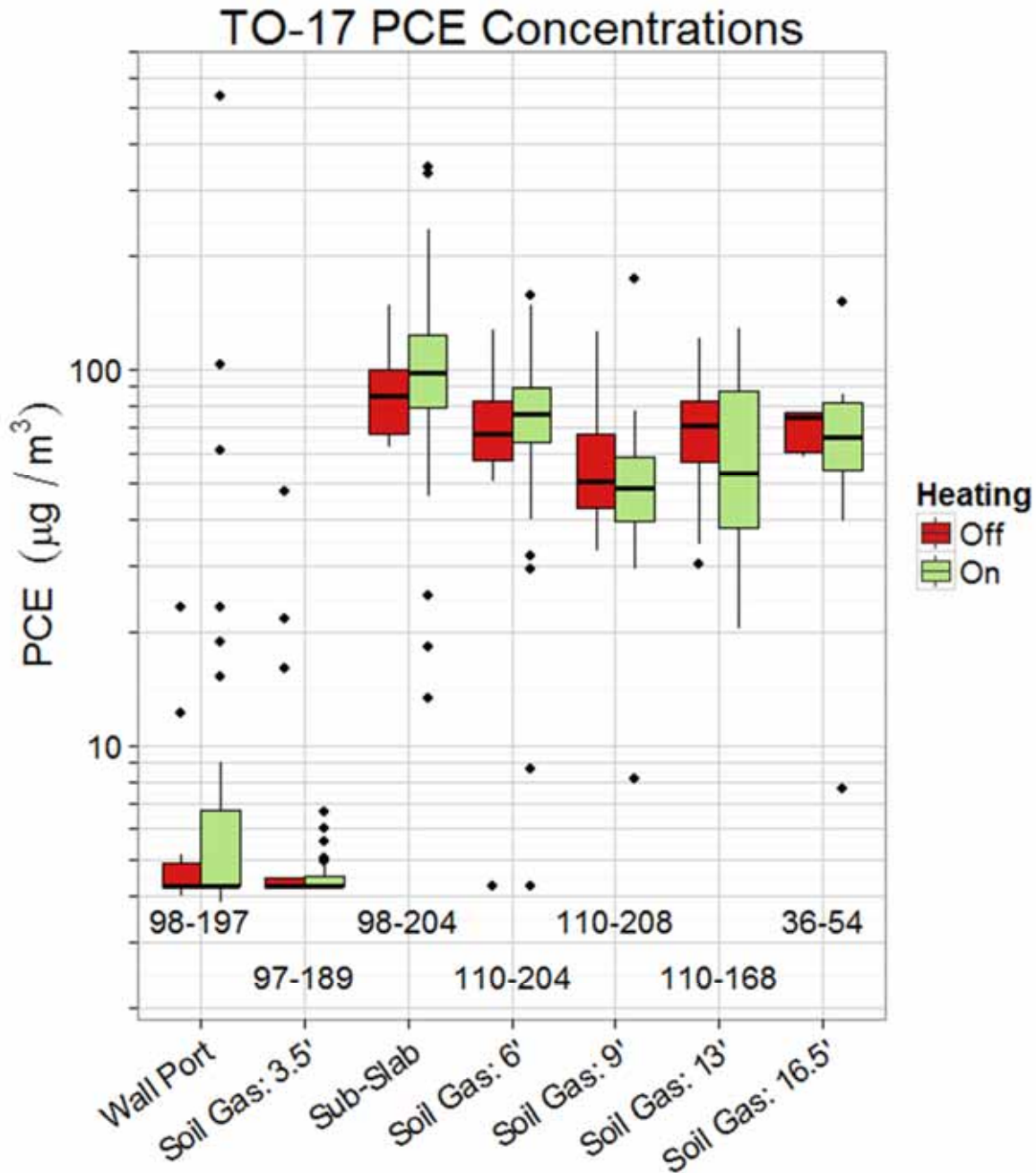


Figure 8-10. TO-17 PCE soil gas concentrations used in indoor air / soil gas attenuation factor calculations with multiple soil gas sample probes averaged at each depth.

Attenuation factors calculated from the weekly data are provided in **Figure 8-11**. As expected, attenuation factors are higher (less attenuation) in the winter (during heating) on the 422 side, with summer levels tending to have less attenuation than winter for the unheated 420 basement.

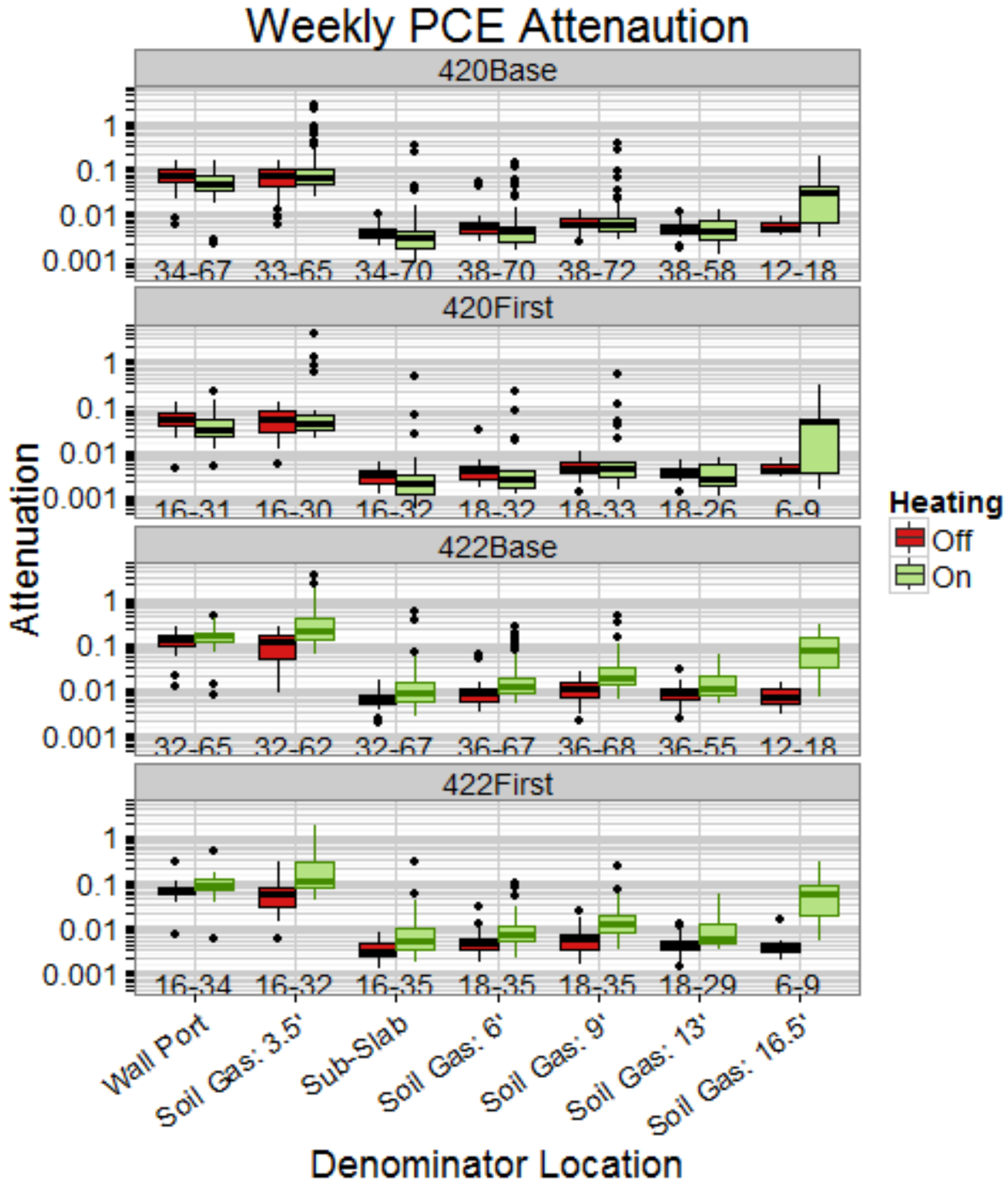


Figure 8-11. Weekly PCE attenuation factors (numbers of samples indicated by numbers beneath each bar graph pair). Soil gas concentrations (denominator) averaged by depth across different soil gas probes.

Figure 8-12 shows the weekly Radiello indoor air samples used for the weekly attenuation factors. Again winter VOC levels are statistically higher ($p = 6e-11$ for basement and $p = 0.0004$ for first floor) due to furnace operation on the 422 side but about the same (with no statistical difference), summer to winter, on the unheated 420 side of the duplex.

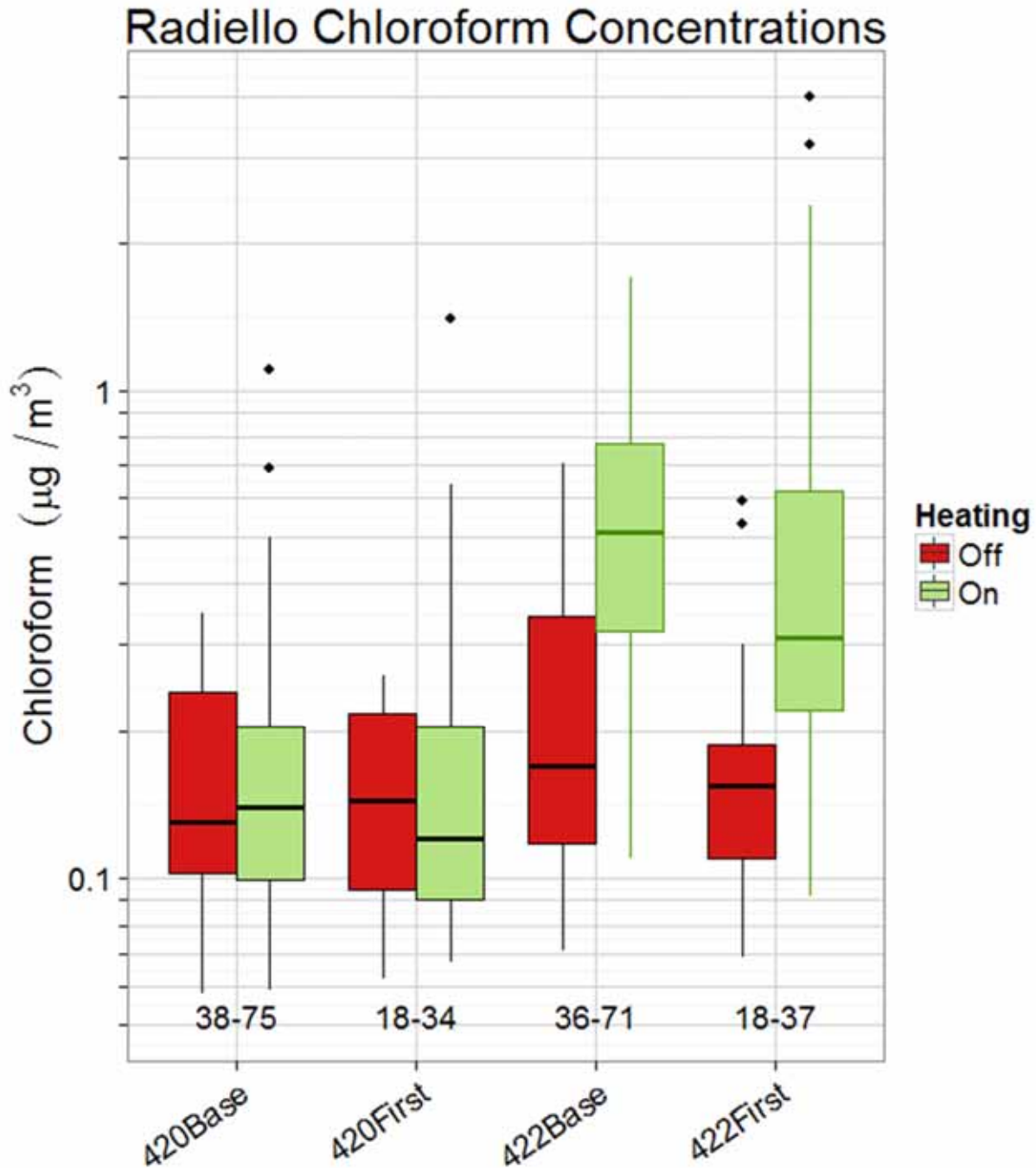


Figure 8-12. Radiello chloroform indoor air concentrations used as numerators for weekly attenuation factor calculations.

Figure 8-13 shows the TO-17 grab samples taken from the subsurface sampling ports used as a denominator in calculating the chloroform attenuation factors. Unlike PCE, chloroform concentrations tend to more or less increase with depth, with winter (heating on) concentrations higher for subslab and 6 ft and 9 ft soil gas samples but about the same as heating off concentrations in the deeper (13 ft and 16.5 ft) soil gas samples.

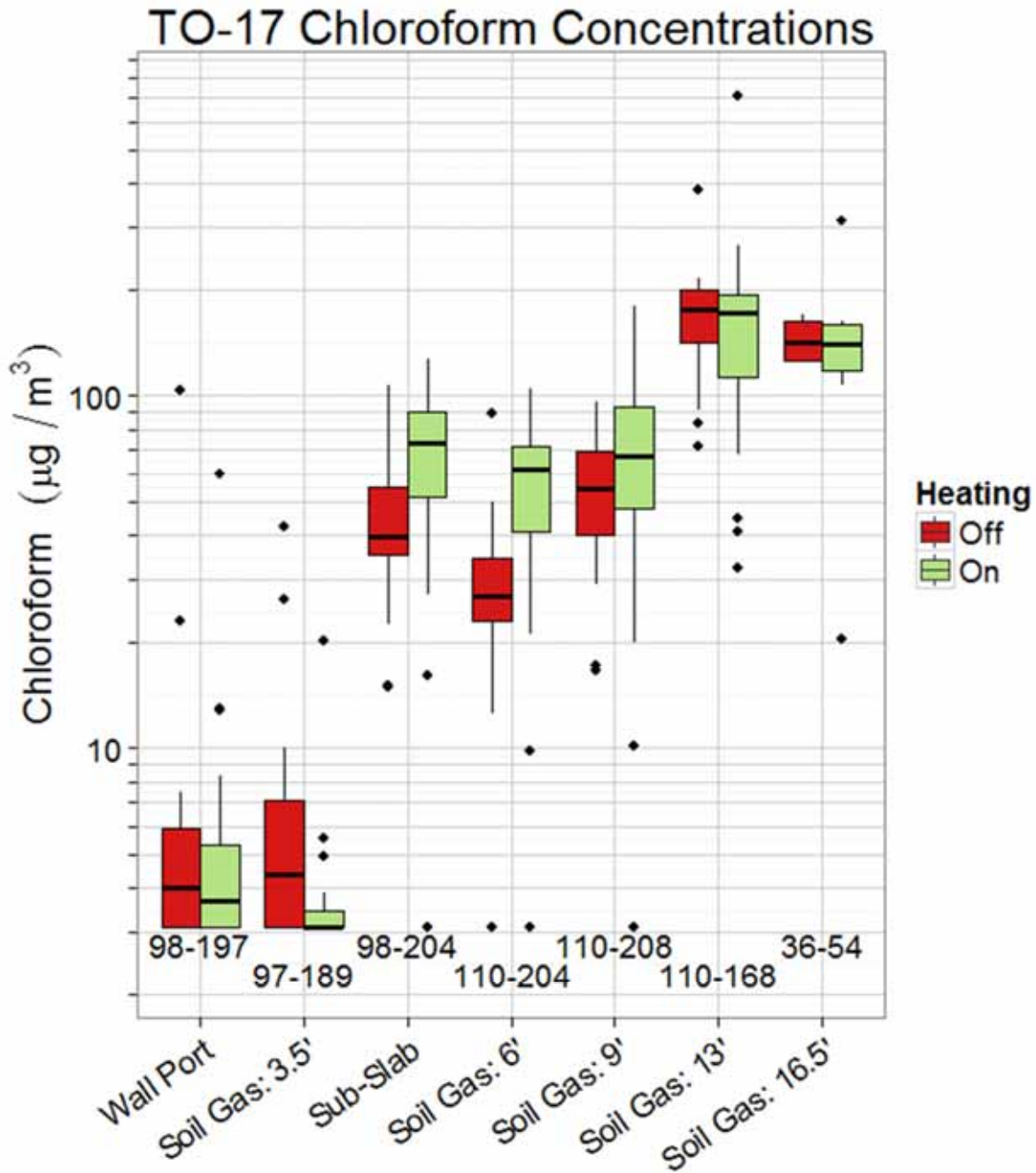


Figure 8-13. TO-17 chloroform soil gas concentrations (averaged by depth across soil gas probes) used as denominators for weekly attenuation factor calculations.

Figure 8-14 shows the weekly chloroform attenuation factors for the 420 and 422 first floors and basements. For the 422 side the attenuation factors tend to decrease with depth from about 0.01 at subslab to 0.002 at 13 and 16.5 ft, with attenuation going down (higher attenuation factors) in the heated winter. For the unheated 420 side the attenuation factors show a similar if slightly lower trend with depth, but tend to show an increase in attenuation (lower attenuation factors) from summer to winter.

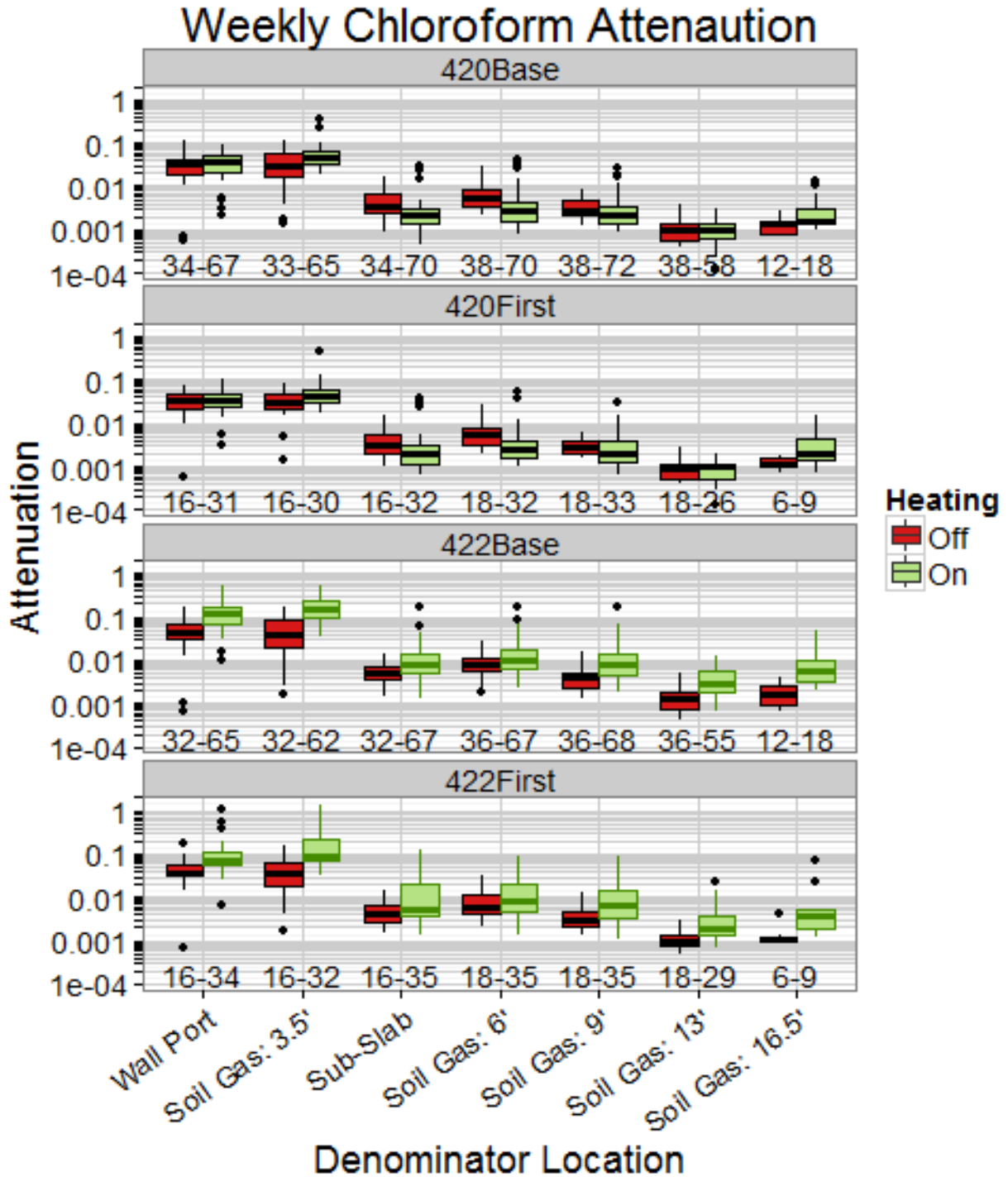


Figure 8-14. Weekly chloroform attenuation factors (number of samples indicated below each bar graph pair).

It is also informative to compare the attenuation of all three compounds. **Figure 8-15** juxtaposes the weekly attenuation factors observed during the study period for radon, chloroform, and PCE for the 420 and 422 basement indoor air concentrations over subslab and near-subslab (6 ft) soil gas. One can see a strong agreement between the different chemicals and house sides, with subslab attenuation factors centering on or just below 0.01 and opposite summer-to-winter (heat off to heat on) trends for the heated (422) and unheated (420) sides of the building.

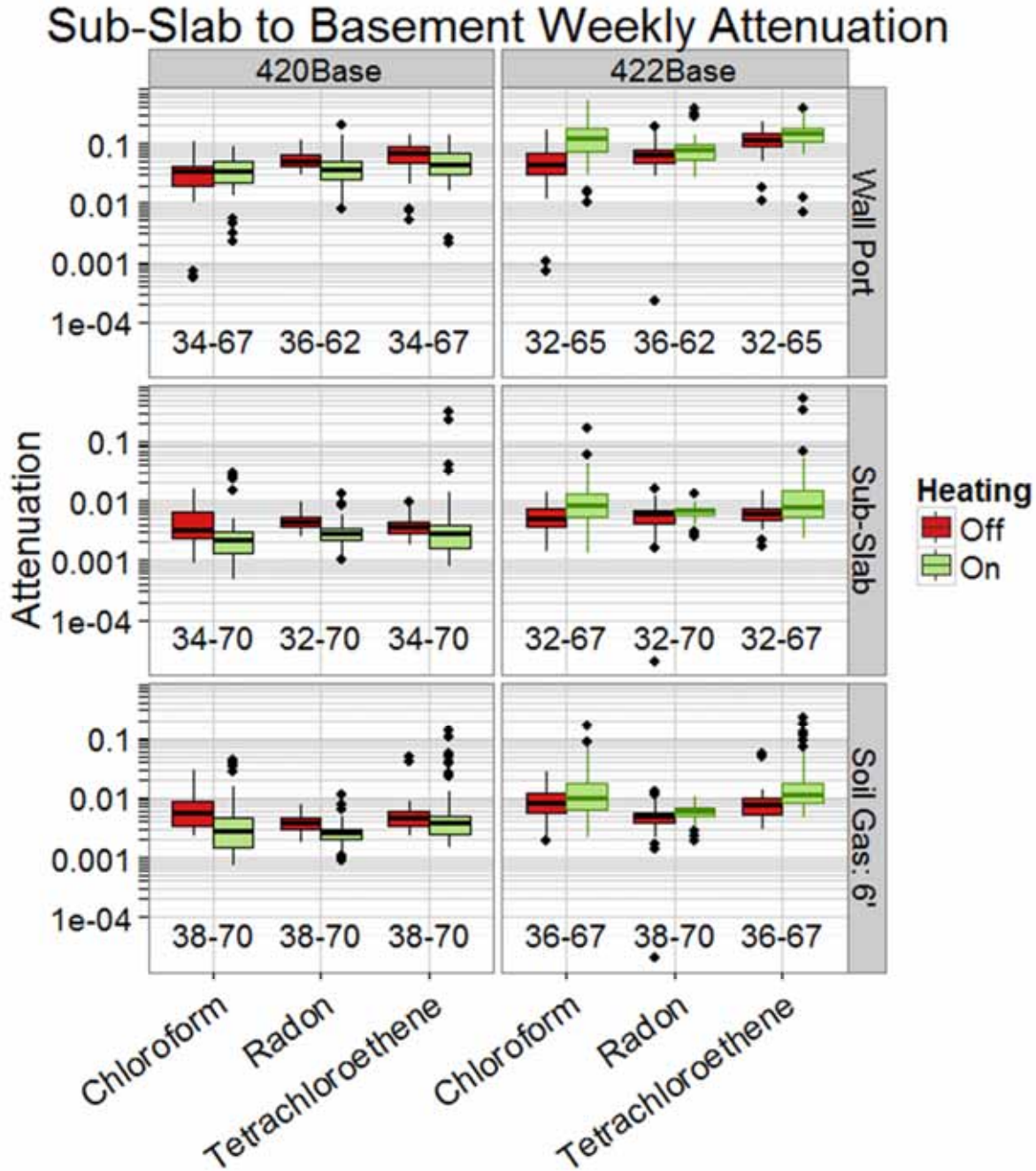


Figure 8-15. Attenuation of PCE, chloroform, and radon juxtaposed.

8.3.1 Subslab to Indoor Air Daily Attenuation

Daily Radon Attenuation Factors

The mitigation system was designed for radon mitigation and it has been proven to be very effective in this regard (see Section 5). Radon attenuation between the subslab and indoor air responded as expected to the mitigation system, with dramatic drops in radon concentrations when the system was turned on and equally rapid increases in radon system when the system was shut off or operated in passive mode. Even with relatively few indoor air and soil gas sample pairs (**Figure 8-17**), the effect of the mitigation on radon attenuation is obvious (**Figure 8-18**), with over an order of magnitude reduction in radon concentrations with mitigation on, which is mainly due to the over an order of magnitude reduction in indoor air radon concentrations (see upper panel of **Figure 8-17**).

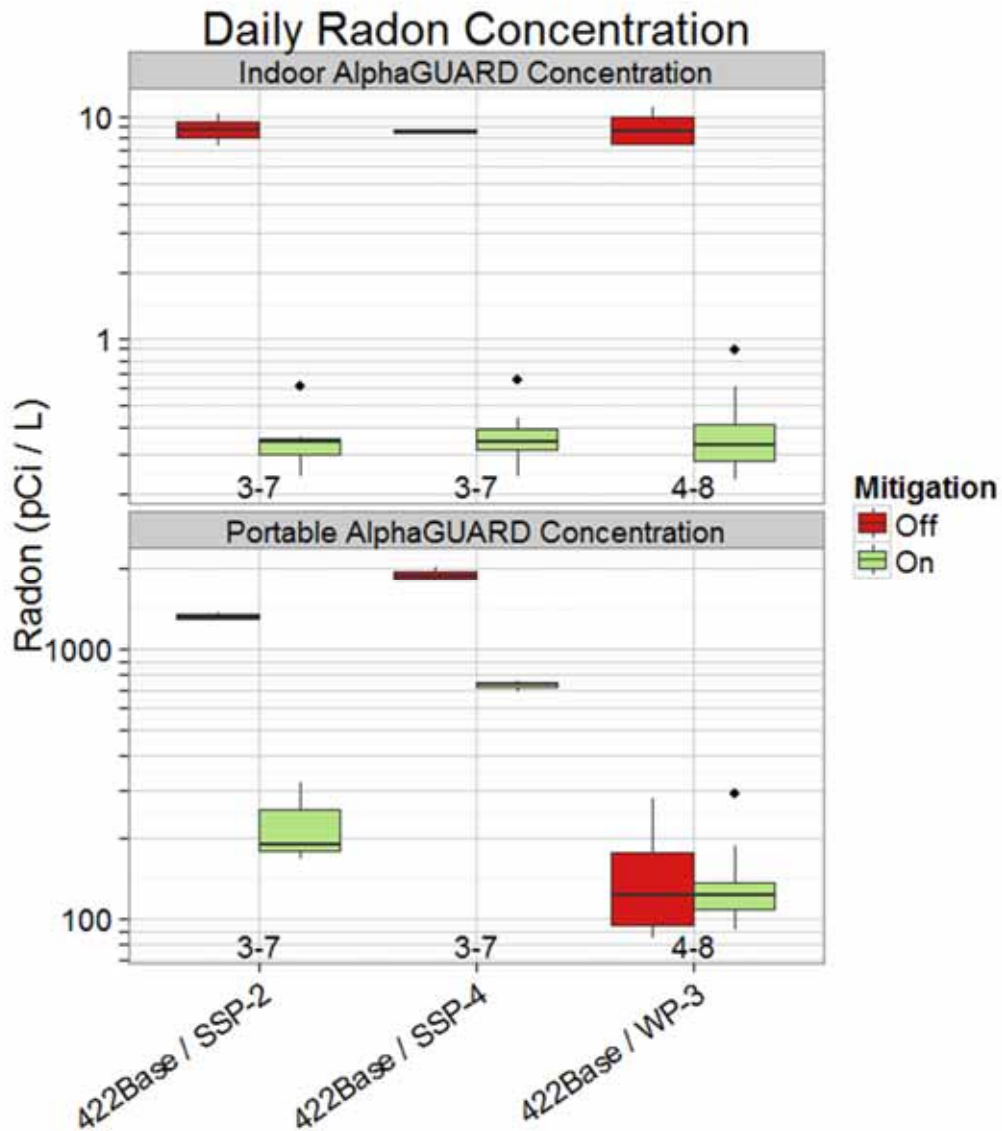


Figure 8-17. Indoor air (AlphaGUARD) and soil gas (portable AlphaGUARD) radon concentrations used in daily attenuation factor calculations.

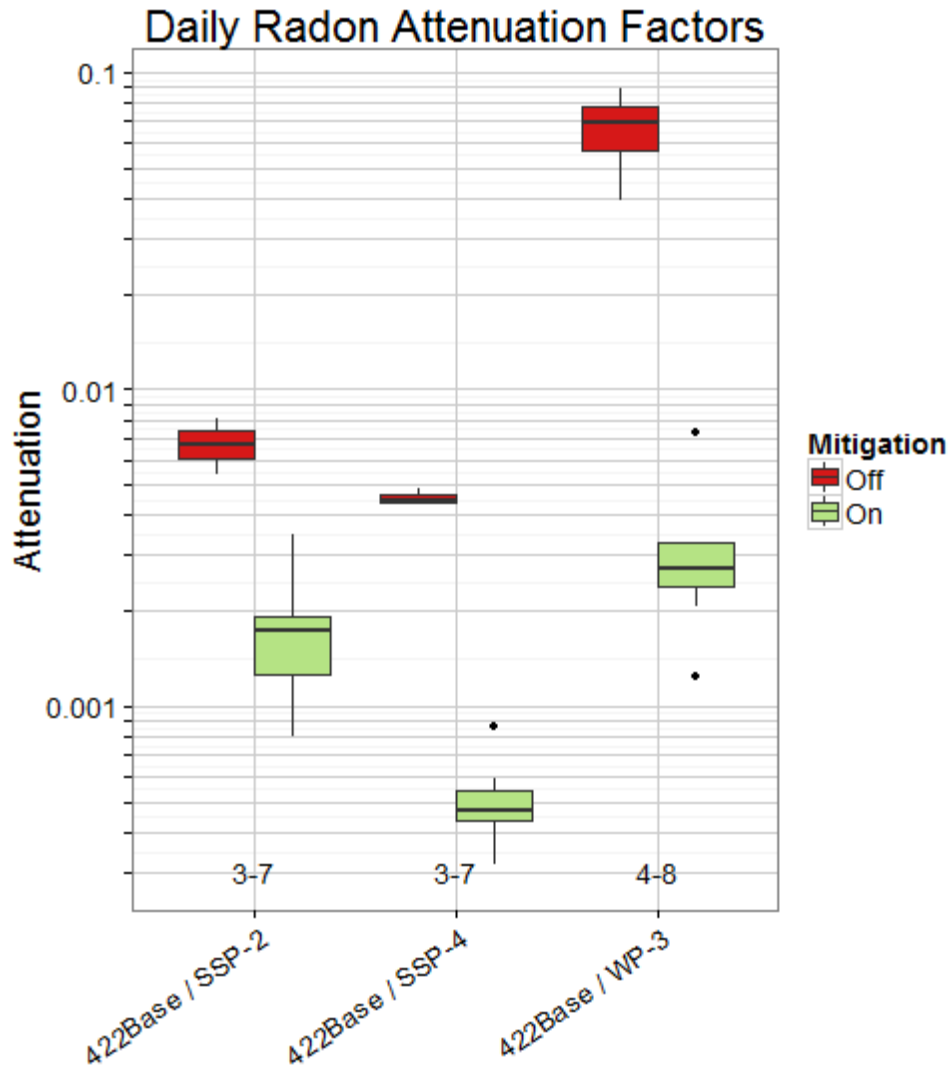


Figure 8-18. Daily radon attenuation factors.

Interestingly, at some locations it appears that mitigation also decreases subslab and wall port radon concentrations (bottom panel of **Figure 8-17**). Even in locations where the exterior concentration dropped, the attenuation factor between exterior locations and indoor air is reduced considerably by mitigation (**Figure 8-18**).

Daily VOC Attenuation Factors

For daily VOC attenuation factors (**Figure 8-19** and **8-20**), turning the mitigation system on decreased the attenuation factors and increased attenuation for all conditions tested. Although the SSP-2 and WP-3 concentrations are suspected low because of dilution, there was an increase in attenuation in both cases for PCE (**Figure 8-19**) and chloroform (**Figure 8-20**). Attenuation factors over 1 in these figures for PCE and (especially) chloroform in SSP-2 are clearly unrealistic and may be reflecting limited connections between the subslab area sampled by SSP-2 and indoor air.

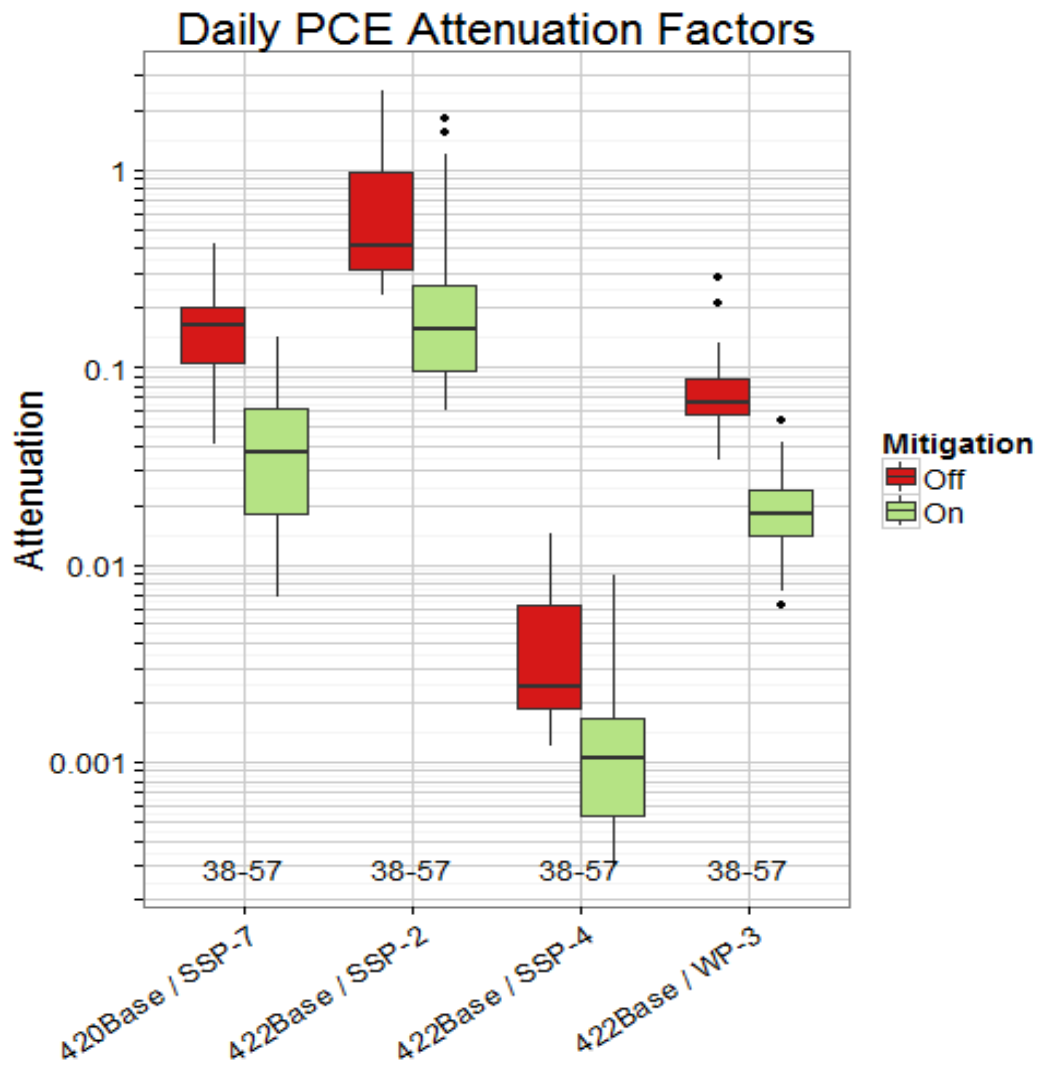


Figure 8-19. Daily PCE attenuation factors.

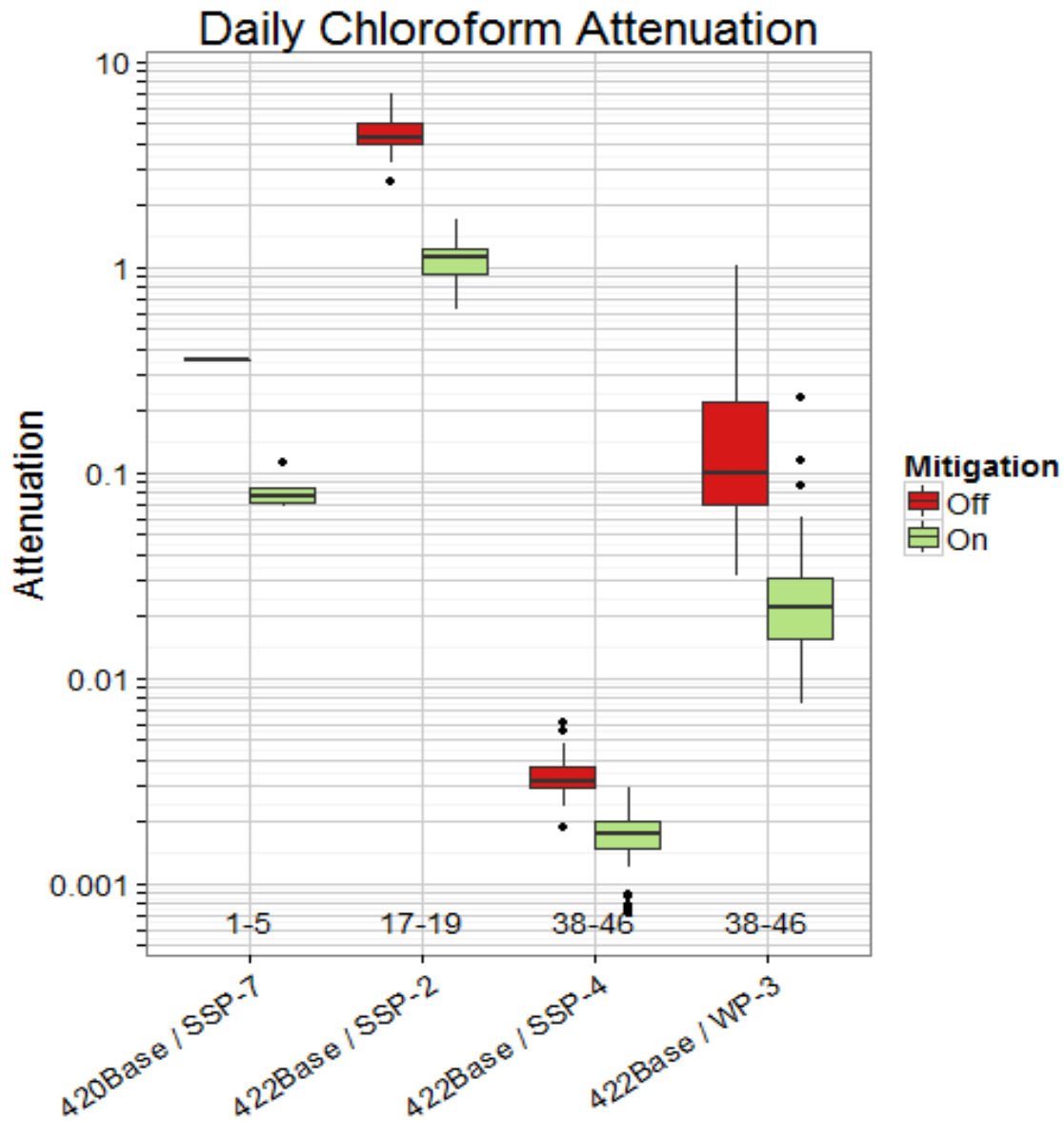


Figure 8-20. Daily chloroform attenuation factors.

8.3.2 Subslab and Soil Gas to Indoor Air Weekly Attenuation

The weekly attenuation factors are assigned a mitigation status based on what mitigation status was most common during the sample’s exposure. For example, a weekly sample that was exposed for 7 days, four of them with the mitigation system off and three of them with the mitigation system in passive mode, is assigned a mitigation status of “Off.” As in previous discussions, weekly attenuation factors were based weekly indoor air electret concentrations for radon and Radiellos for VOC concentrations, with subsurface concentrations being represented by portable AlphaGUARD and TO-17 grab samples.

Radon

The electret indoor air concentrations before and after mitigation are shown in **Figure 8-21**, representing the entire period of electret record available for this study (January 2011 to May 2013).¹⁸ The dramatic reduction of radon in indoor air during mitigation of about an order of magnitude can be seen in the figure, with all post-mitigation radon concentrations being under the 4 pCi/L target concentration.

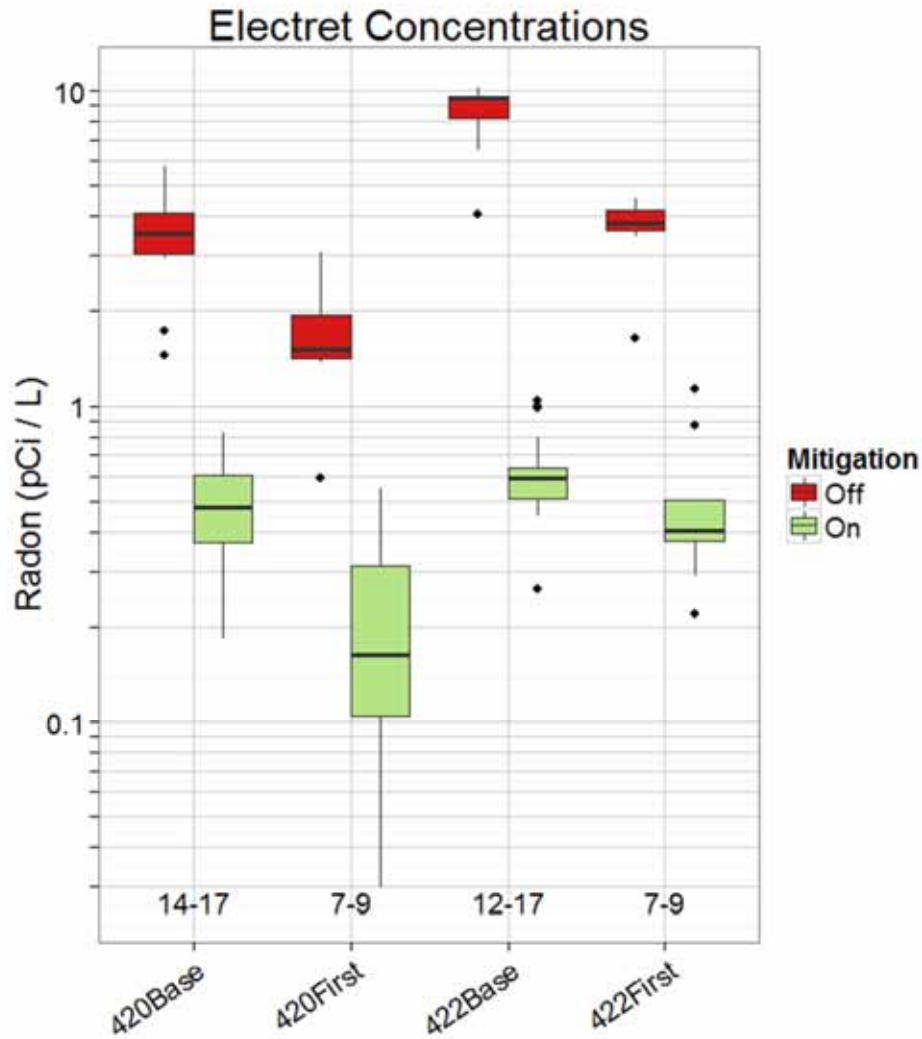


Figure 8-21. Electret indoor air radon concentrations.

Subsurface radon concentrations also show a reduction with mitigation (**Figure 8-22**), but not as great a reduction as observed for indoor air. The attenuation factors calculated from these pairs of measurements (**Figure 8-23**) show that in every case, the lowered indoor air concentration predominates with a decrease in the attenuation factors (and increase in attenuation) as a result.

¹⁸See mitigation on and off periods in **Figure 8-16**.

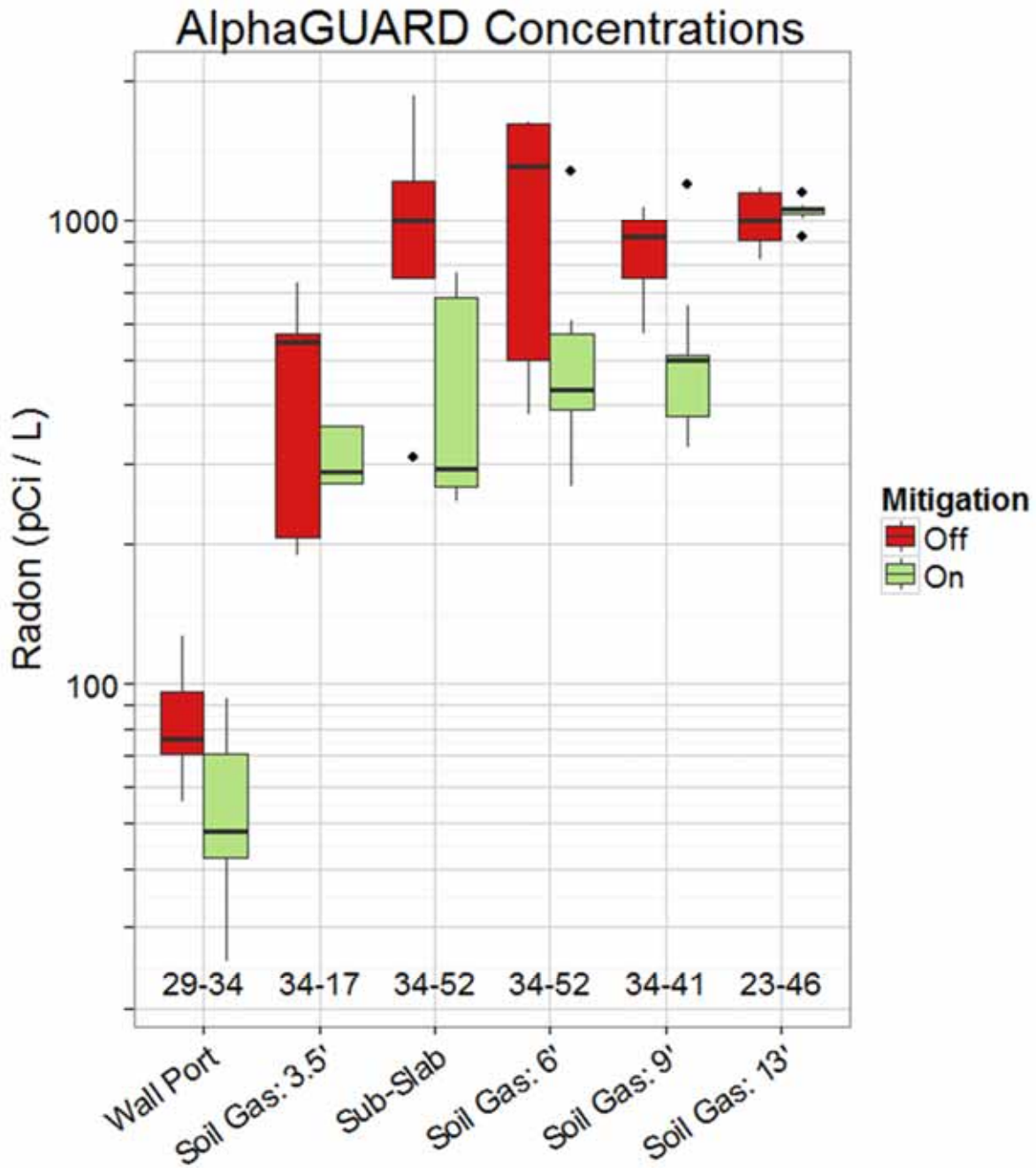


Figure 8-22. AlphaGUARD soil gas radon concentrations (pCi/L) used as denominator in attenuation factor calculations.

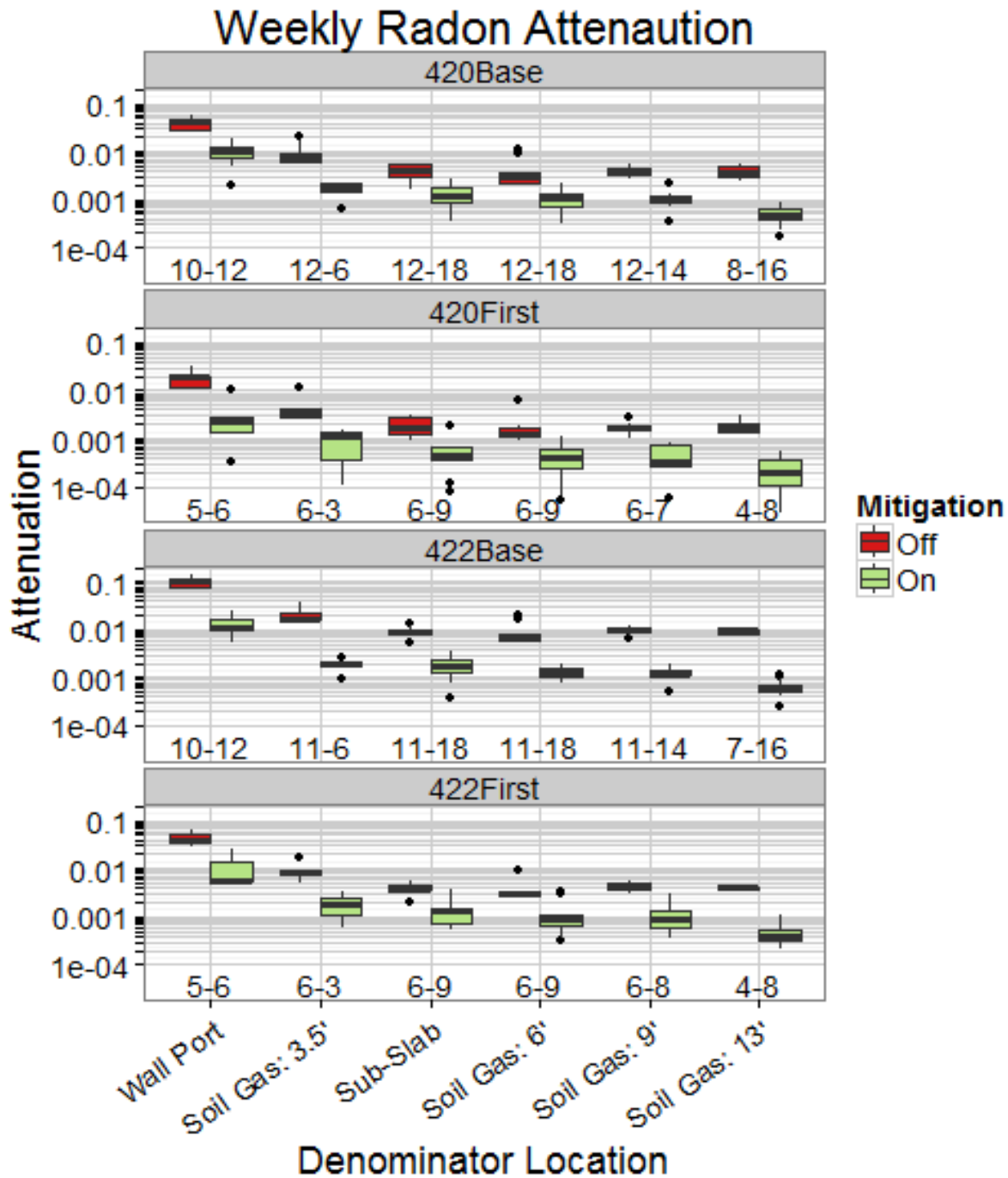


Figure 8-23. Weekly radon attenuation.

Weekly VOC Attenuation Factors

As previously described, the VOC attenuation factors were calculated from the weekly Radiello and corresponding TO-17 grab samples. **Figure 8-24** shows the weekly Radiello indoor air data used as the numerator to calculate VOC attenuation factors. Although the drops in concentration are not as great as for radon, they are lower in every case, indicating that the subslab depressurization mitigation system appears to be effective in reducing VOC as well as radon concentrations on both sides of the duplex.

However, note that the number of samples was too low to determine the statistical significance of these VOC drops for PCE.

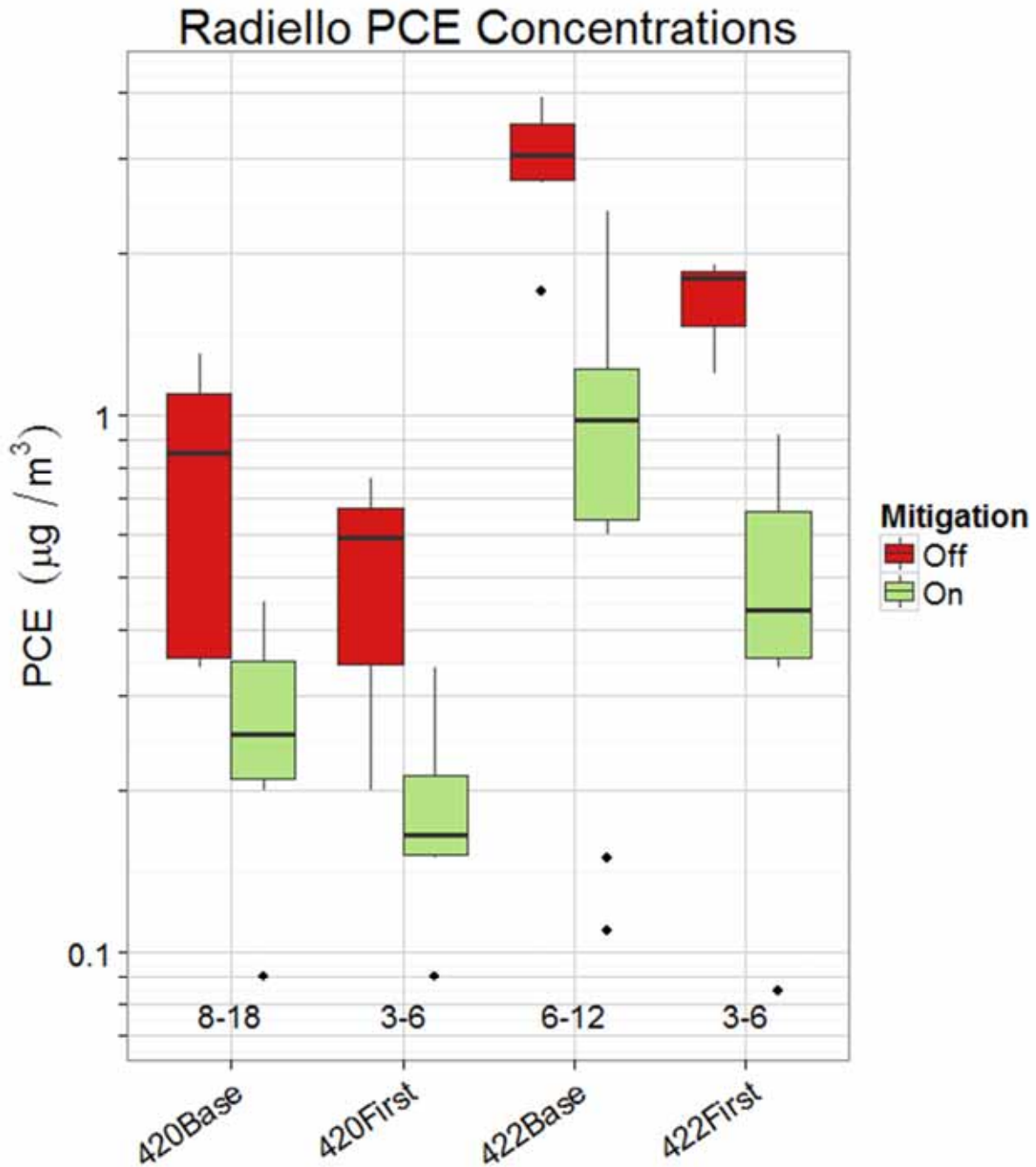


Figure 8-24. Radiello indoor air PCE concentrations.

Figure 8-25 shows that mitigation effects on the subsurface PCE concentrations were not so definitive, with concentrations actually increasing in a few cases, and decreasing in others. These data suggest effects on the distribution of subsurface VOCs that are not consistent with radon and not fully understood

at this time. However, **Figure 8-26**, which shows the effect of mitigation on weekly PCE attenuation, increased attenuation (i.e., decreased the attenuation factor) in every case, although again the sample size was small.

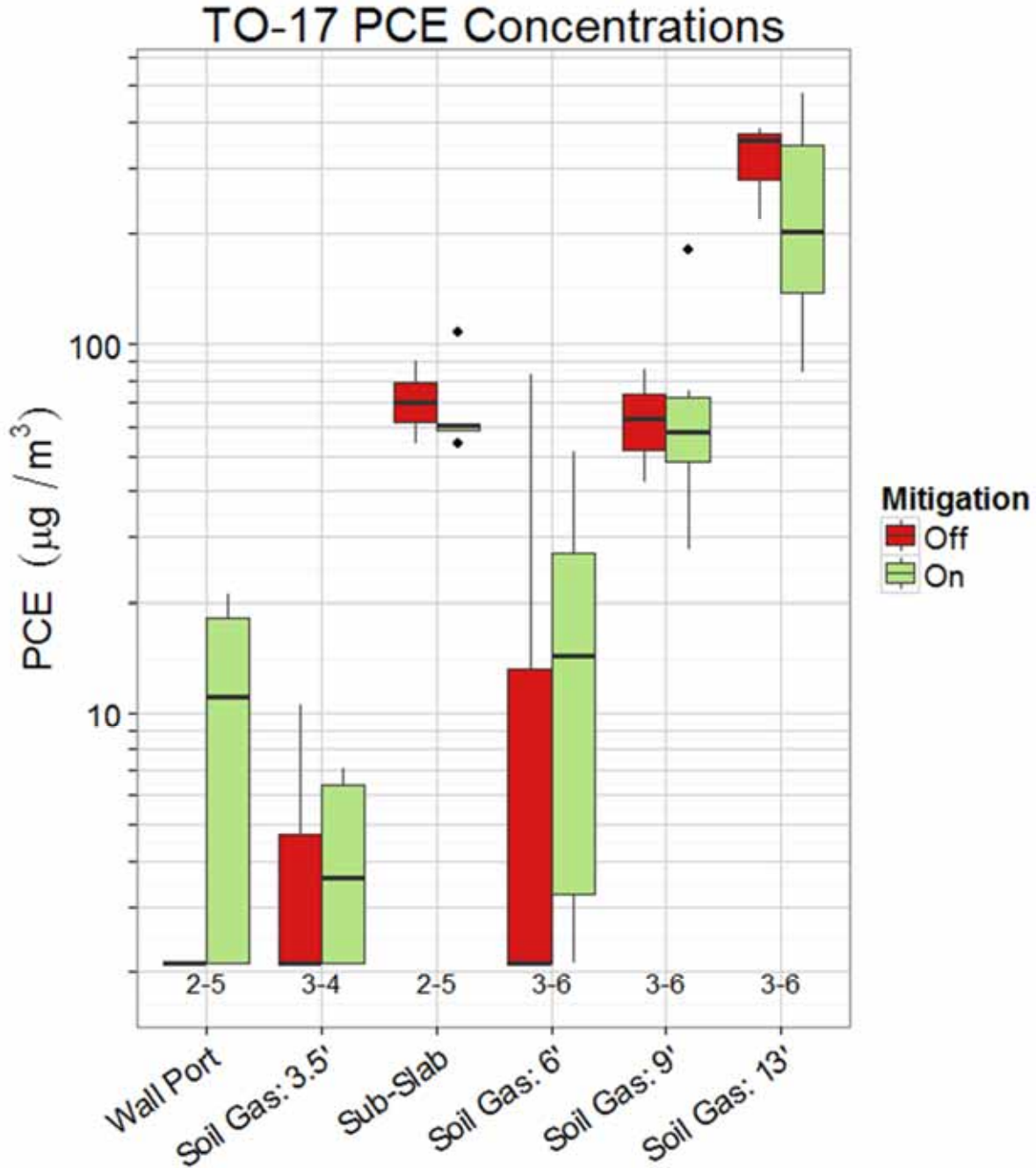


Figure 8-25. TO-17 soil gas PCE concentrations.

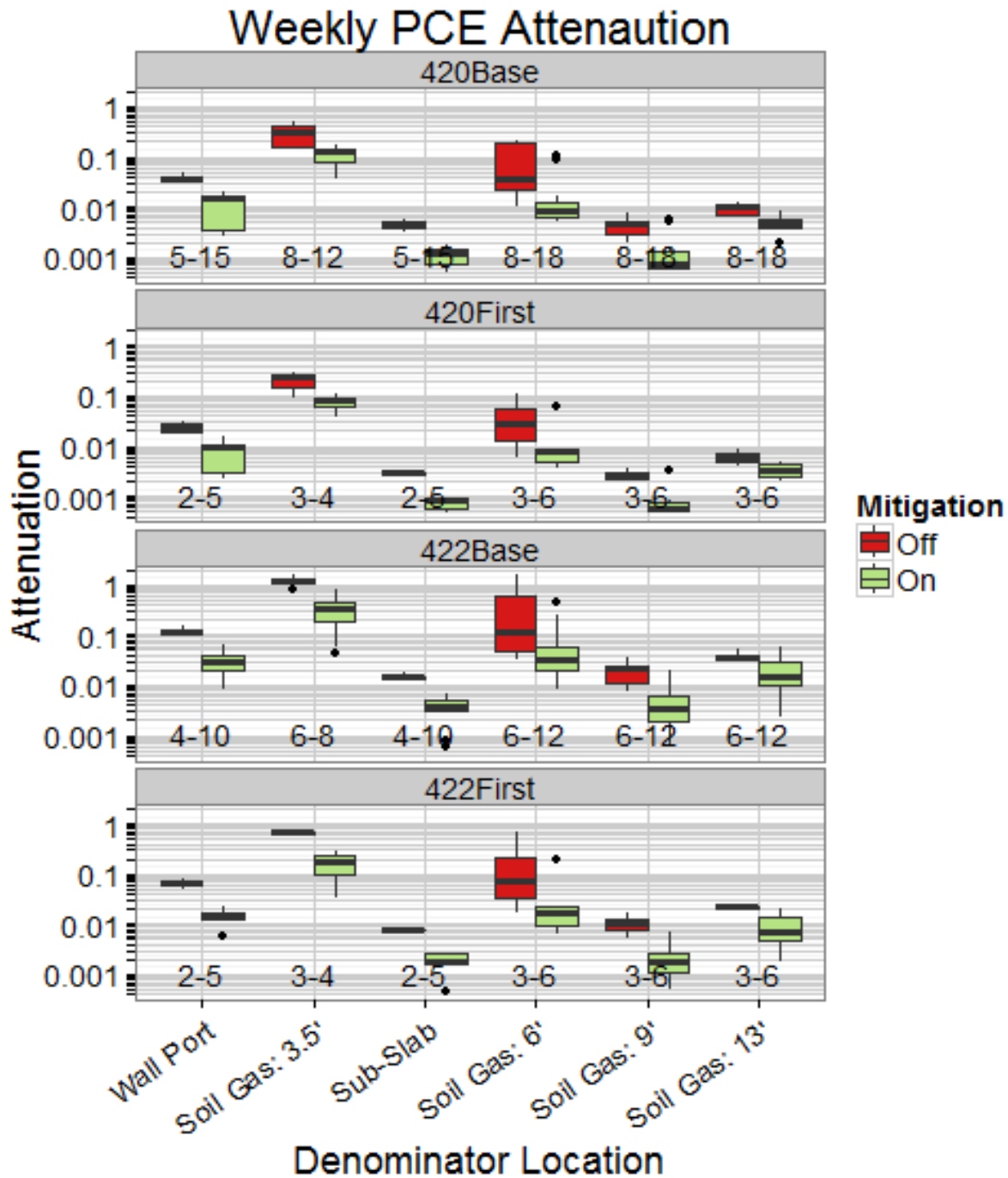


Figure 8-26. Weekly PCE attenuation.

Figures 8-27, 8-28, and 8-29 show the same effects of mitigation on chloroform as was observed for PCE: a consistent decrease in indoor air concentrations (Figure 8-27), variable impacts on the various subsurface soil gas concentrations measured (Figure 8-28), and reductions in the subsurface attenuation factors in every case examined (Figure 8-29). Compared with Figure 8-26 for PCE, Figure 8-29 does show greater variability in chloroform attenuation factors than was observed for PCE. Again, the sample size for the weekly chloroform indoor air data used to calculate the weekly attenuation factors was small,

but in this case there was a statistically significant decrease in chloroform with mitigation for the 422 basement ($p = 6e-11$) and the 422 first floor ($p = 0.004$).

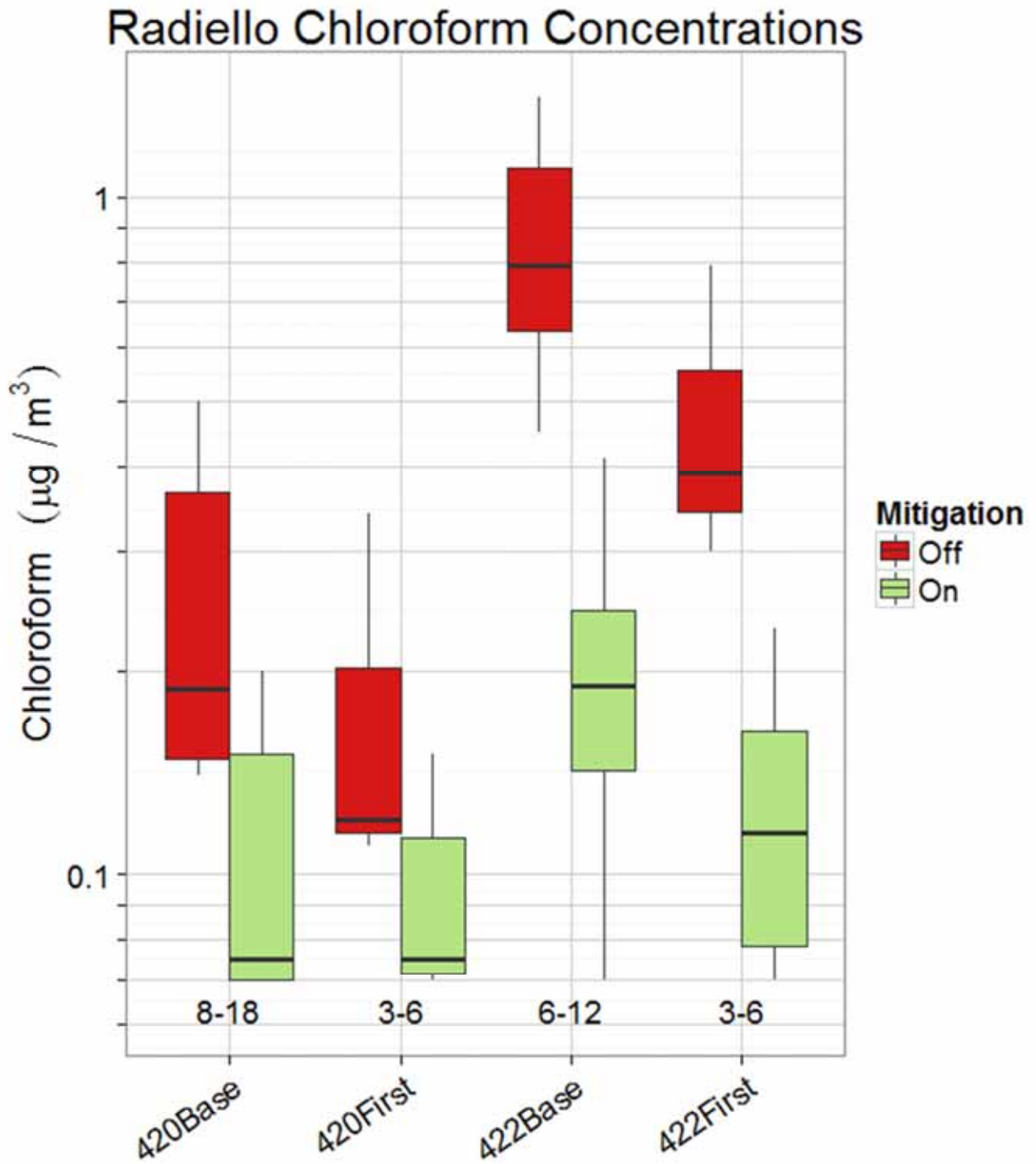


Figure 8-27. Radiello weekly indoor air chloroform concentrations.

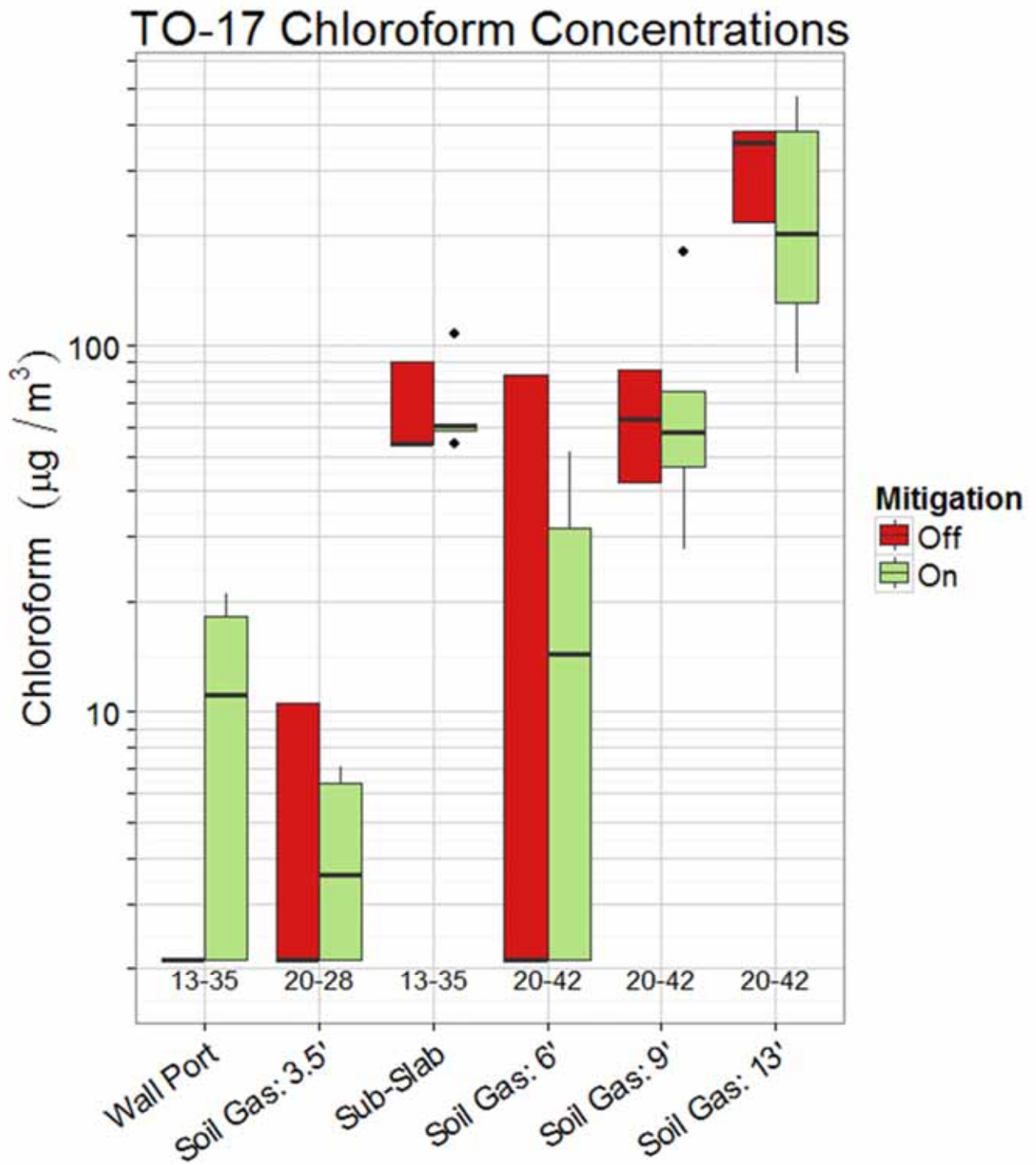


Figure 8-28. TO-17 soil gas chloroform concentrations.

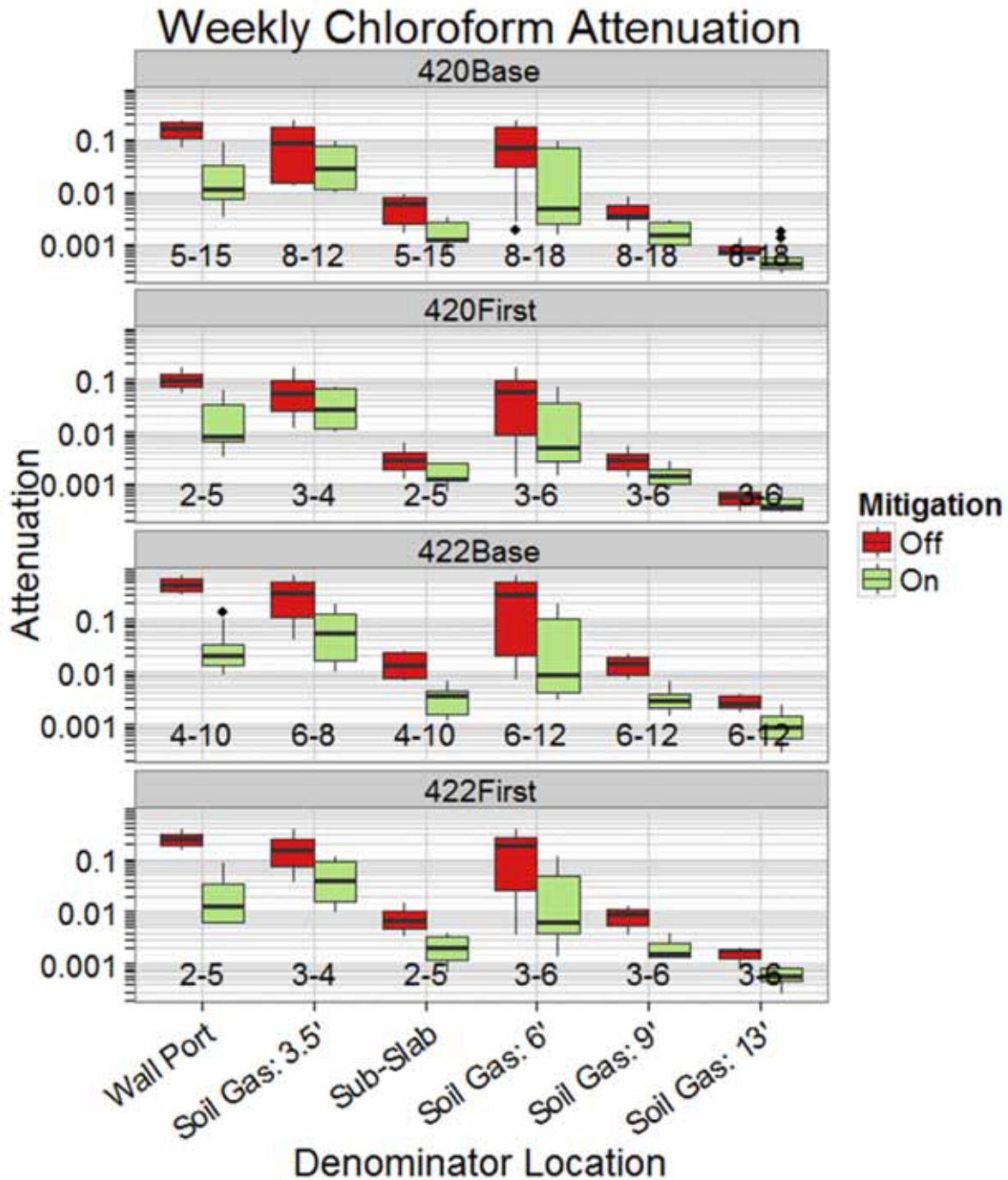


Figure 8-29. Weekly chloroform attenuation factors.

In summary, **Figure 8-30** compares the weekly attenuation of radon and the two VOCs. In general, one can see that attenuation increases with mitigation for all three compounds, with less variable results being identified for radon compared to PCE and for PCE compared to chloroform. However, the influence of the mitigation system on subslab VOC levels (**Figures 8-22, 8-25, and 8-28**) should be considered when evaluating these data as well as whether the attenuation factor is meaningful when an SSD mitigation system is on. Also, the performance of the mitigation system on VOCs at this site is not fully understood

at this point. To better understand VOC attenuation at this site, additional scrutiny of possible VOC entry routes and subslab pressure field variability is warranted, particularly in the vicinity of subsurface structures such as the sanitary sewer.

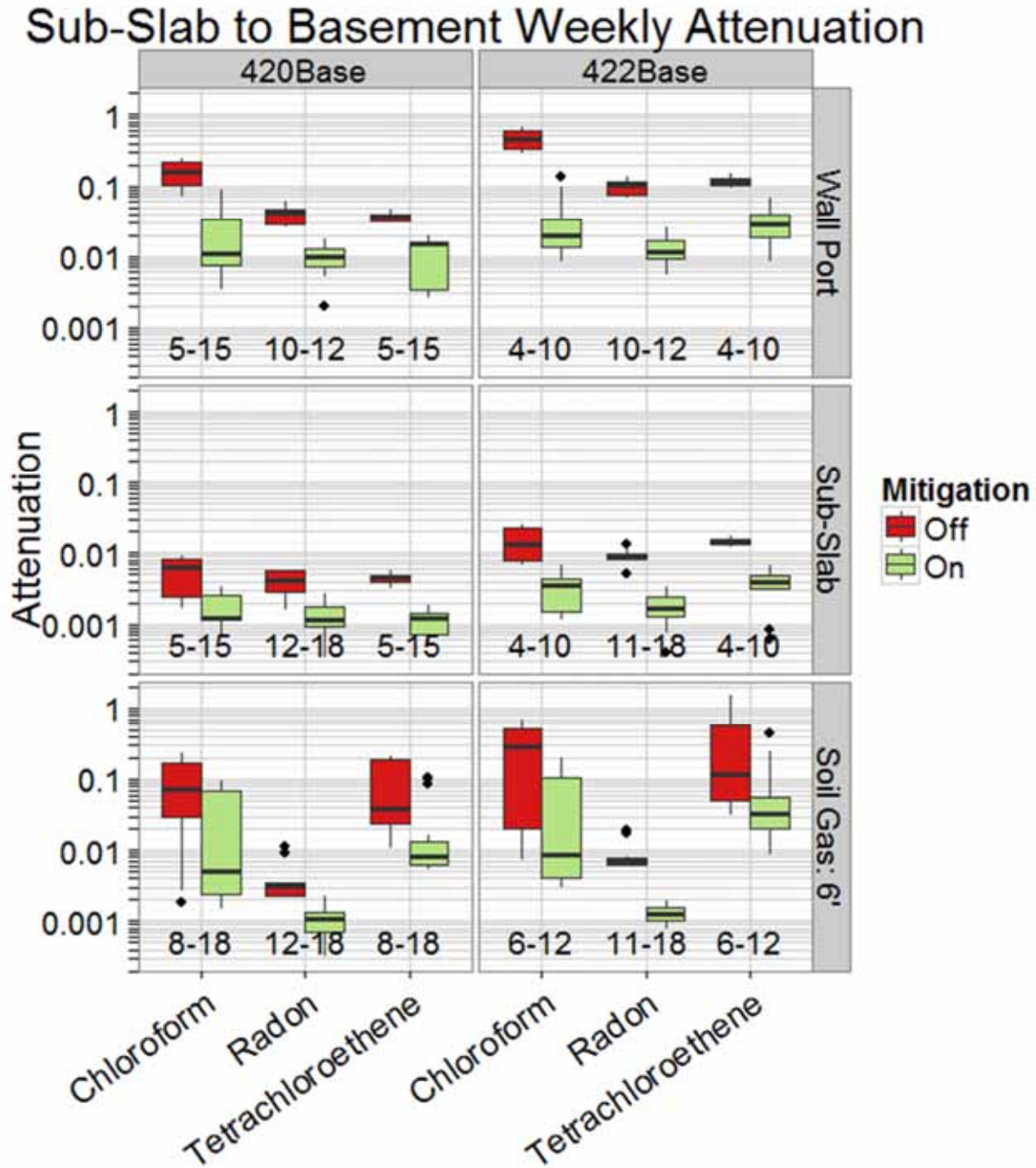


Figure 8-30. Attenuation of PCE, chloroform, and radon juxtaposed.

Table of Contents

| | | |
|-------|---|------|
| 9.0 | Results and Discussion: Determine If Observed Changes in Indoor Air Concentration of Volatile Organics of Interest are Mechanistically Attributable to Changes in Vapor Intrusion | 9-1 |
| 9.1 | Large Differential Pressures, Pressure Changes and Meteorological Factors Analysis with Mitigation Off | 9-1 |
| 9.1.1 | Temperature Effects on Differential Pressure..... | 9-1 |
| 9.1.2 | Barometric Pressure Effects on Differential Pressure..... | 9-4 |
| 9.1.3 | Precipitation Effects on Differential Pressure..... | 9-8 |
| 9.1.4 | Wind Effects on Differential Pressure | 9-10 |
| 9.1.5 | Assessment of Whether High Observed Differential Pressures Could be Artifactual | 9-16 |
| 9.1.6 | Examination of High-Resolution Time Series Data for Individual Extreme Differential Pressure Events | 9-16 |
| 9.2 | Influence of Meteorological Conditions on Indoor VOC Concentration; Mitigation Off | 9-44 |
| 9.2.1 | Temperature Effect on VOCs | 9-44 |
| 9.2.2 | Barometric Pressure Effect on VOCs | 9-47 |
| 9.2.3 | Precipitation Effects on VOCs..... | 9-47 |
| 9.2.4 | Effect of Wind on VOC Concentrations | 9-52 |
| 9.3 | Summary of Meteorological Effects on Vapor Intrusion—Evidence Presented in Sections 6 and 9..... | 9-59 |

List of Figures

| | | |
|-------|--|------|
| 9-1. | Long-term trend in subslab vs. basement differential pressure (Pa) compared with exterior temperature and the first derivative of exterior temperature (°F)..... | 9-2 |
| 9-2. | XY plot of subslab vs. basement differential pressure vs. daily low exterior temperature..... | 9-3 |
| 9-3. | XY plot of daily low exterior temperature vs. (subslab vs. basement differential pressure)..... | 9-4 |
| 9-4. | Long term pressure trends in subslab vs. basement differential pressure (Pa) compared with external barometric pressure (inches) with derivative plots. | 9-5 |
| 9-5. | XY plot of external barometric pressure vs. (422 subslab vs. basement differential pressure)..... | 9-6 |
| 9-6. | XY plot of barometric pressure drop (per hour) vs. (422 subslab vs. basement differential pressure)..... | 9-7 |
| 9-7. | Long term trends in subslab vs. basement pressure (Pa) compared to rainfall and snow depth (inches)..... | 9-8 |
| 9-8. | XY graph of total daily rainfall vs. (subslab vs. basement differential pressure)..... | 9-9 |
| 9-9. | XY graph of total snow depth (inches) vs. differential pressures (Pa). | 9-10 |
| 9-10. | Long-term trends in subslab vs. basement differential pressure (Pa) compared to maximum wind speed and average wind speed data (mph)..... | 9-11 |

Section 9—Results and Discussion: Determine If Observed Changes in Indoor Air Concentration of Volatile Organics of Interest are Mechanically Attributable to Changes in Vapor Intrusion

| | | |
|-------|---|------|
| 9-11. | Long-term trend in subslab vs. basement differential pressure (Pa) vs. wind direction parameters (change in direction, maximum direction, average direction) (degrees)..... | 9-12 |
| 9-12. | XY plot of daily high wind speed vs. (subslab vs. basement differential pressure)..... | 9-13 |
| 9-13. | XY plot of daily average wind speed vs. (subslab vs. basement differential pressure)..... | 9-14 |
| 9-14. | XY plot of wind direction effects on subslab vs. basement differential pressure (upper plot) and radon concentrations in the 422 basement (lower plot)..... | 9-15 |
| 9-15. | Extreme Event 1: subslab vs. basement differential pressure (positive difference indicates flow into the structure)..... | 9-17 |
| 9-16. | Extreme Event 2: subslab vs. basement differential pressure (positive difference indicates flow into the structure)..... | 9-18 |
| 9-17. | Extreme Event 3: subslab vs. basement differential pressure (positive difference indicates flow into the structure)..... | 9-19 |
| 9-18. | Extreme Event 4: subslab vs. basement differential pressure (positive difference indicates flow into the structure)..... | 9-20 |
| 9-19. | Extreme Event 5: subslab vs. basement differential pressure (positive difference indicates flow into the structure)..... | 9-21 |
| 9-20. | Extreme Events 6/7: subslab vs. basement differential pressure (positive difference indicates flow into the structure)..... | 9-22 |
| 9-21. | Detailed time series of unusual pressure Event 1 showing barometric pressure changes (barometric pressure in inches of Hg, differential pressure in Pa)..... | 9-23 |
| 9-22. | Detailed time series of unusual pressure Event 1 showing precipitation events (rainfall in inches, snow depth in inches, differential pressure in Pa)..... | 9-24 |
| 9-23. | Detailed time series of unusual pressure Event 2 showing barometric pressure changes (barometric pressure in inches of Hg, differential pressure in Pa)..... | 9-25 |
| 9-24. | Detailed time series of unusual pressure Event 2 showing temperature changes (differential pressure in Pa, temperature in °F)..... | 9-26 |
| 9-25. | Detailed time series of unusual pressure Event 3 showing barometric pressure changes (barometric pressure in inches of Hg, differential pressure in Pa)..... | 9-27 |
| 9-26. | Detailed time series of unusual pressure Event 3 showing temperature changes (differential pressure in Pa, temperature in °F)..... | 9-28 |
| 9-27. | Detailed time series of unusual pressure Event 3 showing wind direction variables (wind direction-related variables in degrees, differential pressure in Pa)..... | 9-29 |
| 9-28. | Detailed time series of unusual pressure Event 3 showing PCE and radon..... | 9-30 |
| 9-29. | Detailed time series of Event 4 showing wind direction variables (wind direction-related variables in degrees, differential pressure in Pa)..... | 9-32 |
| 9-30. | Detailed time series of Event 4 showing wind speed variables (wind speed variables in MPH, differential pressure in Pa)..... | 9-33 |
| 9-31. | Detailed time series of Event 4 showing temperature variables (differential pressure in Pa, temperature in °F)..... | 9-34 |
| 9-32. | Detailed time series of Event 5 showing precipitation event (rainfall in inches, snow depth in inches, differential pressure in Pa)..... | 9-35 |

Section 9—Results and Discussion: Determine If Observed Changes in Indoor Air Concentration of Volatile Organics of Interest are Mechanically Attributable to Changes in Vapor Intrusion

| | | |
|-------|--|------|
| 9-33. | Detailed time series of Event 5 showing wind speed variables (wind direction-related variables in degrees, differential pressure in Pa). | 9-36 |
| 9-34. | Detailed time series of Event 5 showing wind direction variables. | 9-37 |
| 9-35. | Detailed time series of Event 5 showing temperature variables (differential pressure in Pa, temperature in °F). | 9-38 |
| 9-36. | Detailed time series of Event 5 showing PCE and radon. | 9-39 |
| 9-37. | Detailed time series of Event 6/7 showing barometric pressure (barometric pressure in inches of Hg, differential pressure in Pa). | 9-40 |
| 9-38. | Detailed time series of Event 6/7 showing precipitation (rainfall in inches, snow depth in inches, differential pressure in Pa). | 9-41 |
| 9-39. | Detailed time series of Event 6/7 showing wind speed variables (wind direction-related variables in degrees, differential pressure in Pa). | 9-42 |
| 9-40. | Detailed time series of Event 6/7 showing wind direction variables (wind direction-related variables in degrees, differential pressure in Pa). | 9-43 |
| 9-41. | Detailed time series of Event 6/7 showing radon and PCE. | 9-44 |
| 9-42. | XY graph of total heating degree days per week vs. weekly PCE concentration (Radiello data). | 9-45 |
| 9-43. | XY graph of heating degree days vs. chloroform concentration (weekly Radiello data). | 9-46 |
| 9-44. | XY graph of average weekly barometric pressure vs. PCE concentration. | 9-47 |
| 9-45. | XY graph of weekly average snow depth vs. PCE concentration. | 9-48 |
| 9-46. | XY graph of weekly average snow depth vs. chloroform concentration. | 9-49 |
| 9-47. | XY graph of weekly average snow depth vs. radon concentration. | 9-50 |
| 9-48. | XY graph of total weekly rainfall vs. PCE concentration in indoor air. | 9-51 |
| 9-49. | XY graph of total weekly rainfall vs. chloroform concentration in indoor air. | 9-52 |
| 9-50. | XY graph of wind direction vs. PCE concentration in indoor air in 422 basement. | 9-53 |
| 9-51. | XY graph of wind direction vs. chloroform concentration in indoor air in 422 basement. | 9-54 |
| 9-52. | XY graph of wind direction vs. radon concentration in indoor air in 422 basement. | 9-55 |
| 9-53. | Modeled effect of building wind loads on ground surface and subslab gauge pressure distribution (adapted from U.S. EPA, 2012d). | 9-56 |
| 9-54. | Modeled effect of building wind load on subslab soil vapor distribution for recalcitrant and aerobically biodegradable VOCs (adapted from U.S. EPA, 2012d). | 9-57 |
| 9-55. | XY graph of wind speed vs. PCE concentration in indoor air in 422 basement. | 9-58 |
| 9-56. | XY graph of wind speed vs. chloroform concentration in indoor air in 422 basement. | 9-59 |

List of Tables

| | | |
|------|---|------|
| 9-1. | Summary of Qualitative Lines of Evidence for Meteorological Factors Influencing Vapor Intrusion in This Study. | 9-60 |
|------|---|------|

Section 9—Results and Discussion: Determine If Observed Changes in Indoor Air Concentration of Volatile Organics of Interest are Mechanically Attributable to Changes in Vapor Intrusion

9.0 Results and Discussion: Determine If Observed Changes in Indoor Air Concentration of Volatile Organics of Interest are Mechanistically Attributable to Changes in Vapor Intrusion

9.1 Large Differential Pressures, Pressure Changes and Meteorological Factors Analysis with Mitigation Off

Significant vapor intrusion into the indoor air is normally attributable to an advective driving force across the building envelope—a differential pressure. For this research effort, we gathered a larger high temporal resolution data set on these differential pressures than on indoor air concentrations of VOCs.¹⁹ Thus, we performed a focused analysis of the events surrounding the periods where unusual differential pressure, especially subslab to indoor air differential, pressure was evident using the following criteria:

- great variation (swings of more than 5 Pa in a short time period) and
- the strongest driving forces pushing subslab vapors into the building (> 10 Pa).

A change of 5 Pa is generally seen as the maximum change expected in residential situations (U.S. EPA, 1993; Environmental Quality Management, 2004; U.S. EPA, 2012d; Yao, 2010). However, there are some reports of larger pressure fluctuations of up to 20 Pa in the literature (Environmental Quality Management, 2004; Lutes, 2010).

We identified seven such extreme variation events over nearly 2 years of data collection (typical time resolution of 14 minutes) and reviewed them to determine if they could have been artifactual or if they had the hallmarks of real events. Real causative factors that were examined included extremes in any of these metrological parameters:

- wind velocity gusts
- abrupt significant changes in wind direction (approaching 180 degrees)
- barometric pressure changes
- sudden changes in temperature (outside)
- snowfalls
- rain events.

We used multiple graphing approaches to examine this data, including:

- long time-scale stacked graphs comparing differential pressure trends with time to those of meteorological parameters
- XY graphs of meteorological parameters vs. differential pressure (which were done on the data after aggregating to 1-day time resolution)
- short time-scale stacked graphs comparing differential pressures with time during individual events to meteorological parameters.

9.1.1 Temperature Effects on Differential Pressure

The seven events are clearly visible in the subslab vs. basement differential pressure plot (**Figure 9-1**). They appear to not be distributed randomly over time but to be clustered in midwinter and to occur with much greater frequency on the days with the lowest daily low temperatures (**Figure 9-2**). A related trend

¹⁹In statistical terms, differential pressure can be viewed as an intermediary variable, one that is part of a causal pathway linking a predictor variable such as temperature with an outcome such as indoor air concentration.

is that these high differential pressures occurred on the days that were the coldest overall as measured by heating degree days (Figure 9-3). The occurrence of strong driving forces into the building during cold weather is likely mechanistically related to the stack effect. More rarely, however, a strong differential pressure pushing out of the building was also observed in the daily average differential pressure.²⁰ However, not all low-temperature days exhibited strong differential pressure driving forces on average, suggesting that other meteorological parameters may also be important.

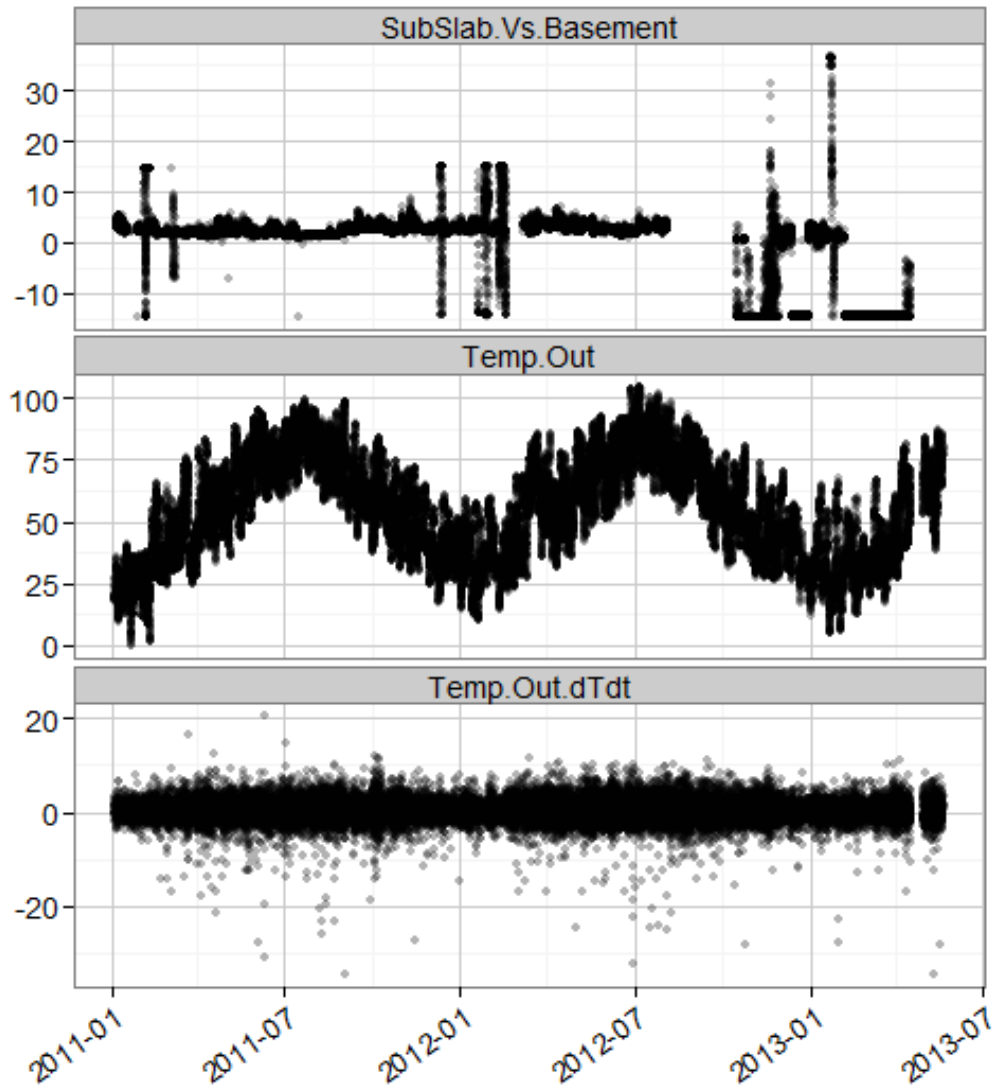


Figure 9-1. Long-term trend in subslab vs. basement differential pressure (Pa) compared with exterior temperature and the first derivative of exterior temperature (°F).

²⁰The meteorological data were examined, but no consistent common factor could be discerned to explain the 4 days with an average differential pressure out of the structure of more than -2Pa : 2/6/11, 2/17/12, 1/30/12, and 1/26/13. Nor do those days stand out as unusual in the AlphaGUARD radon data set.

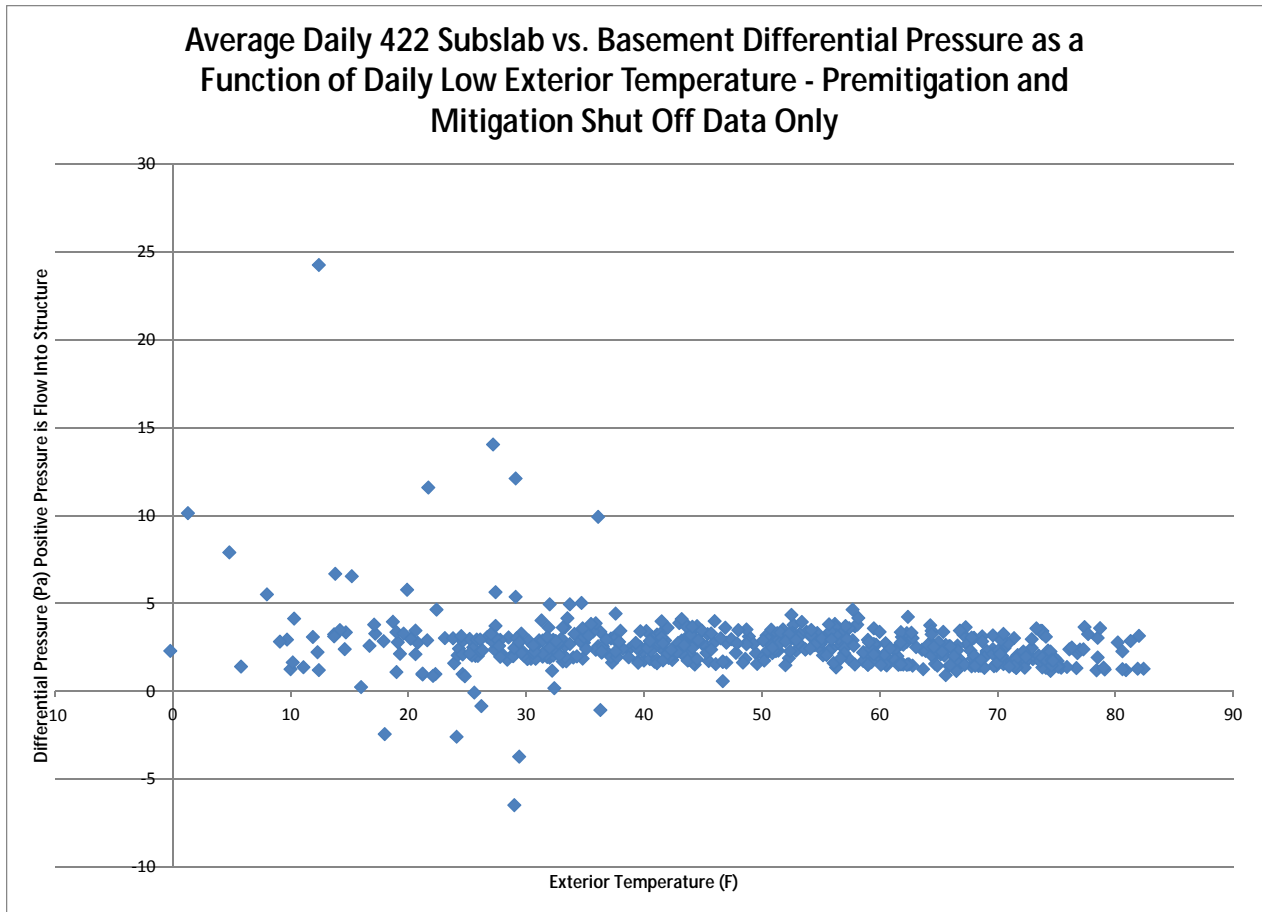


Figure 9-2. XY plot of subslab vs. basement differential pressure vs. daily low exterior temperature.

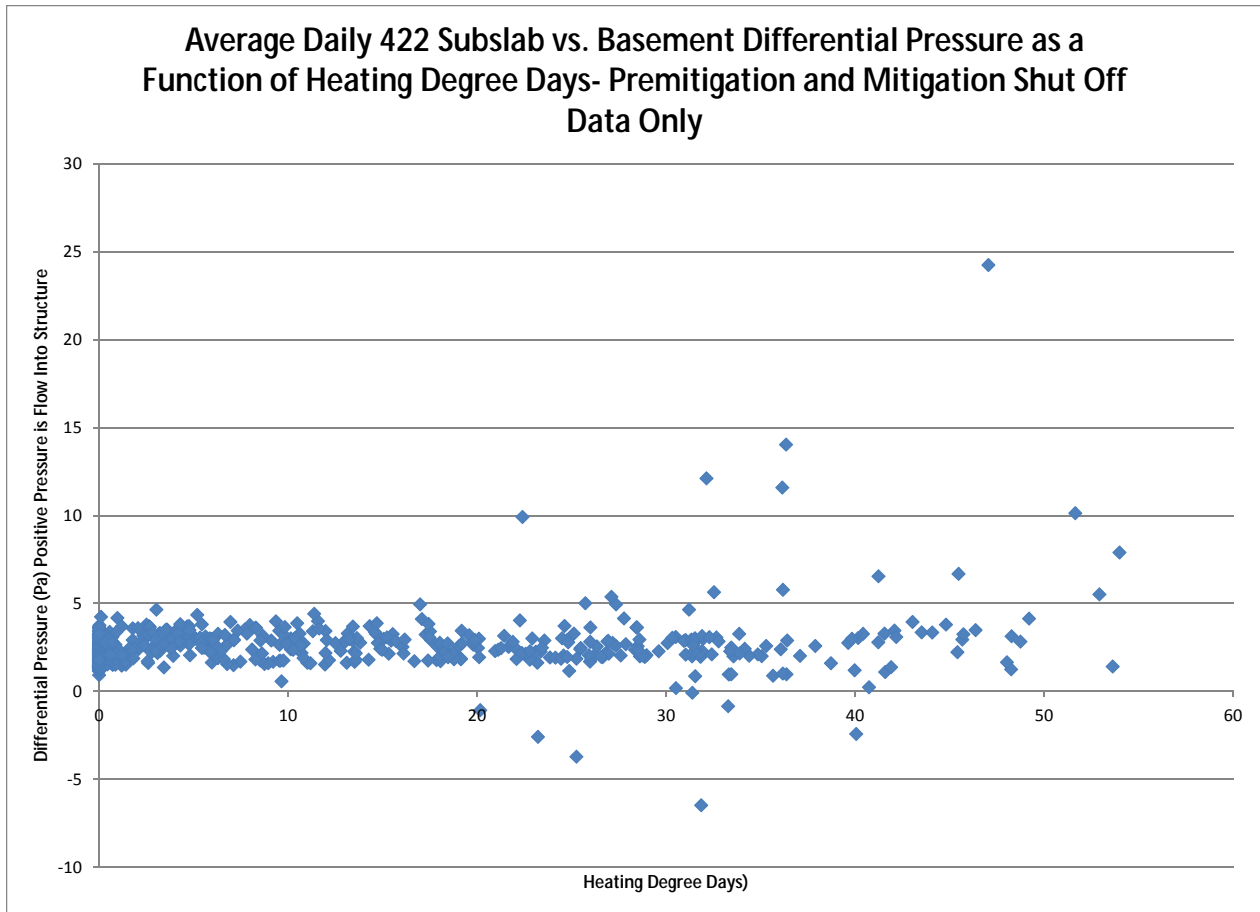


Figure 9-3. XY plot of daily low exterior temperature vs. (subslab vs. basement differential pressure).

9.1.2 Barometric Pressure Effects on Differential Pressure

The greatest degree of barometric pressure variation was observed in winter (Figure 9-4). However, on a scale of days, extreme differential pressures occur under a variety of barometric pressure conditions (Figure 9-5). It might be expected that these extreme differential pressure events would be related to the rate of barometric pressure change, but this did not appear to be the case (Figure 9-6).

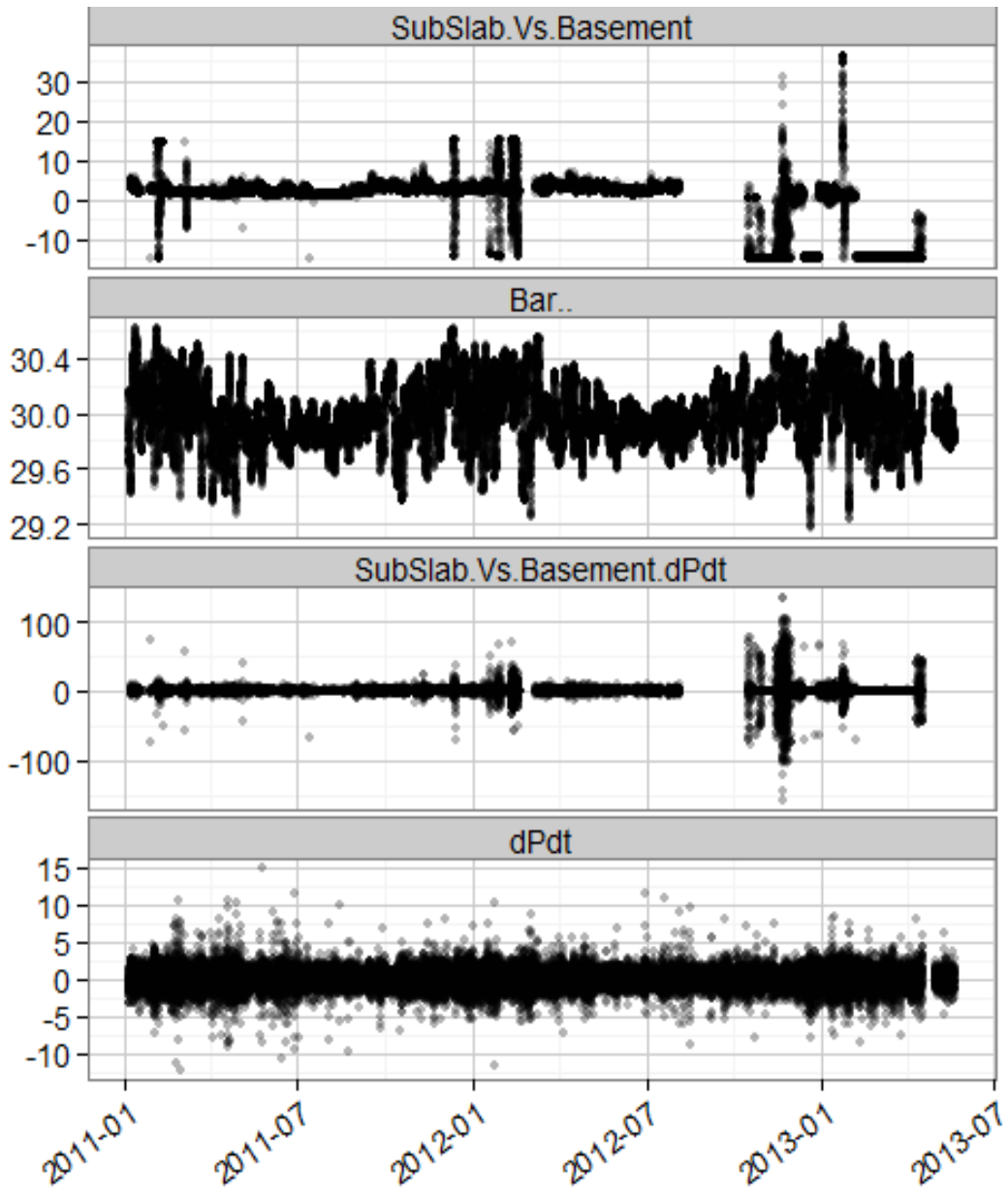


Figure 9-4. Long term pressure trends in subslab vs. basement differential pressure (Pa) compared with external barometric pressure (inches) with derivative plots.

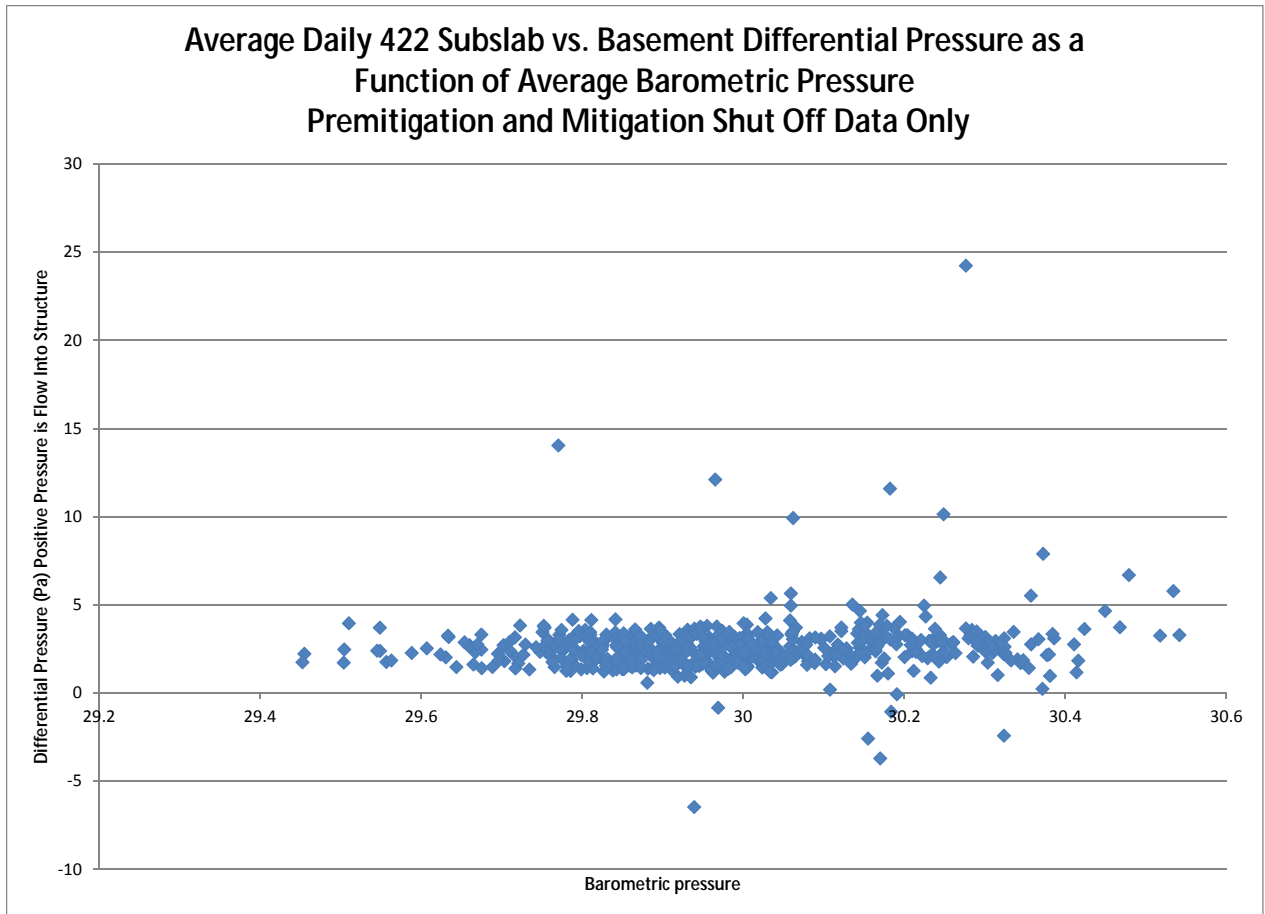


Figure 9-5. XY plot of external barometric pressure vs. (422 subslab vs. basement differential pressure).

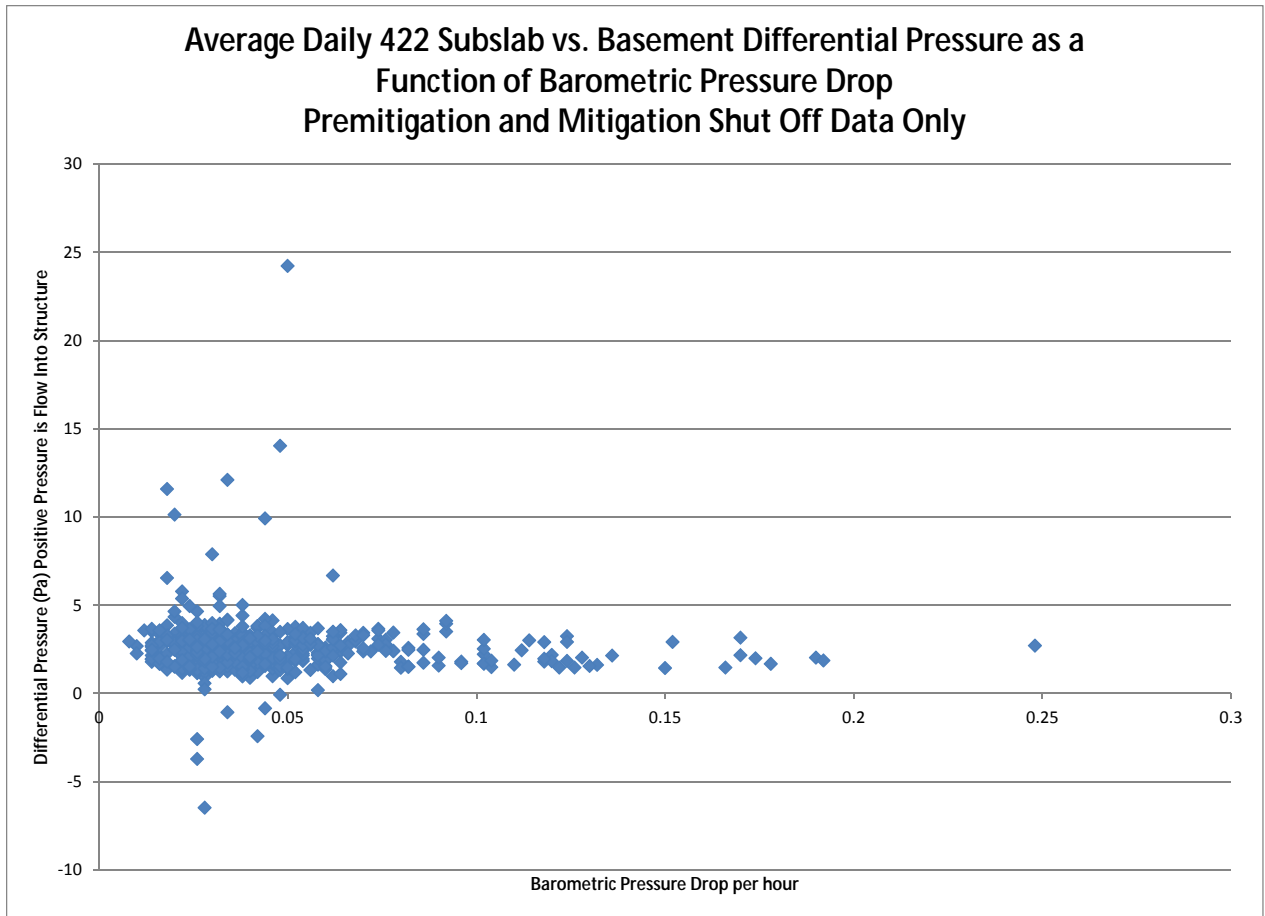


Figure 9-6. XY plot of barometric pressure drop (per hour) against 422 subslab vs. basement differential pressure.

9.1.3 Precipitation Effects on Differential Pressure

There was no apparent relationship between rain events and the extreme differential pressure events. (Figures 9-7 and 9-8). There was no apparent relationship between average differential pressure and snow depth (Figure 9-9) either.

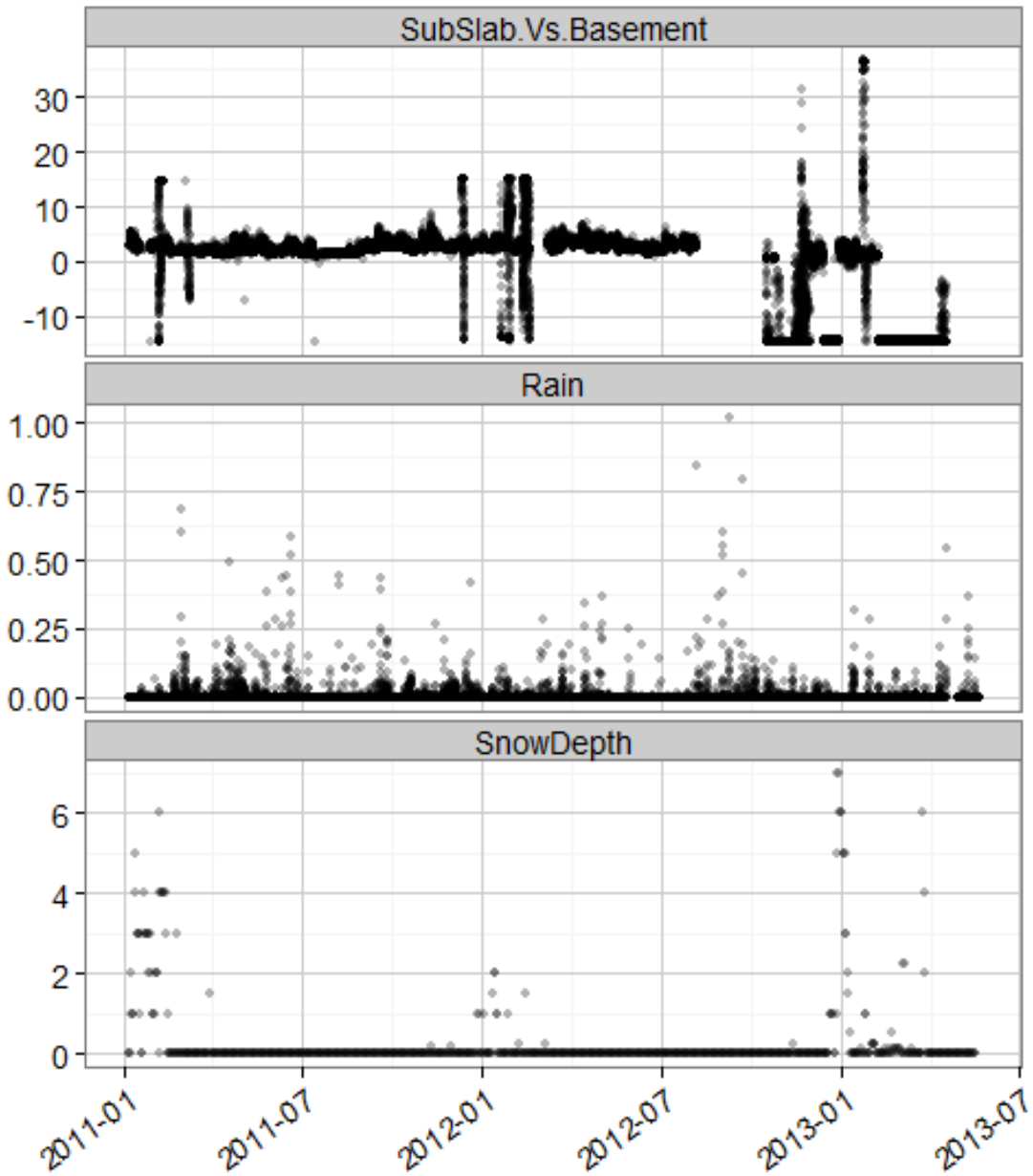


Figure 9-7. Long term trends in subslab vs. basement pressure (Pa) compared to rainfall and snow depth (inches).

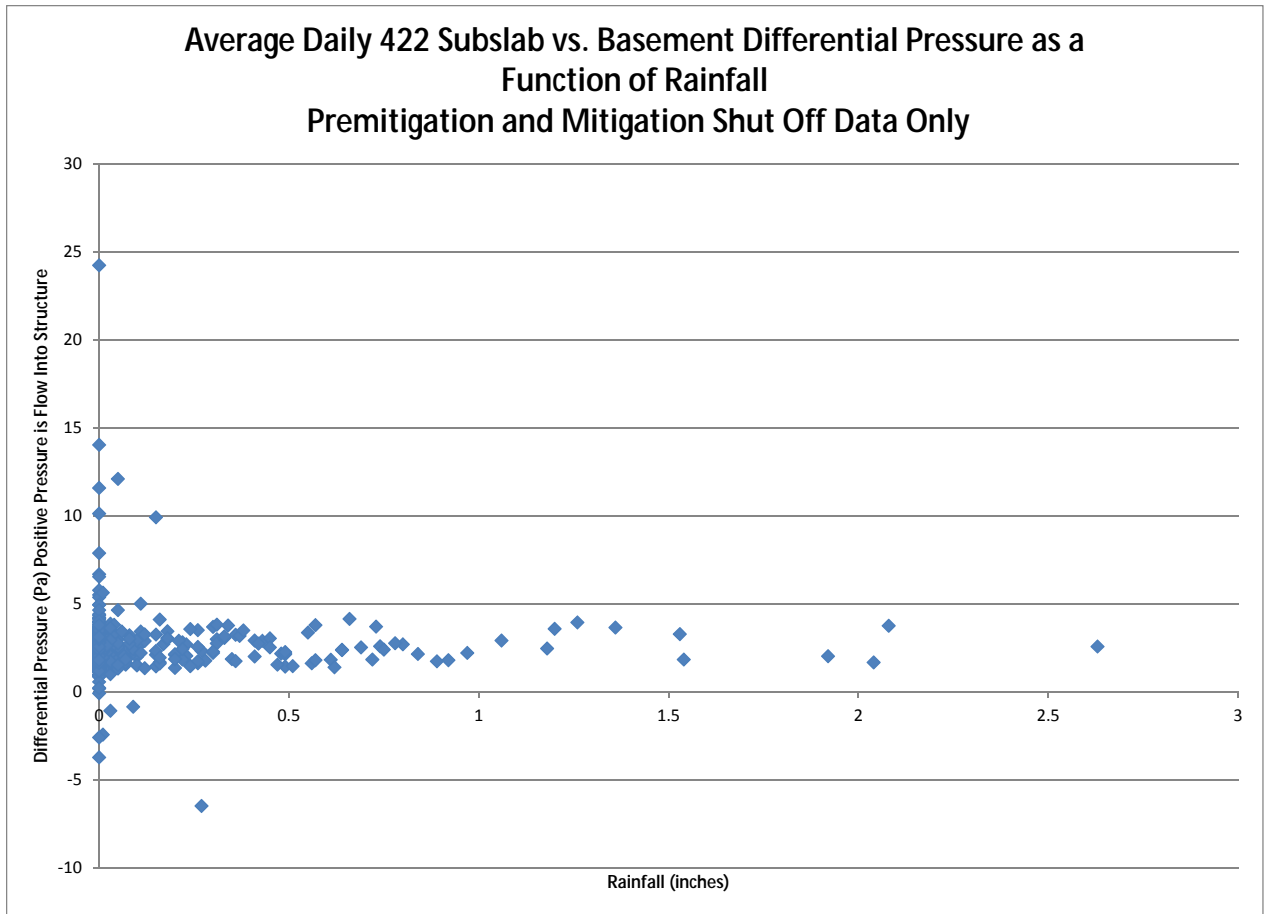


Figure 9-8. XY graph of total daily rainfall against subslab vs. basement differential pressure

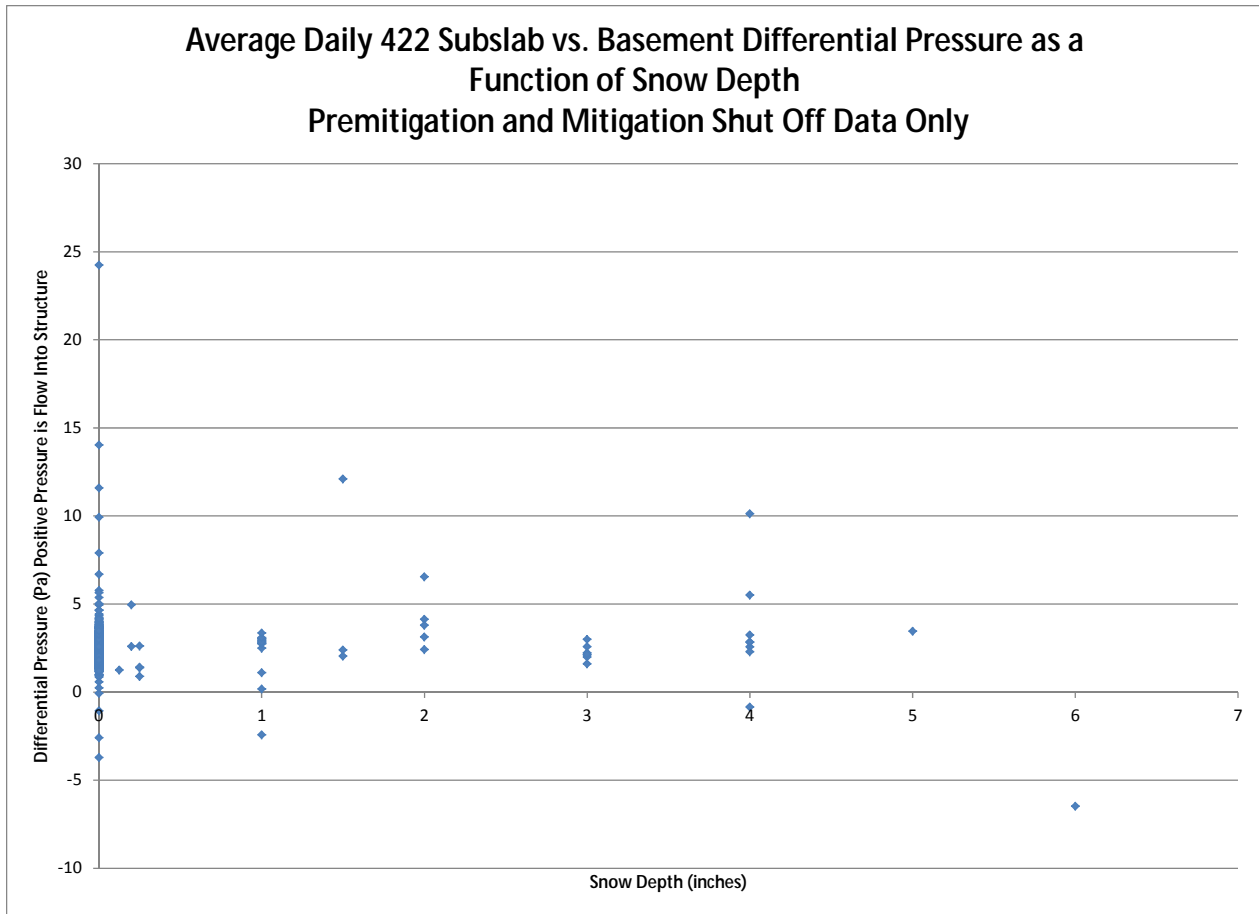


Figure 9-9. XY graph of total snow depth (inches) against differential pressures (Pa).

9.1.4 Wind Effects on Differential Pressure

Based on the long-term time series, it is clear that winter is when these large differential pressure swings occur, which is also the season when the highest wind speeds are experienced (Figure 9-10). When the differential pressure time series was plotted against the wind direction-related time series (Figures 9-11 and 9-14), the highest differential pressures are associated with wind directions between 220 and 320 degrees. Surprisingly, the high differential pressure days appear to occur with moderate average wind speeds and minimal values for the daily high wind speed (Figures 9-12 and 9-13). The clearest relationship on a scale of days, however, is when high differential pressures that are created by average winds from 220 to 320 degrees (roughly SW to NW) draw vapors into the building.

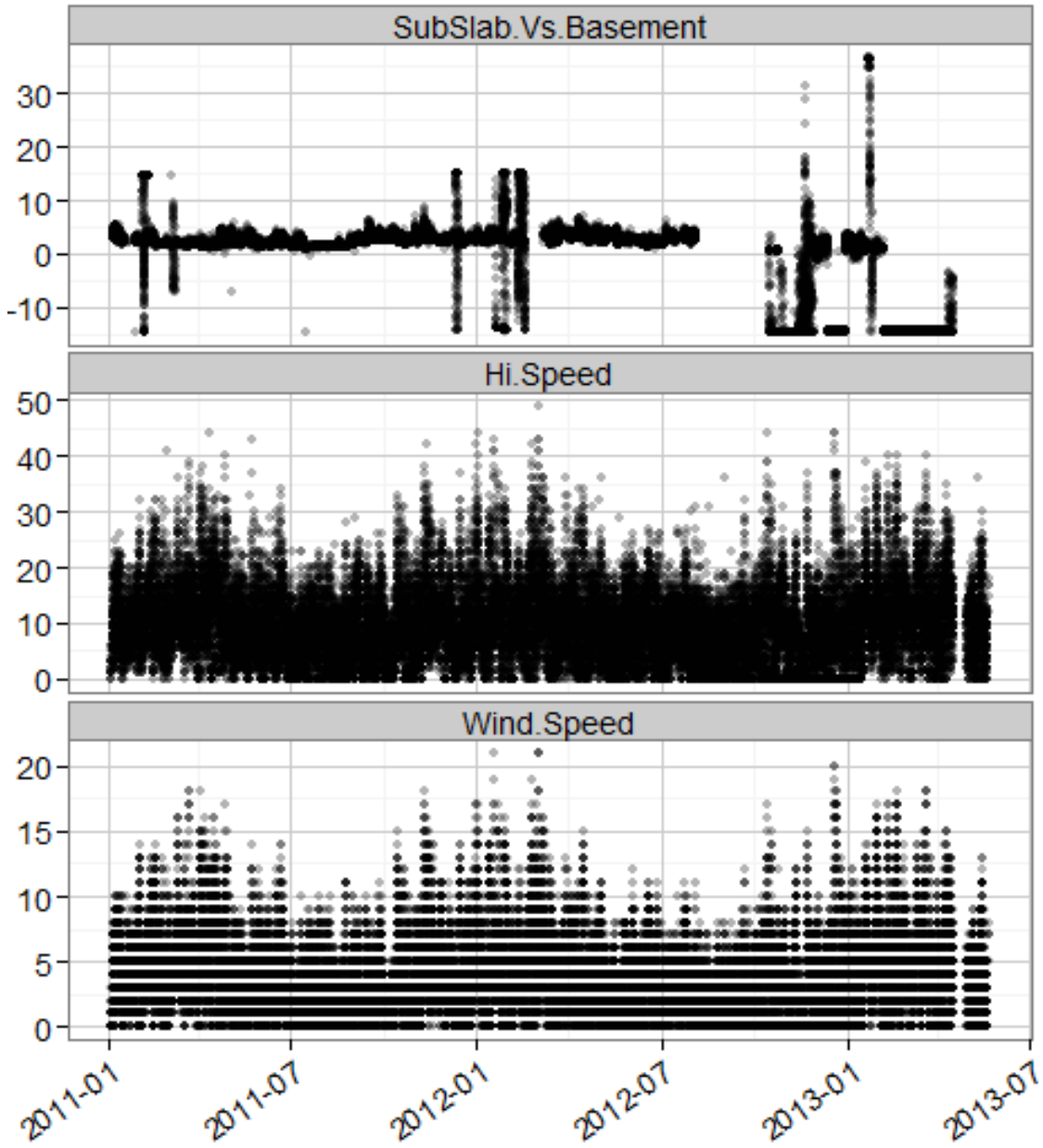


Figure 9-10. Long-term trends in subslab against basement differential pressure (Pa) compared to maximum wind speed and average wind speed data (mph).

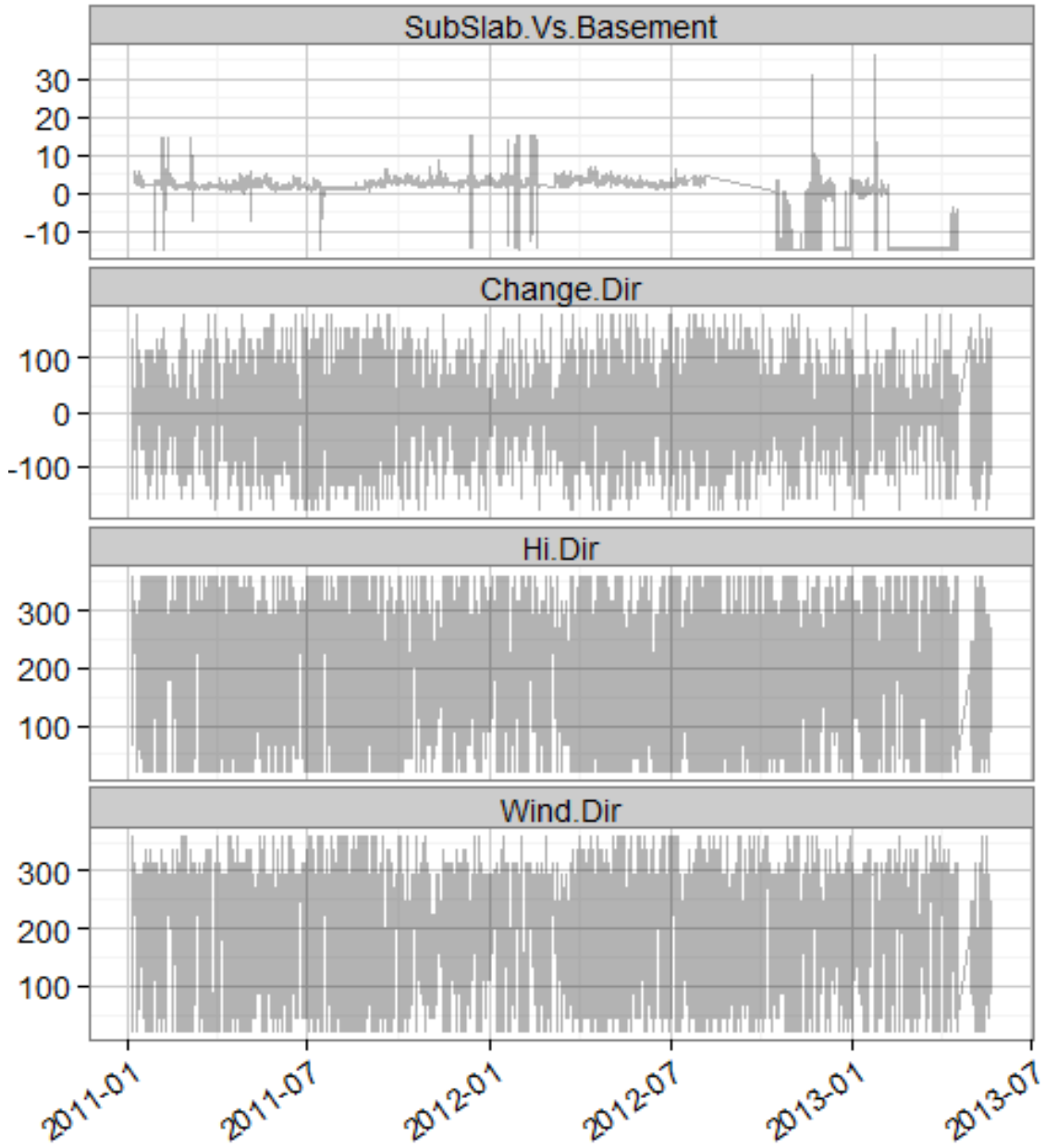


Figure 9-11. Long-term trend in subslab vs. basement differential pressure (Pa) vs. wind direction parameters (change in direction, maximum direction, average direction) (degrees).

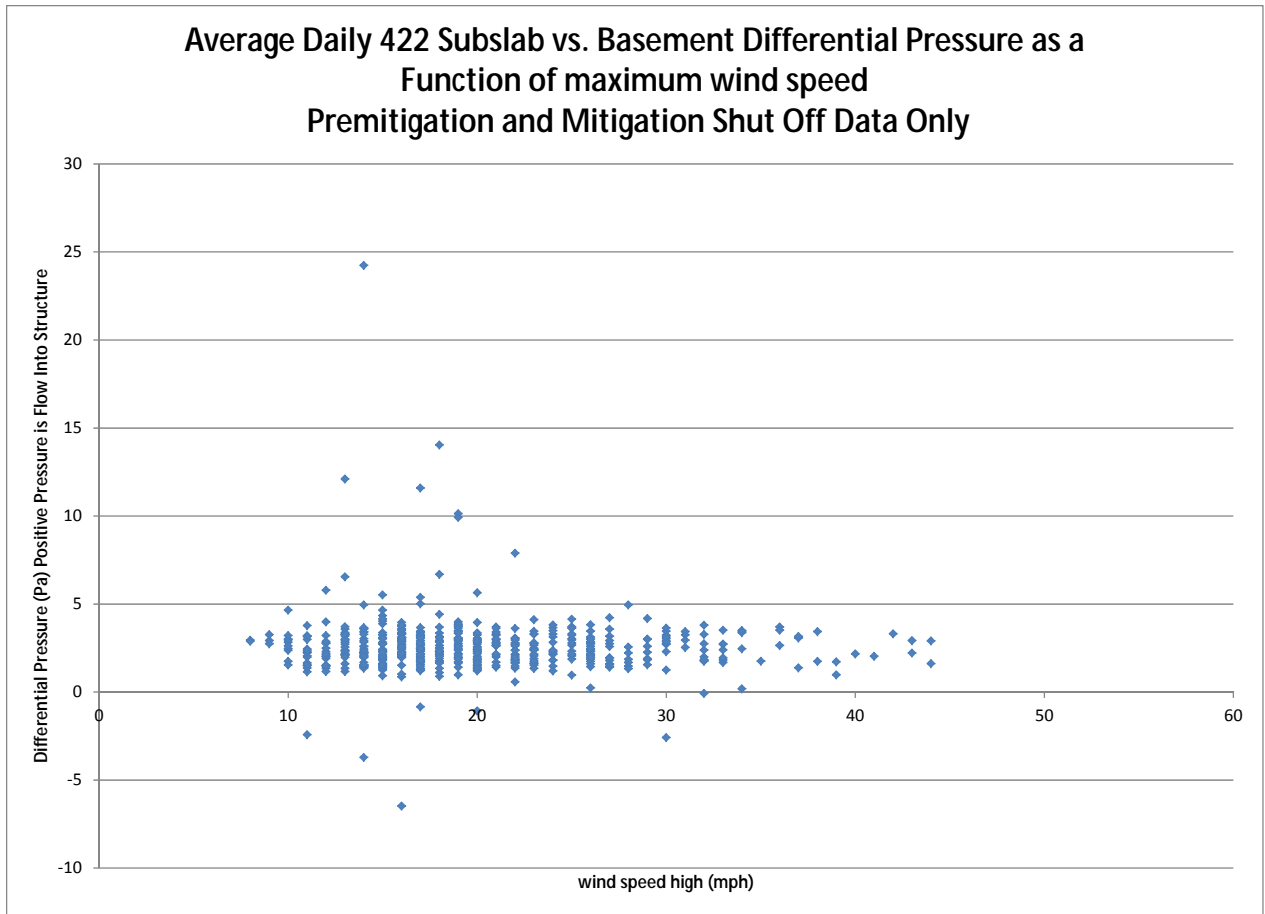


Figure 9-12. XY plot of daily high wind speed against subslab vs. basement differential pressure.

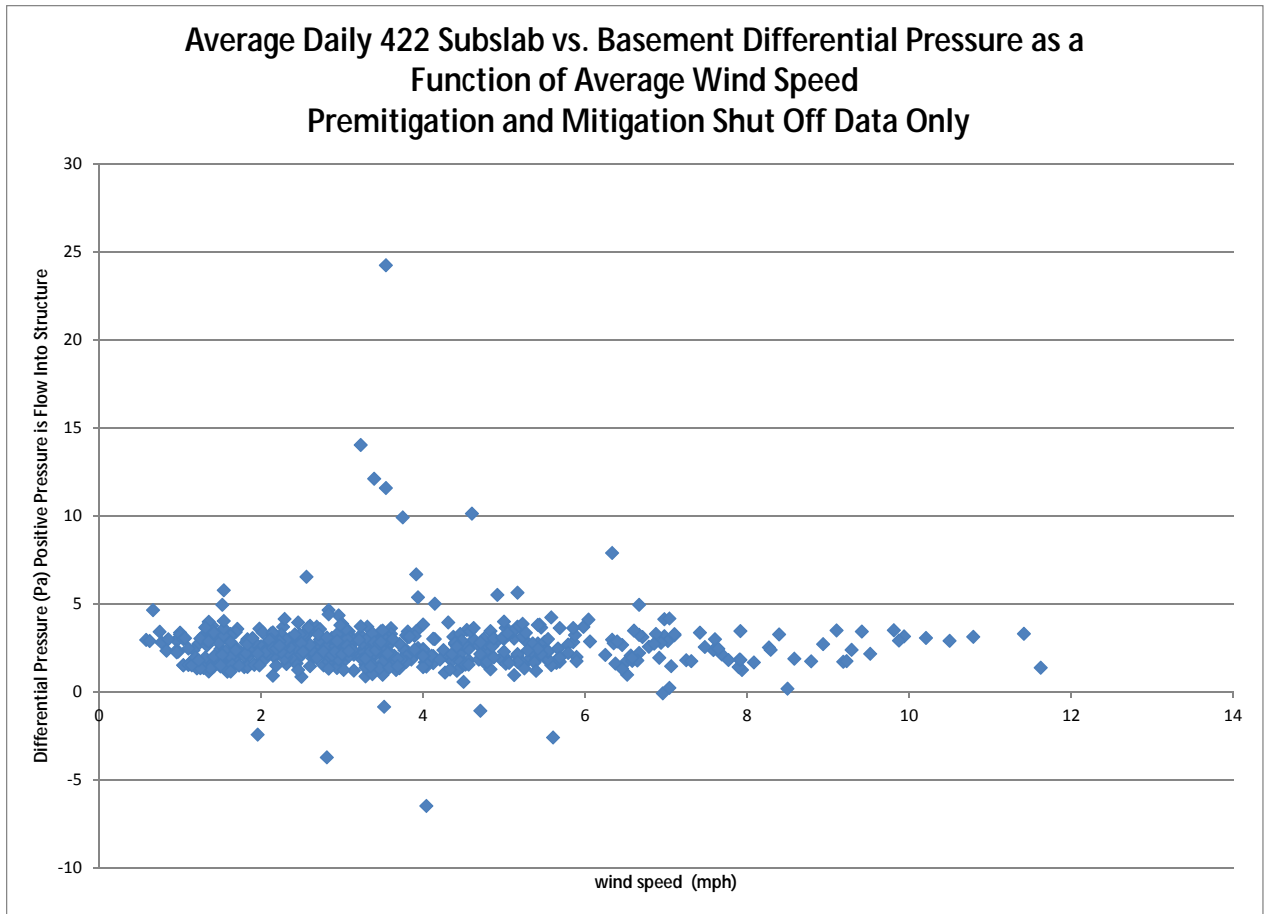


Figure 9-13. XY plot of daily average wind speed against subslab vs. basement differential pressure.

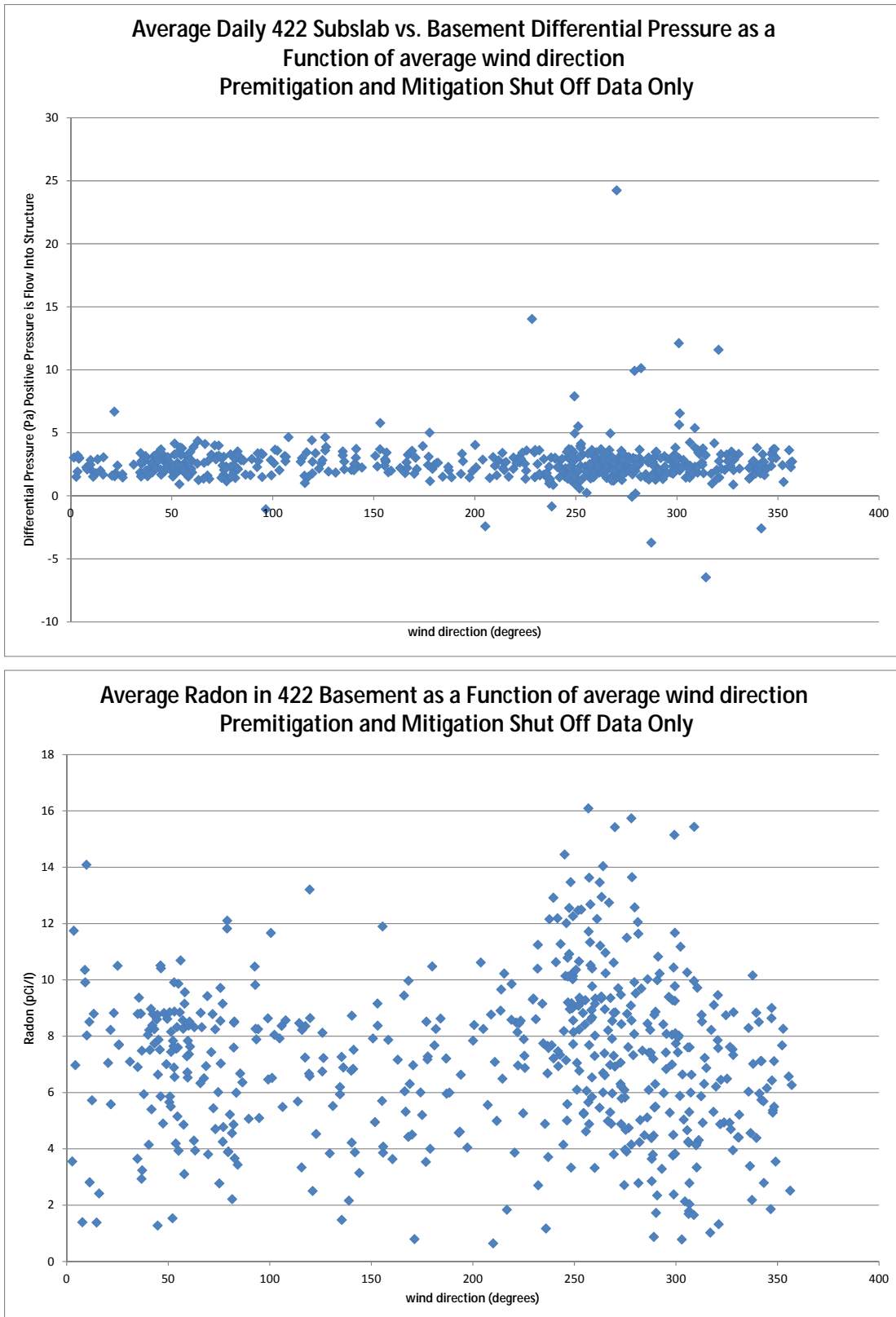


Figure 9-14. XY plot of wind direction effects on subslab vs. basement differential pressure (upper plot) and radon concentrations in the 422 basement (lower plot).

9.1.5 Assessment of Whether High Observed Differential Pressures Could be Artificial

We examined multiple lines of evidence to determine if these differential pressures could be artificial:

- The association between the extreme differential pressures and particular temperature ranges and wind directions discussed above suggests that they are real phenomenon potentially caused by meteorological events.
- The occurrence of these pressure swing events in three winters and the absence in intervening summers would have been unlikely if they were due to an instrument failure.
- The lack of outliers in some of the other meteorological data sets occurring at the same time as the very high/changeable differential pressures tends to eliminate one possible cause of artificial data—power fluctuations or lightning strikes—because all of the instrumentation is located in one room and shares a common building power supply.
- The lack of extreme values in the first derivative of the differential pressure (see **Figure 9-4**) also suggests that these results are not artificial, because an artifact caused by a discrete event (for example, a technician stepping on or tripping over a hose of the differential pressure instrument) should be evidenced by an extremely high rate of change in the differential pressure.
- When examined in detail, the pattern of the data points taken every 14 minutes shows a continuous increase or decrease for 10 or more successive measurements. This would not be characteristic of either random noise or a discrete, inadvertently human-caused event.
- We focused our review presented in this section on extremes that occurred in the time period before the mitigation system was installed, although some extreme events did occur that were not fully managed by the mitigation system. As an additional step to determine if these extreme events were artificial, we reviewed their duration and time of occurrence. We reasoned that hypothetical artifacts caused by human action should be short in duration and occur primarily during regular on-site working hours. Artifacts caused by power system disruptions or spikes should also be of short duration. As discussed in the sections that follow, many of these events extend over multiple days, which suggests a physical as opposed to artificial explanation.
- As discussed in Section 5.1.2, a separate, handheld differential pressure instrument was also used to make some observations. On 2 days, fluctuations of subslab:interior differential pressure of >0.28 inches of water column (70 Pascals) were observed with that instrument.

These lines of evidence taken together strongly suggest that these extreme pressure events are real physical phenomena.

9.1.6 Examination of High-Resolution Time Series Data for Individual Extreme Differential Pressure Events

Since:

- we concluded in Section 9.1.5 that these extreme pressure events were a real physical phenomena
- we expect from theory that high differential pressures toward the structure will lead to high vapor intrusion flux and
- we expect from theory that large changes in differential pressure if sustained over a period of hours or days should be associated with large changes in indoor air concentrations
- we sought to understand the conditions under which these extreme differential pressure events occurred.

The first extreme event lasts at least 3 days, from Friday February 4 at approximately 4 PM to approximately 1 PM on Monday February 7, 2011 (**Figure 9-15**). During that period, two pressure

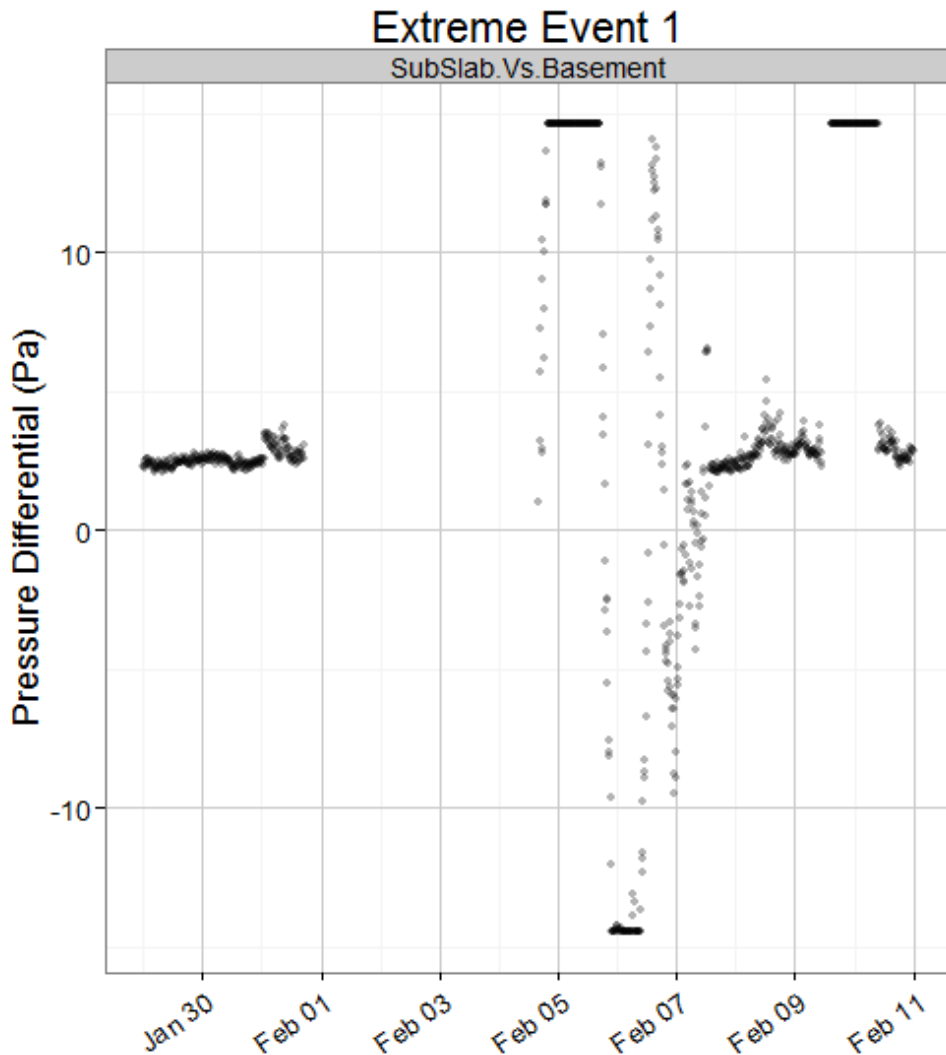


Figure 9-15. Extreme Event 1: subslab vs. basement differential pressure (positive difference indicates flow into the structure).

maximums and two pressure minimums were observed with the first maximum and first minimum showing evidence that the pressure sensor had reached or exceeded its maximum design range (-15 Pa to 15 Pa) for a sustained period (for example, a pressure maximum that included 92 successive data points over approximately 21 hours). The second maximum and second minimum are much more narrow peaks. The exact start time of this event is uncertain because of missing data, perhaps related to the ice storm that occurred on February 1, 2011. During much of the time period of this event (the weekend of February 5 and 6), we have no record of staff working at the facility, suggesting that human causes for the extreme pressures are unlikely.

The second extreme event lasted fewer than 2 days, from the evening of Monday March 7 to the afternoon of Tuesday March 8 (**Figure 9-16**). This was a period of intensive on-site work with staff working on site about 12 hours a day, which suggested some possibility of an association between the on-site work and the pressure observations. However as discussed in Section 9.1.5, because similar differential pressure events occurred during time periods when the site was not occupied, and human activities were more likely to have caused brief pressure fluctuations rather than long-term sustained differentials, we do not believe that site work was the likely cause. The end of this extreme event record is

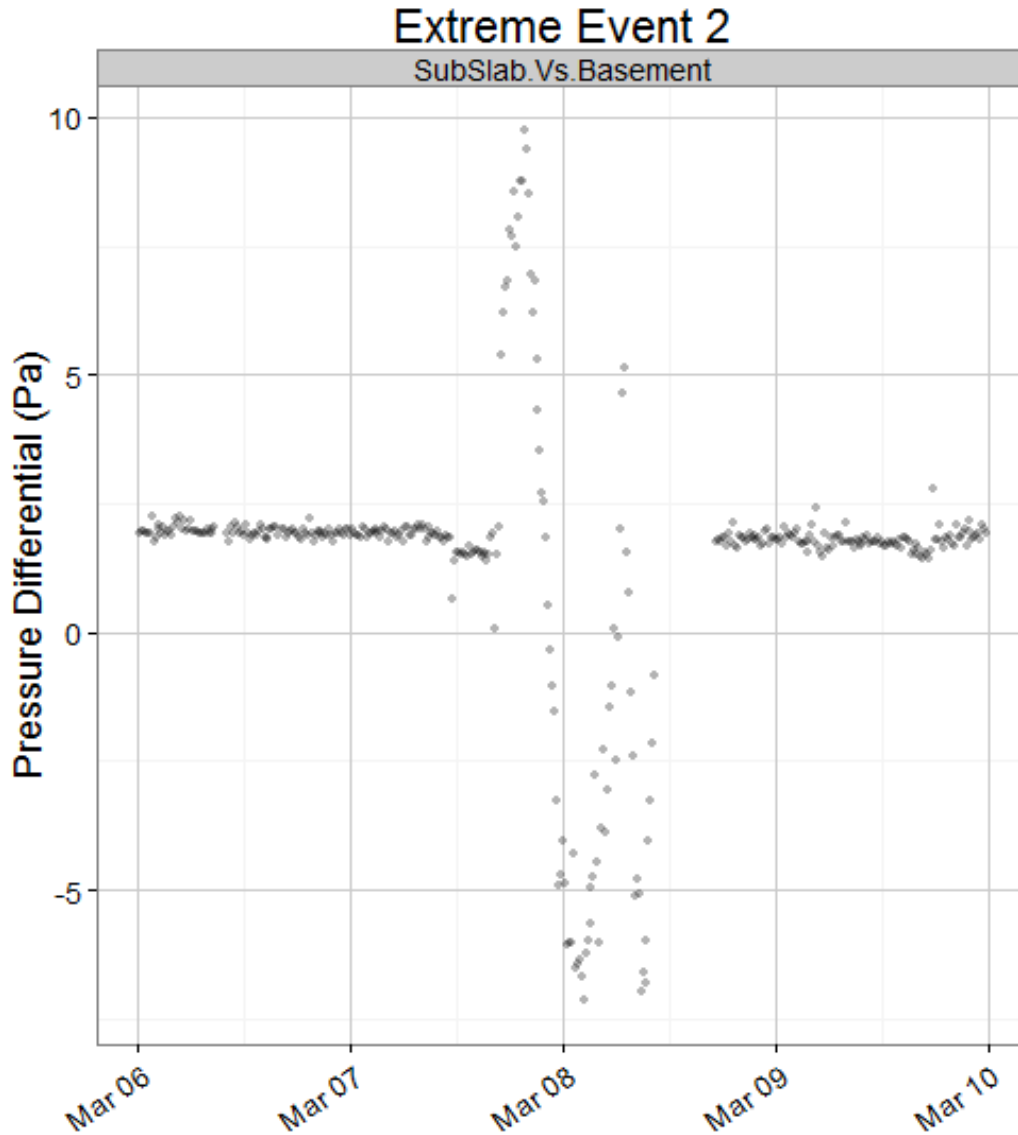


Figure 9-16. Extreme Event 2: subslab vs. basement differential pressure (positive difference indicates flow into the structure).

truncated by a manual disconnection of this pressure sensor on March 8, after which pressures returned to baseline. Such disconnection events would be expected to have caused only a momentary disturbance in the measured pressures, and we removed their influence from the pressure record by deleting rows of data. While this event truncates the data set, it is not expected to change the reliability of the data reported.

The third extreme event (**Figure 9-17**) happened over about 4 days, from Sunday December 11 to Wednesday December 14, 2011. This was also a period of intensive site work, approximately 12 hours per day. During this period, a sewer construction crew was observed approximately one block from the house. Thus, we cannot rule out the potential that their soil excavations had some effect on the differential pressures observed during this period.

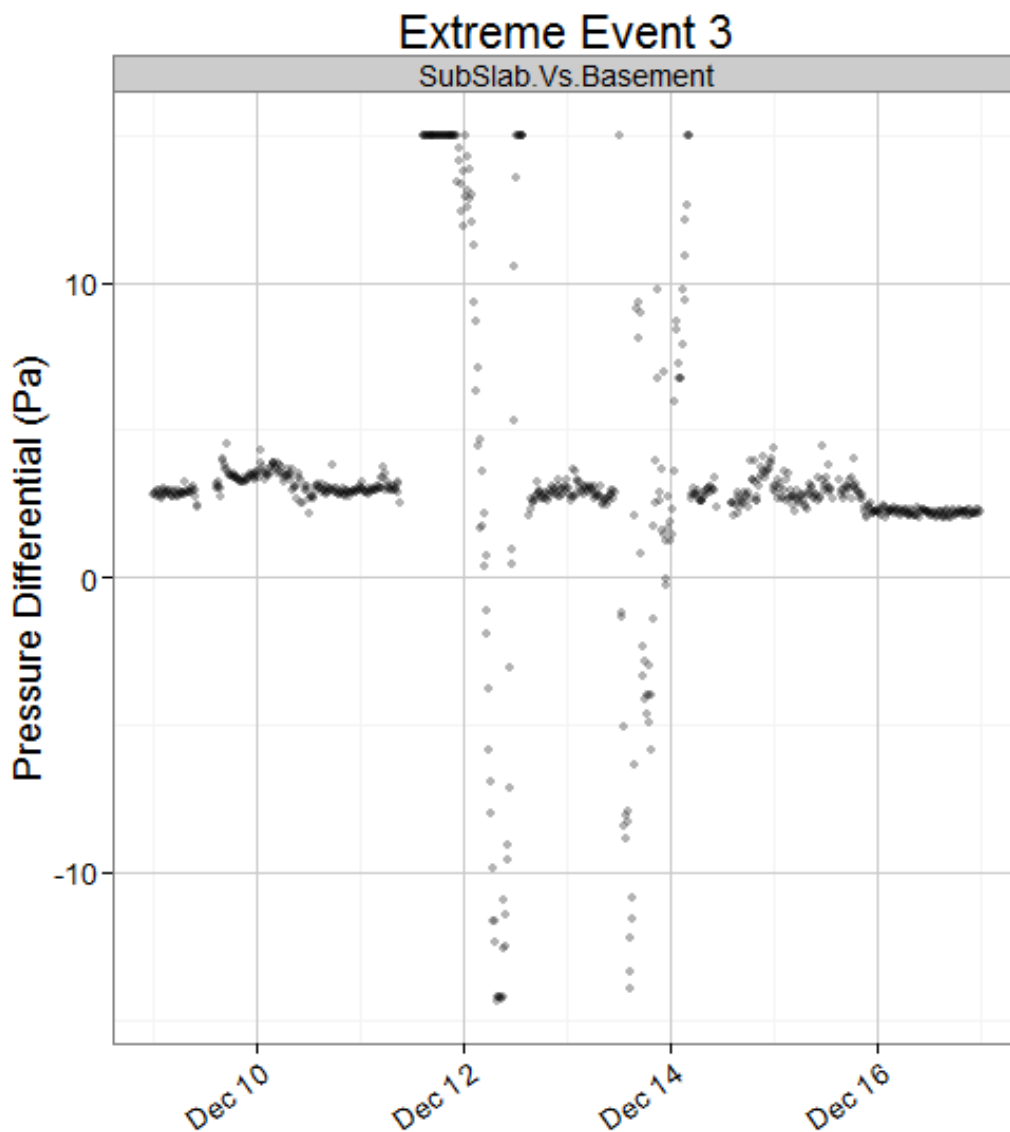


Figure 9-17. Extreme Event 3: subslab vs. basement differential pressure (positive difference indicates flow into the structure).

The fourth event (**Figure 9-18**) lasted just 8 hours, beginning with a brief high positive differential pressure spike and ending with a period of high negative differential pressure that ended abruptly at approximately 9:30 PM local time (later than our staff would typically be at the house). From that we conclude that a human cause was unlikely. There was a period of snow flurries late that day, which, as discussed Section 10, may be associated with vapor intrusion.

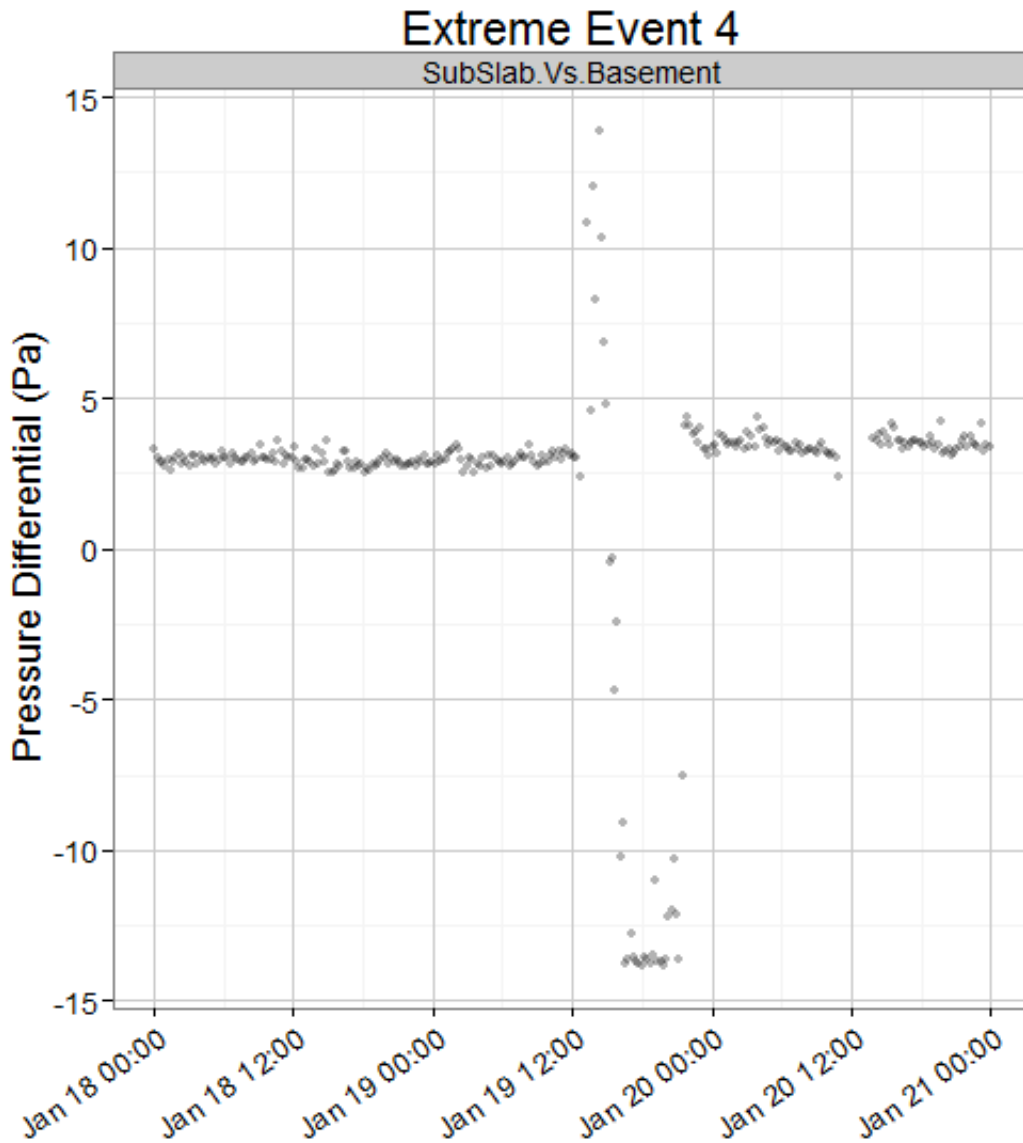


Figure 9-18. Extreme Event 4: subslab vs. basement differential pressure (positive difference indicates flow into the structure).

The fifth event lasted about 5 days (**Figure 9-19**) and has several peaks and troughs, including three separate periods when it appears that the instrument went off range below -15 Pa, as well as two briefer periods that may have been off range at >15 Pa. The long period of extreme values argues against a human artifactual cause. The occurrence of multiple maxima and minima in differential pressure suggests that the associated predictor variable(s) should also display multiple maxima and minima at this time period.

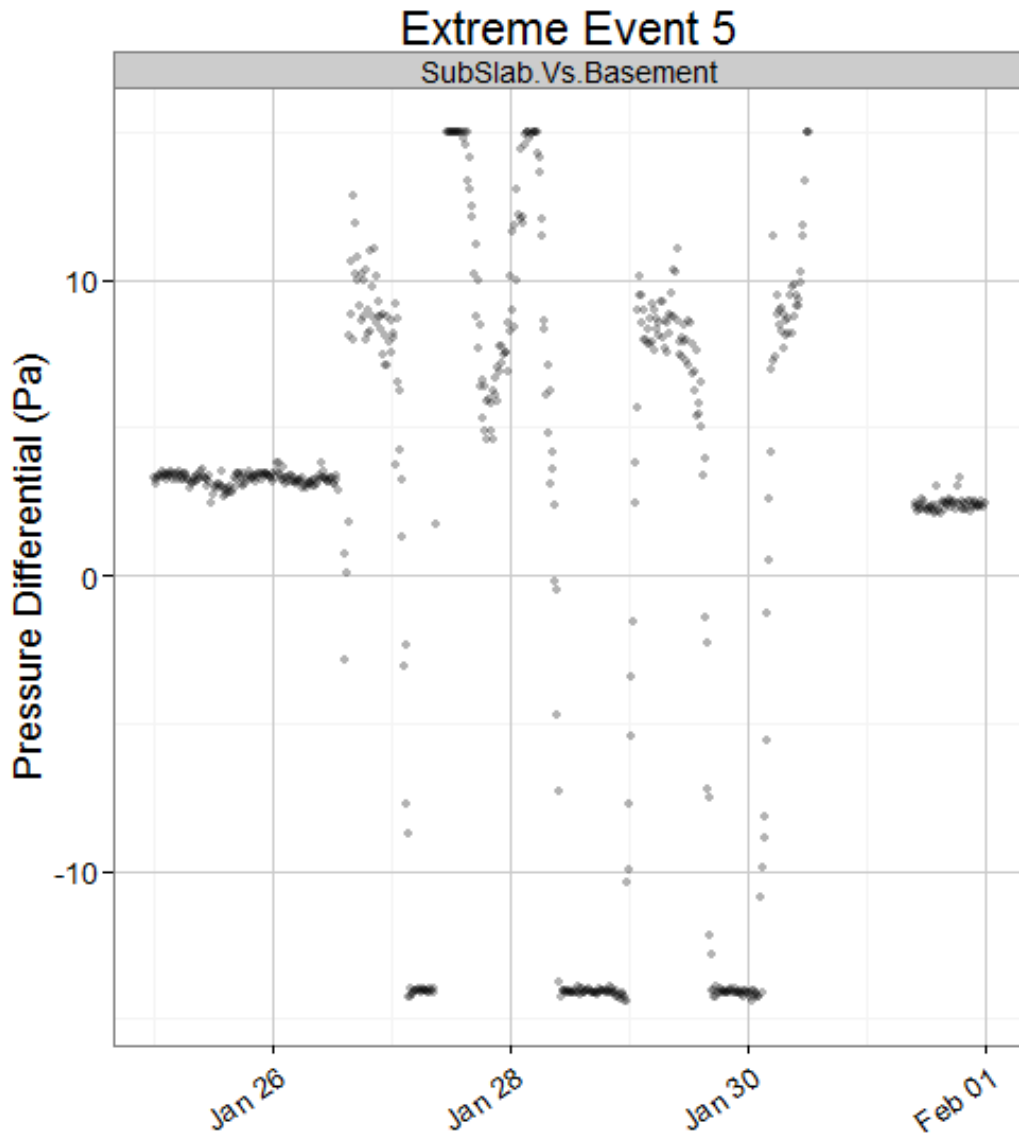


Figure 9-19. Extreme Event 5: subslab vs. basement differential pressure (positive difference indicates flow into the structure).

The sixth and seventh events (**Figure 9-20**) were very close to each other, taking place over about a week. During that time, there were at least five separate peaks to >10 Pa and three troughs to <-10 Pa. This event included several periods during which the pressure likely exceeded the sensors' capacity >15 Pa. As discussed above, the long duration of the events argues against a cause due to human disturbance and suggests that linked predictor variables should also display multiple maxima and minima.

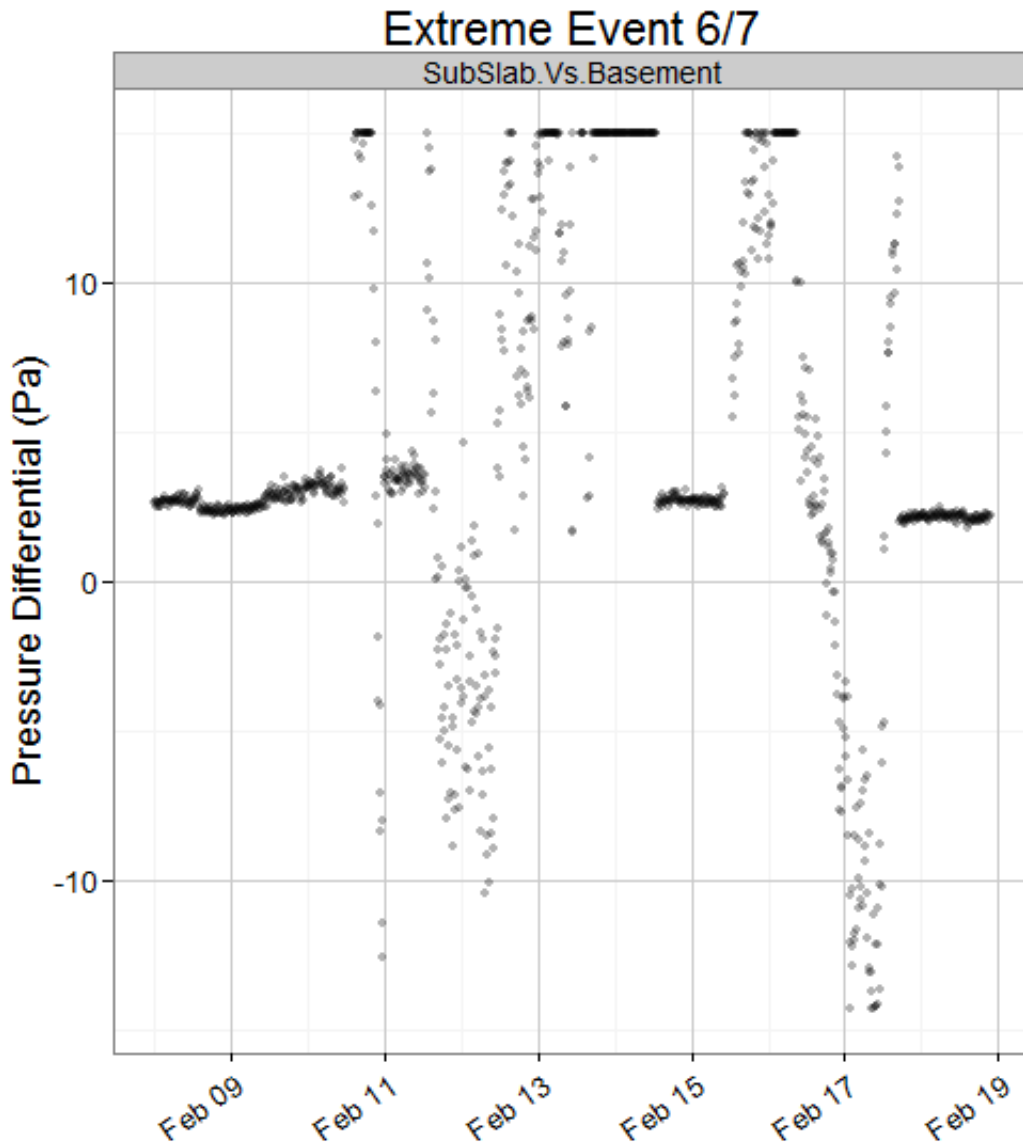


Figure 9-20. Extreme Events 6/7: subslab vs. basement differential pressure (positive difference indicates flow into the structure).

We examined visually the high resolution metrological data for each event, seeking coincidences in time between marked changes in metrological parameters and the differential pressure events. Plots that did not suggest a relationship are not shown.

Event 1 appears to coincide with a substantial drop in barometric pressure and a snowstorm (**Figures 9-21** and **9-22**). Event 2 appears to begin slightly ahead of a substantial drop in barometric pressure and increase in temperature (**Figures 9-23** and **9-24**). Event 3 also appears to begin slightly ahead of a substantial drop in barometric pressure and to coincide with a rise in temperature as well as a wind shift. (**Figures 9-25** through **9-27**). The online GC was available during Event 3 and appears to show some correlation of rising PCE to positive differential pressure (toward the structure).

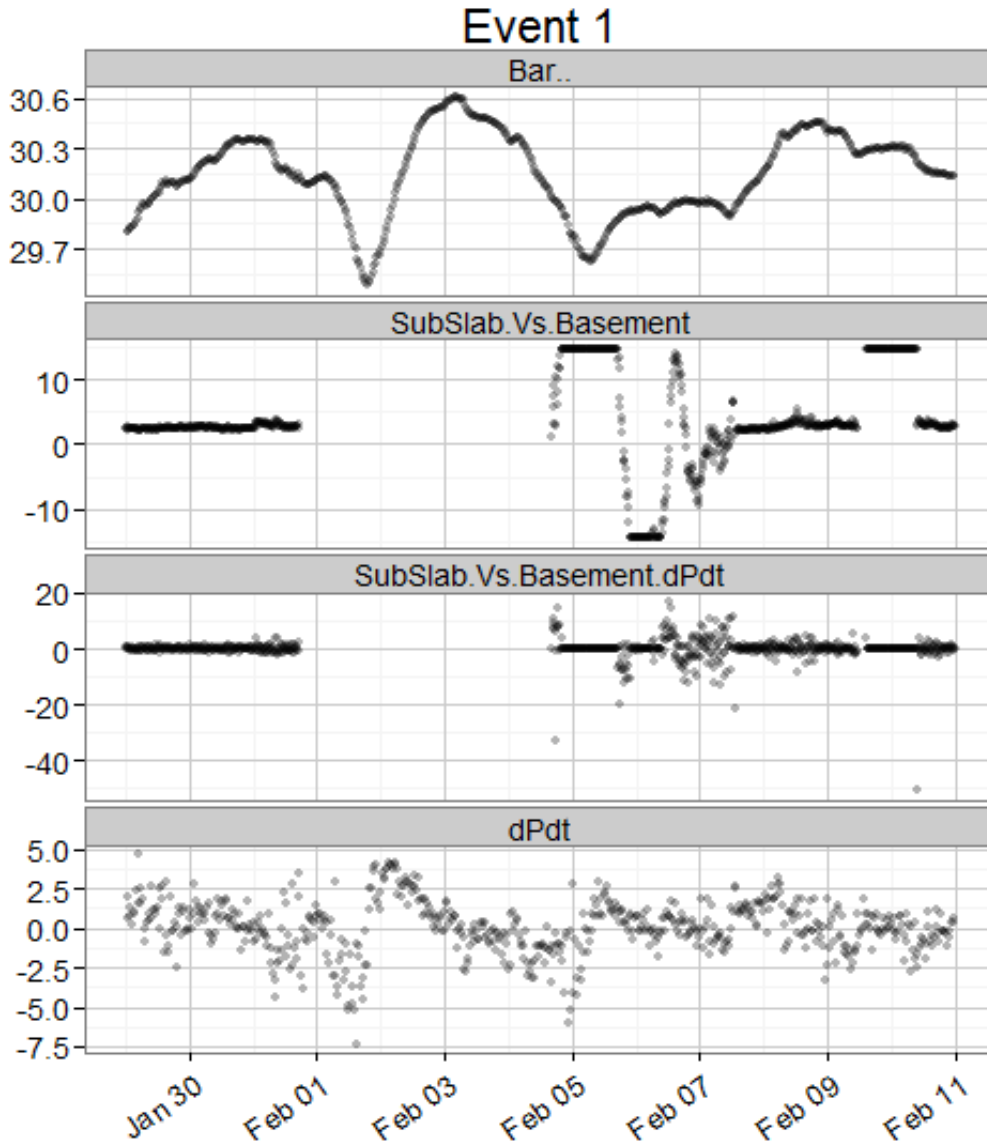


Figure 9-21. Detailed time series of unusual pressure Event 1 showing barometric pressure changes (barometric pressure in inches of Hg, differential pressure in Pa).

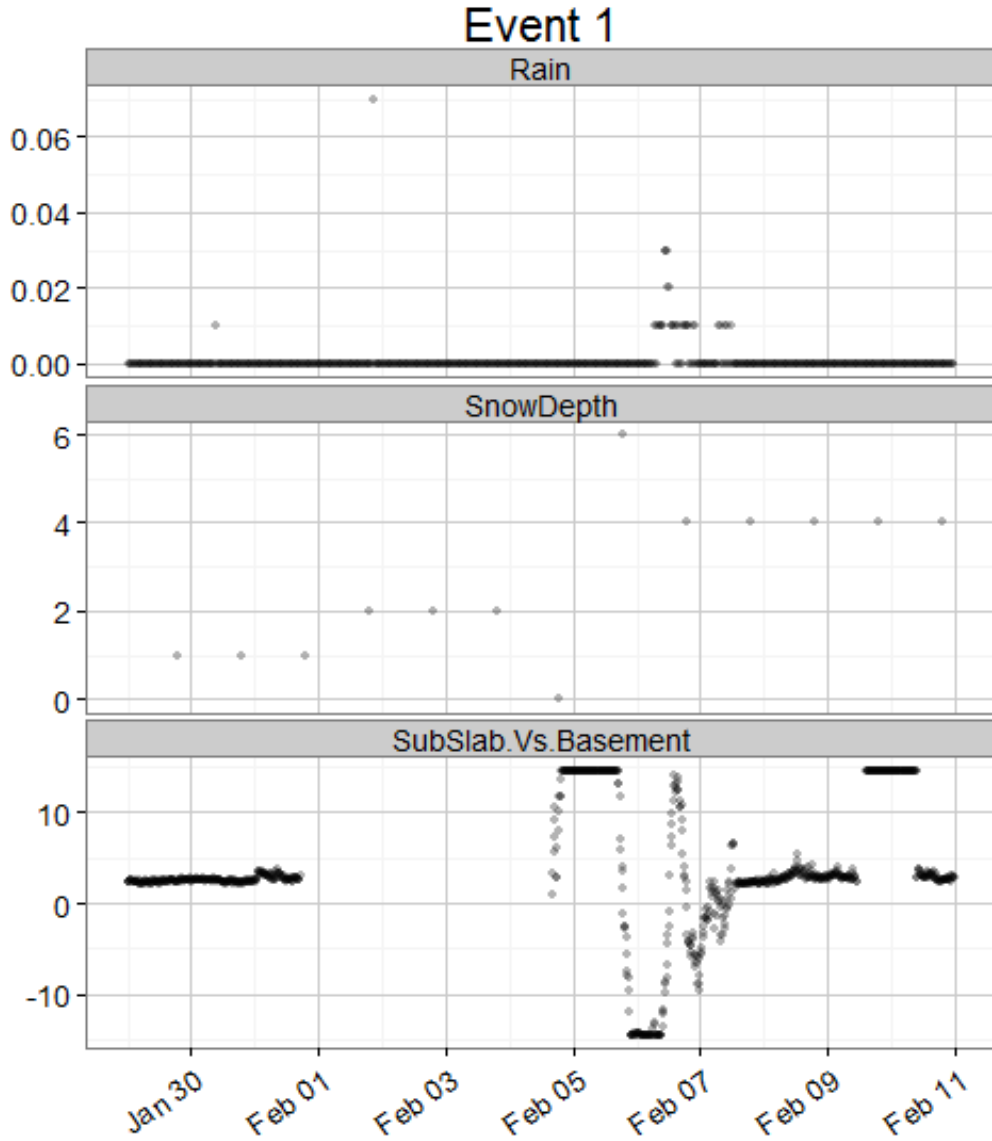


Figure 9-22. Detailed time series of unusual pressure Event 1 showing precipitation events (rainfall in inches, snow depth in inches, differential pressure in Pa).

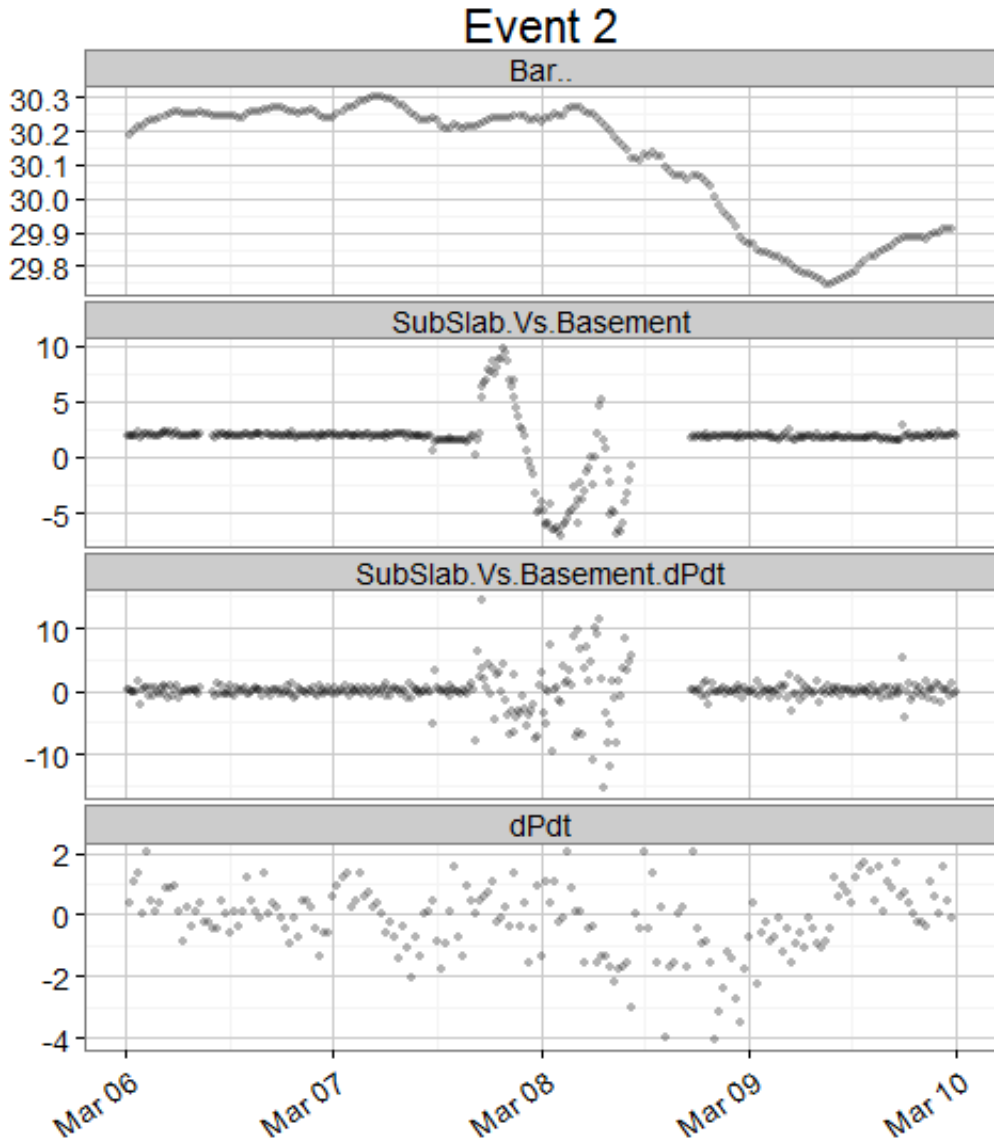


Figure 9-23. Detailed time series of unusual pressure Event 2 showing barometric pressure changes (barometric pressure in inches of Hg, differential pressure in Pa).

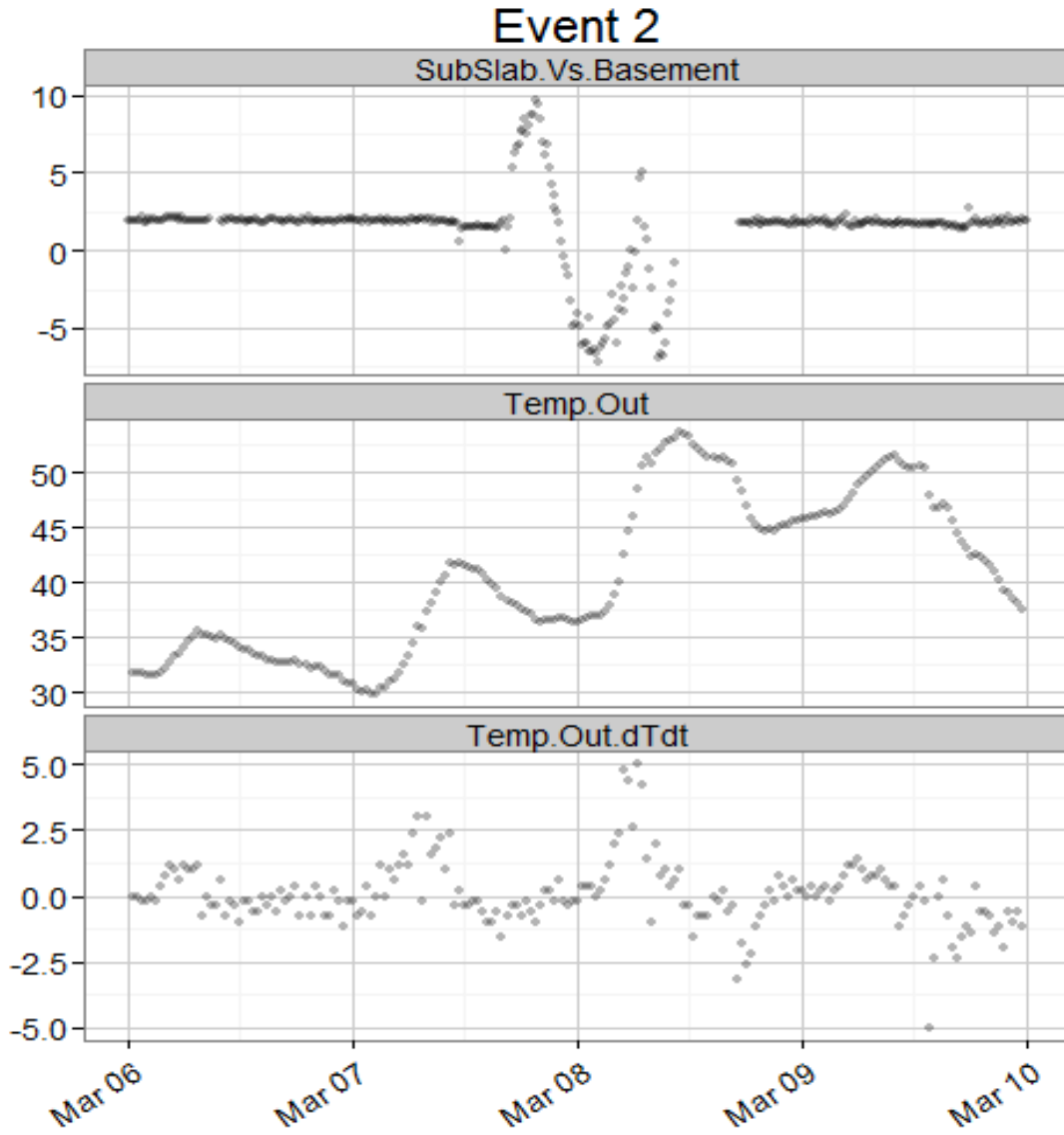


Figure 9-24. Detailed time series of unusual pressure Event 2 showing temperature changes (differential pressure in Pa, temperature in °F).

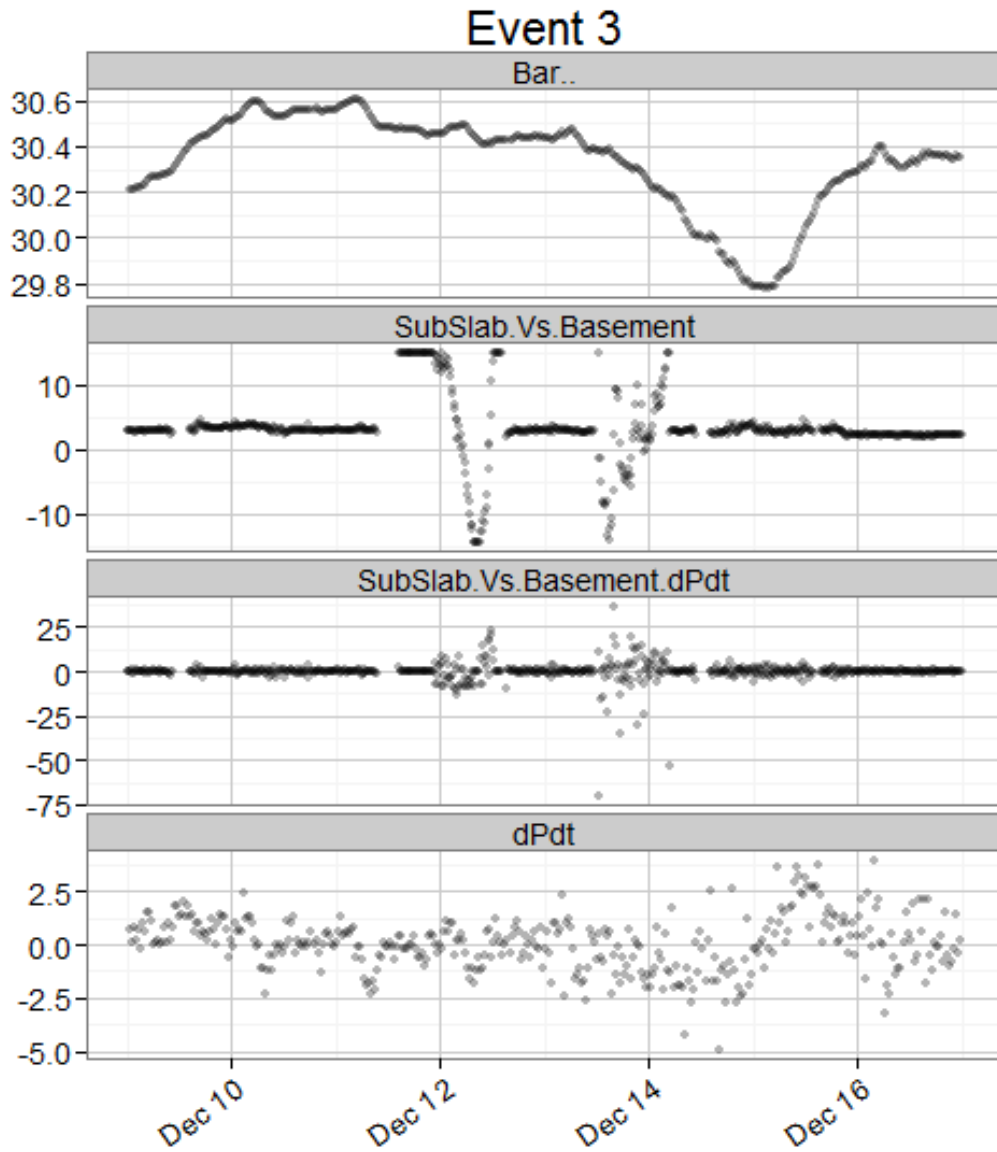


Figure 9-25. Detailed time series of unusual pressure Event 3 showing barometric pressure changes (barometric pressure in inches of Hg, differential pressure in Pa).

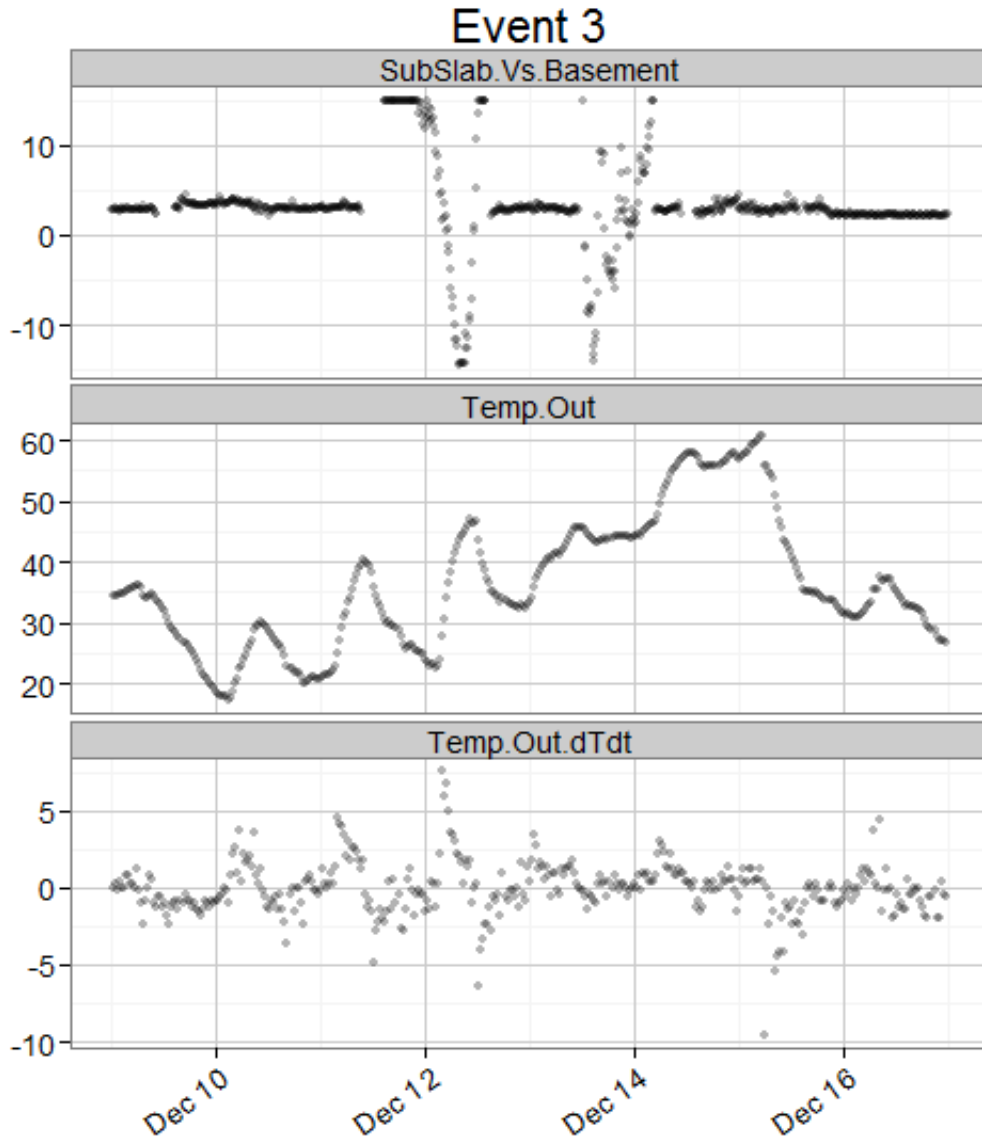


Figure 9-26. Detailed time series of unusual pressure Event 3 showing temperature changes (differential pressure in Pa, temperature in °F).

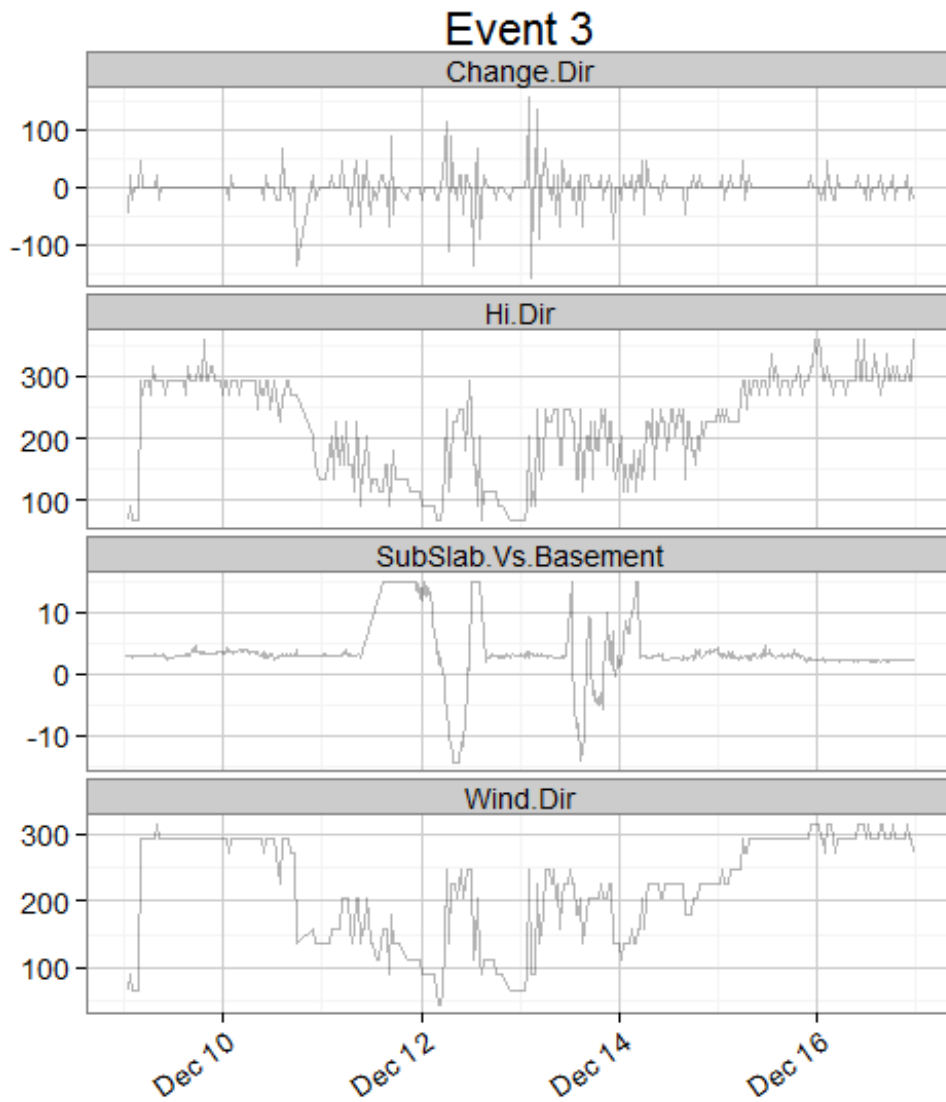


Figure 9-27. Detailed time series of unusual pressure Event 3 showing wind direction variables (wind direction-related variables in degrees, differential pressure in Pa).

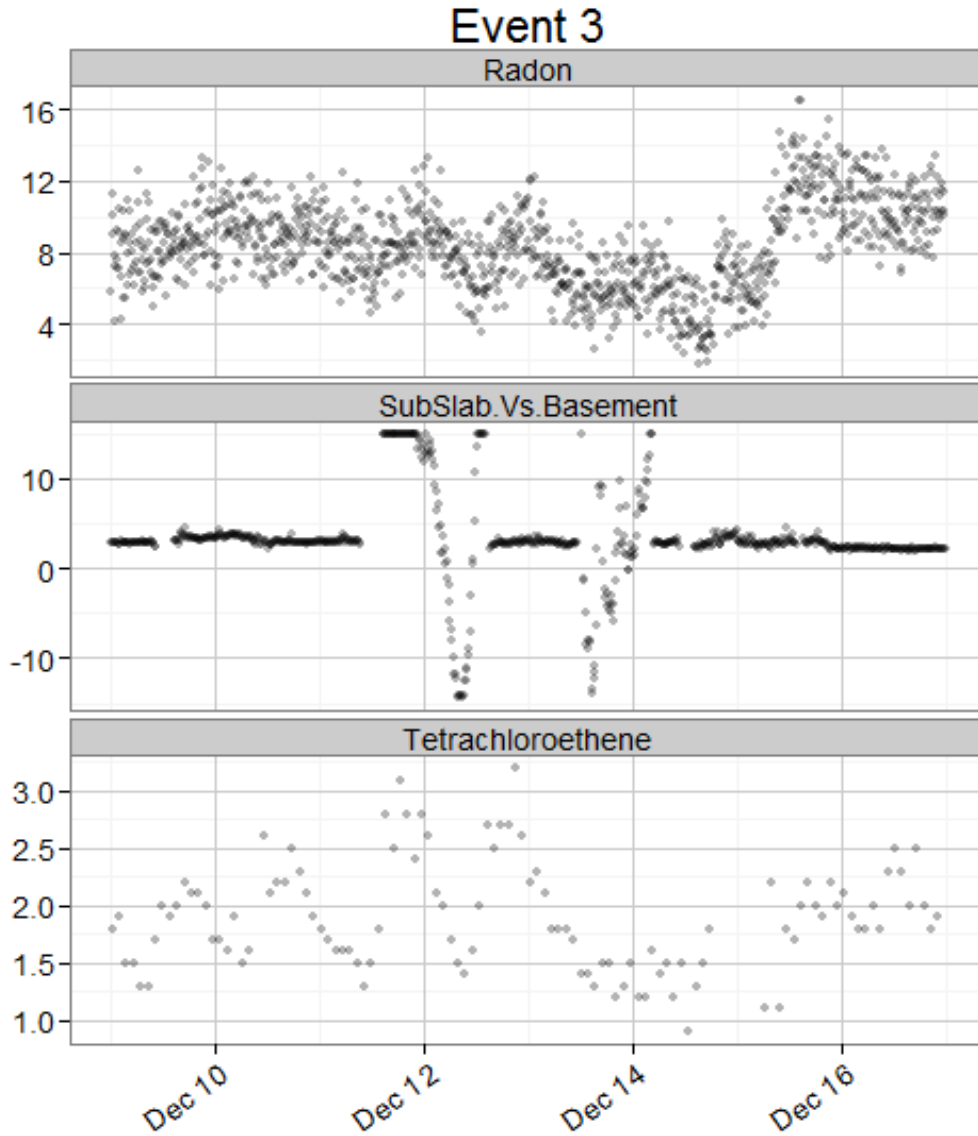


Figure 9-28. Detailed time series of unusual pressure Event 3 showing PCE and radon.

In reviewing the stacked graphs seeking evidence of a cause of these extreme differential pressure values, we noted that Event 4 appears to be associated with a significant drop in temperature and a substantial wind direction shift that was accompanied by a period of calm wind (**Figure 9-29** through **Figure 9-31**). Others have noted an association between a period of calm and a wind shift.²¹ Since subslab to interior differential pressure spatial patterns can vary with wind direction (U.S. EPA, 2012d), this association in the data is reasonable.

Event 5, which shows multiple peaks and troughs in differential pressure, appears to be related to a series of weather events. It appears to have been triggered by a light snow (**Figure 9-32**). The middle fluctuations of the event appear to track with a period of high and shifty winds, including some gusts over 30 mph (**Figures 9-33** and **9-34**). As discussed above, exterior winds are known to be associated with the subslab to interior differential pressure (U.S. EPA, 2012d). The last fluctuation appears to coincide with a substantial temperature rise (**Figure 9-35**). Exterior temperature changes are expected to cause changes in the strength of the stack effect. Event 5 seems to have caused two spikes in the indoor radon concentration that each reached 15 pCi/l (**Figure 9-36**).

²¹gcc.glendale.edu/fire/Documents/ClassMaterials/s190-2.pdf

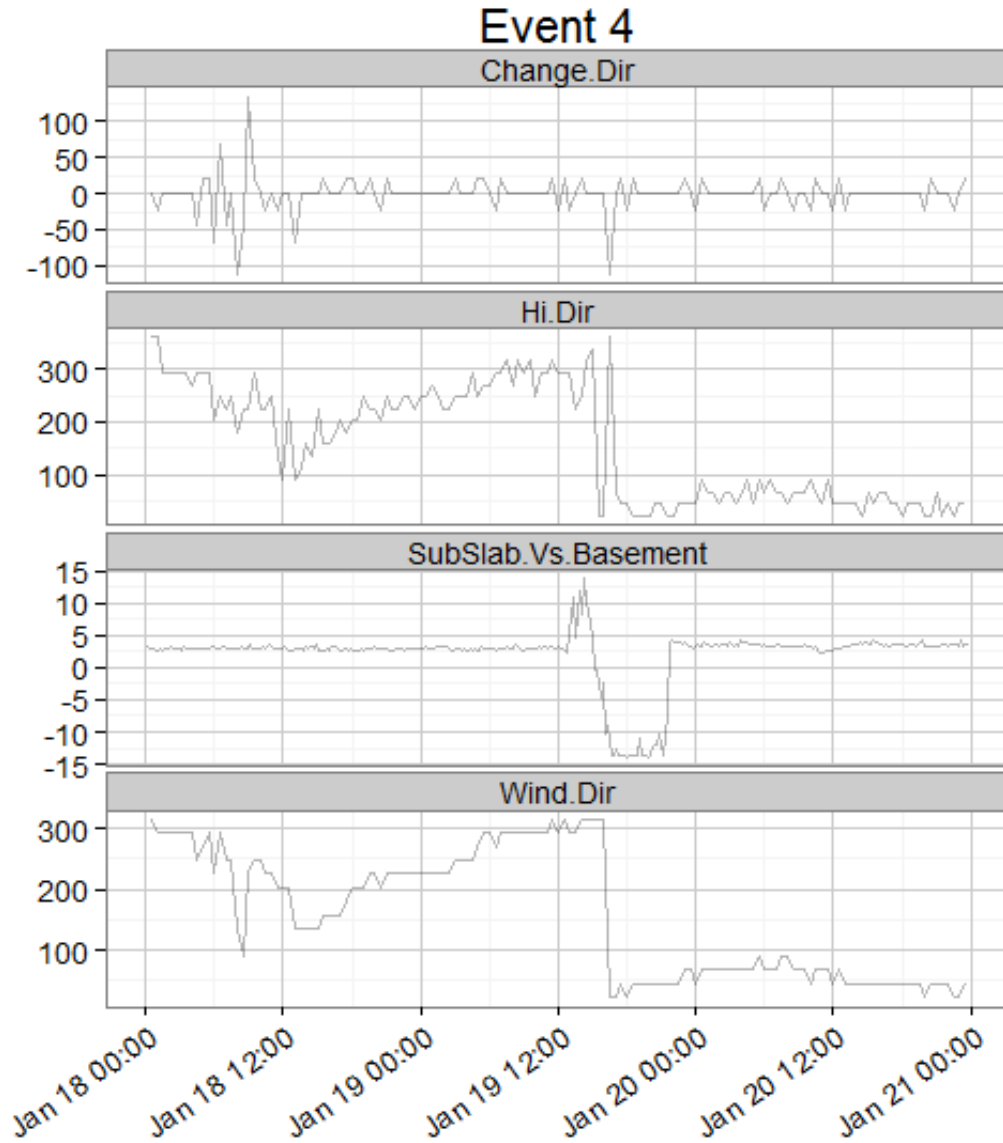


Figure 9-29. Detailed time series of Event 4 showing wind direction variables (wind direction-related variables in degrees, differential pressure in Pa).

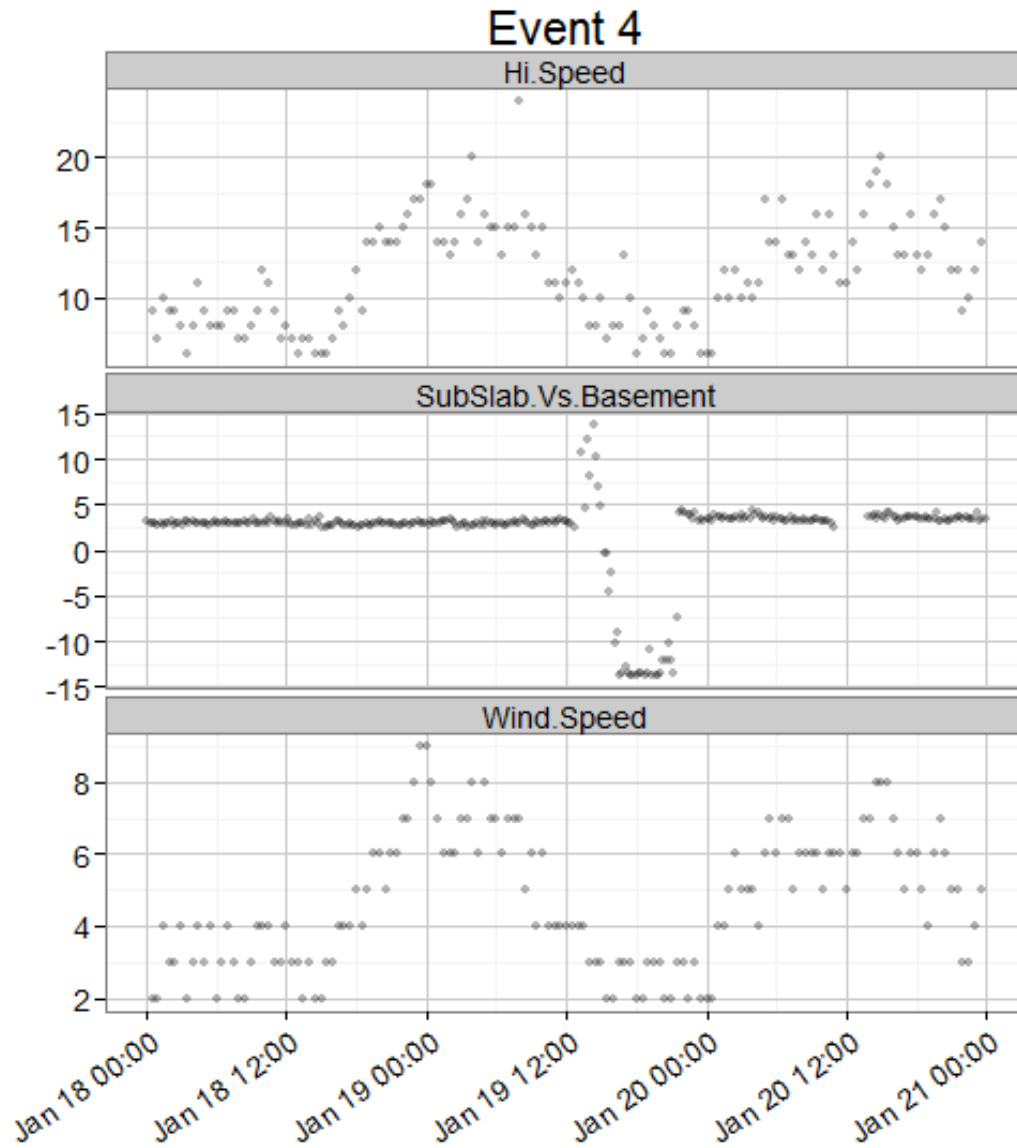


Figure 9-30. Detailed time series of Event 4 showing wind speed variables (wind speed variables in MPH, differential pressure in Pa).

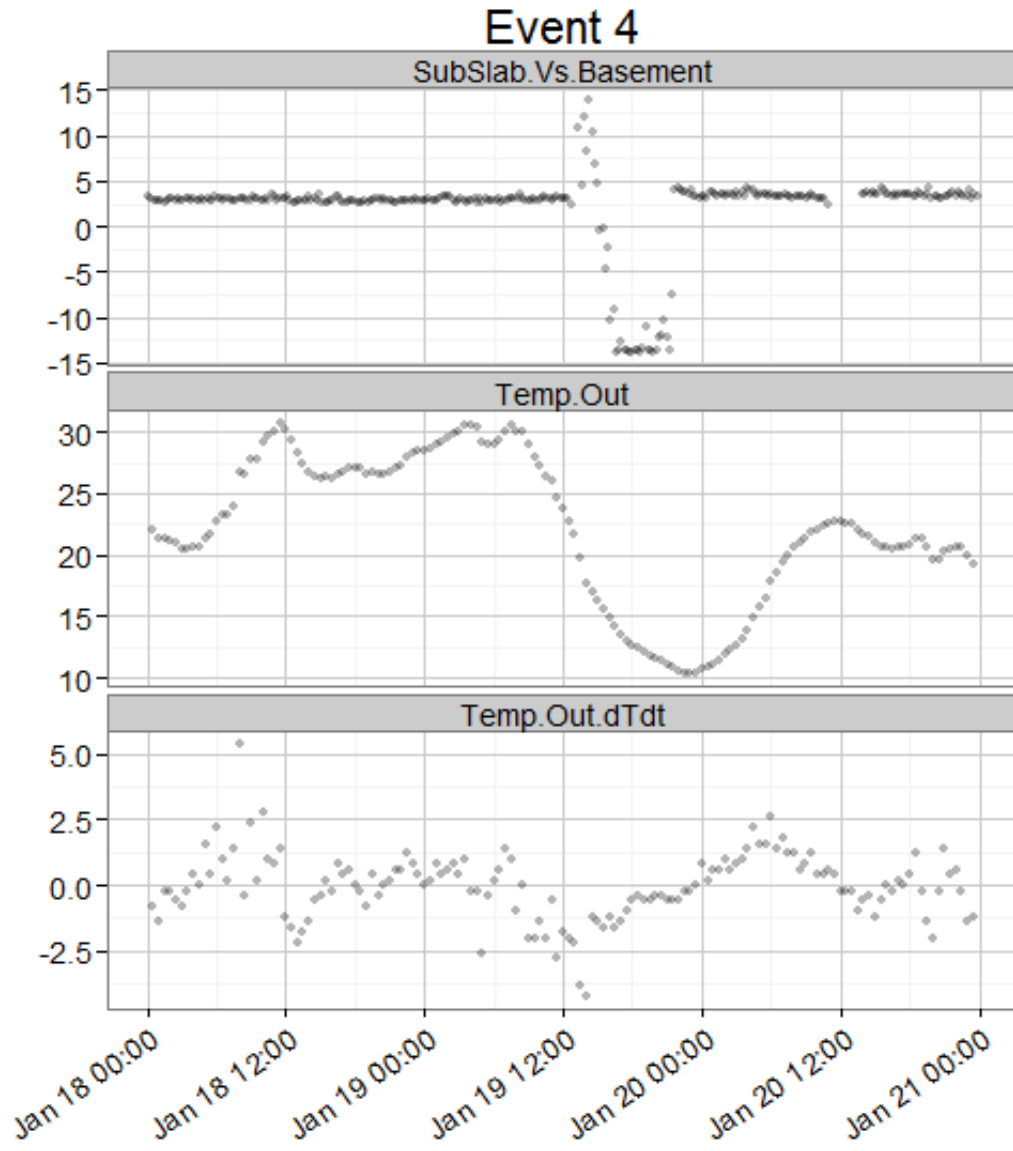


Figure 9-31. Detailed time series of Event 4 showing temperature variables (differential pressure in Pa, temperature in °F).

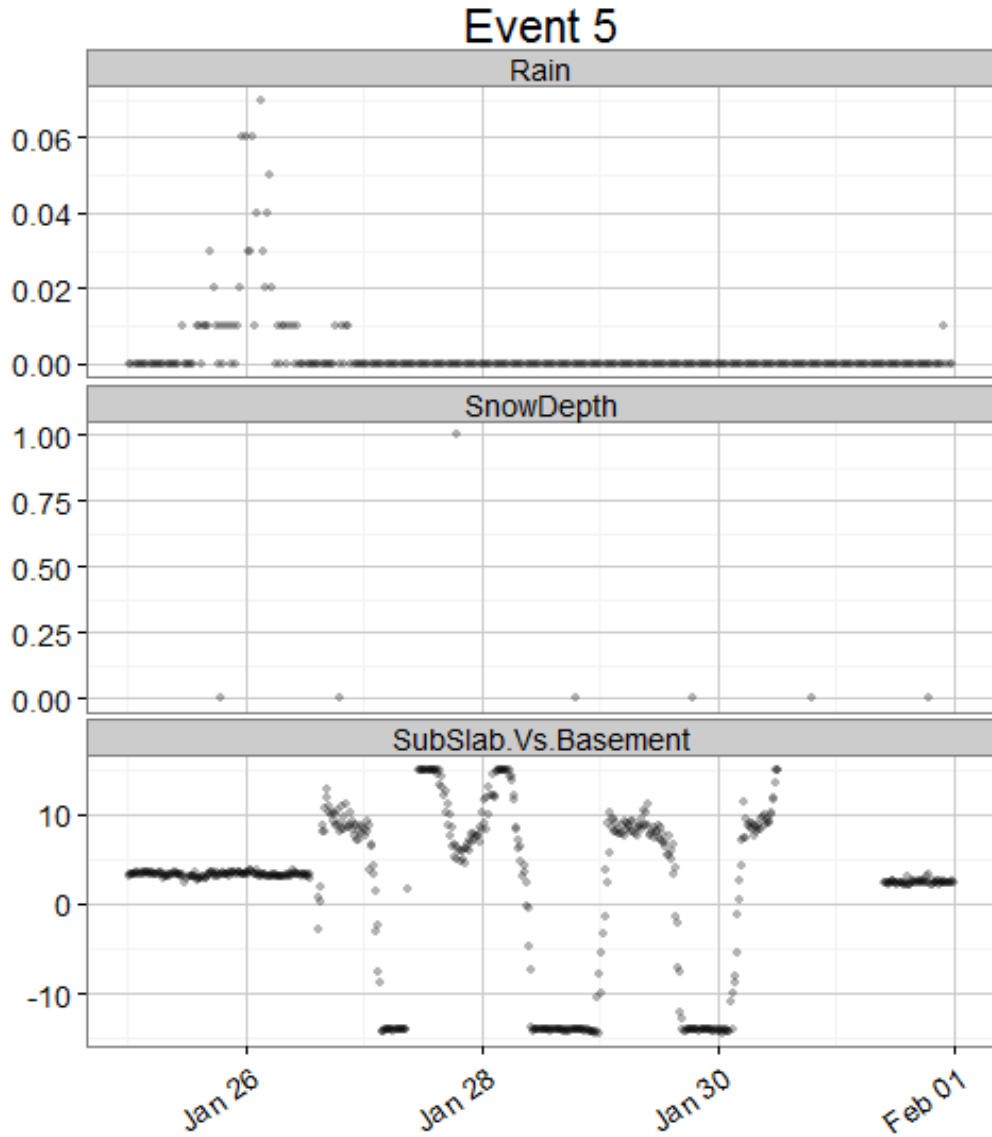


Figure 9-32. Detailed time series of Event 5 showing precipitation event (rainfall in inches, snow depth in inches, differential pressure in Pa).

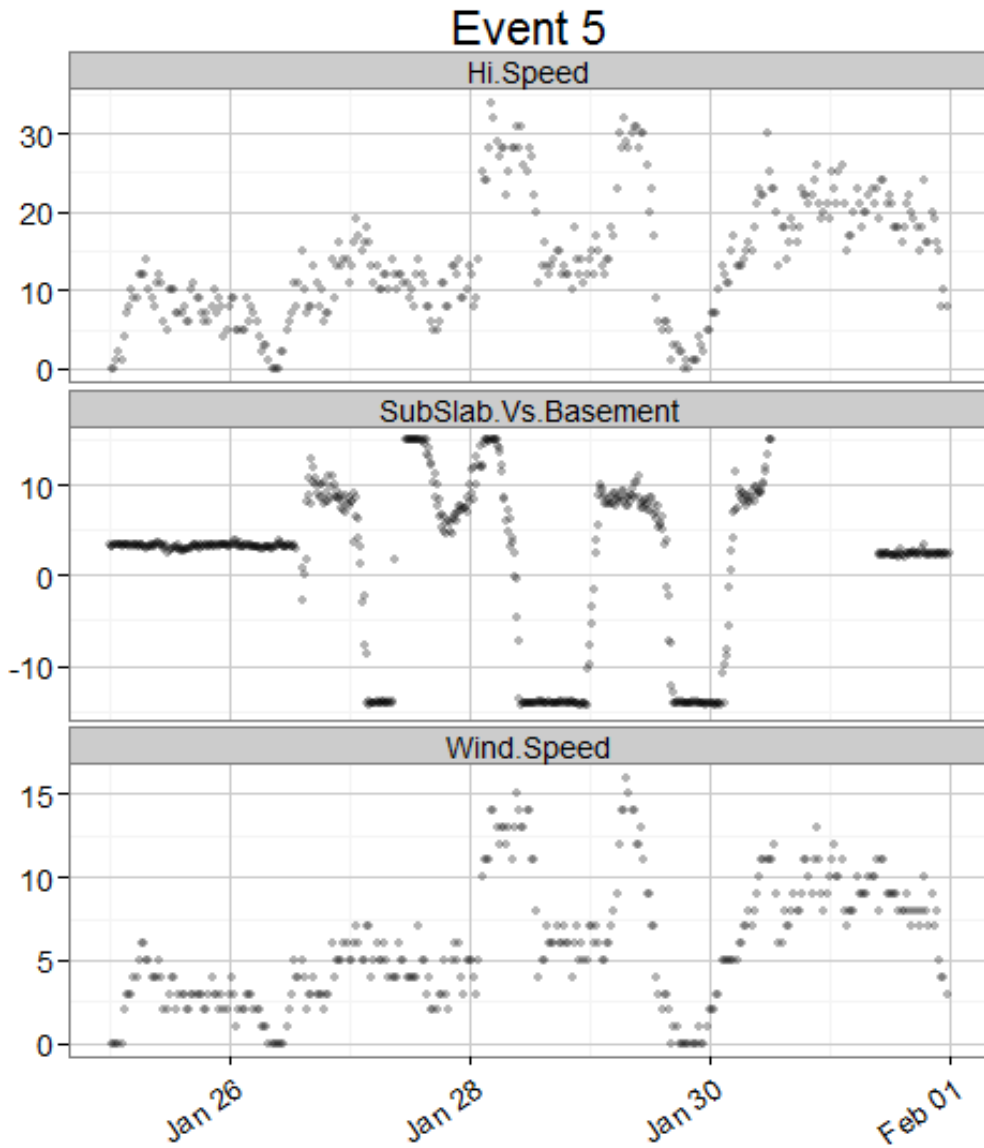


Figure 9-33. Detailed time series of Event 5 showing wind speed variables (wind direction-related variables in degrees, differential pressure in Pa).

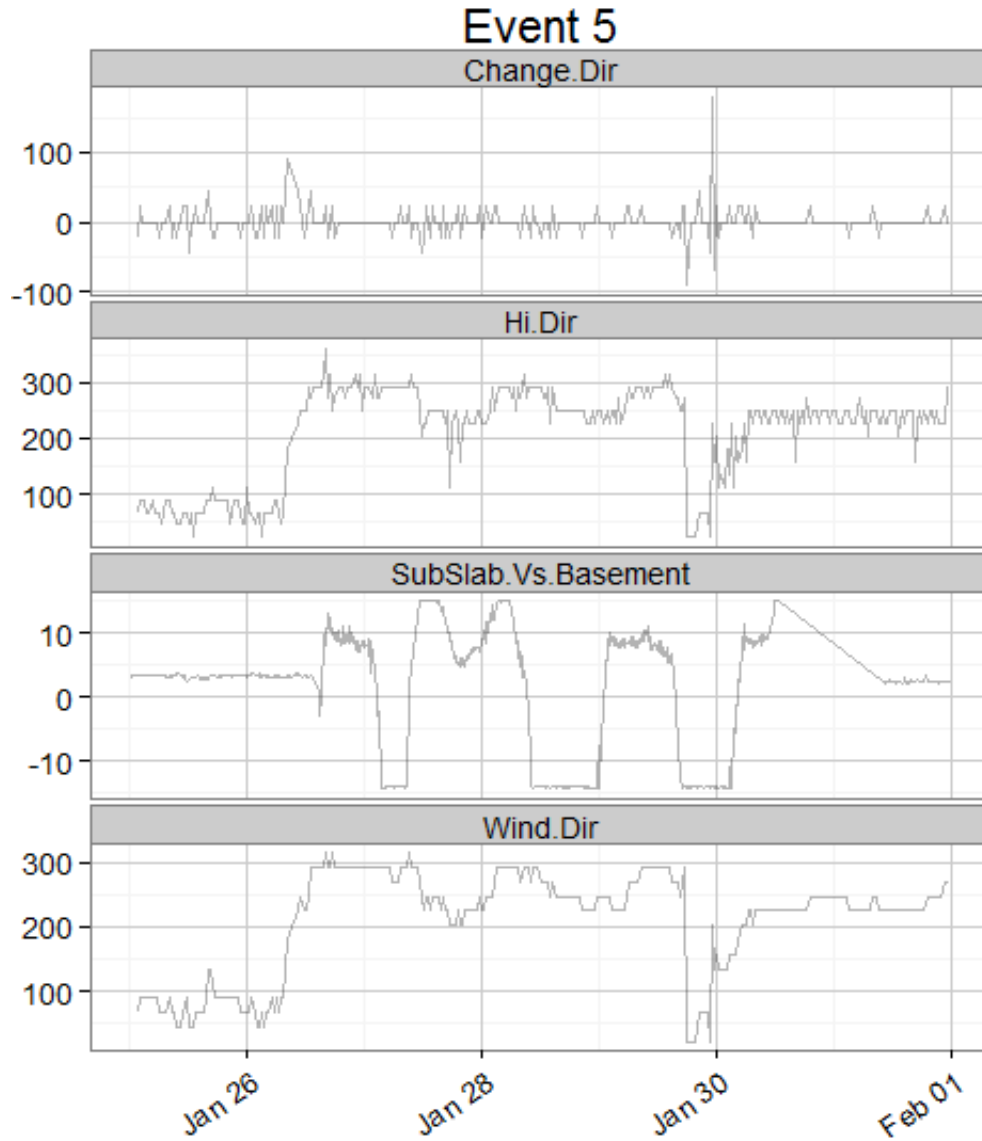


Figure 9-34. Detailed time series of Event 5 showing wind direction variables.

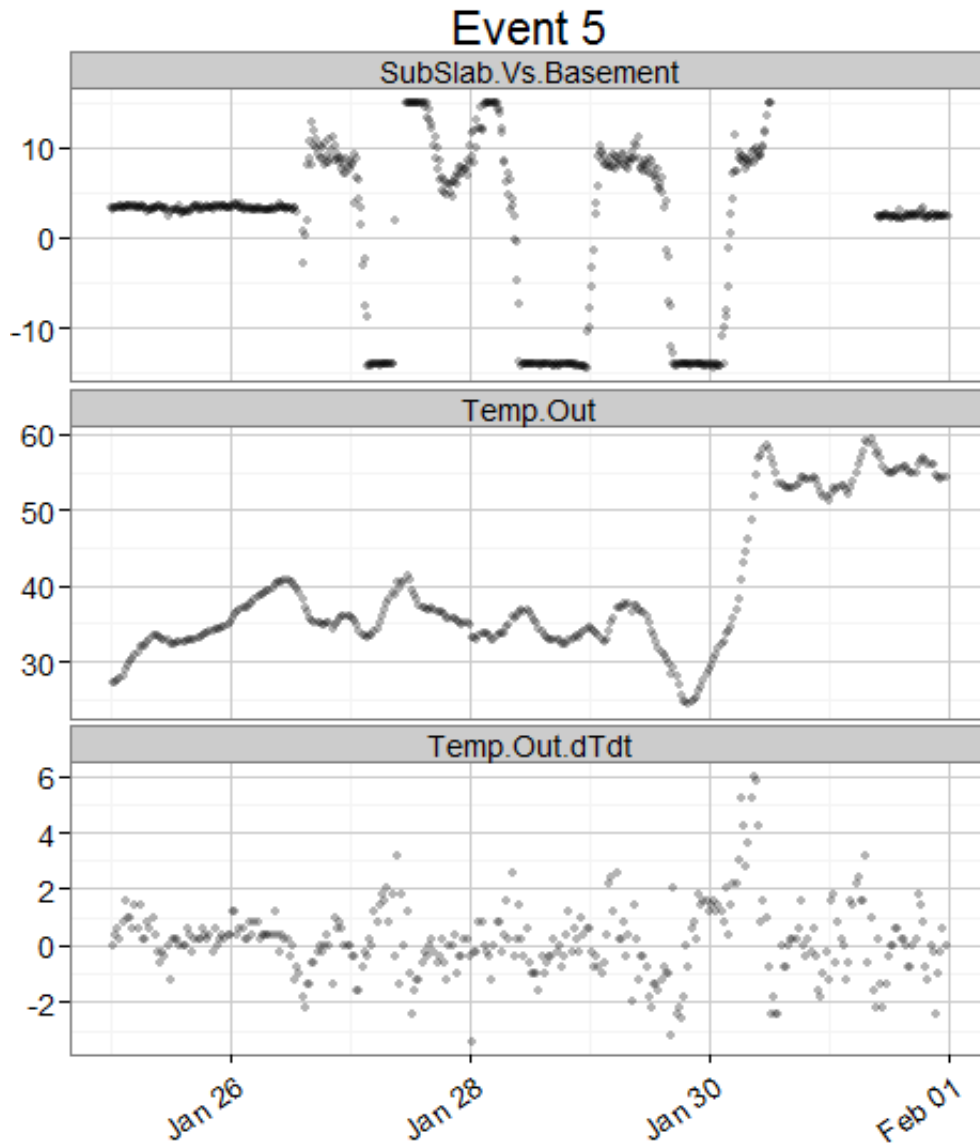


Figure 9-35. Detailed time series of Event 5 showing temperature variables (differential pressure in Pa, temperature in °F).

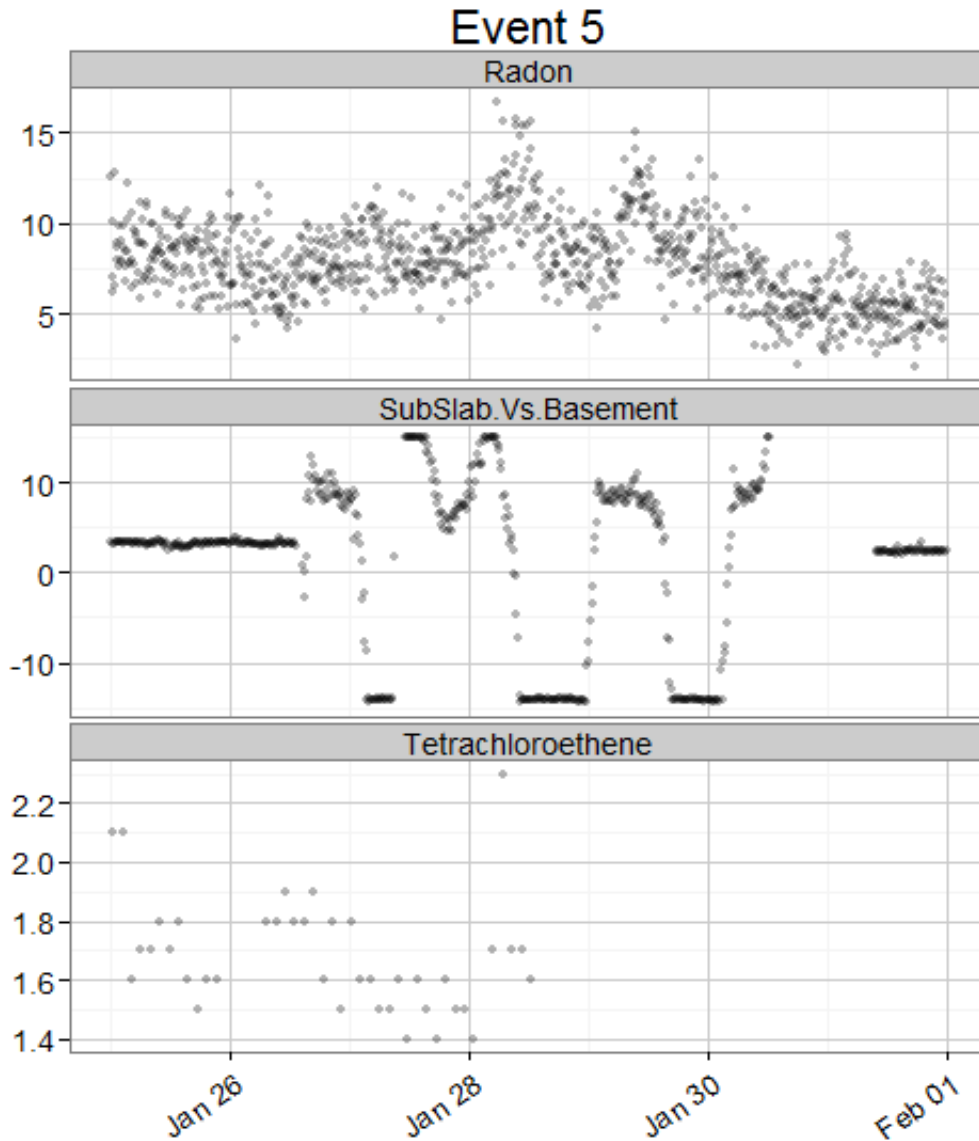


Figure 9-36. Detailed time series of Event 5 showing PCE and radon.

Event 6/7 is more difficult to interpret. Although we initially numbered these events differently, we discuss them together here because they occur in short succession. The event shows some association with substantial barometric pressure changes, with a falling barometer being associated with positive differential pressure as was seen in other events (and is expected from theory) (Figure 9-37). This event appears also to be associated with a light snow (Figure 9-38). There also appears to be some coincident events in the wind speed and direction plots (Figures 9-39 and 9-40). Event 6/7 may have a corresponding radon and PCE peak, but the data for these parameters are quite noisy during this time period, so the evidence shown in Figure 9-41 is weak.

Taken together, the detailed examination of these time series for multiple extreme pressure events suggests that all of these events have some likely relationship to meteorological variables. However, the particular meteorological variables causing each pressure event may be different and multiple. This is not surprising because changes in temperature, barometric pressure, wind speed, and direction are typically associated with a frontal passage or storm event.

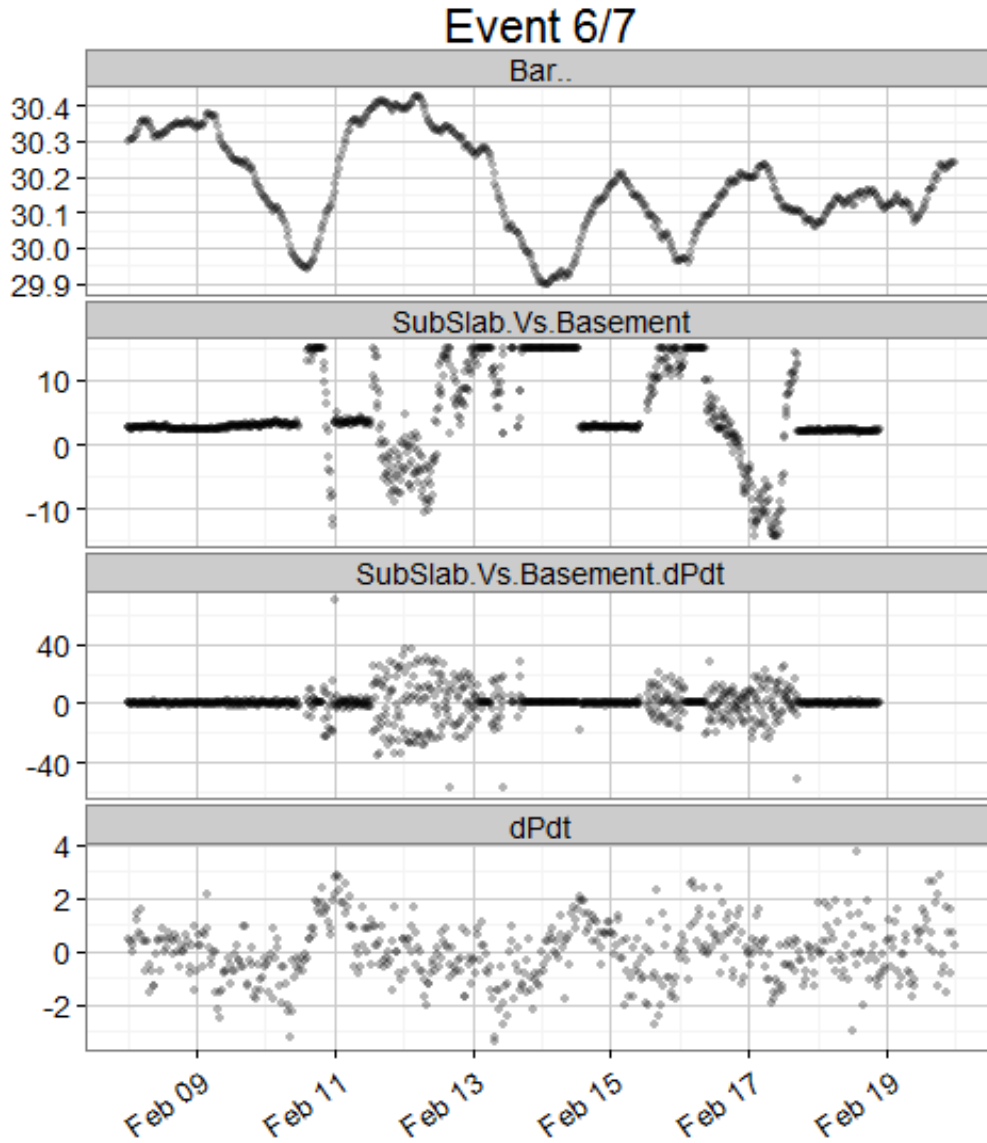


Figure 9-37. Detailed time series of Event 6/7 showing barometric pressure (barometric pressure in inches of Hg, differential pressure in Pa).

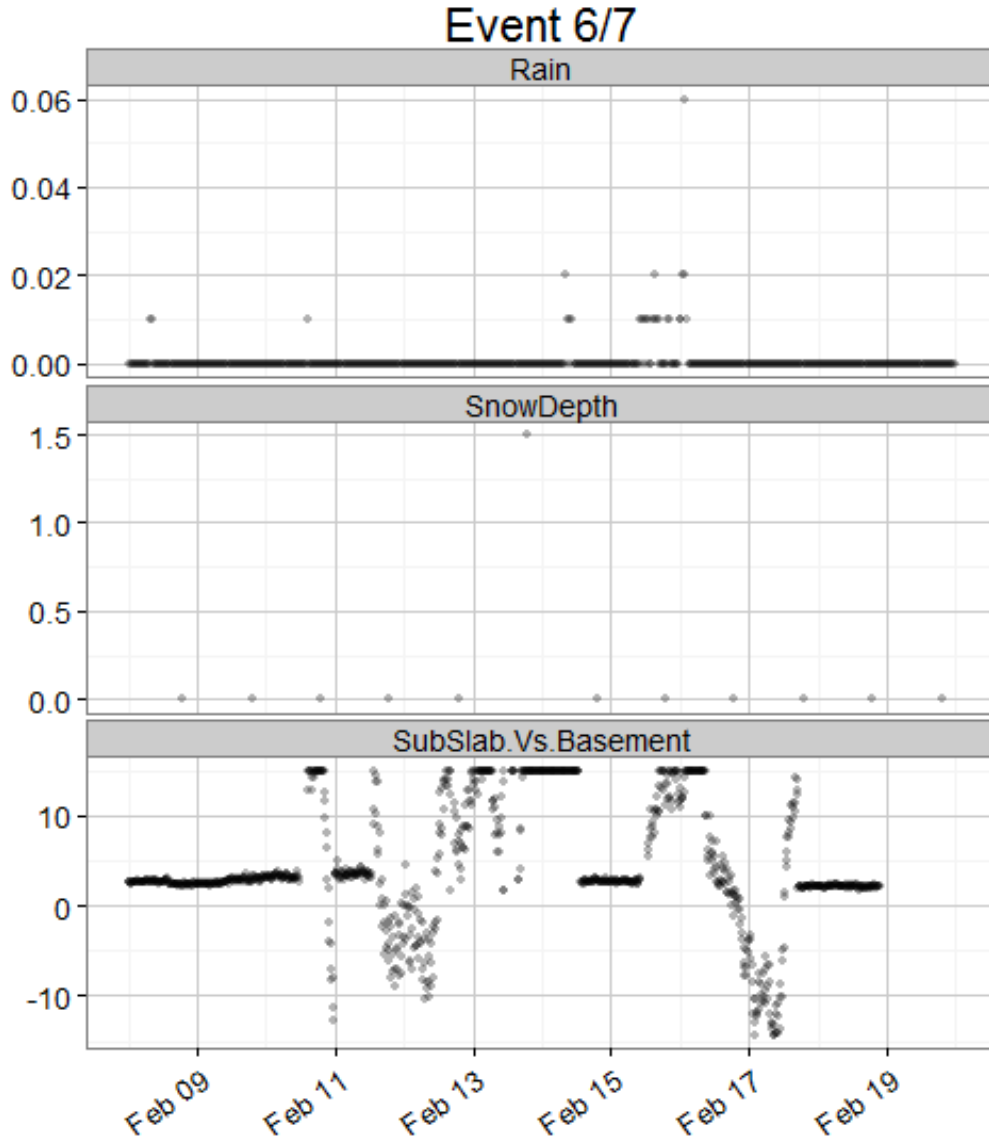


Figure 9-38. Detailed time series of Event 6/7 showing precipitation (rainfall in inches, snow depth in inches, differential pressure in Pa).

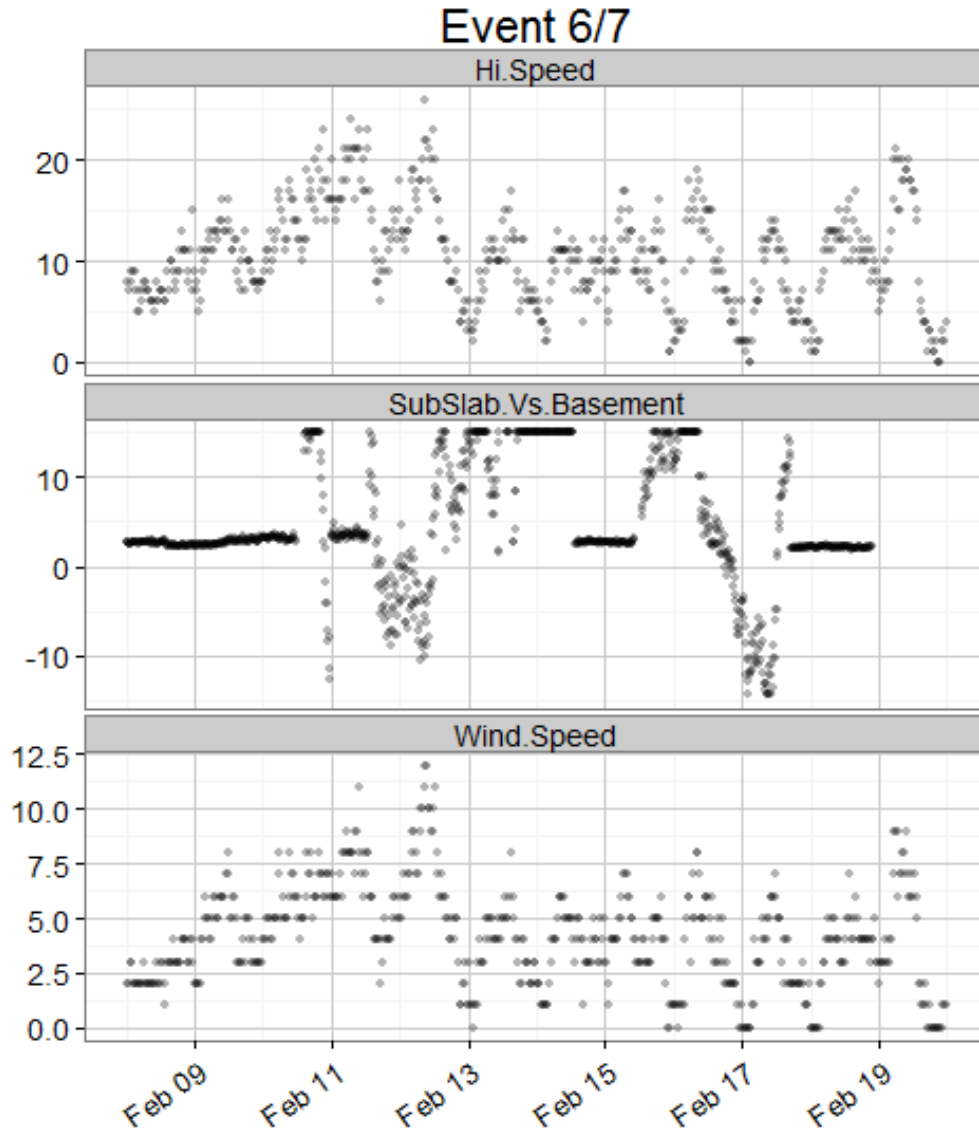


Figure 9-39. Detailed time series of Event 6/7 showing wind speed variables (wind direction-related variables in degrees, differential pressure in Pa).

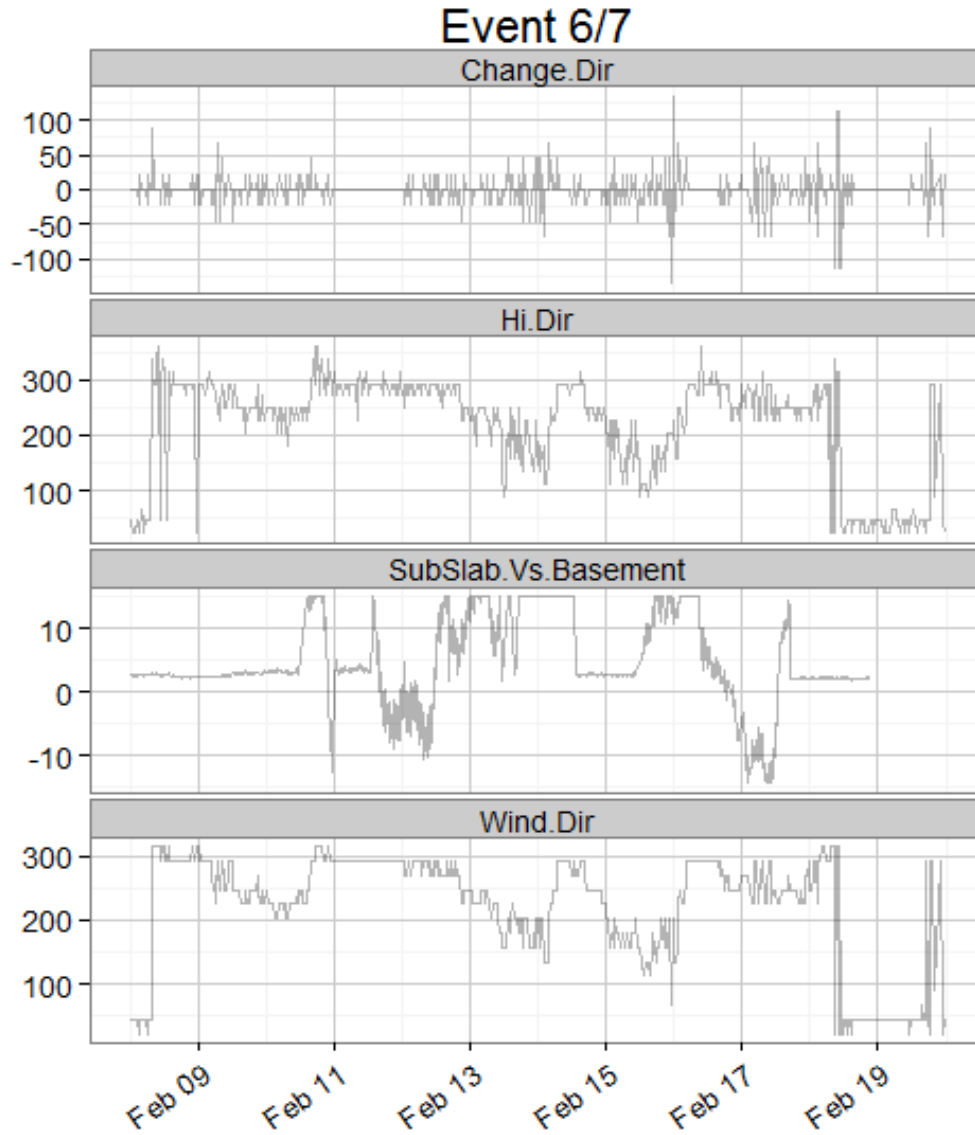


Figure 9-40. Detailed time series of Event 6/7 showing wind direction variables (wind direction-related variables in degrees, differential pressure in Pa).

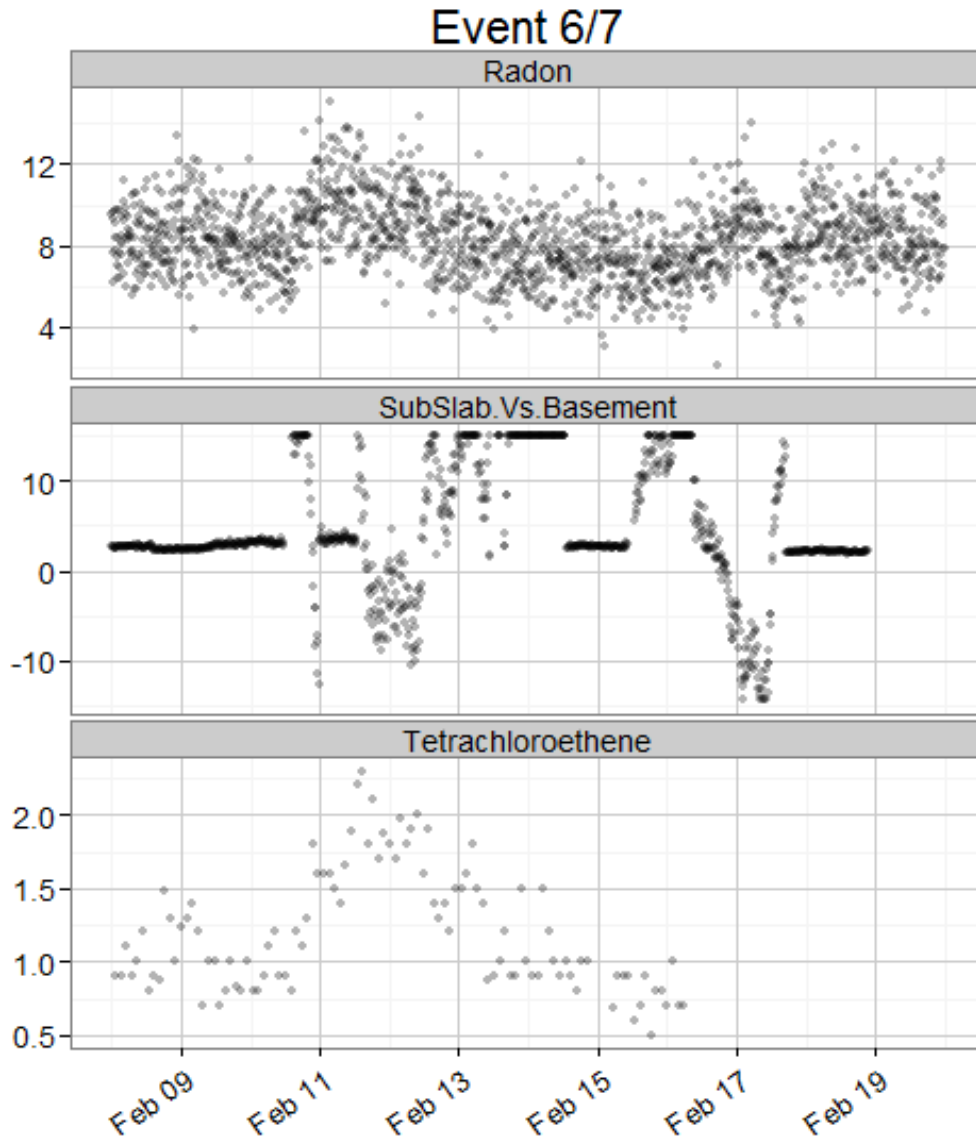


Figure 9-41. Detailed time series of Event 6/7 showing radon and PCE.

9.2 Influence of Meteorological Conditions on Indoor VOC Concentration; Mitigation Off

In Section 6, we examined this topic based on a review of patterns in the high temporal resolution on-site GC data and found evidence that peaks in wind speed and snow events were coincident in time with peak VOC concentrations in WP-3 and indoor air.

9.2.1 Temperature Effect on VOCs

The effect of meteorological variables can also be examined using the weeklong passive Radiello data set. We visually screened our meteorological variables and present here those with an evident correlation. As shown in **Figure 9-42**, there is a visual correlation between PCE and heating degree days, a measure of

sustained cold weather.²² Because the 422 side had thermostatically controlled temperature in winter, this result is expected and is similar in appearance to that based on the analysis of the stack effect driving force provided in Section 10.3 of our previous report (U.S. EPA, 2012a). The analysis according to heating degree days may be a useful one to practitioners and in public communication because it is an easily calculated and widely reported parameter.²³

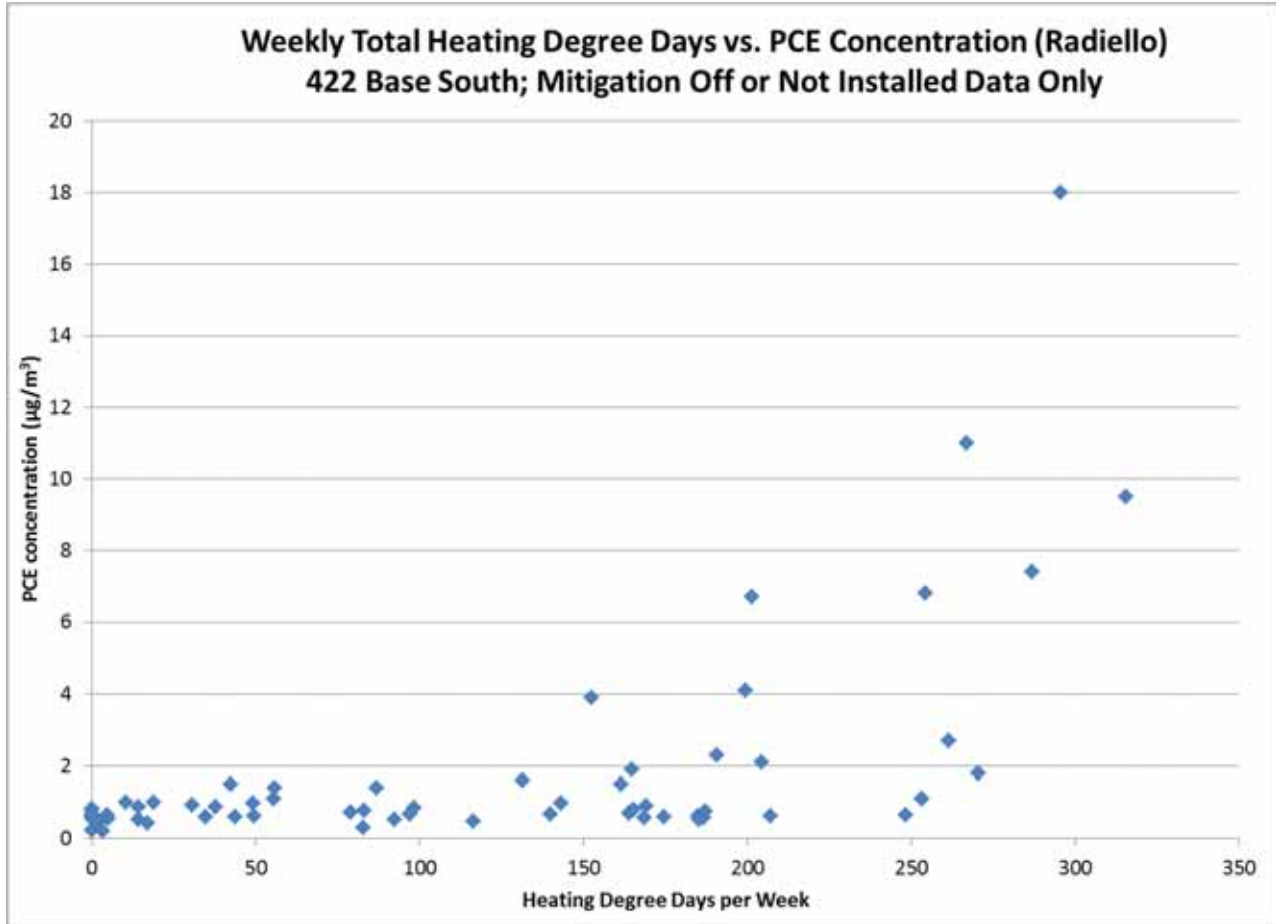


Figure 9-42. XY graph of total heating degree days per week vs. weekly PCE concentration (Radiello data).

²²One heating degree day is the amount of heat required to keep a structure at 65°F when the outside temperature remains one degree below the 65°F threshold for 24 hours.

²³The stack effect driving force calculation discussed in U.S. EPA (2012a) is a slightly more complex calculation (stack effect is proportional to the square root of the indoor outdoor temperature difference divided by the indoor temperature). The data set shown here includes some additional weeks and uses the heating degree day function, which is calculated using the difference between 65°F and average exterior temperature for the half-hour time interval, divided by 48 (to correct from hours to days). The degree days for each half hour are then totaled over the week.

Similarly, the concentration of chloroform is visually correlated to temperature but shows a somewhat different curve shape than PCE (**Figure 9-43**). Four data points that appear above the general trend have been marked in the graph to indicate that they were collected in January through March 2011 before a floor drain sealing procedure was implemented (see discussions of this matter in Sections 3.2 and 10.8 of U.S. EPA [2012a]). The sewer line has been discussed as a potential source of chloroform based on measurements described in the previous report (U.S. EPA, 2012a), although the sealing procedure appears to have been effective in blocking any subsequent vapor entry through the drains in the house. However, as described in the previous report, the contribution of sewer gases to chloroform indoor air concentrations cannot be ruled out prior to when the floor drain was sealed in March 2011.

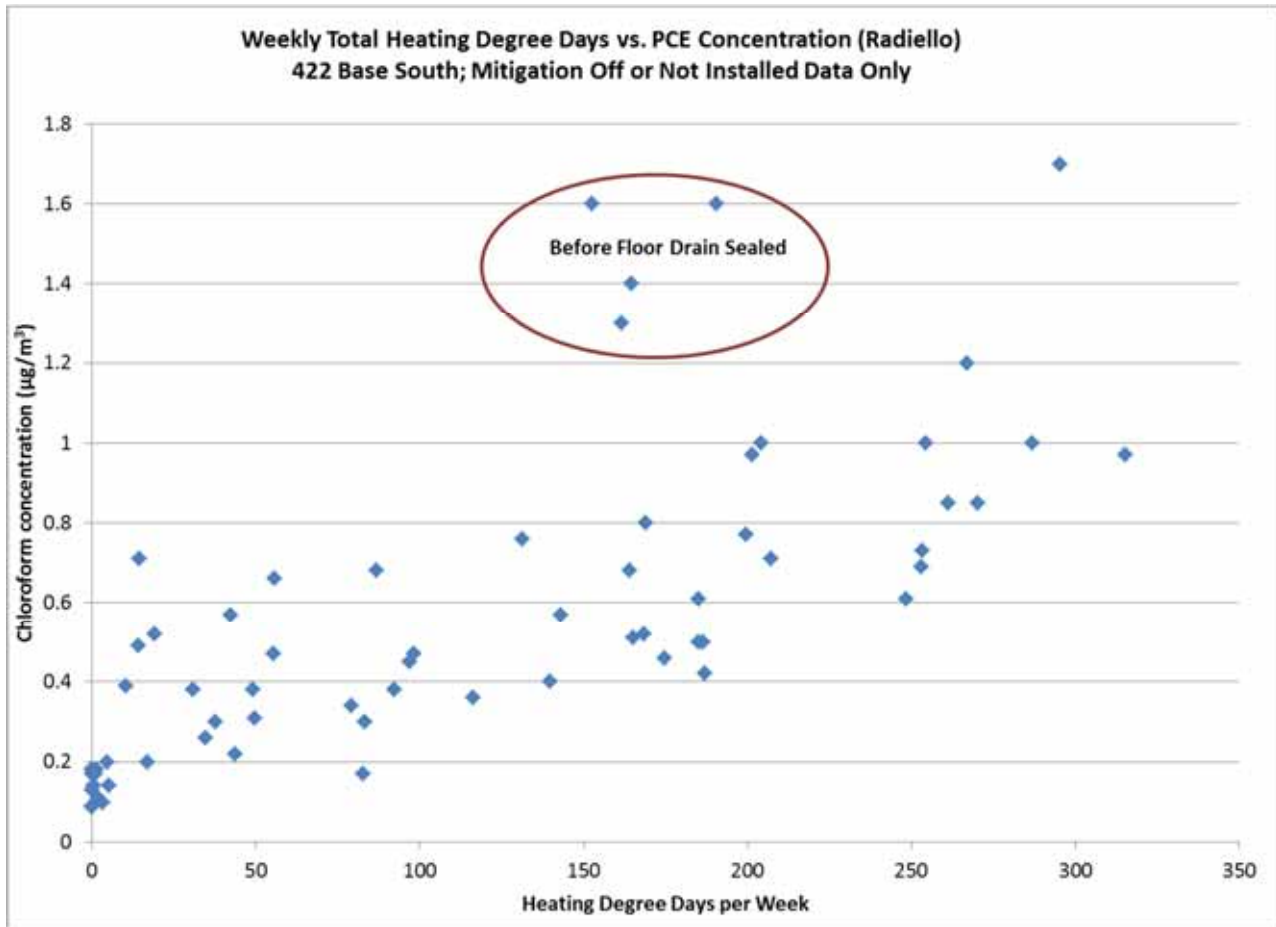


Figure 9-43. XY graph of heating degree days vs. chloroform concentration (weekly Radiello data).

9.2.2 Barometric Pressure Effect on VOCs

The 11 weeks with the highest PCE concentrations were all characterized by average barometric pressures in a relatively narrow range from 30.01 to 30.18 inches of mercury. There is no readily apparent direct physical mechanism to explain why these midrange barometric pressures may be associated with the highest PCE concentrations. Chloroform did not show the same relationship (graph not shown for brevity). It is possible that this is a fortuitous result or that this range of barometric pressures may be serving as a marker for some more causative meteorological variable.

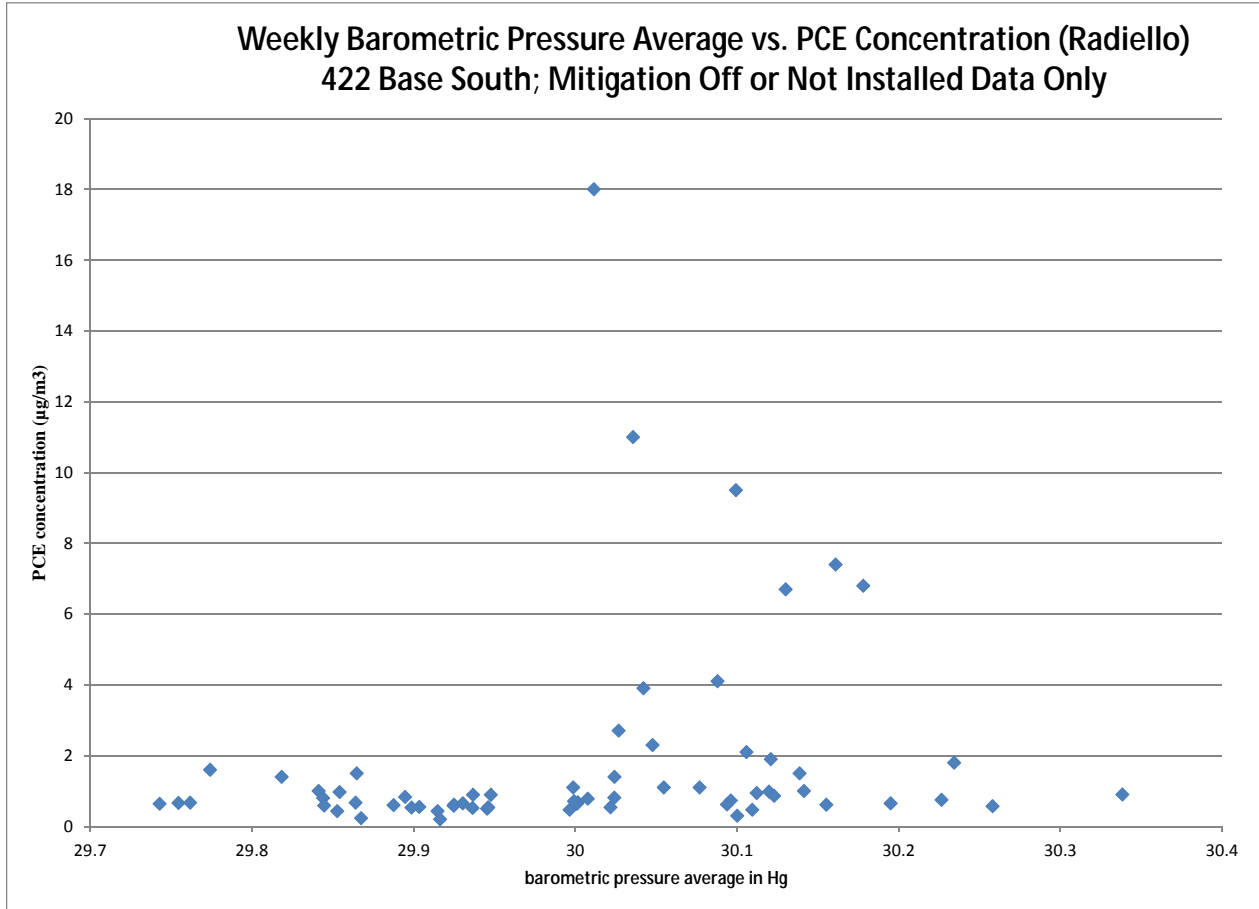


Figure 9-44. XY graph of average weekly barometric pressure vs. PCE concentration.

9.2.3 Precipitation Effects on VOCs

A rough relationship is visually evident between snow depth on the ground averaged over the week of sampling and the PCE concentration in indoor air measured with a passive sampler (Figure 9-45). This effect was less evident for chloroform (Figure 9-46) and absent for radon (Figure 9-47). In Section 6, we present data that indicate a partial agreement in time between the occurrence of even light snowstorms (even those not leaving an accumulation) and peaks in chloroform and PCE on-site GC data as well as radon.

The relationship between rainfall and PCE concentration in our data set is unclear (Figures 9-48 and 949). Although some of the highest PCE concentrations are associated with low rain weeks, which is almost surely attributable to those weeks being very cold, the rain sensor on the Vantage Vue instrument is not designed to melt snow. The chloroform data show no evident correlation to rainfall.

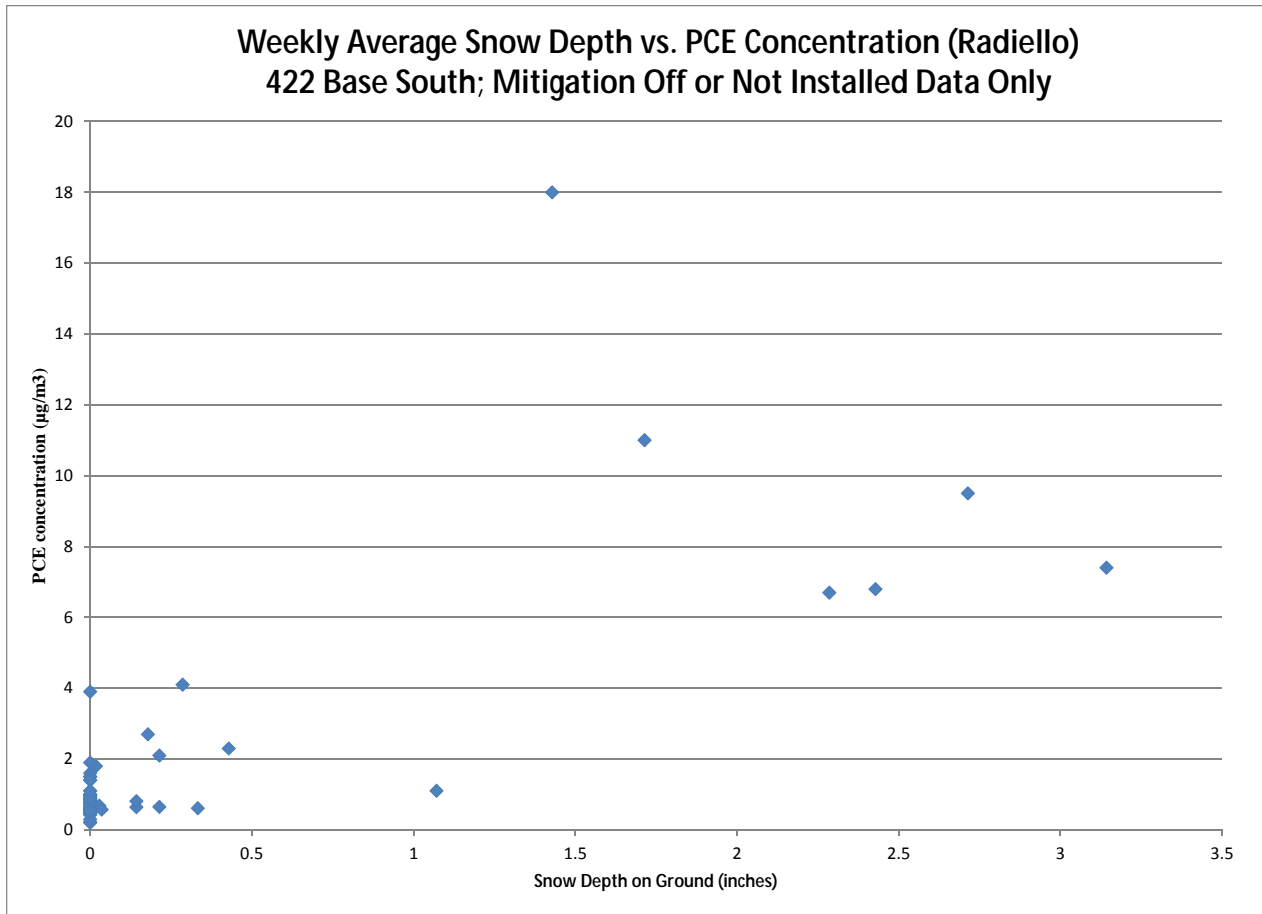


Figure 9-45. XY graph of weekly average snow depth vs. PCE concentration.

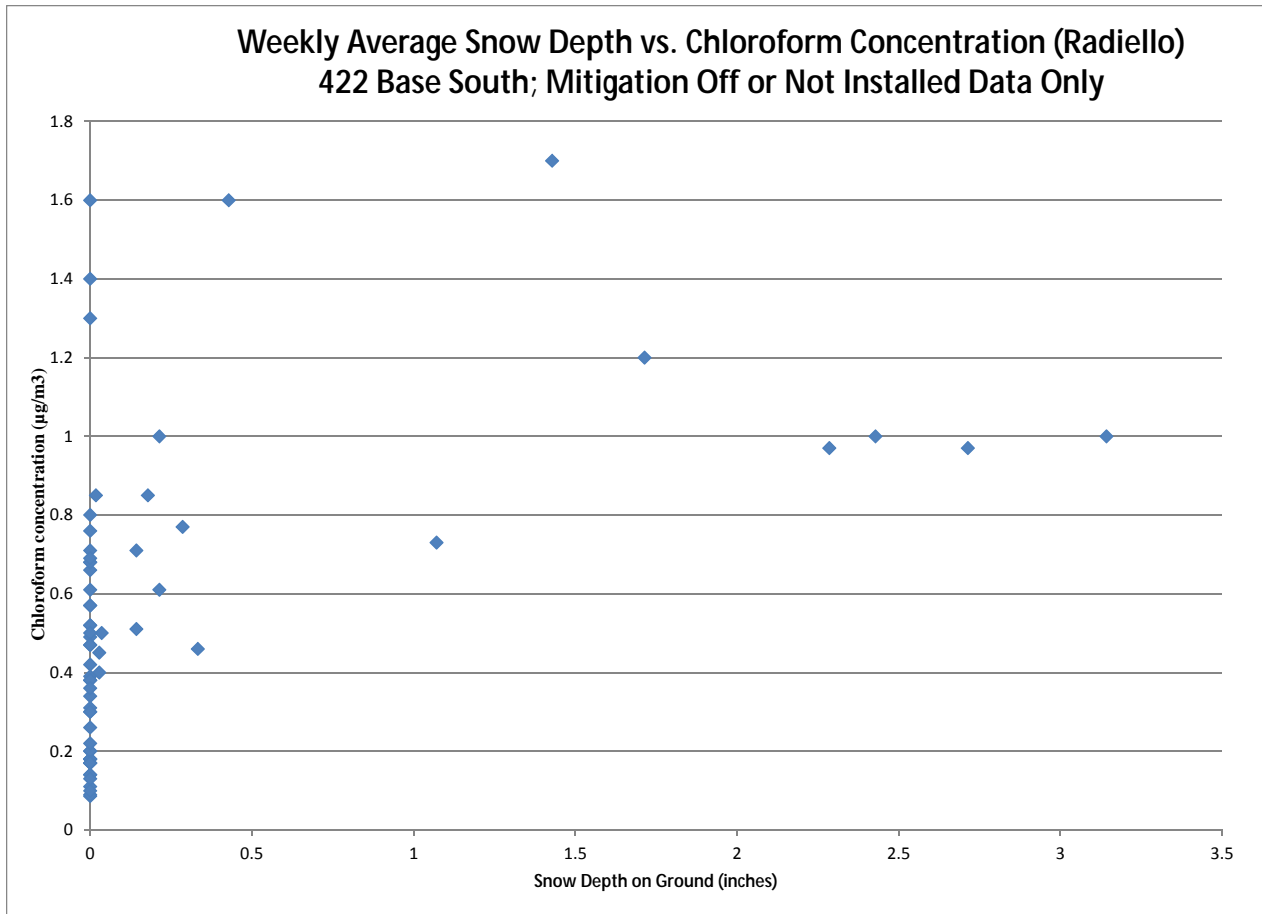


Figure 9-46. XY graph of weekly average snow depth vs. chloroform concentration.

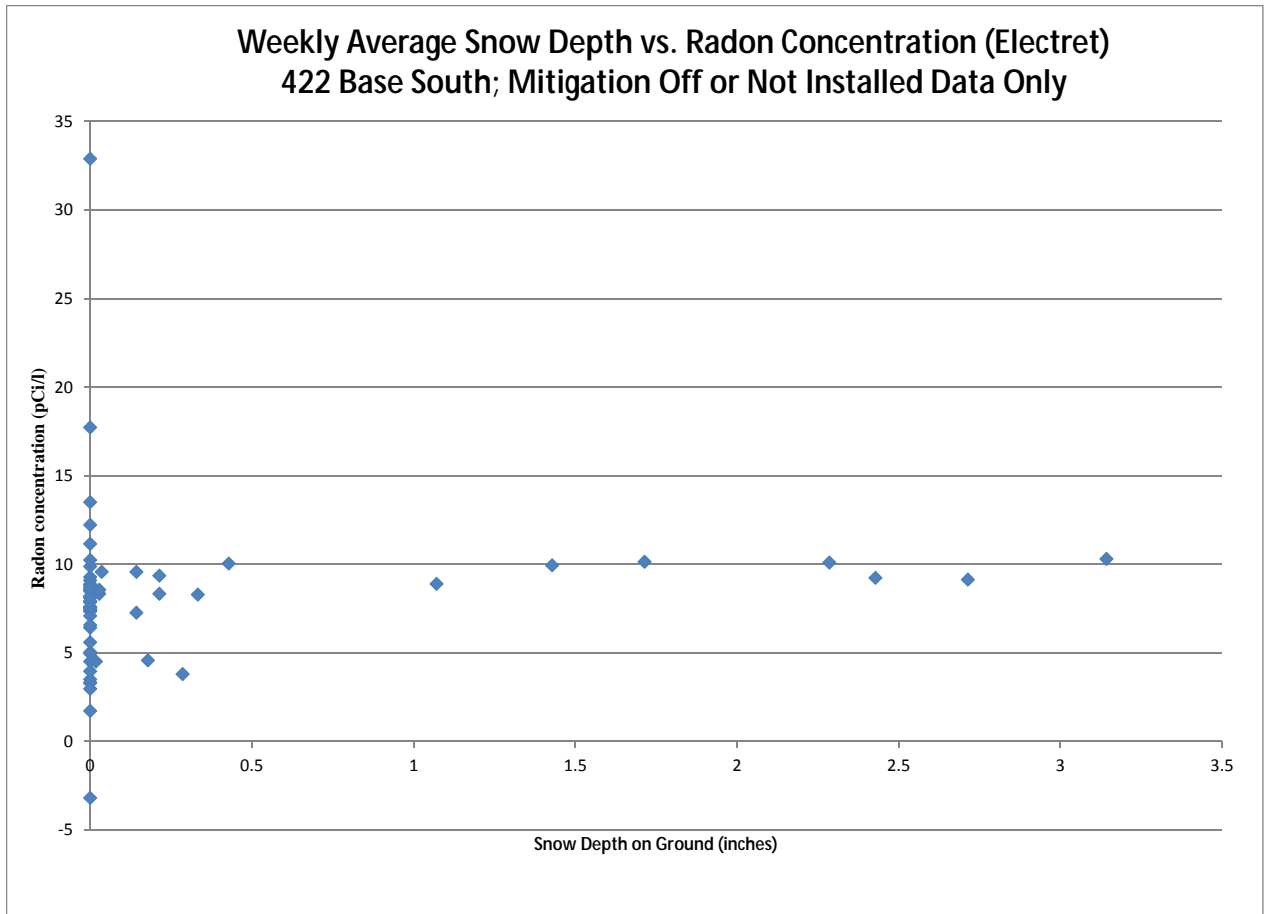


Figure 9-47. XY graph of weekly average snow depth vs. radon concentration.

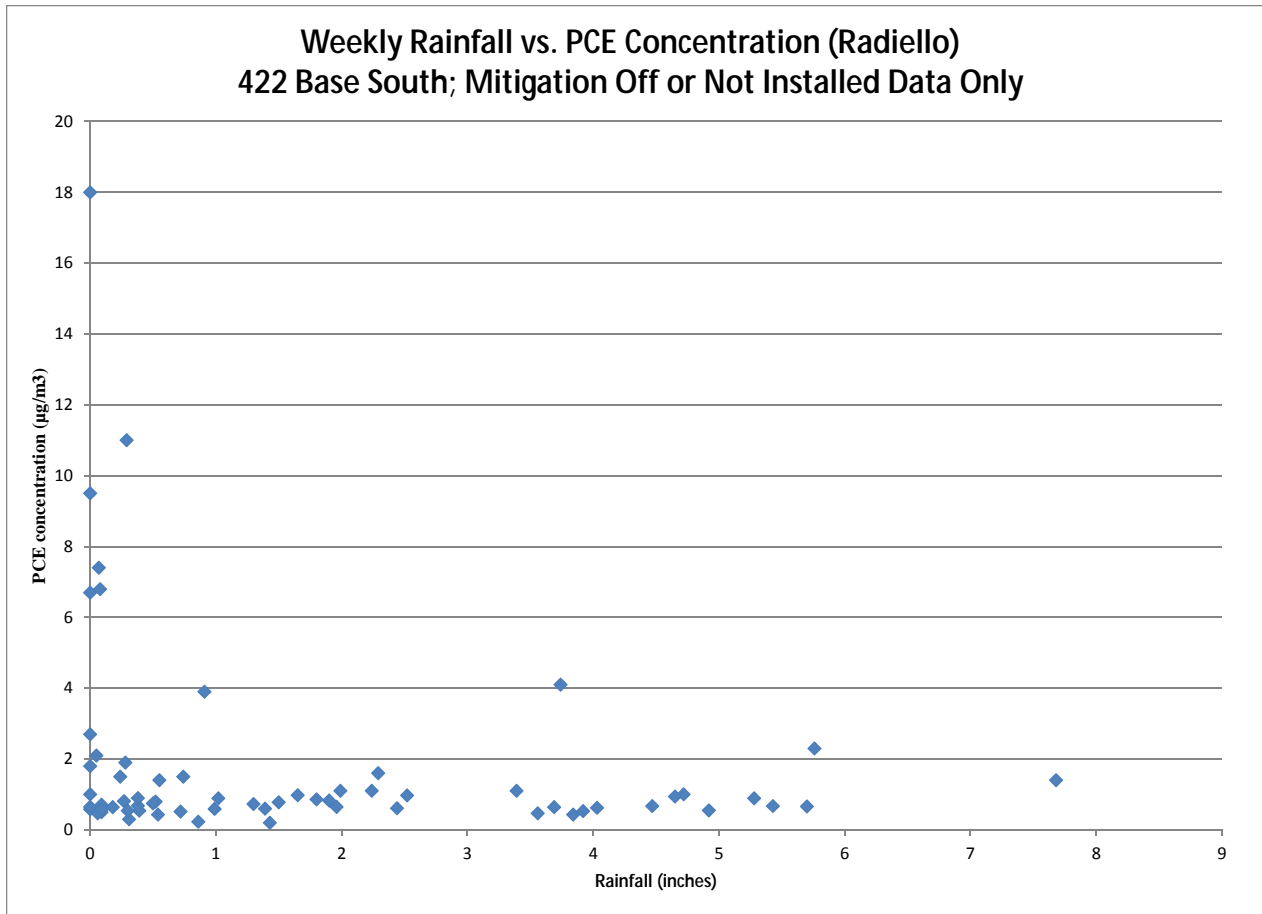


Figure 9-48. XY graph of total weekly rainfall vs. PCE concentration in indoor air.

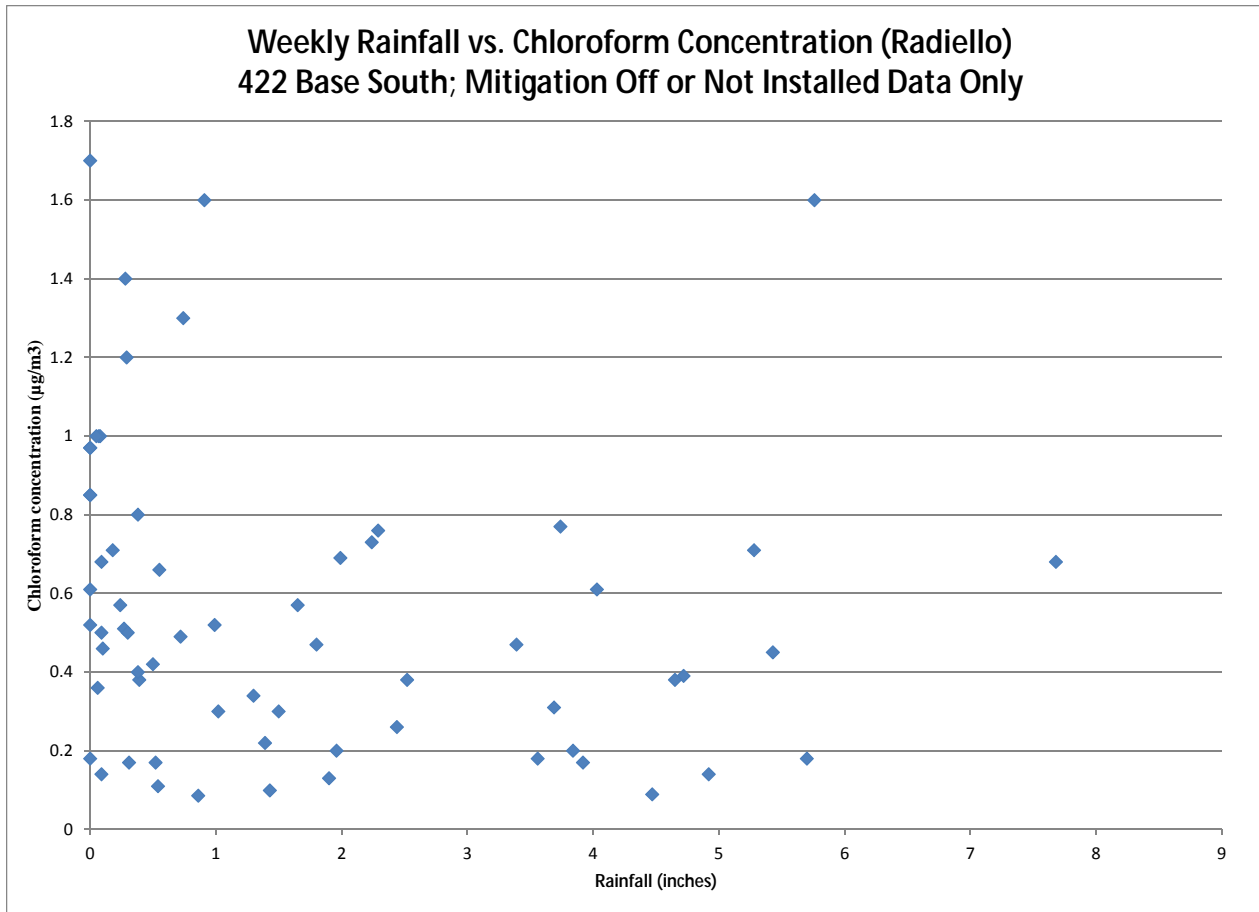


Figure 9-49. XY graph of total weekly rainfall vs. chloroform concentration in indoor air.

9.2.4 Effect of Wind on VOC Concentrations

The six highest weekly PCE concentrations in the 422 basement occurred during average wind weeks that were generally westerly, ranging from 205 to 296 degrees (Figure 9-50). That pattern of directionality agrees with the observations of high differential pressures into the 422 basement during winds in a similar range of direction (see Section 9.1.4), an analysis that used daily averaged data. Chloroform concentrations; however, are apparently independent of wind direction (Figure 9-51). West winds do seem to have some effect on increasing radon concentrations (Figure 9-52) as measured by weekly electret samplers, but the effect is not as dramatic as the effect on PCE. The same trend of west winds increasing radon concentrations was also seen in the daily AlphaGUARD data (Figure 9-14b).

The observed wind direction effects for PCE and radon agree with the predictions of a 3D numerical model (Abreu and Johnson, 2005) presented in U.S. EPA (2012d). As seen in Figures 9-53 and 9-54, VOC concentrations and subslab to indoor differential pressures are expected to increase on the side of the building opposite to the direction from which the wind is blowing. In this case, the 422 side of the duplex lies east of the 420 side. Therefore, the observation of higher vapor intrusion on the 422 side of the duplex under westerly winds fits the model prediction. Note that the modeled wind velocities in U.S. EPA (2012d) were 5 m/s (11 mph), which is very comparable to monthly average wind speeds in Indianapolis (4 to 6 m/s).

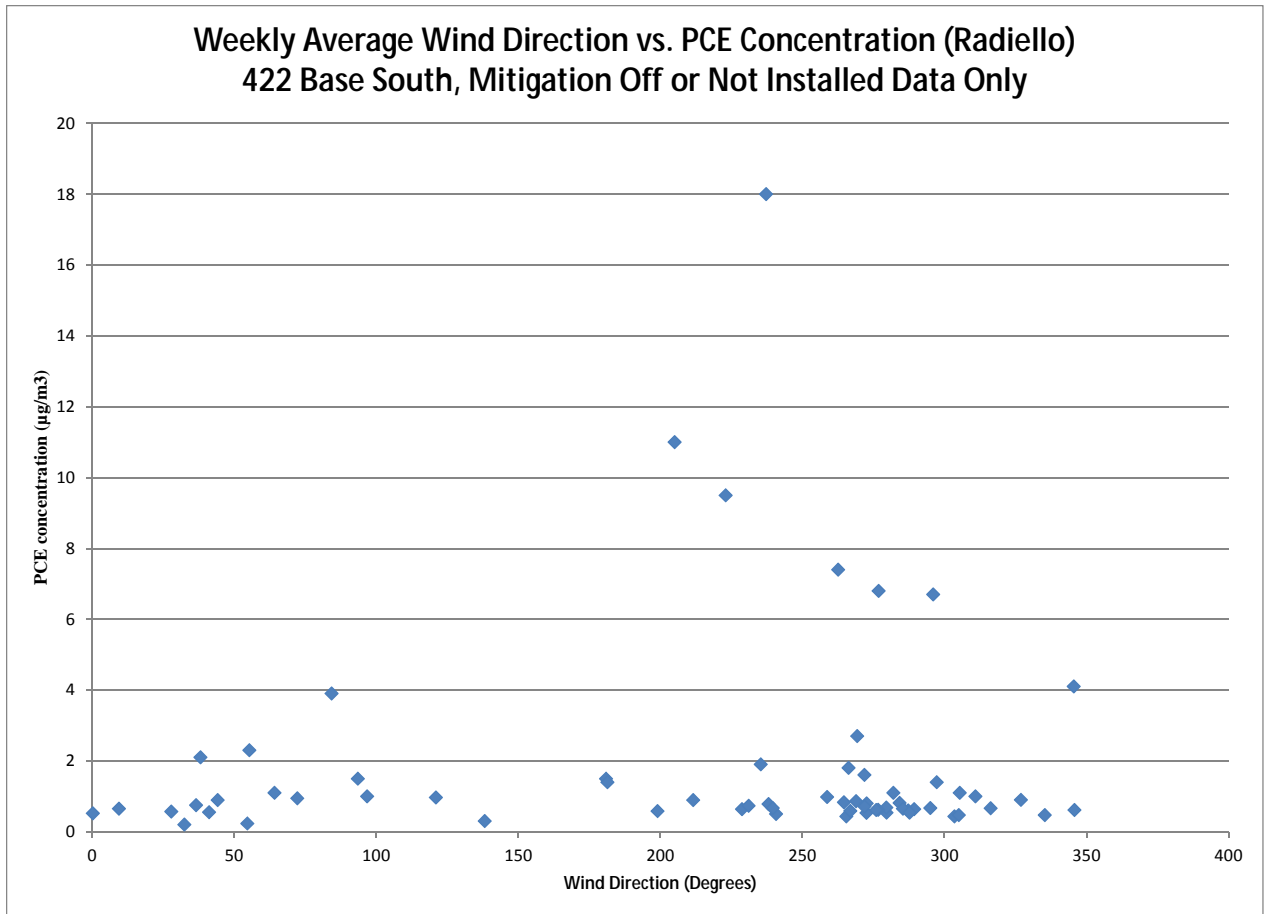


Figure 9-50. XY graph of wind direction vs. PCE concentration in indoor air in 422 basement.

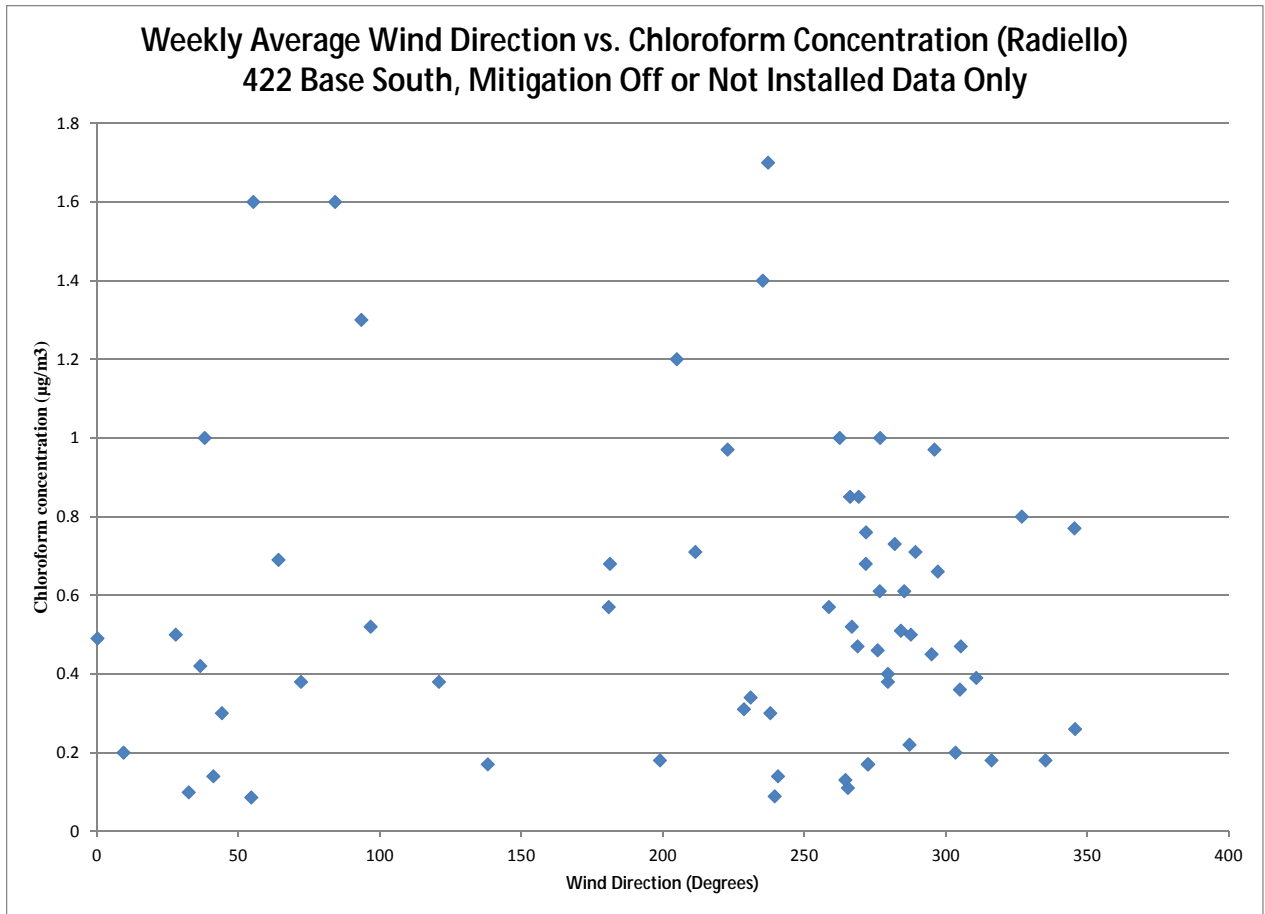


Figure 9-51. XY graph of wind direction vs. chloroform concentration in indoor air in 422 basement.

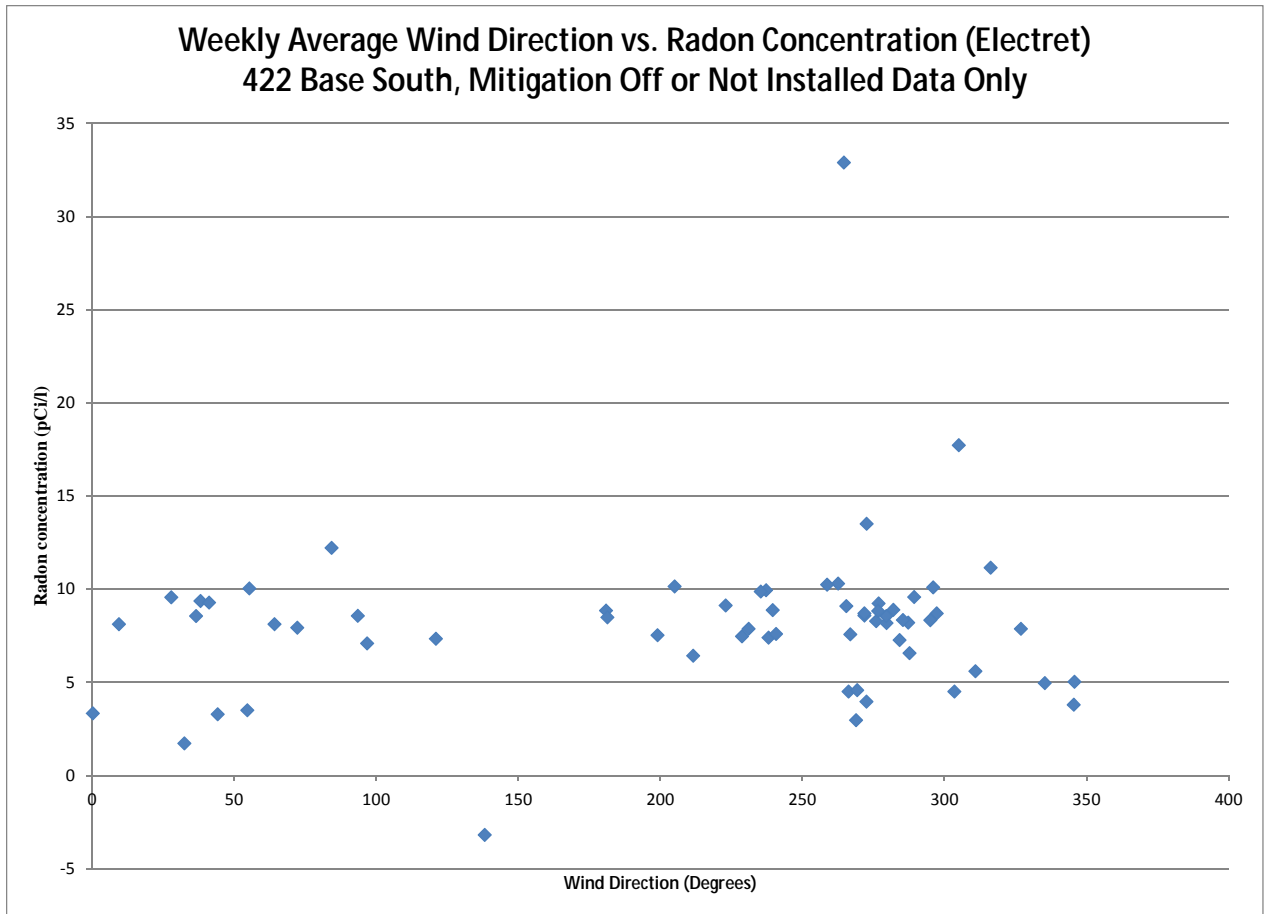


Figure 9-52. XY graph of wind direction vs. radon concentration in indoor air in 422 basement.

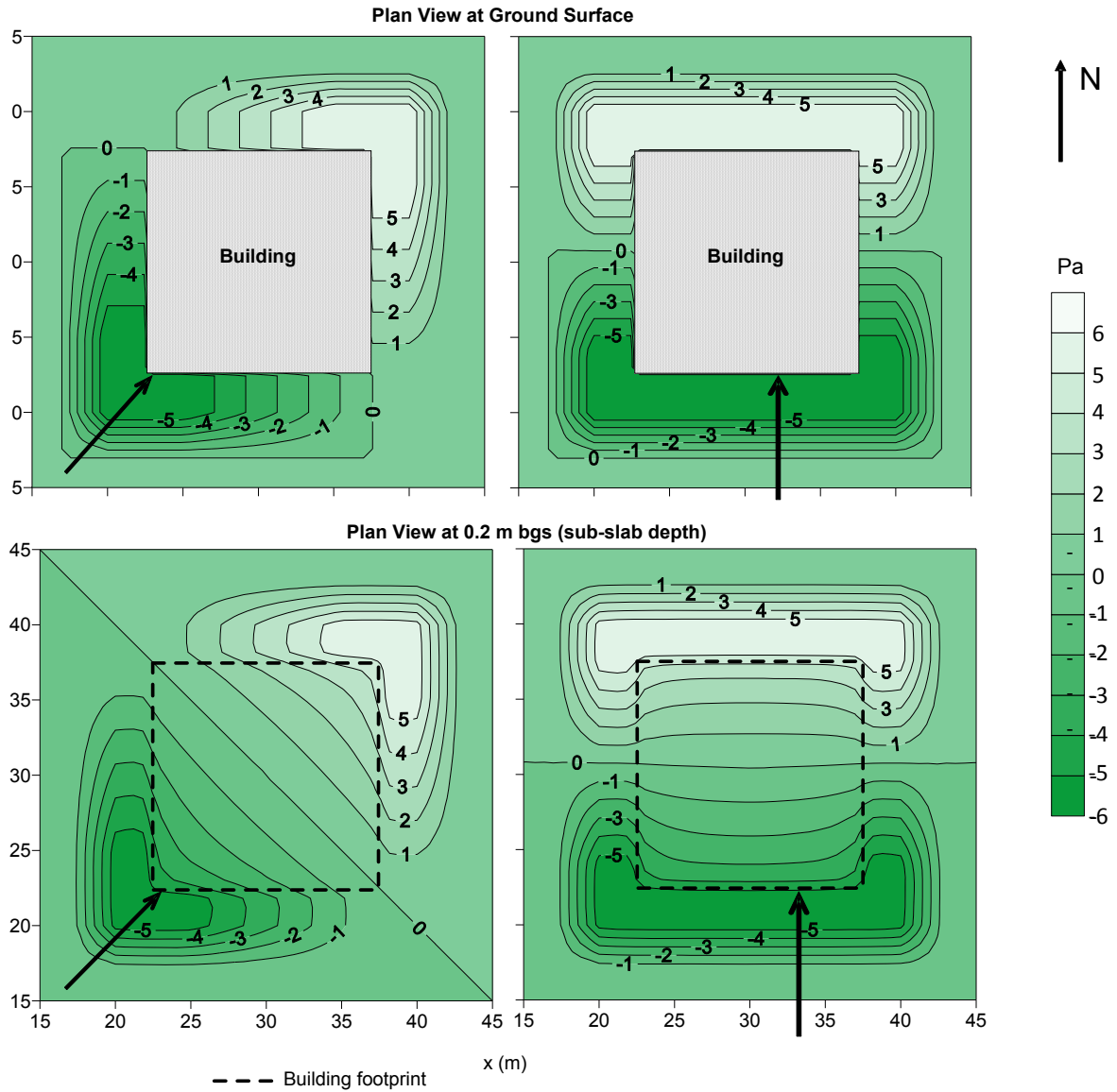


Figure 9-53. Modeled effect of building wind loads on ground surface and subslab gauge pressure distribution (adapted from U.S. EPA, 2012d).

The gauge pressure contour lines are in Pa; negative values reflect over-pressurization and positive values reflect under-pressurization. Wind velocity was constant at 5 m/s (11 mph).

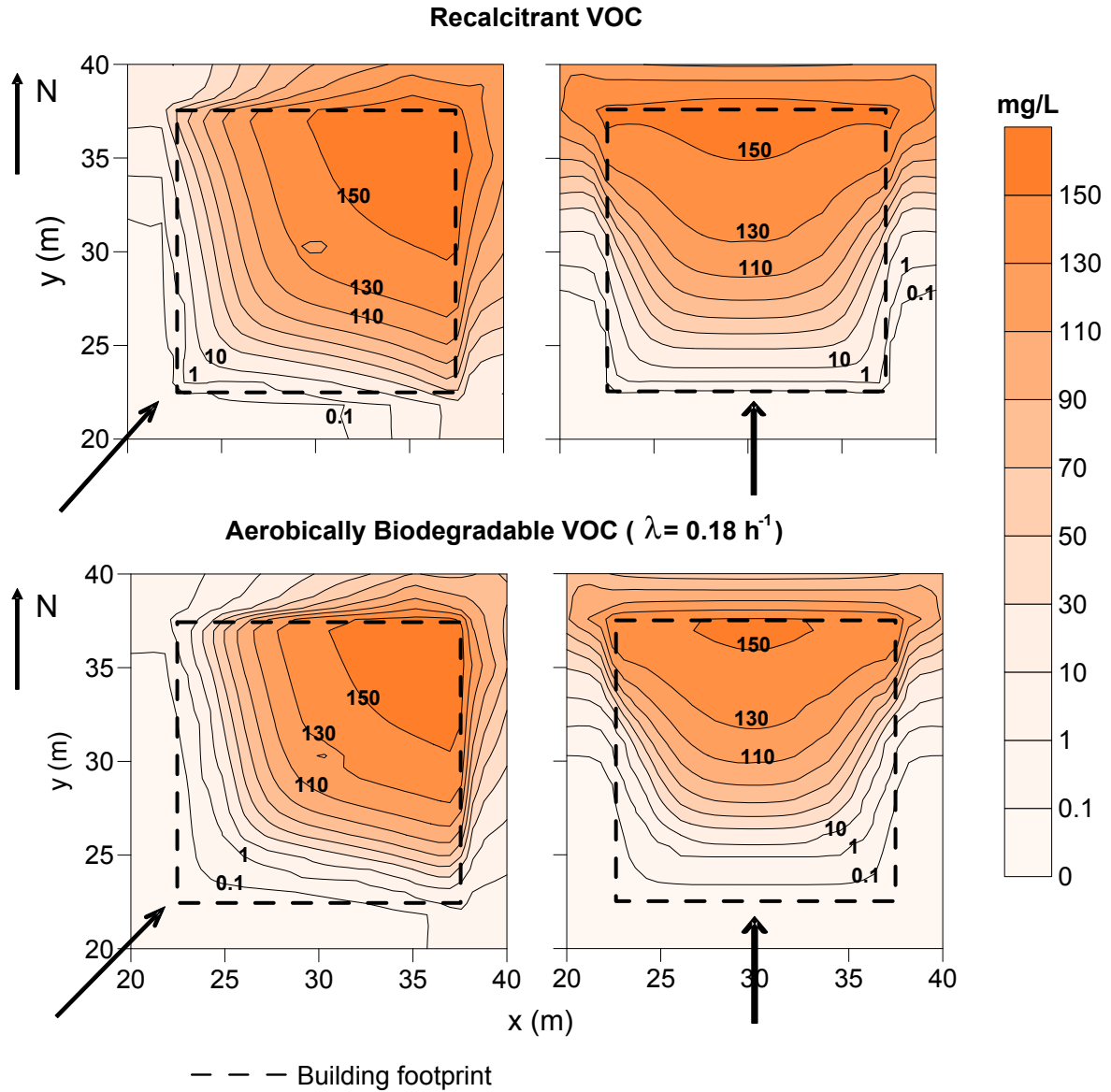


Figure 9-54. Modeled effect of building wind load on subslab soil vapor distribution for recalcitrant and aerobically biodegradable VOCs (adapted from U.S. EPA, 2012d).

The vapor concentration contour lines are in mg/L. The source vapor concentration is 160 mg/L. Wind velocity was constant at 5 m/s (11 mph).

A more subtle aspect of the data that may or may not be significant is that the radon maximum appears to occur under winds with more of a northwesterly component (245 to 309 degrees in **Figure 9-14b**; 264 to 305 degrees in **Figure 9-52**), while the PCE concentrations reach their maximum under somewhat more southwesterly conditions of 205 to 296 degrees in **Figure 9-50**. It is possible that this is attributable to the distribution of PCE in soil gas toward the southern edge of the building and the more uniform distribution of radon along the south-north axis (see Sections 5 and 6 of U.S. EPA [2012a] for a discussion of this spatial data). The 3D model would predict that winds with a southerly component might move more VOCs toward the center of the building.

No clear, physically rational relationship between wind speed and PCE concentration could be discerned (**Figure 9-55**), but a rough relationship of increasing chloroform with increasing wind speed was seen (**Figure 9-56**).

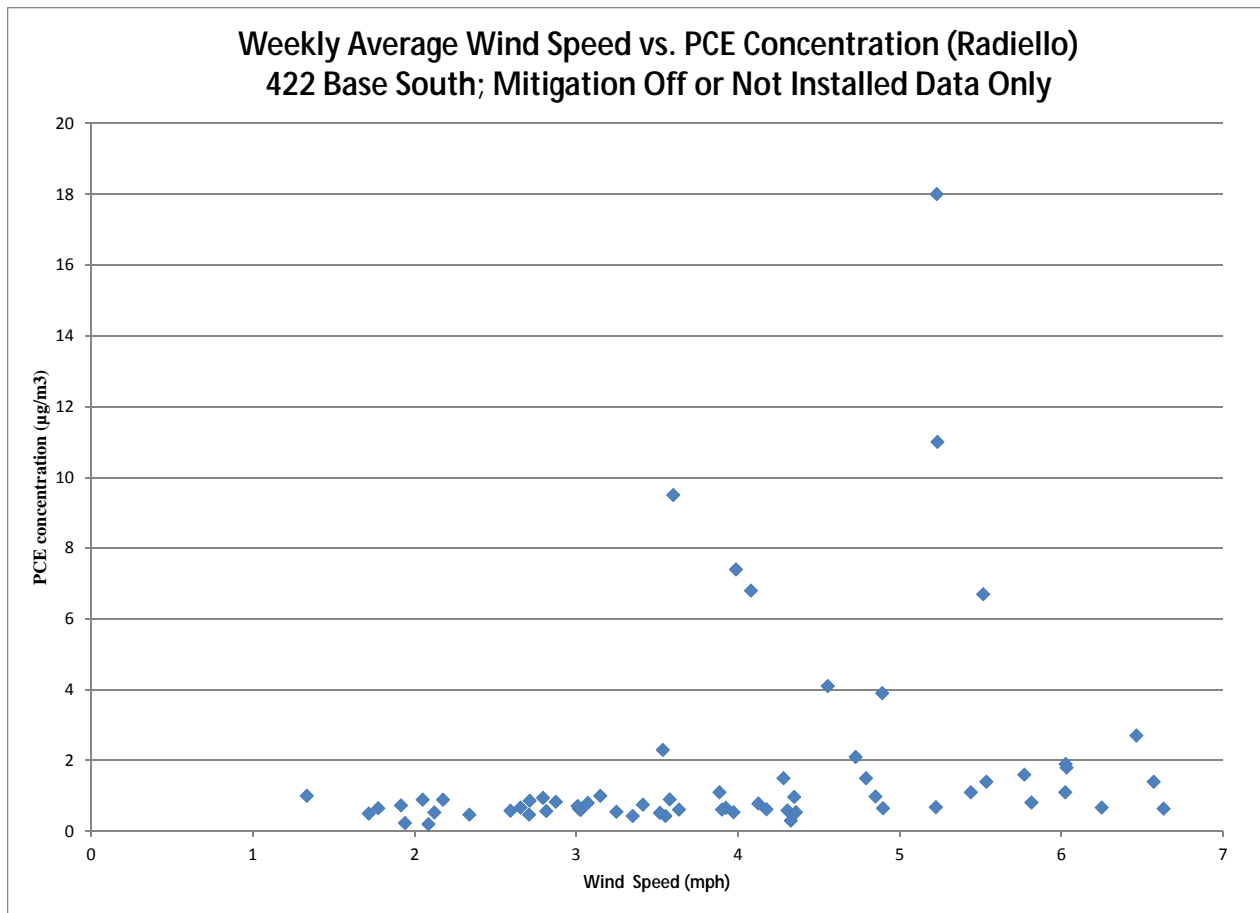


Figure 9-55. XY graph of wind speed vs. PCE concentration in indoor air in 422 basement.

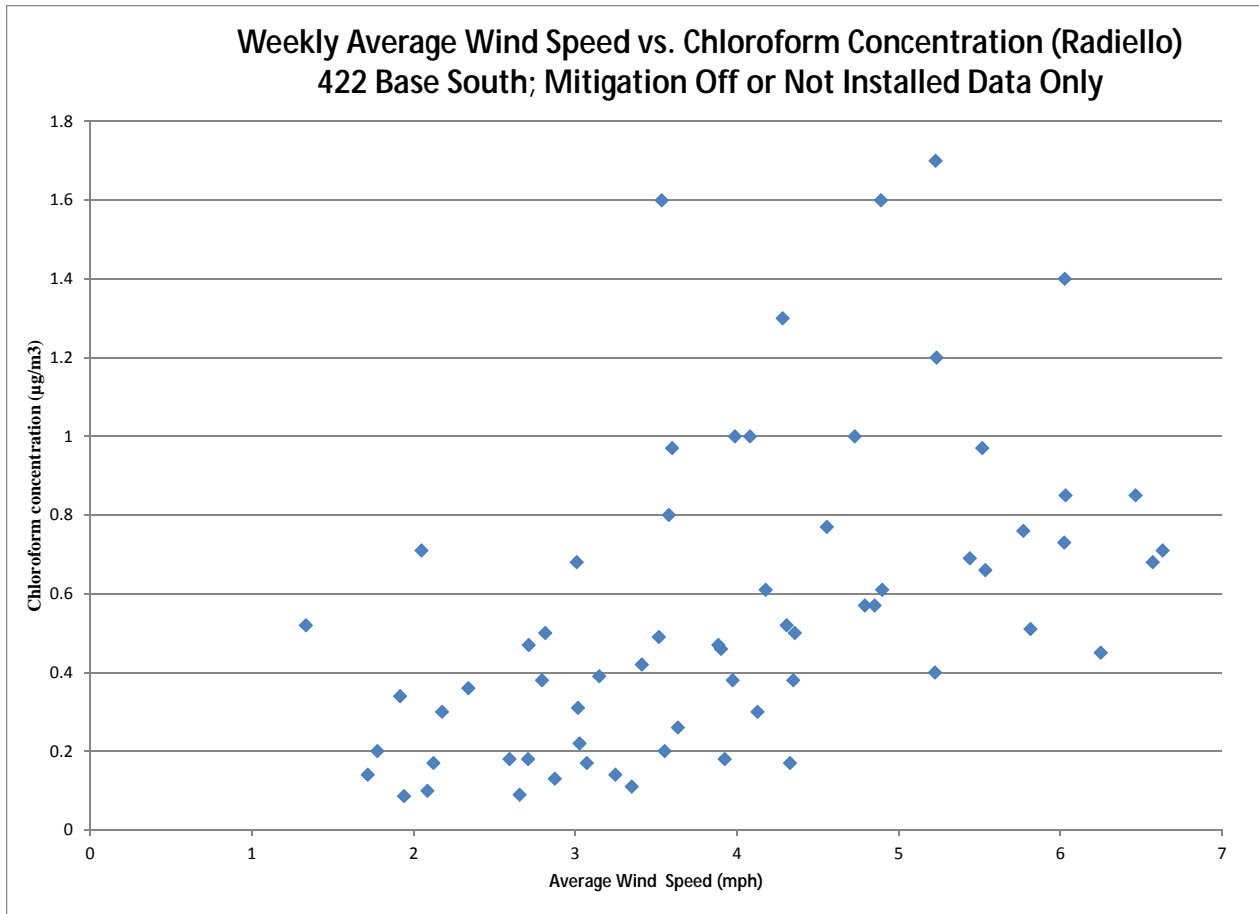


Figure 9-56. XY graph of wind speed vs. chloroform concentration in indoor air in 422 basement.

9.3 Summary of Meteorological Effects on Vapor Intrusion—Evidence Presented in Sections 6 and 9

Up to this point, we have analyzed relationships between meteorological variables and vapor intrusion in several ways in Sections 6 and 9. Before entering into a quantitative time series analysis in Section 10, we pause to provide the reader with a summary of the more qualitative analyses as **Table 9-1**. Similarities are seen, as advective flow considerations would suggest, between the meteorological conditions that drive high differential pressures and those that are associated with higher indoor and subslab concentrations. Although this is speculative at this point, the lines of evidence can be used to select particular variables to focus on in the quantitative analysis described in Section 10.

Table 9-1. Summary of Qualitative Lines of Evidence for Meteorological Factors Influencing Vapor Intrusion in This Study

(Blank cells reflect types of analysis not completed for a given parameter)

| | Snowfall | Snow or Ice Accumulation on Ground | Cold Exterior Temperatures (or substantial change in temperatures) | Rain Events/Rainfall Amount | Barometric Pressure Changes | West to NW Winds | High Wind Velocity |
|--|-------------------|--|--|-----------------------------|-----------------------------|--------------------------------|--------------------------------|
| Apparent Temporal Association with VOC Concentrations in Indoor Air (Section 6, also U.S. EPA, 2012a) | Yes | Yes | Yes | Possibly for chloroform | | | |
| Apparent Temporal Association with VOC Concentrations in Wall Ports or Subslab Ports (Section 6) | Yes | Yes | | | Weak | | Some |
| Apparent Temporal Association with Large Subslab to Indoor Differential Pressure Events (Section 9.1) | Yes in some cases | | Yes in some cases | | Yes in some cases | Yes in a few cases | Yes in a few cases |
| Apparent Trend in XY Graph of Meteorological Parameter vs. Subslab/Indoor Differential Pressure (Section 9.1 and U.S. EPA, 2012a) | | No | Yes | No | | Yes | No |
| Apparent Trend in XY Graph of Meteorological Parameter vs. VOC Concentration (Section 9.2) | | Yes for PCE, not definitive for chloroform | Yes | No clear relationship | Not definitive | Yes for PCE, No for chloroform | No for PCE, Yes for chloroform |

Table of Contents

| | | |
|--------|--|-------|
| 10.0 | Time Series Analysis..... | 10-1 |
| 10.1 | Time Series Analysis of Indoor Radon Data (AlphaGUARD) Aggregated with 1-Day Time Resolution | 10-2 |
| 10.2 | Correlation between Radon Concentration and Categorical Predictors | 10-18 |
| 10.3 | Correlation between Radon Concentration Time Series for 422 Basement South in 2011–2012 (X422BN-1) and Continuous Predictor Variables..... | 10-19 |
| 10.4 | Correlation between Radon Concentration Time Series for 422 2nd Floor Office (2011–2012) and Predictor Variables..... | 10-25 |
| 10.5 | Correlation between Radon Concentration Time Series for 422 Basement South (2012–2013) and Predictor Variables..... | 10-32 |
| 10.6 | Correlation between Radon Concentration Time Series for 422 Office on 2nd Floor and Predictor Variables | 10-37 |
| 10.7 | Correlation between VOC (Radiello) Time Series and Predictor Variables in 422 Basement South..... | 10-41 |
| 10.7.1 | Stationarity and Serial Correlation Analysis..... | 10-41 |
| 10.7.2 | Predictor Variables Modeled and Their Potential for Autocorrelation..... | 10-50 |
| 10.7.3 | Time Series Analysis Results for 2011–2012 Chloroform Data Set..... | 10-53 |
| 10.7.4 | Time Series Analysis Results for 2011–2012 PCE Data Set..... | 10-57 |
| 10.7.5 | Time Series Analysis of 422 Basement South Chloroform Data Set from the period Sept 2012–Apr 2013 | 10-65 |
| 10.7.6 | Time Series Analysis Results of 422 Basement South PCE Data from Sept 2012 through April 2013..... | 10-71 |
| | Addendum..... | 10-78 |

List of Figures

| | | |
|-------|---|------|
| 10-1. | Daily time series of radon concentrations (pCi/L) 422 basement north, 2011–2012 with rolling-averages, and autocorrelation (ACF) and partial autocorrelation function (PACF) plots..... | 10-4 |
| 10-2. | Time series of first difference of daily radon concentrations (pCi/L) 422 basement north, 2011–2012 with rolling-averages, and autocorrelation (ACF) and partial autocorrelation function (PACF) plots..... | 10-5 |
| 10-3. | Daily time series of radon concentrations (pCi/L) 422 basement north, 2012–2013 with rolling-averages, and autocorrelation (ACF) and partial autocorrelation function (PACF) plots..... | 10-6 |
| 10-4. | Time series of first difference of daily radon concentrations (pCi/L) 422 basement north, 2012–2013 with rolling-averages, and autocorrelation (ACF) and partial autocorrelation function (PACF) plots..... | 10-7 |
| 10-5. | Time series of daily radon concentrations: 422 office (2nd floor), 2011–2012 with rolling-averages, and autocorrelation (ACF) and partial autocorrelation function (PACF) plots..... | 10-8 |

| | | |
|--------|---|-------|
| 10-6. | Time series of first difference of daily radon concentrations: 422 office (2nd floor), 2011–2012 with rolling-averages, and autocorrelation (ACF) and partial autocorrelation function (PACF) plots..... | 10-9 |
| 10-7. | Time series of radon concentrations: 422 office (2nd floor), 2012–2013 with rolling-averages, and autocorrelation (ACF) and partial autocorrelation function (PACF) plots. | 10-10 |
| 10-8. | Time series of differences of daily radon concentrations: 422 office (2nd floor), 2012–2013 with rolling-averages, and autocorrelation (ACF) and partial autocorrelation function (PACF) plots..... | 10-11 |
| 10-9. | Correlation between radon concentration and predictors for both sites (basement north and office 2nd floor). Time period 2011–2012. NOTE: See Table 10-2 for “Plain Language” key of abbreviations used in this figure..... | 10-16 |
| 10-10. | Correlation between radon concentration and predictors for both sites (basement north and office 2nd floor). Time period 2012–2013. NOTE: See Table 10-2 for “Plain Language” key of abbreviations used in this figure..... | 10-17 |
| 10-11. | Time series plot, ACF and PACF for weekly Radiello chloroform. Location X422 basement south. Time period: Jan 5, 2011–Feb 15, 2012..... | 10-42 |
| 10-12. | Time series plot, ACF and PACF for first difference of weekly Radiello. Chloroform. Location X422 basement south. Time period: Jan 5, 2011–Feb 15, 2012..... | 10-43 |
| 10-13. | Time series plot, ACF and PACF for weekly Radiello PCE. Location X422 basement south. Time period: Jan 5, 2011–Feb 15, 2012..... | 10-44 |
| 10-14. | Time series plot, ACF and PACF for weekly chloroform. Location X422 basement south. Time period: Sept 26, 2012–April 10, 2013. | 10-46 |
| 10-15. | Time series plot, ACF and PACF for first difference weekly Radiello CHCl ₃ -2 (X422BaseS_Radiello_Weekly_CHCl ₃). Location X422 basement south. Time period: Sept 26, 2012–April 10, 2013. | 10-47 |
| 10-16. | Time series plot, ACF and PACF for weekly Radiello PCE-2 (X422BaseS_Radiello_Weekly_PCE). Location X422 basement south. Time period: Sept 26, 2012–April 10, 2013. | 10-48 |
| 10-17. | Time series plot, ACF and PACF for first difference weekly Radiello PCE-2 (X422BaseS_Radiello_Weekly_PCE). Location X422 basement south. Time period: Sept 26, 2012–April 10, 2013. | 10-49 |
| 10-18. | XY plot of weekly average snow depth vs. PCE concentration. | 10-63 |
| 10-19. | XY Plot of change in weekly average snow depth vs. PCE concentration..... | 10-63 |
| 10-20. | XY Plot of weekly average snow depth vs. change in PCE..... | 10-64 |

List of Tables

| | | |
|-------|--|-------|
| 10-1. | Significant Lags for ACF and PACF for Each Time Series and Regression Model | 10-12 |
| 10-2. | Significant Lag and AR Model by Predictor and Site Location | 10-13 |
| 10-3. | Model Parameters, Standard Errors by Model, Predictor and Time Series: All Radon Time Periods, Categorical Variables | 10-18 |
| 10-4. | Model Parameters, Standard Errors by Model and Predictor for X422baseN_AG_radon (X422BN-1): 2011–2012, Lag 1 Models..... | 10-20 |

| | | |
|--------|--|-------|
| 10-5. | Model Parameters, Standard Errors by Predictor for X422baseN_AG_radon (X422BN-1): 2011–2012, Lag 2 Models | 10-25 |
| 10-6. | Model Parameters, Standard Errors by Predictor for X422baseN_AG_radon (X422BN-1), Lag 4 Models | 10-25 |
| 10-7. | Model Parameters, Standard Errors by Predictor for X422office_2nd_AG_radon Concentration (X422OF2-1): 2011–2012, No Lag Terms in Model | 10-26 |
| 10-8. | Model Parameters, Standard Errors by Model and Predictor for Time Series Analysis of Radon in 422 Office: 2011–2012, Lag 1 Models..... | 10-26 |
| 10-9. | Model Parameters, Standard Errors by Predictor for X422office_2nd_AG_radon Concentration (X422OF2-1): 2011–2012. Lag 2 Models..... | 10-32 |
| 10-10. | Model Parameters, Standard Errors by Predictor for X422baseN_AG_radon (X422OF2-1): 2011–2012. Lag4 Models | 10-32 |
| 10-11. | Model Parameters, Standard Errors by Predictor for 422 Basement Radon: 2012–2013. No Lag Terms in Model..... | 10-33 |
| 10-12. | Model Parameters, Standard Errors by Model and Predictor for 422 Basement Radon: 2012–2013 Lag 1 Models | 10-33 |
| 10-13. | Model Parameters, Standard Errors by Predictor for X422office_2nd_AG_radon Concentration (X422OF2-2): 2012–2013. No Lag Terms in Model | 10-37 |
| 10-14. | Model Parameters, Standard Errors by Model and Predictor for X422office_2nd_AG_radon Concentration (X422OF2-2): 2012–2013 Lag 1 Models..... | 10-38 |
| 10-15. | Name, Periodicity, Time Period, and Location of Time Series (Outcome) Considered..... | 10-41 |
| 10-16. | Transformation and Terms Required by Time Series | 10-45 |
| 10-17. | Continuous Covariates by Time Period | 10-50 |
| 10-18. | Analysis for Outcome First Difference of X422BaseS_Radiello_Weekly_CHCl ₃ . Variables That Did Not Need Lag Terms. Period Jan 5, 2011–Feb 15, 2012..... | 10-53 |
| 10-19. | Analysis for Outcome X422BaseS_Radiello_Weekly_CHCl ₃ . Variables that Needed a lag-1 Term. Period Jan 5, 2011–Feb 15, 2012 | 10-54 |
| 10-20. | Analysis for Outcome X422BaseS_Radiello_Weekly_CHCl ₃ . Variables that Needed Lag-1 and Lag-2 Terms. Period Jan 5, 2011–Feb 15, 2012 | 10-58 |
| 10-21. | Time Series Analysis for Outcome First Difference of 422 Basement South PCE Concentration Variables that Did Not Need Lag Terms. Period Jan 2011 to Feb 2012 | 10-59 |
| 10-22. | Analysis for PCE Concentration at 42 Base South, Variables that Needed a Lag-1 Term. Period Jan 2011 to Feb 2012..... | 10-60 |
| 10-23. | Analysis for PCE Concentration at 422 Base South Variables that Needed Both Lag-1 Week And Lag-2 Week Terms. Period Jan 2011 to Feb 2012..... | 10-64 |
| 10-24. | Analysis for First Difference of Chloroform Concentration at 422 Basement South. Variables that Did Not Need Lag Terms. Period Sept 2012 to April 2013 | 10-66 |
| 10-25. | Analysis Chloroform Concentration at 422 Base South. Variables that Needed A Lag-1 One Week Term. Period Sept 2012 to April 2013 | 10-67 |
| 10-26. | Analysis for Chloroform Concentration at 422 Base South. Variables Needing Lag-1 And Lag-2 Week Terms. Period Sept 2012 to April 2013 | 10-71 |

10-27. Analysis for First Difference of 422 Base South PCE Concentration. Variables that Did Not Need Lag Terms. Period Sept 2012 to April 2013 10-72

10-28. Analysis for 422 Base South PCE Concentration. Variables that Needed A Lag-1 Week Term. Period Sept 2012 to April 2013 10-74

10-29. Analysis for PCE Concentration at 422 Base South. Variables Needing Both Lag-1 And Lag-2 Week Terms. Period Sept 2012 to April 2013 10-78

10.0 Time Series Analysis

Observations in time series are, in general, time-correlated and thus, not independent of each other. Modeling time series data using standard modeling approaches (e.g., usual regression analysis) will produce standard errors estimates that can be wrong and the results of the statistical tests used in hypothesis testing might be biased, which can affect the conclusions derived from them. We considered in this analysis only consecutive, evenly spaced observations (i.e., daily or weekly observations). Having missing and non-evenly spaced data introduces technical complications and requires modifications to the approaches adopted here.

Given the expected correlation between consecutive observations, a time series regression model usually includes past and present observations of the outcome of interest (e.g., radon concentration) as well as other predictors. In statistics, the term “predictor” refers to a variable that is possibly a predictor of the outcome under study, also known as (aka) the independent variable. Models that include past observations of the time series are called autoregressive models. Previous values of a time-ordered variable are referred as lagged terms. The order of the lag of the outcome (aka dependent), or y-variable, in a model determines the order of the time-series model. For example, if the model only includes the previous observation (denoted as $y(t-1)$) and predictors, it will be termed autoregressive model of order 1, first order autoregressive model or AR(1). A model can include lag terms of the predictors as well.

We conducted a statistical analysis to determine if any of the predictors available were good predictors of the variability of the outcome (e.g., radon or VOC concentrations). The analysis included the evaluation of the stationarity of the time series, determination of which autoregressive model to use, and determination of the lags for the predictor functions. Full and reduced model approaches were used to evaluate the significance of the reduced models.

A time series is termed “stationary” if the mean, variance, autocorrelation, etc. are all constant over time. The Augmented Dickey–Fuller test (ADF) (Said and Dickey, 1984) and the Phillips–Perron Unit Root Test (PP) (Perron, 1988) test for stationarity were also calculated to formally evaluate stationarity of the time series. The null hypothesis for the two tests is that the data is non-stationary. Small p-values (p-values < 0.05) suggest evidence favoring stationarity. It is desirable for a time series to be stationary—it does not necessarily mean that it is boring; only amenable to analysis. As Nau (2005a) states:

Most statistical forecasting methods are based on the assumption that the time series can be rendered approximately stationary (i.e., “stationarized”) through the use of mathematical transformations. A stationarized series is relatively easy to predict: you simply predict that its statistical properties will be the same in the future as they have been in the past! ... The predictions for the stationarized series can then be “untransformed,” by reversing whatever mathematical transformations were previously used, to obtain predictions for the original series. ... Thus, finding the sequence of transformations needed to stationarize a time series often provides important clues in the search for an appropriate forecasting model.

Another reason for trying to stationarize a time series is to be able to obtain meaningful sample statistics such as means, variances, and correlations with other variables. Such statistics are useful as descriptors of future behavior only if the series is stationary. For example, if the series is consistently increasing over time, the sample mean and variance will grow with the size of the sample, and they will always underestimate the mean and variance in future periods. And if the mean and variance of a series are not well-defined, then neither are its correlations with other variables. For this reason you should be cautious about trying to extrapolate regression models fitted to nonstationary data.

Predictor variables that are significantly associated with the transformed outcome variable are also associated with the original outcome variable.

10.1 Time Series Analysis of Indoor Radon Data (AlphaGUARD) Aggregated with 1-Day Time Resolution

Four radon time series are analyzed in this section; their time frames of the data and location are described below.

16. daily radon concentrations collected at 422 basement north between March 31, 2011, to July 23, 2012 (referred to as data set 422BN-1). This data set was constructed by averaging the AlphaGUARD data for each day.
17. daily radon concentrations collected at 422 basement north between September 7, 2012, and May 20, 2013 (referred to as data set 422BN-2)
18. daily radon concentrations collected at 422 office (2nd floor) between March 31, 2011, to July 23, 2012 (referred to as data set 422O2F-1)
19. daily radon concentrations collected at 422 office (2nd floor) between September 7, 2012, and May 20, 2013 (referred to as data set 422O2F-2)

The first step in the statistical analysis was the evaluation of the non-stationarity of the time series itself (shown as the left panels **Figures 10-1, 10-3, 10-5, and 10-7**). We evaluated the stationarity (or non-stationarity) of the radon time series using the ADF and PP tests. Small p-values suggest that a time series is stationary. A solution for non-stationarity is to calculate the first differences (y_t (outcome concentration at time t) – y_{t-1} (outcome concentration at time $t-1$)) and to use the difference variable as the outcome. We calculated the first differences ($y_t - y_{t-1}$) and evaluated their stationarity using ADF and PP tests. The first difference series (left panels in **Figures 10-2, 10-4, 10-6, and 10-8**) resulted in small p-values and a time series plot more consistent with the stationarity assumption (constant variance and constant mean). Thus, the first difference series is more suitable for analysis.

The fact that the first differences of our time series are more stationary than the time series themselves can also be seen visually by comparing the left-hand panels between **Figures 10-1 and 10-2; 10-3 and 10-4**, etc. In the case of constant mean, one should be able to have a straight line fit going across all the points in the series from left to right. A constant variance means that the series oscillates about the mean within a band of equal size. So if a time series goes up and down around a constant mean but the width of the max and min values is not constant, then we have non-constant variance.

The second step of the statistical analysis performed was determining the serial correlation. The autocorrelation function (ACF) plot (shown in the central panel in each of the **Figures 10-1 through 10-8**) shows the correlation between a time series and lags of itself. In the ACF plot, the lag 1 (day) is the correlation between all pairs of two consecutive observations. The broken horizontal blue lines on the ACF plots correspond to 95% confidence limits. For example in **Figure 10-1**, we can see that the radon concentration in the 422 basement on any given day is strongly related to what the radon concentration was the day before in the 422 basement. This makes intuitive physical sense because research has shown that radon concentrations can be controlled by weather variables (see Section 2), and the type of weather experienced from 1 day to the next is not completely random. For example, it is very unlikely that a 10°F day will be followed by a 90°F day. This autocorrelation is also to be expected because the indoor air concentrations only change gradually—with an air exchange rate of less than one air exchange per hour (see Section 12.1 in U.S. EPA [2012a] for air exchange rate measurements). Thus, even if the weather conditions did radically change, it would take several hours for that change to have its full influence on the indoor radon concentration.

Partial autocorrelations are shown in the right-most panel in each of the figures from **Figures 10-1** through **10-8**. A spike in the partial autocorrelation function (PACF) plot is the amount of correlation between a variable and a lag of itself that is not already explained by correlations at all lower order lags. For example, partial correlation value for 2 days is the correlation between day 0 and day 2 observations that is not already explained by including the lag 1-day correlation in a model. The broken horizontal blue lines on the PACF plots correspond to 95% confidence limits.

Note that if y_t (outcome concentration at time t) is correlated with y_{t-1} (outcome concentration at time $t-1$), and y_{t-1} is equally correlated with y_{t-2} (outcome concentration at time $t-2$), then we should also expect to find correlation between y_t and y_{t-2} . This behavior is called “propagation.” Thus, in theory, the correlation at lag 1 “propagates” to higher order lags, and as a result, some of the statistical significance (i.e., spikes crossing the 95% confidence bands in the ACF plot) observed in larger autocorrelations in the ACF plot might be the result of this “propagation.”

Figures 10-1 and **10-3** show the time series plots for time series 422BN-1 and 422BN-2, respectively. The ACF plot show significant autocorrelations for a large number of lags (lag 26 days and lag 14 days, **Figures 10-1** and **10-3**, respectively), but, as shown by the PACF plots (right panels in each figure), the autocorrelations at lag 2 days and above may be the result of the propagation of the autocorrelation at lag 1 day. To determine the true correlation between the outcome and the lag of the outcome after removing the effect of previous lags, we look at the PACF plots.

In **Figure 10-1**, the PACF plot for time series 422BN-1 shows significant autocorrelations up to lag 4 days (crossing the blue line either positively or negatively). Thus, the first data set acquired in the 422 basement for radon shows that the radon concentration on any given day is not random; it is related to the radon concentration on the 4 previous days. This also shows that the time series provides at least the equivalent of one independent measurement every 5 days. In **Figure 10-3**, the PACF plot for 422BN-2 shows significance at lag 1 day, suggesting that all the higher order autocorrelations are explained by the lag 1 day autocorrelation. The spike crossing the blue line in lag 3 could be the result of some random noise.

Figure 10-3; for the second data set acquired in 422 basement north shows only one significant autocorrelation at lag 1 day. The spike crossing the blue line in lag 11 could be the result of some random noise. **Figures 10-5** and **10-7** show the time series plots with corresponding ACF and PACF plots for time series data sets from the 422 second floor office, 422O2F-1 and 422O2F-2, respectively. The ACF plots show significant autocorrelations up to lags 26 days and 14 days for time series 422O2F-1 and 422O2F-2, respectively. A closer look at the PACF plots (right most panels) suggests that only lag 1 day was significant for these two time series.

Figures 10-2, 10-4, 10-6, and 10-8 show the ACF and PACF of first difference daily concentrations. PACF plots do not display any significant autocorrelation, suggesting there is no need to include a lag variable in a model using the transformed data. In lay terms, this means that although the radon concentration on Tuesday is dependent on the radon concentration on Monday and the radon concentration on Wednesday is, in turn, dependent on the radon concentration on Tuesday, the direction and magnitude of the *change* in radon that occurs between Monday and Tuesday is not connected to the direction and magnitude of the *change* in radon that occurs between Tuesday and Wednesday.

Daily Time Series of radon concentration (pCi/L). Location: X422 Base N AG
 ADF and PP tests pvalues = (0.01 , 0.01)

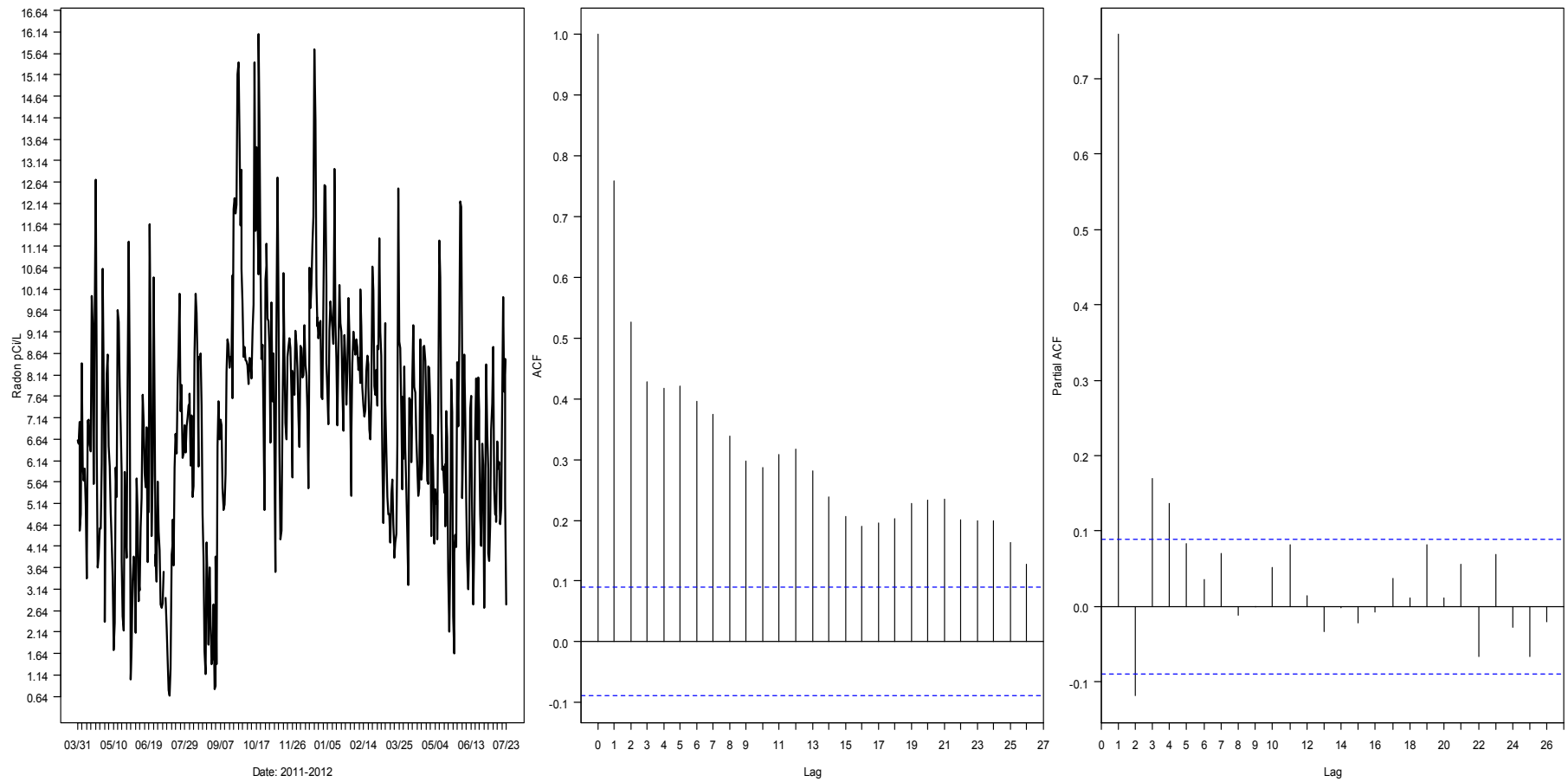


Figure 10-1. Daily time series of radon concentrations (pCi/L) 422 basement north, 2011–2012 with rolling-averages, and autocorrelation (ACF) and partial autocorrelation function (PACF) plots.

First Difference of Daily Time Series of radon concentration (pCi/L). Location: X422 Base N AG
 ADF and PP pvalues = (0.01 , 0.01)

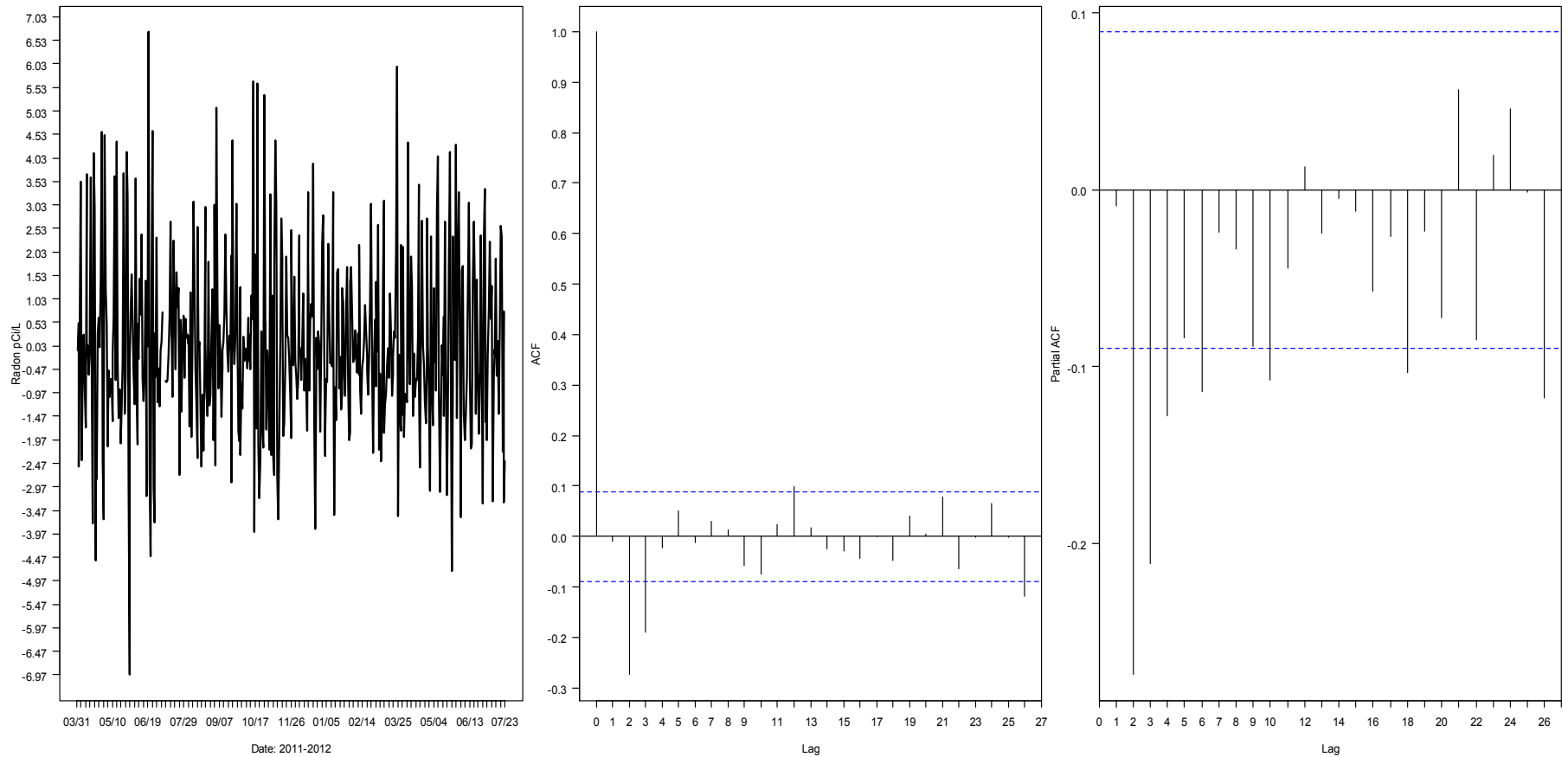


Figure 10-2. Time series of first difference of daily radon concentrations (pCi/L) 422 basement north, 2011–2012 with rolling-averages, and autocorrelation (ACF) and partial autocorrelation function (PACF) plots.

Daily Time Series of radon concentration (pCi/L). Location: X422 Base N AG
 ADF and PP tests pvalues = (0.43 , 0.23)

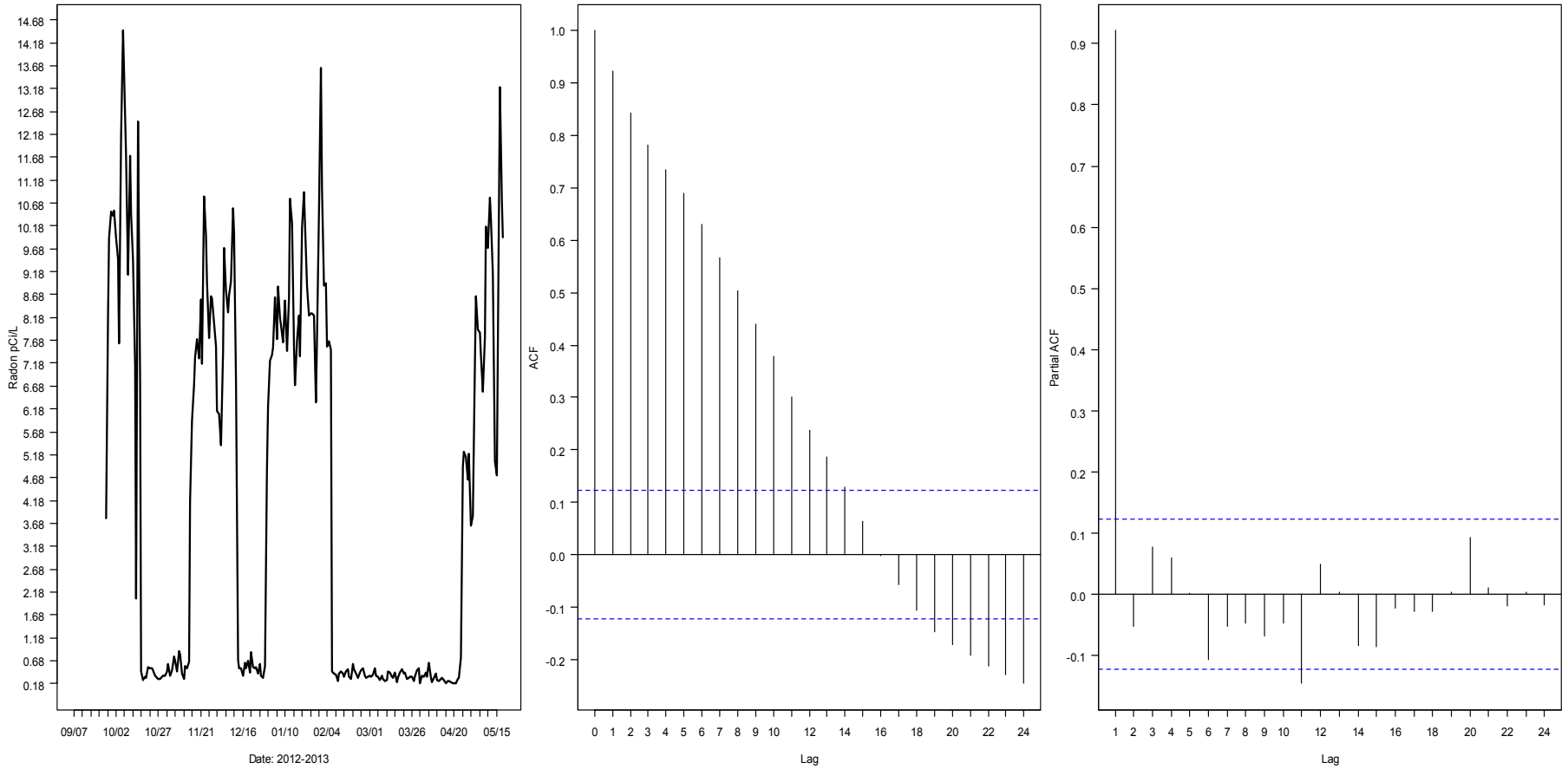


Figure 10-3. Daily time series of radon concentrations (pCi/L) 422 basement north, 2012–2013 with rolling-averages, and autocorrelation (ACF) and partial autocorrelation function (PACF) plots.

First Difference of Daily radon concentration (pCi/L). Location: X422 Base N AG
ADF and PP pvalues = (0.01 , 0.01)

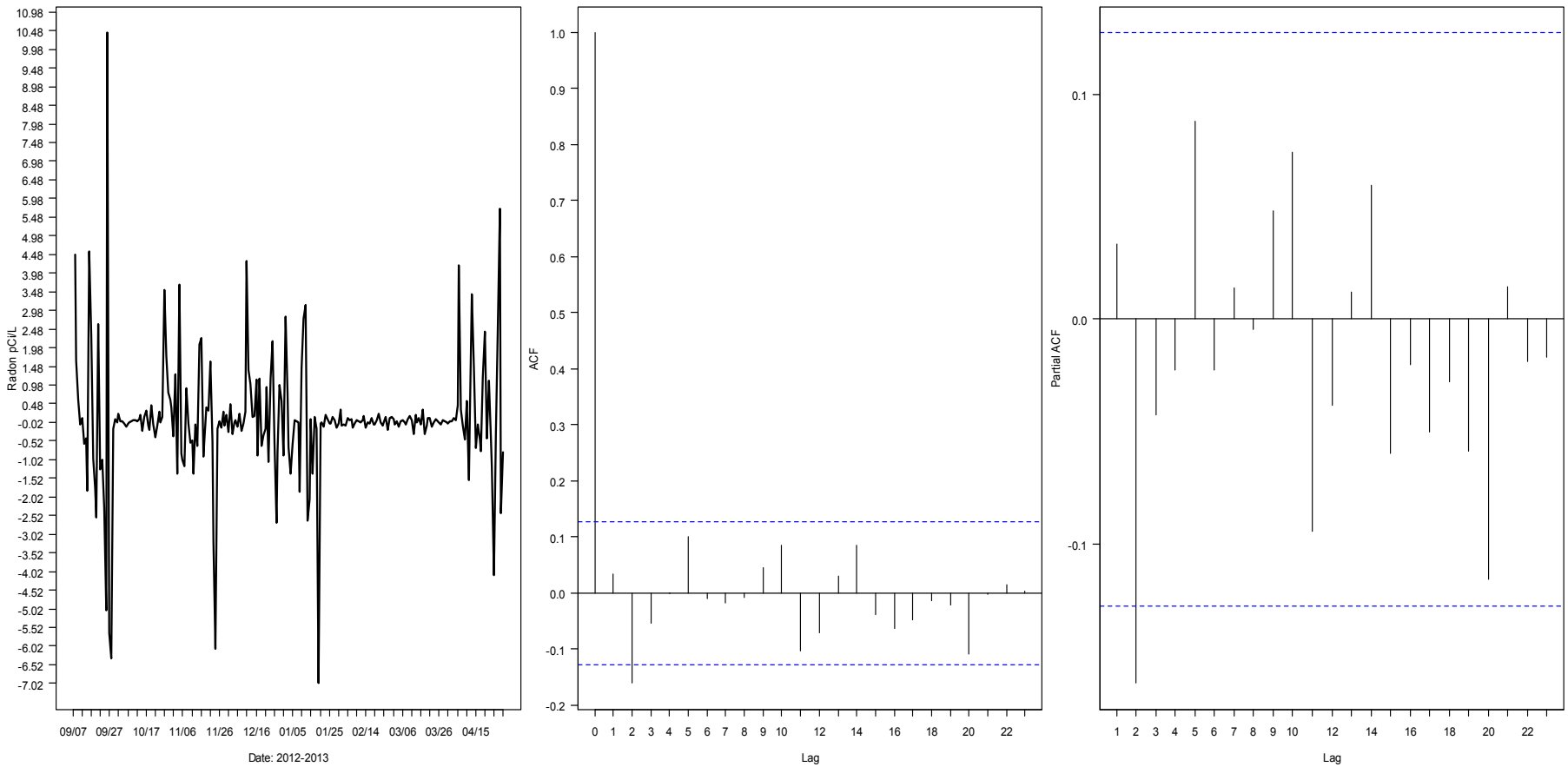


Figure 10-4. Time series of first difference of daily radon concentrations (pCi/L) 422 basement north, 2012–2013 with rolling-averages, and autocorrelation (ACF) and partial autocorrelation function (PACF) plots.

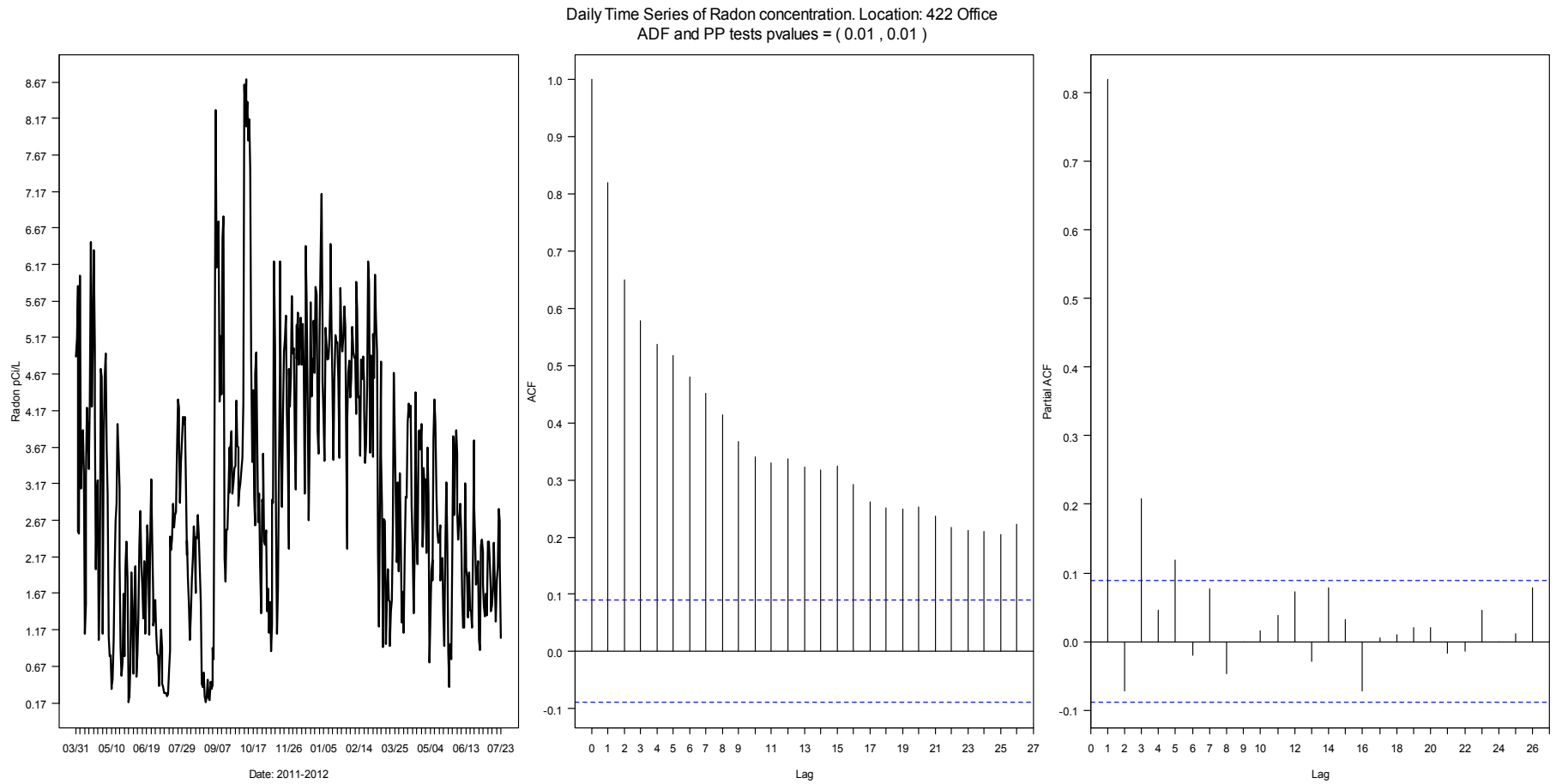


Figure 10-5. Time series of daily radon concentrations: 422 office (2nd floor), 2011–2012 with rolling-averages, and autocorrelation (ACF) and partial autocorrelation function (PACF) plots.

First Difference of Daily radon concentration (pCi/L). Location: X422 Base N AG
ADF and PP pvalues = (0.01 , 0.01)

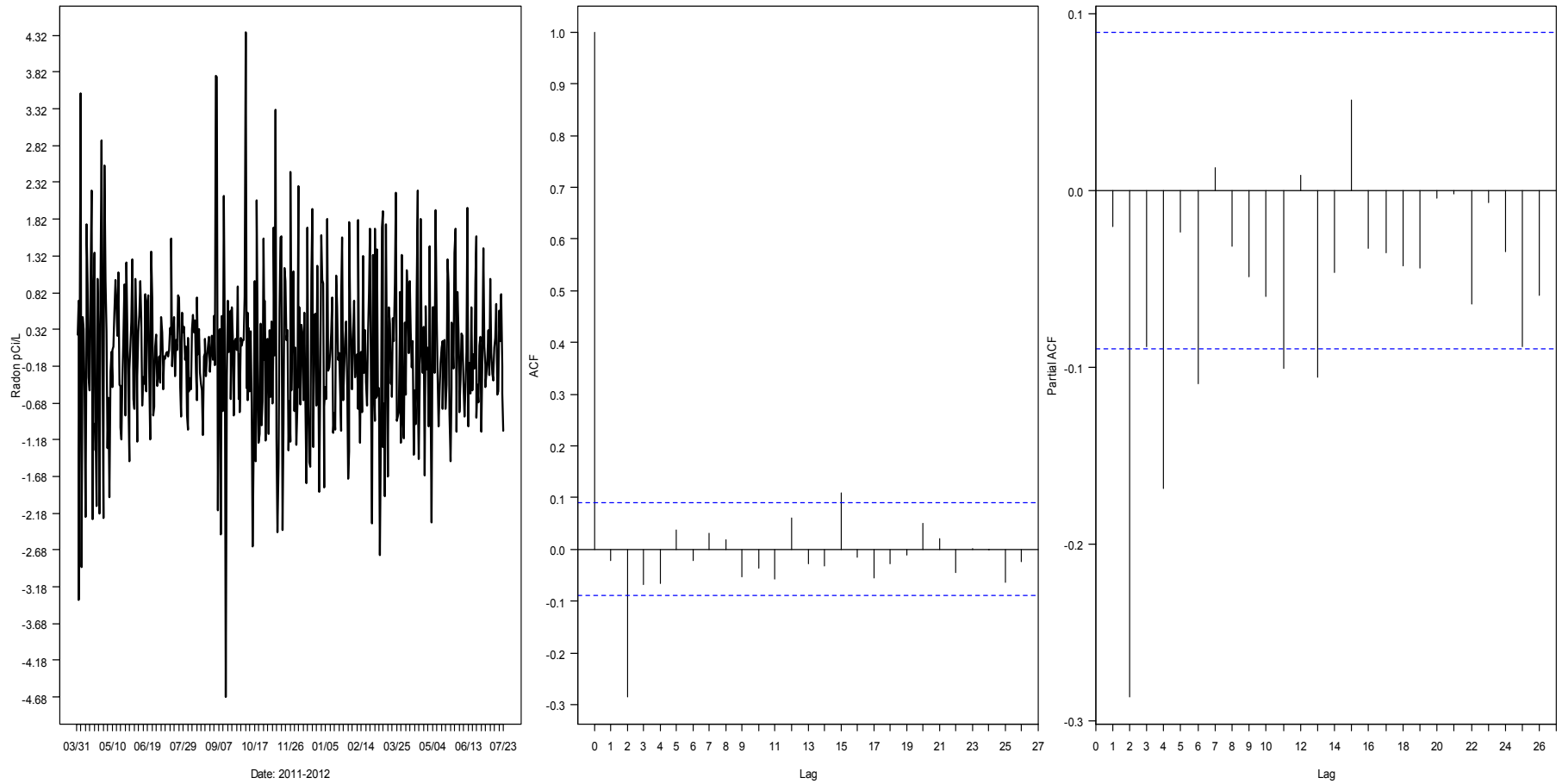


Figure 10-6. Time series of first difference of daily radon concentrations: 422 office (2nd floor), 2011–2012 with rolling-averages, and autocorrelation (ACF) and partial autocorrelation function (PACF) plots.

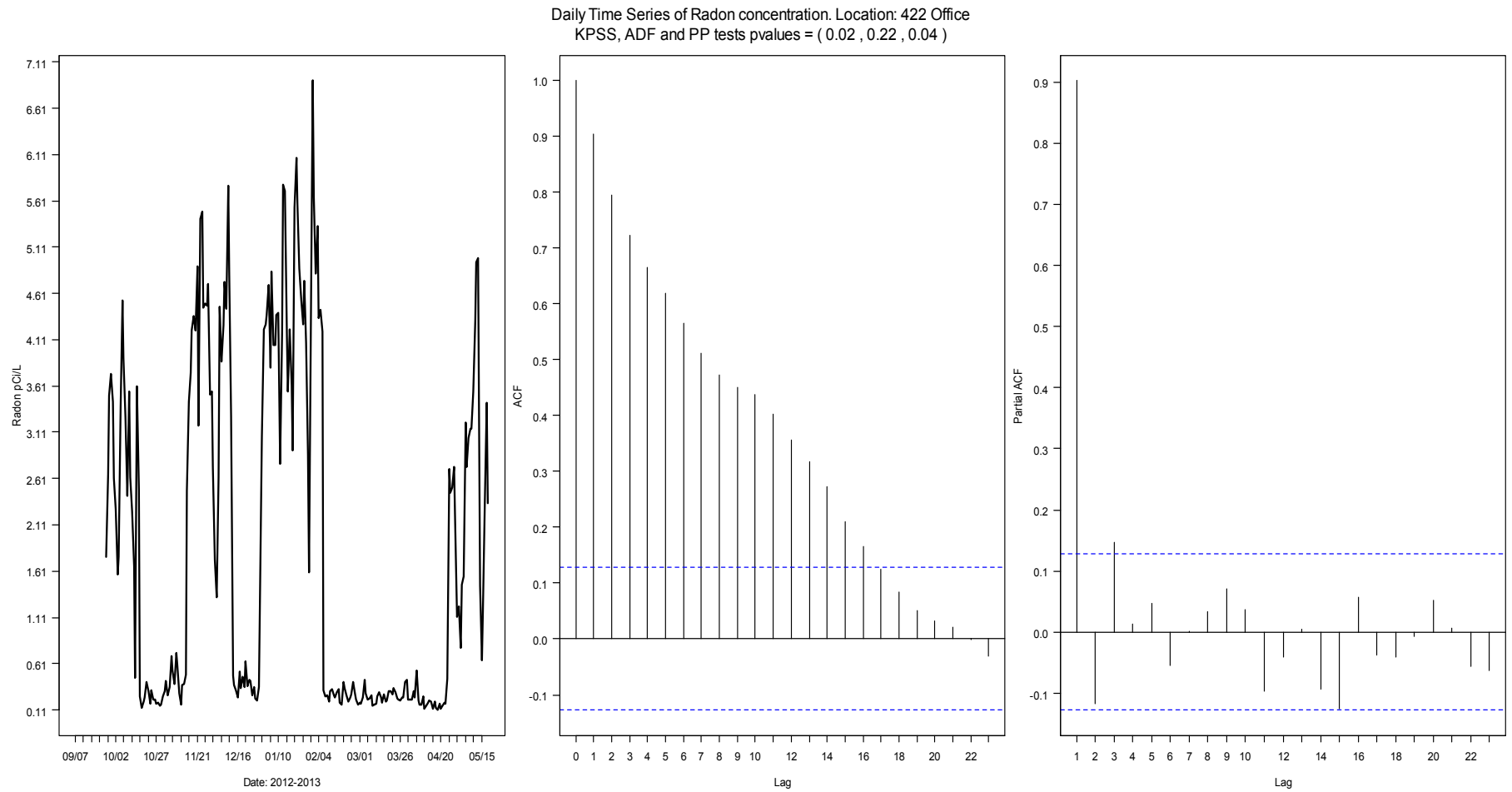


Figure 10-7. Time series of radon concentrations: 422 office (2nd floor), 2012–2013 with rolling-averages, and autocorrelation (ACF) and partial autocorrelation function (PACF) plots.

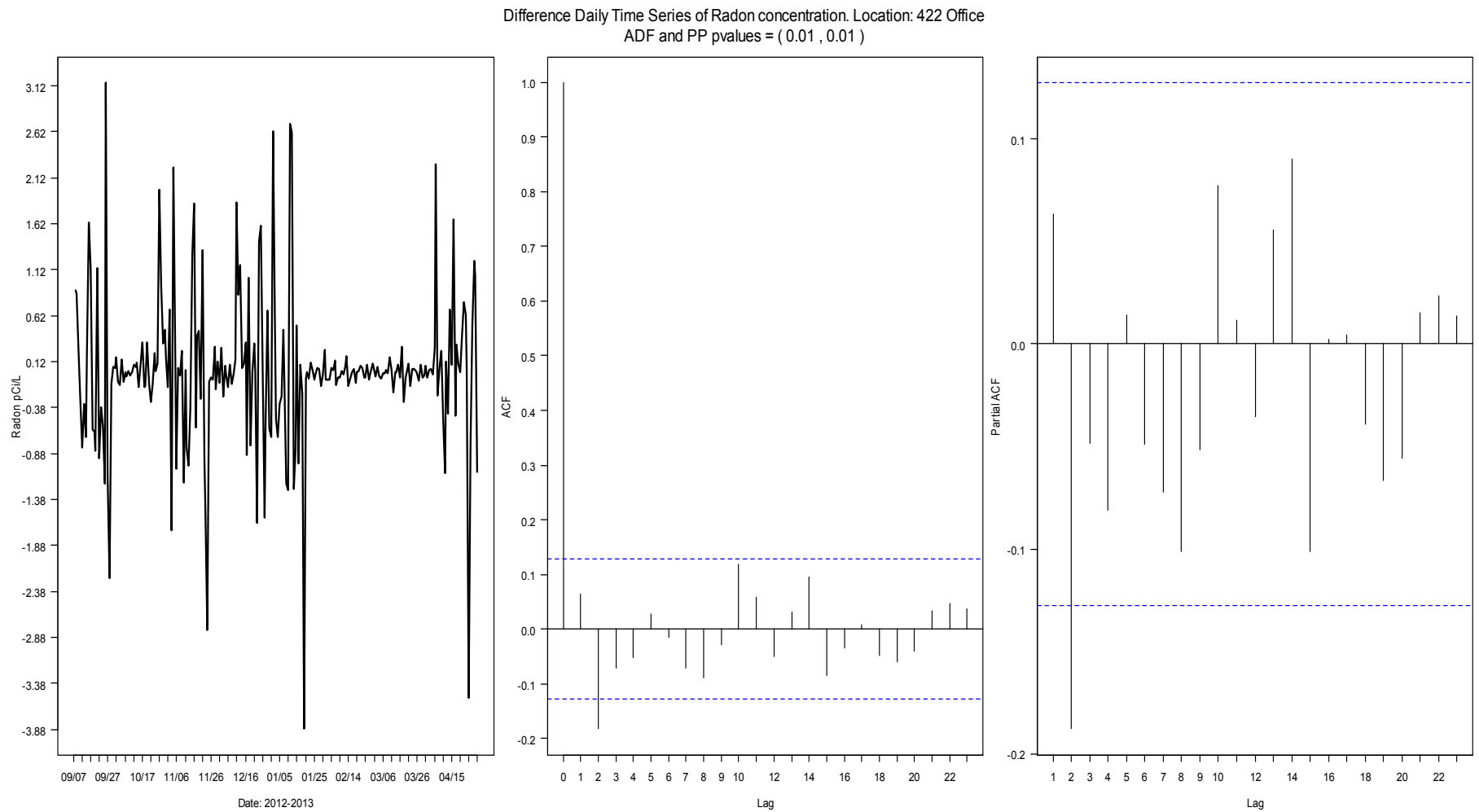


Figure 10-8. Time series of differences of daily radon concentrations: 422 office (2nd floor), 2012–2013 with rolling-averages, and autocorrelation (ACF) and partial autocorrelation function (PACF) plots.

The PACF plots (right-most panel in **Figures 10-1** through **10-8**) indicate the number of autoregressive terms (k) needed to explain the autocorrelation pattern in the time series. If the partial autocorrelation is significant at lag k and not significant at any higher order lags, then this suggests an autoregressive model (AR) of order k . **Table 10-1** shows a summary of the ACF and PACF analysis and the autoregressive model of order k (AR(k)) required for the original and the first difference time series. Since the first differences are stationary, a model with a first difference as the outcome was fit to the data. The shorthand AR model=0 denotes an autoregressive model for the first difference that does not incorporate any lag term of the outcome as predictor. For example: if $\text{Diff}(t) = \text{outcome}(t) - \text{outcome}(t-1)$, then a model with no lag term of the outcome will be $\text{Diff}(t) = \text{intercept} + \text{predictor}(t)$, i.e., $\text{outcome}(t) - \text{outcome}(t-1) = \text{intercept} + \text{predictor}(t)$. The results of this analysis make intuitive sense because the concentration of radon is expected to be influenced by the amount of vapor intrusion occurring over the past 12 hours, given the observed air exchange rate (0.3 to 0.8 air exchanges per hour, see Section 10.1 in U.S. EPA [2012a]).

Table 10-1. Significant Lags for ACF and PACF for Each Time Series and Regression Model

| Time Series Variable Name | Data Period | Original Data | | | First Difference | | |
|---------------------------|-------------|------------------|------|-----------------------------|------------------|------|-----------------------------|
| | | Significant Lags | | Autoregressive Model Chosen | Significant Lags | | Autoregressive Model Chosen |
| | | ACF | PACF | | ACF | PACF | |
| 422BN-1 | 2011–2012 | >26 | 4 | AR(4) | 1 | 0 | 0 |
| 422BN-2 | 2012–2013 | 14 | 1 | AR(1) | 1 | 0 | 0 |
| 422ON-1 | 2011–2012 | >26 | 1 | AR(1) | 1 | 0 | 0 |
| 422ON-2 | 2012–2013 | 14 | 1 | AR(1) | 1 | 0 | 0 |

The third step of the statistical analysis is to determine the order of the serial autocorrelation in each of the continuous predictors. **Table 10-2** displays the type of AR model for each continuous predictor. Most of the continuous predictors required only a lag 1 day term in the model. The significance of the association between radon concentration and the categorical variables available was studied separately.

Also listed in **Table 10-2** are plain language explanations for the predictor variables used in this analysis. Next, for each continuous variable listed in **Table 10-2**, a full or saturated model was fit to the time series. In each time series analysis, the first difference was the dependent or outcome variable modeled because it passed the test for being stationary. The term “full model” or “saturated model” refers to a model that includes an intercept, the predictor, all needed lags of the predictor (as specified in **Table 10-2**), and any control variable. The larger lag term of the predictor variable in the full or saturated model was dropped from the list of predictors and the resulting first “reduced” model was fit. The next lag-term was then dropped from the list of predictors and a second reduced model was fit to the data. This process continued until all lag terms of the predictors were removed from the previous model.

A control variable is a variable that can affect the association between the dependent variable and other predictors in the model. In this analysis, the variable `Mitigation_status_daily` was considered a control variable since it was expected to have a dramatic effect on the behavior of the vapor intrusion process. It was included in the model to account for the testing of subslab depressurization. Since mitigation was not installed in the period 2011 to 2012, none of the models using the 2011 to 2012 data set (422BN-1 and 422OF2-1) included mitigation as a control variable. Mitigation was included as control variable only in models using data from 2012 and 2013. Thus, for the 2012 to 2013 data, the change in radon concentration was modeled separately for each predictor variable, but mitigation was always included in the equation.

For example, the full model for the first predictor in **Table 10-2**, Air Density Interior for data period 2012–2013, is: $\text{Diff}(t) = \text{Intercept} + \text{Air Density Interior}(t) + \text{Air Density Interior}(t-1) + \text{Mitigation}(t)$. The first reduced model is: $\text{Diff}(t) = \text{Intercept} + \text{Air Density Interior}(t) + \text{Mitigation}(t)$; the second reduced model is $\text{Diff}(t) = \text{Intercept} + \text{Mitigation}(t)$. Models for the same predictor using data period 2011 to 2012 contain the same terms except the variable mitigation is not used. The mitigation was coded with on =1 and off = 0.

Table 10-2. Significant Lag and AR Model by Predictor and Site Location

| Predictor Name (Plain Language) | Predictor Name (Abbreviation) | Data Period: 2011–2012 | | Data Period: 2012–2013 | |
|---|----------------------------------|----------------------------|--------------------|---------------------------|--------------------|
| | | Significant Lags (days) | AR Model Chosen | Significant Lags(days) | AR Model Chosen |
| Air density interior | AirDens_422 | 1 | AR(1) | 1 | AR(1) |
| Drop in barometric pressure per hour | Bar_drop_Hg.hr | 0 | 0 | 0 | 0 |
| Barometric pressure in inches of mercury | Bar_in_Hg | 1 | AR(1) | 1 | AR(1) |
| Cooling degree day | Cool_Degree_Day | 1 | AR(1) | 1 | AR(1) |
| Dew point, interior, Fahrenheit | Dew_pt_422_F | 1 | AR(1) | 1 | AR(1) |
| Dew point, exterior | Dew_pt_out_F | 1 | AR(1) | 1 | AR(1) |
| Height measured at Fall Creek stream gauge in feet | Fall_Crk_Gage_ht_ft | 1 | AR(1) | 1 | AR(1) |
| Heating degree days | Heat_Degree_Day | 1 | AR(1) | 1 | AR(1) |
| Exterior heating index—calculated based on temperature and humidity | Heat_Index_F | 1 | AR(1) | 1 | AR(1) |
| Humidity interior | Hum_422_. | 1 | AR(1) | 1 | AR(1) |
| Humidity exterior | Hum_out_. | 1 | AR(1) | 1 | AR(1) |
| Interior heating index | Indoor_Heat_Index | 1 | AR(1) | 1 | AR(1) |
| Rain (inches) totaled during observation period | Rain_In_met | 1 | AR(1) | 0 | 0 |
| Rain highest rate during observation, hperiod | Rain_IPH | 0 | 0 | 0 | 0 |
| 420 side, subslab vs. basement differential pressure | Setra_420ss.base_Pa | 1 | AR(1) | | |
| 422 side basement vs. exterior differential pressure, pascals | Setra_422base.out_Pa | 4 | AR(4) | | |
| 422 side, basement vs. upstairs differential pressure, pascals | Setra_422base.upst_Pa | 1 | AR(1) | | |
| 422 side, deep vs. shallow soil gas differential pressure, pascals | Setra_422SGdp.ss_Pa | 1 | AR(1) | | |
| 422 side, subslab vs. basement differential pressure, pascals | Setra_422ss.base_Pa | 2 | AR(2) | | |

(continued)

Table 10-2. Significant Lag and AR Model by Predictor and Site Location (cont.)

| Predictor Name (Plain Language) | Predictor Name (Abbreviation) | Data Period: 2011–2012 | | Data Period: 2012–2013 | |
|---|----------------------------------|----------------------------|--------------------|---------------------------|--------------------|
| | | Significant Lags (days) | AR Model Chosen | Significant Lags(days) | AR Model Chosen |
| Depth of snow on the ground, inches | Snowdepth_daily | 1 | AR(1) | 1 | AR(1) |
| Soil moisture, 13 ft bls beneath structure, cbar | Soil_H2O_In13._cbar | 1 | AR(1) | 1 | AR(1) |
| Soil moisture 16.5 ft bls beneath structure, cbar | Soil_H2O_In16.5._cbar | 1 | AR(1) | 0 | 0 |
| Soil moisture 6 ft bls beneath structure, cbar | Soil_H2O_In6._cbar | 1 | AR(1) | 1 | AR(1) |
| Soil moisture 13 ft bls exterior, cbar | Soil_H2O_Out13._cbar | 1 | AR(1) | | |
| Soil moisture, 3.5 ft bls exterior, cbar | Soil_H2O_Out3.5._cbar | 1 | AR(1) | 1 | AR(1) |
| Soil moisture 6 ft bls exterior, cbar | Soil_H2O_Out6._cbar | 1 | AR(1) | 1 | AR(1) |
| Soil temperature 13 ft bls beneath structure | Soil_T_C_MW3.13 | 1 | AR(1) | | |
| Soil temperature 16.4 ft bls beneath structure | Soil_T_C_MW3.16.5 | 1 | AR(1) | | |
| Soil temperature 6 ft bls beneath structure | Soil_T_C_MW3.6 | 1 | AR(1) | | |
| Soil temperature 9 ft bls beneath structure | Soil_T_C_MW3.9 | 1 | AR(1) | | |
| Soil temperature 1 ft bls exterior | Soil_T_C_OTC.1 | 1 | AR(1) | | |
| Soil temperature 13 ft bls exterior | Soil_T_C_OTC.13 | 1 | AR(1) | | |
| Soil temperature 16.5 ft bls exterior | Soil_T_C_OTC.16.5 | 1 | AR(1) | | |
| Soil temperature 6 ft bls exterior | Soil_T_C_OTC.6 | 1 | AR(1) | | |
| Temperature at 420 basement north sampling location | T_420baseN_C | 1 | AR(1) | | |
| Temperature at 420 basement south sampling location | T_420baseS_C | 1 | AR(1) | | |
| Temperature at 420 first floor sampling location | T_420first_C | 1 | AR(1) | | |
| Temperature, 422 first floor | T_422_F | 1 | AR(1) | 1 | AR(1) |
| Temperature 422 basement north | T_422baseN_C | 1 | AR(1) | | |
| Temperature 422 first floor | T_422baseS_C | 1 | AR(1) | | |
| Temperature on first floor of 422 side of duplex | T_422first_C | 1 | AR(1) | | |
| Temperature exterior | T_out_C | 1 | AR(1) | | |

(continued)

Table 10-2. Significant Lag and AR Model by Predictor and Site Location (cont.)

| Predictor Name (Plain Language) | Predictor Name (Abbreviation) | Data Period: 2011–2012 | | Data Period: 2012–2013 | |
|--|----------------------------------|----------------------------|--------------------|---------------------------|--------------------|
| | | Significant Lags (days) | AR Model Chosen | Significant Lags(days) | AR Model Chosen |
| Exterior temperature (°F) | T_out_F | 1 | AR(1) | 1 | AR(1) |
| Temperature exterior, high during data collection period | T_out_Hi_F | 1 | AR(1) | 1 | AR(1) |
| Lowest exterior temperature | T_out_Lo_F | 1 | AR(1) | 1 | AR(1) |
| Temperature, humidity and wind index | THW_F | 1 | AR(1) | 1 | AR(1) |
| Wind chill | Wind_Chill_F | 1 | AR(1) | 1 | AR(1) |
| Wind direction (average) | Wind_Dir | 1 | AR(1) | 1 | AR(1) |
| Wind direction (of high during measurement period) | Wind_Dir_Hi | 1 | AR(1) | 1 | AR(1) |
| Wind run is a function of wind speed and duration | Wind_Run_mi | 1 | AR(1) | 1 | AR(1) |
| High wind speed during measurement period | Wind_Speed_Hi_MPH | 1 | AR(1) | 1 | AR(1) |
| Average wind speed during measurement period | Wind_Speed_MPH | 1 | AR(1) | 1 | AR(1) |

Figure 10-9 and **Figure 10-10** show the correlation matrix of the two first-difference radon concentration variables and continuous predictors available for 2011 to 2012 and 2012 to 2013 time periods, respectively. The color and the size of the circles describe the degree of correlation between the variables listed. Blue color denotes positive correlation and red color denotes negative correlation. Clear or almost white circles denote almost no correlation between pair of variables. The size of the circles is proportional to the degree of correlation; therefore, large circles denote large correlations and small circles denote very small correlation. The names of the first difference radon concentrations are listed as X422baseN_AG_radon and X422office_2nd_AG_radon for Base North and Office 2nd floor, respectively; and they are located at the end of the plots.

These figures show that the cross-correlation of the variables generally follows expected mathematical or physical principles. The strong positive correlation among the variables that directly measure temperature (either average or maximum) is unsurprising, as is the link to the variables calculated from temperature such as cooling degree days, heating degree days, heat index, and wind chill. The positive correlation between dew point and temperature also follows from the definition of dew point. The negative correlation of temperature to air density is rational based on both the ideal gas law and the formula used to calculate air density. The strong negative correlation between the temperature related variables and radon concentration likely shows the influence of the stack effect in vapor intrusion—as the temperature decreases, the stack effect increases, bringing in more radon. Similarly, the strong positive correlation between the various rainfall-related variables is expected, and the weak positive correlation between rainfall and humidity is expected. Also, the heat index is positively correlated to humidity by definition.

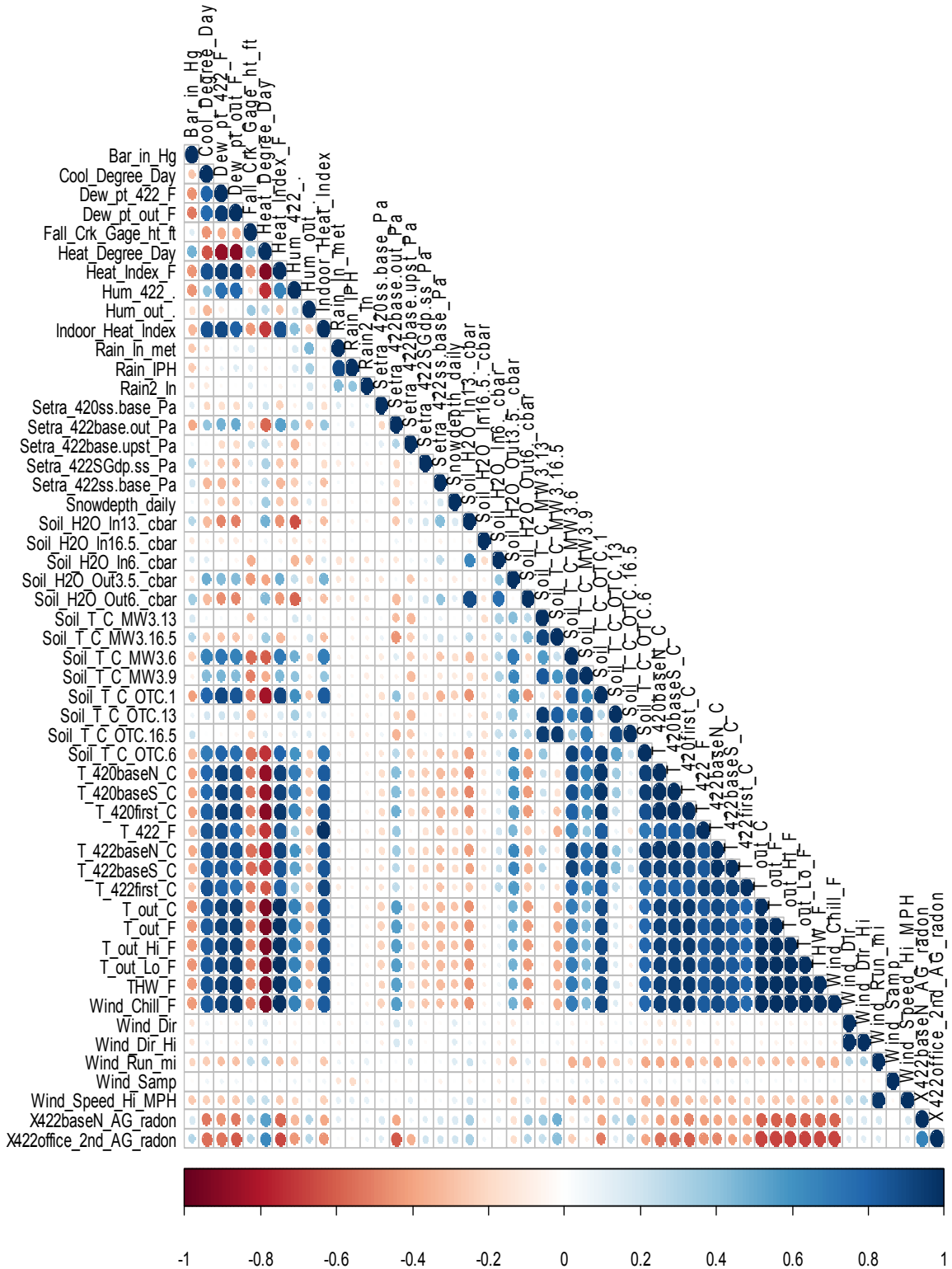


Figure 10-9. Correlation between radon concentration and predictors for both sites (basement north and office 2nd floor). Time period 2011–2012. NOTE: See Table 10-2 for “Plain Language” key of abbreviations used in this figure.

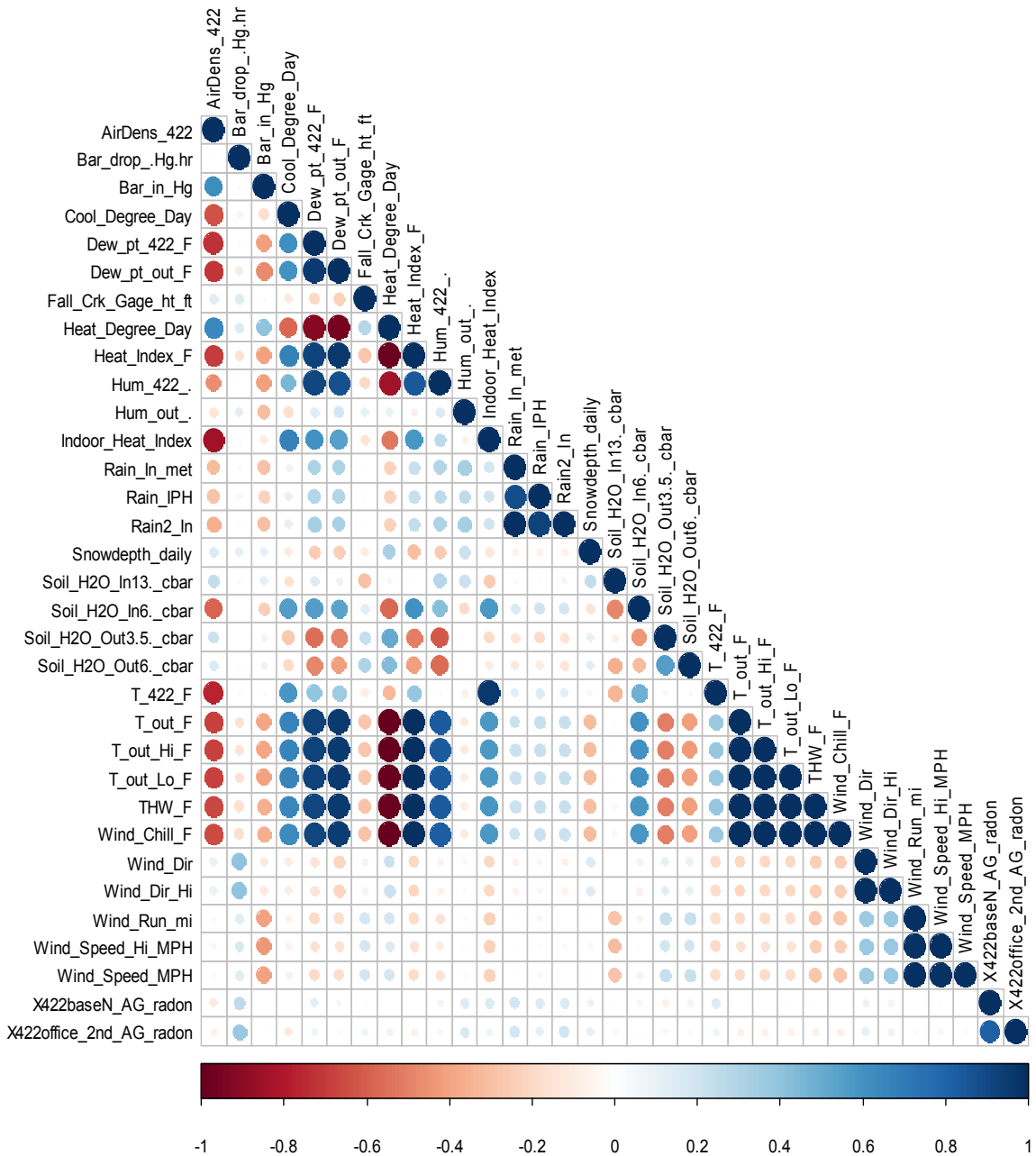


Figure 10-10. Correlation between radon concentration and predictors for both sites (basement north and office 2nd floor). Time period 2012–2013. NOTE: See Table 10-2 for “Plain Language” key of abbreviations used in this figure.

Somewhat less obvious were:

- The negative correlation between barometric pressure and wind speed: This makes sense because storms are frequently associated with a falling barometer.
- The 6-ft interior soil moisture and dew point correlation: The direction of this relationship is intuitive, but one would not necessarily have expected this to have such a rapid response.

- A positive correlation between wind direction and barometric pressure drop: This may suggest that storms consistently arrive from a common direction.

10.2 Correlation between Radon Concentration and Categorical Predictors

Note that some of our predictor variables could be described only with a limited number of values; that is, they are categorical variables. Categorical variables included the status of the air conditioning, fan used in fan testing, and central heating. In each case, these were either “on” or “off.” On was coded as a 1 and off as a 0. **Table 10-3** displays the results of the association between categorical predictors and the four time series. In reading this and subsequent tables an* by the coefficient means that the term is significantly correlated with radon concentration at the 5% significance level. A** denotes significance at the more stringent 1% significance level.

As discussed before, the first difference of the time series was used as the response for the model and mitigation was included only in the analysis of the data set collected from 2012 to 2013.

Table 10-3. Model Parameters, Standard Errors by Model, Predictor and Time Series: All Radon Time Periods, Categorical Variables

| Time Series | Predictor Name = x(t) | Model : $Y(t)-Y(t-1) = \text{Intercept} + \text{Predictor}(t)$ | | |
|-------------|-----------------------|--|-----------|-------|
| | | Model Term | Parameter | SE |
| X422OF2-1 | AC_on.off_420_daily | Intercept | -0.010 | 0.089 |
| | | x(t) | 0.104 | 0.537 |
| | AC_on.off_422_daily | Intercept | 0.003 | 0.098 |
| | | x(t) | -0.048 | 0.218 |
| | Fan_on.off_422_daily | Intercept | -0.024 | 0.090 |
| | | x(t) | 0.344 | 0.400 |
| | Heat_on.off_422_daily | Intercept | -0.037 | 0.140 |
| | | x(t) | 0.050 | 0.179 |
| X422BN-1 | AC_on.off_420_daily | Intercept | -0.007 | 0.048 |
| | | x(t) | -0.036 | 0.265 |
| | AC_on.off_422_daily | Intercept | 0.003 | 0.053 |
| | | x(t) | -0.053 | 0.118 |
| | Fan_on.off_422_daily | Intercept | -0.030 | 0.049 |
| | | x(t) | 0.432* | 0.218 |
| | Heat_on.off_422_daily | Intercept | -0.015 | 0.076 |
| | | x(t) | 0.011 | 0.097 |
| X422BN-2 | Heat_on.off_422_daily | Intercept | 0.146 | 0.294 |
| | | x(t) | 0.210 | 0.301 |
| | | Mitigation(t) | -0.534* | 0.215 |
| X422OF2-2 | Heat_on.off_422_daily | Intercept | 0.042 | 0.148 |
| | | x(t) | 0.070 | 0.151 |
| | | Mitigation(t) | -0.186 | 0.108 |

*Significant at 5% level of significance; ** Significant at 1% level of significance

Red font denotes significance at 1% or 5% level. SE = standard error

An example of how to read the results in **Table 10-3** is as follows: the first pair of rows (blue shaded) on the table are for radon concentration at 422 basement north during the 2011 to 2012 time period. In that model, the effect of having the air conditioning on today is that the predicted difference between today's radon concentration and yesterday's radon concentration is $-0.010 + 1 * .104 = 0.094$ pCi/L (a result that is not statistically significant). Similarly the effect of having the air conditioning off today is that the predicted difference between today's radon concentration and yesterday's radon concentration is that radon will have decreased by 0.01 pCi/L, (a result that is not statistically significant). From this model, we can conclude that air conditioning is not correlated with radon.

The predictor (AC_on.off_420_daily) was not significant, suggesting that it is not correlated with radon concentration. In other words, turning the air conditioning on or off on the 420 side of the duplex did not significantly affect the amount of radon in the 422 basement.

The only models that were shown to be statistically significant were:

- The model using interior fan in the first data set (2011 to 2012) for the 422 basement. When the fan was on, it increased today's radon as compared to yesterday's by 0.43 pCi/L per day. That makes physical sense because, as discussed in Section 12.2 of our previous report (U.S. EPA, 2012a), the fan was setup in the stairway and was being used to simulate a worst case vapor intrusion condition.
- The model in which both mitigation status and heating status were included for the 2012 to 2013 basement data. In that model, the slope of the mitigation term was statistically significant. That suggests that when the mitigation system was on today the radon concentration decreased by -0.534 pCi/L per day, regardless of whether the heating system was on or off. The heating system (on/off) term in that same equation was not statistically significant. That makes physical sense because the mitigation system was designed to reduce radon when it was turned on.

10.3 Correlation between Radon Concentration Time Series for 422 Basement South in 2011–2012 (X422BN-1) and Continuous Predictor Variables

Table 10-4 shows the results of models requiring only a lag 1 day term of the predictors in the model. In this and subsequent tables, a red font and the symbols “*” and “***” adjacent to the numbers in the cell of the “Estimate” column denote a statistically significant coefficients at 5% and more stringent 1% significance level, respectively. Statistically significant coefficients for the predictor variable in the model, suggest that the predictor and the outcome (radon concentrations) are correlated. If the coefficient of $x(t-1)$ (i.e., predictor at time $t-1$, shown in the third column of the table) is significant, that implies that the previous day's observation of the predictor is correlated with the outcome. The sign of the coefficient denotes the direction of the correlation.

If significance of the coefficient of $x(t-1)$ was detected, then there is no need to analyze the reduced model results (which are shown in columns 5 and 6). But if the variable $x(t-1)$ was not statistically significant in the full model (columns 3 and 4), then a reduced model (with all parameters except $x(t-1)$) was fit. In the reduced model (columns 5 and 6), the interest centers in the significance of the coefficient of $x(t)$. This coefficients measures the strength of the association between the first difference of radon concentration ($Y(t)-Y(t-1)$) and the predictor.

Table 10-4. Model Parameters, Standard Errors by Model and Predictor for X422baseN_AG_radon (X422BN-1): 2011–2012, Lag 1 Models

| Predictor Name | Model Term | Model : $Y(t)-Y(t-1) = \text{Intercept} + \text{Predictor (t)} + \text{Predictor (t-1)}$ | | Model : $Y(t)-Y(t-1) = \text{Intercept} + \text{Predictor (t)}$ | |
|--|------------|--|---------|---|--------|
| | | Estimate | SE | Estimate | SE |
| Air density interior | intercept | 10.54412** | 3.184 | 6.494 | 3.310 |
| | x(t-1) | -989.073 | 133.532 | | |
| | x(t) | 845.491 | 133.144 | -88.565 | 45.078 |
| Barometric pressure | intercept | 76.174 | 14.505 | 44.6707** | 13.718 |
| | x(t-1) | -3.330 | 0.608 | NA | NA |
| | x(t) | 0.788 | 0.609 | -1.49088** | 0.458 |
| Cooling degree day | intercept | -0.026 | 0.102 | 0.093 | 0.110 |
| | x(t-1) | 13.280 | 1.370 | | |
| | x(t) | -13.002 | 1.362 | -0.867 | 0.587 |
| Dew point, interior | intercept | -0.9325** | 0.345 | -0.626 | 0.356 |
| | x(t-1) | 0.143 | 0.023 | | |
| | x(t) | -0.124 | 0.023 | 0.012 | 0.007 |
| Dew point, exterior | intercept | -0.74167** | 0.265 | -0.151 | 0.290 |
| | x(t-1) | 0.129 | 0.012 | | NA |
| | x(t) | -0.114 | 0.012 | 0.003 | 0.006 |
| Height measured at Fall Creek stream gauge | intercept | 0.356 | 0.225 | -0.046 | 0.235 |
| | x(t-1) | -1.133 | 0.136 | | |
| | x(t) | 1.026 | 0.136 | 0.012 | 0.064 |
| Heating degree days | intercept | 0.124 | 0.101 | -0.062 | 0.115 |
| | x(t-1) | -9.343 | 0.744 | | NA |
| | x(t) | 8.768 | 0.745 | 0.264 | 0.358 |
| Exterior heating index— calculated based on temperature and humidity | intercept | -0.405 | 0.247 | 0.245 | 0.299 |
| | x(t-1) | 0.171 | 0.011 | | |
| | x(t) | -0.164 | 0.011 | -0.004 | 0.005 |
| Humidity interior | intercept | -0.97832* | 0.407 | -0.729 | 0.404 |
| | x(t-1) | 0.07735** | 0.023 | | |
| | x(t) | -0.05419* | 0.023 | 0.017 | 0.009 |
| Humidity exterior | intercept | -2.28123** | 0.528 | -2.392 | 0.478 |
| | x(t-1) | -0.004 | 0.009 | | |
| | x(t) | 0.03714** | 0.009 | 0.034 | 0.007 |
| Interior heating index | intercept | -1.07508* | 0.495 | -0.676 | 0.512 |
| | x(t-1) | 0.186 | 0.028 | | |
| | x(t) | -0.172 | 0.028 | 0.009 | 0.007 |
| Rain inches totaled during observation period | intercept | -0.29376** | 0.092 | -0.164 | 0.090 |
| | x(t-1) | 72.148 | 14.874 | | |
| | x(t) | 71.053 | 14.872 | 78.302 | 15.144 |

(continued)

Table 10-4. Model Parameters, Standard Errors by Model and Predictor for X422baseN_AG_radon (X422BN-1): 2011–2012, Lag 1 Models (cont.)

| Predictor Name | Model Term | Model : $Y(t)-Y(t-1) = \text{Intercept} + \text{Predictor}(t) + \text{Predictor}(t-1)$ | | Model : $Y(t)-Y(t-1) = \text{Intercept} + \text{Predictor}(t)$ | |
|---|------------|--|-------|--|-------|
| | | Estimate | SE | Estimate | SE |
| 422 side, basement vs. upstairs differential pressure | intercept | -0.9325** | 0.345 | -0.626 | 0.356 |
| | x(t-1) | 0.143 | 0.023 | | |
| | x(t) | -0.124 | 0.023 | 0.012 | 0.007 |
| 422 side, deep vs. shallow soil gas differential pressure | intercept | -0.74167** | 0.265 | -0.151 | 0.290 |
| | x(t-1) | 0.129 | 0.012 | | NA |
| | x(t) | -0.114 | 0.012 | 0.003 | 0.006 |
| 422 side, subslab vs. basement differential pressure | intercept | 0.356 | 0.225 | -0.046 | 0.235 |
| | x(t-1) | -1.133 | 0.136 | | |
| | x(t) | 1.026 | 0.136 | 0.012 | 0.064 |
| Depth of snow on the ground | intercept | 0.010 | 0.088 | -0.001 | 0.088 |
| | x(t-1) | -0.909 | 0.546 | | |
| | x(t) | 0.334 | 0.546 | -0.193 | 0.446 |
| Soil moisture, 13 ft bls beneath structure | intercept | -0.114 | 0.206 | -0.117 | 0.205 |
| | x(t-1) | -0.028 | 0.201 | | |
| | x(t) | 0.054 | 0.201 | 0.028 | 0.047 |
| Soil moisture 16.5 ft bls beneath structure | intercept | -0.009 | 0.089 | 0.004 | 0.089 |
| | x(t-1) | 6.926 | 4.440 | | |
| | x(t) | -8.474 | 5.045 | -1.209 | 1.927 |
| Soil moisture 6 ft bls beneath structure | intercept | 0.053 | 0.201 | 0.028 | 0.195 |
| | x(t-1) | 0.043 | 0.084 | | |
| | x(t) | -0.043 | 0.084 | 0.000 | 0.001 |
| Soil moisture 13 ft bls exterior | intercept | -0.008 | 0.193 | -0.012 | 0.193 |
| | x(t-1) | -0.002 | 0.006 | | |
| | x(t) | 0.002 | 0.006 | 0.000 | 0.001 |
| Soil moisture, 3.5 ft bls exterior | intercept | -0.013 | 0.111 | -0.016 | 0.110 |
| | x(t-1) | -0.001 | 0.004 | | |
| | x(t) | 0.001 | 0.004 | 0.000 | 0.001 |
| Soil moisture 6 ft bls exterior | intercept | 0.033 | 0.152 | 0.042 | 0.152 |
| | x(t-1) | 0.007 | 0.005 | | |
| | x(t) | -0.007 | 0.005 | 0.000 | 0.001 |
| Soil temperature 13 ft bls beneath structure | intercept | -0.665 | 0.875 | -0.298 | 0.897 |
| | x(t-1) | -11.290 | 1.919 | | |
| | x(t) | 11.326 | 1.925 | 0.019 | 0.058 |
| Soil temperature 16.4 ft bls beneath structure | intercept | -0.717 | 1.097 | -0.405 | 1.140 |
| | x(t-1) | -15.470 | 2.391 | | |
| | x(t) | 15.513 | 2.396 | 0.028 | 0.079 |

(continued)

Table 10-4. Model Parameters, Standard Errors by Model and Predictor for X422baseN_AG_radon (X422BN-1): 2011–2012, Lag 1 Models (cont.)

| Predictor Name | Model Term | Model : $Y(t)-Y(t-1) = \text{Intercept} + \text{Predictor}(t) + \text{Predictor}(t-1)$ | | Model : $Y(t)-Y(t-1) = \text{Intercept} + \text{Predictor}(t)$ | |
|---|------------|--|-------|--|-------|
| | | Estimate | SE | Estimate | SE |
| Soil temperature 6 ft bls beneath structure | intercept | -0.221 | 0.541 | -0.450 | 0.578 |
| | x(t-1) | -4.526 | 0.543 | | |
| | x(t) | 4.532 | 0.543 | 0.024 | 0.031 |
| Soil temperature 9 ft bls beneath structure | intercept | -0.131 | 0.710 | -0.177 | 0.724 |
| | x(t-1) | -6.422 | 1.253 | | |
| | x(t) | 6.423 | 1.254 | 0.010 | 0.042 |
| Soil temperature 1 ft bls exterior | intercept | -0.167 | 0.218 | -0.186 | 0.217 |
| | x(t-1) | 0.3096* | 0.141 | | |
| | x(t) | -0.29855* | 0.141 | 0.011 | 0.013 |
| Soil temperature 13 ft bls exterior | intercept | -0.033 | 0.621 | -0.147 | 0.605 |
| | x(t-1) | -0.265 | 1.955 | NA | NA |
| | x(t) | 0.267 | 1.962 | 0.010 | 0.043 |
| Soil temperature 16.5 ft bls exterior | intercept | -0.176 | 1.040 | -0.103 | 1.054 |
| | x(t-1) | 4.09682** | 0.986 | | |
| | x(t) | -4.08292** | 0.987 | 0.007 | 0.075 |
| Soil temperature 6 ft bls exterior | intercept | -0.046 | 0.252 | -0.054 | 0.260 |
| | x(t-1) | -2.922 | 0.478 | | |
| | x(t) | 2.917 | 0.478 | 0.003 | 0.016 |
| Temperature at 420 basement north sampling location | intercept | -0.784 | 0.469 | -0.614 | 0.484 |
| | x(t-1) | 0.323 | 0.054 | | |
| | x(t) | -0.311 | 0.054 | 0.010 | 0.008 |
| Temperature at 420 basement south sampling location | intercept | -0.794 | 0.473 | -0.604 | 0.491 |
| | x(t-1) | 0.345 | 0.054 | | |
| | x(t) | -0.332 | 0.054 | 0.010 | 0.008 |
| Temperature at 420 first floor sampling location | intercept | -0.81561* | 0.388 | -0.459 | 0.424 |
| | x(t-1) | 0.297 | 0.030 | | |
| | x(t) | -0.284 | 0.030 | 0.007 | 0.006 |
| Temperature, 422 first floor | intercept | -1.41954* | 0.653 | -0.808 | 0.684 |
| | x(t-1) | 0.284 | 0.038 | | |
| | x(t) | -0.264 | 0.038 | 0.011 | 0.009 |
| Temperature 422 basement north | intercept | -1.201 | 0.669 | -0.877 | 0.698 |
| | x(t-1) | 0.476 | 0.071 | | |
| | x(t) | -0.457 | 0.071 | 0.013 | 0.011 |
| Temperature 422 first floor | intercept | -1.333 | 0.814 | -1.079 | 0.829 |
| | x(t-1) | 0.41748** | 0.092 | NA | NA |
| | x(t) | -0.39746** | 0.092 | 0.016 | 0.012 |

(continued)

Table 10-4. Model Parameters, Standard Errors by Model and Predictor for X422baseN_AG_radon (X422BN-1): 2011–2012, Lag 1 Models (cont.)

| Predictor Name | Model Term | Model : $Y(t)-Y(t-1) = \text{Intercept} + \text{Predictor}(t) + \text{Predictor}(t-1)$ | | Model : $Y(t)-Y(t-1) = \text{Intercept} + \text{Predictor}(t)$ | |
|--|------------|--|-------|--|-------|
| | | Estimate | SE | Estimate | SE |
| Temperature on first floor of 422 side of duplex | intercept | -1.80372* | 0.831 | -1.027 | 0.879 |
| | x(t-1) | 0.419 | 0.052 | | |
| | x(t) | -0.395 | 0.052 | 0.014 | 0.012 |
| Temperature exterior | intercept | -0.384 | 0.263 | 0.339 | 0.321 |
| | x(t-1) | 0.186 | 0.012 | | |
| | x(t) | -0.179 | 0.012 | -0.006 | 0.005 |
| Exterior temperature (°F) | intercept | -0.384 | 0.263 | 0.339 | 0.321 |
| | x(t-1) | 0.186 | 0.012 | NA | NA |
| | x(t) | -0.179 | 0.012 | -0.006 | 0.005 |
| Temperature exterior, high during data collection period | intercept | -0.395 | 0.264 | 0.326 | 0.322 |
| | x(t-1) | 0.184 | 0.012 | | |
| | x(t) | -0.178 | 0.012 | -0.005 | 0.005 |
| Lowest exterior temperature | intercept | -0.399 | 0.262 | 0.323 | 0.320 |
| | x(t-1) | 0.186 | 0.012 | | |
| | x(t) | -0.180 | 0.012 | -0.005 | 0.005 |
| Temperature, humidity and wind index | intercept | -0.354 | 0.224 | 0.265 | 0.278 |
| | x(t-1) | 0.167 | 0.010 | | |
| | x(t) | -0.161 | 0.010 | -0.005 | 0.004 |
| Wind chill | intercept | -0.332 | 0.237 | 0.350 | 0.295 |
| | x(t-1) | 0.180 | 0.011 | | |
| | x(t) | -0.174 | 0.011 | -0.006 | 0.005 |
| Wind direction (average) | intercept | -0.368 | 0.297 | -0.335 | 0.248 |
| | x(t-1) | 0.000 | 0.001 | | |
| | x(t) | 0.002 | 0.001 | 0.002 | 0.001 |
| Wind direction (of high during measurement period) | intercept | -0.349 | 0.291 | -0.318 | 0.245 |
| | x(t-1) | 0.000 | 0.001 | | |
| | x(t) | 0.002 | 0.001 | 0.002 | 0.001 |
| Wind run (a function of wind speed and duration) | intercept | -0.40685* | 0.199 | -0.3598* | 0.177 |
| | x(t-1) | 0.050 | 0.097 | | |
| | x(t) | 0.169 | 0.097 | 0.19307* | 0.085 |
| High wind speed during measurement period | intercept | -0.71054** | 0.244 | -0.5822** | 0.213 |
| | x(t-1) | 0.024 | 0.022 | | |
| | x(t) | 0.04746* | 0.022 | 0.05863** | 0.020 |
| Average wind speed during measurement period | intercept | -0.40685* | 0.199 | -0.3598* | 0.177 |
| | x(t-1) | 0.025 | 0.048 | | |
| | x(t) | 0.084 | 0.048 | 0.09654* | 0.042 |

Note: Lag 1 models; SE = standard error

** Significant at 1% level of significance * Significant at 5% level of significance

In **Table 10-4**, the correlation of radon concentrations with wind run, high wind speed, and average wind speed is in each case positive, so high winds are predicted to result in high radon. This agrees with a qualitative observation in Section 6—that peaks in wall port VOCs are associated with wind speed. A positive relationship between increasing wind speed and increasing chloroform is shown graphically in Section 9.2.4.

The negative association of barometric pressure with radon shown in **Table 10-4** makes intuitive physical sense since increased barometric pressure should decrease the emanation of soil gas. Barometric pressure changes are associated with some of the unusual subslab-to-interior differential pressure events discussed in Section 9.1. However, the visual analysis of the VOC data in Section 9.2 did not reveal a clear, monotonic barometric pressure trend. Barometric pressure drops, especially those accompanied by rainfall, have been associated with increased indoor radon in several studies (see review by Lewis and Houle [2009]).

Although the relationship between indoor humidity and radon was judged to be statistically significant (not subject to chance), note that the signs of the $X(t-1)$ and $X(t)$ terms are opposite, and the absolute value of those terms is similar and relatively small. Note also that indoor humidity changes slowly from day to day (**Table 10-4**). Therefore, these terms will likely nearly cancel out in many cases. The exterior humidity analysis is thus more interesting, since, although the signs are opposite, the absolute values are very different. The term that would be expected to be dominant would be the term relating to today's humidity, which would be associated with increased radon. An association of greater radon emanation with higher humidity has also been observed in laboratory experiments with soil (Hosoda, 2008).²⁴

Similarly, although relationships with exterior soil temperature at 1 ft and 16.5 ft were judged unlikely to be attributable to chance (**Table 10-4**) because the signs of the terms in the full model are opposite, soil temperatures change relatively slowly, and the magnitude of the slopes was similar; it is unlikely that soil temperature explains a large amount of the radon variation.

Table 10-5 displays the coefficient estimate and standard error for those predictor variables that required a lag 2 day term in the model. The predictor 420 side, subslab vs. basement differential pressure had a relationship unlikely to be due to chance with the 422 basement radon. However, the magnitude of this relationship is likely to be small since the signs of the coefficients for the differential pressures on various days are opposite. For example, in the full model, the radon increases 0.55 pCi/L per pascal of differential pressure measured blowing into the building today. But that is likely to be essentially canceled out in many cases by the effect of the terms for yesterday's differential pressure and the day before yesterday's differential pressure, which are negative. Note, however, that in the first reduced model, the net effect is likely to be positive—the statistically significant term for today's differential pressure is likely to outweigh the term for yesterday's differential pressure.

Table 10-6 displays the models for predictor 422 side basement vs. exterior differential pressure, which necessitated 4 lag days in the model because of the results of the analysis of autocorrelation and partial autocorrelation. The two higher order lags were not significant, so they were dropped from the full model one at a time. Relationships were found between this predictor and radon concentration, which are unlikely to be due to chance. However, these relationships will often cancel and not explain much of the variation in radon because the signs of the slopes of the $x(t)$ and $x(t-1)$ terms are opposite. The meaning of this relationship can perhaps be most easily understood with an example using the model that has been reduced to only the $X(t)$ and $x(t-1)$ terms. Assume a case when the basement vs. exterior pressure is

²⁴Generation and control of radon from soil

1 pascal today and was 0 pascal yesterday. In that simplified case, the model would predict that the radon concentration would be decreased by 0.4 pCi/L. That result is reasonable, because with a basement such

Table 10-5. Model Parameters, Standard Errors by Predictor for X422baseN_AG_radon (X422BN-1): 2011–1012, Lag 2 Models

| Predictor Name | Model Term | Y(t)–Y(t–1) = Intercept + Predictor (t) + Predictor(t–1)+ Predictor(t–2) | | Y(t)–Y(t–1) = Intercept + Predictor (t) + Predictor(t–1)+ | | Y(t)–Y(t–1) = Intercept + Predictor (t) | |
|--|------------|--|-------|---|-------|---|-------|
| | | Estimate | SE | Estimate | SE | Estimate | SE |
| 420 side, subslab vs. basement differential pressure | intercept | 0.006 | 0.243 | –0.190 | 0.223 | –0.364 | 0.203 |
| | x(t) | 0.55596* | 0.223 | 0.58588** | 0.223 | 0.348 | 0.178 |
| | x(t–1) | –0.088 | 0.264 | –0.406 | 0.223 | | |
| | x(t–2) | –0.48452* | 0.223 | | | | |

*Significant at 5% level of significance

**Significant at 1% level of significance

Table 10-6. Model Parameters, Standard Errors by Predictor for X422baseN_AG_radon (X422BN-1), Lag 4 Models

| Predictor Name | Model Term | Y(t)–Y(t–1) = Intercept + Predictor (t) + Predictor(t–1)+ Predictor(t–2) + Predictor(t–3)+ Predictor(t–4) | | Y(t)–Y(t–1) = Intercept + Predictor (t) + Predictor(t–1)+ Predictor(t–2) + Predictor(t–3)+ | | Y(t)–Y(t–1) = Intercept + Predictor (t) + Predictor(t–1)+ Predictor(t–2) | | Y(t)–Y(t–1) = Intercept + Predictor (t) + Predictor(t–1) | | Y(t)–Y(t–1) = Intercept + Predictor (t) | |
|--|------------|---|-------|--|-------|--|-------|--|-------|---|-------|
| | | Estimate1 | SE1 | Estimate2 | SE2 | Estimate3 | SE3 | Estimate4 | SE4 | Estimate5 | SE5 |
| 422 side basement vs. exterior differential pressure | intercept | 0.005 | 0.089 | –0.005 | 0.089 | –0.003 | 0.089 | –0.002 | 0.088 | –0.006 | 0.090 |
| | x(t) | –0.36984** | 0.091 | –0.38245** | 0.090 | –0.3958** | 0.088 | –0.37946** | 0.086 | –0.094 | 0.060 |
| | x(t–1) | 0.35053** | 0.104 | 0.3452** | 0.104 | 0.34485** | 0.103 | 0.39558** | 0.086 | NA | NA |
| | x(t–2) | 0.109 | 0.104 | 0.111 | 0.103 | 0.085 | 0.087 | NA | NA | NA | NA |
| | x(t–3) | 0.051 | 0.104 | –0.053 | 0.088 | NA | NA | NA | NA | NA | NA |
| | x(t–4) | –0.138 | 0.089 | NA | NA | NA | NA | NA | NA | NA | NA |

**Significant at 1% level of significance

as this that is partially above ground, a positive pressure vs. exterior air means that some air is directly leaking out of the basement above ground.

10.4 Correlation between Radon Concentration Time Series for 422 2nd Floor Office (2011–2012) and Predictor Variables

Similarly to the basement time series, the variable “drop in barometric pressure” has a significant correlation with radon concentration (see Table 10-7). The positive coefficients indicate that as barometric pressure goes down, the radon concentration upstairs goes up. This is an expected result.

Table 10-8 shows the results of models including predictors requiring Lag 1 terms to model X422OF2-1 for the period 2011 to 2012.

Table 10-7. Model Parameters, Standard Errors by Predictor for X422office_2nd_AG_radon Concentration (X422OF2-1): 2011–2012, No Lag Terms in Model

| Time Series | Model : $Y(t)-Y(t-1) = \text{Intercept} + \text{Predictor (t)}$ | | | |
|--------------------|---|------------|----------------|-------|
| | Predictor Name = $x(t)$ | Model Term | Estimate | SE |
| X422baseN_AG_radon | Drop in barometric pressure | intercept | -0.009 | 0.044 |
| | | $x(t)$ | 0.986** | 0.102 |
| | Rain highest rate during observation period | intercept | -0.035 | 0.049 |
| | | $x(t)$ | 1.622 | 0.855 |

**Significant at 1% level of significance

Table 10-8. Model Parameters, Standard Errors by Model and Predictor for Time Series Analysis of Radon in 422 Office: 2011–2012, Lag 1 Models

| Predictor Name | Model Term | Model : $Y(t)-Y(t-1) = \text{Intercept} + \text{Predictor (t)} + \text{Predictor (t-1)}$ | | Model : $Y(t)-Y(t-1) = \text{Intercept} + \text{Predictor (t)}$ | |
|--|------------|--|--------|---|--------|
| | | Estimate | SE | Estimate | SE |
| Air density interior | Intercept | 3.98887* | 1.777 | 2.252 | 1.810 |
| | $x(t)$ | 377.08738** | 74.255 | -30.798 | 24.659 |
| | $x(t-1)$ | -431.49046** | 74.388 | | |
| Barometric pressure | Intercept | 31.96701** | 7.873 | 10.989 | 7.550 |
| | $x(t)$ | 1.14704** | 0.330 | -0.367 | 0.252 |
| | $x(t-1)$ | -2.21408** | 0.330 | | |
| Cooling degree day | Intercept | -0.023 | 0.058 | 0.026 | 0.060 |
| | $x(t)$ | -5.26306** | 0.776 | -0.292 | 0.320 |
| | $x(t-1)$ | 5.43776** | 0.781 | | |
| Dew point, interior | Intercept | -0.44352* | 0.193 | -0.336 | 0.194 |
| | $x(t)$ | -0.04195** | 0.013 | 0.007 | 0.004 |
| | $x(t-1)$ | 0.05078** | 0.013 | | |
| Dew point, exterior | Intercept | -0.37804** | 0.146 | -0.065 | 0.158 |
| | $x(t)$ | -0.06071** | 0.006 | 0.001 | 0.003 |
| | $x(t-1)$ | 0.06835** | 0.006 | | |
| Height measured at Fall Creek stream gauge | Intercept | 0.101 | 0.126 | -0.060 | 0.128 |
| | $x(t)$ | 0.43301** | 0.076 | 0.016 | 0.035 |
| | $x(t-1)$ | -0.46503** | 0.076 | | |
| Heating degree days | Intercept | 0.055 | 0.054 | -0.047 | 0.062 |
| | $x(t)$ | 4.91909** | 0.405 | 0.188 | 0.195 |
| | $x(t-1)$ | -5.19542** | 0.404 | | |

(continued)

Table 10-8. Model Parameters, Standard Errors by Model and Predictor for Time Series Analysis of Radon in 422 Office: 2011–2012, Lag 1 Models (cont.)

| Predictor Name | Model Term | Model : $Y(t)-Y(t-1) = \text{Intercept} + \text{Predictor}(t) + \text{Predictor}(t-1)$ | | Model : $Y(t)-Y(t-1) = \text{Intercept} + \text{Predictor}(t)$ | |
|--|------------|--|-------|--|-------|
| | | Estimate | SE | Estimate | SE |
| Exterior heating index— calculated based on temperature and humidity | Intercept | -0.204 | 0.139 | 0.127 | 0.163 |
| | x(t) | -0.08386** | 0.006 | -0.002 | 0.003 |
| | x(t-1) | 0.08723** | 0.006 | | |
| Humidity interior | Intercept | -0.61177** | 0.220 | -0.47041* | 0.218 |
| | x(t) | -0.02534* | 0.012 | 0.011* | 0.005 |
| | x(t-1) | 0.03973** | 0.012 | | |
| Humidity exterior | Intercept | -1.17568** | 0.290 | -1.18449** | 0.262 |
| | x(t) | 0.0172** | 0.005 | 0.01698** | 0.004 |
| | x(t-1) | 0.000 | 0.005 | | |
| Interior heating index | Intercept | -0.390 | 0.279 | -0.272 | 0.280 |
| | x(t) | -0.05113** | 0.016 | 0.004 | 0.004 |
| | x(t-1) | 0.05631** | 0.016 | | |
| Rain inches totaled during observation period | Intercept | -0.12091* | 0.051 | -0.056 | 0.050 |
| | x(t) | 20.3433* | 8.317 | 23.93887** | 8.427 |
| | x(t-1) | 35.95066** | 8.317 | | |
| 422 side, basement vs. upstairs differential pressure | Intercept | 0.000 | 0.047 | 0.008 | 0.049 |
| | x(t) | -0.68146** | 0.100 | -0.10379* | 0.050 |
| | x(t-1) | 0.65764** | 0.100 | | |
| 422 side, deep vs. shallow soil gas differential pressure | Intercept | 0.058 | 0.056 | 0.010 | 0.054 |
| | x(t) | 0.003 | 0.015 | -0.009 | 0.015 |
| | x(t-1) | -0.04185** | 0.015 | | |
| 422 side, slab vs. basement differential pressure | Intercept | -0.041 | 0.135 | -0.068 | 0.120 |
| | x(t) | 0.039 | 0.050 | 0.024 | 0.042 |
| | x(t-1) | -0.024 | 0.050 | | |
| Depth of snow on the ground | intercept | 0.001 | 0.048 | -0.006 | 0.048 |
| | x(t) | 0.256 | 0.298 | -0.076 | 0.244 |
| | x(t-1) | -0.573 | 0.298 | | |
| Soil moisture, 13 ft bls beneath structure | intercept | -0.039 | 0.111 | -0.036 | 0.111 |
| | x(t) | -0.024 | 0.110 | 0.007 | 0.025 |
| | x(t-1) | 0.032 | 0.110 | | |
| Soil moisture 16.5 ft bls beneath structure | intercept | -0.009 | 0.048 | -0.002 | 0.048 |
| | x(t) | -8.04869** | 2.752 | -1.482 | 1.053 |
| | x(t-1) | 6.25195* | 2.422 | | |

(continued)

Table 10-8. Model Parameters, Standard Errors by Model and Predictor for Time Series Analysis of Radon in 422 Office: 2011–2012, Lag 1 Models (cont.)

| Predictor Name | Model Term | Model : $Y(t)-Y(t-1) = \text{Intercept} + \text{Predictor}(t) + \text{Predictor}(t-1)$ | | Model : $Y(t)-Y(t-1) = \text{Intercept} + \text{Predictor}(t)$ | |
|--|------------|--|-------|--|-------|
| | | Estimate | SE | Estimate | SE |
| Soil moisture 6 ft bls beneath structure | intercept | 0.026 | 0.109 | -0.009 | 0.106 |
| | x(t) | -0.058 | 0.046 | 0.000 | 0.001 |
| | x(t-1) | 0.058 | 0.046 | | |
| Soil moisture 13 ft bls exterior | intercept | -0.042 | 0.104 | -0.042 | 0.104 |
| | x(t) | 0.001 | 0.003 | 0.000 | 0.000 |
| | x(t-1) | -0.001 | 0.003 | | |
| Soil moisture, 3.5 ft bls exterior | intercept | -0.015 | 0.060 | -0.013 | 0.060 |
| | x(t) | 0.000 | 0.002 | 0.000 | 0.001 |
| | x(t-1) | 0.001 | 0.002 | | |
| Soil moisture 6 ft bls exterior | intercept | -0.029 | 0.082 | -0.026 | 0.082 |
| | x(t) | -0.002 | 0.003 | 0.000 | 0.000 |
| | x(t-1) | 0.002 | 0.003 | | |
| Soil temperature 13 ft bls beneath structure | intercept | -0.280 | 0.489 | -0.190 | 0.487 |
| | x(t) | 3.25428** | 1.075 | 0.012 | 0.032 |
| | x(t-1) | -3.23827** | 1.072 | | |
| Soil temperature 16.4 ft bls beneath structure | intercept | -0.330 | 0.616 | -0.245 | 0.618 |
| | x(t) | 4.58871** | 1.342 | 0.017 | 0.043 |
| | x(t-1) | -4.56774** | 1.338 | | |
| Soil temperature 6 ft bls beneath structure | intercept | -0.064 | 0.304 | -0.163 | 0.314 |
| | x(t) | 1.89452** | 0.304 | 0.009 | 0.017 |
| | x(t-1) | -1.89359** | 0.305 | | |
| Soil temperature 9 ft bls beneath structure | intercept | -0.057 | 0.395 | -0.091 | 0.393 |
| | x(t) | 1.70464* | 0.696 | 0.005 | 0.023 |
| | x(t-1) | -1.70318* | 0.696 | | |
| Soil temperature 1 ft bls exterior | intercept | -0.071 | 0.118 | -0.081 | 0.118 |
| | x(t) | -0.15712* | 0.077 | 0.005 | 0.007 |
| | x(t-1) | 0.16196* | 0.077 | | |
| Soil temperature 13 ft bls exterior | intercept | 0.019 | 0.337 | -0.105 | 0.329 |
| | x(t) | -1.180 | 1.063 | 0.007 | 0.024 |
| | x(t-1) | 1.180 | 1.059 | | |
| Soil temperature 16.5 ft bls exterior | intercept | -0.248 | 0.571 | -0.228 | 0.574 |
| | x(t) | -1.62806** | 0.540 | 0.016 | 0.041 |
| | x(t-1) | 1.64586** | 0.539 | | |

(continued)

Table 10-8. Model Parameters, Standard Errors by Model and Predictor for Time Series Analysis of Radon in 422 Office: 2011–2012, Lag 1 Models (cont.)

| Predictor Name | Model Term | Model : $Y(t)-Y(t-1) = \text{Intercept} + \text{Predictor}(t) + \text{Predictor}(t-1)$ | | Model : $Y(t)-Y(t-1) = \text{Intercept} + \text{Predictor}(t)$ | |
|--|------------|--|-------|--|-------|
| | | Estimate | SE | Estimate | SE |
| Soil temperature 6 ft bls exterior | intercept | -0.020 | 0.140 | -0.030 | 0.141 |
| | x(t) | 1.00762** | 0.266 | 0.002 | 0.009 |
| | x(t-1) | -1.00914** | 0.267 | | |
| Temperature at 420 basement north sampling location | intercept | -0.404 | 0.256 | -0.312 | 0.264 |
| | x(t) | -0.1692** | 0.030 | 0.005 | 0.004 |
| | x(t-1) | 0.17576** | 0.030 | | |
| Temperature at 420 basement south sampling location | intercept | -0.410 | 0.258 | -0.309 | 0.268 |
| | x(t) | -0.17917** | 0.030 | 0.005 | 0.004 |
| | x(t-1) | 0.18575** | 0.030 | | |
| Temperature at 420 first floor sampling location | intercept | -0.400 | 0.215 | -0.221 | 0.232 |
| | x(t) | -0.14556** | 0.017 | 0.003 | 0.003 |
| | x(t-1) | 0.15167** | 0.017 | | |
| Temperature, 422 first floor | intercept | -0.457 | 0.373 | -0.312 | 0.374 |
| | x(t) | -0.06239** | 0.021 | 0.004 | 0.005 |
| | x(t-1) | 0.06843** | 0.021 | | |
| Temperature 422 basement north | intercept | -0.563 | 0.371 | -0.419 | 0.380 |
| | x(t) | -0.20225** | 0.039 | 0.006 | 0.006 |
| | x(t-1) | 0.21089** | 0.039 | | |
| Temperature 422 first floor | intercept | -0.595 | 0.452 | -0.546 | 0.452 |
| | x(t) | -0.071 | 0.051 | 0.008 | 0.007 |
| | x(t-1) | 0.080 | 0.051 | | |
| Temperature on first floor of 422 side of duplex | intercept | -0.647 | 0.475 | -0.421 | 0.480 |
| | x(t) | -0.11474** | 0.030 | 0.006 | 0.007 |
| | x(t-1) | 0.1235** | 0.030 | | |
| Temperature exterior | intercept | -0.200 | 0.148 | 0.167 | 0.175 |
| | x(t) | -0.09139** | 0.007 | -0.003 | 0.003 |
| | x(t-1) | 0.09471** | 0.007 | | |
| Exterior temperature (°F) | intercept | -0.200 | 0.148 | 0.167 | 0.175 |
| | x(t) | -0.09139** | 0.007 | -0.003 | 0.003 |
| | x(t-1) | 0.09471** | 0.007 | | |
| Temperature exterior, high during data collection period | intercept | -0.206 | 0.149 | 0.159 | 0.175 |
| | x(t) | -0.09043** | 0.007 | -0.003 | 0.003 |
| | x(t-1) | 0.09383** | 0.007 | | |

(continued)

Table 10-8. Model Parameters, Standard Errors by Model and Predictor for Time Series Analysis of Radon in 422 Office: 2011–2012, Lag 1 Models (cont.)

| Predictor Name | Model Term | Model : $Y(t)-Y(t-1) = \text{Intercept} + \text{Predictor}(t) + \text{Predictor}(t-1)$ | | Model : $Y(t)-Y(t-1) = \text{Intercept} + \text{Predictor}(t)$ | |
|--|------------|--|-------|--|-------|
| | | Estimate | SE | Estimate | SE |
| Lowest exterior temperature | intercept | -0.208 | 0.148 | 0.158 | 0.175 |
| | x(t) | -0.09138** | 0.007 | -0.003 | 0.003 |
| | x(t-1) | 0.09487** | 0.007 | | |
| Temperature, humidity and wind index | intercept | -0.178 | 0.129 | 0.128 | 0.152 |
| | x(t) | -0.07969** | 0.006 | -0.002 | 0.002 |
| | x(t-1) | 0.08267** | 0.006 | | |
| Wind chill | intercept | -0.172 | 0.137 | 0.163 | 0.161 |
| | x(t) | -0.08563** | 0.006 | -0.003 | 0.003 |
| | x(t-1) | 0.08853** | 0.006 | | |
| Wind direction (average) | intercept | -0.141 | 0.160 | -0.30692* | 0.134 |
| | x(t) | 0.00203** | 0.001 | 0.0016* | 0.001 |
| | x(t-1) | -0.001 | 0.001 | | |
| Wind direction (of high during measurement period) | intercept | -0.159 | 0.157 | -0.30257* | 0.133 |
| | x(t) | 0.00204** | 0.001 | 0.0016* | 0.001 |
| | x(t-1) | -0.001 | 0.001 | | |
| Wind run is a function of wind speed and duration | intercept | -0.128 | 0.106 | 0.082 | 0.097 |
| | x(t) | -0.16169** | 0.052 | -0.050 | 0.046 |
| | x(t-1) | 0.22816** | 0.052 | | |
| High wind speed during measurement period | intercept | -0.236 | 0.131 | 0.042 | 0.117 |
| | x(t) | -0.02996* | 0.012 | -0.005 | 0.011 |
| | x(t-1) | 0.05337** | 0.012 | | |
| Average wind speed during measurement period | intercept | -0.128 | 0.106 | 0.082 | 0.097 |
| | x(t) | -0.08085** | 0.026 | -0.025 | 0.023 |
| | x(t-1) | 0.11408** | 0.026 | | |

**Significant at 1% level of significance

*Significant at 5% level of significance

The magnitude of effect is large for rain (**Table 10-8**), which increased indoor radon substantially whether it fell on the day in question or the previous day. This effect has been documented by others in other structures. Lewis and Houle (2009), for example, review Nazaroff's work and state:

*In a house with a crawl space, a modest drop in barometric pressure and a period of **heavy rain** caused the indoor radon and crawl space radon to rise to its highest level during a 5-week measurement period. The rain may be acting in one of two ways; it could act by funneling the radon from the soil into the crawl space: with heavy rain, the permeability of the soil surrounding the house is greatly reduced while the permeability of the soil beneath the house remains unchanged; as the barometric pressure falls, soil gas then flows into the crawl space at a higher rate than it does out of the soil surrounding the house. The*

alternative explanation is that the downward movement of water through the soil may act like a piston and displace the radon, which then flows into the crawl space (Lewis & Houle, 1985).

Numerous predictor variables showed the same pattern in the results:

- The results for $x(t)$ and $x(t-1)$ were both judged to be unlikely to be due to chance.
- The results for $x(t)$ and $x(t-1)$ slopes were similar in magnitude but opposite in sign.
- The reduced model is not significant.

Results of this type suggest that the change from day to day in the predictor variable may be associated with a change in radon concentration but that the absolute value of the predictor variable is less important (Nau, 2005b). In at least some cases, this result can make physical sense. For example, let us use the example of exterior temperature. For a day when the temperature is 40°F and yesterday's temperature was 60°F, the model predicts that the radon concentration will have increased 1.9 pCi/L—falling temperatures increase radon, which is consistent with the stack effect. In the opposite case where the temperature yesterday was 40°F and today 60°F, a decrease in radon is predicted.

Another example where the modeled behavior appears reasonable is the height of the Fall Creek stream gauge, which we have shown to be tightly linked to the on-site water table (Chapter 11, U.S. EPA, 2012a). In an example where the stream gauge is 5 ft today and 2 ft yesterday, the model predicts an increase in radon of 1.3 pCi/L. This is what would be expected—the rising stream and; thus, water table would tend to “squeeze” radon containing soil gas up into the structure. It could also be that the rise in the stream gauge is a surrogate parameter for on-site rainfall, which could be expected to have an effect on the vadose zone, increasing radon indoors.

Since the change in so many parameters appears to be related to radon concentrations, it may be more fruitful to examine those that stand out from the pattern. Surprisingly, the parameters that were not significantly associated with radon in this data set included 422 subslab vs. basement differential pressure and the depth of snow on the ground.

The few parameters that were significant even in the reduced model of this data set include rainfall (discussed above as positively correlated), humidity (positively correlated, see discussion in Section 10.3) and wind direction (positively correlated).

Table 10-9 shows the result for models exploring the correlation between predictor 420 side, subslab vs. basement differential pressure, and radon concentration (X422OF2-1) for time period 2011 to 2012. The non-significant results suggest that subslab vs. basement differential pressure on the 420 side of the duplex is not correlated with radon concentrations in the office on the second floor of the 422 side. The range of variation of this differential pressure is shown in our previous report (Figure 10-5 of U.S. EPA 2012a).

Table 10-10 shows the results of the analysis to determine the correlation between 422 side basement vs. exterior differential pressure and radon concentration (X422OF2-1) for time period 2011 to 2012. Current and past observations of the 422 side basement vs. exterior differential pressure are highly correlated with radon concentrations. The current observation has negative correlation and the past observation has a positive correlation. The difference in signs indicates that the change in the predictor variable (differential pressure) is likely more important than its absolute magnitude.

Table 10-9. Model Parameters, Standard Errors by Predictor for X422office_2nd_AG_radon Concentration (X422OF2-1): 2011–2012. Lag 2 Models

| Predictor Name | Model Term | Y(t)-Y(t-1) = Intercept + Predictor (t) + Predictor(t-1)+ Predictor(t-2) | | Y(t)-Y(t-1) = Intercept + Predictor (t) + Predictor(t-1)+ | | Y(t)-Y(t-1) = Intercept + Predictor (t) | |
|---|------------|--|-------|---|-------|---|-------|
| | | Estimate | SE | Estimate | SE | Estimate | SE |
| 420 side, slab vs. basement differential pressure | intercept | -0.016 | 0.131 | -0.086 | 0.120 | -0.106 | 0.109 |
| | x(t) | 0.101 | 0.120 | 0.116 | 0.120 | 0.101 | 0.096 |
| | x(t-1) | 0.109 | 0.142 | -0.034 | 0.120 | | |
| | x(t-2) | -0.203 | 0.120 | | | | |

Table 10-10. Model Parameters, Standard Errors by Predictor for X422baseN_AG_radon (X422OF2-1): 2011–2012. Lag4 Models

| Predictor Name | Model Term | Y(t)-Y(t-1) = Intercept + Predictor (t) + Predictor(t-1)+ Predictor(t-2)+ Predictor(t-3)+ Predictor(t-4) | | Y(t)-Y(t-1) = Intercept + Predictor (t) + Predictor(t-1)+ Predictor(t-2) + Predictor(t-3)+ | | Y(t)-Y(t-1) = Intercept + Predictor (t) + Predictor(t-1)+ Predictor(t-2) | | Y(t)-Y(t-1) = Intercept + Predictor (t) + Predictor(t-1) | | Y(t)-Y(t-1) = Intercept + Predictor (t) | |
|--|------------|--|-------|--|-------|--|-------|--|-------|---|-------|
| | | Estimate | SE | Estimate | SE | Estimate | SE | Estimate | SE | Estimate | SE |
| 422 side basement vs. exterior differential pressure | intercept | -0.001 | 0.047 | -0.011 | 0.047 | -0.008 | 0.047 | -0.007 | 0.047 | -0.008 | 0.049 |
| | x(t) | -0.25521** | 0.048 | -0.25277** | 0.048 | -0.25845** | 0.047 | -0.2452** | 0.046 | -0.052 | 0.032 |
| | x(t-1) | 0.21061** | 0.055 | 0.21655** | 0.055 | 0.21495** | 0.055 | 0.2674** | 0.046 | | |
| | x(t-2) | 0.065 | 0.055 | 0.079 | 0.055 | 0.082 | 0.046 | | | | |
| | x(t-3) | 0.017 | 0.055 | -0.008 | 0.047 | | | | | | |
| | x(t-4) | 0.003 | 0.047 | | | | | | | | |

**Significant at 1% level of significance

*Significant at 5% level of significance

10.5 Correlation between Radon Concentration Time Series for 422 Basement South (2012–2013) and Predictor Variables

For time period 2012 to 2013, the variable mitigation was incorporated in the model as a controlling variable to account for the testing of slab depressurization. Thus, all of the model equations have a mitigation term incorporated. **Table 10-11** displays the results for models that include predictors not needing lag terms. Except for soil moisture 16.5 ft bls beneath structure, all three variables in **Table 10-11** have significant positive association with radon concentration after accounting for the effect of mitigation being on during the time period. This is a reasonable result because, as discussed in previous sections, we expect from the literature that drops in barometric pressure and rainfall increase indoor radon. In all models, mitigation was significant and the coefficients were negative, suggesting the expected negative correlation that falling barometric pressure increases radon concentration.

Table 10-11. Model Parameters, Standard Errors by Predictor for 422 Basement Radon: 2012–2013. No Lag Terms in Model

| Time Series | Model: $Y(t)-Y(t-1) = \text{Intercept} + \text{Mitigation}(t) + \text{Predictor}(t)$ | | | |
|--------------------|--|---------------|----------|--------|
| | Predictor Name = $x(t)$ | Model Term | Estimate | SE |
| X422baseS_AG_radon | Drop in barometric pressure | intercept | 0.299 | 0.157 |
| | | $x(t)$ | 0.798** | 0.193 |
| | | mitigation(t) | -0.518* | 0.216 |
| | Rain inches totaled during observation period | intercept | 0.175 | 0.166 |
| | | $x(t)$ | 65.318** | 24.607 |
| | | mitigation(t) | -0.474* | 0.221 |
| | Rain highest rate during observation period | intercept | 0.207 | 0.167 |
| | | $x(t)$ | 5.1572* | 2.561 |
| | | mitigation(t) | -0.4584* | 0.223 |
| | Soil moisture 16.5 ft bls beneath structure | intercept | 0.32675* | 0.158 |
| | | $x(t)$ | -0.336 | 0.690 |
| | | mitigation(t) | -0.532* | 0.216 |

**Significant at 1% level of significance

*Significant at 5% level of significance

Table 10-12 shows the results of models including predictors Lag 1 terms for radon in the 422 basement for the period 2012 to 2013. In a large number of cases, the patterns seen in the 422 office data set in 2011 to 2012 (**Table 10-8**) are repeated in this basement 2012 to 2013 data set. The sign and magnitude of the coefficients for external temperature, barometric pressure, and height of Fall Creek rain gauge are quite similar for example. Thus, the interpretations provided in Section 10.4 also apply here and will not be repeated for brevity.

Note that in **Table 10-12** the mitigation effect is calculated in each model, but the calculated values are similar to each other although not identical.

The **Table 10-12** data set is also similar to **Table 10-8** in that the depth of snow on the ground is not significant in either data set. As discussed in Section 9, some literature suggests that radon moves easily through snow packs, so this result is reasonable.

Table 10-12. Model Parameters, Standard Errors by Model and Predictor for 422 Basement Radon: 2012–2013 Lag 1 Models

| Predictor Name | Model Term | Model : $Y(t)-Y(t-1) = \text{Intercept} + \text{Mitigation}(t) + \text{Predictor}(t) + \text{Predictor}(t-1)$ | | Model : $Y(t)-Y(t-1) = \text{Intercept} + \text{Mitigation}(t) + \text{Predictor}(t)$ | |
|----------------------|---------------|---|---------|---|---------|
| | | Estimate | SE | Estimate | SE |
| Air density interior | Intercept | 34.46805** | 9.136 | 20.88483* | 8.837 |
| | mitigation(t) | -0.51691* | 0.214 | -0.50571* | 0.221 |
| | $x(t)$ | 354.740 | 187.911 | -276.63943* | 118.699 |
| | $x(t-1)$ | -813.64637** | 191.384 | | |

(continued)

Table 10-12. Model Parameters, Standard Errors by Model and Predictor for 422 Basement Radon: 2012–2013 Lag 1 Models (cont.)

| Predictor Name | Model Term | Model : $Y(t)-Y(t-1) =$ Intercept + Mitigation(t) + Predictor (t) + Predictor (t-1) | | Model : $Y(t)-Y(t-1) =$ Intercept + Mitigation(t) + Predictor (t) | |
|--|---------------|---|--------|---|--------|
| | | Estimate | SE | Estimate | SE |
| Barometric pressure | Intercept | 40.47232* | 18.416 | 10.929 | 16.622 |
| | mitigation(t) | -0.6509** | 0.228 | -0.54489* | 0.230 |
| | x(t) | 0.945 | 0.658 | -0.353 | 0.552 |
| | x(t-1) | -2.27969** | 0.660 | | |
| Cooling degree day | Intercept | 0.154 | 0.159 | 0.293 | 0.172 |
| | mitigation(t) | -0.43284* | 0.208 | -0.51052* | 0.226 |
| | x(t) | -18.75498** | 3.894 | 0.023 | 2.971 |
| | x(t-1) | 26.55995** | 3.950 | | |
| Dew point, interior | Intercept | -0.781 | 0.469 | -0.487 | 0.465 |
| | mitigation(t) | -0.389 | 0.225 | -0.422 | 0.228 |
| | x(t) | -0.049 | 0.026 | 0.020 | 0.011 |
| | x(t-1) | 0.07627** | 0.026 | | |
| Dew point, exterior | intercept | -0.474 | 0.335 | 0.083 | 0.350 |
| | mitigation(t) | -0.413 | 0.210 | -0.48707* | 0.226 |
| | x(t) | -0.067** | 0.014 | 0.006 | 0.008 |
| | x(t-1) | 0.08762** | 0.014 | | |
| Height measured at Fall Creek stream gauge | intercept | 0.438 | 0.350 | 0.217 | 0.341 |
| | mitigation(t) | -0.55895* | 0.221 | -0.53849* | 0.221 |
| | x(t) | 0.411* | 0.166 | 0.030 | 0.081 |
| | x(t-1) | -0.43615** | 0.166 | | |
| Heating degree days | intercept | 0.57716* | 0.233 | 0.296 | 0.244 |
| | mitigation(t) | -0.46499* | 0.209 | -0.51029* | 0.225 |
| | x(t) | 3.89451** | 0.742 | -0.008 | 0.419 |
| | x(t-1) | -4.56292** | 0.739 | | |
| Exterior heating index— calculated based on temperature and humidity | intercept | -0.392 | 0.367 | 0.256 | 0.395 |
| | mitigation(t) | -0.44966* | 0.204 | -0.50762* | 0.226 |
| | x(t) | -0.08667** | 0.014 | 0.001 | 0.008 |
| | x(t-1) | 0.10184** | 0.014 | | |
| Humidity interior | intercept | -0.122 | 0.353 | 0.059 | 0.356 |
| | mitigation(t) | -0.44899* | 0.225 | -0.47586* | 0.229 |
| | x(t) | -0.06728** | 0.025 | 0.007 | 0.010 |
| | x(t-1) | 0.07987** | 0.024 | | |
| Humidity exterior | intercept | -1.370 | 0.840 | -1.249 | 0.749 |
| | mitigation(t) | -0.4653* | 0.224 | -0.47371* | 0.222 |
| | x(t) | 0.019 | 0.012 | 0.02065* | 0.010 |
| | x(t-1) | 0.004 | 0.012 | | |

(continued)

Table 10-12. Model Parameters, Standard Errors by Model and Predictor for 422 Basement Radon: 2012–2013 Lag 1 Models (cont.)

| Predictor Name | Model Term | Model : $Y(t)-Y(t-1) =$ Intercept + Mitigation(t) + Predictor (t) + Predictor (t-1) | | Model : $Y(t)-Y(t-1) =$ Intercept + Mitigation(t) + Predictor (t) | |
|--|---------------|---|-------|---|-------|
| | | Estimate | SE | Estimate | SE |
| Interior Heating Index | intercept | -5.03405** | 1.720 | -3.92999* | 1.647 |
| | mitigation(t) | -0.386 | 0.223 | -0.411 | 0.224 |
| | x(t) | -0.031 | 0.049 | 0.06073* | 0.024 |
| | x(t-1) | 0.10743* | 0.051 | | |
| Depth of snow on the ground | intercept | 0.270 | 0.162 | 0.275 | 0.161 |
| | mitigation(t) | -0.50981* | 0.216 | -0.51539* | 0.215 |
| | x(t) | 0.069 | 0.158 | 0.104 | 0.085 |
| | x(t-1) | 0.042 | 0.159 | | |
| Soil moisture, 13 ft bls beneath structure | intercept | 0.413 | 0.263 | 0.406 | 0.259 |
| | mitigation(t) | -0.54499* | 0.221 | -0.54187* | 0.219 |
| | x(t) | 0.017 | 0.229 | -0.018 | 0.042 |
| | x(t-1) | -0.036 | 0.230 | | |
| Soil moisture 6 ft bls beneath structure | intercept | -0.802 | 0.804 | -0.555 | 0.799 |
| | mitigation(t) | -0.427 | 0.219 | -0.5213* | 0.215 |
| | x(t) | -0.127 | 0.067 | 0.005 | 0.005 |
| | x(t-1) | 0.133 | 0.068 | | |
| Soil moisture, 3.5 ft bls exterior | intercept | 0.347 | 0.290 | 0.464 | 0.283 |
| | mitigation(t) | -0.4946* | 0.233 | -0.46782* | 0.234 |
| | x(t) | -0.005 | 0.002 | -0.001 | 0.001 |
| | x(t-1) | 0.004 | 0.002 | | |
| Soil moisture 6 ft bls exterior | intercept | -0.596 | 0.452 | -0.309 | 0.447 |
| | mitigation(t) | -0.60875** | 0.215 | -0.58545** | 0.218 |
| | x(t) | -0.005 | 0.003 | 0.003 | 0.002 |
| | x(t-1) | 0.00914** | 0.003 | | |
| Temperature, 422 first floor | intercept | -5.207* | 2.017 | -4.3276* | 1.933 |
| | mitigation(t) | -0.435 | 0.223 | -0.44668* | 0.223 |
| | x(t) | -0.013 | 0.057 | 0.06414* | 0.027 |
| | x(t-1) | 0.090 | 0.059 | | |
| Exterior temperature (°F) | intercept | -0.358 | 0.373 | 0.284 | 0.399 |
| | mitigation(t) | -0.45692* | 0.205 | -0.51003* | 0.226 |
| | x(t) | -0.08621** | 0.014 | 0.000 | 0.008 |
| | x(t-1) | 0.10054** | 0.014 | | |
| Temperature exterior, high during data collection period | intercept | -0.374 | 0.375 | 0.260 | 0.401 |
| | mitigation(t) | -0.4561* | 0.205 | -0.50818* | 0.226 |
| | x(t) | -0.08492** | 0.014 | 0.001 | 0.008 |
| | x(t-1) | 0.09949** | 0.014 | | |

(continued)

Table 10-12. Model Parameters, Standard Errors by Model and Predictor for 422 Basement Radon: 2012–2013 Lag 1 Models (cont.)

| Predictor Name | Model Term | Model : $Y(t)-Y(t-1) =$ Intercept + Mitigation(t) + Predictor (t) + Predictor (t-1) | | Model : $Y(t)-Y(t-1) =$ Intercept + Mitigation(t) + Predictor (t) | |
|--|---------------|---|-------|---|-------|
| | | Estimate | SE | Estimate | SE |
| Lowest exterior temperature | intercept | -0.370 | 0.371 | 0.266 | 0.397 |
| | mitigation(t) | -0.45514* | 0.205 | -0.50864* | 0.226 |
| | x(t) | -0.08599** | 0.014 | 0.001 | 0.008 |
| | x(t-1) | 0.10073** | 0.014 | | |
| Temperature, humidity and wind index | intercept | -0.224 | 0.322 | 0.309 | 0.345 |
| | mitigation(t) | -0.45807* | 0.205 | -0.51239* | 0.226 |
| | x(t) | -0.07583** | 0.013 | 0.000 | 0.007 |
| | x(t-1) | 0.08785** | 0.012 | | |
| Wind chill | intercept | -0.197 | 0.326 | 0.331 | 0.348 |
| | mitigation(t) | -0.46436* | 0.206 | -0.51439* | 0.226 |
| | x(t) | -0.07522** | 0.013 | -0.001 | 0.007 |
| | x(t-1) | 0.08654** | 0.013 | | |
| Wind direction (average) | intercept | 0.066 | 0.405 | -0.022 | 0.346 |
| | mitigation(t) | -0.50485* | 0.225 | -0.50827* | 0.223 |
| | x(t) | 0.002 | 0.002 | 0.002 | 0.002 |
| | x(t-1) | -0.001 | 0.002 | | |
| Wind direction (of high during measurement period) | intercept | 0.119 | 0.405 | 0.045 | 0.348 |
| | mitigation(t) | -0.50456* | 0.225 | -0.50736* | 0.224 |
| | x(t) | 0.002 | 0.002 | 0.001 | 0.002 |
| | x(t-1) | -0.001 | 0.002 | | |
| Wind run is a function of wind speed and duration | intercept | 0.092 | 0.256 | 0.244 | 0.236 |
| | mitigation(t) | -0.55184* | 0.229 | -0.52169* | 0.227 |
| | x(t) | -0.064 | 0.113 | 0.027 | 0.096 |
| | x(t-1) | 0.175 | 0.113 | | |
| High wind speed during measurement period | intercept | 0.009 | 0.289 | 0.181 | 0.265 |
| | mitigation(t) | -0.56257* | 0.229 | -0.5332* | 0.228 |
| | x(t) | -0.009 | 0.027 | 0.012 | 0.023 |
| | x(t-1) | 0.040 | 0.027 | | |
| Average wind speed during measurement period | intercept | 0.092 | 0.256 | 0.244 | 0.236 |
| | mitigation(t) | -0.55184* | 0.229 | -0.52169* | 0.227 |
| | x(t) | -0.032 | 0.056 | 0.014 | 0.048 |
| | x(t-1) | 0.088 | 0.056 | | |

**Significant at 1% level of significance

*Significant at 5% level of significance

10.6 Correlation between Radon Concentration Time Series for 422 Office on 2nd Floor and Predictor Variables

For time period 2012 to 2013, the variable mitigation was incorporated in the model for the office as well as a controlling variable to account for the testing of subslab depressurization. **Table 10-13** displays the results for models that include predictors not needing lag terms in the model. Drops in barometric pressure and rainfall have significant positive association with radon concentration after accounting for the effect of mitigation being on during the time period. These results are expected from the literature as discussed earlier in this section.

Table 10-13. Model Parameters, Standard Errors by Predictor for X422office_2nd_AG_radon Concentration (X422OF2-2): 2012–2013. No Lag Terms in Model

| Time Series | Model : $Y(t)-Y(t-1) = \text{Intercept} + \text{Predictor}(t)$ | | | |
|-------------------------|--|---------------|----------|--------|
| | Predictor Name = $x(t)$ | Model Term | Estimate | SE |
| X422office_2nd_AG_radon | Drop in Barometric Pressure | intercept | 0.084 | 0.076 |
| | | $x(t)$ | 0.561** | 0.093 |
| | | mitigation(t) | -0.174 | 0.104 |
| | Rain inches totaled during observation period | intercept | 0.019 | 0.083 |
| | | $x(t)$ | 34.104** | 12.313 |
| | | mitigation(t) | -0.149 | 0.111 |
| | Rain highest rate during observation period | intercept | 0.046 | 0.084 |
| | | $x(t)$ | 2.063 | 1.288 |
| | | mitigation(t) | -0.147 | 0.112 |
| | Soil moisture 16.5 ft bls beneath structure | intercept | 0.099 | 0.079 |
| | | $x(t)$ | 0.055 | 0.347 |
| | | mitigation(t) | -0.182 | 0.108 |

**Significant at 1% level of significance

Table 10-14 shows the results of models including predictors requiring Lag 1 terms to model for the 422 Office for the period 2012 to 2013. The patterns of sign of the $x(t)$ and $x(t-1)$ terms for some of the most interesting parameters, such as exterior temperature and Fall Creek gauge height, parallel those seen in the previous year's data set in **Table 10-8**. The coefficients were somewhat different than for the previous year's data set. Therefore, the qualitative interpretations provided in Section 10.4 for those parameters apply here and will not be repeated for brevity.

There were some modest differences with this 2012–2013 data set as compared to the 2011–2012 data set. For example, the 2012–2013 office data set does not show a statistically significant humidity effect in the full model (**Table 10-14**), although the effect in the reduced model is significant and similar to the result from the 2011–2012 data set (**Table 10-8**).

Mitigation provides a benefit in almost all cases, just as was seen in the basement data set. The magnitude of the mitigation benefit in pCi/L is lower upstairs than in the basement, which is expected since the unmitigated concentrations upstairs are lower than the unmitigated concentrations in the basement.

Table 10-14. Model Parameters, Standard Errors by Model and Predictor for X422office_2nd_AG_radon Concentration (X422OF2-2): 2012–2013 Lag 1 Models

| Predictor Name | Model Term | Model : $Y(t)-Y(t-1) = \text{Intercept} + \text{Predictor}(t) + \text{Predictor}(t-1)$ | | Model : $Y(t)-Y(t-1) = \text{Intercept} + \text{Predictor}(t)$ | |
|--|---------------|--|----------|--|----------|
| | | Estimate | SE | Estimate | SE |
| Air density interior | intercept | 12.06096** | 4.61969 | 4.97669 | 4.47063 |
| | mitigation(t) | -0.17894 | 0.10823 | -0.16696 | 0.11191 |
| | x(t) | 244.35736* | 95.02056 | -65.7802 | 60.05041 |
| | x(t-1) | -405.1163** | 96.77658 | | |
| Barometric pressure | intercept | 22.75505* | 9.1404 | 5.43045 | 8.32925 |
| | mitigation(t) | -0.2547* | 0.11311 | -0.18533 | 0.11525 |
| | x(t) | 0.54341 | 0.32666 | -0.17777 | 0.27675 |
| | x(t-1) | -1.29649** | 0.32735 | | |
| Cooling degree day | intercept | 0.09455 | 0.08373 | 0.13298 | 0.0856 |
| | mitigation(t) | -0.18022 | 0.10915 | -0.19906 | 0.11248 |
| | x(t) | -8.76847** | 2.04811 | -2.8046 | 1.47652 |
| | x(t-1) | 8.48575** | 2.07788 | | |
| Dew point, interior | intercept | -0.3166 | 0.23253 | -0.11388 | 0.23414 |
| | mitigation(t) | -0.12924 | 0.11153 | -0.14608 | 0.11476 |
| | x(t) | -0.03995** | 0.01282 | 0.005 | 0.00565 |
| | x(t-1) | 0.05038** | 0.01287 | | |
| Dew point, exterior | intercept | -0.15241 | 0.16129 | 0.18395 | 0.17534 |
| | mitigation(t) | -0.14079 | 0.10092 | -0.17985 | 0.11346 |
| | x(t) | -0.04584** | 0.0067 | -0.00281 | 0.00421 |
| | x(t-1) | 0.05222** | 0.0067 | | |
| Height measured at Fall Creek stream gauge | intercept | 0.04278 | 0.17284 | -0.08965 | 0.16992 |
| | mitigation(t) | -0.17441 | 0.10914 | -0.15852 | 0.10981 |
| | x(t) | 0.26485** | 0.08217 | 0.04413 | 0.04048 |
| | x(t-1) | -0.25319** | 0.08213 | | |
| Heating degree days | intercept | 0.15756 | 0.11004 | -0.03351 | 0.12186 |
| | mitigation(t) | -0.16145 | 0.09882 | -0.18448 | 0.11256 |
| | x(t) | 2.6996** | 0.35027 | 0.2624 | 0.20917 |
| | x(t-1) | -2.87089** | 0.34897 | | |
| Exterior heating index— calculated based on temperature and humidity | intercept | -0.0601 | 0.1755 | 0.32065 | 0.19695 |
| | mitigation(t) | -0.1603 | 0.09756 | -0.1885 | 0.11278 |
| | x(t) | -0.0554** | 0.00672 | -0.00536 | 0.004 |
| | x(t-1) | 0.05861** | 0.00671 | | |
| Humidity interior | intercept | -0.11104 | 0.17324 | 0.01439 | 0.17854 |
| | mitigation(t) | -0.14609 | 0.11011 | -0.15832 | 0.11465 |
| | x(t) | -0.04852** | 0.0121 | 0.00204 | 0.0049 |
| | x(t-1) | 0.05451** | 0.01196 | | |

(continued)

Table 10-14. Model Parameters, Standard Errors by Model and Predictor for X422office_2nd_AG_radon Concentration (X422OF2-2): 2012–2013 Lag 1 Models (cont.)

| Predictor Name | Model Term | Model : $Y(t)-Y(t-1) = \text{Intercept} + \text{Predictor}(t) + \text{Predictor}(t-1)$ | | Model : $Y(t)-Y(t-1) = \text{Intercept} + \text{Predictor}(t)$ | |
|--|---------------|--|---------|--|---------|
| | | Estimate | SE | Estimate | SE |
| Humidity exterior | intercept | -0.85948* | 0.41918 | -0.77538* | 0.37462 |
| | mitigation(t) | -0.14924 | 0.11204 | -0.1476 | 0.11118 |
| | x(t) | 0.00927 | 0.00617 | 0.01146* | 0.0049 |
| | x(t-1) | 0.00338 | 0.00618 | | |
| Interior heating index | intercept | -1.18663 | 0.87626 | -0.75597 | 0.83561 |
| | mitigation(t) | -0.14504 | 0.11381 | -0.14835 | 0.11368 |
| | x(t) | -0.01957 | 0.02497 | 0.01203 | 0.01196 |
| | x(t-1) | 0.03793 | 0.02575 | | |
| Depth of snow on the ground | intercept | 0.07105 | 0.08145 | 0.07316 | 0.0806 |
| | mitigation(t) | -0.17566 | 0.10847 | -0.17781 | 0.10772 |
| | x(t) | 0.04996 | 0.0795 | 0.06345 | 0.04261 |
| | x(t-1) | 0.01604 | 0.07972 | | |
| Soil moisture, 13 ft bls beneath structure | intercept | 0.08809 | 0.1319 | 0.07184 | 0.13014 |
| | mitigation(t) | -0.18544 | 0.11073 | -0.17751 | 0.11017 |
| | x(t) | 0.09404 | 0.11492 | 0.00574 | 0.02099 |
| | x(t-1) | -0.09041 | 0.11569 | | |
| Soil moisture 6 ft bls beneath structure | intercept | -0.10557 | 0.40645 | -0.01077 | 0.4025 |
| | mitigation(t) | -0.14658 | 0.11059 | -0.18287 | 0.10816 |
| | x(t) | -0.0499 | 0.03399 | 0.00064 | 0.00228 |
| | x(t-1) | 0.05101 | 0.03423 | | |
| Soil moisture, 3.5 ft bls exterior | intercept | 0.07703 | 0.14646 | 0.10444 | 0.14243 |
| | mitigation(t) | -0.18782 | 0.11796 | -0.18157 | 0.11762 |
| | x(t) | -0.00089 | 0.00126 | -2.00E-05 | 0.00067 |
| | x(t-1) | 0.00101 | 0.00124 | | |
| Soil moisture 6 ft bls exterior | intercept | -0.16799 | 0.2302 | -0.07969 | 0.22524 |
| | mitigation(t) | -0.20792 | 0.10957 | -0.20076 | 0.10994 |
| | x(t) | -0.0016 | 0.00169 | 8.00E-04 | 0.00094 |
| | x(t-1) | 0.00281 | 0.00165 | | |
| Temperature, 422 first floor | intercept | -1.03116 | 1.0247 | -0.7593 | 0.97944 |
| | mitigation(t) | -0.15938 | 0.11332 | -0.15652 | 0.11284 |
| | x(t) | -0.00889 | 0.02903 | 0.01166 | 0.01355 |
| | x(t-1) | 0.02443 | 0.02976 | | |
| Exterior Temperature (°F) | intercept | -0.04636 | 0.17824 | 0.33336 | 0.19908 |
| | mitigation(t) | -0.16269 | 0.09789 | -0.18821 | 0.11264 |
| | x(t) | -0.0553** | 0.0068 | -0.00561 | 0.00403 |
| | x(t-1) | 0.0582** | 0.00679 | | |

(continued)

Table 10-14. Model Parameters, Standard Errors by Model and Predictor for X422office_2nd_AG_radon Concentration (X422OF2-2): 2012–2013 Lag 1 Models (cont.)

| Predictor Name | Model Term | Model : $Y(t)-Y(t-1) =$ Intercept + Predictor (t) + Predictor (t-1) | | Model : $Y(t)-Y(t-1) =$ Intercept + Predictor (t) | |
|--|---------------|---|---------|--|---------|
| | | Estimate | SE | Estimate | SE |
| Temperature exterior, high during data collection period | intercept | -0.05542 | 0.18007 | 0.3181 | 0.19999 |
| | mitigation(t) | -0.16208 | 0.09851 | -0.18684 | 0.1127 |
| | x(t) | -0.0542** | 0.00685 | -0.00522 | 0.00401 |
| | x(t-1) | 0.05727** | 0.00684 | | |
| Lowest exterior temperature | intercept | -0.05472 | 0.17769 | 0.32169 | 0.19822 |
| | mitigation(t) | -0.16152 | 0.09804 | -0.18725 | 0.11267 |
| | x(t) | -0.05517** | 0.00684 | -0.0054 | 0.00404 |
| | x(t-1) | 0.05828** | 0.00683 | | |
| Temperature, humidity and wind index | intercept | -0.00968 | 0.1538 | 0.30327 | 0.1718 |
| | mitigation(t) | -0.1647 | 0.0982 | -0.19085 | 0.11272 |
| | x(t) | -0.04851** | 0.00598 | -0.00521 | 0.00354 |
| | x(t-1) | 0.05072** | 0.00597 | | |
| Wind chill | intercept | 0.00109 | 0.1559 | 0.31297 | 0.17335 |
| | mitigation(t) | -0.16674 | 0.09852 | -0.19049 | 0.11259 |
| | x(t) | -0.04828** | 0.00604 | -0.0054 | 0.00356 |
| | x(t-1) | 0.05023** | 0.00603 | | |
| Wind direction (average) | intercept | -0.09544 | 0.2019 | -0.16009 | 0.17276 |
| | mitigation(t) | -0.17169 | 0.11218 | -0.16626 | 0.11159 |
| | x(t) | 0.00137 | 0.00083 | 0.00121 | 0.00077 |
| | x(t-1) | -0.00046 | 0.00083 | | |
| Wind direction (of high during measurement period) | intercept | -0.07846 | 0.20227 | -0.1357 | 0.17383 |
| | mitigation(t) | -0.171 | 0.11235 | -0.1652 | 0.11173 |
| | x(t) | 0.00123 | 0.00085 | 0.00109 | 0.00078 |
| | x(t-1) | -4.00E-04 | 0.00085 | | |
| Wind run is a function of wind speed and duration | intercept | -0.0663 | 0.12726 | 0.03087 | 0.11839 |
| | mitigation(t) | -0.20776 | 0.11376 | -0.17926 | 0.11377 |
| | x(t) | -0.03347 | 0.0561 | 0.02779 | 0.04824 |
| | x(t-1) | 0.11895* | 0.05615 | | |
| High wind speed during measurement period | intercept | -0.12455 | 0.14387 | -0.01764 | 0.13236 |
| | mitigation(t) | -0.21512 | 0.11412 | -0.18769 | 0.1139 |
| | x(t) | -0.00303 | 0.01346 | 0.01074 | 0.01144 |
| | x(t-1) | 0.02608 | 0.01346 | | |
| Average wind speed during measurement period | intercept | -0.0663 | 0.12726 | 0.03087 | 0.11839 |
| | mitigation(t) | -0.20776 | 0.11376 | -0.17926 | 0.11377 |
| | x(t) | -0.01674 | 0.02805 | 0.0139 | 0.02412 |
| | x(t-1) | 0.05948* | 0.02808 | | |

**Significant at 1% level of significance; * Significant at 5% level of significance

10.7 Correlation between VOC (Radiello) Time Series and Predictor Variables in 422 Basement South

The association between four Radiello time series and a series of predictors were investigated in this section. Details of the periodicity, time period and location are displayed in **Table 10-15**. Please refer to the discussion of the terminology, and methods of time series analysis presented earlier in this section in the context of a discussion of the radon time series. Examples of how to read the output tables were also provided earlier in this section.

Table 10-15. Name, Periodicity, Time Period, and Location of Time Series (Outcome) Considered

| Time Series Name | Variable Name in Data Set | Periodicity | Time Period | Location |
|----------------------------|---------------------------------|-------------|------------------------------|----------------|
| X422BaseS Radiello CHCI3-1 | X422BaseS_Radiello_Weekly_CHCI3 | Weekly | Jan 5, 2011–Feb 15, 2012 | Basement south |
| X422BaseS Radiello PCE-1 | X422BaseS_Radiello_Weekly_PCE | Weekly | Jan 5, 2011–Feb 15, 2012 | Basement south |
| X422BaseS Radiello CHCI3-2 | X422BaseS_Radiello_Weekly_CHCI3 | Weekly | Sept 26, 2012–April 10, 2013 | Basement south |
| X422BaseS Radiello PCE-2 | X422BaseS_Radiello_Weekly_PCE | Weekly | Sept 26, 2012–April 10, 2013 | Basement south |

10.7.1 Stationarity and Serial Correlation Analysis

As a first step in the time series data analysis, we explored the stationarity and serial correlation of the time series. The p-values of the stationarity tests suggested the chloroform time series, period Jan 5, 2011–Feb 15, 2012, is non-stationary (**Figure 10-11**). A first difference of that time series was calculated (i.e., $y(t) - y(t-1)$ where $y(t)$ denotes the measurement of 422 Base South Chloroform at time t), and corresponding plots are displayed in **Figure 10-12**. The stationarity tests results suggested the first differences constitute a stationary time series; therefore, no further transformations were needed. None of the partial autocorrelation functions (spikes) in the PACF plot were statistically significant (none of the spikes are crossing blue lines), suggesting no significant serial correlation remained in the first differences time series. As a result, a model for this time series did not include any lag-terms. Note that while autocorrelation was found in the radon analyses, those analyses used daily data sets. Significant autocorrelation in indoor concentrations between one week and the next is not necessarily physically expected.

The plot of the time series 422BaseSouth PCE for the, period Jan 5, 2011–Feb 15, 2012, suggested some non-stationarity in the mean (non-constant means) in the first weeks, and a more stationary mean and variance (more stable plot) in the later weeks (**Figure 10-13**). For example, the average of the first 4 observations is not the same as the average of the last observations. The test for non-stationarity suggests that the deviations for non-stationarity were not significant (both p-values < 0.01). Therefore, no transformation was needed of this data set. The PACF plot suggested serial autocorrelation at lag 2 weeks, this indicates that three weekly consecutive measurements are correlated. We accounted for the serial

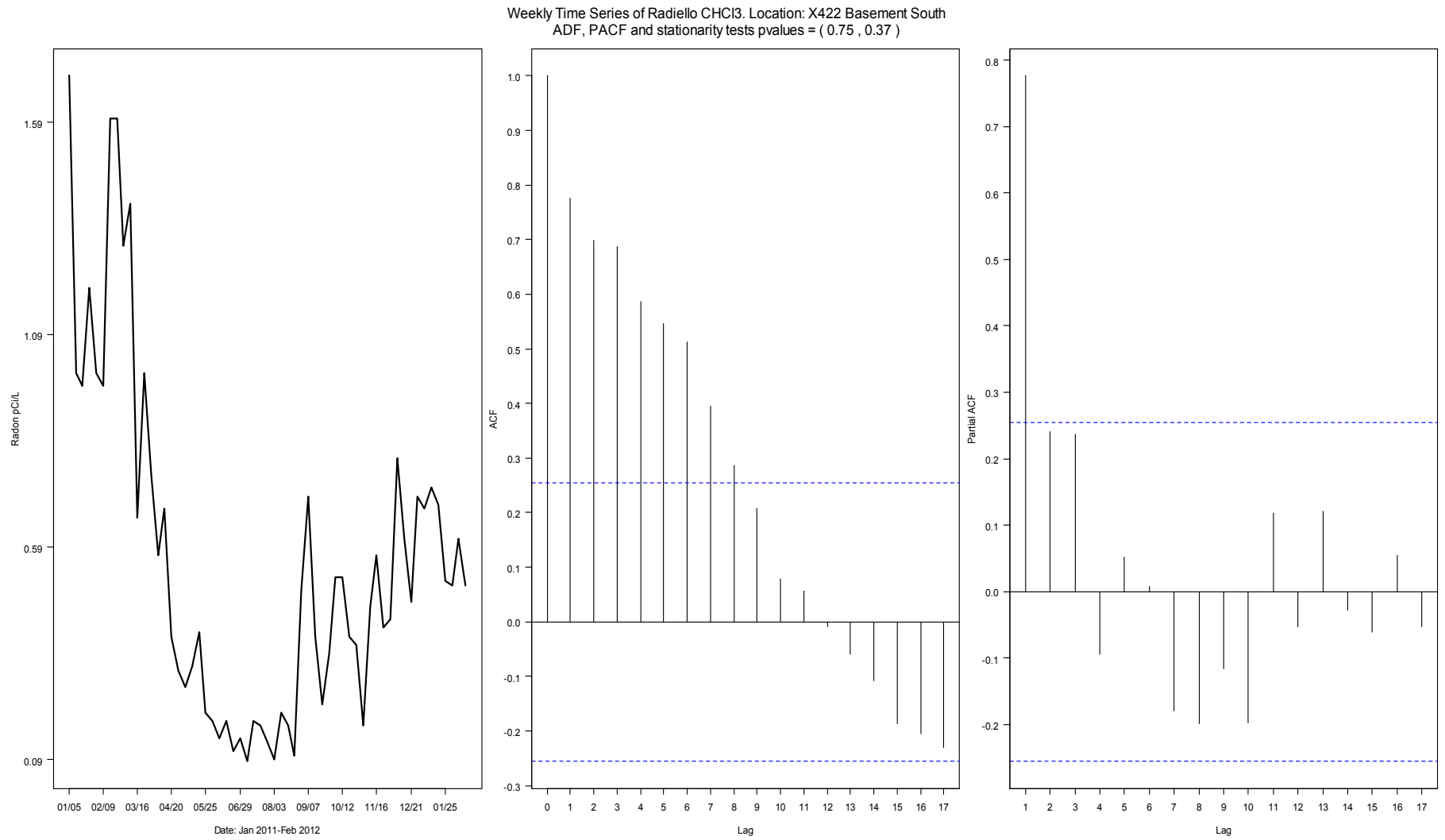


Figure 10-11. Time series plot, ACF and PACF for weekly Radiello chloroform. Location X422 basement south. Time period: Jan 5, 2011–Feb 15, 2012.

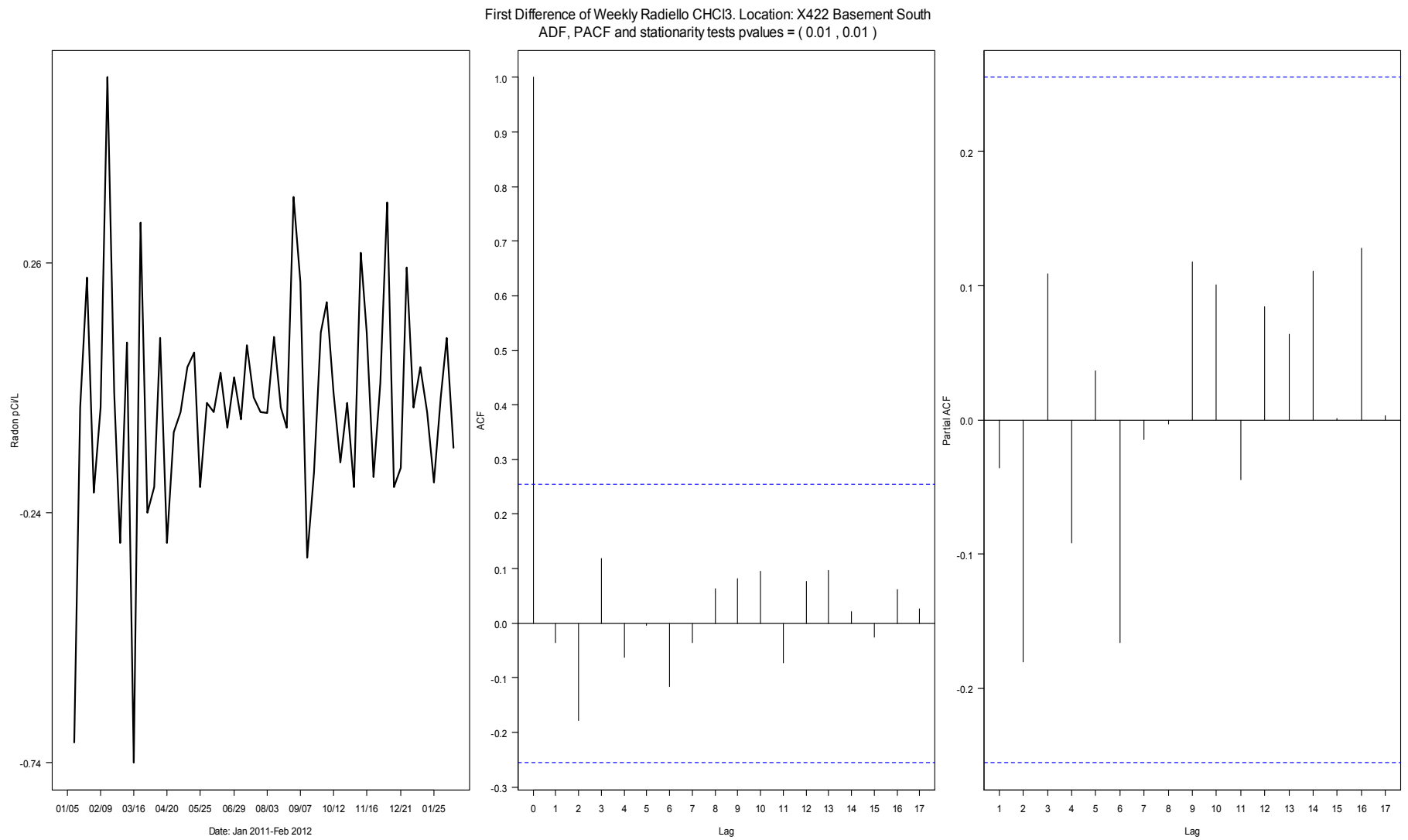


Figure 10-12. Time series plot, ACF and PACF for first difference of weekly Radiello. Chloroform. Location X422 basement south. Time period: Jan 5, 2011–Feb 15, 2012.

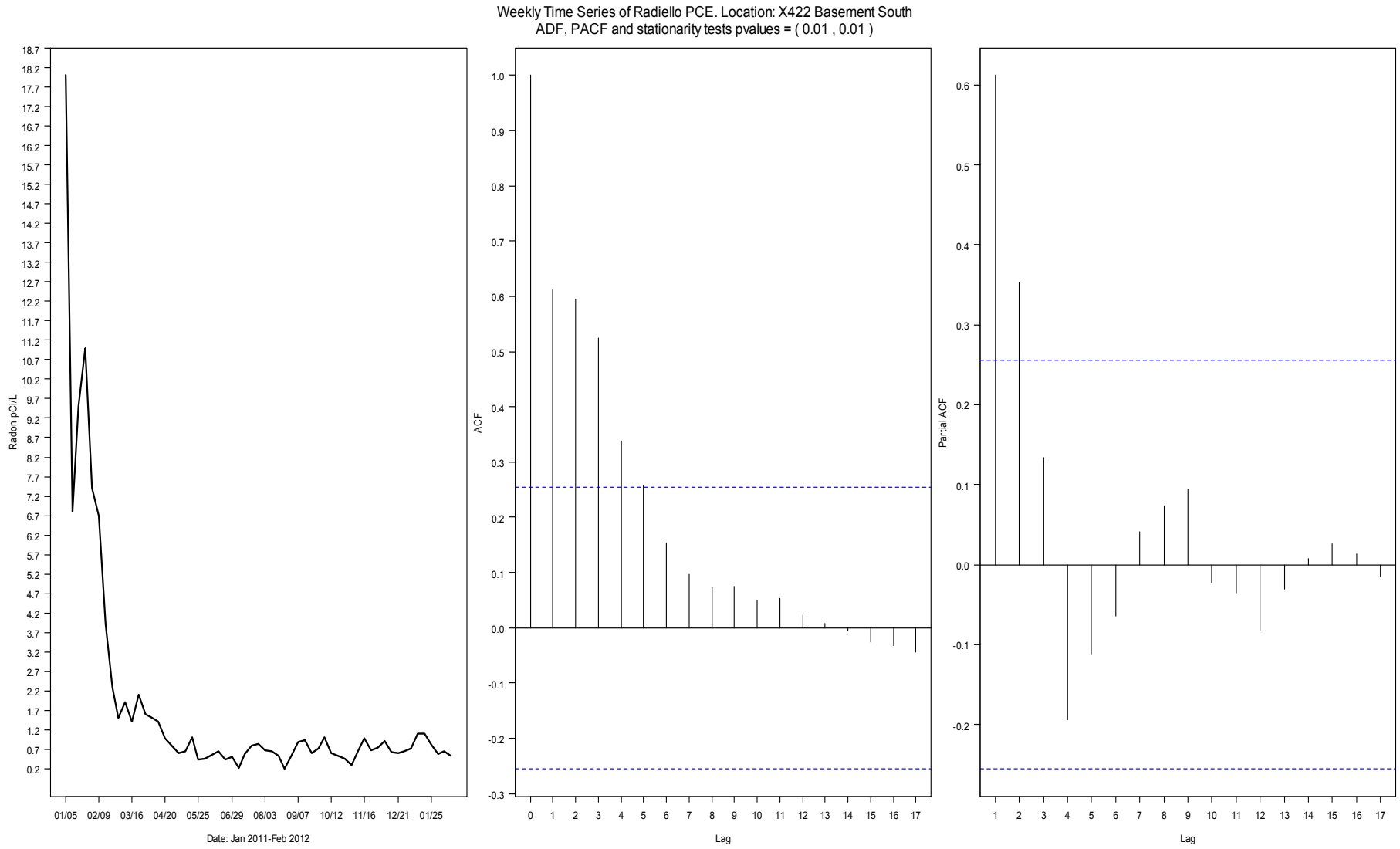


Figure 10-13. Time series plot, ACF and PACF for weekly Radiello PCE. Location X422 basement south. Time period: Jan 5, 2011–Feb 15, 2012.

autocorrelation in the models by modeling the error term²⁵ instead of adding lag terms of the response as predictors (Cochrane and Orcutt, 1949).

Figure 10-14 display the time series and corresponding ACF and PACF plots for 422 Base South chloroform data set for the period Sept 26, 2012–April 10, 2013. The stationarity test results were conflicting (one concluding non-stationarity and the other suggesting stationarity). We investigated the non-stationarity of the first differences time series (**Figure 10-15**), and both tests concluded stationarity at 5% and 1% significance level. None of the partial autocorrelation functions (spikes) in the PACF plot were statistically significant (none of the spikes are crossing blue lines), suggesting no significant serial correlation remained in the first differences time series. A model for X422BaseS Radiello CHCl3-2 thus did not include any lag-term of the outcome.

Similarly, **Figures 10-16** and **10-17** display the time series, and corresponding ACF and PACF plots for the time series and first differences of the 422 Base South PCE data set for the, period Sept 26, 2012–April 10, 2013. The original time series did not pass both stationarity tests. We proceeded to calculate the first differences of the time series, which passed both stationarity tests (**Figure 10-17**). No indication of significant serial correlation was detected from the PACF plot (**Figure 10-17**).

Table 10-16 summarizes the transformation (first difference or no difference needed) and serial correlation determined for each of the four time series data sets. The needed transformations were then applied before modeling the data. The serial correlations identified were used to determine how many lag terms were needed in the equation fit to the data.

Table 10-16. Transformation and Terms Required by Time Series

| Time Series Name | Transformation | Serial Correlation |
|----------------------------|----------------------|--------------------|
| X422BaseS Radiello CHCl3-1 | First difference | None |
| X422BaseS Radiello PCE-1 | No difference needed | Second order |
| X422BaseS Radiello CHCl3-2 | First difference | None |
| X422BaseS Radiello PCE-2 | First difference | None |

²⁵The error term is the difference between the actual value of the independent variable and the value predicted by the regression equation. In the presence of non-significant serial correlation, the outcome is approximately independent, which results in error terms that are approximately independent. The serial correlation also affects the constant variance assumption that is inherent in regression analysis. Having non-constant variance will affect the results of the test-statistics used to evaluate the significance of the parameters in the regression equation. This is addressed at the model level by incorporating a model for the errors that accounts for the serial correlation. Using an appropriate model for the errors results in correct results for the testing of the significance of the parameters (Judge et al., 1985).

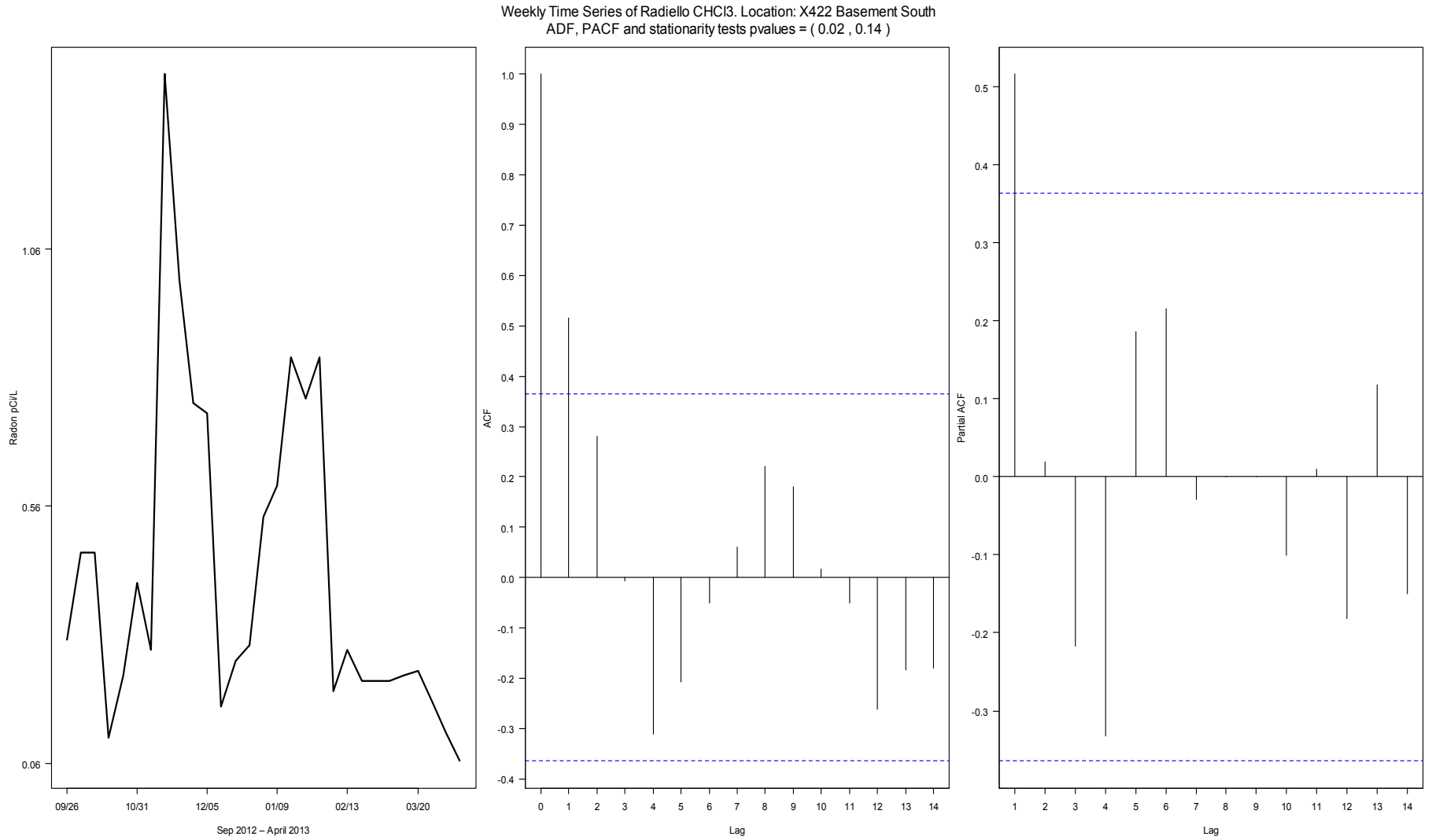


Figure 10-14. Time series plot, ACF and PACF for weekly chloroform. Location X422 basement south. Time period: Sept 26, 2012–April 10, 2013.

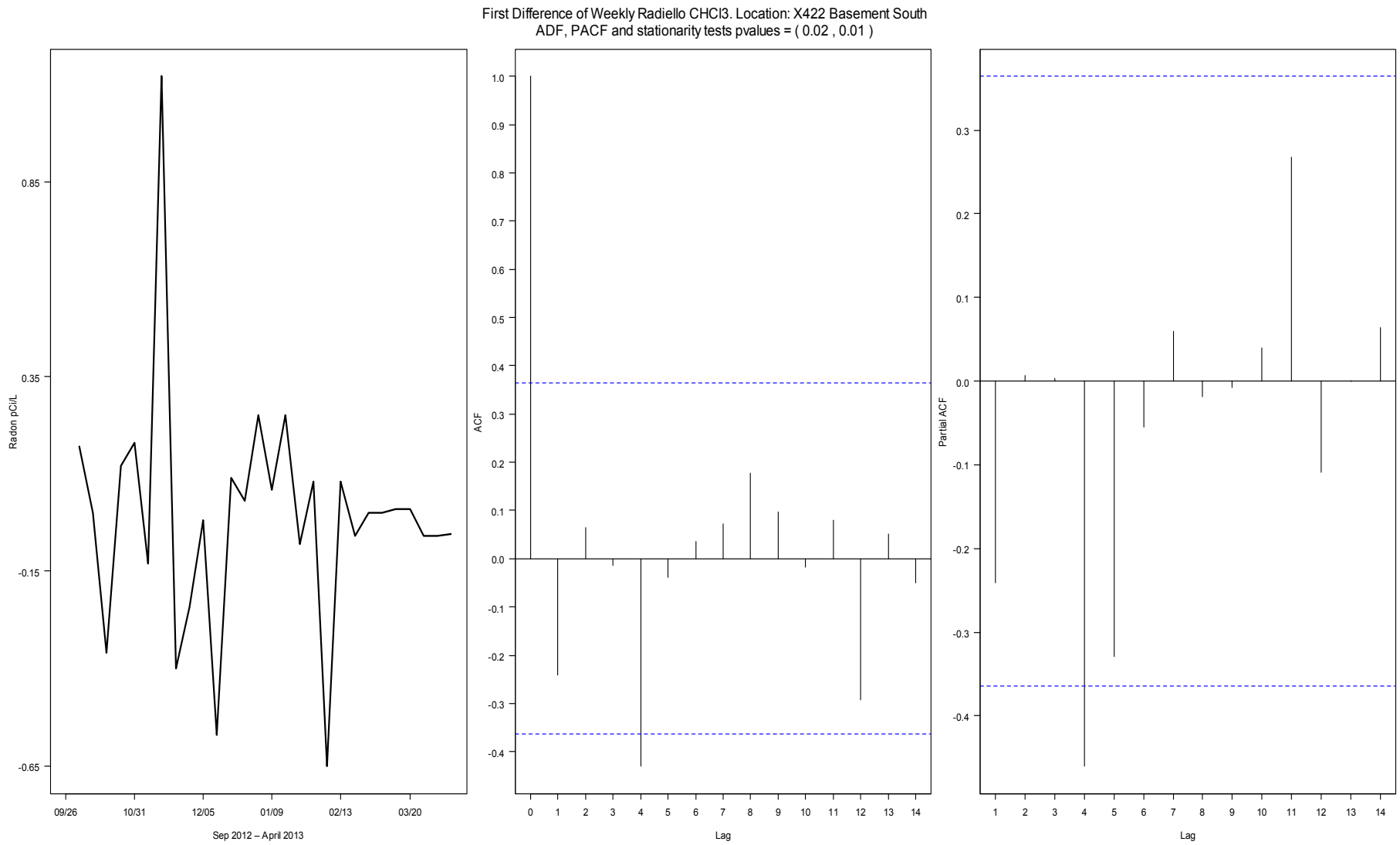


Figure 10-15. Time series plot, ACF and PACF for first difference weekly Radiello CHCl3-2 (X422BaseS_Radiello_Weekly_CHCl3). Location X422 basement south. Time period: Sept 26, 2012–April 10, 2013.

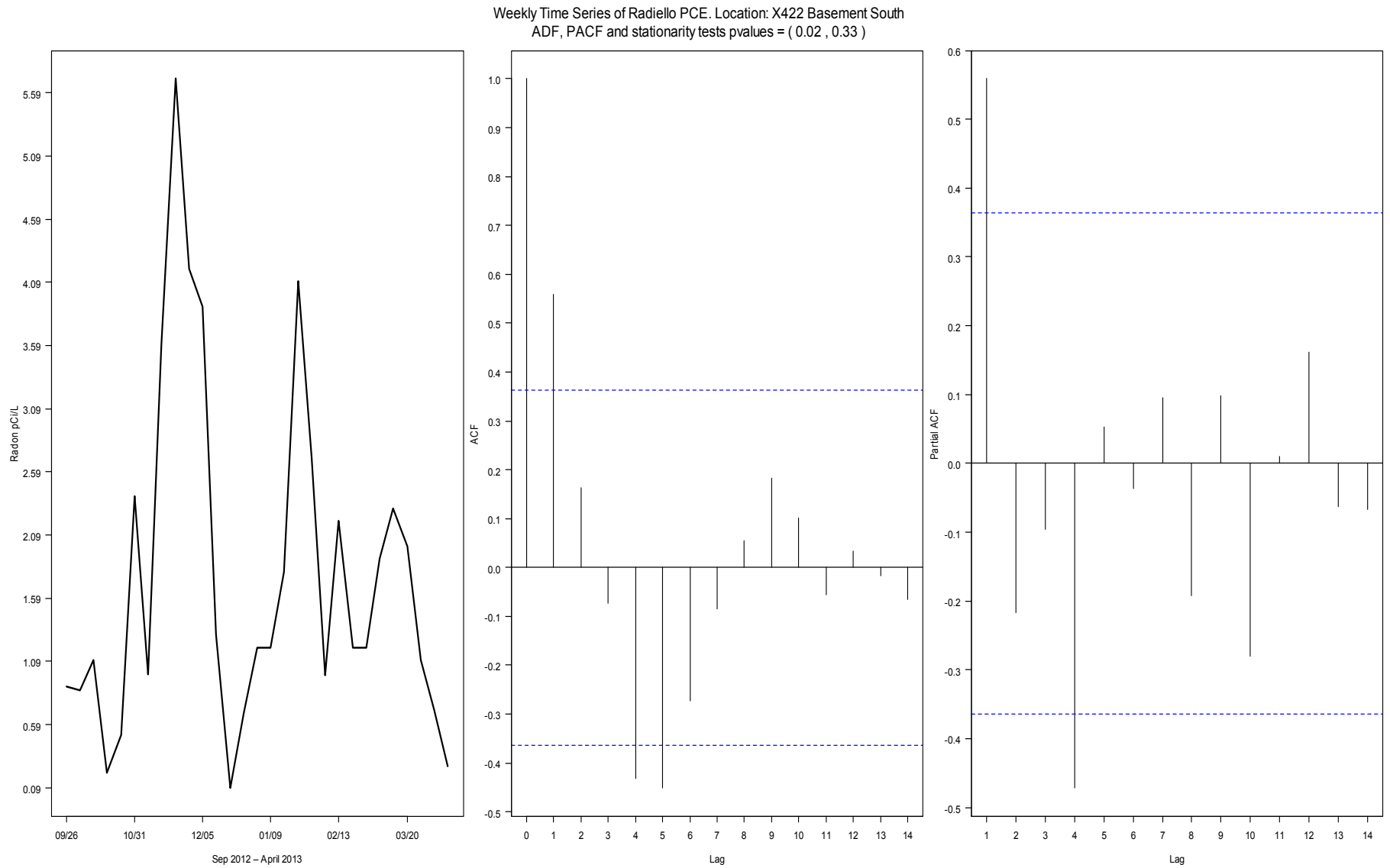


Figure 10-16. Time series plot, ACF and PACF for weekly Radiello PCE-2 (X422BaseS_Radiello_Weekly_PCE). Location X422 basement south. Time period: Sept 26, 2012–April 10, 2013.

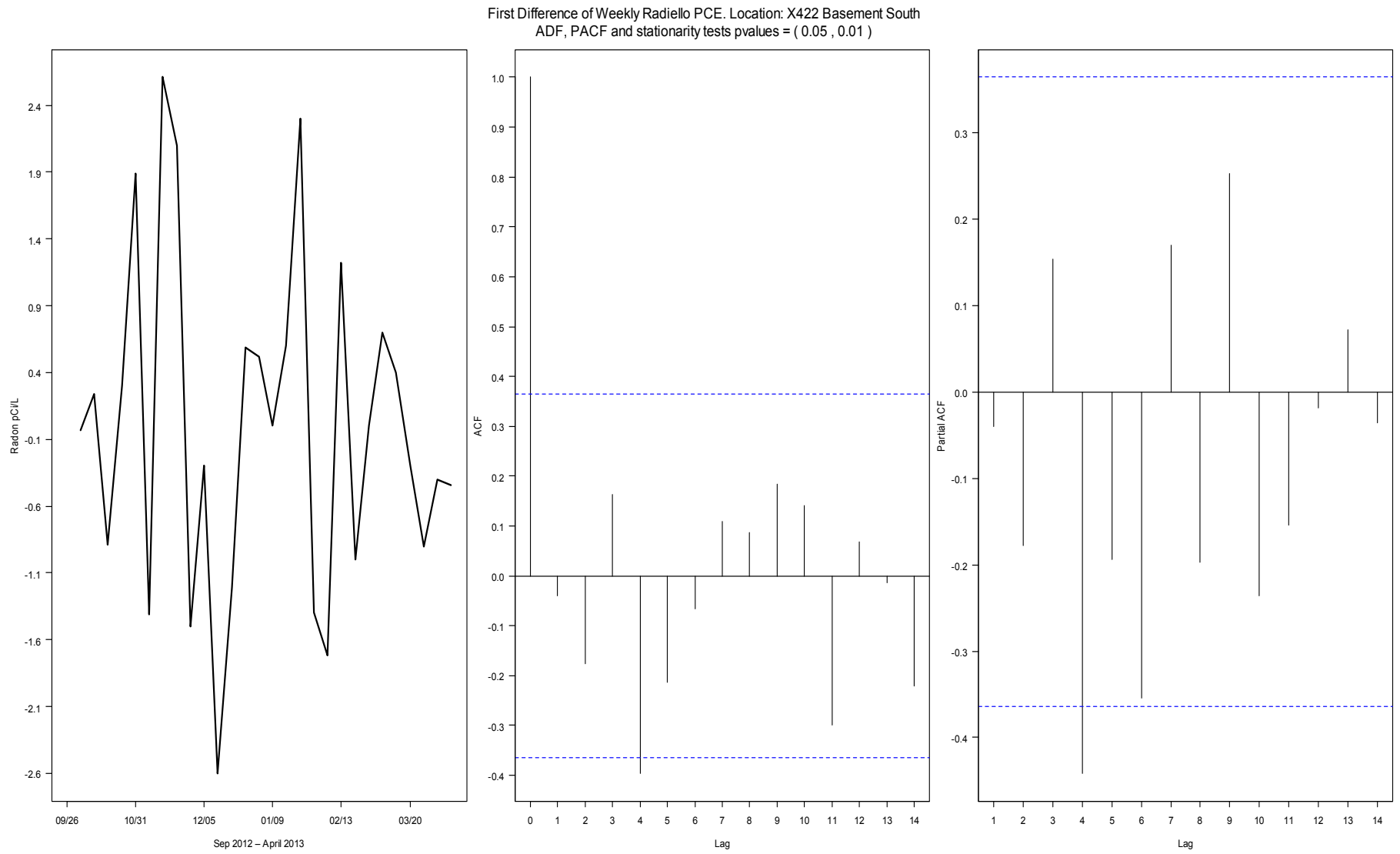


Figure 10-17. Time series plot, ACF and PACF for first difference weekly Radiello PCE-2 (X422BaseS_Radiello_Weekly_PCE). Location X422 basement south. Time period: Sept 26, 2012–April 10, 2013.

10.7.2 Predictor Variables Modeled and Their Potential for Autocorrelation

Table 10-17 lists a set of variables considered potential predictors for the VOC concentrations. We investigated their serial correlation (significant lags) and determined the transformation (e.g., no transformation, include a lag variable (e.g., lag 1 or past observation = $x(t-1)$) needed for the inclusion of each predictor in the model. Variables with 0 significant lags did not show significant serial correlation among consecutive measurements and did not need any lag transformation. Variables with 1 significant lag necessitated two terms in the model, the variable ($x(t)$) and the previous observation ($x(t-1)$). Variables with 2 significant lags required a model with three terms, the variable ($x(t)$), the previous observation ($x(t-1)$) and the second previous observation ($x(t-2)$).

A set of categorical variables were also considered. For the period Jan 5, 2011–Feb 15, 2012, the following variables were considered: AC (on or off), fan (used for fan testing, on or off), and heating system (on or off). In each case, the on was modeled as 1 and the off as zero. The variable for mitigation status was set to OFF during the Jan 2011 to Feb 2012 period (because the mitigation system had not yet been installed). For the period Sept 26, 2012–April 10, 2013, most of the categorical variables were consistently OFF except for heat and mitigation status, which was ON and OFF during the time period. As with the radon analysis, mitigation status was considered as a control variable and was included in all models for variables listed for the period Sept 26, 2012–April 10, 2013. In other words, as each of the predictor variables was individually modeled, a mitigation (on/off) term was always used as part of the equation.

Table 10-17. Continuous Covariates by Time Period

| Plain Language Variable Name | Variable Name | Jan 5, 2011–Feb 15, 2012 | | Sept 26, 2012–April 10, 2013 | |
|--|---------------------|--------------------------|----------|------------------------------|----------|
| | | Significant Lags | AR Model | Significant Lags | AR Model |
| Barometric rate of change in inches of mercury pressure per hour | Bar_drop_Hg.hr | 0 | | 0 | |
| Barometric pressure in inches of mercury | Bar_in_Hg | 1 | AR(1) | 0 | |
| Net pressure change over measurement period in inches of mercury | BP_Net_Change | 0 | | 0 | |
| Standard deviation of pressure change over measurement period in inches of mercury | BP_Pump_Speed | 1 | AR(1) | 0 | |
| Largest pressure change over measurement period (“stroke length” of barometric pumping) in inches of mercury | BP_Stroke_Length | 1 | AR(1) | 0 | |
| Cooling degree day | Cool_Degree_Day | 1 | AR(1) | 0 | |
| Dew point, interior, 422 Fahrenheit | Dew_pt_422_F | 1 | AR(1) | 1 | AR(1) |
| Height measured at Fall Creek stream gauge in feet | Fall_Crk_Gage_ht_ft | 1 | AR(1) | 0 | |

(continued)

Table 10-17. Continuous Covariates by Time Period (cont.)

| Plain Language Variable Name | Variable Name | Jan 5, 2011–Feb 15, 2012 | | Sept 26, 2012–April 10, 2013 | |
|--|-----------------------|--------------------------|----------|------------------------------|----------|
| | | Significant Lags | AR Model | Significant Lags | AR Model |
| Heating degree days | Heat_Degree_Day | 2 | AR(2) | 1 | AR(1) |
| % Humidity in interior of 422 | Hum_422_. | 1 | AR(1) | 1 | AR(1) |
| % Humidity in exterior | Hum_out_. | 1 | AR(1) | 0 | |
| Rain (inches) totaled during observation period | Rain_In_met | 1 | AR(1) | 0 | |
| Rain highest rate during observation period in inches/hour | Rain_IPH | 1 | AR(1) | 0 | |
| 420 side, subslab vs. basement differential pressure | Setra_420ss.base_Pa | 1 | AR(1) | 1 | AR(1) |
| 422 side basement vs. exterior differential pressure, Pascals | Setra_422base.out_Pa | 1 | AR(1) | 1 | AR(1) |
| 422 side, basement vs. upstairs differential pressure, Pascals | Setra_422base.upst_Pa | 1 | AR(1) | 1 | AR(1) |
| 422 side, deep vs. shallow soil gas differential pressure, Pascals | Setra_422SGdp.ss_Pa | 1 | AR(1) | 1 | AR(1) |
| 422 side, subslab vs. basement differential pressure, Pascals | Setra_422ss.base_Pa | 1 | AR(1) | 1 | AR(1) |
| Depth of snow on the ground, inches | Snowdepth_daily | 1 | AR(1) | 1 | AR(1) |
| Soil moisture 6 ft bls beneath structure, cbar | Soil_H2O_In6._cbar | 1 | AR(1) | 1 | AR(1) |
| Soil moisture, 3.5 ft bls exterior, cbar | Soil_H2O_Out3.5._cbar | 1 | AR(1) | 1 | AR(1) |
| Soil moisture 6 ft bls exterior, cbar | Soil_H2O_Out6._cbar | 1 | AR(1) | 1 | AR(1) |
| Soil temperature 9 ft bls beneath structure, C | Soil_T_C_MW3.9 | 1 | AR(1) | 1 | AR(1) |
| Soil temperature 1 ft bls exterior, C | Soil_T_C_OTC.1 | 1 | AR(1) | 1 | AR(1) |
| Soil temperature 6 ft bls exterior, C | Soil_T_C_OTC.6 | 1 | AR(1) | 1 | AR(1) |
| Temperature, 422 first floor from weather station | T_422_F | 1 | AR(1) | 1 | AR(1) |

(continued)

Table 10-17. Continuous Covariates by Time Period (cont.)

| Plain Language Variable Name | Variable Name | Jan 5, 2011–Feb 15, 2012 | | Sept 26, 2012–April 10, 2013 | |
|---|--------------------------------|--------------------------|----------|------------------------------|----------|
| | | Significant Lags | AR Model | Significant Lags | AR Model |
| Temperature 422 basement north from HOBO | T_422baseN_C | 1 | AR(1) | 1 | AR(1) |
| Temperature 422 first floor from HOBO | T_422baseS_C | 1 | AR(1) | 1 | AR(1) |
| Temperature on first floor of 422 side of duplex from HOBO | T_422first_C | 1 | AR(1) | 0 | |
| Temperature exterior | T_out_F | 1 | AR(1) | 1 | AR(1) |
| Temperature exterior, high during data collection period | T_out_Hi_F | 1 | AR(1) | 1 | AR(1) |
| Lowest exterior temperature in Fahrenheit | T_out_Lo_F | 2 | AR(2) | 1 | AR(1) |
| Wind chill | Wind_Chill_F | 1 | AR(1) | 1 | AR(1) |
| Average wind direction in degrees | Wind_Dir | 0 | | 0 | |
| Wind direction of high speed during measurement period in Degrees | Wind_Dir_Hi | 0 | | 0 | |
| Wind run (a function of wind speed and duration) | Wind_Run_mi | 0 | | 2 | AR(2) |
| High wind speed during measurement period | Wind_Speed_Hi_MPH | 0 | | 0 | |
| Average wind speed during measurement period | Wind_Speed_MPH | 2 | AR(2) | 0 | |
| 422 Base North radon measured by electret | X422baseN_Wkly_Elect_radon | 1 | AR(1) | 1 | AR(1) |
| 422 Base south radon measured by electret | X422baseS_Wkly_Elect_radon | 0 | | 1 | AR(1) |
| 422 first floor radon measured by electret | X422first_Wkly_Elect_radon | 1 | AR(1) | 1 | AR(1) |
| Soil temperature from exterior thermocouple at 3.5 ft bls, C | Soil_T_C_OTC.3.5 | | | 1 | AR(1) |
| 422 second floor office radon measured by electret | X422office2nd_Wkly_Elect_radon | | | 1 | AR(1) |

10.7.3 Time Series Analysis Results for 2011–2012 Chloroform Data Set

Table 10-18 lists the results for the analysis of association between the outcome (chloroform concentration in 422 base south) and predictors not needing a lag term in the model. None of these predictors were found to be statistically significant. Note that the finding that indoor radon and chloroform were not significantly correlated in this data set suggests that the mechanisms controlling vapor intrusion for these two pollutants must have differed.

Table 10-18. Analysis for Outcome First Difference of X422BaseS_Radiello_Weekly_CHCl₃. Variables That Did Not Need Lag Terms. Period Jan 5, 2011–Feb 15, 2012

| Predictor Name | Model Term | Estimate | SE |
|----------------------------|------------|----------|-------|
| Wind_Speed_Hi_MPH | intercept | -0.020 | 0.130 |
| | x(t) | 0.000 | 0.000 |
| Rain_IPH | intercept | -0.030 | 0.040 |
| | x(t) | 0.010 | 0.020 |
| Soil_T_C_OTC.6 | intercept | -0.070 | 0.070 |
| | x(t) | 0.000 | 0.000 |
| X422baseN_Wkly_Elect_radon | intercept | -0.080 | 0.100 |
| | x(t) | 0.010 | 0.010 |
| X422baseS_Wkly_Elect_radon | intercept | -0.040 | 0.070 |
| | x(t) | 0.000 | 0.010 |
| X422first_Wkly_Elect_radon | intercept | -0.070 | 0.070 |
| | x(t) | 0.020 | 0.020 |
| BP_Pump_Speed | intercept | 0.100 | 0.080 |
| | x(t) | -0.770 | 0.440 |

Table 10-19 shows the results of the regression analysis of predictor variables that needed a lag-1 week term in the model. Only heating degree days, snow depth, outside soil temperature at one foot bls, exterior temperature, exterior high temperature, and wind chill showed a significant association with the outcome. As discussed previously heating degree days, exterior temperature and daily high exterior temperature are closely linked variables that are all expected to be measures of the strength of the stack effect. The finding that snow depth had a significant correlation but rain did not is valuable. Current sampling guidance often imposes logistically difficult requirements for vapor intrusion related sampling based on rain. For example, California requires that soil gas sampling be delayed for 5 days after any rain of more than ½ inch (California EPA, 2012). The California guidance refers specifically to rain and the term snow does not appear in the guidance. NJ DEP (2012), in contrast, requires documentation of “significant precipitation” but does not further define the types or quantities of precipitation which may be significant.

As discussed earlier in this section, when the slopes of the $x(t)$ and $x(t-1)$ terms differ in sign but are similar in magnitude, that can be interpreted as an indication that the change in the predictor variable from week to week is what is correlated with the change in chloroform concentration. To understand the implications of the model predictions, it is useful to plug in some realistic trial values and compute the outcome.

Example A: If the exterior temperature this week averages 20°F and the temperature last week averaged 0° F, the model predicts this week’s chloroform will be 0.258 $\mu\text{g}/\text{m}^3$ lower than last week’s chloroform. This is consistent with the expected weaker stack effect with warmer temperatures.

Table 10-19. Analysis for Outcome X422BaseS_Radiello_Weekly_CHCl₃. Variables that Needed a lag-1 Term. Period Jan 5, 2011–Feb 15, 2012

| Predictor Name (x(t)) | Model Term | Model $Y(t)-Y(t-1) = \text{intercept} + x(t) + x(t-1)$ | | Model $Y(t) - Y(t-1) = \text{intercept} + x(t)$ | |
|-----------------------|------------|--|--------|---|--------|
| | | Estimate | SE | Estimate | SE |
| Bar_drop_Hg.hr | intercept | -0.018 | 0.029 | -0.019 | 0.029 |
| | x(t) | 17.416 | 16.828 | 28.654 | 14.306 |
| | x(t-1) | -21.010 | 16.782 | NA | NA |
| Bar_in_Hg | intercept | -1.352 | 7.760 | -0.518 | 6.669 |
| | x(t) | -0.012 | 0.259 | 0.017 | 0.222 |
| | x(t-1) | 0.056 | 0.260 | NA | NA |
| BP_Net_Change | intercept | -0.018 | 0.029 | -0.019 | 0.029 |
| | x(t) | -0.129 | 0.100 | -0.18906* | 0.084 |
| | x(t-1) | 0.108 | 0.100 | NA | NA |
| BP_Stroke_Length | intercept | 0.117 | 0.088 | 0.101 | 0.079 |
| | x(t) | -0.156 | 0.145 | -0.192 | 0.117 |
| | x(t-1) | -0.062 | 0.144 | NA | NA |
| Cool_Degree_Day | intercept | -0.035 | 0.036 | -0.032 | 0.036 |
| | x(t) | -0.001 | 0.002 | 0.000 | 0.001 |
| | x(t-1) | 0.001 | 0.002 | NA | NA |
| Dew_pt_422_F | intercept | -0.065 | 0.105 | -0.041 | 0.105 |
| | x(t) | -0.008 | 0.006 | 0.000 | 0.002 |
| | x(t-1) | 0.009 | 0.006 | NA | NA |
| Fall_Crk_Gage_ht_ft | intercept | 0.050 | 0.093 | 0.046 | 0.084 |
| | x(t) | -0.018 | 0.030 | -0.018 | 0.021 |
| | x(t-1) | -0.001 | 0.030 | NA | NA |
| Heat_Degree_Day | intercept | 0.001 | 0.044 | -0.021 | 0.046 |
| | x(t) | 0.00143* | 0.001 | 0.000 | 0.000 |
| | x(t-1) | -0.00161** | 0.001 | NA | NA |
| Hum_422_. | intercept | -0.074 | 0.119 | -0.052 | 0.118 |
| | x(t) | -0.005 | 0.006 | 0.001 | 0.003 |
| | x(t-1) | 0.006 | 0.006 | NA | NA |
| Hum_out_. | intercept | 0.471 | 0.380 | 0.258 | 0.324 |
| | x(t) | -0.001 | 0.005 | -0.004 | 0.004 |
| | x(t-1) | -0.005 | 0.005 | NA | NA |
| Rain_In_met | intercept | 0.029 | 0.045 | 0.010 | 0.041 |
| | x(t) | -0.027 | 0.037 | -0.038 | 0.035 |
| | x(t-1) | -0.035 | 0.037 | NA | NA |

(continued)

Table 10-19. Analysis for Outcome X422BaseS_Radiello_Weekly_CHCl₃. Variables That Needed a lag-1 Term. Period Jan 5, 2011–Feb 15, 2012 (cont.)

| Predictor Name (x(t)) | Model Term | Model $Y(t) - Y(t-1) =$ intercept + x(t) + x(t-1) | | Model $Y(t) - Y(t-1) =$ intercept + x(t) | |
|-----------------------|------------|--|-------|---|-------|
| | | Estimate | SE | Estimate | SE |
| Setra_420ss.base_Pa | intercept | 0.001 | 0.073 | -0.054 | 0.063 |
| | x(t) | 0.057 | 0.056 | 0.032 | 0.053 |
| | x(t-1) | -0.079 | 0.056 | NA | NA |
| Setra_422base.out_Pa | intercept | -0.018 | 0.030 | -0.021 | 0.030 |
| | x(t) | -0.019 | 0.027 | 0.001 | 0.021 |
| | x(t-1) | 0.030 | 0.027 | NA | NA |
| Setra_422base.upst_Pa | intercept | -0.020 | 0.029 | -0.022 | 0.029 |
| | x(t) | -0.051 | 0.031 | -0.041 | 0.030 |
| | x(t-1) | 0.038 | 0.031 | NA | NA |
| Setra_422SGdp.ss_Pa | intercept | 0.015 | 0.049 | -0.020 | 0.045 |
| | x(t) | 0.024 | 0.030 | -0.001 | 0.022 |
| | x(t-1) | -0.047 | 0.035 | NA | NA |
| Setra_422ss.base_Pa | intercept | -0.110 | 0.112 | -0.128 | 0.097 |
| | x(t) | 0.051 | 0.044 | 0.044 | 0.038 |
| | x(t-1) | -0.014 | 0.044 | NA | NA |
| Snowdepth_daily | intercept | -0.019 | 0.030 | -0.006 | 0.031 |
| | x(t) | -0.19513** | 0.063 | -0.057 | 0.042 |
| | x(t-1) | 0.17307** | 0.061 | NA | NA |
| Soil_H2O_In6._cbar | intercept | -0.068 | 0.053 | -0.072 | 0.051 |
| | x(t) | -0.001 | 0.006 | 0.001 | 0.001 |
| | x(t-1) | 0.002 | 0.006 | NA | NA |
| Soil_H2O_Out3.5._cbar | intercept | -0.041 | 0.037 | -0.041 | 0.036 |
| | x(t) | 0.000 | 0.001 | 0.001 | 0.001 |
| | x(t-1) | 0.000 | 0.001 | NA | NA |
| Soil_H2O_Out6._cbar | intercept | -0.037 | 0.040 | -0.038 | 0.039 |
| | x(t) | 0.000 | 0.002 | 0.000 | 0.000 |
| | x(t-1) | 0.000 | 0.002 | NA | NA |
| Soil_T_C_OTC.1 | intercept | -0.061 | 0.050 | -0.002 | 0.062 |
| | x(t) | -0.05861** | 0.015 | -0.001 | 0.004 |
| | x(t-1) | 0.06156** | 0.015 | NA | NA |
| T_422_F | intercept | -0.103 | 0.270 | -0.009 | 0.259 |
| | x(t) | -0.006 | 0.006 | 0.000 | 0.004 |
| | x(t-1) | 0.007 | 0.006 | NA | NA |

(continued)

Table 10-19. Analysis for Outcome X422BaseS_Radiello_Weekly_CHCl₃. Variables That Needed a lag-1 Term. Period Jan 5, 2011–Feb 15, 2012 (cont.)

| Predictor Name (x(t)) | Model Term | Model $Y(t) - Y(t-1) =$ intercept + x(t) + x(t-1) | | Model $Y(t) - Y(t-1) =$ intercept + x(t) | |
|-----------------------|------------|--|-------|---|-------|
| | | Estimate | SE | Estimate | SE |
| T_422baseN_C | intercept | -0.208 | 0.203 | -0.188 | 0.205 |
| | x(t) | -0.016 | 0.012 | 0.003 | 0.003 |
| | x(t-1) | 0.019 | 0.012 | NA | NA |
| T_422baseS_C | intercept | -0.293 | 0.243 | -0.275 | 0.241 |
| | x(t) | -0.006 | 0.013 | 0.004 | 0.004 |
| | x(t-1) | 0.010 | 0.012 | NA | NA |
| T_422first_C | intercept | -0.327 | 0.305 | -0.243 | 0.299 |
| | x(t) | -0.007 | 0.009 | 0.003 | 0.004 |
| | x(t-1) | 0.011 | 0.009 | NA | NA |
| T_out_F | intercept | -0.067 | 0.091 | -0.035 | 0.095 |
| | x(t) | -0.00957* | 0.004 | 0.000 | 0.002 |
| | x(t-1) | 0.01048* | 0.004 | NA | NA |
| T_out_Hi_F | intercept | -0.117 | 0.124 | -0.076 | 0.127 |
| | x(t) | -0.006 | 0.004 | 0.001 | 0.002 |
| | x(t-1) | 0.00757* | 0.003 | NA | NA |
| T_out_Lo_F | intercept | -0.043 | 0.069 | -0.043 | 0.067 |
| | x(t) | 0.001 | 0.004 | 0.001 | 0.002 |
| | x(t-1) | 0.000 | 0.004 | NA | NA |
| Wind_Chill_F | intercept | -0.060 | 0.081 | -0.030 | 0.086 |
| | x(t) | -0.00912* | 0.004 | 0.000 | 0.002 |
| | x(t-1) | 0.00994** | 0.004 | NA | NA |
| Wind_Run_mi | intercept | 0.099 | 0.103 | -0.001 | 0.085 |
| | x(t) | 0.000 | 0.000 | 0.000 | 0.000 |
| | x(t-1) | 0.000 | 0.000 | NA | NA |
| Wind_Speed_MPH | intercept | 0.073 | 0.104 | 0.000 | 0.092 |
| | x(t) | 0.012 | 0.025 | -0.005 | 0.023 |
| | x(t-1) | -0.036 | 0.025 | NA | NA |

**Significant at 1% level of significance

*Significant at 5% level of significance

NA = Not Applicable

Example B: If the exterior temperature this week averages 20° F and the temperature last week averaged 40° F, the model predicts this week's chloroform will be 0.162 $\mu\text{g}/\text{m}^3$ greater than last week's chloroform. This is consistent with the expected stronger stack effect with cooler temperatures.

Example C: If snow depth this week = 2 in and snow depth last week = 0 in, the model predicts that the concentration of chloroform will be 0.41 $\mu\text{g}/\text{m}^3$ LOWER this week than last week. This appears to be the opposite of the effect we might have predicted from our analysis in Section 9.

Only the current observation of the high temperature is significantly associated with the chloroform concentration, not the previous week's concentration.

Table 10-20 displays the results for the analysis of the association between variables needing a Lag 1 and Lag 2 terms in the model. The recent past and current measurement of soil temperature at 9 ft bls (3ft below the basement floor) was associated with the chloroform concentration. Again an example may be needed to interpret the results. Assume the soil temperature at that location was gradually warming so that it averaged 18°C this week, 17°C the week before, and 16°C two weeks ago. The model would predict that the chloroform concentration in indoor air would have increased 0.51 $\mu\text{g}/\text{m}^3$. While the strength of this effect is surprising, the direction is physically reasonable from a consideration of volatility.

10.7.4 Time Series Analysis Results for 2011–2012 PCE Data Set

We encountered convergence issues when fitting the models for PCE during the period Jan 2011 to Feb 2012. These issues were likely the results of the non-constant mean observed at the beginning of the time series (see **Figure 10-3**). We decided to take the first difference to get a more stationary time series and to ensure convergence. The first difference improved the stationarity of the mean but it did not eliminate the serial correlation observed between the consecutive time terms in the time series. To address this issue, we investigated the distribution (specifically the covariance structure) of the error term in the model. We fitted several models using several predictors and explored the corresponding PACF of the error term and determined that a lag-1 error term was required. To incorporate a model term to the error, we specify in the model equation a distribution for the variance of the error terms, in this case an AR(1) structure. A more complex model (AR(2)) was also considered, but convergence issues were encountered likely the result of small variability in some predictors and the small data set.

Table 10-21 shows the results of the analysis of the association between various predictor variables and the PCE concentration in the 422 basement for the period Jan 2011 to Feb 2012. Only the variables soil temperature at 6ft and barometric pressure “pump speed” were significantly associated with the PCE concentration. As shown in Section 3, we defined the variable “barometric pressure pump speed” to be the standard deviation of pressure change over measurement period in inches of mercury. While a relationship between barometric pressure change and vapor intrusion is expected, the negative coefficient is at first counterintuitive. We would have expected that the greater the amount of variability in barometric pressure the more air that would be pumped in and out of the building. However, the negative coefficient of this significant correlation may point to a more subtle interpretation—a pump such as the human heart can be less effective when it has an irregular rapid pumping, described in the human as atrial fibrillation or atrial flutter.²⁶ Further investigation in the literature of barometric pumping, building science and fluid dynamics may be needed to better understand how to correlate the variability of barometric pressure to vapor intrusion.

²⁶<http://www.nlm.nih.gov/medlineplus/ency/article/000184.htm>

Table 10-20. Analysis for Outcome X422BaseS_Radiello_Weekly_CHCl₃. Variables that Needed Lag-1 and Lag-2 Terms. Period Jan 5, 2011–Feb 15, 2012

| Predictor Name | Model Term | Model $Y(t) - Y(t-1) = \text{intercept} + x(t) + x(t-1) + x(t-2)$ | | Model $Y(t) - Y(t-1) = \text{intercept} + x(t) + x(t-1)$ | | Model $Y(t) - Y(t-1) = \text{intercept} + x(t)$ | |
|----------------|------------|---|----------|--|----------|---|----------|
| | | Estimate | SE | Estimate | SE | Estimate | SE |
| Soil_T_C_MW3.9 | intercept | -0.247180 | 0.186580 | -0.333260 | 0.193930 | -0.267510 | 0.190440 |
| | x(t) | 0.25581* | 0.115020 | 0.089320 | 0.084300 | 0.015130 | 0.011550 |
| | x(t-1) | -0.49172* | 0.210950 | -0.070670 | 0.083090 | NA | NA |
| | x(t-2) | 0.25033* | 0.112990 | NA | NA | NA | NA |
| Wind_Dir | intercept | -0.024830 | 0.102390 | 0.128880 | 0.095890 | 0.066990 | 0.068320 |
| | x(t) | -0.000400 | 0.000260 | -0.000440 | 0.000290 | -0.000420 | 0.000290 |
| | x(t-1) | -0.000180 | 0.000260 | -0.000270 | 0.000300 | NA | NA |
| | x(t-2) | 0.00065* | 0.000260 | NA | NA | NA | NA |
| Wind_Dir_Hi | intercept | 0.022160 | 0.135680 | 0.051860 | 0.122550 | -0.066890 | 0.094640 |
| | x(t) | 0.000320 | 0.000350 | 0.000260 | 0.000380 | 0.000200 | 0.000380 |
| | x(t-1) | -0.000520 | 0.000350 | -0.000570 | 0.000380 | NA | NA |
| | x(t-2) | 0.000070 | 0.000350 | NA | NA | NA | NA |

*Significant at 5% level of significance

Table 10-21. Time Series Analysis for Outcome First Difference of 422 Basement South PCE Concentration Variables that Did Not Need Lag Terms. Period Jan 2011 to Feb 2012

| Predictor Name | Model Term | Estimate | SE |
|----------------------------|------------|----------|-------|
| Wind_Speed_Hi_MPH | Intercept | -0.419 | 0.720 |
| | x(t) | 0.006 | 0.024 |
| Rain_IPH | Intercept | -0.352 | 0.202 |
| | x(t) | 0.067 | 0.085 |
| Soil_T_C_OTC.6 | Intercept | -1.048** | 0.271 |
| | x(t) | 0.058** | 0.018 |
| X422baseN_Wkly_Elect_radon | Intercept | 0.289 | 0.498 |
| | x(t) | -0.074 | 0.067 |
| X422baseS_Wkly_Elect_radon | Intercept | -0.041 | 0.366 |
| | x(t) | -0.023 | 0.040 |
| X422first_Wkly_Elect_radon | Intercept | 0.180 | 0.371 |
| | x(t) | -0.123 | 0.103 |
| BP_Pump_Speed | Intercept | 0.593 | 0.405 |
| | x(t) | -5.279* | 2.395 |

**Significant at 1% level of significance

*Significant at 5% level of significance

The positive correlation to soil temperature is a physically reasonable result. It is likely that this reflects the enhanced volatility of PCE at higher temperatures.

Table 10-22 displays the results of an analysis of the association between PCE concentration in the basement of 422 for the period Jan 2011 to Feb 2012, and predictor variables needing a lag-1 week term in their models. Relatively few variables were found to be significantly correlated:

- the previous week's dew point and humidity.
- Several exterior temperature related variables were significant, although the signs of the coefficients were in many cases counterintuitive (and opposite of those observed for radon): exterior temperature, low exterior temperature for the week, heating degree days, and wind chill.
- The positive correlation with the interior basement temperatures is expected: warmer interior temperatures should lead to a stronger stack effect.
- The highly significant correlation to snow depth was expected from a visual examination of the data set but again the negative coefficient was not expected. As shown in **Figure 10-18**, a visual inspection of the XY plot of the weekly data would have suggested a positive correlation. However as shown in **Figures 10-19** and **10-20**, the first difference of snow depth (difference between last week's snow depth and this week's) and first difference in PCE concentration shows a more complex behavior. After examining the data set, we believe that there are some confounding factors that may have affected the results observed in this part of the time series analysis:
 1. There are relatively few weeks with a non-zero amount of snow in the data set.
 2. The project began at a time with snow already on the ground.
 3. The weekly time resolution was probably too coarse.

Table 10-22. Analysis for PCE Concentration at 42 Base South, Variables that Needed a Lag-1 Term. Period Jan 2011 to Feb 2012

| Predictor Name (x(t)) | Model Term | Model $Y(t)-Y(t-1) = \text{intercept} + x(t) + x(t-1)$ | | Model $Y(t)-Y(t-1) = \text{intercept} + x(t)$ | |
|-----------------------|------------|--|---------|---|---------|
| | | Estimate | SE | Estimate | SE |
| Bar_drop_Hg.hr | intercept | -0.223 | 0.137 | -0.232 | 0.134 |
| | x(t) | 67.183 | 122.050 | 96.997 | 122.437 |
| | x(t-1) | -205.252 | 124.905 | | |
| Bar_in_Hg | intercept | 50.044 | 36.234 | 56.164 | 33.303 |
| | x(t) | -2.620 | 1.762 | -1.880 | 1.110 |
| | x(t-1) | 0.944 | 1.764 | | |
| BP_Net_Change | intercept | -0.222 | 0.136 | -0.232 | 0.134 |
| | x(t) | -0.574 | 0.729 | -0.819 | 0.724 |
| | x(t-1) | 1.231 | 0.755 | | |
| BP_Stroke_Length | intercept | 0.574 | 0.388 | 0.386 | 0.404 |
| | x(t) | 0.498 | 0.912 | -0.988 | 0.603 |
| | x(t-1) | -1.763 | 0.896 | | |
| Cool_Degree_Day | intercept | -0.358* | 0.167 | -0.35023* | 0.162 |
| | x(t) | 0.001 | 0.012 | 0.004 | 0.003 |
| | x(t-1) | 0.004 | 0.012 | | |
| Dew_pt_422_F | intercept | -1.235** | 0.460 | -1.201* | 0.454 |
| | x(t) | -0.012 | 0.039 | 0.0213* | 0.010 |
| | x(t-1) | 0.034 | 0.039 | | |
| Fall_Crk_Gage_ht_ft | intercept | -0.151 | 0.417 | -0.008 | 0.411 |
| | x(t) | -0.250 | 0.170 | -0.062 | 0.104 |
| | x(t-1) | 0.229 | 0.169 | | |
| Heat_Degree_Day | intercept | 0.121 | 0.192 | 0.091 | 0.196 |
| | x(t) | 0.005 | 0.005 | -0.003* | 0.001 |
| | x(t-1) | -0.008 | 0.005 | | |
| Hum_422_. | intercept | -1.494** | 0.498 | -1.473** | 0.512 |
| | x(t) | -0.028 | 0.040 | 0.030* | 0.012 |
| | x(t-1) | 0.059 | 0.038 | | |
| Hum_out_. | intercept | 2.069 | 1.926 | 1.876 | 1.727 |
| | x(t) | -0.025 | 0.032 | -0.029 | 0.024 |
| | x(t-1) | -0.007 | 0.031 | | |
| Rain_In_met | intercept | -0.273 | 0.230 | -0.197 | 0.209 |
| | x(t) | -0.150 | 0.234 | -0.047 | 0.194 |
| | x(t-1) | 0.193 | 0.233 | | |

(continued)

Table 10-22. Analysis for PCE Concentration at 42 Base South, Variables that Needed A Lag-1 Term. Period Jan 2011 to Feb 2012 (cont.)

| Predictor Name (x(t)) | Model Term | Model $Y(t)-Y(t-1) =$ intercept + x(t) + x(t-1) | | Model $Y(t)-Y(t-1) =$ intercept + x(t) | |
|-----------------------|------------|--|-------|---|-------|
| | | Estimate | SE | Estimate | SE |
| Setra_420ss.base_Pa | intercept | -0.208 | 0.377 | -0.248 | 0.335 |
| | x(t) | 0.046 | 0.364 | 0.004 | 0.295 |
| | x(t-1) | -0.081 | 0.364 | | |
| Setra_422base.out_Pa | intercept | -0.236 | 0.139 | -0.244 | 0.136 |
| | x(t) | -0.248 | 0.179 | -0.055 | 0.102 |
| | x(t-1) | 0.234 | 0.176 | | |
| Setra_422base.upst_Pa | intercept | -0.226 | 0.137 | -0.231 | 0.136 |
| | x(t) | 0.040 | 0.207 | 0.127 | 0.170 |
| | x(t-1) | 0.157 | 0.207 | | |
| Setra_422SGdp.ss_Pa | intercept | -0.079 | 0.210 | -0.268 | 0.199 |
| | x(t) | 0.331 | 0.183 | 0.044 | 0.103 |
| | x(t-1) | -0.432 | 0.234 | | |
| Setra_422ss.base_Pa | intercept | 0.249 | 0.542 | -0.154 | 0.506 |
| | x(t) | 0.347 | 0.286 | -0.034 | 0.202 |
| | x(t-1) | -0.552 | 0.299 | | |
| Snowdepth_daily | intercept | -0.059 | 0.123 | -0.057 | 0.118 |
| | x(t) | -0.746 | 0.406 | -0.692** | 0.170 |
| | x(t-1) | 0.050 | 0.387 | | |
| Soil_H2O_In6._cbar | intercept | -0.705** | 0.225 | -0.648** | 0.211 |
| | x(t) | 0.027 | 0.027 | 0.005* | 0.002 |
| | x(t-1) | -0.021 | 0.027 | | |
| Soil_H2O_Out3.5._cbar | intercept | -0.342 | 0.173 | -0.334* | 0.166 |
| | x(t) | 0.002 | 0.005 | 0.002 | 0.002 |
| | x(t-1) | 0.001 | 0.005 | | |
| Soil_H2O_Out6._cbar | intercept | -0.41* | 0.180 | -0.397* | 0.175 |
| | x(t) | 0.007 | 0.009 | 0.002 | 0.001 |
| | x(t-1) | -0.006 | 0.009 | | |
| Soil_T_C_OTC.1 | intercept | -0.205 | 0.115 | -0.434 | 0.332 |
| | x(t) | -0.076* | 0.031 | 0.017 | 0.021 |
| | x(t-1) | 0.086** | 0.031 | | |
| T_422_F | intercept | -1.680 | 1.246 | -1.667 | 1.185 |
| | x(t) | 0.019 | 0.041 | 0.020 | 0.017 |
| | x(t-1) | 0.001 | 0.041 | | |

(continued)

Table 10-22. Analysis for PCE Concentration at 42 Base South, Variables that Needed A Lag-1 Term. Period Jan 2011 to Feb 2012 (cont.)

| Predictor Name (x(t)) | Model Term | Model $Y(t)-Y(t-1) = \text{intercept} + x(t) + x(t-1)$ | | Model $Y(t)-Y(t-1) = \text{intercept} + x(t)$ | |
|-----------------------|------------|--|-------|---|-------|
| | | Estimate | SE | Estimate | SE |
| T_422baseN_C | intercept | -2.298* | 0.894 | -2.274* | 0.871 |
| | x(t) | 0.009 | 0.074 | 0.033* | 0.014 |
| | x(t-1) | 0.024 | 0.073 | | |
| T_422baseS_C | intercept | -2.677* | 1.052 | -2.66* | 1.027 |
| | x(t) | 0.047 | 0.074 | 0.078* | 0.016 |
| | x(t-1) | -0.009 | 0.073 | | |
| T_422first_C | intercept | -2.631 | 1.340 | -2.720* | 1.309 |
| | x(t) | 0.061 | 0.056 | 0.035 | 0.018 |
| | x(t-1) | -0.027 | 0.055 | | |
| T_out_F | intercept | -1.077* | 0.407 | -1.063* | 0.416 |
| | x(t) | -0.026 | 0.030 | 0.015* | 0.007 |
| | x(t-1) | 0.041 | 0.029 | | |
| T_out_Hi_F | intercept | -1.380* | 0.536 | -1.340* | 0.573 |
| | x(t) | -0.035 | 0.023 | 0.015 | 0.008 |
| | x(t-1) | 0.051* | 0.022 | | |
| T_out_Lo_F | intercept | -0.826** | 0.295 | -0.809** | 0.287 |
| | x(t) | 0.003 | 0.026 | 0.016* | 0.007 |
| | x(t-1) | 0.014 | 0.026 | | |
| Wind_Chill_F | intercept | -0.980** | 0.360 | -0.973* | 0.375 |
| | x(t) | -0.031 | 0.027 | 0.014* | 0.007 |
| | x(t-1) | 0.045 | 0.026 | | |
| Wind_Run_mi | intercept | 0.222 | 0.496 | -0.091 | 0.465 |
| | x(t) | 0.001 | 0.001 | 0.000 | 0.001 |
| | x(t-1) | -0.001 | 0.001 | | |
| Wind_Speed_MPH | intercept | 0.318 | 0.479 | 0.034 | 0.471 |
| | x(t) | 0.196 | 0.181 | -0.070 | 0.117 |
| | x(t-1) | -0.339 | 0.181 | | |

**Significant at 1% level of significance

*Significant at 5% level of significance

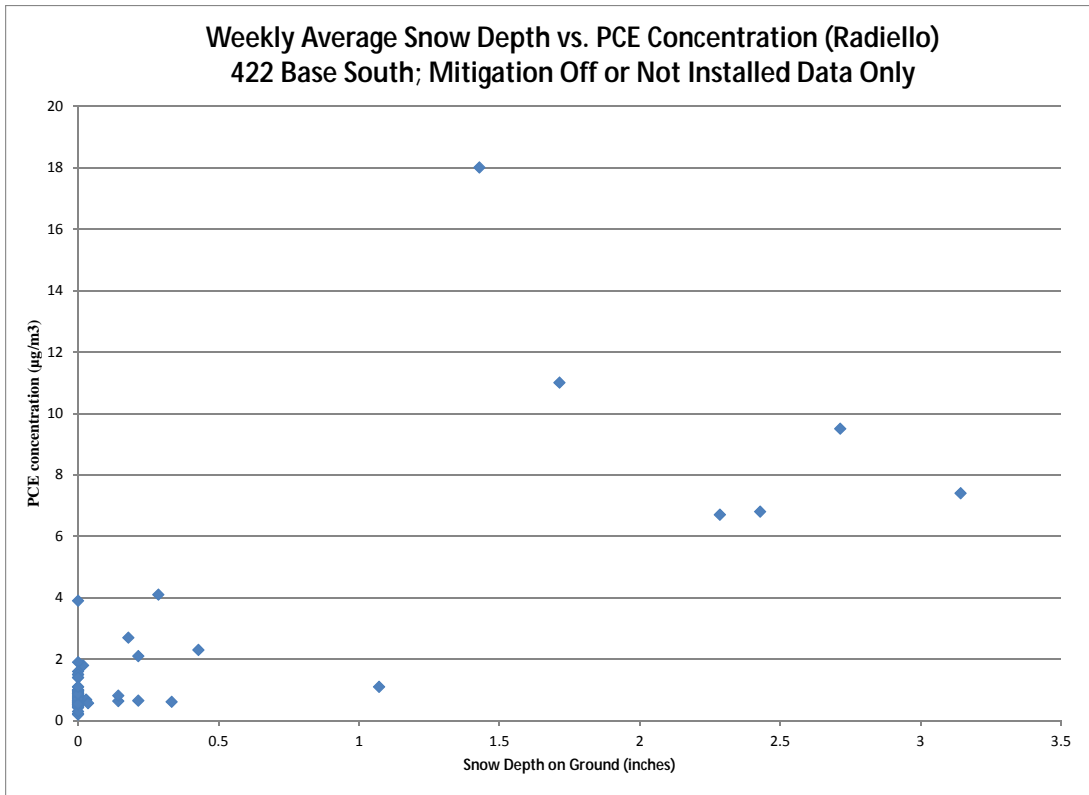


Figure 10-18. XY plot of weekly average snow depth vs. PCE concentration.

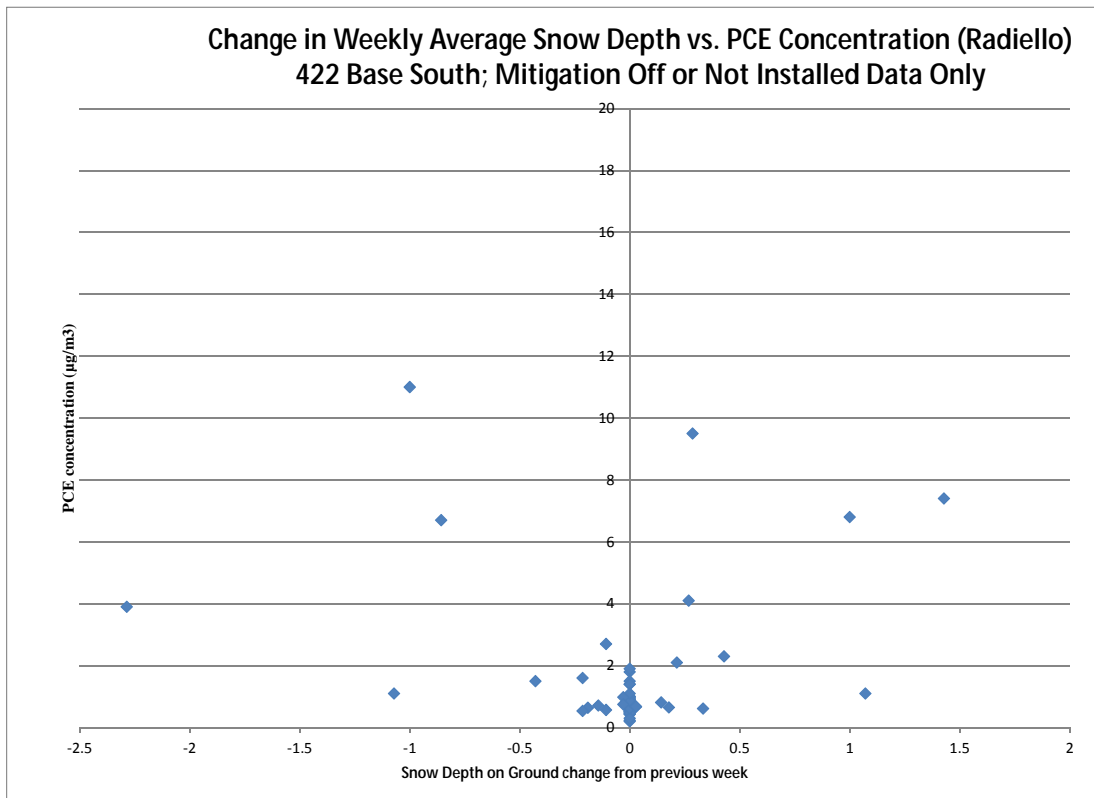


Figure 10-19. XY Plot of change in weekly average snow depth vs. PCE concentration.

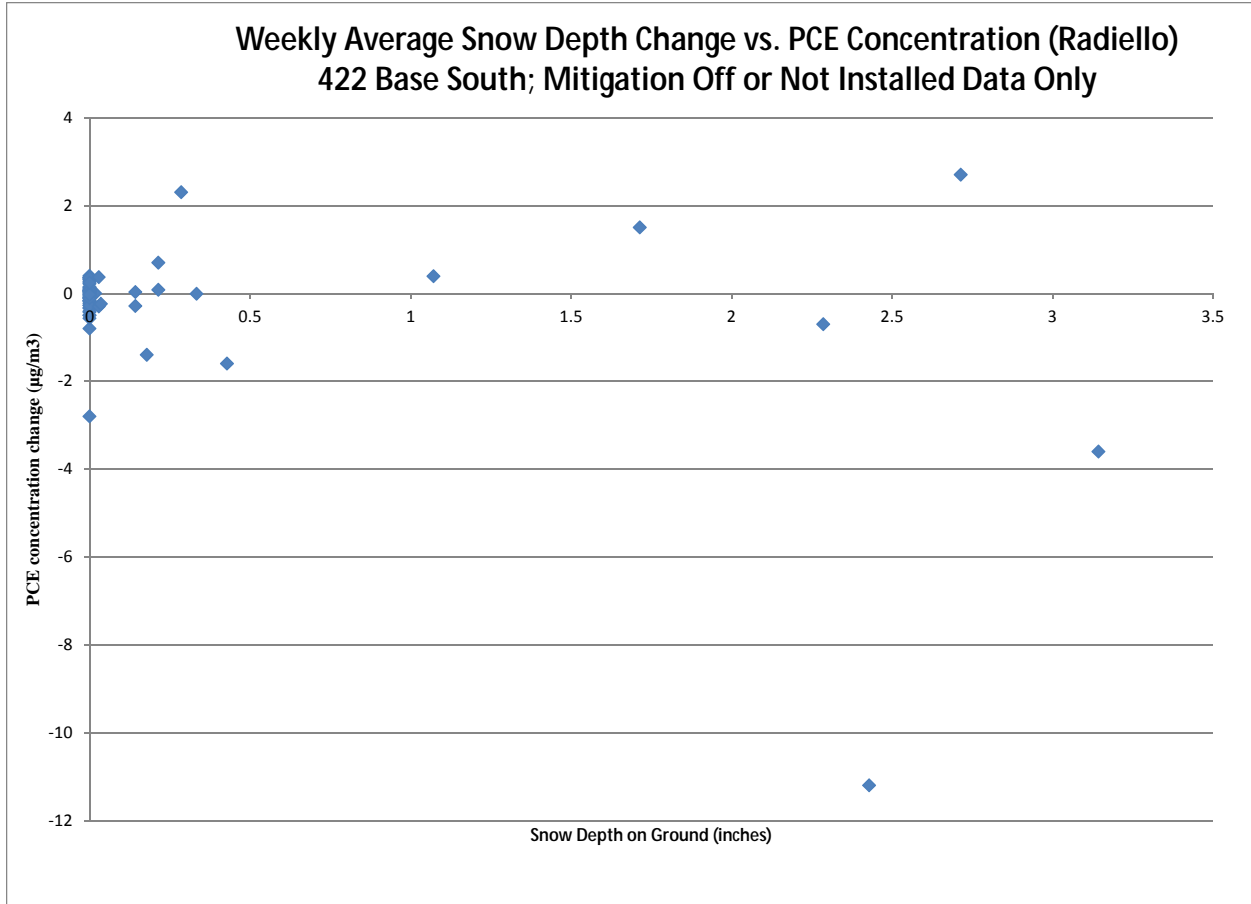


Figure 10-20. XY Plot of weekly average snow depth vs. change in PCE.

As shown in **Table 10-23**, only one significant association was found between predictors needing two lag terms and the PCE concentration. The one case where significance was shown was a correlation between the soil temperature at 9 ft (3 ft directly below the basement floor) in the reduced model. This positive coefficient is physically realistic, most likely suggesting that warmer soils enhanced PCE volatility.

Table 10-23. Analysis for PCE Concentration at 422 Base South Variables that Needed Both Lag-1 Week And Lag-2 Week Terms. Period Jan 2011 to Feb 2012

| Predictor Name | Model Term | Model $Y(t)-Y(t-1) = \text{intercept} + x(t) + x(t-1)+x(t-2)$ | | Model $Y(t)-Y(t-1) = \text{intercept} + x(t) + x(t-1)$ | | Model $Y(t)-Y(t-1) = \text{intercept} + x(t)$ | |
|----------------|------------|---|-------|--|------------|---|-------|
| | | Estimate | SE | Estimate | SE | Estimate | SE |
| Soil_T_C_MW3.9 | Intercept | -1.419* | 0.684 | -2.546 | 20,354.593 | -2.677** | 0.746 |
| | x(t) | 0.326 | 0.255 | 0.543 | 0.683 | 0.14655** | 0.045 |
| | x(t-1) | -0.598 | 0.419 | -0.775 | 0.681 | | |
| | x(t-2) | 0.350 | 0.251 | | | | |

(continued)

Table 10-23. Analysis for PCE Concentration at 422 Base South Variables that Needed Both Lag-1 Week And Lag-2 Week Terms. Period Jan 2011 to Feb 2012 (cont.)

| Predictor Name | Model Term | Model $Y(t)-Y(t-1) = \text{intercept} + x(t) + x(t-1)+x(t-2)$ | | Model $Y(t)-Y(t-1) = \text{intercept} + x(t) + x(t-1)$ | | Model $Y(t)-Y(t-1) = \text{intercept} + x(t)$ | |
|----------------|------------|---|-------|--|-------|---|-------|
| | | Estimate | SE | Estimate | SE | Estimate | SE |
| Wind_Dir | Intercept | -0.322 | 0.501 | -0.172 | 0.506 | -0.239 | 0.423 |
| | x(t) | 0.000 | 0.001 | 0.000 | 0.002 | 0.000 | 0.002 |
| | x(t-1) | 0.000 | 0.001 | -0.001 | 0.002 | | |
| | x(t-2) | 0.000 | 0.001 | | | | |
| Wind_Dir_Hi | Intercept | 0.175 | 0.641 | 0.245 | 0.632 | 0.079 | 0.544 |
| | x(t) | 0.000 | 0.001 | -0.001 | 0.003 | -0.001 | 0.002 |
| | x(t-1) | 0.000 | 0.001 | -0.001 | 0.003 | | |
| | x(t-2) | -0.001 | 0.001 | | | | |

**Significant at 1% level of significance

*Significant at 5% level of significance

10.7.5 Time Series Analysis of 422 Basement South Chloroform Data Set from the period Sept 2012–Apr 2013

In this section, we discussed the evaluation of the association between chloroform concentrations at 422 base south and a list of predictor variables measured weekly during between Sept 2012 and April 2013. All models in this section (period Sept 2013 to April 2013) include mitigation as a control variable. Mitigation was coded as 1 (on both sides of duplex,) and 0 (OFF, passive or not yet installed).

Table 10-24 display the analysis results for the chloroform time series, period Sept 2012 to April 2013 at 422 base south for variables not requiring lag terms in these models. Only barometric pressure was associated with X422BaseS_Radiello_CHCl3-2 after controlling for the effect of mitigation. Note that the mitigation effect was not statistically significant, although it almost always had a consistent coefficient of the expected sign.

Table 10-25 displays the results of the analysis to of the association between basement 422 chloroform for the period Sept 2012 to April 2013, with predictors needing a lag-1 week term in the model. Both the past and current measurements of shallow soil temperature at 1 ft bls and exterior temperature were correlated to the chloroform concentration. The current measurements of predictor heating degree days, and soil moisture at 6 ft were correlated with the chloroform concentrations. Only the previous weeks measurements of the basement temperatures were correlated to chloroform, not the current measurement.

The correlation with heating degree days was in the expected direction and was large in magnitude. An example is helpful to understand the implications of the model of shallow soil temperature. Assume mitigation is off and that the shallow soil temperature is 15°C this week and 10°C last week. The model predicts that the indoor chloroform will be 0.42 µg/m³ higher this week than last week.

As with **Table 10-24**, it is notable that the effect of mitigation being on is almost always to decrease chloroform and usually by a similar amount (less than 0.250 µg/m³) but that this never rises to statistical significance.

Table 10-24. Analysis for First Difference of Chloroform Concentration at 422 Basement South. Variables that Did Not Need Lag Terms. Period Sept 2012 to April 2013

| Predictor Name | Model Term | Model: $Y(t) - Y(t-1) = \text{intercept} + \text{mitigation}(t) + x(t)$ | |
|---------------------|------------|---|--------|
| | | Estimate | SE |
| Bar_drop_Hg.hr | Intercept | 0.086 | 0.143 |
| | Mitigation | -0.117 | 0.158 |
| | x(t) | 9.488 | 27.176 |
| Bar_in_Hg | Intercept | -35.363* | 13.862 |
| | Mitigation | -0.050 | 0.143 |
| | x(t) | 1.177* | 0.460 |
| BP_Net_Change | Intercept | 0.086 | 0.143 |
| | Mitigation | -0.117 | 0.158 |
| | x(t) | -0.060 | 0.167 |
| BP_Pump_Speed | Intercept | 0.384 | 0.252 |
| | Mitigation | -0.146 | 0.154 |
| | x(t) | -1.486 | 1.048 |
| BP_Stroke_Length | Intercept | 0.333 | 0.275 |
| | Mitigation | -0.163 | 0.162 |
| | x(t) | -0.292 | 0.277 |
| Cool_Degree_Day | Intercept | 0.106 | 0.144 |
| | Mitigation | -0.115 | 0.156 |
| | x(t) | -0.011 | 0.014 |
| Fall_Crk_Gage_ht_ft | Intercept | 0.290 | 0.328 |
| | Mitigation | -0.105 | 0.157 |
| | x(t) | -0.006 | 0.009 |
| Hum_out_. | Intercept | 0.025 | 0.283 |
| | Mitigation | -0.111 | 0.158 |
| | x(t) | 0.016 | 0.066 |
| Rain_In_met | Intercept | 0.048 | 0.193 |
| | Mitigation | -0.110 | 0.158 |
| | x(t) | 0.000 | 0.001 |
| Rain_IPH | Intercept | 0.244 | 0.247 |
| | Mitigation | -0.136 | 0.159 |
| | x(t) | -0.005 | 0.006 |
| T_422first_C | Intercept | 0.356 | 0.633 |
| | Mitigation | -0.107 | 0.158 |
| | x(t) | -0.004 | 0.008 |

(continued)

Table 10-24. Analysis for First Difference of Chloroform Concentration at 422 Basement South. Variables that Did Not Need Lag Terms. Period Sept 2012 to April 2013 (cont.)

| Predictor Name | Model Term | Model: $Y(t) - Y(t-1) = \text{intercept} + \text{mitigation}(t) + x(t)$ | |
|-------------------|------------|---|-------|
| | | Estimate | SE |
| Wind_Dir | Intercept | 0.102 | 0.151 |
| | Mitigation | -0.116 | 0.158 |
| | x(t) | -0.035 | 0.096 |
| Wind_Dir_Hi | Intercept | 0.157 | 0.176 |
| | Mitigation | -0.164 | 0.173 |
| | x(t) | -0.041 | 0.059 |
| Wind_Speed_Hi_MPH | Intercept | 0.062 | 0.178 |
| | Mitigation | 0.132 | 0.225 |
| | x(t) | 0.020 | 0.011 |
| Wind_Speed_MPH | Intercept | 0.028 | 0.162 |
| | Mitigation | -0.083 | 0.172 |
| | x(t) | 0.005 | 0.004 |

*Significant at 5% level of significance

Table 10-25. Analysis Chloroform Concentration at 422 Base South. Variables that Needed A Lag-1 One Week Term. Period Sept 2012 to April 2013

| Predictor Name | Model Term | Model: $Y(t) - Y(t-1) = \text{intercept} + \text{mitigation}(t) + x(t) + x(t-1)$ | | Model: $Y(t) - Y(t-1) = \text{intercept} + \text{mitigation}(t) + x(t)$ | |
|-----------------|---------------|--|--------|---|--------|
| | | Estimate | SE | Estimate | SE |
| Dew_pt_422_F | intercept | 0.096 | 0.150 | 0.086 | 0.143 |
| | mitigation(t) | -0.132 | 0.171 | -0.117 | 0.158 |
| | x(t) | 13.751 | 32.226 | 9.488 | 27.176 |
| | x(t-1) | 8.819 | 34.080 | | |
| Heat_Degree_Day | intercept | -28.500 | 17.429 | -35.36332* | 13.862 |
| | mitigation(t) | -0.059 | 0.145 | -0.050 | 0.143 |
| | x(t) | 1.290* | 0.496 | 1.17744* | 0.460 |
| | x(t-1) | -0.341 | 0.514 | | |
| Hum_422_. | intercept | 0.099 | 0.151 | 0.086 | 0.143 |
| | mitigation(t) | -0.136 | 0.170 | -0.117 | 0.158 |
| | x(t) | -0.093 | 0.197 | -0.060 | 0.167 |
| | x(t-1) | -0.069 | 0.207 | | |

(continued)

Table 10-25. Analysis Chloroform Concentration at 422 Base South. Variables that Needed A Lag-1 One Week Term. Period Sept 2012 to April 2013 (cont.)

| Predictor Name | Model Term | Model: $Y(t) - Y(t-1) = \text{intercept} + \text{mitigation}(t) + x(t) + x(t-1)$ | | Model: $Y(t) - Y(t-1) = \text{intercept} + \text{mitigation}(t) + x(t)$ | |
|-----------------------|---------------|--|-------|---|-------|
| | | Estimate | SE | Estimate | SE |
| Setra_420ss.base_Pa | intercept | 0.357 | 0.328 | 0.384 | 0.252 |
| | mitigation(t) | -0.145 | 0.157 | -0.146 | 0.154 |
| | x(t) | -1.483 | 1.069 | -1.486 | 1.048 |
| | x(t-1) | 0.137 | 1.045 | | |
| Setra_422base.out_Pa | intercept | 0.378 | 0.314 | 0.333 | 0.275 |
| | mitigation(t) | -0.164 | 0.165 | -0.163 | 0.162 |
| | x(t) | -0.270 | 0.291 | -0.292 | 0.277 |
| | x(t-1) | -0.086 | 0.273 | | |
| Setra_422base.upst_Pa | intercept | 0.092 | 0.149 | 0.106 | 0.144 |
| | mitigation(t) | -0.112 | 0.158 | -0.115 | 0.156 |
| | x(t) | -0.012 | 0.014 | -0.011 | 0.014 |
| | x(t-1) | 0.007 | 0.014 | | |
| Setra_422SGdp.ss_Pa | intercept | 0.084 | 0.346 | 0.290 | 0.328 |
| | mitigation(t) | -0.032 | 0.160 | -0.105 | 0.157 |
| | x(t) | -0.020 | 0.012 | -0.006 | 0.009 |
| | x(t-1) | 0.018 | 0.012 | | |
| Setra_422ss.base_Pa | intercept | 0.094 | 0.411 | 0.025 | 0.283 |
| | mitigation(t) | -0.124 | 0.170 | -0.111 | 0.158 |
| | x(t) | 0.016 | 0.068 | 0.016 | 0.066 |
| | x(t-1) | -0.017 | 0.071 | | |
| Snowdepth_daily | intercept | 0.086 | 0.198 | 0.048 | 0.193 |
| | mitigation(t) | -0.091 | 0.160 | -0.110 | 0.158 |
| | x(t) | 0.001 | 0.001 | 0.000 | 0.001 |
| | x(t-1) | -0.001 | 0.001 | | |
| Soil_H2O_In6._cbar | intercept | 0.138 | 0.241 | 0.244 | 0.247 |
| | mitigation(t) | -0.082 | 0.153 | -0.136 | 0.159 |
| | x(t) | -0.023* | 0.011 | -0.005 | 0.006 |
| | x(t-1) | 0.020 | 0.010 | | |
| Soil_H2O_Out3.5._cbar | intercept | 0.370 | 0.803 | 0.356 | 0.633 |
| | mitigation(t) | -0.107 | 0.163 | -0.107 | 0.158 |
| | x(t) | -0.004 | 0.009 | -0.004 | 0.008 |
| | x(t-1) | 0.000 | 0.009 | | |

(continued)

Table 10-25. Analysis Chloroform Concentration at 422 Base South. Variables that Needed A Lag-1 One Week Term. Period Sept 2012 to April 2013 (cont.)

| Predictor Name | Model Term | Model: $Y(t) - Y(t-1) = \text{intercept} + \text{mitigation}(t) + x(t) + x(t-1)$ | | Model: $Y(t) - Y(t-1) = \text{intercept} + \text{mitigation}(t) + x(t)$ | |
|---------------------|---------------|--|-------|---|-------|
| | | Estimate | SE | Estimate | SE |
| Soil_H2O_Out6._cbar | intercept | -0.235 | 0.272 | 0.102 | 0.151 |
| | mitigation(t) | 0.145 | 0.235 | -0.116 | 0.158 |
| | x(t) | 0.019 | 0.101 | -0.035 | 0.096 |
| | x(t-1) | 0.267 | 0.182 | | |
| Soil_T_C_MW3.9 | intercept | 0.247 | 0.249 | 0.157 | 0.176 |
| | mitigation(t) | -0.232 | 0.219 | -0.164 | 0.173 |
| | x(t) | -0.051 | 0.063 | -0.041 | 0.059 |
| | x(t-1) | -0.040 | 0.077 | | |
| Soil_T_C_OTC.1 | intercept | 0.075 | 0.117 | 0.062 | 0.178 |
| | mitigation(t) | 0.033 | 0.161 | 0.132 | 0.225 |
| | x(t) | 0.054** | 0.010 | 0.020 | 0.011 |
| | x(t-1) | -0.046** | 0.009 | | |
| Soil_T_C_OTC.3.5 | intercept | -0.231 | 1.657 | -0.461 | 1.387 |
| | mitigation(t) | -0.141 | 0.175 | -0.139 | 0.171 |
| | x(t) | 0.011 | 0.023 | 0.008 | 0.020 |
| | x(t-1) | -0.006 | 0.022 | | |
| Soil_T_C_OTC.6 | intercept | 0.098 | 0.189 | 0.028 | 0.162 |
| | mitigation(t) | -0.155 | 0.204 | -0.083 | 0.172 |
| | x(t) | 0.011 | 0.012 | 0.005 | 0.004 |
| | x(t-1) | -0.005 | 0.011 | | |
| T_422_F | intercept | -0.054 | 0.431 | -0.236 | 0.372 |
| | mitigation(t) | 0.025 | 0.225 | -0.012 | 0.204 |
| | x(t) | 1.721* | 0.629 | 0.464 | 0.514 |
| | x(t-1) | -1.706** | 0.532 | | |
| T_422baseN_C | intercept | -0.053 | 0.181 | 0.054 | 0.165 |
| | mitigation(t) | -0.130 | 0.198 | -0.121 | 0.198 |
| | x(t) | -0.005 | 0.006 | 0.002 | 0.006 |
| | x(t-1) | 0.014* | 0.005 | | |
| T_422baseS_C | intercept | 0.123 | 0.169 | 0.062 | 0.163 |
| | mitigation(t) | -0.275 | 0.228 | -0.062 | 0.211 |
| | x(t) | 0.023 | 0.012 | 0.003 | 0.011 |
| | x(t-1) | -0.036** | 0.012 | | |

(continued)

Table 10-25. Analysis Chloroform Concentration at 422 Base South. Variables that Needed A Lag-1 One Week Term. Period Sept 2012 to April 2013 (cont.)

| Predictor Name | Model Term | Model: $Y(t) - Y(t-1) = \text{intercept} + \text{mitigation}(t) + x(t) + x(t-1)$ | | Model: $Y(t) - Y(t-1) = \text{intercept} + \text{mitigation}(t) + x(t)$ | |
|--------------------------------|---------------|--|-------|---|-------|
| | | Estimate | SE | Estimate | SE |
| T_out_F | intercept | 0.080 | 0.143 | 0.081 | 0.142 |
| | mitigation(t) | -0.139 | 0.161 | -0.126 | 0.158 |
| | x(t) | 0.016 | 0.053 | 0.030 | 0.049 |
| | x(t-1) | 0.039 | 0.053 | | |
| T_out_Hi_F | intercept | 0.245 | 0.811 | 0.233 | 0.661 |
| | mitigation(t) | -0.112 | 0.171 | -0.111 | 0.158 |
| | x(t) | -0.001 | 0.013 | -0.001 | 0.004 |
| | x(t-1) | 0.000 | 0.015 | | |
| T_out_Lo_F | intercept | 0.130 | 0.231 | 0.133 | 0.232 |
| | mitigation(t) | -0.086 | 0.184 | -0.087 | 0.185 |
| | x(t) | -0.002 | 0.002 | 0.000 | 0.001 |
| | x(t-1) | 0.002 | 0.001 | | |
| Wind_Chill_F | intercept | -0.154 | 0.387 | -0.121 | 0.367 |
| | mitigation(t) | -0.174 | 0.187 | -0.170 | 0.183 |
| | x(t) | 0.001 | 0.002 | 0.001 | 0.002 |
| | x(t-1) | 0.000 | 0.001 | | |
| X422baseN_Wkly_Elect_radon | intercept | -0.852 | 0.776 | -0.270 | 0.682 |
| | mitigation(t) | -0.084 | 0.204 | -0.106 | 0.203 |
| | x(t) | 0.184 | 0.441 | 0.023 | 0.043 |
| | x(t-1) | -0.122 | 0.420 | | |
| X422baseS_Wkly_Elect_radon | intercept | 0.019 | 0.197 | 0.086 | 0.194 |
| | mitigation(t) | -0.094 | 0.219 | -0.089 | 0.218 |
| | x(t) | -0.024 | 0.043 | -0.001 | 0.020 |
| | x(t-1) | 0.041 | 0.039 | | |
| X422first_Wkly_Elect_radon | intercept | -0.070 | 0.218 | 0.020 | 0.213 |
| | mitigation(t) | -0.139 | 0.213 | -0.131 | 0.209 |
| | x(t) | 0.030 | 0.084 | 0.013 | 0.020 |
| | x(t-1) | 0.000 | 0.075 | | |
| X422office2nd_Wkly_Elect_radon | intercept | 0.422 | 1.640 | 0.466 | 1.648 |
| | mitigation(t) | -0.029 | 0.206 | -0.111 | 0.193 |
| | x(t) | -0.060 | 0.057 | -0.007 | 0.029 |
| | x(t-1) | 0.052 | 0.048 | | |

**Significant at 1% level of significance; * Significant at 5% level of significance

The only variable that required two lag terms, Wind Run was not correlated with chloroform (see **Table 10-26**).

Table 10-26. Analysis for Chloroform Concentration at 422 Base South. Variables Needing Lag-1 And Lag-2 Week Terms. Period Sept 2012 to April 2013

| Predictor Name (x(t)) | Model Term | Model $Y(t)-Y(t-1) = \text{intercept} + x(t) + x(t-1)+x(t-2)$ | | Model $Y(t)-Y(t-1) = \text{intercept} + x(t) + x(t-1)$ | | Model $Y(t)-Y(t-1) = \text{intercept} + x(t)$ | |
|-----------------------|------------|---|--------|--|--------|---|--------|
| | | Estimate | SE | Estimate | SE | Estimate | SE |
| Wind_Run_mi | intercept | 0.130 | 0.170 | 0.096 | 0.150 | 0.086 | 0.143 |
| | Mitigation | -0.199 | 0.193 | -0.132 | 0.171 | -0.117 | 0.158 |
| | x(t) | 16.281 | 32.314 | 13.751 | 32.226 | 9.488 | 27.176 |
| | x(t-1) | 37.376 | 37.720 | 8.819 | 34.080 | | |
| | x(t-2) | 60.663 | 33.665 | | | | |

10.7.6 Time Series Analysis Results of 422 Basement South PCE Data from Sept 2012 through April 2013

In this section, we discussed the evaluation of the association between PCE a concentrations at 422 base south and a list of predictor variables measured weekly during between Sept 2012 and April 2013. All models in this section (period Sept 2013 to April 2013) include mitigation as a control variable. Mitigation was coded as 1 (on both sides of duplex,) and 0 (OFF, passive or not yet installed).

Table 10-27 displays the analysis results for variables that did not need a lag term. The variable mitigation was included as a control variable but was not statistically significant. Only the barometric pressure predictor variable was significantly associated with PCE.

Table 10-27. Analysis for First Difference of 422 Base South PCE Concentration. Variables that Did Not Need Lag Terms. Period Sept 2012 to April 2013

| Predictor Name | Model Term | Model: $Y(t) - Y(t-1) = \text{intercept} + \text{mitigation} (t) + x(t)$ | |
|----------------|------------|--|---------|
| | | Estimate | SE |
| Bar_drop_Hg.hr | intercept | 0.338 | 0.587 |
| | mitigation | -0.432 | 0.649 |
| | x(t) | -23.020 | 111.636 |
| Bar_in_Hg | intercept | -131.243* | 58.183 |
| | mitigation | -0.211 | 0.599 |
| | x(t) | 4.371* | 1.933 |
| BP_Net_Change | intercept | 0.338 | 0.587 |
| | mitigation | -0.435 | 0.649 |
| | x(t) | 0.110 | 0.686 |
| BP_Pump_Speed | intercept | 0.877 | 1.068 |
| | mitigation | -0.504 | 0.651 |
| | x(t) | -2.652 | 4.436 |

(continued)

Table 10-27. Analysis for First Difference of 422 Base South PCE Concentration. Variables that Did Not Need Lag Terms. Period Sept 2012 to April 2013 (cont.)

| Predictor Name | Model Term | Model: $Y(t) - Y(t-1) = \text{intercept} + \text{mitigation}(t) + x(t)$ | |
|---------------------|------------|---|-------|
| | | Estimate | SE |
| BP_Stroke_Length | intercept | 1.097 | 1.137 |
| | mitigation | -0.598 | 0.670 |
| | x(t) | -0.886 | 1.148 |
| Cool_Degree_Day | intercept | 0.433 | 0.590 |
| | mitigation | -0.454 | 0.639 |
| | x(t) | -0.045 | 0.055 |
| Fall_Crk_Gage_ht_ft | intercept | 1.178 | 1.346 |
| | mitigation | -0.412 | 0.643 |
| | x(t) | -0.025 | 0.036 |
| Hum_out_ | intercept | 1.087 | 1.148 |
| | mitigation | -0.462 | 0.641 |
| | x(t) | -0.203 | 0.269 |
| Rain_In_met | intercept | 0.221 | 0.792 |
| | mitigation | -0.437 | 0.648 |
| | x(t) | 0.001 | 0.003 |
| Rain_IPH | intercept | 1.012 | 1.014 |
| | mitigation | -0.541 | 0.651 |
| | x(t) | -0.021 | 0.026 |
| T_422first_C | intercept | 1.860 | 2.587 |
| | mitigation | -0.411 | 0.645 |
| | x(t) | -0.021 | 0.035 |
| Wind_Dir | intercept | 0.371 | 0.619 |
| | mitigation | -0.450 | 0.648 |
| | x(t) | -0.058 | 0.395 |
| Wind_Dir_Hi | intercept | 0.076 | 0.725 |
| | mitigation | -0.256 | 0.711 |
| | x(t) | 0.149 | 0.241 |
| Wind_Speed_Hi_MPH | intercept | 0.457 | 0.745 |
| | mitigation | -0.258 | 0.945 |
| | x(t) | 0.039 | 0.045 |
| Wind_Speed_MPH | intercept | 0.328 | 0.671 |
| | mitigation | -0.513 | 0.714 |
| | x(t) | 0.014 | 0.017 |

*Significant at 5% level of significance

Among the predictors needing a lag-1 week term in the model (**Table 10-28**), the following predictor variables were statistically significantly related to PCE:

- the current week's total of heating degree days (in the reduced model),
- the past and current weeks' measurement of soil temperature at 1 ft bls, and
- the past week's measurements of temperatures in the 422 basement.

The relationship with heating degree days was in the expected direction: colder weather would result in more heating degree days in the current week and higher PCE in indoor air. Once again since the coefficients for the soil temperature are opposite, a worked example will be beneficial. Assume that the shallow soil is 15°C this week and was 10°C last week. Assume mitigation to be turned off. Under those conditions, the model predicts PCE will increase by 1.4 $\mu\text{g}/\text{m}^3$.

Table 10-28. Analysis for 422 Base South PCE Concentration. Variables that Needed A Lag-1 Week Term. Period Sept 2012 to April 2013

| Predictor Name | Model Term | Model: $Y(t) - Y(t-1) = \text{intercept} + \text{mitigation}(t) + x(t) + x(t-1)$ | | Model: $Y(t) - Y(t-1) = \text{intercept} + \text{mitigation}(t) + x(t)$ | |
|----------------------|---------------|--|---------|---|---------|
| | | Estimate | SE | Estimate | SE |
| Dew_pt_422_F | intercept | 0.352 | 0.619 | 0.338 | 0.587 |
| | mitigation(t) | -0.454 | 0.702 | -0.432 | 0.649 |
| | x(t) | -16.713 | 132.540 | -23.020 | 111.636 |
| | x(t-1) | 13.050 | 140.164 | | |
| Heat_Degree_Day | intercept | -190.689* | 70.939 | -131.243* | 58.183 |
| | mitigation(t) | -0.136 | 0.590 | -0.211 | 0.599 |
| | x(t) | 3.392 | 2.018 | 4.37081* | 1.933 |
| | x(t-1) | 2.954 | 2.094 | | |
| Hum_422_. | intercept | 0.361 | 0.621 | 0.338 | 0.587 |
| | mitigation(t) | -0.467 | 0.702 | -0.435 | 0.649 |
| | x(t) | 0.053 | 0.813 | 0.110 | 0.686 |
| | x(t-1) | -0.117 | 0.854 | | |
| Setra_420ss.base_Pa | intercept | 1.685 | 1.362 | 0.877 | 1.068 |
| | mitigation(t) | -0.545 | 0.653 | -0.504 | 0.651 |
| | x(t) | -2.724 | 4.444 | -2.652 | 4.436 |
| | x(t-1) | -4.167 | 4.344 | | |
| Setra_422base.out_Pa | intercept | 1.720 | 1.274 | 1.097 | 1.137 |
| | mitigation(t) | -0.610 | 0.669 | -0.598 | 0.670 |
| | x(t) | -0.578 | 1.180 | -0.886 | 1.148 |
| | x(t-1) | -1.186 | 1.107 | | |

(continued)

Table 10-28. Analysis for 422 Base South PCE Concentration. Variables that Needed A Lag-1 Week Term. Period Sept 2012 to April 2013 (cont.)

| Predictor Name | Model Term | Model: $Y(t) - Y(t-1) = \text{intercept} + \text{mitigation}(t) + x(t) + x(t-1)$ | | Model: $Y(t) - Y(t-1) = \text{intercept} + \text{mitigation}(t) + x(t)$ | |
|-----------------------|---------------|--|-------|---|-------|
| | | Estimate | SE | Estimate | SE |
| Setra_422base.upst_Pa | intercept | 0.415 | 0.612 | 0.433 | 0.590 |
| | mitigation(t) | -0.450 | 0.653 | -0.454 | 0.639 |
| | x(t) | -0.047 | 0.058 | -0.045 | 0.055 |
| | x(t-1) | 0.009 | 0.057 | | |
| Setra_422SGdp.ss_Pa | intercept | 0.964 | 1.483 | 1.178 | 1.346 |
| | mitigation(t) | -0.336 | 0.685 | -0.412 | 0.643 |
| | x(t) | -0.040 | 0.054 | -0.025 | 0.036 |
| | x(t-1) | 0.019 | 0.050 | | |
| Setra_422ss.base_Pa | intercept | 0.548 | 1.665 | 1.087 | 1.148 |
| | mitigation(t) | -0.362 | 0.687 | -0.462 | 0.641 |
| | x(t) | -0.204 | 0.274 | -0.203 | 0.269 |
| | x(t-1) | 0.131 | 0.288 | | |
| Snowdepth_daily | intercept | 0.223 | 0.825 | 0.221 | 0.792 |
| | mitigation(t) | -0.435 | 0.667 | -0.437 | 0.648 |
| | x(t) | 0.001 | 0.004 | 0.001 | 0.003 |
| | x(t-1) | 0.000 | 0.004 | | |
| Soil_H2O_In6._cbar | intercept | 0.737 | 1.034 | 1.012 | 1.014 |
| | mitigation(t) | -0.402 | 0.657 | -0.541 | 0.651 |
| | x(t) | -0.067 | 0.047 | -0.021 | 0.026 |
| | x(t-1) | 0.051 | 0.043 | | |
| Soil_H2O_Out3.5._cbar | intercept | 3.641 | 3.224 | 1.860 | 2.587 |
| | mitigation(t) | -0.500 | 0.654 | -0.411 | 0.645 |
| | x(t) | -0.011 | 0.036 | -0.021 | 0.035 |
| | x(t-1) | -0.033 | 0.036 | | |
| Soil_H2O_Out6._cbar | intercept | 1.076 | 1.154 | 0.371 | 0.619 |
| | mitigation(t) | -0.997 | 0.998 | -0.450 | 0.648 |
| | x(t) | -0.171 | 0.428 | -0.058 | 0.395 |
| | x(t-1) | -0.560 | 0.771 | | |
| Soil_T_C_MW3.9 | intercept | 1.023 | 0.991 | 0.076 | 0.725 |
| | mitigation(t) | -0.973 | 0.872 | -0.256 | 0.711 |
| | x(t) | 0.040 | 0.250 | 0.149 | 0.241 |
| | x(t-1) | -0.420 | 0.306 | | |

(continued)

Table 10-28. Analysis for 422 Base South PCE Concentration. Variables that Needed A Lag-1 Week Term. Period Sept 2012 to April 2013 (cont.)

| Predictor Name | Model Term | Model: $Y(t) - Y(t-1) = \text{intercept} + \text{mitigation}(t) + x(t) + x(t-1)$ | | Model: $Y(t) - Y(t-1) = \text{intercept} + \text{mitigation}(t) + x(t)$ | |
|------------------|---------------|--|-------|---|-------|
| | | Estimate | SE | Estimate | SE |
| Soil_T_C_OTC.1 | intercept | 0.480 | 0.677 | 0.457 | 0.745 |
| | mitigation(t) | -0.372 | 0.929 | -0.258 | 0.945 |
| | x(t) | 0.138* | 0.056 | 0.039 | 0.045 |
| | x(t-1) | -0.118* | 0.054 | | |
| Soil_T_C_OTC.3.5 | intercept | 0.835 | 6.581 | -3.259 | 5.660 |
| | mitigation(t) | -0.648 | 0.693 | -0.619 | 0.698 |
| | x(t) | 0.098 | 0.090 | 0.053 | 0.083 |
| | x(t-1) | -0.103 | 0.086 | | |
| Soil_T_C_OTC.6 | intercept | 0.515 | 0.730 | 0.328 | 0.671 |
| | mitigation(t) | -0.862 | 0.791 | -0.513 | 0.714 |
| | x(t) | -0.067 | 0.048 | 0.014 | 0.017 |
| | x(t-1) | 0.086 | 0.044 | | |
| T_422_F | intercept | 0.583 | 2.111 | -0.008 | 1.535 |
| | mitigation(t) | -0.381 | 1.102 | -0.355 | 0.843 |
| | x(t) | 3.132 | 3.077 | 0.689 | 2.119 |
| | x(t-1) | -3.598 | 2.604 | | |
| T_422baseN_C | intercept | 0.072 | 0.734 | 0.508 | 0.670 |
| | mitigation(t) | -0.326 | 0.803 | -0.283 | 0.805 |
| | x(t) | -0.043 | 0.023 | -0.016 | 0.023 |
| | x(t-1) | 0.0563* | 0.022 | | |
| T_422baseS_C | intercept | 0.599 | 0.744 | 0.429 | 0.666 |
| | mitigation(t) | -0.994 | 1.003 | -0.349 | 0.862 |
| | x(t) | 0.082 | 0.054 | 0.018 | 0.045 |
| | x(t-1) | -0.11453* | 0.054 | | |
| T_out_F | intercept | 0.330 | 0.595 | 0.331 | 0.583 |
| | mitigation(t) | -0.507 | 0.667 | -0.495 | 0.650 |
| | x(t) | 0.101 | 0.221 | 0.114 | 0.202 |
| | x(t-1) | 0.037 | 0.222 | | |
| T_out_Hi_F | intercept | 2.232 | 3.294 | 2.322 | 2.682 |
| | mitigation(t) | -0.406 | 0.693 | -0.418 | 0.641 |
| | x(t) | -0.015 | 0.054 | -0.012 | 0.016 |
| | x(t-1) | 0.003 | 0.062 | | |

(continued)

Table 10-28. Analysis for 422 Base South PCE Concentration. Variables that Needed A Lag-1 Week Term. Period Sept 2012 to April 2013 (cont.)

| Predictor Name | Model Term | Model: $Y(t) - Y(t-1) = \text{intercept} + \text{mitigation}(t) + x(t) + x(t-1)$ | | Model: $Y(t) - Y(t-1) = \text{intercept} + \text{mitigation}(t) + x(t)$ | |
|--------------------------------|---------------|--|-------|---|-------|
| | | Estimate | SE | Estimate | SE |
| T_out_Lo_F | intercept | 0.404 | 0.944 | 0.421 | 0.954 |
| | mitigation(t) | -0.401 | 0.750 | -0.402 | 0.759 |
| | x(t) | -0.007 | 0.007 | 0.000 | 0.005 |
| | x(t-1) | 0.007 | 0.006 | | |
| Wind_Chill_F | intercept | -1.195 | 1.564 | -1.038 | 1.484 |
| | mitigation(t) | -0.848 | 0.755 | -0.829 | 0.741 |
| | x(t) | 0.006 | 0.008 | 0.007 | 0.007 |
| | x(t-1) | 0.002 | 0.006 | | |
| X422baseN_Wkly_Elect_radon | intercept | -0.520 | 3.133 | 0.086 | 2.722 |
| | mitigation(t) | -0.599 | 0.822 | -0.715 | 0.810 |
| | x(t) | -1.492 | 1.781 | 0.027 | 0.170 |
| | x(t-1) | 1.539 | 1.694 | | |
| X422baseS_Wkly_Elect_radon | intercept | 0.302 | 0.787 | 0.548 | 0.766 |
| | mitigation(t) | -0.515 | 0.877 | -0.591 | 0.863 |
| | x(t) | -0.174 | 0.171 | -0.028 | 0.079 |
| | x(t-1) | 0.194 | 0.154 | | |
| X422first_Wkly_Elect_radon | intercept | 0.137 | 0.896 | 0.370 | 0.851 |
| | mitigation(t) | -0.655 | 0.874 | -0.775 | 0.834 |
| | x(t) | -0.125 | 0.343 | 0.026 | 0.079 |
| | x(t-1) | 0.178 | 0.307 | | |
| X422office2nd_Wkly_Elect_radon | intercept | 1.448 | 6.816 | 1.410 | 6.632 |
| | mitigation(t) | -0.487 | 0.858 | -0.417 | 0.779 |
| | x(t) | 0.026 | 0.235 | -0.019 | 0.116 |
| | x(t-1) | -0.044 | 0.199 | | |

*Significant at 5% level of significance

The variable wind run which required two lag terms was not correlated with PCE (Table 10-29).

Table 10-29. Analysis for PCE Concentration at 422 Base South. Variables Needing Both Lag-1 And Lag-2 Week Terms. Period Sept 2012 to April 2013

| Predictor Name (x(t)) | Model Term | Model $Y(t)-Y(t-1) = \text{intercept} + x(t) + x(t-1)+x(t-2)$ | | Model $Y(t)-Y(t-1) = \text{intercept} + x(t) + x(t-1)$ | | Model $Y(t)-Y(t-1) = \text{intercept} + x(t)$ | |
|-----------------------|------------|---|---------|--|---------|---|---------|
| | | Estimate | SE | Estimate | SE | Estimate | SE |
| Wind_Run_mi | intercept | 0.681 | 0.693 | 0.352 | 0.619 | 0.338 | 0.587 |
| | Mitigation | -0.935 | 0.787 | -0.454 | 0.702 | -0.432 | 0.649 |
| | x(t) | 10.321 | 131.649 | -16.713 | 132.540 | -23.020 | 111.636 |
| | x(t-1) | 151.413 | 153.677 | 13.050 | 140.164 | | |
| | x(t-2) | 262.750 | 137.155 | | | | |

Addendum

To capture the existing serial correlation between consecutive observations, a time series regression model requires incorporating a model for the errors. For example, assume radon concentrations can be modeled as a function of observed predictors and a random error. The random error includes measurement error and any variability not explained by the current variables in the model. A model like that is formulated as $y_t = \sum_{i=1}^n \beta_i x_{it} + \varepsilon_t$ where $x_{it}, i = 1, \dots, n$ denote n time-dependent predictors observed at time t , y_t is the outcome of interest (radon emissions) at time t , and ε_t is the associated error at time t . A standard model for the error term is: $\varepsilon_t = \rho \varepsilon_{t-1} + v_t$, where $-1 < \rho < 1$, and v_t are independent and identically distributed random errors.

Given the expression for ε_t , y_t can be rewritten as: $y_t = \sum_{i=1}^n \beta_i x_{it} + \rho \varepsilon_{t-1} + v_t$ and since

$$y_{t-1} = \sum_{i=1}^n \beta_i x_{it-1} + \varepsilon_{t-1} \text{ then } \varepsilon_{t-1} = y_{t-1} - \sum_{i=1}^n \beta_i x_{it-1}, \text{ which result in}$$

$$y_t = \sum_{i=1}^n \beta_i x_{it} + \rho \left(y_{t-1} - \sum_{i=1}^n \beta_i x_{it-1} \right) + v_t$$

The above model is termed an autoregressive (because it includes lag values of y_t) distributed lag (because it includes lag values of the predictors: $x_{it}, i = 1, \dots, n$).

Table of Contents

| | |
|--|------|
| 11.0 Results and Discussion: Do Groundwater Concentrations Control Soil Gas Concentrations at this Site? And Thus Indoor Air Concentrations? | 11-1 |
| 11.1 Groundwater Level Changes | 11-1 |
| 11.2 Groundwater Concentration Trends | 11-2 |
| 11.2.1 Is the Groundwater Concentration Trend Correlated to Well or Water Table Depth? | 11-5 |
| 11.3 Revision to the Conceptual Model—Is the Groundwater Concentration Related to Soil Gas and Indoor Air Concentrations? | 11-6 |

List of Figures

| | |
|---|------|
| 11-1. Stacked hydrological graph with rainfall in inches (top—green line), depth to water in feet (middle—red circles), and discharge at Fall Creek in ft ³ /s (bottom—blue line). | 11-1 |
| 11-2. Actual groundwater levels along with the daily time series predicted from Fall Creek gage height data. | 11-2 |
| 11-3. Groundwater concentrations over time for Indianapolis duplex. | 11-4 |
| 11-4. PCE groundwater concentrations over time, showing concentrations by individual well and soil gas ports. | 11-4 |
| 11-5. Plot of groundwater PCE and chloroform concentrations against well screen (or soil gas port) depth (well depth measured to top of screen). | 11-5 |
| 11-6. Plot of groundwater PCE and chloroform concentrations against groundwater depth. | 11-6 |

List of Tables

| | |
|--|------|
| 11-1. Groundwater Monitoring Locations. | 11-3 |
|--|------|

11.0 Results and Discussion: Do Groundwater Concentrations Control Soil Gas Concentrations at this Site? And Thus Indoor Air Concentrations?

11.1 Groundwater Level Changes

Figure 11-1 presents the relationship between depth to water readings taken at the 422/420 house, Fall Creek discharge, and the rainfall taken at the house for the duration of the project. Fall Creek discharge was obtained from the online stream gage data collected by the USGS at gaging station number 03352500.²⁷

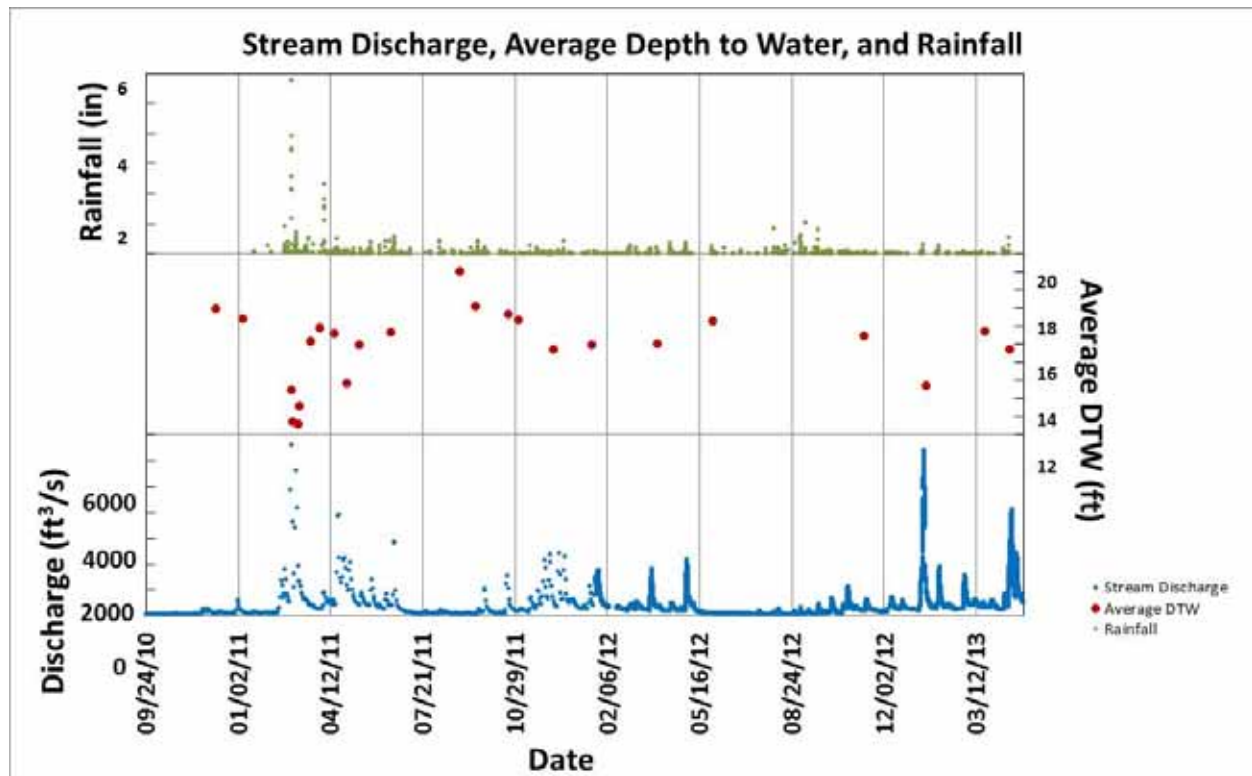


Figure 11-1. Stacked hydrological graph with rainfall in inches (top—green line), depth to water in feet (middle—red circles), and discharge at Fall Creek in ft³/s (bottom—blue line).

The most striking feature is during the heavy rain events that occurred in early March 2011. This rain was immediately reflected in the discharge at Fall Creek and in the rapid decrease in depth to groundwater as the water level responded to the increasing height of the creek. The hotter summer 2011 months that followed were drier, with deepening groundwater levels down to the lowest water table depth recorded during this project (about 20 ft bls). Spikes in Fall Creek discharge in early 2013 also were reflected in a higher water table.

As described in the previous report (U.S. EPA, 2012a), the water table had been expected to be at about 17 ft, just under the deepest of the soil gas ports (16.5 ft), but these deep ports were flooded in 2011. In

²⁷http://waterdata.usgs.gov/in/nwis/uv?site_no=03352500

response, groundwater samples were taken from the deeper soil gas ports (16.5 ft and sometimes 13 ft) when they flooded, analyzed along with the more conventional well samples and included in the groundwater sampling data discussed in this report.

Starting on November 9, 2012, a Solinst water Levellogger Model 3001 was used to obtain higher time resolution, with data recorded each half hour. The device was installed in the deepest well (MW1A). The higher resolution of this instrument enabled us to confirm and model the strong and rapid connection between surface water levels in Fall Creek and groundwater levels at the duplex. The strong correlation between groundwater levels and Fall Creek gauge heights enabled the use of the historic Fall Creek USGS gauge height data to accurately hind cast groundwater levels for the earlier part of the project at a much finer (daily) resolution than was available before. This empirical model was used to create a detailed time series of water table elevations that was used as an independent variable in the statistical analyses discussed in Sections 9 and 10 of this report and compared with groundwater VOC concentration trends in this section. **Figure 11-2** shows the daily time series of actual and predicted groundwater levels from the model.

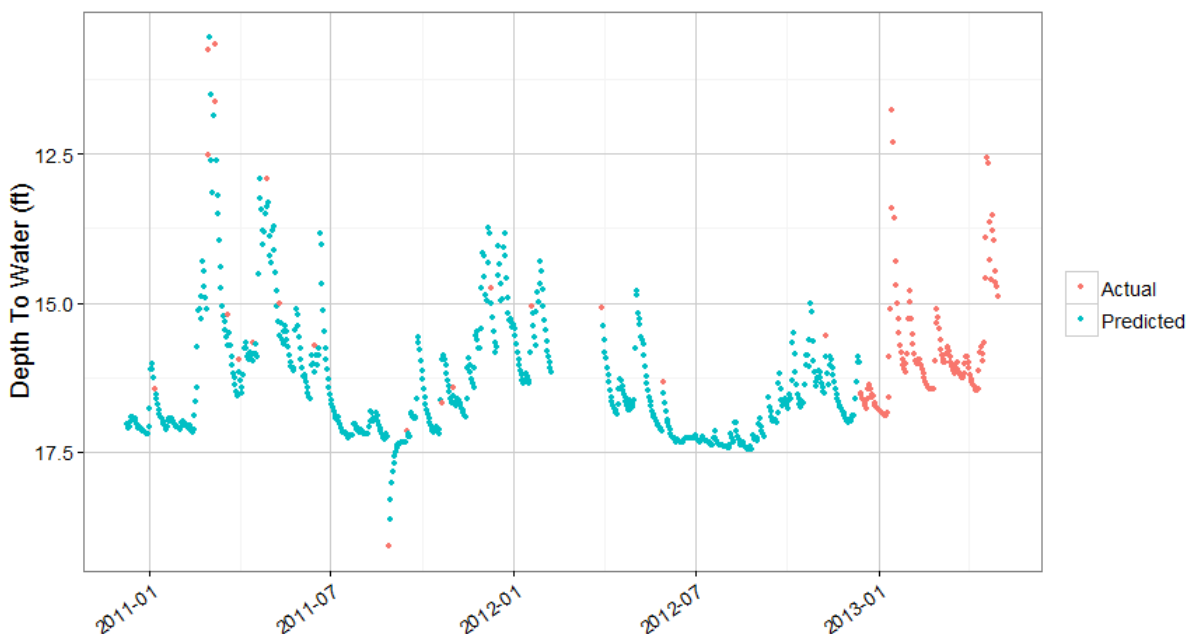


Figure 11-2. Actual groundwater levels along with the daily time series predicted from Fall Creek gage height data.

11.2 Groundwater Concentration Trends

During initial screening conducted in late spring 2010 at the site (U.S. EPA, 2012a), groundwater had detectable but low concentrations of PCE and chloroform, with PCE concentrations ranging from 0.46 to 0.61 $\mu\text{g/L}$ and chloroform levels ranging from 1.9 to 3.0 $\mu\text{g/L}$. Although these data were subject to qualifiers related to the very low levels of analytes in the samples, the analyst believed that the analytes were present. In addition, a June 2005 groundwater sampling event associated with the nearby Mapleton-Fall Creek brownfields site found detectable chloroform (8.9 to 22.1 $\mu\text{g/L}$) in groundwater. However, initial groundwater sampling at the duplex did not find comparable chloroform levels in groundwater, with only nondetects being seen in the earlier phase of this project (U.S. EPA, 2012a). The detectable chloroform concentrations measured in late 2012 and early 2013 were also lower than those observed

during screening. However, PCE levels have remained fairly constant from spring 2010 screening through the spring 2013 measurements presented in this report.

As described in Section 3, groundwater was sampled for VOC analysis approximately monthly during the active project. One hundred eighteen groundwater samples were collected and analyzed over the two project phases from six monitoring wells (two 3-well clusters) and from the flooded soil gas ports. **Table 11-1** shows the sampling locations, screened interval, and number of samples collected from each well and from the soil gas ports.

Table 11-1. Groundwater Monitoring Locations

| Well ID | Screened Interval Depth (ft bls) | No. Measurements | Location |
|----------------------------|----------------------------------|------------------|----------------|
| MW1A | 24–26 | 9 | Exterior South |
| MW1B | 21–24 | 14 | Exterior South |
| MW1C | 16–21 | 15 | Exterior South |
| MW2A | 24–26 | 14 | Exterior North |
| MW2B | 21–24 | 14 | Exterior North |
| MW2C | 16–21 | 13 | Exterior North |
| MW3 | 19.5–24.5 | 12 | 422 Basement |
| SGP GW points ¹ | 13–16.5 | 27 | Various |

¹flooded soil gas ports

Figure 11-3 shows the groundwater concentrations of PCE and chloroform over both phases of the project. Nondetect samples were not plotted for the first phase of this project because the detection limits for PCE (2.8 µg/L) and chloroform (2.0 µg/L) were considerably higher than the detectable concentrations in the figure. As a result of efforts to improve the detection limits and instrument sensitivity at EPA NERL, chloroform was detected beginning in late 2012.

Chloroform concentrations were not detectable until late March through mid-April 2013, when two samples showed detectable concentrations around 0.6 µg/L. Detectable mid-April chloroform concentrations otherwise ranged from 0.07 to 0.37 µg/L. The reason for the difference between the two high samples and the rest of the chloroform detections is not clear at this point in time. Overall, the chloroform groundwater data showed 99 nondetects, or 84% of the 118 groundwater measurements. There were 19 detections and 21 nondetects in the 2013 data for a 48% detection rate.

For PCE, groundwater concentrations were consistent with screening and fairly stable over the course of the project, with almost all detectable concentrations ranging between 0.2 and 0.8 µg/L. A single higher concentration event occurred in September–October 2011 when PCE concentrations in some wells ranged up to 1.3 µg/L. **Figure 11-4** plots the PCE concentrations by well so that one can see the fairly consistent relationship between the wells during a particular sampling event. Note that the groundwater concentrations taken from the soil gas ports generally plot well within the range of the more conventional monitoring well samples. Overall, there were 50 nondetects for PCE for a 42% detection rate. In 2013, PCE was detected in 13 of 40 samples, for a 33% detection rate.

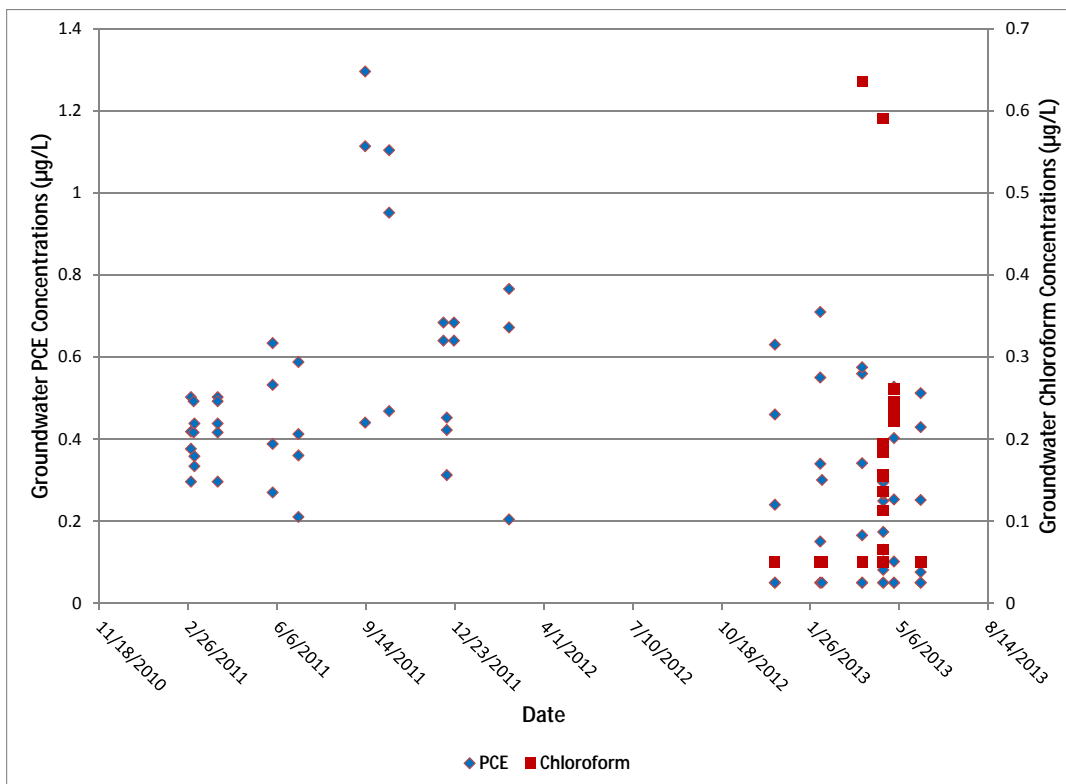


Figure 11-3. Groundwater concentrations over time for Indianapolis duplex.

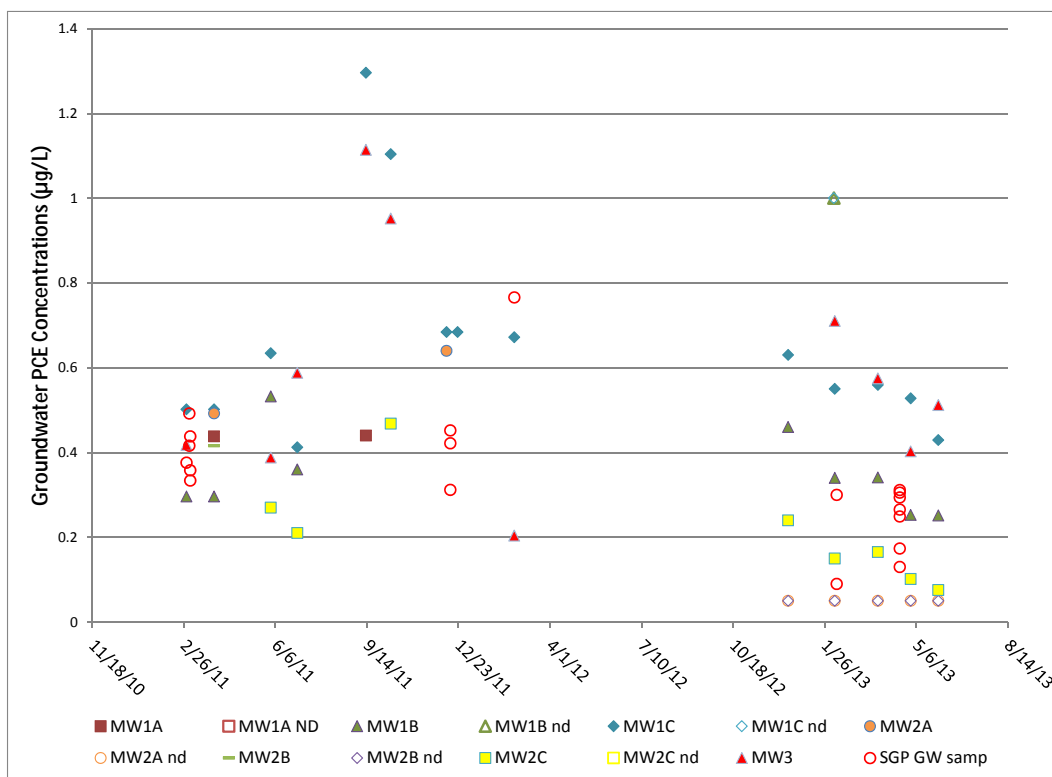


Figure 11-4. PCE groundwater concentrations over time, showing concentrations by individual well and soil gas ports.

11.2.1 Is the Groundwater Concentration Trend Correlated to Well or Water Table Depth?

Figure 11-5 shows the relationship between monitoring well screen depth (or soil gas port depth) and PCE and chloroform groundwater concentration. As the figure shows, there does not appear to be a strong correlation, although the higher concentrations are associated with the 16-ft, 16.5-ft, and 19-ft well screen depths. (Note that the well screen depths discussed here are at the top of the screen.) This supports the hypotheses that this site lacks a “clean water lens” and that the shallowest groundwater contains VOCs available to partition into the soil gas.

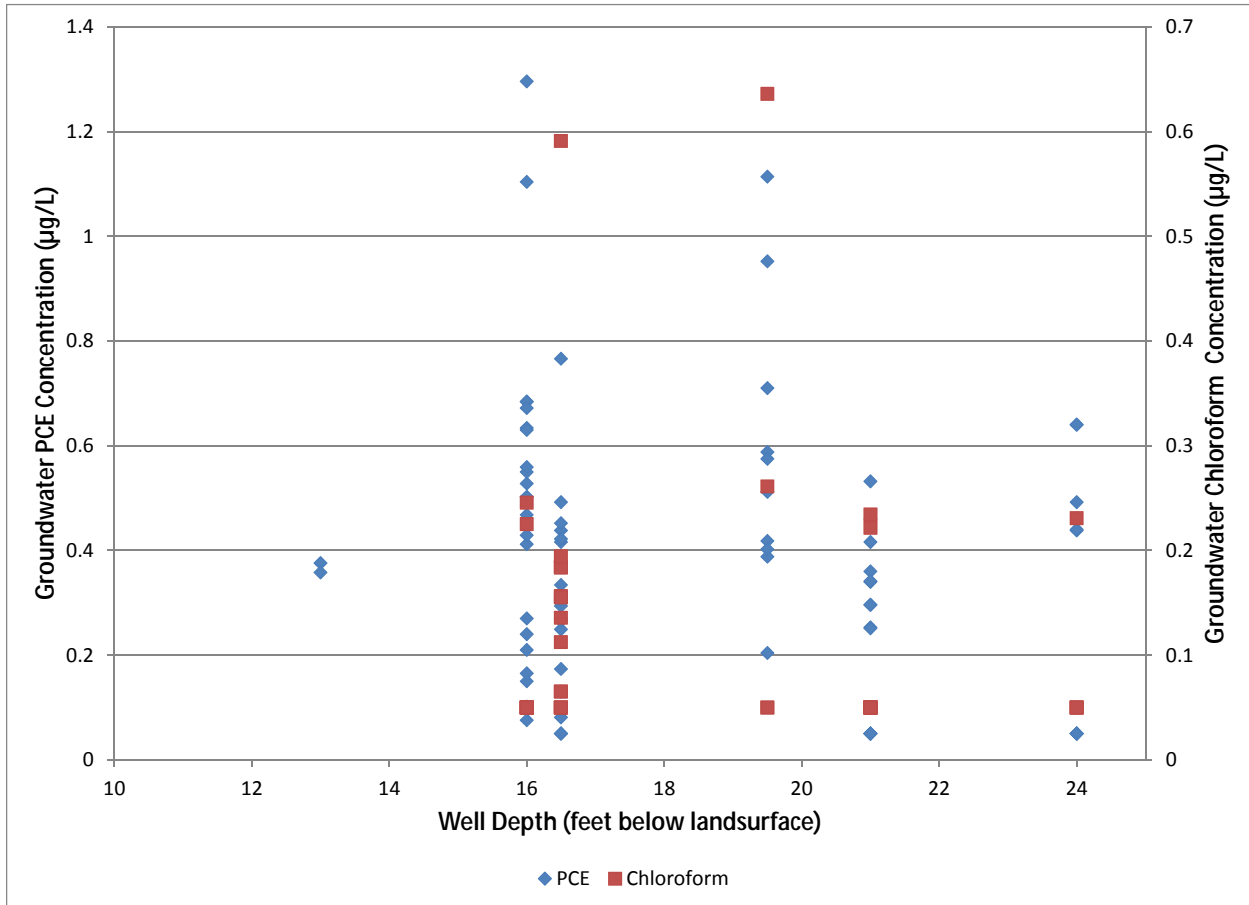


Figure 11-5. Plot of groundwater PCE and chloroform concentrations against well screen (or soil gas port) depth (well depth measured to top of screen).

Figure 11-6 plots the groundwater PCE and chloroform concentration against the water level measured or estimated for the day the groundwater sample was taken. Again, a strong correlation is not visually apparent, but the PCE high concentrations do correspond with the low groundwater levels observed in September–October 2011. This could be related to the extremely rapid groundwater level decrease shown for this time period in Figure 4-2. Possible conceptual models consistent with this finding include:

- When freshwater comes into the aquifer, it is generally low concentration. Over time, the freshwater mixes with existing water and picks up VOCs at a rate faster than it can give them off through volatilization. Thus, the maximum concentration is seen when little freshwater has come in recently. OR

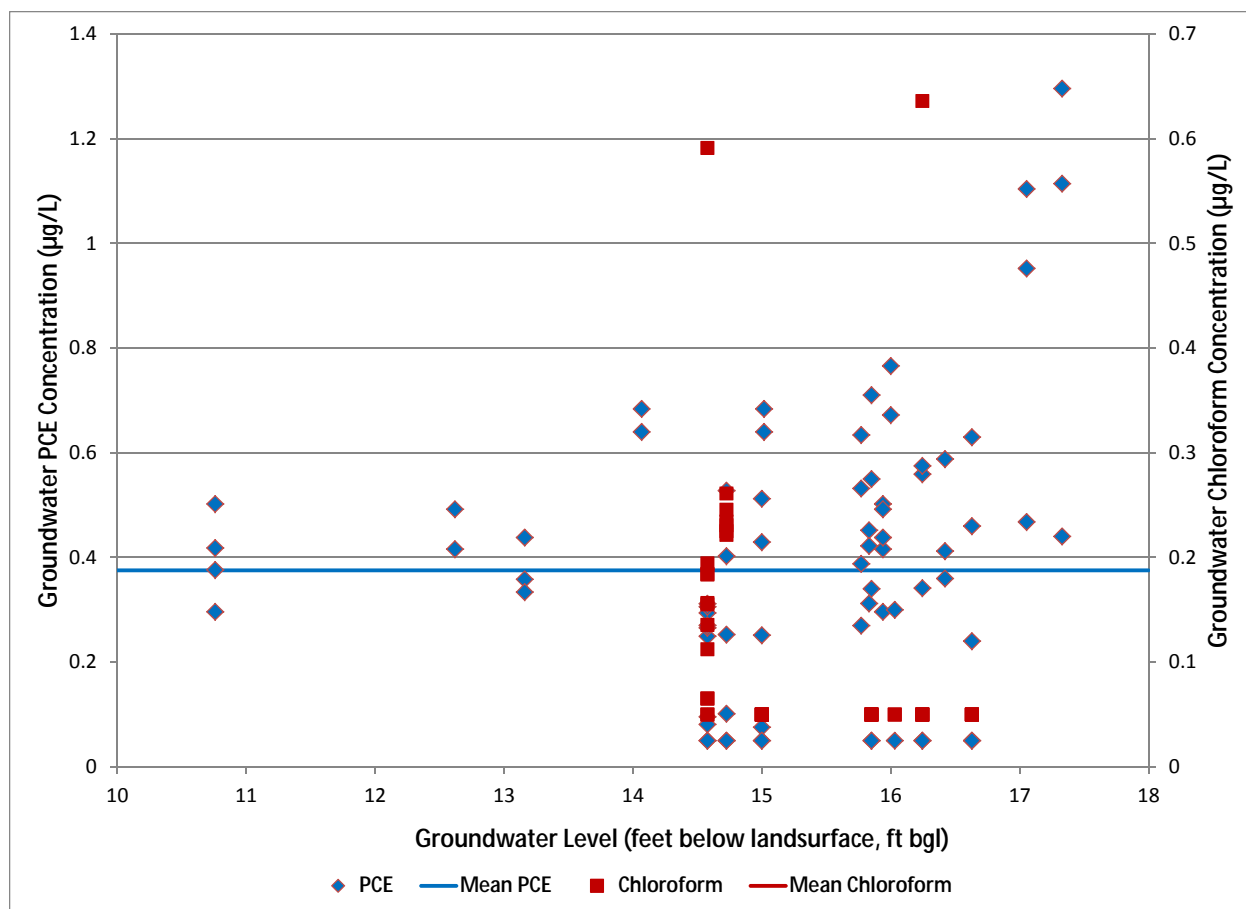


Figure 11-6. Plot of groundwater PCE and chloroform concentrations against ground water depth.

- Figure 11-6. Plot of groundwater PCE and chloroform concentrations against groundwater depth. The well screens are composed as most screens are by materials of varying conductivity. At high water levels in the well, the screens are mostly or completely submerged. The water in the PDB then preferentially comes from the high conductivity parts of the formation within the well screen. At low water levels in the well, it may be that all the water in the well is coming from a lower flow part of the formation. Formation layers with higher hydraulic conductivities can be lower in concentration than the layers with lower hydraulic conductivities because finer grained materials (e.g., clays, organic matter) tend to have higher sorption affinities for VOCs than coarser sand and gravels.

11.3 Revision to the Conceptual Model—Is the Groundwater Concentration Related to Soil Gas and Indoor Air Concentrations?

The monthly or longer sampling intervals make it very difficult to quantitatively assess the correlation of groundwater PCE against soil gas or indoor air concentrations, although the narrow range of variability in PCE concentrations (below an order of magnitude) and stability of this variability over time (see **Figures 11-3 and 11-4**) make it unlikely that changes in groundwater concentrations are strongly related to the changes in soil gas or indoor air concentrations over the time scales observed in this study. Chloroform's limited length of record for detectable concentrations in groundwater severely limits what can be assessed in that regard.

However, given the groundwater concentrations are relatively stable under the site, there are sufficient data to evaluate the potential for groundwater to be the source of indoor air concentrations in the 420/422 duplex on the basis of Henry's law calculations. For PCE, the prevalent range of groundwater concentrations, from 0.2 to 0.8 $\mu\text{g/L}$, and mean of 0.4 $\mu\text{g/L}$, corresponds to vapor concentrations of 175, 579, and 275 $\mu\text{g/m}^3$, respectively, with the maximum groundwater concentration, 1.3 $\mu\text{g/L}$, corresponding to 941 $\mu\text{g/m}^3$. These concentrations are probably sufficient to produce the soil gas and indoor air concentrations observed in this study, especially considering the coarse-grained nature of the subsurface that allow ready diffusion and flow of contaminants from the water table to the building. Thus, the available groundwater data indicate that groundwater is a likely source of the PCE vapors observed in the subsurface and indoor air during this study, although additional vadose zone PCE sources cannot be ruled out based on the groundwater evidence.

As mentioned above, although the groundwater PCE concentrations are sufficient to be the primary source of the PCE measured in indoor air in this study, their observed variability does not explain the variability in the indoor air PCE measurements. As has been shown in this and other studies, the variability in indoor air PCE concentrations is also influenced by subsurface, building-related, and meteorological variables that affect the concentration of PCE as it migrates from the water table, enters the building, and mixes with indoor air. In addition, other sources of PCE that may also exist in the vadose zone or sewer lines cannot be ruled out at this point, and variability in those sources could also influence the PCE concentrations in indoor air. We will continue to test this assertion (that groundwater is the primary source of PCE vapors) as additional data are collected and analyzed at this site.

The same VOC source situation may not hold true for chloroform. Most of the measured concentrations of chloroform in groundwater are nondetects, with the maximum groundwater concentration (0.64 $\mu\text{g/L}$) corresponding to a vapor concentration of 63 $\mu\text{g/m}^3$, and the mean (0.12 $\mu\text{g/L}$) corresponding to 12 $\mu\text{g/m}^3$. These groundwater concentrations are not sufficient to drive the soil gas and indoor air concentrations measured in this study, indicating that other sources, such as vadose zone sources from nearby former businesses using chloroform or disinfection by-products from leaky water mains, may be responsible for the observed peak soil gas and indoor air chloroform concentrations.

Table of Contents

| | | |
|--------|---|-------|
| 12.0 | Results and Discussion: Special Studies | 12-1 |
| 12.1 | Summary of Geophysics Study | 12-1 |
| 12.2 | Summary of Tracer Testing..... | 12-3 |
| 12.2.1 | Introduction to Tracer Testing | 12-3 |
| 12.2.2 | Tracer Testing Objective..... | 12-3 |
| 12.2.3 | Tracer Test Experimental Methods..... | 12-3 |
| 12.2.4 | Tracer Test Results and Discussion | 12-4 |
| 12.2.5 | Summary of Tracer Test Conclusions..... | 12-15 |
| 12.3 | Testing Utility of Consumer Grade Radon Device (Safety Siren Pro)..... | 12-15 |
| 12.3.1 | Introduction to the Use of Consumer Grade Radon Monitoring Equipment in Vapor Intrusion..... | 12-15 |
| 12.3.2 | Objective of Consumer-Grade Radon Device Testing | 12-15 |
| 12.3.3 | Methods of Consumer-Grade Radon Device Testing | 12-15 |
| 12.3.4 | Consumer Grade Radon Detector Results and Discussion | 12-16 |

List of Figures

| | | |
|--------|---|-------|
| 12-1. | Response at all locations to first helium injection in front yard. | 12-5 |
| 12-2. | Response at all locations to second helium injection in front yard..... | 12-6 |
| 12-3. | Response at all locations to third helium injection in backyard..... | 12-6 |
| 12-4. | Response at all locations to fourth helium injection in backyard. | 12-7 |
| 12-5. | Helium response at SGP2 cluster (south of duplex) directly above injection point after injections 1 (top graph, mitigation off) and 2 (bottom graph, mitigation on)..... | 12-8 |
| 12-6. | Helium response at SGP6 cluster at SGP6 cluster (north of duplex) directly above injection point after injections 3 (top graph, mitigation off) and 4 (bottom graph, mitigation on)..... | 12-9 |
| 12-7. | Helium response at SGP1 cluster (south of duplex, approximately 6 ft closer to duplex than injection point) after first Injection (top graph, mitigation off) and second injection (bottom graph, mitigation on)..... | 12-10 |
| 12-8. | Helium response at SGP5 cluster (north of duplex, approximately 6 ft closer to duplex than injection point) after third injection (top graph, mitigation off) and fourth injection (bottom graph, mitigation on)..... | 12-11 |
| 12-9. | Helium response to first and second helium injections at SGP9 (interior). | 12-12 |
| 12-10. | Helium response to third and fourth helium injections at SGP10 (interior). | 12-12 |
| 12-11. | Cross-section view of helium tracer arrival at 6-ft depth intervals. | 12-14 |
| 12-12. | Comparison of electret and Safety Siren results for first phase of the project (top graph) and second project phase (bottom graph). | 12-17 |
| 12-13. | Comparison between the 422 office Safety Siren and electret. | 12-22 |
| 12-14. | Comparison between the 422 basement N Safety Siren and electret. | 12-22 |

List of Tables

12-1. Data Quality Objectives and Performance/Acceptance Criteria for Special Studies..... 12-1
12-2. Comparison of Safety Siren, AlphaGUARD, and Electret Radon Data 12-18
12-3. Comparison of Safety Siren and Electret Radon Data 12-20

12.0 Results and Discussion: Special Studies

We conducted five special studies in the Indianapolis duplex. These studies either go beyond the objectives articulated in Section 2 to address specific EPA research needs or address the primary project objectives using different tools. Two of these special studies were reported completely in our previous report and are not discussed in detail here:

- VOC measurement efficiency of temporary subslab ports as compared with permanent subslab port constructions (Section 12.1 and Appendix B of U.S. EPA [2012a])
- Use of box fans to induce flow into the structure in an attempt to create “worst case” conditions for vapor intrusion (Section 12.2 of U.S. EPA [2012a])

In this section, we present methods, results, and discussion for three special studies:

- An EPA ORD study of this duplex and its subsurface environs using geophysical methods (Section 12.1)
- Helium tracer testing in which helium was injected into deep soil gas ports and its migration observed. (Section 12.2)
- Continued testing of a consumer-grade radon detector as an indicator of vapor intrusion, providing additional data collected since U.S. EPA (2012a) (Section 12.3)

Data quality objectives and criteria for these studies are described in **Table 12-1**.

12.1 Summary of Geophysics Study

In August 2012, the EPA National Exposure Research Laboratory (NERL) in Las Vegas conducted magnetic, electromagnetic induction, and ground penetrating radar (GPR) surveys within the basement and surrounding exterior of the Indianapolis study duplex (U.S. EPA, in press). The exterior surveys included the house property, East 28th Street to the south, the adjacent alley and property to the west, and the property to the north and northeast. The interior surveys were performed in the basement of both the 420 and 422 residences. The objectives of these surveys were to locate anthropogenic objects and identify subsurface conditions that may influence subsurface vapor flow to aid in the conceptual site model refinement.

The exterior magnetic and EMI survey identified known surface objects and known utilities as well as likely utilities. The exterior 200 MHz and 500 MHz GPR results suggested an electrically conductive unsaturated zone with irregular hummocky layers overlaying a more regular horizontally stratified zone at approximately 7.5 ft deep, which likely corresponds to the facies contrast between the underlying sand/gravel layer and the shallower silt/clay layer. This contact may also form local perched water conditions that may also cause such a geophysical response. These stratigraphic features may influence subsurface fluid fate and transport. A large hyperbolic reflection was observed in the middle of the backyard and about 10 ft north of the house. The source of this object is unknown and should be investigated. A sloping feature near the back wall of the house may be a backfill horizon or perhaps old brick stairs formerly used for external access to the basements. Additional observed features are described in U.S. EPA (in press).

Table 12-1. Data Quality Objectives and Performance/Acceptance Criteria for Special Studies

| Task Order Objectives | Study Questions | Measurements Used | Measurement Performance or Acceptance Criteria |
|--|--|--|---|
| Better define the subsurface conditions that influence the movement of VOCs and radon into the study duplex. | What is the nature of the subsurface environment? What stratigraphic and human-made features influence contaminant transport? | Geophysical techniques (i.e., GPR, magnetic, and electromagnetic induction), Helium tracer testing. | Acquire geophysical data from multiple transects within each third of the basement. Perform at least two helium tracer injections with monitoring on 1-hour frequency at five or more locations. |
| Evaluate the ability of a low-cost consumer-grade radon detector (Safety Siren Pro Series 3, Family Safety Products Inc.) to provide continuous indication of soil gas entry into the structure. | Does the measurement of radon concentration using this consumer-based analyzer agree within +/- 30% to the readings from the electret and AlphaGUARD methods >90% of the time? | The Safety Siren has two displays—the “short term” is an average over the previous 7 days, and the “long term” is the average from time of last reset (up to 5 years). Readings are available after a minimum of 48 hours of operation. Record the short-term reading at each of six indoor stations weekly and compare with ongoing electret and AlphaGUARD measurements. | Conduct tests at six stations: 422 south basement (AlphaGUARD), 422 north basement, 420 south basement, 422 first floor (AlphaGUARD), 422 second floor, and 420 first floor. Add an electret measurement during the Safety Siren test period at 422 second floor for additional comparison. At six stations, compare Safety Siren results with weekly electrets. Collect at least 4 weeks of comparative data = 28 pairs of data points. At two stations, compare the Safety Siren against weekly averages of hourly AlphaGUARD data, providing at least 8 additional pairs of data points. |
| | Does the consumer-grade radon detector provide a useful indication of the weekly average infiltration of VOC containing soil gas? | Month-long correlation test between consumer-grade radon detector and other radon detectors as discussed above. Year-long data set on radon/VOC correlation in this house. | Safety Siren adequately correlates with the electrets (see above) and radon correlates to VOCs in the main study data set. |

The interior GPR results suggest the concrete slab varies from 0.5 to 0.7 ft in thickness with an irregular undulating contact with the underlying material. This underlying material is electrically conductive and contains many discontinuities and non-horizontal interfaces, which may govern subsurface fluid fate and transport. This suggests the concrete floor was not poured on well-flattened fill material and may provide pockets into which soil gas may pool or move preferentially. However, the presence of fill material of some sort is evident at many locations beneath the slab. One prominent area of fill lies to the west of the cistern in the 420 basement. This may be consistent with a construction practice in which cuts and fills were incompletely done prior to pouring the slab. The GPR data suggest there is a thicker concrete footing below the doorways that separate the rooms in the basement. The GPR response to the cistern and the covered sewer line is evident as are GPR reflections likely due to fill material or other features related to the cistern. Other anomalous GPR reflections are detailed in U.S. EPA (in press).

12.2 Summary of Tracer Testing

12.2.1 Introduction to Tracer Testing

In addition to geophysical imaging and stratigraphic visualization based on soil logs, an additional line of evidence for understanding subsurface conditions is tracer testing. Tracer testing uses injected gases, like helium, to help determine subsurface air permeability, possible vapor entry pathways into a structure, and potential preferential pathways for vapor migration.

12.2.2 Tracer Testing Objective

During the first phase of this project, three-dimensional characterization and visualization was done on the 422/420 house based on survey maps, soil data, VOC, and radon data. In autumn 2012, geophysical work was performed on the 422/420 house as an additional line of evidence of subsurface conditions in the near- and sub-building environments. A helium tracer test can add to the already acquired evidence by suggesting flow pathways and points of ingress into the 422/420 house. Additionally, tracer testing, by sampling proximally related points, can describe how subsurface conditions change from north to south in the house environment. The following is a quote from the study objectives in U.S. EPA (2012a):

A helium tracer test will also be used in order to gather more information about the conditions beneath the 422/420 house and its immediate surroundings, as well as sewer outflows, utility corridors, and public utility lines (if possible). The sample plan will also incorporate a way of determining the difference in the dynamics of collection and motion of vapors and gases between the 422 and 420 sides of the house and the changes between the north (back yard), central (house basement), and south (front yard) sections of the house.

Helium was selected as a tracer because it was easily obtained and measured and would meet the above objectives. And although helium diffuses much faster than chlorinated VOCs, the coarse (sand and gravel) subsurface beneath the home makes this less of an issue because the system is probably not diffusion driven.

12.2.3 Tracer Test Experimental Methods

Although tracer testing occurred on four separate occasions, the basic structure of the tests remained essentially the same: a measureable volume of pure industrial helium was injected into a 13-ft deep soil gas location and then a handheld helium detector was used to make observations at a preselected series of subslab and soil-gas ports. The 13-ft depth was selected for injection because it is the deepest depth in the nested soil gas points that is normally above the water table. Readings were taken over a period of time, frequently at first, and then with greater temporal spacing as helium concentrations fell to 0 ppm.

Injections were done by a Cole-Parmer rotameter connected to a helium tank and consisted of 18.6 L of helium for injections 1 and 2, 23.25 L for injection 3, and approximately 26 L for injection 4. The first two tests focused on the nested soil gas ports (SGP1, SGP2, and SGP9), WP-3, and SSP-1 and -4; soil gas ports located in the front yard and several soil gas ports, sub-slab ports, and wall ports located within the 422/420 house proximal to the front yard ports. SGP2-13 was used as the injection port.

Tests 3 and 4 switched to the backyard locations, using a series of exterior soil gas ports and proximally related interior soil gas ports, wall ports, and sub-slab ports. SGP6-13 was the injection point in tests 3 and 4. These tests were monitored at SGP5; SGP6; SGP10; SGP8-6; SSP-1, -2, and -6; and WP-1. The sample locations are shown in plan view in Section 3 and in cross section in **Figure 12-11**.

Readings were taken during all four tests with a rented Dielectric MGD-2002 helium detector. However, during the first test, the first MGD-2002 rented suffered from battery and filter issues, so it was returned. Another MGD-2002 was rented immediately from a different rental firm, and all subsequent rentals of the MGD-2002 were from the second firm. After injecting the helium, readings were taken rapidly in order to record the initial stages of helium dispersal. Over the following day or two, the readings would be taken further apart until measurements dropped to 0 ppm.

Test 1 occurred on October 13, 2012, to October 17, 2012. Test 2 occurred on October 17, 2012, to October 22, 2012. Test 3 occurred on November 19, 2012, to November 21, 2012. Test 4 occurred on April 10, 2013, to April 12, 2013. The mitigation system was on during tests 2 and 4, and in passive mode during test 3, and off except for the last two readings during test 1 (the full mitigation system was not running until after all of test 1 was complete).

Given that the geologic material at the 13-ft depth is relatively coarse, it was expected that these injections would generate a brief pulse of advective pressure-driven migration that would then dissipate. Helium would be expected to migrate upward based on its lower gas density than air and due to the driving forces for VOC vapor intrusion such as the stack effect.

12.2.4 Tracer Test Results and Discussion

Figures 12-1 through **12-4** show the combined results of each of the helium injections plotted versus the time from injection in days. Tests that occurred during mitigation system on cycles (tests 2 and 4) had peak concentrations at monitoring points vertically separated from the injection point, approximately 1,800 ppm to 2,500 ppm; however, those that occurred during mitigation system off or passive cycles had concentrations ranging from approximately 3,500 ppm to 4,000 ppm. Recall that our differential pressure measurements show that when the mitigation system is on the deep to shallow soil gas differential pressure is enhanced, pulling soil gas toward the building (Section 5). Thus, it is likely that the mitigation system pulled the injected gasses away from the point of injection (at 13 ft outside the footprint of the house) and helped dilute the tracer in the immediate vicinity of the injection point.

The paired tests have similar patterns for the same injection location (with and without mitigation) when comparing the exterior soil gas ports immediately above the injection point (SGP2 and SGP6 clusters, respectively; see **Figures 12-5** and **12-6**). There is considerable similarity in paired tests at the exterior soil gas clusters that are approximately 6 ft closer to the house than the injection points (SGP1 and SGP5 clusters, respectively; see **Figures 12-7** and **12-8**).

The tests with the injection point in the front yard can be seen in **Figures 12-1** and **12-2** (tests 1 and 2, respectively). Test 1 had its high concentrations of helium at the monitoring points by the end of 24 hours, but the helium was nearly gone after ~48 hours. Test 2 had its highest concentration by the end of 24 hours and showed very low helium concentrations 48 hours later.

Test 3 had its high helium shortly after injection, was low but steady by the end of 24 hours, and roughly steady at 48 hours (**Figure 12-3**). Test 4 showed roughly the same pattern as test 3 (**Figure 12-4**).

In general, the comparisons of these paired tests at the exterior monitoring ports suggest that the mitigation system had a relatively limited effect on the speed of tracer migration. Most often, among all the tests, the ports that showed the highest helium concentrations were the deepest, such as the 9-ft and 13-ft depths. This suggests attenuation during vertical migration by dispersion or dilution. Attenuation was especially pronounced in the 3.5 ft bls soil gas ports, even directly above the injection point. The similarity between paired tests performed in common locations suggests that tracer migration from deep soil gas zones is controlled primarily by localized differences in soil types and/or building structure more than by the mitigation system status.

Figures 12-9 and 12-10 focus on two of the sets of nested soil gas ports located under the building and tell a slightly different story from the exterior soil gas points. **Figure 12-9** shows data from SGP9 (a cluster under the southern portion of the 422 side of the duplex) from the first two injections. Based on its location, it would be expected to be the first soil gas cluster to detect migration from the front yard deep injection point beneath the structure. The data from the first injection (mitigation system off) is on the bottom half of the graph, and the top half plots the second injection data (mitigation system on). The first injection data for SGP9 shows a peak nearly at the time of the injection, which almost immediately drops to 0 ppm. This finding would suggest a very rapid migration propelled by the advective force of the gas injection. However, the second injection shows a peak after 24 hours, with only other minor fluctuations. Also note the helium detection that occurs right before the second injection in SGP9. The explanation for this detection is not clear at this time, but its timing could represent a delayed migration of helium from the first injection to SGP9 or carryover from another nearby injection point.

SGP10 is located under the north side of the 422 duplex and is expected to be the first soil gas cluster to detect migration from the exterior injection point in the backyard beneath the structure. **Figure 12-10** plots SGP10 during the third and fourth injections, the bottom half of the graph showing the third injection (mitigation system off) and the top showing the fourth (mitigation system on). There is considerable fluctuation for the third injection, with helium concentrations at some points rising and falling (SGP10-9 and -13). During test 4, there are initial peaks roughly at the time of injection and then another after ~24 hours. This could indicate a difference between initial injection pressure-driven flow and subsequent buoyant or stack effect flow. The arrival time at the SGP10 cluster appears to be somewhat delayed with the mitigation off vs. mitigation on. The mitigation on results show much less observable concentration at the shallow depths (6 and 9 ft) in this case; this result differs from the results discussed in the previous paragraph from the injection at SGP9. However, SGP10 is similar to SGP9 in that there were elevated helium concentrations prior to the injection time.

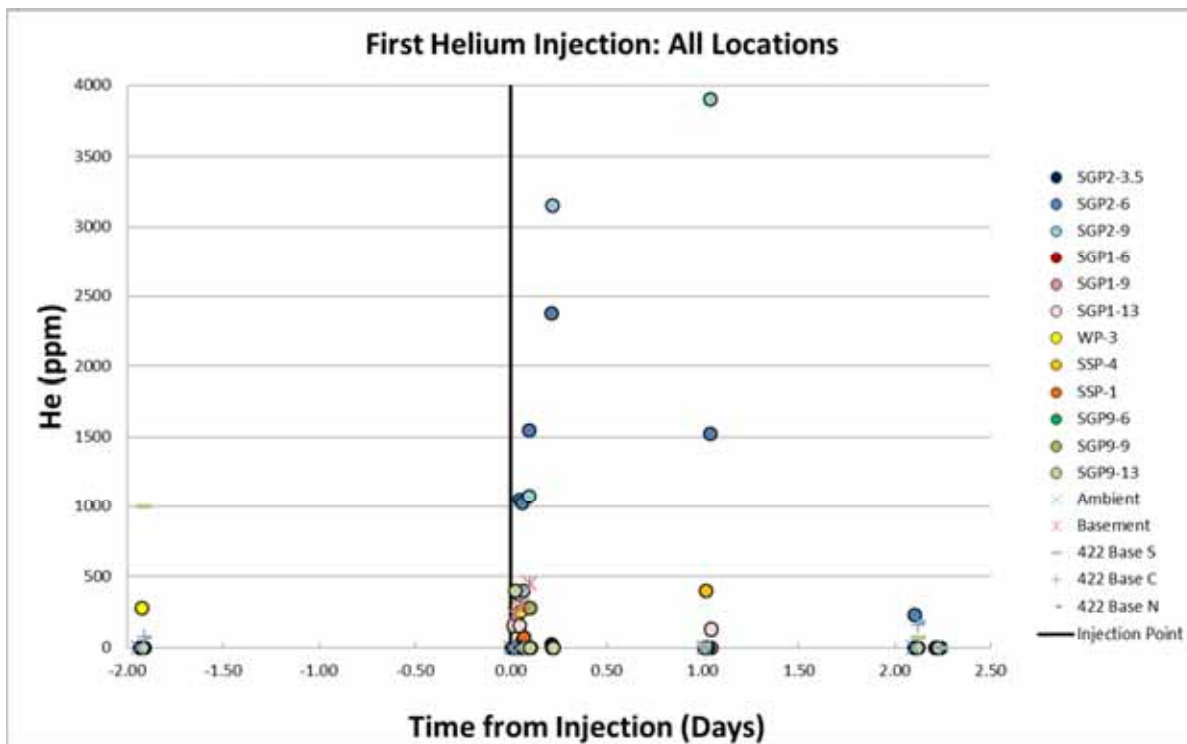


Figure 12-1. Response at all locations to first helium injection in front yard.

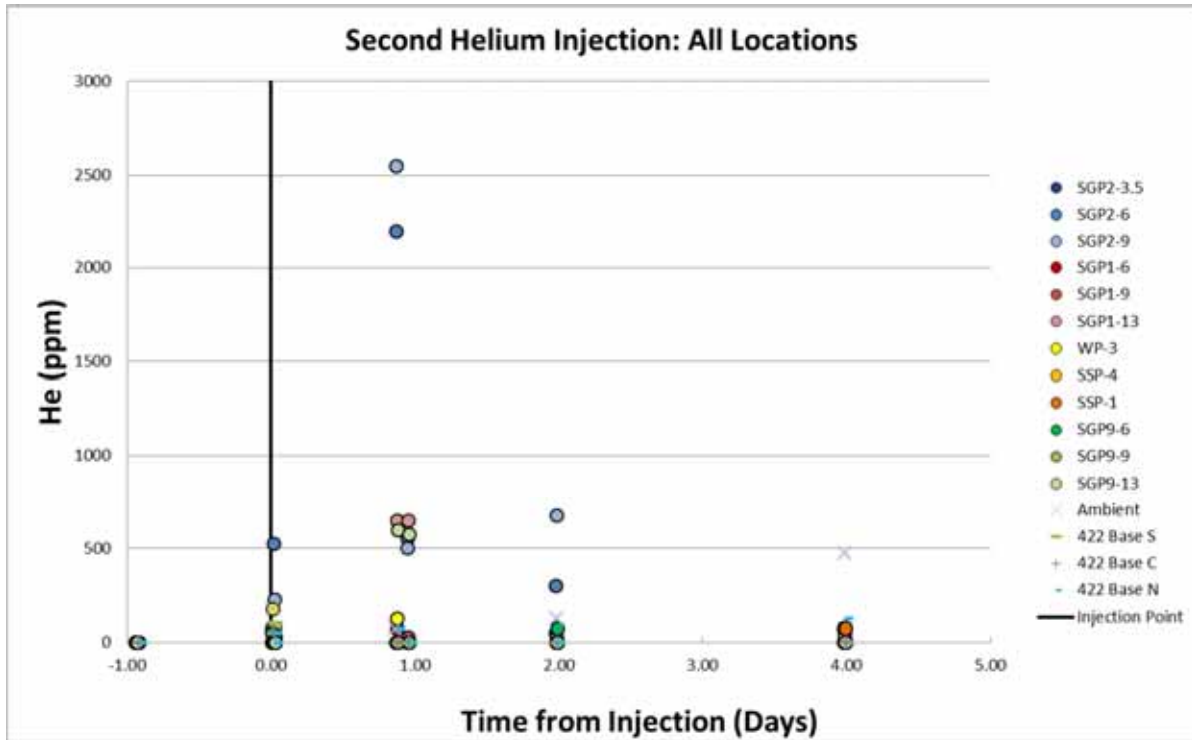


Figure 12-2. Response at all locations to second helium injection in front yard.

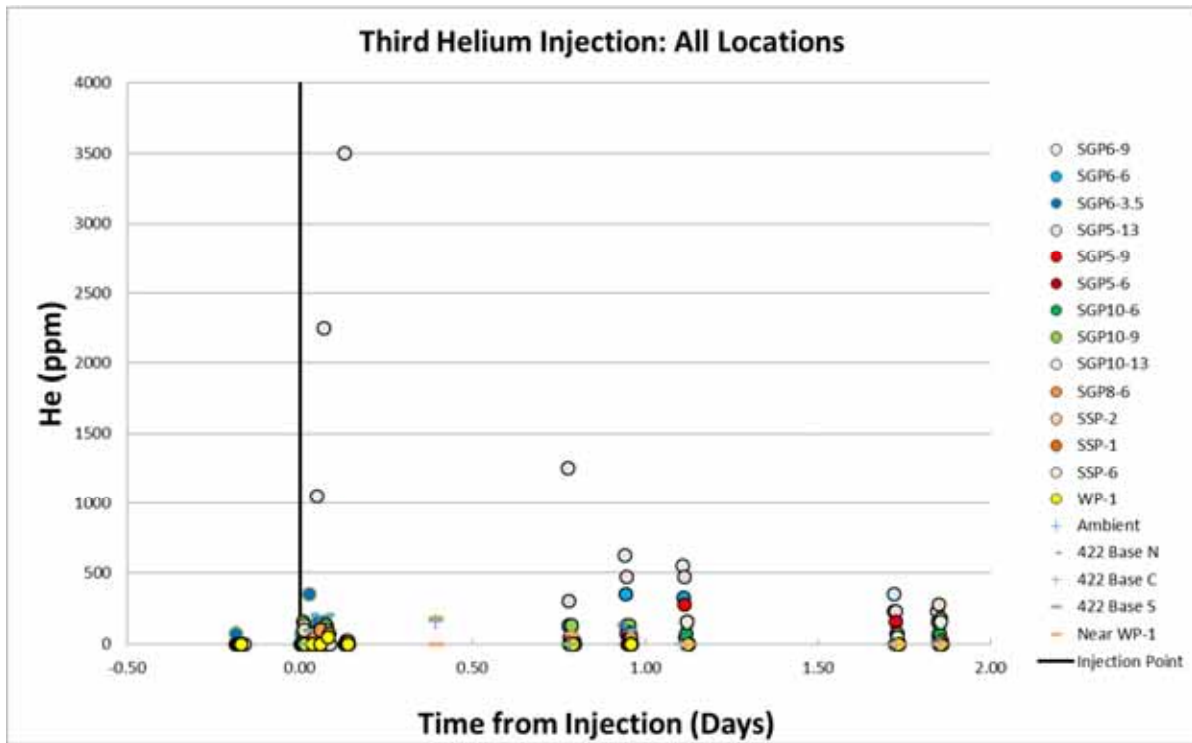


Figure 12-3. Response at all locations to third helium injection in backyard.

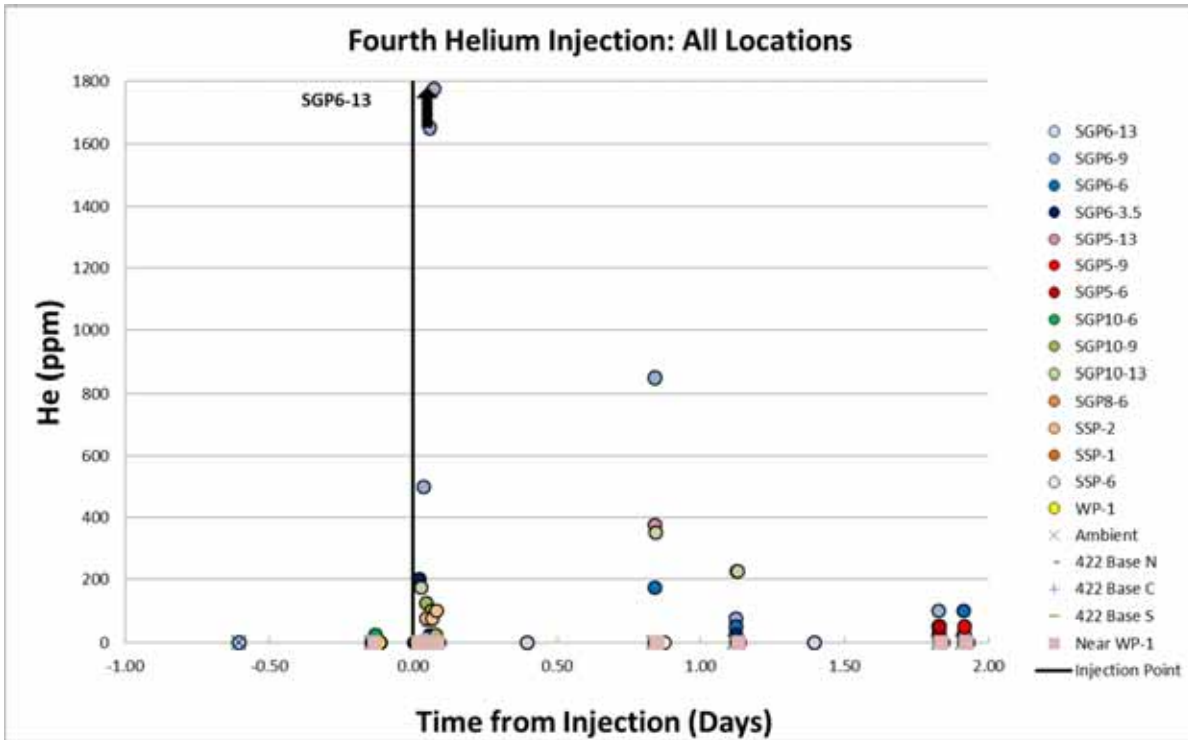


Figure 12-4. Response at all locations to fourth helium injection in backyard.

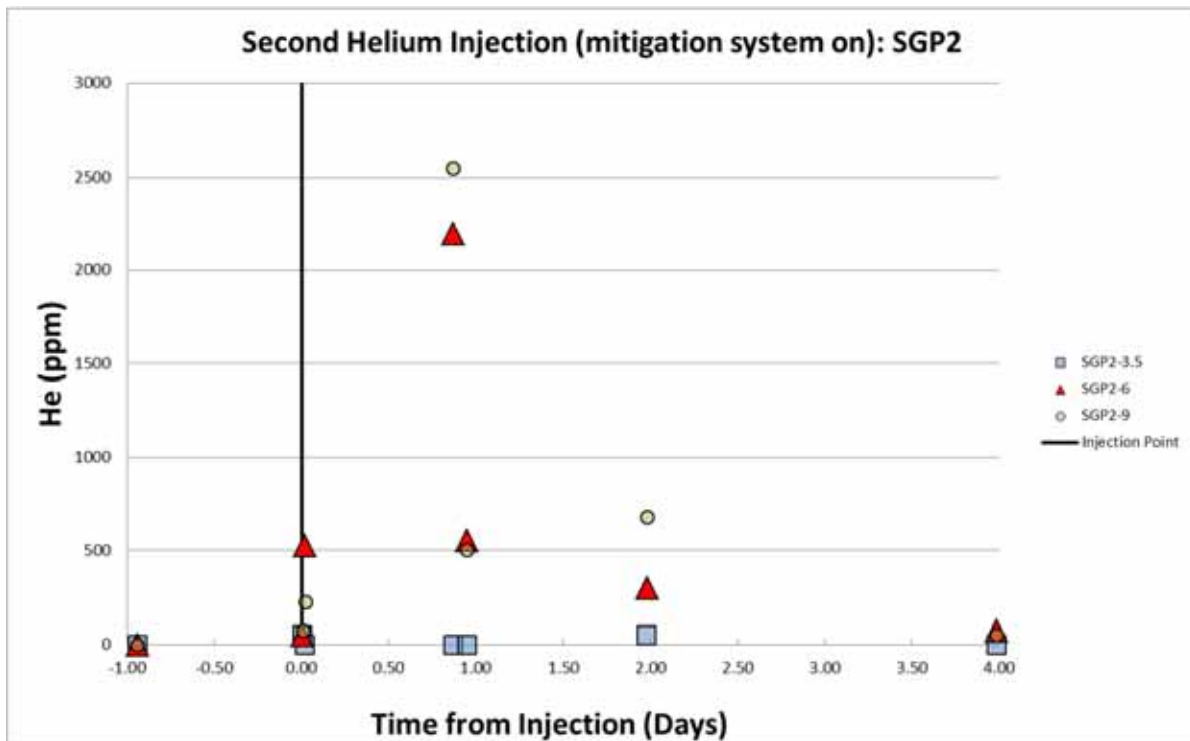
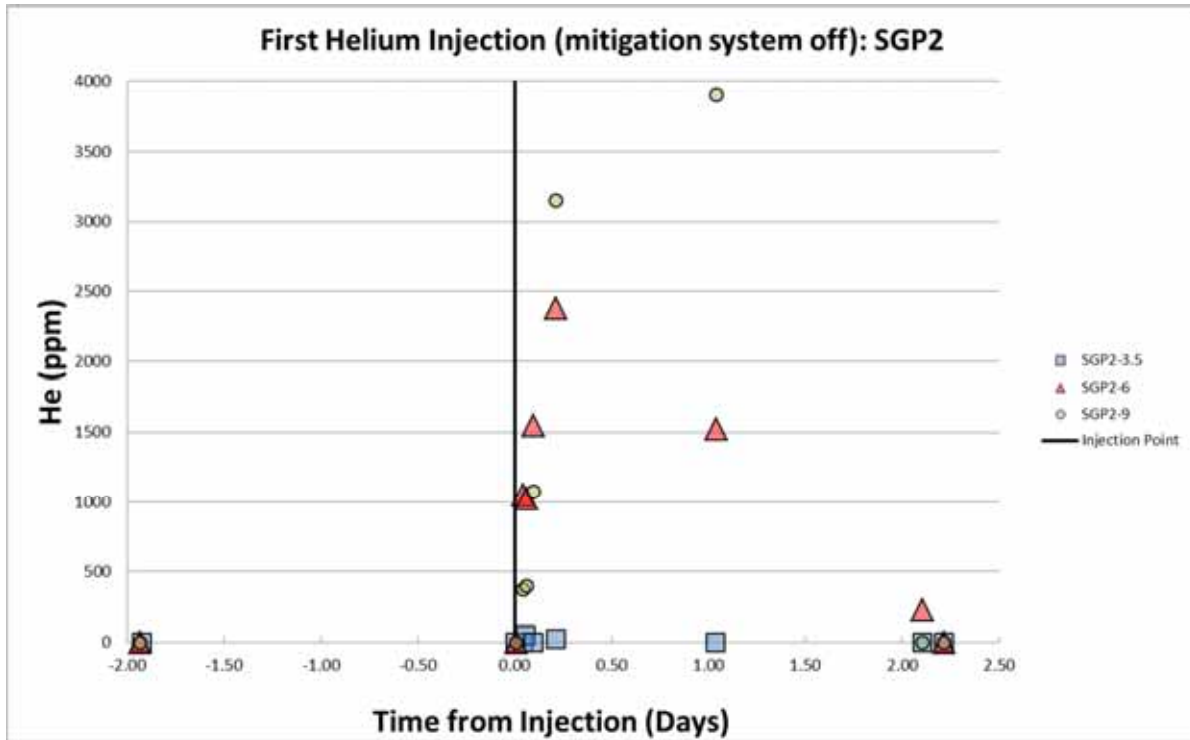


Figure 12-5. Helium response at SGP2 cluster (south of duplex) directly above injection point after injections 1 (top graph, mitigation off) and 2 (bottom graph, mitigation on).

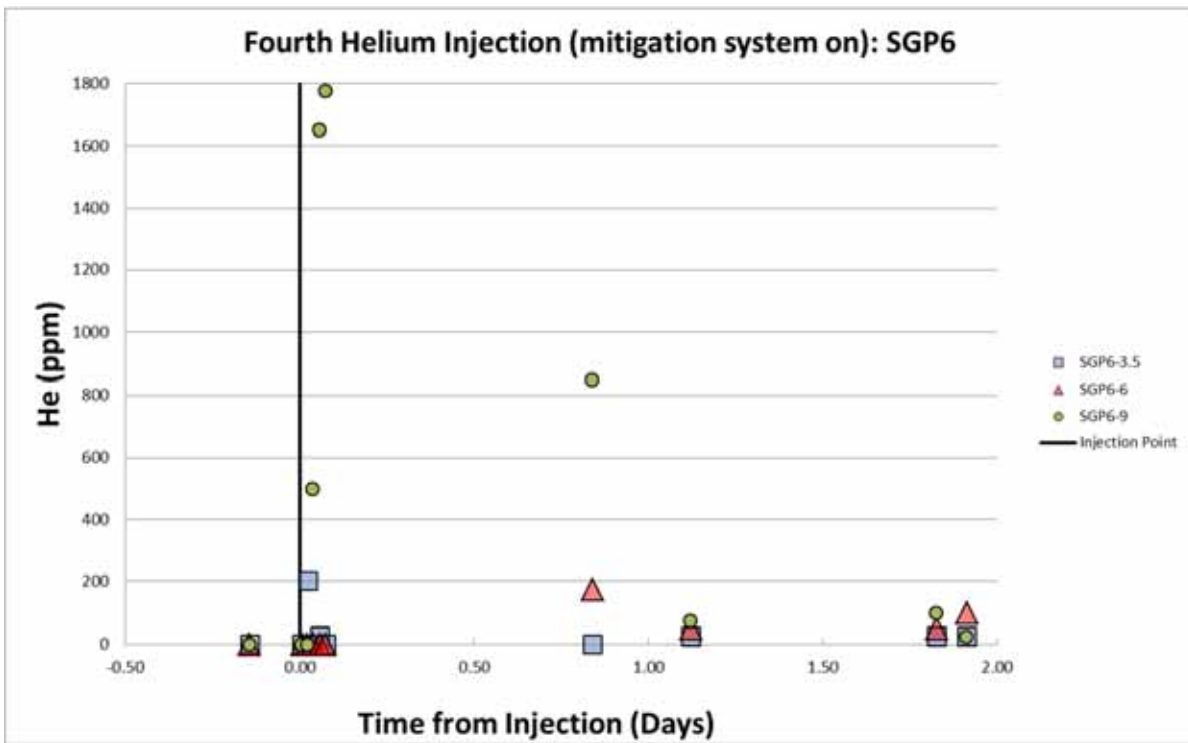
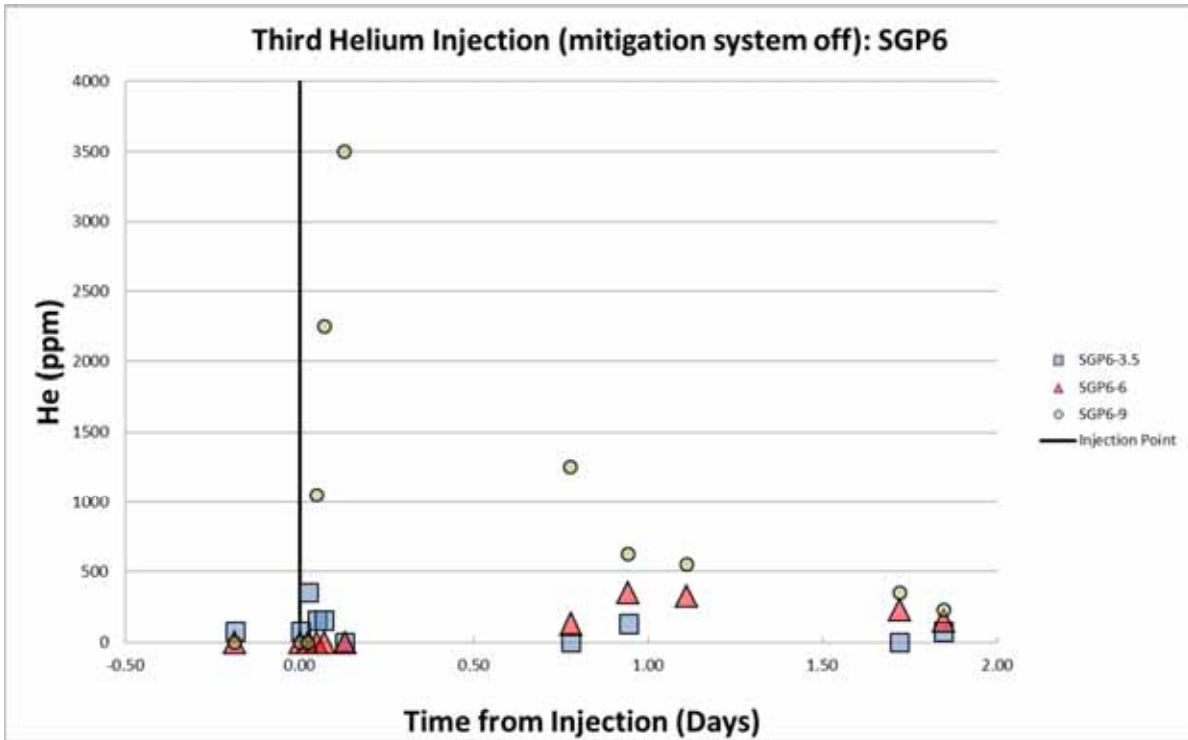


Figure 12-6. Helium response at SGP6 cluster at SGP6 cluster (north of duplex) directly above injection point after injections 3 (top graph, mitigation off) and 4 (bottom graph, mitigation on).

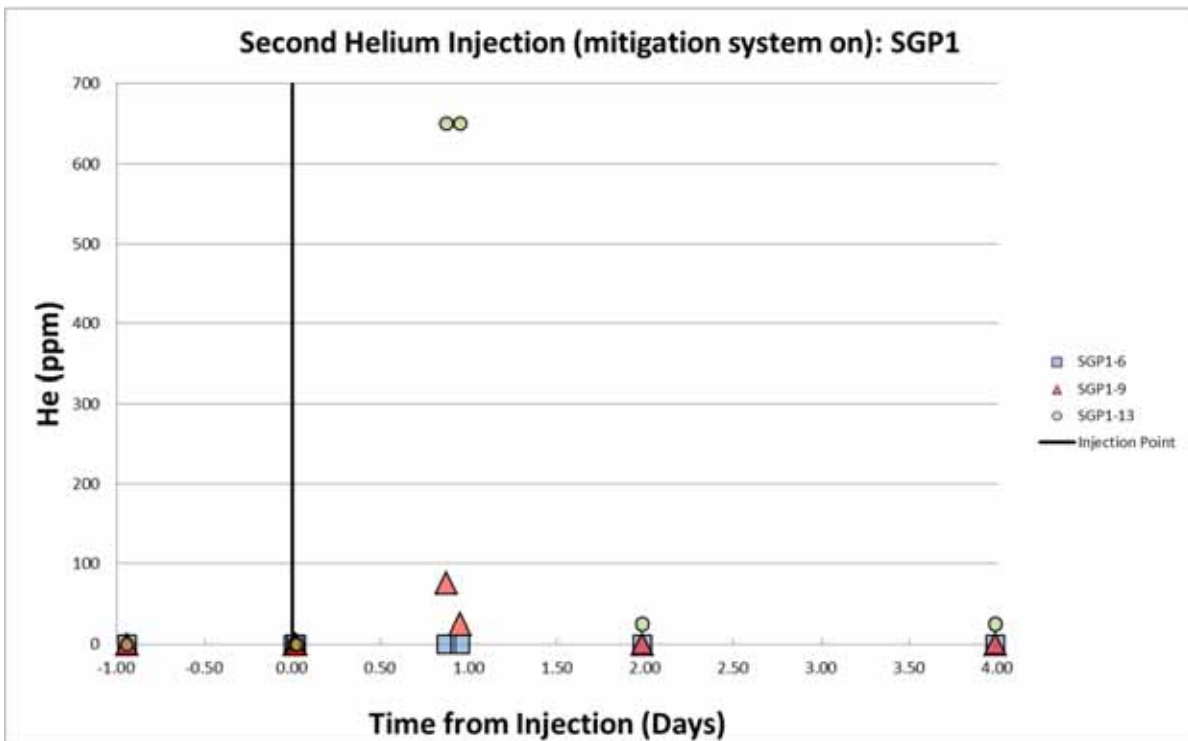
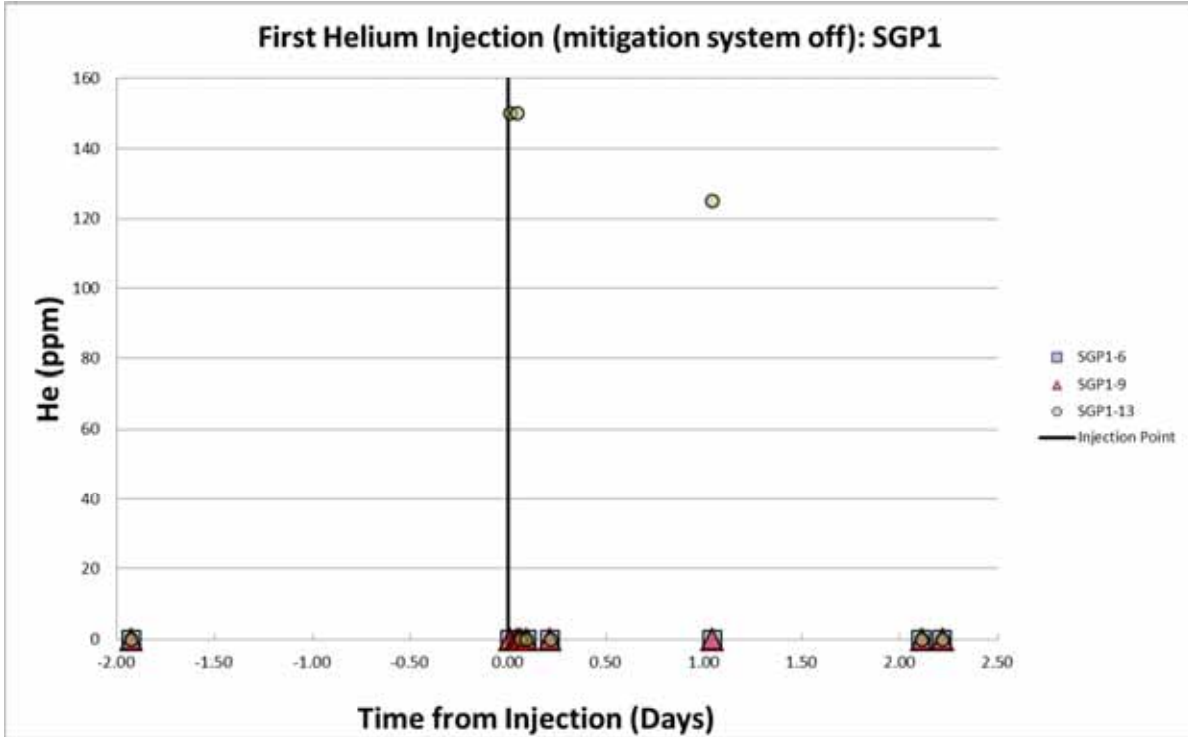


Figure 12-7. Helium response at SGP1 cluster (south of duplex, approximately 6 ft closer to duplex than injection point) after first Injection (top graph, mitigation off) and second injection (bottom graph, mitigation on).

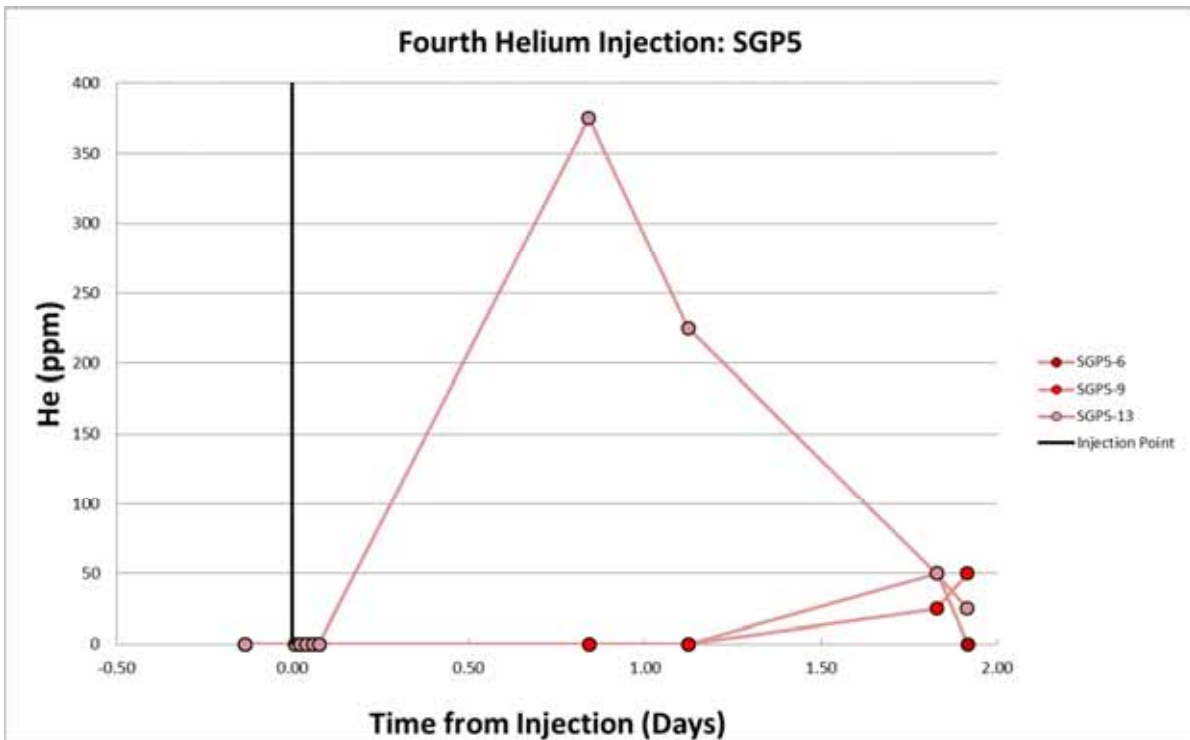
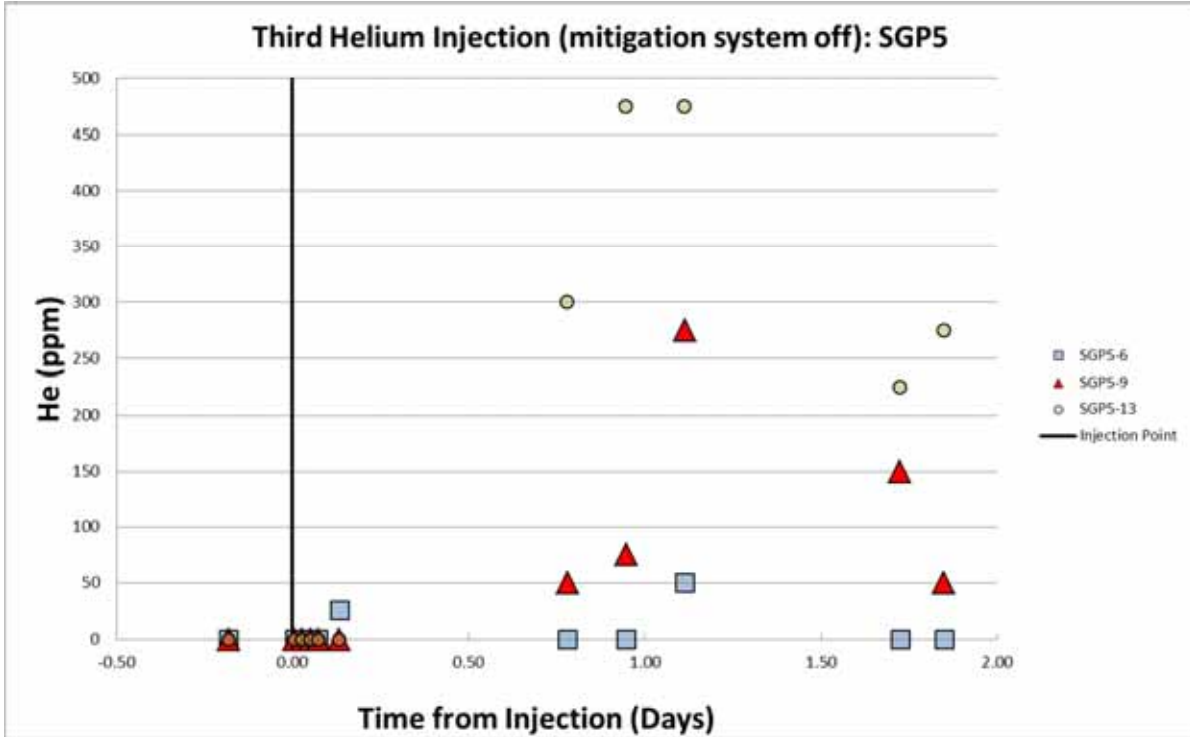


Figure 12-8. Helium response at SGP5 cluster (north of duplex, approximately 6 ft closer to duplex than injection point) after third injection (top graph, mitigation off) and fourth injection (bottom graph, mitigation on).

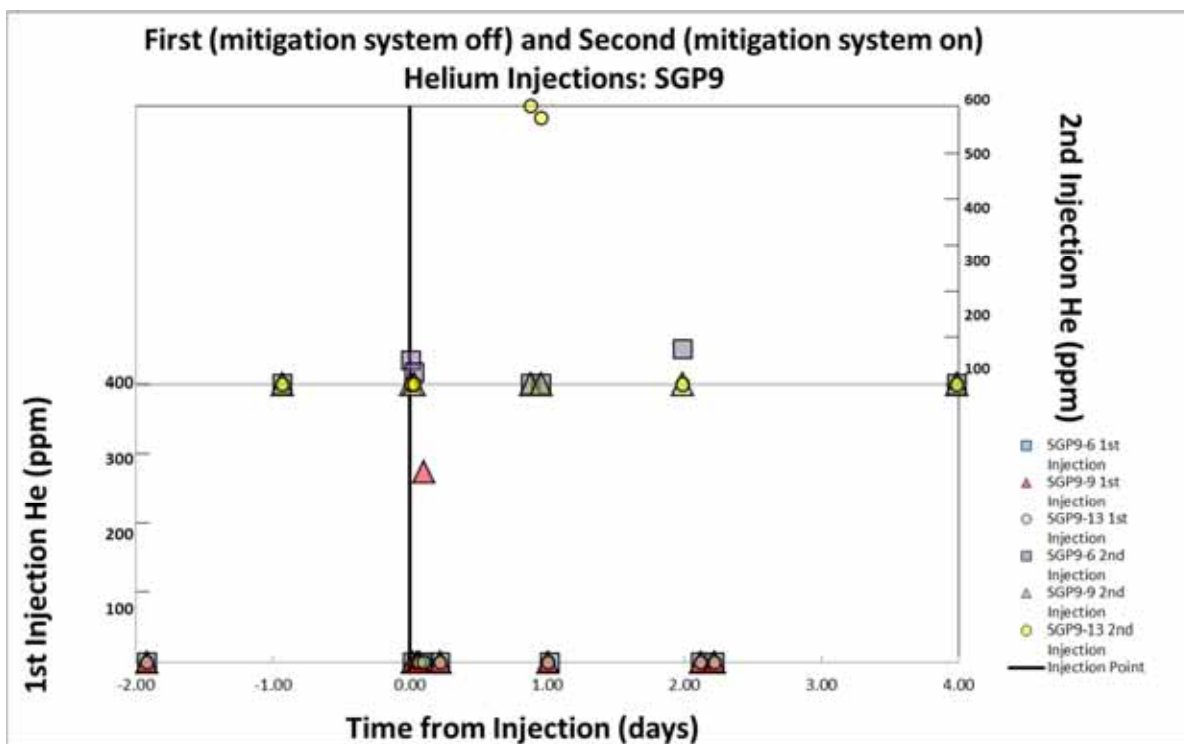


Figure 12-9. Helium response to first and second helium injections at SGP9 (interior).

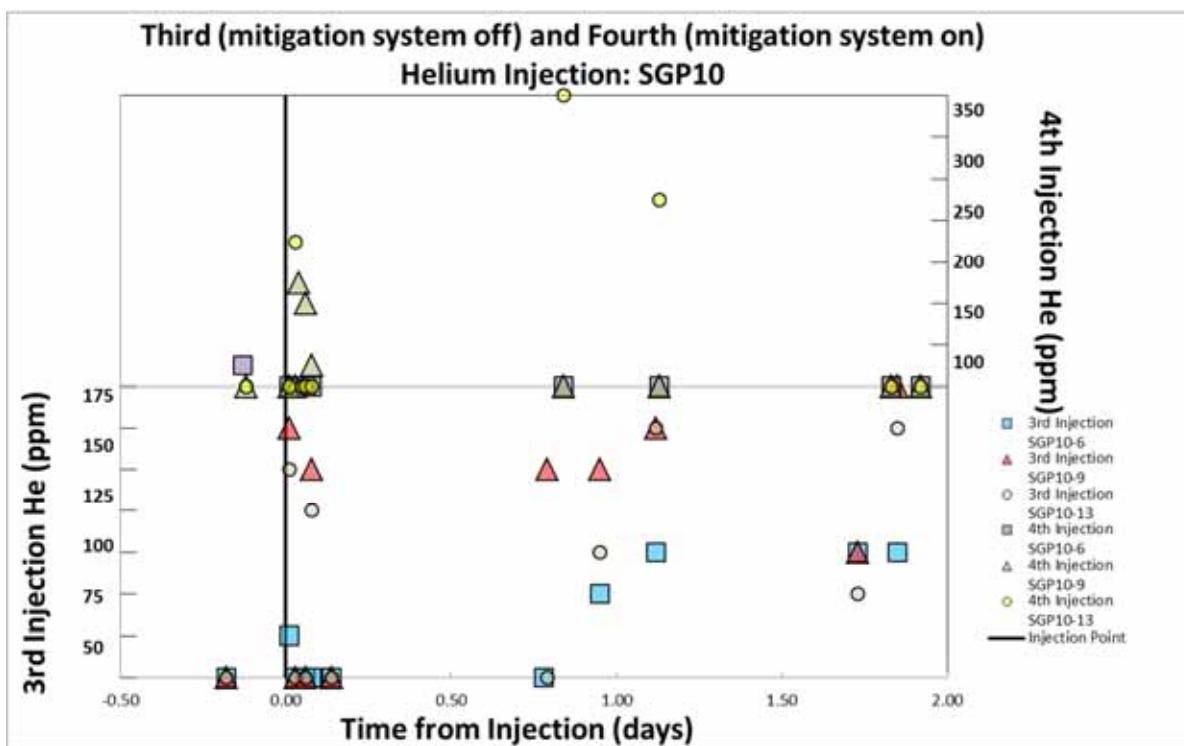


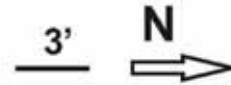
Figure 12-10. Helium response to third and fourth helium injections at SGP10 (interior).

These differences in the time profiles observed at SGP9 and SGP10 within the test groups performed in common locations must be controlled by a factor other than just soil differences or building structure. The first two tests were performed in close sequence, but a considerable amount of time passed between the third and fourth tests, so for the third and fourth tests, differences in soil moisture cannot be ruled out as an explanation for differences in tracer behavior.

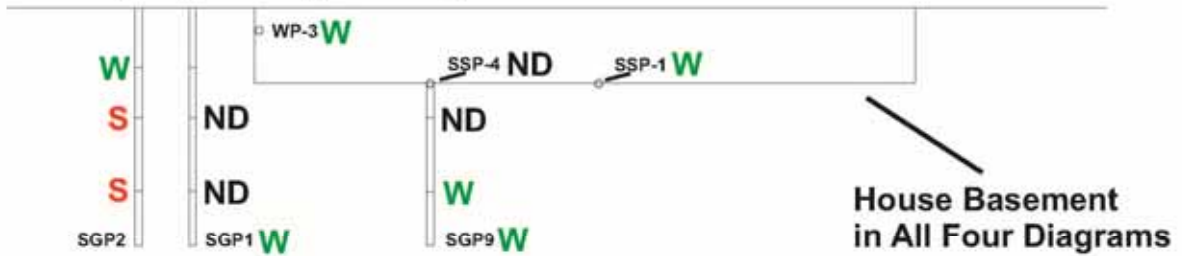
The first three tests showed fleeting but moderately strong detections of helium tracer at the wall ports located closest to the injection locations (WP-3 and WP-1) within the first day after injection. These wall ports are approximately 10 ft above and 10 ft laterally from the injection location. This suggests rapid migration to the building envelope is possible from near the water table if the buoyant and advective driving forces are sufficiently strong.

Observation of tracer arrival at the points immediately below the slab—either conventional subslab ports or the shallow 6-ft intervals of the nested soil gas probes was highly erratic (**Figure 12-11**). Note, for example, in tests 1 and 2 how some tracer was seen at both SGP9-6 and SSP-1 but not at SSP-4, which lies closer to the point of injection than SSP-1 and quite near SGP9-6. Similarly, in test 1, no tracer was observed at SGP1-6 and SGP1-9.

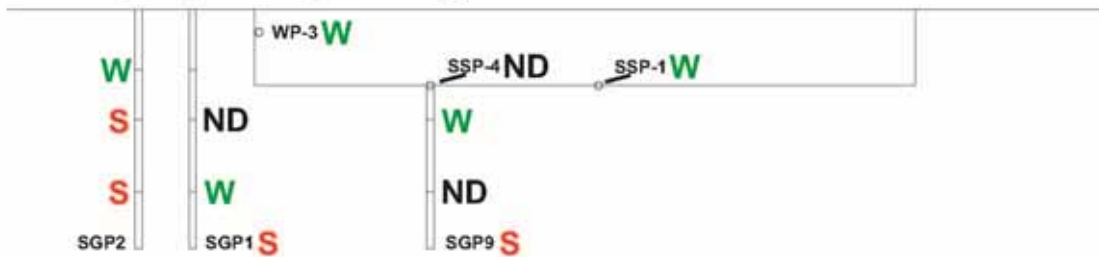
Helium Tests House Cross-section View



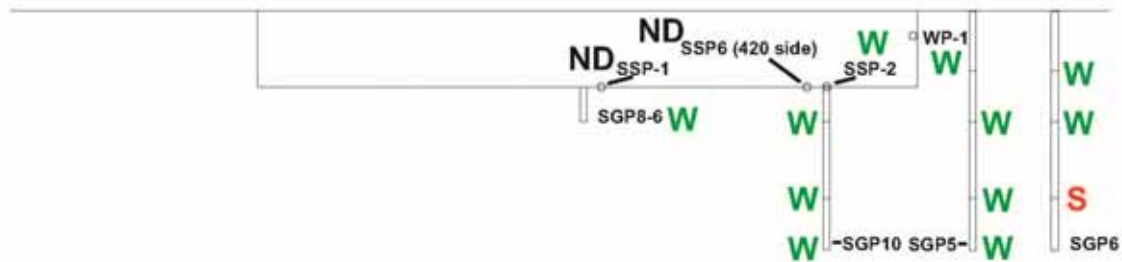
Test 1 (mitigation system off)



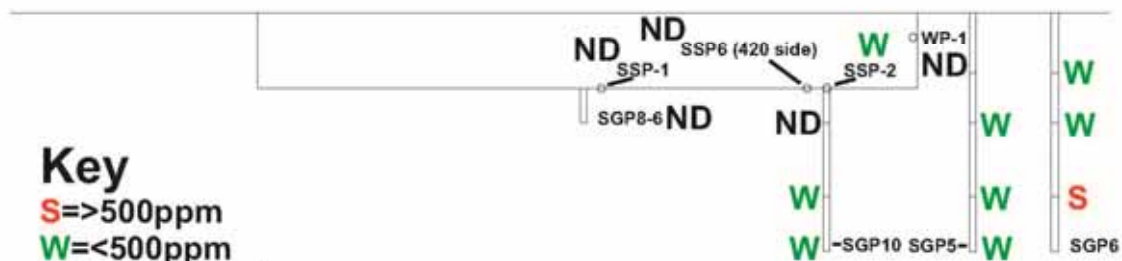
Test 2 (mitigation system on)



Test 3 (mitigation system off)



Test 4 (mitigation system on)



Key

- S=>500ppm
- W=<500ppm
- ND=non detect

Note: soil gas port depths are 3.5', 6', 9', and 13' bgs, except the indoor locations, which omit the 3.5' depths. SGP8-6 is truncated in this figure, since only its 6' depth was sampled during the helium tests.

Figure 12-11. Cross-section view of helium tracer arrival at 6-ft depth intervals.

12.2.5 Summary of Tracer Test Conclusions

The four tracer tests provide more information about the subsurface conditions surrounding the 422/420 house. The tests performed with common injection locations yielded similar overall patterns of tracer distribution with and without mitigation in the exterior soil gas clusters. The variability between paired tests (mitigation on and mitigation off) was more pronounced beneath the building where the mitigation system would be expected to have the most significant influence on airflow. The highest concentrations observed were usually those close to the 13-ft deep injection depth, suggesting attenuation as the tracer migrated upward. The similar patterns between tests performed in different subsurface areas (different injection wells) suggest control by common features of soil stratigraphy or the building envelope because the tests would have these factors in common. The high concentrations observed at the 9-ft and 13-ft depths for all the injections, despite the buoyancy of the helium-enriched soil gas, suggest that transference of helium is easy horizontally toward the building over distances of up to 20 ft typically within 2 days. Vertical migration from 13 ft to 6 ft bls also occurred relatively rapidly at the injection cluster. The lack of influence at certain ports closer to the point of injection and along the same general line to more distant ports suggests subsurface heterogeneity and preferential flow paths. In all cases, tracer concentrations were reduced to baseline concentrations within 2–2.5 days, indicating a rather quick clearing out of trace gas from the subsurface under mitigated and non-mitigated conditions. In two interior probes (SGP9 and SGP10), relatively high concentrations before and after injection at several sample ports suggest either carry-over from previous injections or flow of helium from other nearby injection ports.

12.3 Testing Utility of Consumer Grade Radon Device (Safety Siren Pro)

12.3.1 Introduction to the Use of Consumer Grade Radon Monitoring Equipment in Vapor Intrusion

Schuver and Siegel (2011) have highlighted the role of radon as a potential “general tracer of soil-gas entry” and pointed out that there are multiple benefits from minimizing soil gas entry (including reductions in problems attributable to moisture/mold, radon, and methane as well as reduction in VOCs). They also advocated the active involvement of homeowners in observing the building-specific aspects of vapor intrusion at VOC sites, both as an educational tool (to help homeowners understand temporal and spatial variability) and a way to an efficient solution to which all stakeholders agree.

To address this need we evaluated the ability of a widely available low-cost (\$129) consumer-grade radon detector based on an ionization chamber, the Safety Siren Pro Series 3 manufactured by Family Safety Products Inc., to provide a continuous indication of soil gas entry into the structure.

12.3.2 Objective of Consumer-Grade Radon Device Testing

The objective of this research was to evaluate the ability of a widely available low cost (\$129) consumer grade radon detector based on an ionization chamber to provide a continuous indication of soil gas entry into the structure.

12.3.3 Methods of Consumer-Grade Radon Device Testing

The Safety Siren Pro Series 3 is a consumer-grade radon detection instrument that provides continuous real-time measurement based on an ionization chamber and requires little operator labor. In this test, we sought to compare the performance of the Safety Siren to a well-accepted method (electrets). Secondly, we were able to compare it with the continuous AlphaGUARD data and the weekly electret data.

The following six stations were planned for testing: 422 south basement S, 422 north basement (downstairs AlphaGUARD), 420 south basement, 422 first floor, 422 second floor (upstairs

AlphaGUARD), and 420 first floor (note that the 420 first floor device was stolen on October 17, 2012, and not replaced). According to the instruction manual, the Safety Siren detector may be placed face up on a tabletop, countertop, or any flat surface where the ventilation slots will not be blocked. The detector also must be kept dust free and a proper airflow must be maintained through the detector to obtain an air sample that is representative of the local environment. It was impractical to use the Safety Siren for ambient measurement at this site because of temperature and power issues. The manual restricts the operating environment to 0°C (32°F) to 40°C (104°F). An additional electret was added on December 28, 2011, to the 422 second floor office to include that location in the comparison between the radon detectors and electrets.

The Safety Siren has two displays—the “short term” is an average over the previous 7 days, and the “long term” is the average from time of last reset (up to 5 years). The numeric LED display shows the level of radon gas in pCi/L. The display range is 0.0 to 999.9. Readings are available after a minimum of 48 hours of operation. We manually recorded the short-term reading at each of six indoor stations weekly. Data were assembled in spreadsheet form for comparison to electret and AlphaGUARD results. The audible alarm was muted. Every 24 hours, the detector does a self-test. If there is a failure in this self-test, an error message will appear in the display window.

12.3.4 Consumer Grade Radon Detector Results and Discussion

As shown in **Figure 12-12** and **Tables 12-2** and **12-3**, the Safety Siren consumer-grade detector shows reasonably good agreement with an accepted professional method (electrets) over a range (1 to 5 pCi/L) useful for determining compliance with EPA’s recommend radon action level (4 pCi/L). Above 5 pCi/L, the Safety Siren detector tends to overestimate the radon concentration; however, the overestimation appears less pronounced in the second phase of the project (**Figure 12-12**). Thus, this device would provide an indication of soil gas entry at low concentrations useful for radon management, although in the higher range it might overestimate radon concentrations. Thus, it would be useful in showing a homeowner when radon was being effectively excluded, but it might create a somewhat exaggerated impression of vapor intrusion variability if high concentration peaks occur.

Figures 12-13 and **12-14** show comparisons between the 422 office and 422 north basement Safety Sirens and electrets, along with black and gray bars representing mitigation system on/off periods. From these graphs it is apparent that both the Safety Sirens and the electrets react in a very similar manner to mitigation system on/off cycles: during mitigation on periods, radon concentrations decrease, and during off periods, or passive cycles, radon concentrations increase. At lower concentrations, the Safety Sirens and electrets produce similar readings, but higher concentrations yield a greater absolute difference between readings for a given point in time (**Figures 12-13** and **12-14**). Thus, the Safety Sirens can successfully be used as a means of monitoring whether the mitigation system is functioning, if not as an accurate indicator of the exact degree of mitigation.

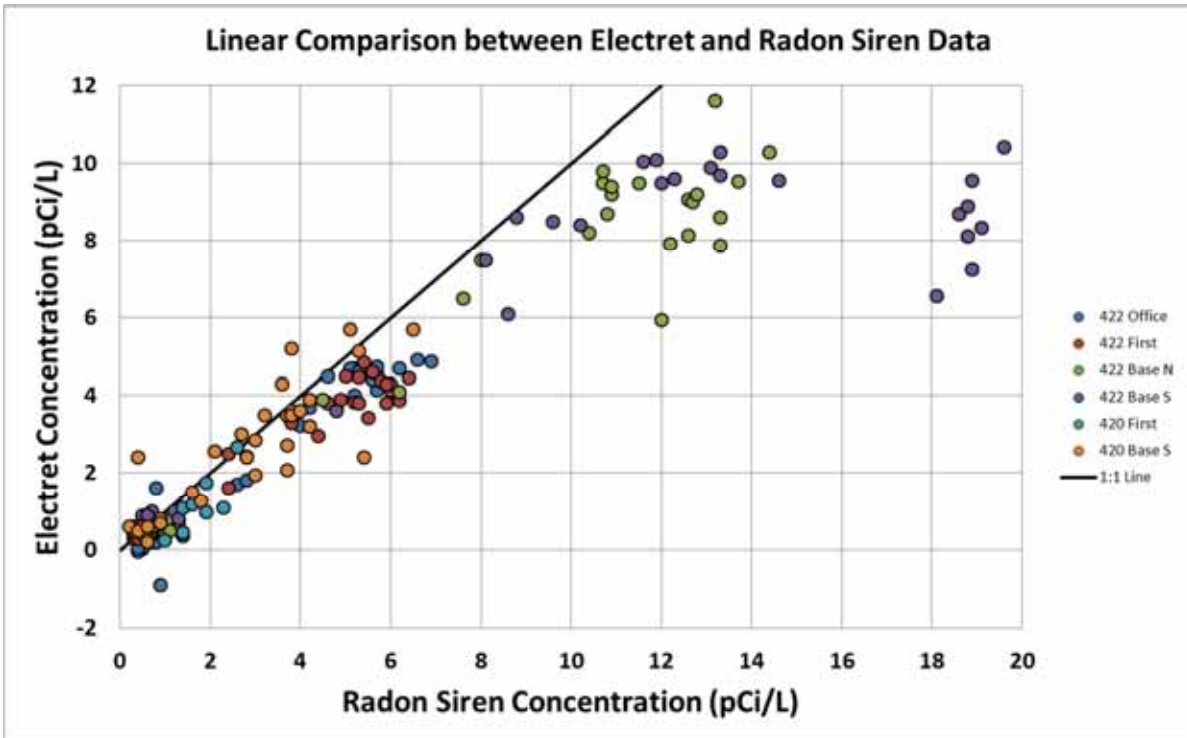
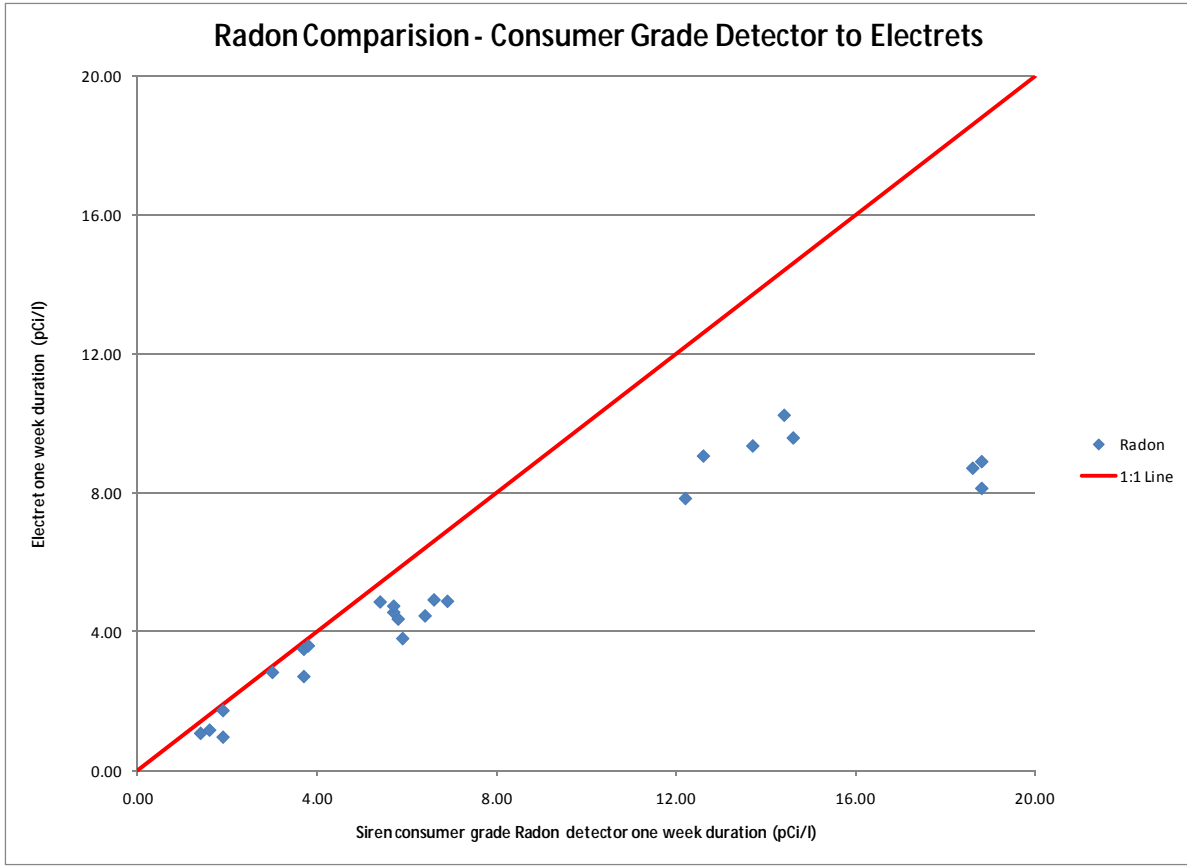


Figure 12-12. Comparison of electret and Safety Siren results for first phase of the project (top graph) and second project phase (bottom graph).

Table 12-2. Comparison of Safety Siren, AlphaGUARD, and Electret Radon Data

| Location | Time | Date | Safety Siren (pCi/L) | AlphaGUARD (pCi/L) | Electrets (pCi/L) | Electret Duplicates (pCi/L) |
|------------------------------------|-------|-----------|----------------------|--------------------|-------------------|-----------------------------|
| 1st Week's Radon Comparison | | | | | | |
| 422 Office | 15:55 | 1/4/2012 | 6.6 | ~5 | 4.92 | |
| 422 First | 16:03 | 1/4/2012 | 5.4 | | 4.86 | |
| 422 Base N | 16:10 | 1/4/2012 | 14.4 | ~10 | 10.22 | 10.35 |
| 422 Base S | 16:08 | 1/4/2012 | 14.6 | | 9.57 | |
| 420 First | 16:13 | 1/4/2012 | 1.4 | | 1.09 | |
| 420 Base S | 16:13 | 1/4/2012 | 3.7 | | 2.72 | |
| 2nd Week's Radon Comparison | | | | | | |
| 422 Office | 13:59 | 1/11/2012 | 5.7 | 4.69 | 4.56 | |
| 422 First | 14:12 | 1/11/2012 | 5.8 | | 4.37 | |
| 422 Base N | 14:18 | 1/11/2012 | 12.6 | 8.78 | 9.05 | 9.11 |
| 422 Base S | 14:19 | 1/11/2012 | 18.6 | | 8.70 | |
| 420 First | 14:21 | 1/11/2012 | 1.6 | | 1.18 | |
| 420 Base S | 14:25 | 1/11/2012 | 3.7 | | 3.50 | |
| 3rd Week's Radon Comparison | | | | | | |
| 422 Office | 11:25 | 1/18/2012 | 6.9 | 5.09 | 4.88 | |
| 422 First | 11:26 | 1/18/2012 | 6.4 | | 4.46 | |
| 422 Base N | 11:27 | 1/18/2012 | 13.7 | 9.73 | 9.34 | 9.73 |
| 422 Base S | 11:28 | 1/18/2012 | 18.8 | | 8.89 | |
| 420 First | 11:40 | 1/18/2012 | 1.9 | | 0.98 | |
| 420 Base S | 11:42 | 1/18/2012 | 3.0 | | 2.84 | |
| 4th Week's Radon Comparison | | | | | | |
| 422 Office | 15:17 | 1/25/2012 | 5.7 | 4.79 | 4.74 | |
| 422 First | 15:18 | 1/25/2012 | 5.9 | | 3.81 | |
| 422 Base N | 15:20 | 1/25/2012 | 12.2 | 8.52 | 7.83 | 7.98 |
| 422 Base S | 15:21 | 1/25/2012 | 18.8 | | 8.12 | |
| 420 First | 15:25 | 1/25/2012 | 1.9 | | 1.74 | |
| 420 Base S | 15:26 | 1/25/2012 | 3.8 | | 3.60 | |
| 5th Week's Rn Comparison | | | | | | |
| 422 Office | 14:41 | 2/1/2012 | 5.7 | 4.46 | 4.15 | |
| 422 First | 14:40 | 2/1/2012 | 5.5 | | 3.42 | |
| 422 Base N | 14:39 | 2/1/2012 | 12.6 | 7.71 | 8.24 | 8.03 |
| 422 Base S | 14:39 | 2/1/2012 | 18.9 | | 7.26 | |
| 420 First | 14:38 | 2/1/2012 | 1.0 | | 0.25 | |
| 420 Base S | 14:36 | 2/1/2012 | 1.8 | | 1.27 | |

(continued)

Table 12-2. Comparison of Safety Siren, AlphaGUARD, and Electret Radon Data (cont.)

| Location | Time | Date | Safety Siren (pCi/L) | AlphaGUARD (pCi/L) | Electrets (pCi/L) | Electret Duplicates (pCi/L) |
|------------------------------------|-------|-----------|----------------------|--------------------|-------------------|-----------------------------|
| 6th Week's Radon Comparison | | | | | | |
| 422 Office | 14:03 | 2/8/2012 | 5.2 | 4.78 | 4.58 | |
| 422 First | 14:04 | 2/8/2012 | 5.3 | | 4.48 | |
| 422 Base N | 14:15 | 2/8/2012 | 13.3 | 8.68 | 8.60 | 8.62 |
| 422 Base S | 14:15 | 2/8/2012 | 18.9 | | 9.56 | |
| 420 First | 14:10 | 2/8/2012 | 2.3 | | 1.09 | |
| 420 Base S | 14:11 | 2/8/2012 | 5.4 | | 2.40 | |
| 7th Week's Radon Comparison | | | | | | |
| 422 Office | 12:19 | 2/15/2012 | 5.6 | 4.80 | 4.41 | |
| 422 First | 12:20 | 2/15/2012 | 6.0 | | 4.15 | |
| 422 Base N | 12:23 | 2/15/2012 | 13.3 | 8.44 | 8.28 | 7.47 |
| 422 Base S | 12:25 | 2/15/2012 | 19.1 | | 8.34 | |
| 420 First | 12:28 | 2/15/2012 | 1.4 | | 0.36 | |
| 420 Base S | 12:30 | 2/15/2012 | 3.0 | | 1.94 | |
| 8th Week's Radon Comparison | | | | | | |
| 422 Office | 14:28 | 2/22/2012 | 4.8 | 4.30 | 3.68 | |
| 422 First | 14:29 | 2/22/2012 | 5.2 | | 3.82 | |
| 422 Base N | 14:30 | 2/22/2012 | 12.0 | 7.74 | 6.08 | 5.82 |
| 422 Base S | 14:31 | 2/22/2012 | 18.1 | | 6.56 | |
| 420 First | 14:26 | 2/22/2012 | 1.4 | | 0.42 | |
| 420 Base S | 14:25 | 2/22/2012 | 3.7 | | 2.08 | |
| 9th Week's Rn Comparison | | | | | | |
| 422 Office | 15:40 | 3/1/2012 | 6.1 | 4.74 | 3.97 | |
| 422 First | 15:40 | 3/1/2012 | 6.2 | | 3.88 | |
| 422 Base N | 15:41 | 3/1/2012 | 12.7 | 8.48 | 9.00 | 9.00 |
| 422 Base S | 15:42 | 3/1/2012 | 19.6 | | 10.43 | |
| 420 First | 15:46 | 3/1/2012 | 1.4 | | 0.45 | |
| 420 Base S | 15:47 | 3/1/2012 | 2.1 | | 2.56 | |

Table 12-3. Comparison of Safety Siren and Electret Radon Data

| End Date | Electret 422 Office | Safety Siren 422 Office | Electret 422 First Floor | Safety Siren 422 First Floor | Electret 422 Basement N | Safety Siren 422 Basement N |
|------------|---------------------|-------------------------|--------------------------|------------------------------|-------------------------|-----------------------------|
| 10/10/2012 | 3.2 | 4.0 | 3.0 | 4.4 | 12 | 13 |
| 10/17/2012 | 2.4 | 2.8 | | 3.1 | 9.2 | 11 |
| 10/25/2012 | 0.2 | 0.8 | 0.6 | 0.3 | 0.7 | 0.8 |
| 10/31/2012 | 0.4 | 0.4 | 0.3 | 0.3 | 0.7 | 0.6 |
| 11/07/2012 | -0.9 | 0.9 | 0.5 | 0.7 | 0.6 | 0.9 |
| 11/14/2012 | 1.6 | 0.8 | 0.2 | 0.6 | 0.95 | 1.2 |
| 11/21/2012 | 3.7 | 4.2 | 3.5 | 3.7 | 6.5 | 7.6 |
| 11/28/2012 | 4.7 | 5.2 | 4.3 | 6 | 9.5 | 11 |
| 12/05/2012 | 3.2 | 4.2 | 3.3 | 3.8 | 7.5 | 8.0 |
| 12/12/2012 | 4.4 | 5.6 | 3.9 | 4.9 | 9.8 | 11 |
| 12/19/2012 | 0.5 | 0.6 | 0.4 | 0.7 | 0.9 | 1.1 |
| 12/26/2012 | 0.2 | 0.7 | 0.4 | 0.7 | 0.8 | 1.1 |
| 01/02/2013 | 1.7 | 2.6 | 1.6 | 2.4 | 3.9 | 4.5 |
| 01/09/2013 | 4.5 | 4.6 | 3.8 | 4.6 | 8.7 | 11 |
| 01/16/2013 | 4.7 | 5.1 | 4.3 | 5.9 | 9.4 | 11 |
| 01/23/2013 | 4.6 | 5.3 | 4.5 | 5 | 9.5 | 12 |
| 01/30/2013 | 4 | 5.2 | 3.8 | 5.3 | 8.2 | 10 |
| 02/06/2013 | 4.7 | 6.2 | 4.6 | 5.6 | 9.2 | 13 |
| 02/13/2013 | 0.2 | 0.8 | 0.3 | 0.6 | 0.7 | 1.3 |
| 02/20/2013 | 0.1 | 0.5 | 0.4 | 0.3 | 0.5 | 0.8 |
| 03/6/2013 | 0.05 | 0.5 | 0.4 | 0.6 | 0.5 | 0.7 |
| 03/14/2013 | 0.03 | 0.5 | 0.5 | 0.5 | 0.5 | 0.5 |
| 03/20/2013 | 0.2 | 0.5 | 0.4 | 0.3 | 0.4 | 1 |
| 03/27/2013 | -0.03 | 0.4 | 0.3 | 0.4 | 0.5 | 0.6 |
| 04/03/2013 | 0.2 | 0.5 | 0.4 | 0.5 | 0.5 | 1.1 |
| 04/10/2013 | 0.06 | 0.4 | 0.7 | 0.5 | 0.5 | 0.6 |
| 05/01/2013 | 1.8 | 2.8 | 2.5 | 2.4 | 4.1 | 6.2 |

(continued)

Table 12-3. Comparison of Safety Siren and Electret Data (cont.)

| End Date | Electret 422 Basement S | Safety Siren 422 Basement S | Electret 420 First Floor | Safety Siren 420 First Floor | Electret 420 Basement S | Safety Siren 420 Basement S |
|-----------------|------------------------------------|--|-------------------------------------|---|------------------------------------|--|
| 10/10/2012 | 10 | 12 | 2.7 | 2.6 | 5.1 | 5.3 |
| 10/17/2012 | 8.6 | 8.8 | 2.4 | 2.8 | 3.5 | 3.8 |
| 10/25/2012 | 0.6 | 0.7 | | | 0.4 | 0.5 |
| 10/31/2012 | 0.9 | 0.5 | | | 2.4 | 0.4 |
| 11/07/2012 | 0.5 | 0.5 | | | 0.2 | 0.6 |
| 11/14/2012 | 1.0 | 1.2 | | | 0.7 | 0.9 |
| 11/21/2012 | 7.5 | 8.1 | | | 3.5 | 3.2 |
| 11/28/2012 | 10 | 13 | | | 5.2 | 3.8 |
| 12/05/2012 | 8.5 | 9.6 | | | 3.9 | 4.2 |
| 12/12/2012 | 9.5 | 12 | | | 5.7 | 5.1 |
| 12/19/2012 | 1 | 0.7 | | | 0.6 | 0.7 |
| 12/26/2012 | 0.9 | 0.6 | | | 0.6 | 0.4 |
| 01/02/2013 | 3.6 | 4.8 | | | 1.5 | 1.6 |
| 01/09/2013 | 8.4 | 10 | | | 3.0 | 2.7 |
| 01/16/2013 | 10 | 12 | | | 5.7 | 6.5 |
| 01/23/2013 | 9.9 | 13 | | | 3.6 | 4.0 |
| 01/30/2013 | 9.6 | 12 | | | 4.3 | 3.6 |
| 02/06/2013 | 9.7 | 13 | | | 3.2 | 4.2 |
| 02/13/2013 | 0.8 | 1.3 | | | 0.8 | 0.9 |
| 02/20/2013 | 0.7 | 0.7 | | | 0.6 | 0.4 |
| 03/06/2013 | 0.7 | 0.7 | | | 0.6 | 0.5 |
| 03/14/2013 | 0.6 | 0.8 | | | 0.5 | 0.3 |
| 03/20/2013 | 0.9 | 0.6 | | | 0.6 | 0.2 |
| 03/27/2013 | 0.6 | 0.8 | | | 0.5 | 0.4 |
| 04/03/2013 | 0.6 | 0.8 | | | 0.7 | 0.9 |
| 04/10/2013 | 0.6 | 0.5 | | | 0.6 | 0.6 |
| 05/01/2013 | 6.1 | 8.6 | | | 2.4 | 2.8 |

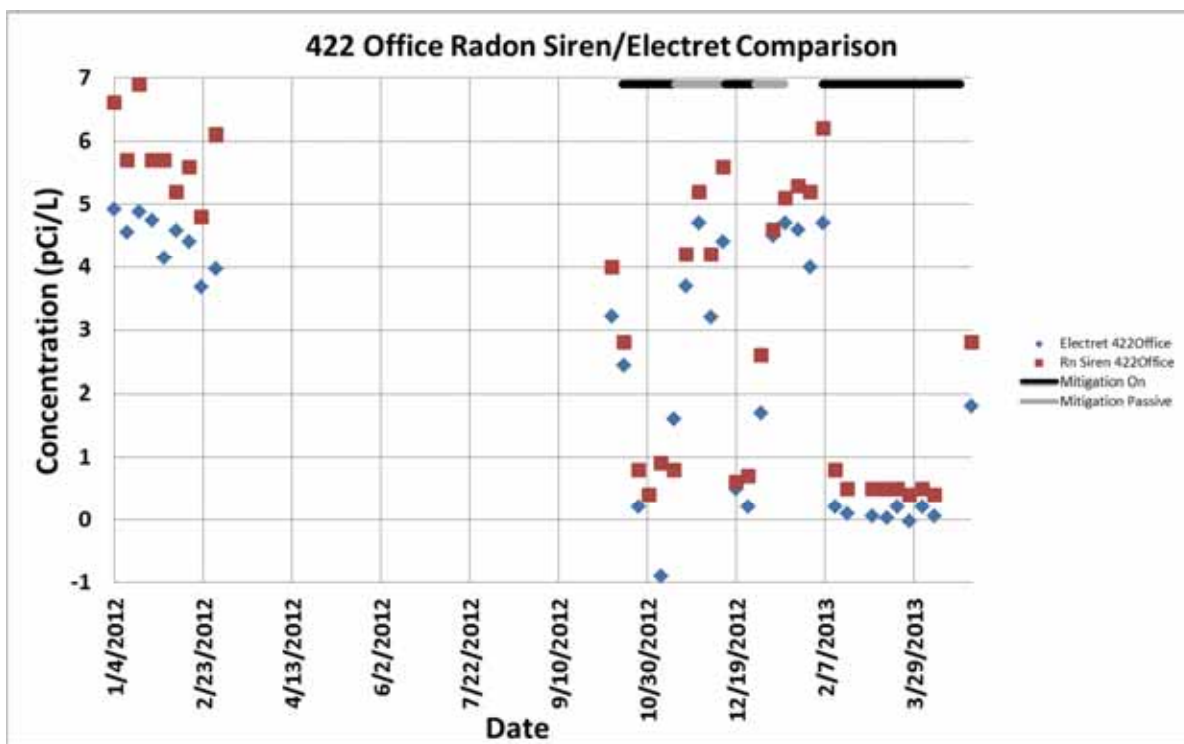


Figure 12-13. Comparison between the 422 office Safety Siren and electret.

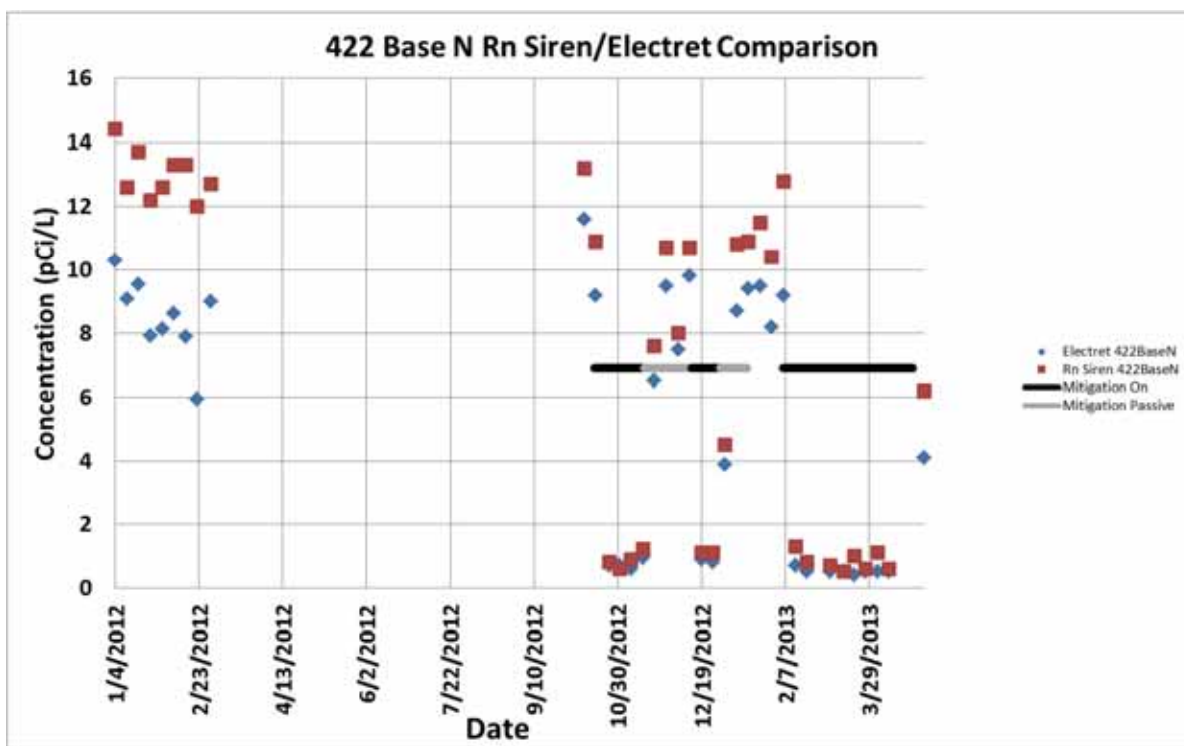


Figure 12-14. Comparison between the 422 basement N Safety Siren and electret.

Table of Contents

13.0 Conclusions and Recommendations..... 13-1

 13.1 Conclusions 13-1

 13.1.1 Mitigation System Performance 13-2

 13.1.2 Meteorological Effects on Vapor Intrusion 13-4

 13.1.3 Preferential Pathways and Revisions to Conceptual Site Model: Helium Tracer
 and Geophysical Tests 13-5

 13.1.4 Revisions to Conceptual Site Model: VOC Data..... 13-7

 13.1.5 Temporal Trends..... 13-8

 13.2 Practical Implications for Practitioners 13-9

 13.2.1 Mitigation Design Implications 13-9

 13.2.2 Sampling Planning Implications 13-9

 13.2.3 Delineating Preferential Pathways..... 13-10

 13.3 Recommendations 13-10

List of Tables

13-1. Summary of Lines of Evidence for Meteorological Factors Influencing Vapor Intrusion in
This Study 13-6

13.0 Conclusions and Recommendations

Conclusions of this phase of the research (results through May 2013) should be considered as a work in progress, because active work at this site is ongoing at the time of this report and additional reports will update (and may change) the study's findings. Also any application of these and other conclusions and results of this study, and especially the "practical implications for practitioners" discussed in Section 13.2, should be carefully considered in light of the facts that (1) this report describes a study on one site of a relatively old urban residence in the Midwest and (2) vapor intrusion is variable in terms of the site-specific conditions that influence vapor intrusion processes and impacts.

13.1 Conclusions

The following summarizes the main conclusions that can be drawn from this study. Additional details can be found in the following subsections.

- **Mitigation system performance—radon.** The mitigation system installed in the duplex met or exceeded all conventional performance tests, as well as more comprehensive tests involving pressure differentials and continuous indoor radon monitoring. Radon reductions greater than 90% were observed, and all measured radon levels were below 4 pCi/L with the mitigation system on.
- **Mitigation system performance—VOCs.** The mitigation system did not perform as well with VOCs as it did with radon. During 7 months of mitigation system operation, immediate VOC reductions in indoor air were observed and were significant overall, but the system only achieved a reduction of just over 60% of VOC indoor air concentrations before mitigation. However, additional decreases in VOC levels were observed near the end of the monitoring period reported in this document (May 2013). During these periods of mitigation system operation, the system was also observed to increase soil gas levels below the slab and at depth below the duplex, suggesting that VOCs are being redistributed by the mitigation system and that soil gas concentrations close to the building may be enhanced by drawing higher concentrations of VOCs from greater depths. In addition, several snow events corresponded to increases in indoor air VOC levels during mitigation that were not observed for radon.
- **Meteorological variables.** Multiple meteorological variables likely interact in complex ways to affect VOC vapor intrusion at this duplex. The evidence is overwhelming that cold temperatures contribute to greater vapor intrusion in this duplex. This was expected from knowledge of the stack effect mechanism. The evidence also indicates that both snowfall and snow/ice accumulation can increase VOC vapor intrusion, although this effect is complex for VOCs and may be absent for radon. There is relatively little evidence of rain effects on VOCs, but some evidence suggests a rain effect on radon. Barometric pressure change appears to have effects on radon and probably VOCs, although the interactions are complex and additional work on the time series data is needed to determine how best to analyze the effects of barometric pumping on vapor intrusion in the duplex. There is evidence of an association between winds from westerly directions with vapor intrusion in the 422 portion of the duplex, but the evidence for an effect of wind velocity is equivocal. Additional study is needed to assess how to best model the complex interactions between meteorological variables and vapor intrusion at this site.
- **Preferential pathways and revisions to conceptual site model: Helium tracer and geophysical tests.** Four helium tracer tests performed pairwise with common subsurface injection locations yielded similar overall patterns of tracer distribution in soil gas outside the building with and without mitigation system operating. The variability between paired tests (mitigation on and mitigation off) was more pronounced beneath the building where the mitigation system would

have been expected to have the most significant influence on airflow. The similar patterns between tests performed in different subsurface areas (i.e., different injection points) suggest control by common features of soil stratigraphy or the building envelope. Helium tracer concentrations suggest easy horizontal migration toward the building over distances of up to 20 ft and rapid vertical migration from 13 ft to 6 ft bls at the injection cluster. However, lower helium concentrations at certain ports suggest subsurface heterogeneity and preferential flow paths that could not be fully mapped with only the four tests conducted. Geophysical tests confirmed the location of many known features in and around the duplex, including the shallow, moist silty clay layer overlying the deeper sand/gravel outwash layer and the shallower (7 to 7.5 ft bls) silt/clay layer. Ground penetrating radar (GPR) results suggest that the concrete slab varies from 0.5 to 0.7 ft in thickness with an irregular undulating contact with the underlying fill material and resulting gaps where soil gas may pool or move preferentially.

- **Revisions to conceptual site model: VOC data.** Although chloroform was detected in groundwater, the measured concentrations were too low to account for the peak chloroform concentrations observed in soil gas (see Section 11). This suggests that there may be other sources of chloroform such as combined sewers²⁸ or drinking water mains²⁹ that leak below grade, higher groundwater concentrations at some locations near the site, or chloroform mass stored in the vadose zone from a historic release. For PCE, the results suggest a groundwater source, but the narrow range of variability in PCE concentrations and stability of this variability over time make it unlikely that variability in groundwater concentrations is the only source of the observed changes in soil gas or indoor air concentrations observed in this study. The variability in indoor air PCE concentrations is also influenced by subsurface, building-related, and meteorological variables. The potential that other sources of PCE may exist in the vadose zone or combined sewer lines cannot be ruled out at this point.
- **Temporal variability.** PCE levels in indoor air follow the general trend of starting higher at the beginning of the project (January 2011), dropping to a low in early summer, and rising slightly and leveling out through the end of the intensive pre-mitigation study period (February 2012). This general trend was attributed primarily to temperature, because the winter of 2010–2011 was much more severe than the winter of 2011–2012. During mitigation testing, which began in October 2012, indoor air PCE concentrations rose to levels above those observed in the March 2011 to September 2012 time period. We postulate that VOCs can be moved close to the structure either by a cumulative stack effect during a severe winter or by operation of an SSD mitigation system. It is unknown whether this VOC migration effect toward the slab will be common at sites with other geological formations or contaminant distributions. Because our mitigation testing included several on-off cycles over one winter, we do not know whether more substantial reductions in indoor air VOC concentrations would be achieved with continued operation of the SSD mitigation system. Spatial patterns changed dramatically when mitigation was operating, indicating that during initial operation the mitigation system was influencing both soil gas and indoor air concentrations.

13.1.1 Mitigation System Performance

An active subslab depressurization system was installed in the duplex, which met conventional tests of mitigation system performance used by practitioners:

²⁸Chloroform can form in sewers that receive bleach-containing products.

²⁹Groundwater chloroform concentrations at this duplex are lower than the mean and peak drinking water concentrations for Indianapolis (19 ppb and 82 ppb).

- Depressurization was observed with handheld micro manometers at 10 locations, which is more locations than are typically monitored for such a small structure. In many cases, the observed depressurization substantially exceeded conventional design criteria (Section 5.1).
- VOC sampling in the week following installation showed a dramatic reduction in VOC concentrations in indoor air as measured by weeklong passive samplers, using methods consistent with those used to monitor concentrations prior to mitigation (Section 5.3).
- Radon concentrations in indoor air were immediately and dramatically reduced, both as measured by directly reading instruments and by weeklong electret samples (Section 5.2).
- A U-tube manometer installed as a visual indication at the extraction points indicated that the system was functional when it was turned on. No sign of difficulty was seen with the U-tube manometer.

A program of SSD testing was then performed involving cycles of active operation, passive operation, and shutoff, with each cycle extending for multiple weeks. Such testing cycles are not conventionally done in installed systems and may not be economically or logistically feasible. An intensive program of monitoring of mitigation system performance was also conducted, more extensive than would normally be done by residential mitigation practitioners. Although this program showed that the mitigation system continued to provide a significant benefit, some aspects of the mitigation performance differed from conventional expectations.

- “Control” of differential pressure as indicated by micro manometers connected to a computerized data acquisition system was constant for long periods of time. During much of the testing, subslab to indoor air differential pressures were observed at a negative 15 Pa or more, indicating a strong driving force out of the structure. However, pressure “control” was lost on periods of up to several days. The pressure control loss during active SSD was observed on each side of the duplex but not on the same dates. The losses of pressure control were generally contemporaneous with either snow or heavy rain events. On at least two occasions, pressure swings of a total of at least 30 Pa were observed. These relatively brief events are most likely not significant in the context of exposures being compared with risk-based standards derived from a 30-year cancer exposure period. However, these events suggest that the conventional design criteria of protection against a 5 Pa differential pressure change may be insufficient if indoor air concentrations attributable to vapor intrusion must be controlled with reference to risk-based standards applicable to a 24-hour or less exposure period (Section 5.1).
- The weeklong integrated passive samples from the mitigation system for the third week of operation, for example, suggested that the indoor air VOC concentrations had reached levels substantially higher than those observed in the first week after operation began. This pattern was not seen with the weeklong integrated radon samples. Initial monitoring of SSD systems in practice is not normally continued for multiple weeks (Sections 5.3 and 6.1).
- Instantaneous VOC concentrations in indoor air, as measured by an on-site GC, exhibited several prominent spikes with durations between 1 and 3 days during active mitigation system operations. These spikes were associated with brief snow storm events and particular wind directions that appear for this house to be connected to higher indoor air concentrations. These same spikes were not clearly seen in any of the radon data sets (Sections 5.3 and 6.5.1).
- The brief excursions in pressure and VOC concentrations were not contemporaneous.
- The overall performance of the mitigation system in reducing indoor concentrations was better for radon than for VOCs. This finding is of possible concern because VOC mitigation design practices and standards are drawn from the radon literature. The estimated reduction for radon was approximately 91%, and the mitigation system consistently controlled radon to well below

the 2 pCi/l limit that EPA believes to be the practical limit of mitigation system effectiveness (which is constrained by ambient levels). For the 7 months of on/off mitigation system operation, average reductions of 68% in chloroform and 61% in PCE in indoor air were observed, considerably lower than that achieved for radon (Section 5.3).

- Concentrations of VOCs in some subslab and soil gas ports rose after mitigation began to levels not seen in more than a year of approximately weekly monitoring. This suggests that VOCs are being redistributed by the mitigation system and that soil gas concentrations close to the building may be enhanced by drawing higher concentrations of VOCs from greater depths (Sections 5.3 and 6.1.2).
- A significant drop off in VOC concentrations (by an order of magnitude or more from the peak VOC levels) was observed for all indoor air concentrations during the last few weeks of mitigation system operation (through mid-May 2013). Whether this trend would continue over a longer mitigation period (e.g., 6 months) is unknown. It is possible that, although initial mitigation system operation does influence and increase soil gas concentrations at this site, VOC concentrations may reach lower values at steady-state with longer term system operation. (Section 5.3).
- The flux of VOCs through the SSD system was dramatically higher than the flux through the building when the mitigation system was not installed (Section 5.4).

Taken together, these observations suggest that a “typical radon style system” would not necessarily achieve the same degree or consistency of protection for VOCs, at least over the initial months of operation that were tested in this study. We caution, however, that the application of this result **should not be** to simply increase the conservatism of the depressurization standard and thus the amount of vacuum routinely applied. Applying more vacuum routinely could have the deleterious effect of drawing more VOC mass near to the structure. These results may suggest additional evaluation to weigh the benefits of the following alternatives:

- automated (pressure controlled) variable speed fans in the SSD system
- a higher powered active SSD system run continuously
- modifications of the system to provide additional extraction points (such as in the basement walls) or to enhance the effectiveness of SSD operation by sealing additional entry paths.³⁰

Future testing could also investigate the possibility of additional and more stable VOC reductions with longer term continuous mitigation system operation than was possible under the time frame of this study.

13.1.2 Meteorological Effects on Vapor Intrusion

In this study, we used multiple analytical tools to assess the relationship between meteorological parameters and vapor intrusion:

- exploratory data analysis through visual examination of the shape of temporal trends in stacked plots of indoor air and certain soil gas ports over the full project period (Section 6)
- detailed examination of temporal trends on stacked plots during unusual differential pressure events (Section 9.1)
- visual examination of XY graphs (Section 9.2)
- quantitative time series methods (Section 10).

³⁰Some sealing activities were performed on this structure in spring 2011 (as described in Section 3.2.2 of U.S. EPA, 2012a), but additional sealing was not performed during the SSD installation.

Not all methods of analysis have yet been completed for all possible meteorological variables. The lines of evidence investigated for the meteorological variables are summarized in **Table 13-1**.

The evidence is overwhelming that cold temperatures contribute to greater vapor intrusion in this duplex. This was expected from knowledge of the stack effect mechanism.

The evidence suggests that both snowfall and snow/ice accumulation have effects on VOC vapor intrusion, although this effect is likely absent for radon. The snow effect is likely to be complex in that snow varies dramatically in moisture content and thus air permeability from one snow event to another and as a snow accumulation ages over time. There is relatively little evidence of rain effects on VOCs, but there is more evidence of a rain effect on radon.

Barometric pressure appears to have effects on radon and probably VOCs, although it is likely a complex function of barometric pressure. Additional work will be required to determine how best to assess the power of barometric pumping from time series data.

There is relatively strong evidence both in the data and from theory to support an association between winds from a range of westerly directions with vapor intrusion in the 422 portion of the duplex. This effect is expected to be different in other structures, depending on their orientation to the wind and the distribution of subsurface contaminants. The evidence for an effect of wind velocity is equivocal.

Thus, multiple meteorological variables likely control VOC vapor intrusion at this duplex. The meteorological variables likely interact in complex ways that would make the system difficult to model completely. Such multiple variable effects are also known in the radon vapor intrusion literature. In a recent review, Lewis and Houle stated:

“This paper identified about thirteen factors that can affect radon variation in the soil and house environment. The thirteen factors being soil moisture content, soil permeability, wind, temperature, barometric pressure, rainfall, frozen ground, snow cover, earth tides, atmospheric tides, occupancy factors, season and time of day. One can see the complexity of understanding and studying radon variability in homes.”

Although radon is not expected to be a highly quantitative tracer for VOC vapor intrusion in most situations, we should not expect VOC vapor intrusion to be a significantly simpler process.

The relationships among the variables may not be purely linear, they could be synergistic. For example, the PCE concentration curve vs. cold temperature related variables appears to curve upward under the most extreme winter conditions. This can be seen in the PCE plots vs. heating degree days (**Figure 9-42**) and vs. stack effect driving force (Figure 10-10 in U.S. EPA, 2012a). That may reflect an additive or synergistic effect between related variables such as cold temperature, frozen ground, and snow cover. In other words, cold could influence vapor intrusion through separate physical mechanisms, such as enhancement of the strength of the stack effect and formation of a lower permeability frozen ground layer near the surface.

13.1.3 Preferential Pathways and Revisions to Conceptual Site Model: Helium Tracer and Geophysical Tests

Two primary methods were used in this study in an attempt to better understand the effects of stratigraphic features on vapor intrusion at this duplex helium tracer tests and geophysical studies.

Table 13-1. Summary of Lines of Evidence for Meteorological Factors Influencing Vapor Intrusion in This Study

(Blank cells reflect types of analysis not completed for a given parameter)

| | Snowfall | Snow or Ice Accumulation on Ground | Cold Exterior Temperatures (or substantial change in temperatures) | Rain Events/ rainfall amount | Barometric Pressure Changes | West to NW Winds | High Wind Velocity |
|--|-------------------|---|--|------------------------------|-----------------------------|--------------------------------|--------------------------------|
| Apparent Temporal Association with VOC Concentrations in Indoor Air (Section 6, also U.S. EPA, 2012a) | Yes | Yes | Yes | Possibly for chloroform | | | |
| Apparent Temporal Association with VOC Concentrations in Wall Ports or Subslab Ports (Section 6) | Yes | Yes | | | Weak | | Some |
| Apparent Temporal Association with Large Subslab to Indoor Differential Pressure Events (Section 9.1) | Yes in some cases | | Yes in some cases | | Yes in some cases | Yes in a few cases | Yes in a few cases |
| Apparent Trend in XY Graph of Meteorological Parameter vs. Subslab/Indoor Differential Pressure (Section 9.1 and U.S. EPA, 2012a) | | | Yes | No | | Yes | No |
| Apparent Trend in XY Graph of Meteorological Parameter vs. VOC Concentration (Section 9.2) | | Yes for PCE, not definitive for chloroform | Yes | No clear relationship | Not definitive | Yes for PCE, No for Chloroform | No for PCE, Yes for Chloroform |
| Correlation with Radon in Quantitative Time Series Analysis (Sections 10.1 to 10.4); 422 Basement and Office | No | No | Yes in most analyses | Yes in some analyses | Yes in most analyses | | Yes in some analyses |
| Correlation with Chloroform in Quantitative Time Series Analysis (Sections 10.5 and 10.7); 422 Basement | | Yes in one of two cases with opposite signs for the coefficients of the current and past weeks. | Yes | No | Yes in some analyses | | |
| Correlation with PCE in Quantitative Time Series Analysis (Sections 10.6 and 10.8), 422 Basement | | Yes in one of two cases but with an unexpectedly negative coefficient for the current week. | Yes, although coefficients are both positive and negative | No | Yes | | No |

No

Helium tracer tests (Section 12.2) performed with common injection locations yielded similar overall patterns of tracer distribution in the exterior soil gas clusters with and without mitigation system operation. The variability between paired tests (mitigation on and mitigation off) was more pronounced beneath the building where the mitigation system would have been expected to have the most significant influence on airflow. The highest concentrations observed were usually those close to the 13-ft deep injection depth, suggesting attenuation as the tracer migrated upward. The similar patterns between tests performed in different subsurface areas (different injection wells) suggest control by common features of soil stratigraphy or the building envelope because the tests would have these factors in common. The high concentrations observed at the 9-ft and 13-ft depths for all the injections, despite the buoyancy of the helium-enriched soil gas, suggest that transference of helium is easy horizontally toward the building over distances of up to 20 ft typically within 2 days. Vertical migration from 13 ft to 6 ft bls also occurred relatively rapidly at the injection cluster. The lack of influence at certain ports closer to the point of injection and along the same general line to more distant ports suggests subsurface heterogeneity and preferential flow paths. However, many more than the four tracer tests performed would likely be needed to fully map the preferential flow paths.

Geophysical studies (Section 12.1) confirmed the location of many known features in and around the duplex. The results suggested an electrically conductive unsaturated zone with irregular hummocky layers overlaying a more regular horizontally stratified zone at approximately 7.5 feet deep, which likely corresponds to the facies contrast between the underlying sand/gravel layer and the shallower silt/clay layer. This contact may also form local perched water conditions which may also cause such a geophysical response. These stratigraphic features may influence subsurface fluid fate and transport.

The interior ground penetrating radar (GPR) results suggest the concrete slab varies from 0.5 to 0.7 ft in thickness with an irregular undulating contact with the underlying material. This underlying material is electrically conductive and contains many discontinuities and non-horizontal interfaces that may govern subsurface fluid fate and transport. This suggests the concrete floor was not poured on well-flattened fill material and may provide pockets into which soil gas may pool or move preferentially. However, the presence of fill material of some sort is evident at many locations beneath the slab. The GPR data suggest there is a thicker concrete footing below the doorways, which separate the three rooms in each of the duplex basements. The GPR response to the cistern and the covered sewer line is evident as are GPR reflections likely due to fill material.

13.1.4 Revisions to Conceptual Site Model: VOC Data

The finding of chloroform in groundwater, but at current concentrations substantially too low to account for the peak chloroform concentrations in soil gas (Section 11), would be consistent with several alternative conceptual models:

20. Chloroform is primarily transported to the site through combined sewers that leak below grade. Chloroform is stripped from these waters as they infiltrate down to the water table. It should be noted that the concentrations observed in groundwater at this duplex are lower than even the mean drinking water concentration for Indianapolis (19 ppb) and are far below the peak reported drinking water concentration (82 ppb).³¹ Additional formation is likely in combined sewers that receive bleach-containing products.
21. Chloroform is present in higher concentration in groundwater at some locations near the site that has not yet been delineated by the three existing groundwater well clusters.
22. Chloroform mass is stored primarily in the vadose zone from a historic release.

³¹NY Times, May 16, 2012 <http://projects.nytimes.com/toxic-waters/contaminants/in/marion/in5249004-indianapolis-water>

23. Groundwater chloroform concentrations at the site were historically (or are periodically but briefly) higher, and the observed soil gas concentrations are a legacy of that period.

Our results suggest a groundwater source for PCE, but the narrow range of variability in PCE concentrations (below an order of magnitude) and stability of this variability over time (see Section 11) make it unlikely that variability in groundwater concentrations is strongly related to the changes in soil gas or indoor air concentrations over the time scales observed in this study. As has been shown in this and other studies, the variability in indoor air PCE concentrations is also influenced by subsurface, building-related, and meteorological variables that affect the concentration of PCE as it migrates from the water table, enters the building, and mixes with indoor air. However, other sources of PCE that may also exist in the vadose zone or combined sewer lines cannot be ruled out at this point, and variability in those sources could also influence the PCE concentrations in indoor air.

13.1.5 Temporal Trends

PCE levels at all six indoor air sampling stations follow the same general trend of starting higher at the beginning of the project (January 2011), dropping to a low in early summer, and rising slightly and leveling out through the end of the pre-mitigation study period (February 2012). This general trend was attributed primarily to temperature, since the winter of 2010–2011 was much more severe than the winter of 2011–2012 (Section 6).

Sampling was discontinued for the spring and summer of 2012 because of funding limitations. However, the concentrations in October 2012 before the mitigation system was installed were very similar to those observed in October 2011, which suggests that the intensive sampling conducted for this project did not distort the observed indoor concentrations. Surprisingly, the concentration levels of PCE in the first period of active mitigation rose to levels above those observed in the March 2011 to February 2012 time period. The concentrations rose somewhat more after the mitigation system was switched into a passive mode. The observation of higher PCE post-mitigation suggests that the geologic formation could yield enough vapor intrusion-derived PCE to account for the January 2011 concentrations. We postulate that VOCs can be moved close to the structure either by a cumulative stack effect during a severe winter or by operation of an SSD mitigation system. It is unknown whether this VOC migration effect toward the slab will be common at sites with other geological formations or contaminant distributions or whether it would continue at this site with continued operation of the mitigation system. Because this project used an experimental design with multiple on-off cycles for mitigation over the course of one winter, it is also unknown whether more stable reductions in indoor air VOC concentrations would be achieved with longer term continuous operation of the SSD mitigation system.

Soil gas concentrations at some sampling locations) vary only within a narrow range of two or three times over 1 year, suggesting that multiple samples or time-integrated samples may have limited benefit. However, at some locations, changes of about a factor of 10 in soil gas concentrations occur over 1 year, suggesting that there would be significant additional information provided from additional soil gas sampling rounds at these locations. However, these changes are gradual, suggesting that sampling rounds should be widely spaced and that time-integrated soil gas sampling over periods of 8 hours to 1 week would have limited benefit.

The soil gas samples showed much more spatial variability in winter than in summer when mitigation was not being operated. Spatial patterns changed dramatically, as might be expected when mitigation was operating.

13.2 Practical Implications for Practitioners

As described in the introduction to this section, the practical implications discussed below should be couched with the caveats that (1) this is a work in progress subject to change as additional information is gathered in the next phase of study and (2) it does not represent an intensive study of a single house and therefore any conclusions may not (or may) be representative of other chlorinated VOC vapor intrusion sites in different environments.

13.2.1 Mitigation Design Implications

The results of our mitigation system testing suggest that the assumption that systems protective for radon will always be equally protective for VOCs could be incorrect, at least during the first few months of system operation. Although this house could be relatively unique (given its old age and very coarse grained geology in the deeper layers) at least in this situation subslab to basement differential pressure variations of at least 30 Pa were observed repeatedly but for a small percentage of the total period of observation. Since these unusual pressure events typically lasted from 1 to 3 days, they may not significantly impact design of systems designed to protect against chronic risks in indoor air, but they are more likely to impact design for systems protecting against short-term risks.

Similarly, if short-term risks are a design driver and the mitigation systems will not have backup electrical power (the majority of SSD systems in our experience), caution may be necessary about the potential for the mitigation system to increase the subslab VOC concentration at least during early system operation. For example, if the subslab VOC concentration increases, then indoor air concentrations could increase if the mitigation system stops operating during a power failure.

It should be stressed that the observations of the effects of mitigation on soil gas and indoor air VOC levels in this report are based on on/off operation cycles of the mitigation system for about 7 months after installation. Also, indoor air VOC concentrations were steadily declining in all sampling locations just before the sampling period in this report was completed (in May 2013). This suggests the possibility that although initial mitigation system operation appeared to move higher VOC soil gas concentrations closer to the building, resulting in lower VOC reductions than were observed for indoor air, continued mitigation system operation could, over time, result in more stable reductions in indoor air levels once more steady state conditions are reached in the subsurface. Alternatively, the decline in VOC concentrations in May 2013 could be attributable to weather changes (indoor VOC concentrations have been shown to decline in the spring time at this site). However, it is clear from these results that at least at sites with similar conditions to this one, VOCs may not respond as rapidly or as completely to mitigation as radon does.

13.2.2 Sampling Planning Implications

The results reported here provide little support of the common guidance that vapor intrusion sampling must be timed around rain events greater than one half inch. While there may have been some effects on vapor intrusion of major seasonal flooding events that changed the local water table by approximately 5 ft, there was not any apparent effect on indoor air concentrations from more moderate rain events. The results reported here do suggest that snow events, snow cover, and/or frozen soils may temporarily and significantly increase vapor intrusion.

Several variables have been shown here to most likely have an interactive effect on VOC vapor intrusion:

- cold temperatures
- snow/ice
- barometric pressure

- wind direction

Given this complexity and variability in vapor intrusion observed at this site, practitioners should not expect to be able to explain in detail temporal patterns drawn from smaller data sets (for example, three or four rounds of VOC sampling). However, as results from this study are confirmed in studies of other buildings, it may be possible to develop recommendations to guide selection of “near worst case” indoor air sampling conditions for specific sites based on the site’s known characteristics such as climate and stratigraphy.

13.2.3 Delineating Preferential Pathways

The results of our geophysics and tracer injection studies show that these tools can provide useful insights in delineating structures beneath a building and ground surfaces. However, the level of effort required to fully understand and map the features that influence subslab gas flow in even a small old building such as this may be too high for routine application of those tools.

13.3 Recommendations

The results presented here suggest several fruitful lines of future inquiry:

24. The results suggest that current chemical vapor intrusion mitigation system designs, based on radon system’s experience, may produce designs that are highly effective for radon but not as effective for VOCs, at least during the initial months of system operation. This finding suggests a need for longer term confirmation of post-mitigation VOC concentrations and replication of this study’s findings in other environments. Specifically, buildings of other ages/designs in conditions similar to this (15 to 20 ft to groundwater, moderate strength source, coarse deep geology) should be tested. This finding should also prompt more intensive studies of long-term mitigation system performance in commercial buildings and in other geographies. The current trend of TCE being managed based on short-term exposure thresholds provides additional impetus for such studies, because radon and other VOCs are not usually managed based on short-term health effects.
25. The finding that the current mitigation system was not at all times able to shut off VOC vapor intrusion as well as it controlled radon leaves open several questions:
 - Would a mitigation system continuously operated over a longer period and/or with a more powerful fan provide additional protection and, ultimately, a reduction in soil gas VOC levels or merely exacerbate the problem of VOCs being drawn toward the foundation?
 - Would a mitigation system with a variable speed fan controlled based on differential pressure provide better performance?
 - Would a degree of sealing beyond what was needed to meet radon standards have produced a more effective VOC mitigation system in this structure?
 - Would a mitigation system that extracted air from behind the basement walls be more effective?
 - Was the on/off testing protocol used in this study unrealistic?
26. Additional statistical analyses could be performed on this data set to:
 - Determine if any of the meteorological parameters cause consistent trends in soil gas concentrations of a sufficient magnitude to effect site management decision making.
 - Examine the optimum spacing of sampling events in indoor air (although the autocorrelation and partial autocorrelation analysis provides some hints, this is not the proper type of statistical analysis to address the question of optimum sample spacing).

- Assess if there are important diurnal effects in indoor air (the current analyses were conducted on data aggregated over 24 hours, but 7 or more samples a day were taken with the on-site GC).
 - Examine whether combinations of predictor variables may predict more of the variance in indoor VOCs than any one variable alone. The most likely first strategy to explore would be to use a function of exterior temperature as a model term in all of the models and see which of the other predictor variables best accounts for the residual variability after temperature (and thus, the stack effect) was modeled.
 - Predict the optimum sampling time based on meteorological conditions.
27. The finding that wind direction effects appear to fit the Abreu and Johnson (2005) model predictions (e.g., U.S. EPA, 2012d) suggest that this data set could be a useful test for validating that model and exploring its utility in site management decision making.
28. Although the information collected under this and the previous project has shown that PCE groundwater levels are high enough to serve as a source for the VOCs in soil gas and indoor air at this site, other vadose zone PCE sources cannot be ruled out. Also, current chloroform groundwater concentrations were not adequate to serve as a source for the soil gas and indoor air concentrations under and in the duplex. Additional work is needed, including additional subsurface borings and soil gas monitoring points, to more positively identify the sources responsible for the vapor intrusion of these VOCs at this site.

14.0 References

- Aaltonen, J., H. Pumpanen, T. Hakola, S. Vesala, R. Rasmus, and J. Back. 2012. Snowpack concentrations and estimated fluxes of volatile organic compounds in a boreal forest. *H. Biogeosciences* 9: 2033–2044.
- Abreu, L.D., and P.C. Johnson. 2005. Effect of vapor source—building separation and building construction on soil vapor intrusion as studied with a three-dimensional numerical model. *Environmental Science and Technology* 39(12):4550–4561.
- Abreu, L.D., and P.C. Johnson. 2006. Simulating the effect of aerobic biodegradation on soil vapor intrusion into buildings: influence of degradation rate, source concentrations. *Environmental Science and Technology* 40(7):2304–2315.
- AFCEE (Air Force Center for Environmental Excellence). 2004. *Principles and Practices of Enhanced Anaerobic Bioremediation of Chlorinated Solvents*. Prepared for AFCEE, Brooks City-Base, TX. Available at http://costperformance.org/remediation/pdf/principles_and_practices_bioremediation.pdf.
- Allen, M.K., D. Grande, and L. Pansch. 2007. *Evaluation of Passive Sampling Techniques for Monitoring Roadway and Neighborhood Exposures to Benzene and Other Mobile Source VOCs*. Wisconsin Department of Natural Resources (WDNR) Publication AM-384 2007. WDNR, Madison, WI. funded by U.S. EPA Community Scale Monitoring Grant. Available at <http://dnr.wi.gov/topic/AirQuality/documents/RoadwayStudyFinal.pdf>.
- Armstrong, R.L., and E. Brun. 2008. *Snow and Climate: Physical Processes, Surface Energy Exchange and Modeling*. Cambridge University Press.
- Arvela, H. 2008. *Radonsafe Foundation, Moisture Prevention and Air Exchange in a Healthy Building*. Finnish Research Programme on Environmental Health. Available at <http://www.ktl.fi/sytty/abstracts/arvela.htm>.
- ATSDR (Agency for Toxic Substances and Disease Registry). 1997. *Toxic Substances Portal—Toxicological Profile for Chloroform*. Available at <http://www.atsdr.cdc.gov/toxprofiles/tp.asp?id=53&tid=16>.
- Batterman, S., T. Metts, and P. Kalliokoski. 2002a. Diffusive uptake in passive and active absorbent sampling using thermal desorption tubes. *Journal of Environmental Monitoring* 4:870.
- Batterman, S., T. Metts, and P. Kalliokoski. 2002b. Low-flow active and passive sampling of VOCs using thermal desorption tubes: Theory and application at an offset printing facility. *Journal of Environmental Monitoring* 4:361–370.
- Begerow, J., E. Jermann, T. Keles, and L. Dunemann. 1999. Performance of two different types of passive samplers for the GC/ECD-FID determination of environmental VOC levels in air. *Fresenius Journal of Analytical Chemistry* 363:399–403.
- Bender, J.A. 1957. *Air Permeability of Snow*. Res. Rep. 37 Snow, Ice and Permafrost Research Establishment (U.S. Army Corps of Engineers) Wilmette, IL. p. 46–62.

- Bertoni, G., R. Tappa, and I. Allegrini. 2001. Internal consistence of the new “Analyst” diffusive sampler: a long term field test. *The Diffusive Monitor* 12:2–5.
- Bozkurt, O., K.G. Pennell, and E.M. Suuberg. 2007a. Evaluation of characterization techniques for vapor intrusion scenarios using a three-dimensional computational fluid dynamics (CFD) model. Air and Waste Management Association, Providence, RI, September.
- Bozkurt, O., K.G. Pennell, and E.M. Suuberg. 2007b. Characterizing vapor intrusion scenarios using a computational fluid dynamics model. ACS National Meeting. Boston, MA. August.
- Brenner, D. 2007. Effect of meteorological and site conditions on, and relationship of diurnal variation to, vapor intrusion at NASA Ames Research Center. Conference Proceeding from *Vapor Intrusion: Learning from the Challenges*—Air and Waste Management Association (AWMA), Providence, RI.
- Brown, V., and D. Crump. 1993. Appropriate sampling strategies to characterize VOCs in indoor air using diffusive samplers. Pp. 241–249 in *Proceedings of International Conference on VOCs*, London, October 27–28.
- Brown, V., and D. Crump. 1993. Appropriate sampling strategies to characterize VOCs in indoor air using diffusive samplers. Pp. 241–249 in *Proceedings of International Conference on VOCs*, London, October 27–28.
- Bruno, P., M. Caputi, M. Caselli, G. de Gennaro, and M. de Rienzo. 2005. Reliability of a BTEX radial diffusive sampler for thermal desorption: Field measurements. *Atmospheric Environment* 39:1347–1355.
- California Environmental Protection Agency. 2012. *Advisory Active Soil Gas Investigations*. Department of Toxic Substances Control, Los Angeles Regional Water Quality Control Board, San Francisco Regional Water Quality Control Board, April.
- Cao, X.L., and C.N. Hewitt. 1994. Study of the degradation by ozone of adsorbents and hydrocarbons adsorbed during the passive sampling of air. *Environmental Science and Technology* 28:757–725.
- Carr, D.B., P.G., Laurent, C. Levy, and A.H. Horneman. 2011. Stylistic modeling of vadose zone transport insight into vapor intrusion processes. Presented at the *AEHS Workshop: Addressing Regulatory Challenges in Vapor Intrusion. A State of the Science Update*. San Diego CA, March 15.
- Case, J., and K. Gorder. 2006. The investigation of vapor intrusion at Hill AFB. Conference Proceeding from *Vapor Intrusion: The Next Great Environmental Challenge—An Update*. Air and Waste Management Association (AWMA), Los Angeles, CA.
- Christ, Maj John A. 2010. Vapor intrusion from entrapped NAPL sources and groundwater plumes : process understanding and improved modeling tools for pathway assessment. Presented at *SERDP Technical Exchange Meeting*, August 16.
- Cleveland, W.S, and S.J. Devlin. 1988. Locally-weighted regression: an approach to regression analysis by local fitting. *Journal of the American Statistical Association* 83(403):596–610.

- Cleveland, W.S. 1981. LOWESS: A program for smoothing scatterplots by robust locally weighted regression. *The American Statistician* 35(1):54.
- Cocheo, C., C. Boaretto, D. Pagani, F. Quaglio, P. Sacco, L. Zaratin, and D. Cottica. 2009. Field evaluation of thermal and chemical desorption BTEX radial diffusive sampler Radiello® compared with active (pumped) samplers for ambient air measurements. *Journal of Environmental Monitoring* 11:297–306.
- Cochrane, D., and G. H. Orcutt. 1949. Application of least squares regression to relationships containing autocorrelated error terms. *Journal of the American Statistical Association* 44:32–61,
- Cody, R.J., A. Lee, and R. Wiley. 2003. Use of radon measurements as a surrogate for relative entry rates of volatile organic compounds in the soil gas. Presented at the *AWMA Conference on Indoor Air Quality Problems and Engineering Solutions*. Research Triangle Park, NC, July 21–23.
- Cohen, A. B. 1971. *Concepts of Nuclear Physics*. McGraw-Hill.
- Colby College. 2009. *Regression: Patterns of Variation*. Colby College Biology Department. Available at <http://www.colby.edu/biology/BI17x/regression.html>.
- Conway, H. and J. Abrahamson. 1984. Air permeability as a textural indicator of snow. *Journal of Glaciology* 30(106):328-333.
- Coyne, L. 2010. Personal communication. SKC, Inc. August 17.
- Dawson, H. 2008. *US EPA's Vapor Intrusion Database—Preliminary Evaluation of Attenuation Factors for Chlorinated VOCs in Residences*. U.S. EPA Office of Superfund Remediation and Technology Innovation (OSRTI).
- Dawson, H., and H. Schuver. 2010. *US EPA's Vapor Intrusion Database: Preliminary Evaluation of Attenuation Factors for Chlorinated VOCs in Residences*. Presented at the 20th Annual International Conference on Soils, Sediments, Water and Energy, March 16.
- DePersio, T., and J. Fitzgerald. 1995. Guidelines for the Design, Installation, and Operation of Sub-Slab Depressurization Systems. Massachusetts Department of Environmental Protection, Northeast Regional Office. Available at <http://www.mass.gov/dep/cleanup/laws/ssd1e.pdf>.
- DeVaull, G.E. 2012. *Analysis and Interpretation of Time-Variable Vapor Intrusion Data: Pressure-Driven Flow Across Building Foundations*. Proceedings paper, AWMA Vapor Intrusion Conference, 2012. Also DeVaull, G.E. 2013. *Analysis and Interpretation of Time-Variable Vapor Intrusion Data: Pressure-Driven Flow Across Building Foundations*. Presented at 23rd Annual International Conference on Soil, Water, Energy and Air, San Diego, CA, March 2013.
- Dickson, J., A. Lonegran, and R. Stetson. 2010. Characterization of multiple chlorinated solvent plumes due to the impact of TCE screening level reduction. *International Journal of Soil, Sediment and Water* 3(2):Section 11.
- Dietz, R.N., and E.A. Cote. 1982. Air infiltration measurements in a home using convenient perfluorocarbon tracer technique. *Environment International* 8(1-6):419–433.

- Dietz, R.N., et al. 1986. Detailed description and performance of a passive perfluorocarbon tracer system for building ventilation and air exchange measurements. Pp. 203–254 in *Measured Air Leakage of Buildings: A Symposium*. Heinz R. Trechsel, Peter L. Lagus, ASTM Committee E-6 on Performance of Building Constructions Contributor Heinz R. Trechsel, Peter L. Lagus. Published by ASTM International.
- DiGiulio, D., C. Paul, R. Cody, R. Willey, S. Clifford, P. Kahn, R. Mosley, A. Lee, and K. Christensen. 2006. *Assessment of Vapor Intrusion in Homes near the Raymark Superfund Site Using Basement and Subslab Air Samples*. EPA/600/R-05/147. U.S. EPA Office of Research and Development, Ada, OK, March.
- Distler, M., and P. Mazierski. 2010. Soil vapor migration through subsurface utilities. *Proceedings 2010 AWMA Vapor Intrusion Specialty Conference*.
- Division of Spill Prevention and Response Contaminated Sites Program. 2012. *Vapor Intrusion Guidance for Contaminated Sites*. October.
<http://dec.alaska.gov/spar/csp/guidance/Vapor%20Intrusion%20Guidance.pdf>.
- Eklund, B., and D. Borrows. 2009. Prediction of indoor air quality from soil-gas data at industrial buildings. *Groundwater Monitoring and Remediation* 29(1):118–125.
- Environmental Quality Management. 2004. *Users Guide for Evaluating Subsurface Vapor Intrusion into Buildings*. Prepared for US EPA under EPA Contract Number: 68-W-02-33, WA No. 004, PN 030224.0002. Available at
http://www.epa.gov/oswer/riskassessment/airmodel/pdf/2004_0222_3phase_users_guide.pdf.
- Falta, R. 2006. “Environmental Remediation of Volatile Organic Compounds” in C. Ho and S. Webb *Gas Transport in Porous Media* p. 354-370. Netherlands: Springer.
- Folkes, D., W. Wertz, J. Kurtz, and T. Kuehster. 2009. Observed spatial and temporal distributions of CVOCs at Colorado and New York vapor intrusion sites. *Ground Water Monitoring & Remediation* 29(1):70–80.
- Forbes, J., J. Havlena, M. Burkhard, and K. Myers. 1993. Monitoring of VOCs in the deep vadose zone using multi-port soil gas wells and multi-port soil gas/ground-water wells. Pp. 557–571 in *Proceedings of the Seventh National Symposium on Aquifer Restoration, Ground-water Monitoring, and Geophysical Methods*, National Ground Water Association, Dublin, OH.
- Garbesi, K., and R.G. Sextro. 1989. Modeling and field evidence of pressure-driven entry of soil gas into a house through permeable below-grade walls. *Environmental Science and Technology* 23(12):1481–1487.
- Greiner, M.A., and R.M. Franza. 2003. Barriers and bridges for successful environmental technology transfer. *The Journal of Technology Transfer* 28(2):167–177(11).
- GSI Environmental. 2008. *Final Report: Detailed Field Investigation of Vapor Intrusion Processes*. ESTCP Project ER-0423, September.
- Hall, S.K., J. Chakraborty, and R.J. Ruch. 1997. *Chemical Exposure and Toxic Responses*. Boca Raton, FL: CRC Press.

- Hosoda, M., A. Sorimachia, S. Tokonamia, T. Ishikawaa, S.K. Sahooa, N.M.M. Hassanb, M. Fukushib, and S. Uchidaa. 2008. Generation and control of radon from soil. *Proceedings of 12th International Congress of the International Radiation Protection Association*. Available at <http://www.irpa12.org.ar/fullpapers/FP0971.pdf>
- Hass, B.S., and R. Herrmann. 1998. Tracing volatile organic compounds in sewers. *Water Science and Technology* 37(1):295–301.
- Hayes, H. 2008. Air Toxics Ltd., personal communication to Chris Lutes, ARCADIS, August.
- Heggie, A.C., and B. Stavropoulos. 2019. Evaluating vapor intrusion risk using comparative dynamic and passive flux chambers at a TCE impacted site in Sydney Australia. <http://events.awma.org/education/Final%20Papers/7-Heggie.pdf>. Paper presented at *AWMA 2010 Vapor Intrusion Specialty Conference*.
- Helsel, D.R. 2005. *Nondetects and Data Analysis: Statistics for Censored Environmental Data*. Hoboken, NJ: Wiley.
- Hers et al. 2011. *Cold Climate Vapor Intrusion Research Study – Results of Seasonal Monitoring of House at North Battleford, Saskatchewan*. <http://indoorairproject.files.wordpress.com/2011/03/sgs-attachment-4.pdf> cited as in preparation in http://www.epa.gov/oust/cat/pvi/PVI_Database_Report.pdf.
- Holton, C., et al. 2013. Multi-year monitoring of a house over a dilute CHC plume: implications for pathway assessment using indoor air sampling and forced under-pressurization tests. Presentation at AEHS conference, March. Available at https://iavi.rti.org/attachments/WorkshopsAndConferences/05_Johnson_03-19-13.pdf.
- Howard, P.H., R.S. Boethling, W.F. Jarvis, W.M. Meylan, and E.M. Michalenko. 1991. *Handbook of Environmental Degradation Rates*. Chelsea, MI: Lewis Publishers, Inc.
- Hui, S.C. 2003. *Lecture: Air Movement and Natural Ventilation*. Department of Mechanical Engineering, The University of Hong Kong. Used by Permission from Dr. Hui. Available at <http://www.arch.hku.hk/teaching/lectures/airvent/sect03.htm>.
- IndyGov. 2012. *My Neighborhood*. Available at <http://maps.indy.gov/myneighborhood/>.
- ITRC (Interstate Technology and Regulatory Council). 2007. Vapor Intrusion Pathway: A Practical Guideline. Prepared by The Interstate Technology & Regulatory Council Vapor Intrusion Team. Available at <http://www.itcreweb.org/documents/VI-1.pdf>.
- Johnson, P.C., et al. 2012. *Vapor Intrusion above a Dilute CHC Plume: Lessons-Learned from Two Years of Monitoring*. Presentation at AEHS Conference, March. Available at https://iavi.rti.org/attachments/WorkshopsAndConferences/09_P%20Johnson%20AEHS%20Talk%20032112.pdf.
- Johnson, P.C., and R.A. Ettinger. 1991. Heuristic model for predicting the intrusion rate of contaminant vapors into buildings. *Environmental Science and Technology* 25:1445–1452.
- Judge, G.G, W.E. Griffiths, R.C. Hill, H. Lutkepohl, and T.C. Lee. 1985. *The Theory and Practice of Econometrics*, Second Edition. New York: Wiley.

- Jury, W.A., D. Russo, G. Streile, and H.E. Abd. 1990. Evaluation of volatilization by organic chemicals residing below the soil surface. *Water Resources Research* 26(1):13–20.
- Koontz, M.D., and H.E. Rector. 1995. *Estimation of Distributions for Residential Air Exchange Rates*. EPA Contract No. 68-D9-0166, Work Assignment No. 3-19. U.S. EPA Office of Pollution Prevention and Toxics. Washington, DC.
- Krewski, D., R. Mallick, J.M. Zielinski, and E.G. Létourneau. 2005. Modeling seasonal variation in indoor radon concentrations. *Journal of Exposure Analysis & Environmental Epidemiology* 15(3):234–243.
- Kuehster, T.E., D.J. Folkes, and E.J. Wannamaker. 2004. Seasonal variation of observed indoor air concentrations due to vapor intrusion. Presented at the *Midwestern States Risk Assessment Symposium*, Indianapolis, IN.
- Kurtz, J.P., and D.J. Folkes. 2008. Empirical data on lag time for vapor intrusion from a chlorinated VOC groundwater plume. Presented at *AEHS San Diego Conference*, March 12.
- Lau, P. 2008. Calculation of flow rate from differential pressure devices – orifice plates. Presented to the *European Metrology Association for Thermal Energy Measurement*, August 2–4.
- Lee, A., K. Baylor, P. Reddy, and M. Plate. 2010. EPA Region 9’s RARE opportunity to improve vapor intrusion indoor air investigations. Presented at the *20th Annual International Conference on Soils, Sediments, Water and Energy*, San Diego, CA. March 16.
- Lewis, R.K. and P.N. Houle. 1985. *A Living Radon Reference Manual*. http://www.dep.state.pa.us/brp/radon_division/LivingRadonReferenceManual.htm reviewing Nazaroff, W. and Doyle, S. Radon Entry into Houses Having a Crawl Space. *Health Physics* 48:265–281.
- Linn, W., L. Appel, R. DeZeeuw, P. Doorn, J. Doyon, T. Evanson, J. Farrell, D. Hanson, R. Jurgens, J. So, C. Spiegel, D. Switek, and S. Yankey. 2010. *Conducting Contamination Assessment Work at Drycleaning Sites*. State Coalition for Remediation of Drycleaners. Available at <http://www.drycleancoalition.org/download/assessment.pdf>.
- Loureiro, C.O., and L.M. Abriola. 1990. Three-dimensional simulation of radon transport into houses with basements under constant negative pressure. *Environmental Science and Technology* 24(9):1338–1348.
- Luo, H., P. Dahlen, P. Johnson, T. Creamer, T. Peargin, P. Lundegard, B. Hartman, L. Abreau, and T. McAlary. 2006. Spatial and temporal variability in hydrocarbon and oxygen concentrations beneath a building above a shallow NAPL source. Presented at the *Battelle Conference on Remediation of Chlorinated and Recalcitrant Compounds*, Monterey, CA, May.
- Luo, H., P. Dahlen, P.C. Johnson, T. Peargin, and T. Creamer. 2009. Spatial variability of soil-gas concentrations near and beneath a building overlying shallow petroleum hydrocarbon-impacted soils. *Ground Water Monitoring & Remediation* 29(1):81–91.
- Lutes, C., Cosky, B., B. Schumacher, J. Zimmerman, H. Hayes, R. Truesdale, S. Lin, and B. Hartman. 2012a. Long-term detailed study of vapor intrusion temporal variability: implications for indoor air and soil gas sampling guidance. Oral Presentation and Short Paper: *AWMA Symposium on Air*

- Quality Measurement Methods and Technology*, Durham, NC. April.
- Lutes, C., Cosky, B., L. Abreu, B. Schumacher, J. Zimmerman, R. Kapucinski, and R. Truesdale. 2012b. Can short-term fan testing provide insight into vapor intrusion. Oral Presentation and Short Paper *AWMA Symposium on Air Quality Measurement Methods and Technology*, Durham, NC. April.
- Lutes, C., Cosky, B., Uppencamp, R., Abreu, L., Schumacher, B., Zimmerman, J. Truesdale, R., Lin, S, Hayes, H. and Hartman, B. 2012c. Recent observations on spatial and temporal variability in the field. Invited presentation at *EPA Workshop: Recent Advances to Vapor Intrusion Application and Implementation* at the 22nd Annual International Conference on Soil, Water, Energy & Air (AEHS) San Diego, March.
- Lutes, C., Cosky, B., Uppencamp, R., Abreu, L., Schumacher, B., Zimmerman, J. Truesdale, R., Lin, S, Hayes, H. and Hartman, B. 2012d. Short-term variability, radon tracer, and long-term passive sampler performance in the field. Invited presentation at *EPA Workshop: Recent Advances to Vapor Intrusion Application and Implementation* at the 22nd Annual International Conference on Soil, Water, Energy & Air (AEHS) San Diego, March.
- Lutes, C.; R. Studebaker, and N. Weinberg. 2010b. *Optimal design of subslab depressurization systems for volatile organic compound vapor intrusion (VI) mitigation*. Poster presented at *AWMA Specialty Conference: Vapor Intrusion 2010*, Chicago, IL, September 28–30. Available at http://events.awma.org/education/Posters/Final/Lutes_OptimalPoster.pdf.
- Lutes, C.C., R. Uppencamp, C. Singer, L. Abreu, R. Mosley, and D. Greenwell. 2009. *Radon Tracer as a Multipurpose Tool to Enhance Vapor Intrusion Assessment and Mitigation*. Poster presented at the Partners in Environmental Technology Technical Symposium and Workshop, Washington, DC, December.
- Lutes, C.C., R. Uppencamp, H. Hayes, D. Greenwell, and R. Mosley. 2010. Long-term integrated samplers for indoor air and sub-slab soil gas at VI sites. Presented at the *2010 Battelle Conference*, Monterey, CA.
- Lutes, C.C., R. Uppencamp, H. Hayes, R. Mosley and D. Greenwell. 2010b. Long-term integrating samplers for indoor air and subslab soil gas at VI sites. Oral Presentation at *AWMA Specialty Conference: Vapor Intrusion 2010*, September 28–30, 2010. Chicago, IL. paper submitted to proceedings. Available at http://events.awma.org/education/Posters/Final/Lutes_RadonPoster.pdf or <http://events.awma.org/education/Final%20Papers/7-Lutes.pdf>
- Lutes, C.C., R. Uppencamp, H. Hayes, R. Mosley and D. Greenwell. 2010. Long-term integrated samplers for indoor air and subslab soil gas at VI sites. Oral presentation at *Seventh International Remediation of Chlorinated and Recalcitrant Compounds Conference*, Monterey, CA; May 24–27.
- MacLeod, G., and J.M. Ames. 1986. Comparative assessment of the artifact background on thermal desorption of Tenax GC and Tenax TA. *Journal of Chromatography* 355:393–398.
- MADEP. 2002. *Indoor Air Sampling and Evaluation Guide*. Boston, MA: Commonwealth of Massachusetts Executive Office of Environmental Affairs, Office of Research and Standards, Department of Environmental Protection.

- Marotta, L., M. Snow, and S. Varisco. 2012. Extending the hydrocarbon range above naphthalene for soil vapor and air samples using automated thermal desorption/gas chromatography/mass spectrometry (*ATD/GC/MS*). Presented at *National Environmental Monitoring Conference*, Washington, DC, August 6–10.
- McAlary, T.A., P. Dollar, P. de Haven, R. Moss, G. Wilkinson, J. Llewellyn, and D. Crump. 2002. *Assessment of subsurface vapour transport through Triassic sandstone and quarry fill into indoor air in Weston Village, Runcorn*. Presented at Indoor Air 2002, Monterey, CA.
- McHugh, T. E., and Nickels, T. N. 2007. Evaluation of spatial and temporal variability in VOC concentrations at vapor intrusion investigation sites. Conference Proceeding from *Vapor Intrusion: Learning from the Challenges*—Air and Waste Management Association (AWMA), Providence, RI.
- McHugh, T., P. De Blanc, and R. Pokluda. 2006. Indoor air as a source of VOC contamination in shallow soils below buildings. *Soil and Sediment Contamination* 15:103–22.
- McHugh, T.E., T.N. Nichols, and S. Brock. 2007. Evaluation of spatial and temporal variability in VOC concentrations at vapor intrusion investigation sites. Pp. 129–142 in *Proceeding of Air & Waste Management Association's Vapor Intrusion: Learning from the Challenges*, Providence, RI, September 26–28.
- Middleditch, B.S. 1989. *Analytical Artifacts: GC, MS, HPLC, TLC and PC*. Journal of Chromatography Library Volume 44. Elsevier, Amsterdam. p. 668-669.
- Moses, H., H.F. Lucas and G.A. Zerbe. 1963. The effect of meteorological variables upon radon concentration three feet above the ground. *J. APCA*. 13(1):12-19.
- Mosley, R.B. 2007. *Use of Radon to Establish a Building-specific Sub-slab Attenuation Factor for comparison with Similar Quantities measured for Other Vapor Intrusion Contaminants*. Presented at the National Environmental Monitoring Conference, Cambridge, MA, August 19–25.
- Mosley, R.B., D. Greenwell, A. Lee, K. Baylor, M. Plate, and C. Lutes. 2008. *Use of Integrated Indoor Radon and Volatile Organic Compounds (VOCs) to Distinguish Soil Sources from Above-Ground Sources*. Extended abstract and oral presentation, AWMA Symposium on Air Quality Measurement and Technology, Chapel Hill NC, November 6.
- Mosley, R.B., D. Greenwell, and C.C. Lutes. 2010. Use of integrated indoor concentrations of tracer gases and volatile organic compounds (VOCs) to distinguish soil sources from above-ground sources. Poster presented at the *Seventh International Remediation of Chlorinated and Recalcitrant Compounds Conference*, Monterey, CA, May 24–27.
- Murry, D.M., and D.E. Burmaster. 1995. Residential air exchange rates in the United States: Empirical and estimated parametric distributions by season and climatic region. *Risk Analysis* 15(4):459–65.
- National Weather Service. 2012. *Excessive Heat - An Underrated Problem*. National Weather Service Regional Office, Central Regional Headquarters. Available at <http://www.crh.noaa.gov/Image/lx/wcm/Heat/ExcessiveHeat.pdf>.

- Nau, R. 2005a. Duke University, Class Notes for Decision 411 Forecasting. Available at <http://people.duke.edu/~rnau/411diff.htm>.
- Nau, R. 2005b. Duke University, Class Notes for Decision 411 Forecasting. Available at <http://people.duke.edu/~rnau/411regou.htm>.
- Nazaroff, W.W. 1988. Predicting the rate of ²²²Rn entry from soil into the basement of a dwelling due to pressure-driven air flow. *Radiation Protection Dosimetry* 22(1/4):199–202.
- Nazaroff, W.W., and A.V. Nero (Eds.). 1988. *Radon and Its Decay Products in Indoor Air*. New York: John Wiley and Sons.
- Nazaroff, W.W., S.R. Lewis, S.M. Doyle, B.A. Moed, and A.V. Nero, 1987. Experiments on pollutant transport from soil into residential basements by pressure-driven airflow. *Environmental Science & Technology* 21:459–466.
- Neptune and Company. 2007. *Report for 2007 Annual Vapor Intrusion Sampling for Buildings N210 and 19 and Additional Baseline Sampling for Building 16*. Prepared for ISSi/SAIC NASA Ames Research Center Moffett Field, California 94035-1100 Neptune Project No 09501.
- New York Times*. 2012. *Toxic Waters: Indianapolis Water*. May 26. Available at <http://projects.nytimes.com/toxic-waters/contaminants/in/marion/in5249004-indianapolis-water>.
- Newton, E., and R. Rudela. 2007. Estimating correlation with multiply censored data arising from the adjustment of singly censored data. *Environmental Science and Technology* 41(1):221–228.
- NJ DEP (New Jersey Department of Environmental Protection). 2012. *Draft Vapor Intrusion Guidance*. January.
- NJ DEP (New Jersey Department of Environmental Protection). 2013. *Vapor Intrusion Technical Guidance*. January. Available at http://www.nj.gov/dep/srp/guidance/vaporintrusion/vig_main.pdf
- Odabasi, M. 2008. Halogenated volatile organic compounds from the use of chlorine-bleach-containing household products. *Environmental Science and Technology* 42:1445–1451.
- Odenchantz, J.E., H. O'Neill, S.J. Steinmacher, J.D. Case, and P.C. Johnson. 2008. Residential vapor intrusion evaluation: long duration passive sampling v. short duration active sampling. *Remediation Journal* 18(4):49–54. Available at <http://onlinelibrary.wiley.com/doi/10.1002/rem.20181/abstract>.
- Oury, B., F. Lhuillier, J. Protois, and Y. Moréle. 2006. Behavior of the GABIE, 3M3500, PerkinElmer Tenax TA, and RADIELLO 145 diffusive samplers exposed over a long time to a low concentration of VOCs. *Journal of Occupational and Environmental Hygiene* 3(10):547–557.
- Parker, G.B. 1985. Measurement of air exchange rates in residential and commercial buildings in the northwest: techniques and results. *PNL-SA-13507*. Presented at *Conference on Conservation in Buildings: Northwest Perspective*, Butte MT, May 20. Abstract available at http://www.osti.gov/energycitations/product.biblio.jsp?osti_id=5567459.

- Pennequin-Cardinala, A. et al. 2005. Performances of the Radiellos diffusive sampler for BTEX measurements: Influence of environmental conditions and determination of modeled sampling rates. *Atmospheric Environment* 39:2535–2544.
- Perron, P. 1988. Trends and random walks in macroeconomic time series. *Journal of Economic Dynamics and Control* 12:297–332.
- R Development Core Team. 2012. *R: A Language and Environment for Statistical Computing*. R Foundation for Statistical Computing, Vienna, Austria. Available at <http://www.R-project.org>.
- Razali, N., and Y.B. Wah. 2011. Power comparisons of Shapiro-Wilk, Kolmogorov-Smirnov, Lilliefors and Anderson-Darling tests. *Journal of Statistical Modeling and Analytics* 2(1):21–33. Available at <http://instatmy.org.my/downloads/e-jurnal%202/3.pdf>. Retrieved 5 June 2012.
- Revzan K.L., W.J. Fisk, and A.J. Gadgil. 1991. Modeling radon entry into houses with basements: model description and verification. *Indoor Air* 2:173–189.
- Robinson A.L., and R.G. Sextro. 1997. Radon entry into buildings driven by atmospheric pressure fluctuations. *Environmental Science and Technology* 31:1742–1748.
- Robinson, A.L., R.G. Sextro, and W.J. Fisk. 1997. Soil-gas entry into an experimental basement driven by atmospheric pressure fluctuations—Measurements, spectral analysis and model comparison. *Atmospheric Environment*, 31(10):1477–1485.
- Robinson, A.L., R.G. Sextro, and W.J. Riley. 1997. Soil-gas entry into houses driven by atmospheric pressure fluctuations - the influence of soil properties. *Atmospheric Environment* 31:1487–1495.
- Rorech, G. J. 2001. Vacuum Extraction and Bioventing, Chapter 3. In E.K. Nyer, et al. (Ed.). *In-situ Treatment Technology*, 2nd edition, Lewis.
- Ryan, J.V, P.M. Lemieux, and W.T Preston. 1998. Near-real-time measurement of trace volatile organic compounds from combustion processes using an on-line gas chromatograph. *Waste Management* 18(6):403–410.
- Said, S.E. and D.A. Dickey. 1984. Testing for unit roots in autoregressive-moving average models of unknown order. *Biometrika* 71:599–607.
- Scheeringa, K., and K. Hudson. 2011–2013. *Monthly Climate Summaries*. Indiana State Climate Office. Available at <http://iclimate.org/summary.asp>.
- Schumacher, B., J. Zimmerman, C. Lutes, B. Cosky, R. Truesdale, R. Norberg and B. Hartman. 2013. Indoor Air and Soil Gas Temporal Variability: Effects on Sampling Strategies Evidence from Controlled and Uncontrolled Conditions. Oral Presentation at an EPA Organized Workshop, *Looking Beyond Natural Variation in Vapor Intrusion: Understanding, Controlling and Addressing Site Variables for Improved Practices and Effective Protection Strategies*, at the 23rd Annual International Conference on Soil, Water, Energy and Air, San Diego, CA. March 19.
- Schumacher, B., J. Zimmerman, G. Swanson, J. Elliot, and B. Hartman. 2010. Field observations on ground covers/buildings. Presented at the 20th Annual International Conference on Soils, Sediments, Water, and Energy, San Diego, CA. March 16.

- Schuver, H. 2013. Radon as a tracer and risk driving co-contaminant in chemical vapor intrusion. Presentation at *RemTec 2013 Summit*, Westminster, CO, March 6.
- Schuver, H., and L. Siegel. 2011. Vapor intrusion: involved-stakeholder awareness of the uncertainty (and multiple benefits of controls). *Community Involvement Training Conference*, Crystal City VA, July. Available at http://epa.gov/ciconference/download/presentations/Wed_OpenTime%20Session_Salon6_SchuverSiegel.pdf.
- Schuver, H.J., and R.B. Mosley. 2009. Investigating vapor intrusion with confidence and efficiency (some observations from indoor air-based radon intrusion studies). *AWMA Vapor Intrusion 2009*, San Diego, CA.
- Sigma-Aldrich. 2012. *Radiello Manual, Volatile Organic Compounds (VOCs) Chemically Desorbed with CS₂, Supelco Edition*. Available at http://www.sigmaaldrich.com/content/dam/sigmaaldrich/docs/Supelco/Application_Notes/radiello_d1_d6.pdf, accessed August 2012.
- Smajstrla, A.G., and D.S. Harrison. 1998. *Tensiometers for Soil Moisture Measurement and Irrigation Scheduling*. CIR487. Agricultural and Biological Engineering Department, Florida Cooperative Extension Service, Institute of Food and Agricultural Sciences, University of Florida. Available at <http://edis.ifas.ufl.edu/ae146>.
- Steck, D.J. 2012. An update on the draft of "Lessons from radon for vapor intrusion research and programs". Presented at EPA-AEHS Workshop, *Recent Advances to VI Application & Implementation*, San Diego, CA. March.
- The Polis Center. 2012. *Study Neighborhoods from the Project on Religion and Urban Culture: Mapleton-Fall Creek*. Footnote 2. The Polis Center, Indianapolis, IN. Available at http://www.polis.iupui.edu/RUC/Neighborhoods/MapletonFallCreek/MFCNarrative.htm#_ftn2.
- Thomas, R.G. 1990. Volatilization from Soil, Chapter 16. In W.J. Lyman, et al. (Eds.). *Handbook of Chemical Property Estimation Methods*. American Chemical Society.
- Thomson, N.R. and D.J. Flynn. 2000. Soil vacuum extraction of perchloroethylene from the Borden aquifer. *Groundwater* 38(5): 673-688.
- Truesdale, R., H. Dawson, and I. Hers. 2005. Vapor intrusion database status and updates. Presented at *Specialty Workshop on Integrating Observed and Modeled Vapor Attenuation, AEHS 15th Annual West Coast Conference on Soils, Sediments and Water*, San Diego, CA. March 14. Available at http://iavi.rti.org/attachments/Resources/1045_-_Truesdale_Vapor_Intrusion_Database_Status_and_Updates.pdf.
- U.S. DOE (Department of Energy). *Innovative Technology Summary Report: Frozen Soil Barrier*. DOE/EM-0483 October 1999.
- U.S. EPA (Environmental Protection Agency). 1990. *NAREL Standard Operating Procedures for Radon-222 Measurement Using Diffusion Barrier Charcoal Canisters*. EPA 520/5-90/032 Stock Number PB91-179002. U.S. EPA National Air and Radiation Environmental Lab., Montgomery AL.

-
- U.S. EPA (Environmental Protection Agency). 1992. *Indoor Radon and Radon Decay Product Measurement, Device Protocols*. EPA 402-R-92-004, Office of Radiation Programs, Washington, DC, July (revised).
- U.S. EPA (Environmental Protection Agency). 1993a. *Protocols for Radon and Radon Decay Product Measurements in Homes*. EPA-402-R-92-003, May 1993a.
- U.S. EPA (Environmental Protection Agency). 1993b. *Radon Reduction Techniques for Existing Detached Houses, Technical Guidance (third edition) for Active Soil Depressurization Systems*. EPA/625/R-93/011.
- U.S. EPA (Environmental Protection Agency). 1999a. *Compendium of Methods for the Determination of Toxic Organic Compounds in Ambient Air, Second Edition, Compendium Method TO-14Ab: Determination of Volatile Organic Compounds (VOCs) in Ambient Air Using Specially Prepared Canisters With Subsequent Analysis By Gas Chromatography*. EPA/625/R-96/010b. Available at <http://www.epa.gov/ttnamti1/files/ambient/airtox/to-14ar.pdf>.
- U.S. EPA (Environmental Protection Agency). 1999b. *Compendium of Methods for the Determination of Toxic Organic Compounds in Ambient Air Second Edition Compendium Method TO-15 Determination of Volatile Organic Compounds (VOCs) in Air Collected in Specially-Prepared Canisters and Analyzed by Gas Chromatography Mass Spectrometry (GC/MS)*. EPA/625/R-96/010b. Available at <http://www.epa.gov/ttnamti1/files/ambient/airtox/to-15r.pdf>.
- U.S. EPA (Environmental Protection Agency). 1999c. *Compendium of Methods for the Determination of Toxic Organic Compounds in Ambient Air, Second Edition, Compendium Method TO-17, Determination of Volatile Organic Compounds in Ambient Air Using Active Sampling Onto Sorbent Tubes*. EPA/625/R-96/010b. Available at <http://www.epa.gov/ttnamti1/files/ambient/airtox/to-17r.pdf>.
- U.S. EPA (Environmental Protection Agency). 2002a. *OSWER Draft Guidance for Evaluating the Vapor Intrusion to Indoor Air Pathway from Groundwater and Soils (Subsurface Vapor Intrusion Guidance)*. EPA530-D-02-004. Available at <http://www.epa.gov/correctiveaction/eis/vapor.htm>
- U.S. EPA (Environmental Protection Agency). 2002b. *Guidance on Environmental Data Verification and Validation*. EPA QA/G-8 EPA/240/R-02/004. November. Available at <http://www.epa.gov/quality/qs-docs/g8-final.pdf>.
- U.S. EPA (Environmental Protection Agency). 2003. *A Standardized EPA Protocol for Characterization of Indoor Air Quality in Large Office Buildings*. U.S. EPA Indoor Air Division and Atmospheric Research and Exposure Assessment Laboratory. Available at http://www.epa.gov/iaq/base/pdfs/2003_base_protocol.pdf.
- U.S. EPA (Environmental Protection Agency). 2005a. *DRAFT Standard Operating Procedure (SOP) for Installation of Sub-Slab Vapor Probes and Sampling Using EPA Method TO-15 to Support Vapor Intrusion Investigations*. Available at http://www.epa.gov/region8/r8risk/pdf/epa_sub-slabvapor.pdf.
- U.S. EPA (Environmental Protection Agency). 2005b. *DRAFT Assessment of Vapor Intrusion in Homes Near the Former Raymark Superfund Site - Recommendations for Testing at Other Sites*.
-

- U.S. EPA (Environmental Protection Agency). 2008. *Engineering Issue: Indoor Air Vapor Intrusion Mitigation Approaches*. EPA/600/R-08-115. National Risk Management Research Laboratory, Cincinnati, OH. <http://www.clu-in.org/download/char/600r08115.pdf>
- U.S. EPA (Environmental Protection Agency). 2008b. *U.S. EPA Contract Laboratory Program National Functional Guidelines for Superfund Organic Methods Data Review*. EPA-540-R-08-01. Office of Superfund Remediation and Technology Innovation, Washington, DC. June. Available at <http://epa.gov/superfund/programs/clp/download/somnfg.pdf>.
- U.S. EPA (Environmental Protection Agency). 2011. *Exposure Factors Handbook 2011 Edition (Final)*. EPA/600/R-09/052F. 2011. Office of Research and Development, Washington, DC.
- U.S. EPA (Environmental Protection Agency). 2012a. *Fluctuation of Indoor Radon and VOC Concentrations Due to Seasonal Variability*. EPA/600/R-12/673. Office of Research and Development, Las Vegas, NV. September. Available at <http://www.clu-in.org/download/contaminantfocus/vi/VI-EPA600-R-09-073.pdf>
- U.S. EPA (Environmental Protection Agency). 2012b. *EPA On-line Tools for Site Assessment Calculation: Johnson and Ettinger Attenuation Factor*. U.S. EPA Ecosystems Research, Athens, GA. Available at http://www.epa.gov/athens/learn2model/part-two/onsite/jne_alpha.htm.
- U.S. EPA (Environmental Protection Agency). 2012c. *EPA's Vapor Intrusion Database: Evaluation and Characterization of Attenuation Factors for Chlorinated Volatile Organic Compounds and Residential Buildings*. EPA 530-R-10-002. Office of Solid Waste and Emergency Response, Washington, DC. March. Available at http://www.epa.gov/oswer/vaporintrusion/documents/OSWER_2010_Database_Report_03-16-2012_Final_witherratum_508.pdf
- U.S. EPA (Environmental Protection Agency). 2012d. *Conceptual Model Scenarios for the Vapor Intrusion Pathway*. Office of Solid Waste and Emergency Response, Washington, DC. Available at <http://www.epa.gov/oswer/vaporintrusion/documents/vi-cms-v11final-2-24-2012.pdf>.
- U.S. EPA (Environmental Protection Agency). 2012e. *Drinking Water Contaminants*. Available at <http://water.epa.gov/drink/contaminants/index.cfm>.
- U.S. EPA (Environmental Protection Agency). 2012f. *Petroleum Hydrocarbons and Chlorinated Hydrocarbons Differ In Their Potential for Vapor Intrusion*. Information Paper. Office of Underground Storage Tanks, Washington, DC. March. Available at <http://www.epa.gov/oust/cat/pvi/pvicvi.pdf>.
- U.S. EPA (Environmental Protection Agency). 2012g. *A Citizen's Guide to Radon*. EPA 402-K-12-002. Office of Air and Radiation, Indoor Environments Division. Washington, DC. May. <http://www.epa.gov/radon/pubs/citguide.html>.
- U.S. EPA (Environmental Protection Agency). *In press. Geophysical Investigations at the Indianapolis Vapor Intrusion Study House, 420 and 422 East 28th St., Indianapolis, IN*. EPA/600/R-13/184. Office of Research and Development, National Exposure Research Laboratory. Las Vegas, NV.
- University of Minnesota. 2008. *Re-Arch: The Initiative for Renewable Energy in Architecture*. Fact Sheet. University of Minnesota Initiative for Renewable Energy in Architecture (re-ARCH). Available at <http://www.rearch.umn.edu/factsheets/VentilationFactSheet.pdf>.

- Wang, F., and I.C. Ward. 2000. The development of a radon entry model for a house with a cellar. *Building and Environment* 35:615–631.
- Wania, F., J.T. Hoff, C.Q. Jia, and D. Mackay. 1998. The effects of snow and ice on the environmental behaviour of hydrophobic organic chemicals. *Environmental Pollution* 102(1):25–41.
- Wertz, W., and T. Festa. 2007. The patchy fog model of vapor intrusion. Pp. 28–36 in *Proceedings of AWMA Conference on Vapor Intrusion: Learning from the Challenges*, Providence, RI, September 26–28. Pittsburgh, PA: Air and Waste Management Association.
- White, R.G. 1964. Determination of carbon disulfide in benzene by ultraviolet spectrophotometry. *Applied Spectroscopy* 18(4):112–113.
- Whitmore, A., and R.L. Corsi. 1994. Measurement of gas-liquid mass transfer coefficients for volatile organic compounds in sewers. *Environmental Progress* May:114–123.
- Wickham, H. 2009. *ggplot2: Elegant Graphics for Data Analysis*. New York: Springer.
- Wilson, L.G., L.G. Everett, and S.J. Cullen (Eds.). 1995. *Handbook of Vadose Zone Characterization and Monitoring*. Boca Raton, FL: Lewis Publishers.
- Winberry, W. T., L. Forehand, N.T. Murphy, A. Ceroli, B. Phinney, and A. Evans. 1990. *Compendium of Methods for the Determination of Air Pollutants in Indoor Air*. EPA/600/4-90/010. U.S. Environmental Protection Agency, Office of Research and Development, Research Triangle Park, NC. April.
- Wisbeck D., C. Sharpe, A. Frizzell, C. Lutes, and N. Weinberg. 2006. Using naturally occurring radon as a tracer for vapor intrusion: a case study. ARCADIS, presented at the 2006 *Society of Risk Analysis (SRA) Annual Meeting*, Baltimore, MD.
- Yamazawaa, H., T. Miyazakia, J. Moriizumia, T. Iidaa, S. Takedab, S. Nagarab, K. Satob, and T. Tokizawab. 2005. High levels of natural radiation and radon areas: radiation dose and health effects. *Proceedings of the 6th International Conference on High Levels of Natural Radiation and Radon Areas*. International Congress Series. 1276:221–222. February. Available at <http://www.sciencedirect.com/science/article/pii/S0531513104017947>
- Yao, Y., K.G. Pennell, and E.M. Suuberg. 2010. *Proceedings of the Air & Waste Management Association's Vapor Intrusion 2010 Conference*. September 29–30. Available at <http://www.clu-in.org/download/contaminantfocus/vi/The%20Influence%20of%20Transient%20Processes.pdf>
- Yeates, G.L., and D.M. Nielsen. 1987. Design and implementation of an effective soil gas monitoring program for four-dimensional monitoring of volatile organics in the subsurface. In *Proceedings of the NWWA Focus Conference on Ground Water Issues*. Indianapolis, IN. April 21–23.
- Zhao, Y., and C. Frey. 2006. Uncertainty for data with non-detects: air toxic emissions from combustion. *Human and Ecological Risk Assessment* 12:1171–1191.

Appendix A.

Radon Mitigation System Photos and Field Diagnostic Report

MITIGATION PHOTOS



#1



#2



#3



#4



#5



#6

MITIGATION PHOTOS



#7



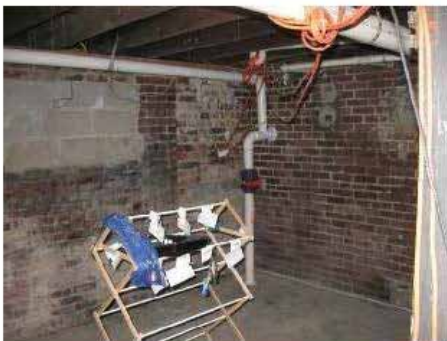
#8



#9



#10



#11



#12

MITIGATION PHOTOS



#13



#14



#15



#16



#17



#18

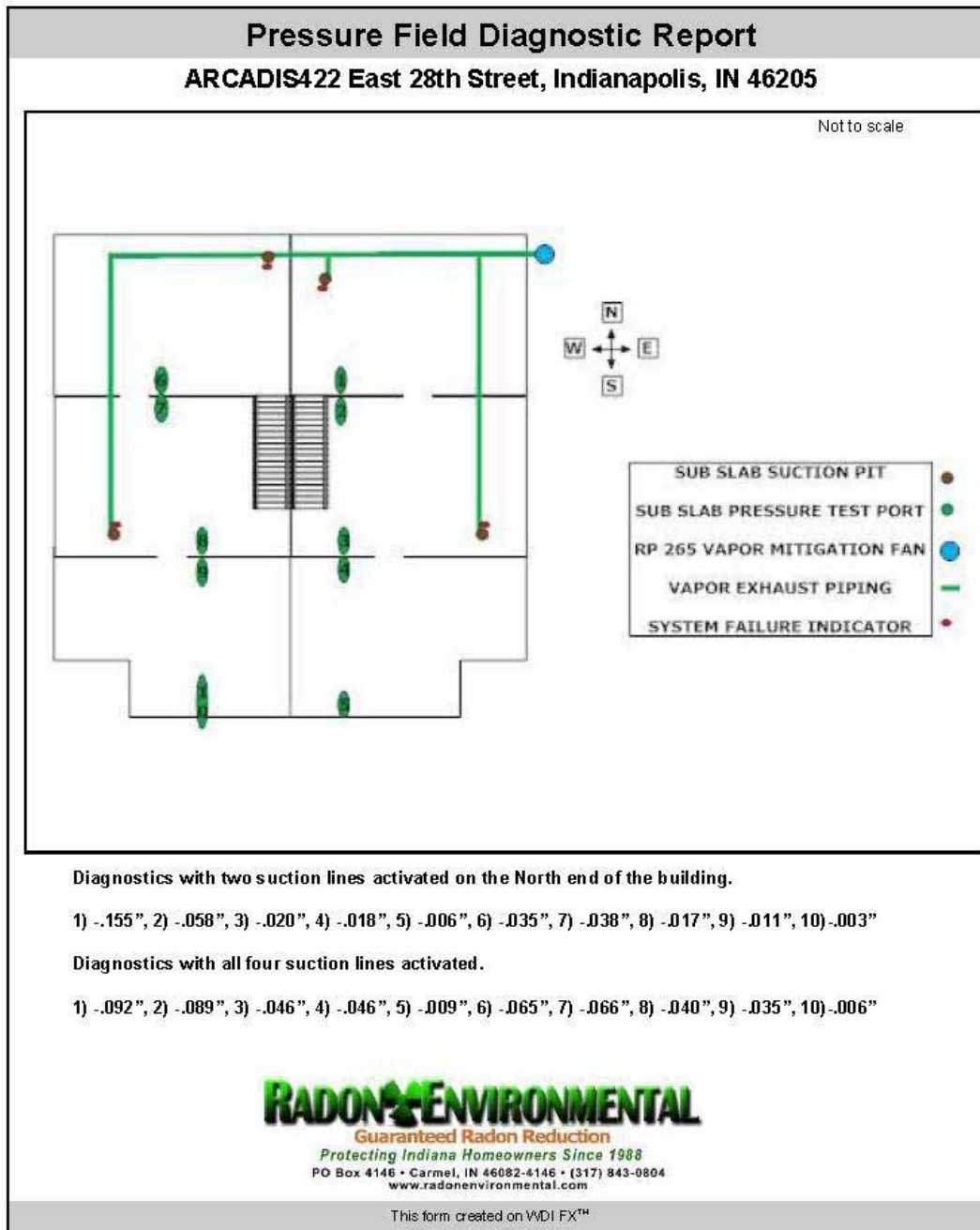
MITIGATION PHOTOS



#19



#20



PDF created with pdfFactory trial version www.pdffactory.com

PDF created with pdfFactory trial version www.pdffactory.com

Air Pressure Field Diagnostic Revised Report

1) The sequence you went through of changing the blower and the reasoning for it?

To determine what style of fan unit to install for our mitigation system we take into account several factors. We look at the age of the building, soil type under the slab, air pressure field diagnostics and the air pressure reading on the system failure indicator (Mini U-Tube). Before any work is performed, we make educated guesses on what type of fan unit by the age of the building. Usually older buildings prove to be more difficult in moving air under the slab. This lack of air flow is typically due to the lack of gravel, and perforated drain tile. Also an older building will usually have tighter soil under the slab. The combination of these factors usually means we will install a high pressure fan unit, which is designed to handle a greater air pressure/work load to pull air through the tighter soil.

In this particular installation process, we had a home built in the early 1900's with Sand/Dirt/Coal Slag as the soil mix. These initial factors normally indicate a high pressure fan will be needed. Chris Jordan, the lead technician installed a high pressure fan in the beginning of the installation process, which seemed to be the right choice with only two suction points according to our air pressure field diagnostics and more importantly our U-Tube pressure readings (Inches Per Water Column). However, Chris discovered that after installing the third and fourth suction points, a high pressure fan was no longer needed as the additional suction points increased the negative air pressures and allowed the fan unit to not have to work as hard to move air through the PVC piping (meaning the pressure readings on the Mini U-Tube monitor dropped below 2").

When the pressure reading on the Mini U-Tube monitor drops below 2 inches per water column (2" is a measurement we use as a company guideline for our installation process. A fan manufacturer lists the max pressure a fan unit can handle and most of the high flow fan units can handle greater pressures than 2", but our experience has found they tend to not have a very long life span if they are running above 2" on the U-Tube monitor), then a high pressure fan unit is no longer required. Chris at that point installed a larger high flow Radon Away fan unit (RP 265 max pressure of 2.5"/water column). The initial high pressure fan unit installed was a Radon Away GP 501 with a max pressure limit of 4.2". The high flow fans move more air than the high pressure fan units. Ultimately the more air we can move under the slab the better chance of success we will have in lower the radon and vapor levels. The pressure readings for each U-Tube after the full installation was complete are written on our company's labels next to the U-Tubes.

2) What instrument was being used?

To measure air pressure under the slab we use an Infiltec Digital Micro-Manometer and to measure the pressures of air flow through the PVC piping we use a Mini U-Tube Failure Indicator Monitor.

3) What date the measurements were made on?

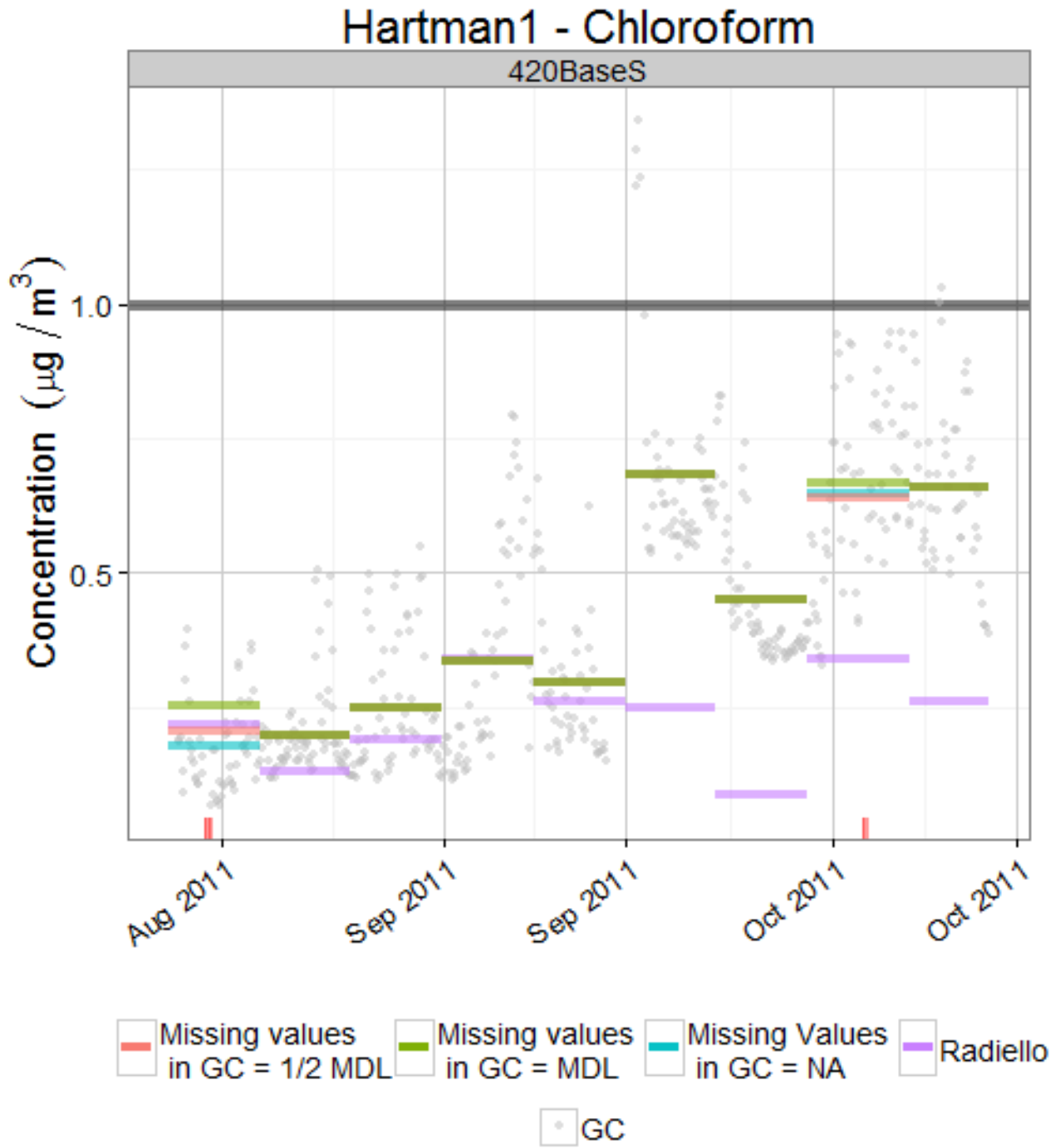
4) Whether these are single data points or averages over some time?

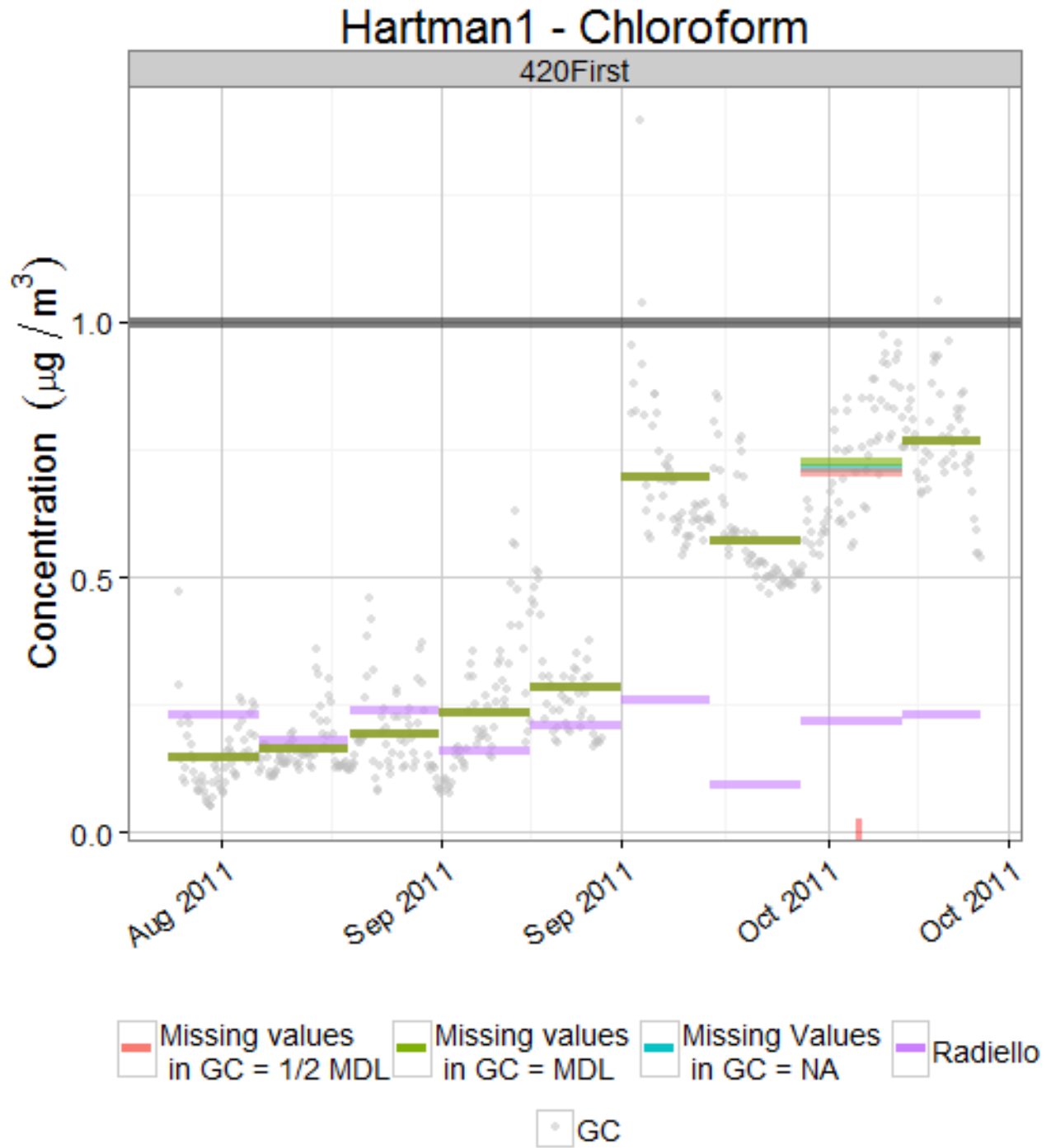
The installation process began on Tuesday, October 16th, 2012. That first day we performed a preliminary air pressure field diagnostic test and air pressure readings after each suction point was installed. The report has two sets of measurements listed. The first set of readings are air pressure measurements after the second suction line was installed. The diagnostic measurements help us gauge

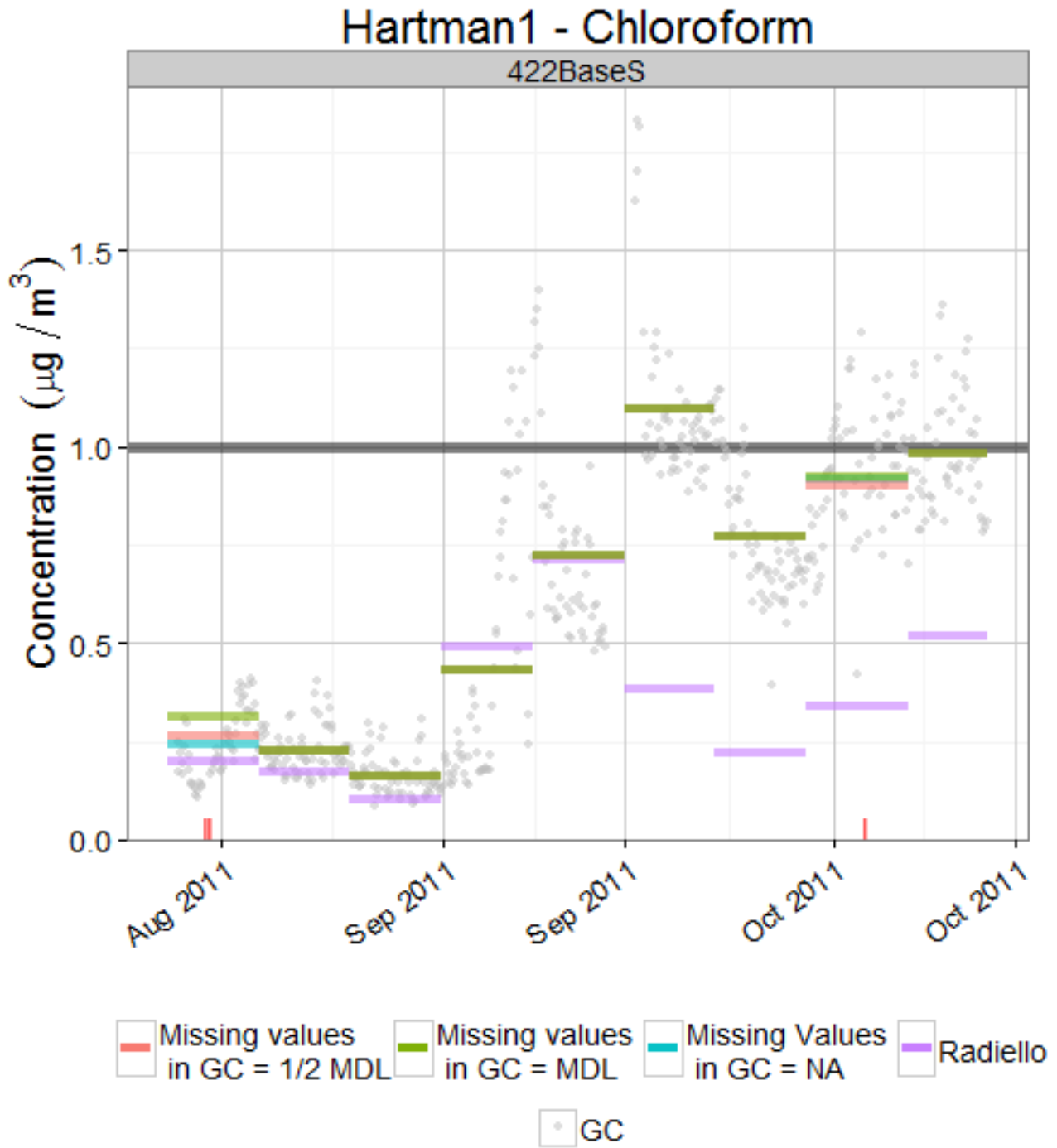
how much dirt/gravel to dig out from each suction point and how many suction points are needed. Wednesday, October 17th was the final day of the installation. The air pressure readings on October 17th were taken after all four suction lines were installed. The measurements provided are not an average, rather one last single reading after the technician was satisfied with the design and performance of the system.

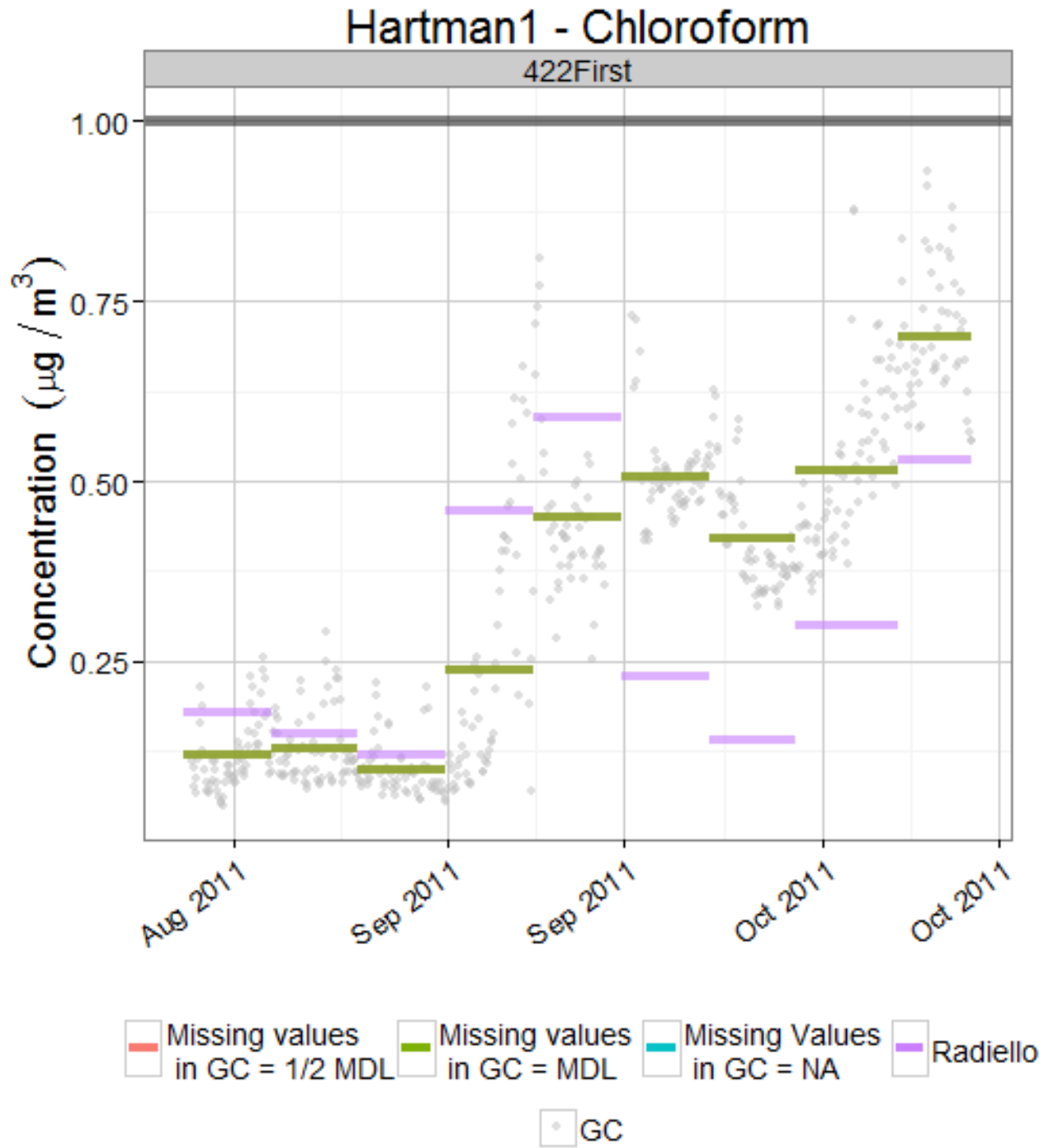
Appendix B.

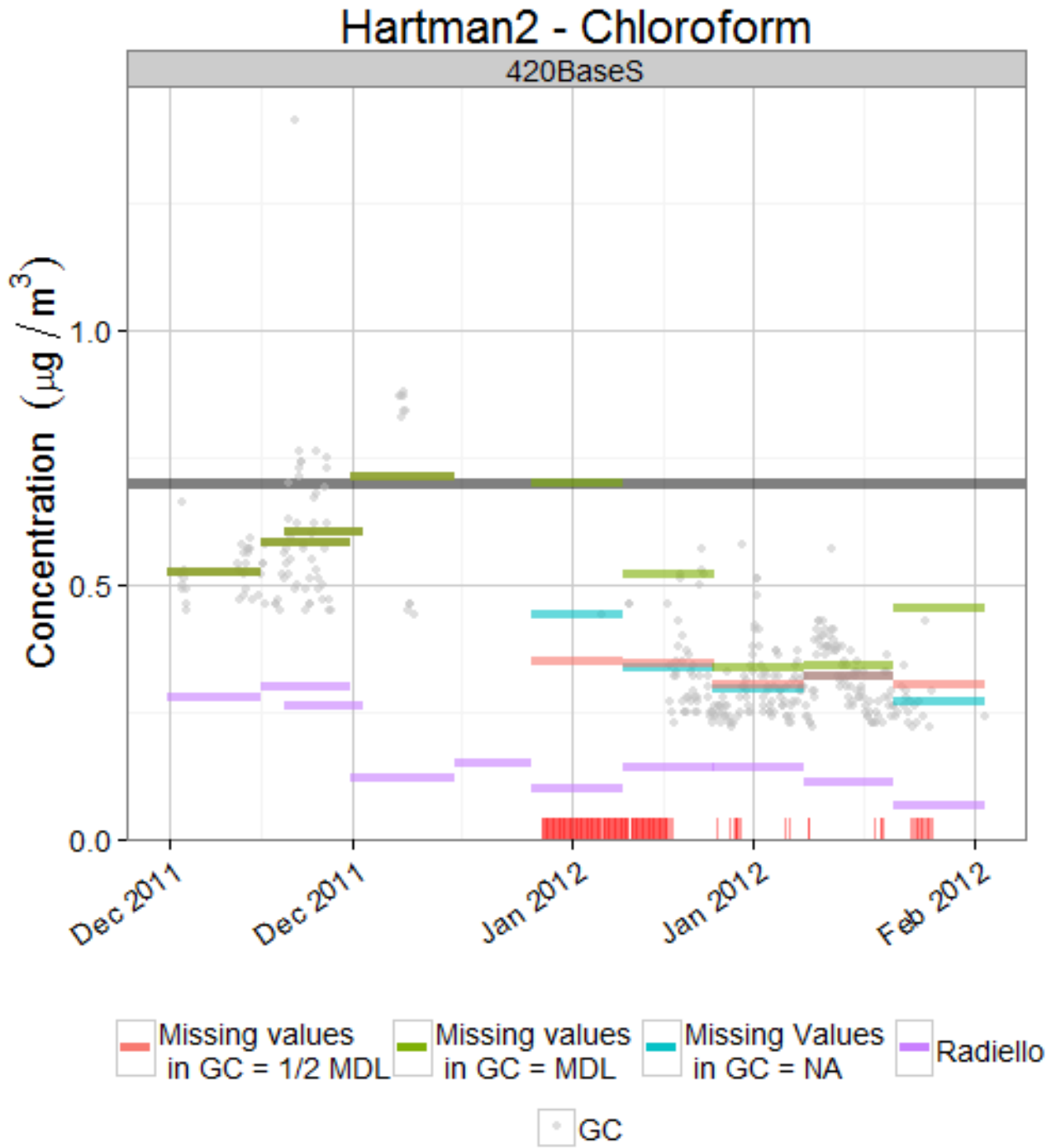
Plots Comparing Onsite GC with Weekly Radiello Indoor Air Results by Chemical, Sampling Period, and Sample Location

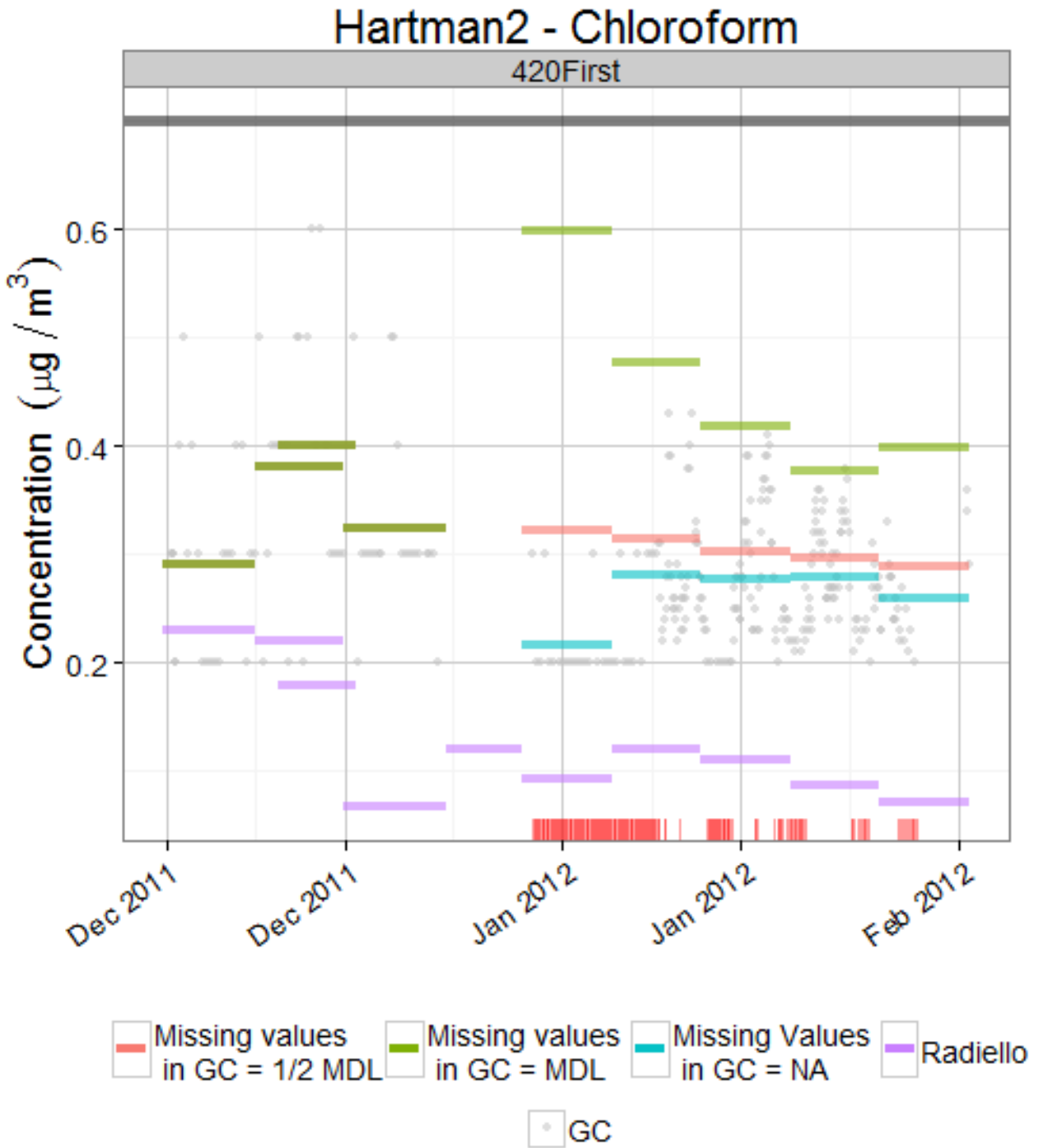


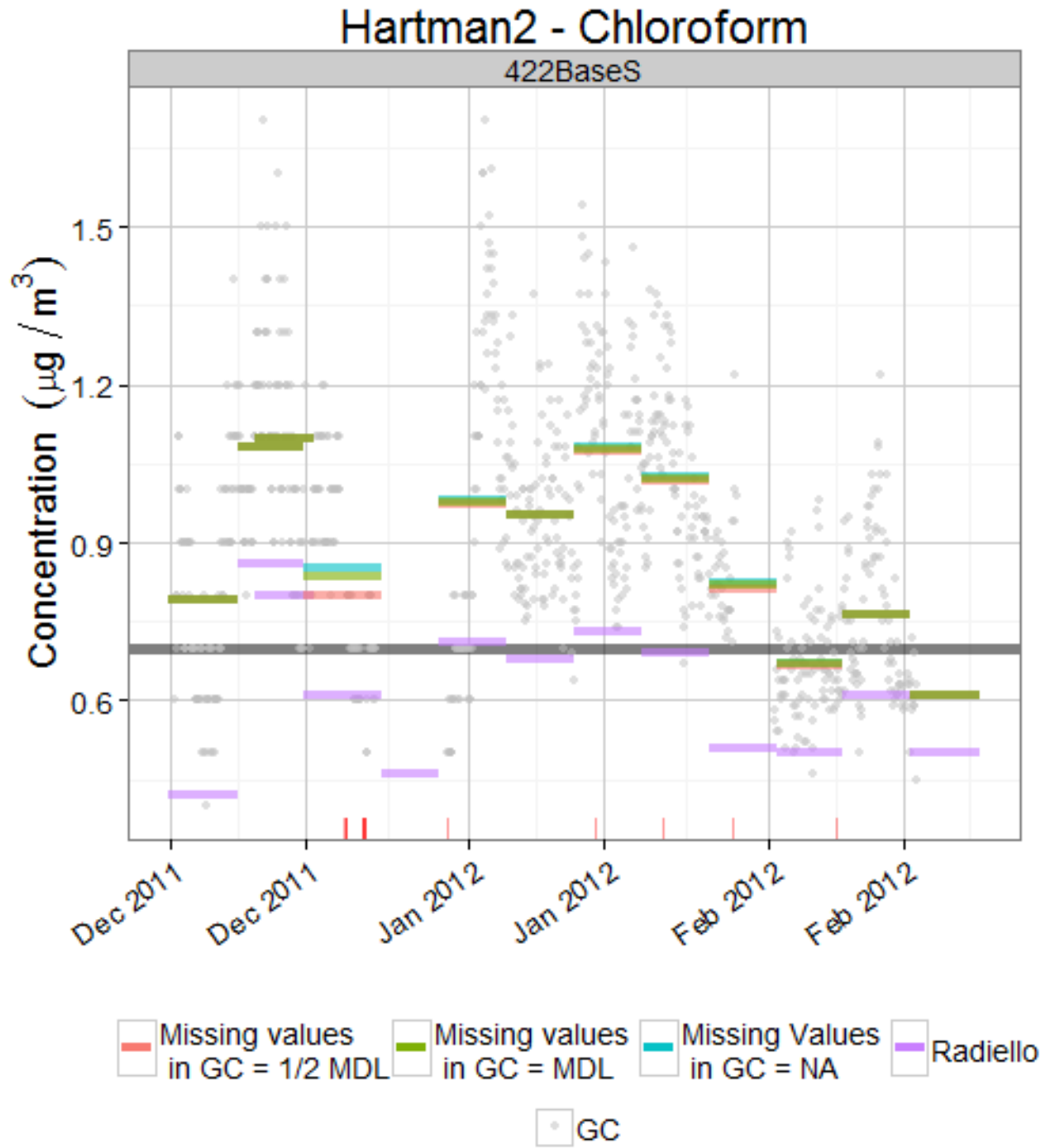


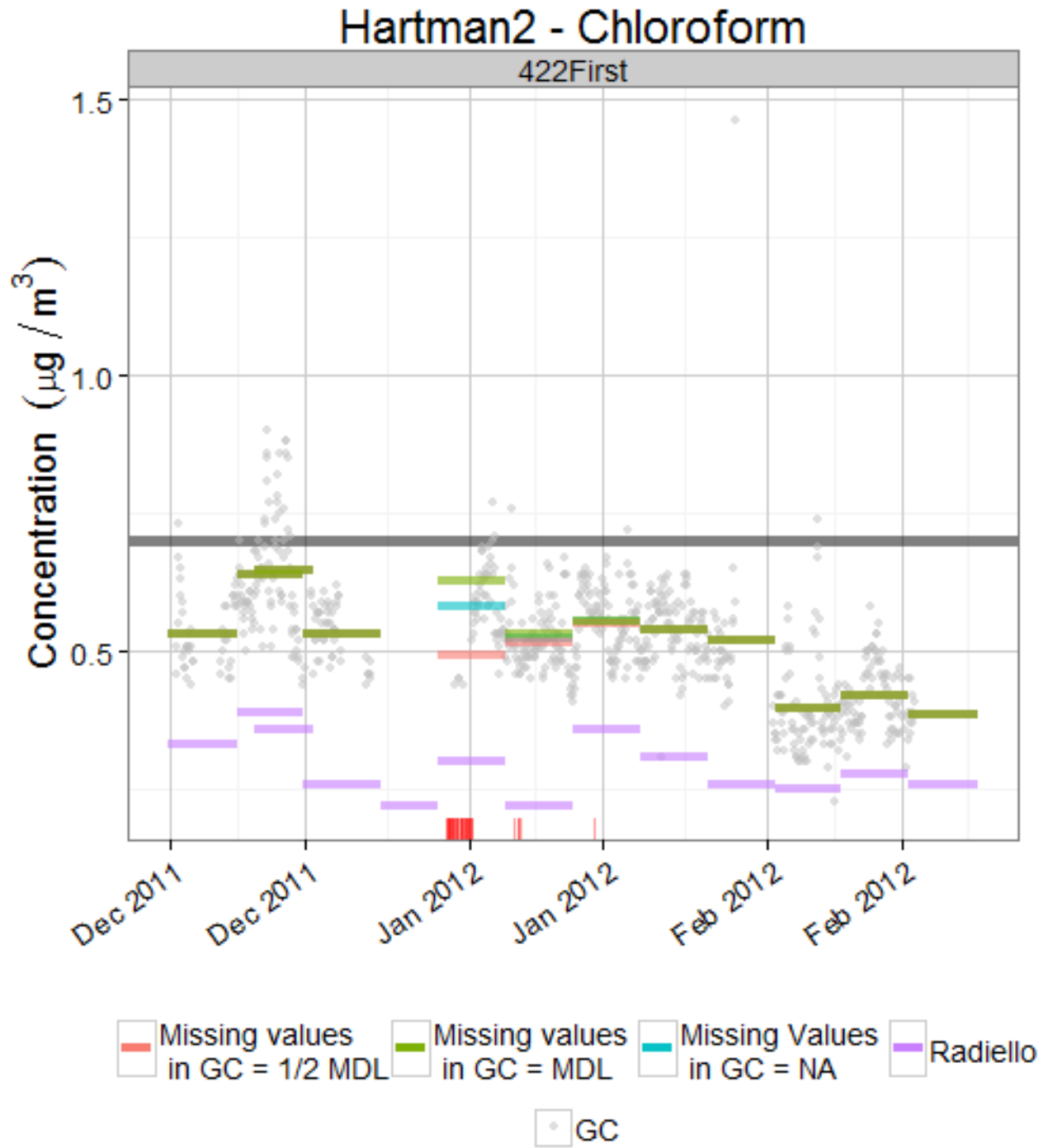


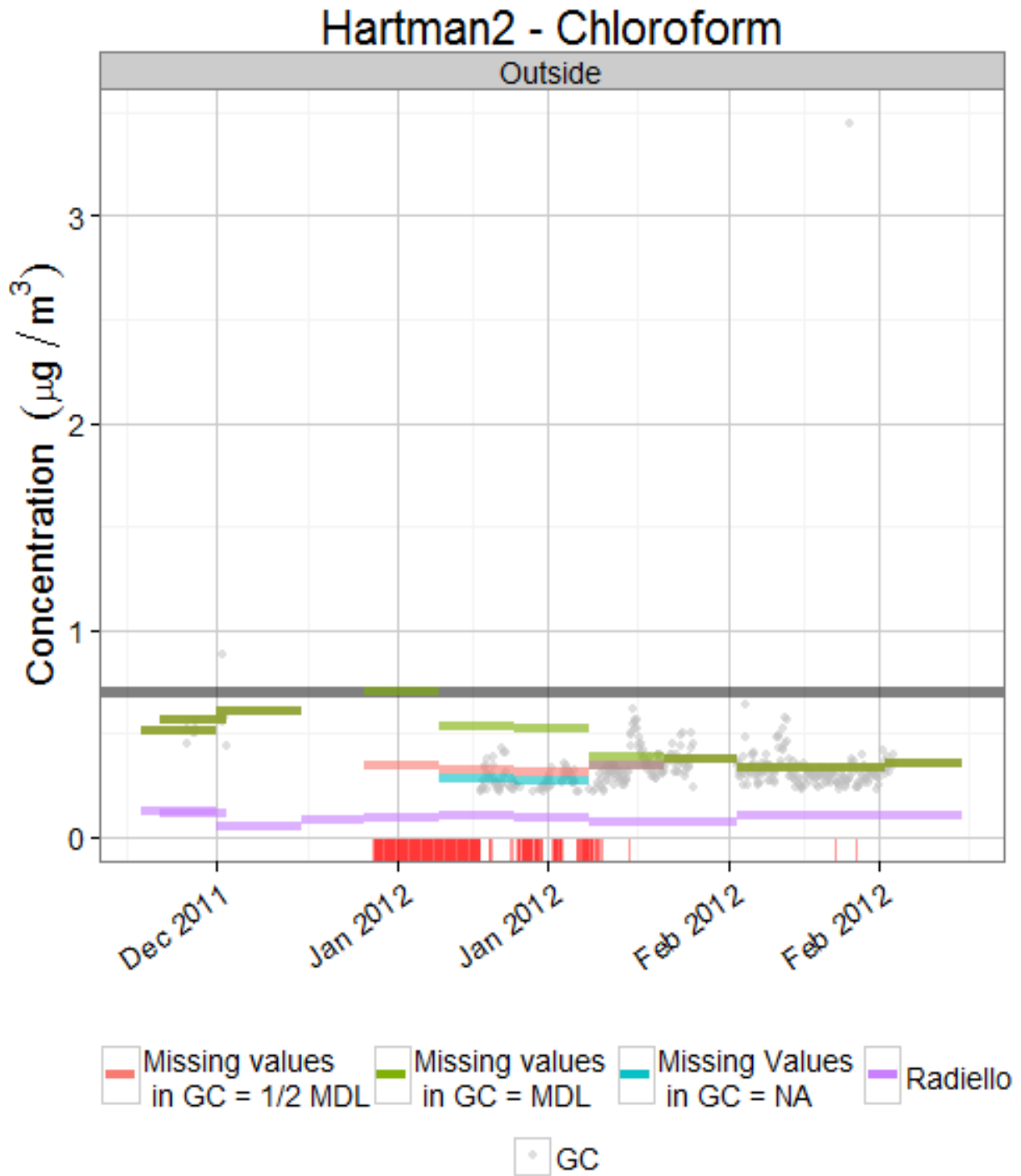


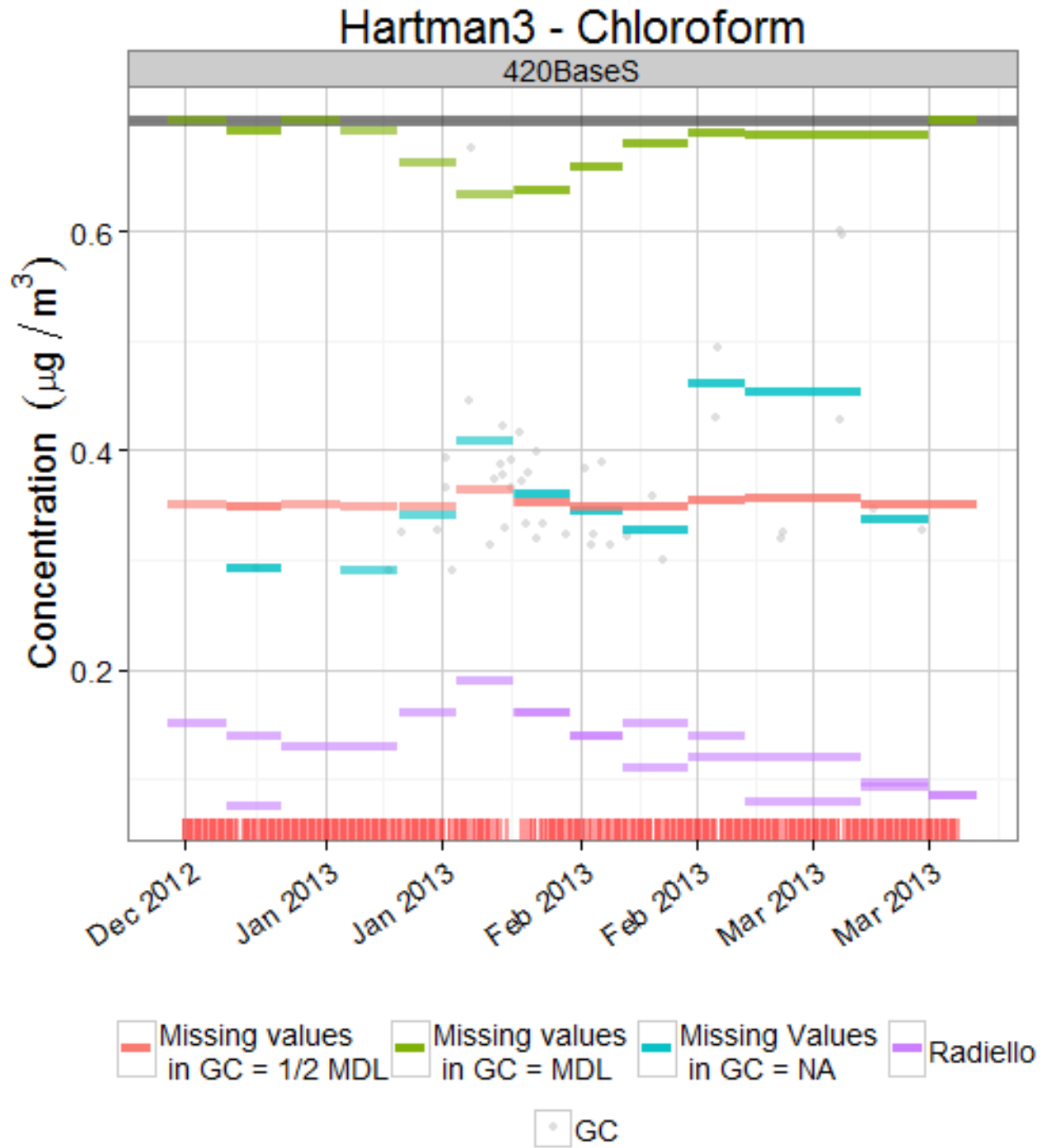


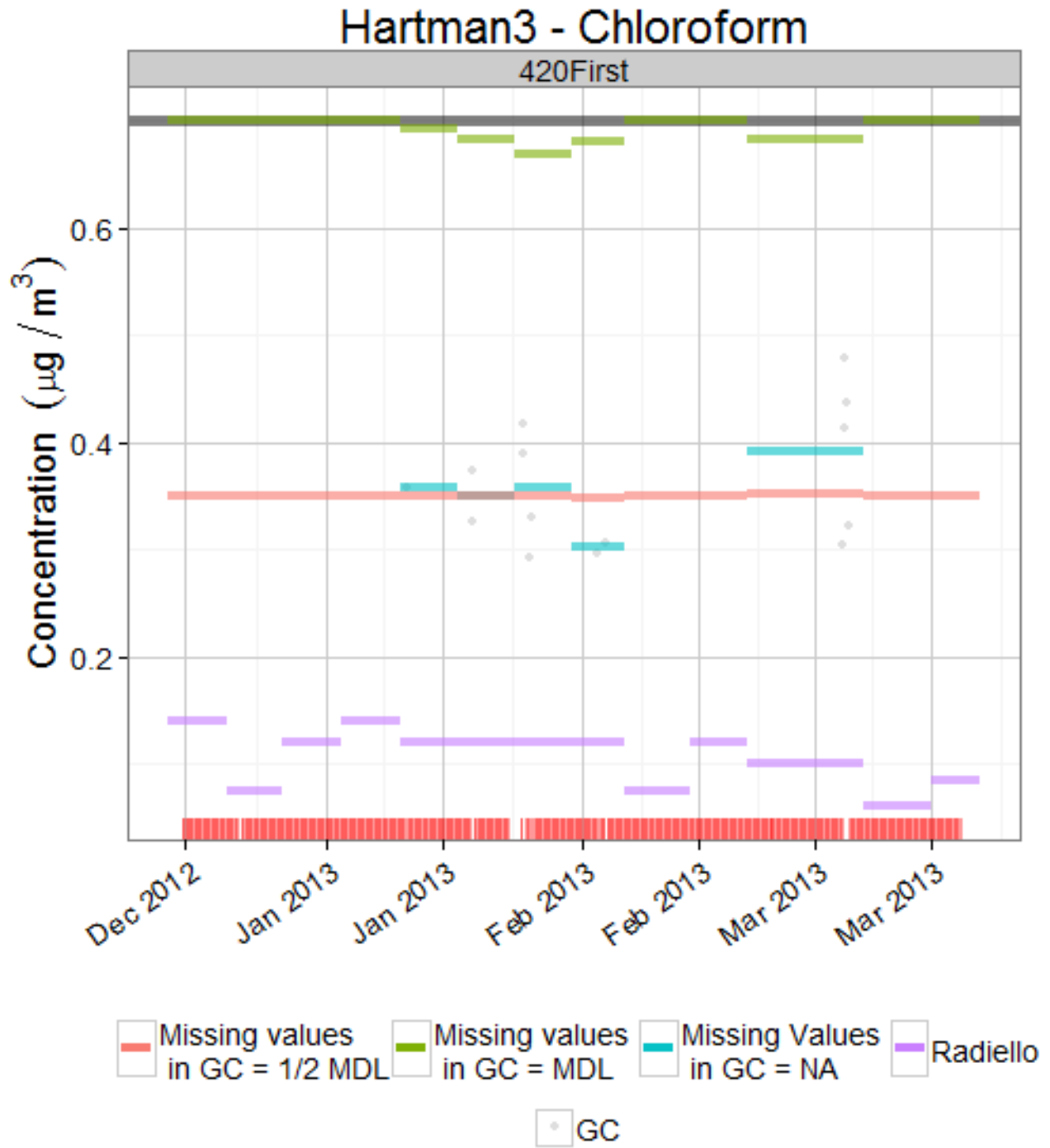


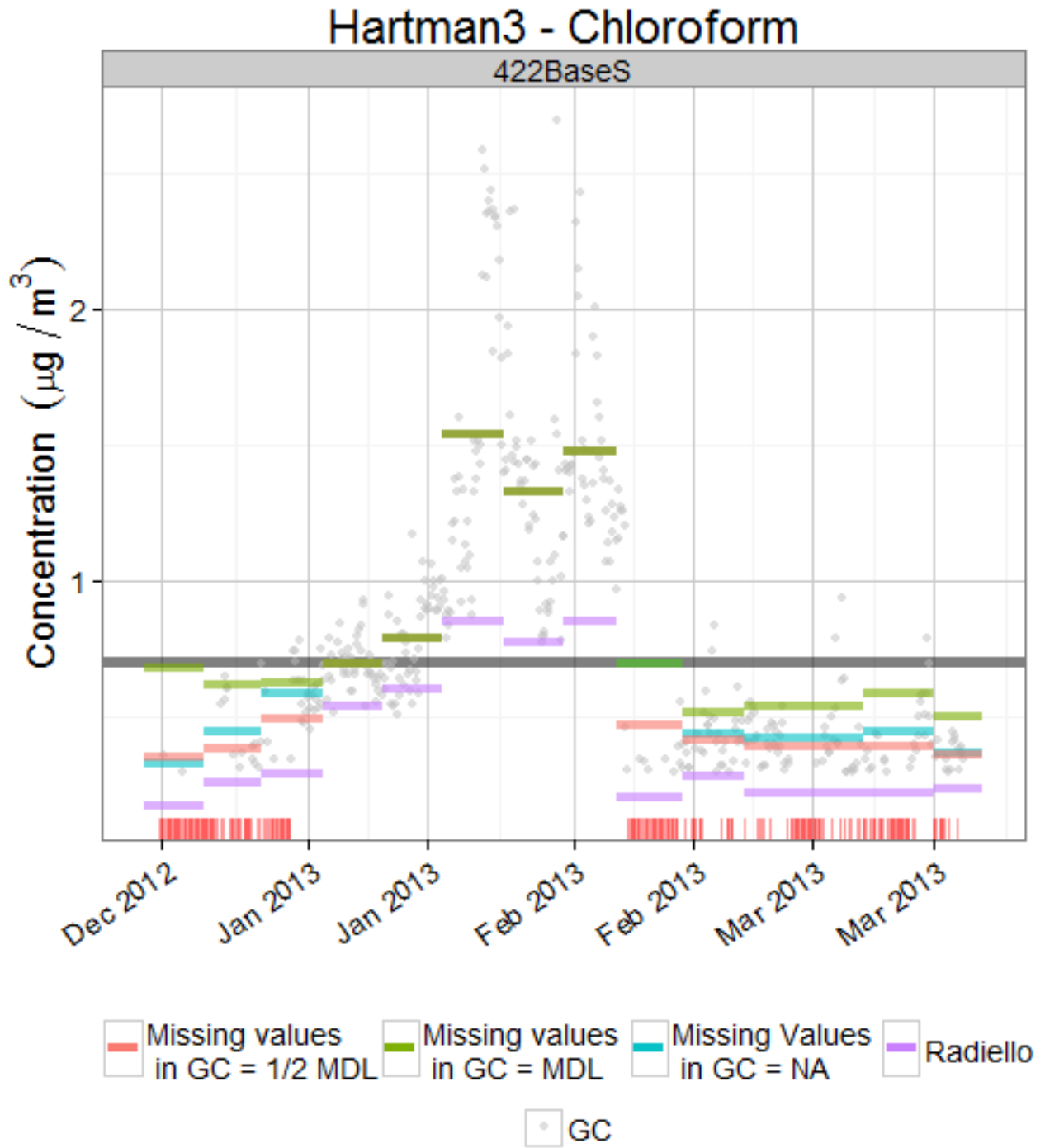


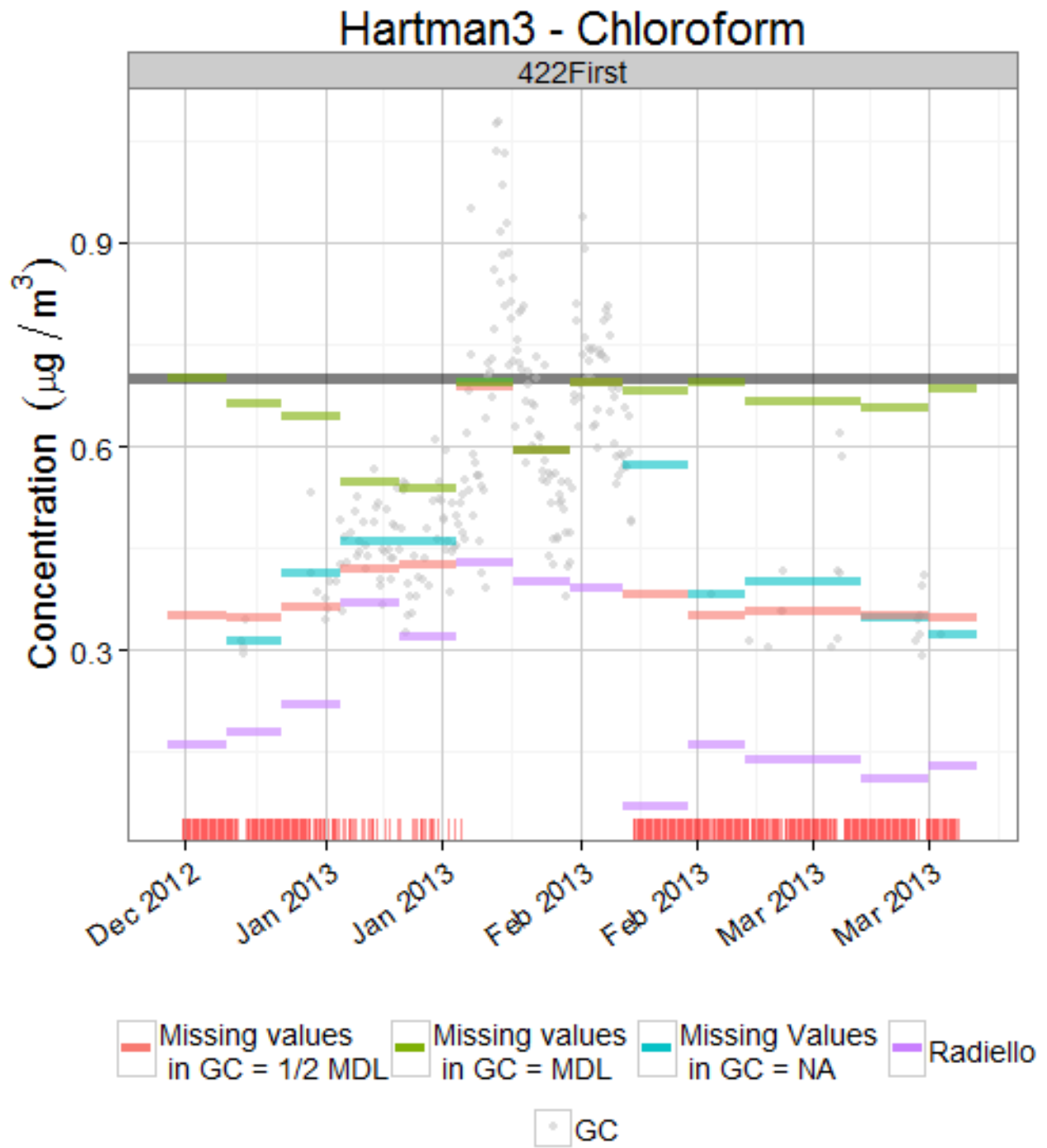


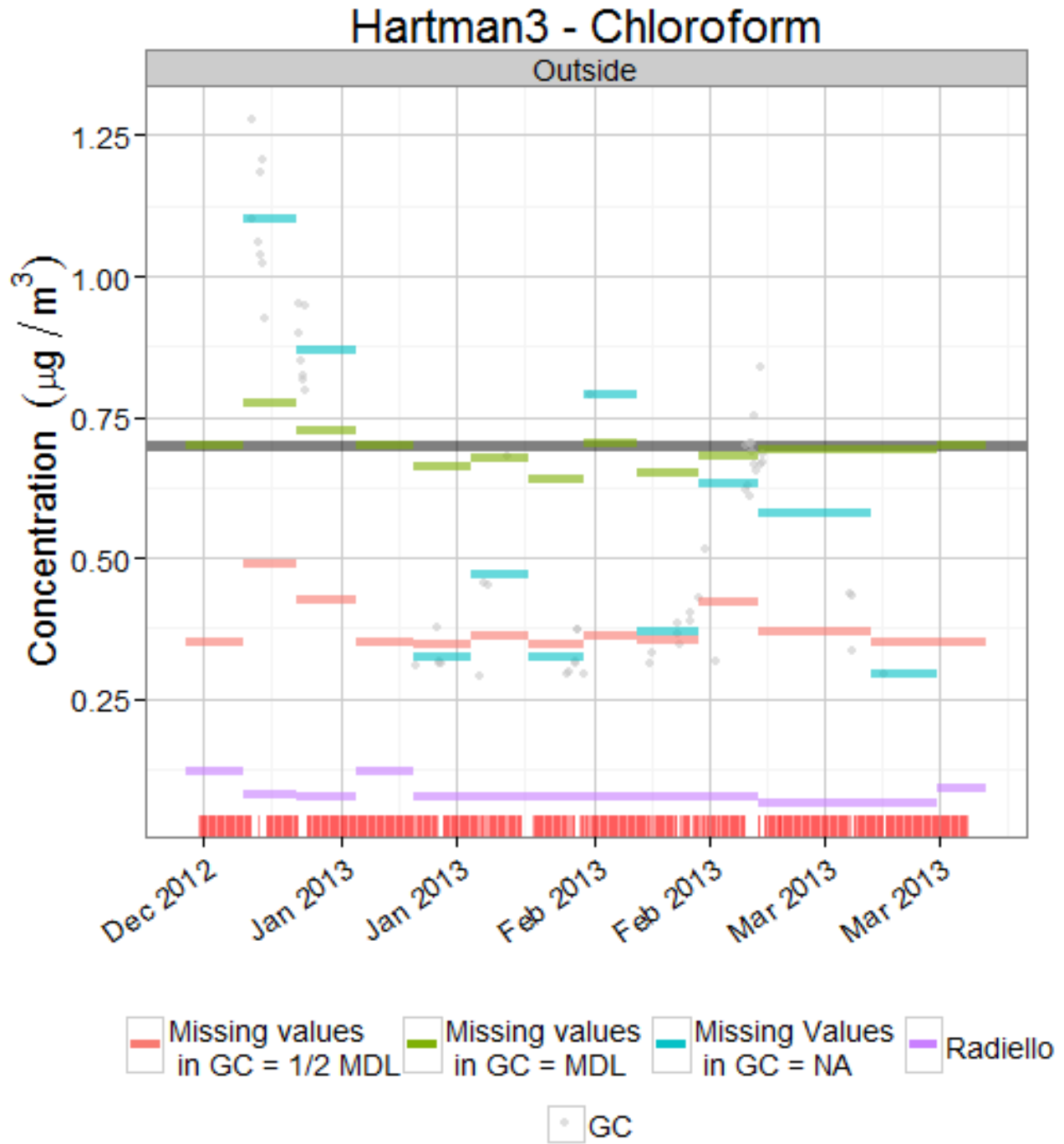


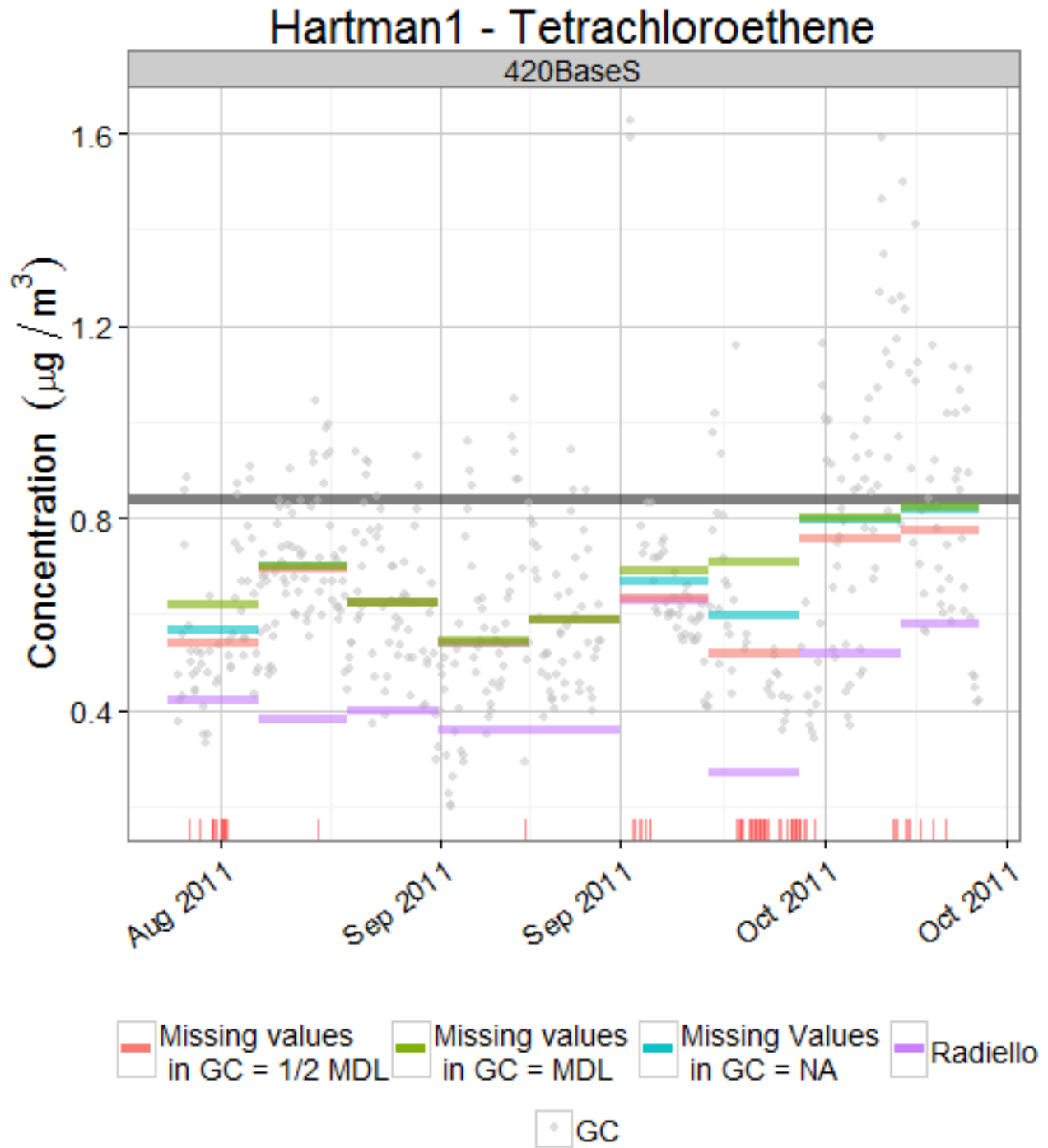


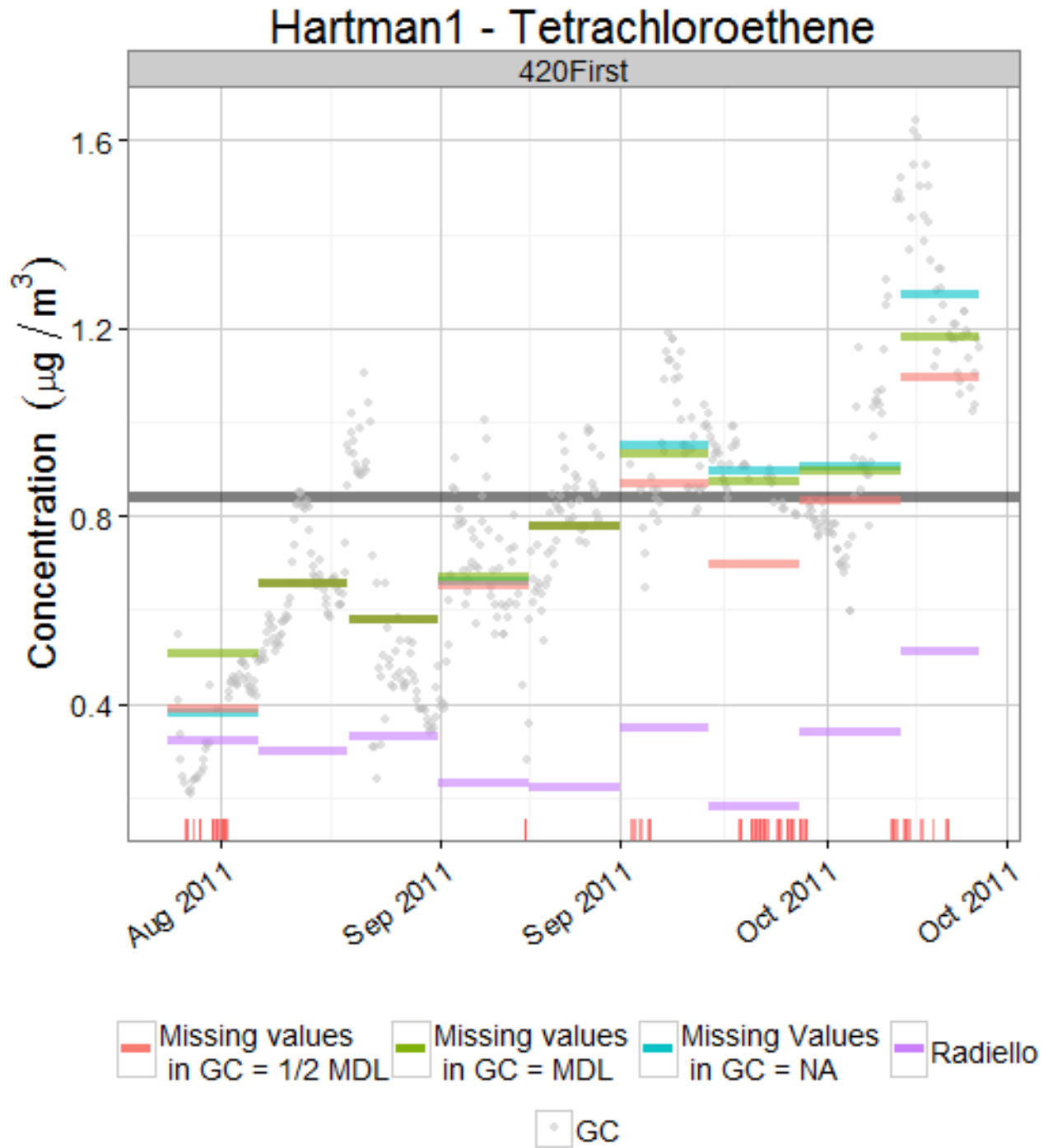


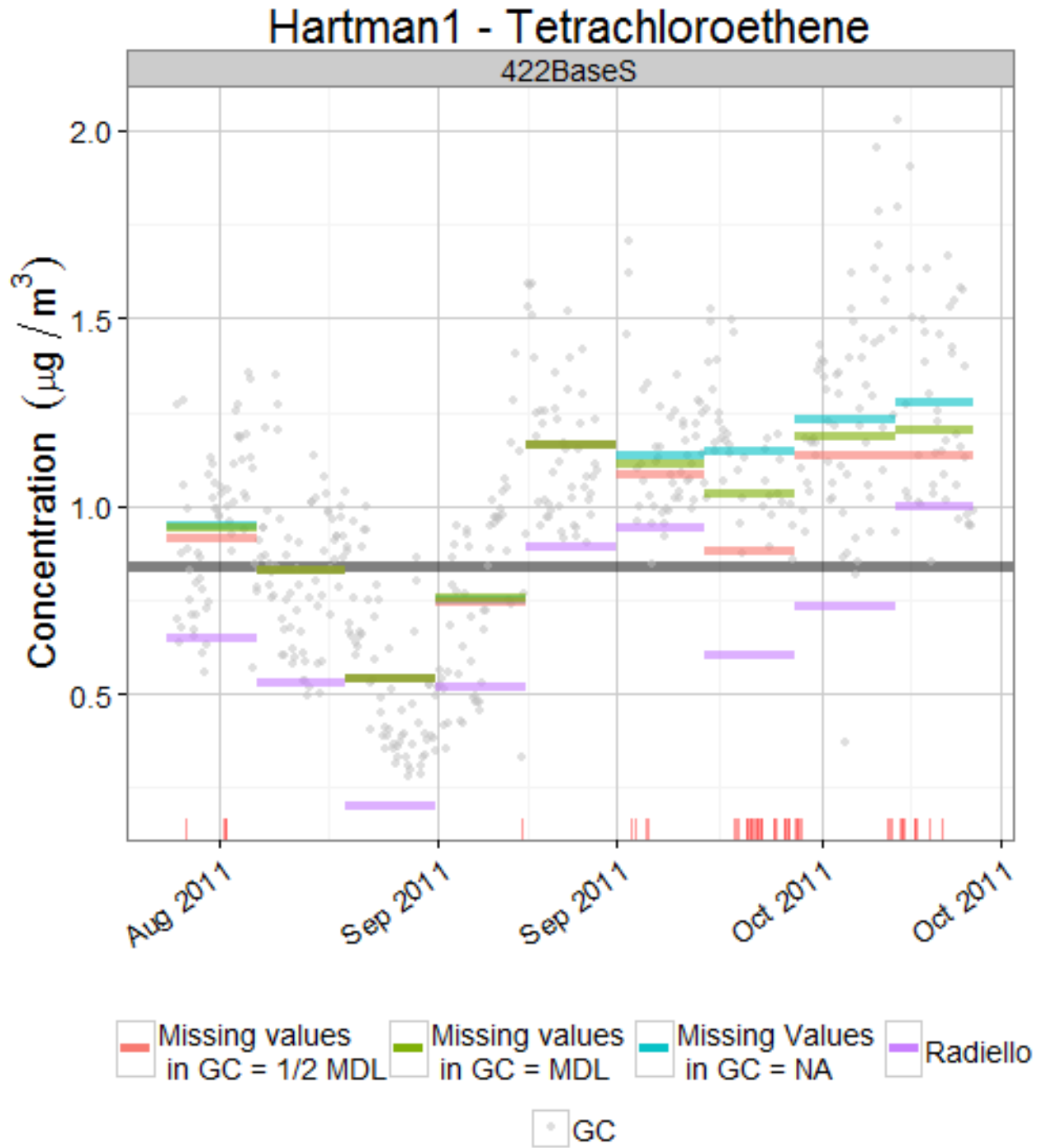


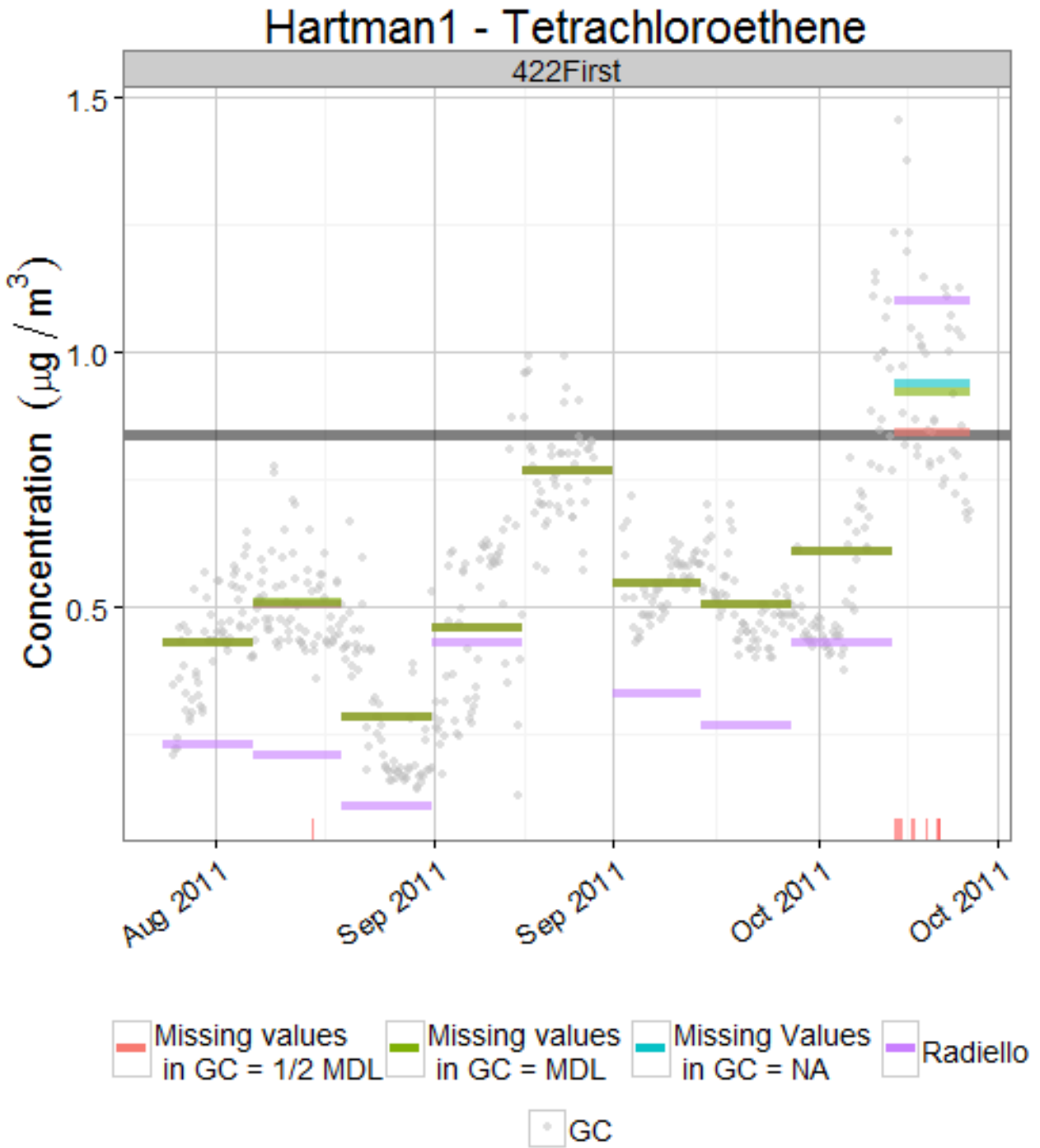


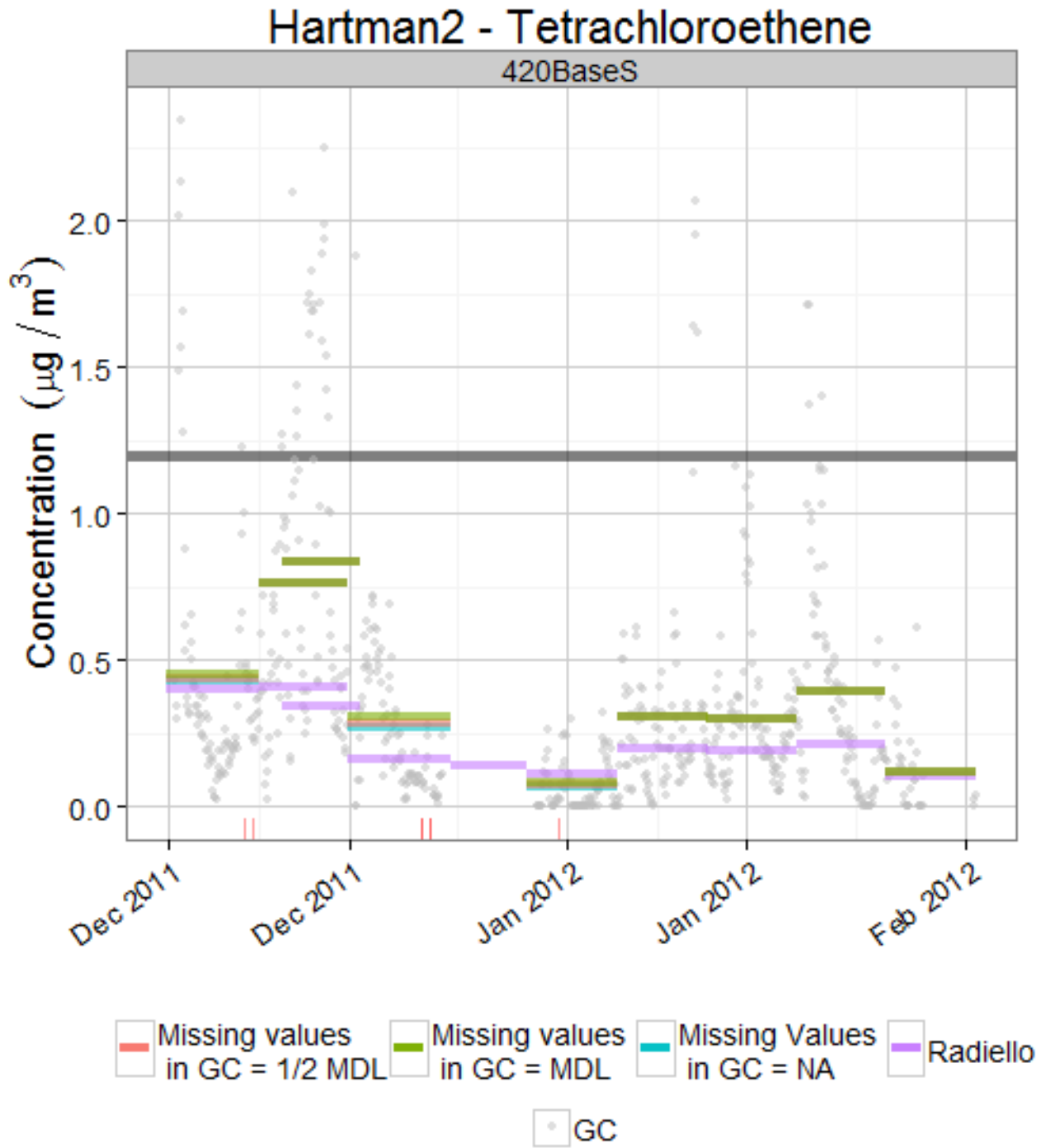


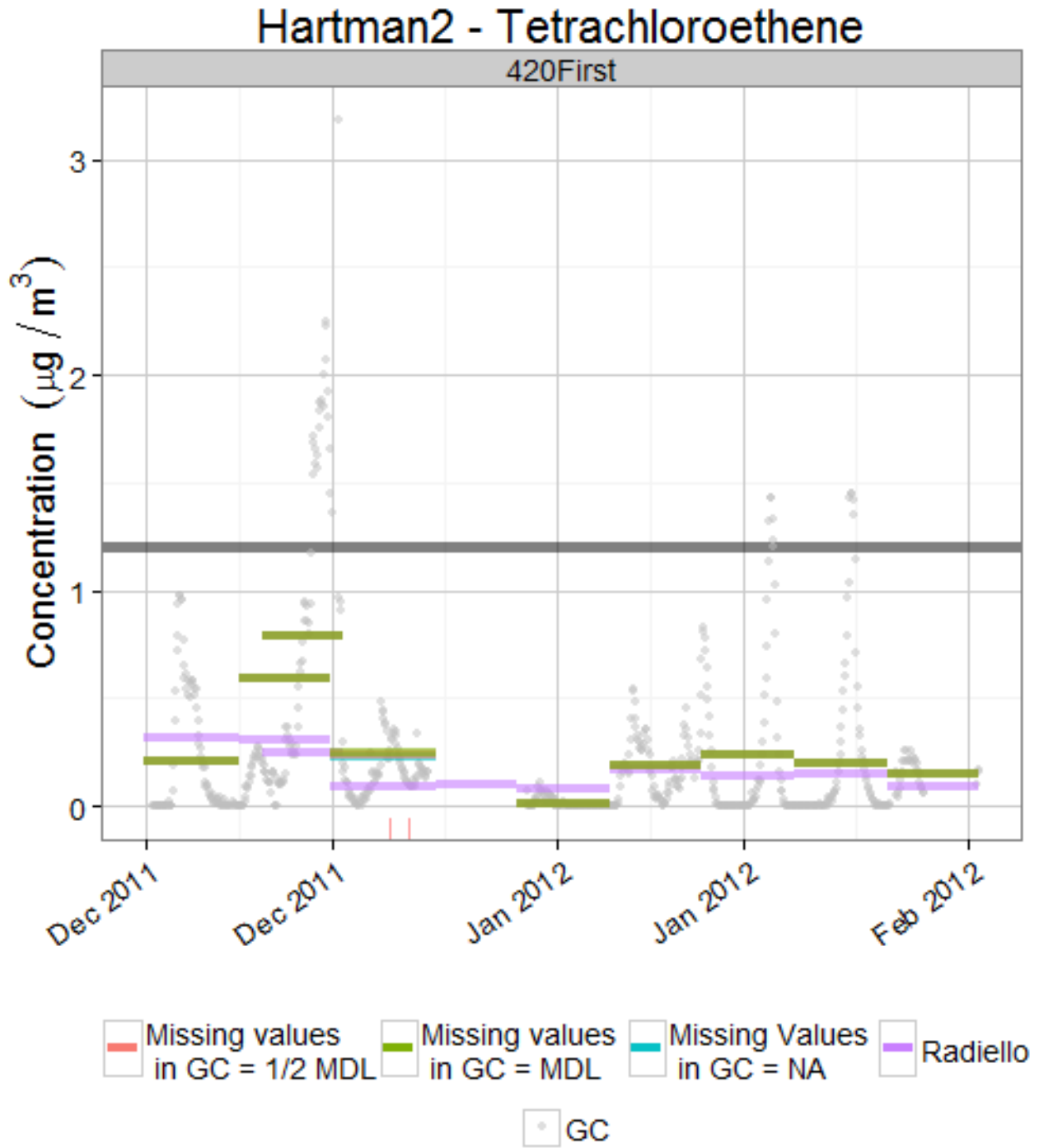


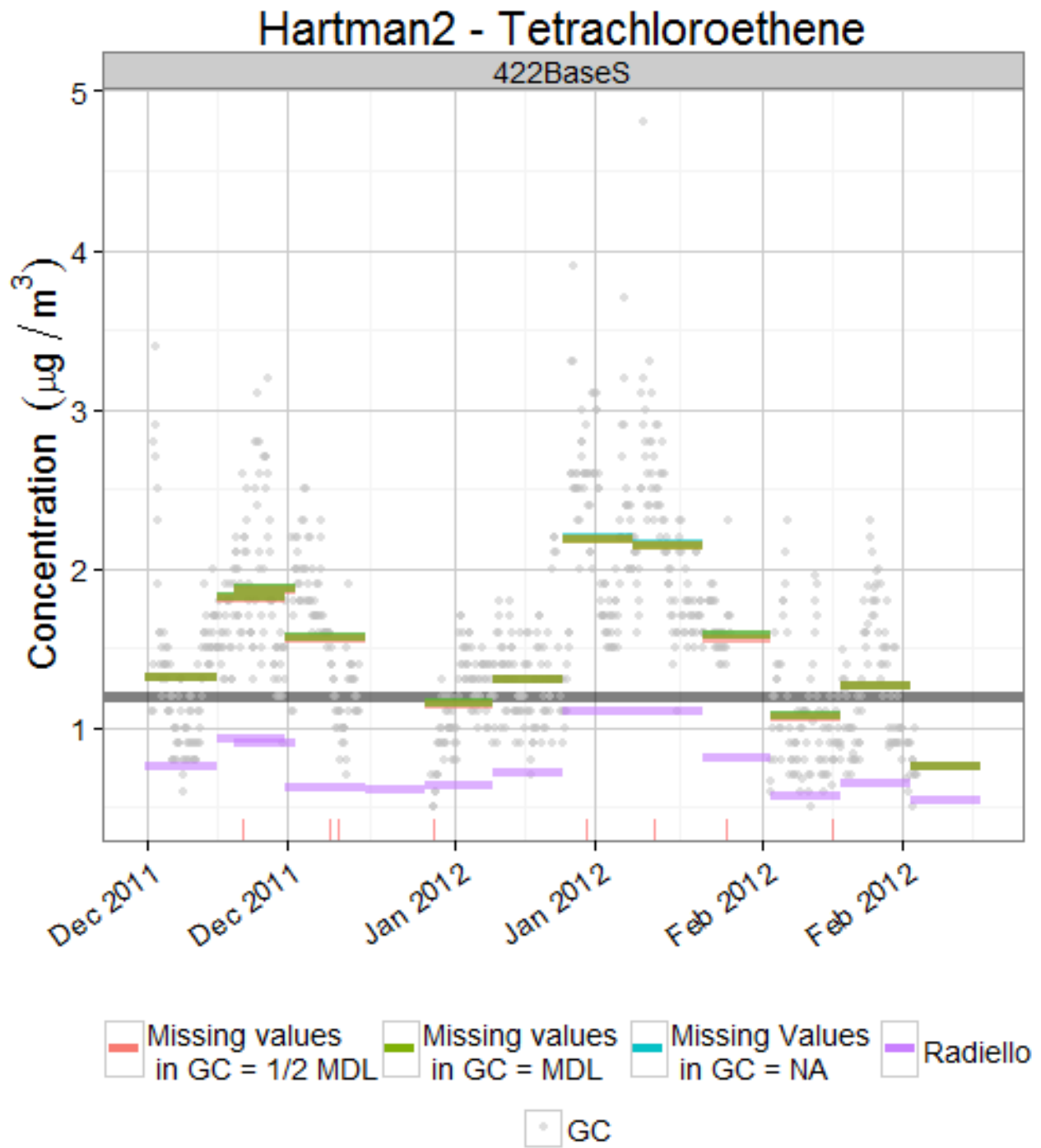


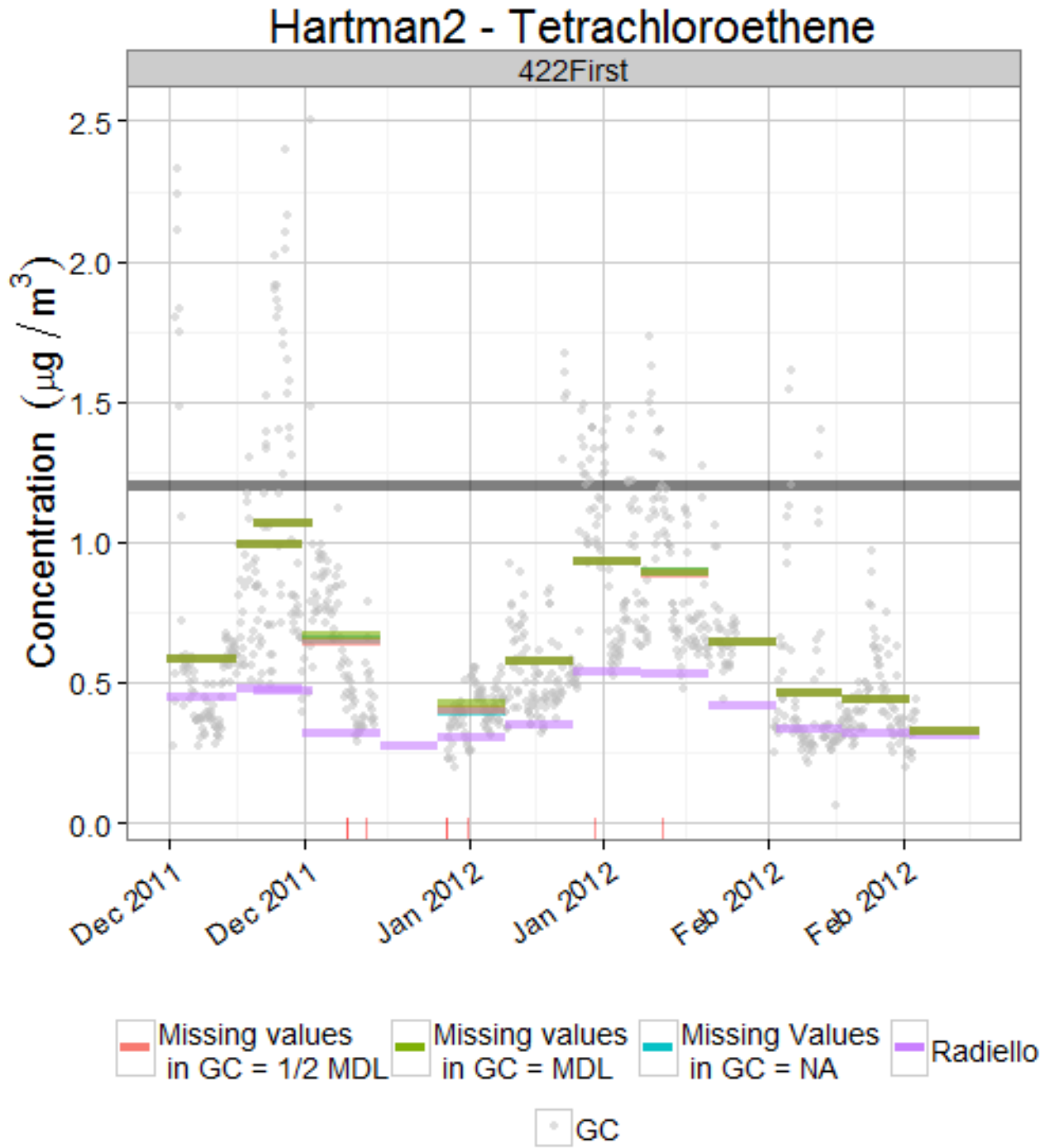


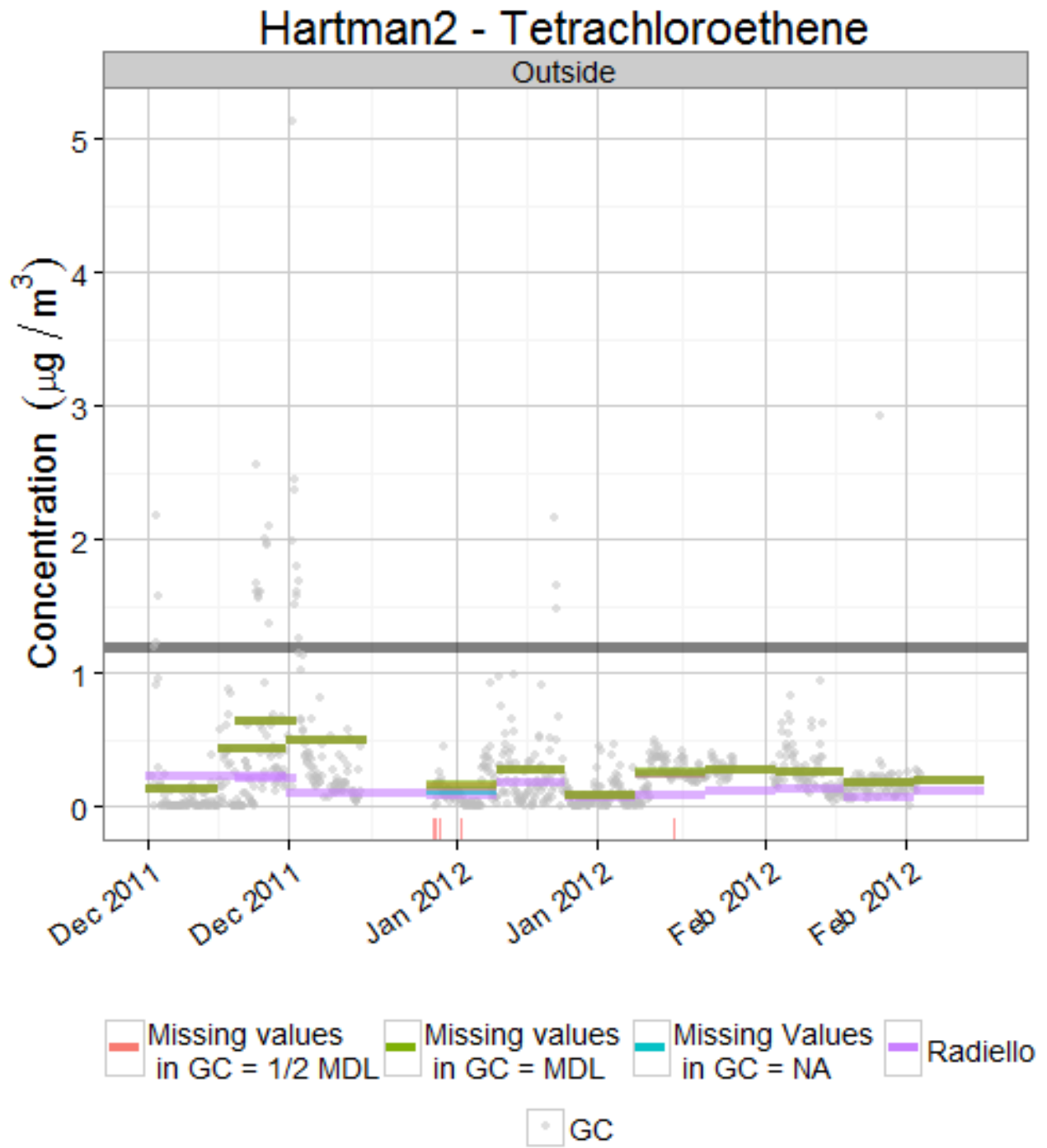


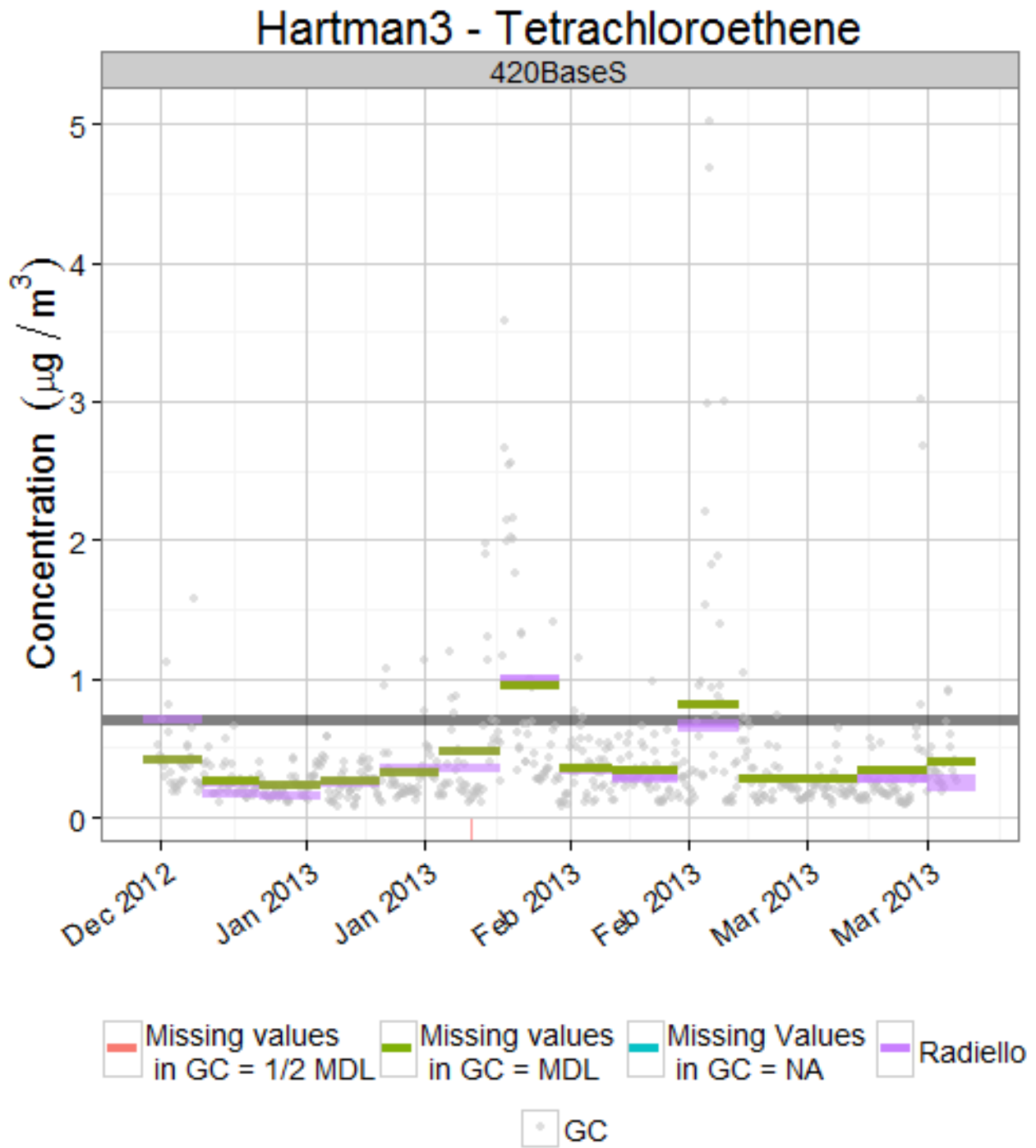


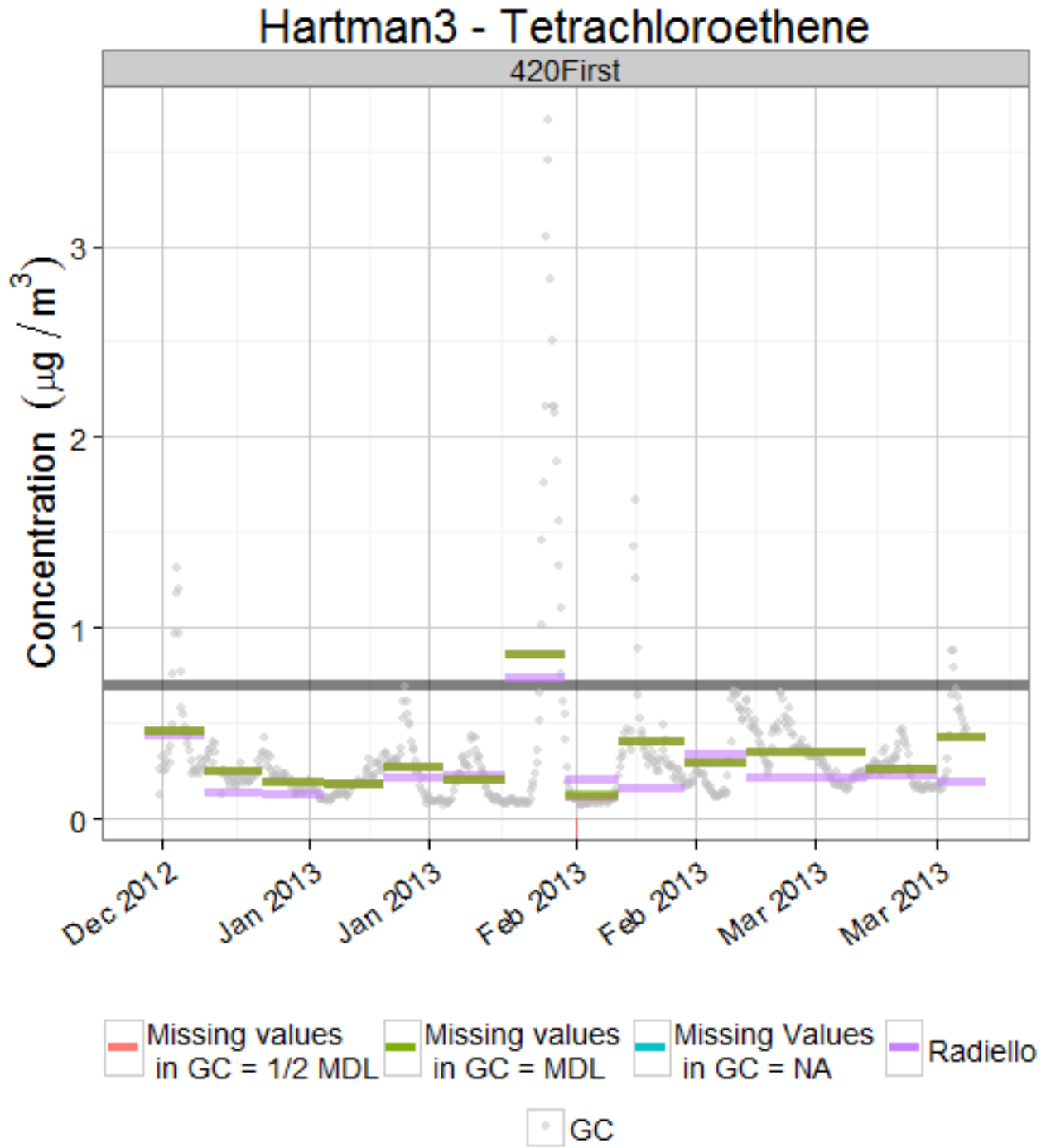


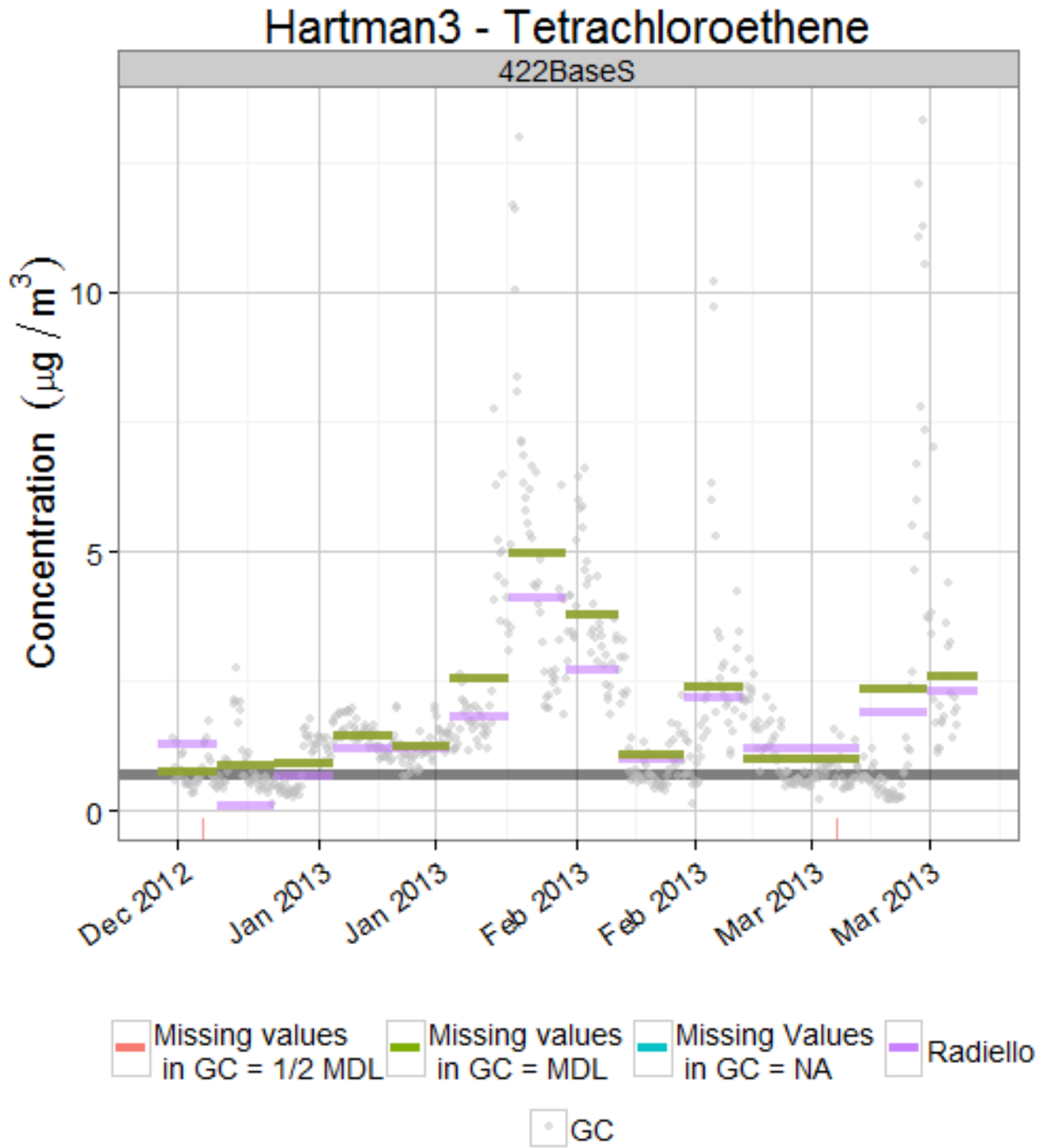


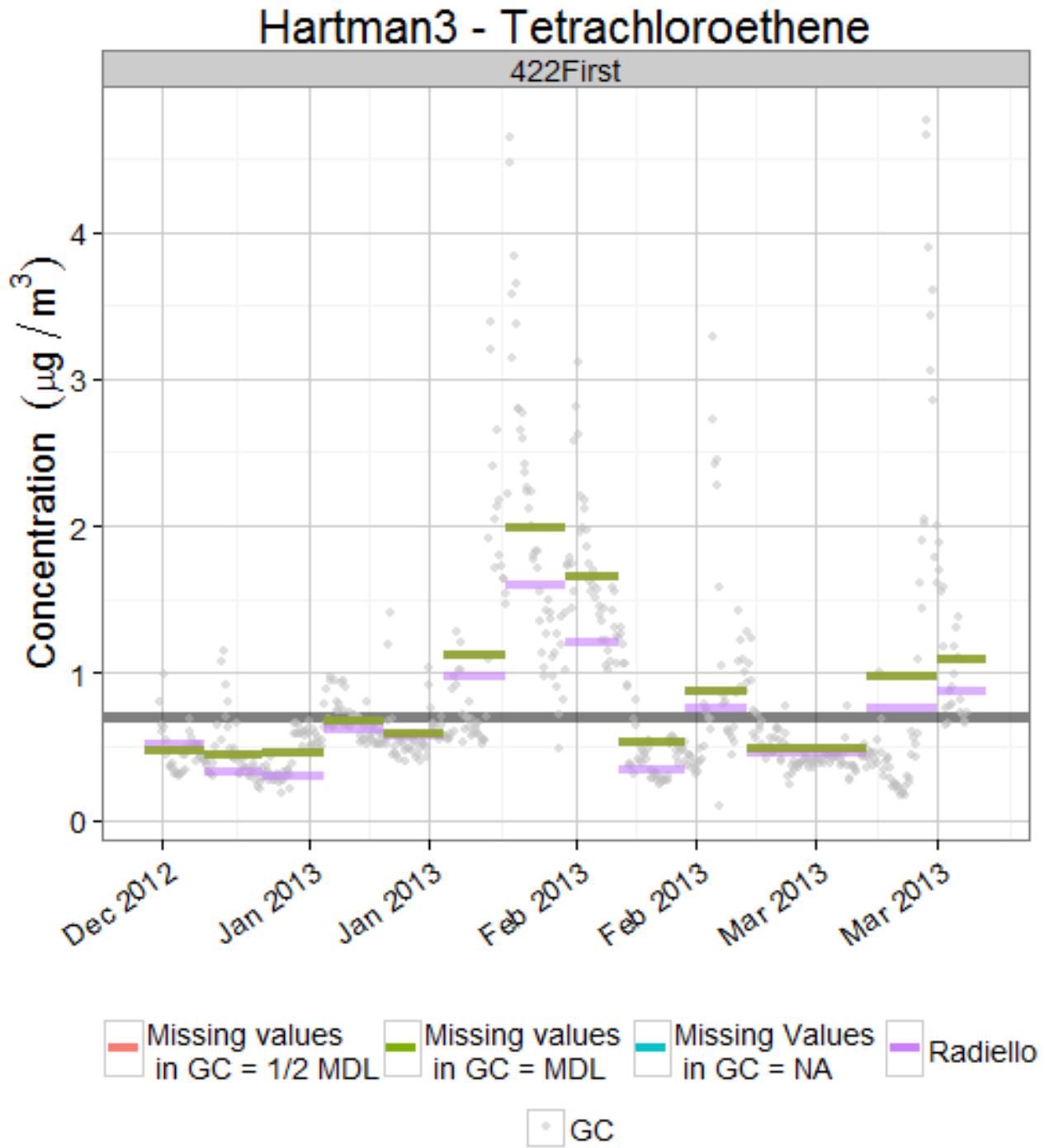












Appendix C

Additional Statistical Analysis of Effect of Mitigation on Indoor VOC Concentrations

Last ran on 09/14/2013

How much do indoor air concentrations differ between mitigation “On” and mitigation “Off”?

To address this question we used the standard VOC measurement in our study: weeklong Radiello passive samplers.

The mitigation system was installed on October 16, 2012 and run on 1 of 3 possible settings: “On,” “Off,” or “Passive.” Based on analyses elsewhere in this report we consider “Not Yet Installed,” “Passive,” and “Off” to be equivalent. These all appear as “Off” in this section. It is also important to consider that the heating system was used during some, but not all, of the mitigation testing. Only the 422 side was heated however, allowing its effect to be isolated. The on/off dates for both mitigation and heating are shown in calendar format in **Figure C-1** below.

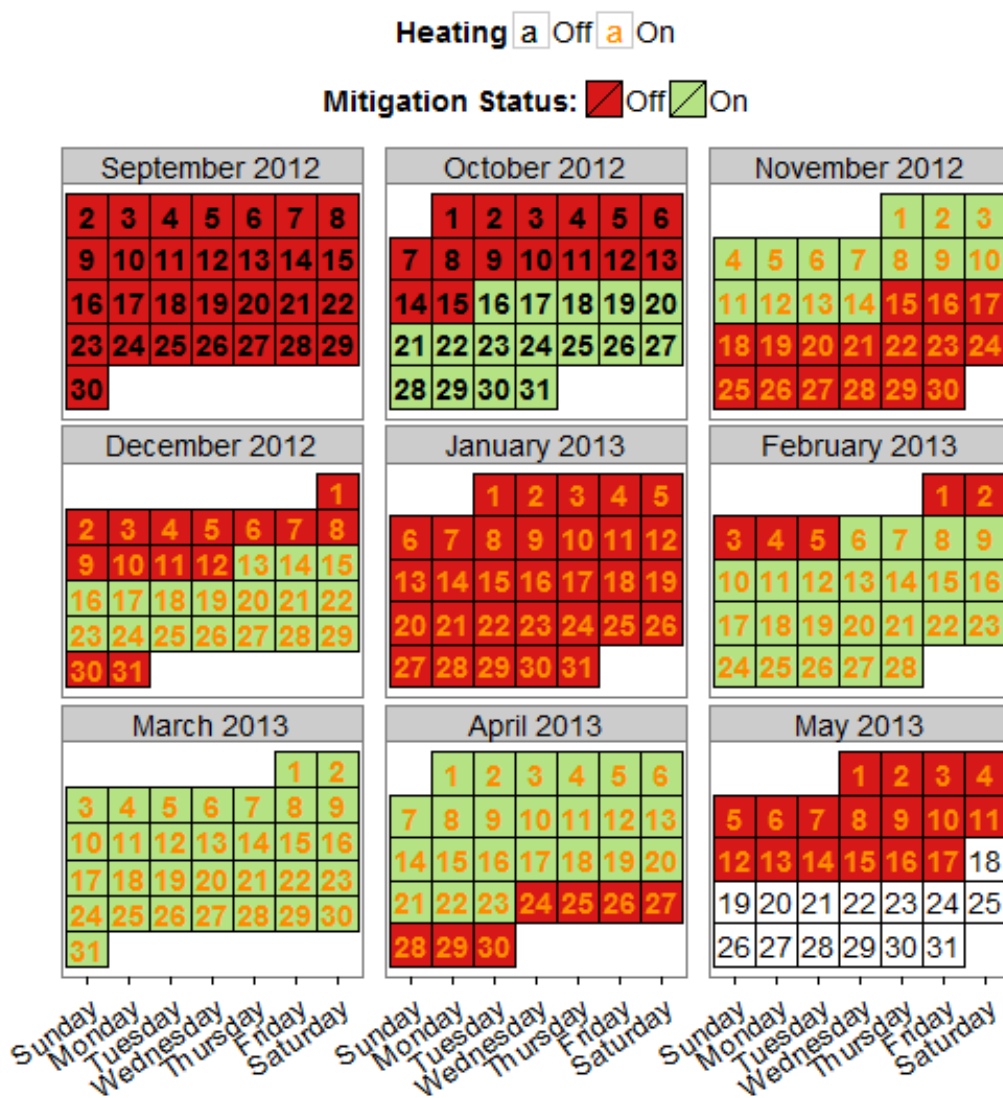


Figure C-1. Calendar of mitigation testing and heating status.

The Radiello samples were taken from several locations on each side of the duplex. The observed chloroform concentrations at each location are graphed in **Figure C-2** and the PCE concentrations are

plotted in **Figure C-3**. Note that both chloroform and PCE show a marked and continuing drop off in all indoor air concentrations corresponding to the last period of mitigation on (February through April).

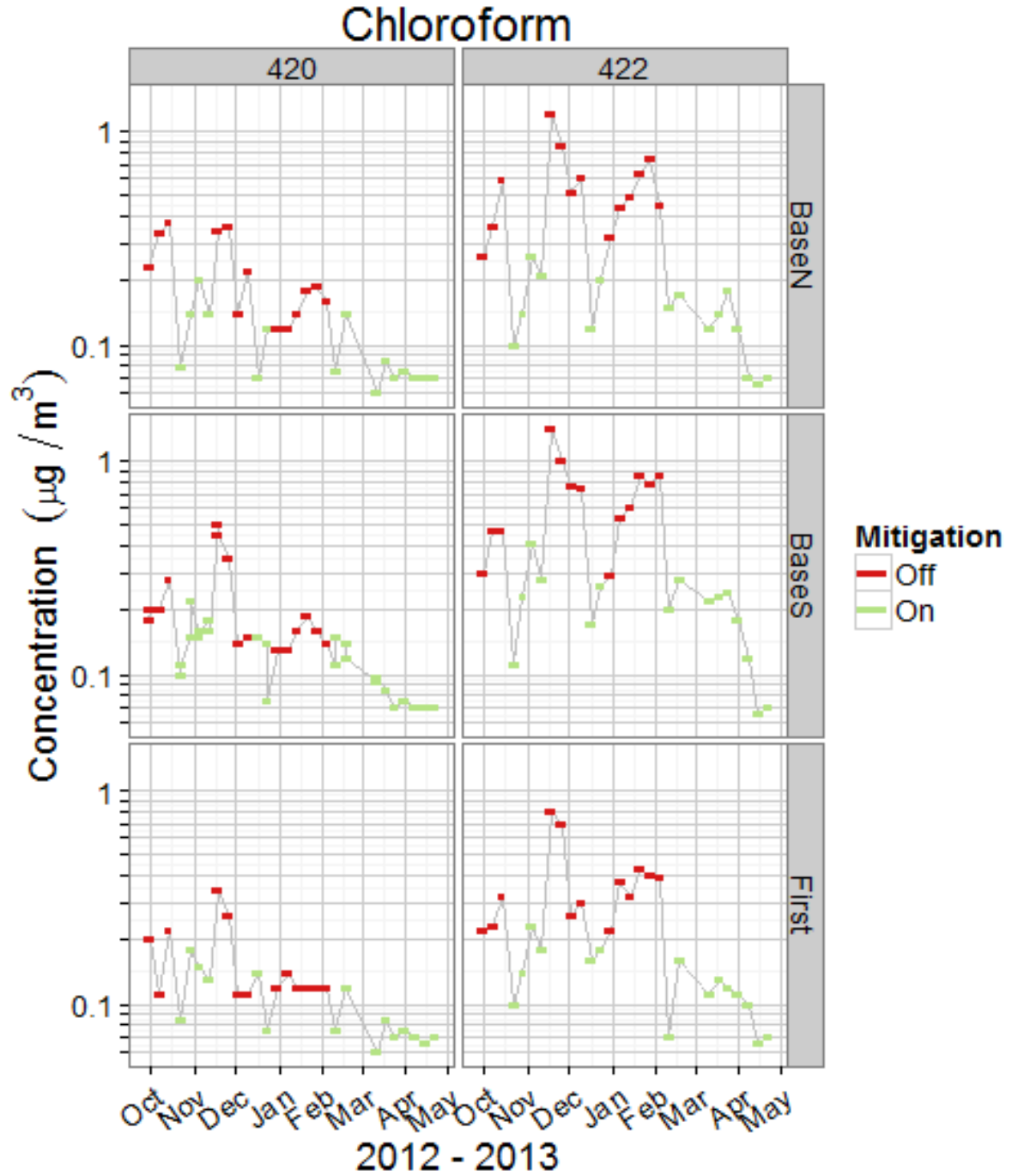


Figure C-2. Radiello chloroform results during mitigation testing.

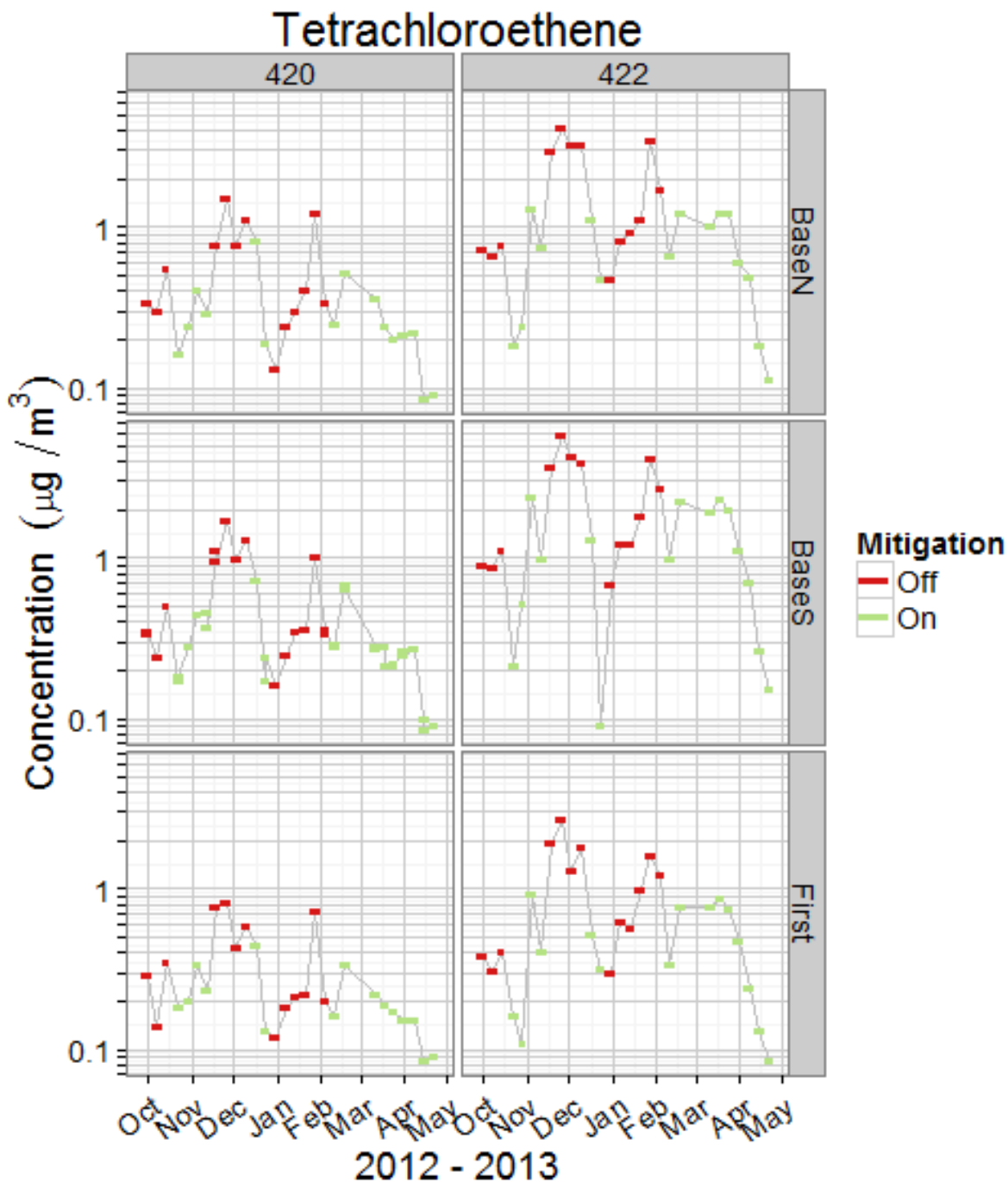


Figure C-3. Radiello PCE results during mitigation testing.

Boxplots juxtaposing the chloroform and PCE concentration values with mitigation “On” and “Off” at each location are given below (Figure C-4). In all cases the distribution of mitigated values is lower than for non-mitigated conditions.

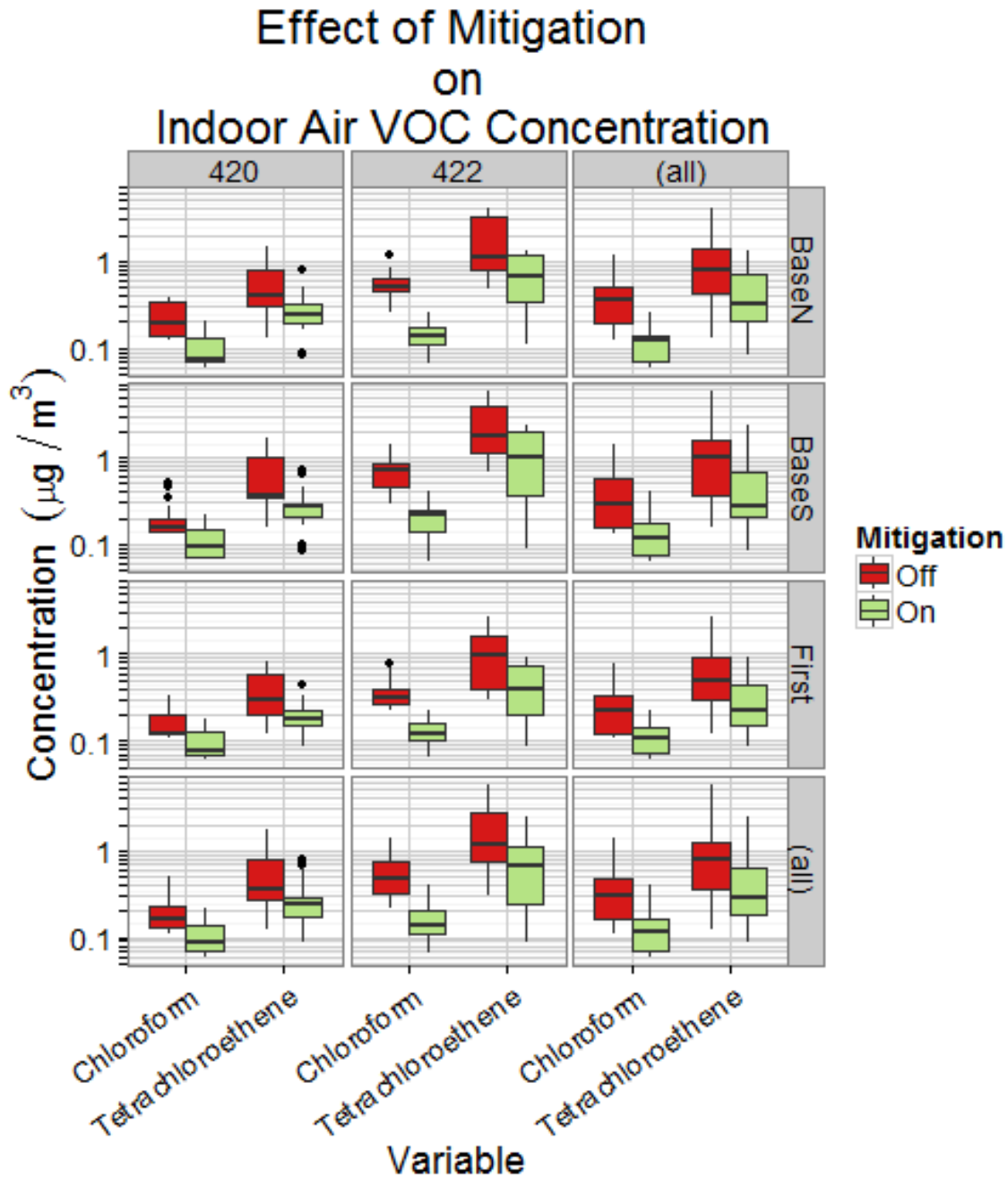


Figure C-4. Boxplots of mitigation effect on indoor air concentrations.

The boxplots suggest that turning the mitigation system on reduces the indoor air concentration of VOCs, but do not prove whether the difference is statistically significant. In order to apply a simple T-test for statistical significance, three assumptions must be made:

- The two populations are normally distributed.
- The two populations have the same variance.
- The sampled values are independent from one another.

These assumptions were checked as discussed below.

The two populations are normally distributed

Chemical concentration data are rarely normal, but often log-normally distributed. This is a simple transformation of the data that has a relevant interpretation, so we tested for both normality and log-normality using the Shapiro-Wilk test (**Table C-1**).

Table C-1. Results of Shapiro-Wilk Normality Testing

| Side | Location | Mitigation | Compound | N | Percent J Flags | P.Lognormal |
|------|----------|------------|-------------------|----|-----------------|-------------|
| 422 | BaseS | Off | CHCl ₃ | 13 | 0 | 0.685 |
| 422 | BaseS | Off | PCE | 13 | 0 | 0.153 |
| 420 | First | Off | CHCl ₃ | 13 | 69.2 | 0.003 |
| 420 | First | Off | PCE | 13 | 23.1 | 0.315 |
| 420 | BaseS | Off | CHCl ₃ | 17 | 17.6 | 0.004 |
| 420 | BaseS | Off | PCE | 17 | 5.9 | 0.101 |
| 422 | BaseN | Off | CHCl ₃ | 13 | 0 | 1 |
| 422 | BaseN | Off | PCE | 13 | 0 | 0.089 |
| 422 | First | Off | CHCl ₃ | 13 | 0 | 0.18 |
| 422 | First | Off | PCE | 13 | 0 | 0.31 |
| 420 | BaseN | Off | CHCl ₃ | 13 | 30.8 | 0.134 |
| 420 | BaseN | Off | PCE | 13 | 7.7 | 0.719 |
| 420 | First | On | CHCl ₃ | 15 | 26.7 | 0.029 |
| 420 | First | On | PCE | 15 | 46.7 | 0.738 |
| 420 | BaseS | On | CHCl ₃ | 29 | 31 | 0.003 |
| 420 | BaseS | On | PCE | 29 | 13.8 | 0.071 |
| 420 | BaseN | On | CHCl ₃ | 15 | 26.7 | 0.008 |
| 420 | BaseN | On | PCE | 15 | 13.3 | 0.69 |
| 422 | BaseN | On | CHCl ₃ | 15 | 33.3 | 0.53 |
| 422 | BaseN | On | PCE | 15 | 6.7 | 0.043 |
| 422 | First | On | CHCl ₃ | 15 | 46.7 | 0.646 |
| 422 | First | On | PCE | 15 | 20 | 0.174 |
| 422 | BaseS | On | CHCl ₃ | 15 | 13.3 | 0.143 |
| 422 | BaseS | On | PCE | 15 | 6.7 | 0.075 |

There are six subsets that “failed” the test (those with $p < 0.05$ are unlikely to have come from a log-normal distribution), but most locations and conditions (75%) do not. These results are encouraging and we will proceed with the assumption that log-normality is a defensible assumption for these data.

The two populations have the same variance

An F-test can be used to test this for each mitigation “On”/“Off” comparison (**Table C-2**). The assumption of equal variances holds in every case.

Table C-2. Results of F-test for Equal Variance

| Location | Side | Compound | p | V2 |
|----------|------|-------------------|---|----|
| BaseN | 420 | CHCl ₃ | 1 | 3 |
| BaseS | 420 | CHCl ₃ | 0 | 3 |
| First | 420 | CHCl ₃ | 1 | 3 |
| BaseN | 422 | CHCl ₃ | 1 | 3 |
| BaseS | 422 | CHCl ₃ | 1 | 3 |
| First | 422 | CHCl ₃ | 1 | 3 |
| BaseN | 420 | PCE | 0 | 3 |
| BaseS | 420 | PCE | 0 | 3 |
| First | 420 | PCE | 0 | 3 |
| BaseN | 422 | PCE | 1 | 3 |
| BaseS | 422 | PCE | 0 | 3 |
| First | 422 | PCE | 1 | 3 |

The sampled values are independent from one another

This is the hardest of the three assumptions to validate. This may not hold if the autocorrelation of the VOC concentrations is longer than a week. We believe that VOC concentrations from consecutive weeks are not autocorrelated due to the known air exchange rate at this house and autocorrelation results from other vapor intrusion studies, but significant autocorrelation beyond a week was found in our data in some cases (see Chapter 10). However, because the data being examined in this section do not span an entire year, the data cannot be detrended and this may contribute to the observed autocorrelation. If the data were indeed autocorrelated across weeks, the data in each of the two populations considered for each comparison (the two populations are mitigation “On” observations and mitigation “Off” observations) would be more similar amongst themselves than truly randomly chosen observations from each population would be and it would be possible to come to an incorrect conclusion as to the significance of the difference between the unmitigated and mitigated datasets.

For example, there are more mitigation “Off” samples preceded by other mitigation “Off” samples than there are preceded by mitigation “On” samples. If the concentration the previous week influenced the current week, the population of mitigation “Off” samples would be artificially heterogeneous causing its variance to be underestimated. This could potentially result in erroneously declaring the difference between two populations significant when it was not significant.

That being said, the results are quite convincing. We used a two-sided two-sample t-test to test the difference between the log-concentrations with mitigation “On” and “Off” with the null hypothesis that the difference between the two populations is 0 (that is to say that the null hypothesis is that mitigation has no effect). This provides a p-value for that hypothesis and an estimate of the difference and a standard error for that estimate which we used to calculate a 95% confidence interval for the estimated differences between populations. The raw estimates and upper/lower confidence limits of the log transformed data are not particularly valuable, but exponentiating them recovers the *factor* by which mitigation increases or decreases VOC concentration in indoor air. The exponentiated results are presented in **Table C-3** and **Figure C-5**.

Table C-3. Estimates of Concentration Reduction Factor with Mitigation On with 95% Confidence Intervals on the Factor

| Location | Side | Compound | p | low95 | estimate | up95 | Warning |
|----------|------|-------------------|-------|-------|----------|-------|---------|
| BaseN | 420 | CHCl ₃ | 0 | 0.327 | 0.443 | 0.601 | * |
| BaseS | 420 | CHCl ₃ | 0 | 0.416 | 0.527 | 0.669 | * |
| First | 420 | CHCl ₃ | 0.001 | 0.459 | 0.609 | 0.81 | * |
| BaseN | 422 | CHCl ₃ | 0 | 0.179 | 0.247 | 0.341 | |
| BaseS | 422 | CHCl ₃ | 0 | 0.196 | 0.288 | 0.422 | |
| First | 422 | CHCl ₃ | 0 | 0.254 | 0.343 | 0.465 | |
| BaseN | 420 | PCE | 0.009 | 0.3 | 0.498 | 0.827 | |
| BaseS | 420 | PCE | 0 | 0.328 | 0.479 | 0.7 | |
| First | 420 | PCE | 0.019 | 0.378 | 0.585 | 0.908 | |
| BaseN | 422 | PCE | 0.004 | 0.21 | 0.389 | 0.721 | * |
| BaseS | 422 | PCE | 0.014 | 0.19 | 0.393 | 0.812 | |
| First | 422 | PCE | 0.007 | 0.228 | 0.418 | 0.767 | |

* Log-normality assumption potentially violated

Effect of Mitigation on Indoor Air VOC Concentrations and 95% Confidence Intervals

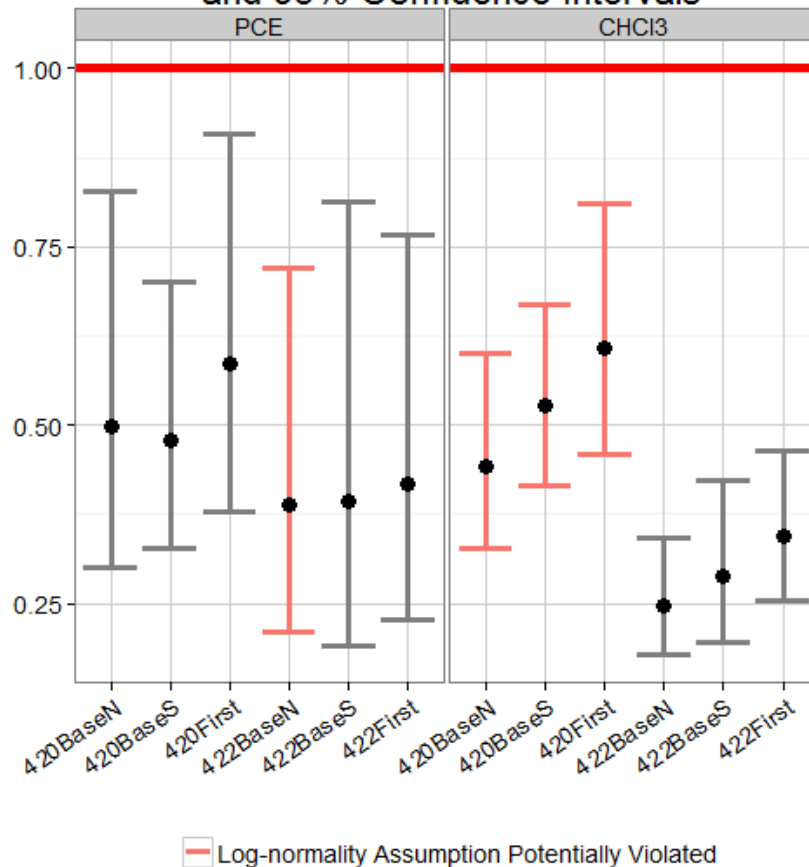


Figure C-5. Graphical presentation of concentration reduction factor with mitigation on.

In **Figure C-5** we include a red horizontal line at 1 because this represents the null hypothesis that turning the mitigation on will have no effect. An example of how one might interpret this figure is:

“We are 95% confident that mitigation decreases indoor air chloroform concentration at 420BaseN by a factor of 0.33 to 0.60.”

Notice the confidence bands are not symmetrical on either side of the point estimate. This is because the confidence intervals are computed in log space and then transformed back into real space.

Although the log-normality assumption is potentially violated in some of the tests and an argument could be made that the independence assumption is violated as well, the results are conclusive. All of the point estimates are below 1 and none of the confidence intervals include 1. A violation of the assumptions might result in a modest increase in the width of the confidence intervals, but certainly not enough to change the overall conclusion that mitigation does reduce indoor air VOC concentrations. Keep in mind that each test is done individually and does not take into account the conclusion of the other tests. The fact that 12 separate tests each corroborate one another inspires more overall confidence than the potential violation of the assumptions inspires doubt.

A summary of the PCE and chloroform geometric means, the estimated effect of mitigation, and the accompanying p-value are presented in **Table C-4**. Note that the difference between the mitigation off and mitigation on geometric mean VOC concentrations are significant in every case, with p-values well below 0.05.

Table C-4. Summary of PCE and Chloroform Geometric Means and Estimated Effect of Mitigation

| Compound | Side | Location | Geo Mean Mitigation Off | GeoMean Mitigation On | Effect (On/Off) | p-value |
|----------|------|----------|-------------------------|-----------------------|-----------------|-----------|
| PCE | 420 | BaseN | 0.484 | 0.2409 | 0.498 | 0.008937 |
| PCE | 420 | BaseS | 0.5294 | 0.2536 | 0.479 | 0.0003092 |
| PCE | 420 | First | 0.3171 | 0.1856 | 0.585 | 0.01871 |
| PCE | 422 | BaseN | 1.424 | 0.5533 | 0.389 | 0.004114 |
| PCE | 422 | BaseS | 1.94 | 0.7617 | 0.393 | 0.01366 |
| PCE | 422 | First | 0.8455 | 0.3537 | 0.418 | 0.006519 |
| CHCl3 | 420 | BaseN | 0.2055 | 0.09112 | 0.443 | 9.499e-06 |
| CHCl3 | 420 | BaseS | 0.1951 | 0.1029 | 0.527 | 2.328e-06 |
| CHCl3 | 420 | First | 0.1491 | 0.09086 | 0.609 | 0.001377 |
| CHCl3 | 422 | BaseN | 0.5283 | 0.1305 | 0.247 | 2.31e-09 |
| CHCl3 | 422 | BaseS | 0.635 | 0.1829 | 0.288 | 4.3e-07 |
| CHCl3 | 422 | First | 0.3505 | 0.1203 | 0.343 | 1.026e-07 |



EPA

United States
Environmental Protection
Agency

Office of Research
and Development (8101R)
Washington, DC 20460

Official Business
Penalty for Private Use
\$300

EPA/600/R-13/241
June 2015
www.epa.gov

Please make all necessary changes on the below label, detach or copy and return to the address in the upper left hand corner.

If you do not wish to receive these reports CHECK HERE ; detach, or copy this cover, and return to the address in the upper left hand corner.

PRESORTED STANDARD
POSTAGE & FEES PAID
EPA PERMIT No. G-35



Recycled/Recyclable

Printed with vegetable-based ink on
paper that contains a minimum of
50% post-consumer fiber content
processed chlorine free